ORGANOMETALLICS

Volume 2, Number 1, January 1983

Intramolecular Reactions of Alkenylsilylenes

Thomas J. Barton* and Gary T. Burns

Department of Chemistry, Iowa State University, Ames, Iowa 50011

Received July 14, 1982

Thermally generated 4-butenylmethylsilylene was found to cyclize in 56% yield to 4-methyl-4-silacyclopentene. This isomerization is proposed to occur through β-CH insertion to form the often postulated vinylsilacyclopropane which then rearranges via 1,3-silyl migration. Methyl-4-(2-pentenyl)silylene also undergoes intramolecular allylic C–H insertion to directly form 3,4-dimethyl-4-silacyclopentene (30%). Methyl-5-(1,3-pentadienyl)silylene undergoes intramolecular π addition to give predominantly (52%) 5-methyl-5-silacyclohexa-1,3-diene. A silabicyclo[3.1.0]hexene intermediate is also proposed for the transformation of methyl-1-(2,4-hexadienyl)silylene to 1-methyl-1-vinyl-1-silacyclopent-2-ene (68%), but C–C rather than Si–C bond homolysis is invoked as the penultimate step.

Introduction

Recently we reported[1] that flash vacuum pyrolysis (FVP) generated allylmethylsilylene (**1**) isomerized to 1-methylsiletene (**3**) and suggested that this occurred via initial intramolecular π addition to form silabicyclo[1.1.0]butane **2** followed by homolysis of the internal Si–C bond and 1,2-hydrogen migration. We now wish to report the extension of this work to selected, longer chain alkenyl and dienyl silylenes.

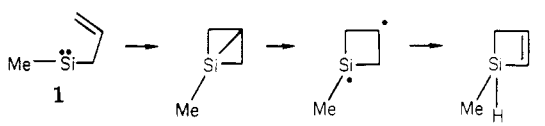

1 **2** **3**

Results and Discussion

4-Butenylmethylsilylene (8). In contrast to the behavior of allylcarbenes, generation of 4-butenylcarbene (**4**) by catalytic decomposition of the corresponding diazo precursor does not lead to the product of intramolecular π addition, bicyclo[2.1.0]pentane (**5**), but rather to 1,4-pentadiene by hydrogen shift.[2] Since the corresponding

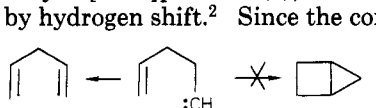

4 **5**

shift by a 4-butenylsilylene would involve the unknown process of thermal rearrangement of a silylene to a silene ($R_2Si{=}CR_2$) via hydrogen migration, it was hoped that the silicon analogue of **4** would exclusively undergo π addition if produced under conditions favoring intramolecular reaction. To this end the desired silylene precursor, disilane **6**, was synthesized by the addition of 1-aziranyl-1-chlorotetramethyldisilane to a solution of 4-butenyl bromide followed by quaternarization with methyl iodide and displacement of the amine by methanol to afford 1-(4-butenyl)-1-methoxytetramethyldisilane (**6**) in 64% yield. The FVP of **6** was conducted at 690 °C (1×10^{-4} torr) with an 81% mass recovery. In addition to the expected product of reductive elimination, Me_3SiOMe (79%), only a single volatile product was obtained: 4-methyl-4-silacyclopentene (**7**) in 56% yield (absolute, GC).

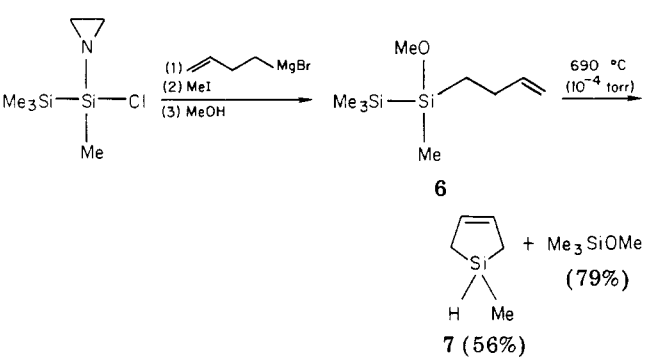

6

+ Me_3SiOMe (79%)

7 (56%)

In consideration of the origin of **7**, it should be first noted that direct insertion of silylene **8** into a vinyl β-CH bond would produce the unobserved isomeric silacyclopentene **9**. Also, a mechanistic route of π addition and central Si–C bond homolysis affords diradical **10**, for which 1,2-hydrogen migration to form **9** would be expected to be at least competitive with a 1,3-hydrogen shift to produce **7**. Thus, we favor initial silylene insertion into an allylic

(1) Burns, G. T.; Barton, T. J., *J. Am. Chem. Soc.*, in press.
(2) Kirmse, W.; Grassman, D. *Chem. Ber.* **1966**, *99*, 1746.

0276-7333/83/2302-0001$01.50/0

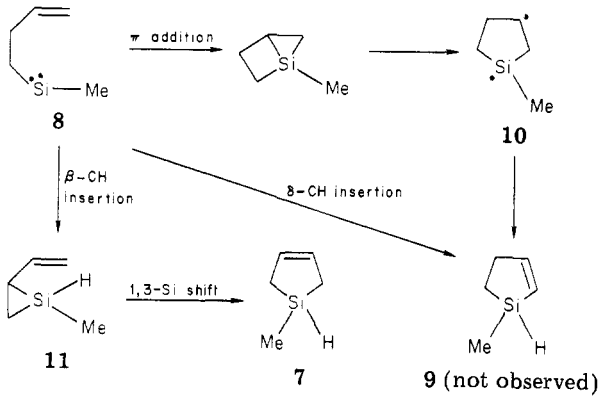

C–H bond to form an intermediate vinylsilacyclopropane **11** which undergoes a formal 1,3-silyl migration to afford **7**. Invocation of **11** is of additional interest in that vinylsilacyclopropanes have long been thought to be the *initial intermediates in the bimolecular reactions of silylenes* and 1,3-dienes to produce 4-silacyclopentenes.[3] Thus, it would appear that we have achieved the same intermediate through an intramolecular silylene reaction.

Methyl-4-(2-pentenyl)silylene (13). Intramolecular allylic C–H insertion by silylene appears also to be involved in the thermochemistry of methyl-4-(2-pentenyl)silylene (**13**). Thus, when 4-(1-methoxytetramethyldisilanyl)-2-pentene (**12**) (synthesized in a similar fashion as for **6** in only an 8% yield) was subjected to FVP (680 °C (10^{-4} torr)) only two volatile products were observed and isolated by gas chromatography. The products were Me_3SiOMe (67%) and 3,4-dimethyl-4-silacyclopentene (**14**) (29%, 43% based on Me_3SiOMe). Formation of **14** is again most easily rationalized as arising from cyclization of silylene **13** through insertion into an allylic C–H bond.

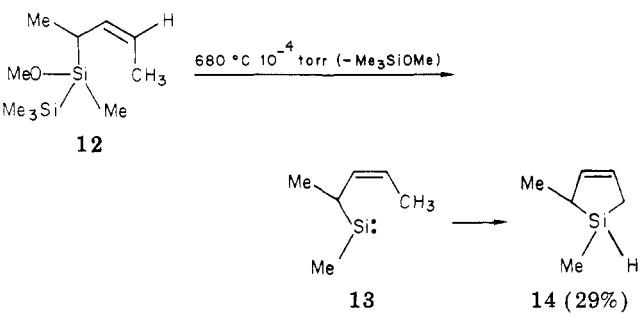

Methyl-5-(1,3-pentadienyl)silylene (16). Extension of this study to dienylsilylenes was accomplished by the FVP of 5-(1-methoxytetramethyldisilanyl)-1,3-pentadiene (**15**) at 700 °C (10^{-4} torr) with 87% mass recovery. In addition to Me_3SiOMe (84%), two volatile products were isolated and found to be isomeric with silylene **16**. The major product was determined to be 5-methyl-5-silacyclohexa-1,3-diene (**18**) and was formed in 52% yield. The minor product (13%) was found to be 3-methylene-4-methyl-4-silacyclopentene (**20**). Both of these products presumably arise from addition of the divalent silicon in **16** to the terminal double bond. The intermediate silabicyclo[3.1.0]hexene **17** apparently undergoes preferential opening of the internal Si–C bond followed by 1,2-hydrogen shift to produce **18**. Competition in the form of external Si–C bond homolysis affords a silacyclopentenyl diradical **19** which rearranges to **20**.

Methyl-1-(2,4-hexadienyl)silylene (22). Increasing the length of the alkadienyl chain of **16** by a single methyl

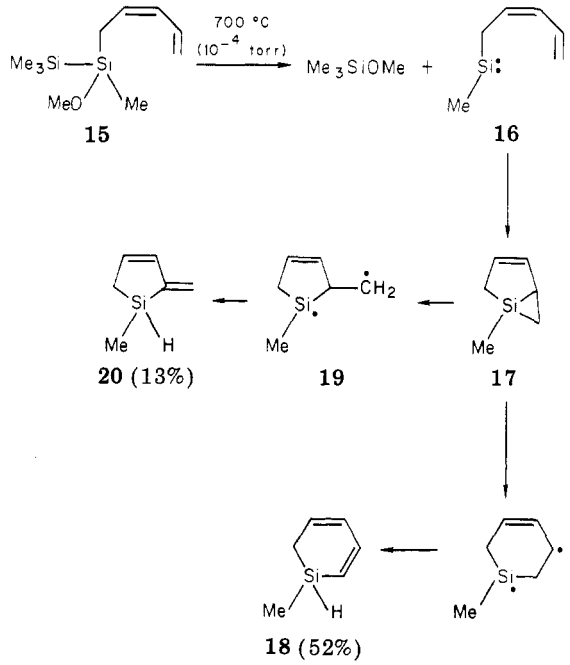

group had a profound and unexpected effect on the observed chemistry. Thus, when methyl-1-(2,4-hexadienyl)silylene (**22**) was generated by FVP of hexadienyldisilane **21** (680 °C (10^{-4} torr)), a very clean formation of 1-methyl-1-vinyl-1-silacyclopent-2-ene (**25**) was obtained. The absolute yield of **25** was 68%, but on the basis of the yield of Me_3SiOMe (73%), hence the amount of silylene **22** formed, the yield of **25** was a remarkable 93%. Formation of **25** is most economically rationalized by initial π addition to form silabicyclo[3.1.0]hexene **23**. Apparently the methyl substitution on **23** is sufficient to alter the course of decomposition from that taken by **17**. Although the carbon–carbon bond rupture required for the conversion of **23** to diradical **24** is not the normal expectation for a monocyclic silacyclopropane, this process has ample precedent in the ring-expansion reactions between silylenes and cyclic dienes such as furans,[4] cyclopentadiene,[5] and 1,3-cyclooctadiene.[6]

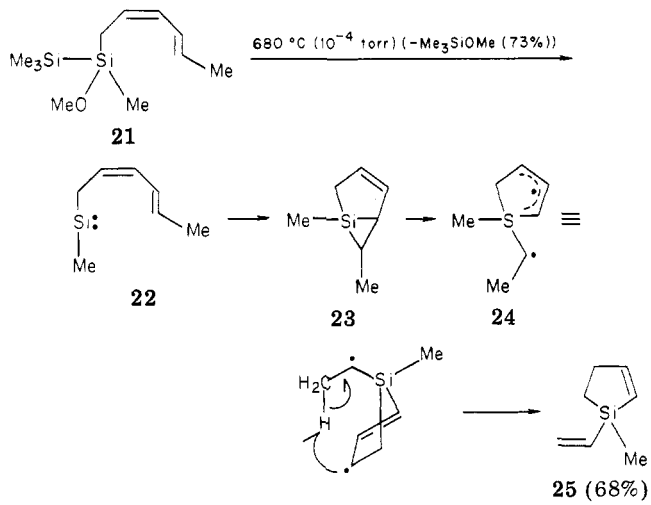

In summary one can conclude that intramolecular π additions of appropriately substituted silylenes can be

(3) Gaspar, P. P.; Hwang, R.-J. *J. Am. Chem. Soc.* **1974**, *96*, 6198. Ishikawa, M.; Ohi, F.; Kumada, M. *J. Organomet. Chem.* **1975**, *86*, C23; and references therein.

(4) Chernyshev, E. A.; Krasnova, T. L.; Stepanov, V. V.; Labartkava, M. O. *Zh. Obshch. Khim.* **1978**, *48*, 2798.

(5) Hwang, R.-J.; Conlin, R. T.; Gaspar, P. P. *J. Organomet. Chem.* **1975**, *94*, C38.

(6) Childs, M. E.; Weber, W. P. *Tetrahedron Lett.* **1974**, 4033.

extremely clean and synthetically useful even under the rather severe thermal conditions of this work. However, it appears from these limited data (and related work from our laboratory) that when allylic C–H bonds are available and suitably located that C–H insertion by the divalent silicon will predominate. Indeed, allylic activation of the C–H bond is not required as Gusel'nikov[7] has recently demonstrated that methyl(trimethylsilylalkyl)silylenes such as **26** react predominantly through β-CH insertion followed by methylsilylene ejection from the transient silacyclopropane to afford the corresponding alkenylsilanes. This is consistent with our finding that *n*-butylsilylene **28** cleanly affords 1-butene.

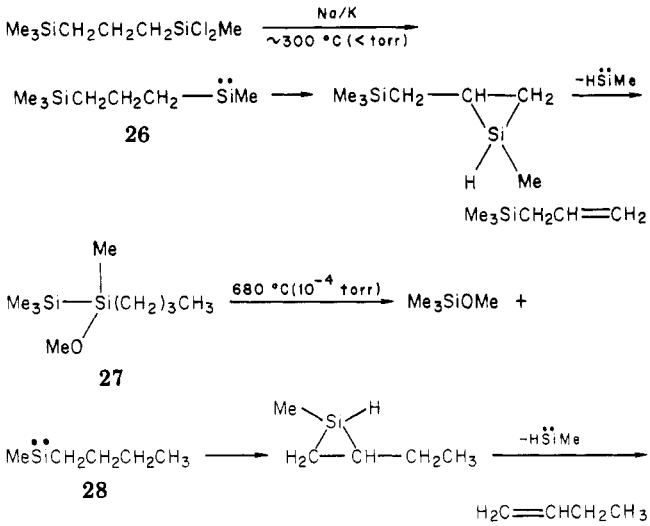

In addition to extensions of this work, we are currently attempting to generate these and other alkenylsilylenes under photochemical conditions in the hopes of observing the bicyclic intermediates.

Experimental Section

General Data. Proton NMR spectra were recorded on a Varian Model EM-360 spectrometer. GC–mass spectral (GC–MS) data were collected at 70 eV on a Finnegan Model 4023 mass spectrometer, and exact mass measurements were obtained on an AEI MS-902 mass spectrometer. Gas chromatographic separations were performed on a Varian-Aerograph Series 1700 instrument. Unless otherwise specified, all yields are calculated from NMR measurements with internal standards and are absolute. Flash vacuum pyrolyses (FVP) were carried out by evaporating the silylene precursor through a horizontal 30-cm quartz tube packed with quartz chips and heated in a tube furnace. Products are collected in a liquid N_2 cooled trap.

1-(4-Butenyl)-1-methoxytetramethyldisilane (6). A solution of 9.85 mmol of 4-butenylmagnesium bromide was prepared by the slow addition of 1.33 g (9.85 mmol) of 4-butenyl bromide to a stirred suspension of excess Mg turnings in anhydrous Et_2O. To this solution was added 1.554 g (8.03 mmol) of 1-aziranyl-1-chlorotetramethyldisilane[8] over a 10-min interval. After the solution was stirred for 8 h at room temperature, 1.0 mL of MeI was added, and this was followed immediately by the addition of 0.8 mL of MeOH. After being stirred for 15 min, the solution was poured into twice its volume of hexane, filtered through celite, and concentrated by rotary evaporation. The residue was GC separated on a 20-ft, 20% SE-30 column programmed from 130 °C at 2 °C/min to afford 0.334 g (21%) of pure **6**. On a larger scale reaction (33 mmol) the product was isolated by distillation (60 °C (1 torr)) in 64% yield: NMR ($DCCl_3$) δ 0.22 (s, 9 H), 0.27 (s, 3 H), 0.67–1.0 (m, 2 H), 1.91–2.49 (m, 2 H), 3.50 (s, 3 H), 4.78–5.21 (m, 2 H), 5.58–6.28 (m, 1 H); mass spectrum, *m/e* (% relative intensity) 202 (10), 187 (38), 147 (41), 133 (75), 98 (90), 97 (81), 89 (70), 75 (85), 73 (100); calcd for $C_9H_{22}Si_2O$ *m/e* 202.120 93, measured *m/e* 202.120 85.

FVP of 6. Disilane **6** (0.3340 g, 1.65 mmol) was distilled (45 °C (1 × 10^{-4} torr)) through a quartz tube heated to 690 °C. The pyrolysate was collected in a N_2-cooled trap and represented an 81% mass recovery (0.2718 g). The pyrolysate was separated by GC on a 20-ft, 20% SE-30/Chromosorb W column using a temperature program of 100 °→ at 2 °C/min. Two products were obtained. The first was identified as Me_3SiOMe (79%) on the basis of spectral comparison with an authentic sample. The second product was identified as 4-methyl-4-silacyclopentene (**7**):[9] 56%; NMR (C_6D_6) δ −0.11 (d, 3 H, *J* = 4 Hz, collapses to s with hν at δ 4.22), 1.35 (center of doubled AB, collapses to broadened AB with hν at δ 4.38, 4 H), 4.38 (SiH, m), 5.88 (br s, 2 H); mass spectrum, *m/e* (% relative intensity) 98 (65), 97 (100), 83 (77), 81 (23), 70 (54), 67 (11), 57 (11), 55 (55), 54 (14), 53 (27); the GC retention time and spectral properties exactly matched those of an authentic sample prepared by $LiAlH_4$ reduction of 4-chloro-4-methyl-4-silacyclopentene.

4-(1-Methoxytetramethyldisilanyl)-2-pentene (12). To a stirred suspension of excess Mg turnings in 30 mL of Et_2O was added a solution of 2.361 g (15.8 mmol) 4-bromo-2-pentene and 2.462 g (12.9 mmol) of 1-chloro-1-aziranyltetramethyldisilane[8] in 20 mL of Et_2O at a rate sufficient to maintain a gentle reflux. After the reaction had subsided, the liquid was decanted from the Mg and excess methyl iodide and methanol were added sequentially. The solution was stirred for 2 h and then diluted with hexane, filtered through celite, and concentrated by rotary evaporation. The residue was separated by GC on a 20-ft, 20% SE-30 on Chromosorb W column by using a temperature program of 150–220 °C at 2 °C/min to afford 0.218 g pure **12** (8%): NMR ($DCCl_3$) δ 0.06 (s, 12 H), 1.01 (d, *J* = 7 Hz, 3 H), 1.59 (d, *J* = 5 Hz, 3 H, collapses to s with hν at δ 5.26), 1.84 (br q, *J* = 7 Hz, collapses to sharp q with hν at d 5.26, 1 H), 3.36 (s, 3 H, OMe) 5.26 (m, 2 H, collapses to brd s with hν at δ 1.59); *m/e* (% relative intensity) 216 (15), 201 (10), 147 (100), 132 (15), 107 (30), 88 (20), 73 (70); calcd for $C_{10}H_{24}OSi_2$ *m/e* 216.136 58, measured *m/e* 216.136 45.

FVP of 12. Disilane **12** (0.2184 g, 1.01 mmol) was distilled (25 °C (10^{-4} torr)) through a quartz tube heated to 680 °C with 68% mass recovery. Two products were isolated by GC using a 20-ft, 20% SE-30 on Chromosorb W column with a temperature program of 100–220 °C at 2 °C/min. The first product was Me_3SiOMe in 67% yield. The other product was identified as 3,4-dimethyl-4-silacyclopentene (**14**): 29% yield, 43% based on Me_3SiOMe; NMR (C_6D_6) δ 0.07 (d, *J* = 4 Hz, collapses to s with hν at δ 4.12, 3 H), 1.12 (d, *J* = 7 Hz, 3 H), 0.89–1.82 (m, 3 H), 4.12 (SiH, m, 1 H), 5.75 (br s, 2 H); mass spectrum, *m/e* (% relative intensity) 112 (35), 111 (11), 97 (100), 95 (34), 84 (32), 83 (15), 71 (30), 70 (21), 69 (27), 67 (12), 59 (16), 58 (30), 55 (23), 53 (15).

5-(1-Methoxytetramethyldisilanyl)-1,3-pentadiene (15). To a stirred solution of 8.92 mmol of pentadienyllithium[11] in 40 mL of Et_2O at −78 °C were added 1.688 g (8.72 mmol) of 1-aziranyl-1-chlorotetramethyldisilane[8] in one portion. The solution was allowed to warm to room temperature, and the consumption of the chlorodisilane was followed by GC. After 40 min, 10 mL of hexane was added followed by the sequential addition of 1.0 mL of MeI and 0.50 mL of MeOH. Within 30 min (GC monitor) the reaction was complete. The reaction mixture was diluted with 5 times its volume of hexane and filtered through celite, and the filtrate was concentrated by rotary evaporation. The residue was GC separated on a 5-ft, 12% SE-30 column at 160 °C to afford 1.070 g of **15** (57%): NMR ($DCCl_3$) δ 0.22 (s, 9 H), 0.27 (s, 3 H), 1.80 (d, *J* = 8 Hz, 2 H), 3.49 (s, 3 H, SiO*Me*), 4.74–6.71 (m, 5 H); mass spectrum, *m/e* (% relative intensity) 214 (5), 199 (6), 147 (100), 117 (33), 89 (37), 73 (54); calcd for $C_{10}H_{22}Si_2O$ *m/e* 214.120 93, measured *m/e* 214.120 41.

(7) Gusel'nikov, L. E.; Lopatnikova, E.; Polyakov, Yu. P.; Nametkin, N. S. *Dokl. Akad. Nauk SSSR* **1980**, *253* (6), 1387.
(8) Burns, G. T.; Barton, T. J., submitted for publication.
(9) Silacyclopentene **7** has been previously reported,[10] but the structural assignment was solely based on the mass spectrum (which was not reported other than the apparent molecular ion).
(10) Jenkins, R. L.; Kedrowski, R. A.; Elliott, I. E.; Tappen, D. C.; Schlyer, D. J.; Ring, M. A. *J. Organomet. Chem.* **1975**, *86*, 347.
(11) Bates, R. B.; Gosselink, D. W.; Kaczynski, J. A. *Tetrahedron Lett.* **1967**, 199, 205.

FVP of 15. Disilane **15** (0.8097 g, 3.78 mmol) was distilled (70 °C (1 × 10^{-4} torr) through a horizontal quartz tube heated at 700 °C. The pyrolysate collected in a N_2-cooled trap weighed 0.7032 g for an 87% mass recovery. The three products were isolated by preparative GC on a 20-ft, 20% SE-30 on Chromosorb W column with a temperature program of 70 °C to 200 °C at 2 °C/min. The first product was Me_3SiOMe (84%). The second product was identified as 5-methyl-5-silacyclohexa-1,3-diene (**18**): 52%; NMR (CCl_4) δ 0.20 (d, J = 4 Hz, 3 H, collapses to s with $h\nu$ at δ 4.16), 1.39–1.76 (m, 2 H), 4.16 (q, 1 H), 5.52–5.98 (m, 3 H), 6.40–6.81 (m, 1 H); mass spectrum, m/e (% relative intensity) 110 (72), 109 (36), 95 (100), 93 (21), 84 (15), 83 (11), 82 (12); calcd for $C_6H_{10}Si$ m/e 110.0552, measured m/e 110.0545; the spectral properties of **18** were identical with those of an authentic sample prepared by $LiAlH_4$ reduction of 5-methyl-5-chloro-5-silacyclohexa-1,3-diene. The third product was identified as 3-methylene-4-methyl-4-silacyclopentene (**20**): 13%; NMR (C_6D_6) δ 0.05 (d, J = 4 Hz, 3 H), 1.30 (center of m, 2 H), 4.42 (m, Si–H, 1 H), 5.28 (br s, 1 H), 5.65 (br s, 1 H), 5.90 (m, 1 H), 6.42 (m, 1 H); mass spectrum, m/e (% relative intensity) 110 (70), 109 (47), 95 (100), 69 (36), 67 (42), 58 (16), 55 (27), 53 (33), 43 (73).

1-(1-Methoxytetramethyldisilanyl)-2,4-hexadiene (21). To a stirred solution of 1.065 g (13 mmol) of 1,4-hexadiene (Aldrich) in 3.0 mL of THF at −78 °C was added 6.0 mL of 1.44 M (8.6 mmol) n-BuLi (Ventron) in one portion. The solution was warmed to room temperature during which time an exothermic reaction occurred and two layers were formed. After addition of enough THF to rehomogenize the orange solution, 1.815 g (8.12 mmol) of 1-chloro-1-(diethylamino)-tetramethyldisilane[8] was added in one portion. The solution was stirred at room temperature for 4 h, and then 4 mL of CH_3I and 3 mL of MeOH were sequentially added. After being stirred an additional 1.5 h, the solution was diluted with hexane, filtered through celite, and concentrated by rotary evaporation. The residue was distilled at 63–68 °C (0.1 torr) to afford 1.253 g of pure **21**: 68%; NMR ($DCCl_3$) δ 0.21 (s, 9 H), 0.27 (s, 3 H), 1.77 (apparent d, overlapped $CH_2C{=}C$ and $C{=}CMe$, collapses to br s with $h\nu$ at ca. δ 5.80, 5 H), 3.47 (s, OMe, 3 H), 5.20–6.33 (vinyl m, 4 H); mass spectrum, m/e (% relative intensity) 228 (8), 213 (5), 147 (100), 117 (32), 89 (25), 73 (55), 59 (30); calcd for $C_{11}H_{24}OSi_2$ m/e 228.1366, measured m/e 228.1360.

FVP of 21. Disilane **21** (0.5010 g, 2.20 mmol) was distilled (40 °C (10^{-4} torr)) through a quartz tube heated at 680 °C with 95% mass recovery (0.4742 g). Two products were isolated by preparative GC. The first product was Me_3SiOMe in 73% yield. The second product was identified as 1-methyl-1-vinyl-1-silacyclopent-2-ene (**25**): 68% yield, 93% based on Me_3SiOMe; NMR ($DCCl_3$) δ 0.32 (s, 3 H), 0.81 (m, 2 H, collapses to br s with $h\nu$ at δ 2.56), 2.56 (m, 2 H, collapses to br s with $h\nu$ at 0.81, collapses to br t with $h\nu$ at ca δ 6), 5.44–6.57 (m, 4 H, C_2H_3 + 1 vinyl H on ring), 6.87 (d of t, J = 10 Hz, 2 Hz, collapses to d with J = 10 Hz with $h\nu$ at δ 2.56, 1 H); mass spectrum, m/e (% relative intensity) 124 (2), 109 (55), 97 (30), 96 (100), 83 (20), 81 (15), 55 (20); calcd for $C_7H_{12}Si$ m/e 124.0708, measured m/e 124.0712.

1-Methoxy-1-*n*-butyltetramethyldisilane (27). To a stirred solution of 3.250 g (14.5 mmol) of 1-chloro-1-(diethylamino)-tetramethyldisilane[8] in 50 mL of Et_2O were added 11.0 mL (0.158 mol) of 1.44 M n-BuLi (Alfa) over a 10-min period. After the solution was stirred for 1 h, 3 mL of MeI was added, followed by excess NaOMe. The solution was stirred for ca. 6 h and then diluted with 100 mL of pentane, filtered through celite, and then concentrated by rotary evaporation. Distillation of the residue at 50–55 °C (0.1 torr) afforded 1.559 g pure **27**: 53% yield; NMR ($DCCl_3$) δ 0.18 (s, 9 H), 0.20 (s, 3 H), 0.51–1.58 (m, 9 H, butyl), 3.44 (s, 3 H, OMe); mass spectrum, m/e (% relative intensity) 204 (3), 189 (4), 131 (20), 117 (100), 75 (67), 73 (28); calcd for $C_9H_{24}Si_2O$ m/e 204.136 58, measured m/e 204.136 61.

FVP of 27. Disilane **27** (0.5626 g) was distilled through a horizontal quartz tube heated to 680 °C with 42% mass recovery (0.2387 g). The volatile products were isolated by preparative GC (20-ft, 20% OV-101 on Chromosorb W at 110 °C) and identified as Me_3SiOMe and 1-butene by spectral comparison with authentic samples. Due to difficulties in quantitative manipulation, no attempt was made to establish yields in this reaction.

Acknowledgment. The support of this research by the National Science Foundation is gratefully acknowledged. We are also thankful for partial support by Dow Corning Corp.

Registry No. **6**, 83134-61-6; **7**, 55544-25-7; **8**, 83134-62-7; **12**, 83134-63-8; **13**, 83134-64-9; **14**, 83134-65-0; **15**, 83134-66-1; **16**, 83134-67-2; **18**, 78698-04-1; **20**, 83134-68-3; **21**, 83134-69-4; **22**, 83134-70-7; **25**, 83134-71-8; **27**, 83151-99-9; **28**, 83134-72-9; 1-aziranyl-1-chlorotetramethyldisilane, 83134-73-0; 4-butenyl bromide, 5162-44-7; 4-bromo-2-pentene, 1809-26-3; pentadienyllithium, 54962-98-0; 1,4-hexadiene, 592-45-0; 1-chloro-1-(diethylamino)tetramethyldisilane, 83134-74-1.

1,5-Silyl Migrations as a Route to Acyclic 1-Sila-1,3-butadienes

Thomas J. Barton,* William D. Wulff, and Stephanie A. Burns

Department of Chemistry, Iowa State University, Ames, Iowa 50011

Received July 15, 1982

cis-1-(Pentamethyldisilanyl)-3-methyl-1,3-butadiene was synthesized in three steps and subjected to flash vacuum pyrolysis at 635 °C. Three of the four products were isomeric silyl hydrides which arose from 1,5 migration of trimethylsilyl from silicon to carbon to produce an intermediate 1-sila-1,3-butadiene which underwent 1,5-hydrogen migration back to doubly bonded silicon. (*Z*)-7,7,8,8-Tetramethyl-7,8-disilanon-5-en-4-one was synthesized in an attempt to extend this rearrangement to 1,5-silicon migration to oxygen. A remarkably clean pyrolysis afforded a 2-sila-2,3-dihydrofuran (86%), most probably resulting from initial oxygen attack on internal silicon followed by 1,2-silyl migration.

In 1979 we reported that 1-methyl-1-(trimethylsilyl)-2,5-diphenylsilole (**1**) underwent a reversible, thermally induced 1,5-migration of trimethylsilyl from silicon to carbon to generate a transient silole **2** which could be removed from the equilibrium with great efficiency by aldehydes, ketones, olefins, and acetylenes.[1]

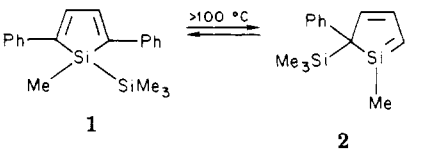

1 **2**

Since 1,5-sigmatropic rearrangements are entropically more favorable on cyclopentadienes, it was not a foregone certainty that acyclic 1-disilanyl-1,3-butadienes would

(1) Barton, T. J.; Wulff, W. D.; Arnold, E. V.; Clardy, J. *J. Am. Chem. Soc.* **1979**, *101*, 2733.

0276-7333/83/2302-0004$01.50/0

FVP of 15. Disilane **15** (0.8097 g, 3.78 mmol) was distilled (70 °C (1 × 10^{-4} torr) through a horizontal quartz tube heated at 700 °C. The pyrolysate collected in a N_2-cooled trap weighed 0.7032 g for an 87% mass recovery. The three products were isolated by preparative GC on a 20-ft, 20% SE-30 on Chromosorb W column with a temperature program of 70 °C to 200 °C at 2 °C/min. The first product was Me_3SiOMe (84%). The second product was identified as 5-methyl-5-silacyclohexa-1,3-diene (**18**): 52%; NMR (CCl_4) δ 0.20 (d, J = 4 Hz, 3 H, collapses to s with $h\nu$ at δ 4.16), 1.39–1.76 (m, 2 H), 4.16 (q, 1 H), 5.52–5.98 (m, 3 H), 6.40–6.81 (m, 1 H); mass spectrum, m/e (% relative intensity) 110 (72), 109 (36), 95 (100), 93 (21), 84 (15), 83 (11), 82 (12); calcd for $C_6H_{10}Si$ m/e 110.0552, measured m/e 110.0545; the spectral properties of **18** were identical with those of an authentic sample prepared by $LiAlH_4$ reduction of 5-methyl-5-chloro-5-silacyclohexa-1,3-diene. The third product was identified as 3-methylene-4-methyl-4-silacyclopentene (**20**): 13%; NMR (C_6D_6) δ 0.05 (d, J = 4 Hz, 3 H), 1.30 (center of m, 2 H), 4.42 (m, Si–H, 1 H), 5.28 (br s, 1 H), 5.65 (br s, 1 H), 5.90 (m, 1 H), 6.42 (m, 1 H); mass spectrum, m/e (% relative intensity) 110 (70), 109 (47), 95 (100), 69 (36), 67 (42), 58 (16), 55 (27), 53 (33), 43 (73).

1-(1-Methoxytetramethyldisilanyl)-2,4-hexadiene (21). To a stirred solution of 1.065 g (13 mmol) of 1,4-hexadiene (Aldrich) in 3.0 mL of THF at −78 °C was added 6.0 mL of 1.44 M (8.6 mmol) n-BuLi (Ventron) in one portion. The solution was warmed to room temperature during which time an exothermic reaction occurred and two layers were formed. After addition of enough THF to rehomogenize the orange solution, 1.815 g (8.12 mmol) of 1-chloro-1-(diethylamino)-tetramethyldisilane[8] was added in one portion. The solution was stirred at room temperature for 4 h, and then 4 mL of CH_3I and 3 mL of MeOH were sequentially added. After being stirred an additional 1.5 h, the solution was diluted with hexane, filtered through celite, and concentrated by rotary evaporation. The residue was distilled at 63–68 °C (0.1 torr) to afford 1.253 g of pure **21**: 68%; NMR ($DCCl_3$) δ 0.21 (s, 9 H), 0.27 (s, 3 H), 1.77 (apparent d, overlapped $CH_2C{=}C$ and $C{=}CMe$, collapses to br s with $h\nu$ at ca. δ 5.80, 5 H), 3.47 (s, OMe, 3 H), 5.20–6.33 (vinyl m, 4 H); mass spectrum, m/e (% relative intensity) 228 (8), 213 (5), 147 (100), 117 (32), 89 (25), 73 (55), 59 (30); calcd for $C_{11}H_{24}OSi_2$ m/e 228.1366, measured m/e 228.1360.

FVP of 21. Disilane **21** (0.5010 g, 2.20 mmol) was distilled (40 °C (10^{-4} torr)) through a quartz tube heated at 680 °C with 95% mass recovery (0.4742 g). Two products were isolated by preparative GC. The first product was Me_3SiOMe in 73% yield. The second product was identified as 1-methyl-1-vinyl-1-silacyclopent-2-ene (**25**): 68% yield, 93% based on Me_3SiOMe; NMR ($DCCl_3$) δ 0.32 (s, 3 H), 0.81 (m, 2 H, collapses to br s with $h\nu$ at δ 2.56), 2.56 (m, 2 H, collapses to br s with $h\nu$ at 0.81, collapses to br t with $h\nu$ at ca δ 6), 5.44–6.57 (m, 4 H, C_2H_3 + 1 vinyl H on ring), 6.87 (d of t, J = 10 Hz, 2 Hz, collapses to d with J = 10 Hz with $h\nu$ at δ 2.56, 1 H); mass spectrum, m/e (% relative intensity) 124 (2), 109 (55), 97 (30), 96 (100), 83 (20), 81 (15), 55 (20); calcd for $C_7H_{12}Si$ m/e 124.0708, measured m/e 124.0712.

1-Methoxy-1-*n*-butyltetramethyldisilane (27). To a stirred solution of 3.250 g (14.5 mmol) of 1-chloro-1-(diethylamino)-tetramethyldisilane[8] in 50 mL of Et_2O were added 11.0 mL (0.158 mol) of 1.44 M n-BuLi (Alfa) over a 10-min period. After the solution was stirred for 1 h, 3 mL of MeI was added, followed by excess NaOMe. The solution was stirred for ca. 6 h and then diluted with 100 mL of pentane, filtered through celite, and then concentrated by rotary evaporation. Distillation of the residue at 50–55 °C (0.1 torr) afforded 1.559 g pure **27**: 53% yield; NMR ($DCCl_3$) δ 0.18 (s, 9 H), 0.20 (s, 3 H), 0.51–1.58 (m, 9 H, butyl), 3.44 (s, 3 H, OMe); mass spectrum, m/e (% relative intensity) 204 (3), 189 (4), 131 (20), 117 (100), 75 (67), 73 (28); calcd for $C_9H_{24}Si_2O$ m/e 204.136 58, measured m/e 204.136 61.

FVP of 27. Disilane **27** (0.5626 g) was distilled through a horizontal quartz tube heated to 680 °C with 42% mass recovery (0.2387 g). The volatile products were isolated by preparative GC (20-ft, 20% OV-101 on Chromosorb W at 110 °C) and identified as Me_3SiOMe and 1-butene by spectral comparison with authentic samples. Due to difficulties in quantitative manipulation, no attempt was made to establish yields in this reaction.

Acknowledgment. The support of this research by the National Science Foundation is gratefully acknowledged. We are also thankful for partial support by Dow Corning Corp.

Registry No. **6**, 83134-61-6; **7**, 55544-25-7; **8**, 83134-62-7; **12**, 83134-63-8; **13**, 83134-64-9; **14**, 83134-65-0; **15**, 83134-66-1; **16**, 83134-67-2; **18**, 78698-04-1; **20**, 83134-68-3; **21**, 83134-69-4; **22**, 83134-70-7; **25**, 83134-71-8; **27**, 83151-99-9; **28**, 83134-72-9; 1-aziranyl-1-chlorotetramethyldisilane, 83134-73-0; 4-butenyl bromide, 5162-44-7; 4-bromo-2-pentene, 1809-26-3; pentadienyllithium, 54962-98-0; 1,4-hexadiene, 592-45-0; 1-chloro-1-(diethylamino)tetramethyldisilane, 83134-74-1.

1,5-Silyl Migrations as a Route to Acyclic 1-Sila-1,3-butadienes

Thomas J. Barton,* William D. Wulff, and Stephanie A. Burns

Department of Chemistry, Iowa State University, Ames, Iowa 50011

Received July 15, 1982

cis-1-(Pentamethyldisilanyl)-3-methyl-1,3-butadiene was synthesized in three steps and subjected to flash vacuum pyrolysis at 635 °C. Three of the four products were isomeric silyl hydrides which arose from 1,5 migration of trimethylsilyl from silicon to carbon to produce an intermediate 1-sila-1,3-butadiene which underwent 1,5-hydrogen migration back to doubly bonded silicon. (*Z*)-7,7,8,8-Tetramethyl-7,8-disilanon-5-en-4-one was synthesized in an attempt to extend this rearrangement to 1,5-silicon migration to oxygen. A remarkably clean pyrolysis afforded a 2-sila-2,3-dihydrofuran (86%), most probably resulting from initial oxygen attack on internal silicon followed by 1,2-silyl migration.

In 1979 we reported that 1-methyl-1-(trimethylsilyl)-2,5-diphenylsilole (**1**) underwent a reversible, thermally induced 1,5-migration of trimethylsilyl from silicon to carbon to generate a transient silole **2** which could be removed from the equilibrium with great efficiency by aldehydes, ketones, olefins, and acetylenes.[1]

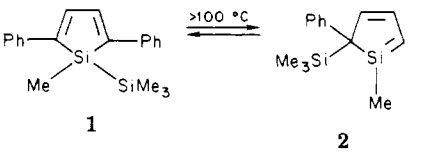

1 **2**

Since 1,5-sigmatropic rearrangements are entropically more favorable on cyclopentadienes, it was not a foregone certainty that acyclic 1-disilanyl-1,3-butadienes would

(1) Barton, T. J.; Wulff, W. D.; Arnold, E. V.; Clardy, J. *J. Am. Chem. Soc.* **1979**, *101*, 2733.

0276-7333/83/2302-0004$01.50/0

Scheme I

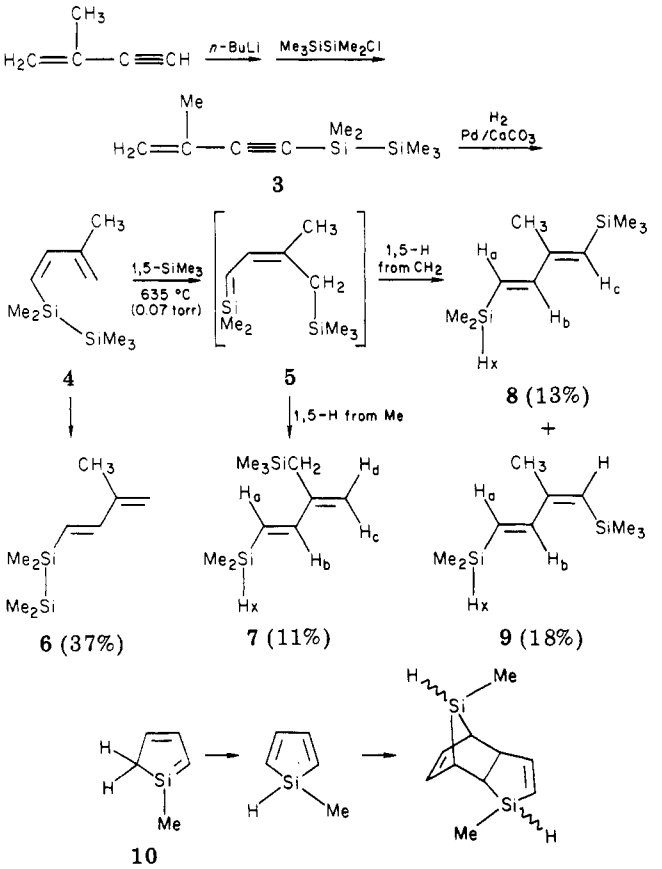

undergo thermally induced rearrangement to 1-sila-1,3-butadienes. Thus, in order to determine generality of this isomerization, we prepared *cis*-1-(pentamethyldisilanyl)-3-methyl-1,3-butadiene (**4**) (Scheme I). Reduction of enyne **3** using Lindlar's catalyst gave a mixture of isomers from which **4** was isolated by preparative GC. Flash vacuum pyrolysis of **4** at 635 °C afforded only four products, all isomeric with **4**, in total yield of 79% (Scheme I). All four products were isolated by preparative GC and assigned the indicated structures on the basis of their NMR, IR, and mass spectra. The major product **6** was simply the trans isomer of the starting diene. However, the other three products clearly arise from isomerization of **4** to 1-sila-1,3-butadiene **5** followed by 1,5-hydrogen migration from methyl to silicon to produce **7** or from methylene to afford **8** or **9**. The apparent 1,5-hydrogen migration on a 1-sila-1,3-butadiene framework is precedented. In all previous literature reports of the generation of acyclic 1-sila-1,3-butadienes[2-4] only closure to silacyclobutenes was observed. However, in none of the literature systems have there been C–H units available for this rearrangement. In the single example of a cyclic 1-sila-1,3-butadiene (**10**) possessing an available proton at the 5-position exclusive 1,5-hydrogen migration apparently occurred.[5] Thus, the generality of the thermal 1,5 migration of silicon from silicon to carbon as a method of silene generation has been extended to a linear system with the expected increase in thermal requirement.

Another example of thermally induced rearrangement of silicon to form a silene is found in the work of Brook,[6]

Scheme II

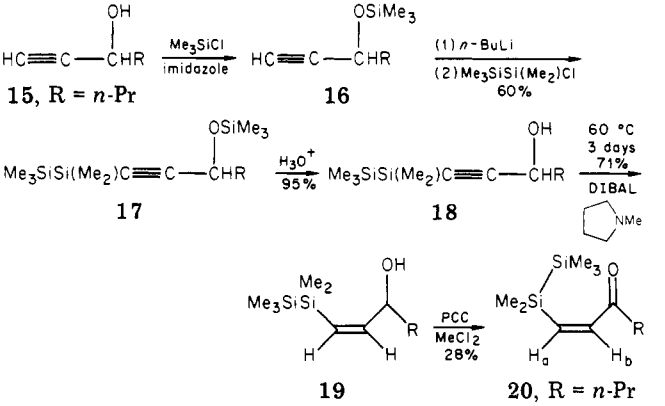

who demonstrated that pivaloylsilane (**11**) isomerized to silene **12** via 1,3 migration of silicon from silicon to oxygen.

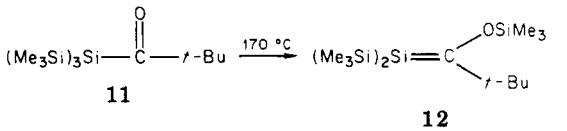

In view of the above results, it seemed obvious that an excellent candidate for silene formation from thermal sigmatropic rearrangement would be a *cis*-disilanyl enone **13**. Although a C–O π bond must be lost in a 1,5 rearrangement of silicon to form silene **14**, it was thought that the formation of the extremely strong Si–O σ bond (128 kcal/mol) would make this a more facile process than the rearrangement of **4** to **5**.

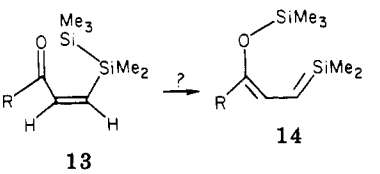

The synthesis of a suitable test molecule was not uneventful, but was eventually accomplished as shown in Scheme II. Commercially available alcohol **15** was protected with Me_3SiCl, and then metalated (*n*-BuLi), and quenched with pentamethylchlorodisilane to afford protected ynol **17** in 60% yield. The reduction of ynol **18** proved quite troublesome as no success was realized with various standard catalytic hydrogenations or borane reductions. However, heating **18** with a fivefold excess of diisobutylaluminum hydride–*N*-methylpyrrolidine for 3 days at 60 °C afforded cis olefin **19** in 71% yield. Oxidation of **19** with pyridinium chlorochromate produced (*Z*)-7,7,8,8-tetramethyl-7,8-disilanon-5-en-4-one (**20**) in an unmaximized yield of 28%.

Thermolysis of **20** was conducted at 430 °C through a 1-ft vertical quartz chip packed tube with a nitrogen stream of 30 mL/min with complete disappearance of **20**. A single product was formed in 86% yield and was assigned structure **21** on the basis of its NMR, IR, and mass spectra. The facility of this remarkable isomerization can be recognized by the observation that attempted GC purification of **20** (injector 250 °C, column 150 °C) results in essentially quantitative conversion to **21**.

Based on literature precedent, we expected that if siladiene **22** were formed it would either cyclize[4] to a silacy-

(2) Nakadaira, Y.; Kanouchi, S.; Sakurai, H. *J. Am. Chem. Soc.* **1974**, *96*, 5621.
(3) Block, E.; Revelle, L. K. *J. Am. Chem. Soc.* **1978**, *100*, 1630.
(4) Burns, G. T.; Barton, T. J. *J. Organomet. Chem.* **1981**, *216*, C5.
(5) Barton, T. J.; Burns, G. T. *J. Organomet. Chem.* **1979**, *179*, C17.
(6) Brook, A. G.; Harris, J. W.; Lennon, J.; El Sheikh, M. *J. Am. Chem. Soc.* **1979**, *101*, 83.
(7) Walsh, R. *Acc. Chem. Res.* **1981**, *14*, 246.
(8) Kumada, M.; Nakajima, J. I.; Ishikawa, M.; Yamamoto, Y. *J. Org. Chem.* **1958**, *23*, 292.

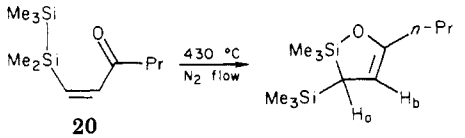

20 21

clobutene or undergo 1,5-hydrogen migration[5] to the doubly bound silicon to form a 1,3-butadiene. Even though such products were not observed, it is still possible that the formation of **21** involves initial 1,5 migration in **20** if, for example, it is assumed that 1,2 migration in zwitterionic intermediate **23** is followed by 1,3-silyl migration in **24**. 1,3-Sigmatropic silyl shifts are well-known;[9] thus, it is a question of relative thermodynamic stability between a vinylsilane (**24**) and an enol ether (**21**). Of course, this is also the question when one considers the possibility of direct rearrangement of **23** to **21** via a 1,4-silyl shift rather than a 1,2-silyl shift to form **24**. To a degree this was subject to experimental test by the synthesis and pyrolysis of a model system, 1,3-bis(trimethylsilyl)-3-phenoxypropene (**26**), which possesses the salient structural features of **24**. Thus, if indeed **24** were rearranging to form enol ether **21**, one would expect **26** to perform the analogous isomerization to **27** under similar conditions. The answer was almost immediately forthcoming as it was possible to purify **26** by preparative GC with a column temperature of 170 °C, a condition of greater severity than necessary to convert **20** to **21**. Flow pyrolysis (N_2, 450 °C) of **26** produced a complex inseparable mixture of products in striking contrast to the clean pyrolysis of **20**. However, the infrared spectrum of the entire pyrolysate revealed no significant band between 1620 and 1700 cm^{-1} as would be demanded for the enol ether **27**. An excellent model for the absent **27** is precursor **25** which displays a sharp C=C—O stretching band of moderate intensity at 1660.6 cm^{-1} (FTIR).

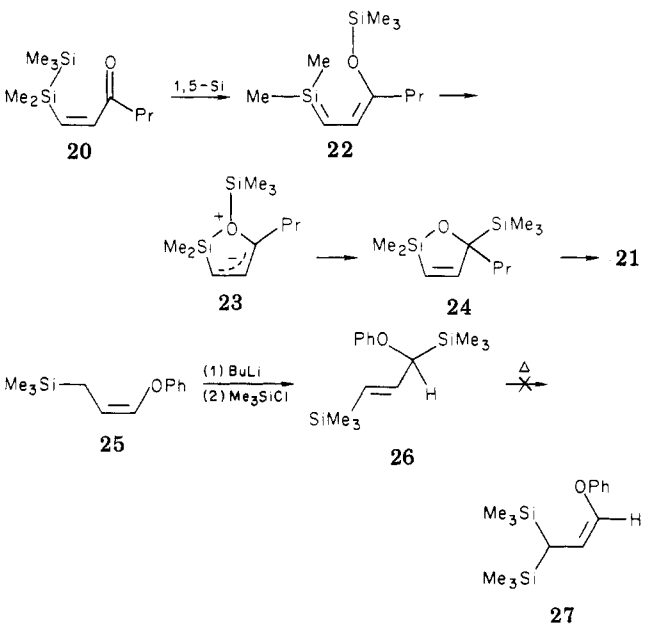

20 22 23 24 25 26 27

Thus, we consider it most likely that the isomerization of **20** to **21** involves initial coordination of the internal silicon and the carbonyl oxygen to form zwitterion **28**. The reaction is then completed by migration of trimethylsilyl to the adjacent carbon. Thus, the favorable thermodynamics did indeed direct the thermal rearrangement but not in the desired direction. The 1,2 migration of silicon to a carbon bearing full or partial positive charge is well-known. For example, (chloromethyl)pentamethyldisilane **29** reacts vigorously with aluminum chloride to afford **30** through exclusive 1,2-migration of the trimethylsilyl group.[8] In keeping with the zwitterionic character proposed for the **20** to **21** transformation is the current belief[10] that the 1,3 migration of silicon in β-ketosilanes involves the zwitterionic transition state **31**.[11]

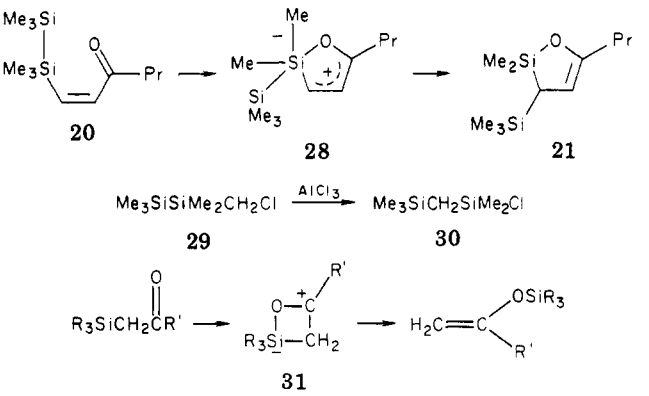

Experimental Section

General Data. Routine proton NMR spectra were recorded on a Varian EM-360 spectrometer. IR spectra were recorded on a Beckman IR-4250 or a Beckman Acculab-2 infrared spectrophotometer. Gas chromatographic mass spectra (GC–MS) were obtained on a Finnegan Model 4023 mass spectrometer. All melting points were obtained with a Thomas-Hoover capillary melting point apparatus and are uncorrected. Gas chromatographic (GC) data were obtained on a Varian-Aerograph Series 1700 gas chromatograph. All GC yields were calculated from predetermined response factors and are based on reacted starting material.

3-Methyl-1-(pentamethyldisilanyl)but-3-en-1-yne (3). To a solution of 1.95 g (0.0295 mol) of 3-methyl-3-en-1-yne in 125 mL of THF was added 0.0295 mol of *n*-butyllithium. The solution was stirred for 10 min and then cooled to 0 °C. To this solution was added 5.0 g (0.030 mol) of pentamethylchlorodisilane. After being stirred for 30 min, the organic solution was quenched with saturated ammonium chloride, washed with saturated sodium chloride, and dried over sodium sulfate. Distillation yielded 4.04 g (69%) of **3** (bp 49–51 °C (4 mm)): NMR (CCl_4) δ 0.12 (s, 9 H), 0.20 (s, 6 H), 1.88 (br s, 3 H), 5.28 (m, 2 H, collapses to AB quartet, J = 1.1 Hz, upon $h\nu$ at δ 1.88); IR (neat) 3110, 2960, 2905, 2150, 1620, 1275, 1250, 980, 900, 855, 830, 800, 775 cm^{-1}; mass spectrum (70 eV), m/e (% relative intensity) 197 (12), 196 (53), 182 (17), 181 (86), 155 (19), 141 (18), 123 (83), 97 (15), 73 (100): calcd for $C_{10}H_{20}Si_2$ m/e 196.110 36, measured 196.110 56.

Synthesis of *cis*-3-Methyl-1-(pentamethyldisilanyl)-1,3-butadiene (4). A mixture of 0.1 g of Lindlar's catalyst, 0.1 mL of quinoline, and 15 mL of hexane was saturated with hydrogen in a hydrogenation apparatus. After 3.0 g (0.0153 mol) of the eneyne **3** was added, it was observed that 1 equiv of hydrogen was taken up in 73 min at which point the reaction was stopped. After filtration and removal of solvent, a GC analysis of the crude reaction mixture indicated the presence of four compounds. The three major compounds of this mixture were isolated by preparative GC on a 12 ft × $^1/_4$ in. 20% DC-550 on Chromosorb P

(9) Barton, T. J.; Vuper, M. *J. Am. Chem. Soc.* **1981**, *103*, 6788.

(10) Kwart, H.; Barnette, W. I. *J. Am. Chem. Soc.* **1977**, *99*, 614.

(11) A reviewer has suggested that **20** thermally rearranges to silacyclopropane **i** by a 1,2-silyl shift, and that **i** proceeds to **21**. Although we would certainly expect **i** to isomerize to **21**, we feel that the contrast between the thermal lability of **20** and the thermal stability of vinyldisilanes (in our hands) argues against this novel proposal.

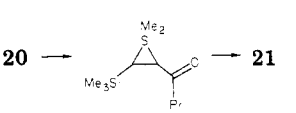

i

column at 150 °C. One of these was determined to be starting material (17.0%, GC yield). The second compound was determined to be isopropylpentamethyldisilanyl acetylene (17.9%, GC yield) on the basis of its spectra: NMR (CCl_4) δ 0.10 (s, 9 H), 0.15 (s, 6 H), 1.18 (d, 3 H, J = 8 Hz), 2.58 (heptet, 1 H, J = 8 Hz, collapses to a singlet upon $h\nu$ at δ 1.18); IR (neat) 2950, 2890, 2160, 1310, 1240, 1195, 960, 830, 790, 760 cm^{-1}; mass spectrum (70 eV), m/e (% relative intensity) 198 (44), 183 (15), 155 (71), 147 (29), 141 (20), 127 (11), 126 (28), 125 (71), 124 (46), 83 (28), 75 (16), 73 (100), 59 (14); calcd for $C_{10}H_{22}Si_2$ m/e 198.126 01, measured 198.125 02. The third compound was determined to be the desired product **4** (18.3%, GC yield) on the basis of its spectra: NMR (CCl_4) δ 0.06 (s, 9 H), 0.16 (s, 6 H), 1.86 (br s, 3 H), 4.94 (br s, 2 H), 5.57 (d, 1 H, J = 16 Hz), 6.83 (d, 1 H, J = 16 Hz); IR (neat) 3080, 2950, 2890, 1630, 1240, 890, 830, 795, 680 cm^{-1}; mass spectrum (70 eV), m/e (% relative intensity) 198 (1.2), 183 (2), 110 (50), 109 (11), 73 (100), 58 (16); calcd for $C_{10}H_{22}Si_2$ m/e 198.126 01, measured 198.124 84.

Pyrolysis of 4. The pyrolysis of **4** was carried out by evaporating it (25 °C (0.07 torr)) through a horizontal quartz tube that was packed with quartz chips and heated to 635 °C. The pyrolysate (0.146 g) was trapped (liquid nitrogen). Four products were obtained that were isolated by preparative GC on a 12 ft × $^1/_4$ in. 20% DC-550 on Chromosorb P column at 125 °C. The major product, **6** (36.8%, GC yield), was identified as the trans isomer of the starting material on the basis of its spectra: NMR (CCl_4) δ 0.07 (s, 9 H), 0.15 (s, 6 H), 1.87 (br s, 3 H), 5.05 (br s, 2 H), 5.82 (d, 1 H, J = 20 Hz), 6.65 (d, 1 H, J = 20 Hz); IR (neat) 3080, 2950, 2890, 1580, 1245, 985, 890, 835, 820, 795 cm^{-1}; mass spectrum (70 eV), m/e (% relative intensity) 198 (4), 183 (3), 110 (52), 109 (9), 73 (100), 59 (18); calcd for $C_{10}H_{22}Si_2$ m/e 198.126 01, measured 198.125 47. One of the products was determined to be *trans*-3-[(trimethylsilyl)methyl]-1-(dimethylsilyl)butadiene (**7**; 11%, GC yield) on the basis of its spectra: NMR (CCl_4) δ −0.03 (s, 9 H), 0.20 (d, 6 H, J = 3.5 Hz), 1.78 (br s, 2 H), 4.05 (m, H_X, J_{AX} = 3.5 Hz), 4.82 (H_C and H_D, collapses to AB quartet, J = 2 Hz, upon $h\nu$ at δ 1.78), 5.62 (d of d, H_A, J_{AX} = 3.5 Hz, J_{AB} = 19 Hz), 6.51 (d, H_B, J = 19 Hz); IR (neat) 3075, 2950, 2890, 2110, 1575, 1245, 980, 885, 850, 830, 795 cm^{-1}; mass spectrum (70 eV), m/e (% relative intensity) 198 (3), 183 (1), 124 (10), 109 (22), 74 (8), 73 (100), 59 (100). Also identified from this reaction was 1-*cis*-3-*trans*-4-(dimethylsilyl)-2-methyl-1-(trimethylsilyl)butadiene (**9**; 18.1%, GC yield): NMR (CCl_4) δ 0.13 (s, 9 H), 0.16 (d, 6 H, J = 3.9 Hz), 1.86 (sharp singlet, 3 H), 4.09 (m, 1 H), 5.53 (br s, 1 H), 5.71 (d of d, H_A, J_{AB} = 19 Hz, J_{AX} = 3.9 Hz), 6.54 (d, H_B, J = 19 Hz); IR (neat) 2980, 2950, 2890, 2110, 1565, 1245, 985, 890, 865, 830, 785, 685 cm^{-1}; mass spectrum (70 eV), m/e (% relative intensity) 198 (0.3), 183 (2), 110 (35), 109 (14), 73 (100), 59 (20); calcd for $C_{10}H_{22}Si_2$ m/e 198.126 01, measured 198.125 39. The last product from this pyrolysis was identified as 1-*trans*-3-*trans*-4-(dimethylsilyl)-2-methyl-1-(trimethylsilyl)butadiene (**8**; 12.7%, GC yield) on the basis of the following spectra: NMR (CCl_4) δ 0.15 (s, 9 H), 0.19 (d, 6 H, J = 3.8 Hz), 1.93 (d, 3 H, J = 1 Hz), 4.15 (m, 1 H), 5.59 (br s, 1 H, J = 1 Hz), 5.84 (d of d, 1 H, J = 19 Hz, J = 3.8 Hz), 6.89 (d, 1 H, J = 19 Hz); IR (neat) 2950, 2890, 2110, 1600, 1555, 1250, 1150, 980, 890, 870, 840 cm^{-1}; mass spectrum (70 eV), m/e (% relative intensity) 183 (0.7), 110 (45), 109 (8), 83 (6), 73 (100), 59 (21); calcd for $C_{10}H_{22}Si_2$ m/e 198.126 01, measured 198.125 03. On the basis of GC retention times, it was determined that when a solution of **4** in diphenyl ether was heated at 226 °C for 90 min, **4** isomerized to **6**.

2,2,3,3-Tetramethyl-6-(trimethylsiloxy)-2,3-disilanon-4-yne (17). To a stirring solution of 5.00 g (0.0510 mol) of **15** in 35 mL of DMF at 0 °C were added 8.67 g (0.127 mol) of imidazole and 6.08 g of trimethylchlorosilane. After the solution was warmed to room temperature, stirring was continued for 18 h. The organic solution was poured into ether, washed with water, and dried with magnesium sulfate. After solvent removal, the residue was eluted through a silica gel column with a 90:10 hexane/ethyl acetate solution to afford 7.26 g (84%) of **16**: NMR (CCl_4) δ 0.13 (s, 9 H), 0.86–1.71 (m, 7 H, $CH_2CH_2CH_3$), 2.24 (d, 1 H, J = 2 Hz), 4.21 (d of t, 1 H, J = 2 Hz, J' = 6 Hz); mass spectrum, m/e (% relative intensity) 169 (0.2), 127 (75), 83 (51), 74 (75), 73 (100).

To a stirring solution of 7.26 g (0.0427 mol) of **16** in 100 mL of dry ether at −78 °C (under a nitrogen atmosphere) was added 18.6 mL (0.0465 mol) of 2.5 M *n*-butyllithium in hexane. After the solution was stirred 30 min at −78 °C, 7.10 g (.0427 mol) of pentamethylchlorodisilane was added. The solution was warmed to room temperature and stirred several hours. After the mixture was poured into hexane, the organic solution was washed with water and dried with magnesium sulfate. The residue was distilled at 68–72 °C (0.1 torr) to afford 7.69 g (60%) of **17**: NMR (CCl_4) δ 0.11 (s, 9 H), 0.14 (s, 9 H), 0.18 (s, 6 H), 0.85–1.75 (m, 7 H, $CH_2CH_2CH_3$), 4.39 (t, 1 H, J = 6 Hz); mass spectrum, m/e (% relative intensity) 285 (2), 199 (47), 183 (25), 155 (44), 149 (45), 148 (89), 147 (100), 133 (61), 109 (58), 75 (65), 73 (99), 55 (45); calcd for (p − CH_3) $C_{13}H_{29}OSi_3$ 285.152 63, measured 285.152 89.

7,7,8,8-Tetramethyl-7,8-disilanon-5-yn-4-ol (18). To a stirring solution of 10% HCl in THF was added 7.69 g of **17** at room temperature. After being stirred 1 h, the organic solution was poured into hexane, washed with water, and dried with magnesium sulfate. Following solvent removal, the residue was eluted through a silica gel column with hexane/ethyl acetate (75:25) to give 5.55 g (95%) of **18**: NMR (CCl_4) δ 0.12 (s, 9 H), 0.18 (s, 6 H), 0.82–1.76 (m, 8 H, $C(OH)CH_2CH_2CH_3$, with added D_2O, 7 H), 4.28 (t, J = 6 Hz); IR (neat) 3700–3050 (br OH), 2960, 2880, 2165, 1240 cm^{-1}; mass spectrum, m/e (% relative intensity) 213 (0.2), 211 (.6), 157 (23), 155 (9), 147 (73), 109 (53), 75 (88), 73 (100), 59 (18); calcd for (D–CH(OH)*n*-Pr) $C_7H_{15}Si_2$ 155.071 24, measured 155.070 98.

(*Z*)-7,7,8,8-Tetramethyl-7,8-disilanon-5-en-4-ol (19). A two-necked round-bottom flask was equipped with a reflux condenser, a drying tube, and a pressure equalized addition funnel. The apparatus was flushed with nitrogen and charged with 120 mL (0.120 mol) of 1 M diisobutylaluminum hydride (DIBAL) in heptane. After the solution was cooled to 0 °C, 10.2 g (0.120 mol) of *N*-methylpyrrolidine were added dropwise, keeping the temperature below 5 °C. After the solution was stirred for 30 min, 5.3 g (0.023 mol) of **18** was added. The solution was warmed to 60 °C and stirred for 3 days. After being cooled to room temperature, the organic solution was poured into a hexane/ice mixture with vigorous stirring for 30 min. The salts were filtered through a pad of celite, and the filtrate was washed with water and dried with magnesium sulfate. After removal of solvent, the residue was eluted through a silica gel column with 75:25 hexane/ethyl acetate solution to afford 3.80 g (71%) of **19**: NMR (CCl_4) δ 0.14 (s, 9 H), 0.23 (s, 6 H), 0.80–1.22 (m, 8 H, $C(OH)CH_2CH_2CH_3$), 3.90–4.28 (m, 1 H), 5.56 (d, 1 H, J = 14 Hz), 6.24 (d of d, J = 14 Hz, J' = 8 Hz, collapses to d, J = 14 Hz with $h\nu$ at *ca.* 4.0); IR (neat) 3390 (br OH), 2960, 2900, 2880, 1608, 1465, 1400, 1255, 1245, 1115, 1095, 1060, 1010, 830, 790, 720 cm^{-1}; mass spectrum, m/e (% relative intensity) 215 (0.1), 139 (18), 133 (10), 113 (13), 75 (100), 73 (95), 61 (14), 59 (31); calcd for (p − 2) $C_{11}H_{24}Si_2O$ 228.136 58, measured 228.137 15.

(*Z*)-7,7,8,8-Tetramethyl-7,8-disilanon-5-en-4-one (20). To a stirring solution of 3.0 g (0.014 mol) of pyridinium chlorochromate (PCC) in 50 mL of methylene chloride at 0 °C was added 2.99 g (0.013 mol) of **19**. The mixture was stirred for 2 h while being warmed to room temperature. The dark brown solid was filtered through a pad of celite and solvent removed. Hexane was added and the newly formed brown precipitate filtered. After removal of solvent, the residue was eluted through silica gel with hexane, affording 0.827 g (28%) of the *cis*-enone **20**: NMR (CCl_4) δ 0.04 (s, 9 H), 0.12 (s, 6 H), 0.91 (t, 3 H, J = 6 Hz), 1.61 (sextet, 2 H, J = 6 Hz), 2.44 (t, 2 H, J = 6 Hz), 6.44 (d, 1 H, J = 14 Hz), 6.80 (d, 1 H, J = 14 Hz); IR (neat) 2980, 2950, 1692, 1570, 1420, 1410, 1372, 1242, 1130, 1055, 830, 800 cm^{-1}; mass spectrum, m/e (% relative intensity) 228 (19), 213 (10), 155 (100), 147 (92), 133 (36), 91 (33); calcd for $C_{11}H_{24}Si_2O$ 228.136 58, measured 228.135 57.

Pyrolysis of *cis*-Enone 20. Compound **20** was slowly dripped into a vertical quartz tube packed with quartz chips and heated at 430 °C. Nitrogen was used as the carrier gas. A flow rate of 30 mL/min was used. The pyrolysate was collected in a trap cooled with liquid nitrogen and represented an 86% mass recovery. The only product in this pyrolysis was isolated by preparative gas chromatography on a 8 ft × $^1/_4$ in. 20% DC-550 column at 180 °C. This product was identified as **21** (86%) on the basis of its spectra: NMR (CCl_4) δ 0.02 (s, 9 H), 0.20 (s, 3 H), 0.30 (s, 3 H), 0.68–1.11 (m, 4 H), 1.48 (center of m, 2 H), 2.1 (center of m, 2 H), 4.50 (d, 1 H_B, J_{AB} = 3 Hz); IR (neat) 2955, 1630, 1245, 1050, 975, 830 (br) cm^{-1}; mass spectrum, m/e (% relative intensity) 228 (8), 155 (61), 147 (70), 139 (40), 133 (28), 111 (21), 75 (27), 73 (100);

calcd for $C_{11}H_{24}Si_2O$ 228.136 58, measured 228.135 79.

Synthesis of (*Z*)-1-Phenoxy-3-(trimethylsilyl)propene (25). To a stirred solution of 3-phenoxypropene (10.0 g, 0.075 mol) and TMEDA (6 mL) in 200 mL of dry THF at −78 °C was slowly added 37 mL (10% excess) of 2.2 M *n*-BuLi. The resulting yellow solution was stirred for 2 h at −78 °C after which 9.4 mL (0.075 mol) of Me_3SiCl was added. After being stirred for 4 h at room temperature, the reaction mixture was poured into hexane, the solution washed three times with H_2O and dried over $MgSO_4$ and the solvent removed by rotary evaporation. Distillation through a 10-cm Vigreux column (135 °C (60 torr)) afforded 3.70 g (24%) of pure **25**: NMR ($DCCl_3$) δ 0.03 (s, 9 H), 1.52 (d, 2 H, J = 9 Hz), 4.77 (d of t, 1 H, J = 9 Hz and 6 Hz), 6.23 (d of t, 1 H, J = 6 Hz and 1 Hz); mass spectrum, m/e (% relative intensity) 206 (9), 191 (8), 151 (11), 77 (13), 73 (100); calcd for $C_{12}H_{18}SiO$ m/e 206.112 70, measured m/e 206.112 19.

Synthesis and Pyrolysis of (*E*)-1,3-Bis(trimethylsilyl)-3-phenoxypropene (26). To a stirred solution of **25** (2.202 g, 0.0107 mol) and TMEDA (1.6 mL) in 50 mL of dry THF at −78 °C was slowly added 5.34 mL of 2.2 M *n*-BuLi. After the solution was stirred for 5 h at −78 °C, 1.48 mL (1.23 g, 0.0113 mol) of Me_3SiCl was added. The solution was stirred for 30 min at room temperature then poured into hexane, the mixture washed three times with H_2O, and the solvent removed by rotary evaporation. It was necessary to separate **26** by preparative GC and this was accomplished on an 8-ft, 12% OV101 column at 170 °C: NMR ($DCCl_3$) δ 0.03 (s, 9 H) 0.10 (s, 9 H), 4.37 (d, 1 H, J = 5 Hz, collapses to s with $h\nu$ at δ 6.09), 5.50 (d, 1 H, J = 19 Hz and 5 Hz, collapses to d with J = 19 Hz with $h\nu$ at δ 4.37); mass spectrum, m/e (% relative intensity) 278 (5), 175 (16), 100 (60); calcd for $C_{15}H_{26}Si_2O$ m/e 278.1522, measured 278.1516. Pyrolysis of **26** (0.1667 g) was conducted by slowly dripping (via syringe) it directly into a vertical 1-ft quartz tube packed with quartz chips heated at 450 °C in a tube furnace, with a continuous N_2 flow of 30 mL/min. The mass recovery was 66%. GC analysis revealed a complex mixture of products for which the IR spectrum showed no significant absorption in the 1620–1700-cm^{-1} region.

Acknowledgment. The support of this work by the National Science Foundation is gratefully acknowledged.

Registry No. **3**, 83135-14-2; **4**, 83135-15-3; **6**, 83159-75-5; **7**, 83135-16-4; **8**, 83135-17-5; **9**, 83135-18-6; **15**, 105-31-7; **16**, 62785-87-9; **17**, 83152-00-5; **18**, 83135-19-7; **19**, 83135-20-0; **20**, 83135-21-1; **21**, 83135-22-2; **25**, 83135-23-3; **26**, 83135-24-4; 3-methylbut-3-en-1-yne, 78-80-8; isopropyl(pentamethyldisilanyl)acetylene, 83135-25-5; 3-phenoxypropene, 1746-13-0; $Me_3SiSiMe_2Cl$, 1560-28-7; Me_3SiCl, 75-77-4.

New Silene Rearrangements from a Study of the Mechanism of Silacyclopentene Formation from [3.3]Silaspirocycloheptane

Thomas J. Barton,* Gary T. Burns, and David Gschneidner

Department of Chemistry, Iowa State University, Ames, Iowa 50011

Received July 23, 1982

In an attempt to unravel the mechanism of silacyclopentene formation in the pyrolysis of [3.3]silaspirocycloheptane, pyrolysis of 1-methoxy-1-[(trimethylsilyl)methyl]-1-silacyclobutane was conducted. Instead of the desired elimination of Me_3SiOMe, extrusion of ethylene occurred followed by a novel isomerization of the resulting silene. Model system studies produced the mechanistic proposal that [(trimethylsilyl)methyl]silenes thermally isomerize via 1,4-hydrogen atom transfer. Pyrolysis of 1-methoxy-1-(trimethylsilyl)-1-silacyclopentane also produced silacyclopent-3-ene, thus confirming the legitimacy of proposing silacyclopentanylidene intermediate in the title transformation.

Recently considerable attention has focused on thermal isomerization of silenes to silylenes.[1] To our knowledge this rearrangement was first proposed when we suggested the rearrangement of silylsilene **1** to silylene **2** via 1,2-silyl migration to explain the ultimate formation of disilacyclobutane **3** in the pyrolysis of allylpentamethyldisilane.[2]

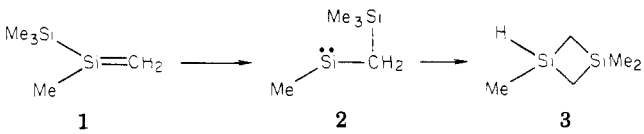

1 2 3

However, there has long existed the possibility that the first example of silene to silylene rearrangement had been unknowingly reported in 1973 when Gusel'nikov[4] observed that the gas-phase pyrolysis of silaspirocycle **4** afforded 1-silacyclopent-3-ene (**9**) as the sole silicon-containing product. Although no mechanism for the formation of **9** was put forth, it was suggested that silene **5** was initially formed and somehow rearranged to **9**. We have long wondered whether this reaction might not be taking place through isomerization of **5** to silacyclopentanylidene **6** via alkyl migration, followed by C–H insertion to form silabicyclo[2.1.0]pentane (**7**). Homolysis of the internal Si–C central bond in **7** would lead to 1,3-diradical **8** from which a 1,3-hydrogen shift to silicon would afford **9**. A both-

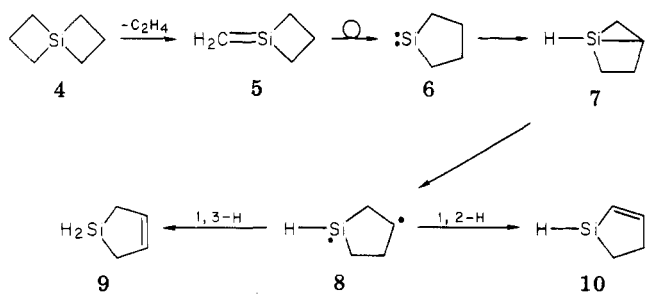

4 5 6 7 9 8 10

ersome feature of this proposal is that one would reasonably expect that from diradical **8** 1,2-hydrogen migration would be competitive with a 1,3 shift, and thus silacyclopent-2-ene (**10**) should also be formed. However, this objection can be overcome if one recognizes that silahausane **7** could undergo isomerization to 4-butenylsilylene **11**, as the thermal decomposition of silacyclopropanes to silylenes and olefins is a long-established process.[4] Silylene

(1) Barton, T. J.; Burns, S. A.; Burns, G. T. *Organometallics* **1982**, *1*, 210.
(2) Barton, T. J.; Jacobi, S. A. *J. Am. Chem. Soc.* **1980**, *102*, 7979.
(3) Nametkin, N. S.; Gusel'nikov, L. E.; Orlov, V. Y.; Ushakova, R. L.; Kuzmin, O. V.; Vdovin, V. M. *Dokl. Adak. Nauk SSSR* **1973**, *211*, 106.
(4) Seyferth, D.; Annarelli, D. C. *J. Am. Chem. Soc.* **1975**, *97*, 7162.

0276-7333/83/2302-0008$01.50/0

calcd for $C_{11}H_{24}Si_2O$ 228.136 58, measured 228.135 79.

Synthesis of (*Z*)-1-Phenoxy-3-(trimethylsilyl)propene (25). To a stirred solution of 3-phenoxypropene (10.0 g, 0.075 mol) and TMEDA (6 mL) in 200 mL of dry THF at −78 °C was slowly added 37 mL (10% excess) of 2.2 M *n*-BuLi. The resulting yellow solution was stirred for 2 h at −78 °C after which 9.4 mL (0.075 mol) of Me_3SiCl was added. After being stirred for 4 h at room temperature, the reaction mixture was poured into hexane, the solution washed three times with H_2O and dried over $MgSO_4$ and the solvent removed by rotary evaporation. Distillation through a 10-cm Vigreux column (135 °C (60 torr)) afforded 3.70 g (24%) of pure **25**: NMR ($DCCl_3$) δ 0.03 (s, 9 H), 1.52 (d, 2 H, J = 9 Hz), 4.77 (d of t, 1 H, J = 9 Hz and 6 Hz), 6.23 (d of t, 1 H, J = 6 Hz and 1 Hz); mass spectrum, m/e (% relative intensity) 206 (9), 191 (8), 151 (11), 77 (13), 73 (100); calcd for $C_{12}H_{18}SiO$ m/e 206.112 70, measured m/e 206.112 19.

Synthesis and Pyrolysis of (*E*)-1,3-Bis(trimethylsilyl)-3-phenoxypropene (26). To a stirred solution of **25** (2.202 g, 0.0107 mol) and TMEDA (1.6 mL) in 50 mL of dry THF at −78 °C was slowly added 5.34 mL of 2.2 M *n*-BuLi. After the solution was stirred for 5 h at −78 °C, 1.48 mL (1.23 g, 0.0113 mol) of Me_3SiCl was added. The solution was stirred for 30 min at room temperature then poured into hexane, the mixture washed three times with H_2O, and the solvent removed by rotary evaporation. It was necessary to separate **26** by preparative GC and this was accomplished on an 8-ft, 12% OV101 column at 170 °C: NMR ($DCCl_3$) δ 0.03 (s, 9 H) 0.10 (s, 9 H), 4.37 (d, 1 H, J = 5 Hz, collapses to s with $h\nu$ at δ 6.09), 5.50 (d, 1 H, J = 19 Hz and 5 Hz, collapses to d with J = 19 Hz with $h\nu$ at δ 4.37); mass spectrum, m/e (% relative intensity) 278 (5), 175 (16), 100 (60); calcd for $C_{15}H_{26}Si_2O$ m/e 278.1522, measured 278.1516. Pyrolysis of **26** (0.1667 g) was conducted by slowly dripping (via syringe) it directly into a vertical 1-ft quartz tube packed with quartz chips heated at 450 °C in a tube furnace, with a continuous N_2 flow of 30 mL/min. The mass recovery was 66%. GC analysis revealed a complex mixture of products for which the IR spectrum showed no significant absorption in the 1620–1700-cm^{-1} region.

Acknowledgment. The support of this work by the National Science Foundation is gratefully acknowledged.

Registry No. **3**, 83135-14-2; **4**, 83135-15-3; **6**, 83159-75-5; **7**, 83135-16-4; **8**, 83135-17-5; **9**, 83135-18-6; **15**, 105-31-7; **16**, 62785-87-9; **17**, 83152-00-5; **18**, 83135-19-7; **19**, 83135-20-0; **20**, 83135-21-1; **21**, 83135-22-2; **25**, 83135-23-3; **26**, 83135-24-4; 3-methylbut-3-en-1-yne, 78-80-8; isopropyl(pentamethyldisilanyl)acetylene, 83135-25-5; 3-phenoxypropene, 1746-13-0; $Me_3SiSiMe_2Cl$, 1560-28-7; Me_3SiCl, 75-77-4.

New Silene Rearrangements from a Study of the Mechanism of Silacyclopentene Formation from [3.3]Silaspirocycloheptane

Thomas J. Barton,* Gary T. Burns, and David Gschneidner

Department of Chemistry, Iowa State University, Ames, Iowa 50011

Received July 23, 1982

In an attempt to unravel the mechanism of silacyclopentene formation in the pyrolysis of [3.3]silaspirocycloheptane, pyrolysis of 1-methoxy-1-[(trimethylsilyl)methyl]-1-silacyclobutane was conducted. Instead of the desired elimination of Me_3SiOMe, extrusion of ethylene occurred followed by a novel isomerization of the resulting silene. Model system studies produced the mechanistic proposal that [(trimethylsilyl)methyl]silenes thermally isomerize via 1,4-hydrogen atom transfer. Pyrolysis of 1-methoxy-1-(trimethylsilyl)-1-silacyclopentane also produced silacyclopent-3-ene, thus confirming the legitimacy of proposing silacyclopentanylidene intermediate in the title transformation.

Recently considerable attention has focused on thermal isomerization of silenes to silylenes.[1] To our knowledge this rearrangement was first proposed when we suggested the rearrangement of silylsilene **1** to silylene **2** via 1,2-silyl migration to explain the ultimate formation of disilacyclobutane **3** in the pyrolysis of allylpentamethyldisilane.[2]

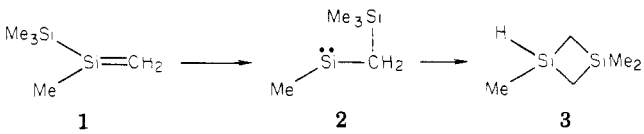

1 2 3

However, there has long existed the possibility that the first example of silene to silylene rearrangement had been unknowingly reported in 1973 when Gusel'nikov[4] observed that the gas-phase pyrolysis of silaspirocycle **4** afforded 1-silacyclopent-3-ene (**9**) as the sole silicon-containing product. Although no mechanism for the formation of **9** was put forth, it was suggested that silene **5** was initially formed and somehow rearranged to **9**. We have long wondered whether this reaction might not be taking place through isomerization of **5** to silacyclopentanylidene **6** via alkyl migration, followed by C–H insertion to form silabicyclo[2.1.0]pentane (**7**). Homolysis of the internal Si–C central bond in **7** would lead to 1,3-diradical **8** from which a 1,3-hydrogen shift to silicon would afford **9**. A both-

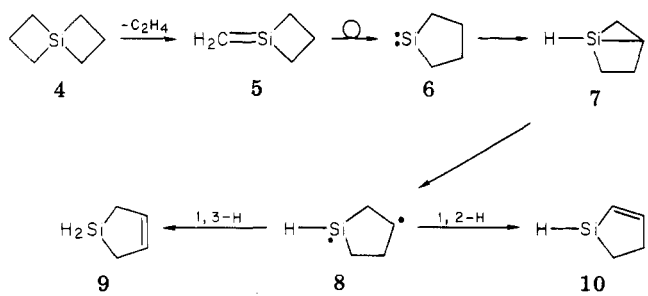

4 5 6 7 9 8 10

ersome feature of this proposal is that one would reasonably expect that from diradical **8** 1,2-hydrogen migration would be competitive with a 1,3 shift, and thus silacyclopent-2-ene (**10**) should also be formed. However, this objection can be overcome if one recognizes that silahausane **7** could undergo isomerization to 4-butenylsilylene **11**, as the thermal decomposition of silacyclopropanes to silylenes and olefins is a long-established process.[4] Silylene

(1) Barton, T. J.; Burns, S. A.; Burns, G. T. *Organometallics* **1982**, *1*, 210.
(2) Barton, T. J.; Jacobi, S. A. *J. Am. Chem. Soc.* **1980**, *102*, 7979.
(3) Nametkin, N. S.; Gusel'nikov, L. E.; Orlov, V. Y.; Ushakova, R. L.; Kuzmin, O. V.; Vdovin, V. M. *Dokl. Adak. Nauk SSSR* **1973**, *211*, 106.
(4) Seyferth, D.; Annarelli, D. C. *J. Am. Chem. Soc.* **1975**, *97*, 7162.

0276-7333/83/2302-0008$01.50/0

11 could undergo β-CH insertion to form vinylsilacyclopropane **12**, and a 1,3-silyl migration would produce exclusively **9**. Indeed we have recently[5] generated the methyl derivative of **11**, methyl-4-(1-butenyl)silylene **13**, which afforded a remarkable 56% yield of silacyclopent-3-ene **14** and none of the 2-ene isomer.

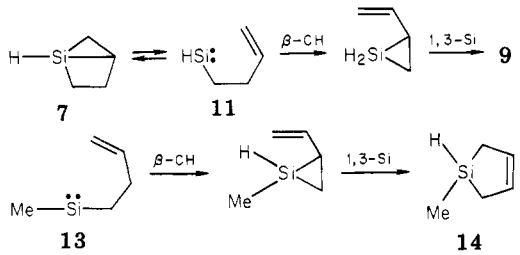

In order to probe the mechanism of the formation of **9**, we have attempted the synthesis of silene **5**. To this end we chose the thermally induced β elimination of Me_3SiOMe from silacyclobutane **15** as this method has proved quite successful for us in the synthesis of a variety of silenes.[6] Precursor **15** was prepared by sequential addition of [(trimethylsilyl)methyl]magnesium chloride and methanol to 1,1-dichloro-1-silacyclobutane. Flash vacuum pyrolysis (FVP) of **15** (780 °C (10^{-4} torr)) afforded, in addition to unreacted **15**, a 42% yield of 1-methoxy-1,3,3-trimethyl-1,3-disilacyclobutane (**16**) which was identified from its spectral characteristics and comparison of these with those of an authentic sample. Thus, instead of the desired elimination of Me_3SiOMe, **15** had lost ethylene. This is the normal course of silacyclobutane pyrolysis and apparently takes precedent over β elimination in this system. Indeed, the methoxy substituent plays no role in this reaction for we find that FVP (790 °C (10^{-4} torr)) of the methyl analogue, **17**, also results in extrusion of ethylene, here to produce 1,1,3,3-tetramethyl-1,3-disilacyclobutane (**18**) in 27% yield.

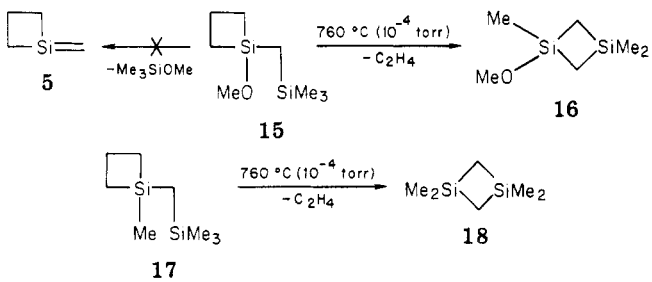

The formation of both **16** and **18** clearly arise from the respective intermediacy of silenes **19a,b**. These unprecedented rearrangements can be envisioned as arising from a hydrogen atom transfer from methyl (of $SiMe_3$) to the terminal methylene to yield 1,4-diradical **20**, which closes to product. Alternatively, a concerted six-electron decomposition of **19** to yield two molecules of silene which then cycloadd would also account for the observed products. However, we consider this retroene process unlikely as it would be necessary to demand exclusive geminate cycloaddition as the cross product **21** is not observed.

Further evidence that these reactions proceed through isomerization of initially formed silenes is found in the FVP (770 °C (10^{-4} torr)) of silacyclobutane **22**. The major product of the reaction is 1-ethyl-1,3,3-tetramethyl-1,3-disilacyclobutane (**24**) as expected from the predominant

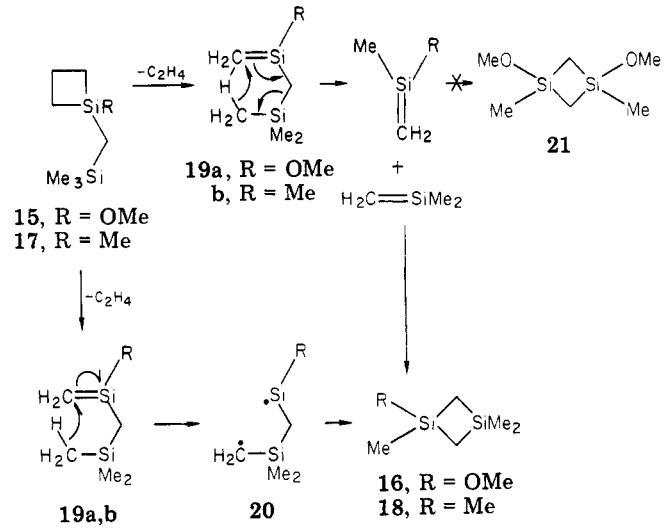

formation[7] of silene **23** followed by 1,4-hydrogen shift to create the ethyl group and closure of the 1,4 diradical. An interesting minor product, vinylsilane **25** can be rationalized as arising by the isomerization of silene **23** via a 1,3-hydrogen migration.[8] The product from apparent radical rearrangement of the minor silene **26**, **18**, was formed in only 5% yield. Again no evidence of the retroene process was found since no 1,3-diethyl-1,3-dimethyl-1,3-disilacyclobutane could be detected.

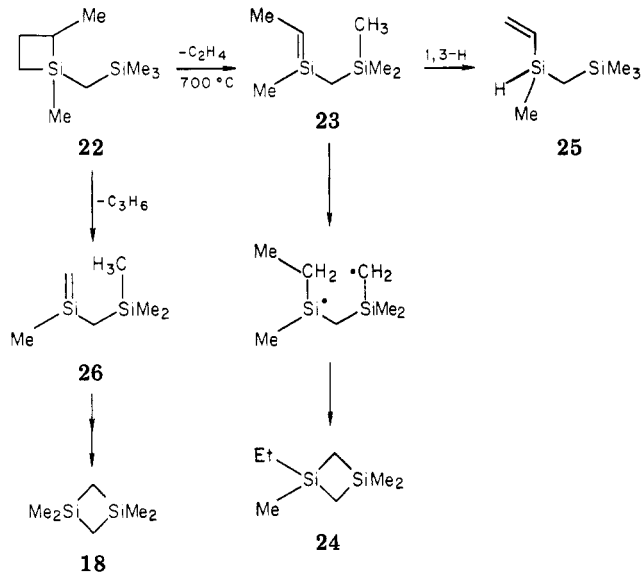

It is of interest to note that this novel rearrangement of a silene via 1,4-hydrogen shift is dependent upon the presence of a suitably located Me_3Si group. Thus, when the analogous *n*-propylsilacyclobutane **27** was pyrolyzed (780 °C (10^{-4} torr)), only **29**, the normal product of head-to-tail dimerization of the *n*-propylmethylsilene **28**, was formed, with no products consistent with hydrogen transfer being observed. We would argue that since a retroene reaction of **28** would afford both a new silene and a stable C–C double bond, that this process would be more likely for **28** than for silenes **19a,b**, **23**, or **26**, each of which would yield two relatively unstable silicon–carbon double bonds.

(5) Barton, T. J.; Burns, G. T., *Organometallics*, preceding article in this issue.

(6) Barton, T. J.; Burns, G. T.; Arnold, E. V.; Clardy, J. *Tetrahedron Lett.* **1981**, 7. Burns, G. T.; Barton, T. J. *J. Organomet. Chem.* **1981**, C5. Barton, T. J.; Vuper, M. *J. Am. Chem. Soc.* **1981**, *103*, 6788.

(7) Barton, T. J.; Marquardt, G.; Kilgour, J. A. *J. Organomet. Chem.* **1975**, *85*, 317.

(8) A possible precedent for this rearrangment exists in the work of Shechter.[9] who reported that (trimethylsilyl)carbene produced a small amount (3–4%) of vinyldimethylsilane, possibly by rearrangement of intermediate 1,3,3-trimethylsilene (Me_2Si=CHMe).

(9) Kreeger, R. L.; Shechter, H. *Tetrahedron Lett.* **1975**, 2061.

Thus, the absence of the retroene reaction for **28** speaks for the radical mechanism of hydrogen transfer.

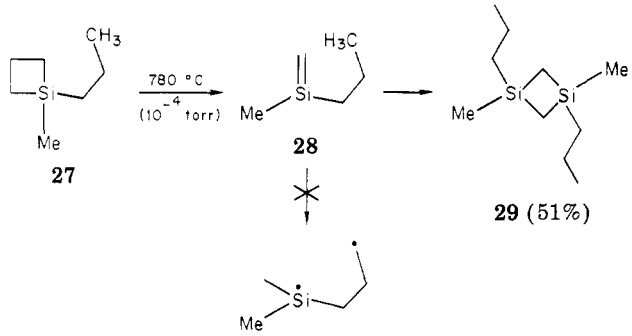

Although thwarted in our attempt to generate silene **5**, we set out to produce silylene **6** to determine the legitimacy of its inclusion in our mechanistic scheme for the formation of silacyclopentene **9**. This was accomplished by the synthesis and FVP (680 °C (10^{-4} torr)) of 1-methoxy-1-(trimethylsilyl)-1-silacyclopentane **30**. The mass recovery was exceptionally low (a reproducible 23%), but the major volatile products were Me_3SiOMe (24% from reductive elimination) and silacyclopent-3-ene (**9**, 7.9%). Due to small amounts of sample and the low yield we can not say whether or not any of **10** is formed in this reaction as a yield of perhaps 2% could have gone undetected. However, this turns out to be of less importance than we originally thought, since we find that in our hands the pyrolysis of silaspirocycle **4** affords both **9** and **10** in a 3:1 ratio.

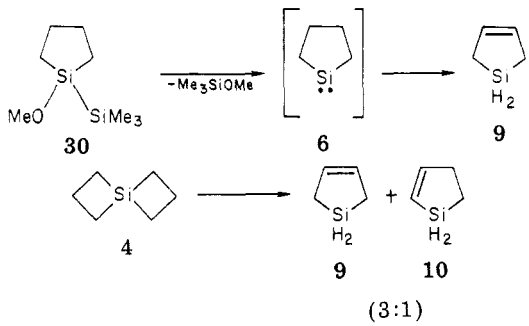

Thus, although it remains to unambiguously generate silene **5**, it appears very likely that conversion of **4** to silacyclopentenes does indeed involve a thermally induced silene (**5**) to silylene (**6**) rearrangement. In this regard it is perhaps of interest to note that we[10] have recently found it necessary to invoke an analogous reverse rearrangement for silacyclobutanylidenes **31** and **33** to methylenesilacyclopropane **32** to explain the complex interconversions observed in the thermochemistry of C_3H_5 silylsilylenes. Our data do not allow a definitive statement

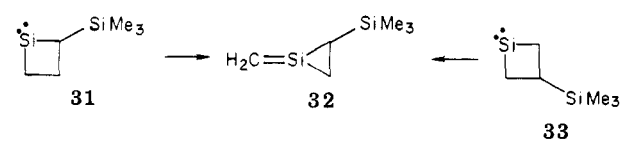

to be made concerning the possible intermediacy of silylene **11**. Indeed, it is entirely possible that **8** could be an immediate precursor of **9**, **10**, and **11**.

Experimental Section

General Data. Proton NMR spectra were recorded on a Varian Model EM-360 spectrometer. GC–mass spectral (GC–MS) data were collected at 70 eV on a Finnegan Model 4023 mass spectrometer, and exact mass measurements were obtained on an AEI MS-902 mass spectrometer. Gas chromatographic separations were performed on a Varian-Aerograph Series 1700 instrument. Unless otherwise specified, all yields are GC yields calculated from predetermined response factors and are absolute. Flash vacuum pyrolyses (FVP) were carried out by evaporating the silylene precursor through a horizontal 30-cm quartz tube packed with quartz chips and heated in a tube furnace. Products are collected in a liquid N_2 cooled trap.

Synthesis of 1-Methoxy-1-[(trimethylsilyl)methyl]-1-silacyclobutane (15). To a stirred suspension of excess Mg turnings in 100 mL of dry THF was added 5.10 g (41 mmol) of trimethylchlorosilane in 20 mL of THF over a 90-min period. After being stirred for an additional 30 min, the solution was transferred by syringe to a stirred solution of 5.85 g (41.5 mmol) of 1,1-dichloro-1-silacyclobutane in 250 mL of THF. The solution was stirred for 1.5 h at room temperature, and a solution consisting of 2.0 mL of MeOH and 4.0 mL of pyridine was added. After the mixture was stirred for an additional 30 min, 250 mL of hexane was added, the mixture filtered through celite, the filtrate concentrated by rotary evaporation, and the residue distilled at 73–74 °C (10–12 torr) to afford 2.37 g (30%) of pure **15**: NMR (CCl_4) δ −0.05 (br s, 2 H), 0.05 (s, 9 H, $SiMe_3$), 0.71–2.11 ($CH_2CH_2CH_2$ m, 6 H), 3.47 (s, 3 H, OMe); mass spectrum *m/e* (% relative intensity) 188 (0.01), 173 (22), 160 (55), 146 (29), 145 (67), 131 (14), 119 (11), 117 (39), 115 (42), 73 (32), 59 (100); calcd for $Si_2C_7H_{17}O$ (M − CH_3) *m/e* 173.0818, measured *m/e* 173.0816.

Flash Vacuum Pyrolysis (FVP) of 15. FVP of **15** (0.7461 g, 3.97 mmol) was conducted by slowly distilling (25 °C (1×10^{-4} torr)) the material through a horizontal 1-ft quartz tube packed with quartz chips and heated at 780 °C. A 78% (0.5790 g) mass recovery was achieved by liquid N_2 trapping. The pyrolysate was separated by preparative GC on a $^1/_4$ in. × 16 ft, 20% SE-30 on Chromosorb W column using a temperature program of 120 → 210 °C at 2 °C/min to afford, in addition to unreacted **15**, a 42% yield of 1-methoxy-1,3,3-trimethyl-1,3-disilacyclobutane (**16**):[11] ^1H NMR ($DCCl_3$) δ 0.22 (s, 4 H), 0.28 (s, 9 H), 3.44 (s, 3 H); ^{13}C NMR ($DCCl_3$) 0.95, 1.17, 1.65, 5.82, 49.81 ppm; mass spectrum, *m/e* (% relative intensity) 160 (41), 145 (77), 119 (16), 117 (47), 115 (100), 73 (39), 59 (80); calcd for $Si_2C_6H_{16}O$ *m/e* 160.073 98; measured *m/e* 160.074 18.

Further confirmation of the identity of **16** was obtained by independent synthesis. To a stirred solution of 2.23 g (13.6 mmol) of 1-chloro-1,3,3-trimethyl-1,3-disilacyclobutane[11] in 20 mL of Et_2O at 25 °C was added an equimolar mixture of methanol and pyridine (1 equiv each) over a 10-min period. The solution was stirred for several hours and filtered and the filtrate concentrated by rotary evaporation. Analytically pure **16**[11] was obtained by preparative GC on a 16-ft, 20% SE-30 on Chromosorb W column with a temperature program from 120 °C at 2 °C/min.

Synthesis of 17. To a stirred solution of 43.3 mmol of Me_3SiCH_2MgCl in 200 mL of Et_2O was added 5.081 g (42.2 mmol) of 1-chloro-1-methyl-1-silacyclobutane in one portion. After being stirred for 1.5 h, the reaction was quenched with saturated NH_4Cl, washed with H_2O, dried over $MgSO_4$, and filtered and the filtrate concentrated by rotary evaporation. Distillation of the residue at 99–100 °C (53 torr) afforded 2.194 g (30%) of **17**: NMR (CCl_4) δ 0.04 (s, 11 H), 0.27 (s, 3 H), 0.90 (t, J = 8 Hz, 4 H), 1.70–2.30 (m, 2 H); mass spectrum, *m/e* (% relative intensity) 172 (0.1), 157 (85), 131 (35), 129 (100), 73 (36); calcd for $Si_2C_8H_{20}$ *m/e* 172.110 36, measured *m/e* 172.110 02.

FVP of 17. FVP of **17** (0.2559 g, 1.49 mmol) of **17** was conducted at 790 °C in the same fashion as described for **15** (vide supra). The pyrolysate (0.1708 g) was collected in a liquid N_2 cooled trap and represented a 67% mass recovery. The major product was identified as tetramethyldisilacyclobutane (18, 27%) by spectral comparison with an authentic sample.

Synthesis of 22. A solution of 4.43 g (36 mmol) of trimethylchloromethylsilane (Petrarch) and 4.578 g (34 mmol) 1,2-dimethyl-1-chloro-1-silacyclobutane[13] in 10 mL Et_2O was added

(10) Burns, S. A.; Burns, G. T.; Barton, T. J., *J. Am. Chem. Soc.*, in press.

(11) Nametkin, N. S.; Babich, E. D.; Karel'skii, V. N.; Vdovin, V. M. *Izv. Akad. Nauk SSSR* **1971**, 5, 1033.

(12) Kriner, W. A. *J. Org. Chem.* **1964**, *29*, 160.

(13) Dubac, J.; Mazerolles, P.; Serres. B. *Tetrahedron Lett.* **1972**, 525.

to a stirring suspension of excess Mg turnings in 60 mL of Et_2O at a rate sufficient to maintain a gentle reflux. The solution was then refluxed for 15 h, hydrolyzed with 10% NH_4Cl, washed with H_2O, dried over $MgSO_4$, filtered, and concentrated by rotary evaporation. The residue was separated by preparative GC on an 8-ft, 20% DC-550 column at 150 °C to afford pure **22** as a mixture of the cis and trans isomers: NMR (CCl_4) δ −0.05 (s, 2 H, SiCH_2Si), 0.00 (s, 9 H), 0.15 and 0.18 (two singlets, total 3 H), 0.48–1.68 (m, 8 H); mass spectrum, *m/e* (% relative intensity) 186 (0.1), 171 (12), 143 (11), 131 (100), 129 (67), 73 (26), 59 (19); calcd for $Si_2C_9H_{22}$ *m/e* 186.126 01, measured 186.126 32.

FVP of 22. FVP of **22** (0.3517 g, 1.89 mmol) was conducted at 770 °C in the same fashion as for **15** and **17** with a 71% (0.2493 g) mass recovery. Three products were isolated by preparative GC on an 8-ft, 20% DC-550 on Chromosorb W column at 130 °C. The first product was 3,5,5-trimethyl-3,5-disila-1-hexene (**25**): 7%; NMR ($DCCl_3$) δ −0.06 (d, J = 4 Hz, 2 H, collapses to s with *h*ν at δ 4.15), 0.18 (s, 9 H), 0.27 (d, J = 4 Hz, 3 H, collapses to s with *h*ν at δ 4.15), 4.15 (m, 1 H, Si*H*), 5.47–6.34 (m, 3 H, vinyl); mass spectrum, *m/e* (% relative intensity) 158 (0.03), 157 (0.4), 144 (15), 143 (100), 117 (14), 116 (11), 115 (73), 103 (8), 101 (9), 85 (13), 73 (57), 59 (40). The second product, **18**, 5%, was identified solely by spectral comparison with an authentic sample. The third product, 1-ethyl-1,3,3-tetramethyl-1,3-disilacyclobutane (**24**), was formed in 23% yield: NMR ($DCCl_3$) δ 0.08 (s, 3 H), 0.31 (s, 3 H), 0.36 (s, 3 H), 0.58–1.31 (m, 5 H); mass spectrum *m/e* (% relative intensity) 158 (21), 143 (21), 130 (23), 129 (100), 115 (59), 101 (18), 73 (19), 65 (11), 59 (41), 57 (11); calcd for $Si_2C_7H_{18}$ *m/e* 158.094 71, measured *m/e* 158.094 67. Product **24** was independently prepared by the addition of EtMgBr to a stirred solution of 1-chloro-1,3,3-trimethyl-1,3-disilacyclobutane in Et_2O. All spectra exactly matched.

Synthesis of 1-*n*-Propyl-1-methyl-1-silacyclobutane (27). To a stirred solution of 55 mmol of *n*-propylmagnesium bromide in 80 mL of Et_2O at room temperature was added 4.933 g (41 mmol) of 1-chloro-1-methyl-1-silacyclobutane. After 3 h the reaction was hydrolyzed with H_2O. The two layers were separated, and the ether layer was dried over $MgSO_4$ and filtered, and the filtrate was concentrated by rotary evaporation. Distillation of the residue at 103–104 °C afforded 1.83 g (35%) of **27**: NMR (CCl_4) δ 0.22 (s, 3 H), 0.47–2.31 (m, 13 H); mass spectrum, *m/e* (% relative intensity) 128 (15), 100 (45), 85 (30), 72 (100), 59 (40), 58 (60); calcd for SiC_7H_{16} *m/e* 128.102 13, measured *m/e* 128.101 82.

FVP of 27. FVP of **27** (0.6677 g, 5.22 mmol) was conducted at 760 °C in the same fashion as for **15**, **17**, and **22**, with a 68% mass recovery. In addition to unreacted **27**, one product was isolated by preparative GC (8-ft, 20% DC-550 on Chromosorb W at 150 °C), 1,3-dimethyl-1,3-diethyl-1,3-disilacyclobutane (**29**): 51% yield; NMR ($DCCl_3$) δ −0.19 (s, 4 H), 0.05 (s, 6 H), 0.31–1.61 (m, 14 H); mass spectrum *m/e* (% relative intensity) 200 (6), 185 (2), 159 (15), 158 (19), 157 (30), 143 (10), 115 (100); calcd for $Si_2C_{10}H_{24}$ *m/e* 200.141 66, measured *m/e* 200.141 31.

Synthesis of 1-Methoxy-1-(trimethylsilyl)-1-silacyclopentane (30). A solution of 1,4-dibromobutane (9.00 g, 41.6 mmol) and 2,2-dichlorohexamethyltrisilane (10.0 g, 40.8 mmol) in 40 mL of THF was added to a stirring suspension of excess Mg turnings over a 1- period. The reaction mixture was stirred for 1 day, then hydrolyzed, diluted with hexane, separated, dried over $MgSO_4$, and filtered, solvent removed by rotary evaporation, and the residue distilled at 79–81 °C (0.1 torr) to afford 5.58 g (59%) of 1,1-bis(trimethylsilyl)-1-silacyclopentane: NMR ($DCCl_3$) δ 0.17 (s, 18 H), 0.62–0.99 (m, 4 H), 1.43–1.97 (m, 4 H); mass spectrum, *m/e* (% relative intensity) 230 (28), 215 (17), 157 (48), 129 (33), 97 (71), 73 (100); calcd for $Si_3C_{10}H_{26}$ *m/e* 230.134 24, measured *m/e* 230.133 51. The entire sample (5.58 g, 24.2 mmol) was heated with 5.40 g (26 mmol) PCl_5 in 60 mL of CCl_4 at 70 °C for ca. 2 h. The CCl_4 and PCl_3 were removed in vacuo, and the residue was distilled over at ca. 50–60 °C (0.1 torr) and used without further purification. To the resulting distilled chlorosilane in hexane solution was added a solution consisting of 1 equiv of methanol and 1 equiv of pyridine followed by stirring the reaction mixture overnight. After dilution with hexane, the mixture was filtered through celite, the solvent was removed by rotary evaporation, and the residue was separated by preparative GC (20 ft, 20% OV-101, programmed from 120–180 °C at 2 °C/min to afford pure **30** in ca. 4% yield: NMR (CCl_4, no internal standard, peaks given relative to Me_3Si singlet) δ 0.3 (s, 9 H), 0.36–0.72 (m, 4 H), 1.26–1.66 (m, 4 H), 3.18 (s, OMe, 3 H); mass spectrum *m/e* (% relative intensity) 188 (9), 173 (71), 145 (49), 119 (92), 115 (45), 73 (91), 58 (100); calcd for $Si_2C_8H_{20}O$ *m/e* 188.105 28, measured *m/e* 188.105 15.

FVP of 30. FVP of **30** (0.1848 g, 0.983 mmol) was conducted at 680 °C as described above with a mass recovery of 43.9 mg. The yields of Me_3SiOMe (23.5%) and **9** (7.9%) were obtained by NMR integration relative to an internal toluene standard. Silacyclopentene **9** was isolated by preparative GC (20 ft, 20% OV-101): ^1H NMR (CCl_4, 300 MHz, Me_4Si capillary) δ 1.76 (d of t, J = 3.4 and 1.8 Hz, 4 H), 4.19 (1.4.6.4.1 pentet, J = 3.4 Hz, 2 H, SiH_2) 6.11 (broadened s, 2 H, vinyl); ^{13}C NMR (CCl_4, 300 MHz) 11.5 and 130.9 ppm; GC–MS, *m/e* (% relative intensity) 84 (83), 83 (100), 82 (29), 81 (14), 69 (17), 58 (22), 57 (16), 56 (72), 55 (50), 54 (16), 53 (36). Our observed chemical shift values for **9** are consistent with those reported by Ring[14] for **9** in $DCCl_3$ solution, but each is approximately 0.35-ppm upfield. Presumably, this is due to the difference in solvents and internal vs. external reference. In D_6C_6 solvent we find the resonances of **9** shifted upfield from 0.1 and 0.3 ppm relative to the spectrum in CCl_4.

FVP of 4. FVP of **4** (1.6348 g, 14.6 mmol) was conducted at 780 °C (10^{-4} torr) with a 23% (0.430 g) mass recovery. From the complex product mixture (at least 20 products) only one major silicon-containing product could be isolated by preparative GC (20 ft, 20% OV-101, programmed 85–190 °C at 2 °C/min), and the retention time matched that of **9**. However, the NMR spectrum (C_6D_6) clearly revealed it to be a clean 3:1 mixture of **9** and **10**. The presence of silacyclopent-2-ene (**10**) was revealed by the unique vinyl proton adjacent to Si as a doubled triplet (J_{H-SiH} = 2.5 Hz and $J_{HC=CH}$ = 10 Hz), the β-vinyl H was obscured by the vinyl absorption of **9**, but the SiH_2 unit was observed as a multiplet at δ 4.45 (apparent septet). The two CH_2 units were fortuitously observable as they flanked the CH_2 absorption of **9** as multiplets at δ 2.17–2.57 and 0.83–1.10. Separation of **9** and **10** was not accomplished. Attempts to trap silene **5** by copyrolysis of **4** and butadiene were unsuccessful.

Acknowledgment. The support of the National Science Foundation is gratefully acknowledged.

Registry No. **4**, 33317-66-7; **5**, 83292-09-5; **9**, 7049-25-4; **10**, 6572-33-4; **15**, 83292-10-8; **16**, 33432-33-6; **17**, 63647-94-9; **18**, 1627-98-1; **22**, 83292-11-9; **24**, 25261-25-0; **25**, 83292-12-0; **27**, 63647-86-9; **29**, 83292-13-1; **30**, 83292-14-2; Me_3SiCH_2Cl, 2344-80-1; 1,1-dichloro-1-silacyclobutane, 2351-33-9; 1-chloro-1-methyl-1-silacyclobutane, 2351-34-0; 1,2-dimethyl-1-chloro-1-silacyclobutane, 35741-74-3; propyl bromide, 106-94-5; 1,4-dibromobutane, 110-52-1; 2,2-dichlorohexamethyltrisilane, 5181-42-0; 1,1-bis(trimethylsilyl)-1-silacyclopentane, 83292-15-3.

(14) Jenkins, R. L.; Kedrowski, R. A.; Elliot, L. E.; Tappen, D. C.; Schlyer, D. J.; Ring, M. A. *J. Organomet. Chem.* **1975**, *86*, 347.

Acid-Promoted Cleavage of 2-Silanorborn-5-enes

Paul Ronald Jones,* Richard A. Pierce, and Albert H. B. Cheng

Department of Chemistry, North Texas State University, Denton, Texas 76203

Received June 7, 1982

The acid-promoted cleavage of both *exo*- and *endo*-2,2-dimethyl-3-neopentyl-2-silanorborn-5-ene under a variety of experimental conditions gives clean and nearly quantitative formation of the ring-opened 3-(3-cyclopenten-1-yl)-2,5,5-trimethyl-2-silahex-2-yl products **4** (X = OH, OMe, F, OSO_3H, OSO_2CF_3, and in Me_2SO, presumably $OSMe_2^+$). No evidence requiring the intermediacy of a silanorbornyl cation was obtained.

Introduction

Unsaturated organosilanes often exhibit unusual reactivity toward electrophiles in comparison to their carbon analogues in that they usually react with electrophiles to give products consistent with the formation of a carbocation to silicon.

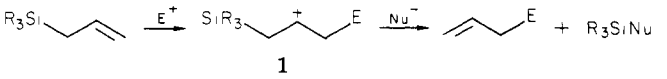

1

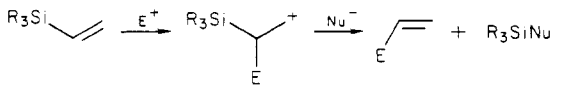

2

These cations are presumably formed because of stabilization of the cation by overlap of the Si–C bonding orbital with the vacant p orbital of the cation.[1,2] However, there is little evidence for the free cations as intermediates. We report here our studies of a related system, the acid-promoted cleavage of the exo and endo isomers 2,2-dimethyl-3-neopentyl-2-silabicyclo[2.2.1]hept-5-ene (**3**).

Results and Discussion

In the preparation of **3**[3] a minor impurity was observed whose concentration appeared to be dependent on the length of time employed in the hydrolytic workup. This product was identified as the ring-opened hydroxide **4**, X = OH, subsequent experiments showed that **4**, X = OH,

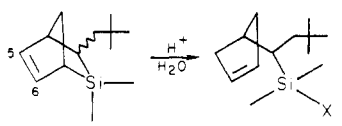

3 **4**, X = OH

could not be prepared from **3** by treatment with water or aqueous base. However, treatment of **3** with dilute aqueous acid gave **4**, X = OH, in good yield.

The methoxy derivative of **4**, X = OMe, could be prepared in good yield (>75%) by bubbling dry HCl through a solution of **3** in dry methanol. In the absence of acid no reaction occurred. **4**, X = OMe, was also observed in ^1H NMR experiments by treatment of the sulfuric acid or trifluoromethanesulfonic acid esters of **4**, X = OH, OSO_3H, or OSO_2CF_3, with methanol.

Likewise, **4**, X = F, could be formed by acid-promoted reactions. Treatment of **3** with $BF_3{\cdot}OEt_2$ or reaction of **4**, X = OSO_3H, with ammonium fluoride gave the fluoro derivative in good yields. The sulfate and trifluoromethanesulfonate derivatives of **4** were identified in ^1H NMR experiments and were formed by the addition of sulfuric acid or trifluoromethanesulfonic acid, respectively, to **3**. Scheme I summarizes the conversions which were carried out.

Of interest is the conversion of **4**, X = F, to **4**, X = OMe. When **4**, X = F, was stirred in dry methanol for a period of 24 h, only 15% conversion to the methoxy derivative occurred. However, upon addition of a single drop of concentrated HCl, the reaction rapidly went to completion giving a 92% isolated yield of **4**, X = OMe. Usually in the absence of base, the alcoholysis of organosilyl fluorides is slow with the equilibrium favoring the fluorosilane.[4] To our knowledge, this is the first example of alcoholysis of a fluorosilane which is promoted by acid.[5]

In light of the many examples of reactions of electrophiles with allyl silanes, including our own studies of the hydroboration of allylsilanes,[6] it seems reasonable that initial protonation of **3** at C-5 would give the carbocation **5** stabilized by the β-silyl substituent. Subsequent nucleophilic attack at silicon would give rise to the observed products. In none of our experiments did we observe products arising from the cation **6** which would result from protonation at C-6. It is well-known that reaction of

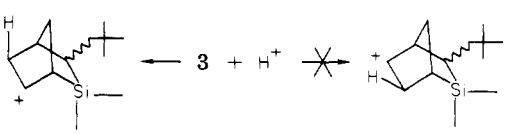

5 **6**

norbornene with electrophiles gives rise to the norbornyl cation. Thus, the addition of DCl to norbornene gave *exo*-norbornyl chloride with deuterium incorporated 57% in the *exo*-**3** and 41% in the syn-7-positions.[7] Under appropriate experimental conditions the cation has been characterized spectroscopically.[8] By analogy, a similar σ stabilization of **5** might explain the facile acid-promoted cleavage reactions of **3** and the unusual acid-promoted alcoholysis of **4**, X = F, which we have observed.

In our system, the formation of an equilibrating or delocalized cation such as **5** could provide a pathway for the exo- and endo isomerization of **3** if proton loss from the cation was competitive with nucleophilic attack at silicon.

(1) Chan, T. H.; Fleming, I. *Synthesis* **1979**, 761.
(2) Fleming, I.; Langley, J. A. *J. Chem. Soc., Perkin Trans. 1* **1981**, 1421–3.
(3) Jones, P. R.; Lim, T. F. O.; Pierce, R. A. *J. Am. Chem. Soc.* **1980**, *102*, 4970–72.
(4) Eaborn, C. *J. Chem. Soc.* **1952**, 2840–2846, 2846–2849.
(5) Acid catalysis of the hydrolysis of silyl fluorides has been observed. "Stereochemistry, Mechanism and Silicon"; Sommer, L. H., Ed.; McGraw-Hill: New York, 1964; pp 139–41. We thank Professor Colin Eaborn for pointing this out.
(6) Jones, P. R.; Myers, J. K. *J. Organomet. Chem.* **1972**, *34*, C9–10.
(7) Brown, H. C.; Liu, K. J. *J. Am. Chem. Soc.* **1975**, *97*, 600–10.
(8) Olah, G. A.; White, A. M.; DeMember, J. R.; Commeyras, A.; Lui, C. Y. *J. Am. Chem. Soc.* **1970**, *92*, 4627–40.

0276-7333/83/2302-0012$01.50/0

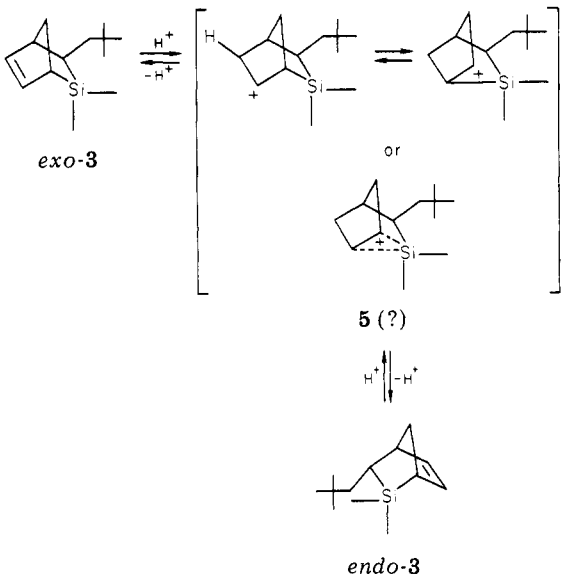

The exo and endo isomers of **3** are readily distinguished in the PMR spectrum by the chemical shifts of the silicon methyl protons. For *exo*-**3** these appear at δ 0.02 and 0.17, while in *endo*-**3** the resonances occur at −0.03 and 0.24 ppm[3] In an attempt to observe isomerization of **3** the following ^{1}H NMR experiments were carried out.

A solution 99% pure *exo*-**3** in carbon tetrachloride with a small amount of chloroform present as an internal standard was treated with one drop of fuming sulfuric acid. The peaks due to *exo*-**3** diminished in intensity immediately and the peaks due to **4**, X = OSO_3H, appeared. After 2 days at room temperature the spectrum was essentially unchanged. No new peaks were observed, and no evidence for isomerization of *exo*-**3** to *endo*-**3** was obtained. Treatment with additional fuming sulfuric acid converted *exo*-**3** completely to **4**, X = OSO_3H. When this solution was quenched with methanol, a spectrum corresponding to **4**, X = OMe, was obtained. Separate experiments starting with a mixture of **3** containing >90% of the endo isomer gave similar results. No isomerization to the exo isomer was observed. Experiments involving carbon tetrachloride solutions of **3** treated with trifluoromethanesulfonic acid gave only the ring-opened **4**, X = OSO_2CF_3. In order to verify that the singlets in the PMR spectra at δ 0.63 and 0.77 were indeed due to the silicon methyl protons of **4**, X = OSO_3H and OSO_2CF_3, respectively, solutions of hexamethyldisiloxane in carbon tetrachloride were treated with fuming sulfuric acid or trifluoromethanesulfonic acid. The ^{1}H NMR spectra of these solutions showed new peaks at δ 0.63 and 0.76 corresponding to the silicon methyl protons of trimethylsilyl hydrogen sulfate and trimethylsilyl trifluoromethanesulfonate, respectively.

With analogous carbon compounds, treatment of ring-opened compounds similar to **4** with strong acids provides an alternate route to the norbornyl cation system.[8] However, treatment of carbon tetrachloride solutions of **4**, X = OMe, with either fuming sulfuric acid or with trifluoromethanesulfonic acid gave only **4**, X = OSO_3H or OSO_2CF_3, respectively. No evidence for ring closure to a delocalized or equilibrating silyl cation was obtained.

In an effort to determine the extent to which the low polarity of the carbon tetrachloride solvent contributed to the results given above, analogous experiments were carried out by using dimethyl sulfoxide (Me_2SO) as the solvent. To our surprise, in this solvent, neither fuming sulfuric acid nor trifluoromethane sulfonic acid gave rise to the ring-opened compounds **4**, X = OSO_3H or OSO_2CF_3. Instead, treatment of a Me_2SO solution of the exo or endo isomers of **3** with either acid gave rise to a ^{1}H NMR spectrum of a new species, which showed the vinyl protons for a ring-opened analogue of **4** and a new peak for the silicon methyl protons at δ 0.12, midway between the peaks for the exo- and endo-silicon methyl protons of the silanorbornene **3**. It was tempting to assign this peak to the rapidly equilibrating isomers of *exo*- and *endo*-**3** or to some form of the cation **5**. However, we believe it more reasonable to attribute the new peaks to a ring-opened species, **4**, X = $OSMe_2^+$, for the following reasons.

Equilibration of the exo and endo isomers of **3** which was rapid on the ^{1}H NMR time scale would give rise to broadening and coalescence of the peaks due to the silicon methyl protons of the isomers of **3**. With trace amounts of acid we observed a sharp peak at 0.12 appearing *between* the peaks due to the silicon methyl groups of **3**.

In the norbornyl cation, 6, 1, and 2 hydride shifts are rapid even at low temperatures and the protons give rise to a ^{1}H NMR signal at δ 5.01.[8] In 6-substituted norbornyl cations, H_1 appears in the region δ 4.64 to 4.83.[9] For the species which we are assigning as **4**, X = $OSMe_2^+$, the peaks due to the silylmethyl, *tert*-butyl, and vinyl protons are more shielded than for any of the other derivatives of **4** (Table I) but still are not at the higher field observed for characterized norbornyl cations.

Consistent with this assignment the spectrum of **4**, X = $OSMe_2^+$, is also obtained when **4**, X = OMe, is dissolved in acidified Me_2SO. Quenching of this solution with dry methanol regenerates **4**, X = OMe. Similar interactions between silanes and Me_2SO have been observed in the hydrolysis or racemization of silyl halides,[10] and in the cleavage of cyclopentadienyltrimethylsilane by Me_2SO which gives rise to cyclopentadienylidenedimethylsulfurane.[11]

When hexane solutions of mixtures of **3** enriched in either the exo or the endo isomer to which one drop of purified boron trifluoride etherate had been added were monitored by gas chromatography over a period of 24 h, no exo–endo isomerization was observed. However, the slow formation of **4**, X = F, occurred. The same compound was obtained in 80% yield by treating **4**, X = OSO_3H, with ammonium fluoride.

The failure to observe exo–endo isomerization of **3** in a variety of solvents with a variety of acids provides no evidence for the existence of a cationic intermediate such as **5** in the cleavage reactions of the 2-silanorbornenes. However, if nucleophilic attack on **5** is significantly faster than the bond reorganization and proton loss required for isomerization, the same results would be obtained. To test this possibility, cleavage reactions of **3** were conducted by using deuteriosulfuric acid (ca. 80% D_2) in both carbon tetrachloride and dimethyl sulfoxide to approximately 50% completion. Under these conditions one would anticipate that, if proton loss from **5** was at all competitive with nucleophilic attack on the cation, deuterium incorporation in the unreacted silanorbornene would be observed. After derivatization of the reaction mixtures with tetra-*n*-butylammonium fluoride, they were analyzed by using GC/MS.[12] There was no deuterium incorporation in the re-

(9) In our system, because of numbering differences due to the silicon heteroatom these correspond to the cations designated as 2-substituted norbornyl cations in the original reports. Reference 7 and Farnum, D. G.; Mehta, G. *J. Am. Chem. Soc.* **1969**, *91*, 3256–3261.

(10) Corriu, R. J.; Dabosi, G.; Martineau, M. *J. Organomet. Chem.* **1978**, *150*, 27–38; **1980**, *186*, 25–37; *J. Chem. Soc., Chem. Commun.* **1977**, 649–650.

(11) McLean, S.; Reed, G. W. B. *Can. J. Chem.* **1970**, *48*, 3110–3111.

(12) Details of these analyses are given in the Ph.D. Dissertation of Richard A. Pierce, North Texas State University, December 1981.

Scheme I

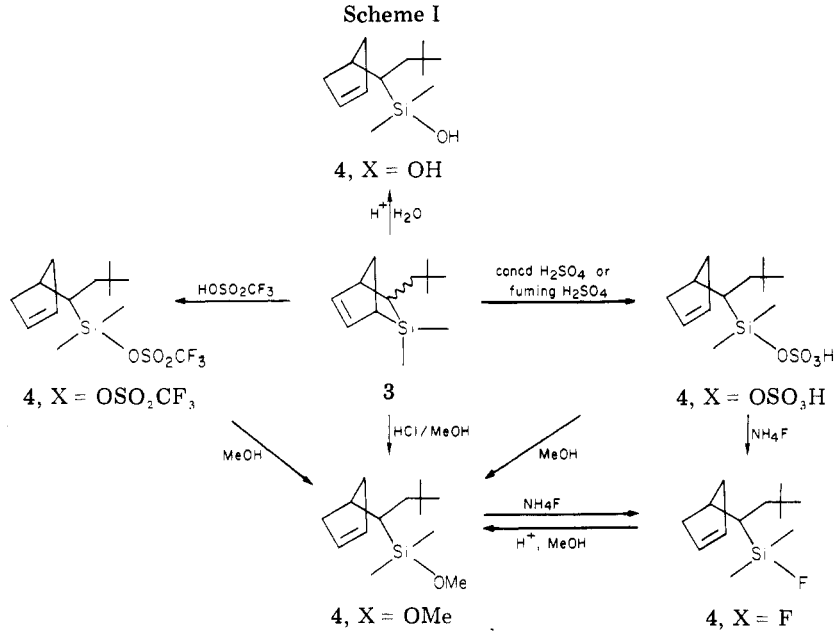

Table I. Proton NMR Data for the Compounds[a]

compd	$Si(CH_3)_2$[b]	$C(CH_3)_3$[b]	vinyl[c] protons	other protons
exo-3[d]	0.02, 0.17	0.95	5.85	0.46 (m, 1 H), 1.05-1.24 (m, 2 H), 1.60 (m, 2 H), 1.96 (m, 1 H), 2.60 (m, 1 H)
endo-3[d]	−0.03, 0.24	0.96	5.85	0.80-0.95 (m, 1 H), 1.18 (m, 2 H), 1.53 (m, 2 H), 2.05 (m, 1 H), 2.83 (m, 1 H)
4, X = OH	0.24	1.03	5.69	1.29-1.59 (m, 4 H), 2.19-2.79 (m, 5 H)
4, X = OMe	0.22	1.00	5.67	1.30-1.58 (m, 4 H), 2.15-2.70 (m, 4 H), 3.44 (s, 3 H)
4, X = F	0.37 (J = 7.2 Hz)	1.05	5.69	1.03-1.07 (m, 4 H), 2.26-2.56 (m, 4 H)
4, X = OSO_3H	0.63	1.11	5.71	1.24-1.70 (m, 4 H), 2.19-2.91 (m, 4 H)
4, X = OSO_2CF_3	0.77	1.16	5.75	1.34-1.75 (m, 4 H), 2.21-2.95 (m, 4 H)
4, X = OS^+Me_2[e]	0.12	0.91	5.59	1.0-2.4 (m)

[a] Chemical shifts in ppm downfield from Me_4Si, carbon tetrachloride solvent, chloroform internal standard. [b] Singlets with the exception of 4, X = F. [c] Broad singlets. [d] Reference 5. [e] Me_2SO as the solvent which obscured the 2.4-3.1 ppm region of the spectrum.

covered starting material. The derivatized cleavage product 4, X = F, showed deuterium incorporation, although it was not quantitative. The diminished intensity of the peaks in the δ 2.26–2.56 region of the ^1H NMR spectra of the products indicated that deuterium had been incorporated in the allylic position(s?) of the cyclopentene ring.

Thus, in contrast to the results of Fleming and Langley, who were able to obtain evidence for a cationic intermediate in the protodesilylation of allylsilanes,[2] we have found no evidence requiring a cationic intermediate, **5**, in the acid cleavage of 2-silanorbornenes. Our results are consistent with their conclusion that the loss of a silyl group is faster than loss of a proton from such an intermediate. Recently, Olah and co-workers reported the failure of attempts to observe β-silyl carbocations in stable ion media and observed cations resulting from the loss of the silyl group even at temperatures as low at −140 °C.[13] In addition, Lambert and Finzel have shown that in the rate enhancement produced by β-silyl substituents in the solvolysis of cyclohexyl trifluoroacetates, only a small factor of about 75 in acceleration can be ascribed to neighboring group participation by the silyl substituent.[14] It seems highly likely that if any significant cationic component were involved in the solvolysis reactions, cleavage of the silicon would be observed.

Experimental Section

Materials and Equipment. In all reactions where air-sensitive chemicals were used, the reagents and solvents were dried prior to use. Methanol was purified by vacuum distillation from barium oxide. Boron trifluoride etherate was vacuum distilled from calcium hydride.

For the reactions in which moisture sensitive materials were used, the glassware was flame or oven dried, and the experiments were carried out under an inert atmosphere.

The preparation of 2,2-dimethyl-3-neopentyl-2-silabicyclo-[2.2.1]hept-5-ene has been described previously.[3] Deuteriosulfuric acid, trifluoromethanesulfonic acid, ammonium fluoride, and deuterium oxide were obtained from Aldrich.

GLC preparative and analytical work was done as described previously.[3] ^1H NMR spectra were obtained on a Hitachi Perkin-Elmer R24B 60 MHz spectrometer using chloroform as the internal standard and carbon tetrachloride or dimethyl sulfoxide (Me_2SO) as the solvent. Mass spectra were obtained by using a Hitachi Perkin-Elmer RMU-6E mass spectrometer or a Finnegan 9500 automated gas chromatography/mass spectra system. Elemental analyses were performed by Galbraith Laboratories, Inc., Nashville, TN., or Midwest Microlab. Ltd., Indianapolis, IN.

General Procedure for the Preparation of the Ring Cleavage Products. All of the compounds shown in Scheme I were prepared either in ^1H NMR tubes or by normal synthetic methods. The synthetic methods vary in some ways; however,

(13) Olah, G. A.; Berrier, A. L.; Field, L. D.; Surya Prakash, G. K. *J. Am. Chem. Soc.* **1982**, *104*, 1349–1355.
(14) Lambert, J. B.; Finzel, R. B. *J. Am. Chem. Soc.* **1982**, *104*, 2020–2022.

all of the NMR experiments were conducted in the same manner. In each ^1H NMR experiment an acid was added to a substrate in a 5-mm tube. In some cases the acid was used as the solvent. In others, the acid was added dropwise by using a capillary tube as a pipette. In some cases, methanol was added dropwise after the acid had been added. The acids, the amount of acid added, the substrate, and the solvents were varied and have been reported above.

Preparation of 3-(3-Cyclopenten-1-yl)-2,5,5-trimethyl-2-silahex-2-yl Hydroxide (4, X = OH). 1. 3-(3-Cyclopenten-1-yl)-2,5,5-trimethyl-2-silahex-2-yl hydroxide (4, X = OH) was first found as a byproduct in the reaction of chlorodimethylvinylsilane with *tert*-butyllithium in the presence of cyclopentadiene.[3] Presumably the product was formed by the acid-promoted ring cleavage reaction of *exo*- and *endo*-2,2-dimethyl-3-neopentyl-2-silabicyclo[2.2,1]hept-5-ene.

2. A three-necked 25-mL flask was charged with 2.5 g (0.012 mol) of 3 and 10 mL of distilled water. The mixture was stirred vigorously and GLC of the organic layer after 2 h of stirring showed no reaction. Further stirring overnight produced no reaction. At this point the aqueous layer was separated from the organic layer, and the organic layer was mixed with 10 mL of 0.01 M sodium hydroxide solution. Stirring for 3 h produced no reaction.

3. A three-necked 25-mL flask was charged with 2.5 g (0.012 mol) of 3 and 10 mL of diluted HCl. The mixture was stirred vigorously for 2 h. The mixture was washed with three 20-mL portions of ether. The combined organic layers were dried and filtered, and the excess solvent was stripped off. GLC of the residue indicated a 95% yield of a water white liquid 4, X = OH; IR (neat, cm^{-1}) 3700–3100, 3050–2800, 1610, 1475, 1360, 1250, 830; MS, *m/e* (M^+) 226, (base) 73. The slow formation of the disiloxane prevented obtaining a satisfactory elemental analysis for this compound.

Preparation of 3-(3-Cyclopenten-1-yl)-2,5,5-trimethyl-2-silahex-2-yl Methoxide (4, X = OMe). 1. **From 3.** A 100-mL three-necked flask was fitted with a gas inlet and septum and flame dried while flushing with dry nitrogen. Then, 50 mL of freshly distilled methanol and 2.5 mL (0.01 mol) of 3 was added. Dry hydrogen chloride gas was then added until pH paper showed the solution to be acidic. The solution became brown and gave off heat. The solution was washed with hexane and the hexane evaporated, leaving a residue containing the product 4, X = OMe, in 72% yield: MS, *m/e* (M^+) 240. Anal. Calcd for $SiC_{14}H_{28}O$: C, 69.93; H, 11.74. Found: C, 70.08; H, 11.54.

4, X = OMe, was also prepared from 4, X = OSO_3H, OSO_2CF_3, or $OSMe_2^+$, when methanol was used as a quenching reagent in some of the ^1H NMR experiments.

2. **From 4, X = F.** In a dry 25-mL three-necked flask equipped with a reflux condensor/gas inlet and septum was placed 0.5 g (0.003 mol) of 4, X = F, and 10 mL of dry methanol. The mixture was stirred vigorously for 24 h but reaction was only 15% complete. A single drop of concentrated was added, and the reaction rapidly went to completion, giving 92% of 4, X = OMe.

Preparation of 3-(3-Cyclopenten-1-yl)-2,5,5-trimethyl-2-silahex-2-yl Fluoride (4, X = F). 1. Two 100-mL three-necked flasks were set up, fitted with gas inlets, and septa, and flame dried while flushing with dry nitrogen. Then 35 mL of freshly distilled hexane was added to each. Into one flask was added 1.5 mL of a mixture of 3 enriched in the exo isomer while 1.5 mL of a mixture of 3 enriched in the endo isomer was added to the other flask. Flask A contained 77% *exo*-3 and 23% endo-3 while flask B contained 19% exo-3 and 81% endo-3. At this point, a single drop of boron trifluoride etherate was added to each mixture. The GLC of each mixture was run periodically and showed approximately 40% conversion to 4, X = F, after 24 h. No exo–endo isomerization was observed in either mixture.

2. To a solution of 5 g (0.024 mol) of 3 in 25 mL of hexane was added dropwise 5 mL of concentrated sulfuric acid. Smoke and heat were given off, and the mixture turned black. Then, 5.0 g of ammonium fluoride was added followed by the addition of 5 mL of water. The mixture was stirred for 5 min, and the aqueous layer was then extracted with ether. The organic layer was dried over sodium sulfate and filtered, and the solvent stripped away, leaving a residue which contained 4, X = F, a colorless liquid, in 80% yield: MS, *m/e* (M^+) 228, (base) 171. Anal. Calcd for $SiC_{13}H_{25}F$: C, 68.42; H, 10.97. Found: C, 68.12; H, 11.15.

Cleavage Reactions with Deuteriosulfuric Acid. To NMR tubes containing 150 L of 3, 50 L of chloroform, and either 250 L of carbon tetrachloride or 250 L of dimethyl sulfoxide was added deuteriosulfuric acid, 80% D_2, until the ^1H NMR spectra of the mixtures indicated the ca. 50% of 3 had been converted to 4, X = OSO_3H. The mixtures were then treated with excess *tetra-n*-butylammonium fluoride,[15] and the entire mixture was subjected to GC/MS analysis. The mass spectral data was first obtained by scanning the full range of masses. In subsequent runs the detection range was limited to 200–250 mass units to enhance the sensitivity with which the M, M + 1 and M + 2 ions were observed. The intensities of these peaks for the P, P – Me, P – *t*-Bu, and cyclopentadienyldimethylsilyl ions for both isomers of recovered 3 showed no deuterium incorporation in the starting material. For the product, 4, X = F, the intensities of the M, M + 1, and M + 2 peaks for the P, P – Me, P – *t*-Bu, and P – neopentyl ions compared with calculated intensities for these peaks for undeuterated compounds showed 38 ± 2% deuterium incorporation in the product when carbon tetrachloride was used as the solvent and 10 ± 2% deuterium incorporation when dimethyl sulfoxide was used as the solvent.[12]

Acknowledgment. We thank the Robert A. Welch Foundation and the North Texas State University Organized Research Fund for their support of this work. Dr. Priscilla C. Jones is acknowledged for her assistance with the GC/MS studies.

Registry No. *exo*-3, 74107-87-2; *endo*-3, 74107-88-3; 4 (X = OH), 83562-35-0; 4 (X = OMe), 83562-36-1; 4 (X = OSO_3H), 83562-37-2; 4 (X = OSO_2CF_3), 83562-38-3; 4 (X = $OSMe_2^+$), 83562-39-4; 4 (X = F), 83562-40-7; NH_4F, 12125-01-8; boron trifluoride etherate, 109-63-7.

(15) Nakamura, E.; Murofushi, T.; Shimigu, M.; Kuwajima, I. *J. Am. Chem. Soc.* **1976**, *98*, 2346–2348.

Dialkyl Bis[bis(trimethylsilyl)amido] Group 4A Metal Complexes. Preparation of Bridging Carbene Complexes by γ Elimination of Alkane. Crystal Structure of $\{\overline{ZrCHSi(Me)_2NSiMe_3[N(SiMe_3)_2]}\}_2$

Roy P. Planalp, Richard A. Andersen,* and Allan Zalkin

Chemistry Department and Materials and Molecular Research Division of Lawrence Berkeley Laboratory, University of California, Berkeley, California 94720

Received July 30, 1982

The dialkyls of zirconium of the type $R_2Zr[N(SiMe_3)_2]_2$, where R is Me, Et, or CH_2SiMe_3, thermally decompose (60 °C (10^{-2} mm)) by elimination of alkane (MeH, EtH, or Me_4Si, respectively) to give the bridging carbene compound $\{\overline{ZrCHSi(Me_2)NSiMe_3[N(SiMe_3)_2]}\}_2$. The 1:1 complex with pyridine is described. The related hafnium dialkyls decompose in a related manner though in this case the decomposition product could only be characterized as its pyridine complex, $\{\overline{HfCHSi(Me)_2NSiMe_3[N(SiMe_3)_2]}NC_5H_5\}_2$. The NMR spectra of the pyridine complexes of zirconium and hafnium are similar. In contrast, $Me_2Ti[N(SiMe_3)_2]_2$ is thermally stable to 190 °C. The titanium-carbene $\{\overline{TiCHSi(Me)_2NSiMe_3[N(SiMe_3)_2]}\}_2$ may be prepared by sodium amalgam reduction of $Cl_2Ti[N(SiMe_3)_2]_2$. The crystal structure of $\{\overline{ZrCHSi(Me)_2NSiMe_3[N(SiMe_3)]}\}_2$ was determined by single-crystal X-ray crystallography. The crystals are orthorhombic of space group *Pbca* with cell dimensions a = 18.307 (7) Å, b = 26.036 (6) Å, and c = 19.425 (6) Å; for Z = 8, d_{calcd} = 1.18 g cm^{-3}. The structure was refined to a conventional R factor of 0.061 by using 3149 data where $F^2 > 3\sigma(F^2)$. The structure consists of three, fused planar, four-membered rings giving the molecule a "tub" conformation. The Zr-C distances are 2.16 and 2.21 Å, and the Zr-N distances range from 2.04 to 2.09 Å.

The hafnium dialkyls $R_2Hf[N(SiMe_3)_2]_2$, where R = Me, Et, or Me_3SiCH_2, have been described recently.[1] Isolation of the methyl or (trimethylsilyl)methyl derivatives is not surprising. However, isolation of the thermally stable diethyl derivative (the complex melts without decomposition at 68 °C) is rather surprising since diethyl derivatives of transition metals are rather rare due to facile β elimination of ethylene and ethane.[2] We suggested that the thermal stability was due to steric congestion about the metal atom due to the sterically large $(Me_3Si)_2N$ groups preventing the β hydrogens atoms of the ethyl groups from getting close enough to the metal center to react. Thus, $Et_2Hf[N(SiMe_3)_2]_2$ is kinetically stable as a result of steric effects. In a related class of thermally stable amido alkyls, $Et_2Mo_2(NMe_2)_4$, molybdenum to nitrogen π bonding, pπ $\rightarrow$ dπ, was suggested as the reason for the stability.[3] Though metal to nitrogen π bonding may play a role in the stability of silylamido alkyls, we think it is a minor one since we have shown that this type of bonding is insignificant in M-N$(SiMe_3)_2$ complexes.[4a] Others, however, have shown that π bonding is very important in M-NR_2 complexes where R is an alkyl group.[4b] In order to gain insight into the reasons for the thermal stability of $Et_2Hf[N(SiMe_3)_2]_2$ and related dialkyls, we began a study of the thermal decomposition reactions of $R_2M[N(SiMe_3)_2]_2$ where R is Me, Et, or Me_3SiCH_2 when M is Zr or Hf and R is Me when M is Ti.

Synthetic Studies. The three hafnium compounds and $Me_2Zr[N(SiMe_3)_2]_2$ have been described.[1] The diethyl and bis(trimethylsilyl)methyl derivatives of zirconium were prepared in a similar fashion. It is of interest to note that $Et_2Hf[N(SiMe_3)_2]_2$ is rather more thermally stable than its zirconium analogue; the former melts without decomposition at 68 °C, while the latter melts with decomposition at 25 °C. This relative thermal stability trend is also observed for the Me_3SiCH_2 derivatives; $(Me_3SiCH_2)_2Hf[N(SiMe_3)_2]_2$ melts without decomposition at 91-92 °C, whereas the zirconium analogue melts with decomposition at 53-55 °C.

We wished to prepare the corresponding titanium derivatives so that the properties of all the group 4A derivatives could be compared. Though $Cl_3TiN(SiMe_3)_2$[5] and $ClTi[N(SiMe_3)_2]_3$[6] are known, $Cl_2Ti[N(SiMe_3)_2]_2$ is unknown. The latter compound was isolated as a dark red liquid that solidified to a red, waxy material after distillation (138 °C at 10^{-2} mm). The $Me_2Ti[N(SiMe_3)_2]_2$ was isolated as a pale yellow solid from reaction of $Cl_2Ti[N(SiMe_3)_2]_2$ and the methyl Grignard reagent. It is noteworthy that $Me_2Ti[N(SiMe_3)_2]_2$ is a solid at room temperature (20 °C) with a melting point of 46-48 °C, whereas the zirconium and hafnium complexes are liquids at that temperature. We have been unable to prepare, in pure form, $Et_2Ti[N(SiMe_3)_2]_2$ or $(Me_3SiCH_2)_2Ti[N(SiMe_3)_2]_2$.

All three zirconium alkyls decompose at comparable rates at ca. 60 °C under reduced pressure (10^{-2} mm) to give

(1) Andersen, R. A. *Inorg. Chem.* **1979**, *18* 2928-2932; *J. Organomet. Chem.* **1980**, *192*, 189-193.

(2) (a) Tamura, M.; Kochi, J. K. *J. Organomet. Chem.* **1971**, *29*, 111-129; *Bull. Chem. Soc. Jpn.* **1971**, *44*, 3063-3073. (b) Lau, W.; Huffman, J. C.; Kochi, J. K. *Organometallics* **1982**, *1*, 155-169. (c) Ikariya, T.; Yamamoto, A. *J. Organomet. Chem.* **1976**, *120*, 257-284; **1976**; *116*, 239-250. (d) Yamamoto, T.; Yamamoto, A.; Ikeda, S. *J. Am. Chem. Soc.* **1971**, *93*, 3350-3359. (e) Ozawa, F.; Ito, T.; Yamamoto, A. *Ibid.* **1980**, *102*, 6457-6463. (f) Ozawa, F.; Ito, T.; Nakamura, Y.; Yamamoto, A. *Bull. Chem. Soc. Jpn.* **1981**, *54*, 1868-1880. (g) Miyashita, A.; Yamamoto, T.; Yamamoto, A. *Ibid.* **1977**, *50*, 1109-1117. (h) Komiya, S.; Yamamoto, A.; Yamamoto, T. *Chem. Lett.* **1978**, 1273-1276. (i) McCarthy, T. J.; Nuzzo, R. G.; Whitesides, G. M. *J. Am. Chem. Soc.* **1981**, *103*, 3396-3403. (j) McDermott, J. X.; Wilson, M. E.; Whitesides, G. M. *Ibid.* **1976**, *98*, 6529-6536. (k) Kochi, J. K. "Organometallic Mechanisms and Catalysis" Academic Press: New York, 1978.

(3) Chisholm, M. H.; Haitko, D. A.; Folting, K.; Huffman, J. C. *J. Am. Chem. Soc.* **1981**, *103*, 4046-4053.

(4) (a) Green, J. C.; Payne, M.; Seddon, E. A.; Andersen, R. A. *J. Chem. Soc., Dalton Trans.*, **1982**, 887-892. (b) Chisholm, M. H.; Cowley, A. H.; Lattman, M. *J. Am. Chem. Soc.* **1980**, *102*, 46-50.

(5) (a) Bürger, H.; Wannagat, U. *Monatsh. Chem.* **1963**, *94*, 761-771. (b) Alcock, N. W.; Pierce-Butler, M.; Wiley, G. R. *J. Chem. Soc., Dalton Trans.* **1976**, 707-713.

(6) (a) Airoldi, C.; Bradley, D. C. *Inorg. Nucl. Chem. Lett.* **1975**, *11*, 155. (b) Airoldi, C.; Bradley, D. C.; Chudzynska, H.; Hursthouse, M. B.; Malik, K. M. A.; Raithby, P. R. *J. Chem. Soc., Dalton Trans.* **1980**, 2010-2015.

0276-7333/83/2302-0016$01.50/0

alkane and a yellow material whose empirical composition is derived from $R_2Zr[N(SiMe_3)_2]_2$ less 2 molar equiv of alkane, viz., I. The ^1H NMR spectrum of I, isolated in

$$R_2Zr[N(SiMe_3)_2]_2 \triangleq 2RH + Zr[N(SiMe_3)(SiMe_2CH)]_2$$
$$\text{I}$$

R = Me, Et, Me_3SiCH_2

quantitative yield after crystallization from pentane, consists of singlets at δ 7.08, 1.14, 0.44, 0.40, and 0.28 in area ratio of 1:3:9:18:3. The four upfield resonances are most reasonably ascribed to methyl groups on silicon, and the downfield singlet of area one suggests that a methine group is present.[7] This inference is supported by the ^{13}C NMR spectrum which yields a downfield doublet centered at δ 201.4 (J_{CH} = 122 Hz). The other resonances in the ^{13}C NMR spectrum are quartets clustered between δ 5 and δ 10 and are due to methyl groups bound to silicon (see Experimental Section for details). A structural unit that is consistent with these data is $\overline{Zr(CHSi(Me)_2NSiMe_3)N(SiMe_3)_2}$, in which the methyl groups on the Me_2Si group are diastereotropic. In addition, the mass spectrum shows that I is dimeric. Two structural formulas that are consistent with all of the spectroscopic data are II and III, where M is zirconium. These data, however do not allow us to make a distinction between the two valence isomers, but a crystal structure (see below) shows that III is the correct structural isomer.

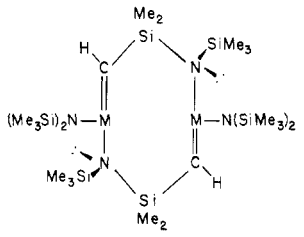

II

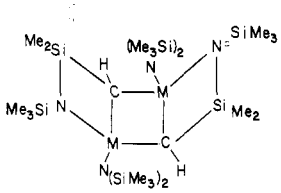

III

Thus, thermal decomposition of all three zirconium alkyls gives the same compound, III, derived by a *formal* elimination of alkane, the hydrogen atoms of the alkane coming from the methyl group of a $(Me_3Si)_2N$ ligand. It is important to note that we are describing the events in a phenomenological way; we intend to address the mechanistic question later. A single hydrogen γ elimination from a coordinated $(Me_3Si)_2N$ group[8] or a β elimination from a Me_2N or Et_2N group[9] is a well-known thermal decomposition pathway. Elimination of both hydrogen atoms from the same methyl group is without precedent in metal amide chemistry, though some examples of this are known in alkyl chemistry.[10]

The dimeric unit in III cannot be cleaved by pyridine, since a 1:2 coordination complex is isolated (see Experimental Section for details).

The three hafnium alkyls may be thermally decomposed at ca. 70 °C under reduced pressure (10^{-2} mm), eliminating alkane and forming a yellow substance. We have not been able to crystallize this material though we have been able to isolate a pyridine complex. The similarity of the ^1H and ^{13}C NMR spectrum of the pyridine complex of hafnium to that of the zirconium pyridine complex suggests that they are isostructural (see Experimental Section for details). Thus, the zirconium and hafnium dialkyls decompose at similar rates to give the dimeric, bridging, carbene-like metallacycles III, where M is zirconium or hafnium.

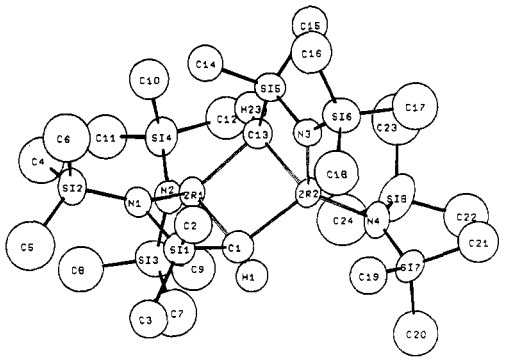

Figure 1. An ORTEP diagram of $\{\overline{ZrCHSi(Me)_2NSiMe_3}[N(SiMe_3)_2]\}_2$ showing the atom numbering scheme.

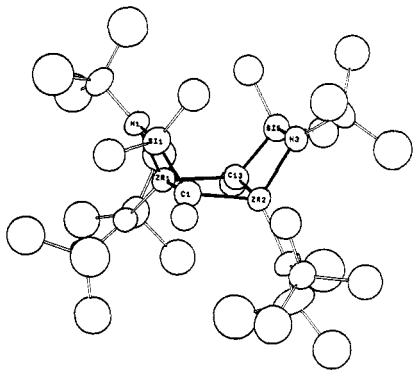

Figure 2. An ORTEP diagram showing a side-on view.

In contrast, the titanium alkyl $Me_2Ti[N(SiMe_3)_2]_2$ is thermally stable. This dialkyl may be recovered unchanged after heating at 190 °C for prolonged periods of time. This observation may be rationalized by noting that tetravalent titanium (IV) is smaller than either zirconium or hafnium. As a consequence, the steric congestion about the titanium atom in $Me_2Ti[N(SiMe_3)_2]_2$ is greater than that around the two heavier group 4A metal complexes, and a hydrogen atom of the $(Me_3Si)_2N$ group cannot get close enough to the titanium atom to become "activated". This explanation is a kinetic one, and it implies that a titanium metallacycle, III (M = Ti), should exist if a suitable preparative route could be found. Sodium amalgam reduction of $TiCl_2[N(SiMe_3)_2]_2$ yields orange-red III (M = Ti). The similarity of the NMR spectral properties of the titanium complex to those of its zirconium or hafnium congeners (see Experimental Section) shows that they are isostructural. The titanium complex does not react with pyridine, a result consistent with steric effects.

The inability to get $Me_2Ti[N(SiMe_3)_2]_2$ to thermally decompose whereas the related zirconium and hafnium dimethyls readily decompose to III has some mechanistic significance. Titanium–carbon bond strengths are less than the corresponding zirconium- or hafnium–carbon bond strengths.[11] This suggests that radical processes are not involved.

(7) (a) Andersen, R. A. *Inorg. Chem.* **1979**, *18*, 3622–3623. (b) Tebbe, F. N.; Parshall, G. W.; Reddy, G. S. *J. Am. Chem. Soc.* **1978**, *100*, 3611–3613. (c) Schrock, R. R.; Sharp, P. R. *Ibid.* **1978**, *100*, 2389–2399. (d) Schwartz, J.; Gell, K. I. *J. Organomet. Chem.* **1980**, *184*, C1–C2. (e) Gell, K. I.; Schwartz, J. *Inorg. Chem.* **1980**, *19*, 3207–3211.

(8) (a) Bennett, C. R.; Bradley, D. C. *J. Chem. Soc., Chem. Commun.* **1974**, 29–30. (b) Simpson, S. J.; Andersen, R. A. *Inorg. Chem.* **1981**, *20*, 3627–3629. (c) Simpson, S. J.; Turner, H. W.; Andersen, R. A. *Ibid.* **1981**, *20*, 2991–2995.

(9) (a) Bürger, H.; Neese, H. J. *J. Organomet. Chem.* **1970**, *21*, 381–388. (b) Takahashi, Y.; Onoyama, N.; Ishikawa, Y.; Motojima, S.; Sugiyama, K. *Chem. Lett.* **1978**, 525–528.

(10) (a) Fellmann, J. D.; Turner, H. W.; Schrock, R. R. *J. Am. Chem. Soc.* **1980**, *102*, 6608–6609. (b) Sharp, P. R.; Holmes, S. J.; Schrock, R. R.; Churchill, M. R.; Wasserman, H. J. *Ibid.* **1981**, *103*, 965–966. (c) Wengrovis, J. H.; Sancho, J.; Schrock, R. R. *Ibid.* **1981**, *103*, 3932–3934.

(11) (a) Lappert, M. F.; Patil, D. S.; Pedley, J. B. *J. Chem. Soc., Chem. Commun.* **1975**, 830–831. (b) Connor, J. A. *Top. Curr. Chem.* **1977**, *71*, 71–110.

Table I. Positional Parameters[a]

atom	x	y	z
Zr (1)	0.12720 (6)	0.06047 (4)	0.21461 (5)
Zr (2)	0.15127 (6)	0.17194 (4)	0.14944 (6)
Si(1)	0.1641 (2)	0.12331 (14)	0.3251 (2)
Si(2)	0.0540 (2)	0.0400 (2)	0.3786 (2)
Si(3)	0.2325 (2)	−0.0406 (2)	0.1943 (2)
Si(4)	0.0827 (2)	−0.04306 (13)	0.1282 (2)
Si(5)	0.0003 (2)	0.16088 (13)	0.1522 (2)
Si(6)	0.0301 (2)	0.2768 (2)	0.1740 (2)
Si(7)	0.2815 (2)	0.23425 (14)	0.0872 (2)
Si(8)	0.2216 (3)	0.1514 (2)	−0.0089 (2)
N(1)	0.1003 (5)	0.0719 (3)	0.3155 (5)
N(2)	0.1501 (5)	−0.0126 (3)	0.1759 (5)
N(3)	0.0574 (5)	0.2140 (3)	0.1684 (4)
N(4)	0.2226 (6)	0.1859 (3)	0.0679 (4)
C(1)	0.1974 (8)	0.1256 (5)	0.2344 (7)
C(2)	0.1153 (9)	0.1832 (5)	0.3558 (8)
C(3)	0.2400 (8)	0.1077 (6)	0.3870 (6)
C(4)	0.029 (2)	−0.023 (1)	0.348 (1)
C(5)	0.107 (2)	0.032 (1)	0.461 (2)
C(6)	−0.029 (2)	0.074 (1)	0.400 (2)
C(7)	0.292 (1)	0.0079 (7)	0.241 (1)
C(8)	0.223 (1)	−0.0953 (7)	0.257 (1)
C(9)	0.279 (1)	−0.0631 (7)	0.1147 (9)
C(10)	−0.0084 (9)	−0.0157 (6)	0.1524 (8)
C(11)	0.080 (1)	−0.1160 (7)	0.1388 (9)
C(12)	0.0952 (9)	−0.0325 (6)	0.0298 (9)
C(13)	0.0724 (7)	0.1106 (5)	0.1386 (6)
C(14)	−0.0626 (7)	0.1451 (6)	0.2271 (7)
C(15)	−0.0563 (8)	0.1706 (5)	0.0725 (7)
C(16)	−0.0708 (9)	0.2829 (6)	0.2011 (8)
C(17)	0.048 (1)	0.3116 (7)	0.091 (1)
C(18)	0.083 (1)	0.3127 (7)	0.2452 (9)
C(19)	0.2586 (8)	0.2555 (6)	0.1779 (8)
C(20)	0.379 (1)	0.2154 (7)	0.087 (1)
C(21)	0.2683 (9)	0.2921 (6)	0.0303 (8)
C(22)	0.275 (1)	0.182 (1)	−0.078 (1)
C(23)	0.124 (1)	0.1496 (9)	−0.046 (1)
C(24)	0.247 (1)	0.0816 (9)	0.011 (1)
H(1)	0.237 (5)	0.128 (4)	0.234 (5)
H(23)	0.048 (7)	0.085 (5)	0.104 (6)

[a] Here and in the following tables the number in parentheses is the estimated deviation in the least significant digit.

Table II. Selected Interatomic Distances (Å)

Zr(1)-N(1)	2.04 (1)	Zr(2)-N(3)	2.07 (1)
-N(2)	2.09 (1)	-N(4)	2.08 (1)
-C(1)	2.16 (2)	-C(13)	2.16 (2)
-C(13)	2.21 (2)	-C(1)	2.21 (2)
N(1)-Si(1)	1.79 (1)	N(3)-Si(5)	1.76 (1)
-Si(2)	1.70 (1)	-Si(6)	1.71 (1)
N(2)-Si(3)	1.71 (1)	N(4)-Si(7)	1.70 (1)
-Si(4)	1.74 (1)	-Si(8)	1.74 (1)
Si(1)-C(1)	1.87 (2)	Si(5)-C(13)	1.88 (2)
-C(2)	1.89 (2)	-C(14)	1.90 (2)
-C(3)	1.88 (2)	-C(15)	1.88 (1)
Si(2)-C(4)	1.80 (3)	Si(6)-C(16)	1.93 (2)
-C(5)	1.89 (4)	-C(17)	1.87 (2)
-C(6)	1.80 (4)	-C(18)	1.93 (2)
Si(3)-C(7)	1.90 (2)	Si(7)-C(19)	1.89 (2)
-C(8)	1.89 (2)	-C(20)	1.85 (2)
-C(9)	1.86 (2)	-C(21)	1.88 (2)
Si(4)-C(10)	1.87 (2)	Si(8)-C(22)	1.85 (3)
-C(11)	1.91 (2)	-C(23)	1.92 (3)
-C(12)	1.95 (2)	-C(24)	1.92 (3)

Structural Studies of III (M = Zr). An ORTEP diagram showing the atom numbering scheme is shown in Figure 1. Figure 2 shows a "side-on" view that illustrates the overall stereochemistry. Table I lists the positional parameters, and Tables II and III list some important bond angles and bond distances.

The molecular structure consists of two planar four-membered ZrCSiN rings fused to the central planar, four-membered Zr_2C_2 ring along the Zr–C edges. The deviations of the atoms in each of the three planes is shown in Table IV. The angles formed by the intersection of the Zr(1)N(1)Si(1)C(1) and Zr(2)N(3)Si(5)C(13) planes with the Zr(1)C(1)Zr(2)C(13) plane are 124° and 111°, respectively. The overall conformation of the eight-membered ring is that of a "tub" reminiscent of that found for cyclooctatetraene in the gas phase.[12]

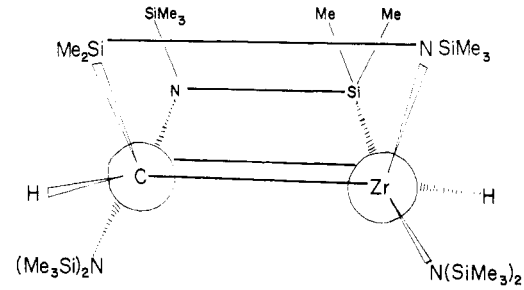

Figure 3. A line drawing showing the diastereotopic Me_2Si groups.

A line drawing of III (M = Zr) looking toward the Zr_2C_2 ring is shown in Figure 3. As can be seen no symmetry plane bisects the Me_2Si groups and the methyl groups are diastereotopic as described earlier. This conformation is consistent with the solution ^1H NMR spectrum which is invarient from −90 to +60 °C. The molecule is either stereochemically rigid or highly fluxional on the NMR time scale in this temperature range.

The averaged terminal Zr–N[N(2,4)] bond length of 2.09 ± 0.01 Å lies at the low end of zirconium–amido nitrogen bond lengths which range from 2.05 to 2.20 Å.[6b,13] The averaged Zr–N[N(1,3)] bond length of 2.06 ± 0.02 Å, which is part of the metallacyclic ring, is also within this range. Given the uncertainty in the individual bond lengths (Table II) this difference is probably not chemically significant.

The zirconium–carbon bond lengths in the Zr_2C_2 unit are unsymmetrical. The two Zr–C bonds that are part of the ZrCSiN framework, Zr(1)–C(1) and Zr(2)–C(13), are 2.16 (2) Å, and they are not significantly (3σ) shorter than the two Zr–C bonds that are not part of the metallacyclic framework. The latter two distances, Zn(1)–C(13) and Zr(2)–C(1), are both 2.21 (2) Å. These bond lengths are shorter than Zr–C(sp^3) bond lengths in compounds of the type Cp_2ZrR_2 which vary from 2.25 to 2.37 Å.[14] The zirconium–carbon bond lengths in III (M = Zr) are close to those found for Zr–C(sp^2) of 2.20 Å.[15] It is well-known that the coordination number of a metal atom plays a

(12) Traetteberg, M. *Acta Chem. Scand.* **1966**, *20*, 1724–1726.
(13) (a) Nugent, W. A.; Harlow, R. L. *Inorg. Chem.* **1979**, *18*, 2030–2032. (b) Bynum, R. V.; Hunter, W. E.; Rogers, R. D.; Atwood, J. L. *Ibid.* **1980**, *19*, 2368–2374. (c) Brauer, D. J.; Bürger, H.; Essig, E.; Geschwandtner, W. *J. Organomet. Chem.* **1980**, *190*, 343–351.
(14) Atwood, J. L.; Hunter, W. E.; Hrncir, D. C.; Samuel, E.; Alt, H.; Rausch, M. D. *Inorg. Chem.* **1975**, *14*, 1757–1763. (b) Lappert, M. F.; Riley, P. I.; Yarrow, P. I. W.; Atwood, J. L.; Hunter, W. E.; Zaworotko, M. J. *J. Chem. Soc., Dalton Trans.* **1981**, 814–821. (c) Jeffrey, J.; Lappert, M. F.; Luong-Thi, N. T.; Webb, M.; Atwood, J. L.; Hunter, W. E. *Ibid.* **1981**, 1593–1605. (d) Jeffrey, J.; Lappert, M. F.; Luong-Thi, N. T.; Atwood, J. L.; Hunter, W. E. *J. Chem. Soc., Chem. Commun.* **1978**, 1081–1083. (e) Atwood, J. L.; Barker, G. K.; Holton, J.; Hunter, W. E.; Lappert, M. F.; Pearce, R. *J. Am. Chem. Soc.* **1977**, *99*, 6645–6652. (f) Lappert, M. F.; Martin, T. R.; Atwood, J. L; Hunter, W. E. *J. Chem. Soc., Chem. Commun.* **1980**, 476–477. (g) Schmidt, R.; Duggan, D. M. *Inorg. Chem.* **1981**, *20*, 318–323. (h) Erker, G. Wicher, J.; Engel, K.; Rosenfeldt, F.; Dietrich, W.; Krüger, C. *J. Am. Chem. Soc.* **1980**, *102*, 6344–6346. (i) Davies, G. R.; Jarvis, J. A. J.; Kilbourn, B. T.; Pioli, A. J. P. *J. Chem. Soc., Chem. Commun.* **1971**, 677.
(15) (a) Atwood, J. L.; Hunter, W. E.; Alt, H.; Rausch, M. D. *J. Am. Chem. Soc.* **1976**, *98*, 2454–2459. (b) Fachinetti, Floriani, C.; Marchetti, F.; Merlino, S. *J. Chem. Soc., Chem. Commun.* **1976**, 522–523.

Table III. Selected Angles (deg)

N(1)-Zr(1)-N(2)	121.7 (4)	N(3)-Zr(2)-N(4)	124.3 (4)
N(1)-Zr(1)-C(1)	81.9 (5)	N(3)-Zr(2)-C(13)	81.6 (4)
N(1)-Zr(1)-C(13)	116.5 (4)	N(3)-Zr(2)-C(1)	118.2 (5)
N(2)-Zr(1)-C(1)	131.2 (5)	N(4)-Zr(2)-C(13)	118.2 (4)
N(2)-Zr(1)-C(13)	112.8 (4)	N(4)-Zr(2)-C(1)	115.0 (5)
C(1)-Zr(1)-C(13)	85.8 (5)	C(1)-Zr(2)-C(13)	85.7 (5)
N(1)-Si(1)-C(1)	98.1 (6)	N(3)-Si(5)-C(13)	99.0 (6)
N(1)-Si(1)-C(2)	110.0 (6)	N(3)-Si(5)-C(14)	113.2 (6)
N(1)-Si(1)-C(3)	112.8 (6)	N(3)-Si(5)-C(15)	111.6 (6)
C(1)-Si(1)-C(2)	115.2 (7)	C(13)-Si(5)-C(14)	112.5 (6)
C(1)-Si(1)-C(3)	111.6 (7)	C(13)-Si(5)-C(15)	111.4 (6)
C(2)-Si(1)-C(3)	108.9 (7)	C(14)-Si(5)-C(15)	109.0 (7)
Zr(1)-N(1)-Si(1)	92.9 (4)	Zr(2)-N(3)-Si(5)	92.6 (4)
Zr(1)-N(1)-Si(2)	127.6 (6)	Zr(2)-N(3)-Si(6)	139.3 (6)
Si(1)-N(1)-Si(2)	128.0 (6)	Si(5)-N(3)-Si(6)	126.0 (6)
Zr(1)-C(1)-Zr(2)	93.9 (6)	Zr(1)-C(13)-Zr(2)	93.9 (5)
Zr(1)-C(1)-Si(1)	87.0 (6)	Zr(2)-C(13)-Si(5)	86.6 (5)
Zr(2)-C(1)-Si(1)	126.7 (8)	Zr(1)-C(13)-Si(5)	129.5 (6)

Table IV. Deviations (Å) of Atoms from Selected Least Squares Planes

plane		
Zr(1),C(1), C(13),Zr(2)	Zr(1),C(1), N(1),Si(1)	Zr(2),C(13), N(3),Si(5)
Zr(1) −0.06	Zr(1) −0.02	Zr(2) −0.03
C(1) 0.06	C(1) 0.02	C(13) 0.03
Zr(2) −0.06	Si(1) −0.02	Si(5) −0.04
C(13) 0.06	N(1) 0.02	N(3) 0.03

significant role in determining bond lengths. In the Cp_2ZrR_2 compounds the coordination number of zirconium is eight, defining the coordination number of a Cp group as three,[16] whereas the coordination number of the zirconium atom in III (M = Zr) is only four. Since the ionic or covalent radius of Zr(IV) in eight coordination is estimated to be 0.78 or 0.92 Å, respectively, and 0.59 or 0.73 Å, respectively, in four coordination, the zirconium–carbon bond lengths in III (M = Zr) should be ca. 0.2 Å shorter than in the cyclopentadienyl derivatives.[17] Thus, adjusting the Zr–C bond lengths in the metallacycle for the coordination number change puts them within the region for Zr–C(sp^3) bond lengths.

It is probably best to view the bridging methine (carbene) group in III as a sp^3-hybridized carbon atom. This view is consistent with the C–H coupling constant and chemical shifts and with the bond length data which imply that the carbon atoms carry a negative charge, as found in $Cp_2ZrCl(CHPPh_3)$.[18]

Experimental Section

All operations were performed under argon. Elemental analyses were done by the microanalytical laboratory of this department. The ^1H and ^{13}C nuclear magnetic resonance spectra were recorded on a JEOL FX90Q instrument operating at 89.56 and 22.50 MHz, respectively, in benzene-d_6 solutions at 26 °C.

$TiCl_2[N(SiMe_3)_2]_2$. Titanium tetrachloride (6.5 g, 0.034 mol) in pentane (50 mL) at −30 °C was added to a solution of lithium bis(trimethylsilyl)amide (11.4 g, 0.0683 mol) in pentane (150 mL) also at −30 °C. The mixture was warmed to 0 °C, stirred at that temperature for 40 min, and then warmed to room temperature. The solution was filtered, and the residue was extracted with pentane (50 mL). The red extracts were combined, and the pentane was removed under reduced pressure, giving a red, viscous liquid. The oil was fractionated, and the fraction that distilled at 136–140 °C (10^{-3} mm) was collected. The distillate solidified as a dark red, waxy solid in 61% yield (9.1 g): mp 60–62 °C; IR ν(M–N) 438, ν(M–Cl) 350 cm^{-1}; ^1H NMR δ 0.53 (s); ^{13}C NMR δ 5.10 (q, J = 119 Hz). Anal. Calcd for $C_{12}H_{36}Cl_2N_2Si_4Ti$: C, 32.8; H, 8.20; Cl, 16.2; N, 6.38. Found: C, 30.6; H, 8.10; Cl, 14.7; N, 5.91.

$TiMe_2[N(SiMe_3)_2]_2$. Methylmagnesium chloride (5.7 mL of a 0.62 M solution in diethyl ether, 0.0035 mol) was added to dichlorobis[bis(trimethylsilyl)amido]titanium (0.70 g, 0.0032 mol) in pentane (50 mL) at −35 °C. The mixture was stirred at that temperature for 50 min and then allowed to warm to 0 °C. The volatile material was removed under reduced pressure at 0 °C. The dark solid was extracted with pentane (20 mL) and filtered, and the filtrate was concentrated to ca. 4 mL and cooled (−70 °C). The yellow prisms (0.97 g, 77% yield) were collected and dried under reduced pressure: mp 46–48 °C; ^1H NMR δ 1.63 (s, 6 H), 0.47 (s, 36 H); ^{13}C NMR δ 66.1 (q, J = 114 Hz), 5.41 (q, J = 121 Hz), due to Me and Me_3Si, respectively. Anal. Calcd for $C_{14}H_{42}N_2Si_4Ti$: C, 42.2; H, 10.5; N, 7.03. Found: C, 42.0; H, 10.5; N, 6.63.

$ZrEt_2[N(SiMe_3)_2]_2$. Diethylmagnesium (2.2 mL of a 1.0 M solution in diethyl ether, 0.0022 mol) was added to dichlorobis[bis(trimethylsilyl)amido]zirconium (1.0 g, 0.0021 mol) in pentane (20 mL) at −30 °C. The suspension was stirred at that temperature for 40 min, and then the volatile material was evaporated. The solid was extracted at −30 °C with cold (−30 °C) pentane (20 mL), filtered (−30 °C), concentrated to ca. 3 mL (−30 °C), and then cooled (−70 °C). The white prisms (0.41 g, 40% yield) were collected and dried under reduced pressure. The crystals were stored at 5 °C since they decompose at ca. 25 °C, and reliable elemental analyses could not be obtained: ^1H NMR (PhMe-d_8, −50 °C) δ 1.64 (t, J = 7 Hz, 6 H), 1.12 (q, J = 8 Hz, 4 H), 0.43 (s, 36 H); ^{13}C NMR (PhMe-d_8, −40 °C) δ 63.5 (s), 13.9 (s), 3.80 (s), due to CH_2, CH_3, and Me_3Si, respectively.

$Zr(CH_2SiMe_3)_2[N(SiMe_3)_2]_2$. Bis[(trimethylsilyl)methyl]magnesium (2.6 mL of a 1.3 M diethyl ether solution, 0.0034 mol) was added to dichlorobis[bis(trimethylsilyl)amido]zirconium (1.5 g, 0.0035 mol) in pentane (60 mL) at −30 °C. The mixture was slowly allowed to warm to 0 °C (3 h) with stirring. The volatile material was removed under reduced pressure (0 °C), and the solid was extracted with cold (0 °C) pentane (50 mL). The extract was filtered (0 °C), and the filtrate was concentrated to ca. 6 mL (0 °C) and cooled (−70 °C). The white prisms (1.7 g, 83% yield) were collected and dried under reduced pressure: mp 53–55 °C dec; ^1H NMR δ 1.04 (s, 4 H), 0.34 (s, 36 H), 0.27 (s, 18 H); $^{13}C\{^1H\}$ NMR δ 69.4 (s), 5.70 (s), 3.30 (s), due to CH_2, $SiMe_3$, and $(Me_3Si)_2N$, respectively. The compound did not give satisfactory elemental analyses, possibly due to thermal decomposition.

$\{\overline{TiCHSi(Me)_2NSiMe_3}[N(SiMe_3)_2]\}_2$. Sodium amalgam (0.78 mL of a 1% amalgam, 0.0046 mol) was added to dichlorobis[bis(trimethylsilyl)amido]titanium (1.0 g, 0.0023 mol) in toluene (30 mL) under argon. The red solution turned green then back to red over 5 h. After being stirred for 72 h, the red solution was filtered, and the filtrate was evaporated to dryness, giving a red oil. The oil was extracted with pentane (50 mL), filtered, concentrated to ca. 5 mL, and cooled (−70 °C). The red material that

(16) Raymond, K. N.; Eigenbrot, C. E. *Acc. Chem. Res.* **1980**, *13*, 276–283.
(17) Shannon, R. D. *Acta Crystallogr.* **1976**, *32A*, 751–767.
(18) Baldwin, J. C.; Keder; Strouse, C. E.; Kaska, W. C. *Z. Naturforsch., B: Anorg. Chem., Org. Chem.* **1980**, *35B*, 1289–1297.

crystallized was recrystallized twice from pentane (−70 °C), giving 0.44 g (58%) of bright orange-red prisms: mp 168–169 °C; the mass spectrum consisted of a molecular ion at 732; ^{1}H NMR δ 10.5 (s, 1 H), 1.43 (s, 3 H), 0.12 (s, 3 H), 0.42 (s, 18 H), 0.43 (s, 9 H); ^{13}C NMR δ 271.4 (d, J = 128 Hz), 8.10 (q, J = 117 Hz), 3.40 (q, J = 118 Hz), 4.90 (q, J = 117 Hz), 4.60 (q, J = 120 Hz), due to CH, $SiMe_2$ (diastereotropic), $(Me_3Si)_2N$, and Me_3SiN, respectively. The complex does not form an adduct with pyridine. Anal. Calcd for $C_{12}H_{34}N_2Si_4Ti$: C, 39.3; H, 9.28; N, 7.64. Found: C, 40.4; H, 9.45; N, 7.35.

{ZrCHSi(Me)$_2$NSiMe$_3$[N(SiMe$_3$)$_2$]}$_2$. Dimethylbis[bis(trimethylsilyl)amido]zirconium (1.2 g, 0.0027 mol) was heated to 60 °C under dynamic vacuum (10^{-2} mm). Within 5 min the clear, colorless liquid turned yellow and began to froth. After the liquid was heated for 6 h the frothing ceased and a light yellow, clear glassy solid remained. The gases that were evolved were collected (liquid nitrogen) and shown to be methane by gas-phase infrared spectroscopy. The solid was dissolved in pentane (30 mL), the solution filtered, and the yellow filtrate was concentrated to ca. 7 mL and cooled (−20 °C). The yellow needles were collected and dried under reduced pressure. The yellow mother liquor yielded an additional crop of yellow needles, and the combined yield was 1.0 g (94%): mp 150–151 °C. ^{1}H NMR δ 7.08 (s, 1 H), 1.14 (s, 3 H), 0.28 (s, 3 H), 0.44 (s, 9 H), 0.40 (s, 18 H); ^{13}C NMR δ 201.4 (d, J = 122 Hz), 9.50 (q, J = 119 Hz), 4.50 (q, J = 117 Hz), 4.90 (q, J = 117 Hz), 4.30 (q, J = 117 Hz), due to CH, Me_2Si (diastereotropic), Me_3SiN, and $(Me_3Si)_2N$, respectively. Elemental analyses were not satisfactory. Pyrolyses of diethyl- and bis((trimethylsilyl)methyl)bis[bis(trimethylsilyl)amido]zirconium were performed similarly, yielding the metallacycle in essentially quantitative yield, as shown by the melting point and ^{1}H NMR spectroscopy. The gaseous materials were identified as ethane and tetramethylsilane, respectively, by gas-phase infrared spectroscopy. Monitoring the course of the reaction by ^{1}H NMR spectroscopy showed no detectable amount of hydrogen evolution.

{ZrCHSi(Me)$_2$NSiMe$_3$[N(SiMe$_3$)$_2$][NC$_5$H$_5$]}$_2$. Pyridine (0.4 mL, 0.0052 mol) was added to a solution of the metallacycle (1.0 g) in pentane (15 mL). The yellow precipitate was collected and dried under reduced pressure. Toluene (10 mL) was added, the solution was heated and then filtered, and the filtrate was cooled to −20 °C and then to −70 °C, giving 1.2 g (95%) of bright yellow prisms: mp 133–134 °C dec; the mass spectrum contained a molecular ion at 897 due to M − NC_5H_5; ^{1}H NMR δ 8.80 (m, 2 H), 7.02 (m, 2 H), 6.77 (m, 1 H), 7.11 (s, 1 H), 1.24 (s, 3 H), 0.53 (s, 3 H), 0.55 (s, 18 H), 0.25 (s, 9 H); ^{13}C{^{1}H} NMR δ 195.7 (s), 11.0 (s), 5.60 (s), 6.30 (s), 5.00 (s), 151.4 (s), 137.5 (s), 124 (s), due to CH, Me_2Si (diastereotropic), $(Me_3Si)_2N$, Me_3SiN, and the ortho, meta, and para resonances of pyridine, respectively.

{HfCHSi(Me)$_2$NSiMe$_3$[N(SiMe$_3$)$_2$]NC$_5$H$_5$}$_2$. Dimethylbis[bis(trimethylsilyl)amido]hafnium (1.1 g, 0.0021 mol) was heated to 70 °C under dynamic vacuum (10^{-2} mm) for 6 h. The pale yellow material was dissolved in pentane (10 mL), and the solution was filtered. Pyridine (0.2 mL, 0.0025 mol) was added, and the small, bright yellow prisms were isolated by filtration. The prisms, 0.94 g (78%), were crystallized from toluene (10 mL) at −70 °C: mp 137–139 °C dec; the mass spectrum contained a molecular ion at 1073 amu due to M − py$^+$; ^{1}H NMR δ 8.96 (m, 2 H), 7.18 (m, 2 H), 6.79 (m, 1 H), 4.95 (s, 1 H), 2.32 (s, 3 H), 1.36 (s, 3 H), 0.63 (s, 18 H), 0.34 (s, 9 H); ^{13}C NMR δ 180.3 (d, J = 166 Hz), 10.8 (q, J = 118 Hz), 3.20 (q, J = 119 Hz), 6.60 (q, J = 118 Hz), 5.40 (q, J = 117 Hz), 151.8 (d, J = 182 Hz), 138.0 (d, J = 116 Hz), 124.1 (d, J = 168 Hz), due to CH, Me_2Si (diastereotopic), $(Me_3Si)_2N$, Me_3SiN, and o-, p-, and m-CH of pyridine, respectively. The pyridine complex was also prepared by a similar pyrolysis of diethylhafnium bis[bis(trimethylsilyl)amide], as shown by the melting point and ^{1}H NMR spectroscopy.

X-ray Study. Yellow crystals of the zirconium complex were grown from heptane (−20 °C) and loaded into quartz capillaries at room temperature under an atmosphere of argon and sealed. A crystal was examined with a Picker FACS-I automated diffractometer equipped with a graphite monochromator and a Mo X-ray tube (λ(Kα_1) 0.709 30 Å). The space group is *Pbca*. The setting angles of 12 manually centered reflections (41° < 2θ < 45°) were used to determine the cell parameters by least-squares. The cell dimension are a = 18.307 (7) Å, b = 26.036 (6) Å, and c = 19.425 (6) Å. For Z = 8 the calculated density is 1.18 g/cm^3.

Intensity data were collected by using a θ–2θ scan technique with a scan speed of 2°/min on 2θ. Each peak was scanned 0.7° before the Kα_1 peak to 0.7° after the Kα_2 peak, and backgrounds were counted for 10 s at each end of the scan range. The temperature during the data collection was 23 ± 1 °C. Three standard reflections were measured every 250th scan, and no significant variations of their intensities were observed. A total of 10 589 scans (4° < 2θ < 45°) yielded 5966 unique data of which 3149 had $F^2 > 3\sigma(F^2)$. An absorption correction (μ = 6.6 cm^{-1}) was applied[19] which ranged from 1.35 to 1.43.

A three-dimensional Patterson calculation showed the two zirconium positions, and subsequent least-squares refinements and electron density calculation revealed all of the non-hydrogen atoms in the structure. The least-squares function used minimizes the function $\sum w(|F_o| - |F_c|)^2/\sum wF_o^2$. The expressions used in processing the data and estimating weights are given in the supplementary material; the "ignorance factor" p was set to 0.065. An extinction correction was made; $F_c = F_o(1 + 0.167 \times 10^{-6}I)$, where I is the raw intensity and F is the structure factor. The scattering factors were from ref 20. In the final refinements the zirconium, silicon, nitrogen C(1)–C(3), and C(13)–C(15) atoms were assigned anisotropic thermal parameters, and hydrogen atoms H(1) and H(23) were included. Only the carbons atoms C(1)–C(3) and C(13)–C(15) were given anisotropic thermal parameter as they are in the region of the fused rings, and confirmation of the hydrogen atoms on the bridging atoms C(1) and C(13) was sought. In the difference electron density maps the hydrogen atoms H(1) and H(23) were found and were included in the least-squares refinements. Because of the large computer costs no more parameters were added and the refinment was terminated at this point.

The discrepancy indices for the data where $F^2 > 3\sigma$ are $R = \sum||F_o| - |F_c||/\sum|F_o| = 0.061$ and $R_w = |\sum w(|F_o| - |F_c|)^2/\sum w|F_o|^2]^{1/2} = 0.082$. R for all the data is 0.12. The error in the observation of unit weight is 1.71.

Tables of the thermal parameters and a list of observed structure factors is given in the supplementary materials.

Acknowledgment. This crystallographic work was supported by the Director, Office of Energy Research, Office of Basic Energy Sciences, Chemical Sciences Division, of the U.S. Department of Energy under Contract No. DE-AC03-76SF00098. The synthetic studies were supported by a grant from the Gas Research Institute.

Registry No. $TiCl_2[N(SiMe_3)_2]_2$, 83666-31-3; $TiCl_4$, 7550-45-0; $TiMe_2[N(SiMe_3)_2]_2$, 83666-32-4; $ZrEt_2[N(SiMe_3)_2]_2$, 83666-33-5; $Zr(CH_2SiMe_3)_2[N(SiMe_3)_2]_2$, 83681-35-0; {TiCHSi(Me)$_2$NSiMe$_3$[N(SiMe$_3$)$_2$]}$_2$, 83666-34-6; {ZrCHSi(Me)$_2$NSiMe$_3$[N(SiMe$_3$)$_2$]}$_2$, 83666-35-7; {ZrCHSi(Me)$_2$NSiMe$_3$[N(SiMe$_3$)$_2$][NC$_5$H$_5$]}$_2$, 83666-36-8; {HfCHSi(Me)$_2$NSiMe$_3$[N(SiMe$_3$)$_2$]NC$_5$H$_5$}$_2$, 83681-36-1; $ZrCl_2[N(SiMe_3)_2]_2$, 70969-28-7; $ZrMe_2[N(SiMe_3)_2]_2$, 70969-30-1; $HfMe_2[N(SiMe_3)_2]_2$, 71000-84-5; $HfEt_2[N(SiMe_3)_2]_2$, 70969-31-2; $Li[N(SiMe_3)_2]$, 4039-32-1; $Mg(CH_2SiMe_3)_2$, 51329-17-0; $MgEt_2$, 557-18-6; methyl chloride, 74-87-3.

Supplementary Material Available: Data processing formulas, a table of thermal parameters, and the listing of structure factor amplitudes (17 pages). Ordering information is given on any current masthead page.

(19) Templeton, L. K.; Templeton, D. H. "Abstracts of Papers", Proceedings of the American Crystallographic Association, 1973, Series 2, Vol. 1, p 143.
(20) Doyle, P. A.; Turner, P. S. *Acta Crystallogr., Sect. A* **1968**, *24A*, 390–395.

Stereo-Controlled Multiple Trimethylsilylation of Pentadienyl Anions and the Structure of Polysilylated Anions

H. Yasuda, T. Nishi, K. Lee, and A. Nakamura*

Department of Macromolecular Science, Faculty of Science, Osaka University, Toyonaka, Osaka 560, Japan

Received July 9, 1982

Trimethylsilylation of ((trimethylsilyl)pentadienyl)- and (1,3,5-tris(trimethylsilyl)pentadienyl)lithium with $(CH_3)_3SiCl$ gave conjugated (*E,E*)-1,5-di- and 1,1,3,5-tetrasilylated 1,3-pentadienes, respectively, while 1,5-bis(trimethylsilyl)pentadienyl anions gave a 1,3,5-trisilylated 1,4-pentadiene. The regio- and stereoselectivity were >90% in every case. The structures of monosilylated pentadienyllithium and 1,5-disilylated pentadienyllithium, -potassium, and -cesium are of the W forms as confirmed by the ^1H and ^{13}C NMR spectra, but (1,3,5-tris(trimethylsilyl)pentadienyl)lithium assumes the S-shaped structure in THF. Alkylation of these silylated pentadienyllithiums with *tert*-butyl bromide occurred selectively at the central carbon while protonation with *tert*-butyl alcohol proceeded at the terminal carbon.

As an extension of allyl anion chemistry, the reactions and structures of pentadienyl anions have attracted much attention in both organic and inorganic chemistry. Pentadienyl anions are useful reagents for the preparation of "open metallocenes"[1] and related complexes[2,3] and are valuable precursors for pentadienylsilanes or -stannanes which are capable of converting ketones or aldehydes to dienyl alcohols.[4,5] The use of silylated allyl anions,[6] silylated pentadienyl anions,[7a] and (silyloxy)pentadienyl anions[7b] is of increasing importance in synthetic chemistry since the regioselectivity in the reaction with various electrophiles is significantly improved by the introduction of trialkylsilyl groups. The usefulness of a silylated cyclopentadienyl ligand was also reported recently in lanthanide chemistry.[8] Nevertheless, structural knowledge of the silylated dienyl anions is still limited. This paper describes the chemistry and structures of silylated dienyl anions obtained by sequential metalation–trimethylsilylation cycles starting from a pentadiene mixture. The mode of alkylation and protonation also was examined for comparison.

Results and Discussion

Multiple Trimethylsilylation of Pentadienyl Anions. Pentadienyl anions can be silylated to give silylpentadienes which are then readily converted to anions and silylated again to effect multiple silylation.[9a] Regio- and stereoselective trimethylsilylation of pentadienyllithium (**1a**), pentadienylpotassium (**1b**),[7a,9b,c] and (((trialkylsilyl)oxy)pentadienyl)lithium[7b] has been reported previously. Thus, the reaction of **1a** with chlorotrimethylsilane in THF gave (*E*)-2,4-pentadienyltrimethylsilane exclusively while the reaction of potassium analogue **1b** in THF gave the *Z* isomer, reflecting their structures in solution.[9-12] The resulting 2,4-pentadienyltrimethylsilane underwent metalation on treatment with *n*-BuLi in THF as reported by Oppolzer et al.[7a] The metalation occurred readily to the exclusion of the well-known alkyllithium-catalyzed polymerization of dienes[14] when a silyl group is attached (eq 1). Thus, monosilylated pentadienyllithium **2a** was

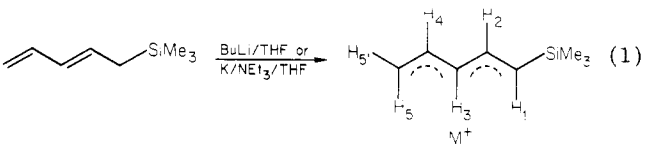

(1)

2a, M = Li
b, M = K

obtained as yellow crystals in good yield. The preparation of the potassium analogue also was successful by direct metalation of (*Z*)- or (*E*)-2,4-pentadienyltrimethylsilane with potassium in the presence of a stoichiometric amount of triethylamine. (The reaction mechanism will follow that given in ref 9d.)

The ^1H NMR chemical shifts and coupling constants of the complexes were determined by iterative computer simulation of the spectrum as shown in Table I. The spectrum of **2a** is given in Figure 1 as a typical example. The variable-temperature ^1H NMR spectra of **2a** clearly indicate that it exists as a single torsional isomer with *E,E,E* configuration (exo W-shaped structure) in THF in the temperature range from 50 to −70 °C. The coupling constant of $J_{4,5}$ (16.0 Hz) and $J_{2,3(3,4)}$ (11.5 Hz) are nearly equal to the corresponding values for the parent penta-

(1) (a) D. R. Wilson, A. A. DiLullo, and R. D. Ernst, *J. Am. Chem. Soc.*, **102**, 5928 (1980); (b) D. R. Wilson, Ju-Z. Liu, and R. D. Ernst, *ibid.*, **104**, 1120 (1982); (c) M. C. Böhn, M. Eckert-Maksic, R. D. Ernst, D. R. Wilson, and R. Gleiter, *ibid.*, **104**, 2699 (1982).

(2) D. Seyferth, E. W. Goldman, and J. Pornet, *J. Organomet. Chem.*, **208**, 189 (1981).

(3) M. A. Paz-Sandoval and P. Powell, *J. Organometal. Chem.*, **219**, 81 (1981).

(4) D. Seyferth and J. Pornet, *J. Org. Chem.*, **45**, 1721 (1980).

(5) A. Hosomi, M. Saito, and H. Sakurai, *Tetrahedron Lett.*, 3783 (**1980**).

(6) (a) E. Ehlinger and P. Magnus, *J. Am. Chem. Soc.*, **102**, 5004 (1980) and literatures cited therein; (b) D. Seyferth and R. E. Mammarella, *J. Organomet. Chem.*, **156**, 278 (1978); (c) R. J. P. Corriu, C. Guerin, and J. M'Boula, *Tetrahedron Lett.*, 2985 (**1981**); (d) H. Yatagai, Y. Yamamoto, and K. Maruyama, *J. Am. Chem. Soc.*, **102**, 4548 (1980).

(7) (a) W. Oppolzer, S. C. Burford, and F. Marazza, *Helv. Chim. Acta*, **63**, 555 (1980); (b) W. Oppolzer, R. L. Snowden, and D. P. Simmons, *ibid.*, **64**, 2002 (1981).

(8) M. L. Lappert, A. Singh, J. L. Atwood, and W. E. Hunter, *J. Chem. Soc., Chem. Commun.*, 1190 (**1981**).

(9) (a) For a preliminary report, H. Yasuda and A. Nakamura, "Proceedings of the Tenth International Conference on Organometallic Chemistry", Toronto, 1981, Abstr 2E52. (b) H. Yasuda, M. Yamauchi, Y. Ohnuma, and A. Nakamura, *Bull. Chem. Soc. Jpn.* **54**, 1481 (1981); (c) H. Yasuda, M. Yamauchi, and A. Nakamura, *J. Organomet. Chem.*, **202**, C1 (1981). (d) H. Yasuda, Y. Ohnuma, M. Yamauchi, H. Tani, and A. Nakamura, *Bull. Chem. Soc. Jpn.*, **52**, 2036 (1979).

(10) (a) R. B. Bates, D. W. Gosselink, and J. A. Kaczynski, *Tetrahedron Lett.*, 199 (**1967**); (b) *ibid.*, 205 (**1967**); (c) R. B. Bates, S. Brenner, C. M. Cole, E. W. Davidson, G. D. Forsythe, D. A. McCombs, and A. S. Roth, *ibid.*, **95**, 926 (1973).

(11) W. T. Ford and M. Newcomb, *J. Am. Chem. Soc.*, **96**, 309 (1974).

(12) (a) M. Schlosser and G. Rauchschwalbe, *J. Am. Chem. Soc.*, **100**, 3258 (1978); (b) V. H. Bosshardt and M. Schlosser, *Helv. Chem. Acta*, **63**, 2393 (1980); (c) M. Schlosser and M. Stähle, *Angew. Chem. Suppl.*, 198 (**1982**).

(13) ^1H NMR assignment of **2c** was made from the decoupled spectra: δ 6.47 (m, 1, H_2), 6.36 (m, 1, H_4), 4.10 (d of d, 1, J_{45} = 16.0 Hz, anti-H_5), 3.91 (d of d, $J_{4,5'}$ = 11.0 Hz, syn-H_5), 3.76 (d of d, $J_{2,3}$ = 11.2, $J_{3,4}$ = 9.0 Hz), 3.62 (d, J = 16.5 Hz, H_1).

(14) For example, (a) A. V. Tobolsky and C. E. Rogers, *J. Polym. Sci.*, **40**, 73 (1959); (b) S. Bywater, *Pure Appl. Chem.*, **4**, 319 (1962).

0276-7333/83/2302-0021$01.50/0

Table I. ^{1}H NMR Chemical Shifts and Coupling Constants (Hz) for 1-4[a]

complex	temp, °C	ν_1	ν_2	ν_3	ν_4	ν_5	ν_5'	$J_{1,2}$	$J_{1,3}$ ($J_{3,5}$)	$J_{2,3}$	$J_{2,4}$	$J_{3,4}$	$J_{4,5}$	$J_{4,5'}$
1a	30	3.08	6.32	4.31	6.32	3.08	3.05	12.1	−0.2	10.8	−0.2	10.8	12.1	12.1
	−70	3.04	6.22	4.65	6.22	3.04	2.69	15.5	−0.2	11.5	−0.2	11.5	15.5	9.0
2a	−40	2.95	6.46	4.67	6.25	3.36	3.00	16.3	−0.2	11.5	−0.2	11.5	16.0	9.3
2b	−40	3.02	6.49	4.68	6.28	3.44	3.14	16.2	−0.2	11.6	−0.2	11.6	16.0	9.5
3a	−40	3.25	6.44	4.78	6.44	3.25		16.7	−0.2	11.0	−0.2	11.0	16.7	
3b	−40	3.34	6.45	4.77	6.45	3.34		16.8	−0.2	11.2	−0.2	11.2	16.8	
3c	−40	3.38	6.44	4.77	6.44	3.38		16.8	−0.2	11.2	−0.2	11.2	16.8	
4	30	4.10	6.95		6.95	4.10		18.1			−0.4		18.1	
	−70	3.89	6.39		7.35	4.07		17.5			−0.4		18.5	

[a] Parameters were determined by the computer simulation of the 100-MHz ^{1}H NMR spectra. In ppm downfield from external Me_4Si in THF-d_8 (calibrated by using the downfield THF peak as the internal standard, assumed to be 3.75 ppm). ν_1, ν_5, and ν_5' express the chemical shift values of anti-H_1, anti-H_5, and syn-H_1 signals, respectively.

Table II. ^{1}H NMR Parameters for Silylated Allyllithium in THF-d_8 at −40 °C[a]

	ν_1	ν_2	ν_3	ν_3'	$J_{1,2}$	$J_{1,3}$	$J_{2,3}$	$J_{2,3'}$
allyllithium[b]	2.24	6.38	2.24	1.78	15.2	~0	15.2	8.6
(1-(trimethylsilyl)allyl)lithium	2.21	6.40	2.78	2.48	15.6	−0.2	14.5	8.0
(1,3-bis(trimethylsilyl)allyl)lithium	2.73	6.55	2.73		16.0	−0.2	16.0	

[a] Parameters were determined by the computer simulation of the spectrum (100 MHz) in THF-d_8 J values in hertz. [b] Data reported by P. West.[29] See also ref 30. ν_1, ν_3, ν_3' express the chemical shift values of anti-H_1, anti-H_3, and syn-H_3, respectively.

dienyllithium which has the *E,E* configuration (W form).[10b,11] The corresponding potassium complex consists of two isomers in THF below 50 °C; i.e., ((*E,E,E*)-1-trimethylpentadienyl)potassium (**2b**; 70%) and ((*E,Z,E*)-1-(trimethylsilyl)pentadienyl)potassium (**2c**; 30%), as analyzed by the ^{1}H NMR spectrum.[13] The configuration of the C_1/C_2 bond of **2a–c** is *E*. The value of $J_{1,2}$ (16.3 Hz) is consistent with those of (*E*)-(trimethylsilyl)allyl and 1,3-bis(trimethylsilyl)allyl anions (J = 15.6–15.8 Hz) as shown in Table II. When the trimethylsilyl group is attached to olefinic carbons, the proton–proton coupling constant for the *E* configuration increases to 16–19 Hz.[15] A similar geometrical change has been observed for allyl anions whn the countercation Li was replaced with K^+; i.e., crotyllithium assumes the *E*-allylic configuration while potassium analogue prefers the *Z*-allylic configuration.[16]

The excellent regio- and stereoselection observed in the trimethylsilylation of **1a** and **1b** prompted us to examine the trimethylsilylation of **2**. If any significant difference in electron densities or in steric hindrance exists among three carbon atoms (C_1, C_3, and C_5), a regioselective reaction will occur. Actually, trimethylsilylation of **2a** proceeded in high regioselectivity (97%) to give (*E,E*)-1,5-bis(trimethylsilyl)-1,3-pentadiene in 92% yield. A mixture of potassium analogues **2b,c** also gave the same product exclusively (94% regioselectivity, 95% yield). This result

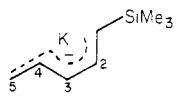

2c

or **2a,b** $\xrightarrow{Me_3SiCl}$

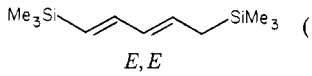

E,E (2)

supports the above-mentioned ^{1}H NMR implication that

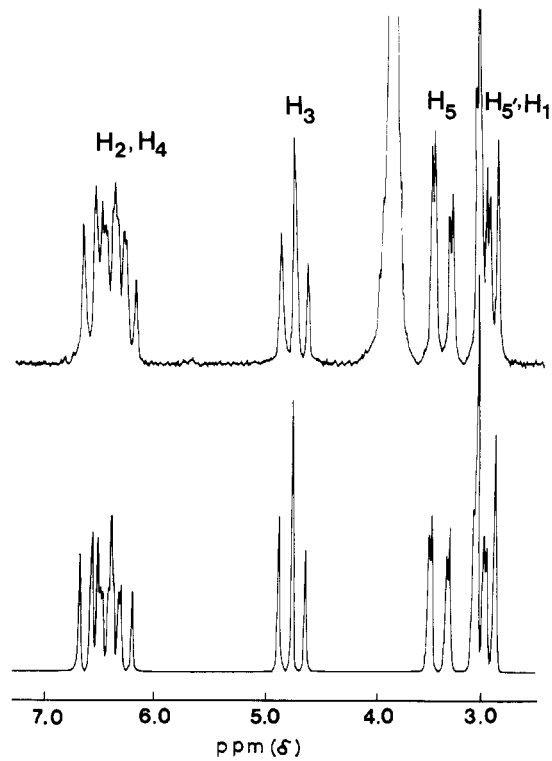

Figure 1. ^{1}H NMR (100 MHz) spectrum of (1-(trimethylsilyl)pentadienyl)lithium (**2a**) in THF-d_8 at −70 °C (above) and the simulated spectrum (below). The numbering system follows that given in eq 1 (see the parameter listed in Table I).

the minor species **2c** has the *E,Z,E* configuration of the S (sickle)-shaped structure and the major species **2b** has the *E,E,E* configuration. If **2** has another type of S-shaped structure (**2d**) or the U-shaped structure (**2e**), the species must afford the *E,Z*-disilylated compound (eq 3). The yield of (*E,Z*)-, (*Z,E*)-, or (*Z,Z*)-1,5-bis(trimethylsilyl)-1,3-pentadiene was lower than 6% for both lithium and potassium derivatives.

The metalation of 1,5-disilylated 1,3-pentadiene occurred at relatively higher temperatures (30 °C) by the addition of *n*-butyllithium or M/NEt_3 (M = K, Cs) as shown in eq 4. The resulting (1,5-bis(trimethylsilyl)pentadienyl)lith-

(15) M. L. Maddox, S. L. Stafford, and H. D. Kaesz, *Adv. Organomet. Chem.*, **3**, 1 (1965). For non-siylated allyl anions, see ref 16.

(16) (a) S. Bank, A. Schriesheim, and C. A. Rowe, Jr., *J. Am. Chem. Soc.*, **87**, 3244 (1965); (b) G. J. Heiszwolf, J. A. A. Van Drunen, and H. Kloosterziel, *Recl. Trav. Cheim. Pays-Bas*, **88**, 1377 (1969); (c) M. Schlosser and J. Hartmann, *J. Am. Chem. Soc.*, **98**, 4674 (1976); (d) M. Stähle, J. Hartmann, and M. Schlosser, *Helv. Chim. Acta*, **60**, 1730 (1977); (e) T. B. Thompson and W. T. Ford, *J. Am. Chem. Soc.*, **101**, 5459 (1979).

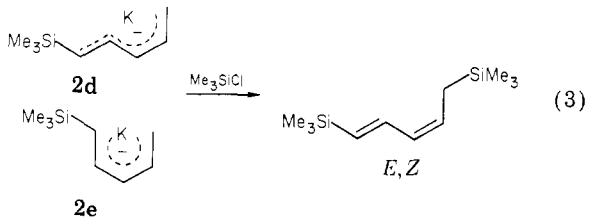

(3)

ium, -potassium, and -cesium (**3a–c**) were purified by recrystallization. The ^{1}H NMR data of **3a–c** indicate that these complexes comprise a single torsional isomer which has the *E,E,E,E* configuration. The values of $J_{2,3(3,4)}$

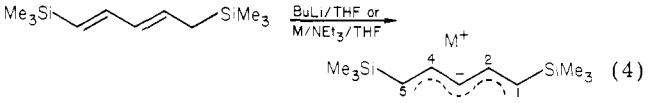

(4)

3a, M = Li
b, M = K
c, M = Cs

(11.0–11.6 Hz) are comparable to those of *E* inner bonds observed for **1a** and **2a**. No significant change was observed in the spectral pattern and coupling constants by lowering the temperature from 50 to −70 °C or raising the temperature from −70 to 60 °C.

The mode of trimethylsilylation of **3** is quite different from that of **1** and **2**. The silylation occurred preferentially at the central C_3 atom and gave (*E,E*)-1,3,5-tris(trimethylsilyl)-1,4-pentadiene. The regioselectivity was 98%.

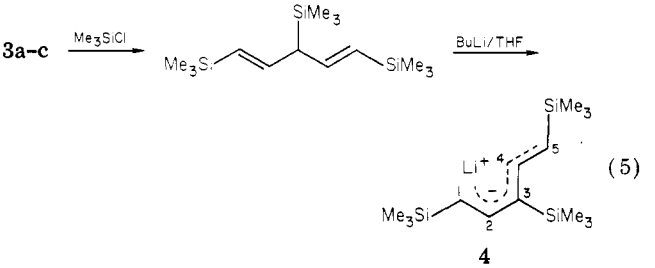

(5)

4

Thus, stereo- and regio-controlled triple trimethylsilylation of pentadienyl anions was realized by repeated metalation–trimethylsilylation sequences starting from 1,3-pentadiene. Similar high regioselectivity has been reported also in the sequential trimethylsilylation of allyllithium which gives monosilylated or 1,3-disilylated propene of the *E* configuration.[17]

The lithiation of the resulting trisilylated 1,4-pentadiene occurred at 30 °C in THF to give (1,3,5-tris(trimethylsilyl)pentadienyl)lithium (**4**) in good yield (98%). The ^{1}H NMR spectrum of **4** is temperature dependent. At 30 °C, the signals assigned to C_1–H and C_5–H appeared at 4.10 ppm as a doublet (J = 18.1 Hz) and the signal of C_2–H (C_4–H) at 6.95 ppm as a doublet. However, when the temperature was lowered to −20 °C, the spectrum coalesced and, at −70 °C, the signal of C_1–H, C_5–H and C_2–H, C_4–H split into two doublets. (3.89, 4.07 and 6.39, 7.35 ppm, respectively) (Figure 2). The signal intensity ratio between $C_1(C_2)$–H and $C_5(C_4)$–H was just 1:1 irrespective of the concentration. The coupling constants were 17.5- and 18.5-Hz values for trans configuration. Therefore, the limiting structure of **4** was taken to the S form. The peak splitting does not indicate the presence of the symmetrical W- or U-shaped structures. Until fairly recently, the anion of 1-methyl-1,4-cyclohexadiene was an unique example of the S-shaped pentadienyl anion.[10b] η^2-Coordination of Li atom to C_1–C_5 is sterically possible for the U-shaped anion

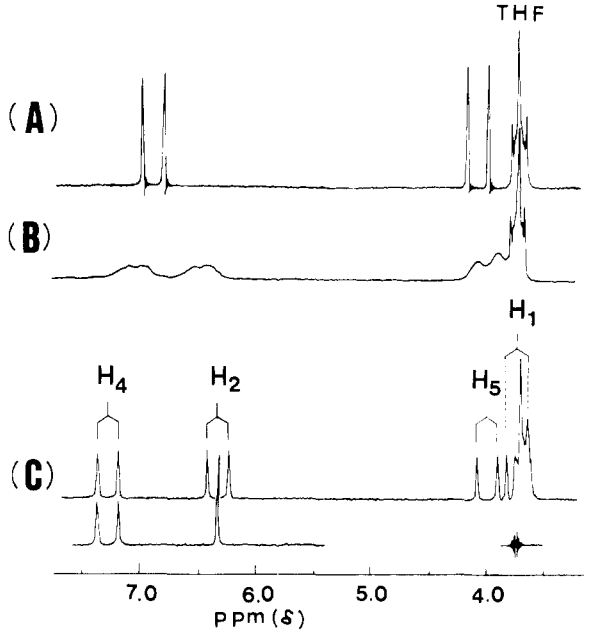

Figure 2. Variable-temperature ^{1}H NMR (100 MHz) spectra of (1,3,5-tris(trimethylsilyl)pentadienyl)lithium (**4**) in THF-d_8: (A) 30 °C, (B) −30 °C, (C) −70 °C (decoupled spectrum is shown below). Numbering system is given in eq 6.

but is impossible for the W- and S-shaped ones. Therefore, the following metallotropy was considered for the S-shaped isomer as was estimated theoretically for the W-formed pentadienyllithium.[18] The equilibrium should shift to the left (**4a**) because the signals of C_5–H, C_4–H appeared at

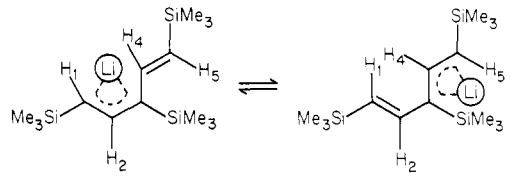

(6)

4a **4b**

a significantly lower field than those of C_1–H, C_2–H, respectively. The species **4a** appears to be favored over **4b** because of the following reasons. (1) The ^{13}C NMR chemical shift difference between C_1 and C_3 (0.8 ppm at 30 °C and 8.6 ppm at −70 °C) is close to the values (0.9–1.1 ppm) observed for (*Z*)-pentadienyl- and (*Z*)-hexadienylpotassium[9b,12c] rather than the values (17–21 ppm) observed for **1a** and **3a–c** of the *E* configuration, indicating that the C_2–C_3 bond has the *Z* configuration. (2) The ionic character of the M–C bond of **4** is larger than that of **1** by the inductive effect of three trimethylsilyl groups. The increased ionic character generally results in the *Z* configuration as was found for monoalkyl-substituted allylpotassium[16b] and pentadienylpotassium.[9b,12c] (3) The ab initio SCF computation on pentadienyllithium with STO/3G atomic orbital suggested that the nonplanar S-shaped structure which is similar to **4a** is more stable (12 kcal/mol) than the W-shaped structure if the effect of solvation or aggregation is negligible.[19] On this bases, the structure of **4** was concluded to be the nonplanar S-shaped structure.

Trimethylsilylation of **4** in THF produced (*E*)-1,1,3,5-tetrakis(trimethylsilyl)-1,3-pentadiene in 99% regioselec-

(17) G. T. Burns and T. J. Barton, *J. Organomet. Chem.*, **216**, C5 (1981).

(18) (a) R. J. Bushby and A. S. Patterson, *J. Organomet. Chem.*, **132**, 163 (1977). (b) J. F. Sebastian, B. Hsu, and J. R. Grunwell, *ibid.*, **105**, 1 (1976).

(19) A. Bongini, G. Cainelli, G. Cardillo, P. Palmieri, and A. Umani-Ronch, *J. Organomet. Chem.*, **92**, C1 (1975).

Table III. ^{13}C NMR Chemical Shift Values for 1-4[a]

complex	temp, °C	C_1	C_2	C_3	C_4	C_5	$Si(CH_3)_3$
1a	−40	66.0	144.0	87.3	144.0	66.0	
2a	−30	69.7	149.7	91.0	143.4	75.5	1.9
3a	−30	78.1	149.7	95.0	149.7	78.1	1.5
3b	−30	79.6	150.4	96.6	150.4	79.6	1.7
3c	−30	80.4	151.0	100.6	151.0	80.4	1.7
4	30	85.5	150.9	86.3	150.9	85.5	1.8
	−70	77.5	150.1	86.1	152.3	90.8	1.9

[a] Data were collected at 22.6 MHz in THF by using the high-field THF peak (25.8 ppm) as internal standard.

tivity (90% yield), while the reaction in hexane gave a mixture of 1,1,3,5-tetrakis(trimethylsilyl)-1,3-pentadiene (55%) and 1,3,3,5-tetrakis(trimethylsilyl)-1,4-pentadiene (45%). Thus, the medium effect was appreciable in this case.

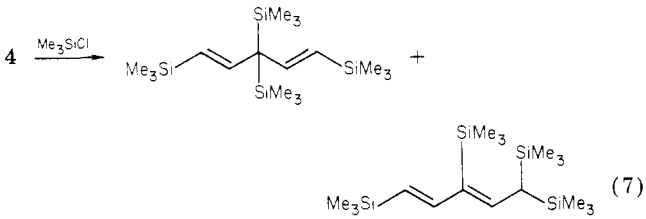

(7)

^{13}C NMR Spectral Studies on Silylated Dienyl Anions. ^{13}C NMR spectra of allyl and pentadienyl anions have been extensively studied since the chemical shifts provide useful information on the configuration and conformation. The ^{13}C NMR assignment of the present silylated pentadienyl anions was made with nondecoupled spectra as listed in Table III. The data show that **1a**, **2a**, **3a–c**, and **4** exist as a single torsional isomer in THF. The C_3 signal of **3a–c** appeared at relatively higher field by 17–20 ppm than the C_1 or C_5 signal, as was found for the W-shaped pentadienyllithium.[9b,11,12c] In U-shaped anions such as pentadienyl- and hexadienylpotassium, the chemical shift difference was known to reduce to 1–2 ppm.[9b,12c] Thus, the chemical shift values observed for **2a** and **3a–c** suggest that they have the W-shaped structure in THF.

Introduction of a Me_3Si group into the dienyl anion results in a downfield shift of the C_1, C_3, and C_5 signals. This will be due to the $p\pi$–$d\pi$ conjugation in the Si–C bond which allows the extensive delocalization of electrons over the pentadienyl group. However, the chemical shift value for C_1 of **2a** did not approach to that of **3a–c**, suggesting that the negative charge density on C_1 is larger than that on C_5 of **2a**. It is noteworthy that **3a–c** assume the W-shaped structure irrespective of the counter cation, whereas, in the parent pentadienyl anion systems, the Li complex favors the W form and the K analogue assumes the U-shaped structure. The observed preference for the W form is ascribed to the repulsion between the two Me_3Si groups at the C_1 and C_5 positions which diminishes the stability of the U form. The chemical shifts of C_1 and C_3 of **3** were little affected by changing the countercation from Li to the more positive Cs. The upfield shift (2.3–5.1 ppm) is significantly smaller than that (30 ppm) observed between (*tert*-butylallyl)lithium and -cesium.[20]

The ^1H NMR supposition that **4** has the S-shaped structure was also confirmed from the ^{13}C NMR spectrum. Five peaks assigned to C_1–C_5 atom were observed at −70 °C while it gave an averaged spectrum at 30 °C.

Electronic Spectra of Silylated Pentadienyl Anions. The $p\pi$–$d\pi$ interaction in C–Si bonds present in the silylated pentadienyl anion systems may be reflected in the electronic spectra as it will cause extensive delocalization of electrons over the pentadienyl group. To evaluate the effect of the silyl group, we measured the spectra of a series of silylated pentadienyl anions in THF. The absorption maximum shifted to higher wavelength with increasing substitution in the order of **4 > 3c > 3b > 3a > 2a** (Table IV). The effect of countercations on the absorption maximum was rather small as was shown in the case of **3a–c**. The difference in wavelength (10 nm with respect to Li and Cs analogues) is comparable to the value (15 nm) for "living" anions of polystyrene[21] but smaller than that (20–21 nm) observed for pentadienyl anions[9b] and fluorenyl anions.[22] The large value of the absorption maximum for **4** may be a result of extensive $p\pi$–$d\pi$ conjugation in Si–C bonds. The geometrical change is assumed to be of little effect on the wavelength because only a small difference (9 nm) exists between (*Z*)-pentadienylpotassium and (*E*)-pentadienyllithium[9b] (this difference is ascribable merely to the effect of the countercations).

Table IV. Electronic Spectral Data for 1-4[a]

	λ_{max}, nm	ϵ_{max}
1a	358	5400
2a	370	3400
3a	386	6100
3b	393	4200
3c	396	4000
4	423	4700

[a] Data were collected in THF at 25 °C. Electronic spectral data for nonmetalated starting dienes are given in Experimental Section.

Table V. Product Distribution in the Alkylation of 2a and 3a with Butyl Halides[a]

complex	RX	product distributn, % 5a (6a)	5b (6b)	5c	yield,[b] %
2a	*t*-BuBr	99–100	0–1	0	98
	sec-BuBr	85	15	0	99
	i-BuBr	85	15	0	99
	n-BuBr	70	10	20	99
3a	*t*-BuBr	100	0		98
	sec-BuBr	99	1		97
	i-BuBr	95	5		99
	n-BuBr	60	40		99

[a] Reaction was carried out in THF at 0 °C. [b] Determined by the gas chromatographic analysis.

Alkylation of Silylated Pentadienyl Anions. The alkylation of silylated dienyl anions with *tert*-butyl, *sec*-butyl, isobutyl, and *n*-butyl bromides was examined in order to compare with the results of the silylation with chlorotrimethylsilane. The reaction occurred at the central

(20) S. Bywater and D. J. Worsfold, *J. Organomet. Chem.*, **159**, 229 (1978).

(21) (a) S. Bywater, A. F. Johnson, and D. J. Worsfold, *Can. J. Chem.*, **42**, 1255 (1964); (b) J. E. L. Roovers and S. Bywater, *Trans faraday Soc.*, **62**, 701 (1966).

(22) T. E. Hogen-Esch and J. Smid, *J. Am. Chem. Soc.*, **88**, 307 (1966).

carbon to give **5a** or **6a** exclusively (99–100%) when *tert*-butyl bromide was added to **2a** or **3a**. Benzyl bromide is known to attack the central carbon of **2a** in 100% regioselectivity.[7a] However, when *sec*-butyl, isobutyl, and *n*-butyl bromides were used, alkyl substitution occurred not only at the central carbon but also at the terminal carbon atoms to give **5b–c** or **6b** (Table V). This trend

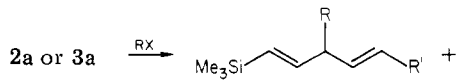

5a, R′ = H
6a, R′ = Me_3Si

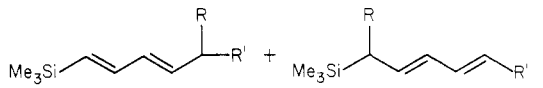

5b, R′ = H **5c**, R′ = H
6b, R′ = Me_3Si (8)

R = *n*-, *i*-, *sec*-, or *t*-C_4H_9

also has been observed in the alkylation of nonsilylated pentadienyl anions **1a,b** as reported previously; i.e., the reaction of pentadienylpotassium with *t*-BuBr gave 3-alkylated 1,4-pentadiene in 78% yield and occurred with MeI in 35% regioselectivity.[9d] Thus compounds **1–3** showed similar trends in the alkylation and protonation reactions (described later), irrespective of the presence of trimethylsilyl group on the pentadienyl unit, suggesting that the negative charge is predominantly localized on the central C_3 atom of **1–3** as predicted for **1** by EH,[23] CNDO/II,[18] and MINDO/III[24] calculations. It should be noted that the regioselection observed in reaction of *sec*-butyl or isobutyl bromide with **2a** was much improved when **3a** was used. This will be due to the increased electron density on the C_3 atom by the inductive and the steric effects of the two methyl groups. In the (trimethylsilyl)allyl anions, both alkylation and silylation occurred at the nonsilylated γ-position to give vinylsilane derivatives.[6] However, alkylation of **1–3** is essentially different from that of allyl anions as mentioned above. Since chlorotrialkylsilanes are known to react with allyl anions by the S_N2 mechanism with inversion of configuration at silicon,[25] the trimethylsilylation of **1** and **2** may be explained by assuming intermediate A. The substitution proceeds by attack by Me_3SiCl on the C_1 or C_5 atom from the apical position to form A, followed by pseudorotation around the Si atom which allows the elimination of Cl from the apical position. Intermediate B will be less stable for steric and electronic reasons (Li^+ will be in the vicinity of the C_3 atom on which the highest negative charge is present).

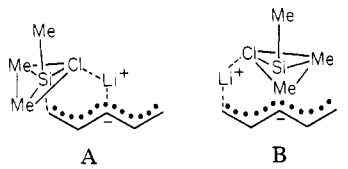

Protonation of Silylated Pentadienyl Anions. Hydrolysis of nonsilylated pentadienylpotassium and its alkylated derivatives always gave conjugated dienes selectively (97–99%);[9d] i.e., protonation occurred predominantly at the terminal carbon. In general, the protonation of a series of pentadienylmetal compounds showed that terminal carbon attack was favored when the ionic character of the M–C bond was increased. The ratio of 1,3- to 1,4-pentadiene obtained by the hydrolysis of C_5H_7K, C_5H_7Na, C_5H_7Li,[9d] $(C_5H_7)_2Mg$,[26] $(C_5H_7)_2Zn$, and $(C_5H_7)_2Be$[27] was 99/1, 99/1, 90/10, 80/20, 70/30, and 15/85, respectively. In the case of the beryllium analogue, the negative charge is localized on the terminal atom, where the metal makes a covalent bond (cf. negative charge is highest on the central carbon in the case of alkali-metal derivatives). Thus, protonation generally proceeds in a 1,3 fashion.

Table VI. Product Distribution in the Protonation of 2a and 3a[a]

complex	reagent	product distributn, % 7a (8a)	7b (8b)
2a	Ph_3COH	95	5
	Ph_2CHOH	90	10
	$(CH_3)_3COH$	89	11
	H_2O	87	13
3a	Ph_3COH	100	0
	Ph_2CHOH	99	1
	$(CH_3)_3COH$	99	1
	H_2O	99	1

[a] Protonation was carried out in THF at 0 °C, and the distribution was determined by GC. Yields were >99% as confirmed by GC.

The protonation of mono- and disilylated pentadienyl anions **2a** and **3a** occurred at the terminal carbons and gave **7a** or **8a** predominantly (Table VI). The use of a

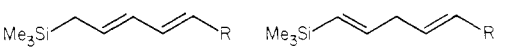

7a, R = H **7b**, R = H
8a, R = Me_3Si **8b**, R = Me_3Si

bulky protonation agent such as triphenylmethanol raised the regioselectivity to 95–100%. The product distribution for complex **2a** indicates that the negative charge on C_1 atom is larger than that on C_5; i.e., $C_3 > C_1 > C_5$. On this basis the protonation of **2a** is explained as depicted in eq 9. A similar transition state has been proposed for the

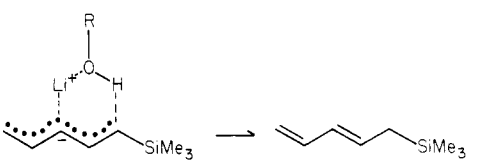

(9)

isomerization of allyl ether with KO-*t*-Bu.[28] The high selectivity observed in protonation of **3a** may have arisen from the steric effect as well as the inductive effect of the Me_3Si group.

Experimental Section

General Remarks. All operations were conducted with Schlenk techniques under an argon atmosphere. Tetrahydrofuran and hexane were dried over Na/K alloy and distilled before use. GC analysis was effected with a Hitachi Model 163 gas chro-

(23) R. Hoffmann and R. A. Olofson, *J. Am. Chem. Soc.*, **88**, 943 (1966).
(24) M. J. S. Dewar, M. A. Fox, and D. J. Nelson, *J. Organomet. Chem.*, **185**, 157 (1980).
(25) R. Corriu and J. Masse, *J. Organomet. Chem.*, **35**, 51 (1972) and literatures cited therein.
(26) H. Yasuda, M. Yamauchi, A. Nakamura, T. Sei, Y. Kai, N. Yasuoka, and N. Kasai, *Bull. Chem. Soc. Jpn.* **53**, 1089 (1980).
(27) H. Yasuda, Y. Ohnuma, A. Nakamura, Y. Kai, N. Yasuoka, and N. Kasai, *Bull. Chem. Soc. Jpn.* **53**, 1101 (1980).
(28) (a) T. J. Prosser, *J. Am. Chem. Soc.*, **83**, 1701 (1961); (b) C. C. Price and W. H. Synder, *ibid.*, **83**, 1773 (1961).
(29) P. West, J. I. Purmort, and S. V. McKinley, *J. Am. Chem. Soc.*, **90**, 797 (1968).
(30) D. A. Hutchison, K. R. Beck, R. A. Benkeser, and J. B. Grutzner, *J. Am. Chem. Soc.*, **95**, 7075 (1973).

matograph using capillary columns (45 m) OV-1, CW-45, or HB-2000, and the separation of the reaction products was accomplished with a Varian-Aerograph Model 700 gas chromatograph using a column (4 m) of 5% Benton-34 on 60/80 mesh Uniport-B (Gasukuro Kogyo Co.). ^1H and ^{13}C NMR spectra were recorded on a Varian XL-100 instrument and analyzed with a Varian spin simulation program. Electronic spectra were recorded on a JASCO Model UVIDEC-5A spectrometer and the mass spectra on a JEOL 01SG-2 spectrometer.

Preparation of (*Z*)- and (*E*)-2,4-Pentadienyltrimethylsilane. Preparation of pentadienylpotassium (**1b**) and its trimethylsilylation were carried out in essentially the same way as described before.[9b] Chlorotrimethylsilane (0.6 mL, 4.9 mmol) in THF (5 mL) was dropwise added over a 30-min period to the stirred THF (100 mL) solution of **1b** (0.5 g, 4.7 mmol) at −20 °C. The solution changed from orange to colorless at the equivalence point. The solution was concentrated to 20 mL by evaporation, and pentane (100 mL) was added to induce precipitation of the salt which then was removed by filtration. The pentane solution was distilled in vacuo to give (*Z*)-2,4-pentadienyltrimethylsilane (45 °C (6 mmHg)) in 70% isolated yield. The *Z*/*E* ratio was 94/6 as confirmed by gas chromatographic analysis.

(*E*)-2,4-Pentadienyltrimethylsilane was prepared by using THF-free powdered pentadienylpotassium obtained by heating the crystals of **1b** at 80 °C in vacuo (see ref 9b). To the suspension of THF-free **1b** (0.8 g, 7.5 mmol) in hexane (30 mL) was added chlorotrimethylsilane (1 mL, 7.6 mmol) dissolved in hexane (10 mL) at 0 °C over a 20-min period. The mixture was stirred for 6 h at 20 °C, and the resulting salt was removed by filtration. The hexane fraction was distilled in vacuo to give (*E*)-2,4-pentadienyltrimethylsilane (50 °C (7 mmHg)) in 85% yield. The content of the *E* isomer was 97–99%. Great care is necessary in handling the hexane dispersion of **1b** because of the flammability of THF-free **1b** in the air. Analytical data were given in ref 9b and 7a: UV (THF) λ_{max} 236 nm (ϵ_{max} 2.6 × 10^4).

Preparation of Monosilylated Anion 2a. To a stirred mixture of *n*-butyllithium (58 mL of 1.7 M hexane solution, 0.10 mol) and THF (58 mL) was added dropwise 2,4-pentadienyltrimethylsilane [14.0 g (17.5 mL), 0.10 mol] dissolved in THF (18 mL) at 0 °C over 30 min. The mixture was stirred for 1 h at ambient temperature. The resulting solution was evaporated to dryness, and the residue was washed with dry pentane (20 mL) twice at 0 °C to give **2a** as yellow solid. Recrystallization from THF–hexane at −20 °C gave **2a** as yellow crystals. Typical yield is 70% as determined by acid titration.

Preparation of Monosilylated Anion 2b. (*E*)- or (*Z*)-2,4-Dimethylpentadienyltrimethylsilane (8.8 mL, 50 mmol) was dropwise added at 0 °C to the potassium (1.0 g, 25 mmol) dispersed in a mixture of THF (10 mL, 125 mmol) and triethylamine (7 mL, 50 mmol). The mixture was stirred for 5 h at 25 °C and refluxed for 30 min to complete the reaction. The solution was evaporated to dryness, and the residue was washed twice with hexane (10 mL) to give **2b** as an orange powder. The yield was 90% based on potassium. One recrystallization from THF–hexane at −20 °C suffices for the purification of **2b**.

Preparation of (*E*,*E*)-1,5-Bis(trimethylsilyl)-1,3-pentadiene. To the THF (15 mL) solution of **2a** or **2b**,**c** (10 mmol) was added at 0 °C chlorotrimethylsilane (1.3 mL, 10 mmol) dissolved in THF (5.0 mL). After the usual workup, (*E*,*E*)-1,5-bis(trimethylsilyl)-1,3-pentadiene was separated by distillation. Yields from **2a** and **2b**,**c** were 92 and 95%, respectively: bp 98 °C (10 mmHg); mp 5 °C; ^1H NMR ($CDCl_3$) δ 6.47 (d of d, *J* = 7.7 Hz, CH), 5.94 (d of d, 1, *J* = 14.3 Hz, CH), 5.68 (d of t, 1, *J* = 7.7 Hz, CH), 5.58 (d, 1, *J* = 17.7 Hz, CH), 1.53 (d, 2, CH_2), 0.04 (s, 9, $SiCH_3$), −0.01 (s, 9, $SiCH_3$); mass spectrum (EI), *m*/*e* 212 (M^+); UV (THF) λ_{max} 249 nm (ϵ_{max} 2.6 × 10^4). Anal. Calcd for $C_{11}H_{24}Si_2$: C, 62.18; H, 11.38. Found: C, 62.16; H, 11.40.

Preparation of Di- and Trisilylated Anions 3a–c and 4. (1,5-Bis(trimethylsilyl)pentadienyl)lithium **3a** was prepared by the metalation of 1,5-bis(trimethylsilyl)-1,3-pentadiene with BuLi at 30 °C according to the procedure described for **2a**; yield 85%. Potassium and cesium analogues **3b** and **3c** were synthesized by direct metalation of 1,5-bis(trimethylsilyl)-1,3-pentadiene with potassium and cesium, respectively, in essentially the same way as described for **1b**; yield 92% based on the metal. (1,3,5-Tris(trimethylsilyl)pentadienyl)lithium (**4**) was prepared in 90% yield by a 1:1 reaction of 1,3,5-tris(trimethylsilyl)-1,3-pentadiene with butyllithium. All the anions were purified by recrystallization from THF–hexane at −20 °C.

Preparation of (*E*,*E*)-1,3,5-Tris(trimethylsilyl)-1,4-pentadiene. To a THF solution (12 mL) of 1,5-bis(trimethylsilyl)-pentadienyl anion (**3a**) (4.50 g, 20 mmol) or **3b** (20 mmol) was dropwise added at 0 °C chlorotrimethylsilane (2.4 mL, 22 mmol) dissolved in pentane (8 mL). After the solution was stirred for 1 h at 0 °C followed by filtration, the products were distilled in vacuo to give (*E*,*E*)-1,3,5-tris(trimethylsilyl)-1,4-pentadiene in 90% yield (99% GC yield). Regioselectivity was 98% as confirmed by GC: bp 80 °C (3 mmHg); IR (neat) 1593 (C=C), 1405, 1244 ($SiCH_3$), 993 (trans CH=CH), 838, 800 cm^{-1} ($SiCH_3$); ^1H NMR ($CDCl_3$) δ 6.07 (d of d, 2, *J* = 8.6 Hz, CH), 5.41 (d, 2, *J* = 18.7 Hz, CH), 2.51 (t, 1, CH), 0.02 (s, 18, $SiCH_3$), −0.06 (s, 9, $SiCH_3$); mass spectrum (EI), *m*/*e* 284 (M^+); UV (THF) λ_{max} 219 nm (ϵ_{max} 1.0 × 10^4). Anal. Calcd for $C_{14}H_{32}Si_3$: C, 59.07; H, 11.33. Found: C, 59.1; H, 11.39.

Preparation of 1,1,3,5- and 1,3,3,5-Tetrakis(trimethylsilyl)pentadienes. The medium effect was examined with THF and hexane as solvents. (a) To a mixture of **4** (1.2 g, 4 mmol) and THF (10 mL) was dropwise added at 0 °C chlorotrimethylsilane (0.45 mL, 4 mmol) diluted with THF (2 mL). After being stirred for 30 min and filtered, the solution was distilled to give 1,1,3,5-tetrakis(trimethylsilyl)-1,3-pentadiene in 90% yield (regioselectivity, 99%): bp 110 °C (1 mmHg); IR(neat) 1585, 1551 (C=C), 1407, 1250 ($SiCH_3$), 989 (trans C=C), 863, 840 ($SiCH_3$); ^{1}NMR ($CDCl_3$) δ 6.74 (d, 1, *J* = 19.8 Hz, CH), 5.76 (d, 1, *J* = 12.6 Hz, CH), 5.68 (d, 1, CH), 1.78 (d, 1, CH), 0.09 (s, 9, $SiCH_3$), 0.06 (s, 9, $SiCH_3$), 0.00 (s, 18, $SiCH_3$); mass spectrum (EI), *m*/*e* 356 (M^+); UV (THF) λ_{max} 262 nm (ϵ_{max} 2.8 × 10^4). Anal. Calcd for $C_{17}H_{40}Si_4$: C, 57.22; H, 11.30. Found: C, 56.88; H, 11.34. (b) To a mixture of **4** (4 mmol) and hexane (10 mL) was added at 0 °C chlorotrimethylsilane (0.5 mL). The solution was stirred for 1 h and distilled; bp 140 °C (3 mmHg). The distillate contained 1,3,3,5-tetrakis(trimethylsilyl)-1,4-pentadiene (45%) and 1,1,3,5-tetrakis(trimethylsilyl)-1,3-pentadiene (55%). ^1H NMR ($CDCl_3$) of the former: δ 6.14 (d, 2, *J* = 19.0 Hz, CH), 5.47 (d, 2, CH), 0.06 (s, 18, $SiCH_3$), 0.00 (s, 18, $SiCH_3$).

Alkylation of 2a and 3a. *tert*-Butyl bromide (1.0 mL, 8.0 mmol) was dissolved in THF (4 mL) and was dropwise added at 0 °C to the THF (8 mL) solution of **2a** (8 mmol) with magnetic stirring. The mixture was stirred for 1 h at 25 °C, and then ether (20 mL) was added. After separation of the salt by filtration, the ether fraction was distilled to give (3-*tert*-butyl-1,4-pentadienyl)trimethylsilane in 88% yield: bp 100 °C (25 mmHg); IR (neat) 1635, 1607 (C=C), 1245 ($SiCH_3$), 997 (trans CH=CH), 913 (CH_2=C), 864, 837 cm^{-1} ($SiCH_3$); NMR ($CDCl_3$) δ 5.99 (d of d, 1, *J* = 19.0 Hz, CH), 5.79 (d of d of d, 1, *J* = 8.0 Hz, CH), 5.55 (d, 1, CH), 4.98 (d of d, 1, *J* = 8.9 Hz, *J* = 3.2 Hz, =CH_2 cis), 4.92 (d of d, 1, *J* = 17.7 Hz, =CH_2 trans), 2.40 (t, 1, *J* = 8.0 Hz, CH), 0.82 (s, 9, CH_3), 0.00 (s, 9, $SiCH_3$); mass spectrum (EI), *m*/*e* 196 (M^+); UV (THF) λ_{max} 194 nm (ϵ_{max} 2.0 × 10^3). Anal. Calcd for $C_{12}H_{24}Si$: C, 73.38; H, 12.32. Found: C, 73.64; H, 12.37.

The reaction of **2a** with *sec*-butyl, isobutyl, or *n*-butyl bromide gave the following products, respectively, which are separated by preparative gas chromatography.

(3-*sec*-Butyl-1,4-pentadienyl)trimethylsilane: IR (neat) 1642, 1610 (C=C), 1244 ($SiCH_3$), 995 (trans CH=CH), 913 (CH_2=CH), 845, 837 cm^{-1} ($SiCH_3$); NMR ($CDCl_3$) δ 5.98 (d of d of d, 1, *J* = 17.5 Hz, 3.0 Hz, CH) 5.73 (d of d, 1, CH), 5.60 (d, 1, CH), 5.01 (d, 1, *J* = 9.7 Hz, =CH_2 cis), 4.97 (d, 1, *J* = 18.0 Hz, =CH_2 trans), 2.65 (d of d, 1, *J* = 6.8 Hz, CH), 1.45 (m, 3, CH, CH_2), 0.88 (m, 6, CH_3), 0.04 (s, 9, $SiMe_3$); mass spectrum, *m*/*e* 196 (M^+); UV (THF) λ_{max} 196 nm (ϵ_{max} 9 × 10^3). Anal. Calcd for $C_{12}H_{24}Si$: C, 73.38; H, 12.32. Found: C, 73.72; H, 12.32.

(3-Isobutyl-1,4-pentadienyl)trimethylsilane: IR (neat) 1637, 1611 (C=C), 1245 ($SiCH_3$), 992 (trans CH=CH), 912 (CH_2=CH), 868, 847 cm^{-1} ($SiCH_3$); NMR ($CDCl_3$) δ 5.88 (d of d, 1, *J* = 18.6 Hz, CH), 5.64 (d of d of d, 1, *J* = 8.0 Hz, CH), 5.58 (d, 1, CH), 4.95 (d, 1, *J* = 9.8 Hz, =CH_2 cis), 4.95 (d, 1, *J* = 17.7 Hz, =CH_2 trans), 2.79 (quint, 1, *J* = 8.0 Hz, CH), 1.59 (m, 1, CH), 1.26 (d of d, 2, *J* = 7.6 Hz, CH_2), 0.86 (d, 6, *J* = 6.6 Hz, CH_3); mass spectrum, *m*/*e* 196 (M^+); UV (THF) λ_{max} 194 nm (ϵ_{max} 6.0 × 10^3). Anal. Calcd for $C_{12}H_{24}Si$: C, 12.32; H, 73.38. Found: C, 12.37; H, 73.64.

(5-Isobutyl-1,3-pentadienyl)trimethylsilane: NMR ($CDCl_3$) δ 6.44 (d of d, 1, J = 9.5 Hz, CH), 6.02 (d of d, 1, J = 15.5 Hz, CH), 5.64 (d, 1, J = 17.8 Hz, CH), 5.66 (d of t, 1, J = 7.0 Hz, CH), 2.05 (m, 2, CH_2), 1.54 (m, 1, CH), 1.27 (m, 2, CH_2), 0.84 (d, 6, J = 6.8 Hz, CH_3), 0.00 (s, 9, $SiCH_3$); mass spectrum, m/e 196 (M^+).

(3-*n*-Butyl-1,4-pentadienyl)trimethylsilane: IR (neat) 1638, 1612 (C=C), 1245 ($SiCH_3$), 992 (trans CH=CH), 913 (CH_2=CH), 868, 838 cm^{-1} ($SiCH_3$); NMR ($CDCl_3$) δ 5.89 (d of d, 1, J = 19.2 Hz, CH), 5.70 (d of d of d, 1, J = 6, 3 Hz, CH), 5.55 (d, 1, CH), 4.95 (d, 1, J = 11.0 Hz, $=CH_2$ cis), 4.93 (d, 1, J = 16.3 Hz, $=CH_2$ trans), 2.65 (quint, 1, J = 6.3 Hz, CH), 1.30 (m, 6, CH_2), 0.76 (t, 3, J = 6.4 Hz, CH_3), 0.00 (s, 9, $SiCH_3$); mass spectrum, m/e 196 (M^+); UV (THF) λ_{max} 96 (ϵ_{max} nm 7.1 × 10^3). Anal. Calcd for $C_{12}H_{24}Si$: C, 73.38; H, 12.32. Found: C, 73.55; H, 12.24.

(1-*n*-Butyl-2,4-pentadienyl)trimethylsilane: NMR ($CDCl_3$) δ 6.27 (d of d of d, J = 10.0 Hz, CH), 5.87 (d of d, 1, J = 15.0 Hz, CH), 5.48 (d of d, 1, J = 8.3 Hz, CH), 4.95 (d, 1, J = 17.9 Hz, $=CH_2$ trans), 4.80 (d, 1, J = 10.6 Hz, $=CH_2$ cis), 1.33 (m, 6, CH_2), 0.83 (t, 3, J = 6.4 Hz, CH_3), 0.08 (s, 9, $SiCH_3$); mass spectrum, m/e 196 (M^+); UV (THF) λ_{max} 238 nm (ϵ_{max} 4.3 × 10^3). Anal. Calcd for $C_{12}H_{24}Si$: C, 73.38; H, 12.32. Found: C, 73.55; H, 12.29.

(5-*n*-Butyl-1,3-pentadienyl)trimethylsilane: NMR ($CDCl_3$) δ 6.45 (d of d, 1, J = 8.9 Hz, CH), 6.01 (d of d, 1, J = 14.8 Hz, CH), 5.65 (d, 1, J = 17.7 Hz, CH), 5.64 (d of d, 1, J = 6.3 Hz), 2.03 (m, 2, CH_2), 1.28 (m, 6, CH_2), 0.84 (t, 3, J = 6.5 Hz, CH_3), 0.01 (s, 9, $SiCH_3$); mass spectrum, m/e 196 (M^+).

The reaction of **3a** with *tert*-butyl, *sec*-butyl, isobutyl, and *n*-butyl bromides in THF at 25 °C for 3 h gave the following products.

3-*tert*-Butyl-1,5-bis(trimethylsilyl)-1,4-pentadiene: bp 110 °C (5 mmHg); IR (neat) 1602 (C=C), 1245 ($SiCH_3$), 995 (trans CH=CH), 865, 836 cm^{-1} ($SiCH_3$); NMR ($CDCl_3$) δ 6.05 (d of d, 2, J = 7.9 Hz, CH), 5.58 (d, 2, J = 18.9 Hz, CH), 2.47 (t, 1, CH), 0.87 (s, 9, *t*-Bu), 0.06 (s, 18, $SiCH_3$); mass spectrum, m/e 268 (M^+). Anal. Calcd for $C_{15}H_{32}Si_2$: C, 67.08; H, 12.01. Found: C, 67.39; H, 12.06.

3-*sec*-Butyl-1,5-bis(trimethylsilyl)-1,4-pentadiene: IR (neat) 1605 (C=C), 1248 ($SiCH_3$), 993 (trans CH=CH), 865, 837 cm^{-1} ($SiCH_3$); NMR ($CDCl_3$) δ 5.97 (d of d of d, 2, J = 6.7 Hz, 2.2 Hz, CH), 5.58 (d, 2, J = 18.2 Hz, CH), 2.65 (m, 1, CH), 1.52 (m, 3, CH, CH_2), 0.87 (m, 6, CH_3), 0.05 (s, 18, $SiCH_3$); mass spectrum, m/e 268 (M^+). Anal. Calcd for $C_{15}H_{32}Si_2$: C, 67.08; H, 12.01. Found: C, 67.39; H, 11.92.

3-Isobutyl-1,5-bis(trimethylsilyl)-1,4-pentadiene: IR (neat) 1604 (C=C), 1244 ($SiCH_3$), 990 (trans CH=CH), 867, 837 cm^{-1} ($SiCH_3$); NMR ($CDCl_3$) δ 5.87 (d of d, 2, J = 6.5 Hz, CH), 5.57 (d, 2, J = 18.5 Hz, CH), 2.80 (m, 1, CH), 1.62 (m, 1, CH), 1.26 (m, 2, CH_2), 0.86 (d, 6, J = 6.5 Hz, CH_3), 0.03 (s, 18, $SiMe_3$); mass spectrum, m/e 268 (M^+). Anal. Calcd for $C_{15}H_{32}Si_2$: C, 67.08; H, 12.01. Found: C, 67.43; H, 12.04.

3-*n*-Butyl-1,5-bis(trimethylsilyl)-1,4-pentadiene: IR (neat) 1605 (C=C), 1244 ($SiCH_3$), 990 (trans CH=CH), 865, 838 cm^{-1} ($SiCH_3$); NMR ($CDCl_3$) δ 5.90 (d of d, 2, J = 6.6 Hz, CH), 5.56 (d, 2, J = 18.0 Hz, CH), 2.68 (quint, 1, J = 6.6 Hz, CH), 1.29 (m, 6, CH_2), 0.88 (t, 3, J = 6.0 Hz, CH_3) 0.04 (s, 18, $SiCH_3$); mass spectrum, m/e 268 (M^+). Anal. Calcd for $C_{15}H_{32}Si_2$: C, 67.08; H, 12.01. Found: C, 67.29, H, 12.03.

1-*n*-Butyl-1,5-bis(trimethylsilyl)-2,4-pentadiene: IR (neat) 1628, 1573 (C=C), 1243 ($SiCH_3$), 999 (trans CH=CH), 867, 837 cm^{-1} ($SiCH_3$); NMR ($CDCl_3$) δ 6.46 (d of d, 1, J = 9.2 Hz, CH), 5.90 (d of d, 1, J = 14.8 Hz, CH), 5.55 (d, 1, J = 18.2 Hz, CH), 5.51 (d of d, 1, J = 8.2 Hz, CH), 1.35 (m, 7, CH_2, CH), 0.86 (t, 3, J = 6.2 Hz, CH_3), 0.03 (s, 9, $SiCH_3$), −0.06 (s, 9, $SiCH_3$); mass spectrum, m/e 268 (M^+). Anal. Calcd for $C_{15}H_{32}Si_2$: C, 67.08; H, 12.01. Found: C, 67.33; H, 12.05.

Protonation of 2a and 3a. To the THF (4 mL) solution of **2a** or **3a** (4 mmol) was added at 0 °C a protic agent (0.1 mL, 5.5 mmol) dissolved in THF (1 mL). After the usual workup, the products were distilled and then separated with preparative gas chromatography. The structure of the products was analyzed with reference to the spectral data described above.

Registry No. **1a**, 54932-98-0; **1b**, 51391-25-4; **2a**, 75150-96-8; **2b**, 83573-32-4; **2c**, 83573-37-9; **3a**, 83573-33-5; **3b**, 83573-34-6; **3c**, 83573-35-7; **4**, 83573-36-8; **5a** (R = *t*-C_4H_9, R′ = H), 83573-40-4; **5a** (R = *sec*-C_4H_9, R′ = H), 83573-41-5; **5a** (R = *i*-C_4H_9, R′ = H), 83573-42-6; **5a** (R = *n*-C_4H_9, R′ = H), 83573-44-8; **5b** (R = *i*-C_4H_9, R′ = H), 83573-43-7; **5b** (R = *n*-C_4H_9, R′ = H), 70960-90-6; **5c** (R = *n*-C_4H_9, R′ = H), 83573-45-9; **6a** (R = *t*-C_4H_9, R′ = Me_3Si), 83573-46-0; **6a** (R = *sec*-C_4H_9, R′ = Me_3Si), 83573-47-1; **6a** (R = *i*-C_4H_9, R′ = Me_3Si), 83573-48-2; **6a** (R = *n*-C_4H_9, R′ = Me_3Si), 83573-49-3; **6b** [R = *n*-C_4H_9, R′ = Me_3Si), 83573-50-6; **7a**, 72952-73-9; **7b**, 83573-51-7; **8a**, 71813-99-5; Ph_3COH, 76-84-6; Ph_2CHOH, 91-01-0; $(CH_3)_3COH$, 75-65-0; H_2O, 7732-18-5; Me_3SiCl, 75-77-4; BuLi, 109-72-8; K, 7440-09-7; Ce, 7440-46-2; *t*-C_4H_9Br, 507-19-7; *sec*-C_4H_9Br, 78-76-2; *i*-C_4H_9Br, 78-77-3; *n*-C_4H_9Br, 109-65-9; (*Z*)-2,4-pentadienyltrimethylsilane, 73400-23-4; (*E*,*E*)-1,3,5-tris(trimethylsilyl)-1,4-pentadiene, 83585-37-9; 1,1,3,5-tetrakis(trimethylsilyl)pentadiene, 83573-38-0; 1,3,3,5-tetrakis(trimethylsilyl)pentadiene, 83573-39-1.

Synthesis, Structure, and Fluxional Behavior of [1-4-η-*exo*-7-(R_3E)-cyclohepta-1,3,5-triene]tricarbonyliron (R_3E = Me_3Si, Me_3Ge, and Ph_3Ge)

L. K. K. LiShingMan,[1a] Johannes G. A. Reuvers,[1a] Josef Takats,*[1a] and Giulio Deganello[1b]

Department of Chemistry, University of Alberta, Edmonton, Alberta, Canada T6G 2G2, and Istituto di Chimica Generale ed Inorganica, Facoltà di Scienze dell'Università, 90123 Palermo, Italy

Received July 19, 1982

The reaction of $[C_7H_7Fe(CO)_3]^-$ with group 4A electrophiles yields ring-substituted (cycloheptatriene)tricarbonyliron complexes $[1\text{-}4\text{-}\eta\text{-}7\text{-}(R_3E)C_7H_7]Fe(CO)_3$ (E = Si, R = Me, **2a**; E = Ge, R = Me, **2b**; E = Ge, R = Ph, **2c**). Unambiguous assignment of the stereochemistry of the substituents at C(7) on the basis of ^1H NMR and mass spectra of the molecules was not feasible. The orientation of the R_3E groups was shown to be exo by single-crystal X-ray crystallography on **2c**. Crystal data: monoclinic, $P2_1/n$; a = 7.0699 (7) Å, b = 28.634 (2) Å, c = 12.154 (2) Å, β = 103.26 (1)°; Z = 4, ρ_{calcd} = 1.48 g/cm^3. Full-matrix least-squares refinement on 2768 reflections, $F_o^2 > 3\sigma(F_o^2)$, gave R_1 = 0.026 and R_2 = 0.033. Analysis of the bond distances showed a significantly stronger and more asymmetric metal–diene bonding in **2c** than in unsubstituted (cycloheptatriene)tricarbonyliron (CHT = cycloheptatriene), the asymmetry manifesting in a movement of the $Fe(CO)_3$ group toward the C(3)–C(4) bond. The molecules exhibit surprisingly facile oscillation of the $Fe(CO)_3$ moiety which was probed by variable-temperature ^1H and ^{13}C NMR spectroscopy and ^{13}C NMR spin saturation transfer experiments. The values of $\Delta G^{\ddagger}$ are approximately 75 kJ mol^{-1} for all three compounds. Possible pathways for the rearrangement are explored, and on the basis of ^{13}CO incorporation and PPh_3 substitution studies, the molecular structure of **2c**, the remarkable lowering of $\Delta G^{\ddagger}$ relative to $(CHT)Fe(CO)_3$, and comparison with activation barriers in other substituted $(CHT)Fe(CO)_3$ derivatives, it is concluded that direct 1,3-iron shift is most appropriate in describing the mechanism of fluxionality.

Introduction

The preparation of $[C_7H_7Fe(CO)_3]^-$ (1) in 1971 by Maltz and Kelly[2] provided yet another excellent example of the stability imparted upon a reactive organic ligand by the $Fe(CO)_3$ unit.[3] The free anion $(C_7H_7)^-$ is not easily prepared and, as expected from its antiaromatic nature, is rather unstable.[4] As a result, the cycloheptatrienide anion has received only scant attention for the synthesis of organic derivatives of the type C_7H_7R and has yet to be used as a precursor to cycloheptatrienyl derivatives of the transition metals.

In contrast, 1 can be prepared easily by the deprotonation of $(\eta^4\text{-}C_7H_8)Fe(CO)_3$ with a variety of strong bases (eq 1).

$$\underset{\text{yellow}}{(\eta^4\text{-}C_7H_8)Fe(CO)_3} \xrightarrow[\text{THF}]{\text{base}} \underset{\text{red}}{[C_7H_7Fe(CO)_3]^-} \qquad (1)$$

base = *n*-BuLi (−60 °C), KH (25° °C), K-*t*-BuO (25 °C)

Although air-sensitive solutions of 1 in THF can be kept under pure nitrogen at room temperature for long periods of time, the bis(triphenylphosphine)nitrogen(1+) salt (PPN^+) is stable enough to be handled briefly in air.

There are two bonding alternatives that can be written for 1 which satisfy the 18-electron rule. In structure **1a** the $Fe(CO)_3$ moiety is bonded to an η^4-diene unit with the negative charge formally localized on the allyl part of the seven-membered ring. Structure **1b** corresponds to an $(\eta^3$-allyl$)Fe(CO)_3$ unit carrying the negative charge, while the remaining diene fragment of the ring remains uncoordinated to the metal. A recent X-ray crystallographic study[5] has revealed form **1b** as the preferred bonding mode of the anion in the solid state. This result is in accord with molecular orbital calculations[6] which predicted form **1b** to be more stable than **1a**. However, the energy difference between the two bonding modes was calculated to be very small, ~14 kJ mol^{-1}, and this last result is in agreement with the highly nonrigid character of 1. The room-temperature ^1H NMR spectrum of 1 shows a sharp singlet for the seven-ring protons at δ 4.90 which coalesces only at −140 °C and remains in the base line down to −160 °C.[7] The rearrangement of 1 probably proceeds by rapid 1,2 shifts of the $Fe(CO)_3$ moiety which, based on the aforementioned theoretical study, may involve the intermediacy of form **1a**.

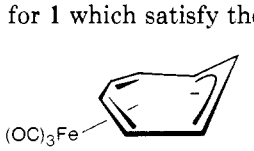

1a

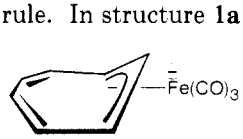

1b

A final point of interest concerns the reactivity of 1. Irrespective of the solution structure of 1, exclusively **1b** or an equilibrium mixture of **1a** and **1b**, the anion can be looked upon as an ambident nucleophile capable of reacting both at the iron center and/or at the ring carbon atoms. Indeed, this dual characteristic of 1 toward electrophiles has been observed already. Takats et al. have reported[8] that 1 reacts with transition-metal carbonyl halides to form heterodimetallic cycloheptatrienyl complexes of the type $(\eta\text{-}C_7H_7)Fe(CO)_3M(CO)_x$ (M = Mn, Re, x = 3; M = Rh, x = 2). These complexes contain a met-

(1) (a) University of Alberta. (b) Università di Palermo.
(2) Maltz, H.; Kelly, B. A. *J. Chem. Soc., Chem. Commun.* **1971**, 1390.
(3) (a) Landesberg, J. M. In "The Organic Chemistry of Iron"; Koerner von Gustorf, E. A., Grevels, F.-W; Fischler, I., Eds.; Academic Press: New York, 1978; Vol. 1, p 627. (b) Deganello, G. "Transition Metal Complexes of Cyclic Polyolefins"; Academic Press: New York, 1979.
(4) (a) Dauben, H. J.; Rifi, M. R. *J. Am. Chem. Soc.* **1963**, *85*, 3041. (b) Doering, W. E.; Gaspar, P. P. *J. Am. Chem. Soc.* **1963**, *85*, 3043.
(5) Sepp, E.; Pürzer, A.; Thiele, G.; Behrens, H. *Z. Naturforsch., B: Anorg. Chem., Org. Chem.* **1978**, *33B*, 261.
(6) Hofmann, P. *Z. Naturforsch., B: Anorg. Chem., Org. Chem.* **1978**, *33B*, 251.
(7) The variable-temperature 100-MHz ^1H NMR spectrum was recorded in a 4:1 mixture of $CHFCl_2/CD_2Cl_2$ by using the more stable and more soluble $PPN^+[C_7H_7Fe(CO)_3]^-$: Henderson-Lypkie, J.; Reuvers, J. G. A.; Takats, J. unpublished observations.
(8) Bennett, M. J.; Pratt, J. L.; Simpson, K. A.; LiShingMan, L. K. K.; Takats, J. *J. Am. Chem. Soc.* **1976**, *98*, 4810.

0276-7333/83/2302-0028$01.50/0

al–metal bond with both metal carbonyl moieties coordinated to the same face of the seven-membered ring and thus formally arise from nucleophilic displacement of the halide ion in $M(CO)_xX$ by the iron center of 1. In contrast the reactions with Me_3SiCl and Me_3GeBr were reported to proceed by carbon attack with concomitant formation of $[1\text{-}4\text{-}\eta\text{-}7\text{-}(R_3E)C_7H_7]Fe(CO)_3$ (2) complexes.[9] Similar ring attack has been observed by Deganello et al.[10] in the reaction of 1 with $[C_7H_7M(CO)_3]^+$ (M = Cr, Mo, W, Fe) and by Behrens et al.[11] with RCOCl, Et_3SiCl, Et_3GeCl, and $[C_6H_7Fe(CO)_3]^+$.

It is the purpose of this article to describe completely the synthesis and characterization of the complexes obtained from the reaction of 1 and group 4A electrophiles, R_3EX (E = Si, X = Cl, R = Me; E = Ge, X = Br, R = Ph and Me), to discuss the solid-state structure and fluxional behavior of the compounds.

Experimental Section

All experimental procedures were performed in standard Schlenk ware under a static atmosphere of rigorously purified nitrogen.[8] All solvents were dried by refluxing under nitrogen with the appropriate drying agent and distilled just prior to use.

Pentacarbonyliron (Ventron Corp.) was filtered, while cycloheptatriene (Aldrich) was distilled before use. All other chemicals were either prepared according to literature procedures or purchased from commercial sources and used as received.

Infrared spectra were obtained with a Perkin-Elmer 337 grating spectrophotometer and were recorded in expanded form on a Hewlett-Packard 7127A recorder. The spectra were measured in matched NaCl or KBr cells and were calibrated with gaseous carbon monoxide.

Proton magnetic resonance spectra were obtained on the following spectrometers: Varian HA-100 (32 °C), Varian HA-100 Digilab (32 °C), and Perkin-Elmer R-32 (35 °C). Variable-temperature spectra were recorded on the Varian HA-100 or the Varian HA-100 Digilab spectrometers, using sealed or serum-capped NMR tubes. Temperature calibration was achieved with a copper/Constantan thermocouple with one junction immersed in ice water and the other in the NMR probe below the sample tube. The ^1H NMR chemical shifts were measured relative to Me_4Si or to the internal solvent resonance. The following conversions were used: $\delta_{Me_4Si} = \delta_{CH_2Cl_2} - 5.32$, $\delta_{Me_4Si} = \delta_{C_6D_5CHD_2} - 2.09$, and $\delta_{Me_4Si} = \delta_{THF(H_{2,5})} - 3.58$.

Carbon-13 NMR spectra were recorded on a deuterium-lock Bruker HFX-90/Nicolet 1085 FT or a Bruker WP-60 FT spectrometer. The former operates at 22.628 MHZ, the latter at 15.086 MHz. For variable-temperature work, depending on the solvent and the temperature, serum-capped or sealed 10-mm tubes were employed. Temperature measurements and calibration were made with a Bruker temperature control unit, Model B-5T 100/700, and are believed to be accurate to ±1 K. The ^{13}C NMR chemical shifts were measured relative to Me_4Si or to the internal solvent resonance. In the latter case the following conversion were used: $\delta_{Me_4Si} = \delta_{CHDCl_2} - 53.63$, $\delta_{Me_4Si} = \delta_{THF(C_{2,5})} - 68.05$, and $\delta_{Me_4Si} = \delta_{C_6D_5CD_3} - 20.4$.

Forsén–Hoffmann experiments were carried out as described in the text. Good reviews of the experimental procedures, the assumptions involved, and the sources of error are available.[12] A time interval of at least $5T_1$ was applied between pulses.

Mass spectra were recorded on an Associated Electrical Industries MS-12 mass spectrometer, usually operating at 70 eV. The samples were introduced into the ion source by using the direct inlet technique at a temperature just sufficient to record the data. Field ionization mass spectra were recorded on an AEI-MS-9 spectrometer. The intensity ratios within the clusters were calculated by using the computer program "ISOC", written by Drs. R. S. Gay and E. H. Brooks, University of Alberta.

Melting points are uncorrected and were determined on a Thomas-Hoover apparatus on samples which were sealed in a capillary.

Analyses were performed by the Microanalytical Laboratory of this department or at the Analytische Laboratorien, Engelskirchen, West Germany.

Preparation of Potassium Cycloheptatrienyltricarbonylferrate(1−). Extremely air-sensitive solutions of 1 were prepared by dropwise addition of a THF solution of $CHTFe(CO)_3$ to a slurry of KH or K-t-BuO in the same solvent. The formation of 1 is conveniently followed by infrared spectroscopy. The absorption bands due to $CHTFe(CO)_3$ (2048 (s), 1974 (s, br) cm^{-1} in THF) rapidly decrease in intensity while new intense bands of 1 appear at 1942 (vs) and 1868 (vs, br) cm^{-1}. With KH the reaction is complete in approximately 1–2 h, K-*t*-BuO requires longer reaction times.

If desired, filtration followed by removal of all volatile components under vacuum leaves 1 as a red, pyrophoric solid. ^1H NMR spectrum in THF-d_8 shows the presence of one molecule of THF per anion even after prolonged vacuum drying at room temperature.

The extreme air sensitivity of the anion prevented its characterization by elemental analysis. However, the spectroscopic measurements conclusively prove its formation, and we believe the absence of other peaks in the IR and NMR spectra bespeak for its purity. In subsequent reactions it was assumed that anion 1 is formed quantitatively with no other iron-containing byproducts being present.

Although the use of commercial KH is more cumbersome than that of K-*t*-BuO,[13] it is the deprotonating reagent of choice. The other product of the reaction, dihydrogen gas, evolves from solution leaving nothing but pure 1 behind. On the other hand, with K-*t*-BuO, the also formed *t*-BuOH apparently can inhibit some reactions of 1. For instance, almost no yield of the $SiMe_3$-substituted compound was obtained when K-*t*-BuO is used to form 1, no such difficulties were encountered with KH.

Preparation of (7-Triphenylgermylcycloheptatriene)tricarbonyliron, 2c. A solution of 1 (0.0476 mol in 140 mL of THF) was added dropwise over a period of 2 h to a magnetically stirred solution of 18.25 g (0.0476 mol) of Ph_3GeBr in 60 mL of THF. As the reaction proceeded the deep red color of the anion rapidly disappeared. The mixture was stirred for an additional 4 h to ensure completion of the reaction. Potassium bromide was allowed to settle and the greenish brown supernatant solution filtered; solvent was removed in vacuo, yielding a yellow-brown oily substance which solidified upon prolonged drying. The residue was stirred for 4 h at room temperature with 100 mL of hexane, the hexane removed with a syringe, and the residue dried to give 21.4 g of yellow solid. The solid was Soxhlet extracted with 200 mL of pentane for 5 h. Cooling the mixture to room temperature followed by filtration and drying gave 16.7 g (65% yield) of pure **2c** as a bright yellow solid.

Various amounts of bis(triphenylgermyl) ether, $Ph_3GeOGePh_3$, were obtained, in this reaction. All attempts to separate $Ph_3GeOGePh_3$ and **2c** chromatographically (alumina of activity II, florisil) failed. Only fractional crystallization from hexane or the sequence hexane washing and Soxhlet extraction described above proved successful in obtaining pure products (as evidenced by a correct integration ratio in the ^1H NMR spectra, phenyl/ring

(9) LiShingMan, L. K. K.; Takats, J. *J. Organomet. Chem.* **1976**, *117*, C104.

(10) (a) Deganello, G.; Boschi, T.; Toniolo, L. *J. Organomet. Chem.* **1975**, *97*, C46. (b) Airoldi, M.; Deganello, G.; Dia, G.; Saccone, P.; Takats, J. *Inorg. Chim. Acta* **1980**, *41*, 171.

(11) (a) Moll, M.; Behrens, H.; Kellner, R.; Knöckel, H.; Würstl, P. *Z. Naturforsch., B: Anorg. Chem., Org. Chem.* **1976**, *31B*, 1019. (b) Moll, M.; Würstl, P.; Behrens, H.; Merbach, P. *Ibid.* **1978**, *33B*, 1304.

(12) (a) Hoffman, R. A.; Forsen, S. *Prog. Nucl. Magn. Reson. Spectrosc.* **1966**, *1*, 15. (b) Faller, J. W. In "Determination of Organic Structures by Physical Methods"; Zuckermann, J. J., Nachod, F. C., Eds.; Academic Press: New York, 1973; Vol. 5. (c) Mann, B. E. *J. Magn. Reson.* **1976**, *21*, 17. (d) Mann, B. E. *Prog. Nucl. Magn. Reson. Spectrosc.* **1977**, *11*, 95.

(13) Commercial KH is freed from paraffin oil by twice washing with petroleum ether and dried in vacuo. To ensure the success of the deprotonation excess of KH is used, routinely twofold stoichiometric amounts were employed. At the completion of the reaction, excess KH is filtered or alternatively the solution is allowed to settle and the required volume of 1 is carefully removed with an air-tight syringe. Freshly sublimed K-*t*-BuO is used in stoichiometric amounts, and when possible, the so-obtained solution of 1 used directly.

= 15/7, and the absence of $Ph_3GeOGePh_3$ in the mass spectra): IR (cyclohexane) ν_{CO} 2046 (s), 1978 (s), 1965 (s) cm^{-1}. Anal. Calcd for $C_{28}H_{22}O_3GeFe$: C, 62.92; H, 4.12. Found: C, 62.98; H, 4.18.

Preparation of (7-$Me_3SiC_7H_7$)$Fe(CO)_3$, 2a, and (7-$Me_3GeC_7H_7$)$Fe(CO)_3$, 2b. These compounds were synthesized according to the procedure outlined above for **2c**. No traces of $Me_3SiOSiMe_3$ or $Me_3GeOGeMe_3$ were encountered; however, various amounts of the dimeric $[C_7H_7Fe(CO)_3]_2$ were also obtained. The latter was separated from **2a** and **2b** by chromatography on alumina of activity II. Crystallization from pentane at −78 °C gave yellow crystals of **2a** and **2b** in 50% yield. If necessary, the materials can be further purified by sublimation at 50 °C and 10^{-3} mmHg. **2a**: IR (cyclohexane) ν_{CO} 2044 (s), 1983 (s), 1969 (s) cm^{-1}. Anal. Calcd for $C_{13}H_{16}O_3SiFe$: C, 51.33; H, 5.30. Found: C, 51.61; H, 5.40. **2b**: IR (cyclohexane) ν_{CO} 2043 (s), 1982 (s), 1968 (s) cm^{-1}. Anal. Calcd for $C_{13}H_{16}O_3GeFe$: C, 44.78; H, 4.63. Found: C, 44.96; H, 4.65.

The Interaction of $[C_7H_7Fe(CO_3]^-$ with Chlorotriphenylsilane. A 4.74-mmol sample of $[C_7H_7Fe(CO)_3]^-$ in 20 mL of THF was added dropwise to chlorotriphenylsilane (1.55 g, 5.23 mmol) in 20 mL of THF at ambient temperature. The red color of the anion persisted and infrared spectra showed the continued presence of $[C_7H_7Fe(CO)_3]^-$.

The Interaction of $[C_7H_7Fe(CO)_3]^-$ with Me_3SiCH_2Cl. A 14.28-mmol sample of $[C_7H_7Fe(CO)_3]^-$ in 60 mL of THF was slowly added over a period of 3 h to a magnetically stirred solution of Me_3SiCH_2Cl (2.1 mL, 1.85 g, 20.0 mmol) in 60 mL of THF. No color change was observed. After the solution was stirred for 24 h at ambient temperature, infrared spectra indicated the presence of **1** only.

Attempted Exchange of ^{13}CO with 2. **2a** and **2c** were heated in toluene for 24 h under an atmosphere of ^{13}CO. No ^{13}CO enrichment was observed as evidenced by IR and mass spectral analyses.

X-ray Diffraction Study of 2c. A yellow crystal of (7-$Ph_3GeC_7H_7$)$Fe(CO)_3$, **2c**, having approximate dimensions of 0.14 × 0.18 × 0.35 mm was secured to a glass fiber and mounted in a nonspecific orientation on an Enraf-Nonius CAD4 computer controlled diffractometer. All intensity measurements were performed by using Mo Kα radiation (λ = 0.710 73 Å) with a graphite crystal, incident beam monochromator. Preliminary measurements showed the crystal to be monoclinic and from the systematic absences of $h0l$, $h + l = 2n + 1$, and $0k0$, $k = 2n + 1$, the space group was determined to be $P2_1/n$, an alternative setting of $P2_1/c$ with the equivalent positions $\pm(x, y, z; {}^1/_2 + x, {}^1/_2 - y, {}^1/_2 + z)$.[14] Cell constants were obtained from a least-squares refinement of the setting angles of 25 reflections in the range $29 < 2\theta < 36°$. The cell constants and calculated volume are a = 7.0699 (7) Å, b = 28.634 (2) Å, c = 12.154 (2) Å, β = 103.26 (1)°, V = 2394.8 Å^3. For Z = 4 and fw = 534.324 the calculated density is 1.48 cm^{-1}.

The data were collected at room temperature using an ω–2θ scan ranging in speed from 0.7 to 10 deg min^{-1} (in ω). The variable scan rate was adjusted to give $\sigma(I)/I \leq 0.03$ within a time limit of 100 s in order to achieve optimum counting statistics for both intense and weak reflections in a minimum time. The scan range and aperture width were determined as a function of θ to compensate for the α_1–α_2 dispersion: ω scan width = (0.75 + 0.35 tan θ)° and aperture width = (2.0 + 0.5 tan θ) mm. Peak backgrounds were measured by extending the scan 25% on either side of the calculated range to give a peak to background counting time of 2:1. Intensity measurements were made on reflections of the type $h,k,\pm l$ to a 2θ limit of 55°. Three reflections were remeasured every 60 min of exposure time to check on crystal and electronic stability over the course of data collection. These intensities remained constant within experimental error. A total of 6013 unique reflections were collected, and these were corrected for Lorentz, polarization, and background effects to give 2768 reflections with $F_o^2 \geq 3\sigma(F_o^2)$ which were used in the structure solution and refinement. The following relationships were used: $F_o^2 = SR(SC - R*B)/Lp$ and $\sigma^2(F_o^2) = [SR(SC + R^2B) + (pF_o^2)^2]/Lp^2$, where SR is the scan rate, SC is the total scan count, R is the ratio of scan time to background time, B is the total background count, p is a factor to downweight intense reflections (chosen as 0.04 in this experiment), and Lp is the Lorentz–polarization correction term.

The structure was solved by using the direct methods program MULTAN[15] which gave positional parameters for the Ge and Fe atoms. The remaining non-hydrogen atoms were located by the usual combination of least-squares refinement and difference Fourier synthesis. Refinement of atomic parameters was carried out by using full-matrix least-squares techniques on F_o minimizing the function $\sum w(|F_o| - |F_c|)^2$ where $|F_o|$ and $|F_c|$ are the observed and calculated structure factor amplitudes, respectively, and the weighting factor w is given by $w = 4F_o^2/\sigma^2(F_o^2)$. The neutral atom scattering factors were calculated from the analytical expression for the scattering factor curves.[16] The f' and f'' components of anomalous dispersion were those of Cromer and Liberman[17] and were included in the calculations for the Ge and Fe atoms. Preliminary refinement of the model in which all non-hydrogen atoms were present with isotropic thermal parameters gave agreement factors of $R_1 = \sum||F_o| - |F_c||/\sum|F_o| = 0.063$ and $R_2 = [\sum w(|F_o| - |F_c|)^2/\sum wF_o^2]^{1/2} = 0.082$. All 22 H atoms were located in a subsequent difference Fourier. The hydrogens of the seven-membered ring had their positional and isotropic thermal parameters refined in subsequent cycles while the phenyl H atoms were included as fixed contributions to the structure factors at "idealized" calculated positions (C–H = 0.95 Å, sp^2 geometry). In the final cycle 326 parameters were refined by using 2768 observations to give agreement factors of $R_1 = 0.026$ and $R_2 = 0.033$. The largest shift in any parameter was 0.5 times its estimated standard deviation and was associated with the thermal parameter of HC(1). The error in an observation of unit weight is 0.96 e. The largest peak in a difference Fourier calculated from the final structure factors was 0.4 e Å^{-3} and located at the fractional coordinates 0.51, 0.26, and 0.13. Final positional and thermal parameters are tabulated in Table III.

Results and Discussion

Synthetic and Spectral Studies. The reaction of **1** with Me_3SiCl, Me_3GeBr, and Ph_3GeBr(R_3EX) in THF at ambient temperature gives, after workup, moderate yields of yellow crystalline solids. On the basis of their characteristic IR and NMR spectra, vide infra, the complexes are assigned structure **2**, eq 2, instead of the isomeric form **3**

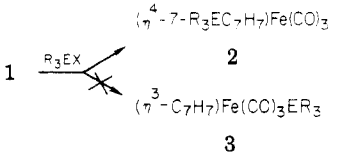

(2)

which could also arise from the known ambident nucleophilic character of **1**. The compounds are soluble in common organic solvents giving moderately air-sensitive solutions. However, the solid complexes can be handled in air for several days without apparent decomposition and they can be stored at room temperature under nitrogen.

In contrast to these electrophiles, no reaction was observed between **1** and Ph_3SiCl and Me_3SiCH_2Cl. The failure of Ph_3SiCl to react is, by itself, not surprising since similar behavior toward other transition-metal carbonylates has been observed already by Graham et al.[18] However, the additional lack of reaction toward Me_3SiCH_2Cl, coupled with the fact that the so far reported

(14) "International Tables for X-ray Crystallography"; Kynoch Press: Burmingham, England, 1969; Vol. I.

(15) The computer programs used include locally written ones and versions of MULTAN 78 by P. Main, ORFE by W. R. Busing, K. O. Martin, and H. A. Levy, NUCLS by J. A. Ibers, FORDAP by A. Zalkin, and ORTEP II by C. K. Johnson.

(16) "International Tables for X-ray Crystallography"; Kynoch Press: Birmingham, England, 1974; Vol. IV, p 99.

(17) Cromer, D. T.; Liberman, D. L. *J. Chem. Phys.* **1970**, *53*, 1891.

(18) Ph_3SiCl did not react with $[C_7H_7Mo(CO)_2]^-$: Isaacs, E. E.; Graham, W. A. G. *Can. J. Chem.* **1975**, *53*, 975, and with $[C_3H_5Fe(CO)_3]^-$: N. O. Okamoto, Ph.D. Thesis, University of Alberta, 1971, and failed to give the expected product with $[Mn(CO)_5]^-$: Jetz, W.; Simons, P. B.; Thompson, J. A. J.; Graham, W. A. G. *Inorg. Chem.* **1966**, *5*, 2217.

Table I. ^1H and ^{13}C NMR Data[a] of $(1\text{-}4\text{-}\eta\text{-}7\text{-}R_3EC_7H_7)Fe(CO)_3$ (2a, $SiMe_3$; 2b, $GeMe_3$; 2c, $GePh_3$)

	assign[b]								
compd	H(1)	H(2)	H(3)	H(4)	H(5)	H(6)	H(7)	Me/Ph	solvent
2a	3.36	4.37-4.48		2.97	5.56	5.10	1.68	−0.10	toluene
2b	3.41	4.34-4.59		2.96	5.51	5.02	1.81	−0.10	toluene
2c	3.75	4.06-4.42		2.80	5.56-5.26		2.94	7.50-7.25	toluene

	assign[b]										
compd	C(1)	C(2)	C(3)	C(4)	C(5)	C(6)	C(7)	Ph	CO	Me	solvent
2a	67.0	84.8	91.4	59.6	126.0	128.3	35.5		213.3	−2.5	toluene
2b	67.4	84.4	91.7	59.2	125.6	128.5	36.4		212.4	−2.6	n-decane
2c	65.8	85.4	91.8	58.6	*c*	*c*	36.2	127.0-136.4	212.5		toluene

[a] Chemical shifts (δ) in ppm from Me_4Si by appropriate conversion from internal solvent references. [b] Assignments are based on homonuclear (^1H) and heteronuclear (^{13}C) decoupling experiments. The overlapping of the H(2) and H(3) signals precludes the application of this technique to differentiate between C(2) and C(3); this ambiguity was resolved in the Forsen-Hoffman spin-saturation transfer experiment[12] on compound **2c** (see text). [c] The resonances due to C(5) and C(6) are obscured by the phenyl resonances in **2c**.

reactions of **1** all involved strong electrophiles, bespeaks for only moderate nucleophilic power for **1**. The presence of the seven-membered ring and the concomitant delocalization of the negative charge are not inconsistent with this observation.

The infrared spectra of the complexes exhibit three strong absorption bands in the terminal carbonyl region (see Experimental Section). Two of the bands are only separated by 13 cm^{-1} and are reminescent of the doubly degenerate E stretching mode of an $Fe(CO)_3$ moiety under local C_{3v} symmetry. The appearance of the spectra is quite compatible with structure **2** for the compounds but can not be reconciled with structural isomer **3** for which three well separated bands are expected ($Fe(CO)_3$ having C_s local symmetry) and found experimentally.[19]

Confirmation and unequivocal proof for structure **2** (**2a**, $SiMe_3$; **2b**, $GeMe_3$; **2c**, $GePh_3$) come from the room-temperature ^1H and ^{13}C NMR spectra of the compounds. The complicated nature of the spectra, Table I and Figure 1, is clearly incompatible with structural alternative **3** since it is known that similar η^3-bonded cycloheptatrienyl complexes are fluxional and exhibit a single averaged resonance in their NMR spectra at room temperature.[20] However, the spectra are in complete accord with the presence of a static 1-4-η-bonded and 7-substituted cycloheptatriene ring in which all hydrogen and carbon atoms reside in different chemical environments, i.e., structure **2**. Reference to the table reveals the well-known upfield shift of the signals of the atoms associated with the coordinated diene fragments (H(1)–H(4) and C(1)–C(4)) from their usual positions in the free organic ligands. As expected, the outer diene positions experience a considerably larger displacement than the inner signals.[21,22] Not surprisingly then, a comparison of the ^1H NMR spectra of compounds **2** and the parent molecule, $CHTFe(CO)_3$,[21] reveals substantial similarities in the positions and multiplicities of the respective resonances; naturally the H(7) signal in **2** has relative intensity one. The only exceptions to this correlation are some signals in complex **2c**. As can be seen in Table I, the H(7) resonance experiences a remarkably large *downfield* shift (~1.2 ppm) upon replacing the Me_3E groups by the Ph_3Ge substituent. Similar, but greatly reduced, downfield shifts (0.3–0.4 ppm) are also experienced by protons H(1) and H(6), the protons closest to the Ph_3Ge substituent. Both the inductive effect of the phenyl groups and the possible orientation of these hydrogens toward the deshielding region of the phenyl rings could contribute to this effect.

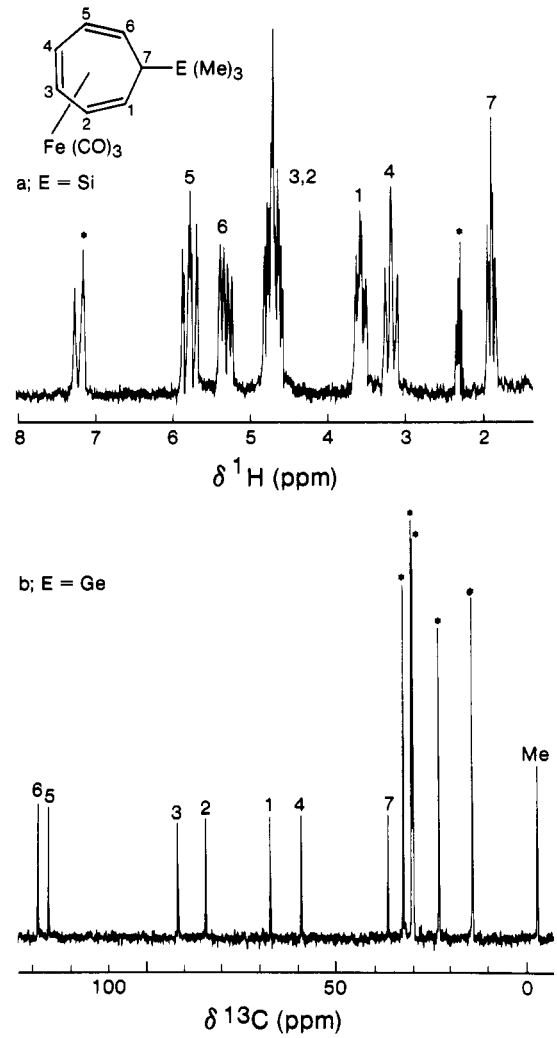

Figure 1. (a) ^1H NMR spectrum of $(1\text{-}4\text{-}\eta\text{-}7\text{-}Me_3SiC_7H_7)Fe(CO)_3$ in toluene-d_8 (*) at ambient temperature. (b) ^{13}C NMR spectrum of $(1\text{-}4\text{-}\eta\text{-}7\text{-}Me_3GeC_7H_7)Fe(CO)_3$ in *n*-decane (*) at ambient temperature.

With the gross bonding features of the complexes secured, the question that remains to be resolved is the stereochemistry of the ER_3 substituents at the saturated carbon atom, C(7). As shown below, the ER_3 group and

(19) Reuvers, J. G. A.; Takats, J., manuscript in preparation.
(20) Calderon, J. L.; Cotton, F. A.; Shaver, A. *J. Organomet. Chem.* **1972**, *42*, 419.
(21) (a) Manual, T. A.; Stone, F. G. A. *J. Am. Chem. Soc.* **1960**, *82*, 366. (b) Burton, R.; Pratt, L.; Wilkinson, G. *J. Chem. Soc.* **1961**, 594. (c) Karel, K. J.; Brookhart, M. *J. Am. Chem. Soc.* **1978**, *100*, 1619.
(22) Kruczynski, L.; Takats, J. *Inorg. Chem.* **1976**, *15*, 3140 and references therein.

Table II. Mass Spectra of $(1\text{-}4\text{-}\eta\text{-}7\text{-}R_3EC_7H_7)Fe(CO)_3$ and Major Fragmentation Processes for 2c[a]

	2a[b]		2b[c]		2c[d]	
assignt	*m/e*	rel abund, %	*m/e*	rel abund, %	*m/e*	rel abund, %
parent$^+$			350	0.2	536[f]	<0.1
P − R$^+$			335	0.2		
P − CO$^+$	276[e]	82.6	322	10.0	508	14.8
P − CO − R$^+$			307	0.3		
P − 2CO$^+$	248	35.4	294	4.6	480	14.2
P − 2CO − R$^+$			279	0.2		
P − 3CO$^+$	220	100	266	19.4	452	100
P − 3CO − R$^+$			251	7.5		
P − 3CO − $C_6H_6^+$					374	3.6
P − 3CO − 2$C_6H_6^+$					296	2.5
$C_7H_7ER_3^+$	164	11.6	210	0.3	396	0.3
$C_7H_7Fe^+$	147	68.4	147	100	147	99.9
$C_6H_6Fe^+$	134	45.2				
$C_5H_5Fe^+$	121	15.2				
$C_7H_7^+$	91	100	91	62.6	91	83.9
R_3E^+	73	93.5	119	4.1	305	52.6

	metastable peaks	
process	calcd	obsd
$(C_7H_7GePh_3)Fe(CO)_2^+ \rightarrow (C_7H_7GePh_3)Fe(CO)^+ + CO$	453.5	452
$(C_7H_7GePh_3)Fe(CO)^+ \rightarrow (C_7H_7GePh_3)Fe^+ + CO$	425.6	425.5
$(C_7H_7GePh_3)Fe^+ \rightarrow C_{14}H_{16}GeFe^+ + C_6H_6$	309.5	309.0

[a] Not corrected for ^{13}C; all ions with $m/e > 91$ are shown. The nominal mass corresponding to the most abundant *m/e* value within each cluster is reported. [b] $T = 110$ °C. [c] $T = 95$ °C. [d] $T = 140$ °C. [e] Measured mass for this ion is 276.0254. The calculated mass for $C_{12}H_{16}O_2SiFe$ is 276.0269. [f] Determined by field ionization mass spectrometry.

$Fe(CO)_3$ moiety can either be on the same side of the cycloheptatriene ring, *endo*-**2**, or they can occupy opposite faces of the cyclic polyene, *exo*-**2**. Successful stereochemical assignments in substituted (cycloheptatriene)-metal carbonyl complexes have been made before on the basis of the ^1H NMR[23] and mass spectra[24] of the respective complexes. However, in all cases the complexes involved η^6-bonded cycloheptatriene ring and innocent, carbon-based substituents. An extension of these empirical correlations to include η^4-bonded cycloheptatriene rings would be of obvious interest. Unfortunately, a brief examination of the pertinent data of complexes **2** reveals that this does not appear to be feasible.

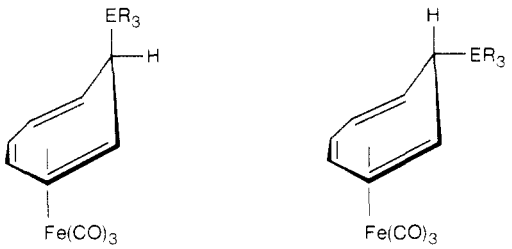

exo-**2** *endo*-**2**

In a series of chromium complexes $(\eta^6\text{-}7\text{-}RC_7H_7)Cr(CO)_3$, Pauson et al.[23] have shown that the chemical shift of H(7) and the magnitude of its coupling constant to H(1) and H(6) lead to consistent and unambiguous stereochemical predictions. In the endo isomer the H(7) proton, occupying the axial position and being shielded by the triene system, resonates at high field, $\delta \simeq 1.8$. The signal is shifted downfield by 1.0–1.5 ppm in the exo isomer where H(7) is now equatorial and the shielding effect of the ring is absent. Straight extrapolation of this correlation to compounds **2** is, however, hampered by the effect of the ER_3 substituents on the chemical shift of H(7). It is known that the replacement of a proton at C(7) by $SiMe_3$ in cycloheptatriene causes a 0.7-ppm upfield shift in the resonance position of the remaining H(7) proton.[25] Also, the electron-withdrawing and anisotropic nature of the phenyl groups in $GePh_3$ have been noted before. Thus it is not clear whether the high-field position of H(7) in **2a** and **2b** and its shift to low field in **2c** are the results of substitution effects or arise because of the respective endo and exo stereochemistries of the complexes. In view of the rather unlikely reversal of configuration at C(7), in what we anticipate to be isostructural complexes, the former explanation appears to be more plausible for the observed chemical shifts of H(7). Considerations of the vicinal H(7)–H(1),H(6) coupling constants also fail to give a consistent stereochemical picture. The application of the empirical Karplus curve[26] to the dihedral angle between H(7) and H(1),H(6) in the chromium complexes predicted coupling constants of ~4 and ~8 Hz for the endo and exo isomers, respectively, in excellent agreement with the observed values.[23] In compounds **2**, the values of $J_{H(7)-H(1)H(6)}$ are 5.2 Hz in **2a**, 5.0 Hz in **2b**, and 4.0 Hz in **2c**. It is clear that the intermediate size of the coupling constant in **2a** and **2b** has no practical predictive value. Furthermore, the magnitude of the vicinal coupling in **2c** seems to indicate endo stereochemistry, a result which is diametrically opposed to the chemical shift prediction. Although vicinal coupling constants are known to vary with substitution, the effects are expected to be minor in the present compounds and we attribute the breakdown of this NMR correlation to the different bonding mode of cycloheptatriene in complexes **2** and $(\eta^6\text{-}7\text{-}RC_7H_7)Cr(CO)_3$. The additional degree of freedom introduced by the free double bond in complexes **2**, and presumable in other η^4-bonded cycloheptatriene compounds, is apparently capable of supporting a larger range of dihedral angles and hence the size of the vicinal coupling is no longer characteristic of

(23) Pauson, P. L.; Smith, G. H.; Valentine, J. H. *J. Chem. Soc. C* **1967**, 1061.
(24) (a) Müller, J. *Angew. Chem. Int. Ed. Engl.* **1972**, *11*, 653. (b) Müller, J.; Mertschenk, B. *J. Organomet. Chem.* **1972**, *34*, 165.
(25) Ashe, A. J., III *J. Org. Chem.* **1972**, *37*, 2053.
(26) (a) Karplus, M. *J. Chem. Phys.* **1959**, *30*, 11. (b) Lynden-Bell, R. M.; Harris, R. K. In "Nuclear Magnetic Resonance Spectroscopy"; Nelson and Sons: London, 1969; p 111.

Table III. Atomic Positional and Thermal Parameters for (1-4-η-*exo*-7-$Ph_3GeC_7H_7$)$Fe(CO)_3$ (2c)[a]

atom	x	y	z	U(11)	U(22)	U(33)	U(12)	U(13)	U(23)
Ge	2254.1 (6)	8946.1 (1)	7459.7 (3)	42.1 (3)	34.1 (2)	37.7 (2)	0.8 (2)	5.4 (2)	0.1 (2)
Fe	4426.1 (8)	7285.9 (2)	7852.5 (4)	43.7 (4)	34.3 (3)	38.2 (3)	−1.6 (3)	10.1 (3)	0.6 (2)
O(1)	1200 (6)	6700 (1)	6660 (3)	88 (3)	83 (2)	78 (2)	−36 (2)	−15 (2)	2 (2)
O(2)	6791 (5)	6489 (1)	8854 (3)	75 (3)	67 (2)	99 (3)	23 (2)	16 (2)	28 (2)
O(3)	6449 (7)	7529 (1)	6107 (3)	150 (4)	73 (2)	109 (3)	−7 (2)	95 (3)	−1 (2)
C(1)	2821 (6)	7934 (1)	7488 (3)	38 (2)	37 (2)	47 (2)	0 (2)	2 (2)	−4 (2)
C(2)	2623 (7)	7710 (1)	8505 (4)	45 (3)	43 (2)	61 (3)	−3 (2)	25 (2)	−6 (2)
C(3)	4258 (7)	7593 (1)	9335 (3)	70 (3)	45 (2)	36 (2)	−4 (2)	20 (2)	0 (2)
C(4)	6128 (7)	7700 (1)	9178 (3)	52 (3)	47 (2)	41 (2)	2 (2)	−2 (2)	0 (2)
C(5)	6801 (7)	8146 (1)	8828 (4)	36 (3)	47 (2)	61 (3)	−6 (2)	1 (2)	−9 (2)
C(6)	5849 (6)	8442 (1)	8063 (3)	40 (3)	38 (2)	60 (3)	−7 (2)	12 (2)	−3 (2)
C(7)	3873 (6)	8375 (1)	7364 (3)	40 (3)	34 (2)	37 (2)	0 (2)	11 (2)	0 (2)
C(8)	2454 (7)	6933 (1)	7108 (3)	60 (3)	46 (3)	47 (2)	−4 (2)	3 (2)	6 (2)
C(9)	5821 (7)	6792 (1)	8474 (3)	50 (3)	47 (2)	53 (2)	0 (2)	11 (2)	3 (2)
C(10)	5679 (7)	7420 (1)	6795 (4)	74 (3)	38 (2)	63 (3)	−1 (2)	32 (3)	−4 (2)
C(11)	1339 (6)	8976 (1)	8845 (3)	40 (2)	33 (2)	40 (2)	−4 (2)	5 (2)	−4 (2)
C(12)	−239 (6)	9252 (1)	8896 (3)	45 (3)	61 (3)	49 (2)	6 (2)	3 (2)	1 (2)
C(13)	−887 (7)	9291 (2)	9882 (4)	44 (3)	81 (3)	78 (3)	9 (3)	16 (3)	−18 (3)
C(14)	5 (7)	9045 (2)	10838 (4)	62 (3)	68 (3)	55 (3)	−18 (3)	23 (2)	−17 (2)
C(15)	1581 (7)	8775 (1)	10802 (3)	70 (3)	49 (2)	40 (2)	−11 (2)	9 (2)	−3 (2)
C(16)	2246 (6)	8737 (1)	9825 (3)	50 (3)	38 (2)	47 (2)	3 (2)	4 (2)	−3 (2)
C(21)	3907 (6)	9489 (1)	7398 (3)	46 (3)	34 (2)	46 (2)	1 (2)	2 (2)	5 (2)
C(22)	4173 (7)	9829 (1)	8232 (3)	65 (3)	50 (3)	48 (2)	−9 (2)	6 (2)	−1 (2)
C(23)	5393 (8)	10204 (2)	8202 (4)	85 (4)	53 (3)	57 (3)	−18 (3)	6 (3)	−7 (2)
C(24)	6355 (7)	10245 (2)	7350 (4)	54 (3)	52 (3)	77 (3)	−16 (2)	−8 (3)	15 (2)
C(25)	6112 (7)	9913 (2)	6511 (4)	49 (3)	56 (3)	72 (3)	3 (2)	15 (2)	18 (2)
C(26)	4879 (7)	9537 (1)	6532 (3)	57 (3)	38 (2)	56 (2)	4 (2)	12 (2)	2 (2)
C(31)	78 (6)	8954 (1)	6137 (3)	47 (2)	36 (2)	39 (2)	10 (2)	8 (2)	−3 (2)
C(32)	−76 (7)	9298 (1)	5311 (3)	61 (3)	42 (2)	48 (2)	5 (2)	7 (2)	1 (2)
C(33)	−1589 (8)	9292 (1)	4363 (3)	83 (4)	52 (3)	46 (2)	17 (3)	−2 (2)	8 (2)
C(34)	−2964 (7)	8942 (2)	4220 (3)	62 (3)	61 (3)	55 (3)	19 (3)	−9 (2)	−12 (2)
C(35)	−2835 (7)	8604 (1)	5021 (4)	42 (3)	60 (3)	60 (3)	6 (2)	−1 (2)	−13 (2)
C(36)	−1349 (6)	8608 (1)	5978 (3)	43 (3)	47 (2)	54 (2)	3 (2)	6 (2)	0 (2)

atom	x	y	z	B, Å²	atom	x	y	z	B, Å²
HC(1)	1712 (56)	7917 (12)	6903 (30)	48 (11)	HC(16)	3392	8552	9819	60
HC(2)	1441 (56)	7600 (11)	8574 (28)	38 (10)	HC(22)	3461	9805	8828	70
HC(3)	4130 (60)	7420 (13)	9951 (31)	58 (12)	HC(23)	5589	10437	8793	78
HC(4)	7114 (55)	7531 (12)	9639 (29)	42 (11)	HC(24)	7202	10510	7323	78
HC(5)	7995 (61)	8237 (13)	9141 (31)	51 (12)	HC(25)	6821	9933	5918	72
HC(6)	6504 (61)	8743 (14)	7988 (31)	62 (12)	HC(26)	4674	9303	5939	62
H1C(7)	3879 (56)	8404 (11)	6727 (29)	39 (11)	HC(32)	895	9542	5387	65
HC(12)	−897	9422	8238	63	HC(33)	−1693	9537	3796	75
HC(13)	−1996	9490	9904	80	HC(34)	−4022	8937	3549	77
HC(14)	−496	9062	11509	72	HC(35)	−3809	8362	4924	72
HC(15)	2242	8604	11469	66	HC(36)	−1291	8374	6556	61

[a] Estimated standard deviations in this and other tables are given in parentheses and correspond to the least significant digits. The positional parameters are $\times 10^4$ and the thermal parameters are $\times 10^3$. $U(ij) = B(ij)/(2\pi^2 a^*(i)a^*(j))$ Å². The thermal ellipsoid is given by $\exp\{-(B(11)h^2 + B(22)k^2 + B(33)l^2 + 2B(12)hk + 2B(13)hl + 2B(23)kl)\}$.

a unique stereochemical configuration.

The mass spectra data of the complexes are summarized in Table II. The parent ion was detected for **2b** and for **2c** only under field ionization condition. As expected, the fragmentation pattern of each compound is dominated by successive loss of three carbonyl groups and, particularly for **2c**, by the characteristic breakdown of the ER_3 substituents. In all cases the ions $C_7H_7Fe^+$, $R_3EC_7H_7^+$, ER_3^+, and $C_7H_7^+$ are observed and belong to the more intense fragments.

Müller and co-workers have applied mass spectrometry to the determination of the position, exo or endo, of the substituent in (η^6-7-RC_7H_7)$Cr(CO)_3$[24a] and (η^6-7-RC_7H_7)-$V(\eta^5$-$C_5H_5)$[24b] complexes. It was found that in the exo isomers two competitive fragmentation processes were operating: (i) successive carbonyl losses from the molecular ion and (ii) radical elimination of the exo substituent to produce the stable [η^7-$C_7H_7Cr(CO)_3$]$^+$, where the positive charge is carried by the 6π-electron tropylium cation. On the other hand, in the endo complexes, fragmentation of the RC_7H_7 moiety occurred only after the loss of all three carbonyl ligands. Again it is not known whether the above correlation can be extended to the complexes **2**, especially in view of the fact that the stabilizing influence of the 6π-electron tropylium cation is not present in these derivatives after the elimination of $R_3E\cdot$. [$C_7H_7Fe(CO)_3$]$^+$ is known,[27] but it is a fluxional molecule in which only five carbon atoms of the C_7H_7 ring are coordinated to the iron center forming a five-electron pentadienyl radical donor moiety. Thus, although the complexes **2** do not show the simultaneous loss of carbonyl ligands and $R_3E\cdot$ radical species, a deduction of endo stereochemistry for these compounds without supporting evidence would be premature at best.

Since none of the previously employed spectroscopic techniques yielded a reliable indication of the stereochemistry of the complexes **2**, single-crystal X-ray structural analyses of **2b** and **2c** were carried out to establish unequivocally the position of the ER_3 substituent at C(7).[28]

(27) Mahler, J. E.; Jones, D. A. K.; Pettit, R. *J. Am. Chem. Soc.* **1964**, *86*, 3589.

(28) The structure of **2b** will be published separately by V. W. Day and co-workers.

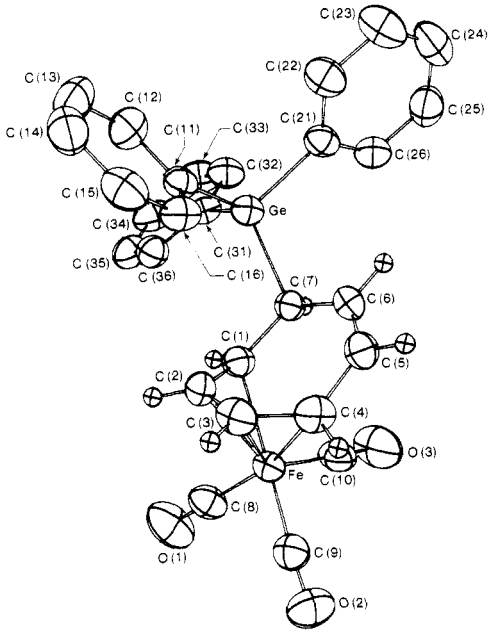

Figure 2. Perspective drawing of (1-4-η-*exo*-7-$Ph_3GeC_7H_7$)Fe-$(CO)_3$ showing the atom numbering scheme. Thermal ellipsoids are drawn at 50% probability level for non-hydrogen atoms.

Molecular Structure of (1-4-η-7-$Ph_3GeC_7H_7$)Fe-$(CO)_3$, 2c. A perspective view of the molecule is shown in Figure 2, along with the atomic numbering scheme. It is clear from the figure that the structural study corroborates the η^4-bonding mode between the ring and the $Fe(CO)_3$ moiety which was deduced on the basis of the previously discussed spectral data. More important, the study unequivocally establishes that the orientation of the $GePh_3$ substituent at C(7) is exo with respect to the Fe-$(CO)_3$ moiety. A similar arrangement is seen in the $GeMe_3$-substituted complex,[28] **2b**, and in (1-4-η-*exo*-7-phenylcycloheptatriene)tricarbonyliron,[29] **2Ph**, the only other simple (cycloheptatriene)tricarbonyliron complex structurally characterized to date. Although detailed mechanistic studies are lacking, the simplest physical pathway that accounts for the observed stereochemistry at C(7) is direct and specific exo addition of the Si and Ge electrophiles to the cycloheptatrienyl ring system of **1**.[30] The alternate pathway, addition to iron, followed by ER_3 group migration is expected to give the endo-substituted material. It is noteworthy that deuteration of **1** also appears to proceed by stereospecific attack of the coordinated cycloheptatrienyl ring to yield (1-4-η-*exo*-7-DC_7H_7)Fe-$(CO)_3$.[2,31]

Selected bond distances and angles are listed in Table IV. The geometry around the iron can be described as approximately tetragonal pyramidal with the midpoints of the two "*cis*-diene" double bonds and two carbonyl moieties forming the base of the pyramid, the apical carbonyl group is directed toward the "open" side of the bound diene. The Fe–C bond length to the apical carbonyl group is shorter (Fe–C(10) = 1.762 (5) Å) than the distances to the basal carbonyl groups (Fe–C(8) = 1.790 (5), Fe–C(9) = 1.790 (5) Å), and the two OC–Fe–CO angles involving the apical carbonyl group are larger (103° and 99°) than the third such angle. Finally, the Fe–C(diene) bond lengths to the inner carbon atoms are shorter (Fe–C(2) = 2.048 (4), Fe–C(3) = 2.032 (4) Å) than the similar distances to the outer carbon atoms (Fe–C(1) = 2.166 (4), Fe–C(4) = 2.135 (4) Å). These features are unexceptional and indeed form the common link among all previously investigated (*cis*-diene) $Fe(CO)_3$ structures.[29,32] However,

Table IV. Selected Bond Distances (Å) and Bond Angles (Deg) in (1-4-η-*exo*-7-$Ph_3GeC_7H_7$)$Fe(CO)_3$

Bond Distances

Fe-C(1)	2.166 (4)	Ge-C(7)	2.015 (4)
Fe-C(2)	2.048 (4)	Ge-C(11)	1.940 (4)
Fe-C(3)	2.032 (4)	Ge-C(21)	1.956 (4)
Fe-C(4)	2.135 (4)	Ge-C(31)	1.954 (4)
Fe-C(8)	1.790 (5)	C(8)-O(1)	1.144 (5)
Fe-C(9)	1.790 (4)	C(9)-O(2)	1.136 (4)
Fe-C(10)	1.762 (5)	C(10)-O(3)	1.140 (5)
C(1)-C(2)	1.426 (6)	C(1)-HC(1)	0.93 (4)
C(2)-C(3)	1.390 (6)	C(2)-HC(2)	0.92 (4)
C(3)-C(4)	1.412 (6)	C(3)-HC(3)	0.92 (4)
C(4)-C(5)	1.460 (6)	C(4)-HC(4)	0.92 (4)
C(5)-C(6)	1.323 (6)	C(5)-HC(5)	0.88 (4)
C(6)-C(7)	1.472 (6)	C(6)-HC(6)	0.99 (4)
C(7)-C(1)	1.492 (5)	C(7)-H1C(7)	0.78 (3)
C(11)-C(12)	1.381 (5)	C(21)-C(22)	1.388 (5)
C(12)-C(13)	1.382 (6)	C(22)-C(23)	1.382 (6)
C(13)-C(14)	1.381 (6)	C(23)-C(24)	1.369 (7)
C(14)-C(15)	1.365 (6)	C(24)-C(25)	1.375 (6)
C(15)-C(16)	1.378 (5)	C(25)-C(26)	1.391 (6)
C(16)-C(11)	1.395 (5)	C(26)-C(21)	1.390 (6)
C(31)-C(32)	1.393 (5)	C(34)-C(35)	1.360 (6)
C(32)-C(33)	1.381 (6)	C(35)-C(36)	1.378 (5)
C(33)-C(34)	1.379 (6)	C(36)-C(31)	1.394 (5)

Bond Angles

Fe-C(8)-O(1)	179.0 (4)	C(8)-Fe-C(9)	93.3 (2)
Fe-C(9)-O(2)	176.3 (4)	C(8)-Fe-C(10)	102.6 (2)
Fe-C(10)-O(3)	176.6 (4)	C(9)-Fe-C(10)	99.2 (2)
C(1)-Fe-C(2)	39.4 (2)	C(1)-C(2)-C(3)	120.5 (4)
C(1)-Fe-C(3)	71.1 (2)	C(2)-C(3)-C(4)	119.8 (4)
C(1)-Fe-C(4)	81.8 (2)	C(3)-C(4)-C(5)	127.4 (4)
C(1)-Fe-C(8)	94.0 (2)	C(4)-C(5)-C(6)	128.2 (4)
C(1)-Fe-C(9)	167.2 (2)	C(5)-C(6)-C(7)	125.7 (4)
C(1)-Fe-C(10)	89.5 (2)	C(6)-C(7)-C(1)	118.8 (3)
C(2)-Fe-C(3)	39.8 (2)	C(7)-C(1)-C(2)	128.2 (4)
C(2)-Fe-C(4)	70.8 (2)	C(7)-Ge-C(11)	113.1 (2)
C(2)-Fe-C(8)	92.8 (2)	C(7)-Ge-C(21)	106.9 (2)
C(2)-Fe-C(9)	129.6 (2)	C(7)-Ge-C(31)	108.2 (2)
C(2)-Fe-C(10)	127.9 (2)	C(11)-Ge-C(21)	108.6 (2)
C(3)-Fe-C(4)	39.5 (2)	C(11)-Ge-C(31)	110.9 (2)
C(3)-Fe-C(8)	119.7 (2)	C(21)-Ge-C(31)	108.9 (2)
C(3)-Fe-C(9)	96.1 (2)	Ge-C(7)-C(1)	112.2 (3)
C(3)-Fe-C(10)	133.9 (2)	Ge-C(7)-C(6)	109.7 (3)
C(4)-Fe-C(8)	159.0 (2)	Ge-C(7)-H1C(7)	96 (3)
C(4)-Fe-C(9)	87.7 (2)	C(1)-C(7)-H1C(7)	108 (3)
C(4)-Fe-C(10)	98.0 (2)	C(6)-C(7)-H1C(7)	110 (3)

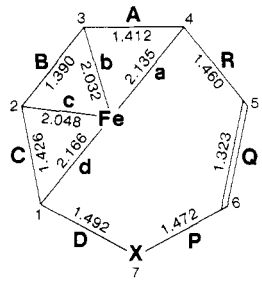

Figure 3. Bond designation in derivatives of (1-4-η-cycloheptatriene)tricarbonyliron. Numbering scheme is the same as in Figure 2; the distances are those observed in **2c**.

(29) Jeffreys, J. A. D.; Metters, Ch. *J. Chem. Soc., Dalton Trans.* **1977**, 729.

(30) This of course is just a different way of saying that the reaction proceeds by the well-known S_N2 displacement of halide ion from R_3EX (E = Si, Ge) by a carbon nucleophile.

(31) Brookhart, M.; Karel, K. J.; Nance, L. E. *J. Organomet. Chem.* **1977**, *140*, 203.

(32) (a) Churchill, M. R.; Bird, P. H. *Inorg. Chem.* **1969**, *8*, 1941. (b) Johnson, S. M.; Paul, I. C. *J. Chem. Soc. B* **1970**, 1783. (c) Cotton, F. A.; Day, V. W.; Frenz, B. A.; Hardcastle, K. J.; Troup, J. M. *J. Am. Chem. Soc.* **1973**, *95*, 4522.

Table V. Least-Squares Planes in (1-4-η-*exo*-7-$Ph_3GeC_7H_7$)$Fe(CO)_3$

plane	atoms defining the plane	eq of mean plane[a]
I	C(1), C(4), C(5), C(6), C(7)	$3.981x - 12.93y - 9.76z - 16.46 = 0$
II	C(1), C(2), C(3), C(4)	$0.981x - 25.54y - 5.473z - 24.09 = 0$

Displacement of Atoms from Mean Plane (Å)

plane I		plane II	
C(1)	0.014 (4)	C(1)	0.002 (4)
C(4)	−0.016 (4)	C(2)	−0.003 (4)
C(5)	0.018 (4)	C(3)	0.003 (4)
C(6)	0.002 (4)	C(4)	−0.002 (4)
C(7)	−0.017 (4)		

[a] The equations of the planes refer to the fractional atomic coordinates.

the variations in the individual Fe–C and C–C bond distances reflect the nature of the bonding between the iron atom and the *cis*-diene fragment which, of course, is related to the nature of the substituents on the organic ligands. The relevant bond distances in structures containing formal cycloheptatriene ligand system have been summarized by Jeffreys in his study on **2Ph**[29] and following his convention we designate the bonds as in Figure 3.

Jeffreys has observed that the difference between the iron–outer carbon bond lengths (bonds a and d in Figure 3) appears to correlate with the inductive effect of the substituent at C(7). The present value of −0.031 Å is consistent with the well-known electron-donating ability of germyl and silyl substituents via both inductive and hyperconjugative mechanisms.[33] This effect is especially noticeable when, as in the present case, the substituent is β to the unsaturated system. The resulting bonding asymmetry in the Fe–diene interaction (see Figure 3) is such that the $Fe(CO)_3$ moiety moves slightly but significantly toward the C(3)–C(4) bond. It is extremely interesting to note that precisely such a geometrical distortion for this type of system was predicted by Albright on the basis of molecular orbital calculations.[34]

The variations in the C–C bond distances of the complexed diene fragment are a sensitive indicator of the strength of the diene-to-iron bonding. Although it is tenuous to draw conclusions on the nature of the diene substituent on the basis of the observed C–C bond lengths because of the synergic donation and back-acceptance of electron density between the $Fe(CO)_3$ and diene moieties, it is well-known and lucidly discussed elsewhere[35] that as the difference, Δ, between the average value of the "outer" C–C distance (bonds A and C) and the "inner" C–C distance (bond B) increases, so does the strength of the diene-to-iron interaction. In the present compound, the value of Δ is 0.029 Å and indicates a significantly stronger bonding than in **2Ph**, $\Delta = -0.035$ Å, and by inference in the parent molecule, $CHTFe(CO)_3$. The reason for this increased diene-to-iron bonding is presumably due to the greater electron-donating ability of the germyl- and silyl-substituted cycloheptatriene ligands, vide supra. It is noteworthy that concurrent with the increased metal–diene bonding interaction there appears to be an increased bond localization in the uncomplexed part of the cycloheptatriene ring. The lengths of the R and Q bonds are 1.460 (6) and 1.323 (6) Å, respectively, which are typical values for $C(sp^2)$–$C(sp^2)$ single and double bonds, the corresponding distances in **2Ph** are 1.39 and 1.36 Å.

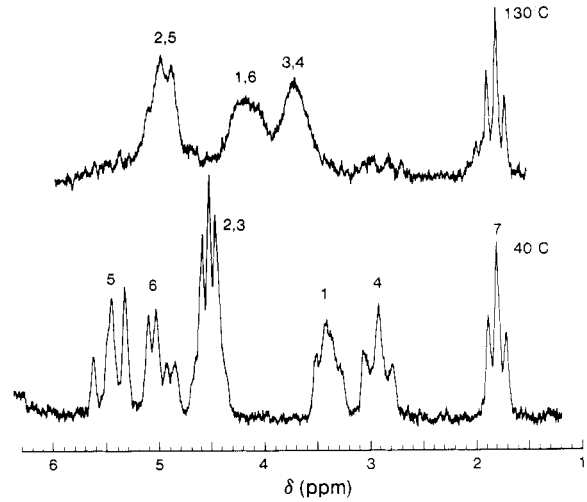

Figure 4. Variable-temperature ^1H NMR spectra of (1-4-η-*exo*-7-$Me_3GeC_7H_7$)$Fe(CO)_3$ in diphenyl ether. Numbering is the same as in Figure 1.

The atoms of the seven-membered ring form, as usual, two planar systems. The equations of these planes and the distances of the atoms from the planes are given in Table V. The dihedral angle between these planes is 38.9° which is substantially less than the 46° found in **2Ph**, the corresponding angle in [η^4-*N*-(methoxycarbonyl)azepine]tricarbonyliron[32b] is 42.5°. The somewhat variable nature of this angle seems to bear out our contention, vide supra, that in these η^4-bonded cycloheptatriene complexes the dihedral angle between protons H(7) and H(1),H(6) is also variable and thus renders vicinal coupling considerations as stereochemical guide suspect. The dihedral angles between H(7)–H(1) and H(7)–H(6) are 43 (4) and 57 (4)°, respectively. These are indeed quite different from the anticipated ~4° in (η^6-*exo*-7-RC_7H_7)$Cr(CO)_3$.[23] The predicted vicinal coupling constants based on the observed dihedral angles are 6 and 4 Hz, respectively, with an average value of 5 Hz which compares well with the observed 4 Hz in **2c**.

Finally, it is tempting to find an explanation for the downfield shifts in the resonance portion of H(7), H(1), and H(6) protons in terms of the observed orientations of the phenyl rings in the solid state. However, arguments along these lines are beset with uncertainties because of the rapid Ge–C(Ph) bond rotation in solution. Perhaps it is significant that the stable conformation about the Ge–C(7) bond is such that two phenyl groups are in close proximity to H(7) while there is only one next to H(1) and H(6), the much larger downfield shift of the H(7) proton is not inconsistent with this observation.

Stereochemical Nonrigidity or the "Performing Dogs in the Nighttime".[36,37] In contrast to $CHTFe(CO)_3$, the proton NMR spectrum of which shows no line broadening up to 100 °C,[38] complexes **2** show temperature-dependent behavior in their NMR spectra. This is demon-

(33) Mollère, P.; Bock, H.; Becker, G.; Fritz, G. *J. Organomet. Chem.* **1972**, *46*, 89.
(34) Karel, K. J.; Albright, T. A.; Brookhart, M. *Organometallics* **1982**, *1*, 419.
(35) (a) Churchill, M. R.; Mason, R. *Proc. R. Soc. London, Ser. A* **1967**, *301*, 433. (b) Cotton, F. A.; Wilkinson, G. "Advanced Inorganic Chemistry", 3rd. ed.; Interscience-Wiley: New York, 1972; pp 731–733.
(36) Cotton, F. A. In "Dynamic Nuclear Magnetic Resonance Spectroscopy"; Jackman, L. M., Cotton, F. A. Eds.; Academic Press: New York, 1975; p 435.
(37) Mann, B. E. *J. Organomet. Chem.* **1977**, *141*, C33.
(38) See ref 25 in: Brookhart, M.; Davis, E. R.; Harris, D. L. *J. Am. Chem. Soc.* **1972**, *94*, 7853.

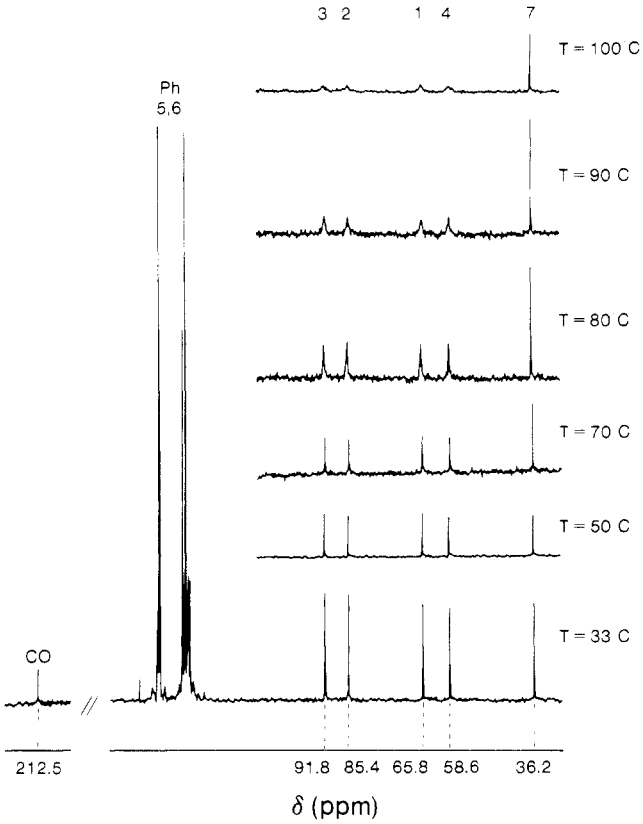

Figure 5. Variable-temperature ^{13}C NMR spectra of (1–4-η-*exo*-7-$Ph_3GeC_7H_7$)$Fe(CO)_3$ in toluene-d_8. Numbering is the same as in Figure 1.

strated in Figure 4 which shows the ^1H NMR spectrum of (η^4-*exo*-7-$Me_3GeC_7H_7$)$Fe(CO)_3$, **2b**, at 40 and 130 °C, respectively. As the temperature is raised the resonances due to H(1)–H(6) protons broaden, coalesce, and reform into three new broad peaks. It is evident that the resonance due to H(7) remains sharp over the entire temperature range and does not participate in the fluxional process. The positions of the three new peaks are in good agreement with the calculated averages from the room-temperature chemical shifts values of H(1) and H(6), H(2) and H(5), and H(3) and H(4), respectively. The observed line-shape changes demonstrate that the molecule is fluxional and undergoes some rearrangement process which imparts a time-averaged mirror plane to the molecule at high temperatures.

In addition to this thermally reversible process, irreversible hydrogen atom shifts, but *no* R_3E group migrations, were also observed for complexes **2a** and **2b**. Qualitatively, it appears that the process was more facile for **2a** than for **2b**. The mechanisms and energetics of these rearrangements were not investigated further. Nevertheless, it is interesting to note that in the metal free ligand, 7-$Me_3SiC_7H_7$, hydrogen migration also occurs in preference to Me_3Si group migration.[25] The process in this case is known to proceed by exclusive [1,5] H shifts.

The proton-decoupled variable temperature ^{13}C NMR spectra of **2c** are shown in Figure 5. The ^{13}C NMR spectra exhibit temperature-dependent behavior which is similar to the previously described proton spectra. It is seen that the resonances due to C(1)–C(4) coalesce into the base line at a temperature slightly higher than 100 °C (resonances C(5) and C(6) are hidden by the phenyl group resonances). Due to the much larger chemical shift separations in the ^{13}C spectra, compared to the proton NMR spectra, the formation of the new averaged sets of resonances is not observed. That is, the high-temperature limiting spectrum

Table VI. Chemical Shift Differences,[a] Coalescence Temperatures,[b] and $\Delta G^\ddagger$ Values[c] for Complexes 2

	^1H spectra			^{13}C spectra		
compd	$\Delta\nu$	T_c	$\Delta G^\ddagger$	$\Delta\nu$	T_c	$\Delta G^\ddagger$
2a	145	105	75	719	115	72
2b	150	95	73	735	115	72
2c	155	100	74	750	120	73

[a] In Hz. [b] The chemical shift differences and temperatures quoted refer to the exchanging H(3)–H(4) and C(3)–C(4) pairs, respectively. T_c in °C, ±5 °C. [c] In kJ mol^{-1} at T_c, ±3 kJ mol^{-1}.

of **2c** could not be obtained since at the required higher temperatures substantial decomposition of the complex occurs. Again, the sharpness of the resonance attributed to C(7) over the entire temperature range is evident.

An approximate value for the energetics of the rearrangement process can be gained by the application of eq 3[39] where T_c is the coalescence temperature and $\Delta\nu$ the

$$\Delta G^\ddagger = -RT_c \ln (h\pi\Delta\nu/\sqrt{2}kT_c) = 19.13\ T_c[9.97 + \log (T_c/\Delta\nu)]\ \text{J mol}^{-1} \quad (3)$$

chemical shift difference in hertz between the two exchanging sites in the absence of exchange and the other constants have their usual meanings. The coalescence temperatures for the complexes **2** and the calculated $\Delta G^\ddagger$ values obtained from the ^1H and ^{13}C NMR spectra are tabulated in Table VI. The good agreement between the values calculated based on the ^1H and ^{13}C NMR data is gratifying. However, because of the uncertainties involved in the calculations, the neglect of coupling constants in the proton data and our inability to accurately determine the T_c values in the ^{13}C spectra, we felt it was necessary to determine $\Delta G^\ddagger$ by another independent means.

Since it enables one to obtain the desired activation parameters at the *onset* of chemical exchange, the Forsen–Hoffman technique of spin-saturation transfer (SST) is an ideal method for determining the energetics of the rearrangement processes in thermolabile molecules. This technique was applied to complex **2c** where substantial decomposition at higher temperatures rendered the value of T_c particularly suspect.

In addition to being useful for the above purpose, the SST technique also constitutes a convenient way of labeling specific nuclei. In our case this proved to be especially effective in confirming the initial assignment of carbon atoms C(2) and C(3) by selective proton-decoupling experiments. Due to the very similar chemical shift values of the protons H(2) and H(3), only a tentative assignment for C(2) and C(3) could be made. Selective irradiation of carbon atom C(4) of **2c** at 50 °C resulted in a drastic decrease in the intensity of the resonance tentatively assigned to C(3), no other resonances were affected. This establishes C(3) and C(4) as a pair of exchanging carbon atoms and thus confirms the assignment of the resonance at δ 91.8 as C(3).

The energetics of the rearrangement in **2c** were obtained by selectively irradiating the resonance due to C(4) at various temperatures in the range 35–65 °C, thus avoiding any complications due to thermal decomposition. The lifetime at C(3), $\tau_{(3)}$, is given by eq 4,[12] where $M_{z(3)}(0)$ is

$$\tau_{(3)} = \frac{M_{z(3)}(\infty)}{M_{z(3)}(0) - M_{z(3)}(\infty)} T_{1(3)} \quad (4)$$

(39) Kost, D.; Carlson, E. H.; Roban, M. *J. Chem. Soc., Chem. Commun.* **1971**, 656.

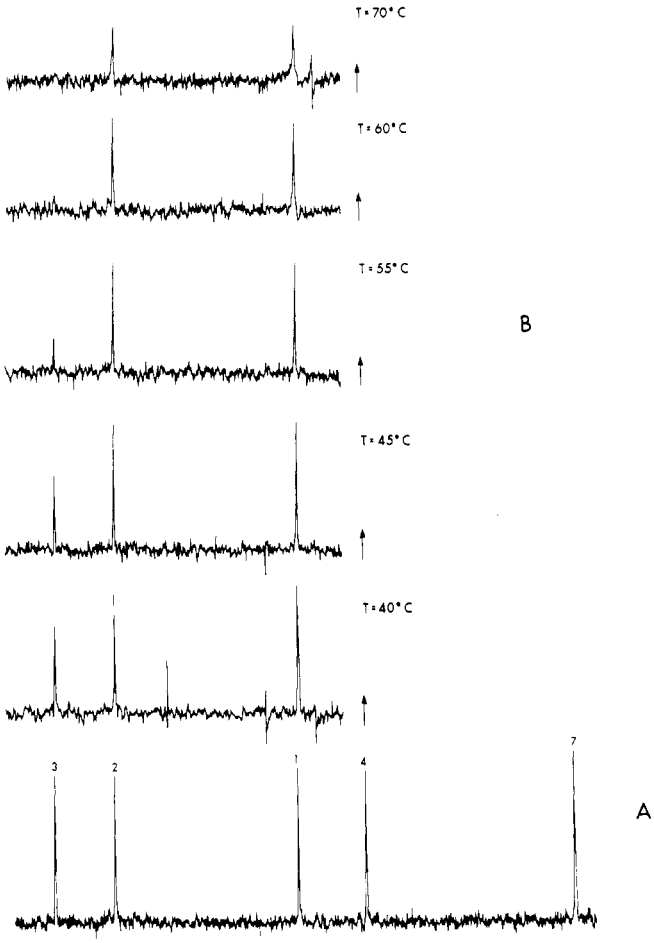

Figure 6. The Forsén–Hoffman spin-saturation transfer technique applied to (1–4-η-*exo*-7-$Ph_3GeC_7H_7$)$Fe(CO)_3$: A, ^{13}C NMR spectrum at 50 °C showing the assignment of the signals; B, as A but with an irradiating field applied at C(4) (at different temperatures).

the normal equilibrium magnetization of carbon C(3) in the absence of irradiation at C(4) and $T_{1(3)}$ is the spin–lattice relaxation time of carbon C(3) and is measured by the (180°–τ–90°–(sample)–T)$_n$ pulse sequence with $T \geq 5T_1$. The spin–lattice relaxation times of the carbon atoms C(1) through C(4) and C(7) were measured at different temperatures and subsequently plotted as a function of temperature. Straight line behavior was observed and intermediate values of T_1 were extracted from these graphs. It was found that $T_{1(3)}$ and $T_{1(4)}$ were comparable at all temperatures. From the lifetime, the rate of leaving site C(3), i.e., the rate for the exchange between C(3) and C(4), is given by eq 5. Experimentally $M_{z(3)}(0)/M_{z(3)}(\infty)$ is de-

$$k_{ex} = k_{34} = \frac{1}{\tau_{(3)}} = \left(\frac{M_{z(3)}(0)}{M_{z(3)}(\infty)} - 1 \right) \frac{1}{T_{1(3)}} \qquad (5)$$

termined by comparing the signal areas of C(3) without and with saturation of carbon atom C(4). In the present case the heights of the ^{13}C signals were taken as a measure of $M_{z(3)}$.[12c,d]

The SST experiment is shown in Figure 6 while the data for T_1, $M_{z(3)}(\infty)/(M_{z(3)}(0) - M_{z(3)}(\infty))$ and the calculated values of k_{ex} are summarized in Table VII. Three independent SST experiments were performed with identical results. The activation energies were determined from a least-squares fit of ln k_{ex}/T vs. $1/T$ and are $\Delta H^{\ddagger}$ = 84 (4) kJ mol^{-1} and $\Delta S^{\ddagger}$ = 18 (2) J K^{-1} mol^{-1} which lead to a value of 77 (4) kJ mol^{-1} for $\Delta G^{\ddagger}$ at 120 °C. This compares favorably with the parameters obtained previously by the

Table VII. Spin-Saturation Transfer Data, Rate Constants, and Free Energy of Activation for (1–4-η-*exo*-7-$Ph_3GeC_7H_7$)$Fe(CO)_3$ [a]

T, °C	$T_{(3)}$, s	$M_{z(3)}(\infty)/(M_{z(3)}(0) - M_{z(3)}(\infty))$	k_{ex}, s
40	0.868	2.69	0.428
45	0.994	1.44	0.699
55	1.309	0.44	1.754
60	1.462	0.20	3.367

[a] $\Delta H^{\ddagger}$ = 84 (4) kJ mol^{-1}, $\Delta S^{\ddagger}$ = 18 (2) J K^{-1} mol^{-1}, and $\Delta G^{\ddagger}_{393}$ = 77 (4) kJ mol^{-1}.

Scheme I

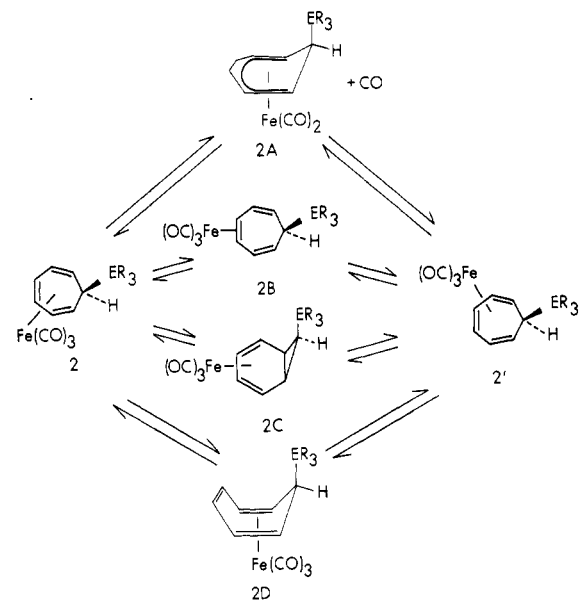

application of the approximate expression at the coalescence temperatures and lends support for the validity of the values listed in Table VI. The remarkable lowering of the $\Delta G^{\ddagger}$ values for the iron shift in these complexes compared to the unsubstituted parent molecule CHTFe$(CO)_3$, $\Delta G^{\ddagger} \simeq 95$ kJ mol^{-1},[34,37] is noted and will be discussed later in the paper.

The temperature dependence of the ^1H and ^{13}C NMR line shapes and especially the unchanging nature of H(7) and C(7) resonances, indicating nonparticipation of these atoms in the rearrangement, allow the elimination of processes involving hydrogen and R_3E group migrations from further consideration as possible mechanisms for the dynamic behavior of complexes **2**. Indeed, both of these processes would effect the line shapes of the H(7) and C(7) signals. The latter process, by averaging the environment of *all* hydrogen and carbon atoms, would give rise to a single peak in the respective ^1H and ^{13}C NMR spectra.

We can think of four other processes to explain the observed temperature dependence of the NMR spectra, and these are depicted in Scheme I. The first process involves the reversible dissociation of carbon monoxide with the simultaneous formation of the (η^6-$R_3EC_7H_7$)Fe$(CO)_2$ intermediate. Rapid recombination of this short-lived species **2A** with CO leads to rearranged **2'**. The reported isolation of (η^6-C_7H_8)$Ru(CO)_2$ gives support for the consideration of this process.[40] The second feasible process involves dechelation of the $Fe(CO)_3$ moiety leading to the 16-electron coordinatively unsaturated intermediate

(40) Deganello, G.; Mantovani, A.; Sandrini, P. L.; Petrici, P.; Vitulli, G. *J. Organomet. Chem.* **1977**, *135*, 215.

2B which contains an η^2-bound cycloheptatriene ring. Collapse of **2B** can again give **2'** and constitutes an overall 1,3-iron shift. The next process, involving two consecutive 1,2-metal shifts with the intermediacy of (norcaradiene)-tricarbonyliron intermediate, **2C**, also has the effect of a net 1,3-iron shift. Finally, it is also possible that **2** and **2'** are interconverted through the intermediacy of **2D** which contains the unusual and rarely observed nonconjugated chelating diene bonding mode of cycloheptatriene,[41] (1,2,5,6-η-C_7H_7R). We should note, however, the above represent *limiting* mechanisms for the rearrangement. It is, of course, conceivable that the interchange **2** $\rightleftharpoons$ **2'** proceeds without the intervention of well-defined η^2, **2B**, or η^4, **2C**, and/or **2D** intermediates but lies closer to a direct 1,3-iron shift pathway. 1,3-Metal shifts have been identified as major rearrangement processes in (η^6-C_8H_8)$Cr(CO)_3$,[42] [$(C_{16}H_{16})Ru_2(CO)_5$],[43] and cycloheptatrienyl and cyclooctadienyl complexes of palladium.[44]

As a first step toward elucidating the mechanism of the rearrangement, ^{13}CO enrichment of the complexes **2** under thermal conditions was attempted. Heating the complexes under an atmosphere of 95% ^{13}CO in refluxing benzene or toluene for 4 h, a time perid much longer than that required for the NMR investigation, resulted in *no* ^{13}CO incorporation as evidenced by infrared spectroscopy and mass spectrometry. This then rules out process A as a plausible mechanism for the rearrangement. In this regard we note that heating **2C** in the presence of 2 equiv of triphenylphosphine for 3 days in benzene at 80 °C did not result in any reaction, refluxing in toluene at 112 °C for 3 days gave only an approximately 10% yield of $Fe(CO)_3(PPh_3)_2$. These experiments further corroborate our contention that path A is not the dominant operative mechanism for the rearrangement. They also seem to mitigate against the dechelation mechanism B. Indeed, it is not unreasonable to expect that intermediates **2A** and **2B**, albeit short-lived, would react with PPh_3, leading to substituted products. This, in the case of path B, would first give an expectedly labile olefin complex, (η^2-$R_3EC_7H_7$)$Fe(CO)_3PPh_3$, which would further react with triphenylphosphine, eliminating $R_3EC_7H_7$ and producing $Fe(CO)_3(PPh_3)_2$. There is some experimental support for this expectation. Whitesides et al.,[45] in their study of the cis–trans isomerization and hydrogen scrambling reactions in cyclic and acyclic (diene)$Fe(CO)_3$ complexes, noted that the isomerization of **4**, for which a dechelation step was

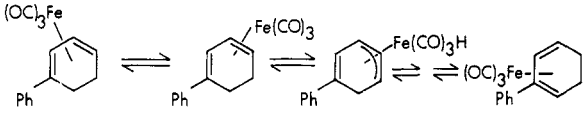

4 **5**

proposed, was greatly inhibited by excess PPh_3. In addition, a 71% yield of $Fe(CO)_3(PPh_3)_2$ was isolated when **4** was heated in the presence of a 10-fold excess of PPh_3 at 145 °C for several hours. On the other hand, Whitlock et al.,[46] in their study on the 1,3-$Fe(CO)_3$ shift in acyclic (polyene)$Fe(CO)_3$ complexes (**6**, **7**), apparently did not

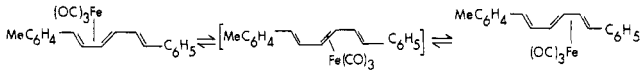

6 **7**

observe noticeable degradation of the complexes in the presence of PPh_3. However, the activation energies for the above process, which constitute essentially the energy required for the dechelation of the $Fe(CO)_3$ moiety, are around 140 kJ mol^{-1}, a value much higher than the ones observed in the present system. Although the rearrangement in the acyclic complexes must proceed via a coordinatively unsaturated η^2 intermediate, it is not known how accurate of a model these complexes are for the compounds **2**. Nevertheless, we feel that the startling decrease in the activation energies on going from **6** to **2** is most probably due to a change in the operative mechanism in the latter. Thus based on the changes in the activation energies and the inertness of complexes **2** toward PPh_3 substitution, we would tend to disfavor process B as the dominant path for rearrangement for this class of compounds. The solid-state structure of **2c** offers further support for this conclusion. As discussed before, the substitution by a silyl or germyl moiety results in a substantially stronger diene–metal bonding in complexes **2** relative to $CHTFe(CO)_3$.[47] Concurrent with these changes is the expectation of an increase in the dechelation energy of the $Fe(CO)_3$ moiety in compounds **2**, and hence an *increase* in the activation energy for $Fe(CO)_3$ movement should **2B** be a true intermediate in the rearrangement. However, ΔG^* in **2** is some 20 kJ mol^{-1} *less* than in $CHTFe(CO)_3$, a change *opposite* to what is expected for process B.

The significant decrease in the activation energy for the iron shift on going from the unsubstituted molecule to complexes **2** and the well-known fact that substituents at the C(7) carbon can have a dramatic effect on the position of the cycloheptatriene $\rightleftharpoons$ norcaradiene equilibrium[48] appear to indicate that path C, with the norcaradiene intermediate **2C**, could be an attractive alternative for the mechanism of fluxional behavior. Albeit electron-withdrawing substituents are most noted to shift the equilibrium toward the bicyclic species,[48,49] recent studies seem to indicate that π-electron donors can also cause a relative stabilization of the norcaradiene structure.[50] However, there are now irrefutable experimental results which mitigate against serious consideration of pathway C. Karel, Albright, and Brookhart,[34] in an elegant **2c** with specifically designed substituted cycloheptatrienetricarbonyliron complexes, have shown that the variation in barriers for rearrangement are clearly inconsistent with an intermediate which resembles a (norcaradiene)tricarbonyliron species. Furthermore, the syntheses of both *syn*- and *anti*-(norcaradiene)tricarbonyliron have just been communicated by Grimme and Koser.[51] Although both rearrange irreversibly to $CHTFe(CO)_3$, indicating that the latter is thermodynamically more stable, the rate of isomerization is approximately 10^8 times slower than the 1,3-iron shift. Thus neither of them can be an intermediate

(41) Brown, J. M.; Coles. D. G. *J. Organomet. Chem.* **1973**, *60*, C31 and references therein.
(42) (a) Mann, B. E. *J. Chem. Soc., Chem. Commun.* **1977**, 626. (b) Gibson, J. A.; Mann, B. E. *J. Chem. Soc., Dalton Trans.* **1979**, 1021.
(43) Humphries, A. P.; Knox, S. A. R. *J. Chem. Soc., Dalton Trans.* **1978**, 1514.
(44) Mann, B. E.; Maitlis, P. M. *J. Chem. Soc., Chem. Commun.* **1976**, 1058.
(45) Whitesides, T. H.; Neilan, J. P. *J. Am. Chem. Soc.* **1976**, *98*, 63.
(46) (a) Whitlock, H. W.; Chuah, Y. N. *J. Am. Chem. Soc.* **1965**, *87*, 3605. (b) Whitlock, H. W.; Reich, C.; Woessner, W. D. *Ibid.* **1971**, *93*, 2483.
(47) The stronger metal–diene bonding in **2** relative to $CHTFe(CO)_3$ is also supported by the UV photoelectron spectra of the molecules. Fragalà, I. L.; Takats, J., manuscript in preparation.
(48) (a) Ciganek, E. *J. Am. Chem. Soc.* **1971**, *93*, 2207. (b) Hall, G. E.; Roberts, J. D. *J. Am. Chem. Soc.* **1971**, *93*, 2203.
(49) Hoffmann, R. *Tetrahedron Lett.* **1970**, 2907.
(50) Staley, S. W.; Fox, M. A.; Cairncross, A. *J. Am. Chem. Soc.* **1977**, *99*, 4524.
(51) Grimme, W.; Köser, H. G. *J. Am. Chem. Soc.* **1981**, *103*, 5919.

in the pathway of the fluxional process.

No firm experimental evidences can be offered for or against pathway D. We note, however, that in his theoretical treatment of the subject, Albright[34] has considered the (1,2,5,6-η-C_7H_7R), **2D**, bonding mode an unlikely intermediate in the rearrangement because of the high-energy unoccupied ligand orbitals involved with this geometry.

Thus none of the limiting pathways depicted in Scheme I seem to fit the experimental observations or calculations concerning the fluxional behavior of (η^4-C_7H_7R)$Fe(CO)_3$ complexes. We are left with the inescapable conclusion that these molecules represent yet another example of the growing number of fluxional organometallic compounds which rearrange by direct 1,3-metal shifts. Although our study does not allow an unambiguous identification of the intimate mechanism nor a precise description of the details of the intermediate involved in the rearrangement, we again refer the reader to the theoretical analysis of Albright,[34] who concludes that the fluxionality is manifested by essentially direct 1,3-metal shifts. He also shows that electron-donating substituents at C(7) are expected to lower the barrier for rearrangement and do so by causing the $Fe(CO)_3$ moiety to move toward the C(3)–C(4) bond and the "way-point" of the 1,3 shift. We think it is no accident that this is the exact arrangement which is seen in the ground-state molecular structure of **2c**.

Without further dwelling on the mechanism, we would like to close this contribution by reiterating the experimental observation that relatively small substitutional changes at the C(7) position are apparently sufficient to produce quite visible changes in the fluxional character of this class of molecules. Or to put it another way, it does not take much to change whimpering to "performing dogs in the nighttime".[37]

Acknowledgment is made to NSERC of Canada (J.T.), Italian CNR (G.D.), and NATO (Grant No. 1209 to G.D. and J.T.) for financial support and the Killam Foundation for a postgraduate fellowship (J.G.A.R.). We wish to thank Dr. T. Nakashima and Mr. T. Brisbane for recording the NMR spectra and their help with the SST experiments, Dr. R. Ball for the X-ray structure of **2c**, Mr. L. Ramsay for experimental assistance, and Professors Albright and Brookhart for a preprint of ref 34.

Registry No. **1**, 36594-73-7; **2a**, 83006-17-1; **2b**, 83058-33-7; **2c**, 83058-34-8; $CHTFe(CO)_3$, 36343-88-1.

Supplementary Material Available: Listings of structure factor amplitudes and a table of bond distances and angles of the phenyl groups in **2c** (16 pages). Ordering information is given on any current masthead page.

Excited-State Chemistry of 1,1-Dimethylsilacyclobutane. The Role of Singlet and Triplet States at 254 nm

Clayton George and R. D. Koob*

Department of Chemistry, North Dakota State University, Fargo, North Dakota 58105

Received July 27, 1982

Direct photolysis of 1,1-dimethylsilacyclobutane (SCB) at a variety of excitation energies is compared with benzene-sensitized dissociation of SCB in the gas phase. Directly photolyzed SCB decomposes predominately to ethene and 2-methyl-2-silapropene. In the presence of benzene, SCB decomposes to cyclopropane and dimethylsilylene as well as C_2H_4 and $(CH_3)_2SiCH_2$. The relative amounts of the two sets of products depend strongly on other additives. The use of Xe in benzene causes the c-C_6H_6/C_2H_4 to increase proportionately to the Xe concentration. For a given Xe/benzene/SCB ratio, c-C_3H_6/C_2H_4 varies inversely with added *cis*-butene-2. From these observations we have concluded that C_2H_4 and $(CH_3)_2SiCH_2$ arise predominately from singlet SCB while c-C_3H_6 and $(CH_3)_2Si$ are the result of sensitization of SCB by triplet benzene. We have estimated that SCB quenches singlet benzene with a rate constant of $\sim 1 \times 10^{11}$ M^{-1} s^{-1}. SCB quenches triplet benzene with a rate constant of about 1.5×10^8 M^{-1} s^{-1}. Both numbers are based on $k_{ISC}^{Xe} = 3.58 \times 10^8$ M^{-1} s^{-1}, and the latter value also requires knowledge of the quenching rate constant for *cis*-butene.

Introduction

Identification of the multiplicity of electronic states participating in photoreactions is a common practice in physical organic chemistry. However, little has been said about the multiplicity of states participating in the observed photochemistry of organosilanes. This is the case even though photochemical investigations of organosilanes is not uncommon.[1-4]

There are a number of practical reasons why this situation exists. Carbonyl and aromatic molecules form the bulk of known photochemical systems for which conclusions have been drawn concerning reactive singlet and triplet states.[5] Siliconyl (>Si=O) and π-bonded silicon

(1) (a) O. P. Strausz, K. Obi, and W. Duholke, *J. Am. Chem. Soc.*, **90**, 1359 (1968); (b) A. G. Alexander and O. P. Strausz, *J. Phys. Chem.*, **80**, 2531 (1976); (c) S. K. Tokach and R. D. Koob, *ibid.*, **83**, 774 (1979).

(2) (a) H. P. Schuchmann, A. Ritter, and C. Von Sonntag, *J. Organomet. Chem.*, **148**, 213 (1978); (b) T. J. Barton and E. Kline, *ibid.*, **42**, C21 (1972); (c) I. M. T. Davidson and N. A. Ostah, *ibid.*, **206**, 149 (1981).

(3) (a) M. Ishikawa, K. I. Nakagawa, and M. Kumada, *J. Organomet. Chem.*, **190**, 117 (1980); (b) M. Ishikawa, T. Fuchikami, and M. Kumada, *ibid.*, **127**, 261 (1977); (c) M. Ishikawa, T. Fuchikami, and M. Kumada, *Tetrahedron Lett.*, **16**, 1299 (1976); (d) P. Boudjouk and L. H. Sommer, *J. Chem. Soc., Chem. Commun.*, 54 (1973).

(4) (a) M. A. Nay, G. N. C. Woodall, O. P. Strausz, and H. E. Gunning, *J. Am. Chem. Soc.*, **87**, 179 (1965); (b) S. K. Tokach and R. D. Koob, *ibid.*, **102**, 376 (1980).

(5) P. J. Wagner and G. S. Hammond, Properties and Reactions of Organic Molecules in their Triplet State, in "Advances in Photochemistry", W. A. Nayes, G. S. Hammond, and J. N. Pitts, Jr., Eds., Wiley, New York, 1968, p 21.

0276-7333/83/2302-0039$01.50/0

Excited-state chemistry of 1,1-dimethylsilacyclobutane. The role of singlet and triplet states at 254 nm

Clayton George, and R. D. Koob

Organometallics, **1983**, 2 (1), 39-43• DOI: 10.1021/om00073a008 • Publication Date (Web): 01 May 2002

in the pathway of the fluxional process.

No firm experimental evidences can be offered for or against pathway D. We note, however, that in his theoretical treatment of the subject, Albright[34] has considered the (1,2,5,6-η-C_7H_7R), **2D**, bonding mode an unlikely intermediate in the rearrangement because of the high-energy unoccupied ligand orbitals involved with this geometry.

Thus none of the limiting pathways depicted in Scheme I seem to fit the experimental observations or calculations concerning the fluxional behavior of (η^4-C_7H_7R)$Fe(CO)_3$ complexes. We are left with the inescapable conclusion that these molecules represent yet another example of the growing number of fluxional organometallic compounds which rearrange by direct 1,3-metal shifts. Although our study does not allow an unambiguous identification of the intimate mechanism nor a precise description of the details of the intermediate involved in the rearrangement, we again refer the reader to the theoretical analysis of Albright,[34] who concludes that the fluxionality is manifested by essentially direct 1,3-metal shifts. He also shows that electron-donating substituents at C(7) are expected to lower the barrier for rearrangement and do so by causing the $Fe(CO)_3$ moiety to move toward the C(3)–C(4) bond and the "way-point" of the 1,3 shift. We think it is no accident that this is the exact arrangement which is seen in the ground-state molecular structure of **2c**.

Without further dwelling on the mechanism, we would like to close this contribution by reiterating the experimental observation that relatively small substitutional changes at the C(7) position are apparently sufficient to produce quite visible changes in the fluxional character of this class of molecules. Or to put it another way, it does not take much to change whimpering to "performing dogs in the nighttime".[37]

Acknowledgment is made to NSERC of Canada (J.T.), Italian CNR (G.D.), and NATO (Grant No. 1209 to G.D. and J.T.) for financial support and the Killam Foundation for a postgraduate fellowship (J.G.A.R.). We wish to thank Dr. T. Nakashima and Mr. T. Brisbane for recording the NMR spectra and their help with the SST experiments, Dr. R. Ball for the X-ray structure of **2c**, Mr. L. Ramsay for experimental assistance, and Professors Albright and Brookhart for a preprint of ref 34.

Registry No. **1**, 36594-73-7; **2a**, 83006-17-1; **2b**, 83058-33-7; **2c**, 83058-34-8; $CHTFe(CO)_3$, 36343-88-1.

Supplementary Material Available: Listings of structure factor amplitudes and a table of bond distances and angles of the phenyl groups in **2c** (16 pages). Ordering information is given on any current masthead page.

Excited-State Chemistry of 1,1-Dimethylsilacyclobutane. The Role of Singlet and Triplet States at 254 nm

Clayton George and R. D. Koob*

Department of Chemistry, North Dakota State University, Fargo, North Dakota 58105

Received July 27, 1982

Direct photolysis of 1,1-dimethylsilacyclobutane (SCB) at a variety of excitation energies is compared with benzene-sensitized dissociation of SCB in the gas phase. Directly photolyzed SCB decomposes predominately to ethene and 2-methyl-2-silapropene. In the presence of benzene, SCB decomposes to cyclopropane and dimethylsilylene as well as C_2H_4 and $(CH_3)_2SiCH_2$. The relative amounts of the two sets of products depend strongly on other additives. The use of Xe in benzene causes the c-C_6H_6/C_2H_4 to increase proportionately to the Xe concentration. For a given Xe/benzene/SCB ratio, c-C_3H_6/C_2H_4 varies inversely with added *cis*-butene-2. From these observations we have concluded that C_2H_4 and $(CH_3)_2SiCH_2$ arise predominately from singlet SCB while c-C_3H_6 and $(CH_3)_2Si$ are the result of sensitization of SCB by triplet benzene. We have estimated that SCB quenches singlet benzene with a rate constant of $\sim 1 \times 10^{11}$ M^{-1} s^{-1}. SCB quenches triplet benzene with a rate constant of about 1.5×10^8 M^{-1} s^{-1}. Both numbers are based on $k_{ISC}^{Xe} = 3.58 \times 10^8$ M^{-1} s^{-1}, and the latter value also requires knowledge of the quenching rate constant for *cis*-butene.

Introduction

Identification of the multiplicity of electronic states participating in photoreactions is a common practice in physical organic chemistry. However, little has been said about the multiplicity of states participating in the observed photochemistry of organosilanes. This is the case even though photochemical investigations of organosilanes is not uncommon.[1-4]

There are a number of practical reasons why this situation exists. Carbonyl and aromatic molecules form the bulk of known photochemical systems for which conclusions have been drawn concerning reactive singlet and triplet states.[5] Siliconyl (>Si=O) and π-bonded silicon

(1) (a) O. P. Strausz, K. Obi, and W. Duholke, *J. Am. Chem. Soc.*, **90**, 1359 (1968); (b) A. G. Alexander and O. P. Strausz, *J. Phys. Chem.*, **80**, 2531 (1976); (c) S. K. Tokach and R. D. Koob, *ibid.*, **83**, 774 (1979).

(2) (a) H. P. Schuchmann, A. Ritter, and C. Von Sonntag, *J. Organomet. Chem.*, **148**, 213 (1978); (b) T. J. Barton and E. Kline, *ibid.*, **42**, C21 (1972); (c) I. M. T. Davidson and N. A. Ostah, *ibid.*, **206**, 149 (1981).

(3) (a) M. Ishikawa, K. I. Nakagawa, and M. Kumada, *J. Organomet. Chem.*, **190**, 117 (1980); (b) M. Ishikawa, T. Fuchikami, and M. Kumada, *ibid.*, **127**, 261 (1977); (c) M. Ishikawa, T. Fuchikami, and M. Kumada, *Tetrahedron Lett.*, **16**, 1299 (1976); (d) P. Boudjouk and L. H. Sommer, *J. Chem. Soc., Chem. Commun.*, 54 (1973).

(4) (a) M. A. Nay, G. N. C. Woodall, O. P. Strausz, and H. E. Gunning, *J. Am. Chem. Soc.*, **87**, 179 (1965); (b) S. K. Tokach and R. D. Koob, *ibid.*, **102**, 376 (1980).

(5) P. J. Wagner and G. S. Hammond, Properties and Reactions of Organic Molecules in their Triplet State, in "Advances in Photochemistry", W. A. Nayes, G. S. Hammond, and J. N. Pitts, Jr., Eds., Wiley, New York, 1968, p 21.

0276-7333/83/2302-0039$01.50/0

Table I. Hydrocarbon Products Relative to Ethene from the Photolysis of 1,1-Dimethylsilacyclobutane under a Variety of Conditions

	$h\nu$, nm								
	147[a]	147[a]	185–210[b]	254	254	254	254	254	147
p_{total}, torr	30	30	50	10	10	10	10	80	300
additive[g]		O_2 (0.05)			O_2 (0.03)	B (0.9)[d]	O_2/B (0.05/0.9)	Xe/B (0.89/Q1)	O_2 (0.98)
CH_4	0.07	0.05	c	0.09	0.05	0.15	0.04	0.09	f
C_2H_4	1.0	1.0	1.0	1.0	1.0	1.0	1.0	1.0	1.0
C_2H_6	0.03	0.0	c	0.04	0.0	0.05	0.0	e	
C_3H_6	0.03	0.03	0.05	0.09	0.09	0.09	0.08	0.08	0.37
c-C_3H_6	0.01	0.01	c	0.03	0.03	0.02	0.14	0.14	2.85
C_3H_8	0.02	0.0	c	0.01	0.0	0.01	0.0	0.0	0.15

[a] Reference 10. [b] Reference 11. [c] Not reported. [d] B = benzene. [e] Obscured by xenon elution. [f] Not measured. [g] Number in parentheses is fraction of total pressure contributed by additive.

compounds are stable only in rare examples.[6] Thus, the direct analogy between carbon and organosilicon chemistry is unavailable. Many of the simple diagnostics of triplet state chemistry, sensitization and/or quenching by carbonyl compounds, for example, are complicated by the tendency for functionalized organosilicon molecules to react rapidly with polar oxygen-containing species.[7]

A close analogy to what follows is the work of Lee et al. on cyclobutanone (CB).[8] By a careful combination of photochemical and sensitization experiments, this group was able to elucidate a reasonably detailed mechanism for cyclobutanone dissociation. Upon initial examination SCB would not appear to be a good choice for comparable work. This molecule absorbs strongly only below 200 nm.[9] Direct pholysis has been reported only at 147 and 185–210 nm,[10,11] and chemical methods for distinguishing between singlet and triplet states are not well developed for this energy region. However, close examination of the gas-phase absorption spectrum reveals the presence of a low intensity diffuse band extending well into the far-UV. The molar extinction coefficient of SCB at 254 nm is $\simeq 0.2\ M^{-1}\ cm^{-1}$. This value is 100 times smaller than for cyclobutanone (CB) at 254 nm.[8] Nonetheless, the analogy between the silacyclobutane and cyclobutanone is strong enough to allow fruitful application of the techniques used by Lee for CB to SCB.

Experimental Section

All samples were prepared on a Hg free vacuum line by using standard procedures. Pressures were measured by using a Wallace and Tiernan Model 61-C pressure gauge. Typical sample pressures were 10 torr. Samples were allowed to equilibrate for approximately 2 h to achieve uniform mixtures. A cylindrical sample cell, 10 cm long × 3 cm diameter, fitted with a quartz window was used for photolyses in a Rayonet photochemical reactor equipped with one low-pressure mercury arc lamp. Typical exposure times were 600 s with conversions less than 0.1%.

Analyses of samples were performed by gas chromatography using flame ionization detection. A 15-m, 25% squalane column at 25 °C separated methane, ethane, ethene, propane, propene, and cyclopropane. Retention times for each product were verified by authentic samples.

All starting compounds were vacuum distilled to a minimum of 98% purity, with the exception of oxygen, which was used without further purification.

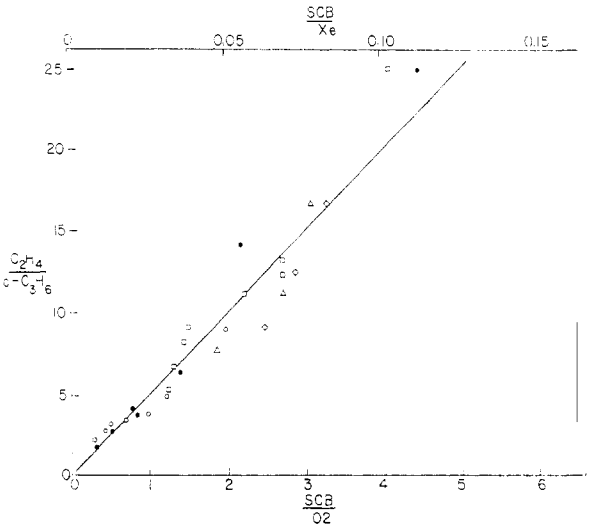

Figure 1. The product ratio C_2H_4/c-C_3H_6 (corrected, see text) is plotted vs. SCB/O_2 concentration (open symbols and lower scale) and SCB/Xe concentrations (closed symbols and upper scale) at a variety of benzene concentrations: ●, SCB/C_6H_6 = 0.1; ○, SCB/C_6H_6 = 0.1; □, SCB/C_6H_6 = 0.5; △, SCB/C_6H_6 = 1.0; ◇, SCB/C_6H_6 = 2.0. The slope for the Xe data is 2.4×10^2. Intercepts are zero.

Results

Table I compares results from the direct photolysis of SCB at 147,[10] 185–210,[11] and 254 nm, respectively. In addition, selected conditions with O_2, benzene, O_2/benzene mixtures, and Xe/benzene mixtures are included. Ethene remains the predominant hydrocarbon product under all photochemical conditions. Thermally induced dissociation of SCB also gives C_2H_4 as the predominant product.[12] The other products, always minor, are remarkably independent of excitation energy. The possible exception is the yield of propene which increases from 3% to 9% of the ethene yield as excitation energy decreases from 147 to 254 nm. A comparable trend exists for cyclopropane, but the yield of c-C_3H_6 is a factor of 3 smaller. Propane, ethane, and a fraction of methane may be ascribed to the reaction of methyl radicals. The radical nature of the precursors to these products is confirmed by their depletion with the addition of small amounts of oxygen. A small yield of methane remains in the presence of O_2 and must derive

(6) (a) L. E. Gusel'nikov and N. S. Nametkin, *Chem. Rev.*, **79**, 531 (1979); (b) A. G. Brook, F. Abdesaken, B. Gutekunst, G. Gutekunst, and R. Kallury, *J. Chem. Soc., Chem. Commun.*, **4**, 191 (1981). (c) R. West, 15th Annual Silicon Symposium, Durham, N.C., March 15, 1981. (d) $R_2Si{=}O$ species at present have only been postulated as reactive intermediates. See: T. H. Lane and C. L. Frye, *J. Organomet. Chem.*, **172**, 213 (1979).

(7) L. H. Sommer, "Stereochemistry, Mechanism and Silicon"; McGraw-Hill: New York, 1965.

(8) E. K. C. Lee, Role of Singlet and triplet states in photochemistry of Gaseous Molecules with π-bonds, in "Excited States Chemistry", J. N. Pitts, Jr., Ed., Gordon and Breach, New York, 1970, p 59.

(9) V. A. Petukov, V. I. Zav, and V. M. Vdovin, *Khim. Geterotsikl. Soedin.*, 164 (1968).

(10) S. K. Tokach, P. Boudjouk, R. D. Koob, *J. Phys. Chem.*, **82**, 1203 (1978).

(11) H. C. Low and P. John, *J. Organomet. Chem.*, **201**, 363 (1980).

(12) M. C. Flowers and L. E. Gusel'nikov, *J. Chem. Soc. B*, **419**, 1396 (1968).

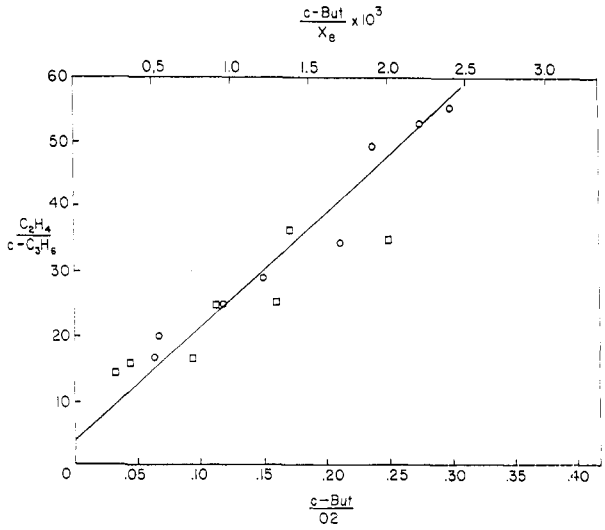

Figure 2. The product ratio (C_2H_4/c-C_3H_6) is plotted vs. the additive ratios *cis*-butene/O_2 (□; lower scale) and *cis*-butene/Xe (○; upper scale). For all of the data SCB/O_2 = 0.4 and SCB/Xe = 0.02. For the xenon data the slope is 2.2×10^4 and the intercept is 3.7.

from an unimolecular process.

While only minor changes in product distribution are observed with changing excitation energy, significant changes are noted when benzene is added along with O_2 or xenon. Benzene alone has little effect on the product distribution. Small amounts of oxygen and modest amounts of xenon added to the SCB/benzene mixture effect a marked increase in c-C_3H_6 relative to all other products. Relative to ethene, all other products, except c-C_3H_6, remain constant when xenon is added. The effect of these additives is displayed further in Figure 1. The ratio C_2H_4/c-C_3H_6 is plotted vs. SCB/O_2 (lower abscissa scale) and SCB/Xe (upper abscissa scale) for a given benzene concentration. The direct relationship between additives, Xe or O_2, and c-C_3H_6 yield is immediately apparent. Addition of 1 atm of N_2 has no effect on the product distribution. The absolute amount of benzene present in a given system appears to have little effect on the C_2H_4/c-C_3H_6 ratio. Addition of methanol does not affect the hydrocarbon distribution but does result in the appearance of trimethylmethoxysilane, an indicator of the presence of $(CH_3)_2SiCH_2$. The last two observations demonstrate that secondary reactions of silicon-containing intermediates are not the cause of the increasing cyclopropane/ethene ratio.

The C_2H_4/c-C_3H_6 ratio that is plotted is actually a slight modification of the observed values. For purposes of the plot, the cyclopropane produced in the direct photolysis is subtracted from the cyclopropane observed in the sensitized experiments. The effect of leaving this "background" cyclopropane incorporated in the ratio would be to flatten the right-hand portion of the plot.

For ease of presentation, both oxygen and xenon additive experiments are presented in the same figure, but relative to different abscissa.

For reasons that will be obvious from the discussion, *cis*-butene-2 was used as an additive for fixed ratios of SCB/O_2/B and SCB/Xe/B. Figure 2 plots these results. C_2H_4/c-C_3H_6 is directly proportional to *cis*-butene-2 concentration. Said another way, the importance of c-C_3H_6 to the overall product distribution is diminished in the presence of *cis*-butene-2.

Discussion

While ethene dominates the SCB photoproducts, other reaction channels exist as indicated by reactions 1–4. C_3H_6

$$\text{SCB} \xrightarrow[254\text{ nm}]{h\nu} \text{SCB}^*$$

$$\text{SCB}^* \xrightarrow{1.0} C_2H_4 + [Me_2Si{=}CH_2] \quad (1)$$

$$\text{SCB}^* \xrightarrow{0.04} CH_4 + SiC_4H_8 \quad (2)$$

$$\text{SCB}^* \xrightarrow{0.13} CH_3 + SiC_4H_9 \quad (3)$$

$$\text{SCB}^* \xrightarrow{0.12} C_3H_6 + SiC_2H_6 \quad (4)$$

appears as both propene and cyclopropane, but in a constant ratio. Thus, it is written as a single channel. There is remarkably little variation in the relative importance of each of these channels with excitation energies which range from ~115 to 191 kcal/mol. One presumes that even at the lowest excitation value, energies are well in excess of the E_{min} for any channel and that other factors control the relative population of these channels. Increasing excitation energy then just increases the internal energy of each product but is insufficient to open new paths. Evidence for internal excitation is available in earlier work on SCB.[10]

The initially populated state(s) for SCB is (are) certainly singlet. There is no evidence for intersystem crossing in SCB indicated from the benzene sensitization work discussed below. Internal conversion to a highly excited ground state, S_0*, is possible in that the most important product of pyrolysis of SCB is also ethene. We have no real evidence concerning this possibility, but it is interesting to note that the photochemistry[13] and thermochemistry[14] of 1,1,3,3-tetramethyl-1,3-disilacyclobutane are completely different.

The observation that the hydrocarbon product distribution is virtually unchanged when a system containing ninefold excess of benzene over SCB is irradiated at 254 nm is somewhat surprising. Certainly all light is absorbed by benzene ($A_B/A_{SCB} > 10^3$) so that any products observed from SCB dissociation must arise by an energy-transfer step

$$B^* + \text{SCB} \rightarrow \text{SCB}^* + B$$

Considerable information is available concerning B* produced by 254-nm light. In pure gas phase benzene at 10 torr and λ_{excite} = 254 nm, the fluorescence quantum yield, $^1B_{2u} \rightarrow {}^1A_{1g} + h\nu$, is 0.18[15] with a lifetime, τ_f, of about 70 ns.[16] Cundall and Davies determined the triplet benzene ($^3B_{1u}$) quantum yield at 254 nm and 2–17 torr to be 0.72 by measuring the cis ↔ trans isomerization of butene-2.[17] A variety of values have been obtained for triplet state lifetimes of benzene under these conditions, but all are in the microsecond range. Clearly, the steady-state concentration of $^3B_{1u}$ benzene will exceed that of $^1B_{2u}$ in the gas phase at 10 torr excited at 254 nm. Yet, energy transfer to SCB under these conditions provide a product distribution indistinguishable from direct photolysis which "intuitively" would be expected to arise from singlet states.

One can maintain the hypothesis of a singlet source of photoproducts in the direct photolysis if the relative rate constant for quenching of $^1B_{2u}$ benzene by SCB is considerably larger than that for $^3B_{1u}$. The experiments with

(13) S. K. Tokach and R. D. Koob, unpublished results.
(14) L. E. Gusel'nikov, V. K. Potapov, L. A. Volniva, V. Yu. Orlov, U. M. Vdovin, and N. S. Nametkin, *Dokl. Akad. Nauk SSSR*, **229**, 1364 (1976).
(15) (a) H. Ishikawa and W. A. Noyes, Jr., *J. Chem. Phys.*, **37**, 583 (1962); (b) J. A. Poole, *J. Phys. Chem.*, **69**, 1343 (1965).
(16) C. S. Burton and H. E. Hunziker, *J. Chem. Phys.*, **52**, 3302 (1970).
(17) R. B. Cundall and A. S. Davis, *Trans. Faraday Soc.*, **62**, 1151 (1966).

Xe probe that possibility. This additive assists intersystem crossing in benzene.[18] By increasing the concentration of triplet benzene at the expense of singlet, it should be possible to increase the contribution of triplet sensitized reaction. This is realized in this system as illustrated by Figure 1. We are fortunate, but not surprised, to find a specific product, c-C_3H_6, apparently associated with triplet sensitization. This finding is reminiscent of cyclobutanone where a similar conclusion is reached.[8] In contrast to the cyclobutanone example, c-C_3H_6 appears to be produced with too little excess energy to isomerize to propene. The propene yield remains unchanged from that found in the direct photolysis and independent of the cyclopropane yield.

Sensitization of SCB with triplet benzene adds a new reaction channel, cyclopropane produced without associated propene. From this point forward it is assumed that (cyclopropane − propene/3, as discussed in results) is directly proportional to the yield of the reaction initiated by triplet benzene.

As verification of the hypothesis that triplet benzene is the precursor to c-C_3H_6 and to provide an alternate measure of the rate constant for quenching of triplet by SCB, competitive quenching experiments were performed with *cis*-butene-2.[15] The results of these experiments are plotted as Figure 2. The expected dependence of C_2H_4/c-C_3H_6 is apparent. As the concentration of cis-butene-2 increases, the singlet/triplet product ratio increases.

While qualitative agreement is found between the hypothesis of triplet enhancement in benzene/oxygen mixtures as is found in benzene/xenon mixtures based on increased triplet sensitized product, cyclopropane, comparison of rate constants derived from the data and those available in the literature cause further examination of the simple interpretation when oxygen is used. For example, oxygen is reported to be 180 times more efficient than xenon in converting singlet to triplet benzene. Yet, from a comparison of the slopes of the lines in Figure 1, only a factor of 43 is obtained. Further, the triplet quenching rate constant for oxygen is large enough to compete with other triplet quenchers, particularly SCB. This expectation is not consistent with experimental observation, which indicates little depression of overall product yield even when oxygen concentration exceeds that of SCB. The implication of both of these findings is that the mechanism involving oxygen is more complex than that involving xenon, and oxygen must play additional roles beyond facilitating singlet–triplet transfer in benzene. Potential complications include the following: (a) Triplet benzene has been shown to sensitize emission of O_2 ($^1\Delta_g$).[19] This, of course, implies quenching of triplet benzene by O_2. (b) Photolysis of O_2/SCB mixtures with O_2 in considerable excess leads to the product distribution found in the last column of Table I. Note the large relative yield of cyclopropane under these conditions. (c) O_2 is a demonstrated radical scavenger and may intercept long-lived diradical intermediates.

From the xenon data of Figures 1 and 2 we are able to calculate the singlet and triplet quenching efficiencies of SCB. These are reported in Table II. (See Appendix for calculation details.) Several groups have measured triplet benzene quenching efficiencies of a number of π-bonded molecules,[8] and the values for SCB fall about 2 orders of magnitudes below typical alkenes, aldehydes, or ketones.

(18) R. B. Cundall and S. M. Ogilvie, The photophysics of benzene in fluid media, in "Organic Molecular Photophysics", T. B. Buks, Ed., Wiley, New York, 1975, p 33.
(19) D. R. Snelling, *Chem. Phys. Lett.*, **2**, 346 (1968).

Table II

	Xe/B/SCB	Xe/B/SCB/ *cis*-butene
k_{Qs},[a] M^{-1} s^{-1}	8.6×10^{10}	1.3×10^{11}
k_{Q1},[a] M^{-1} s^{-1}		1.5×10^{8}

[a] Value based on $K_{isc}^{Xe} = 3.58 \times 10^{8}$ as reported in ref 18. [b] Value based on k_{isc} as above and *cis*-butene $k_c = 9 \times 10^{9}$ as reported in ref 15.

Relative to cyclobutanone, which exhibits similar chemistry, SCB is comparably efficient in quenching singlet benzene but only 0.07 times as efficient in quenching triplet benzene based on our measurements and Lee's reported values for cyclobutanone.[8]

The following mechanism for the Xe/B/SCB system is proposed on the basis of the experiments done up to this time.

$$C_6H_6(^1A_{1g}) \xrightarrow[254\text{ nm}]{h\nu} C_6H_6(^1B_{2u}) \quad (5)$$

$$C_6H_6(^1B_{2u}) \xrightarrow{k_{ISC}^{B}} C_6H_6(^3B_{1u}) \quad (6)$$

$$C_6H_6(^1B_{2u}) + Xe \xrightarrow{k_{ISC}^{BXe}} C_6H_6(^3B_{1u}) + Xe \quad (7)$$

$$C_6H_6(^1B_{2u}) + SCB \xrightarrow{k_Q^S} SCB^{(*)} + C_6H_6(^1A_{1g}) \quad (8)$$

$$C_6H_6(^3B_{1u}) + SCB \xrightarrow{k_Q^T} c\text{-}C_3H_6 + Me_2Si + C_6H_6(^1A_{1g}) \quad (9)$$

$$SCB^{(*)} \xrightarrow{k_{D^*}} \text{reactions 1–4} \quad (10)$$

At this stage we are unable to distinguish beyond two distinct routes to silacyclobutane dissociation, one arising from singlet benzene sensitization or photolysis (SCB*) and the second arising from triplet benzene sensitization. SCB* is a species which dissociates predominately to C_2H_4 and $Me_2Si{=}CH_2$ but also yields other minor products. Within the resolution of our data, the SCB* product spectrum is approximately independent of excitation energy. All of the same minor products are observed along with ethene regardless of initial excitation over the range of 105–190 kcal/mol. Similar minor products have not been reported in examples of gas-phase pyrolyses[12] so one cannot immediately yield to the temptation of assigning SCB* to a vibrationally excited ground-state singlet. On the other hand, this possibility is not excluded by pyrolysis experiments as the activation for this reaction is only of the order of 64 kcal/mol.

Throughout this paper we have referred to an increase in relative cyclopropane yield to be a result of triplet benzene sensitization of SCB dissociation. We believe that the experiments presented provide a convincing case that triplet benzene is the precursor to enhanced cyclopropane yields. The temptation is strong, based on analogy to cyclobutanone studies, to suggest that a triplet SCB is produced in the sensitization step by direct energy transfer. If this proves to be the case, this is among the first reactions producing a triplet organosilane to be reported. Unfortunately, the present state of our data does not allow us to draw this conclusion. The small value for the triplet benzene quenching rate constant and the possibility for direct chemical interaction between the relatively long-lived triplet benzene and SCB force us to delay drawing conclusions about the nature of the triplet sensitization reaction.

Because the singlet quenching efficiency of SCB is approximately 3 orders of magnitude greater than its triplet quenching efficiency, it is experimentally not possible to

completely suppress all dissociation arising from the singlet channel using xenon. The intersystem crossing rate constant due to oxygen addition is considerably larger for oxygen than for xenon,[18] but the use of oxygen is complicated by, among other things, the onset of additional routes to product introduced by oxygen's ability to quench triplet benzene. The energy thus transferred to oxygen apparently enables it to attack SCB successfully and produce cyclopropane. Essentially all previously known reactions of excited oxygen involve unsaturated molecules.[20] The possibility of direct reaction between excited molecular oxygen and silicon centers in saturated molecules as suggested by the benzene sensitized and direct O_2/SCB photolysis experiments certainly merits further investigation. Should reactions similar to those found for SCB and oxygen appear for other alkylsilanes, a new class of reactions of excited oxygen would have to be added to the already extensive list.

The disilane "photolyses" of Kumada and co-workers[3] are of special note in the context of the results reported above. As pointed out before,[21] the rearrangement products in the disilane photochemistry are not inconsistent with a diradical mechanism. While this work does not bear directly on the solution photolyses of Kumada's group, it is clear that it would be improper to interpret photoinitiated dissociation in excess benzene as a direct photolysis. All products from reacting organosilanes must derive ultimately from energy transfer from or interaction with the benzene solvent. Recent work by Kumada and co-workers also suggests that more than one state may be responsible for the range of products observed when aryldisilanes are photolyzed.[22]

(20) E. A. Ogryzlo, Gaseous Singlet Oxygen, in "Singlet Oxygen", H. H. Wasserman and R. W. Murray, Eds., Academic Press, New York, 1979, p 35.

(21) (a) P. Boudjouk, J. S. Kiely, and R. D. Koob, 13th International Organosilicon Symposium, Ann Arbor, Mich., March 30, 1979. (b) R. D. Koob, C. George, J. S. Kiely, and P. Boudjouk, 15th International Organosilicon Symposium, Midland, Mich., 1982.

(22) (a) M. Ishikawa, N. Sugisawa, T. Fuchikami, M. Kumada, T. Yamabe, N. Kawakami, K. Fukui, Y. Ueki, and K. Shizuka, *J. Am. Chem. Soc.* **104**, 2872 (1982); (b) H. Shizuka, Y. Sato, M. Ishikawa, and M. Kumada, *J. Chem. Soc., Chem. Commun.*, 439 (1982).

Appendix

With the assumption of a steady state for all intermediates, the C_2H_4/c-C_3H_6 ratio can be derived from the proposed mechanisms.

$$\frac{[C_2H_4]}{[c\text{-}C_3H_6]} = \frac{k_{D^*}[SCB^{(*)}]}{k_Q^T[SCB][C_6H_6(^3B_{1u})]} = \frac{k_Q^S[C_6H_6(^1B_{2u})]}{k_Q^T[C_6H_6(^3B_{1u})]}$$

$$\frac{d[C_6H_6(^3B_{1u})]}{dt} = k_{ISC}[C_6H_6(^1B_{2u})] + k_{ISC}^{B1Xe}[C_6H_6(^1B_{2u})][Xe] - k_Q^T[C_6H_6(^3B_{1u})][SCB] = 0$$

$$\frac{[C_6H_6(^1B_{2u})]}{C_6H_6(^3B_{1u})]} = \frac{k_Q^T[SCB]}{k_{ISC} + k_{ISC}^{B1Xe}[Xe]}$$

$$\frac{[C_2H_4]}{[c\text{-}C_3H_6]} = \frac{k_Q^S}{k_Q^T}\left\{\frac{k_Q^T[SCB]}{k_{ISC} + k_{ISC}^{B1Xe}]}\right\}$$

If we assume $k_{ISC} < k_{ISC}^{B1Xe}[Xe]$, then

$$\frac{[C_2H_4]}{[c\text{-}C_3H_6]} = \frac{k_Q^S}{k_{ISC}^{B1Xe}}\frac{[SCB]}{[Xe]}$$

From the slope of Figure 1, one calculates k_Q^S (Table II). Adding *cis*-butene-2 to the mixture requires an additional mechanistic step.

$$C_6H_6(^3B_{1u}) + cis\text{-butene} \xrightarrow[k_{cis\text{-butene}}]{} C_6H_6(^1A_{1g}) + cis\text{-butene}^{(*)}$$

$[C_2H_4]/[c\text{-}C_3H_6]$ then becomes

$$\frac{[C_2H_4]}{[c\text{-}C_3H_6]} = \frac{k_Q^S}{k_Q^T}\left\{\frac{k_{cis\text{-butene}}}{k_{ISC}^{B1Xe}}\frac{[cis\text{-butene}]}{[Xe]} + \frac{k_Q^T}{k_{ISC}^{B1Xe}}\frac{[SCB]}{[Xe]}\right\}$$

For a constant [SCB]/[Xe], the slope and intercept terms from Figure 2 then allows calculation of both singlet and triplet quenching rates (Table II).

Registry No. SCB, 2295-12-7.

Five-Coordinate Bent Metallocenes. Crystal and Molecular Structure of Bis(η^5-cyclopentadienyl)chloro-(*N*,*N*-dimethylmonothiocarbamato)zirconium(IV)

Michael E. Silver and Robert C. Fay*

Department of Chemistry, Cornell University, Ithaca, New York, 14853

Received June 21, 1981

Bis(η^5-cyclopentadienyl)chloro(*N*,*N*-dimethylmonothiocarbamato)zirconium(IV), $(\eta^5\text{-}C_5H_5)_2ZrCl[SOCN(CH_3)_2]$, has been prepared by reaction of $(\eta^5\text{-}C_5H_5)_2ZrCl_2$ with anhydrous $Na[SOCN(CH_3)_2]$ and has been characterized by chemical analysis and ^1H NMR and IR spectroscopy. The crystal and molecular structure of $(\eta^5\text{-}C_5H_5)_2ZrCl[SOCN(CH_3)_2]$ has been determined by X-ray diffraction and has been refined anisotropically by least-squares methods to $R_1 = 0.061$ and $R_2 = 0.078$ using 2302 independent diffractometer data having $2\theta_{MoK\alpha} \leq 55.1°$ and $|F_o| > 2.0\sigma_F$. The compound crystallizes in the orthorhombic space group *Pbca* with eight molecules in a cell having dimensions $a = 13.440$ (3) Å, $b = 15.425$ (2) Å, and $c = 14.143$ (4) Å ($\rho_{obsd} = 1.645$ and $\rho_{calcd} = 1.636$ g cm^{-3}). The molecules have a five-coordinate bent metallocene structure with the Zr atom, Cl atom, and S and O atoms of the bidentate monothiocarbamate ligand lying in an equatorial plane that is nearly perpendicular to the plane defined by the Zr atom and the centroids of the two symmetrically attached η^5-C_5H_5 groups. The monothiocarbamate ligand is oriented so as to place the smaller O atom in the sterically more congested, lateral coordination site and the larger S atom in the less congested, interior site adjacent to the Cl atom. Bond lengths in the $ZrClSOC_{10}$ coordination group are Zr–Cl = 2.550 (2), Zr–O = 2.249 (4), Zr–S = 2.641 (2), and Zr–C (av) = 2.521 (4) Å. The bonds to the lateral coordination sites (Zr–Cl and Zr–O) are long, indicative of considerable crowding in the coordination group.

Introduction

The vast majority of bis(η^5-cyclopentadienyl) group 4 transition-metal complexes are 16-electron complexes with two additional ligands, $(\eta^5\text{-}C_5H_5)_2ML_2$.[1] "Five-coordinate", 18-electron complexes of the type $(\eta^5\text{-}C_5H_5)_2ML_3$ are rare,[2-4] perhaps due to the steric requirements of the three additional ligands. Recently, the structures of two $(\eta^5\text{-}C_5H_5)_2ZrL_3$ complexes that contain chelating ligands, $(\eta^5\text{-}C_5H_5)_2Zr(COCH_3)(CH_3)$[5] (1) and $(\eta^5\text{-}C_5H_5)_2ZrCl[S_2CN(C_2H_5)_2]$[6] (2) have been determined by X-ray diffraction.

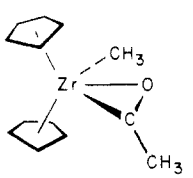

1

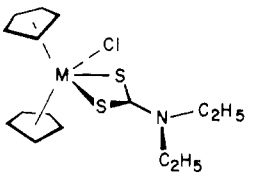

2

The coordination group of the dithiocarbamate complex **2** is severely congested, resulting in unusually long Zr–Cl and Zr–S bonds to the lateral coordination sites (2.556 (2) and 2.723 (2) Å, respectively). Indeed, these are the longest terminal Zr–Cl and Zr–S bond lengths yet observed for any structure involving Zr(IV).

In order to explore the effect of donor atom size on steric crowding in $(\eta^5\text{-}C_5H_5)_2ML_3$ complexes, we have prepared and determined the X-ray crystal structure of the analogous monothiocarbamate complex, $(\eta^5\text{-}C_5H_5)_2ZrCl[SOCN(CH_3)_2]$. The present study confirms the expected bent metallocene geometry **3** and reveals that the smaller oxygen atom occupies the sterically more congested, lateral coordination site.

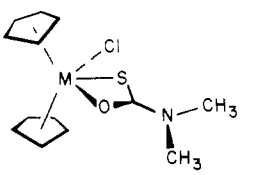

3

Experimental Section

Reagents and General Techniques. Sodium *N*,*N*-dimethylmonothiocarbamate was prepared as previously described.[7] Solvents were dried by refluxing for at least 24 h over phosphorus(V) oxide (dichloromethane and carbon tetrachloride) or calcium hydride (hexane). The synthesis and subsequent handling of $(\eta^5\text{-}C_5H_5)_2ZrCl[SOCN(CH_3)_2]$ was conducted under anhydrous conditions in a dry nitrogen atmosphere.

Bis(η^5-cyclopentadienyl)chloro(*N*,*N*-dimethylmonothiocarbamato)zirconium(IV). This compound was prepared by reaction for 24 h of equimolar amounts of $(\eta^5\text{-}C_5H_5)_2ZrCl_2$ (Alfa Products) and anhydrous $Na[SOCN(CH_3)_2]$ in refluxing dichloromethane. Recrystallization from dichloromethane–hexane afforded clear, colorless crystals of $(\eta^5\text{-}C_5H_5)_2ZrCl[SOCN(CH_3)_2]$: mp 219–222 °C; ^1H NMR (ppm, $CDCl_3$ solution) –2.99 (CH_3), –3.08 (CH_3), –6.16 (C_5H_5); IR (cm^{-1}, Nujol mull) ν(C=O) and ν(C=N) 1568 (s), ν(C=S) 939 (w), ν(Zr–O) 559 (s), ν(Zr–Cl) and ν(Zr–S), 333 (s), other bands, 1418 (w), 1403 (m), 1322 (w), 1256 (m), 1140 (s), 1062 (w), 1019 (s), 847 (m), 823 (s), 815 (s), 803 (s), 713 (s), 663 (w), 610 (w), 482 (m), 402 (m). Anal. Calcd for $Zr(C_5H_5)_2(C_3H_6NOS)Cl$: C, 43.25; H, 4.47; Cl, 9.82; N, 3.88; S, 8.88; Zr, 25.27. Found: C, 42.98; H, 4.56; Cl, 10.01; N, 3.82; S, 8.99; Zr, 24.96.

Nuclear Magnetic Resonance Spectra. Proton chemical shifts were measured at ambient probe temperature (~34 °C)

(1) Wailes, P. C.; Coutts, R. S. P.; Weigold, H. "Organometallic Chemistry of Titanium, Zirconium, and Hafnium"; Academic Press: New York, 1974.

(2) The most familiar examples are the trihydride complexes of group 5 and group 6 metallocenes, $(\eta^5\text{-}C_5H_5)_2NbH_3$,[3] $(\eta^5\text{-}C_5H_5)_2TaH_3$,[3,4] and $[(\eta^5\text{-}C_5H_5)_2WH_3]^+$.[3,4]

(3) Wilson, R. D.; Koetzle, T. F.; Hart, D. W.; Kvick, A.; Tipton, D. L.; Bau, R. *J. Am. Chem. Soc.* **1977**, *99*, 1775.

(4) Green, M. L. H.; McCleverty, J. A.; Pratt, L.; Wilkinson, G. *J. Chem. Soc.* **1961**, 4854.

(5) (a) Fachinetti, G.; Floriani, C.; Marchetti, F.; Merlino, S. *J. Chem. Soc., Chem. Commun.* **1976**, 522. (b) Fachinetti, G.; Fochi, G.; Floriani, C. *J. Chem. Soc., Dalton Trans.* **1977**, 1946.

(6) Silver, M. E.; Eisenstein, O.; Fay, R. C. *Inorg. Chem.*, in press.

(7) Hawthorne, S. L.; Bruder, A. H.; Fay, R. C. *Inorg. Chem.* **1978**, *17*, 2114.

0276-7333/83/2302-0044$01.50/0

relative to an internal reference of tetramethylsilane with a Varian EM-390 90-MHz spectrometer. The sweep width was calibrated with a sample of chloroform-*d*, 99.8 atom % dueterium, and tetramethylsilane.

Infrared Spectra. The infrared spectrum was recorded in the region 4000–300 cm^{-1} with a Perkin-Elmer 521 grating spectrophotometer. The estimated uncertainty in reported frequencies is ±4 cm^{-1}.

Crystallography. Several clear, colorless crystals of $(\eta^5\text{-}C_5H_5)_2ZrCl[SOCN(CH_3)_2]$ were sealed in 0.5-mm diameter Lindemann glass capillaries under an atmosphere of dry nitrogen. Axial photographs indicated the crystal system to be orthorhombic, and the systematically absent reflections ($0kl$ for $k \neq 2n$, $h0l$ for $l \neq 2n$, and $hk0$ for $h \neq 2n$) identified the space group as *Pbca*. The lattice constants of $a = 13.440$ (3) Å, $b = 15.425$ (2) Å, and $c = 14.143$ (4) Å were determined by least-squares refinement of the diffraction geometry for 15 reflections ($2\theta > 20°$) centered on a computer-controlled four-circle Syntex $P2_1$ diffractometer using graphite-monochromated Mo K$\bar{\alpha}$ radiation ($\lambda = 0.71069$ Å). The calculated density based on eight molecules of $(\eta^5\text{-}C_5H_5)_2ZrCl[SOCN(CH_3)_2]$ per unit cell is 1.636 g cm^{-3}; the observed density, measured by flotation using a solution of carbon tetrabromide and carbon tetrachloride, was 1.645 g cm^{-3}.

A rectangular-shaped prism of dimensions 0.40 × 0.20 × 0.18 mm was chosen for collection of intensity data. The data were collected on the Syntex $P2_1$ diffractometer by using the θ–2θ scan technique with graphite-monochromated Mo K$\bar{\alpha}$ radiation at a takeoff angle of 6.3° and a glancing angle of 2.5°. A variable scan rate ranging from 2°/min for reflections of intensity ≤150 counts/s to 29.3°/min for reflections of intensity ≥1500 counts/s was employed. The range of each scan consisted of a base width of 2.0° at $2\theta = 0°$ and an increment of $\Delta(2\theta) = (0.692 \tan \theta)°$ to allow for spectral dispersion; background counts of duration equal to half the total scan time were taken at both limits of the scan. The intensities of three standard reflections, measured at 63-reflection intervals, indicated slight misalignments of the crystal which required recentering three times during the data collection. The resulting four data sets were combined by using scale factors obtained from the intensities of the standard reflections; the scale factors were 1.00, 1.02, 1.16, and 0.98, respectively.

A total of 2792 unique reflections having $2\theta \leq 55.1°$ (0.83 times the number of data in the limiting Cu K$\bar{\alpha}$ sphere) was scanned. On the basis of cited dimensions of the crystal and a linear absorption coefficient of 10.41 cm^{-1}, the maximum error resulting from neglect of absorption corrections was estimated to be <2.4% in any intensity and <1.2% in any structure factor amplitude. Therefore, absorption corrections were neglected. The intensity data were reduced to a set of relative squared amplitudes, $|F_o|^2$, by the application of standard Lorentz and polarization factors. Those 2302 reflections having $|F_o| > 2\sigma_F$, where σ_F is defined elsewhere,[8] were retained as "observed" for the structure analysis.

Structure Determination and Refinement. The structure was solved by application of Patterson and Fourier techniques and was refined by full-matrix least squares using anisotropic thermal parameters for all 18 non-hydrogen atoms, anomalous dispersion corrections for the Zr, Cl, and S atoms, and $w = 1/\sigma^2$ weighting. The function minimized was $\sum w(|F_o| - |F_c|)^2$. A difference Fourier synthesis upon convergence permitted location of the 16 hydrogen atoms. In subsequent cycles of refinement, the H atoms were assigned fixed positions and isotropic thermal parameters 1.0 $Å^2$ larger than the equivalent isotropic thermal parameter of the attached C atom; the coordinates and anisotropic thermal parameters of the 18 non-hydrogen atoms were allowed to vary as before. In the final cycle of refinement no parameter varied by more than 0.02 (the average was 0.01) of its estimated standard deviation, and the discrepancy indicies $R_1 = \sum||F_o| - |F_c||/\sum|F_o|$ and $R_2 = [\sum w(|F_o| - |F_c|)^2/\sum w|F_o|^2]^{1/2}$ were 0.061 and 0.078, respectively. A final difference Fourier showed no anomalous features; the strongest peak had a density of 0.75 e/$Å^3$.

Scattering factors were taken from Cromer and Mann[9] for Zr^0, Cl^0, S^0, O^0, N^0, and C^0 and from Stewart, Davidson, and Simpson[10] for H^0. Anomalous dispersion corrections, real and imaginary, for Zr, Cl, and S were obtained from Cromer.[11] Calculations were performed on PRIME 300 and IBM 370/168 computers using programs listed in a previous paper.[12]

Table I. Final Atomic Fractional Coordinates for $(\eta^5\text{-}C_5H_5)_2ZrCl[SOCN(CH_3)_2]$[a]

atom	10^4x	10^4y	10^4z
Zr	2453.8 (4)	337.3 (3)	989.7 (4)
Cl	915 (1)	42 (1)	1994 (2)
S	2758 (1)	1260 (1)	2536 (1)
O	3884 (3)	1086 (3)	1107 (3)
N	4469 (4)	2091 (3)	2138 (4)
C	3802 (5)	1502 (4)	1886 (4)
C_1	4418 (6)	2546 (5)	3024 (6)
C_2	5305 (6)	2285 (5)	1540 (6)
C_{1a}	2878 (7)	−1068 (5)	189 (5)
C_{2a}	3761 (7)	−720 (5)	468 (8)
C_{3a}	3770 (9)	−760 (6)	1459 (10)
C_{4a}	2910 (11)	−1090 (6)	1726 (6)
C_{5a}	2335 (7)	−1276 (5)	963 (7)
C_{1b}	2440 (7)	820 (6)	−707 (5)
C_{2b}	2480 (6)	1571 (5)	−190 (6)
C_{3b}	1625 (6)	1685 (4)	307 (5)
C_{4b}	1002 (6)	984 (6)	85 (7)
C_{5b}	1518 (7)	428 (5)	−550 (6)

[a] Numbers in parentheses are estimated standard deviations in the last significant figure.

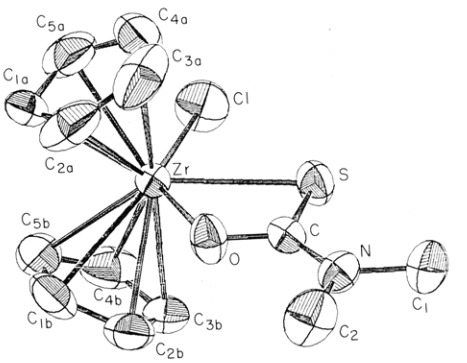

Figure 1. Model in perspective of the $(\eta^5\text{-}C_5H_5)_2ZrCl[SOCN(CH_3)_2]$ molecule. Each atom is represented by an ellipsoid consistent with the thermal parameters in Table II.

Results and Discussion

Final atomic coordinates and thermal parameters are presented in Tables I and II,[13] respectively. A table of observed and calculated structure factor amplitudes is available.[13] A perspective view of the molecule showing the atom numbering scheme is illustrated in Figure 1; atoms of the two η^5-cyclopentadienyl ligands are distinguished by a literal subscript (a or b). Bond distances, nonbonded contacts, and bond angles in the coordination group are listed in Table III.

Molecules of $(\eta^5\text{-}C_5H_5)_2ZrCl[SOCN(CH_3)_2]$ have the bent metallocene geometry **3**, with the Zr atom attached to a Cl atom, a bidentate *N,N*-dimethylmonothiocarbamate ligand, and two symmetrically bound $\eta^5\text{-}C_5H_5$ ligands. The structure is closely similar to that of the dithiocarbamate analogue[6] **2**, and the Zr atom may be regarded as five-coordinate if each $\eta^5\text{-}C_5H_5$ group is considered to occupy a

(8) Radonovich, L. J.; Bloom, A.; Hoard, J. L. *J. Am. Chem. Soc.* **1972**, *94*, 2073.
(9) Cromer, D. T.; Mann, J. B. *Acta Crystallogr., Sect. A* **1968**, *A24*, 321.
(10) Stewart, R. F.; Davidson, E. R.; Simpson, W. T. *J. Chem. Phys.* **1965**, *42*, 3175.
(11) Cromer, D. T. *Acta Crystallogr., Sect. A* **1965**, *A18*, 17.
(12) Steffen, W. L.; Fay, R. C. *Inorg. Chem.* **1978**, *17*, 2120.
(13) See paragraph at end of paper regarding supplementary material.

Table III. Bond Distances (Å), Nonbonded Contacts (Å), and Bond Angles (Deg) Subtended at the Zr(IV) Atom in the Coordination Group of $(\eta^5\text{-}C_5H_5)_2ZrCl[SOCN(CH_3)_2]$[a]

Bond Distances and Nonbonded Contacts			
Zr-Cl	2.550 (2)	Cl···C_{4a}	3.222 (13)
Zr-S	2.641 (2)	Cl···C_{5a}	3.147 (9)
Zr-O	2.249 (4)	Cl···C_{4b}	3.069 (10)
Zr-C_{1a}	2.511 (7)	Cl···S	3.202 (3)
Zr-C_{2a}	2.508 (9)	O···C_{2a}	2.934 (10)
Zr-C_{3a}	2.536 (11)	O···C_{3a}	2.894 (11)
Zr-C_{4a}	2.511 (10)	O···C_{2b}	2.736 (9)
Zr-C_{5a}	2.494 (8)	S···O[b]	2.540 (5)
Zr-C_{1b}	2.512 (8)	Zr-cent Cp_a[c]	2.230 (9)
Zr-C_{2b}	2.531 (8)	Zr-cent Cp_b	2.236 (8)
Zr-C_{3b}	2.548 (7)		
Zr-C_{4b}	2.538 (9)		
Zr-C_{5b}	2.518 (9)		
Zr-C_a(av)	2.512 (9, 10, 24)[d]		
Zr-C_b(av)	2.529 (8, 12, 19)[d]		

Bond Angles			
S-Zr-O	62.0 (1)	Cl-Zr-O	138.1 (1)
Cl-Zr-S	76.1 (1)	cent Cp_a-Zr-cent Cp_b	128.5 (3)

[a] Numbers in parentheses are estimated standard deviations in the last significant figure. [b] The "bite" of the ligand. [c] Cent refers to the centroid of the cyclopentadienyl ring. [d] The numbers in parentheses following each averaged value are the estimated root-mean-square standard deviation for an individual datum and the mean and maximum deviation from the average value.

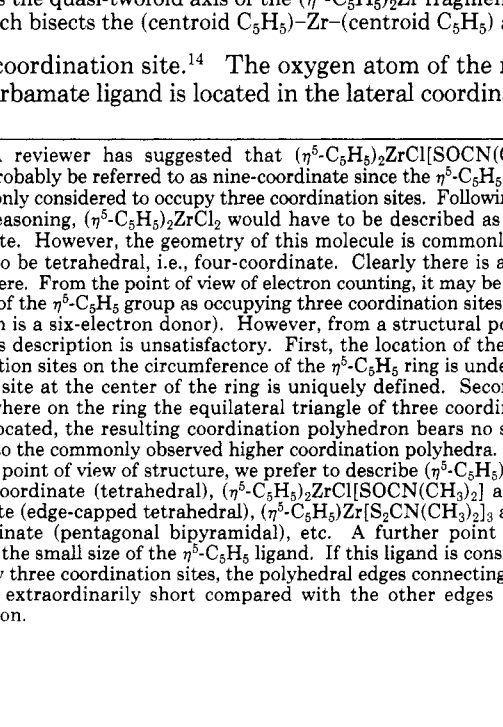

Figure 2. Projection of the $ZrClSOC_{10}$ coordination group onto the equatorial plane defined by the atoms Zr, Cl, S, and O. Also shown is the quasi-twofold axis of the $(\eta^5\text{-}C_5H_5)_2Zr$ fragment, the line which bisects the (centroid C_5H_5)–Zr–(centroid C_5H_5) angle.

single coordination site.[14] The oxygen atom of the monothiocarbamate ligand is located in the lateral coordination site, while the sulfur atom takes the interior site adjacent to the chlorine atom. The Zr, Cl, S, and O atoms lie in an equatorial plane (atomic displacements ≤0.020 Å, cf. Table VI[13]) which is nearly perpendicular to the plane defined by the Zr atom and the centroids of the $\eta^5\text{-}C_5H_5$ rings; the dihedral angle between these two planes is 89.2°. The $\eta^5\text{-}C_5H_5$ rings are staggered, as is shown in Figure 2, which is a projection of the $ZrClSOC_{10}$ coordination group onto the equatorial plane; in $(\eta^5\text{-}C_5H_5)_2ZrCl[S_2CN(C_2H_5)_2]$, the $\eta^5\text{-}C_5H_5$ rings are eclipsed.[6] Both $\eta^5\text{-}C_5H_5$ rings are planar (atomic displacements ≤0.016 Å; cf. Table VI). The (centroid C_5H_5)–Zr–(centroid C_5H_5) angle (128.5 (3)°) is nearly the same as that in $(\eta^5\text{-}C_5H_5)_2ZrCl[S_2CN(C_2H_5)_2]$ (129.4 (3)°). The angle between the normals to the planes of the two $\eta^5\text{-}C_5H_5$ ligands (126.7°) is slightly smaller, indicating that the $\eta^5\text{-}C_5H_5$ rings tip slightly about the Zr–(centroid C_5H_5) vector so as to increase nonbonded contacts between the cyclopentadienyl C atoms and the Cl and O atoms.

As expected, the $ZrClSOC_{10}$ coordination group in $(\eta^5\text{-}C_5H_5)_2ZrCl[SOCN(CH_3)_2]$ is less crowded than the $ZrClS_2C_{10}$ coordination group in $(\eta^5\text{-}C_5H_5)_2ZrCl[S_2CN(C_2H_5)_2]$. This is evidenced by a larger Cl–Zr–S angle (76.1° vs. 72.9°) and a longer Cl···S contact (3.202 Å vs. 3.084 Å). Nevertheless, the nonbonded contacts in $(\eta^5\text{-}C_5H_5)_2ZrCl[SOCN(CH_3)_2]$ are indicative of considerable crowding. The Cl···S distance is still 0.33 Å less than the sum of the van der Waals radii.[15] The three shortest cyclopentadienyl C···Cl and C···O contacts (cf. Table III) average 0.35 and 0.25 Å, respectively, less than the sum of the van der Waals radii, and two cyclopentadienyl C···C contacts ($C_{1a}\cdots C_{1b}$ = 3.23 Å; $C_{1a}\cdots C_{5b}$ = 3.12 Å) are 0.2–0.3 Å less than the van der Waals contact between two aromatic rings. The observed orientation of the monothiocarbamate ligand places the smaller oxygen atom in the sterically more congested coordination site and locates the larger sulfur atom in the interior site where it makes no repulsive contacts with the cyclopentadienyl C atoms.

Because of the crowding in the coordination group, the Zr–Cl and Zr–O bond lengths are long. The Zr–Cl distance (2.550 (2) Å) is closely similar to that in $(\eta^5\text{-}C_5H_5)_2ZrCl[S_2CN(C_2H_5)_2]$ (2.556 (2) Å)[6], which is the longest terminal Zr–Cl bond length yet observed for any structure involving Zr(IV); typical Zr–Cl bond lengths are in the range 2.4–2.5 Å.[17-24] The Zr–O distance (2.249 (4) Å) is longer than the

Table IV. Bond Lengths (Å) and Bond Angles (Deg) in the *N,N*-Dimethylmonothiocarbamate Ligand[a]

Bond Lengths			
S···O[b]	2.540 (5)	C_1-N	1.438 (10)
C-S	1.719 (6)	C_2-N	1.438 (10)
C-O	1.279 (7)		
C-N	1.325 (8)		

Bond Angles			
S-C-O	115.0 (5)	O-C-N	121.1 (6)
C-S-Zr	78.5 (2)	C_1-N-C	122.5 (6)
C-O-Zr	104.3 (4)	C_2-N-C	120.9 (6)
S-C-N	123.9 (5)	C_1-N-C_2	116.6 (6)

[a] Numbers in parentheses are estimated standard deviations in the last significant figure. [b] The bite of the ligand.

(14) A reviewer has suggested that $(\eta^5\text{-}C_5H_5)_2ZrCl[SOCN(CH_3)_2]$ should probably be referred to as nine-coordinate since the $\eta^5\text{-}C_5H_5$ group is commonly considered to occupy three coordination sites. Following this line of reasoning, $(\eta^5\text{-}C_5H_5)_2ZrCl_2$ would have to be described as eight-coordinate. However, the geometry of this molecule is commonly considered to be tetrahedral, i.e., four-coordinate. Clearly there is an ambiguity here. From the point of view of electron counting, it may be useful to think of the $\eta^5\text{-}C_5H_5$ group as occupying three coordination sites (since the anion is a six-electron donor). However, from a structural point of view, this description is unsatisfactory. First, the location of the three coordination sites on the circumference of the $\eta^5\text{-}C_5H_5$ ring is undefined; only the site at the center of the ring is uniquely defined. Second, no matter where on the ring the equilateral triangle of three coordination sites is located, the resulting coordination polyhedron bears no simple relation to the commonly observed higher coordination polyhedra. Thus, from the point of view of structure, we prefer to describe $(\eta^5\text{-}C_5H_5)_2ZrCl_2$ as four-coordinate (tetrahedral), $(\eta^5\text{-}C_5H_5)_2ZrCl[SOCN(CH_3)_2]$ as five-coordinate (edge-capped tetrahedral), $(\eta^5\text{-}C_5H_5)Zr[S_2CN(CH_3)_2]_3$ as seven-coordinate (pentagonal bipyramidal), etc. A further point worth noting is the small size of the $\eta^5\text{-}C_5H_5$ ligand. If this ligand is considered to occupy three coordination sites, the polyhedral edges connecting these sites are extraordinarily short compared with the other edges in the polyhedron.

(15) We take the van der Waals radii of a cyclopentadienyl carbon atom, chlorine, oxygen, and sulfur to be 1.7 Å,[16a] 1.80 Å,[16a] 1.40 Å,[16a] and 1.73 Å,[16b] respectively.

(16) (a) Pauling, L. "The Nature of the Chemical Bond", 3rd ed; Cornell University Press: Ithaca, N.Y., 1960; p 260. (b) van der Helm, D.; Lessor, A. E., Jr.; Merritt, L. L., Jr. *Acta Crystallogr.* **1962**, *15*, 1227.

(17) Prout, C. K.; Cameron, T. S.; Forder, R. A.; Critchley, S. R.; Denton, B.; Rees, G. V. *Acta Crystallogr., Sect. B* **1974**, *B30*, 2290.

(18) Muir, K. W. *J. Chem. Soc. A* **1971**, 2663.

averaged Zr–O bond length in typical eight-coordinate complexes such as $Zr[SOCN(C_2H_5)_2]_4$ (2.190 Å),[12] $[Zr(C_2O_4)_4]^{4-}$ (2.199 Å),[25] and $Zr(acac)_4$ (2.198 Å)[26] but not as long as the Zr–O bond to the η^2-acetyl ligand in $(\eta^5\text{-}C_5H_5)_2Zr(COCH_3)(CH_3)$ (2.290 (4) Å).[5] The Zr–S bond length (2.641 (2) Å) is nearly the same as the interior Zr–S distance in $(\eta^5\text{-}C_5H_5)_2ZrCl[S_2CN(C_2H_5)_2]$ (2.635 (2) Å)[6] and slightly less than the averaged Zr-S bond length in $Zr[S\text{-}OCN(C_2H_5)_2]_4$ (2.679 Å).[12] Because the bite of the monothiocarbamate ligand (2.540 (5) Å) is appreciably shorter than the Cl···S distance, the Zr–S bond does not lie along the quasi-C_2 axis of the $(\eta^5\text{-}C_5H_5)_2Zr$ fragment but is displaced through a solid angle of 12.3° toward the oxygen atom (cf. Figure 2). The ten Zr–C distances are quite uniform (2.494 (8)–2.548 (7) Å; cf. Table III) and are typical of Zr–C distances in other (η^5-cyclopentadienyl)zirconium structures.[5,6,17-19,27-30] The distances from the Zr atom to the centroids of the C_5H_5 rings are 2.230 (9) and 2.236 (8) Å.

Bond lengths and angles within the monothiocarbamate ligand (Table IV) are in agreement with values found in other monothiocarbamate structures.[12,31-33] Delocalized π bonding in the SOCN portion of the ligand is indicated by the C–N (1.325 Å), C–S (1.719 Å), and C–O (1.279 Å) distances, which are intermediate between single-bond and double-bond distances.[34] The $SOCNC_1C_2$ framework is nearly planar (atomic displacements ≤0.028 Å, cf. Table VI), with the small departures from planarity corresponding to a slight twisting of the ligand about the C···N bond; the dihedral angle between the SOCN and CNC_1C_2 mean planes is 2.5°. There is some folding of the chelate ring about the S···O vector so as to bend the ligand toward C_5H_5 group b; the dihedral angle between the $SOCNC_1C_2$ plane and the ZrSO plane is 6.5°.

Bond distances and angles within the cyclopentadienyl ligands are listed in Table V.[13] The averaged C–C bond length (1.374 Å) is in good agreement with values obtained for other (η^5-cyclopentadienyl)zirconium structures.[5,6,17-19,27-30]

There are no unusually short intermolecular contacts. The shortest ($C_2\cdots C_{3b}$ = 3.54 Å) is between a methyl and a cyclopentadienyl carbon atom for which the sum of the van der Waals radii is 3.7 Å.[16a]

Acknowledgment. The X-ray diffractometer used in this research was obtained with support from the National Science Foundation Instrumentation Program (Grant CHE-77-09756). M.E.S. thanks Dow Chemical for a fellowship.

Registry No. 3, 83096-20-2.

Supplementary Material Available: Final thermal parameters for $(\eta^5\text{-}C_5H_5)_2ZrCl[SOCN(CH_3)_2]$ (Table II), bond lengths and bond angles in the η^5-cyclopentadienyl ligands (Table V), least-squares mean planes of the form $AX + BY + CZ = D$ (Table VI), and a listing of structure factor amplitudes for $(\eta^5\text{-}C_5H_5)_2ZrCl[SOCN(CH_3)_2]$ (14 pages). Ordering information is given on any current masthead page.

(19) Saldarriaga-Molina, C. H.; Clearfield, A.; Bernal, I. *J. Organomet. Chem.* **1974**, *80*, 79.
(20) Kowala, C.; Wunderlich, J. A. *Acta Crystallogr., Sect. B* **1976**, *B32*, 820.
(21) Dusausoy, Y.; Protas, J.; Renaut, P.; Gautheron, B.; Tainturier, G. *J. Organomet. Chem.* **1978**, *157*, 167.
(22) VonDreele, R. B.; Stezowski, J. J.; Fay, R. C. *J. Am. Chem. Soc.* **1971**, *93*, 2887.
(23) Brauer, D. J.; Kruger, C. *Inorg. Chem.* **1975**, *14*, 3053.
(24) Stezowski, J. J.; Eick, H. A. *J. Am. Chem. Soc.* **1969**, *91*, 2890.
(25) Glen, G. L.; Silverton, J. V.; Hoard, J. L. *Inorg. Chem.* **1963**, *2*, 250.
(26) Silverton, J. V.; Hoard, J. L. *Inorg. Chem.* **1963**, *2*, 243.
(27) Petersen, J. L. *J. Organomet. Chem.* **1979**, *166*, 179.
(28) Bruder, A. H.; Fay, R. C.; Lewis, D. F.; Sayler, A. A. *J. Am. Chem. Soc.* **1976**, *98*, 6932.
(29) Sim, G. A.; Bush, M. A. *J. Chem. Soc. A* **1971**, 2225.
(30) Anderson, S. J.; Brown, D. S.; Finney, K. J. *J. Chem. Soc., Dalton Trans.* **1979**, 152.
(31) Hawthorne, S. L.; Fay, R. C. *J. Am. Chem. Soc.* **1979**, *101*, 5268.
(32) Pierpont, C. G.; Dickinson, R. C.; McCormick, B. J. *Inorg. Chem.* **1974**, *13*, 1674.
(33) Ahmed, J.; Ibers, J. A. *Inorg. Chem.* **1977**, *16*, 935.
(34) Reference 16a, pp 224–229.

Bent Metallocenes Containing Potentially Bidentate Ligands. The Crystal and Molecular Structure of Bis(η-cyclopentadienyl)bis(benzoato)titanium(IV)

David M. Hoffman, Nicholas D. Chester, and Robert C. Fay*

Department of Chemistry, Cornell University, Ithaca, New York 14853

Received June 29, 1982

The crystal and molecular structure of bis(η-cyclopentadienyl)bis(benzoato)titanium(IV), (η-$C_5H_5)_2Ti(O_2CC_6H_5)_2$, has been determined by X-ray diffraction and has been refined anisotropically by least-squares methods to $R_1 = 0.086$ and $R_2 = 0.077$ using 2373 independent diffractometer data having $2\theta_{MoK\bar{\alpha}} \leq 50.0°$ and $|F_o| > 2.0\sigma_F$. The compound crystallizes in the monoclinic space group $P2_1/c$ with four molecules in a cell having dimensions $a = 16.078$ (3) Å, $b = 12.853$ (3) Å, $c = 16.076$ (2) Å, $\beta = 142.685$ (7)° ($\rho_{obsd} = 1.395$ and $\rho_{calcd} = 1.386$ g cm^{-3}). The molecules have a distorted tetrahedral structure in which the Ti atom is attached to two η-C_5H_5 groups and two monodentate benzoate ligands (Ti–C = 2.337–2.393 Å; Ti–O = 1.922 (7) and 1.930 (5) Å; (centroid C_5H_5)–Ti–(centroid C_5H_5) = 131.7 (5)°; and O–Ti–O = 91.4 (3)°). The relatively short Ti–O bond lengths and large Ti–O–C bond angles (148.6 (4) and 147.9 (7)°) suggest that the Ti atom achieves an effective 18-electron configuration via Ti–O π bonding. Extended Hückel molecular orbital (EHMO) calculations confirm the existence of a strong π-type interaction involving the $1a_1$ orbital of the (η-$C_5H_5)_2Ti^{2+}$ fragment and in-plane p orbitals of the coordinated benzoate oxygen atoms. EHMO calculations and geometrical considerations indicate that the alternate coordination geometry having one monodentate and one bidentate carboxylate ligand is precluded by O···C steric interactions.

Introduction

Many Ti(IV) complexes of the type (η-$C_5H_5)_2TiX_2$ have been reported where X is a potentially bidentate ligand.[1] The structures of some of these complexes have not been definitively determined. In the present study, we are concerned with the complexes where X is a carboxylate,[2] compounds whose structures are a matter of some controversy.

On the basis of IR data Chandra et al. assigned structure **1** to the compounds (η-$CH_3C_5H_4)_2Ti(O_2CR)_2$ for R = $CHCl_2$ or CH_2Cl. For R = CH_3, C_2H_5, n-C_3H_7, or C_6H_5

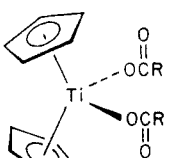

1

a different structure was proposed having one η^5-$CH_3C_5H_4$ ligand, one η^1-$CH_3C_5H_4$ ligand, and two bidentate carboxylate ligands.[3] Interestingly, in an early IR study by Vyshinskii et al., (η-$C_5H_5)_2Ti(O_2CC_6H_5)_2$ and (η-$C_5H_5)_2Ti(O_2CC_6H_4$-p-$NO_2)_2$ were both assigned structure **1**.[4] This formulation was later confirmed for the *p*-nitrobenzoate derivative by X-ray diffraction.[5]

In order to further delineate the structure of (η-$C_5H_5)_2Ti(O_2CR)_2$ complexes, we have synthesized and determined by X-ray crystallography the structure of (η-$C_5H_5)_2Ti(O_2CC_6H_5)_2$.

Experimental Section

Reagents and General Techniques. Triethylamine was refluxed for 18 h over calcium hydride and then distilled from calcium hydride. It was stored under nitrogen until needed. Benzoic acid was dried under vacuum over phosphorus(V) oxide for 6 days at room temperature and then stored under nitrogen. Bis(η-cyclopentadienyl)titanium dichloride was purchased from Alfa Products and used without further purification. Solvents were dried by refluxing for at least 24 h over sodium/benzophenone (tetrahydrofuran) or potassium/benzophenone (hexanes). The synthesis and handling of (η-$C_5H_5)_2Ti(O_2CC_6H_5)_2$ was carried out under anhydrous conditions in a dry nitrogen atmosphere.

Bis(η-cyclopentadienyl)bis(benzoato)titanium(IV). Triethylamine (1.6 mL, 11.5 mmol) was added by syringe to a mixture of (η-$C_5H_5)_2TiCl_2$ (1.4 g, 5.6 mmol) and benzoic acid (1.37 g, 11.2 mmol) in 100 mL of tetrahydrofuran at room temperature. The clear blood-red reaction mixture became cloudy and bright orange after being stirred for 4 h. $[(C_2H_5)_3NH]Cl$ was removed by filtration, and the solvent was removed by pumping. Recrystallization of the resulting orange solid from tetrahydrofuran/hexanes afforded orange crystals of (η-$C_5H_5)_2Ti(O_2CC_6H_5)_2$: mp 198–201 °C dec (lit.[2a] 188–192 °C dec); ^{1}H NMR (ppm, $CDCl_3$ solution) –6.62 (C_5H_5), multiplets at –7.5 and –8.1 (C_6H_5); IR (cm^{-1}, Nujol mull) ν_{asym}(COO) 1642 (s), ν_{sym}(COO) 1350 (s), 1320 (m), 1298 (s), other bands 3090 (w), 3069 (w), 1590 (w), 1287 (s), 1170 (w), 1130 (m), 1063 (w), 1017 (w), 1022 (w), 870 (w), 829 (m), 713 (m), 671 (w), 591 (w), 568 (m), 450 (vw), 419 (m).

Nuclear Magnetic Resonance Spectra. Proton chemical shifts were measured at ambient probe temperature (~34 °C) relative to an internal reference of tetramethylsilane with a Varian

(1) See for instance: (a) Klein, H.-P.; Thewalt, U. *J. Organomet. Chem.* **1981**, *206*, 69–75. (b) Thewalt, U.; Klein, H.-P. *Z. Kristallogr.* **1980**, *153*, 307–315. (c) Bhushan, B.; Mittal, I. P.; Chhatwal, G. R.; Kaushik, N. K. *J. Inorg. Nucl. Chem.* **1979**, *41*, 159–160. (d) Sharan, R.; Gupta, G.; Kapoor, R. N. *Transition Met. Chem. (Weinheim, Ger.)* **1978**, *3*, 282–285. (e) Sharma, R. K.; Singh, R. V.; Tandon, J. P. *J. Inorg. Nucl. Chem.* **1980**, *42*, 1382–1384.

(2) (a) Razuvaev, G. A.; Latyaeva, V. N.; Vyshinskaya, L. I. *Dokl. Akad. Nauk SSSR, Ser. Khim.* **1961**, *138*, 1126–1129; *Dokl. Chem. (Engl. Transl.)* **1961**, *138*, 592–594. (b) Razuvaev, G. A.; Latyaeva, V. N.; Lineva, A. N. *Dokl. Akad. Nauk SSSR, Ser. Khim.* **1969**, *187*, 340–342; *Dokl. Chem. (Engl. Transl.)* **1969**, *187*, 545–547. Razuvaev, G. A.; Latyaeva, V. N.; Lineva, A. N. *Zh. Obshch. Khim.* **1971**, *41*, 1556–1560; *J. Gen. Chem. USSR (Engl. Transl.)* **1971**, *41*, 1560–1564.

(3) Chandra, K.; Sharma, R. K.; Garg, B. S.; Singh, R. P. *J. Inorg. Nucl. Chem.* **1980**, *42*, 187–193.

(4) Vyshinskii, N. N.; Ermolaeva, T. I.; Latyaeva, V. N.; Lineva, A. N.; Lukhton, N. E. *Dokl. Akad. Nauk SSSR, Ser. Khim.* **1971**, *198*, 1081–1084; *Dokl. Chem. (Engl. Transl.)* **1971**, *198*, 487–490.

(5) (a) Gladkikh, E. A.; Kuntsevich, T. S. *Zh. Strukt. Khim.* **1973**, *14*, 949–950; *J. Struct. Chem. (Engl. Transl.)* **1973**, *14*, 898–899. (b) Kuntsevich, T. S.; Gladkikh, E. A.; Lebedev, V. A.; Lineva, A. N.; Belov, N. V. *Kristallografiya* **1976**, *21*, 80–88; *Sov. Phys.—Crystallogr. (Engl. Transl.)* **1976**, *21*, 40–44.

0276-7333/83/2302-0048$01.50/0

EM-390 90-MHz spectrometer. The sweep width was calibrated with a sample of chloroform-*d*, 99.8 atom % deuterium, and tetramethylsilane.

Infrared Spectra. The infrared spectrum was recorded in the region 4000–400 cm^{-1} with a Perkin-Elmer 337 grating spectrophotometer. The estimated uncertainty in reported frequencies is ±4 cm^{-1}.

Crystallography. Several orange crystals of $(\eta\text{-}C_5H_5)_2Ti(O_2CC_6H_5)_2$ were sealed in 0.5-mm diameter Lindemann glass capillaries under an atmosphere of dry nitrogen. Axial photographs indicated the crystal system to be monoclinic, and the systematically absent reflections ($h0l$ for $h \neq 2n$ and $0k0$ for $k \neq 2n$) identified the space group as $P2_1/a$. The data were reindexed to give the standard space group $P2_1/c$. The lattice constants of a = 16.078 (3) Å, b = 12.853 (3) Å, c = 16.076 (2) Å, and β = 142.685 (7)° were determined by least-squares refinement of the diffraction geometry for 15 reflections ($2\theta > 20°$) centered on a computer-controlled four-circle Syntex $P2_1$ diffractometer using graphite-monochromated Mo K$\bar{\alpha}$ radiation (λ = 0.71069 Å). The calculated density based upon four molecules of $(\eta\text{-}C_5H_5)_2Ti(O_2CC_6H_5)_2$ per unit cell is 1.386 g cm^{-3}. The observed density, measured by flotation using a solution of carbon tetrachloride and hexanes, was 1.395 g cm^{-3}.

An irregularly shaped crystal of approximate dimensions 0.32 × 0.26 × 0.16 mm was chosen for collection of intensity data. The data were collected on the Syntex $P2_1$ diffractometer using the θ–2θ scan technique with graphite-monochromated Mo K$\bar{\alpha}$ radiation at a takeoff angle of 6.3° and a glancing angle of 2.5°. A variable scan rate ranging from 2°/min for reflections of intensity ≤150 counts/s to 29.3°/min for reflections of intensity ≥1500 counts/s was employed. The range of each scan consisted of a base width of 2.0° at 2θ = 0° and an increment of $\Delta(2\theta)$ = (0.692 tan θ)° to allow for spectral dispersion; background counts of duration equal to half the total scan time were taken at both limits of the scan. The intensities of three standard reflections, measured at 63-reflection intervals, indicated no crystal decomposition or misalignment.

A total of 3741 unique reflections having $2\theta \leq 50.0°$ were scanned. The linear absorption coefficient was calculated to be 4.72 cm^{-1}. The maximum error resulting from neglect of absorption corrections was estimated to be <3.8% in any intensity and <1.9% in any structure factor amplitude. Therefore, absorption corrections were neglected. The intensity data were reduced to a set of relative squared amplitudes, $|F_o|^2$, by the application of standard Lorentz and polarization factors. Those 2373 reflections having $|F_o| > 2.0\sigma_F$, where σ_F is defined elsewhere,[6] were retained as "observed" for the structure analysis.

Structure Determination and Refinement. The structure was solved by application of Patterson and Fourier techniques and was refined by full-matrix least squares using anisotropic thermal parameters for all 29 non-hydrogen atoms, an anomalous dispersion correction for the Ti atom, and $w = 1/\sigma^2$ weighting. The function minimized was $\sum w(|F_o| - |F_c|)^2$. A difference Fourier synthesis upon convergence permitted location of 17 of the 20 hydrogen atoms. In subsequent cycles of refinement, the 20 hydrogen atoms were assigned fixed positions (based on C atom positions) and isotropic thermal parameters 1.0 $Å^2$ larger than the equivalent isotropic thermal parameter of the attached C atom; the coordinates and anisotropic thermal parameters of the 29 non-hydrogen atoms were allowed to vary as before. In the final cycle of refinement no parameter varied by more than 0.03 of its estimated standard deviation (the average was 0.01) and the discrepancy indices $R_1 = \sum||F_o| - |F_c||/\sum|F_o|$ and $R_2 = [\sum w(|F_o| - |F_c|)^2/\sum w|F_o|^2]^{1/2}$ were 0.086 and 0.077, respectively. A final difference Fourier showed no anomalous features; the strongest peak had a density of 0.48 e $Å^{-3}$.

Scattering factors were taken from Cromer and Mann[7] for Ti^0, O^0, and C^0 and from Stewart, Davidson, and Simpson[8] for H^0. The anomalous dispersion correction, real and imaginary, for Ti was obtained from Cromer.[9] Calculations were performed on a PRIME 750 computer using programs listed previously.[10]

Table I. Final Atomic Fractional Coordinates for $(\eta\text{-}C_5H_5)_2Ti(O_2CC_6H_5)_2$[a]

atom	10^4x	10^4y	10^4z
Ti	6094 (1)	2598.4 (8)	3098 (1)
O_{1a}	7153 (4)	3680 (4)	3422 (4)
O_{2a}	6410 (6)	5231 (4)	2444 (7)
O_{1b}	7536 (4)	1595 (4)	4061 (4)
O_{2b}	7315 (5)	−84 (4)	4197 (5)
C_{1a}	5241 (7)	2388 (7)	1042 (7)
C_{2a}	4431 (8)	3135 (6)	779 (6)
C_{3a}	3733 (6)	2667 (6)	874 (7)
C_{4a}	4136 (7)	1628 (5)	1219 (6)
C_{5a}	5039 (7)	1458 (6)	1279 (7)
C_{6a}	7186 (7)	4507 (5)	2984 (7)
C_{7a}	8263 (6)	4478 (5)	3168 (6)
C_{8a}	9164 (7)	3654 (5)	3805 (7)
C_{9a}	10128 (8)	3648 (8)	3952 (9)
C_{10a}	10192 (9)	4421 (10)	3445 (10)
C_{11a}	9303 (10)	5243 (7)	2790 (9)
C_{12a}	8323 (8)	5288 (5)	2644 (7)
C_{1b}	7311 (8)	2783 (7)	5350 (7)
C_{2b}	6629 (9)	3681 (5)	4680 (8)
C_{3b}	5236 (8)	3497 (6)	3567 (8)
C_{4b}	5064 (8)	2444 (7)	3611 (9)
C_{5b}	6358 (11)	1997 (6)	4706 (10)
C_{6b}	8011 (7)	659 (5)	4573 (6)
C_{7b}	9541 (6)	602 (5)	5718 (6)
C_{8b}	10373 (7)	1486 (5)	6361 (7)
C_{9b}	11761 (7)	1380 (6)	7400 (8)
C_{10b}	12360 (8)	418 (8)	7828 (7)
C_{11b}	11567 (8)	−461 (7)	7208 (8)
C_{12b}	10164 (7)	−375 (5)	6170 (7)

[a] Numbers in parentheses are estimated standard deviations in the last significant figure.

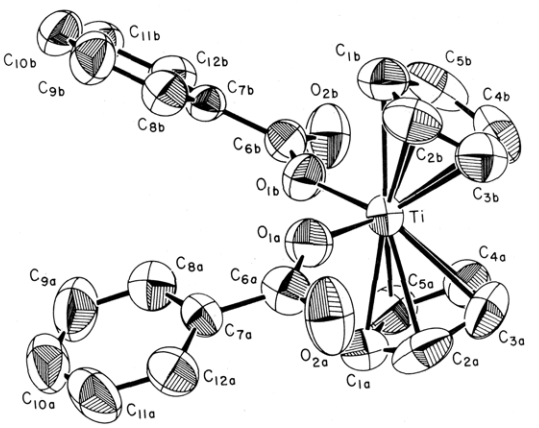

Figure 1. Model in perspective of the $(\eta\text{-}C_5H_5)_2Ti(O_2CC_6H_5)_2$ molecule. Each atom is represented by an ellipsoid consistent with the thermal parameters in Table II.

Results and Discussion

Solid-State Structure. Final atomic coordinates and thermal parameters are presented in Tables I and II,[11] respectively. A table of observed and calculated structure factor amplitudes is available.[11] A perspective view of the molecule showing the atom numbering scheme is displayed in Figure 1; atoms of the two η-cyclopentadienyl and the two benzoate ligands are distinguished by a literal subscript (a or b). Bond distances, nonbonded contacts, and bond angles in the coordination group are listed in Table III.

(6) Radonovich, L. J.; Bloom, A.; Hoard, J. L. *J. Am. Chem. Soc.* **1972**, *94*, 2073–2078.
(7) Cromer, D. T.; Mann, J. B. *Acta Crystallogr., Sect. A* **1968**, *A24*, 321–324.
(8) Stewart, R. F.; Davidson, E. R.; Simpson, W. T. *J. Chem. Phys.* **1965**, *42*, 3175–3187.
(9) Cromer, D. T. *Acta Crystallogr., Sect. A* **1965**, *A18*, 17–23.
(10) Steffen, W. L.; Fay, R. C. *Inorg. Chem.* **1978**, *17*, 2120–2127.
(11) See paragraph at end of paper regarding supplementary material.

Table III. Bond Distances (Å), Nonbonded Contacts (Å), and Bond Angles (Deg) Subtended at the Ti Atom in the Coordination Group of $(\eta\text{-}C_5H_5)_2Ti(O_2CC_6H_5)_2$[a]

Bond Distances and Nonbonded Contacts

Ti-O_{1a}	1.922 (7)	Ti···O_{2a}	3.696 (7)
Ti-O_{1b}	1.930 (5)	Ti···O_{2b}	3.653 (5)
Ti-C_{1a}	2.381 (12)	O_{1a}···O_{1b}	2.758 (7)
Ti-C_{2a}	2.381 (7)	O_{1a}···C_{1a}	2.853 (9)
Ti-C_{3a}	2.369 (5)	O_{1a}···C_{2a}	2.850 (7)
Ti-C_{4a}	2.337 (6)	O_{1a}···C_{1b}	3.123 (17)
Ti-C_{5a}	2.384 (9)	O_{1a}···C_{2b}	2.742 (20)
Ti-C_{1b}	2.393 (11)	O_{1b}···C_{1b}	2.818 (16)
Ti-C_{2b}	2.381 (13)	O_{1b}···C_{5b}	2.838 (24)
Ti-C_{3b}	2.338 (15)	O_{1b}···C_{1a}	3.118 (9)
Ti-C_{4b}	2.374 (18)	O_{1b}···C_{5a}	2.755 (6)
Ti-C_{5b}	2.391 (20)	Ti-cent Cp_a[b]	2.057 (7)
av Ti-Cp_a	2.370 (8, 14, 33)[c]	Ti-cent Cp_b	2.065 (17)
av Ti-Cp_b	2.375 (15, 16, 37)[c]		

Bond Angles

O_{1a}-Ti-O_{1b}	91.4 (3)	cent Cp_a-Ti-cent Cp_b	131.7 (5)

[a] Numbers in parentheses are estimated standard deviations in the last significant figure. [b] Cent refers to the centroid of the cyclopentadienyl ring. [c] The numbers in parentheses following each averaged value are the estimated root-mean-square standard deviation for an individual datum and the mean and maximum deviation from the average value.

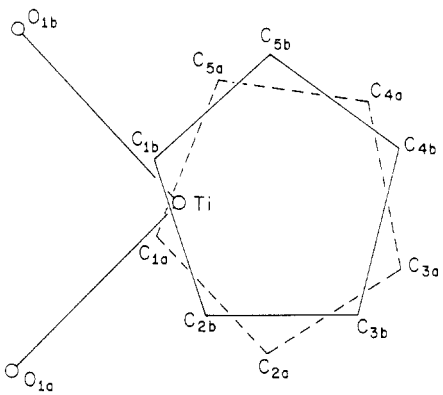

Figure 2. Projection of the TiO_2C_{10} coordination group onto the plane defined by the atoms Ti, O_{1a}, and O_{1b}.

Molecules of $(\eta\text{-}C_5H_5)_2Ti(O_2CC_6H_5)_2$ have the bent metallocene structure 1 in which the Ti atom is attached to two monodentate benzoate ligands and two $\eta\text{-}C_5H_5$ groups. The centroids of the C_5H_5 ligands and the coordinated oxygen atoms define a distorted tetrahedron with the (centroid C_5H_5)–Ti–centroid C_5H_5) angle being 131.7 (5)° and the O_{1a}–Ti–O_{1b} angle being 91.4 (3)°. The plane defined by the atoms Ti, O_{1a}, and O_{1b} bisects the (centroid C_5H_5)–Ti–(centroid C_5H_5) angle and is nearly perpendicular to the plane defined by the Ti atom and the centroids of the C_5H_5 rings; the dihedral angle between these two planes is 88.8°.

The $\eta\text{-}C_5H_5$ rings are more nearly staggered than eclipsed, and they are oriented such that the TiO_2C_{10} coordination group has a quasi-twofold axis which bisects the O_{1a}–Ti–O_{1b} angle. These features are illustrated in Figure 2, which is a projection of the coordination group onto the $TiO_{1a}O_{1b}$ plane. Both $\eta\text{-}C_5H_5$ ligands are planar (atomic displacements ≤0.019 Å; cf. Table VI[11]). The angle between the normals to the planes of the two $\eta\text{-}C_5H_5$ ligands (129.4°) is slightly smaller than the (centroid C_5H_5)–Ti–(centroid C_5H_5) angle (131.7°), indicating that the $\eta\text{-}C_5H_5$ rings tip slightly about the Ti–(centroid C_5H_5) vector so as to increase nonbonded contacts between the cyclopentadienyl C atoms and the benzoate oxygen atoms O_{1a} and O_{1b}. This tipping is reflected in the Ti–C distances, which vary slightly from 2.337 to 2.393 Å (Table III). The Ti–C distances and the distances from the Ti atom to the centroids of the C_5H_5 rings (2.057 (7) and 2.065 (17) Å) are in excellent agreement with the corresponding distances in other $(\eta\text{-}C_5H_5)_2Ti^{IV}$ structures.[1a,b,5,12-14]

There is considerable crowding in the TiO_2C_{10} coordination group, as is evidenced by six O···C nonbonded contacts in the range 2.74–2.85 Å (Table III), 0.3 Å less than the sum of the van der Waals radii.[15] In addition there are three contacts between cyclopentadienyl carbon atoms (C_{3a}···C_{4b} = 3.01 Å; C_{3a}···C_{3b} = 3.01 Å; C_{4a}···C_{4b} = 3.00 Å) which are 0.4 Å less than the van der Waals contact between two aromatic rings. Despite the crowding, the Ti–O bond lengths, 1.922 (7) and 1.930 (5) Å, are relatively short compared to Ti–O bond lengths in other $(\eta\text{-}C_5H_5)_2Ti^{IV}$ structures;[1a,b,5,12-14] typical Ti–O distances range from 1.829 Å in $[\{(\eta\text{-}C_5H_5)_2Ti(H_2O)\}_2O](ClO_4)_2\cdot 2H_2O$ for the bonds to the bridging oxygen atom[13] to 2.146 Å in $(\eta\text{-}C_5H_5)_2Ti(NO_3)_2$.[1a] The two uncoordinated oxygen atoms are far removed from the Ti atom (Ti···O_{2a} = 3.696 (7) Å; Ti···O_{2b} = 3.653 (5) Å) and the nonbonded contacts between these oxygen atoms and the cyclopentadienyl C atoms are longer than 3.3 Å.

A particularly interesting feature of this structure is the large angle at the coordinated oxygen atoms (Ti–O_{1a}–C_{6a} = 148.6 (4)°; Ti–O_{1b}–C_{6b} = 147.9 (7)°). These values are similar to those in $(\eta\text{-}C_5H_5)_2Ti(O_2CC_6H_4\text{-}p\text{-}NO_2)_2$ (136 and 157°)[5] but larger than typical M–O–C angles (114–137°) in coordinatively saturated complexes that contain monodentate carboxylate ligands.[16] The large Ti–O–C angles and relatively short Ti–O bond lengths suggest that $(\eta\text{-}C_5H_5)_2Ti(O_2CR)_2$ complexes, which are formally 16-electron complexes if only Ti–O σ bonding is considered, achieve an effective 18-electron configuration via Ti–O π bonding. This point has been explored by extended Hückel molecular orbital calculations (vide infra). The importance of Ti–O π bonding in organotitanium(IV) alkoxides has been emphasized recently by Caulton and co-workers.[12] It is interesting to note that the Ti–O–C angle in $(\eta\text{-}C_5H_5)_2Ti(O_2CC_6H_5)_2$ is larger than that in $(\eta\text{-}C_5H_5)_2Ti(OC_2H_5)Cl$ (133.2°) though it is not as large as the 166.2° Ti–O–C angle in the formally 12-electron complex $[(\eta\text{-}C_5H_5)Cl_2Ti]_2O_2C_2(CH_3)_4$.

Bond lengths and angles within the benzoate ligands are presented in Table IV. In agreement with other structures that contain monodentate carboxylate ligands,[5,16,17] there is a substantial (0.10-Å) difference between the lengths of the C–O bonds to the coordinated and uncoordinated oxygen atoms. The benzoate ligands exhibit small deviations from planarity (Table VI) owing to a small twisting about the O_2C···C_6H_5 bonds. The O_2C···C and C···C_6 moieties are

(12) Huffman, J. C.; Moloy, K. G.; Marsella, J. A.; Caulton, K. G. *J. Am. Chem. Soc.* **1980**, *102*, 3009–3014.
(13) Thewalt, U.; Kebbel, B. *J. Organomet. Chem.* **1978**, *150*, 59–66.
(14) (a) Thewalt, U.; Klein, H.-P. *J. Organomet. Chem.* **1980**, *194*, 297–307. (b) Klein, H.-P.; Thewalt, U. *Z. Anorg. Allg. Chem.* **1981**, *176*, 62–68. (c) Thewalt, U.; Schleussner, G. *Angew. Chem.* **1978**, *90*, 559; *Angew. Chem., Int. Ed. Engl.* **1978**, *17*, 531. (d) Aleksandrov, G. G.; Struchkov, Yu. T. *Zh. Strukt. Khim.* **1971**, *12*, 667–675; *J. Struct. Chem. (Engl. Transl.)* **1971**, *12*, 605–612. (e) Fachinetti, G.; Biran, C.; Floriani, C.; Chiesi Villa, A.; Guastini, C. *J. Chem. Soc., Dalton Trans.* **1979**, 792–800. (f) Schmid, G.; Bätzel, V.; Stutte, B. *J. Organomet. Chem.* **1976**, *113*, 67–74.
(15) Pauling, L. "The Nature of the Chemical Bond", 3rd ed.; Cornell University Press: Ithaca, NY, 1960, p 260.
(16) (a) Schultz, A. J.; Khare, G. P.; Meyer, C. D.; Eisenberg, R. *Inorg. Chem.* **1974**, *13*, 1019–1024. (b) Dawans, F.; Dewailly, J.; Meunier-Piret, J.; Piret, P. *J. Organomet. Chem.* **1974**, *76*, 53–63. (c) Herrmann, W. A.; Schweizer, I.; Skell, P. S.; Ziegler, M. L.; Weidenhammer, K.; Nuber, B. *Chem. Ber.* **1979**, *112*, 2423–2435. (d) Del Piero, G.; Cesari, M. *Acta Crystallogr., Sect. B.* **1979**, *B39*, 2411–2413. (e) Atwood, J. L.; Hunter, W. E. *J. Organomet. Chem.* **1977**, *127*, 403–414.
(17) Garner, C. D.; Hughes, B.; King, T. J. *J. Chem. Soc., Dalton Trans.* **1975**, 562–566.

Table IV. Bond Lengths (Å) and Bond Angles (Deg) in the Benzoate Ligands[a]

atoms	ligand a	ligand b	av[b]	atoms	ligand a	ligand b	av[b]
$O_1\cdots O_2$	2.210 (7)	2.226 (8)	2.218 (8, 8, 8)	Ti-O_1-C_6	148.6 (4)	147.9 (7)	148.2 (6, 4, 4)
O_1-C_6	1.299 (12)	1.308 (8)	1.304 (10, 5, 5)	O_1-C_6-O_2	124.0 (13)	124.7 (7)	124.4 (10, 4, 4)
				O_1-C_6-C_7	114.1 (7)	112.6 (6)	113.4 (7, 8, 8)
O_2-C_6	1.204 (10)	1.206 (10)	1.205 (10, 1, 1)	O_2-C_6-C_7	121.9 (11)	122.7 (6)	122.3 (9, 4, 4)
C_6-C_7	1.509 (19)	1.497 (9)	1.503 (15, 6, 6)	C_6-C_7-C_8	121.9 (9)	122.7 (6)	122.3 (8, 4, 4)
				C_6-C_7-C_{12}	119.0 (7)	118.7 (6)	118.8 (7, 2, 2)
C_7-C_8	1.381 (10)	1.396 (9)		C_7-C_8-C_9	120.5 (10)	119.8 (7)	
C_8-C_9	1.370 (22)	1.363 (11)		C_8-C_9-C_{10}	120.9 (10)	121.2 (7)	
C_9-C_{10}	1.340 (22)	1.369 (13)		C_9-C_{10}-C_{11}	120.1 (17)	120.2 (8)	
C_{10}-C_{11}	1.369 (16)	1.370 (13)	1.377 (16, 13, 37)	C_{10}-C_{11}-C_{12}	120.6 (14)	119.7 (8)	120.0 (10, 7, 15)
C_{11}-C_{12}	1.397 (24)	1.377 (12)		C_{11}-C_{12}-C_7	118.6 (8)	120.6 (7)	
C_{12}-C_7	1.390 (15)	1.397 (9)		C_{12}-C_7-C_8	119.1 (11)	118.5 (6)	

[a] Numbers in parentheses are estimated standard deviations in the last significant figure. [b] Numbers in parentheses following each averaged value are the root-mean-square estimated standard deviation for an individual datum and the mean and maximum deviation from the average value.

Table V. Bond Lengths (Å) and Bond Angles (Deg) in the η-Cyclopentadienyl Ligands[a]

atoms	ligand a	ligand b	atoms	ligand a	ligand b
C_1-C_2	1.385 (16)	1.348 (11)	C_5-C_1-C_2	108.5 (12)	108.3 (7)
C_2-C_3	1.386 (19)	1.378 (12)	C_1-C_2-C_3	108.3 (8)	109.9 (7)
C_3-C_4	1.393 (10)	1.394 (13)	C_2-C_3-C_4	107.3 (10)	106.5 (6)
C_4-C_5	1.393 (19)	1.390 (12)	C_3-C_4-C_5	107.9 (10)	107.9 (8)
C_5-C_1	1.369 (14)	1.385 (15)	C_4-C_5-C_1	108.0 (8)	107.3 (7)
av C-C[b]	1.385 (16, 7, 16)	1.379 (12, 13, 31)	av C-C-C[b]	108.0 (10, 3, 7)	108.0 (7, 9, 19)

[a] Numbers in parentheses are estimated standard deviations in the last significant figure. [b] The numbers in parentheses following each averaged value are the root-mean-square estimated standard deviation for an individual datum and the mean and maximum deviation from the average value.

planar within 0.012 Å, but the dihedral angle between these mean planes is 3.5° in ligand a and 14.1° in ligand b. Twisting about the $O_2C\text{-}C_6H_5$ bonds and some rotation of the $O_2C\text{-}C$ groups out of the $TiO_{1a}O_{1b}$ plane combine to decrease the nonbonded contact between the ortho-hydrogen atoms on C_{8a} and C_{8b} (cf. Figure 1); in the observed structure the $C_{8a}\cdots C_{8b}$ distance is 3.97 Å, and the dihedral angle between the two phenyl rings is 51.4°. There are no unusually short intermolecular contacts in this structure.

Our X-ray study confirms the monodentate attachment of the benzoate ligands, which Vyshinskii et al.[4] predicted on the basis of the large ($\sim$320-cm^{-1}) difference between the ν_{asym}(COO) and ν_{sym}(COO) infrared frequencies.[18] We do not understand the small ($\sim$100-cm^{-1}) difference between ν_{asym}(COO) and ν_{sym}(COO) which Chandra et al.[3] have reported for the methylcyclopentadienyl analogue $(\eta\text{-}CH_3C_5H_4)_2Ti(O_2CC_6H_5)_2$, but we believe that a change to a bidentate attachment of the benzoate ligands is unlikely.

Bond distances and angles within the cyclopentadienyl ligands are listed in Table V. The averaged C–C bond length (1.382 Å) is in good agreement with values obtained for other (η-cyclopentadienyl)titanium structures.[1a,b,5,12-14]

Molecular Orbital Calculations. Extended Hückel (EH) calculations were performed on a model compound, $(\eta\text{-}C_5H_5)_2Ti(O_2CH)_2$, to probe the question of Ti–O multiple bonding.[19] As a first step in our analysis, we allowed $(\eta\text{-}C_5H_5)_2Ti^{2+}$ to interact with $(O_2CH)_2^{2-}$ to form the composite model complex. The frontier molecular orbitals (MO's) of the bent d^0 $(\eta\text{-}C_5H_5)_2Ti^{2+}$ fragment are given in **2**. They have been discussed in detail elsewhere.[20]

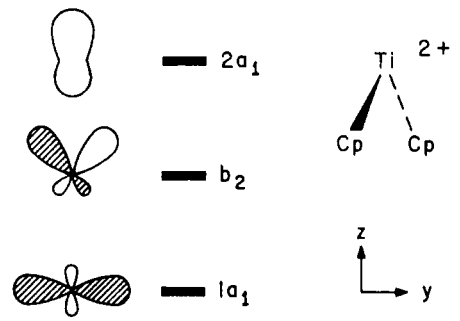

2

Besides the usual σ-type interactions between the $(O_2CH)_2^{2-}$ fragment MO's and b_2 and $2a_1$ in **2**,[20] there is also a strong in-plane π-type interaction involving $1a_1$ of $(\eta\text{-}C_5H_5)_2Ti^{2+}$. This is illustrated schematically in **3**.

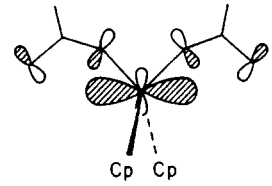

3

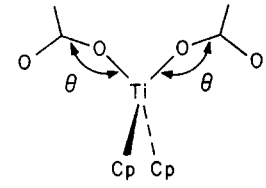

4

A variation of the angle θ as defined in **4** gave a total energy minimum of θ = 180°. However, the total energy did not vary be more than 0.40 eV between θ = 140° and

(18) For a recent review of the relationships between C–O stretching frequencies in carboxylate complexes and the type of carboxylate coordination, see: Deacon, G. B.; Phillips, R. J. *Coord. Chem. Rev.* **1980**, *33*, 227–250.

(19) Details pertinent to the calculations may be found in the Appendix.

(20) Lauher, J. W.; Hoffmann, R. *J. Am. Chem. Soc.* **1976**, *98*, 1729–1742.

θ = 210°. At θ = 180° the Ti–O overlap population, a measure of bonding, was at a maximum, increasing by +0.0149 from its value at the experimental θ of 148°. Interestingly, variation of the Ti–O–H angle in a model alkoxide complex, $(\eta\text{-}C_5H_5)_2Ti(OH)_2$, gave maximum Ti–O bonding and an energy minimum at a Ti–O–H angle of 180°. In both cases the Ti–O bonding is maximized at θ = 180° because of increased bonding interactions involving $1a_1$ (**2** and **3**). As θ increases, the bound oxygen evolves from the canonical sp^2 hybrid, thus allowing for more in-plane π interaction as in **3**.[21]

We also calculated for the same model complex the geometry shown in **5** where one O_2CH^- ligand is bidentate, the other monodentate. The geometry in **5** gives an 18-electron count at the Ti atom and would seem to be an attractive alternative geometry to the experimentally determined structure. However, the EH calculated total

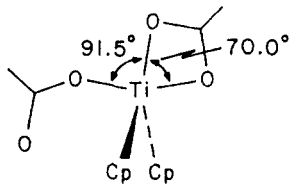

5

energy for **5** is 2.0 eV above that for the experimental geometry. Most of the energy difference cay be traced to interactions involving an occupied $(\eta\text{-}C_5H_5)_2Ti^{2+}$ orbital not normally of importance, **6**.

Orbital **6** is mainly C_5H_5 in character and lies below the important frontier orbitals of $(\eta\text{-}C_5H_5)_2Ti^{2+}$ in **2**. It interacts with low-lying filled carboxylate orbitals and is pushed up in energy. This destabilizing interaction, less

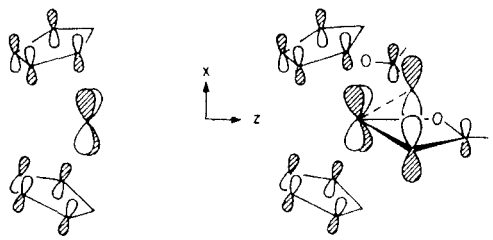

6 **7**

important when both O_2CH^- ligands are monodentate, is shown schematically in **7**. In MO **7**, the $(O_2CH)_2^{2-}$ orbital contributions to the wave function are out-of-phase with both the Ti and C_5H_5 contributions. The oxygen–C_5H_5 carbon repulsion in **7** is a manifestation of close O···C contacts for structure **5**.

We have calculated the O···C contacts for structure **5** assuming several likely eclipsed and staggered conformations of the cyclopentadienyl rings. In each case, four O···C contacts were found in the range 2.32–2.42 Å. These contacts are prohibitively short, 0.7–0.8 Å less than the sum of the van der Waals radii, and they rule out the possibility of forming an 18-electron complex containing one bidentate and one monodentate carboxylate ligand. The titanium atom appears to do the next best thing. It is coordinated by only two oxygen atoms, but it achieves an effective 18-electron count via Ti–O π bonding.

Acknowledgment. The X-ray diffractometer used in this research was obtained with support from the National Science Foundation Instrumentation Program (Grant CHE 77-09756). D.M.H. and N.D.C. wish to thank Professor Roald Hoffmann for graduate and undergraduate assistantships, respectively (NSF Grant CHE 7828048). Timely advice from Michael E. Silver is gratefully acknowledged.

Appendix

All calculations were performed by using the extended Hückel method,[22] with weighted H_{ij}'s.[23] The following distances were assumed for all calculations on the model complex $(\eta\text{-}C_5H_5)_2Ti(O_2CH)_2$: Ti–(centroid C_5H_5) = 2.061 Å; Ti–O = 1.926 Å; C–O = 1.255 Å; C–H = 1.09 Å. The angle between the normals to the planes of the two $\eta\text{-}C_5H_5$ rings was set equal to 131.7°. When the O_2CH ligand was made monodentate the angles Ti–O–C and O–C–O were 148.2° and 123.4°, respectively.

The parameters for C, O, and H are from the literature.[22] The Ti parameters were taken from Lauher and Hoffmann.[20]

Registry No. $(\eta\text{-}C_5H_5)_2Ti(O_2CC_6H_5)_2$, 12156-48-8; $(\eta\text{-}C_5H_5)_2TiCl_2$, 1271-19-8.

Supplementary Material Available: Table II, final thermal parameters, Table VI, least-squares mean planes, and a listing of structure factor amplitudes for $(\eta\text{-}C_5H_5)_2Ti(O_2CC_6H_5)_2$ (15 pages). Ordering information is given on any current masthead page.

(21) Silver, M. E.; Eisenstein, O.; Fay, R. C. *Inorg. Chem.*, in press.

(22) Hoffmann, R. *J. Chem. Phys.* **1963**, *39*, 1397–1412. Hoffmann, R.; Lipscomb, W. N. *Ibid.* **1962**, *36*, 2179–2195; **1962**, *37*, 2872–2883.

(23) Ammeter, J. H.; Bürgi, H.-B.; Thibeault, J. C.; Hoffmann, R. *J. Am. Chem. Soc.* **1978**, *100*, 3686–3692.

Interconversion of Phosphido-Bridged Polynuclear Cobalt Carbonyl Complexes. Cleavage of the Phosphido Bridge during Hydroformylation Catalysis

A. Dale Harley, Gerald J. Guskey, and Gregory L. Geoffroy*

Department of Chemistry, The Pennsylvania State University, University Park, Pennsylvania 16802

Received September 9, 1982

The interconversions of a series of phosphido-bridged cobalt carbonyl complexes have been examined. The oligomeric complex $[Co(\mu\text{-}PPh_2)(CO)_3]_x$, **1**, originally prepared by Hayter[1] but incorrectly given the binuclear formulation $Co_2(\mu\text{-}PPh_2)_2(CO)_6$, **2**, was found to lose CO upon heating to form trinuclear $Co_3(\mu\text{-}PPh_2)_3(CO)_6$, **3**, in near quantitative yield. Both **1** and **3** react with PEt_2Ph upon heating to yield the new binuclear complex $Co_2(\mu\text{-}PPh_2)_2(CO)_2(PEt_2Ph)_2$, **4**, which has been spectroscopically characterized. Under milder conditions, trinuclear **3** reacts with PEt_2Ph to produce mono- and disubstituted clusters $Co_3(\mu\text{-}PPh_2)_3(CO)_5(PEt_2Ph)$, **5**, and $Co_3(\mu\text{-}PPh_2)_3(CO)_4(PEt_2Ph)_2$, **6**. Binuclear **4** was observed to react with CO to displace PEt_2Ph and reform trinuclear **3**. An authentic sample of binuclear $Co_2(\mu\text{-}PPh_2)_2(CO)_6$, **2**, was prepared by heating either **1** or **3** under CO pressure (1000 psi). This compound has been spectroscopically characterized and was shown to be distinct from Hayter's oligomeric species **1**. Complex **1** functions as a catalyst/catalyst precursor for the hydroformylation of 1-hexene (1000 psi of H_2/CO (1:1), 110 °C). However, it is irreversibly transformed into $Co_2(CO)_6(P(n\text{-}C_6H_{13})Ph_2)_2$ under hydroformylation conditions.

Binuclear and polynuclear transition-metal complexes are currently of high interest because of their potential to induce unique catalytic and stoichiometric transformations as a result of cooperative interaction between adjacent metals.[1] One of the problems with many of these compounds, however, is the relative ease with which they fragment under reaction conditions, thereby destroying the integrity of the initial complex.[1,2] One way to retard such fragmentation tendencies is to use bridging ligands to assist in holding the metals together.[3,4] In this regard we have been interested in the preparation of phosphido-bridged heteronuclear complexes[4] and sought to use $Co(CO)_4PPh_2$ as a reagent for the preparation of such compounds containing cobalt. While this species apparently results from the low-temperature reaction of $Na[Co(CO)_4]$ with PPh_2Cl[5] (eq 1) upon warmup to 25 °C, it loses CO to give other

$$Na[Co(CO)_4] + PPh_2Cl \xrightarrow[-60\ °C]{THF} Co(CO)_4PPh_2 + NaCl \quad (1)$$

products. In the course of investigating this reaction and its products, it rapidly became apparent that there are a series of phosphido-bridged cobalt carbonyl complexes which interconvert by rearrangement of the phosphido bridges under relatively mild conditions. We have studied these interconversions, Scheme I, and they are described in detail herein. Also discussed are other examples of reactions which irreversibly cleave the phosphido bridges, including such bridge elimination during the course of hydroformylation catalysis.[6]

A number of phosphido-bridged cobalt carbonyl complexes have been described previously in the literature.[7-10]

Scheme I

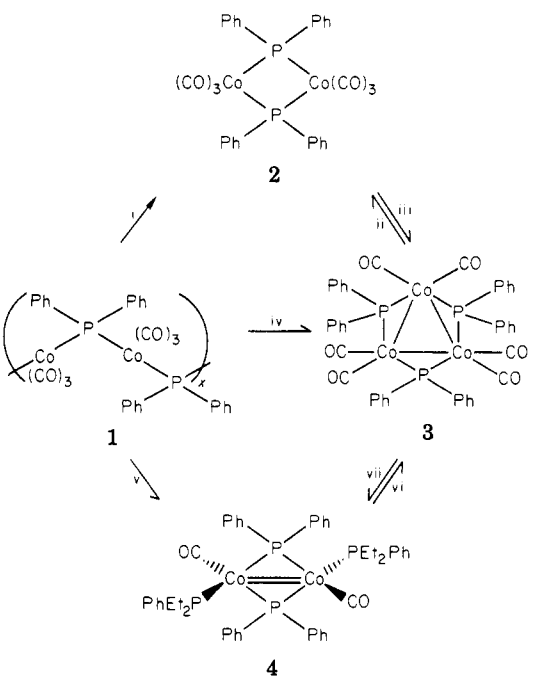

(i) CO (1000 psi), 110 °C, 24 h; (ii) CO (1000 psi), 110 °C, 24 h; (iii) *hν* (366 nm); (iv) 80 °C, 2–3 h, N_2 (1 atm); (v) PEt_2Ph, 110 °C, 48 h; (vii) PEt_2Ph, 110 °C, 3 h; (vi) CO (1 atm), 25 °C, 30 min; all reactions were conducted in toluene solution

(1) (a) Johnson, B. F. G., Ed. "Metal Clusters"; Wiley: New York, 1980. (b) Chisholm, M. H.; Rothwell, I. P. *Prog. Inorg. Chem.* **1982**, *29*, 1. (c) Muetterties, E. L. *Bull Soc. Chim. Belg.* **1976**, *85*, 451. (d) Roberts, D. A.; Geoffroy, G. L. In "Comprehensive Organometallic Chemistry"; Wilkinson, G., Stone, F. G. A., Abels, E., Eds.; Pergamon Press: London, 1982; Chapter 40.

(2) (a) Roberts, D. A.; Mercer, W. L.; Zahurak, S. M.; Geoffroy, G. L.; DeBrosse, C. W.; Cass, M. E.; Pierpont, C. G. *J. Am. Chem. Soc.* **1982**, *104*, 910. (b) Fox, J. R.; Gladfelter, W. L.; Geoffroy, G. L. *Inorg. Chem.* **1980**, *19*, 2574.

(3) (a) Carty, A. J. *Adv. Chem. Ser.* **1982**, *No. 196*, 163. (b) *Pure Appl. Chem.* **1982**, *No. 54*, 113. (c) Finke, R. B.; Gaughan, G.; Pierpont, C.; Cass, M. E. *J. Am. Chem. Soc.* **1981**, *103*, 1394 and references therein. (d) Huttner, G.; Schneider, J.; Muller, H. D.; Mohr, G.; von Seyerl, J.; Wolfhart, L. *Angew. Chem., Int. Ed. Engl.* **1979**, *18*, 76. (e) Werner, H.; Hofmann, W. *Ibid.* **1979**, *18*, 158. (f) Beurich, H.; Madach, T.; Richter, F.; Vahrenkamp, H. *Ibid.* **1979**, *18*, 690.

(4) (a) Breen, M. J.; Duttera, M. R.; Geoffroy, G. L.; Novotnak, G. C.; Roberts, D. A.; Shulman, P. M.; Steinmetz, G. R. *Organometallics* **1982**, *1*, 1008. (b) Breen, M. J.; Geoffroy, G. L. *Ibid.*, in press. (c) Foley, H. C.; Finch, W. C.; Pierpont, C. G.; Geoffroy, G. L. *Ibid.*, in press.

(5) (a) Müller, R.; Vahrenkamp, H. *Chem. Ber.* **1980**, *113*, 3359. (b) Burt, J. C.; Schmid, G. *J. Chem. Soc., Dalton Trans.* **1978**, 1385.

(6) Evidence is beginning to accumulate that these ligands are not as inert and as strongly binding as once thought. See ref 3a,b, for example.

0276-7333/83/2302-0053$01.50/0

Of particular relevance to this study is the oligomeric compound $[Co(\mu\text{-}PPh_2)(CO)_3]_x$, **1**, prepared by Hayter in 1964 by the reaction shown in eq 1 carried out at 25 °C or by reaction of $Co_2(CO)_8$ with P_2Ph_4.[8,9] The binuclear formulation **2** (Scheme I) was originally given to Hayter's product although anomalously high molecular weight values (6000–8000) were obtained for this compound.[8] These were attributed[8] to decomposition during the measurements, although other workers[11,12] have instead suggested an oligomeric structure such as that drawn in Scheme I for Hayter's product. Our observations reported herein are consistent with such a structure for **1**, and we have as well isolated and characterized an authentic sample of binuclear **2** and shown its spectral properties to be different from those of **1**. From the reaction of $Co_2(CO)_8$ with P_2Ph_4, Huntsman and Dahl[10] were also able to isolate a green compound of formula $Co_3(\mu\text{-}PPh_2)_3(CO)_6$ which was shown to have the triangular phosphido-bridged structure **3** (Scheme I) by a single-crystal X-ray diffraction study. A similar compound with bridging μ-PMe_2 ligands has been described by Vahrenkamp and co-workers.[7b]

Experimental Section

$Co_2(CO)_6(PMePh_2)_2$,[14] $Co_4(\mu\text{-}PPh_2)_2(CO)_{10}$,[7c,15] and $Na[Co(CO)_4]$[16] were prepared by literature procedures. PPh_2H, PPh_2Cl, $PHexPh_2$ (Hex = n-C_6H_{13}), PEt_2Ph, $P(OEt)Ph_2$, and $Co_2(CO)_8$ were purchased from Strem Chemical Co. The phosphines were used as received but $Co_2(CO)_8$ was resublimed (25 °C (0.1 mmHg)) before use. $Co_2(CO)_6(PHexPh_2)_2$ and $Co_2(CO)_6(P(OEt)Ph_2)_2$ were prepared by substituting $PHexPh_2$ and $P(OEt)Ph_2$ for $PMePh_2$ in the literature procedure for $Co_2(CO)_6(PMePh_2)_2$.[14,17] Solvents were dried by standard methods, and all reactions were conducted under a prepurified N_2 atmosphere. All transfers of air-sensitive materials were carried out in an N_2-filled glovebox.

IR spectra were recorded on a Perkin-Elmer 580 grating IR spectrophotometer by using 0.5-mm NaCl solution IR cells. These were sealed with Luer-Lock fittings and purged with N_2 to record spectra of air-sensitive solutions. Electron-impact (EI) mass spectra were obtained by using an AEI-MS9 mass spectrometer with a source voltage of 70 eV and probe temperatures in the 100–200 °C range. Field desorption (FD) mass spectra were obtained on a MAT 731 mass spectrometer by Dr. Thomas Criswell at the Eastman Kodak Research Laboratories, Rochester, N.Y. Gas chromatography mass spectra (GC/MS) were recorded on a Finigan 2200 spectrometer. NMR spectra were recorded on JEOL PS-100 FT, Bruker WH200, and Bruker WM360 NMR spectrometers. All reported ^1H chemical shifts are relative to Me_4Si. ^{31}P NMR chemical shifts are relative to external H_3PO_4 with downfield chemical shifts reported as positive. Elemental analyses were performed by Schwarzkopf Laboratories, Woodside, N.Y.

Preparation of $[Co(\mu\text{-}PPh_2)(CO)_3]_x$, 1. Method 1. $Na[Co(CO)_4]$ was prepared in situ by stirring $Co_2(CO)_8$ (2.00 g, 5.84 mmol) with NaOH (2.33 g, 58.4 mmol) in THF (75 mL) for 2.5 h until the color of $Co_2(CO)_8$ was discharged.[16] The suspension was filtered, and PPh_2Cl (2.56 g, 11.68 mmol) was added via syringe, giving formation of a white precipitate (presumably NaCl) and an orange solution. Evolution of gas was noted during the addition time of 10 min. After being stirred for 5 h, the solution was filtered and THF removed in vacuo to give an orange solid. This material was extracted with 2–50-mL portions of toluene. Addition of 60 mL of hexane to the extract gave **1** as an orange solid (1.60 g, 4.87 mmol for x = 1, 42%): IR ν_{CO} (hexane) 2060 (vw), 2045 (m), 2007 (m), 1990 (vs), 1980 (w, sh), 1955 (w, sh), ν_{CO} (CH_2Cl_2) 2065 (vw), 2045 (m), 1995 (vs, br) cm^{-1}; $^{31}P\{^1H\}$ NMR (25 °C, benzene-d_6) δ 61.7 (s).

Method 2. $Co_2(CO)_8$ (2.00 g, 5.84 mmol) was dissolved in toluene (10 mL) in a 125-mL Erlenmeyer flask in an N_2-filled glovebox. To this solution was added dropwise by syringe 2.0 mL of PPh_2H (10.6 mmol, d = 1.07 g cm^{-3}) resulting in vigorous gas evolution, presumably CO and H_2. After the solution had stirred for 8 h, hexane (70 mL) was added and **1** precipitated as an orange powder. This was removed by filtration, washed with 2–10-mL portions of hexane, and dried under N_2 for 12 h (**1**, 3.22 g, 9.81 mmol for x = 1, 78%). If this reaction is carried out in a closed reaction vessel under the pressure of the CO and H_2 released during the reaction, the product **1** is contaminated with significant amounts of **2**.

Preparation of $Co_2(\mu\text{-}PPh_2)_2(CO)_6$, 2. Orange crystals of **2** slowly form when the supernatant solution from the preparation of $[Co(\mu\text{-}PPh_2)(CO)_3]_x$ (method 2, above) is allowed to stand for several days. These were removed to give **2** in 5.6% yield (0.23 g, 0.35 mmol). Alternatively, **2** quantitatively forms upon stirring **1** (0.328 g, 1 mmol) in toluene (30 mL) at 110 °C under 1000 psi of CO pressure for 24 h in a Parr Model 4561 T31S5 pressure reactor. Mixtures of **1** and **2** can be separated by chromatography on silica gel using CH_2Cl_2/hexane (70/30) in red light. Under these conditions **1** sticks to the top of the column, but **2** moves as an orange band: IR ν_{CO} (hexane) 2060 (m), 2040 (s), 2007 (vs), 1995 (vs) cm^{-1}; $^{31}P\{^1H\}$ NMR (25 °C, benzene-d_6) δ 114 (s); mp 148–150 °C; mass spectrum, m/e (FD) = 656 (M^+) + fragment ions corresponding to loss of four CO's. Anal. Calcd for $C_{30}H_{20}Co_2O_6P_2$: C, 54.90; H, 3.13; Found: C, 54.85; H, 3.17.

Preparation of $Co_3(\mu\text{-}PPh_2)_3(CO)_6$, 3. $Co_2(CO)_8$ (2.00 g, 5.84 mmol) was dissolved in toluene (50 mL), and 2.0 mL of PPh_2H (10.6 mmol, d = 1.007 g cm^{-3}) was added via syringe resulting in vigorous gas evolution. This solution was stirred at reflux for 2 h. Hexane (25 mL) was added after the solution was cooled to give **3** as a green microcrystalline solid (2.9 g, 3.22 mmol, 83%): IR ν_{CO} (CH_2Cl_2) 2027 (m), 1990 (vs, br), 1985 (m, sh), 1960 (w, sh) cm^{-1}; $^{31}P\{^1H\}$ NMR (25 °C, benzene-d_6) δ 244 (s);[10] mass spectrum, m/e (EI) = 900 (M^+) + fragment ions corresponding to loss of six CO's.

Preparation of $Co_2(\mu\text{-}PPh_2)_2(CO)_2(PEt_2Ph)_2$, 4. Method 1. To **1** (0.328 g, 0.5 mmol) in tetrahydrofuran (THF, 35 mL) was added 0.3 mL of PEt_2Ph (0.24 g, 1.44 mmol), and the reaction mixture was refluxed for 7 h. The solution was concentrated in vacuo to ca. 5 mL, and 20 mL of hexane was added. The solution was filtered and stored at 0 °C for 24 h during which time black crystals of **4** deposited. The supernatant was decanted, and the black solid was washed with 2–10-mL portions of hexane and then dried under N_2 to give **4** in 18% yield (0.08 g, 0.09 mmol): IR ν_{CO}(THF) 1905 (vs, br) cm^{-1}; $^{31}P\{^1H\}$ NMR (25 °C, benzene-d_6) $\delta(\mu\text{-}PPh_2)$ 175.8 (s), $\delta(PEt_2Ph)$ 48.5 (s); mass spectrum, m/e (EI) = 876 (M^+) + fragment ions corresponding to loss of two CO's. Anal. Calcd for $C_{46}H_{50}O_2P_4Co_2$: C, 63.02; H, 5.75. Found: C, 63.18; H, 5.88.

Method 2. $Co_2(CO)_8$ (2.00 g, 5.84 mmol) and PPh_2H (2.00 mL) were dissolved in toluene (40 mL) in a 250-mL Carius tube. After the solution was stirred for 30 min at 25 °C 2.5 mL of PEt_2Ph

(7) (a) Vizi-Orosz, A.; Palyi, G.; Marko, L. *J. Organomet. Chem.* **1973**, *60*, C25. (b) Marko, L.; Marko, B. *Inorg. Chim. Acta* **1975**, *14*, L39. (c) Ryan, R. C.; Dahl, L. F. *J. Am. Chem. Soc.* **1975**, *97*, 6904. (d) Burt, J. C.; Boese, R.; Schmid, G. *J. Chem. Soc., Dalton Trans.* **1978**, 1387. (e) Keller, E.; Vahrenkamp, H. *Chem. Ber.* **1979**, *112*, 1626. (f) *J. Organomet. Chem.* **1978**, *155*, C41. (g) *Chem. Ber.* **1979**, *112*, 2347. (h) *Angew. Chem., Int. Ed. Engl.* **1977**, *16*, 731. (i) Dobbie, R. C.; Whittaker, D. *J. Chem. Soc., Dalton Trans.* **1973**, 2427. (j) Hutching, L. D.; Light, R. W.; Paine, R. T. *Inorg. Chem.* **1982**, *21*, 266. (k) Grobe. J.; Stierand, H. *Z. Anorg. Chem.* **1969**, *371*, 99.

(8) Hayter, R. G. *J. Am. Chem. Soc.* **1964**, *86*, 823.

(9) An apparently similar compound was described in: Hieber, W.; Duchatsch, H. *Z. Naturforsch., B: Anorg. Chem., Org. Chem., Biochem., Biophys., Biol.* **1963**, *B18*, 1132. Schweckendiek, W. German Patent 1 072 244, Dec 31, 1959.

(10) Huntsman, J. R. Ph.D. Thesis, University of Wisconsin, Madison, Wisc., 1973.

(11) Ginsberg, R. E.; Rothrock, R. K.; Finke, R. G.; Collman, J. P.; Dahl, L. F. *J. Am. Chem. Soc.* **1979**, *101*, 6550.

(12) Private communication from H. Vahrenkamp to L. F. Dahl, cited as ref 24 in ref 11.

(13) Cerriani, S.; Ratcliff, B.; Ugo, R. *Gazz. Chim. Ital.* **1974**, *104*, 1161.

(14) $[Co_4(\mu\text{-}PPh)_2(CO)_{10}]$: mass spectrum, m/e 732 (parent ion) + ions corresponding to loss of 10 CO's; IR (toluene) 2042 (vs), 2032 (vs), 2019 (vs), 1995 (w), 1878 (m) cm^{-1} (lit.[7c] 2040 (vs), 2032 (s), 2016 (s), 1876 (w) cm^{-1}).

(15) Edgell, W. F., Lyford, J. *Inorg. Chem.* **1970**, *9*, 1932.

(16) (a) $[Co_2(CO)_6(PHexPh_2)_2]$: IR 1955 (s, br) cm^{-1}; $^{31}P\{^1H\}$ NMR δ 59.6 (s). (b) $[Co_2(CO)_6[P(OEt)Ph_2]_2]$: IR 1970 (m, sh), 1955 (s, br) cm^{-1}; $^{31}P\{^1H\}$ NMR δ 165.3; ^1H NMR δ(Ph), 7.67, 7.5, $\delta(CH_2)$ 4.04 (m), $\delta(CH_3)$ 1.42 (t, $J_{^1H\text{-}^1H}$ = 6.5 Hz).

(17) Klug, H. P.; Alexander, L. E. "X-Ray Diffraction Procedures for Polycrystalline and Amorphous Materials"; Wiley: New York, 1974.

was added and the Carius tube evacuated. This mixture was heated to 140 °C for 8 h and then cooled to 25 °C. Hexane (25 mL) was added and the Carius tube sealed, heated to 100 °C for 30 min, cooled to 25 °C, and stirred for 6 h. The black crystalline product which formed was filtered, washed with 5–10-mL portions of hexane, and dried in vacuo (**4**, 3.63 g, 4.14 mmol, 71%).

Preparation of $Co_3(\mu\text{-}PPh_2)_3(Co)_5(PEt_2Ph)$, 5. To **3** (0.450 g, 0.50 mmol) dissolved in CH_2Cl_2 (20 mL) in a 75-mL Carius tube was added 0.25 mL of PEt_2Ph (0.20 g, 1.20 mmol). The Carius tube was evacuated, sealed, and heated to 80 °C for 2 h. After the solution was cooled the green residue was dissolved in toluene (20 mL), filtered, and chromatographed under N_2 on a 2 × 30 cm column of silica gel (230–400 mesh) using 30% toluene/hexane as eluant. A green fraction of **5** elutes first followed by a small green fraction of **3**. Evaporation of solvent from the first fraction yields **5** in 64% yield (0.33 g, 0.32 mmol): IR ν_{CO} (CH_2Cl_2) 1995 (m), 1965 (vs br), 1930 (m sh) cm^{-1}; $^{31}P\{^1H\}$ NMR (25 °C, benzene-d_6) $\delta(\mu\text{-}PPh_2)$ 274.5 (s, 1), $\delta(\mu\text{-}PPh_2)$ 198.8 (s, 2), $\delta(PEt_2Ph)$ 31.1 (s, 1); mass spectrum m/e (FD) = 1038 (M^+). Anal. Calcd for $C_{51}H_{45}O_5P_4Co_3$: C, 59.00; H, 4.35. Found: C, 59.21; H, 4.53.

Hydroformylation Catalysis. To the glass liner of a Parr Model 4561 T31S5 300-mL pressure reactor was added the complex to be studied, toluene (50 mL), and 1-hexene (50 mL). The complex concentration was ~4×10^{-3} M in Co in all reactions examined. The reactor was purged three times with carbon monoxide and hydrogen and then pressurized to 1000 psi with a 1:1 mixture of CO and H_2. The reactor was heated to 110 °C and stirred for 24 h. At operating temperature, an initial pressure of 1250 psi was obtained. The reaction mixture following catalysis was analyzed by gas chromatography using a Varian Model 1440 gas chromatograph with a flame ionization detector and a 6 ft × $^1/_8$ in. stainless-steel column of 10% Carbowax on Chromosorb W at a column temperature of 65 °C.

Results

Preparation and Further Characterization of $[Co(\mu\text{-}PPh_2)(CO)_3]_x$, 1. The reaction of $Na[Co(CO)_4]$ with PPh_2Cl, eq 1, was examined initially as a potential route to the desired $Co(CO)_4PPh_2$ synthetic reagent. At −60 °C in THF solution these reagents react to give a pale orange solution which most likely contains $Co(CO)_4PPh_2$.[5] However, upon warm-up to −20 °C, carbon monoxide begins to be evolved and the solution darkens. Gas evolution ceases after 1.5 h at this temperature with a total of 0.93 mol of CO evolved per mol of Co, indicating the transformation shown in eq 2. No further changes occur upon warm-up to 25 °C.

$$x\,Co(CO)_4PPh_2 \xrightarrow{-20\ °C} x\,CO + [Co(\mu\text{-}PPh_2)(CO)_3]_x \quad (2)$$

The orange-brown solid which precipitates from this solution upon addition of hexane shows IR bands (CH_2Cl_2) at 2065 (vw), 2045 (m), and 1995 (vs, br) cm^{-1} (Figure 1a), indicative of terminal but not bridging CO's. Its $^{31}P\{^1H\}$ NMR spectrum shows a single resonance at δ 61.7. This material appears similar to the compound isolated by Hayter[8] and originally given the binuclear formation $Co_2(\mu\text{-}PPh_2)_2(CO)_6$, **2**, although other workers[11,12] have instead suggested the oligomeric structure $[Co(\mu\text{-}PPh_2)(CO)_3]_x$, **1**.

Hayter's[8] high molecular weight values (6000–8000) are consistent with an oligomeric formulation as are also our observations of a markedly decreasing solubility of the compound as it is repeatedly dissolved and precipitated from solution, implying an increasing degree of oligomerization. Further support for its oligomeric character comes from its X-ray powder diffraction pattern. *No diffraction lines were observed* over the scan range $10° \leq 2\theta \leq 60°$, implying an amorphous rather than a crystalline material.[17] The most convincing evidence that this material is not the binuclear complex **2** is our isolation and structural characterization[18] of **2** and our demonstration

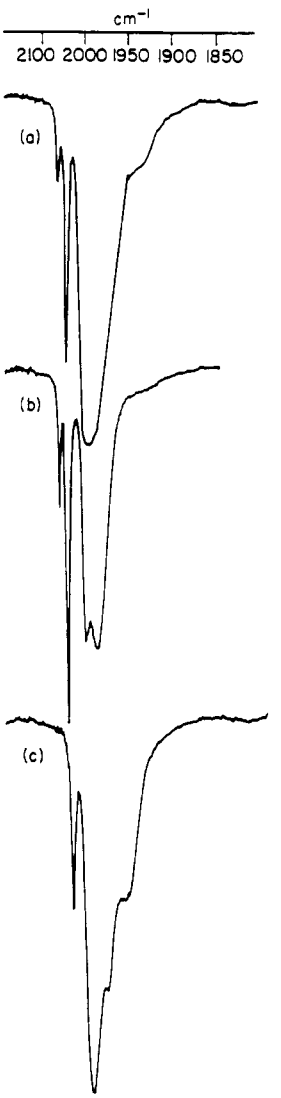

Figure 1. Infrared spectra of (a) $[Co(\mu\text{-}PPh_2)(CO)_3]_x$, **1**, (b) $Co_2(\mu\text{-}PPh_2)_2(CO)_6$, **2**, and (c) $Co_3(\mu\text{-}PPh_2)_3(CO)_6$, **3**, in CH_2Cl_2 solution.

that the spectral properties of **2** are significantly different from those of **1** (see below).

The oligomeric complex **1** is most conveniently prepared by the direct reaction of PPh_2H with $Co_2(CO)_8$ (eq 3).

$$Co_2(CO)_8 + 2PPh_2H \xrightarrow[\text{toluene}]{25\ °C} [Co(\mu\text{-}PPh_2)(CO)_3]_x + 2CO + H_2 \quad (3)$$
$$85\text{–}90\%$$

Simply stirring these reagents together in toluene solution at 25 °C under an N_2 atmosphere results in vigorous gas evolution, presumably H_2 and CO, and precipitation of **1**. Temperature control of this reaction is critical since the trinuclear cluster $Co_3(\mu\text{-}PPh_2)_3(CO)_6$, **3**, forms at elevated temperatures (see below).

Preparation and Characterization of $Co_2(\mu\text{-}PPh_2)_2(CO)_6$, 2. An authentic sample of the *binuclear* complex $Co_2(\mu\text{-}PPh_2)_2(CO)_6$, **2**, was first obtained by allowing the supernatant solution from the preparation of **1** via eq 3 to stand for several days *in the dark*. During this time reddish orange crystals of **2** slowly form and can be isolated in ~6% yield by decantation of the mother liquor. This complex has been fully characterized spec-

(18) Harley, A. D.; Whittle, R.; Geoffroy, G. L. *Organometallics*, submitted for publication.

troscopically and shown to have the binuclear structure **2** by a complete single-crystal X-ray diffraction study, details of which are described separately.[18] Its IR spec-

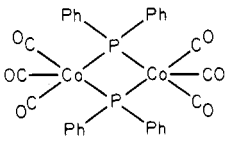

2

trum shows only terminal ν_{CO} bands (Figure 1b), and its $^{31}P\{^1H\}$ NMR spectrum shows a single resonance at δ −114.2. The far upfield position of the μ-PPh_2 resonance is consistent with this ligand bridging two metals not joined by a metal–metal bond. Numerous correlations have shown that the μ-PR_2 ligands in compounds with metal–metal bonds generally display downfield (δ 50 → δ 300) ^{31}P NMR resonances, whereas upfield (δ 50 → δ −200) resonances are observed for compounds in which the μ-PR_2 ligand bridges two metals not joined by a metal–metal bond.[3a,19] A parent ion at m/e 656 and fragment ions corresponding to successive loss of four CO's are apparent in the field desorption mass spectrum of **2**. In contrast to **1**, the binuclear complex **2** is air stable in the solid state and in solution and can be readily purified by chromatography on silica gel under red darkroom lights. Binuclear complex **2** is *extremely* light sensitive, losing CO and rearranging to trinuclear **3** upon photolysis (eq 4). Both IR

$$\underset{\mathbf{2}}{3Co_2(\mu\text{-}PPh_2)_2(CO)_6} \xrightarrow[CH_2Cl_2]{h\nu} 2Co_2(\mu\text{-}PPh_2)_3(CO)_6 + 6CO \quad (4)$$

and ^{31}P NMR monitoring show the conversion of **2** into **3** to be complete following 30 min photolysis with Pyrex-filtered medium-pressure Hg arc lamp irradiation ($\lambda \geq 300$ nm). Even solid samples of **2** are light sensitive and slowly decompose to **3** upon standing under fluorescent room lights.

Complex **2** is most conveniently prepared simply by heating toluene solutions of the oligomeric complex **1** or the trinuclear complex **3** under CO pressure (eq 5 and 6).

$$\underset{\mathbf{1}}{[Co(\mu\text{-}PPh_2)(CO)_3]_x} \xrightarrow[\text{CO, 1000 psi}]{\text{110 °C, 24 h, toluene}} (x/2)Co_2(\mu\text{-}PPh_2)_2(CO)_6 \quad (5)$$

$$\underset{\mathbf{3}}{2Co_3(\mu\text{-}PPh_2)_3(CO)_6} + 6CO \xrightarrow[\text{1000 psi}]{\text{110 °C, 24 h, toluene}} 3Co_2(\mu\text{-}PPh_2)_2(CO)_6 \quad (6)$$

2

From such reactions **1** and **3** can be quantitatively transformed into **2**. The CO pressure is necessary for the **1** → **2** conversion since otherwise **1** loses CO and rearranges to the trinuclear cluster **3** (see below).

Preparation of $Co_3(\mu$-$PPh_2)_3(CO)_6$, 3. Huntsman and Dahl[10] isolated the trinuclear cluster **3** from the reaction of $Co_2(CO)_8$ with P_2Ph_4 and characterized it by an X-ray diffraction study. We find that this complex is most conveniently prepared in high yield simply by heating $Co_2(CO)_8$ with PPh_2H (eq 7). Note that this is the same reaction used to prepare the oligomeric complex **1** (eq 3) except for the different temperatures involved (25 °C for **1**; 110 °C for **3**). The oligomeric complex **1** may be an

$$3Co_2(CO)_8 + 6PPh_2H \xrightarrow[N_2]{\text{110 °C, 2 h, toluene}} \underset{\mathbf{3}\ (83\%)}{2Co_3(\mu\text{-}PPh_2)_3(CO)_6} + 12CO + 3H_2 \quad (7)$$

intermediate in the synthesis of **3** via eq 7 since we find that **1** loses CO and is quantitatively converted into **3** upon heating under N_2 (eq 8). The trinuclear complex **3** shows

$$\underset{\mathbf{1}}{[Co(\mu\text{-}PPh_2)(CO)_3]_x} \xrightarrow[N_2, \text{ toluene}]{\text{80 °C, 2–3 h}} (x/3)\underset{\mathbf{3}}{Co_3(\mu\text{-}PPh_2)_3(CO)_6} + 3CO \quad (8)$$

only terminal ν_{CO} bands (Figure 1c) and a singlet at δ 244 in its $^{31}P\{^1H\}$ NMR spectrum.[10] A parent ion at m/e 900 and fragment ions corresponding to stepwise loss of the six CO's are apparent in its electron-impact mass spectrum. Trinuclear complex **3** is thermally stable up to ~110 °C under an N_2 atmosphere, although when heated under CO pressure it rearranges to give **2** in quantitative yield (see eq 6). Prolonged heating of **3** under N_2 at 150 °C induces an irreversible transformation into $Co_4(\mu\text{-}PPh)_2(CO)_{10}$, a compound previously characterized by Dahl and Ryan.[7c]

Preparation and Characterization of $Co_2(\mu$-$PPh_2)_2(CO)_2(PEt_2Ph)_2$, 4. Reaction of the oligomeric complex **1** with PEt_2Ph was found to result in the formation of the new binuclear complex $Co_2(\mu\text{-}PPh_2)_2(CO)_2(PEt_2Ph)_2$, **4**, albeit in relatively low yield (eq 9).

$$\underset{\mathbf{1}}{[Co(\mu\text{-}PPh_2)(CO)_3]_x} + PEt_2Ph \xrightarrow[THF]{66\ ^\circ C} xCO + (x/2)\underset{\mathbf{4}\ (18\%)}{Co_2(\mu\text{-}PPh_2)_2(CO)_2(PEt_2Ph)_2} \quad (9)$$

This complex is most conveniently prepared in 70% yield by the direct reaction of a 1:2:2 mixture of $Co_2(CO)_8$, PEt_2Ph, and PPh_2H (eq 10). Complex **4** also forms when

$$Co_2(CO)_8 + 2PEt_2Ph + 2PPh_2H \xrightarrow[\text{toluene}]{\text{110 °C, 4 h}} \underset{\mathbf{4}\ (70\%)}{Co_2(\mu\text{-}PPh_2)_2(CO)_2(PEt_2Ph)_2} + 6CO + H_2 \quad (10)$$

trinuclear **3** is heated to 140 °C in a sealed Carius tube containing excess PEt_2Ph (eq 11).

$$\underset{\mathbf{3}}{2Co_3(\mu\text{-}PPh_2)_3(CO)_6} + 6PEt_2Ph \xrightarrow[\text{Carius tube}]{\text{140 °C, toluene}} 3\underset{\mathbf{4}}{Co_2(\mu\text{-}PPh_2)_2(CO)_2(PEt_2Ph)_2} + 6CO \quad (11)$$

This new complex has been characterized spectroscopically and by a complete single-crystal X-ray diffraction study, details of which are given in the following paper.[20] The latter showed it to have the binuclear structure sketched. The coordination geometry about Co is pseu-

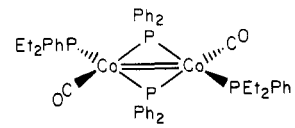

4

dotetrahedral (neglecting the metal–metal bond) with each Co ligated by two μ-PPh_2 ligands, one CO, and one PEt_2Ph. The $Co_2(\mu\text{-}P)_2$ core is planar, and the very short Co–Co bond length of 2.343 (2) Å implies a formal metal–metal double bond.[20] The $^{31}P\{^1H\}$ NMR spectrum of **4** shows two

(19) (a) Petersen, J. L.; Stewart, R. P., Jr. *Inorg. Chem.* **1980**, *19*, 186. (b) Carty, A. J.; MacLaughlin, S. A.; Taylor, N. J. *J. Organomet. Chem.* *1981*, *204*, C27. (c) Garrou, P. E. *Chem. Rev.* **1981**, *81*, 229. (d) Johannsen, G.; Stelzer, O. *Chem. Ber.* **1977**, *110*, 3438.

(20) Harley, A. D.; Whittle, R.; Geoffroy, G. L. *Organometallics*, submitted for publication.

broad singlets at δ 173.4 ($\nu_{1/2}$ = 42 Hz) and δ 48.5 ($\nu_{1/2}$ = 65 Hz) that integrate in a 1:1 intensity ratio and are respectively assigned to the equivalent bridging μ-PPh_2 ligands and to the equivalent terminal phosphines. The downfield position of the former is consistent with this ligand bridging a metal–metal bond.[19,20] Upon allowing the protons to couple to the phosphorus nuclei in the ^{31}P NMR spectrum, only the δ 48.5 resonance shows significant broadening, as expected because of coupling to the C_2H_5 protons. Although the $^{31}P\{^1H\}$ resonances of **4** are inherently broad, no discernible coupling was observed between the phosphorus nuclei, consistent with the pseudotetrahedral arrangement of these ligands about Co with relatively little s character in the metal–ligand bonding orbitals. The $^{31}P\{^1H\}$ NMR resonances sharpen upon cooling to −80 °C and shift slightly in position to δ 176.5 ($\nu_{1/2}$ = 34 Hz) and 53.3 ($\nu_{1/2}$ = 22 Hz), respectively. The broadening is apparently due to quadrapolar coupling to the ^{59}Co nuclei rather than to some fluxional process. A parent ion at m/e 876 and fragment ions corresponding to stepwise loss of the two CO's are apparent in the EI mass spectrum of **4**.

Although not as completely characterized as **4**, spectroscopic data imply that a complex analogous to **4** forms with P(*n*-Bu)$_3$. When the oligomeric complex **1** is heated with excess P(*n*-Bu)$_3$, a brownish orange solid is isolated which shows a parent ion at m/e 916 and fragment ions corresponding to loss of two CO's in its EI mass spectrum. This corresponds to the formula $Co_2(\mu\text{-}PPh_2)_2(CO)_2[P(n\text{-}Bu)_3]_2$, analogous to **4**. The IR spectrum of this material shows a strong ν_{CO} band at 1900 cm^{-1} (cf. **4**, ν_{CO} = 1905 cm^{-1}) with a weak shoulder at 1912 cm^{-1}. Whether or not a PR_3 derivative of structure **4** can form is apparently dependent upon the size of the PR_3 ligand since when **1** is heated with excess PPh_3, only trinuclear **3** is produced.

Although the binuclear complex **4** appears thermally stable when heated to 110 °C under N_2, it rapidly reacts with CO at 25 °C and 1 atm of pressure to displace PEt_2Ph and quantitatively yield the trinuclear cluster **3** (eq 12).

$$\underset{\mathbf{4}}{3Co_2(\mu\text{-}PPh_2)_2(CO)_2(PEt_2Ph)_2} + CO \xrightarrow[\text{1 atm}]{\text{25 °C, toluene}} \underset{\mathbf{3}}{2Co_3(\mu\text{-}PPh_2)_3(CO)_6} + 6PEt_2Ph \quad (12)$$

In contrast to the reactivity with CO, **4** is apparently inert toward H_2. No net reaction was observed when **4** was heated in the presence of H_2 (110 °C, 1000 psi, 24 h), and **4** was recovered unchanged.

Reaction of $Co_3(\mu\text{-}PPh_2)_3(CO)_6$, 3, with PEt_2Ph. As noted above when **3** is heated with excess PEt_2Ph at 140 °C in a Carius tube, the binuclear complex **4** is produced. However, when less severe conditions are used, substituted derivatives of **3** form. When **3** is heated at 80 °C in the presence of a 2.4 molar excess of PEt_2Ph, the monosubstituted derivative $Co_3(\mu\text{-}PPh_2)_3(CO)_5(PEt_2Ph)$, **5**, is produced in 64% isolated yield (eq 13). This species has been

$$\underset{\mathbf{3}}{Co_3(\mu\text{-}PPh_2)_3(CO)_6} + PEt_2Ph \xrightarrow[\text{Carius tube}]{\text{80 °C, 2 h, } CH_2Cl_2} \underset{\mathbf{5}\ (64\%)}{Co_3(\mu\text{-}PPh_2)_3(CO)_5(PEt_2Ph)} + CO \quad (13)$$

characterized spectroscopically and by a satisfactory C, H analysis. Its field desorption mass spectrum shows a parent ion at the expected m/e 1038. Only terminal ν_{CO} bands are seen in its IR spectrum (see Experimental Section), and three broad resonances ($\nu_{1/2} \simeq$ 130 Hz) are observed in its 25 °C $^{31}P\{^1H\}$ NMR spectrum at δ 274.5 (s), 198.8 (s), and 31.1 (s) in a 1:2:1 relative intensity ratio. The downfield resonances are attributed to one nonequivalent and two equivalent μ-PPh_2 ligands, and the δ 31.1 singlet is assigned to the terminal PEt_2Ph ligand. The structure sketched is implied. Coupling between the terminal

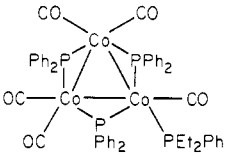

5

PEt_2Ph resonance and the two equivalent μ-PPh_2 bridging ligands was not resolved, although all the resonances are extremely broad, presumably because of coupling to the quadrapolar ^{59}Co nuclei.

When the reaction of **3** with PEt_2Ph was monitored by $^{31}P\{^1H\}$ NMR spectroscopy, in addition to the resonances due to **5**, less intense broad singlets were observed at δ 248.3, ($\nu_{1/2} \simeq$ 134 Hz), 177.6 ($\nu_{1/2} \simeq$ 134 Hz), and 51.8 ($\nu_{1/2} \simeq$ 64 Hz) which integrate in an approximate 2:1:2 ratio. The complex which gives these resonances has not been isolated, but the $^{31}P\{^1H\}$ NMR pattern is consistent with formation of a small amount of the disubstituted cluster $Co_3(\mu\text{-}PPh_2)_3(CO)_4(PEt_2Ph)_2$, **6**. The downfield $^{31}P\{^1H\}$ NMR resonances are assigned to two equivalent and one inequivalent μ-PPh_2 ligand, and the δ 51.8 resonance is assigned to two equivalent PEt_2Ph ligands. A reasonable structure is that sketched.

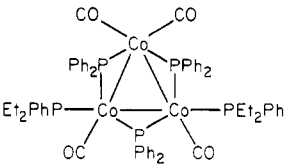

6

When the reaction of $Co_2(\mu\text{-}PPh_2)_2(CO)_2(PEt_2Ph)_2$, **4**, with CO (eq 12) is monitored by $^{31}P\{^1H\}$ NMR spectroscopy, resonances due to **5** and **6** grow in and then decrease in intensity as the resonance due to **3** appears. In an independent experiment it was observed that a solution containing **5** and **6** quantitatively reacts with CO to form **3** and release free PEt_2Ph (eq 14). Thus, both complexes **5** and **6** are likely intermediates in the **4** → **3** conversion (eq 12).

$$\underset{\mathbf{5}}{Co_3(\mu\text{-}PPh_2)_3(CO)_5(PEt_2Ph)} + \underset{\mathbf{6}}{Co_3(\mu\text{-}PPh_2)_3(CO)_4(PEt_2Ph)_2} + CO \xrightarrow[\text{1 atm}]{\text{25 °C, 15 min, } CH_2Cl_2} \underset{\mathbf{3}}{Co_3(\mu\text{-}PPh_2)_3(CO)_6} + PEt_2Ph \quad (14)$$

Hydroformylation Catalysis. Complex **1** has been found to function as a hydroformylation catalyst/catalyst precursor. A mixture of C_7 aldehydes is produced from 1-hexene and **2** under the hydroformylation conditions given in eq 15. Table I gives the relative rates of product

$$1\text{-hexene} + CO + H_2 \xrightarrow[\text{1250 psi, toluene}]{\text{catalyst, 110 °C}} C_7 \text{ aldehydes} \quad (15)$$

formation and isomer yield of **1** compared to $Co_2(CO)_8$, $Co_2(CO)_6(PMePh_2)_2$, and $Co_2(CO)_6(PHexPh_2)_2$, (Hex = *n*-C_6H_{13}). $Co_2(CO)_8$ is a far more efficient catalyst than the other three complexes, in accord with published data,[21]

(21) Slaugh, L. H.; Mullineaux, R. D. *J. Organomet. Chem.* **1968**, *13*, 469.

Table I. Relative Rates and Isomer Yields upon Hydroformylation of 1-Hexene[a]

catalyst precursor	relative rate	linear/branched C-aldehyde ratio[b]
$Co_2(CO)_6(PMePh_2)_2$	1.0	3.50
$Co_2(CO)_6(PHexPh_2)_2$	1.3	2.78
$[Co(\mu\text{-}PPh_2)(CO)_3]_x$	2.0	3.33
$Co_2(CO)_8$	130	2.05

[a] [1-hexene] = 4 M; catalyst concentration = 0.004 M in Co; 1250 psi of 1:1 CO/H_2 at 110 °C; toluene solvent. [b] 1-Heptanal/a mixture of 2-methylhexanal and 3-ethylpentanal.

but its linear/branched product ratio is of course inferior to the phosphine-substituted derivatives. The high linear/branched ratio of 3.33 found by using **1** as catalyst precursor compared to the 2.05 value of $Co_2(CO)_8$ strongly argues against catalysis through decomposition of **1** to produce a small amount of highly active $Co_2(CO)_8$. If this did occur, the product ratio would reflect $Co_2(CO)_8$ catalysis, i.e., 2.05. Furthermore, IR spectra of reaction solutions following 12-h catalysis with **1** as a catalyst precursor show no evidence for $HCo(CO)_4$ or $Co_2(CO)_8$ formation. Likewise, there is no visible metal deposition.

However, $^{31}P\{^1H\}$ NMR spectra of reaction solutions following 12-h catalysis using **1** as catalyst precursor show only a single resonance at δ 59.6 which is not due to **1** but which may be assigned to $Co_2(CO)_6(PHexPh_2)_2$, by comparison to an authentic sample.[16a] Reactions run for shorter time periods show two ^{31}P NMR singlets at δ 61.7 and 59.6 due to **1** and $Co_2(CO)_6(PHexPh_2)_2$, respectively. Thus, **1** is transformed irreversibly into $Co_2(CO)_6(PHexPh_2)_2$ during the course of the catalysis reaction (eq 16). The experimental data do not allow an unambiguous

$$[Co(\mu\text{-}PPh_2)(CO)_3]_x + \text{1-hexene} + H_2 \rightarrow (x/2)Co_2(CO)_6(PHexPh_2)_2 \quad (16)$$

distinction as to the extent of hydroformylation catalysis by **1** and $Co_2(CO)_6(PHexPh_2)_2$ in these solutions. However, the different product ratio obtained by using **1** as a catalyst precursor compared to the use of $Co_2(CO)_6(PHexPh_2)_2$ alone implies that **1** or some other derivative of **1** must have hydroformylation activity. It was also observed that binuclear $Co_2(\mu\text{-}PPh_2)_2(CO)_6$ reacts with 1-hexene under hydroformylation conditions to also give $Co_2(CO)_6(PHexPh_2)_2$.

A similar bridge elimination reaction was observed when **1** was heated under a 1:1 H_2/CO atmosphere (110 °C, 1000 psi) in toluene solution containing 10% ethanol. The product formed was $Co_2(CO)_6(P(OEt)Ph_2)_2$, as determined by comparison of its spectra data to that of an authentic sample[16b] (eq 17). No reaction of **1** with EtOH occurs at 25 °C under 1 atm of H_2/CO.

$$\underset{\mathbf{1}}{[Co(\mu\text{-}PPh_2)(CO)_3]_x} + 2EtOH \xrightarrow[1000\text{ psi, }CO/H_2]{110\text{ °C, 8 h}} (x/2)Co_2(CO)_6\{P(OEt)Ph_2\}_2 \quad (17)$$

Discussion

We were led into the chemistry described herein during our attempts to use "$Co(CO)_4PPh_2$" as a reagent for the synthesis of phosphido-bridged mixed-metal compounds containing Co. While this species can apparently be generated at low temperature by the reaction of $[Co(CO)_4]^-$ with PPh_2Cl,[5] it is not stable above −20 °C. Upon warmup it loses CO and gives rise to a series of phosphido-bridged Co carbonyl complexes. A perusal of the literature demonstrates that the complexity of this chemical system is not generally appreciated, as it was not to us at the onset of this study. In particular, a number of reports have described studies of the compound prepared according to Hayter's recipe[8] and in which Hayter's binuclear $Co_2(\mu\text{-}PPh_2)_2(CO)_6$ formulation was accepted as correct.[10,22] Our data and that of others,[11,12] including Hayter's own molecular weight measurements,[8] clearly show that the compound obtained from Hayter's synthetic procedure is not binuclear but rather must have an oligomeric structure such as that drawn in Scheme I.

One of the most significant achievements of the present study was our discovery of methods for obtaining authentic binuclear $Co_2(\mu\text{-}PPh_2)_2(CO)_6$, **2**, and its complete characterization via the X-ray diffraction study described in a separate paper.[18] As described above, this species can be prepared in essentially quantitative yield by heating either oligomeric **1** or trinuclear **3** under CO pressure. It is a well-behaved compound which can be easily purified by chromatography on silica gel and is only moderately air sensitive, although it is extremely light sensitive.

As illustrated by the spectra presented in Figure 1, compounds **1**–**3** are not easily distinguished by infrared spectroscopy and this may have led to some of the confusion which has existed. They all show broad absorption in the 1970–2010-cm^{-1} region and a sharp peak in the 2020–2060-cm^{-1} region. Furthermore, both oligomeric complex **1** and binuclear complex **2** have similar melting points, melting with decomposition in the 148–151 °C range, and they both give orange solutions. However, trinuclear complex **3** gives green solutions and is thus easily distinguished from **1** and **2**. The best method for distinguishing **1** from **2** is via $^{31}P\{^1H\}$ NMR spectroscopy since the resonance for **1** (δ 61.7 (s)) is far downfield from that of **2** (δ −114 (s)).

We were also surprised to find that these phosphido-bridged cobalt carbonyl complexes can be induced to interconvert under relatively mild conditions. The various transformations observed are summarized in Scheme I. The oligomeric complex **1** can be readily converted into binuclear **2** and trinuclear **3** by heating in the absence or presence of CO, respectively, and reaction of **1** with PEt_2Ph yields the binuclear complex **4**. However, we have not found any reaction conditions in which **1** can be reformed from either **2**, **3**, or **4**. These results suggest that **2** is the more thermodynamically stable form of $[Co(\mu\text{-}PPh_2)(CO)_3]_x$ but that **1** is the kinetically preferred product in the initial synthesis. In contrast, complexes **2** and **3** undergo essentially quantitative interconversion (eq 18).

$$\underset{\mathbf{3}}{2Co_3(\mu\text{-}PPh_2)_3(CO)_6} + 6CO \underset{h\nu,\ N_2}{\overset{\Delta,\ 1000\text{ psi}}{\rightleftharpoons}} \underset{\mathbf{2}}{3Co_2(\mu\text{-}PPh_2)_3(CO)_6} \quad (18)$$

Although binuclear complex **2** is thermally stable at least up to 110 °C, 366-nm photolysis induces loss of CO and formation of **3**. Even room light will slowly induce this conversion to occur, and the compound must be protected from light if it is to be preserved. When **3** is heated to 110 °C under CO pressure, **2** is quantitatively produced. Indeed, in the presence of CO complex **2** is the most stable of all the complexes examined.

Both the oligomeric complex **1** and the trinuclear complex **3** react with PEt_2Ph to form **4** although much more stringent conditions are required with **3**. Under less vig-

(22) (a) Bamford, C. H.; Maltman, W. R. *Trans. Faraday Soc.* **1966**, *62*, 2823. (b) Abel, E. W.; Hutson, G. V. *J. Inorg. Nucl. Chem.* **1968**, *30*, 2339. (c) See also ref 7d.

Scheme II

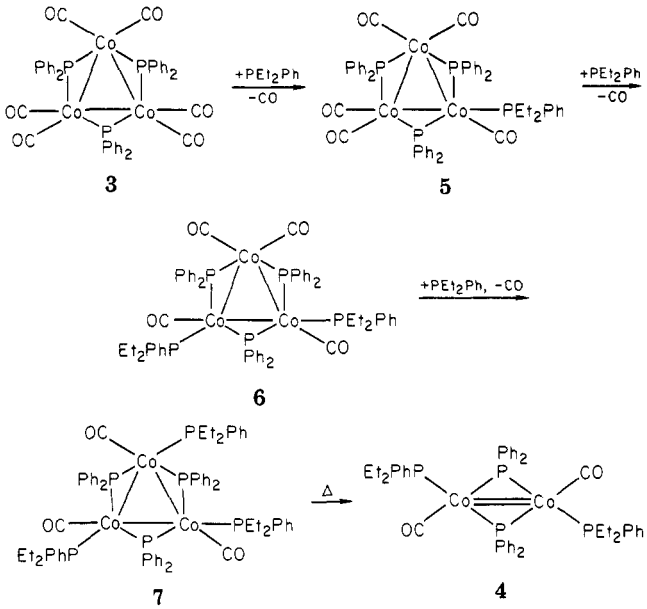

orous conditions trinuclear complex **3** reacts with PEt_2Ph to form first a monosubstituted derivative, **5**, and tentative evidence was obtained for the formation of a disubstituted product, **6**. It would seem likely that these are intermediates in the **3** → **4** conversion, Scheme II, with severe steric crowding in the substituted clusters forcing fragmentation to produce binuclear **4**. A trisubstituted cluster such as **7** should be quite crowded since it has nine phenyl rings and six ethyl groups packed around a relatively small Co_3 core. Likewise, the disubstituted cluster **6** posssesses eight phenyl and four ethyl substituents. Note that **7** and **4** have the same empirical formula $[Co(\mu\text{-}PPh_2)(CO)(PEt_2Ph)]_x$. Surprisingly, binuclear complex **4** was found to easily and quantitatively reform trinuclear complex **3** simply upon exposure to 1 atm of CO at 25 °C, Scheme I, but we have no evidence to bear on the mechanism of this transformation. However **4** is coordinatively unsaturated and would be expected to add nucleophiles such as CO, and the **4** → **3** transformation may proceed through such CO adducts.

The most significant conclusion to be drawn from the interconversions of these phosphido-bridged cobalt carbonyl derivatives discussed herein is that the bridging phosphido ligands are *not* sufficient to retard fragmentation and rearrangement reactions of these complexes. While there are reported examples of *chemical* transformations of phosphido ligands,[3a,b] to our knowledge there has been no other clear demonstration of the interconvertability of phosphido-bridged complexes in which the complex nuclearity changes as it does with this chemical system. There are, however, indications in the literature that such reactions may also occur for other metal derivatives,[23-25] as exemplified by the rearrangements which must occur during the syntheses of $[Rh_4(\mu\text{-}PPh_2)_5(CO)_5]^-$[24] and $Rh_3(\mu\text{-}PPh_2)_3(CO)_5$[23d] from the reactions of $Rh_2(\mu\text{-}Cl)_2(CO)_4$ with $LiPPh_2$ and PPh_2H/Et_2NH, respectively. We have no direct experimental evidence to bear on the *mechanism* of these rearrangement reactions, but it is clear that some Co–phosphido bonds must be broken in the course of the observed transformations, implying the formation of intermediates with pendant PPh_2 ligands (eq 19).

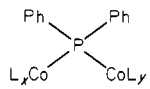

$$\longrightarrow L_xCo\text{-}PPh_2 + CoL_y \qquad (19)$$

The irreversible transformation of the $\mu\text{-}PPh_2$ ligands of **4** and **2** into $PHexPh_2$ under 1-hexene hydroformylation catalysis conditions illustrates the care that must be exercised when interpreting the results of catalytic experiments employing phosphido-bridged complexes. These results further illustrate the fact that phosphido-bridged complexes may find only limited usefulness in catalysis because of such irreversible transformations which destroy the polynuclear character of the complex.[26]

Acknowledgment. This research was supported by the National Science Foundation (Grant CHE-8201160) and in part by grants from the Standard Oil Co. (Ohio) and Air Products and Chemicals, Inc. G.L.G. gratefully acknowledges the Camille and Henry Dreyfus Foundation for a Teacher-Scholar Award (1978-1983), The John Simon Guggenheim Foundation for a fellowship (1982), and Drs. Thomas Criswell and Henry Gysling at the Eastman Kodak research laboratories for assistance in obtaining field desorption mass spectra.

Registry No. 1, 83562-08-7; **2**, 15553-97-6; **3**, 83562-09-8; **4**, 83462-95-7; **5**, 83562-10-1; **6**, 83572-96-7; $Na[Co(CO)_4]$, 14878-28-5; PPh_2Cl, 1079-66-9; $Co_2(CO)_8$, 10210-68-1; PPh_2H, 829-85-6; 1-hexene, 592-41-6.

(23) (a) Haines, R. J.; Steen, N. D. C. T.; English, R. B. *J. Chem. Soc., Chem. Commun.* **1981**, 587. (b) Haines, R. J.; Steen, N. D. C. T.; Laing, M.; Sommerville, P. *J. Organomet. Chem.* **1980**, *198*, C72. (c) Haines, R. J.; Steen, N. D. C. T.; English, R. B. *J. Chem. Soc., Chem. Commun.* **1981**, 407. (d) Haines, R. J.; Steen, N. D. C. T.; English, R. B. *J. Organomet. Chem.* **1981**, *209*, C34.

(24) Kreter, P. E.; Meek, D. W.; Christoph, G. G. *J. Organomet. Chem.* **1980**, *188*, C27.

(25) Jamerson, J. C.; Pruett, R. L.; Billig, E.; Fiato, F. A. *J. Organomet. Chem.* **1980**, *193*, C43.

(26) A similar conclusion has been drawn by Carty and co-workers: Maclaughlin, S. A.; Carty, A. J.; Taylor, N. J. *Can. J. Chem.* **1982**, *60*, 87.

Crystal and Molecular Structure of Binuclear $Co_2(\mu\text{-}PPh_2)_2(CO)_2(PEt_2Ph)_2$, a Phosphido-Bridged Compound with a Formal Cobalt–Cobalt Double Bond

A. Dale Harley, Robert R. Whittle, and Gregory L. Geoffroy*

Department of Chemistry, The Pennsylvania State University, University Park, Pennsylvania 16802

Received September 9, 1982

The new phosphido-bridged cobalt carbonyl complex $Co_2(\mu\text{-}PPh_2)_2(CO)_2(PEt_2Ph)_2$, **1**, has been characterized by a complete single-crystal X-ray diffraction study. It crystallizes in the space group $P\bar{1}$ with a = 11.565 (3) Å, b = 12.356 (5) Å, c = 8.993 (5) Å, α = 108.30 (3)°, β = 108.50 (3)°, γ = 64.79 (3)°, V = 1078 (1) Å^3, and Z = 1. The structure was refined by using the 2927 reflections with $I \geq 2\sigma(I)$ to give final residuals of R = 0.051 and R_w = 0.078. Each Co in **1** is coordinated by one CO, one PEt_2Ph, two bridging μ-PPh_2 ligands, and the other Co. The three phosphorus ligands and the carbonyl are in a psuedotetrahedral arrangement about each cobalt. The $Co_2(\mu\text{-}P)_2$ core is rigorously planar as imposed by a crystallographic inversion center in the middle of the dimer. The Co–Co bond length of 2.343 (2) Å implies a formal metal–metal double bond as required by the effective atomic number rule. The structure is discussed in its relationship to other known and hypothetical compounds of similar structure.

Although numerous compounds with single, triple, and quadruple metal–metal bonds have been prepared and characterized, compounds with metal–metal double bonds are still relatively rare.[1] This is unfortunate since such compounds have proven extremely useful for the directed synthesis of polynuclear organometallic clusters via addition of mononuclear metal fragments across the metal–metal double bonds,[2,3] e.g., eq 1[3b] and 2.[3e] Such coordinatively unsaturated binuclear and polynuclear compounds also react with olefins, alkynes, and other organic substrates to give interesting organometallic derivatives.[4]

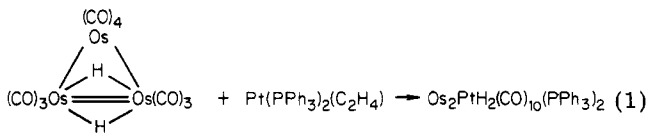

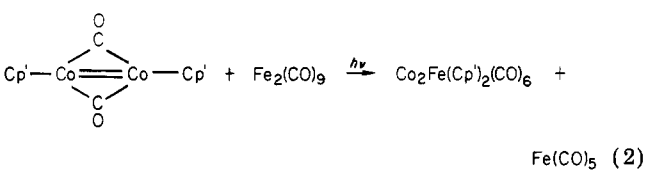

During the course of our investigations into the chemistry of a series of phosphido-bridged cobalt carbonyl complexes,[5] we isolated and spectroscopically characterized the new complex $Co_2(\mu\text{-}PPh_2)_2(CO_2)(PEt_2Ph)_2$, **1**, by the reaction of either $Co_2(\mu\text{-}PPh_2)_2(CO)_6$, $Co_3(\mu\text{-}PPh_2)_3(CO)_6$, or $[Co(\mu\text{-}PPh_2)(CO)_3]_x$ with PEt_2Ph. The complex is most conveniently prepared in high yield via the direct reaction shown in eq 3.[5] This new complex is particularly interesting since it should possess a formal cobalt–cobalt double bond in order to satisfy the effective atomic number rule. A single-crystal X-ray diffraction study was thus undertaken in order to fully characterize this new species, and those results are described herein.

$$Co_2(CO)_8 + 2PEt_2Ph + 2PPh_2H \xrightarrow[\text{toluene}]{110\ ^\circ\text{C},\ 4\ \text{h}} Co_2(\mu\text{-}PPh_2)_2(CO)_2(PEt_2Ph)_2 + 6CO + H_2 \quad (3)$$
$$\mathbf{1}\ (70\%)$$

Table I. Crystal and Intensity Data for the X-ray Diffraction Study of $Co_2(\mu\text{-}PPh_2)_2(CO)_2(PEt_2Ph)_2$, **1**

Crystal Parameters	
cryst system: triclinic	V = 1078.3 (1) Å^3
space group $P\bar{1}$	Z = 1
a = 11.565 (5) Å	ρ(calcd) = 1.350 g cm^3
b = 12.356 (5) Å	abs coeff 9.850, not corrected
c = 8.993 (3) Å	T = 25 °C
α = 108.30 (3)°	
β = 108.50 (3)°	
γ = 64.79 (3)°	

Measurement of Intensity Data	
diffractometer:	Enraf-Nonius CAD4
radiation:	Mo Kα (λ 0.710 73 Å)
monochromator:	graphite crystal
scan type:	θ–2θ
scan speed:	variable[a]
takeoff angle:	28°
std reflctns:	3 std reflctns measd every 3 h; no significant variation
data limits:	$3° \leq 2\theta \leq 60°$
reflctns measd:	$+h,\pm k,\pm l$
unique data:	6428
nonzero data:	2927 ($I \geq 2\sigma(I)$)
R = 0.051; R_w = 0.077	

[a] See ref 7.

Experimental Section

X-ray Structure Determination of $Co_2(\mu\text{-}PPh_2)_2(CO)_2(PEt_2Ph)_2$, 1. Black crystals of **1**, prepared as described in ref 4 (eq 3), were grown by slow evaporation of solvent from a saturated CH_2Cl_2 solution of the complex under N_2. An irregularly shaped crystal of approximately 0.25 mm per side was sealed in a glass capillary under N_2, fixed into an aluminum pin, and

(1) (a) Cotton, F. A.; Walton, R. A. "Multiple Bonds Between Metal Atoms"; Wiley: New York, 1982. (b) Chisholm, M. H., Ed. "Reactivity of Metal–Metal Bonds", American Chemical Society: Washington, D.C., 1981; *ACS Symp. Ser. No. 155.*

(2) Roberts, D. A.; Geoffroy, G. L. In "Comprehensive Organometallic Chemistry"; Wilkinson, G., Stone, F. G. A., Abel, E. W., Eds., Pergamon Press: Oxford, 1982; Chapter 40.

(3) (a) Curtis, M. D.; Klingler, R. J. *J. Organomet. Chem.* **1978**, *161*, 23. (b) Farrugia, L. J.; Howard, J. A. K.; Mitrprachachon, P.; Spencer, J. L.; Stone, F. G. A.; Woodword, P. *J. Chem. Soc., Chem. Commun.* **1978**, 260. (c) Burkhardt, E.; Geoffroy, G. L. *J. Organomet. Chem.* **1980**, *198*, 179. (d) Byers, L. R.; Uchtman, V. A.; Dahl, L. F. *J. Am. Chem. Soc.* **1981**, *103*, 1942. (e) Cirjak, L. M.; Huang, J.-S.; Zhu, Z.-H.; Dahl, L. F. *Ibid.* **1980**, *102*, 6623.

(4) (a) Tachikawa, M.; Shapley, J. R.; Pierpont, C. G. *J. Am. Chem. Soc.* **1975**, *97*, 7172. (b) Deeming, A. J.; Hasso, S.; Underhill, M. *J. Chem. Soc., Dalton Trans.* **1975**, 1614. (c) Dawoodi, Z.; Henrick, K.; Mays, M. J. *J. Chem. Soc., Chem. Commun.* **1982**, 696.

(5) Harley, A. D.; Guskey, G. J.; Geoffroy, G. L. *Organometallics*, submitted for publication.

0276-7333/83/2302-0060$01.50/0

Table II. Atomic Positional and Thermal Parameters for $Co_2(\mu\text{-}PPh_2)_2(CO)_2(PEt_2Ph)_2$, 1[a]

atom	x	y	z	U(1,1)	U(2,2)	U(3,3)	U(1,2)	U(1,3)	U(2,3)
Co	0.06861 (9)	0.03205 (7)	0.6172 (1)	0.0476 (4)	0.0287 (3)	0.0347 (4)	−0.0162 (3)	0.0058 (3)	0.0067 (3)
P1	0.1170 (2)	−0.1576 (1)	0.4886 (2)	0.0482 (8)	0.0303 (6)	0.0416 (8)	−0.0154 (5)	0.0086 (7)	0.0073 (6)
P2	0.2228 (3)	0.1010 (2)	0.6512 (2)	0.0494 (9)	0.0339 (7)	0.0441 (9)	−0.0179 (6)	0.0066 (7)	0.0053 (6)
O1	0.1031 (7)	0.0400 (6)	0.9514 (7)	0.171 (5)	0.104 (3)	0.041 (3)	−0.078 (3)	0.016 (3)	0.012 (2)
C1	0.0903 (8)	0.0383 (6)	0.8189 (9)	0.082 (4)	0.049 (3)	0.048 (4)	−0.033 (3)	0.004 (3)	0.011 (3)
C2	0.1308 (7)	−0.2800 (5)	0.5753 (9)	0.049 (3)	0.033 (2)	0.056 (4)	−0.014 (2)	0.009 (3)	0.015 (2)
C3	0.1367 (7)	−0.3928 (6)	0.4750 (10)	0.061 (4)	0.037 (3)	0.069 (4)	−0.017 (2)	0.022 (3)	0.008 (3)
C4	0.1466 (8)	−0.4871 (6)	0.5344 (11)	0.067 (4)	0.035 (3)	0.095 (5)	−0.022 (2)	0.020 (4)	0.015 (3)
C5	0.1500 (8)	−0.4709 (6)	0.6925 (11)	0.077 (5)	0.053 (3)	0.092 (5)	−0.030 (3)	0.002 (4)	0.038 (3)
C6	0.1428 (10)	−0.3614 (7)	0.7903 (10)	0.117 (6)	0.081 (4)	0.060 (4)	−0.054 (3)	0.004 (4)	0.032 (3)
C7	0.1334 (9)	−0.2651 (7)	0.7332 (10)	0.095 (5)	0.054 (3)	0.052 (4)	−0.039 (3)	0.003 (4)	0.018 (3)
C8	0.2557 (7)	−0.2405 (6)	0.3914 (9)	0.053 (3)	0.031 (2)	0.054 (4)	−0.021 (2)	0.013 (3)	0.002 (2)
C9	0.2518 (9)	−0.2234 (8)	0.2445 (10)	0.054 (4)	0.067 (4)	0.063 (4)	−0.020 (3)	0.013 (3)	0.015 (3)
C10	0.3592 (9)	−0.2840 (9)	0.1738 (11)	0.071 (4)	0.109 (6)	0.075 (5)	−0.032 (4)	0.036 (3)	0.018 (4)
C11	0.4718 (8)	−0.3629 (9)	0.2465 (12)	0.060 (4)	0.073 (5)	0.104 (6)	−0.018 (3)	0.042 (4)	0.009 (4)
C12	0.4792 (8)	−0.3793 (7)	0.3924 (12)	0.050 (4)	0.048 (4)	0.114 (6)	−0.005 (3)	0.028 (4)	0.025 (4)
C13	0.3728 (7)	−0.3204 (6)	0.4625 (10)	0.054 (4)	0.045 (3)	0.079 (4)	−0.014 (3)	0.019 (3)	0.022 (3)
C14	0.2426 (7)	0.2189 (5)	0.8328 (8)	0.057 (3)	0.032 (2)	0.046 (3)	−0.018 (2)	0.008 (3)	0.009 (2)
C15	0.3560 (8)	0.2438 (7)	0.8900 (10)	0.065 (4)	0.053 (3)	0.056 (4)	−0.029 (3)	0.013 (3)	0.007 (3)
C16	0.3679 (8)	0.3361 (7)	1.0229 (10)	0.084 (4)	0.066 (4)	0.057 (5)	−0.049 (3)	0.010 (4)	0.000 (3)
C17	0.2692 (9)	0.4011 (8)	1.1010 (11)	0.104 (6)	0.065 (4)	0.054 (5)	−0.048 (3)	0.017 (4)	−0.009 (4)
C18	0.1560 (9)	0.3772 (8)	1.0455 (12)	0.089 (5)	0.060 (4)	0.074 (5)	−0.031 (4)	0.033 (4)	−0.009 (4)
C19	0.1414 (8)	0.2872 (7)	0.9117 (10)	0.062 (4)	0.049 (3)	0.063 (4)	−0.025 (3)	0.014 (3)	0.004 (3)
C20	0.2122 (8)	0.1777 (7)	0.4996 (9)	0.064 (4)	0.061 (3)	0.057 (4)	−0.026 (3)	0.017 (3)	0.017 (3)
C21	0.2142 (10)	0.1025 (9)	0.3352 (12)	0.111 (6)	0.102 (6)	0.067 (5)	−0.053 (4)	0.019 (5)	0.015 (4)
C22	0.3863 (8)	−0.0155 (7)	0.6577 (12)	0.047 (4)	0.038 (3)	0.095 (6)	−0.014 (3)	0.008 (4)	−0.000 (4)
C23	0.4314 (11)	−0.0847 (9)	0.7893 (14)	0.093 (7)	0.059 (5)	0.100 (7)	−0.018 (5)	−0.028 (6)	0.024 (5)

[a] The form of the anisotropic thermal parameter is $\exp[-2\pi^2(U_{11}h^2a^{*2} + U_{22}k^2b^{*2} + U_{33}l^2c^{*2} + 2U_{12}hka^*b^* + 2U_{13}hla^*c^* + 2U_{23}klb^*c^*)]$.

Table III. Selected Bond Distances (Å) in $Co_2(\mu\text{-}PPh_2)_2(CO)_2(PEt_2Ph)_2$, 1

Co-Co′	2.343 (2)	Co-P2	2.187 (2)
Co-P1	2.176 (2)	Co-C1	1.731 (7)
Co-P1′	2.172 (2)	C1-O1	1.148 (8)

Table IV. Selected Bond Angles (Deg) in $Co_2(\mu\text{-}PPh_2)_2(CO)_2(PEt_2Ph)_2$, 1

P1-Co-P1′	114.77 (5)	Co-P1-Co′	65.23 (5)
P1-Co-P2	112.14 (7)		
P1-Co-P2′	108.99 (6)	C2-P1-C8	98.5 (3)
P1-Co-C1	109.2 (2)	Co-P1-C2	122.6 (2)
P1′-Co-C1	115.2 (3)	Co′-P1-C2	123.4 (2)
P2-Co-C1	95.0 (2)	Co′-P1-C8	123.7 (2)
P1-Co-Co′	57.30 (5)	Co-P1-C8	123.6 (2)
P1′-Co-Co′	57.48 (5)		
P2-Co-Co′	130.66 (7)	Co-C1-O1	178.1 (7)
C1-Co-Co′	134.4 (2)		

mounted onto an eucentric goniometer. Diffraction data were collected on an Enraf-Nonius four-circle CAD4 automated diffractometer controlled by a PDP8a computer coupled to a PDP11/34 computer. The Enraf-Nonius program SEARCH was used to obtain 25 accurately centered reflections which were then used in the program INDEX to obtain an orientation matrix for data collection and to provide cell dimensions.[6] Pertinent crystal and intensity data are listed in Table I. Details of the data collection and reduction procedures have been previously described.[7]

Of the two possible triclinic space groups $P1$ and $P\bar{1}$, the latter was indicated for $Z = 1$ and subsequently verified as correct by the successful solution of the structure. The coordinates of the Co and P atoms and several of the phenyl carbon atoms were located by the use of the direct methods program MULTAN.[8] The heavy-atom positions were subsequently verified in a three-dimensional Patterson map. The coordinates of the remaining 17 non-hydrogen atoms were located by successive least-squares refinements and difference Fourier maps. After three cycles of least squares with anisotropic temperature factors, the phenyl and methylene hydrogen atoms were fixed at their calculated positions with C–H = 0.97 Å and given fixed isotropic temperature factors (B) of 5.0 Å^2. Refinement was continued for two additional least-squares cycles, and a difference Fourier map at this point located the methyl hydrogens H21A and H23A. The positions of the remaining four methyl hydrogens were calculated from these positions, and all six methyl hydrogens were then fixed with C–H = 0.97 Å and an isotropic temperature factor of 5.0 Å^2. In the final least-squares refinement, 244 parameters were varied including the overall scale factor and positional and anisotropic thermal parameters for all non-hydrogen atoms. Convergence was achieved with $R = 0.051$ and $R_w = 0.078$. The residuals are defined as $R = \sum(||F_o| - |F_c||)/\sum|F_o|$ and $R_w = [\sum w(|F_o| - |F_c|)^2/\sum w|F_o|^2]^{1/2}$. In the last cycle of refinement the maximum shift per error was 0.346, and the average shift per error was 0.024. A final difference Fourier map showed the largest peak to be less than 0.11 times the height of a carbon atom. The final error of an observation of unit weight was 1.71. Atomic positional and anisotropic temperature parameters are listed in Table II. Selected bond lengths and angles are given in Tables III and IV, respectively. The derived positions of the hydrogen atoms (Table A) and the structure factors (Table B) are given in the supplementary material.

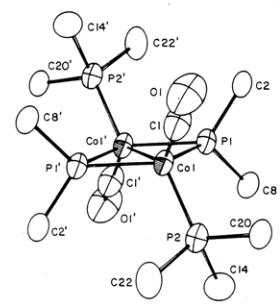

Figure 1. An ORTEP drawing of $Co_2(\mu\text{-}PPh_2)_2(CO)_2(PEt_2Ph)_2$, 1, showing the atom numbering scheme. Thermal ellipsoids are drawn at the 25% probability level.

(6) Programs used in this study are either part of the Enraf-Nonius Structure Determination Package (SDP), Enraf-Nonius, Delft, Holland, 1975, or a local version of X-Ray 67, Stewart, J. M., University of Maryland, Crystallographic Computer Systems.

(7) Steinhardt, P. C.; Gladfelter, W. L.; Harley, A. D.; Fox, J. R.; Geoffroy, G. L. *Inorg. Chem.* **1980**, *19*, 332.

(8) Main, P. "MULTAN 78, A System of Computer Programs for the Automatic Solutions of Crystal Structures", Department of Physics, University of York, York, England, 1978.

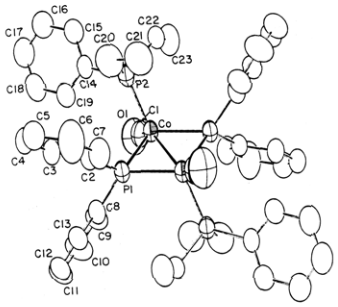

Figure 2. An ORTEP drawing of $Co_2(\mu\text{-}PPh_2)_2(CO)_2(PEt_2Ph)_2$, **1**, showing the core of the molecule. Thermal ellipsoids are drawn at the 25% probability level.

Results

An ORTEP drawing showing the molecular structure and atom numbering scheme for $Co_2(\mu\text{-}PPh_2)_2(CO)_2(PEt_2Ph)_2$, **1**, is shown in Figure 1. Figure 2 shows a different view with the phosphorus organic substituents removed for clarity. Relevant bond distances and angles are listed in Tables III and IV, respectively. With one molecule per unit cell in the space group $P\bar{1}$, the complex has a crystallographically imposed inversion center in the middle of the molecule. The $Co_2(\mu\text{-}P)_2$ core is thus rigorously planar and the virtual symmetry of the complex is C_{2h}. The two $\mu\text{-}PPh_2$ ligands, the Co, and the PEt_2Ph ligand are arranged in a pseudotetrahedral fashion about each cobalt. The P1–Co–P1′, P1–Co–P2, and P1–Co–C1 bond angles of 114.77 (5)°, 112.12 (7)°, and 109.2 (2)° closely approximate the ideal tetrahedral angle of 109.5°. Only the P2–Co–C1 angle of 95.0 (2)° differs significantly from this value. The latter angle is apparently suppressed because of steric crowding induced by the substituents on the phosphorus ligands. The angle between the P1–Co–P1′ and C1–Co–P2 planes is 86.6°, close to the 90° angle expected for pseudotetrahedral coordination.

The Co–Co bond length of 2.343 (2) Å is quite short and implies a formal double bond between the Co atoms, as required to achieve 18 valence electrons about each metal. This distance compares well with the Co–Co distance in two other molecules for which the effective atomic number rule requires a Co–Co double bond. $Co_2(\eta^5\text{-}C_5Me_5)_2(\mu\text{-}CO)_2$ has a Co–Co bond length of 2.338 (2) Å,[9] and in $[Co_2H_3(1,1,1\text{-tris((diphenylarsino)methyl)ethane})_2]BPh_4$, the Co–Co separation is 2.377 (8) Å.[10] Notably, these distances are less than the Co–Co separation of 2.506 Å in Co metal.[11]

The Co–P1–Co bond angle of 65.23 (5)° in $Co_2(\mu\text{-}PPh_2)_2(CO)_2(PEt_2Ph)_2$ is the most acute M–P–M angle found in any compound with a bridging $\mu\text{-}PR_2$ ligand. Likewise the metal–metal distance which this ligand bridges is the shortest observed in any known $\mu\text{-}PR_2$ structure.

Discussion

It is interesting to consider the structure of $Co_2(\mu\text{-}PPh_2)_2(CO)_2(PEt_2Ph)_2$, **1**, in its relationship to other metal–metal doubly bonded compounds. $Co_2(\mu\text{-}PPh_2)_2(CO)_2(PEt_2Ph)_2$ is isoelectronic with $Ir_2(\mu\text{-}PPh_2)_2(CO)_2(PPh_3)_2$, **2**, which has been prepared by the pyrolysis reaction shown in eq 4 and structured by two independent research groups.[12,13] The latter complex has a structure

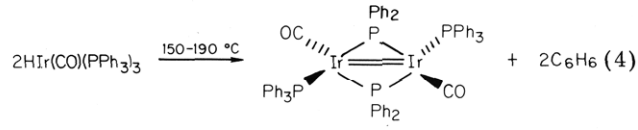

2

analogous to that of **1** with a short Ir–Ir separation (2.551 (1) Å,[12] 2.554 Å[13]) consistent with a metal–metal double bond and a pseudotetrahedral ligand arrangement about each iridium. The $Ir_2(\mu\text{-}P)_2$ core of the latter is also rigorously planar with an inversion center in the middle of the molecule. The isoelectronic complex $Ir_2(\mu\text{-}PPh_2)_2(COD)_2$[14] (COD = 1,5-cyclooctadiene) has not been structured, but its electron count would predict an Ir–Ir double bond. The far downfield ^{31}P NMR chemical shift of the bridging $\mu\text{-}PPh_2$ ligands at δ 166 imply a strong metal–metal interaction in the latter complex.[14,15]

A Rh analogue of **1** and **2** is not known, but there is no reason why it should not exist, providing the PR_3 ligands are sufficiently small. Such a compound does not form upon pyrolysis of $HRh(CO)(PPh_3)_3$, analogous to the preparation of **2** via reaction 4, presumably because of too severe steric crowding induced by the PPh_3 and $\mu\text{-}PPh_2$ ligands in such a complex.[16] We also find that a Co derivative analogous to **1** and **2** cannot be prepared by using PPh_3 instead of PEt_2Ph, for apparently similar steric reasons, although a $P(n\text{-}Bu)_3$ derivative does form.[5] The closest known Rh analogue to **1** and **2** is $Rh_2(\mu\text{-}PPh_2)_2(COD)(PEt_3)_2$, **3**, which was recently structured by Meek and co-workers.[17] Although **3** is isoelectronic with **1** and **2**, the 2.752 (2)-Å Rh–Rh separation does not imply a Rh–Rh double bond. Rather this molecule appears best described as having a donor–acceptor bond between Rh(1–) and Rh(1+) centers.[17]

The first characterized complex with a structure analogous to **1** and **2** is $Ru_2(\mu\text{-}PPh_2)_2(NO)_2(PPh_3)_2$, **3**, a com-

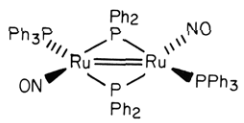

3

pound prepared and structured by Eisenberg and coworkers[18] in 1972. This complex also has a crystallographically imposed planar $Ru_2(\mu\text{-}P)_2$ core with a pseudotetrahedral ligand arrangement about each metal. The short Ru–Ru separation of 2.629 (2) Å is consistent with a Ru–Ru double bond, as required by the effective atomic number rule. Interestingly, a satisfactory synthesis of **3** has never been achieved, and the complex was only ob-

(9) Ginsberg, R. E.; Cirjak, L. M.; Dahl, L. F. *J. Chem. Soc., Chem. Commun.* **1979**, 468.
(10) Dapporto, P.; Midollini, S.; Sacconi, L. *Inorg. Chem.* **1975**, *14*, 1643.
(11) "International Tables for X-Ray Crystallography"; Kynoch Press: Birmingham, England, 1962; Vol. III, p 282.
(12) Belon, P. L.; Benedicenti, C.; Caglio, G.; Manassero, M. *J. Chem. Soc., Chem. Commun.* **1973**, 946.
(13) Mason, R.; Sotofte, I.; Robinson, S. D.; Uttley, M. R. *J. Organomet. Chem.* **1972**, *46*, C61.
(14) (a) Kreter, P. E.; Meek, D. W., submitted for publication. (b) Kreter, P. E. Ph.D. Thesis, The Ohio State University, Columbus, Ohio, 1980.
(15) (a) The $\mu\text{-}PR_2$ ligands in compounds with metal bonds generally show down-field (δ 50–300) ^{31}P NMR resonances, whereas upfield (δ 50 → δ −200) resonances are observed for compounds in which the $\mu\text{-}PR_2$ ligand bridges two metals not joined by a metal–metal bond.[4b-f] (b) Petersen, J. L.; Stewart, R. P., Jr. *Inorg. Chem.* **1980**, *19*, 186. (c) Carty, A. J.; MacLaughlin, S. A.; Taylor, N. J. *J. Organomet. Chem.* **1981**, *204*, C27. (d) Carty, A. J. *Adv. Chem. Ser.* **1982**, *196*, 163. (e) Garrou, P. *Chem. Rev.* **1981**, *81*, 299. (f) Johannsen, G.; Stelzer, O. *Chem. Ber.* **1977**, *110*, 3438. (g) Mott, G. N. Ph.D. Thesis, University of Waterloo, Waterloo, Ontario, Canada, 1981.
(16) Private communication from Jack Jamerson, Union Carbide Corp., South Charleston, WV.
(17) Meek, D. W.; Kreter, P. E.; Christoph, G. G. *J. Organomet. Chem.* **1982**, *231*, C53.

tained in exceedingly low yield.[18,19] Although they have not been reported, Fe and Os analogues to **3** should also exist.

The only other compound with a double metal–metal bond and with two μ-PR_2 bridging ligands which has structured is $V_2(\mu\text{-}PMe_2)_2(CO)_8$, **4**.[20] This complex results from the direct reaction of $V(CO)_6$ with Me_2PH (eq 5) and

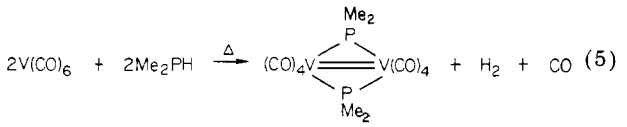

4

has a planar $V_2(\mu\text{-}P)_2$ core with a V–V separation of 2.733 Å (average of four independent molecules). Nb and Ta analogues of **4** have not been reported. Notable missing members of the expected series of bis(phosphido)-bridged doubley bonded binuclear compounds are $Mn_2(\mu\text{-}PPh_2)_2L_6$ and $Re_2(\mu\text{-}PPh_2)_2L_6$ (L = CO, PR_3), e.g., **5**.

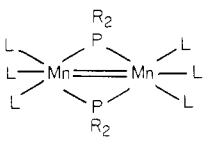

5

The position of the ^{31}P NMR resonances for bridging μ-PPh_2 ligands has been correlated with the M–P–M bond angles and the metal–metal bond distances which these ligands bridge.[15] In general, the resonances have been observed to progressively move to lower field as the bond angles and metal–metal distances decrease.[15d,f] One would thus expect the ^{31}P NMR resonance for the bridging μ-PPh_2 ligands in **1** to be far downfield, since the Co–P1–Co′ bond angle is so acute and the Co–Co separation is very small. Indeed, the resonance is downfield at δ 173.4.[5] This bond angle/distance–^{31}P NMR chemical shift correlation is not perfect, however, since the resonance of the μ-PPh_2 ligands in $Co_3(\mu\text{-}PPh_2)_3(CO)_6$ is much further downfield at δ 244 even though the Co–P–Co angles (average 73.9 (1)°) and Co–Co distances (average 2.610 (3) Å) in the latter complex are much greater than in **1**.[23] Even so, the chemical shift position of the resonance of bridging μ-PR_2 ligands is a useful qualitative indicator of the presence or absence of significant metal–metal bonding in compounds of unknown structure.[15,24]

Even though $Co_2(\mu\text{-}PPh_2)_2(CO)_2(PEt_2Ph)_2$ possesses a formal metal–metal double bond and would appear useful for the synthesis of polynuclear organometallic clusters in reactions similar to those of eq 1 and 2,[2,3] such will probably not be the case since the dimer is easily disrupted. As detailed in ref 5, we find that exposure of solutions of **1** to CO results in rapid loss of PEt_2Ph and rearrangement to form $Co_3(\mu\text{-}PPh_2)_3(CO)_6$ in quantitative yield (eq 6).

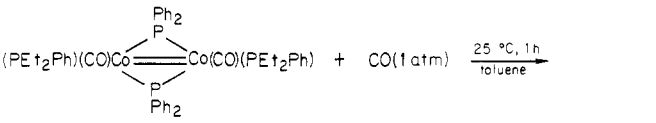

1

$Co_3(\mu\text{-}PPh_2)_3(CO)_6$ (6)

>95%

This reaction presumably proceeds through initial addition of CO to coordinatively unsaturated **1**, but the bridging μ-PPh_2 ligands are simply not sufficient to hold the binuclear complex together and rearrangement occurs.

Acknowledgment. This research was supported by the National Science Foundation (Grant CHE8201160) and in part by grants from the Standard Oil Co. of Ohio, Celanese, Union Carbide, and Air Products, and Chemicals, Inc. G.L.C. gratefully acknowledges the Camille and Henry Dreyfus Foundation for a Teacher-Scholar Award (1978–1983) and the John Simon Guggenheim Memorial Foundation for a fellowship (1982–1983).

Registry No. 1, 83462-95-7; Co, 7440-48-4.

Supplementary Material Available: Listings of the derived positions of the hydrogen atoms (Table A) and the structure factors (Table B) for $Co_2(\mu\text{-}PPh_2)_2(CO)_2(PEt_2Ph)_2$ (14 pages). Ordering information is given on any current masthead page.

(18) Eisenberg, R.; Gaughan, A. P., Jr.; Pierpont, C. G.; Reed, J.; Schultz, A. J. *J. Am. Chem. Soc.* **1972**, *94*, 6240.
(19) Eisenberg, R., private communication.
(20) Vahrenkamp, H. *Chem. Ber.* **1978**, *111*, 3472.
(21) (a) Hayter, R. G. *J. Am. Chem. Soc.* **1964**, *86*, 823. (b) Green, M. L. H.; Moelwyn-Hughes, J. T. *Z. Naturforsch., B:* **1962**, *17b*, 783.
(22) (a) Abel, E. W.; Sabherwal, I. H. *J. Organomet. Chem.* **1967**, *10*, 491. (b) Hieber, W.; Opasky, W. *Chem. Ber.* **1968**, *101*, 2966.
(23) Huntsman, J. R. Ph.D. Thesis, University of Wisconsin, Madison, Wisc., 1973.
(24) Breen, M. J.; Duttera, M. R.; Geoffroy, G. L.; Novotnak, G. L.; Roberts, D. A.; Shulman, P. M.; Steinmetz, G. R. *Organometallics* **1981**, *1*, 1008.

Synthesis and Characterization of Some Rhodium(I) Dimers Containing (Diphenylarsino)(diphenylphosphino)methane as the Bridging Ligand

Paul D. Enlow and Clifton Woods*

Department of Chemistry, University of Tennessee, Knoxville, Tennessee 37996

Received May 18, 1982

Binuclear Rh(I) complexes have been prepared by using the unsymmetrical bridging ligand (diphenylarsino)(diphenylphosphino)methane (DADPM). On the basis of infrared, $^{31}P\{^1H\}$ NMR, and $^{13}C\{^1H\}$ NMR data, the complex $[RhCl(CO)(DADPM)]_2$ and its derivatives have been shown to contain the head-to-tail arrangement of the bridging ligands. The complex $[Rh_2(\mu\text{-}Cl)(\mu\text{-}CO)(CO)_2(DADPM)_2]PF_6$ has been shown to be unstable to loss of CO in the solid state, producing $[Rh_2(\mu\text{-}Cl)(CO)_2(DADPM)_2]PF_6$. The mono- and diisocyanide derivatives, $[Rh_2Cl(CO)_2(t\text{-}C_4H_9NC)(DADPM)_2]PF_6$ and $[Rh_2Cl(CO)_2(t\text{-}C_4H_9NC)_2(DADPM)_2]PF_6$, have been shown to be analogous to the bis(diphenylarsino)methane (DAM) derivatives. Tetrakis(isocyanide) derivatives containing DADPM are also described. Ultraviolet–visible, infrared, and $^{31}P\{^1H\}$ NMR spectroscopic techniques have been used to characterize the DADPM complexes. The $^{31}P\{^1H\}$ NMR spectra have demonstrated the lack of long-range rhodium–phosphorus coupling in the rhodium(I) dimers of the DADPM ligand.

In recent years there has been growing interest in the binuclear Rh(I) complexes *trans*-$[RhCl(CO)(DPM)]_2$, **1**, and *trans*-$[RhCl(CO)(DAM)]_2$, **2** (DPM = $Ph_2PCH_2PPh_2$; DAM = $Ph_2AsCH_2AsPh_2$).[1-4] A great deal of this interest

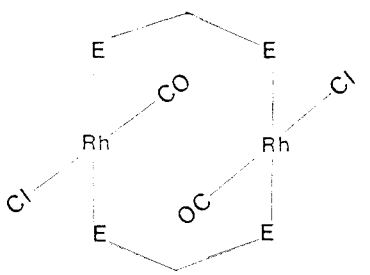

1, E = P
2, E = As

has been focused on the ability of **1** and **2** to form "A-frame" complexes[5-13] which readily add small molecules. Investigations of **1** and **2** have revealed some interesting differences in the nature and stabilities of some of their derivatives.[12,13] Structural studies have shown that **1** and **2** are structurally similar,[1,3] with slight structural differences apparently due to differences in the bite sizes of the DPM and DAM ligands. With the DAM having the larger bite, it is expected that **2** should have the larger rhodium–rhodium separation. In derivatives where small molecules, such as CO, bridge the two metal centers, the metal–metal separations imposed by the DPM and DAM ligands are believed to play a role in determining the stabilities of these derivatives.[4,11,14-17]

In view of the differences exhibited by **1** and **2**, and their derivatives, it was of interest to prepare the ligand (diphenylarsino)(diphenylphosphino)methane (DADPM) and its complex, *trans*-$[RhCl(CO)(DADPM)]_2$. The existence of *trans*-$[RhCl(CO)(DADPM)]_2$ would allow a comparison of the nature and stabilities of derivatives of *trans*-$[RhCl(CO)(DADPM)]_2$ with analogous derivatives of **1** and **2**. Since each bridging DADPM ligand will have a phosphorus bound to one rhodium and an arsenic bound to the other rhodium, the bite of DADPM is expected to be between that of DAM and that of DPM. Therefore, the rhodium–rhodium separation is expected to be between that of **1** and that of **2**. This raises the question of whether the nature and stabilities of the DADPM derivatives are similar to those of DAM, those of DPM, or whether the DADPM derivatives will exhibit a behavior intermediate between those of the analogous DAM and DPM derivatives.

We report in this paper the preparation of $[RhCl(CO)(DADPM)]_2$ and some of its derivatives. We also compare the nature and stabilities of these derivatives with analogous derivatives of **1** and **2**.

Experimental Section

Materials. Methyldiphenylphosphine, chlorodiphenylarsine, *tert*-butyl isocyanide, isopropyl isocyanide, and rhodium(III) chloride trihydrate were obtained from Strem Chemicals. Cyclohexyl isocyanide was obtained from Aldrich Chemicals, and *n*-butyllithium was obtained from Alfa-Ventron Corp.

Preparation of $(C_6H_5)_2AsCH_2P(C_6H_5)_2$: This compound was prepared in a manner similar to that used to prepare some unsymmetrical diphosphines.[18] *N,N,N',N'*-Tetramethylethylenediamine (22.2 g, 191 mmol) was added dropwise under nitrogen to a rapidly stirred solution of 79.5 mL of 2.4 M *n*-butyllithium in hexane. To this yellow solution was added methyldiphenylphosphine (38.2 g, 191 mmol), and after about 10 min a yellow precipitate formed. The slurry was stirred for 3 h, after which 75 mL of freshly distilled tetrahydrofuran (THF) was added, yielding a deep red solution. This solution was added dropwise under nitrogen to a solution of 50.5 g (191 mmol) of chlorodiphenylarsine in 50 mL of benzene. The resulting orange slurry

(1) Mague, J. T. *Inorg. Chem.* **1969**, *8*, 1975.
(2) Balch, A. L.; Tulyathan, B. *Inorg. Chem.* **1977**, *16*, 2840.
(3) Cowie, M.; Dwight, S. K. *Inorg. Chem.* **1980**, *19*, 2500.
(4) Cowie, M.; Dwight, S. K. *Inorg. Chem.* **1981**, *20*, 1534.
(5) Kubiak, C. P.; Eisenberg, R. *J. Am. Chem. Soc.* **1977**, *99*, 6129.
(6) Cowie, M.; Mague, J. T.; Sanger, A. R. *J. Am. Chem. Soc.* **1978**, *100*, 3628.
(7) Cowie, M. *Inorg. Chem.* **1979**, *18*, 286.
(8) Cowie, M.; Dwight, S. K.; Sanger, A. R. *Inorg. Chim. Acta* **1978**, *31*, L407.
(9) Cowie, M.; Dwight, S. K. *Inorg. Chem.* **1979**, *18*, 1209.
(10) Cowie, M.; Dwight, S. K. *Inorg. Chem.* **1979**, *18*, 2700.
(11) Cowie, M.; Dwight, S. K. *Inorg. Chem.* **1980**, *19*, 209.
(12) Mague, J. T.; Sanger, A. R. *Inorg. Chem.* **1979**, *18*, 2060.
(13) Mague, J. T.; DeVries, S. H. *Inorg. Chem.* **1980**, *19*, 3743.
(14) Cowie, M.; Southern, T. G. *J. Organomet. Chem.* **1980**, *193*, C46.
(15) Colton, R.; McCormick, M. J.; Pannan, C. D. *J. Chem. Soc., Chem. Commun.* **1977**, 823.
(16) Colton, R.; McCormick, M. J.; Pannan, C. D. *Aust. J. Chem.* **1978**, *31*, 1425.
(17) Brown, M. P.; Keith, A. N.; Manojlović-Muir, Lj.; Muir, K. W.; Puddephatt, R. J.; Seddon, K. R. *Inorg. Chim. Acta* **1979**, *34*, L223.
(18) Grim, S. O.; Mitchell, J. D. *Inorg. Chem.* **1977**, *16*, 1770.

0276-7333/83/2302-0064$01.50/0

Table I. Analytical Data

no.	compd	C calcd	C found	H calcd	H found	N calcd	N found	other calcd	other found
4	$Rh_2Cl_2(CO)_2((C_6H_5)_2PCH_2As(C_6H_5)_2)_2$	52.50	53.12	3.72	3.85			5.20 (P) 5.96 (Cl)	5.51 6.18
6	$[Rh_2Cl(CO)_2((C_6H_5)_2PCH_2As(C_6H_5)_2)_2]PF_6$	48.08	49.06	3.41	3.91			2.73 (Cl)	2.94
13	$[Rh_2Cl(CO)_2(C_4H_9NC)((C_6H_5)_2PCH_2As(C_6H_5)_2)_2]PF_6$	49.54	49.08	3.87	3.96	1.01	0.86	2.57 (Cl)	2.71
14	$[Rh_2Cl(CO)(C_4H_9NC)_2((C_6H_5)_2PCH_2As(C_6H_5)_2)_2]PF_6$	50.98	50.43	4.35	4.37	1.95	1.81	2.47 (Cl)	2.62
15	$[Rh_2(C_3H_7NC)_4((C_6H_5)_2PCH_2As(C_6H_5)_2)_2][PF_6]_2$	48.46	47.56	4.46	4.30	3.44	3.26		
16	$[Rh_2(C_6H_{11}NC)_4((C_6H_5)_2PCH_2As(C_6H_5)_2)_2][PF_6]_2$	52.36	52.65	4.96	5.16	3.13	3.11	6.92 (P)	7.26
17	$[Rh_2(C_4H_9NC)_4((C_6H_5)_2PCH_2As(C_6H_5)_2)_2][PF_6]_2$	49.90	48.39	4.79	4.87	3.32	2.98		

was refluxed 1 h and allowed to stir ca. 10 h. The mixture was reduced in volume, and the resulting oil was dissolved in 150 mL of dichloromethane. The dichloromethane solution was washed with four 100-mL portions of water to extract the lithium chloride. The dichloromethane layer was dried over Na_2SO_4, after which the dichloromethane was removed under vacuum, yielding a heavy oil. Crystallization from hot ethanol produced white crystals: yield 27.0 g (33%). Anal. Calcd for $C_{25}H_{22}AsP$: C, 70.10; H, 5.18; P, 7.23. Found: C, 69.74; H, 5.10; P 7.17.

Preparation of $[RhCl(CO)(DADPM)]_2$ (4). This compound was prepared by a procedure similar to that used for the preparation of the analogous DPM complex.[19] A mixture of $RhCl_3 \cdot 3H_2O$ (1.00 g, 3.8 mmol) in 200 mL of aqueous ethanol was refluxed under carbon monoxide ca. 4 h until it became lemon yellow. This solution was cooled to room temperature, and a solution of $(C_6H_5)_2AsCH_2P(C_6H_5)_2$ (1.63 g, 3.8 mmol) in a minimum volume of acetone was added. An orange precipitate appeared upon rapid stirring, and it was collected by filtration and washed with ether: yield, 1.76 g (77%).

Preparation of $[Rh_2Cl(CO)_3(DADPM)_2]PF_6$ (5). Rhodium trichloride trihydrate (200 mg, 0.76 mmol) was refluxed in 25 mL of ethanol for 4 h under carbon monoxide. To the yellow solution were added $(C_6H_5)_2AsCH_2P(C_6H_5)_2$ (326 mg, 0.76 mmol) in 4 mL of THF and ammonium hexafluorophosphate (126 mg, 0.77 mmol) in 3 mL of ethanol in quick succession. The resulting orange precipitate was collected by filtration under carbon monoxide and washed with water, ethanol, and ether: yield, 374 mg (74%). The solid product loses CO overnight to produce compound **6**. Elemental analysis cannot distinguish between **5** and **6**.

Preparation of $[Rh_2Cl(CO)_2(DADPM)_2]PF_6$ (6). This compound was made by dissolving compound **5** in a 2.5:1 mixture of THF/acetone and bubbling it with nitrogen for 10 min. Equal volumes of ether and ligroin were added until the cloud point was reached, and the mixture was cooled to 0 °C for 90 min. The resulting orange solid was collected and washed with ether. The yield for this reaction is quantitative.

Preparation of $[Rh_2Cl(CO)_2(t\text{-}C_4H_9NC)(DADPM)_2]PF_6$ (9). *tert*-Butyl isocyanide (7.64 mg, 0.092 mmol) in 1.8 mL of acetone was added to a rapidly stirred solution of compound **6** (116 mg, 0.092 mmol) in 5 mL of acetone under carbon monoxide. An orange precipitate appeared upon addition of 3 mL of ether and 8 mL of ligroin. The mixture was cooled to 0 °C, and the solid was collected by filtration under an atmosphere of carbon monoxide: yield, 101 mg (71%).

Preparation of $[Rh_2Cl(CO)(t\text{-}C_4H_9NC)_2(DADPM)_2]PF_6$ (10). A procedure similar to that used for the preparation of compound **9** was employed, except that *tert*-butyl isocyanide was added in a 2:1 molar ratio with compound **6**: yield, 94.2 mg (70%).

Preparation of $[Rh_2(RNC)_4(DADPM)_2][PF_6]_2$ ($R = i\text{-}C_3H_7$, C_6H_{11}, $t\text{-}C_4H_9$). The procedure for preparing these complexes is analogous to that used to prepare similar DAM and DPM complexes.[2,15] The preparation of the cyclohexyl isocyanide complex is described here. Cyclohexyl isocyanide (167 mg, 1.53 mmol) in 3 mL of methanol was added dropwise to a stirred slurry of $[RhCl(CO)(DADPM)]_2$ (454 mg, 0.38 mmol) in 50 mL of methanol. The deep purple solution was stirred for 20 min, and 126 mg (0.77 mmol) of ammonium hexafluorophosphate in 5 mL of methanol was added. Reddish purple crystals precipitated after 10 min of stirring; they were collected by filtration. The product was recrystallized from acetone/*n*-propanol: yield, 168 mg (25%).

(19) Mague, J. T.; Mitchner, J. P. *Inorg. Chem.* **1969**, *8*, 119.

Physical Measurements. Ultraviolet and visible spectra were recorded on a Cary 17 or Cary 219 spectrophotometer. Infrared (IR) spectra were obtained with a Digilab FTS-20 C/V Fourier transform spectrometer. All NMR spectra were recorded on a JEOL FX90Q Fourier transform spectrometer. The ^{31}P NMR spectra were proton decoupled and recorded at 36.19 MHz with 85% phosphoric acid as an external reference. Proton-decoupled ^{13}C NMR spectra were recorded at 22.51 MHz with tetramethylsilane (Me_4Si) as the reference. All elemental analyses were performed by Galbraith Laboratories, Inc., Knoxville, TN.

Results and Discussion

The reaction of Ph_2PCH_2Li with Ph_2AsCl yielded (diphenylarsino)(diphenylphosphino)methane (DADPM). The DADPM is readily recrystallized from hot ethanol. The addition of DADPM to an ethanolic solution of $[Rh(CO)_2Cl_2]^-$ under carbon monoxide yielded an orange solid. The analytical data in Table I are consistent with the formulation $[RhCl(CO)(DADPM)]_2$. By analogy with the DPM and DAM complexes, the DADPM complex is presumed to have a chloride trans to a CO at each rhodium, with the two chlorides in a trans disposition about the dimeric framework.

Unlike the DPM and DAM complexes, the DADPM complex can exist with two different arrangements of the bridging ligand. One isomer contains the head-to-head arrangement of structure **3** and the other contains the head-to-tail arrangement of structure **4**.

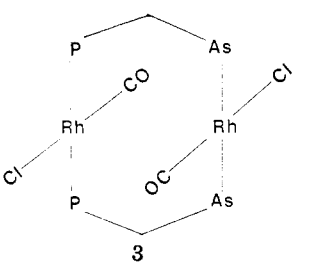

3

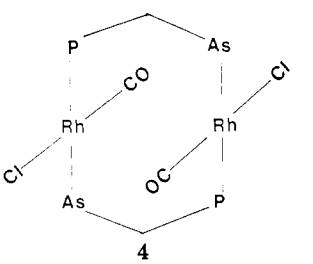

4

In the absence of long-range rhodium–phosphorus coupling, the $^{31}P\{^1H\}$ NMR spectra of **3** and **4** are expected to exhibit simple AX patterns. Therefore, it is possible that $^{31}P\{^1H\}$ NMR cannot distinguish between structures **3** and **4**. The $^{31}P\{^1H\}$ NMR spectrum of $[RhCl(CO)(DADPM)]_2$ exhibits a doublet centered at 27.3 ppm with $^1J(Rh\text{–}P) = 149$ Hz (Table II). The observed spectrum is consistent with the lack of a formal rhodium–rhodium bond. By analogy with **1** and **2**, the DADPM complex is considered to exist without a formal metal–metal bond since each rhodium is a 16-electron system (eight from the rhodium, two from the terminal chloride, two from the CO, and two from each of the bridging ligand donor atoms).

Dinuclear Rh(I) complexes containing an unsymmetrical bridging ligand have recently been reported[20] for the bidentate ligand 2-(diphenylphosphino)pyridine, $Ph_2P(py)$.

(20) Farr, J. P.; Olmstead, M. M.; Hunt, C. H.; Balch, A. L. *Inorg. Chem.* **1981**, *20*, 1182.

Table II. ^{31}P NMR Parameters

no.	compd	δ[a]	^1J(Rh–P)[b]
4	$[RhCl(CO)(DADPM)]_2$	27.3	149
5	$[Rh_2Cl(CO)_3(DADPM)]PF_6$	27.6	142
6	$[Rh_2Cl(CO)_2(DADPM)_2]PF_6$	27.0	146
15	$[Rh_2(i\text{-}C_3H_7NC)_4(DADPM)_2][PF_6]_2$	25.7	144
16	$[Rh_2(C_6H_{11}NC)_4(DADPM)_2][PF_6]_2$	25.7	144
17	$[Rh_2(t\text{-}C_4H_9NC)_4(DADPM)_2][PF_6]_2$	25.5	141

[a] Chemical shifts were measured in CH_2Cl_2 solution with respect to external 85% H_3PO_4. [b] Coupling constants ±0.6 Hz.

The isolated isomers contained the head-to-tail arrangement of two $Ph_2P(py)$ ligands. These complexes contained additional bridging molecules, such as CO and SO_2; therefore, no analogues of **3** or **4** have been reported for $Ph_2P(py)$ or other unsymmetrical bridging ligands. The $Ph_2P(py)$ dimers are considered to contain a formal Rh–Rh bond and exhibit $^{31}P\{^1H\}$ NMR spectra consistent with the AA′XX′ spin system.[20] The lack of a formal rhodium–rhodium bond in structures **3** and **4** could be responsible for the simplicity of the $^{31}P\{^1H\}$ NMR spectrum of $[RhCl(CO)(DADPM)]_2$.

The IR spectrum of $[RhCl(CO)(DADPM)]_2$ shows a strong absorption at 1967 cm^{-1} which is assigned to the carbonyl stretching frequency. This frequency is approximately centered between ν(CO) of **1** at 1971 cm^{-1} and ν(CO) of **2** at 1962 cm^{-1}. Structure **3** is expected to exhibit two CO stretching frequencies. The IR spectrum is therefore consistent with the formulation of $[RhCl(CO)(DADPM)]_2$ as structure **4**.

Carbon-13 NMR spectra were obtained on $[RhCl(CO)(DADPM)]_2$ prepared from 90% enriched CO. The carbonyl resonance occurs at 188 ppm (from Me_4Si) and appears as a doublet-of-doublets. The larger coupling constant of 73 Hz is assigned to ^1J(Rh–C), and the smaller coupling constant of 14 Hz is assigned to the two-bond coupling constant, ^2J(P–C), between the phosphorus and the carbonyl carbon. The ^2J(P–C) value is confirmed from the $^{31}P\{^1H\}$ spectrum which exhibits the expected doublet-of-doublets. The ^{13}C NMR results suggest that the isomer of $[RhCl(CO)(DADPM)]_2$ which has been isolated is that given by structure **4** since in the absence of splitting due to rhodium–rhodium interaction, structure **3** is expected to give a ^{13}C NMR spectrum consisting of a doublet and a doublet-of-triplets for the carbonyl carbons.

Orange crystals are formed when an ethanolic solution of $[Rh_2(CO)_2Cl_2]^-$ is treated, under an atmosphere of CO, with equal molar quantities of DADPM and ammonium hexafluorophosphate. When the IR spectrum of the crystals is obtained immediately after isolation, absorption bands are observed at 1981, 1967, and 1843 cm^{-1}, suggesting the presence of two terminal carbonyl ligands and one bridging carbonyl ligand. This complex has been formulated as $[Rh_2(CO)_2(\mu\text{-}CO)(\mu\text{-}Cl)(DADPM)_2]PF_6$ (**5**).

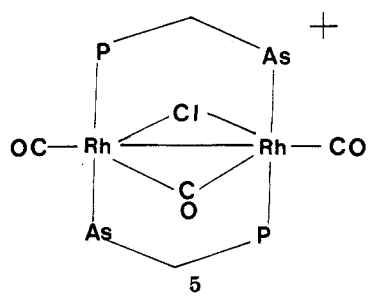

5

Structure **5** is analogous to a tricarbonyl derivative of **1**.[6,7] The $^{31}P\{^1H\}$ NMR spectrum of a CH_2Cl_2 solution of **6** which is saturated with CO and sealed under an atmosphere of CO shows a doublet (Table II) for the ligand phosphorus atoms. Apparently rapid CO exchange reduces the rhodium–rhodium interaction such that the expected second-order spectrum is not observed. If **5** is allowed to stand overnight, loss of CO occurs from the solid state and the IR spectrum of the resulting product shows only terminal carbonyl stretching frequencies at 1981 and 1965 cm^{-1}. This product has been formulated as $[Rh_2(CO)_2(\mu\text{-}Cl)(DADPM)_2]PF_6$ (**6**). The hexafluorophosphate salt of

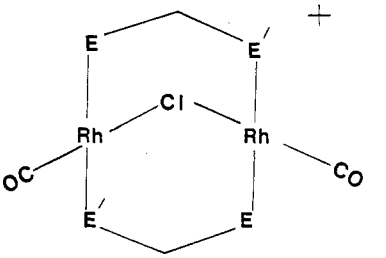

6, E = P, E′ = As
7, E = E′ = P
8, E = E′ = As

the DPM analogue of **5** has been isolated and found to be stable to loss of CO in the solid but is converted to **7** by bubbling nitrogen through a solution of the DPM tricarbonyl dimer.[12] The hexafluorophosphate salt of the DAM analogue of **5** cannot be isolated and characterized. Attempts to isolate the DAM salt result in the isolation of **8**.[13] However, the DAM analogue of **5** is stable to loss of CO in the solid state when isolated as the tetraphenylborate salt.[12] The differences in the stabilities of the tricarbonyl DAM salts have been discussed in terms of packing phenomena in the solid.[13] It is interesting that the behavior of **5** is intermediate between that of $[Rh_2(CO)_2(\mu\text{-}Cl)(\mu\text{-}CO)(DPM)_2]PF_6$, which is stable to loss of CO in the solid state, and $[Rh_2(CO)_2(\mu\text{-}Cl)(\mu\text{-}CO)(DAM)_2]PF_6$, which apparently is too unstable to be isolated as the pure solid.

In view of the intermediate behavior of **5** between the stable DPM analogue and the unstable DAM analogue, it was of interest to see how **6** behaved under conditions where **7** and **8** give stable complexes, but of different types.

The products obtained when **7** is treated with 1 and 2 equiv of $t\text{-}C_4H_9NC$ have been formulated as **9** and **10**, respectively.[13] The behavior of **8** differs from that of **7**

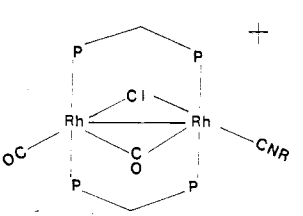

9, R = $t\text{-}C_4H_9$

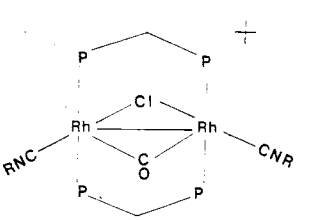

10, R = $t\text{-}C_4H_9$

in that treatment of **8** with 1 and 2 equiv of $t\text{-}C_4H_9NC$ leads to products assigned structures **11** and **12**, respectively.[13] The lack of a bridging CO in **11** is probably due,

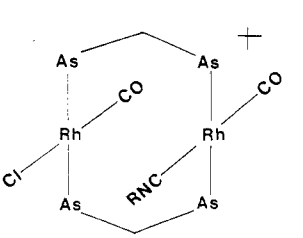

11, R = $t\text{-}C_4H_9$

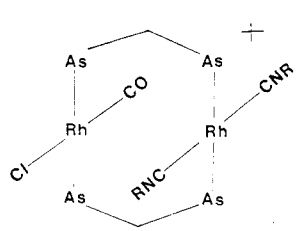

12, R = $t\text{-}C_4H_9$

Table III. Infrared and Electronic Spectral Data for DADPM Complexes

no.	compd	ν(CO),[a] cm^{-1}	ν(CN),[a] cm^{-1}	λ_{max}, nm (ϵ)[b]
4	$[RhCl(CO)(DADPM)]_2$	[1967 (s)]		455 (6740), 283 sh (17 300)
6	$[Rh_2Cl(CO)_2(DADPM)_2]PF_6$	1981 (s), 1965 (s)		435 (10 600), 305 sh (12 700)
13	$[Rh_2Cl(CO)_2(t\text{-}C_4H_9NC)(DADPM)_2]PF_6$	2005 (s), 1954 (s)	2209 (m)	443 (5750),[c] 380 (3700),[d] 305 sh (10 200)
14	$[Rh_2Cl(CO)(t\text{-}C_4H_9NC)_2(DADPM)_2]PF_6$	1954 (s)	2120 (s)	515 (3650),[c] 458 (4860),[d] 383 (3540), 302 sh (12000)
15	$[Rh_2(i\text{-}C_3H_7NC)_4(DADPM)_2][PF_6]_2$		2144 (s)	545 (9160), 322 (13 000), 264 sh (13 400)
16	$[Rh_2(C_6H_{11}NC)_4(DADPM)_2][PF_6]_2$		2166 (m), 2137 (s)	548 (1500), 322 (1300), 265 sh (20 600)
17	$[Rh_2(t\text{-}C_4H_9NC)_4(DADPM)_2][PF_6]_2$		2153 (m), 2125 (s)	517 (11 300), 385 (4650), 323 (14 500), 265 (16 300)

[a] Infrared frequencies in brackets were recorded from KBr spectra; all other frequencies were recorded from Nujol mull spectra. [b] Recorded from degassed CH_2Cl_2 solution spectra. [c] Molar absorptivity rapidly decreases with time. [d] Molar absorptivity rapidly increases with time.

in part, to the larger bite of the DAM compared to that of DPM. It has been noted that DAM complexes with bridging CO groups are less stable than their DPM counterparts and that CO exchange in DAM complexes is more facile than in the DPM complexes.[12]

Treatment of **6** with 1 equiv of t-C_4H_9NC yields orange crystals which analyze as $[Rh_2Cl(CO)_2(t\text{-}C_4H_9NC)(DADPM)_2]PF_6$ (**13**). The IR data (Table III) indicate that there are terminal carbonyl ligands (ν(CO) = 1954 (vs), 2005 (s) cm^{-1}) and terminal isocyanide ligands (ν(CN) = 2209 (m) cm^{-1}). Peaks which could be assigned to bridging CO ligands were not observed. On the basis of these data, **13** is presumed to be similar to **11** and is formulated as

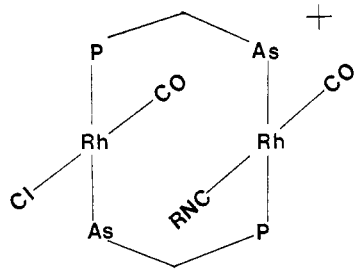

13, R = t-C_4H_9

The 51-cm^{-1} difference in the two CO stretching frequencies suggests that the two CO ligands are in different environments and are therefore coordinated to different metal centers. With use of a rationale similar to that used in making assignments for complex **11**,[13] the lower energy CO absorption band is assigned to the carbonyl ligand trans to the Cl$^-$. For structure **13**, the environment of the rhodium coordinated to Cl$^-$ is expected to be similar to the environment of the rhodium atoms in **4**. The CO ligands coordinated to rhodium atoms in such an environment should have similar stretching frequencies, 1954 cm^{-1} for **13** and 1968 cm^{-1} for **4**. Therefore, the CO ligand trans to t-C_4H_9NC in **13** is assigned the stretching frequency of 2005 cm^{-1}. These assignments are consistent with the view that t-C_4H_9NC is a better π acceptor than Cl$^-$. Through π back-bonding, t-C_4H_9NC competes more efficiently with CO for electron density on the metal than does Cl$^-$ and as a result is more efficient in reducing the backbonding between the rhodium and the CO. The result is a higher energy stretching frequency of the CO trans to t-C_4H_9NC compared to the frequency of the CO trans to Cl$^-$.

Treatment of **6** with 2 equiv of t-C_4H_9NC yields burgundy crystals which analyze as $[Rh_2Cl(CO)(t\text{-}C_4H_9NC)_2(DADPM)_2]PF_6$ (**14**). The IR spectrum of **14** shows CO and isocyanide absorption bands at 1954 and 2120 cm^{-1}, respectively. Again, the proximity of ν(CO) for **14** to that of **4** suggests that the CO ligand is trans to a Cl$^-$. Complex **14** appears to be similar to **12** and is therefore formulated as

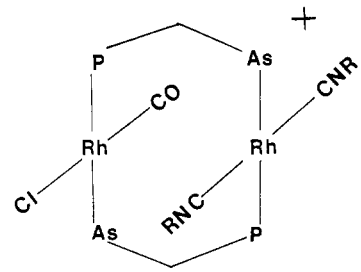

14, R = t-C_4H_9

Time-dependent UV–visible spectra of **13** and **14** in degassed CH_2Cl_2 show that **13** and **14** are not stable in this solvent. The nature of this transformation is not presently known.

The addition of 4 equiv of RNC to **4**, followed by the addition of 2 equiv of BF_4^-, $B(C_6H_5)_4^-$, or PF_6^- salts, results in the formation of tetrakis(isocyanide) dimers. These dimers are similar to those reported[21,22] with DPM and DAM bridging the two rhodium centers and are formulated as

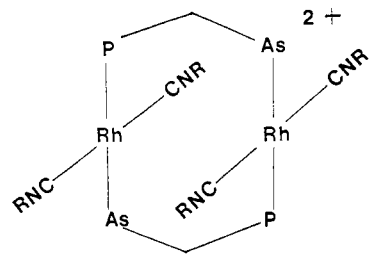

15, R = i-C_3H_7
16, R = C_6H_{11}
17, R = t-C_4H_9

The $^{31}P\{^1H\}$ NMR spectra of **15–17** show simple doublets (Table II), indicating that long-range rhodium–phosphorus coupling is negligible, as was concluded for complex **4**. The electronic spectral data (Table III) of complexes **15–17** are similar to those of the DPM and DAM analogues for which the lowest energy transition is assigned to a "proximity shifted" metal-to-ligand charge-transfer (MLCT) transition.[2] The "proximity shifted" MLCT transition results from the face-to-face approach of the two square-planar rhodium moieties. This approach causes the HOMO and

(21) Olmstead, M. M.; Balch, A. L. *J. Am. Chem. Soc.* **1976**, *98*, 2354.
(22) Balch, A. L.; Labadie, J. W.; Delker, G. *Inorg. Chem.* **1979**, *18*, 1224.

LUMO of the monomeric units to move closer together in the dimer, lowering the energy of the MLCT transition into the 500–550-nm region, thus, giving these complexes their brilliant colors.

Summary. This work has resulted in the preparation of rhodium dimers of the phosphorus–arsenic mixed-ligand DADPM. These dimers, each containing two DADPM ligands, have been shown to exist with the bridging ligands in a head-to-tail arrangement.

The properties, reactivities, and structures of these new complexes are similar to those of the previously known DAM and DPM analogues. Several interesting observations have been made concerning the DADPM complexes studied in this work. The $^{31}P\{^1H\}$ NMR spectra indicate that for the rhodium(I) DADPM dimers long-range rhodium–phosphorus coupling is negligible. Another interesting observation is that the nature of the DADPM complexes appears to parallel that of the DAM complexes more than the DPM complexes. These observations invite the question of how do the structural parameters of the complex $[RhCl(CO)(DADPM)]_2$ compare to those of $[RhCl(CO)(DAM)]_2$ and $[RhCl(CO)(DPM)]_2$, since it is believed that the difference in the bite of DAM and DPM is responsible, in part, for the different behaviors of the DAM and DPM complexes.

Acknowledgment. This work was supported by Research Corp. and The Dow Chemical Co. Foundation. We acknowledge NSF for providing funds to help purchase the FTIR spectrometer. P.D.E. wishes to thank the Chemistry Division of Oak Ridge National Laboratories (ORNL) for partial financial support in the form of a graduate stipend. We thank Dr. Devon Meek of The Ohio State University for obtaining some of the early $^{31}P\{^1H\}$ NMR spectra for us. We are grateful to Dr. Gilbert M. Brown (ORNL) for his helpful comments.

Registry No. **4**, 83153-27-9; **5**, 83153-29-1; **6**, 83159-88-0; **7**, 80448-77-7; **8**, 74965-10-9; **13**, 83153-31-5; **14**, 83174-74-7; **15**, 83153-33-7; **16**, 83153-35-9; **17**, 83153-37-1; $RhCl_3$, 10049-07-7; $(C_6H_5)_2AsCH_2P(C_6H_5)_2$, 69783-37-5; t-C_4H_9NC, 7188-38-7; methyldiphenylphosphine, 1486-28-8; chlorodiphenylarsine, 712-48-1; cyclohexyl isocyanide, 931-53-3; isopropyl isocyanide, 598-45-8.

Oxidative Electrochemistry of Compounds of the Type $(\eta^5\text{-}C_5H_5)_2MX_2$ Where M = Ti(IV), Mo(IV), and W(IV) and X = Halide, Thiolate, or Ferrocenyl

John C. Kotz,* William Vining, William Coco, and Richard Rosen

Department of Chemistry, State University College, Oneonta, New York 13820

Alberto Romão Dias* and Maria Helena Garcia

Centro de Quimica Estrutural, Instituto Superior Tecnico, Lisboa, Portugal

Received January 13, 1982

The oxidative electrochemistry of compounds of the type Cp_2MX_2 has been examined by cyclic voltammetry and coulometry. When M = Mo(IV) and W(IV), X is a halide or thiolate, and when M = Ti(IV), X is a thiolate or a ferrocenyl group. For the group 6B dihalides, the one-electron oxidation in CH_3CN was always quasi-reversible, but all ultimately gave $[Cp_2M(NCMe)X]^+$, the rate of substitution being in the order Cl < Br < I. The substitution is thought to occur by reductive elimination of a halogen atom (which previous work has suggested is photochemically induced). In the case of the group 6B dithiolate complexes $Cp_2M(SR)_2$, three redox waves were always observed in the range 0.0 to +1.4 V in CH_3CN. The wave at least positive potentials was ascribed to M(IV) $\rightleftarrows$ M(V), and it was always at least quasi-reversible; however, the other two waves had varying degrees of reversibility and current relative to the M(IV) $\rightleftarrows$ M(V) wave. The second redox wave was found to be due to the second, one-electron oxidation of the compounds *and* to the oxidation of the product of the first one-electron oxidation $[Cp_2M(NCMe)SR]^+$. The latter ion, based on M(IV), was isolated and characterized as was the ion $[Cp_2Mo(\mu\text{-}SR)_2MoCp_2]^{2+}$ apparently responsible for the most positive wave. It is argued that these ions arise by a reductive elimination of ·SR from $[Cp_2M^V(SR)_2]^+$. Complexes of the type $Cp_2Ti(SR)_2M(CO)_4$ (M = Cr, Mo, W) were studied; both metal sites undergo only quasi-reversible redox, the trends in potentials being explicable in terms of the usual electronic effects. Finally, $Cp_2Ti[(C_5H_4)Fe(C_5H_5)]_2$ was found to be photochemically stable but oxidatively unstable, in contrast with its phenyl analogue. Oxidation of the compound in CH_2Cl_2 leads ultimately to ferrocene and biferrocene, products assumed to arise by an oxidatively induced reductive elimination.

Introduction

Our research groups have long been interested in molecules that can properly be called "organometallic ligands", that is, molecules which contain a site or sites of electron-donating or -accepting capacity and which also contain a metal–carbon bond somewhere in their framework.[1,2] Among the most broadly successful classes of these ligands are compounds of the type $(\eta^5\text{-}C_5H_5)_2M(SR)_2$ (I) where M = Ti(IV), Mo(IV), and W(IV). Several complexes of these ligands, II–IV, are illustrated.

(1) J. Kotz, C. Nivert, J. Lieber, and R. Reed, *J. Organomet. Chem.*, 84, 255 (1975).

(2) A. R. Dias and M. L. H. Green, *J. Chem. Soc. A*, 1951 (1971).

(3) A. R. Dias and M. L. H. Green, *J. Chem. Soc. A*, 2807 (1971).

(4) P. S. Braterman, V. A. Wilson, and K. K. Joshi, *J. Chem. Soc. A*, 191 (1971); H. Köpf and K. H. Rathlein, *Angew. Chem., Int. Ed. Engl.* 8, 908 (1969).

0276-7333/83/2302-0068$01.50/0

LUMO of the monomeric units to move closer together in the dimer, lowering the energy of the MLCT transition into the 500–550-nm region, thus, giving these complexes their brilliant colors.

Summary. This work has resulted in the preparation of rhodium dimers of the phosphorus–arsenic mixed-ligand DADPM. These dimers, each containing two DADPM ligands, have been shown to exist with the bridging ligands in a head-to-tail arrangement.

The properties, reactivities, and structures of these new complexes are similar to those of the previously known DAM and DPM analogues. Several interesting observations have been made concerning the DADPM complexes studied in this work. The $^{31}P\{^1H\}$ NMR spectra indicate that for the rhodium(I) DADPM dimers long-range rhodium–phosphorus coupling is negligible. Another interesting observation is that the nature of the DADPM complexes appears to parallel that of the DAM complexes more than the DPM complexes. These observations invite the question of how do the structural parameters of the complex $[RhCl(CO)(DADPM)]_2$ compare to those of $[RhCl(CO)(DAM)]_2$ and $[RhCl(CO)(DPM)]_2$, since it is believed that the difference in the bite of DAM and DPM is responsible, in part, for the different behaviors of the DAM and DPM complexes.

Acknowledgment. This work was supported by Research Corp. and The Dow Chemical Co. Foundation. We acknowledge NSF for providing funds to help purchase the FTIR spectrometer. P.D.E. wishes to thank the Chemistry Division of Oak Ridge National Laboratories (ORNL) for partial financial support in the form of a graduate stipend. We thank Dr. Devon Meek of The Ohio State University for obtaining some of the early $^{31}P\{^1H\}$ NMR spectra for us. We are grateful to Dr. Gilbert M. Brown (ORNL) for his helpful comments.

Registry No. **4**, 83153-27-9; **5**, 83153-29-1; **6**, 83159-88-0; **7**, 80448-77-7; **8**, 74965-10-9; **13**, 83153-31-5; **14**, 83174-74-7; **15**, 83153-33-7; **16**, 83153-35-9; **17**, 83153-37-1; $RhCl_3$, 10049-07-7; $(C_6H_5)_2AsCH_2P(C_6H_5)_2$, 69783-37-5; t-C_4H_9NC, 7188-38-7; methyldiphenylphosphine, 1486-28-8; chlorodiphenylarsine, 712-48-1; cyclohexyl isocyanide, 931-53-3; isopropyl isocyanide, 598-45-8.

Oxidative Electrochemistry of Compounds of the Type $(\eta^5\text{-}C_5H_5)_2MX_2$ Where M = Ti(IV), Mo(IV), and W(IV) and X = Halide, Thiolate, or Ferrocenyl

John C. Kotz,* William Vining, William Coco, and Richard Rosen

Department of Chemistry, State University College, Oneonta, New York 13820

Alberto Romão Dias* and Maria Helena Garcia

Centro de Quimica Estrutural, Instituto Superior Tecnico, Lisboa, Portugal

Received January 13, 1982

The oxidative electrochemistry of compounds of the type Cp_2MX_2 has been examined by cyclic voltammetry and coulometry. When M = Mo(IV) and W(IV), X is a halide or thiolate, and when M = Ti(IV), X is a thiolate or a ferrocenyl group. For the group 6B dihalides, the one-electron oxidation in CH_3CN was always quasi-reversible, but all ultimately gave $[Cp_2M(NCMe)X]^+$, the rate of substitution being in the order Cl < Br < I. The substitution is thought to occur by reductive elimination of a halogen atom (which previous work has suggested is photochemically induced). In the case of the group 6B dithiolate complexes $Cp_2M(SR)_2$, three redox waves were always observed in the range 0.0 to +1.4 V in CH_3CN. The wave at least positive potentials was ascribed to M(IV) $\rightleftarrows$ M(V), and it was always at least quasi-reversible; however, the other two waves had varying degrees of reversibility and current relative to the M(IV) $\rightleftarrows$ M(V) wave. The second redox wave was found to be due to the second, one-electron oxidation of the compounds *and* to the oxidation of the product of the first one-electron oxidation $[Cp_2M(NCMe)SR]^+$. The latter ion, based on M(IV), was isolated and characterized as was the ion $[Cp_2Mo(\mu\text{-}SR)_2MoCp_2]^{2+}$ apparently responsible for the most positive wave. It is argued that these ions arise by a reductive elimination of ·SR from $[Cp_2M^V(SR)_2]^+$. Complexes of the type $Cp_2Ti(SR)_2M(CO)_4$ (M = Cr, Mo, W) were studied; both metal sites undergo only quasi-reversible redox, the trends in potentials being explicable in terms of the usual electronic effects. Finally, $Cp_2Ti[(C_5H_4)Fe(C_5H_5)]_2$ was found to be photochemically stable but oxidatively unstable, in contrast with its phenyl analogue. Oxidation of the compound in CH_2Cl_2 leads ultimately to ferrocene and biferrocene, products assumed to arise by an oxidatively induced reductive elimination.

Introduction

Our research groups have long been interested in molecules that can properly be called "organometallic ligands", that is, molecules which contain a site or sites of electron-donating or -accepting capacity and which also contain a metal–carbon bond somewhere in their framework.[1,2] Among the most broadly successful classes of these ligands are compounds of the type $(\eta^5\text{-}C_5H_5)_2M(SR)_2$ (I) where M = Ti(IV), Mo(IV), and W(IV). Several complexes of these ligands, II–IV, are illustrated.

(1) J. Kotz, C. Nivert, J. Lieber, and R. Reed, *J. Organomet. Chem.*, 84, 255 (1975).

(2) A. R. Dias and M. L. H. Green, *J. Chem. Soc. A*, 1951 (1971).

(3) A. R. Dias and M. L. H. Green, *J. Chem. Soc. A*, 2807 (1971).

(4) P. S. Braterman, V. A. Wilson, and K. K. Joshi, *J. Chem. Soc. A*, 191 (1971); H. Köpf and K. H. Rathlein, *Angew. Chem., Int. Ed. Engl.* 8, 908 (1969).

0276-7333/83/2302-0068$01.50/0

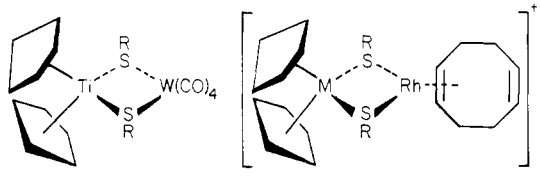

II[4-6] III[2] (M = Mo, W)

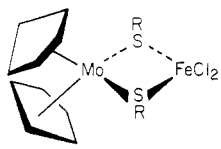

IV[3]

Our examination of organometallic ligands has three objectives: (i) the synthesis and study of new ligands of this type and the study of their chemistry; (ii) the synthesis and study of the complexes formed by these ligands; and (iii) the study of the possibility that such ligands can influence the reactivity of the coordinated metal, especially in reactions of catalytic interest. In our previous work on such compounds we have occasionally examined the electrochemistry of the ligands, their complexes, and closely related compounds, and we frequently found interesting and unique behavior.[7] For this reason we have studied the electrochemistry of compounds of the type $(\eta^5\text{-}C_5H_5)_2MX_2$, and we now wish to report in detail on this aspect of the chemistry of the ligands such as I, complexes such as II and III, and closely related compounds where X and Cl, Br, I, or ferrocenyl (V) in $(\eta^5\text{-}C_5H_5)_2MX_2$. We

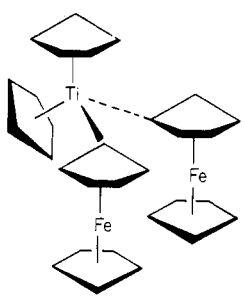

V[8]

have emphasized their oxidative electrochemistry and find that many of these compounds provide excellent examples of *oxidatively induced reductive elimination* reactions.

Results and Discussion

The Electrochemistry of $Cp_2M(halide)_2$ (M = Mo, W; halide = Cl, Br, I). The electrochemical behavior of this series of compounds is not only interesting in itself, but it is also helpful in understanding the behavior of the series of $Cp_2M(SR)_2$ complexes to be described below.

All of the dihalides undergo reversible oxidation in acetonitrile, in the range 0.5–0.55 V for the Mo compounds and in the range 0.3–0.4 V for the W compounds. However, all give evidence for a second reversible wave of very small current (no more than 1–5% of the total) at about

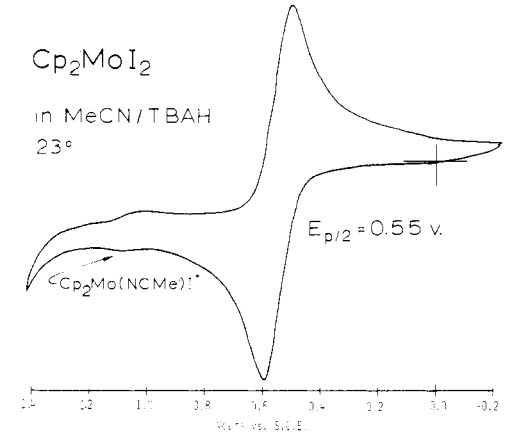

Figure 1. Cyclic voltammogram of Cp_2MoI_2, 1 mM in CH_3CN, containing 0.1 M Bu_4NPF_6. Sweep rate was 200 mv/s.

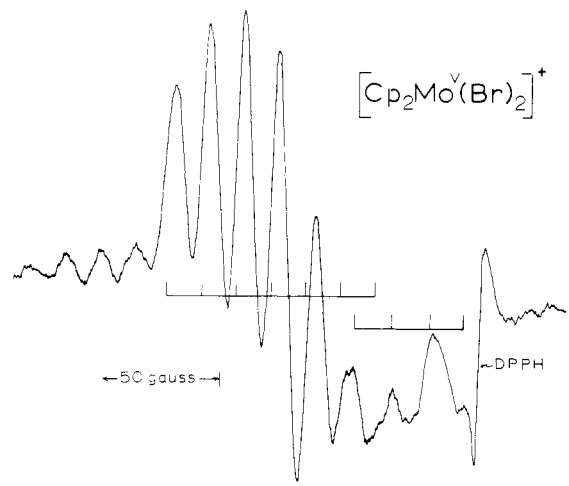

Figure 2. ESR spectrum of $[Cp_2MoBr_2]^+$ after electrochemical generation. Sample, dissolved in CH_3CN with a trace of THF, was frozen and then allowed to warm for 2 min before spectrum was observed. A portion of the satellite lines from $^{95}Mo/^{97}Mo$ coupling is seen at the left. DPPH was the external standard.

1.1 V (Figure 1). The following ECE scheme, rationalized below, indicates the origin of the observed electrochemical reactions.

$$Cp_2M^{IV}X_2 \rightleftarrows [Cp_2M^{V}X_2]^+ + e^- \quad E_1 \qquad (1)$$

$$[Cp_2M^{V}X_2]^+ + MeCN \rightarrow [Cp_2M^{IV}(NCMe)X]^+ + {}^1/_2X_2 \quad C \qquad (2)$$

$$[Cp_2M^{IV}(NCMe)X]^+ \rightleftarrows [Cp_2M^{V}(NCMe)X]^{2+} \quad E_2 \qquad (3)$$

Two comments should be made concerning this scheme before continuing with a detailed discussion of individual compounds. (a) The second process (C) is the *oxidatively induced reductive elimination* of a halogen atom (which then produces X_2). Such reactions have been widely observed in organometallic chemistry but systematically studied in only a few cases;[9] reaction 2 and others we have observed will be compared with the literature in the Summary and Conclusions. There is also experimental evidence that this reaction is photochemically induced.[10] (b) The ion $[Cp_2M(NCMe)X]^+$ can also be prepared by simply stirring the metal dihalide in acetonitrile for several days in vacuo (eq 4). The extent of this solvolysis reaction

(5) T. S. Cameron, C. K. Prout, G. V. Rees, M. L. H. Green, K. K. Joshi, G. R. Davies, B. T. Kilbourn, P. S. Braterman, and V. A. Wilson, *J. Chem. Soc., Chem. Commun.*, 14 (1971).
(6) G. R. Davies and B. T. Kilbourn, *J. Chem. Soc. A*, 87 (1971).
(7) J. Kotz, C. L. Nivert, J. M. Lieber, and R. C. Reed, *J. Organomet. Chem.*, **91**, 87 (1975).
(8) G. A. Razuvaev, G. A. Domrachev, V. V. Sharutin, and O. N. Suvorova, *J. Organomet. Chem.*, **141**, 313 (1977). See also: A. G. Osborne and R. H. Whiteley, *ibid.*, **181**, 425 (1979). The latter paper details the properties of $Cp_2Ti(FcCl_2)_2$ where $FcCl_2$ is the 1,1'-dichloroferrocenyl group; this compound is apparently more air stable than Cp_2TiFc_2.
(9) J. P. Collman and L. S. Hegedus, "Principles and Applications of Organotransition Metal Chemistry", University Science Books, Mill Valley, CA, 1980, p 236.
(10) S. M. B. Costa, A. R. Dias, and F. J. S. Pina, *J. Organomet. Chem.*, **175**, 193 (1979); **217**, 357 (1981).

$$Cp_2MX_2 + MeCN \rightarrow [Cp_2M(NCMe)X]^+ + X^- \quad (4)$$

is in the order Cl ≪ Br < I.

A light green solution of Cp_2MoCl_2 in acetonitrile can be oxidized at about 0.7 V to the extent of 0.98 faraday/mol. The stability of the $[Cp_2MoCl_2]^+$ ion is indicated by the fact that, if the solution is reduced at 0.0 V, 0.82 faraday/mol is passed.

The product of the oxidation of Cp_2MoCl_2, that is, $[Cp_2Mo^{V}Cl_2]^+$, is red in acetonitrile (λ_{max} 482 nm (ϵ 1000)) and gives rise to an ESR spectrum with a center line (g_{obsd} = 2.000) split into seven equally spaced lines (splitting(obsd) = 3.5 G = 9.8 MHz); six satellite lines from coupling with ^{95}Mo and ^{97}Mo (splitting (obsd) = 37.3 G) are also observed.[11] The spectrum persists over several days of standing at room temperature.

The dibromide, Cp_2MoBr_2, also undergoes Mo(IV) → Mo(V) oxidation at 0.54 V, and a wave of very small current is again noted at about 1.1 V. The $[Cp_2Mo^{V}Br_2]^+$ cation is a beautiful deep blue in acetonitrile (λ_{max} 567 nm). Its ESR spectrum in acetonitrile is more complex than that for the oxidized dichloride. The main line is split into a distorted eight-line pattern (Figure 2). We suggest that this arises from a seven-line pattern, which comes from coupling to two equivalent Br atoms in $[Cp_2Mo^{V}Br_2]^+$ (g_{obsd} = 2.056; splitting(obsd) = 16 G), and an underlying four-line pattern of almost identical splitting arising from $[Cp_2Mo^{V}(NCMe)Br]^{2+}$; the latter ion could come from a reaction competing with eq 2 above, that is, the substitution of Br^- in $[Cp_2Mo^{V}Br_2]^+$.

Costa, Dias, and Pina[10] have recently studied the substitution reactions of neutral and oxidized Cp_2MoBr_2 and have reported the following results.

$$[Cp_2Mo^{V}Br_2]PF_6 \xrightarrow[h\nu,\ \lambda > 390\ nm]{MeCN} [Cp_2Mo^{IV}(NCMe)Br]PF_6 \quad (5)$$

$$[Cp_2Mo^{V}Br_2]PF_6 \xrightarrow[h\nu,\ \lambda > 220\ nm]{MeCN} [Cp_2Mo^{IV}(NCMe)_2](PF_6)_2 \quad (6)$$

$$Cp_2MoBr_2 \xrightarrow[h\nu,\ \lambda > 220\ nm]{MeCN} [Cp_2Mo(NCMe)_2]Br_2 \quad (7)$$

$$Cp_2MoBr_2 \xrightarrow[heat]{MeCN} [Cp_2Mo^{IV}(NCMe)Br]Br \quad (8)$$

Our electrochemical results are in agreement with this series of reactions. We find that the Mo(IV) ion in an authentic sample of $[Cp_2Mo^{IV}(NCMe)Br]^+$ undergoes at least quasi-reversible redox at 1.07 V. Following electrochemical oxidation of Cp_2MoBr_2 (0.96 faraday/mol), the quasi-reversible wave at about 1.1 V is considerably larger in current, and the rereduction of the monocation $[Cp_2Mo^{V}Br_2]^+$ after 75 min involved fewer electrons (0.61 faraday/mol) than we had removed in the original oxidation. If the acetonitrile solution of $[Cp_2MoBr_2]^+$ is stirred for 3 days in vacuo (in normal laboratory illumination) the color fades, and roughly half of the material observable electrochemically is the species giving rise to the 1.1-V wave.[12] In another experiment, we found that about half of unoxidized Cp_2MoBr_2 is converted to the species at 1.1 V if the parent compound is simply stirred in acetonitrile for 3 days (in vacuo, normal laboratory illumination).[12] The other possible product of substitution is $[Cp_2Mo^{IV}(NCMe)_2]^{2+}$. However, we find that an authentic sample of this ion does not give rise to any electrochemistry in the +2 to −1-V range; if it were a product in our experiments, it would not be detected.

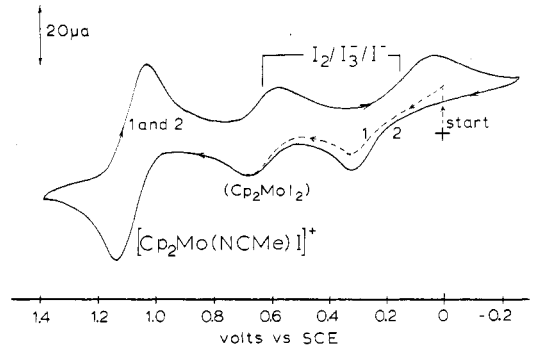

Figure 3. Cyclic voltammogram of Cp_2MoI_2 solution 30 min after controlled potential electrolysis at +0.7 V (CH_3CN containing 0.1 M Bu_4NPF_6; sweep rate = 200 mV/s). Cross indicates position of zero current at zero applied potential. On turning on the potentiostat, a cathodic current was observed. First sweep (1) indicated by a dashed line and second sweep (2) by a solid line. The two less positive waves are assigned to the $I_2/I_3^-/I^-$ system, with some Cp_2MoI_2 contributing to the middle wave.

The diiodides of both molybdenum and tungsten were available and were quite informative. The cyclic voltammogram of Cp_2MoI_2 shows a quasi-reversible wave at 0.54 V and a much smaller wave at 1.1 V (Figure 1). ($[Cp_2WI_2]PF_6$ was similar, having waves at 0.375 and 0.845 V; it is invariably the case that tungsten(V) compounds are reduced at more negative potentials.) Bulk electrolysis at 0.7 v results in the removal of 0.8–0.9 electrons/molecule. We believe the reason the electron count is not more nearly 1 faraday/mol is that some of the Cp_2MoI_2 solvolyzes to $[Cp_2Mo(NCMe)I]^+$. Indeed, stirring an acetonitrile solution of the neutral diiodide in vacuo for 3 days leads to extensive solvolysis to $[Cp_2Mo(NCMe)I]^+$.[13] Loss of I_2 by the oxidized material is more rapid than loss of I^- by the parent in the presence of normal laboratory illumination. We estimate the half-life of $[Cp_2Mo^{V}I_2]^+$ to be less than 60 min in acetonitrile, while the tungsten analogue is somewhat more −1 V its half-life being about 75 min.

As noted above, the ultimate products of reductive elimination from $[Cp_2Mo^{V}I_2]^+$ are $[Cp_2Mo^{IV}(NCMe)I]^+$ and I_2. It is the monosolvent cation that is responsible for the redox wave at about 1.1 V, while I_2 is largely responsible for the two less positive waves seen in Figure 3.[14] That it is in fact I_2 that is in solution and not I^- was proved by comparing the voltammetric behavior of I_2 and an authentic iodide salt in acetonitrile.[13]

As an adjunct to this study of the dihalides, we have examined the cyclic voltammetric behavior of complexes of the type $[Cp_2MLX]PF_6$ (see Table I). It is important to notice that, for L = various nitriles, M = Mo, and X =

(11) Our esr results are in essential agreement with a previous study of compounds of the type Cp_2MX_2 (M = Mo, W): W. E. Lindsell, *J. Chem. Soc., Dalton Trans.* 2548 (1975).

(12) Br_2 is a product of reactions 5 and 6, while Br^- is a product of reactions 7 and 8. Both Br_2 and Br^- have two-wave cyclic voltammograms, neither wave being reversible [$E_{pa}(1)$ = +0.8 V and $E_{pa}(2)$ = +1.1 V]. After either Cp_2MoBr_2 or $[Cp_2MoBr_2]^+$ was allowed to stir in acetonitrile, the wave at about 0.8 V was clearly visible.

(13) Solvolysis of Cp_2MoI_2 gives I^- and $[Cp_2Mo(NCMe)I]^+$, whereas reductive elimination from $[Cp_2MoI_2]^+$ should give I_2 and $[Cp_2Mo(NCMe)I]^+$. Both I_2 and I^- give rise to a two-wave cyclic voltammogram under steady-state cycling conditions in acetonitrile. (Wave 1: E_{pa} = 0.3 V and E_{pc} = 0.1 V. Wave 2: E_{pa} = 0.7 and E_{pc} = 0.55 V. See Figures 3 and 4.) One can differentiate I^- and I_2 in solution by setting the potentiostat at 0 V and observing the current when the potentiostat is activated. A cathodic current indicates the presence of I_2, whereas no current flow at this potential is characteristic of a solution containing I^-. This procedure showed that I_2 was a product of the oxidation of Cp_2MoI_2, whereas I^- came from the solvolysis of Cp_2MoI_2 or from its reduction (Figure 4).

(14) The more positive wave of the $I_2/I_3^-/I^-$ system is of lower current than the less positive wave. Since the current represented by the two less positive waves in Figure 3 are not quite in this ratio, this indicates that some $[Cp_2MoI_2]^+$ remains in solution.

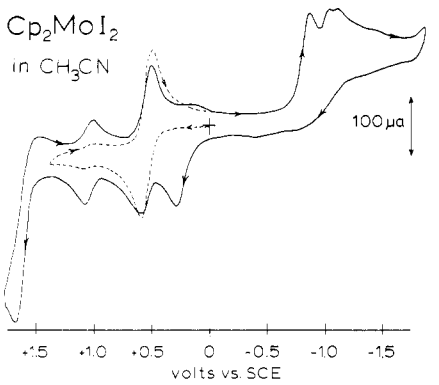

Figure 4. Cyclic voltammogram for Cp_2MoI_2 in CH_3CN containing 0.1 M Bu_4NPF_6. Sweep rate was 500 mV/s. Initial sweep, which started at 0 V, is indicated by a dashed line.

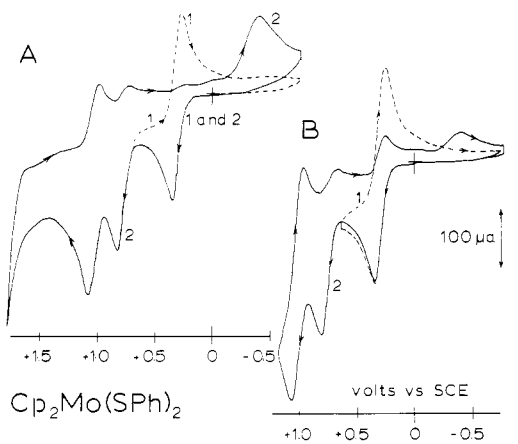

Figure 5. Cyclic voltammogram for $Cp_2Mo(SPh)_2$ in CH_3CN with 0.1 M Bu_4NPF_6 (sweep rate = 500 mV/s). Initial sweep, toward positive potentials, started at 0 V. Numbers 1 and 2 indicate first and second sweeps, respectively. A and B compare the effect of switching potential on the cathodic currents at E_{pc} +0.26 and −0.35 V.

I, all of the compounds undergo quasi-reversible redox in the range 1.1 ± 0.1 V (in general $E_{pa} - E_{pc}$ = 80–100 mV; I_a/I_c = 1).

The reduction of the dicyclopentadienylmolybdenum dihalides was not as thoroughly studied as their oxidation. However, we did note that, if Cp_2MoI_2 was reduced by sweeping past the two irreversible, cathodic waves at E_{pc} = −0.88 and −1.07 V, I^- was a product of the reduction (see Figure 4).[13] It is also interesting that the ion $[Cp_2Mo(NCMe)I]^+$ was also apparently a product. Similar results were obtained with Cp_2MoBr_2. The only analogous compounds studied have been Cp_2TiCl_2[15] and Cp_2VCl_2.[16] In both cases, two-electron reduction led to loss of Cl^-.

One final interesting feature of the dihalide electrochemistry is the relative insensitivity of the $[Cp_2MX_2]^+/Cp_2MX_2$ reduction potential to the nature of the halide. This is presumably owing to the fact that the HOMO in Cp_2MX_2 (M = Mo, W), that is, the MO involved in the redox process, is a relatively nonbonding, metal-based orbital.[17]

The Oxidative Electrochemistry of Dicyclopentadienyl Dithiolates $Cp_2M(SR)_2$ (M = Mo, W). The

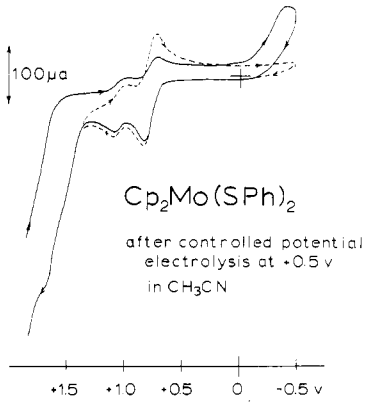

Figure 6. Cyclic voltammogram of $Cp_2Mo(SPh)_2$ solution after controlled potential electrolysis at +0.5 V (CH_3CN containing 0.1 M Bu_4NPF_6; sweep rate = 500 mV/s). Initial voltage sweep indicated by dashed line.

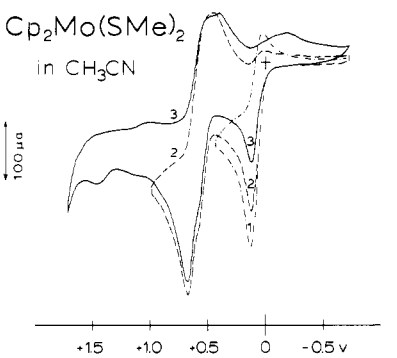

Figure 7. Cyclic voltammogram of $Cp_2Mo(SMe)_2$ in CH_3CN containing 0.1 M Bu_4NPF_6 (sweep rate = 500 mV/s). Numbers 1, 2, and 3 indicate first, second, and third sweeps, respectively.

electrochemistry of the compounds listed in Table II was investigated in acetonitrile with tetrabutylammonium salts as supporting electrolytes. Their oxidative electrochemistry is considerably more complex than that of the dihalides, and, in spite of having done a large number of experiments, we have as yet come to only a partial understanding of the result of mono- and dioxidation of compounds of the type $Cp_2M(SR)_2$. What follows is an account of the results obtained and our tentative interpretations.

Because their patterns are representative of the oxidative electrochemistry of the metal dithiolates, the voltammograms of $Cp_2Mo(SPh)_2$ and $Cp_2Mo(SMe)_2$ are illustrated in Figures 5–7. All of the compounds exhibited redox processes of varying current and reversibility in the following approximate ranges: (1) 0–0.4 V, (2) 0.5–0.8 V, (3) 0.9–1.1 V; additional minor products waves were also observed. The molybdenum thiophenol was the most thoroughly studied and is described first.

The reversibility of the first oxidation of $Cp_2Mo(SPh)_2$ [$E_{p/2}$ = +0.31 V] was found to depend on the switching potential. If the potential sweep was switched at about 0.7 V, or less, the I_a/I_c ratio was nearly 1, and $E_{pa} - E_{pc}$ was about 90 mV, both observations suggesting at least quasi-reversible behavior. However, no matter what the sweep rate, once the potential reached E_{pa} (+0.81 V) for the second, irreversible oxidation, the first wave no longer had a current ratio of 1. One implication of this observation is that the product of the second oxidation rapidly decomposed (in an EEC process) and depleted the diffusion layer of all $Cp_2M(SR)_2$ species. Another implication is that the product of the second oxidation reacted with the parent compound in an irreversible manner.

(15) N. El Murr, A. Chaloyard, and J. Tirouflet, *J. Chem. Soc., Chem. Commun.*, 446 (1980) and references therein; see also A. Chaloyard, A. Dormond, J. Tirouflet, and N. El Murr, *ibid.*, 214 (1980).

(16) J. D. L. Holloway and W. E. Geiger, Jr., *J. Am. Chem. Soc.*, **101**, 2038 (1979).

(17) J. W. Lauher and R. Hoffmann, *J. Am. Chem. Soc.*, **98**, 1729 (1976).

Table I. Electrochemical Data for Cp_2MX_2 and Cp_2MXL^+ (M = Mo, W; X = Cl, Br, I; L = NCR, PPh_3, py)[a]

compd	E_{pa}, V	E_{pc}, V	$E_{pa} - E_{pc}$, mV	$E_{p/2}$, V	faraday/mol (V of bulk electrolysis)	comments
			Molybdenum Compounds			
Cp_2MoCl_2		−1.45				reduction is totally irreversible
	0.56	0.47	90	0.51	0.98 (0.7)	oxidized solution is red; λ_{max} 482 nm
	1.13	1.04	90	1.08		only a trace of this wave observed in CV of fresh solution; after 16 h in vacuo current of this wave is approximately equal to that of the $E_{p/2}$ = 0.51 V wave.
Cp_2MoBr_2		−1.18				reduction is totally irreversible
	0.59	0.49	100	0.54	0.98 (0.7)	oxidized solution is blue; λ_{max} 567 nm
	1.12	1.05	70	1.09		
Cp_2MoI_2		−0.88				see Figures 1, 3, and 4.
		−1.07				reduction is totally irreversible
	0.61	0.51	100	0.56	0.89 (0.75)	half-life for conversion of $[Cp_2MoI_2]^+$ to $[Cp_2Mo(NCMe)I]^+$ is less than 60 min
	1.10	1.04	60	1.07		
$[Cp_2MoBr(NCMe)]^+$	1.11	1.03	80	1.07		
$[Cp_2MoI(NCPh)]^+$	1.12	1.01	110	1.07		
$[Cp_2MoI(NCPh\text{-}Ph)]^+$	1.09	1.01	80	1.05		
$[Cp_2MoI(NCPhBr)]^+$	1.11	1.01	100	1.06		
$[Cp_2MoBr(py)]PF_6$	1.03	0.93	100	0.98		
$[CP_2MoI(PPh_3)]PF_6$	1.04	0.96	80	1.00		
			Tungsten Compounds			
$[Cp_2WCl_2]PF_6$	0.34	0.27	70	0.305		
$[Cp_2WI_2]PF_6$	0.41	0.34	70	0.375		cathodic waves also observed at −1.6 and −1.75 V; half-life for transformation to $[Cp_2WI(NCMe)]^+$ is about 75 min at room temperature
	0.88	0.81	70	0.845		
$[Cp_2WI(py)]PF_6$	0.82	0.75	70	0.785		

[a] All electrochemical data were obtained in CH_3CN containing 0.1 M Bu_4NPF_6 and are referenced to a calomel electrode saturated with NaCl. The sweep rate commonly employed was 200 mV/s. The temperature was 23 ± 2 °C. Unless noted otherwise, I_a/I_c for observed waves was approximately 1. Solute concentration was generally 1 mM.

The anodic current of the second oxidation wave was approximately equal to the anodic current of the first oxidation wave, but the second was clearly irreversible. Since the first oxidation wave represents a one-electron process (see below), the second wave therefore represents the irreversible dioxidation of the original compound to give $[Cp_2Mo(SPh)_2]^+$ which then decays in some manner, at least one product of the decay being the species responsible for the third wave at $E_{p/2}$ = +1.07 V.

If the potential sweep was reversed at any point after passing through the irreversible wave at E_{pa} = +0.81 V, a cathodic wave at E_{pc} = −0.38 V was observed, and it was especially visible on sweeping to about +1.75 V. Bond and co-workers, who thoroughly studied the electrochemistry of compounds of the type $[MO(SR)_4]^-$ (M = Mo, W), observed a similar wave and assigned it to the reduction of hydrogen ions, these ions being a product of a radical reaction with solvent, supporting electrolyte or adventitious water.[18] Bond also observed, and we confirm, that this wave is a product of the irreversible oxidation of PhSSPh at +1.75 V.

When $Cp_2Mo(SPh)_2$ was electrochemically oxidized (at E < +0.7 V) in a cell in the cavity of an ESR spectrometer, the Mo(V) cation $[Cp_2Mo^V(SPh)_2]^+$ was generated. The spectrum consists of a central line (g = 2.0080) with six satellite lines arising from coupling with ^{95}Mo and ^{97}Mo ($I = {}^5/_2$) (observed line separation = 27.5 G = 77.3 MHz). When the potentiostat was turned off, the signal decayed with a half-life estimated to be about 6 min; the decay was first-order in $[Cp_2Mo(SPh)_2]^+$. Thus, the Mo(V) cation decays to one or more ESR silent species, one of which is $[Cp_2Mo(SPh)(NCMe)]^+$ as described below.

Following bulk oxidation of $Cp_2Mo(SPh)_2$ at +0.55 V (1 faraday/mol; the solution changes from amber to purple to yellow-green to yellow), the cyclic voltammogram in Figure 6 was observed. A new electroactive species, having a reversible redox reaction, was seen at almost exactly the same potential as the second irreversible wave for the parent.[19] The species responsible for the third wave was still observed, and a new irreversible wave appeared at about +1.7 V. This latter wave is the same as that seen in the electrochemistry of PhSSPh and is apparently due to $PhSSPh \rightarrow [PhSSPh]^+ + e^-$.[18] The cathodic wave at −0.38 V was especially prominent if the sweep was reversed at E > +1.7 V, a feature seen in the oxidation of PhSSPh.

The tungsten analogue of $Cp_2Mo(SPh)_2$ exhibited a three-wave pattern similar to that of the molybdenum compounds. However, the middle wave for $Cp_2W(SPh)_2$ (at $E_{p/2}$ = +0.69 V) was considerably more reversible for W–SPh than for Mo–SPh, and the final wave at $E_{p/2}$ = 1.00 V represented less current relative to the first wave than in the Mo–SPh case. Upon bulk oxidation of $Cp_2W(SPh)_2$ at 0.4 V, the solution color changed from light green to dark purple, and 0.91 faraday/mol was observed; the cyclic voltammogram following bulk oxidation was unchanged from that observed for the neutral parent. If the oxidized solution was then reduced at 0.0 V, 0.81 faraday/mol was required, indicating that the tungsten(V) ion, $[Cp_2W^V(SPh)_2]^+$, is relatively more stable than the mol-

(18) J. R. Bradbury, A. F. Masters, A. C. McDonell, A. A. Brunette, A. M. Bond, and A. G. Wedd, *J. Am. Chem. Soc.*, **103**, 1959 (1981).

(19) W. L. Bowden, J. D. L. Holloway, and W. E. Geiger, Jr., *Inorg. Chem.*, **17**, 256 (1978). These authors observed a very similar situation in the reduction of $Pt(sacsac)_2$. That is, reduction of the parent complex resulted in a chemical reaction which gave a new species which was reduced at the same potential as the *second* reduction potential of the parent compound.

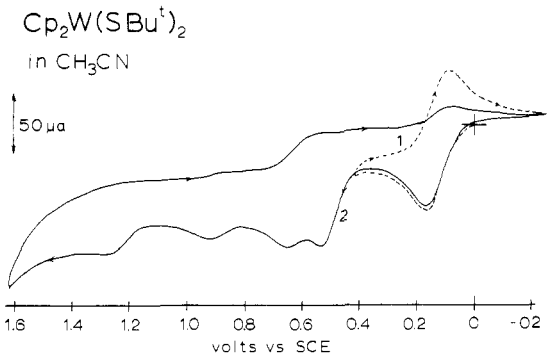

Figure 8. Cyclic voltammogram of $Cp_2W(S\text{-}t\text{-}Bu)_2$ in CH_3CN containing 0.1 M Bu_4NPF_6 (sweep rate = 200 mV/s).

ybednum analogue. In general, we observe that tungsten compounds have more negative reduction potentials and the oxidized species are kinetically more stable than their molybdenum counterparts.

When the $Cp_2W(SPh)_2$ solution described above was reoxidized, this time at 0.86 V, 1.74 faradays/mol passed (giving a yellow solution), and the cyclic voltammogram showed only the presence of the species having $E_{p/2}$ = 1.00 V. This latter species was relatively stable as suggested by the observation that oxidation of the yellow solution at 1.1 V (passing 1.07 faradays) gave rise to a dark red solution; when this red solution was reduced the color changed back to yellow, and 0.54 faraday was required.

The tungsten *tert*-butyl thiolate, $Cp_2W(S\text{-}t\text{-}Bu)_2$, was especially useful in helping to develop some understanding of the electrochemistry of the metal dithiolates (Figure 8). Two distinct waves were observed in the 0.5–0.7-V region, whereas only one was generally observed in this region for all other compounds. [An exception is $Cp_2Mo(SMe)_2$ where there is also evidence for two waves in this region; see Figure 7.] The first of these waves (E_{pa} = 0.51 V) was ascribed to the dioxidation of the parent compound, whereas the second must arise from a product of the one-electron oxidation of the parent. This must be the case since, when $Cp_2W(S\text{-}t\text{-}Bu)_2$ is bulk oxidized at 0.3 V (0.97 faraday/mol observed), the waves for the parent and the species at 0.51 V disappear (as does the wave at 0.87 V, thereby suggesting this was a product of the one-electron oxidation of the parent), leaving only the wave at 0.64 V.

The methyl thiolate $Cp_2Mo(SMe)_2$ once again has a wave that is at least quasi-reversible in the range 0–0.5 V, apparently two waves in the region 0.5–0.7 V, the suggestion of a process at +1 V, and a fourth wave at about +1.45 V (Figure 7). Again, the cathodic process at −0.38 V was observed if the voltage sweep was more positive than 0.5 V. With some variation in complexity and reversibility of the process or processes at 0.5–0.7 V, and the significance of a process in the region around +1.5 V, this basic pattern was observed for all the compounds $Cp_2M(SR)_2$ (M = Mo, W) when R was an alkyl group. Only when R was phenyl was the redox wave in the 0.9–1.1-V range of significant current.

Bulk oxidation of $Cp_2Mo(SMe)_2$ at 0.4 V led to loss of 1 electron/molecule and the total disappearance of the parent. In contrast, following the controlled potential electrolysis of $Cp_2W(SMe)_2$ at 0.25 V (1 faraday/mol), the three-wave pattern persisted. The middle wave of the $Cp_2W(SMe)_2$ voltammogram was seemingly more reversible (presumably owing to the presence of a new species arising from the decay of the oxidized parent where the new species has an E_{pa} the same as E_{pa} for dioxidation), and the third wave at 0.94 V displayed a greater relative current. An irreversible process was observed at about 1.5

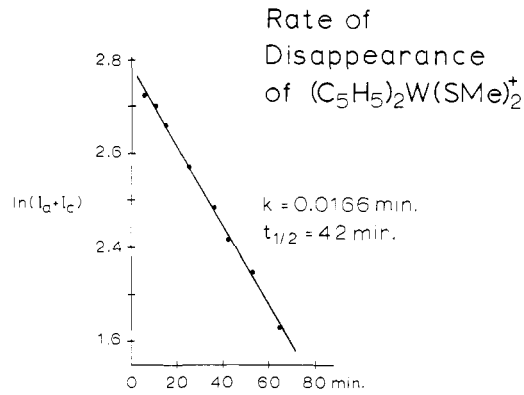

Figure 9. Variation of the current of the −0.01-V redox wave of $[Cp_2W(SMe)_2]^+$ as a function of time. The current is plotted at the ln of the sum of the anodic and cathodic currents. Sample was dissolved in CH_3CN and contained 0.1 M Bu_4NPF_6.

V. Since a similar process was observed for $Cp_2Mo(SMe)_2$ (see also the wave at ~+1.3 V in Figure 8) and is in a region appropriate for the oxidation of MeSSMe, it seems likely that this disulfide is a product of $Cp_2M(SMe)_2$ oxidation, just as PhSSPh was observed in the case of $Cp_2Mo(SPh)_2$.

The decay of the tungsten(V) ion $[Cp_2W(SMe)_2]^+$ was followed for approximately 2 h after controlled potential electrolysis by observing the change in peak current. The disappearance of this species followed first-order kinetics with a rate constant of 0.062 min^{-1} mol^{-1} and a half-life of about 40 min at 22 °C (Figure 9). When the ion had virtually disappeared, there remained approximately equal amounts of the species giving rise to the second ($E_{p/2}$ = 0.54 V) and third ($E_{p/2}$ = 0.85 V) redox waves. Thus, one-electron oxidation of the parent leads to the formation of at least one, if not two, new materials.

The molybdenum thiophenol $Cp_2Mo(SPh)_2$ was chemically oxidized in order to attempt to isolate some of the reaction products. When oxidized with ferricenium ion in CH_3CN, the isolated material was $[Cp_2Mo(SPh)(NCMe)]PF_6$; this species gave rise to a reversible couple at 0.81 V (Table II), a potential identical with that observed for one of the products which appear following controlled potential oxidation of $Cp_2Mo(SPh)_2$ in acetonitrile at 0.5 V. [Notice in Table II that other compounds of the type $[Cp_2Mo(SR)L]^+$ (L = NH_3 when R = *t*-Bu and L = PPh_3 when R = Ph) have redox potentials in this range.] Thus, it is our contention that the wave or waves seen in the range 0.5–0.7 V in all of the cyclic voltammograms of the compounds studied is due to the following:[19] the second, one-electron oxidation of the parent compound

$$[Cp_2M(SR)_2]^+ \rightleftarrows [Cp_2M(SR)_2]^{2+} + e^- \quad (9)$$

and/or the oxidation–reduction of the ion $[Cp_2M^{IV}(SR)(NCMe)]^+$ which arises from decay of the mono-oxidized parent

$$[Cp_2M^{IV}(SR)(NCMe)]^+ \rightleftarrows [Cp_2M^{V}(SR)(NCMe)]^{2+} + e^- \quad (10)$$

If the ferricenium oxidation of $Cp_2Mo(SPh)_2$ was carried out in CH_2Cl_2, on the other hand, a yellow-brown solid was isolated which had an analysis corresponding to $[Cp_4Mo_2(SPh)_4](PF_6)_2$ and an NMR spectrum appropriate for a thiolate-bridged dimer of the type $[Cp_2Mo(\mu\text{-}SPh)_2MoCp_2]^{2+}$. Just as importantly, this same material was isolated upon photolysis of $[Cp_2Mo(CO)(SPh)]PF_6$ in CH_2Cl_2 (eq 11). Although thiolate-bridged dimers have

$$2[Cp_2Mo(CO)(SPh)]PF_6 \xrightarrow{h\nu} [Cp_2Mo(\mu\text{-}SPh)_2MoCp_2](PF_6)_2 + 2CO \quad (11)$$

Table II. Electrochemical Data for $Cp_2M(SR)_2$ (M = Mo, W)[a-c]

compd	E_{pa}	E_{pc}	$E_{pa} - E_{pc}$, mV	$E_{p/2}$, V	faradays/mol (V of electrol)	comments
			Molybdenum Compounds[d]			
$Cp_2Mo(SMe)_2$	0.13	−0.03	100	0.08	1.0 (0.4)	wave disappears after bulk electrolysis at 0.4 V
	0.69	0.55				two overlapping waves; E_{pc} ill-defined; see Figure 7
	1.13	1.06	70	1.09		small I relative to $E_{p/2}$ = 0.08 V; I increases after bulk oxidation at 0.4
$Cp_2Mo(S\text{-}n\text{-}Pr)_2$	0.092	0.024	68	0.058	0.82 (0.25)	I_a/I_c = 1 if switching potential is less than about 0.5 V; oxidized solution is orange
	0.67					totally irreversible; no third wave observed
$Cp_2Mo(S\text{-}i\text{-}Pr)_2$	0.20	0.08	120	0.14	1.03 (0.4)	I_a/I_c = 1 if switching potential is less than about 0.6 V; wave disappears after bulk oxidation at 0.4
	0.76	0.66	100	0.71		I_a/I_c only slightly less than 1
	1.17	1.10	70	1.14		only observed (but with I less than I for 0.71-V wave) after bulk oxidation at 0.4 V
$Cp_2Mo(S\text{-}t\text{-}Bu)_2$	0.28	0.20	80	0.24	1.01 (0.5)	I_a/I_c = 1 if switching potential is less than about 0.6 V
	0.79	0.7 (?) 0.65 (?)				before bulk oxidation at 0.5 V: two cathodic waves observed; total I_c is only slightly less than I_a
	0.83	0.70	130	0.77		after bulk oxidation at 0.5 V: cathodic wave is now clean
$[Cp_2Mo(NH_3)S\text{-}t\text{-}Bu]^+$	0.67	0.54	130	0.61	2.06 (0.7)	new wave at about $E_{p/2}$ = 0.2 V after bulk electrolysis
			Before Bulk Electrolysis at 0.5 V (see Figure 5)			
$Cp_2Mo(SPh)_2$	0.35	0.26	90	0.31	1.03 (0.5)	I ratio is about 1 if switching potential is ≤0.7 V
	0.81					no cathodic wave
	1.07	0.99	80	1.04		
			After Bulk Electrolysis at 0.5 V (see Figure 6)			
	0.41	0.30	110	0.36		
	0.85	0.78	70	0.82		I_a/I_c about 1
	1.11	1.03	80	1.07		
$[Cp_2Mo(NCMe)SPh]^+$	0.86	0.76	100	0.81	1.10 (0.9)	color changes from orange to blue-green on oxidation
$[Cp_2Mo(PPh_3)SPh]^+$	0.90	0.80	100	0.85		
$Cp_2Mo(SC_7H_{15})_2$	0.09	0.01	80	0.05		I ratio is 1 if switching potential is less than about 0.4 V
	0.76					no cathodic wave
			Tungsten Compounds[e]			
			Before Bulk Oxidation at 0.25 V			
$Cp_2W(SMe)_2$	0.04	−0.05	90	−0.01	1.01 (0.25)	
	0.59					I_a about equal to I_a of first wave
	0.98	0.90	80	0.94		small current relative to first two waves
			18 h After Bulk Electrolysis at 0.25 V			
$Cp_2W(SMe)_2$	0.64	0.54	100	0.59		note that wave at $E_{p/2}$ = −0.01 V has disappeared; unlike second wave in initial solution, wave at 0.59 V is reversible
	0.94	0.85	90	0.90		
			Before Bulk Oxidation at 0.3 V (see Figure 8)			
$Cp_2W(S\text{-}t\text{-}Bu)_2$	0.16	0.09	70	0.12	0.97 (0.3)	I ratio is 1 if switching potential is less than 0.4 V; on oxidation, solution goes from yellow to dark green to yellow-green
	0.51					no cathodic wave
	0.64					poorly defined cathodic wave
	0.87					no cathodic wave
			After Bulk Electrolysis at 0.3 V			
	0.67	~0.55	~120	0.61		E_{pc} poorly defined; wave at 0.12 V has disappeared
$Cp_2W(SC_5H_{11})_2$	0.00	−0.07	70	−0.04	0.8 (0.2)	I ratio is 1 if switching potential is less than about 0.4 V; oxidized solution is green-brown
	0.58					no cathodic wave before or after bulk oxidation at 0.2 V
	1.05	0.97	80	1.01		current ratio is about 1
$Cp_2W(SPh)_2$	0.28	0.18	100	0.23	0.91 (0.4)	I ratio is 1 if switching potential is less than 0.6 V; on oxidation solution goes from light green to dark purple

Table II (*Continued*)

compd	E_{pa}	E_{pc}	$E_{pa} - E_{pc}$, mV	$E_{p/2}$, V	faradays/mol (V of electrol)	comments
	0.74	0.64	100	0.69		*I* ratio is about 0.9
	1.04	0.95	90	1.00		

[a] All electrochemistry performed in CH_3CN containing 0.1 M Bu_4NPF_6. Potentials are referenced to a calomel electrode containing a saturated sodium chloride solution. E_{pa} and E_{pc} are in V vs. SCE. Sweep rates of 200 or 500 mV/s were commonly used, and the temperature was 23 ± 2 °C. Solution concentration was generally about 1 mM. [b] Unless noted otherwise, I_a/I_c was about 1 for all waves observed. [c] All compounds underwent irreversible reduction in the range −1 to −2 V. [d] When R = alkyl, all molybdenum compounds had an anodic wave in the region +1.4 to +1.7 V and a cathodic wave at about −0.35 V before controlled potential, one-electron oxidation. (For R = phenyl, the +1.7-V wave was observed only after controlled potential oxidation.) The cathodic wave was generally dependent on switching potential and scan rate, the wave being prominent if the switching potential was > +1.5 V and for scan rates > 200 mV/s. [e] An irreversible anodic wave at +1.2 to +1.7 V and a cathodic wave at about −0.3 V were seen for all tungsten compounds after controlled potential, one-electron oxidation.

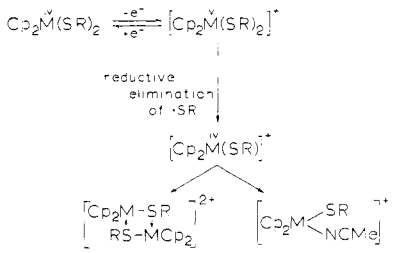

Figure 10. A possible scheme for the reactions following one-electron oxidation of $Cp_2M(SR)_2$ in CH_3CN.

been observed in group 6B chemistry,[20] the suspected dimer isolated herein is of a type not yet observed.) The yellow-brown solid was poorly soluble in CH_3CN, so its electrochemistry was not cleanly defined in this solvent. However, there was a quasi-reversible wave at about +1 V, a wave of smaller current at E_{pa} = +0.8 V, and a multielectron wave at a potential >+1.5 V. While this does not completely correspond to the species responsible for the most anodic wave in $Cp_2Mo(SPh)_2$, we believe that an ion such as $[Cp_2Mo^{IV}(\mu\text{-}SPh)_2Mo^{IV}Cp_2]^{2+}$ is a candidate.

Any reaction scheme devised to account for the oxidative electrochemistry of the dicyclopentadienylmetal dithiolates should agree with the following observations and requirements. (i) Initial oxidation is apparently metal based and not ligand based. (ii) The isolated products are a monosolvent ion, $[Cp_2M^{IV}(SR)(NCMe)]^+$, and possibly a dimer of the type $[Cp_2M^{IV}(\mu\text{-}SR)_2M^{IV}Cp_2]^{2+}$ (although this dimer was found only on reaction in the noncoordinating solvent CH_2Cl_2). (iii) In order to leave the metal ion in the +4 oxidation state in the product ions, the initial one-electron oxidation must be followed by a reductive elimination of ·SR; such radicals are the source of the observed disulfide. (iv) Preliminary experiments indicate that the decay of the one-electron oxidation product, $[Cp_2M(SR)_2]^+$, is first order in the ion.

One possible scheme to account for the reactions following one-electron oxidation is outlined in Figure 10. In this scheme $[Cp_2M^V(SR)_2]^+$ reductively eliminates ·SR in a reaction similar to that of the dihalides. (In this connection it is important to note that Bond and co-workers have observed the reductive elimination of ·SR (with subsequent formation of RSSR) on oxidation of $[MoO(SR)_4]^-$ (R = phenyl and benzyl),[18] and other examples have been reported.[21]) The product of elimination, $[Cp_2M(SR)]^+$, could add a molecule of solvent or couple with another such ion to form a thiolate-bridged dimer. As noted in the case of $Cp_2W(SMe)_2$ above and in most other cases, the species giving rise to the most anodic wave (in the region 0.9–1.1 V), as well as that responsible for the middle wave, was, at least in part, a product of the first one-electron oxidation of the parent. As noted above, a dimer seems a reasonable possibility for the wave in the region 0.9–1.1 V, but other ions or molecules must also be considered.

We can only speculate about the consequences of the second, one-electron oxidation. If this step is ligand based, a reaction, eq 12, between the resulting cation radical and

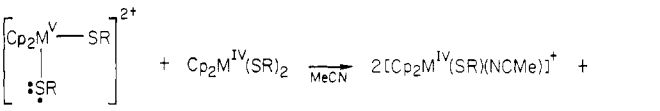

RSSR (12)

the parent compound would give the observed monosolvent ion. Such a reaction is one way to account for the observation tht the cathodic current for the reduction of $[Cp_2M^V(SR)_2]^+$ (see Figures 5 and 7) is severely reduced if the potential for the second oxidation is exceeded. Alternatively, coupling of two ligand radicals could lead to an ion with a bridging disulfide (eq 13), a reaction sim-

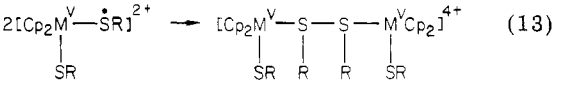

(13)

ilar to that observed by Treichel and Rosenhein[22] for the ion from the one-electron oxidation of CpFe(CO)(L)SPh. They found that, when L was a phosphine, the monomeric cation radical $[CpFe(CO)(L)SPh]^+$ and the dimer $[CpFe(CO)(L)(\mu\text{-}PhSSPh)(L)(CO)FeCp]^{2+}$ were in equilibrium; when L was CO, in contrast, the dimer decomposed to $[CpFe(CO)_2(PhSSPh]^+$ and $[CpFe(CO)_2(NCMe)]^+$ in acetonitrile. A similar reaction could occur on dioxidation of $Cp_2M(SR)_2$, but we currently have no direct evidence for this possibility.

If the second, one-electron oxidation is metal based, giving $[Cp_2M^{VI}(SR)_2]^{2+}$, reductive elimination of RSSR

(20) F. Y. Petillon, J. L. le Quere, and J. E. Guerchais, *J. Organomet. Chem.*, **204**, 207 (1981) and references therein; I. B. Benson, S. D. Killops, S. A. R. Knox, and A. J. Welch, *J. Chem. Soc., Chem. Commun.*, 1137 (1980).

(21) Reductive elimination of RSSR was previously proposed as the key to the formation of thiolate-bridged dimers of group 6B metals according to the equation

$$2MCl_x(SR)_y \rightarrow M_2Cl_{2x}(SR)_{2y-2} + RSSR$$

P. R. Boorman, T. Chivers, K. N. Mahadev, and B. D. O'Dell, *Inorg. Chim. Acta*, **19**, L35 (1976); see also P. M. Boorman, V. D. Patel, K. A. Kerr, P. W. Codding, and P. Van Roey, *Inorg. Chem.*, **19**, 3508 (1980).

(22) P. M. Treichel and L. D. Rosenhein, *J. Am. Chem. Soc.*, **103**, 691 (1981).

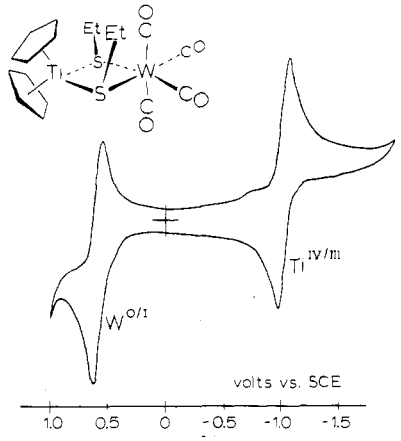

Figure 11. Cyclic voltammogram of $Cp_2Ti(SEt)_2W(CO)_4$ in CH_2Cl_2. The solution was also 0.1 M in Bu_4NPF_6; sweep rate = 200 mV/s.

would give $[Cp_2M^{IV}]^{2+}$, and this ion could couple with $Cp_2M^{IV}(SR)_2$ to provide the thiolate-bridged dimer. Such a reaction apparently occurs on combining $Cp_2Ti(CO)_2$ and $Cp_2Ti(SR)_2$.[23]

$$Cp_2M^{IV}(SR)_2 \rightarrow [Cp_2M^{VI}(SR)_2]^{2+} + 2e^-$$

$$Cp_2M^{VI}(SR)_2]^{2+} \rightarrow [Cp_2M^{IV}]^{2+} + RSSR$$

$$[Cp_2M^{IV}]^{2+} + Cp_2M^{IV}(SR)_2 \rightarrow [Cp_2M^{IV}(\mu\text{-}RSSR)M^{IV}Cp_2]^{2+} \quad (14)$$

The Electrochemistry of Complexes of Dicyclopentadienylmetal Dithiolates. Numerous complexes of the group 6B metal dithiolates have been synthesized; examples include compounds such as III and IV. We were of course interested in the influence of complexation on the electrochemistry at the molybdenum and tungsten atoms or at the coordinated metal. Although our survey of the electrochemistry of the metal dithiolates was far from comprehensive, we generally observed irreversible behavior. For example, complex III shows completely irreversible waves at +0.6 V and 1.2 v (sweep rate = 200 mV/s). Thus, one of our goals of oxidizing the ligand metal and observing the reactions at the coordinated metal, especially catalytic reactions, was thwarted.

In contrast, the group 6B metal carbonyl complexes of the titanium(IV)-based ligand $Cp_2Ti(SR)_2$ (II) displayed quasi-reversible electrochemistry at both the Ti(IV) and M(0) (M = Cr, Mo, W) sites (see Figure 11, for example). By comparison with the free ligands and compounds such as Cp_2TiCl_2, we know that the reduction potential for the Ti(IV) center is in the range −0.5 to −1.0 V. Thus, we assign the wave at −1.03 V to the process Ti(IV) ⇄ Ti(III). Unfortunately, reducing these complexes at room temperature and at potentials more negative than the reduction potential resulted in the uptake of a number of electrons and destruction of the complex. The redox wave at more positive potentials (+0.63 V for M = W and R = Et) is ascribed to oxidation of M(0). This can be assigned with assurance, since complexes such as $L_2M(CO)_4$ (M = Cr, Mo) and the group 6B dicyclopentadienylmetal dithiolates all oxidize in the range 0 to +1.2 V.[7,24] Once again, it is unfortunate that bulk oxidation results in destruction of the complex.

Table III. Electrochemical and Spectroscopic Results for Complexes of the Type $Cp_2Ti(SR)_2M(CO)_4$ and Related Materials

R	M	$E_{p/2}$[a] $Ti^{IV/III}$	$E_{p/2}$[a] $M^{I/0}$	λ_{max},[b] nm
Et	Cr	−0.97	0.48	635
	Mo	−1.06	0.65	595
	W	−1.03	0.63	593
Ph	Mo	−0.79	0.73	
	W	−0.76	0.72	
$(EtSC_2H_4SEt)Mo(CO)_4$			0.87	
$(PhSC_2H_4SPh)Mo(CO)_4$			0.94	

[a] All potentials are referenced to a calomel electrode containing a saturated solution of sodium chloride. CH_2Cl_2 solutions were approximately 2 mM in solute and 0.1 M in $Bu_4N^+PF_6^-$. $E_{p/2}$ is the average of the cathodic and anodic potentials of the cyclic voltammetry wave. In all cases, the anodic and cathodic currents in each wave were equal. The working electrode was a 2-mm piece of Pt wire. [b] Spectroscopic data were obtained in toluene.

As seen in Table III, the complexes $Cp_2Ti(SR)_2M(CO)_4$ all exhibited quasi-reversible electrochemistry at both metal sites. A number of interesting points emerge on examining these data. For example, as one might expect, the Ti(IV) ⇄ Ti(III) and M(I) ⇄ M(0) processes occur at more negative potentials for R = Et than for R = Ph, an understandable shift considering the +I effect of the ethyl group.

Relatively few studies have been made of the electrochemical properties of an entire series of group 6B metal complexes. However, from our previous work,[7] and a few other reports,[24] it would appear to be a general observation that Cr(0) complexes oxidize at less positive potentials than their Mo(0) or W(0) counterparts, the latter usually having nearly identical redox potentials. This is of course the trend noted for the complexes in Table III.

Yet another interesting observation is the change in the M(I) ⇄ M(0) potential on going from the simple complex $(RSC_2H_4Sr)_2Mo(CO)_4$ to the titanium dithiolate analogue: the reduction potential for M(I) is less positive [M(0) is easier to oxidize] by 0.2–0.4 V. Although we can speculate on the reasons for this shift in potential, such as the reputed presence of a M(0) → Ti(IV) donor–acceptor bond in these complexes,[4-6] an experimentally supportable rationalization has eluded us.

The Electrochemistry of Diferrocenyldicyclopentadienyltitanium(IV), Cp_2TiFc_2. When the synthesis of the ferrocenyl derivative of titanocene (V) was first published,[8] it seemed to us an unusual molecule. Unlike the vast number of ferrocenyl compounds that are various shades of orange, V was deep green in color. Compounds of the type Cp_2TiR_2 are also most often shades of orange, although a few are in fact green.[25] It occurred to us that, since oxidized ferrocenyl compounds are usually green or blue-green, V could be a mixture of valence isomers $Cp_2Ti^{IV}(Fc^{II})_2$, $Cp_2Ti^{III}(Fc^{III})(Fc^{II})$, or $Cp_2Ti^{II}(Fc^{III})_2$ (in these compounds Fc^{II} denotes a ferrocenyl group wherein the iron is in the +2 formal oxidation state, for example).[26]

We soon found that V has a chemical behavior that contrasts sharply with its phenyl analogue, Cp_2TiPh_2. The latter is apparently stable in air and moisture, but it is thermally and photochemically unstable.[27] In contrast,

(23) G. Fachinetti and C. Floriani, *J. Chem. Soc., Dalton Trans.*, 2433 (1974).

(24) M. K. Lloyd, J. A. McCleverty, D. G. Orchard, J. A. Connor, M. B. Hall, I. M. Hillier, E. M. Jones, and G. K. McEwen, *J. Chem. Soc., Dalton Trans.*, 1743 (1973).

(25) H. Masai, K. Sonogashira, and N. Hagihara, *Bull. Chem. Soc. Jpn.*, 41, 750 (1968).

(26) Considering the reduction potentials of Fe(III) and Ti(III), however, it is clear that very little if any valence isomer such as $Cp_2Ti^{III}(Fc^{III})(Fc^{II})$ is likely.

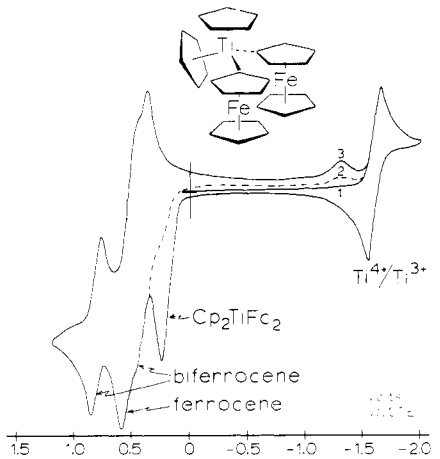

Figure 12. Cyclic voltammogram of $Cp_2Ti[(\eta^5\text{-}C_5H_4)Fe(\eta^5\text{-}C_5H_5)]_2$ in CH_2Cl_2 containing 0.1 M Bu_4NPF_6 (sweep rate = 200 mV/s). The potential was first swept in a cathodic direction (sweep 1), reversed at +0.3 V (dotted line marked 2), and the final sweep covered the entire potential range (sweep 3).

we find that, when exposed to air, Cp_2TiFc_2 is degraded rapidly in solvents such as $CHCl_3$ and CH_2Cl_2 but more slowly in toluene or benzene. Cyclic voltammetry shows that the ferrocenyl derivative is oxidized irreversibly at E_{pa} = +0.25 V (coulometry gives 0.9 faraday/mol) (Figure 12); the irreversibility persisted at the maximum sweep rates available (20 V/sc). As seen in Figure 12, there are also three reversible waves at more anodic potentials. The waves at $E_{p/2} \simeq 0.38$ and 0.78 V are ascribed to one product of the irreversible oxidation of the parent, that is, to biferrocene, while the wave at $E_{p/2} \simeq 0.52$ V is due to another product, ferrocene. (Authentic biferrocene and ferrocene were added to the solution, and an increase in the current under their respective waves was observed.) Finally, if the potential is first swept past the irreversible wave at E_{pa} = +0.25 V, a small wave is observed at E_{pc} = −1.3 V; we ascribe this to an as yet unidentified titanium-containing species.

The following scheme is our rationalization for the electrochemical processes observed in Figure 12. In this scheme we have chosen to use the valence isomer $Cp_2Ti^{IV}(Fc^{II})_2$ as the starting point, but we emphasize that any of the isomers would lead to the same final result; the difference is only a matter of the point of the initial oxidation.

(a) Oxidation of Cp_2TiFc_2 at one ferrocenyl group at E_{pa} = 0.25 V (or oxidation at Ti^{III} in one of the valence isomers):

$$Cp_2Ti^{IV}(Fc^{II})_2 \rightarrow [Cp_2Ti^{IV}(Fc^{III})(Fc^{II})]^+ + e^- \quad (15)$$

(b) Reductive elimination of a ferrocenyl cation radical:

$$[Cp_2Ti^{IV}(Fc^{III})(Fc^{II})]^+ \rightarrow Cp_2Ti^{IV}(Fc^{II}) + Fc^{+}\cdot \quad (16)$$

(c) The observation of ferrocene can be explained if the ferrocenyl cation radical captures an H· from the solvent, electrolyte, or titanium-containing compound.

$$Fc^{+}\cdot + \text{source of H}\cdot \rightarrow FcH^+ \quad (17)$$

(d) Biferrocene can be produced by the reductive elimination of biferricenium ion from the oxidized parent.

$$[Cp_2Ti^{IV}(Fc^{III})(Fc^{II})]^+ \rightarrow [Fc^{III}\text{–}Fc^{II}]^+ + Cp_2Ti^{II} \quad (18)$$

As detailed in the next section, such processes are not uncommon in organometallic chemistry.[28] (Although less likely, it is possible that biferrocene can be produced by coupling of two Fc^+·cation cation radicals from step b above.)

(e) We propose that the biferricenium ion produced in (d), or the ferricenium ion produced in (c), is reduced to the neutral species by a reduced Ti-containing material, Cp_2Ti^{II} for esample, a species which is likely to be a powerful reducing agent.[29] In any event, the ferrocenes are apparently not reduced at the electrode (even though they are produced at a potential appropriate for their reduction). If this were the case, there would be no net current flow on oxidation at +0.25 V; instead, we observed 0.9 faraday/mol.

(f) The most negative redox wave ($E_{p/2}$ = −1.66 V) is most likely the quasi-reversible reduction of the parent $Cp_2Ti^{IV}(Fc^{II})_2$ to $[Cp_2Ti^{III}(Fc^{II})_2]^-$. We might note that the ferrocenyl complex is more difficult to reduce than its phenyl analogue ($E_{p/2}$ = −1.53 V), apparently owing to the +I effect of the ferrocenyl group.

It was pointed out above that Cp_2TiPh_2 is photochemically active, giving Ph· and $[Cp_2TiH]_x$ (and/or other reactive species) upon photolysis in an ESR cavity.[30,31] In contrast, no analogous species were seen when Cp_2TiFc_2 was photolyzed under the same conditions; we have no reason to believe that the ferrocenyl derivative is not indefinitely stable to photolysis.

Summary and Conclusions

From the detailed discussion of the electrochemistry of compounds of the type Cp_2MX_2, several interesting points emerge. The most important of these is that the oxidative electrochemistry of Cp_2MX_2 (M = Mo, W; X = halide, SR) and Cp_2TiFc_2 (V) is governed by an ECE process wherein the original oxidation of the compound gives a species of varying stability, and this oxidized material eventually loses a metal-bound ligand, X, SR, or Fc, to give one or more electrochemically active materials. Especially in the case of Cp_2MX_2 (X = halide, SR), it is clear that X is lost in a reductive elimination reaction which our preliminary evidence suggests is first order in Cp_2MX_2. As such these reactions are excellent examples of oxidatively induced reductive eliminations (or OXIRE), a reaction class broadly important in organometallic chemistry.[9,32,33] Because reductive elimination is an important step in a great many metal-catalyzed reactions, the reductive elimination of groups has been increasingly studied of late, and a number of examples of reductive eliminations that are oxidatively induced have been uncovered. In general, such reactions are of two types: (i) reactions where there is electron abstraction by chemical or electrochemical means; that is, an "outer-sphere mechanism"; (ii) reductive elimination following oxidative addition ("inner sphere mechanism").[9] Some well-defined examples of the first type of reaction are as

$$L_2Ni^{II}(Ar)(R) \xrightarrow{-e^-} [L_2Ni^{III}(Ar)(R)]^+ \rightarrow Ar\cdot + [L_2Ni^{II}(R)]^+ \quad (19)^{34}$$

(27) H. C. Beachell and S. A. Butter, *Inorg. Chem.*, **4**, 1133 (1965).

(28) T. T. Tsou and J. K. Kochi, *J. Am. Chem. Soc.*, **100**, 1634 (1978) and references therein. See also ref 9.

(29) P. C. Wailes, R. S. P. Coutts, and H. Weigold, "Organometallic Chemistry of Titanium, Zirconium, and Hafnium"; Academic Press: New York, 1974.

(30) M. Peng and C. H. Brubaker, Jr., *Inorg. Chim. Acta*, **26**, 231 (1978).

(31) E. Samuel, P. Maillard, and C. Giannotti, *J. Organomet. Chem.*, **142**, 289 (1977).

(32) J. K. Kochi, "Organometallic Mechanisms and Catalysis"; Academic Press: New York, 1978; pp 282, 350.

(33) G. W. Daub, *Prog. Inorg. Chem.*, **22**, 409 (197); see also M. D. Johnson, *Acc. Chem. Res.*, **11**, 57 (1978).

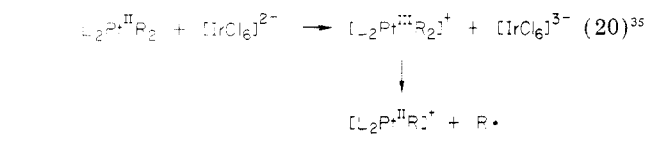

$$CpFe(CO)_2R + 2CuX_2 \rightarrow CpFe(CO)_2X + RX + 2CuX \quad (21)^{36}$$

$$(bpy)_2FeR_2 + Br_2 \rightarrow (bpy)_2FeBr_2 + R\text{-}R \quad (22)^{37}$$

It seems clear that oxidatively induced reductive elimination (OXIRE) of a σ-bound ligand (or ligands) should occur whenever the central metal has a reasonably accessible higher oxidation and if the σ bond is unstable in that higher oxidation state. The mechanisms of such reactions have been thoroughly studied in only a few instances; a great deal is known, for example, about the $CpFe(CO)_2R$ system.[36] However, many more such cases should exist, and our objectives are (i) to search for other, well-defined cases of OXIRE and (ii) to examine in greater detail the mechanism of the $Cp_2M(SR)_2$ class of compounds reported in this paper.

One final point of interest concerns the isolation of a material we suspect to be the thiolate-bridged dimer $[Cp_2Mo(\mu\text{-}SPh)_2MoCp_2]^{2+}$. Such compounds represent a new class of compounds in group 6B chemistry and deserve more careful study. Further, the formation of this material by an OXIRE process suggests that other metal thiolates can be induced to give thiolate-bridged dimers by an oxidatively induced reaction.[21]

Experimental Section

Electrochemical Techniques. The electrochemical instrumentation consisted of a PAR 174 polarographic analyzer, a PAR 175 voltage programmer, and a Hewlett-Packard Moseley 135 X-Y recorder. In coulometry experiments, the number of coulombs passed was determined by graphical integration of the current–time curve or with a PAR 379 digital coulometer.

Potentials were referred to a calomel electrode containing a saturated solution of sodium chloride. A 2-mm piece of Pt wire served as the working electrode for cyclic voltammograms while the working electrode for the coulometry experiments was Pt gauze. The auxiliary electrode in all experiments was a Pt wire coil.

Cyclic voltammetry experiments were done in a PAR polarographic cell or in a three-compartment cell; in the latter, the working electrode compartment was separated from the compartments for auxiliary and reference electrodes by medium porosity glass frits. Unless noted otherwise, all experiments were done at room temperature (23 ± 2 °C).

Solutions were typically 1 mM in solute and 0.1 M in supporting electrolyte, tetrabutylammonium hexafluorophosphate, Bu_4NPF_6. The electrolyte was prepared from Bu_4NBr and KPF_6 (both purchased from Aldrich Chemical Co.) and was recrystallized from ethanol–acetone; it was thoroughly washed with diethyl ether and dried in vacuo. The solvents, CH_3CN and CH_2Cl_2, were reagent grade materials, were dried over P_2O_5, and were distilled before use. Solutions were degassed with dry nitrogen before each experiment, and a nitrogen atmosphere was maintained over the solution during the experiment.

The ESR spectra of electrochemically generated ions were obtained with a Wilmad Glass Co. ESR electrochemical cell equipped with a Pt wire working electrode. Spectra were observed with a Varian E-4 spectrometer.

Chemicals. The following compounds were prepared by published methods: Cp_2MX_2 and $[Cp_2MX_2]PF_6$;[38] $Cp_2M(SR)_2$ (M = Mo, W);[39,40] $[Cp_2Mo(py)Br]PF_6$ and $[Cp_2W(py)I]PF_6$;[41] $Cp_2Ti(SR)_2$, its metal carbonyl complexes, and those of the type $(RSC_2H_4SR)M(CO)_4$;[4] and Cp_2TiFc_2.[8] The group 6B halo nitrile complexes were prepared by the general reaction $Cp_2MX_2 + TlPF_6 + RCN \rightarrow [Cp_2MX(NCR)]PF_6 + TlX$.[42]

In general, Schlenk techniques were used throughout and all reactions were carried out under dry nitrogen or in vacuo.

$[Cp_2Mo(NCMe)SPh]PF_6$. A filtered solution of $[Cp_2Fe]PF_6$[43] (0.35 g, 1.01×10^{-3} mol) in CH_3CN was slowly added to a stirred suspension of $Cp_2Mo(SPh)_2$ (0.45 g, 1.01×10^{-3} mol) in the same solvent at room temperature. After the reaction mixture was filtered, the solvent was removed from the deep red solution in vacuo to leave a red crystalline precipitate. The precipitate was washed with diethyl ether several times until the washings were colorless, and the solid was then recrystallized from acetone–ethanol. (Anal. Calcd for $C_{18}H_{18}F_6MoNPS$: C, 41.47; H, 3.48; N, 2.69. Found: C, 41.00; H, 3.4; N, 2.81.) Proton NMR spectrum in deuterioacetone: τ 3.40 (m, phenyl protons), 4.05 (s, η^5-C_5H_5 protons), 7.53 (s, CH_3 of CH_3CN).

$[Cp_2Mo(\mu\text{-}SPh)_2MoCp_2](PF_6)_2$. (a) Preparation by Oxidation. A filtered solution of $[Cp_2Fe]PF_6$ (0.35 g, 1.01×10^{-3} mol) in CH_2Cl_2 (30 mL) was slowly added to a stirred suspension of $Cp_2Mo(SPh)_2$ (0.45 g, 1.01×10^{-3} mol) in 50 mL of CH_2Cl_2 at room temperature. The solution became brownish yellow, and a small amount of a microcrystalline precipitate of the same color formed. The solvent was removed in vacuo, and the residue was repeatedly washed with CH_2Cl_2 and diethyl ether. Brown microcrystals were obtained after recrystallization from acetone–ethanol.

(b) Preparation from $[Cp_2Mo(CO)SPh]PF_6$. A filtered solution of $[CP_2Mo(CO)SPh]PF_6$[44] (0.600 g, 1.01×10^{-3} mol) in CH_2Cl_2 was irradiated for an hour with an ultraviolet lamp. After that time the solution was filtered and the solvent removed in vacuo. The brown residue was recrystallized from acetone–ethanol to give a brown microcrystalline compound. (Anal. Calcd for $C_{32}H_{30}F_{12}Mo_2S_2P_2$: C, 40.01; H, 3.15. Found: C, 39.73; H, 3.41.) Proton NMR spectrum in deuterioacetonitrile: τ 2.80 (m, six phenyl protons), 3.71 (d, four phenyl protons), 3.99 (s, 20 η^5-C_5H_5 protons).

$[Cp_2Mo(NH_3)S\text{-}t\text{-}Bu]PF_6$. A solution of $Cp_2Mo(S\text{-}t\text{-}Bu)_2$ (0.45 g, 1.11×10^{-3}) mol) in acetone–CH_2Cl_2 was refluxed in the presence of excess NH_4PF_6 (0.30 g, 1.84×10^{-3} mol) for about 2 h. When the solvent was removed in vacuo, a red microcrystalline precipitate remained. The compound was purified by recrystallization from acetone–ethanol, washed with ethanol, and dried in vacuo. The complex was identified by ^1H NMR, infrared spectroscopy, and conductivity. (Anal. Calcd for $C_{14}H_{22}F_6MoNPS$: C, 35.23; H, 4.64; N, 2.93. Found: C, 35.61; H, 4.24; N, 2.83.)

$[Cp_2Mo(PPh_3)SPh]PF_6$. A solution of $[Cp_2Mo(NCMe)SPh]PF_6$ (0.45 g, 1.01×10^{-3} mol) in CH_3CN was stirred at room temperature with excess PPh_3 (0.370 g, 1.4×10^{-3} mol) for 1 h. The solvent was removed in vacuo, and the red crystalline precipitate was recrystallized from acetone–ethanol. (Anal. Calcd for $C_{34}H_{30}F_6MoP_2S$: C, 54.99; H, 4.08. Found: C, 55.22; H, 4.08.) The proton NMR spectrum of the ion at room temperature shows a doublet at τ 5.05 for the η^5-C_5H_5 protons split by spin coupling with ^{31}P.

Acknowledgment is made to the donors of the Petroleum Research Fund, administered by the American Chemical Society, for support of this research. Acknowledgment is also made to the Fulbright Program for a Senior Fellowship to J.C.K. and for a Travel Grant to

(34) M. Almemark and B. Åkermark, *J. Chem. Soc. Chem. Commun.*, 66 (1978); D. G. Morrell and J. K. Kochi, *J. Am. Chem. Soc.*, **97**, 7262 (1977).
(35) J. Y. Chen and J. K. Kochi, *J. Am. Chem. Soc.*, **99**, 1450 (1977).
(36) W. N. Rogers, J. A. Page, and M. C. Baird, *Inorg. Chem.*, **20**, 3521 (1981).
(37) A. Yamamoto, K. Morifuji, S. Ikeda, T. Saito, Y. Uchida, and A. Misano, *J. Am. Chem. Soc.*, **90**, 1878 (1968). See also ref 28.
(38) R. L. Cooper and M. L. H. Green, *J. Chem. Soc. A*, 1155 (1967).
(39) M. L. H. Green and W. C. Lindsell, *J. Chem. Soc. A*, 1455 (1967).
(40) A. R. Dias and M. H. Garcia, *Rev. Port. Quim.* **21**, 145 (1979).
(41) M. J. Calhorda and A. R. Dias, *Rev. Port. Quim.*, **20**, 77 (1978).
(42) C. C. Romão, Ph.D. Thesis, Lisbon, 1979. M. J. Calhorda, Ph.D. Thesis, Lisbon, 1980. F. Pina, private communication.
(43) W. H. Morrison, Jr., and D. N. Hendrickson, *Inorg. Chem.* 14. 2331 (1975).
(44) A. R. Dias and M. H. Garcia, Proceedings of the 4th Annual Meeting of the Portuguese Chemical Society, Lisbon, 1981.

M.H.G. M.H.G. was also supported by the Gulbenkian Foundation of Portugal and by the College at Oneonta, support which we acknowledge with much appreciation. We also wish to thank Professors Richard Reed and William E. Geiger, Jr., for their advice and assistance and the Chemistry Department, Hartwick College, Oneonta, NY, for the generous loan of electrochemical equipment. Finally, we wish to thank the Physics Department, SUNY, Oneonta, for the use of their ESR spectrometer.

Registry No. $[Cp_2Mo(NCMe)SPh]PF_6$, 83136-35-0; $[Cp_2Mo(\mu\text{-}SPh)_2MoCp_2](PF_6)_2$, 83136-37-2; $[Cp_2Mo(CO)SPh]PF_6$, 83136-39-4; $[Cp_2Mo(NH_3)S\text{-}t\text{-}Bu]PF_6$, 83136-41-8; $[Cp_2Mo(PPh_3)SPh]PF_6$, 83136-43-0; $[Cp_2Fe]PF_6$, 11077-24-0; $Cp_2Mo(SPh)_2$, 12246-18-3; $Cp_2Mo(S\text{-}t\text{-}Bu)$, 11082-51-2; Cp_2MoCl_2, 12184-22-4; Cp_2MoBr_2, 12184-15-5; Cp_2MoI_2, 12184-29-1; $[Cp_2MoBr(NCMe)]^+$, 72287-16-2; $[Cp_2MoI(NCPh)]^+$, 79542-67-9; $[Cp_2MoI(NCPh\text{-}Ph)]^+$, 83136-44-1; $[Cp_2NoI(NCPhBr)]^+$, 83136-45-2; $[Cp_2MoBr(Py)]PF_6$, 11133-00-9; $[Cp_2MoI(PPh_3)]PF_6$, 11133-13-4; $[Cp_2WCl_2]PF_6$, 12184-28-0; $[Cp_2WI_2]PF_6$, 83136-47-4; $[Cp_2WI(Py)]PF_6$, 83136-49-6; $Cp_2Mo(SMe)_2$, 83136-50-9; $Cp_2Mo(S\text{-}n\text{-}Pr)_2$, 78305-74-5; $Cp_2Mo(S\text{-}i\text{-}Pr)_2$, 78305-75-6; $[Cp_2Mo(NH_3)S\text{-}t\text{-}Bu]^+$, 83136-51-0; $[Cp_2Mo(NCMe)SPh]^+$, 83136-34-9; $[Cp_2Mo(PPh_3)SPh]^+$, 83136-42-9; $Cp_2Mo(SC_7H_{15})_2$, 79453-25-1; $Cp_2W(SMe)_2$, 37328-16-8; $Cp_2W(S\text{-}t\text{-}Bu)_2$, 79453-21-7; $Cp_2W(SC_5H_{11})_2$, 79453-22-8; $Cp_2W(SPh)_2$, 12246-20-7; $Cp_2Ti(SEt)_2Cr(CO)_4$, 83136-52-1; $Cp_2Ti(SEt)_2Mo(CO)_4$, 83136-53-2; $Cp_2Ti(SEt)_2W(CO)_4$, 83136-54-3; $Cp_2Ti(SPh)_2Mo(CO)_4$, 83136-55-4; $Cp_2Ti(SPh)_2W(CO)_4$, 83136-56-5; $(EtSC_2H_4SEt)Mo(CO)_4$, 61411-31-2; $(PhSC_2H_4SPh)Mo(CO)_4$, 31027-15-3; Cp_2TiFc_2, 65274-19-3.

Intervalent Transfer in Ferrocenyl-Substituted (η^4-Cyclobutadiene)(η^5-cyclopentadienyl)cobalt

John Kotz,* Gregory Neyhart, and William J. Vining

Department of Chemistry, State University of New York, Oneonta, New York 13820

Marvin D. Rausch

Department of Chemistry, University of Massachusetts, Amherst, Massachusetts 01003

Received January 26, 1982

The cis and trans isomers of $(\eta^5\text{-}C_5H_5)Co(\eta^4\text{-}C_4Fc_2Ph_2)$ (Fc = ferrocenyl group) both undergo two successive redox reactions at almost identical potentials in the range 0.30–0.55 V, a range appropriate for the Fe(II)–Fe(III) couple in a ferrocenyl group. In the oxidized form, *both* the 1+ *and* 2+ ions of both isomers give rise to a band in the near-infrared region (in cm^{-1} in CH_2Cl_2: cis 1+, 8000; cis 2+, 8930; trans 1+, 6950; trans 2+, 9260). These bands have the position, intensity, width, and solvent dependence expected for intervalent transfer bands of class II mixed-valence species. Since an Fe–Fe interaction is not possible in the 2+ ions, it is proposed that the IT bands arise predominantly from a Co(I)–Fe(III) interaction. Similar, but less well-defined, results are obtained for $(\eta^5\text{-}C_5H_5)Co(\eta^4\text{-}C_4Fc_4)$.

Introduction

Mixed-valence compounds contain two or more metal ions in different oxidation states. Such compounds have been the subject of continuing interest for the insight they provide into the electronic structure of compounds and the factors affecting electron transfer between interacting sites.[1,2]

Some years ago Robin and Day[2] proposed a classification of mixed-valence compounds according to the extent of delocalization of the valence electrons. Class I compounds have no interaction between sites of different formal oxidation number; the valences are trapped, and the properties of the mixed-valence compound are simply the sum of the properties of the two different sites. In contrast, in class III ions there is extensive delocalization between sites, and two different oxidation states are no longer distinguishable. The electronic spectrum of a class III compound arises from transitions between completely delocalized molecular orbitals. Class II compounds are intermediate between those of classes I and III. There is a weak but nonnegligible interaction between the adjacent oxidation states; to a first approximation, different integral oxidation states can be ascribed to the two sites. However, there is a valency interchange in class II compounds by two different mechanisms: (i) photon-driven electron transfer (this usually gives rise to a broad band of low energy called an intervalent transfer or IT band); (ii) an associated, thermally activated process.

Although intervalence transfer is known for compounds where metal ions of different elements interact,[3] the compounds most thoroughly studied are those having two or more metal ions of the same element. In organometallic chemistry the most commonly studied group of compounds is that based on ferrocene,[4-7] because ferrocenyl groups are usually stable when the iron is in the formal oxidation states of 2+ and 3+. Furthermore, it has been possible to examine the mixed-valence behavior of such compounds as a function of distance between two or more interacting ferrocenyl groups, as a function of the nature of the nature

(1) Brown, D. B., ed. "Mixed Valence Compounds"; D. Reidel Publishing Co.: Boston, 1980.
(2) Robin, M. B.; Day, P. *Adv. Inorg. Chem. Radiochem.* **1967**, *10*, 247.
(3) Dowling, N.; Henry, P. M.; Lewis, N. A.; Taube, H. *Inorg. Chem.* **1981**, *20*, 2345.
(4) Powers, M. J.; Meyer, T. J. *J. Am. Chem. Soc.* **1978**, *100*, 4393.
(5) Kramer, J. A.; Hendrickson, D. N. *Inorg. Chem.* **1980**, *19*, 3330.
(6) LeVanda, C.; Bechgaard, K.; Cowan, D. O. *J. Org. Chem.* **1976**, *41*, 2700.
(7) Cowan, D. O.; LeVanda, C.; Park, J.; Kaufman, F. *Acc. Chem. Res.* **1973**, *6*, 1.

0276-7333/83/2302-0079$01.50/0

M.H.G. M.H.G. was also supported by the Gulbenkian Foundation of Portugal and by the College at Oneonta, support which we acknowledge with much appreciation. We also wish to thank Professors Richard Reed and William E. Geiger, Jr., for their advice and assistance and the Chemistry Department, Hartwick College, Oneonta, NY, for the generous loan of electrochemical equipment. Finally, we wish to thank the Physics Department, SUNY, Oneonta, for the use of their ESR spectrometer.

Registry No. $[Cp_2Mo(NCMe)SPh]PF_6$, 83136-35-0; $[Cp_2Mo(\mu\text{-}SPh)_2MoCp_2](PF_6)_2$, 83136-37-2; $[Cp_2Mo(CO)SPh]PF_6$, 83136-39-4; $[Cp_2Mo(NH_3)S\text{-}t\text{-}Bu]PF_6$, 83136-41-8; $[Cp_2Mo(PPh_3)SPh]PF_6$, 83136-43-0; $[Cp_2Fe]PF_6$, 11077-24-0; $Cp_2Mo(SPh)_2$, 12246-18-3; $Cp_2Mo(S\text{-}t\text{-}Bu)$, 11082-51-2; Cp_2MoCl_2, 12184-22-4; Cp_2MoBr_2, 12184-15-5; Cp_2MoI_2, 12184-29-1; $[Cp_2MoBr(NCMe)]^+$, 72287-16-2; $[Cp_2MoI(NCPh)]^+$, 79542-67-9; $[Cp_2MoI(NCPh\text{-}Ph)]^+$, 83136-44-1; $[Cp_2NoI(NCPhBr)]^+$, 83136-45-2; $[Cp_2MoBr(Py)]PF_6$, 11133-00-9; $[Cp_2MoI(PPh_3)]PF_6$, 11133-13-4; $[Cp_2WCl_2]PF_6$, 12184-28-0; $[Cp_2WI_2]PF_6$, 83136-47-4; $[Cp_2WI(Py)]PF_6$, 83136-49-6; $Cp_2Mo(SMe)_2$, 83136-50-9; $Cp_2Mo(S\text{-}n\text{-}Pr)_2$, 78305-74-5; $Cp_2Mo(S\text{-}i\text{-}Pr)_2$, 78305-75-6; $[Cp_2Mo(NH_3)S\text{-}t\text{-}Bu]^+$, 83136-51-0; $[Cp_2Mo(NCMe)SPh]^+$, 83136-34-9; $[Cp_2Mo(PPh_3)SPh]^+$, 83136-42-9; $Cp_2Mo(SC_7H_{15})_2$, 79453-25-1; $Cp_2W(SMe)_2$, 37328-16-8; $Cp_2W(S\text{-}t\text{-}Bu)_2$, 79453-21-7; $Cp_2W(SC_5H_{11})_2$, 79453-22-8; $Cp_2W(SPh)_2$, 12246-20-7; $Cp_2Ti(SEt)_2Cr(CO)_4$, 83136-52-1; $Cp_2Ti(SEt)_2Mo(CO)_4$, 83136-53-2; $Cp_2Ti(SEt)_2W(CO)_4$, 83136-54-3; $Cp_2Ti(SPh)_2Mo(CO)_4$, 83136-55-4; $Cp_2Ti(SPh)_2W(CO)_4$, 83136-56-5; $(EtSC_2H_4SEt)Mo(CO)_4$, 61411-31-2; $(PhSC_2H_4SPh)Mo(CO)_4$, 31027-15-3; Cp_2TiFc_2, 65274-19-3.

Intervalent Transfer in Ferrocenyl-Substituted (η^4-Cyclobutadiene)(η^5-cyclopentadienyl)cobalt

John Kotz,* Gregory Neyhart, and William J. Vining

Department of Chemistry, State University of New York, Oneonta, New York 13820

Marvin D. Rausch

Department of Chemistry, University of Massachusetts, Amherst, Massachusetts 01003

Received January 26, 1982

The cis and trans isomers of $(\eta^5\text{-}C_5H_5)Co(\eta^4\text{-}C_4Fc_2Ph_2)$ (Fc = ferrocenyl group) both undergo two successive redox reactions at almost identical potentials in the range 0.30–0.55 V, a range appropriate for the Fe(II)–Fe(III) couple in a ferrocenyl group. In the oxidized form, *both* the 1+ *and* 2+ ions of both isomers give rise to a band in the near-infrared region (in cm^{-1} in CH_2Cl_2: cis 1+, 8000; cis 2+, 8930; trans 1+, 6950; trans 2+, 9260). These bands have the position, intensity, width, and solvent dependence expected for intervalent transfer bands of class II mixed-valence species. Since an Fe–Fe interaction is not possible in the 2+ ions, it is proposed that the IT bands arise predominantly from a Co(I)–Fe(III) interaction. Similar, but less well-defined, results are obtained for $(\eta^5\text{-}C_5H_5)Co(\eta^4\text{-}C_4Fc_4)$.

Introduction

Mixed-valence compounds contain two or more metal ions in different oxidation states. Such compounds have been the subject of continuing interest for the insight they provide into the electronic structure of compounds and the factors affecting electron transfer between interacting sites.[1,2]

Some years ago Robin and Day[2] proposed a classification of mixed-valence compounds according to the extent of delocalization of the valence electrons. Class I compounds have no interaction between sites of different formal oxidation number; the valences are trapped, and the properties of the mixed-valence compound are simply the sum of the properties of the two different sites. In contrast, in class III ions there is extensive delocalization between sites, and two different oxidation states are no longer distinguishable. The electronic spectrum of a class III compound arises from transitions between completely delocalized molecular orbitals. Class II compounds are intermediate between those of classes I and III. There is a weak but nonnegligible interaction between the adjacent oxidation states; to a first approximation, different integral oxidation states can be ascribed to the two sites. However, there is a valency interchange in class II compounds by two different mechanisms: (i) photon-driven electron transfer (this usually gives rise to a broad band of low energy called an intervalent transfer or IT band); (ii) an associated, thermally activated process.

Although intervalence transfer is known for compounds where metal ions of different elements interact,[3] the compounds most thoroughly studied are those having two or more metal ions of the same element. In organometallic chemistry the most commonly studied group of compounds is that based on ferrocene,[4-7] because ferrocenyl groups are usually stable when the iron is in the formal oxidation states of 2+ and 3+. Furthermore, it has been possible to examine the mixed-valence behavior of such compounds as a function of distance between two or more interacting ferrocenyl groups, as a function of the nature of the nature

(1) Brown, D. B., ed. "Mixed Valence Compounds"; D. Reidel Publishing Co.: Boston, 1980.
(2) Robin, M. B.; Day, P. *Adv. Inorg. Chem. Radiochem.* **1967**, *10*, 247.
(3) Dowling, N.; Henry, P. M.; Lewis, N. A.; Taube, H. *Inorg. Chem.* **1981**, *20*, 2345.
(4) Powers, M. J.; Meyer, T. J. *J. Am. Chem. Soc.* **1978**, *100*, 4393.
(5) Kramer, J. A.; Hendrickson, D. N. *Inorg. Chem.* **1980**, *19*, 3330.
(6) LeVanda, C.; Bechgaard, K.; Cowan, D. O. *J. Org. Chem.* **1976**, *41*, 2700.
(7) Cowan, D. O.; LeVanda, C.; Park, J.; Kaufman, F. *Acc. Chem. Res.* **1973**, *6*, 1.

0276-7333/83/2302-0079$01.50/0

Table I. Electrochemical and Spectroscopic Data for Derivatives of (η^4-Cyclobutadiene)(η^5-cyclopentadienyl)cobalt[a]

compd	$E_{p/2}$,[b] V	ΔE_p,[c] mV	faraday/mol[d]	Z[e]	electronic spectral data λ_{max}, nm (ϵ_{max}, M^{-1} cm^{-1})
$CpCo[Ph_4C_4]$	0.88	190	4.5 (irrev)	0	285 (29 100), 260 (32 100)
cis-$CpCo[Fc_2Ph_2C_4]$ (I)	0.33	130	0.97	0	298 (28 100)
	0.52	130	0.96	1+	287 (29 200), 248 (32 400), 1250 (1010)
	1.38	irrev		2+	287 (30 800), 248 (32 400), 1120 (1140)
trans-$CpCo[Fc_2Ph_2C_4]$ (II)	0.33	150	0.96	0	300 (28 100)
	0.50	150	1.01	1+	254 (23 600), 1440 (812)
	1.44	irrev		2+	258 (33 700), 1080 (840)
$CpCo[Fc_4C_4]$ (III)	0.29	115	0.96	0	
	remaining 3 redox waves blend into a broad wave centered at $E_{p/2} \simeq 0.4$ V			1+	292 (30 900), 1480 (960)
				2+	285 (31 300), 1025 (800)
				3+	280 (25 300), 750 (918)

[a] All data collected in CH_2Cl_2 containing 0.1 M tetrabutylammonium hexafluorophosphate. [b] $E_{p/2}$ values calculated by averaging the anodic (E_{pa}) and cathodic peak potentials (E_{pc}); in volts vs. SCE. [c] $\Delta E_p = E_{pa} - E_{pc}$ in millivolts. [d] Number of faradays passed per mole on bulk oxidation at an appropriate potential. [e] Charge on the compound, where Z is defined as $[CpCo(R_4C_4)]^Z$.

of the bridge between them, and as a function of their relative orientation.[4-9]

Recently Rausch and co-workers described the synthesis of several compounds wherein ferrocenyl groups are substituted on the cyclobutadiene ring of (η^4-cyclobutadiene)(η^5-cyclopentadienyl)cobalt (I–III).[10] Two of

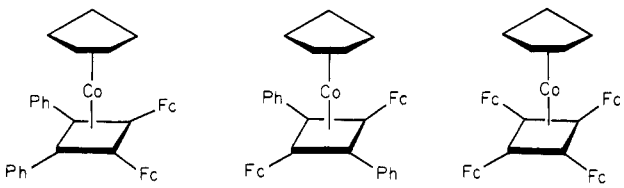

these compounds, I and II, were especially interesting to us, because the mixed-valence behavior of ferrocenyl compounds wherein the groups are attached to an aromatic ring has never been described. Furthermore, compounds I and II would allow us to examine the effect of positional isomerism on the properties of the mixed valence species. However, the actual results of this study have proven even more interesting than expected: one- or two-electron oxidation of I and II, where the electrons are removed from the ferrocenyl groups, leads to ions where the predominant interaction is thought to be between Co(I) and the Fe(III) ion of an oxidized ferrocenyl group.

Results

The cyclic voltammogram of the trans isomer II in CH_2Cl_2 is illustrated in Figure 1 (see also Table I). There are two reversible waves at $E_{p/2} = 0.33$ and 0.50 V (an anodic–cathodic peak separation of 130–150 mV is often observed for reversible processes in CH_2Cl_2, a high dielectric solvent) and one irreversible wave at 1.44 V. The cis isomer shows almost identical behavior (see Table I). Based on analogy with numerous other ferrocenyl compounds, the two reversible waves are assigned to redox reactions of the ferrocenyl groups. The third, irreversible wave is probably due to the Co(I) oxidation, since we observed that the tetraphenyl analogue of III, i.e., (η^5-C_5H_5)Co(η^4-C_4Ph_4), has a quasi-reversible wave at $E_{p/2}$ = 0.88 V in CH_2Cl_2.

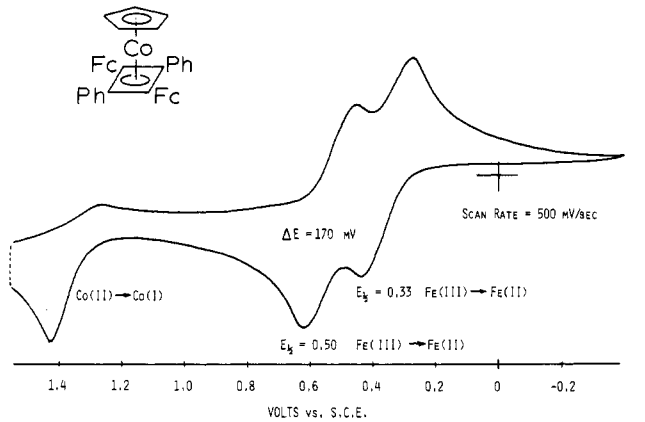

Figure 1. Cyclic voltammogram of *trans*-(η^5-C_5H_5)Co(η^4-$C_4Fc_2Ph_2$) in CH_2Cl_2 containing 0.1 M Bu_4NPF_6 (25 ± 2 °C).

In the case of I and II, controlled potential oxidation at E_{pa} for the first wave leads to the removal of one electron per molecule; in each case oxidation was accompanied by a color change from pale yellow to very dark brown-red. Reduction of the monooxidized species at 0.0 V also occurs with the passage of 1 faraday/mol, showing that little decomposition of the mixed-valence species has occurred.

Controlled potential oxidation of I and II at a potential slightly more anodic than E_{pa} for the second wave leads to removal of a second electron; the color remains very dark brown-red. The 2+ ion is stable in CH_2Cl_2; reduction of the dioxidized species occurs with the passage of 2 faraday/mol.

In the cyclic voltammogram of the tetraferrocenyl compound, III, we observe a one-electron, reversible wave at 0.29 V in CH_2Cl_2, but the waves representing the next three electrons blend into one broad wave centered at about 0.4 V.

The only other solvent medium in which the compounds dissolved and which was also suitable for electrochemistry was a 1:1 mixture of CH_2Cl_2 and CH_3CN. The voltammetric behavior of the compounds in this mixture was the same as in pure CH_2Cl_2 with the exception that the ions of 2+ or higher charge were considerably less stable in the mixed solvent.

Electronic spectra of the 1+ and 2+ ions of compounds I and II were recorded in CH_2Cl_2 and in the CH_2Cl_2/CH_3CN mixture (Tables I–III). Both isomers in *both* charge states (1+ and 2+) exhibited a significant absorption band of Gaussian shape in the near infrared region (12000–5000 cm^{-1}); such bands were not observed in the neutral compounds I and II nor in (η^5-C_5H_5)Co(η^4-C_4Ph_4).

(8) Morrison, W. H.; Hendrickson, D. N. *Inorg. Chem.* **1975**, *14*, 2331.
(9) Rudie, A. W. Thesis, Massachusetts Institute of Technology, 1978.
(10) Rausch, M. D.; Higbie, F. A.; Westover, G. F.; Clearfield, A.; Gopal, R.; Troup, J. M.; Bernal, I. *J. Organomet. Chem.* **1978**, *149*, 245. In addition to the synthesis of compounds I–III, the molecular structure of the trans isomer is reported in detail.

Table II. Near-Infrared Spectral Data for Some Ferrocenyl-Containing Ions[a]

compd	ν_{max}, cm^{-1}	ϵ,[b] M^{-1} cm^{-1}	$\Delta\nu_{1/2}$,[c] cm^{-1} obsd	$\Delta\nu_{1/2}$,[c] cm^{-1} calcd	$10^3\alpha^2$ [c]
$[Fc—Fc]^+$	5000	919	3700	3400	9.3
	(5680)	(···)	(3900)	(3620)	(···)
$[FcC{\equiv}CFc]^+$ [d]	6180	487	5200	3780	2.4
	(7470)	(···)	(5460)	(4150)	(···)
$[FcC{\equiv}CC{\equiv}CFc]^+$ [e]	8475	570	···	···	···
cis-$[CpCo(Fc_2Ph_2C_4)]^+$ (I)	8000	1010	4620	4300	10.3 (10.7)[g]
	(8300)[f]	(1260)	(4700)	(4390)	(12.6)
trans-$[CpCo(Fc_2Ph_2C_4)]^+$ (III)	6950	812	5800	4010	4.3 (12.4)[g]
	(7140)[f]	(965)	(5720)	(4060)	(4.9)

[a] All data are obtained in CH_2Cl_2 (or CH_3CN) (containing a tetrabutylammonium salt as supporting electrolyte unless otherwise noted.) [b] Molar absorptivity values for cyclobutadiene compounds (at 25 ± 2 °C) regarded as accurate within 10%. [c] See text for appropriate equations. α^2 values assume Fe(II)-Fe(III) interaction unless noted otherwise. Values of d used given in ref 13. [d] Data from ref 4. [e] Data from ref 6. [f] All data in parentheses in this line obtained in a 1:1 mixture of CH_2Cl_2 and CH_3CN. [g] Values of α^2 in parentheses in this line calculated assuming a Co(I)-Fe(III) interaction; d = 5 Å.

Table III. Near-Infrared Data for the Doubly Charged Ions *cis*- and *trans*-$[CpCo(Fc_2Ph_2C_4)]^{2+}$ in CH_2Cl_2

compd	ν, cm^{-1}	ϵ, M^{-1} cm^{-1}	$\Delta\nu_{1/2}$, cm^{-1} obsd	$\Delta\nu_{1/2}$, cm^{-1} calcd
cis-$[CpCo(Fc_2Ph_2C_4]^{2+}$	8930	1140	6240	4540
trans-$[CpCo(Fc_2Ph_2C_4]^{2+}$	9260	840	5300	4600

The tetraferrocenyl compound III shows a near-infrared band for the 2+ and 3+ ions as well as for the 1+ ion in CH_2Cl_2. However, the band positions in Table I are only approximate, since the band intensity did not drop appreciably on the low-energy side of the band.

Discussion

The original objective of this study was to oxidize I and II and examine the effect on the expected Fe(II)–Fe(III) interaction of connecting two ferrocenyl groups to an aromatic nucleus in two different locations. Both ferrocenyl groups were found to oxidize at slightly different potentials, and intervalent transfer bands are observed in the near-infrared region for the 1+ *and* 2+ ions of compounds I and II (as well as for oxidized III) (Tables I–III). It is our current hypothesis that such bands arise predominantly from a Co(I)–Fe(III) interaction rather than one between two iron ions in different oxidation states.

Since we expected an Fe(II)–Fe(III) interaction when beginning this work, it seemed best to compare our results with those obtained on other compounds as closely related to I and II as possible. Thus, the mixed-valence ions $[Fc—Fc]^+$, $[FcC{\equiv}CFc]^+$, and $[FcC{\equiv}CC{\equiv}CFc]^+$ (where Fc is a ferrocenyl group) were chosen; the first two in particular have been thoroughly studied,[4,5,7,8] and all have been classified as class II mixed-valence ions.

Table IV compares the reduction potentials observed for $[Fc—Fc]^{2+}$ and $[FcC{\equiv}CFc]^{2+}$ with those of $[I]^{2+}$ and $[II]^{2+}$. This comparison shows that the difference between the first and second reduction potentials of $[I]^{2+}$ and $[III]^{2+}$ and for dioxidized diferrocenylacetylene are nearly the same. Thus, if the disproportionation reaction

$$2[2,3]^+ \rightleftarrows [2,2] + [3,3]^{2+}$$

occurs, the Nernst equation indicates that the equilibrium mixture should contain more than 90% of the $[2,3]^+$ ion.

In Table II we compare the spectroscopic data for $[I]^+$ and $[II]^+$ with that for the mixed-valence ions based on biferrocene and diferrocenylacetylene. The band widths in Table II are calculated from the Hush theory.[11] This

Table IV. Electrochemical Parameters for Some Compounds Containing Two Ferrocenyl Groups[a,b]

compd	$E_{p/2}$,[c] V	$\Delta E_{p/2}$,[d] mV
Fc—Fc	0.44	350
	0.79	
FcC≡CFc	0.46	140
	0.60	
cis-$[CpCo(Fc_2Ph_2C_4)]$	0.33	190
	0.52	
trans-$[CpCo(Fc_2Ph_2C_4)]$	0.33	170
	0.50	

[a] All data obtained in CH_2Cl_2 containing tetrabutylammonium hexafluorophosphate (0.1 M). [b] Data for Fc—Fc and FcC≡CFc taken from ref 4. [c] See Table I. [d] Difference in $E_{p/2}$ for the two reduction processes.

theory predicts that, for class II mixed-valence species, the width of the intervalent transfer band at half-height is approximately given by

$$\nu_{max} = (\Delta\nu_{1/2})^2/2310$$

where ν_{max} is the frequency of the IT band maximum and $\Delta\nu_{1/2}$ is the half-height band width; all parameters are in inverse centimeters. With use of this equation, the expected band width has been calculated for the 1+ ions of I and II. As seen in Table II, the observed[12] band widths are 1.1 to 1.4 times larger than the calculated band widths. Similar agreement has been previously found for observed and calculated band widths in class II mixed-valence species.[3,4] (Nearly the same results are observed for the 2+ ions in Table III.)

Another indication that the 1+ ions are class II mixed-valence species is the solvent dependence of the IT band. The data in Table II for $[Fc—Fc]^+$ and $[FcC{\equiv}CFc]^+$ show that the band energy drops on going from CH_3CN to CH_2Cl_2, and a similar effect is observed for $[I]^+$ and $[II]^+$. This behavior is also predicted by the Hush theory for weakly interacting or class II mixed-valence species.[11]

The Hush theory also suggests that, for class II species, the extent of interaction between sites or the extent of electron delocalization (α^2) can be calculated from[7]

$$\alpha^2 = \frac{(4.6 \times 10^{-4})\epsilon_{max}\Delta\nu_{1/2}}{\nu_{max}d^2}$$

(11) Hush, N. S. *Prog. Inorg. Chem.* **1967**, *6*, 391.

(12) The half-height band widths were usually measured by using the following procedure: the width of the band from the maximum frequency to the band edge was measured at half-height on the high-energy side of the band, and this value was doubled.

where ϵ_{max} is the molar absorptivity, $\Delta\nu_{1/2}$ is the band width of the IT band at half-height, ν_{max} is the position of the IT band maximum, and d is the distance between the interacting sites in angstroms (all other parameters in inverse centimeters).[13] The delocalization parameter α^2 has been calculated for the ions $[I]^+$ and $[II]^+$ for two possibilities: Fe(II)–Fe(III) or Co(I)–Fe(III) intervalent transfer.[14] With the assumption of an Fe(II)–Fe(III) interaction, the values of α^2 are in the range observed for class II ferrocenyl compounds, and, since α^2 is heavily influenced by the estimated Fe–Fe distance, the α^2 value for the cis isomer is greater than that for the trans isomer as might be expected.[13] Although no great significance should be attached to these values, we might note that for the cis isomer and $[Fc–Fc]^+$, where the Fe–Fe distances are estimated to be almost identical, the values of α^2 are comparable. If, on the other hand, a Co(I)–Fe(III) interaction is assumed, the α^2 values are still reasonable and are quite similar to one another, again as would be expected. Finally, we note that these latter values are similar to that for the biferricenium ion (with a metal–metal distance identical with that estimated for Fe–Co).

Previous work on $[Fc—Fc]^+$, $[FcC{\equiv}CFc]^+$, and $[FcC{\equiv}CC{\equiv}CFc]^+$ and several Ru(II)—Ru(III) compounds has indicated that, in a series of *closely* related mixed-valence compounds, the intensity of the IT band decreases and the energy of the transition increases as the distances between interacting centers increases.[4,15] (The latter effect has been explained as being due to the fact that more reorganizational energy is required for electron transfer as the distance between interacting centers increases.) The data in Table II show that the cyclobutadiene compounds both have IT transitions of higher energy than diferrocenylacetylene, and the transition for the cis isomer is of higher energy than that of the trans isomer. Since the estimated Fe–Fe distances in these molecules are in the order $[FcC{\equiv}CC{\equiv}CFc]^+$ (10 Å; ν_{max} = 8475 cm^{-1}) > [trans isomer]$^+$ (8.5 Å; ν_{max} = 6950 cm^{-1}) > $[FcC{\equiv}CFc]^+$ (7.3 Å; ν_{max} = 6180 cm^{-1}) > [cis isomer]$^+$ (5.1 Å; ν_{max} = 8000 cm^{-1}), it is evident that there is no correlation between band energy and distance. Indeed, in the cyclobutadiene compounds there is an inverse correlation to that expected: the energy of the IT band falls as the Fe–Fe distance increases.

Of greatest interest in this study is the existence of a near-infrared band for the 2+ ions of I and II (Table III) (and bands for the 2+ and 3+ ions of III) where none exists for the neutral compounds or $(\eta^5\text{-}C_5H_5)Co(\eta^4\text{-}C_4Ph_4)$. In these ions both ferrocenyl iron atoms have been oxidized to the 3+ formal oxidation state, so Fe–Fe intervalent transfer is not possible. It was this band—and the lack of the appropriate band energy/distance correlation as noted above—that forced us to consider Co(I)–Fe(III) intervalent transfer as a distinct possibility in both the 1+ [Co(I)–Fe(II)–Fe(III)] and 2+ [Co(I)–Fe(III)–Fe(III)] ions. This possibility is further reinforced by noting that the difference in reduction potentials for the Co(II) center and that for the first Fe(III) reduction is about 1.1 eV; the energies of the IT bands are all in the range 0.9–1.1 eV (1 eV = 8067.5 cm^{-1}).

To further test our conclusion that Co(I)–Fe(III) intervalence transfer is a possibility in the 1+ and 2+ ions of I and II, we are now beginning a synthesis program to build systems having a single ferrocenyl group attached to a Co(I) center.[16]

Experimental Section

Electrochemical Techniques. The electrochemical instrumentation consisted of a PAR 174 polarographic analyzer, a PAR 175 voltage programmer, and a Hewlett-Packard Moseley 135 X-Y recorder. In coulometry experiments, the number of coulombs passed was determined by graphical integration of the current–time curve or with a PAR 379 digital coulometer.

Potentials were referred to a calomel electrode containing a saturated solution of sodium chloride. A 2-mm piece of Pt wire served as the working electrode for cyclic voltammetry while the working electrode for coulometry experiments was Pt gauze. The auxiliary electrode in all experiments was a Pt wire coil.

Cyclic voltammetry experiments were done in a PAR polarographic cell or in a three-compartment cell; in the latter, the working electrode compartment was separated from the compartments for auxiliary and reference electrodes by medium porosity glass frits. All experiments were done at room temperature (25 ± 2 °C).

Solutions were 0.1 M in supporting electrolyte, tetrabutylammonium hexafluorophosphate, Bu_4NPF_6. The electrolyte was prepared from Bu_4NBr and KPF_6 (both purchased from Aldrich Chemical Co.) and was recrystallized from ethanol–acetone; it was thoroughly washed with diethyl ether and dried in vacuo. The solvents CH_3CN and CH_2Cl_2 were reagent grade materials which were dried over P_2O_5 and distilled before use. Solutions were degassed with dry nitrogen before each experiment, and a nitrogen atmosphere was maintained over the solution during the experiment.

Near-infrared, visible, and ultraviolet spectra were obtained on a Cary 14 at room temperature. Following bulk electrolysis at an appropriate potential, solutions were syringed into a nitrogen-filled cuvette.

Chemicals. The cobalt(I) compounds used in this study were prepared and characterized as described in ref 10.

Acknowledgment is made to the donors of the Petroleum Research Fund, administered by the American Chemical Society, for support of this research. We wish to express our great appreciation to Professor Richard Reed for his advice and assistance and to the Chemistry Department of Hartwick College for the generous loan of some electrochemical equipment. We also thank L. Rosenzweig and W. Van Der Sluys for experimental assistance.

Registry No. I, 62842-88-0; $[I]^+$, 83573-12-0; $[I]^{2+}$, 83573-13-1; II, 62842-87-9; $[II]^+$, 83585-35-7; $[II]^{2+}$, 83585-36-8; III, 66672-86-4; $[III]^+$, 83649-31-4; $[III]^{2+}$, 83573-14-2; $[III]^{3+}$, 83649-32-5.

(13) Iron–iron distances in $[Fc—Fc]^+$ and $[FcC{\equiv}CFc]^+$ were taken from ref 4. For compounds I and II, the following distances were estimated from the information in ref 10: Fe–Fe in the cis isomer = 5.1 Å; Fe–Fe in the trans isomer = 8.5 Å; Co–Fe = 5.0 Å.

(14) Cowan and his co-workers[6] have previously noted a rough correlation between α^2 and the difference in the $[3,3]^{2+}$ and $[2,3]^+$ reduction potentials for compounds having two interacting ferrocenyl groups. Tables II and IV show that, if iron–iron interaction is assumed in $[I]^+$ and $[II]^+$, these compounds and the mixed-valence ions based on biferrocene and diferrocenylacetylene show only the roughest of trends.

compd	$[Fc–Fc]^+$	[cis isomer]$^+$	[trans isomer]$^+$	$[FcC{\equiv}CFc]^+$
$\Delta E_{1/2}$, mV	350	190	170	140
$10^3\alpha^2$	9	10.3	4.3	2.4

(15) Powers, M. J.; Salmon, D. J.; Callahan, R. W.; Meyer, T. J. *J. Am. Chem. Soc.* **1976**, *98*, 6731.

(16) **Note added in proof.** We have recently obtained a sample of $(\eta^5\text{-}C_5H_5)Co(\eta^4\text{-}C_4Ph_3Fc)$ from K. Yasafuku of the Institute of Physical and Chemical Research, Japan. We find the compound undergoes reversible, one-electron oxidation at the ferrocenyl group ($E_{p/2}$ = 0.35 V vs. SCE in CH_2Cl_2), and the oxidized species exhibits a near-infrared band (ν_{max} = 7843 cm^{-1}; ϵ = 1097 M^{-1} cm^{-1} in CH_2Cl_2) similar to those seen in I and II. The electrochemical and spectroscopic properties of this compound, and some analogues, will be the subject of a future publication.

Structural Characterization of the Helical Ferrocene (±)-[(1,2,3,3a,13a,14,15,16,16a,16f-η)-Diindeno[5,4-*c*:4′,5′-*g*]-phenanthrene]iron[1]

John C. Dewan*

Department of Chemistry, Columbia University, New York, New York 10027

Received September 20, 1982

The crystal structure of the title compound 1 is reported and represents the first ferrocene wherein the two cyclopentadienyl rings are linked by unbroken conjugation. Each of the two terminal cyclopentadienyl rings of the helicene bind iron(II) in a η^5 fashion, and thus the helicene, taken as a whole, binds to the metal in an overall η^{10} fashion. The molecule of 1 possesses approximate C_2 symmetry but has no crystallographically imposed symmetry. The Fe–C distances range from 2.008 (4) to 2.087 (4) Å for ring A and from 2.007 (4) to 2.104 (4) Å for ring G and the dihedral angle, or angle of tilt, between the terminal cyclopentadienyl rings is 19.8°. The Fe–Ω distances are 1.652 Å to ring A and 1.655 Å to ring G and the Ω(A)–Fe–Ω(G) angle is 165.4°, where Ω represents the centroid of each of the two cyclopentadienyl rings. The angle of twist between the two rings averages 26.7°. Torsion angles around the inner core of the helicene are 15.8, 19.1, 27.8, 17.1, and 15.1° and around the periphery are 10.0, 7.4, 14.4, 6.3, and 9.0°. The dihedral angles between least-squares planes of consecutive rings are 8.3, 11.7, 12.5, 12.6, 9.5, and 10.2°. Crystal data for 1 are as follows: a = 15.631 (4) Å, b = 12.462 (3) Å, c = 18.399 (4) Å, V = 3584.0 Å^3, Z = 8, orthorhombic, space group *Pbca*, final R = 0.040 for 1837 X-ray diffractometer data with $F_o > 4\sigma(F_o)$.

Introduction

Past experiments by Katz and co-workers, using various dicyclopentadienyl dianions and aimed at synthesizing potential one-dimensional electrical conductors in which conjugated arrays and metal atoms alternate, only resulted in dimer formation.[2] A strategy devised to overcome this problem was to synthesize helical dicyclopentadienyl dianions that would force metal ions to bind to opposite faces of the cyclopentadienyl rings in the hope of producing the desired polymerization.[3] Although such polymers have not yet been obtained, it was realized[4] that the dianion of helicene 2 would present a unique situation in that the two

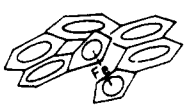

1

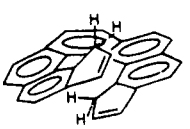

2

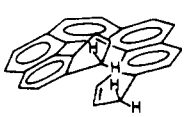

3

cyclopentadienyl rings would lie on top of one another and that reaction of this dianion with iron(II) might well produce the novel helical ferrocene 1. The synthesis[5] and structural characterization[6] of 2 have been effected, and its dianion does indeed lead to 1[5] which represents the first reported ferrocene wherein the two cyclopentadienyl rings are linked by unbroken conjugation. Related molecules are known,[7,8] but they contain alternating single and double bonds where adjacent double bonds are not constrained to be parallel. No structural data appear to have been reported for these compounds.

An examination of the Cambridge Crystallographic Data File[9,10] reveals that the crystal structures of approximately 85 compounds containing the ferrocene moiety have been reported. Of these, about 14 represent studies on ferrocene itself[11–14] and about 25 represent studies on compounds

* To whom correspondence should be addressed at the Laboratory of Molecular Biology, Medical Research Council Centre, University Medical School, Cambridge CB2 2QH, England.

(1) Given here is the Chemical Abstracts name for the compound which is derived from the fundamental ring system Diindeno[5,4-*c*:4′,5′-*g*]phenanthrene whose structural formula and numbering system system are as

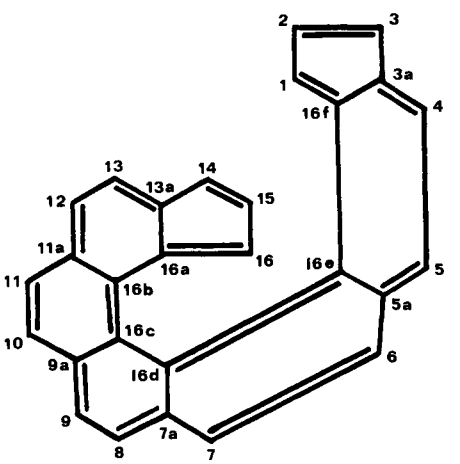

Note that the numbering scheme used throughout this paper in describing the structure of the title compound, 1, is the crystallographic numbering which is depicted in Figure 1.

(2) Katz, T. J.; Slusarek, W. *J. Am. Chem. Soc.* **1980**, *102*, 1058 and references cited therein.
(3) Katz, T. J.; Slusarek, W. *J. Am. Chem. Soc.* **1979**, *101*, 4259.
(4) Slusarek, W. Ph.D. Dissertation, Columbia University, New York, 1977.
(5) Katz, T. J.; Pesti, J. *J. Am. Chem. Soc.* **1982**, *104*, 346.
(6) Dewan, J. C. *Acta Crystallogr., Sect. B* **1981**, *B37*, 1421.
(7) Kasahara, A.; Izumi, T.; Shimizu, I. *Chem. Lett.* **1979**, 1119.
(8) Tanner, D.; Wennerstrom, O. *Acta Chem. Scand., Ser. B* **1980**, *B34*, 529.
(9) Allen, F. H.; Bellard, S.; Brice, M. D.; Cartwright, B. A.; Doubleday, A.; Higgs, H.; Hummelink, T.; Hummelink-Peters, B. G.; Kennard, O.; Motherwell, W. D. S.; Rodgers, J. R.; Watson, D. G. *Acta Crystallogr., Sect B* **1979**, *B35*, 2331.
(10) Machin, P. A.; Mills, J. N.; Mills, O. S.; Elder, M. "Crystal Structure Search Retrieval Manual"; SERC Daresbury Laboratory: Warrington, England, 1978.
(11) Dunitz, J. D.; Orgel, L. E.; Rich, A. *Acta Crystallogr.* **1956**, *9*, 373.
(12) Seiler, P.; Dunitz, J. D. *Acta Crystallogr., Sect. B* **1979**, *B35*, 1068.
(13) Takusagawa, F.; Koetzle, T. F. *Acta Crystallogr., Sect B* **1979**, *B35*, 1074.

0276-7333/83/2302-0083$01.50/0

Table I. Experimental Details of the X-ray Diffraction Study of the Title Compound, 1

(A) Crystal Parameters[a] at 24 °C

a = 15.631 (4) Å	mol wt 408.3
b = 12.462 (3) Å	space group $Pbca$
c = 18.399 (4) Å	Z = 8
V = 3584.0 Å^3	ρ(calcd) = 1.513 g cm^{-3}

(B) Measurement of Intensity Data

instrument	Enraf-Nonius CAD-4F κ geometry diffractometer
radiation	Mo Kα ($\lambda_{\bar{\alpha}}$ = 0.710 73 Å) graphite monochromated
detector aperture	vertical, 4.0 mm; horizontal, variable (3.0 + tan θ) mm
scan technique	coupled ω(crystal)-2θ(counter)
scan rate	variable from 1.26 to 6.71° min^{-1} in ω
scan width	variable, $\Delta\omega$ = (0.7 + 0.35 tan θ)°
prescan rejection limit	1σ
prescan acceptance limit	100σ
max counting time	50 s
bkgd measurements	moving crystal-moving detector, 25% added to scan width at both ends of each scan
standards	three reflections (200), (222), and (008), measured every 3600 s of X-ray exposure time, showed no decay
no. of reflections collected	[3° ≤ 2θ ≤ 50° (+h, +k, +l)] 3153 unique, non-space-group extinguished
reorientation control	the three reflections (884), (1,11,6), and (409) were recentered every 250 data, and if the position of any scattering vector deviated by more than 0.08° from its calculated position, a new orientation matrix was calculated on the basis of the recentering of a further 19 reflections

(C) Treatment of Intensity Data

reduction to F_o and $\sigma(F_o)$	correction for background, attenuator, and Lorentz-polarization of monochromated X radiation as described previously[b]
absorption correction	not applied, μ = 8.48 cm^{-1}
observed data	1837 unique reflections with $F_o > 4\sigma(F_o)$ were used in the structure refinement

[a] From a least-squares fit to the setting angles of 25 reflections with 2θ > 30°. [b] Reference 48.

wherein there is some form of bridge between the two cyclopentadienyl rings.[15-44] These bridges range from rather complex arrangements of atoms[15,16] through heteroatoms such as Si, P, S, Ge, and Se[20-26] to purely hydrocarbon links.[31-44] For the most part these bridges do not prevent the cyclopentadienyl rings from being parallel, or approximately parallel, to one another. Where the bridge is less than the 3.31-Å inter-ring separation observed in ferrocene,[12] however, significant deviations are observed and an "angle of tilt" is thereby introduced into the molecule.

The relatively large number of studies on ferrocene itself[12-14] has arisen because of the realization that the original room-temperature structure of the monoclinic modification of ferrocene[11] was in error due to disorder present in the crystals. This original work reported a staggered conformation of the cyclopentadienyl rings (i.e., an "angle of twist" of 36°). The current position, however, is that the cyclopentadienyl rings in ferrocene are either exactly eclipsed or very nearly eclipsed (i.e., an "angle of twist" between 0 and 10°) in all crystals examined, and these extensive studies have been performed at various temperatures on different crystalline modifications and have used both X-ray and neutron diffraction techniques.[12-14]

Three reviews[45-47] concerned with various aspects of the

(14) (a) Seiler, P.; Dunitz, J. D. *Acta Crystallogr., Sect. B* **1979**, *B35*, 2020. (b) *Ibid.* **1982**, *B38*, 1741.
(15) Nesmeyanov, A. N.; Sedova, N. N.; Struchkov, Y. T.; Andrianov, V. G.; Stakheeva, E. N.; Sazonova, V. A. *J. Organomet. Chem.* **1978**, *153*, 115.
(16) Nesmeyanov, A. N.; Struchkov, Y. T.; Sedova, N. N.; Andrianov, V. G.; Volgin, Y. V.; Sazonova, V. A. *J. Organomet. Chem.* **1977**, *137*, 217.
(17) McKechnie, J. S.; Maier, C. A.; Bersted, B.; Paul, I. C. *J. Chem. Soc., Perkin Trans. 2* **1973**, 138.
(18) Lippard, S. J.; Martin, G. *J. Am. Chem. Soc.* **1970**, *92*, 7291.
(19) Churchill, M. R.; Wormald, J. *Inorg. Chem.* **1969**, *8*, 1970.
(20) Osborne, A. G.; Hollands, R. E.; Bryan, R. F.; Lockhart, S. *J. Organomet. Chem.* **1982**, *224*, 129.
(21) Osborne, A. G.; Hollands, R. E.; Howard, J. A. K.; Bryan, R. F. *J. Organomet. Chem.* **1981**, *205*, 395.
(22) Stoeckli-Evans, H.; Osborne, A. G.; Whiteley, R. H. *J. Organomet. Chem.* **1980**, *194*, 91.
(23) Stoeckli-Evans, H.; Osborne, A. G.; Whiteley, R. H. *Helv. Chim. Acta* **1976**, *59*, 2402.
(24) Abramovitch, R. A.; Atwood, J. L.; Good, M. L.; Lampert, B. A. *Inorg. Chem.* **1975**, *14*, 3085.
(25) Pierpont, C. G.; Eisenberg, R. *Inorg. Chem.* **1972**, *11*, 828.
(26) Davis, B. R.; Bernal, I. *J. Cryst. Mol. Struct.* **1972**, *2*, 107.
(27) Cameron, T. S.; Cordes, R. E. *Acta Crystallogr., Sect. B* **1979**, *B35*, 748.
(28) Sal'nikova, T. N.; Andrianov, V. I.; Struchkov, Y. T. *Koord. Khim.* **1977**, *3*, 768.
(29) Lecomte, C.; Dusausoy, Y.; Protas, J.; Moise, C. *Acta Crystallogr., Sect. B* **1973**, *B29*, 1127.
(30) Jones, N. D.; Marsh, R. E.; Richards, J. H. *Acta Crystallogr.* **1965**, *19*, 330.
(31) Hisatome, M.; Kawajiri, Y.; Yamakawa, K.; Mamiya, K.; Harada, Y.; Iitaka, Y. *Inorg. Chem.* **1982**, *21*, 1345.
(32) Hisatome, M.; Kawaziri, Y.; Yamakawa, K.; Iitaka, Y. *Tetrahedron Lett.* **1979**, 1777.
(33) Spaulding, L. D.; Hillman, M.; Williams, G. J. B. *J. Organomet. Chem.* **1978**, *155*, 109.
(34) Hillman, M.; Fujita, E. *J. Organomet. Chem.* **1978**, *155*, 99. Table 6 of this reference summarizes various parameters from a variety of bridged ferrocenes.
(35) Hillman, M.; Fujita, E. *J. Organomet. Chem.* **1978**, *155*, 87.
(36) Sal'nikova, T. N.; Andrianov, V. I.; Antipin, M. Y.; Struchkov, Y. T. *Koord. Khim.* **1977**, *3*, 939.
(37) Yasufuku, K.; Aoki, K.; Yamazaki, H. *Inorg. Chem.* **1977**, *16*, 624.
(38) Batail, P.; Grandjean, D.; Astruc, D.; Dabard, R. *J. Organomet. Chem.* **1976**, *110*, 91.
(39) Batail, P.; Grandjean, D.; Astruc, D.; Dabard, R. *J. Organomet. Chem.* **1975**, *102*, 79.
(40) Churchill, M. R.; Lin, K.-K. G. *Inorg. Chem.* **1973**, *12*, 2274.
(41) Lectome, C.; Dusausoy, Y.; Protas, J.; Moise, C.; Tirouflet, J. *Acta Crystallogr., Sect B* **1973**, *B29*, 488.
(42) Churchill, M. R.; Wormald, J. *Inorg. Chem.* **1969**, *8*, 716. Table VIII of this reference summarizes the configurations of ferrocene derivatives published before ca. 1969.
(43) Paul, I. C. *J. Chem. Soc., Chem. Commun.* **1966**, 377.
(44) Laing, M. B.; Trueblood, K. N. *Acta Crystallogr.* **1965**, *19*, 373.
(45) Marr, G.; Rockett, B. W. *J. Organomet. Chem.* **1982**, *227*, 373.

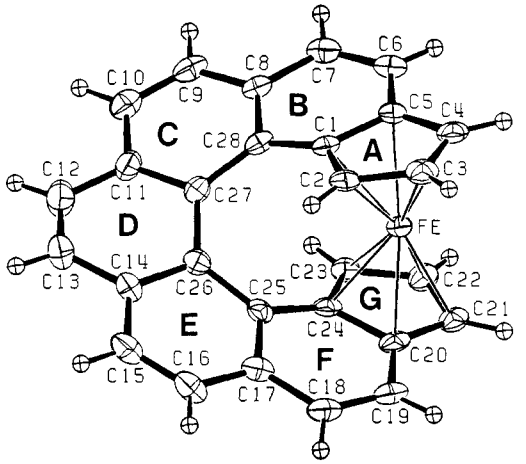

Figure 1. Diagram of the title compound, 1, showing the atom labeling scheme. This does *not* correspond to the Chemical Abstracts numbering (see ref 1). The 40% probability thermal ellipsoids are depicted for the iron and carbon atoms. Hydrogen atoms have been assigned as arbitrary spheres with $B = 1.0$ Å^2 and are labeled according to the carbon atom to which they are bound. The molecule possesses approximate C_2 symmetry but has no crystallographically imposed symmetry. The approximate twofold axis is the line joining the midpoints of the C(12)–C(13) and C(26)–C(27) bonds.

chemistry and structure of complexes containing the ferrocene moiety have appeared recently, and they cover the subject in part. This paper presents the results of a crystallographic study on the title compound, 1.

Experimental Section

Collection and Reduction of X-ray Data. Crystals of the title compound, 1, were provided by Professor T. J. Katz and Dr. J. Pesti, who have described the synthesis of the compound elsewhere.[5] The dark red crystal used in the diffraction study had approximate dimensions 0.17 mm × 0.13 mm × 0.80 mm and was sealed in a capillary under nitrogen to minimize possible decomposition. Open-counter ω scans of several strong low-angle reflections showed that the crystal quality was excellent, the average width of the peaks at half-height being 0.10°. Further details of the data collection and reduction appear in Table I and ref 48.

Determination and Refinement of the Structure. Study on the diffractometer showed that the crystal belonged to the orthorhombic system, and the systematic absences $0kl$ when $k \neq 2n$, $h0l$ when $l \neq 2n$, and $hk0$ when $h \neq 2n$ uniquely define the space group as *Pbca* (D_{2h}^{15}, No. 61).[49] The structure was solved by using the heavy-atom method. Neutral atom scattering factors and anomalous dispersion corrections for the non-hydrogen atoms were obtained from ref 50. Scattering factors for the hydrogen atoms were those of Stewart et al.[51] All non-hydrogen atoms were refined anisotropically, and no evidence for disorder was observed in any part of the structure. Hydrogen atoms were placed in calculated positions (C–H = 0.95 Å) and were constrained to "ride" on the carbon atom to which they are bound. A common isotropic temperature factor for all the hydrogen atoms converged at $U = 0.039$ (3) Å^2.

Table II. Final Positional Parameters for the Atoms of the Title Compound, 1[a,b]

atom	x	y	z
Fe	0.32250 (3)	0.36465 (5)	−0.31579 (3)
C(1)	0.4233 (2)	0.4135 (4)	−0.3748 (2)
C(2)	0.3742 (3)	0.5039 (4)	−0.3503 (2)
C(3)	0.3735 (3)	0.5044 (4)	−0.2731 (3)
C(4)	0.4215 (3)	0.4147 (4)	−0.2483 (3)
C(5)	0.4558 (2)	0.3604 (4)	−0.3103 (2)
C(6)	0.5147 (3)	0.2737 (4)	−0.3171 (3)
C(7)	0.5440 (3)	0.2481 (4)	−0.3832 (3)
C(8)	0.5089 (3)	0.2932 (4)	−0.4495 (3)
C(9)	0.5407 (3)	0.2603 (4)	−0.5177 (3)
C(10)	0.5058 (3)	0.2986 (4)	−0.5800 (3)
C(11)	0.4311 (3)	0.3619 (4)	−0.5786 (2)
C(12)	0.3977 (4)	0.4067 (4)	−0.6447 (3)
C(13)	0.3318 (3)	0.4755 (4)	−0.6431 (3)
C(14)	0.2804 (3)	0.4873 (4)	−0.5785 (2)
C(15)	0.2053 (3)	0.5492 (4)	−0.5806 (3)
C(16)	0.1522 (3)	0.5557 (4)	−0.5218 (3)
C(17)	0.1676 (3)	0.4915 (4)	−0.4600 (2)
C(18)	0.1116 (3)	0.4998 (4)	−0.3971 (3)
C(19)	0.1246 (3)	0.4458 (4)	−0.3353 (3)
C(20)	0.1896 (2)	0.3646 (4)	−0.3338 (2)
C(21)	0.2124 (3)	0.2855 (4)	−0.2810 (3)
C(22)	0.2707 (3)	0.2131 (3)	−0.3142 (3)
C(23)	0.2875 (3)	0.2485 (3)	−0.3858 (2)
C(24)	0.2403 (2)	0.3450 (3)	−0.3985 (2)
C(25)	0.2395 (3)	0.4228 (3)	−0.4580 (2)
C(26)	0.3038 (3)	0.4326 (4)	−0.5140 (2)
C(27)	0.3911 (3)	0.3868 (3)	−0.5110 (2)
C(28)	0.4395 (2)	0.3661 (4)	−0.4457 (2)
Ω(A)	0.40965	0.43940	−0.31136
Ω(G)	0.24008	0.29133	−0.34266
H(2)	0.3465	0.5546	−0.3808
H(3)	0.3462	0.5563	−0.2433
H(4)	0.4291	0.3936	−0.1991
H(6)	0.5327	0.2347	−0.2754
H(7)	0.5895	0.1980	−0.3875
H(9)	0.5870	0.2110	−0.5195
H(10)	0.5321	0.2827	−0.6253
H(12)	0.4231	0.3878	−0.6898
H(13)	0.3185	0.5169	−0.6849
H(15)	0.1913	0.5872	−0.6238
H(16)	0.1048	0.6034	−0.5222
H(18)	0.0629	0.5450	−0.4006
H(19)	0.0928	0.4624	−0.2928
H(21)	0.1925	0.2827	−0.2323
H(22)	0.2945	0.1513	−0.2917
H(23)	0.3234	0.2136	−0.4201

[a] Atoms are labeled as shown in Figure 1. Estimated standard deviations, in parentheses, occur in the last significant figure for each parameter. Ω(A) and Ω(G) represent the centroids of rings A and G, respectively. [b] Hydrogen atoms are labeled according to the carbon to which they are bound.

Full-matrix least-squares refinement of 263 variables, using SHELX-76,[52] converged to final residual indices[53] of $R_1 = 0.040$ and $R_2 = 0.043$. The function minimized in the least squares was $\sum w(|F_o| - |F_c|)^2$, where $w = 1.0981/[\sigma^2(F_o) + 0.000\,400F_o^2]$. In the final cycles of refinement, no parameter shifted by more than 0.001 of its estimated standard deviation, and the largest peak on the final difference Fourier map was 0.37 e Å^{-3}. The average $w\Delta^2$ for groups of data sectioned according to parity group, $|F_o|$, $(\sin\theta)/\lambda$, $|h|$, $|k|$, or $|l|$, showed good consistency, and the weighting scheme was considered to be satisfactory.

Final positional parameters, together with their estimated standard deviations, appear in Table II. Interatomic distances and angles, with estimated standard deviations, are given in Table III. A listing of final observed and calculated structure factors, a table of anisotropic thermal parameters, and the results of

(46) Cullen, W. R.; Woollins, J. D. *Coord. Chem. Rev.* **1981**, *39*, 1.
(47) (a) Omae, I. *Coord. Chem. Rev.* **1982**, *42*, 31. The references in Table 2 of this review appear to be in error. Structure **45** should be equated with ref 59 and structure **64** with ref 78, and thereafter each reference number incremented by unity and equated with the next structure in the table until, finally, structure **69** equates with ref 84. Also, ref 75 in this review is misprinted and should correspond to ref 23 in this paper. (b) Omae, I., personal communication.
(48) Silverman, L. D.; Dewan, J. C.; Giandomenico, C. M.; Lippard, S. J. *Inorg. Chem.* **1980**, *19*, 3379.
(49) "International Tables for X-ray Crystallography", 3rd ed.; Kynoch Press: Birmingham, England, 1976; Vol. I, p 150.
(50) "International Tables for X-ray Crystallography"; Kynoch Press: Birmingham, England, 1974; Vol. IV, pp 99, 149.
(51) Stewart, R. F.; Davidson, E. R.; Simpson, W. T. *J. Chem. Phys.* **1965**, *42*, 3175.
(52) Sheldrick, G. M. In "Computing in Crystallography"; Schenk, H., Olthof-Hazekamp, R., van Koningsveld, H., Bassi, G. C., Eds.; Delft University Press: Delft, Holland, 1978; p 34.
(53) $R_1 = \sum||F_o| - |F_c||/\sum|F_o|$; $R_2 = [\sum w(|F_o| - |F_c|)^2/\sum w|F_o|^2]^{1/2}$.

least-squares plane calculations are available as supplementary material in Tables S1–S3, respectively. Figure 1 depicts the geometry in 1 along with the atom labeling scheme.

Discussion

The structure of the title compound, 1, consists of discrete molecules as shown in Figure 1 wherein an iron atom is bound in a η^5 fashion by each of the two cyclopentadienyl rings at either extremity of the doubly deprotonated helicene **2**. Specifically, the iron is bound to atoms C(1) through C(5) of ring A and to atoms C(20) through C(24) of ring G which means that the helicene, taken as a whole, binds iron in an overall η^{10} fashion. The space group, uniquely defined by its systematic absences as *Pbca*, requires equal numbers of both enantiomers of 1 to be present in each crystal which was also the case for the structure of **2**.[6] In contrast to the structure of **2**, however, in which the molecule has crystallographically required twofold symmetry (i.e., C_2 symmetry), the molecule in the present case has no crystallographically imposed symmetry although the approximation to C_2 symmetry is good. The approximate twofold axis in 1 is the line joining the midpoints of the C(12)–C(13) and C(26)–C(27) bonds. There are no unusually short intermolecular contacts in the structure the closest non-hydrogen atom contact being 3.350 (6) Å between C(2) and C(10), where the latter atom is at $(1 - x, 1 - y, 1 + z)$. All remaining contacts are greater than 3.484 (6) Å.

The angle of tilt, or dihedral angle, between cyclopentadienyl rings A and G in **1** is 19.8°. As a result of this tilt the Fe–C distances to rings A and G vary systematically and range from 2.008 (4) to 2.087 (4) Å for ring A and from 2.007 (4) to 2.104 (4) Å for ring G with the shorter distances being closer to the inner core of the molecule. The deviations between equivalent distances to rings A and G are comparable and in no case is this difference greater than ca. 4σ, thus maintaining the approximate C_2 symmetry of the molecule. The range of Fe–C distances in **1** is quite comparable to that observed in a large number of similar complexes.[15-44] The complex with which **1** is most comparable is (1,1′-ferrocenediyl)diphenylsilane,[23] having an angle of tilt of 19.2°, where the Fe–C distances range from 2.01 (1) to 2.11 (1) Å. The Ω–Fe–Ω angle in this compound is 167.3° while that in **1** is 165.4°, where Ω represents the centroid of each cyclopentadienyl ring. The Fe–C distances observed in the most recent room-temperature structure determination of the monoclinic modification of ferrocene[12] range rather widely from 2.009 to 2.054 Å. The shorter distance is comparable to the shortest distance observed in **1** although the longer distance in **1** is greater than that in ferrocene by some 0.05 Å.

The Fe–Ω distance tends to be fairly constant at between 1.64 and 1.66 Å throughout the large range of bridged ferrocene complexes that have been structurally characterized. The Fe–Ω distance in ferrocene[12] is 1.655 Å which compares well with Fe–Ω(A) = 1.652 Å and Fe–Ω(G) = 1.655 Å in **1**. In certain ferrocene complexes the bridges between the cyclopentadienyl rings are such that the rings are forced closer together than is usually observed, examples being [4](1,1′)[4](3,3′)[4](5,5′)[3](4,4′)ferrocenophane,[32] 1,1′,2,2′,3,3′,4,5,4′,5′-pentakis(trimethylene)ferrocene,[33] 1,1′,2,2′,3,4,4′,5′-tetrakis(trimethylene)ferrocene,[34] and 1,1′,2,2′,4,4′-tris(trimethylene)ferrocene[35] where the Fe–Ω distances are, respectively, 1.618, 1.60, 1.616, and 1.573 Å. Fe–C distances shorter than ca. 2.0 Å are observed, and they tend to be found in these complexes where the cyclopentadienyl rings have been forced closer together than is usual. One of the shortest Fe–C distances observed is 1.968 (6) Å in 1,1′,2,2′,4,4′-tris(trimethylene)ferrocene, and in this case the Fe–Ω distance is the very short 1.573 Å.[35]

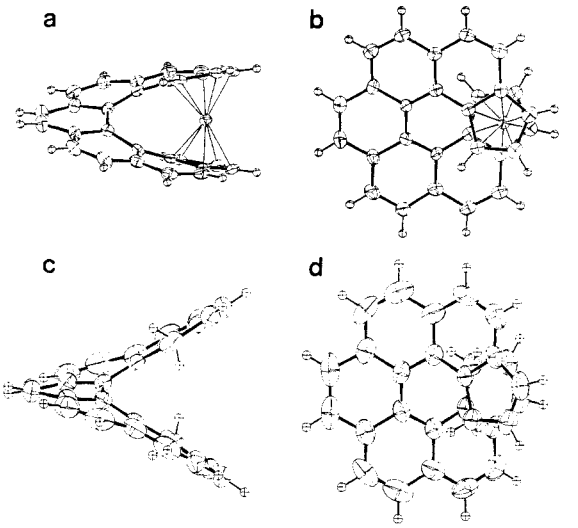

Figure 2. (a) Side view of the title compound, **1**. (b) Top view of **1**. (c) Side view of **2**. (d) Top view of **2**. The 40% probability thermal ellipsoids are depicted for all iron and carbon atoms while all hydrogen atoms are depicted as arbitrary spheres with B = 1.0 Å^2. The structure of **2** has been reported in ref 6.

Comparison between **1** and **2** (Figure 2) shows a dramatic decrease in the dihedral angle between the two terminal cyclopentadienyl ring planes upon complexation of iron(II). The angle of tilt in **2**[6] is 69.1° while that for **1** is 19.8°. The value in **2** is very much larger than that normally observed in similar hexahelicenes and heptahelicenes because two methylene hydrogen atoms on either cyclopentadiene ring are projected into the inner core of the molecule thus forcing the helix arms apart to prevent close intramolecular contacts with carbon atoms. The dihedral angle between terminal ring planes for hexahelicene[54] is 58.5°, for 2-methylhexahelicene 54.8°,[55] and for tribenzo[*f*,*l*,*r*]heptahelicene 33.2°[56] and for heptahelicene averages 32.3°.[57,58] It was suggested previously[6] that helicene **3** should be much less strained than **2** since the two methylene hydrogen atoms are now projected away from the inner core of the molecule. This proposal has not been experimentally verified although, by comparison with heptahelicene itself,[57,58] a dihedral angle of aroung 30° might be expected for **3**. The 19.8° observed in **1** suggests, therefore, that the introduction of iron(II) has served to close the helix arms and clamp rings A and G at a distance closer than might be expected for **3**. It was also suggested previously[6] that the dianion of **2**, produced by deprotonation of both cyclopentadiene rings, should show less strain in the helix. While this argument seems sound on steric grounds, it appears that the two negative charges on the terminal cyclopentadienyl rings serve to keep the helix arms splayed apart, a fact that is suggested by the experimental observation[5] that deuterated acids attack almost as often from the inside of the molecule as from the outside.

The decreased strain in **1**, compared to the highly strained helix in **2**, can also be seen by comparing the

(54) de Rango, C.; Tsoucaris, G.; Declercq, J.-P.; Germain, G.; Putzeys, J. P. *Cryst. Struct. Commun.* **1973**, *2*, 189.
(55) Frank, G. W.; Hefelfinger, D. T.; Lightner, D. A. *Acta Crystallogr., Sect. B* **1973**, *B29*, 223.
(56) van den Hark, Th. E. M.; Noordik, J. H.; Beurskens, P. T. *Cryst. Struct. Commun.* **1974**, *3*, 443.
(57) Beurskens, P. T.; Beurskens, G.; van den Hark, Th. E. M. *Cryst. Struct. Commun.* **1976**, *5*, 241.
(58) van den Hark, Th. E. M.; Beurskens, P. T. *Cryst. Struct. Commun.* **1976**, *5*, 247.

Table III. Interatomic Distances (Å) and Angles (deg) for the Non-Hydrogen Atoms of the Title Compound, 1[a]

Coordination Sphere

Bond Distances

Fe-C(1)	2.008 (4)	Fe-C(5)	2.087 (4)	Fe-C(23)	2.013 (4)
Fe-C(2)	2.017 (4)	Fe-C(20)	2.104 (4)	Fe-C(24)	2.007 (4)
Fe-C(3)	2.070 (4)	Fe-C(21)	2.084 (4)	Fe-Ω(A)	1.652
Fe-C(4)	2.079 (4)	Fe-C(22)	2.055 (4)	Fe-Ω(G)	1.655

Bond Angles

C(1)-Fe-C(2)	41.8 (2)	C(4)-Fe-C(5)	40.1 (2)	Fe-C(1)-C(5)	72.2 (2)
C(1)-Fe-C(3)	69.3 (2)	C(4)-Fe-C(20)	146.0 (2)	Fe-C(1)-C(28)	119.9 (3)
C(1)-Fe-C(4)	69.4 (2)	C(4)-Fe-C(21)	125.0 (2)	Fe-C(2)-C(1)	68.8 (2)
C(1)-Fe-C(5)	41.5 (2)	C(4)-Fe-C(22)	124.1 (2)	Fe-C(2)-C(3)	71.7 (3)
C(1)-Fe-C(20)	133.6 (2)	C(4)-Fe-C(23)	143.1 (2)	Fe-C(3)-C(2)	67.7 (3)
C(1)-Fe-C(21)	163.2 (2)	C(4)-Fe-C(24)	165.0 (2)	Fe-C(3)-C(4)	70.3 (3)
C(1)-Fe-C(22)	126.6 (2)	C(5)-Fe-C(20)	173.6 (2)	Fe-C(4)-C(3)	69.6 (3)
C(1)-Fe-C(23)	94.9 (2)	C(5)-Fe-C(21)	142.9 (2)	Fe-C(4)-C(5)	70.2 (2)
C(1)-Fe-C(24)	97.4 (2)	C(5)-Fe-C(22)	111.7 (2)	Fe-C(5)-C(1)	66.3 (2)
C(2)-Fe-C(3)	40.6 (2)	C(5)-Fe-C(23)	106.5 (2)	Fe-C(5)-C(4)	69.6 (2)
C(2)-Fe-C(4)	68.4 (2)	C(5)-Fe-C(24)	132.3 (2)	Fe-C(5)-C(6)	131.3 (3)
C(2)-Fe-C(5)	68.7 (2)	C(20)-Fe-C(21)	39.9 (2)	Fe-C(20)-C(19)	134.6 (3)
C(2)-Fe-C(20)	110.3 (2)	C(20)-Fe-C(22)	67.2 (2)	Fe-C(20)-C(21)	69.3 (2)
C(2)-Fe-C(21)	146.6 (2)	C(20)-Fe-C(23)	68.3 (2)	Fe-C(20)-C(24)	65.8 (2)
C(2)-Fe-C(22)	162.4 (2)	C(20)-Fe-C(24)	41.3 (1)	Fe-C(21)-C(20)	70.8 (2)
C(2)-Fe-C(23)	121.8 (2)	C(21)-Fe-C(22)	40.1 (2)	Fe-C(21)-C(22)	68.8 (2)
C(2)-Fe-C(24)	97.1 (2)	C(21)-Fe-C(23)	68.4 (2)	Fe-C(22)-C(21)	71.0 (2)
C(3)-Fe-C(4)	40.1 (2)	C(21)-Fe-C(24)	69.3 (2)	Fe-C(22)-C(23)	68.1 (2)
C(3)-Fe-C(5)	67.5 (2)	C(22)-Fe-C(23)	40.7 (2)	Fe-C(23)-C(22)	71.3 (2)
C(3)-Fe-C(20)	116.1 (2)	C(22)-Fe-C(24)	69.3 (2)	Fe-C(23)-C(24)	68.9 (2)
C(3)-Fe-C(21)	126.9 (2)	C(23)-Fe-C(24)	41.7 (2)	Fe-C(24)-C(20)	72.9 (2)
C(3)-Fe-C(22)	156.9 (2)	Ω(A)-Fe-Ω(G)	165.4	Fe-C(24)-C(23)	69.4 (2)
C(3)-Fe-C(23)	162.2 (2)	Fe-C(1)-C(2)	69.4 (2)	Fe-C(24)-C(25)	119.4 (3)
C(3)-Fe-C(24)	129.6 (2)				

Ligand Geometry

Bond Distances

C(1)-C(2)	1.436 (6)	C(12)-C(13)	1.340 (7)	C(24)-C(25)	1.462 (6)
C(1)-C(5)	1.451 (6)	C(13)-C(14)	1.443 (6)	C(25)-C(26)	1.445 (5)
C(1)-C(28)	1.454 (6)	C(14)-C(15)	1.406 (6)	C(26)-C(27)	1.479 (6)
C(2)-C(3)	1.419 (6)	C(14)-C(26)	1.415 (6)	C(27)-C(28)	1.443 (6)
C(3)-C(4)	1.421 (6)	C(15)-C(16)	1.366 (6)	C(1)···C(23)	2.963 (6)
C(4)-C(5)	1.430 (6)	C(16)-C(17)	1.411 (6)	C(1)···C(24)	3.017 (5)
C(5)-C(6)	1.426 (6)	C(17)-C(18)	1.455 (6)	C(2)···C(20)	3.381 (6)
C(6)-C(7)	1.338 (6)	C(17)-C(25)	1.413 (5)	C(2)···C(24)	3.015 (6)
C(7)-C(8)	1.451 (6)	C(18)-C(19)	1.337 (6)	C(3)···C(20)	3.542 (6)
C(8)-C(9)	1.411 (6)	C(19)-C(20)	1.434 (6)	C(3)···C(21)	3.716 (6)
C(8)-C(28)	1.417 (6)	C(20)-C(21)	1.428 (6)	C(4)···C(21)	3.693 (6)
C(9)-C(10)	1.357 (6)	C(20)-C(24)	1.451 (5)	C(4)···C(22)	3.651 (6)
C(10)-C(11)	1.410 (6)	C(21)-C(22)	1.420 (6)	C(5)···C(22)	3.428 (6)
C(11)-C(12)	1.436 (6)	C(22)-C(23)	1.414 (6)	C(5)···C(23)	3.286 (6)
C(11)-C(27)	1.428 (6)	C(23)-C(24)	1.430 (5)		

Bond Angles

C(2)-C(1)-C(5)	106.7 (4)	C(12)-C(11)-C(27)	119.9 (4)	C(21)-C(22)-C(23)	108.7 (4)
C(2)-C(1)-C(28)	133.9 (4)	C(11)-C(12)-C(13)	120.0 (4)	C(22)-C(23)-C(24)	108.6 (4)
C(5)-C(1)-C(28)	119.2 (4)	C(12)-C(13)-C(14)	120.0 (4)	C(20)-C(24)-C(23)	106.8 (4)
C(1)-C(2)-C(3)	108.8 (4)	C(13)-C(14)-C(15)	123.3 (4)	C(20)-C(24)-C(25)	119.8 (4)
C(2)-C(3)-C(4)	108.3 (4)	C(13)-C(14)-C(26)	118.6 (4)	C(23)-C(24)-C(25)	133.2 (4)
C(3)-C(4)-C(5)	108.3 (4)	C(15)-C(14)-C(26)	132.6 (4)	C(17)-C(25)-C(24)	115.4 (4)
C(1)-C(5)-C(4)	107.8 (4)	C(14)-C(15)-C(16)	119.6 (4)	C(17)-C(25)-C(26)	118.9 (4)
C(1)-C(5)-C(6)	120.0 (4)	C(15)-C(16)-C(17)	120.6 (5)	C(24)-C(25)-C(26)	125.7 (4)
C(4)-C(5)-C(6)	132.2 (4)	C(16)-C(17)-C(18)	120.8 (5)	C(14)-C(26)-C(25)	117.3 (4)
C(5)-C(6)-C(7)	118.8 (4)	C(16)-C(17)-C(25)	119.8 (4)	C(14)-C(26)-C(27)	117.1 (4)
C(6)-C(7)-C(8)	122.8 (4)	C(18)-C(17)-C(25)	119.8 (4)	C(25)-C(26)-C(27)	125.5 (4)
C(7)-C(8)-C(9)	120.1 (4)	C(17)-C(18)-C(19)	120.3 (4)	C(11)-C(27)-C(26)	117.0 (4)
C(7)-C(8)-C(28)	119.8 (4)	C(18)-C(19)-C(20)	121.1 (5)	C(11)-C(27)-C(28)	117.2 (4)
C(9)-C(8)-C(28)	120.0 (4)	C(19)-C(20)-C(21)	120.1 (4)	C(26)-C(27)-C(28)	125.8 (4)
C(8)-C(9)-C(10)	120.6 (4)	C(19)-C(20)-C(24)	119.4 (4)	C(1)-C(28)-C(8)	116.0 (4)
C(9)-C(10)-C(11)	121.0 (4)	C(21)-C(20)-C(24)	107.8 (4)	C(1)-C(28)-C(27)	125.6 (4)
C(10)-C(11)-C(12)	120.2 (4)	C(20)-C(21)-C(22)	107.9 (4)	C(8)-C(28)-C(27)	118.4 (4)
C(10)-C(11)-C(27)	120.0 (4)				

[a] See footnote *a*, Table II. Values reported have not been corrected for thermal motion.

terminus to terminus torsion angles around the inner core of the molecules which are 15.8, 19.1, 27.8, 17.1, and 15.1° for the torsion angles C(2)–C(1)–C(28)–C(27), C(1)–C(28)–C(27)–C(26), C(28)–C(27)–C(26)–C(25), C(27)–C(26)–C(25)–C(24), and C(26)–C(25)–C(24)–C(23) in **1**. The similar angles for **2**, which has crystallographically imposed C_2 symmetry, are 4.8, 20.2, 40.8, 20.2, and 4.8°. Thus the strain at the C(28)–C(27)–C(26)–C(25) torsion angle, being 27.8° in **1** compared with 40.8° in **2**, is now much more in line with that observed in heptahelicene where this angle averages 25.0° over two independent structure determinations.[57,58] The similar angles in 2-methylhexahelicene[55] are 26 and 30° while in 2-bromohexahelicene[59] they are 26.6 and 27.9°. Torsion angles around the periphery of the helicene in **1** are 10.0, 7.4, 14.4, 6.3, and 9.0° for the torsion angles C(5)–C(6)–C(7)–C(8), C(8)–C(9)–C(10)–C(11), C(11)–C(12)–C(13)–C(14), C(14)–C(15)–C(16)–C(17), and C(17)–C(18)–C(19)–C(20).

Although in a less dramatic fashion than noted above, the release of helical strain in **1** compared with **2** is also seen in the dihedral angles between consecutive least-squares planes through rings A to G which for **1** are 8.3, 11.7, 12.5, 12.6, 9.5, and 10.2° and for **2** are 6.8, 14.1, 17.4, 17.4, 14.1, and 6.8°. The largest deviations from the least-squares planes through rings A to G are 0.023, 0.117, 0.100, 0.133, 0.094, 0.111, and 0.028 Å in **1**, while the comparable deviations in **2** are 0.013, 0.050, 0.124, 0.142, 0.124, 0.050, and 0.013 Å. Thus the deviations from planarity are greater in the outer ring planes for **1** when compared with **2**. The large helical strain in **2** means, however, that for the inner rings of the helix these deviations become larger in **2**, although only by about 0.11 Å.

The C–C distances in the cyclopentadienyl rings of **1** range from 1.419 (6) to 1.451 (6) Å for ring A (average = 1.431 Å) and from 1.414 (6) to 1.451 (5) Å for ring G (average = 1.429 Å). These average values agree well with the accepted[40] η^5-cyclopentadienyl C–C bond length of ca. 1.43 Å. The cyclopentadienyl distances in **1** are obviously different from those observed in **2** where the nonaromatic nature of the cyclopentadiene rings in this latter compound is reflected in a much larger range of C–C bond lengths. As was noted in the structure of **2**,[6] and indeed with most helicene structures reported to date, the structure of **1** shows the usual pattern of shortened bond lengths along the periphery of the helix and lengthened bonds around the inner core of the molecule. In **1** these shorter peripheral C–C bond lengths are 1.338 (6), 1.357 (6), 1.340 (7), 1.366 (6), and 1.337 (6) Å (average = 1.348 Å) for the bonds C(6)–C(7), C(9)–C(10), C(12)–C(13), C(15)–C(16), and C(18)–C(19). The average value for the similar bonds in **2** is 1.338 Å. The longer inner core C–C bond lengths for **1** are 1.454 (6), 1.443 (6), 1.479 (6), 1.445 (5), and 1.462 (6) Å (average = 1.457 Å) for the bonds C(1)–C(28), C(27)–C(28), C(26)–C(27), C(25)–C(26), and C(24)–C(25) with the average value for the similar bonds in **2** being 1.437 Å. Thus the agreement between these average values for **1** and **2** is quite reasonable.

A compilation of the angles of tilt for several bridged ferrocenes appearing in Table 2 of ref 47 suggests that a two-carbon atom bridge induces an angle of tilt of about 24° into the ferrocene molecule while a three-carbon atom bridge produces an angle of tilt of around 10°. The 19.8° observed in **1** suggests, therefore, that the five benzene rings of the helicene, which are effectively bridging the two cyclopentadienyl rings, are behaving somewhere between a two- and three-carbon atom bridge although closer to the former than the latter. The only compound to have an angle of tilt close to that of **1** is the single silicon atom bridged compound (1,1′-ferrocenediyl)diphenylsilane[23] where the angle of tilt is 19.2°. This value in the similar germanium and phosphorus compounds is 16.6 and 26.7°, respectively.[22]

The angle of twist in **1** (see end of paragraph) averages 26.7° while that in **2** is 24.1°. This difference of 2.6° is probably not a significant deviation especially when one considers that the two structures being compared have angles of tilt differing by some 49.3° and that the cyclopentadienyl rings in **1** are aromatic while those in **2** are not. The conformation of the helicene would seem to be the major factor in determining the angle of twist in **1** and **2**, and the helicene appears to be rather rigid in the sense that the closing of the helix arms by the large 49.3° appears to have little effect on values such as the average peripheral bond lengths and inner core bond lengths of the molecules which, as was seen above, agree quite well between **1** and **2**. Put alternatively, the top views (Figure 2) reveal few differences between **1** and **2** when compared with the dramatic change revealed by a comparison of the side views of **1** and **2**. The angle of twist in **1** was calculated by averaging the five torsion angles C(1)–Ω(A)–Ω(G)–C(23) = 27.3°, C(2)–Ω(A)–Ω(G)–C(24) = 27.3°, C(3)–Ω(A)–Ω(G)–C(20) = 26.4°, C(4)–Ω(A)–Ω(G)–C(21) = 26.4°, and C(5)–Ω(A)–Ω(G)–C(22) = 26.2°.

It is interesting to speculate as to whether complexes that actually require a large angle of tilt between their cyclopentadienyl rings could be formed by the dianion of **2**. The Ω(A)···Ω(G) distance in **1** is 3.28 Å with an angle of tilt of 19.8°, and for **2** the corresponding values are much larger at 4.44 Å and 69.1°. Examination of the recent literature shows that in the uranium complex[60] $\{U[\eta^5\text{-}(CH_3)_5C_5]_2(\mu\text{-}Cl)\}_3$ the Ω···Ω distance is 4.47 Å with an angle of tilt of 48.4° while these values are 4.82 Å and 76.2° in the zirconium complex[61] $[(\eta^5\text{-}C_5H_4CH_3)_2ZrH(\mu\text{-}H)]_2$. This suggests that the dianion of **2** should be capable of forming such complexes, certainly in that the Ω···Ω distance seems to be quite expandable and it may be possible to open this up even further than 4.44 Å, thus inducing further distortions into the helicene. It would be of interest to see how far the helicene could be distorted.

Acknowledgment. I thank Professor S. J. Lippard (Columbia University) for the use of his X-ray diffraction facilities, Professor T. J. Katz and Dr. J. Pesti (Columbia University) for providing the crystals of **1**, Dr. K. Henrick (Polytechnic of North London) for supplying information from the Cambridge Crystallographic Data File[9] via the Crystal Structure Search Retrieval[10] system, and Dr. K. L. Loening (Chemical Abstracts Service) for advice concerning nomenclature.

Registry No. **1**, 83633-75-4.

Supplementary Material Available: Tables S1–S3, listings of final observed and calculated structure factors, anisotropic thermal parameters, and least-squares planes, respectively (11 pages). Ordering information is given on any current masthead page.

(59) Lightner, D. A.; Hefelfinger, D. T.; Powers, T. W.; Frank, G. W.; Trueblood, K. N. *J. Am. Chem. Soc.* **1972**, *94*, 3492.

(60) Fagan, P. J.; Manriquez, J. M.; Marks, T. J.; Day, C. S.; Vollmer, S. H.; Day, V. W. *Organometallics* **1982**, *1*, 170.

(61) Jones, S. B.; Petersen, J. L. *Inorg. Chem.* **1981**, *20*, 2889.

Reactions of the SH^- and S^{2-} Ligands in $W(CO)_5(SH)^-$ and μ-$S[W(CO)_5]_2^{2-}$ with Organic Electrophiles

Robert J. Angelici* and Richard G. W. Gingerich

Department of Chemistry, Iowa State University, Ames, Iowa 50011

Received July 28, 1982

The $W(CO)_5SH^-$ complex reacts at room temperature with heterocumulenes to give products in which the S atom adds to the central carbon of the heterocumulene. Thus, $W(CO)_5SH^-$ reacts with isocyanates (RN=C=O) to give monodentate thiocarbamate complexes $(CO)_5W[SC(=O)NHR]^-$, with the ketene $Ph_2C=C=O$ to give the thioacetate complex $(CO)_5W[SC(=O)CPh_2H]^-$, with isothiocyanates (RN=C=S) to yield bidentate dithiocarbamate complexes $(CO)_4W(S_2CNHR)^-$ via the monodentate intermediate $(CO)_5W[SC(=S)NHR]^-$, with the ketenimine $Ph_2C=C=NPh$ to give the bidentate thioimidate complex $(CO)_4W[SC(=NPh)CPh_2H]^-$ which is transformed to the thioamide complex $(CO)_5W[S=C(NPhH)(CPh_2H)]$ upon reaction with H^+ and CO, and with carbodiimides (RN=C=NR) and H^+ to yield thiourea complexes $(CO)_5W[S=C(NHR)_2]$. The reaction of $W(CO)_5SH^-$ with perfluoroacetone and perfluorocyclohexene gives the F-substituted products $(CO)_5W[SCF_2C(=O)CF_3]^-$ and $(CO)_5W[SC=CF(CF_2)_3CF_2]^-$, respectively. With nitriles (MeCN, MeSCN, H_2NCN) and H^+, the SH^- group is replaced to give $(CO)_5W(N\equiv CR)$ products. With PhOCN, the PhO^- is displaced to give $W(CO)_5(NCS)^-$. Alkylation with $MeOSO_2F$ converts the SH^- complex to $W(CO)_5(SMe_2)$. The dinuclear complex with a bridging S^{2-} ligand, μ-$S[W(CO)_5]_2^{2-}$, reacts with MeN=C=O to give the S-bridged monothiocarbamate complex $[(CO)_5W]_2SC(=O)NMeH^-$ and with $Ph_2C=C=O$ to yield the S-bridged acetate complex $[(CO)_5W]_2SC(=O)CPh_2H^-$. Results of several other attempted reactions of $W(CO)_5SH^-$ with electrophiles are also reported. These studies indicate that the SH^- and μ-S^{2-} ligands in $W(CO)_5SH^-$ and μ-$S[W(CO)_5]_2^{2-}$ are very reactive toward organic electrophiles, while μ-$HS[W(CO)_5]_2^-$ is much less reactive.

Introduction

In 1979, we described the preparations and some reactions of $W(CO)_5SH^-$ and μ-$S[W(CO)_5]_2^{2-}$.[2] At that time, there were few known complexes with SH^- ligands, and very little was known about the reactivity of the coordinated SH^- ligand. More recently, there has been increasing interest in the chemistry of SH^--containing complexes,[3,4] in part because of interest in possible modes of reaction of SH groups on metal sulfide hydrodesulfurization catalysts.

Since this report is concerned with reactions of $W(CO)_5SH^-$ and μ-$S[W(CO)_5]_2^{2-}$, their previously reported reactions are summarized in Scheme I. The bridging sulfido complex μ-$S[W(CO)_5]_2^{2-}$ is reported to react with electrophiles as shown in eq 1, where E = Me_3Sn, MeHg, MeC(=O), $PhCH_2$, or Ph_2P. The related SH^--bridged complex μ-$HS[Cr(CO)_5]_2^-$ reacts with Et_3O^+ to give $(CO)_5Cr(SEt_2)$.[3c]

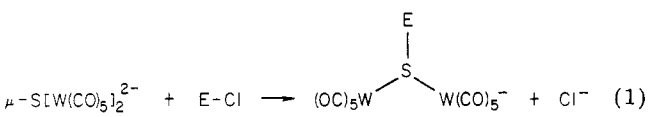

Scheme I[a]

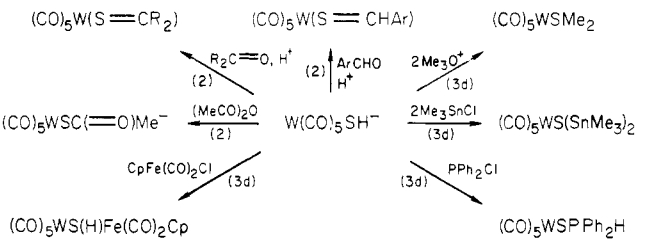

[a] Literature references are given in parentheses.

In this paper, we describe reactions of $W(CO)_5SH^-$ and μ-$S[W(CO)_5]_2^{2-}$ with heterocumulenes and a variety of other organic electrophiles.

Experimental Section

General Procedures. Infrared spectra of solutions and KBr disks were obtained on Perkin-Elmer 237 or 337 and Beckman 4250 spectrophotometers, respectively. The ν(CO) region was calibrated with the 2124-cm^{-1} band of gaseous CO. ^1H NMR Spectra were recorded on Varian A-60 and HA-100 or Perkin-Elmer R20B spectrometers using tetramethylsilane (Me_4Si) as an internal standard. Proton-decoupled ^{13}C NMR spectra of solutions containing added $Cr(acac)_3$[5] and using Me_4Si as the standard were measured on a Bruker HX-90E Fourier transform instrument. This instrument was also used for ^{19}F NMR spectra using hexafluorobenzene as an internal reference; peak positions are reported in δ units relative to $CFCl_3$.

Mass spectra at 18, 50, and 70 eV were obtained on an AEI MS-902 spectrometer. A Cary 14 instrument was used to record visible spectra on 10^{-4} M solutions of the compounds. Conductivities were measured on an Industrial Instruments Model RC 16B2 conductivity bridge at 25.0 °C on 10^{-4} M solutions.

Tetrahydrofuran (THF) was distilled from $LiAlH_4$ under an N_2 atmosphere; absolute EtOH was distilled from CaH_2 also under N_2. Acetone dried over Drierite for 24 h and Et_2O dried over $MgSO_4$ were purged with N_2 before use. Hexanes and *n*-pentane were bubbled with N_2, while CH_2Cl_2 and $CHCl_3$ were dried over

(1) Based on the Ph.D. dissertation submitted by R.G.W.G to Iowa State University, 1977.

(2) Gingerich, R. G. W.; Angelici, R. J. *J. Am. Chem. Soc.* **1979**, *101*, 5604.

(3) (a) Rauchfuss, T. B.; Ruffing, C. J. *Organometallics* **1982**, *1*, 400. (b) McCall, J. M.; Shaver, A. *J. Organomet. Chem.* **1980**, *193*, C37. (c) Hausmann, H.; Höfler, M.; Kruck, T.; Zimmermann, H. W. *Chem. Ber.* **1981**, *114*, 975. (d) Höfler, M.; Hausmann, H.; Heidelberg, H. A. *J. Organomet. Chem.* **1981**, *213*, C1. (e) Cooper, M. K.; Duckworth, P. A.; Henrick, K.; McPartlin, M. *J. Chem Soc., Dalton Trans.* **1981**, 2357. (f) Hartgerink, J.; McCall, J. M.; Shaver, A. In "Abstracts of The Tenth International Conference on Organometallic Chemistry", Toronto, Canada, Aug 9–14, 1981, p 155.

(4) (a) Schmidt, M.; Hoffmann, G. G. *Z. Anorg. Allg. Chem.* **1980**, *464*, 209. (b) Briant, C. E.; Hughes, G. R.; Minshall, P. C.; Mingos, D. M. P. *J. Organomet. Chem.* **1980**, *202*, C18. (c) Kury, R.; Vahrenkamp, H. *J. Chem. Res. Synop.* **1982**, 30. (d) Beck, W.; Grenz, R.; Guetzfried, F.; Vilsmaier, E. *Chem. Ber.* **1981**, *114*, 3184. (e) Harris, R. O.; Yaneff, P. *J. Organomet. Chem.* **1977**, *134*, C40. (f) DiVaira, M.; Midollini, S.; Sacconi, L. *Inorg. Chem.* **1979**, *18*, 3466. (g) Gaffney, T. R.; Ibers, J. A. *Ibid.* **1982**, *21*, 2857. (h) Danzer, W.; Fehlhammer, W. P.; Liu, A. T.; Thiel, G.; Beck, W. *Chem. Ber.* **1982**, *115*, 1682.

(5) (a) Mann, B. E. *Adv. Organomet. Chem.* **1974**, *12*, 135. (b) Todd, L. J. *J. Organomet. Chem.* **1974**, *77*, 1.

0276-7333/83/2302-0089$01.50/0

type 4A molecular sieves. Manipulations of reaction mixtures and residues were performed under an N_2 atmosphere.

Difficult-to-crystallize complexes, of which there were a substantial number in this study, were isolated by a partitional crystallization procedure under N_2. This procedure first involved filtering the reaction solution containing the complex through a glass frit into a 125-mL Erlenmeyer flask equipped with a side-arm stopcock. A volume of Et_2O equal to half the volume of the filtrate (X mL) was floated on top of the filtrate. After being left standing in the freezer (−20 °C) for 1 day, the biphasic mixture became a single phase, which was decanted from precipitated materials. The solution phase was treated as above by floating X mL of Et_2O and collecting another precipitate. Then X-mL portions of a hydrocarbon (frequently hexanes) were repeatedly floated on top of previous solutions until the solutions were free of metal carbonyl products. Precipitated fractions which had the same IR spectra in the ν(CO) region were combined and characterized.

Preparations of the following starting materials are described elsewhere: [PPN][W(CO)$_5$SH] (where PPN$^+$ = $(Ph_3P)_2N^+$),[2] [Et$_4$N]{[μ-HS[W(CO)$_5$]$_2$]},[2] μ-S[W(CO)$_5$]$_2^{2-}$,[2] [Et$_4$N][W(CO)$_5$I],[6] $Ph_2C{=}C{=}NPh$,[7] $PhOC{\equiv}N$,[8] $Ph_2C{=}C{=}O$,[9] and NaSH.[10] The salt [PPN][S_2CNEtH] precipitated when an aqueous solution of Na[S_2CNEtH] was added to a saturated aqueous solution of [PPN]Cl; the product was dried under vacuum.

Preparations. [PPN]{(CO)$_5$W[SC(=O)CPh$_2$H]} and [PPN]{(CO)$_5$W[SC(=O)NPhH]}. A yellow solution of 0.448 g (0.500 mmol) of [PPN][W(CO)$_5$SH] in 20 mL of THF was treated with a 5-mL solution of $Ph_2C{=}C{=}O$ (0.50 mmol) in n-heptane (0.10 M) or 40 μL (0.52 mmol) of $PhN{=}C{=}O$. The mixtures were stirred for 2 h; the resultant yellow suspension was filtered through a frit containing Celite. The filtrate was evaporated to dryness, and the residue was dissolved in acetone. The products were obtained from the acetone solution by partitional crystallization with Et_2O and hexanes. Properties of the yellow needles of [PPN]{(CO)$_5$W[SC(=O)CPh$_2$H]} (66% yield) and yellow powder of [PPN]{(CO)$_5$W[SC(=O)NPhH]} (28%) are given in Tables I and II. Other complexes, whose preparations are given in this section, are also characterized in these tables.

[Et$_4$N]{(CO)$_5$W[SC(=O)NMeH]} and [Et$_4$N][(CO)$_4$W(S$_2$CNRH)] (R = Me, Et, or Ph). A suspension of 0.166 g (1.00 mmol) of Et_4NCl, 0.084 g (1.5 mmol) of NaSH, and 10 mL of EtOH was stirred for 1 h. After vacuum evaporation to a white powder, 0.352 g (1.00 mmol) of $W(CO)_6$ and 10 mL of acetone were added, and the suspension was refluxed for 2 h. The resulting yellow mixture, containing [Et$_4$N][W(CO)$_5$SH], was cooled to room temperature and treated with 80 μL (1.1 mmol) of $MeN{=}C{=}O$, 1.1 mL of a solution of $MeN{=}C{=}S$ (1.0 mmol) in acetone (0.95 M), 87 μL (1.0 mmol) of $EtN{=}C{=}S$, or 0.12 mL (1.0 mmol) of $PhN{=}C{=}S$. After the mixture was refluxed for 2 h, the resulting brown suspensions were filtered through Celite; the yellow filtrates were partitionally crystallized to give yellow plates of [Et$_4$N]{(CO)$_5$W[SC(=O)NMeH]} (17% yield), yellow needles of [Et$_4$N][(CO)$_4$W(S$_2$CNMeH)] (78% yield), or yellow oils of [Et$_4$N][(CO)$_4$W(S$_2$CNEtH)] and [Et$_4$N][(CO)$_4$W(S$_2$CNPhH)].

[PPN][(CO)$_4$W(S$_2$CNPhH)] and [PN]{(CO)$_4$W[SC(=NPh)CPh$_2$H]}. To a 50-mL flask were added consecutively 0.448 g (0.500 mmol) of [PPN][W(CO)$_5$SH], 15 mL of THF, and 62 μL (0.52 mmol) of $PhN{=}C{=}S$ or 0.138 g (0.511 mmol) of $PhN{=}C{=}CPh_2$. After being stirred for 18 h at room temperature, the yellow mixture was filtered through Celite; the solution was evaporated to dryness. The residue was dissolved in acetone and partitionally crystallized with Et_2O and hexanes to give an oil of [PPN]{(CO)$_4$W[SC(=NPh)CPh$_2$H]} and transparent yellow crystals of [PPN][(CO)$_4$W(S$_2$CNPhH)]·0.61$Me_2C{=}O$·0.47Et_2O (26% yield). The presence of $Me_2C{=}O$ and Et_2O of crystallization in the latter compound was established by elemental analysis and ^{1}H NMR spectrometry (Tables I and II).

(CO)$_5$W[S=C(NPhH)(CPh$_2$H)]. To a suspension of 0.185 g (0.207 mmol) of [PPN][W(CO)$_5$SH] in 10 mL of THF was added 0.0782 g (0.291 mmol) of $PhN{=}C{=}CPh_2$ followed by 20 μL (0.23 mmol) of CF_3SO_3H. After being stirred 4 h, the mixture was evaporated to dryness under vacuum. The soluble portion was chromatographed in 20% CH_2Cl_2/hexanes (v/v) on a silica gel (60–200 mesh) column (1.0 × 35 cm), which gave a yellow eluate. The yellow powder, which was obtained upon vacuum evaporation, was washed with 2.5 mL of hexanes at −78 °C to give yellow (CO)$_5$W[S=C(NPhH)(CPh$_2$H)] in 26% yield. This complex was also characterized by its 70-eV mass spectrum which shows m/e values for M$^+$, (M − 3CO)$^+$, and (M − 5CO)$^+$.

(CO)$_5$W[S=C(NH-*i*-Pr)$_2$]. A mixture prepared from 0.451 g (0.504 mmol) of [PPN][W(CO)$_5$SH], 1.2 mL of a solution of i-$PrN{=}C{=}N$-i-Pr (0.505 mmol) in THF (0.421 M), and 10 mL of THF was treated with 49 μL (0.55 mmol) of CF_3SO_3H. The resultant brown mixture was stirred for 18 h. The solution was vacuum evaporated to dryness, and the residue was extracted and chromatographed in 50% $CHCl_3$/hexanes (v/v) on a column (1.5 × 35 cm) of silica gel (60–200 mesh) of Brockman Activity Grade II.[11] The yellow eluate was collected and evaporated to dryness leaving solid (CO)$_5$W[S=C(NH-i-Pr)$_2$] (60% yield) which was washed twice with 5 mL of hexanes and dried. Its mass spectrum shows a parent ion (M$^+$) for the complex.

The same complex was prepared by treating a mixture of 0.163 g (0.201 mmol) of [Et$_4$N]{μ-HS[W(CO)$_5$]$_2$}, 32 μL (0.211 mmol) of i-$PrN{=}C{=}N$-i-Pr, and 10 mL of THF with 18 μL (0.203 mmol) of CF_3SO_3H. After being stirred for 1 h, the mixture was evaporated to dryness, and the residue was chromatographed in $CHCl_3$ on a Florisil (60–100 mesh) column (1 × 20 cm). Evaporation of the yellow eluate gave yellow (CO)$_5$W[S=C(NH-i-Pr)$_2$] (58% yield), whose melting point and spectra were identical with those of the same compound prepared above.

(CO)$_5$W[S=C(NH$_2$)$_2$] and (CO)$_5$W(N≡CNH$_2$). A solution of 0.581 g (1.00 mmol) of [Et$_4$N][W(CO)$_5$I] in 10 mL of acetone was cooled in an ice bath (0 °C) for 10 min. Dropwise addition of 1 mL of $AgBF_4$ (1.0 mmol) in acetone (1.0 M) gave an immediate yellow precipitate of AgI. After being stirred for 1 h, the suspension was treated with 0.0420 g (1.00 mmol) of $N{\equiv}CNH_2$ or 0.152 g (2.00 mmol) of $S{=}C(NH_2)_2$. The solution was stirred for 1.5 h at room temperature. The solvent was evaporated, and the residue was chromatographed on Florisil in $CHCl_3$, giving (CO)$_5$W(N≡CNH$_2$) and (CO)$_5$W[S=C(NH$_2$)$_2$] as yellow powders in 72% and 73% yields, respectively.

(CO)$_5$W(N≡CNH$_2$). To a mixture of 0.177 g (0.198 mmol) of [PPN][W(CO)$_5$SH], 0.0104 g (0.248 mmol) of $N{\equiv}CNH_2$, and 10 mL of THF was added 20 μL (0.225 mmol) of CF_3SO_3H. The mixture was stirred at room temperature for 1 h and then reduced to dryness. The residue was chromatographed in 50/50 (v/v) CH_2Cl_2/hexanes on a 1 × 20 cm Florisil column. The yellow eluate was dried under a stream of N_2 to give yellow needles of (CO)$_5$W[N≡CNH$_2$] in 68% yield. The compound was identical with that prepared above.

(CO)$_5$W(N≡CMe). When a solution of 0.288 g (0.321 mmol) of [PPN][W(CO)$_5$SH] in 15 mL of MeCN was treated with 31 μL of CF_3SO_3H, the reaction solution immediately turned red. After being stirred overnight, the reaction mixture was evaporated to dryness under vacuum. The residue was chromatographed in 50/50 (v/v) CH_2Cl_2/hexanes on silica gel (Activity II); the yellow fraction was evaporated to dryness, giving 0.0762 g (65%) of (CO)$_5$W(NCMe), whose identity was established by its IR spectrum.[12]

(CO)$_5$W(N≡CSMe). The addition of 18 μL (0.203 mmol) of CF_3SO_3H to a mixture of 0.181 g (0.202 mmol) of [PPN][W(CO)$_5$SH] and 14 μL (0.204 mmol) of MeSCN in 10 mL of THF caused an immediate change to dark brown. The mixture was stirred overnight and then chromatographed in 50/50 CH_2Cl_2/hexanes on silica gel (Activity II). The first fraction from the column was evaporated to give 8.6 mg (11%) of yellow-green (CO)$_5$W(NCSMe), which was identified by its IR spectrum.[12]

[PPN][(CO)$_5$W(NCS)]. To a mixture of 0.0445 g (0.0497 mmol) of [PPN][W(CO)$_5$SH] in 5 mL of THF was added 6 μL (0.0548 mmol) of PhOCN. After being stirred overnight, the solution was evaporated to dryness, and the residue was washed

(6) Abel, E. W.; Butler, I. S.; Reid, J. G. *J. Chem. Soc.* **1963**, 2068.
(7) Bestmann, H. J.; Lienert, J.; Mott, L. *Justus Liebigs Ann. Chem.* **1968**, *718*, 24.
(8) Grigat, E.; Putter, R. *Chem. Ber.* **1964**, *97*, 3012.
(9) Darling, S. D.; Kidwell, R. L. *J. Org. Chem.* **1968**, *33*, 3974.
(10) Eibeck, R. E. *Inorg. Synth.* **1963**, *7*, 128.
(11) Abbott, D.; Andrews, R. S. "An Introduction to Chromatography" Longman, Green, and Company: London, 1970.
(12) Quick, M. H.; Angelici, R. J. *Inorg. Chem.* **1976**, *15*, 160.

Table I. Analyses, Physical Properties, and UV-Visible Spectra of the Complexes[a]

complex	mp, °C	anal.[b] % C	anal.[b] % H	Λ_M[c]	nm (M^{-1} cm^{-1})[d]
$(CO)_5W[SC(=O)CPh_2H]^-$ [e]	116–119	60.84 (60.62)	4.02 (3.79)	105	410 (sh), 378 (1510)
$(CO)_5W[SC(=O)NMeH]^-$ [f]	105–108	32.89 (33.10)	4.17 (4.44)[g]	155	424 (1065), 377 (1126)
$(CO)_5W[SC(=O)NPhH]^-$ [e]	99–101			125	417 (775), 376 (1300)
$(CO)_5W[SCF_2C(=O)CF_3]^-$ [f]	96–98	30.92 (30.35)	3.38 (3.18)	151	446 (408), 380 (844)
$(CO)_5W[SC=CF(CF_2)_3CF_2]^-$ [e]	98–100	50.06 (49.62)	2.64 (2.66)	121	443 (537), 376 (1480)
$(CO)_5W[S=C(NPhH)(CPh_2H)]$	42–44	48.07 (47.87)	2.76 (2.73)		400 (4570), 374 (4470)[j]
$(CO)_5W[S=C(NH_2)_2]$	136–139	18.20 (18.02)	1.07 (1.01)		413 (1040), 376 (1950)
$(CO)_5W[S=C(NH\text{-}i\text{-}Pr)_2]$	131–134	29.87 (29.77)	3.36 (3.33)		416 (869), 376 (1650)
$(CO)_5W(N\equiv C\text{-}NH_2)$	105–107	19.85 (19.69)	0.57 (0.55)		412 (sh), 384 (2620)
$(CO)_4W(S_2CNMeH)^-$ [f]	99–101[h]	30.28 (31.59)	4.49 (4.55)		
$(CO)_4W(S_2CNPhH)^-$ [e]	80–82	55.29 (56.76)	4.21 (4.17)[i]	126	394 (991)
$[(CO)_5W]_2SC(=O)NHMe^-$ [f]	120–122[h]	27.69 (27.67)	2.87 (2.79)	158	444 (1520), 375 (2960)

[a] All are yellow. [b] Found (calculated). [c] Molar conductivity (~10^{-4} M in MeCN), cm^2 Ω^{-1} M^{-1}. [d] Visible maxima (ϵ values) in 350–600-nm range; in MeCN solvent. [e] $(Ph_3P)_2N^+$ cation (PPN$^+$). [f] Et_4N^+ cation. [g] % S: 6.12 (5.89). [h] Decomposition temperature. [i] % N: 2.60 (2.61). % S: 6.03 (5.98). Contains 0.61 $Me_2C{=}O$ and 0.47 Et_2O as established by ^1H NMR. [j] In hexanes solvent.

Table II. Infrared and NMR Spectral Features of the Complexes

complex	ν(CO),[a] cm^{-1}	^1H NMR (τ)[b,c]
$(CO)_5WSH^-$ [d]	2056 (w), 1912 (vs), 1843 (m)	12.93 (s, 1, SH)[e]
$(CO)_5W[SC(=O)Me]^-$ [d]	2060 (w), 1968 (sh), 1917 (vs), 1854 (m)[f]	7.55 (s, 1, CH_3)[g]
$(CO)_5W[SC(=O)CPh_2H]^-$ [d]	2060 (w), 1968 (sh), 1916 (vs), 1853 (m)[h]	4.24 (s, 1, CH), 2.64 (m, 40, Ph)
$(CO)_5W[SC(=O)NMeH]^-$ [i]	2062 (w), 1968 (sh), 1916 (vs), 1858 (m)[j]	6.85 (q, 8, NCH_2), 7.41 (s, 3, NCH_3), 8.77 (t, 12, CH_3)[k,l]
$(CO)_5W[SC(=O)NPhH]^-$ [d]	2061 (w), 1968 (sh), 1917 (vs), 1856 (m)[m]	
$(CO)_5W[SCF_2C(=O)CF_3]^-$ [i]	2063 (w), 1924 (vs), 1865 (m)[n]	6.81 (q, 8, NCH_2), 8.81 (t, 12, CH_3)
$(CO)_5W[SC=CF(CF_2)_3CF_2]^-$ [d]	2066 (w), 1971 (sh), 1925 (vs), 1862 (m)[o]	
$(CO)_5W[S=C(NPhH)(CPh_2H)]$	2073 (m), 1988 (w), 1945 (vs), 1934 (s), 1923 (m)[p]	2.82 (m, 16, Ph and NH), 4.49 (s, 1, CH)
$(CO)_5W[S=C(NH_2)_2]$	2072 (w), 1980 (w), 1933 (vs), 1901 (sh)	2.55 (m, NH_2)[q]
$(CO)_5W[S=C(NH\text{-}i\text{-}Pr)_2]$	2071 (w), 1979 (w), 1930 (vs), 1895 (sh)	4.22 (m, NH), 5.98 (m, 1, CH), 8.67 (d, 6, CH_3)
$(CO)_5W(N\equiv C\text{-}NH_2)$	2077 (w), 1975 (w), 1935 (vs), 1894 (m)[r]	4.62 (m, NH_2)[k]
$(CO)_4W(S_2CNMeH)^-$ [i]	2000 (m), 1874 (vs), 1841 (s), 1796 (s)	6.85 (q, NCH_2), 7.14 (s, NCH_3), 8.80 (t, 12, CH_3)[k]
$(CO)_4W(S_2CNPhH)^-$ [d]	2000 (m), 1874 (vs), 1848 (s), 1804 (s)	2.02 (m, NH), 2.58 (m, Ph)[s]
$(CO)_4W[SC(=NPh)CPh_2H]^-$ [d]	1995 (m), 1868 (vs), 1843 (s), 1801 (s)[t]	2.60 (m, Ph), 4.83 (s, CH)
$[(CO)_5W]_2SH^-$ [i]	2068 (sh), 2056 (w), 1969 (sh), 1933 (vs), 1908 (sh), 1859 (m)	11.70 (s, 1, SH), 6.72 (q, 8, NCH_2), 8.58 (t, 12, CH_3)[u]
$[(CO)_5W]_2SC(=O)NMeH^-$ [i]	2072 (sh), 2060 (w), 1974 (sh), 1936 (vs), 1909 (sh), 1866 (m)	3.45 (br, NH), 6.48 (q, 8, NCH_2), 7.25 (d,[w] 3, NCH_3), 8.58 (t, 12, CH_3)[q]
$[(CO)_5W]_2SC(=O)Me^-$ [d]	2073 (sh), 2064 (w), 1976 (sh), 1941 (vs), 1914 (sh), 1872 (m)	7.39 (s, 1, CH_3)

[a] In $CHCl_2$ solvent unless indicated otherwise. [b] Chemical shift (splitting, relative intensity, assignment). $[(Ph_3P)_2N^+]$ peaks not given. Solvent is $CDCl_3$ unless indicated otherwise. [c] Abbreviations for splittings: singlet, s; doublet, d; triplet, t; quartet, q; multiplet, m. [d] $(Ph_3P)_2N^+$ cation (PPN$^+$). [e] ^{13}C NMR ($CDCl_3$): δ 203.4 (trans CO), 199.8 (cis CO). [f] ν(C=O): 1604 (w) cm^{-1} in KBr. [g] ^{13}C NMR ($CDCl_3$): δ 206.2 (SC(=O)), 204.9 (trans CO), 199.5 (cis CO), 34.4 (CH_3). [h] ν(C=O): 1605 (w) cm^{-1} in KBr. [i] Et_4N^+ cation. [j] ν(C=O): 1590 (w) cm^{-1} in KBr. [k] In CD_3CN solvent. [l] ^{13}C NMR (CD_3CN): δ 204.1 (trans CO), 199.6 (cis CO), 199.2 (SC(=O)), 25.8 (NCH_3), 51.8 (NCH_2), 6.5 (CH_3). [m] ν(C=O): 1620 (w) cm^{-1} in KBr. [n] ν(C=O): 1680 (w) cm^{-1} in KBr. [o] ν(C=C): 1639 (vw) cm^{-1} in CH_2Cl_2. [p] In hexanes solvent. [q] In $(CD_3)_2C{=}O$ solvent. [r] ν(C≡N): 2315 (sh), 2270 (w) cm^{-1} in KBr. [s] ^{13}C NMR ($CDCl_3$): δ 199.9 (CN), 197.7 (CO), 188.8 (CO). [t] ν(C=N): 1500 (w) cm^{-1} in KBr. [u] ^{13}C NMR (CD_3CN): δ 201.2 (trans CO), 199.3 (cis CO), 51.8 (NCH_2), 6.4 (CH_3). [v] ν(C=O): 1664 (w) cm^{-1} in KBr. [w] J(HCNH) = 5 Hz.

twice with 5 mL of Et_2O. After the mixture was dried under vacuum, a yield of 0.0270 g (59%) of $[PPN][(CO)_5W(NCS)]$ was obtained. The product was identified by its IR spectrum.[12]

Reaction of $W(CO)_5SH^-$ with MeHgCl/$AgNO_3$. Silver nitrate (0.0177 g, 0.104 mmol) was added to a solution of MeHgCl (0.0264 g, 0.105 mmol) in 5 mL of MeCN. This mixture immediately turned gray when 0.0830 g (0.0926 mmol) of $[PPN][W(CO)_5SH]$ was added. After being stirred overnight, the mixture was evaporated to dryness under vacuum, and the residue was extracted with Et_2O. Filtration and evaporation of the extract yielded 0.0149 g (44%) of $W(CO)_5(NCMe)$ which was characterized by its infrared spectrum.

Reaction of $W(CO)_5SH^-$ with MeHgCl/$AgBF_4$. When 0.846 g (0.945 mmol) of $[PPN][W(CO)_5SH]$ was added to a mixture of 0.252 g (1.01 mmol) of MeHgCl and 0.198 g (1.02 mmol) of $AgBF_4$ in 10 mL of CH_2Cl_2, the mixture became black immediately. After being stirred 1.5 h, the solution was filtered, and the filtrate was treated with 75 mL of hexanes. This solution was filtered, and the filtrate was evaporated to dryness. An IR spectrum (1972 (s) cm^{-1} in CH_2Cl_2) of the slightly yellow residue (0.228 g, 64%) indicated the product to be $W(CO)_6$.

$[Et_4N]\{(CO)_5W[SCF_2C(=O)CF_3]\}$. A suspension of 0.245 g (1.50 mmol) of Et_4NCl and 0.158 g (2.80 mmol) of NaSH in 10 mL of EtOH was stirred for 2 h and then evaporated to dryness. To the residue was added 0.522 g (1.50 mmol) of $W(CO)_6$ and 20 mL of acetone. This mixture was refluxed 2.5 h, and the brown mixture containing $W(CO)_5SH^-$ was cooled to −72 °C in an *i*-PrOH/Dry Ice bath. Then an excess of $(CF_3)_2C{=}O$ was condensed into the solution for 10 min. The mixture was slowly allowed to warm to room temperature and stirred for 16 h. The mixture was filtered, and the product $[Et_4N]\{(CO)_5W[SCF_2C(=O)CF_3]\}$ was isolated from the filtrate as yellow needles in 8% yield by partitional crystallization. The ^{19}F NMR spectrum of the compound in $CDCl_3$ solution showed two peaks: δ 68.5 (s, CF_3), 78.5 (s, CF_2). These assignments are consistent with those made for other $XCF_2C(=O)CF_3$ compounds.[13]

$[PPN]\{(CO)_5W(SC{=}CF(CF_2)_3CF_2]\}$. Perfluorocyclohexene, $CF{=}CF(CF_2)_3CF_2$ (0.10 mL, 0.50 mmol), was added to a suspension of 0.448 g (0.500 mmol) of $[PPN][W(CO)_5SH]$ in 10 mL of THF. The mixture was stirred for 3 h, and partitional crystallization of the resulting black-green solution gave yellow crystals of $[PPN]\{(CO)_5W[SC{=}CF(CF_2)_3CF_2]\}$ in 46% yield. The ^{19}F NMR spectrum of the compound in $CDCl_3$ showed five types of F atoms: δ 109.4 (m, 2, $3CF_2$), 117.4 (m, 2, $6CF_2$), 126.1 (m, 1, 2CF), 134.8 (m, 2, $5CF_2$), 135.6 (m, 2, $4CF_2$). These assignments were made by analogy with those for other $XC{=}CF(CF_2)_3CF_2$ molecules.[14]

$[Et_4N]\{\mu\text{-}HMeNC(=O)S[W(CO)_5]_2\}$. The anion μ-$S[W(CO)_5]_2^{2-}$ was generated by adding 0.0243 g (0.577 mmol) of NaH (in a 57% oil dispersion) to 0.406 g (0.500 mmol) of $[Et_4N]\{\mu\text{-}HS[W(CO)_5]_2\}$ in 10 mL of THF. The reaction mixture turned green immediately; then 43 μL (0.58 mmol) of MeN=C=O was added, and the mixture was stirred for 3 h. To the resulting brown-black suspension was added 0.502 mmol of gaseous HCl, which gave a yellow-brown mixture. The solution was evaporated to dryness, and the residue was dissolved in acetone. This solution was added to 50 mL of an aqueous solution of Et_4NBr (0.27 M, 13.5 mmol) to give an immediate precipitate. After being stirred for 1 h, the mixture was filtered through Celite on a glass frit; the precipitate was then washed through the frit with acetone; the acetone was evaporated to leave a yellow powder. Repeated crystallizations of the powder from mixtures of $CHCl_3$ and hexanes gave the yellow $[Et_4N]\{\mu\text{-}HMeNC(=O)S[W(CO)_5]_2\}$ in 38% yield.

Results and Discussion

Reactions of $W(CO)_5SH^-$, μ-$HS[W(CO)_5]_2^-$, and μ-$S[W(CO)_5]_2^{2-}$ with electrophilic organic compounds are described in the following sections.

Isocyanates (RN=C=O). Alkanethiols (R'SH) are known[15] to react with RN=C=O in the presence of a base catalyst to give thiocarbamates, R'SC(=O)NRH. Even without a base catalyst, $W(CO)_5SH^-$ reacts similarly (eq 2). The thiocarbamate complex product with R = Ph is

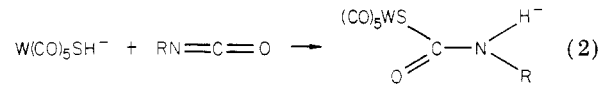

(2)

R = CH_3 or Ph

isolated in 28% yield as the PPN^+ salt, whereas the product with R = Me is isolated in 17% yield as the Et_4N^+ salt. The $[PPN]\{(CO)_5W[SC(=O)NMeH]\}$ salt could be obtained only as an oil, whose IR and UV–visible spectra confirmed the presence of the thiocarbamate complex. Although IR studies indicate that the reactions proceed essentially quantitatively, the extreme reluctance of these and other ionic products reported in this paper to solidify led to low isolated yields.

The 1:1 ionic nature of the products is supported[16] by their molar conductivities (Table I). In the ν(CO) region of the IR spectrum, one expects three allowed absorptions for the pseudo C_{4v} geometry, although another unallowed B_1 band is sometimes observed;[17] all four bands are observed for the thiocarbamate complexes (Table II). Weak bands for the thiocarbamate ν(C=O) vibration are observed about 1600 cm^{-1}. The NCH_3 group in the $^-SC(=O)NMeH$ ligand occurs as a singlet in the ^1H NMR spectrum of the complex in CD_3CN but as a doublet (τ 7.23), presumably due to NH coupling in $CDCl_3$ solvent. There is no evidence for two NCH_3 resonances as would be expected for the presence of two isomers resulting from restricted rotation around the CN amide bond.[18] The ^{13}C NMR spectrum (Table II) of $(CO)_5W[SC(=O)NMeH]^-$ is also consistent with the presence of only one isomer or rapid interconversion of both isomers.

While a full kinetic study of reaction 2 was not conducted, the half-lives for the reactions of MeNCO and PhNCO in THF at room temperature were approximately 1 h and 5 min, respectively. No intermediates were observed in the ν(CO) region during the reactions. Of some interest is whether the SH^- group reacts with RNCO when it is in the $W(CO)_5SH^-$ complex or after it has dissociated to give free SH^-. The latter mechanism could involve free SH^- reaction with RNCO to give $SC(=O)NRH^-$ which would combine with $W(CO)_5$(solvent) to give the product complex. To answer the crucial question of whether SH^- dissociates during reaction 2 to give $W(CO)_5$(solvent), $W(CO)_5SH^-$ was reacted with a 50-fold excess of PPh_3 or with CO in THF at room temperature. During the time (2 h) when reaction 2 would have been complete or nearly complete, there was no evidence for the substitution products $W(CO)_5(PPh_3)$ or $W(CO)_6$. When the mixture was stirred for 48 h, approximately 25% of the $W(CO)_5SH^-$ was converted to $W(CO)_5(PPh_3)$. These results suggest, but do not prove, that SH^- is probably not dissociating from $W(CO)_5SH^-$ during reaction 2 and possibly other reactions discussed in this paper. Mechanisms for reactions of isocyanates with organic nucleophiles have been reviewed.[19]

(13) Dungan, C. H.; Van Wazer, J. R. "Compilation of Reported ^{19}F NMR Chemical Shifts"; Interscience: New York, 1970.
(14) (a) Campbell, S. F.; Hudson, A. G.; Mooney, E. F.; Pedler, A. E.; Stephens, R.; Wood, K. N. *Spectrochim. Acta, Part A* **1967**, *23A*, 2119. (b) Mooney, E. F. "An Introduction to ^{19}F NMR Spectroscopy"; Sadtler Research Laboratories Inc.: New York, 1970.
(15) (a) Dyer, E.; Glenn, J. F. *J. Am. Chem. Soc.* **1957**, *79*, 366. (b) Ozaki, S. *Chem. Rev.* **1972**, *72*, 457.
(16) Geary, W. J. *Coord. Chem. Rev.* **1971**, *7*, 81.
(17) Adams, D. M. "Metal-Ligand and Related Vibrations"; St. Martin's Press: New York, 1967.
(18) (a) Stewart, W. E.; Siddall, T. H. *Chem. Rev.* **1970**, *70*, 523. (b) Kessler, H. *Angew. Chem., Int. Ed. Engl.* **1970**, *9*, 219.

All evidence indicates that μ-$HS[W(CO)_5]_2^-$ is less reactive toward organic electrophiles than is $W(CO)_5SH^-$. This is apparent from the lack of reaction of μ-$HS[W(CO)_5]_2^-$ with MeN=C=O when stirred at room temperature for 18 h. However, when μ-$HS[W(CO)_5]_2^-$ is deprotonated, the resulting green anion reacts rapidly with MeN=C=O to give a brown mixture (eq 3). Although the intermediate was not isolated, protonation with HCl allowed the isolation of the bridging thiocarbamate product.

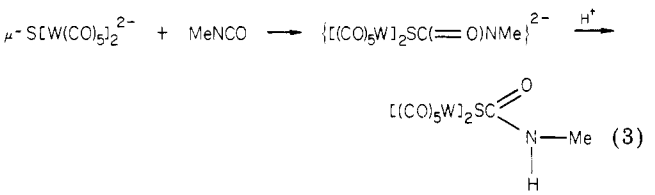

(3)

The formulation of this product as a binuclear complex with the sulfur atom bridging both tungsten atoms is supported by its ν(CO) spectrum which shows the six-band pattern[2] characteristic of the related S-bridged complexes, $[(CO)_5W]_2SH^-$[3e] and $[(CO)_5W]_2SC_6Cl_5^-$,[20] whose structures have been established by X-ray diffraction studies. The presence of a weak band at 1664 cm^{-1} assigned to ν(C=O) of the bridging thiocarbamate indicates that the oxygen of this ligand is not coordinated to a metal.

In the ^1H NMR spectrum, the NCH_3 protons occur as a doublet due to coupling with the NH proton. An attempt to find low-temperature evidence of the two possible isomers resulting from restricted rotation around the C–N amide bond showed only one NCH_3 doublet down to −58 °C.

Ketenes (Ph_2C=C=O). Ketenes react with a variety of organic nucleophiles.[19,21] Similarly, $W(CO)_5SH^-$ reacts instantaneously with diphenylketene at room temperature to give the expected thioacetate complex in 66% yield (eq 4). The molar conducitivity (Table I) is consistent with

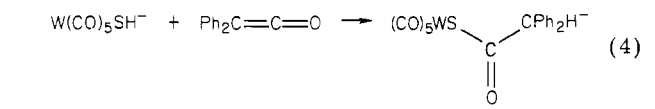

(4)

a 1:1 ionic compound. The IR spectrum in the ν(CO) region (Table II) is very similar to that for the previously reported[2] $(CO)_5WSC(=O)Me^-$ complex.

As for MeN=C=O, Ph_2C=C=O does not react with μ-$HS[W(CO)_5]_2^-$ in 18 h at room temperature. However, the deprotonated complex rapidly reacts with Ph_2C=C=O as shown in eq 5. Treatment of the solution with a

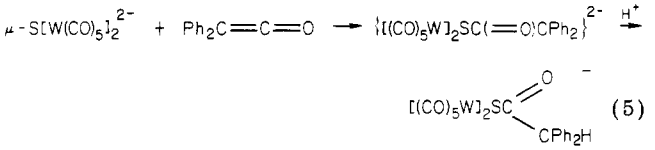

(5)

stoichiometric amount of gaseous HCl yields a product that can be precipitated with Et_4NBr. Repeated attempts to separate the binuclear product $[Et_4N]\{[(CO)_5W]_2SC(=O)CPh_2H\}$ from the mononuclear $[Et_4N]\{(CO)_5W[SC(=O)CPh_2H]\}$ byproduct were unsuccessful. However, the IR spectrum of the binuclear complex in the ν(CO) region (2072 (vw), 2061 (w), 1973 (sh), 1937 (vs), 1913 (s), 1870 (m), and 1680 (vw) cm^{-1}) is nearly identical with the $^-SC(=O)Me$- and $^-SC(=O)NMeH$-bridged complexes (Table II) which suggests that reaction 5 proceeds by analogy with reaction 3.

Isothiocyanates (RN=C=S). Nucleophiles are known to react with alkyl and aryl isothiocyanates.[22,23] When $PPN[W(CO)_5SH]$ is stirred with MeN=C=S in $CHCl_3$ for 18 h at room temperature, the IR spectrum of the solution in the ν(CO) region (2061 (w), 1966 (sh), 1916 (vs), 1869 (s,br) cm^{-1} is almost identical with the spectrum (Table II) of $[PPN]\{W(CO)_5[SC(=O)NMeH]\}$, which indicates that $(CO)_5W[SC(=S)NMeH]^-$ has formed almost quantitatively at this stage. However, attempts to isolate this complex yielded only tars. If the reaction is allowed to continue for 10 days, the spectrum changes to indicate the displacement of a CO group and the formation of the chelated dithiocarbamate complex, $(CO)_4W(S_2CNMeH)^-$. These solution studies indicate that the reaction proceeds in two stages (eq 6). The final chelated complexes may

$$W(CO)_5SH^- + RN{=}C{=}S \rightarrow (CO)_5W[SC(=S)NRH]^- \xrightarrow{-CO} (CO)_4W(S_2CNRH)^- \quad (6)$$

be prepared, isolated, and characterized for R = Me or Ph. For R = Et, only oils are obtained, although IR spectra of reaction solutions indicate that the chelated dithiocarbamate product is formed.

The $W(CO)_4(S_2CNRH)^-$ complexes are characterized by their ionic conductivity and IR spectra. The four ν(CO) absorptions expected for the C_{2v} local symmetry are observed in the ν(CO) region. Bands at 1500 and 1525 cm^{-1} for the complexes with R = Me and Ph, respectively, are characteristic of ν(CN) absorptions in chelated dithiocarbamate complexes.[24]

Ketenimines (Ph_2C=C=NPh). Thiols (RSH) react with ketenimines to give thioimidates.[25,26] The reaction of $[PPN][W(CO)_5SH]$ with Ph_2C=C=NPh in THF at room temperature occurs with a half-life of approximately 2 h according to eq 7. Although it was not detected,

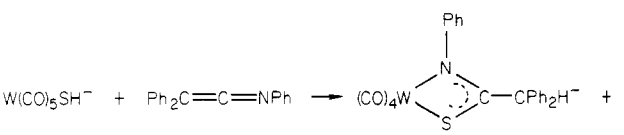

(7)

$(CO)_5W[SC(=NPh)CPh_2H]^-$ presumably forms initially, and it is then converted to the chelated product with loss of CO. Attempts to isolate $[PPN][(CO)_4W(SC(=NPh)CPh_2H)]$ as a solid were unsuccessful; however, the close similarity of its ν(CO) spectrum to that of $(CO)_4W(S_2CNRH)^-$ (Table II) strongly supports the structure in eq 7. The ν(CN) band of the complex at 1500 cm^{-1} is also close to the 1484-cm^{-1} absorption of the S,N-coordinated ligand in $Cp(CO)_2MoSC(=NPh)Me$.[27] When a THF solution of $[(CO)_4W(SC(=NPh)CPh_2H)]^-$ under an atmosphere of CO at room temperature is treated with equimolar CF_3SO_3H, the thioamide complex $(CO)_5[S=C(NPhH)(CPh_2H)]$ is formed within 15 min (eq 8) and is isolated as a yellow powder in 36% yield by evaporating the reaction solution to dryness and recrystallizing the

(19) Satchell, D. P. N.; Satchell, R. S. *Chem. Soc. Rev.* **1975**, *4*, 231.
(20) Cooper, M. K.; Duckworth, P. A.; Saporta, M.; McPartlin, M. *J. Chem. Soc., Dalton Trans.* **1980**, 570.
(21) (a) Lillford, P. J.; Satchell, D. P. N. *J. Chem. Soc. B* **1970**, 1303. (b) "The Chemistry of Ketenes, Allenes, and Related Compounds"; Patai, S., Ed.; Wiley: New York, 1980.
(22) Ulrich, H. "Cycloaddition Reactions of Heterocumulenes"; Academic Press: New York, 1967.
(23) (a) Assony, S. J. "Organic Sulfur Compounds"; Pergamon Press: Oxford, 1961; Vol. I. (b) "Chemistry of Cyanates and Their Thio Derivatives"; Patai, S., Ed.; New York, 1977.
(24) O'Connor, C.; Gilbert, J. D.; Wilkinson, G. *J. Chem. Soc. A* **1969**, 84.
(25) Barker, M. W.; Lauderdale, S. C.; West, J. R. *J. Org. Chem.* **1973**, *38*, 3951.
(26) Krow, G. R. *Angew. Chem., Int. Ed. Engl.* **1971**, *10*, 435.
(27) Abel, E. W.; Towle, I. D. H. *J. Organomet. Chem.* **1976**, *122*, 253.

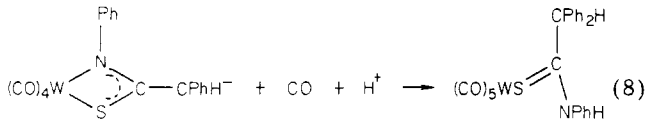

(8)

residue from 50/50 Et_2O/hexanes. The formation of the thioamide complex in this ring-opening reaction supports the proposed formulation of the reacting thioimidate complex. The same thioamide complex may also be isolated from the direct reaction of $W(CO)_5SH^-$, $Ph_2C{=}C{=}NPh$, and CF_3SO_3H as described in the Experimental Section. The close similarity of its ν(CO) spectrum (Table II) to those of other $(CO)_5W$(thioamide) complexes supports the above structure for the product of reaction 8.

Carbodiimides (RN=C=NR). Unlike PhSH[28] and H_2S,[29] which react with carbodiimides, $W(CO)_5SH^-$ does not react with RN=C=NR (R = *i*-Pr or C_6H_{11}) at room temperature. However, when CF_3SO_3H is added to the mixture, a rapid reaction occurs to give the thiourea complex (eq 9). The complex with R = *i*-Pr was isolated in

$$W(CO)_5SH^- + RN{=}C{=}NR + H^+ \rightarrow (CO)_5W[S{=}C(NHR)_2] \quad (9)$$

$$R = i\text{-Pr},\ C_6H_{11}$$

60% yield, while the R = cyclohexyl complex did not solidify and was only characterized by its ν(CO) spectrum (2071 (w), 1978 (w), 1929 (vs), 1895 (sh) cm^{-1} in CH_2Cl_2), which is very similar to that of the isopropyl analogue and to other $(CO)_5W$(thiourea) complexes reported in the literature.[30,31] It is also very similar to that of $(CO)_5W[S{=}C(NH_2)_2]$ prepared from $W(CO)_5I^-$, Ag^+, and thiourea as described in the Experimental Section.

When μ-$HS[W(CO)_5]_2^-$ and *i*-PrN=C=N-*i*-Pr are stirred in THF at room temperature, there is no reaction. Addition of CF_3SO_3H gives in 58% yield the thiourea complex obtained above (eq 10). Other than being required for the formation of the thiourea ligands in eq 9 and 10, the role of the acid in facilitating these reactions is not known.

$$\mu\text{-}HS[W(CO)_5]_2^- + i\text{-PrN}{=}C{=}N\text{-}i\text{-Pr} + H^+ \rightarrow (CO)_5W[S{=}C(NH\text{-}i\text{-Pr})_2] + \{W(CO)_5(THF)\} \quad (10)$$

Perfluoroorganics ($CF_3C(=O)CF_3$ and $\overline{FC{=}CF(CF_2)_3CF_2}$). The carbonyl carbon of $CF_3C(=O)CF_3$ is commonly attacked by nucleophiles to give addition products,[32] but displacement of F^- in fluorocarbons by nucleophiles is also a well-known reaction.[33] Hexafluoroacetone reacts with H_2S at 80 °C to give the hemithioacetal $(CF_3)_2C(OH)(SH)$.[34] When $CF_3C(=O)CF_3$ is allowed to react with $W(CO)_5SH^-$ in acetone for 16 h at room temperature, a low yield (8%) of the F^--substituted product is obtained (eq 11). The molar conductivity

$$W(CO)_5SH^- + CF_3C(=O)CF_3 \rightarrow (CO)_5WSCF_2C(=O)CF_3^- + (HF) \quad (11)$$

(Table I) of the Et_4N^+ salt of the complex supports the 1:1 ionic formula. The three ν(CO) bands of the CO ligands, the 1680 cm^{-1} absorption tentatively assigned to the ν(C=O) vibration, and the ^{19}F NMR spectrum (Experimental Section) of the complex indicate that it has the structure shown in eq 11.

Fluoro olefins are known to undergo F^- substitution by RS^- and addition of RSH to the double bond.[33] The reaction of $W(CO)_5SH^-$ with perfluorocyclohexene in THF at room temperature for 3 h yields the vinyl fluoride substituted product (46%; eq 12). Conductivity, IR

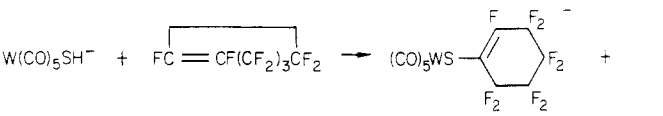

(HF) (12)

measurements, and ^{19}F NMR (see Experimental Section) results support the structure given in eq 12.

Other Electrophiles. Like the reported reaction[3d] of $W(CO)_5SH^-$ with Me_3O^+ to give $(CO)_5W(SMe_2)$, PPN[W(CO)$_5$SH] reacts rapidly with $MeOSO_2F$ in $CDCl_3$ in an NMR tube to give a 33% yield of $(CO)_5W(SMe_2)$, which was identified[3d,31] by its NMR and IR spectra.

Mercaptans (RSH) react in the presence of acid with nitriles R'CN to form iminothioesters R'C(=NH)SR.[35] No reaction occurs between $W(CO)_5SH^-$ and the nitriles MeCN, MeSCN, or H_2NCN at room temperature in THF for at least 4 h. However, upon addition of 1 equiv of CF_3SO_3H, the mixture immediately turns brown; however, only the following nitrile complexes were isolated: $(CO)_5W$(NCMe), 65%; $(CO)_5W$(NCSMe), 11% $(CO)_5W(N{\equiv}CNH_2)$, 68%. Thus, these reactions are represented by eq 13. The cyanamide complex $(CO)_5W(N{\equiv}CNH_2)$

$$W(CO)_5SH^- + N{\equiv}CR + H^+ \rightarrow (CO)_5W(N{\equiv}CR) + (H_2S) \quad (13)$$

is obtained in 72% yield by an independent route involving treatment of $W(CO)_5I^-$ first with Ag^+ and then with $NCNH_2$. The cyanamide ligand is probably coordinated to the W atom through the nitrile N atom. This structure is supported by the IR spectrum of the complex which shows a $\nu(C{\equiv}N)$ band at 2270 cm^{-1} with a shoulder at 2315 cm^{-1} as compared with the free ligand whose comparable bands are reported[36] at 2190 and 2150 cm^{-1}. The substantial increase in $\nu(C{\equiv}N)$ upon coordination of $N{\equiv}C\text{-}NH_2$ is indicative of coordination through the nitrile N atom. Evidence for noncoordination of the NH_2 group is the small shift in the ν(NH) frequencies which are at 3425 and 3335 cm^{-1} in the complex and at 3430 and 3342 cm^{-1} in free $NCNH_2$,[37] both in CH_2Cl_2 solvent.

Unlike tne nitrile compounds discussed above, phenyl cyanate (PhOCN) reacts with equimolar $W(CO)_5SH^-$ in THF over an 18-h period at room temperature to give a 59% yield of the thiocyanate complex $W(CO)_5(NCS)^-$ (eq 14). Infrared spectra of the compound are identical with

$$W(CO)_5SH^- + N{\equiv}COPh \rightarrow W(CO)_5(NCS)^- + (HOPh) \quad (14)$$

those of an authentic sample of $[PPN][W(CO)_5(NCS)]$[12] and are very similar to other salts[38] of the $W(CO)_5(NCS)^-$

(28) Schlack, P.; Keil, G. *Liebigs Ann. Chem.* **1963**, *661*, 164.
(29) Kurzer, F.; Douraghi-Zadeh, K. *Chem. Rev.* **1967**, *67*, 107. Wolman, Y. in "The Chemistry of Ketenes, Allenes, and Related Compounds"; Patai, S., Ed.; Wiley: 1980; p 721.
(30) Granifo, J.; Costamagna, J.; Garrao, A.; Pieber, M. *J. Inorg. Nucl. Chem.* **1980**, *42*, 1587 and references therein.
(31) Dombek, B. D.; Angelici, R. J. *Inorg. Chem.* **1976**, *15*, 2403.
(32) Krespan, C. G.; Middleton, W. J. *Fluorine Chem. Rev.* **1967**, *1*, 145.
(33) Chambers, R. D.; Mobbs, R. H. *Adv. Fluorine Chem.* **1965**, *4*, 50.
(34) Harris, J. F. *J. Org. Chem.* **1965**, *30*, 2190.
(35) Reid, E. E. "Organic Chemistry of Bivalent Sulfur"; Chemical Publishing Co.: New York, 1962; Vol. 4.
(36) "Atlas of Spectral Data and Physical Constants for Organic Compounds"; Grasselli, J. G., Ed.; CRC Press: Cleveland, OH, 1974.
(37) Nakamoto, K. "Infrared Spectra of Inorganic and Coordination Compounds", 2nd ed.; Interscience: New York, 1970.

complex. The observation of a band at 818 (w) cm^{-1} in the product indicates[39] that the NCS^- is coordinated through the N atom. This reaction presumably proceeds via a $W(CO)_5SCN^-$ intermediate formed by displacement of ^-OPh by $W(CO)_5SH^-$. The S-bound intermediate must then rapidly rearrange to give the observed N-bound product.

Phenylacetylene is reported[40] to react with $(\eta$-$C_5H_5)$-$Ni(PBu_3)SH$ to give $(\eta$-$C_5H_5)Ni(PPu_3)[SC(Ph)=CH_2]$. In contrast, $W(CO)_5SH^-$ does not react with PhC≡CH, PhC≡CPh, or HC≡CCO_2Et at room temperature in THF over an 18-h period. Under the same conditions, $W(CO)_5SH^-$ also does not react with the olefins H_2C=$CHCO_2Me$, CH_2=C=CH_2, or CH_2=CHCN.

We had previously reported[2] that μ-$S[W(CO)_5]_2^{2-}$ reacts with MeHgCl to give μ-$MeHgS[W(CO)_5]_2^-$. In contrast, the reaction of $W(CO)_5SH^-$ with equimolar MeHgCl at room temperature for 6 h yields $W(CO)_5Cl^-$. Treatment of $W(CO)_5SH^-$ with $MeHgCl/AgNO_3$ in MeCN gives a 44% yield of $W(CO)_5(NCMe)$. In CH_2Cl_2 solvent, the reaction of $W(CO)_5SH^-$ with $MeHgCl/AgBF_4$ gives $W(CO)_6$ in 64% yield. These results indicate that, if the $W(CO)_5SHgMe^-$ complex is formed, it is rapidly converted to other products.

In an attempt to prepare $W(CO)_5(SMe)^-$, $W(CO)_5SH^-$ was stirred with excess CH_2N_2 at 0 °C in THF for 2 h, but there was no reaction. The attempted preparation of the disulfide $W(CO)_5(SSPh)^-$ by reaction of $W(CO)_5SH^-$ with PhSSPh gave only $[PPN][W(CO)_5(SPh)]$[41] in 29% yield. It was hoped that oxidation of $W(CO)_5SH^-$ with I_2 would give the disulfide complex $(CO)_5WSSW(CO)_5^{2-}$; although a rapid reaction occurred, the only identified carbonyl-containing product was $W(CO)_5I^-$. Unlike its reaction with the other heterocumulenes, $W(CO)_5SH^-$ did not react with either CO_2 or COS in THF at room temperature over an 18-h period. A reaction did occur between equimolar $W(CO)_5SH^-$ and CS_2, but the products could not be isolated or characterized.

Conclusions. The complex $W(CO)_5SH^-$ reacts with a range of organic electrophiles. Mechanisms of these reactions have not been studied, but some evidence suggests that the more rapid reactions probably proceed by nucleophilic attack of the coordinated SH^- group at the electrophilic center. The reactions involving acid (H^+), however, may proceed by other pathways because of the known rapid reaction of $W(CO)_5SH^-$ with H^+ to form μ-$HS[W(CO)_5]_2^-$.[2]

In contrast to the high reactivity of $W(CO)_5SH^-$, μ-$HS[W(CO)_5]_2^-$ is unreactive toward even the more electrophilic reagents (Ph_2C=C=O and MeN=C=O), perhaps reflecting the low basicity of the sulfur atom and the low field position of the SH^- in the ^1H NMR spectrum.[2] The deprotonated binuclear complex μ-$S[W(CO)_5]_2^{2-}$, however, is reactive toward both Ph_2C=C=O and MeN=C=O, as well as other electrophiles reported previously.[2] While the SH^- group in $W(CO)_5SH^-$ is very reactive, it will be of interest to explore the reactivity of SH^- groups in complexes with metals in positive oxidation states. In this connection, it might be noted that the coordinated sulfur atom of thiolate (SR^-) ligands in Co(III) complexes are moderate nucleophiles toward CH_3I.[42]

Acknowledgment. This material is based upon work supported by the National Science Foundation under Grant CHE75-15147 and by the National Institute of General Medical Sciences (Grant No. GM 12626).

Registry No. $[PPN][W(CO)_5SH]$, 71771-28-3; $[PPN]\{(CO)_5W[SC(=O)CPh_2H]\}$, 83477-39-8; $[PPN]\{(CO)_5W[SC(=O)NPhH]\}$, 83477-41-2; Ph_2C=C=O, 525-06-4; PhN=C=O, 103-71-9; $[Et_4N]\{(CO)_5W[SC(=O)NMeH]\}$, 83477-43-4; $[Et_4N][(CO)_4W(S_2CNMeH)]$, 83477-45-6; $[Et_4N][(CO)_4W(S_2CNEtH)]$, 83477-47-8; $[Et_4N][(CO)_4W(S_2CNPhH)]$, 83477-49-0; $[Et_4N][W(CO)_5SH]$, 65198-81-4; MeN=C=S, 556-61-6; EtN=C=S, 542-85-8; PhN=C=S, 103-72-0; MeN=C=O, 624-83-9; $[PPN][(CO)_4W(S_2CNPhH)]$, 83477-50-3; $[PPN]\{(CO)_4W[SC(=NPh)CPh_2H]\}$, 83477-52-5; PhN=C=$CPh_2$, 14181-84-1; $(CO)_5W[S=C(NPh_4)(CPh_2H)]$, 83477-53-6; $(CO)_5W[S=C(NH$-i-$Pr)_2]$, 83477-54-7; Pr-i-N=C=N-i-Pr, 693-13-0; $[Et_4N]\{\mu$-$HS[W(CO)_5]_2\}$, 71688-51-2; $(CO)_5W[S=C(NH_2)_2]$, 69244-65-1; $(CO)_5W(N\equiv CNH_2)$, 83477-55-8; $[Et_4N][W(CO)_5I]$, 14781-01-2; $(CO)_5W(N\equiv CMe)$, 15096-68-1; $(CO)_5W(N\equiv CSMe)$, 57196-05-1; $[PPN][(CO)_5W(NCS)]$, 21948-45-8; $[Et_4N]\{(CO)_5W[SCF_2C(=O)CF_3]\}$, 83477-62-7; $(CF_3)_2C$=O, 684-16-2; $[PPN]\{(CO)_5W[(S\overline{C=CF(CF_2)_3CF_2}]\}$, 83477-57-0; $\overline{CF=CF(CF_2)_3CF_2}$, 355-75-9; $[Et_4N]\{\mu$-$HMeNC(=O)S[W(CO)_5]_2\}$, 83477-59-2; μ-$S[W(CO)_5]_2^{2-}$, 83477-60-5; $[PPN]\{(CO)_5W[SC(=O)Me]\}$, 71688-53-4; $[PPN]\{\mu$-$MeC(=O)S[W(CO)_5]_2\}$, 71688-63-6; PhOCN, 1122-85-6.

(38) Wojcicki, A.; Farona, M. F. *J. Inorg. Nucl. Chem.* **1964**, *26*, 2289.
(39) (a) Bailey, R. A.; Kozak, S. L.; Michelsen, T. W.; Mills, W. N. *Coord. Chem. Rev.* **1971**, *6*, 407. (b) Burmeister, J. L. *Ibid.* **1968**, *3*, 225.
(40) Sato, M.; Sato, F.; Takemoto, N.; Iida, K. *J. Organomet. Chem.* **1972**, *34*, 205.
(41) Schlientz, W. J.; Ruff, J. K. *Inorg. Chem.* **1972**, *11*, 2265.
(42) Root, M. J.; Deutsch, E. *Inorg. Chem.* **1981**, *20*, 4376.

Asymmetrical Sandwich Compounds. The Preparation and Characterization of (η^6-Benzene)(η^6-1,2,3,4,5-pentafluoro-6-(diphenylphosphino)-benzene)chromium(0) and Its Reaction with $[Rh(CO)_2Cl]_2$

Romolo Faggiani,[1a] Nguyen Hao,[1b] Colin J. L. Lock,*[1a] Brian G. Sayer,[1b] and Michael J. McGlinchey*[1b]

Department of Chemistry and the Institute for Materials Research, McMaster University, Hamilton, Ontario, Canada L8S 4M1

Received June 28, 1982

Metal atom synthesis of $(C_6H_6)Cr(C_6F_5H)$, followed by lithiation and treatment with chlorodiphenylphosphine, gave (η^6-benzene)(η^6-1,2,3,4,5-pentafluoro-6-(diphenylphosphino)benzene)chromium(0), **2**. Crystals of **2** were monoclinic of space group $P2_1/c$ with cell dimensions a = 8.341 (1) Å, b = 12.472 (2) Å, c = 21.033 (2) Å, and β = 115.13 (9)° and had four formula units in the unit cell. The crystal structure was determined by standard methods and refined to R_1 = 0.0595 and R_2 = 0.0694 on the basis of 2126 reflections. The data were collected with use of Mo Kα radiation and a Syntex $P2_1$ diffractometer. The benzene and pentafluorophenyl rings sandwich the chromium atom, which lies closer to the pentafluorophenyl ring (Cr–C(F) range = 2.083 (6)–2.104 (6) Å vs. Cr–C(H) range = 2.142 (8)–2.164 (6) Å). The bound phosphorus atom causes distortion of the pentafluorophenyl ring so that the carbon atom bound to phosphorus is 2.149 (2) Å from the chromium atom; the internal ring angle at the carbon atom bound to phosphorus is reduced to 114.3 (5)°, and adjacent internal ring angles are increased (122.4 (5), 123.3 (5)°). Other bond lengths and angles are normal. The 235-MHz ^{19}F NMR spectrum of **2** showed enormous increases in the fluorine–fluorine coupling constants relative to those in the free arene. **2** reacted with $[Rh(CO)_2Cl]_2$ to give the trimetallic complex $[(C_6H_6)Cr(C_6F_5PPh_2)]_2Rh(CO)Cl$, **3**.

Introduction

Two questions stimulated this work. One concerned the relative lengths of metal–carbon bonds in markedly asymmetric sandwich compounds. The second was whether one could use the availability of functionalized chromium–arene sandwich complexes (chromarenes[1c]) to synthesize molecules containing both a chromarene moiety and another catalytic centre such as a 16-electron square-planar rhodium atom. The ability of a chromarene system to catalyze polymerization[2] or hydrogenation processes[3] is well-known. It appeared that the metal-vapor cocondensation procedure might yield compounds suitable for both studies.[4]

An attempt was made to study the first problem by the synthesis[4b,5] and characterization of (η^6-benzene)(η^6-hexafluorobenzene)chromium(0), $(C_6F_6)Cr(C_6H_6)$. A detailed vibrational spectroscopic study has already been reported[6] which showed the asymmetry of the compound along the sixfold axis. Crystallographic studies were unsuccessful, however, in determining the differences in the metal–carbon bond lengths to the fluorinated and nonfluorinated rings. The compound crystallizes in a hexagonal space group, and the structure is markedly disordered. The sandwich compound is stacked up the hexagonal axis, but a translationally equivalent stacks may be inverted. Thus at z = 0 and $^1/_2$, one has averages of benzene and hexafluorobenzene rings, and at z = $^1/_4$ and $^3/_4$ one has half chromium atoms. This problem arises because both the inter- and intramolecule distances between the sandwich rings are roughly 3.4 Å. In order to study this problem further, it was necessary to introduce some asymmetry into one of the rings. Fortunately, from our attempts to study the second problem, a compound was available, namely, the (diphenylphosphino)pentafluorochromarene **2**.

Experimental Section

^1H and ^{31}P NMR spectra were obtained at 2.114 T on a Bruker WH90 at 90 and 36.43 MHz, respectively; tetramethylsilane and 85% H_3PO_4 were used as external references. ^{19}F NMR spectra were obtained at 5.872 T on a Bruker WM 250 at 235.38 MHz; C_6D_6 was used as the solvent and $CFCl_3$ as the external reference. Spectral simulation was achieved with Bruker's "PANIC" iterative software and an ASPECT 2000 computer. Mass spectrometry was performed on a VG micromass 7070 spectrometer equipped with a VG2035 data system. Infrared spectra were recorded on a Perkin-Elmer 337 grating spectrometer. Melting points were uncorrected. Microanalysis results were from Guelph Chemical Laboratories Ltd., Guelph, Ontario.

Preparation of 6-(Diphenylphosphino)-1,2,3,4,5-pentafluorochromarene, 2. To a solution of $(C_6H_6)Cr(C_6F_5Li)$ (1 mmol) in ether at −78 °C was added a very slight excess of chlorodiphenylphosphine. The solution was stirred under an atmosphere of nitrogen for 2 h by which time the starting red-brown solution had turned orange. The solution was allowed to warm to room temperature, stirred a further 3 h, and filtered and the ether removed in vacuo. The residue was taken up in benzene and chromatographed on a silica gel column. Elution of a red band with 50% benzene, 40% hexane, and 10% ether gave **2** (145

(1) (a) Institute for Materials Research. (b) Department of Chemistry. (c) Agarwal, A.; McGlinchey, M. J.; Tan, T.-S. *J. Organomet. Chem.* **1977**, *141*, 85–97.

(2) Tsutsui, M.; Koyano, T. *J. Polym. Sci., Part A* **1967**, *5*, 683–684.

(3) Sneeden, R. P. A. "Organochromium Compounds"; Academic Press: New York, 1975; pp 169–171.

(4) (a) Skell, P. S.; Williams-Smith, D. L.; McGlinchey, M. J. *J. Am. Chem. Soc.* **1973**, *95*, 3337–3340. (b) Middleton, R.; Hull, J. F.; Simpson, S. R.; Tomlinson, C. H.; Timms, P. L. *J. Chem. Soc., Dalton Trans.* **1973**, 120–124. (c) McGlinchey, M. J.; Tan, T.-S. *Can. J. Chem.* **1974**, *52*, 2439–2443. (d) Klabunde, K. J.; Efner, H. F. *Inorg. Chem.* **1975**, *14*, 789–791. (e) Graves, V.; Lagowski, J. J. *Ibid.* **1976**, *15*, 577–586. (f) Nesmeyanov, A. N.; Yur'eva, L. P.; Zaitseva, N. N.; Vasynkova, N. I. *J. Organomet. Chem.* **1978**, *153*, 341–344. (g) Moeckel, R.; Elschenbroich, C. *Angew. Chem., Int. Ed. Engl.* **1977**, *16*, 870–871. (h) Kündig, E. P.; Timms, P. L. *J. Chem. Soc., Dalton Trans.* **1980**, 991–995. (i) Nguyen, Hao; McGlinchey, M. J. *J. Organomet. Chem.* **1979**, *165*, 225–231. (j) Gastinger, R. G.; Klabunde, K. J. *Transition Met. Chem.* **1979**, *4*, 1–13.

(5) McGlinchey, M. J.; Tan, T.-S. *J. Am. Chem. Soc.* **1976**, *98*, 2271–2275.

(6) Laposa, J. D.; Nguyen Hao; Sayer, B. G.; McGlinchey, M. J. *J. Organomet. Chem.* **1980**, *195*, 193–201.

0276-7333/83/2302-0096$01.50/0

Table I. Crystal Data

compd	$C_{24}H_{16}CrF_5P$
fw	482.35
cryst size, mm	cylinder, $r = 0.15$; $l = 0.36$
systematic absences	$h0l$, $l = 2n + 1$; $0k0$, $k = 2n + 1$
space group	$P2_1/c$ (No. 14)
unit cell parameters	
a	8.341 (1)
b	12.473 (2)
c	21.033 (2)
β	115.13 (9)
vol, Å^3	1981.1 (5)
radiation, Å; temp, °C	0.709 26; −70 (1)
Z	4
ρ_{calcd}, g cm^{-3}	1.617
ρ_{obsd}, g cm^{-3}	1.6
linear abs coeff, cm^{-3}	7.43
2θ (max); reflctns collctd	45°, h, k, $\pm l$
std reflctns (esd, %)	2,3,−8 (1.4), 304 (1.4)
no. of independent reflctns	2611 [a]
no. with $I > 3\sigma(I)$	1904
$3\sigma(I) > I > 0$, $F_c > F_o$	222 } used in refinement
$3\sigma(I) > I > 0$, $F_c < F_o$	303
$I < 0$, rejected	181
final R_1, [b] R_2 [b]	0.0595, 0.0694
final shift/error(max); average [c]	0.042; 0.002
final difference map	
highest peak (e Å^{-3}); location	0.94; 0.50, 0.45, 0.30
lowest valley (e Å^{-3}); location	−0.33; 0.45, 0.50, 0.70
weighting	$w = (\sigma^2 + (0.025F_o)^2)^{-1}$
error in an observn of unit weight	1.778

[a] Reflection 002 was too strong to measure. [b] $R_1 = \Sigma ||F_o| - |F_c||/\Sigma |F_o|$; $R_2 = \{\Sigma w(|F_o| - |F_c|)^2/\Sigma wF_o^2\}^{1/2}$. [c] Non-hydrogen atoms.

mg, 0.301 mol; 30%). After recrystallization from benzene, dark cherry-red crystals were obtained: mp 185 °C (with decomposition); Anal. Calcd for $C_{24}H_{16}CrF_5P$; C, 59.75; H, 3.32. Found: C, 59.9; H, 3.5. mass spectrum, m/z (%) 482 ($C_{24}H_{16}CrF_5P^+$, 35), 464 ($C_{24}H_{17}CrF_4P^+$, 45), 404 ($C_{18}H_{10}CrF_5P^+$, 45), 386 ($C_{18}H_{11}CrF_4P^+$, 30), 352 ($C_{18}H_{10}F_5P^+$, 15), 334 ($C_{18}H_{11}F_4P^+$, 17), 275 ($C_{12}H_5F_5P^+$, 14), 219 ($C_6F_5Cr^+$, 10), 201 ($C_6HF_4Cr^+$, 35), 185 ($C_{12}H_{10}P^+$, 60), 168 ($C_6HF_5^+$, 25), 149 ($C_6HF_4^+$, 50), 130 ($C_6H_6Cr^+$, 70), 78 ($C_6H_6^+$, 100), (Cr^+, 90).

Preparation of Chlorocarbonylbis(η^6-6-(diphenylphosphino)-1,2,3,4,5-pentafluorochromarene)rhodium(I), 3. $[Rh(CO)_2Cl]_2$ (0.04 mmol) and **2** (0.08 mmol) were stirred in benzene at room temperature for 4 h under an atmosphere of nitrogen. Removal of the solvent in vacuo gave **3**, mp 212 °C, as brown microcrystals in 90% yield. Anal. Calcd for $C_{49}H_{32}ClCr_2F_{10}OP_2Rh$: C, 52.01; H, 2.83. Found: C, 51.8; H, 3.1. The spectroscopic data are collected in Table IV.

Collection of the X-ray Data. Precession photographs showed the crystal was monoclinic and unit cell parameters were obtained from a fit of χ, ϕ, and 2θ for 15 reflections ($18.2 < 2\theta < 30.2$) recorded on a Syntex $P2_1$ diffractometer with use of graphite-monochromated Mo $K\alpha_1$ radiation (0.709 26 Å at −70 °C). Measurements were made at low temperature because insufficiently precise structure solution was obtained at room temperature. Crystal data and other numbers related to data collection are summarized in Table I. The density was obtained by flotation in aqueous zinc bromide solution. Intensities were measured by using a coupled θ(crystal)−2θ(counter) scan. The methods of scan rates and initial data treatment have been described.[7,8] Corrections were made for Lorentz–polarization effects but not for absorption: this will introduce a maximum error in F_o of < 1%.

Table II. Atomic Positional Coordinates for Non-Hydrogen Atoms (× 10^4)

atom	x	y	z
Cr	2472 (1)	2743.7 (7)	−158.6 (5)
C(1)	1174 (7)	2562 (4)	526 (3)
C(2)	2780 (7)	3122 (4)	859 (3)
C(3)	3218 (8)	4018 (5)	565 (3)
C(4)	2053 (8)	4378 (5)	−93 (3)
C(5)	440 (8)	3882 (4)	−433 (3)
C(6)	5 (8)	2990 (4)	−141 (3)
F(2)	3992 (4)	2804 (3)	1496 (2)
F(3)	4804 (4)	4504 (3)	913 (2)
F(4)	2465 (5)	5263 (3)	−366 (2)
F(5)	−747 (4)	4245 (3)	−1072 (2)
F(6)	−1593 (4)	2527 (3)	−504 (2)
C(11)	2768 (8)	1068 (5)	−354 (3)
C(12)	4417 (8)	1482 (5)	109 (3)
C(13)	5072 (9)	2396 (5)	−76 (3)
C(14)	4104 (9)	2897 (5)	−713 (3)
C(15)	2429 (9)	2507 (5)	−1175 (3)
C(16)	1768 (8)	1579 (5)	−991 (3)
C(21)	−353 (7)	2129 (4)	1466 (3)
C(22)	−223 (8)	3217 (5)	1582 (3)
C(23)	−953 (9)	3703 (5)	1994 (3)
C(24)	−1803 (9)	3091 (6)	2297 (4)
C(25)	−1918 (9)	2011 (6)	2201 (4)
C(26)	−1225 (8)	1511 (5)	1779 (3)
C(31)	2392 (8)	734 (5)	1485 (3)
C(32)	3343 (8)	1028 (5)	2183 (3)
C(33)	4863 (9)	451 (6)	2607 (4)
C(34)	5387 (10)	−400 (6)	2323 (4)
C(35)	4421 (10)	−708 (6)	1636 (4)
C(36)	2908 (9)	−152 (5)	1213 (3)
P	384 (2)	1426 (1)	875.2 (8)

Solution of the Structure. The coordinates of the chromium atom were found from a three-dimensional Patterson synthesis, and a series of full-matrix least-squares refinements followed by electron density difference syntheses revealed all the atoms. The temperature factors of the chromium and phosphorus atoms were made anisotropic, and further refinement (not refining hydrogen atoms) minimizing $w(F_o - F_c)^2$ was terminated when the maximum shift/error fell below 0.05. These results are reported here. One further cycle, the refinement of x, y, z of the hydrogen atoms, was performed to give a rough estimate of the errors on the hydrogen atom positions. No correction was made for secondary extinction. Scattering curves were taken from ref 9, and anomalous dispersion corrections from ref 10 were applied to the curves for Cr and P. Atom parameters for non-hydrogen atoms are listed in Table II.[11]

Results and Discussion

Syntheses. 1,2,3,4,5-Pentafluorochromarene, **1**, prepared by cocondensing benzene, pentafluorobenzene and chromium vapor at −196 °C, is known to possess a relatively acidic proton in the fluorinated ring.[1,12] Lithiation

(7) Lippert, B.; Lock, C. J. L.; Rosenberg, B.; Zvagulis, M. *Inorg. Chem.* **1977**, *16*, 1525–1529.

(8) Hughes, R. P.; Krishnamachari, N.; Lock, C. J. L.; Powell, J.; Turner, G. *Inorg. Chem.* **1977**, *16*, 314–319.

(9) Cromer, D. T.; Waber, J. T. "International Table for X-ray Crystallography"; Ibers, J. A., Hamilton, W. C., Eds.; Kynoch Press: Birmingham, England, 1974; Vol. IV, Table 2.2A, p 72 ff.

(10) Cromer, D. T., ref 9, Table 2.3.1, pp 149–150.

(11) All calculations were carried out on a CYBER 170/730 computer. Initial data treatment used programs from the XRAY 76 package (Stewart, J. M. Technical Report TR-446, Computer Science Center, University of Maryland: College Park, MD, 1976). The structure was solved with use of SHELX (Sheldrick, G. M. "A Programme for Crystal Structure Solution and Refinement"; University of Cambridge: Cambridge, England, 1976). Final refinement and difference maps used the full-matrix least-squares program CUDLS and Fourier program SYMFOU, written internally by J. S. Stephens and J. S. Rutherford, respectively. Planes and interplanar angles were calculated with use of NRC-22 (Pippy, M. E.; Ahmed, F. R. "NRC-22"; National Research Council of Canada: Ottawa, Ontario (1978). Diagrams were prepared by using ORTEP-II (Johnson, C. K. Report ORNL-5138; Oak Ridge National Laboratory: Oak Ridge, TN, 1976).

(12) Tan, T.-S.; McGlinchey, M. J. *J. Chem. Soc., Chem. Commun.* **1976**, 155–156.

Table III. Interatomic Distances (Å) and Angles (Deg)

Bond Distances

C(1)-C(2)	1.406 (8)	C(2)-C(3)	1.399 (9)	C(3)-C(4)	1.386 (7)
C(4)-C(5)	1.373 (8)	C(5)-C(6)	1.392 (9)	C(6)-C(1)	1.428 (7)
C(11)-C(12)	1.403 (8)	C(12)-C(13)	1.389 (10)	C(13)-C(14)	1.384 (9)
C(14)-C(15)	1.407 (8)	C(15)-C(16)	1.404 (10)	C(16)-C(11)	1.396 (8)
		C(2)-F(2)	1.350 (6)	C(3)-F(3)	1.353 (6)
C(4)-F(4)	1.355 (8)	C(5)-F(5)	1.365 (6)	C(6)-F(6)	1.352 (6)
P-C(1)	1.842 (6)	P-C(21)	1.828 (7)	P-C(31)	1.836 (5)
Cr-C(1)	2.149 (7)	Cr-C(2)	2.098 (6)	Cr-C(3)	2.104 (6)
Cr-C(4)	2.083 (6)	Cr-C(5)	2.095 (6)	Cr-C(6)	2.096 (7)
Cr-C(11)	2.164 (6)	Cr-C(12)	2.157 (7)	Cr-C(13)	2.144 (8)
Cr-C(14)	2.143 (9)	Cr-C(15)	2.142 (8)	Cr-C(16)	2.156 (6)

Bond Angles

C(1)-C(2)-C(3)	123.2 (5)	C(2)-C(3)-C(4)	119.8 (5)	C(3)-C(4)-C(5)	119.4 (6)
C(4)-C(5)-C(6)	120.8 (5)	C(5)-C(6)-C(1)	122.4 (5)	C(6)-C(1)-C(2)	114.3 (5)
C(11)-C(12)-C(13)	119.6 (6)	C(12)-C(13)-C(14)	120.3 (6)	C(13)-C(14)-C(15)	120.8 (7)
C(14)-C(15)-C(16)	119.1 (5)	C(15)-C(16)-C(11)	119.7 (5)	C(16)-C(11)-C(12)	120.6 (6)
P-C(1)-C(6)	118.0 (4)	P-C(1)-C(2)	127.6 (4)	F(2)-C(2)-C(1)	120.1 (5)
F(2)-C(2)-C(3)	116.6 (5)	F(3)-C(3)-C(2)	119.8 (4)	F(3)-C(3)-C(4)	120.3 (6)
F(4)-C(4)-C(3)	119.4 (5)	F(4)-C(4)-C(5)	121.0 (5)	F(5)-C(5)-C(4)	120.3 (6)
F(5)-C(5)-C(6)	119.0 (5)	F(6)-C(6)-C(5)	118.1 (4)	F(6)-C(6)-C(1)	119.5 (5)
C(1)-Cr-C(11)	99.0 (3)	C(2)-Cr-C(12)	98.4 (2)	C(3)-Cr-C(13)	96.7 (3)
C(4)-Cr-C(14)	96.4 (3)	C(5)-Cr-C(15)	98.6 (2)	C(6)-Cr-C(16)	100.5 (2)
C(1)-Cr-C(14)	172.0 (3)	C(2)-Cr-C(15)	172.5 (2)	C(3)-Cr-C(16)	172.6 (2)
C(4)-Cr-C(11)	173.5 (2)	C(5)-Cr-C(12)	175.8 (2)	C(6)-Cr-C(13)	173.9 (3)
C(1)-P-C(21)	100.5 (3)	C(1)-P-C(31)	105.4 (3)	C(21)-P-C(31)	102.8 (3)

and reaction with chlorodiphenylphosphine gave a 30% yield of 1,2,3,4,5-pentafluoro-6-(diphenylphosphino)chromarene, **2**, as cherry-red, air-stable crystals which are readily soluble in benzene but somewhat unstable when left in chloroform or methylene chloride for extended periods. Treatment of a benzene solution of $[Rh(CO)_2Cl]_2$ with **2** at room temperature gave a 90% yield of *trans*-chlorocarbonylbis((pentafluorochromarenyl)diphenylphosphine)rhodium(I), **3**, as brown, air-stable microcrystals.

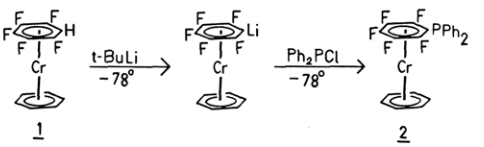

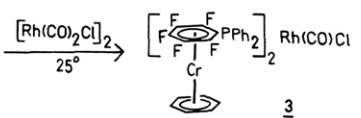

2. Crystallography. The molecule is shown in Figure 1, and selected bond angles and distances are given in Table III. The chromium atom is sandwiched between the benzene ring and the pentafluorophenyl ring which are nearly parallel (dihedral angle = 2.7 (5)°). The rings nearly eclipse one another; torsional angles, C(*i*)–ring center(*i*)–ring center(1*i*)–C(1*i*), are about 10°. The chromium atom is significantly closer to the pentafluorophenyl ring (Cr, 1.573 (1) Å, out of ring plane and Cr–C(F) range = 2.083 (6)–2.104 (6) Å vs. Cr, 1.635 (1) Å, out of ring plane and Cr–C(H) range = 2.142 (8)–2.164 (6) Å). We assume the strongly electronegative fluorine atoms caused electron density to be drawn from the chromium atom into the antibonding π^* orbitals of the phenyl ring, giving stronger Cr–C(F) bonds. This does not cause any detectable differences in the C–C distances in the ring, but the phenyl ring is distorted because of the presence of the phosphorus atom bond to C(1). There is an apparent decrease in C–C bond lengths in the phenyl ring as one moves away from C(1). The errors are too large to say with certainty although C(1)–C(6) (1.428 (7) Å) is significantly longer than

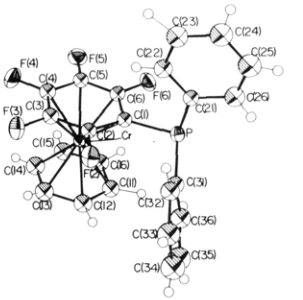

Figure 1. The molecule **2** showing the atom numbering.

C(3)–C(4) or C(4)–C(5) (1.386 (7), 1.373 (8) Å). The values fall in the normal range.[13] The bonding to the pentafluorophenyl ring must be partly localized since C(1), to which phosphorus is bound, is 2.149 (7) Å from the chromium atom, significantly longer than the Cr–C(F) distances and equal to the Cr–C(H) distances. This extra distance is not achieved by bending C(1) out of the plane of the ring but by decreasing the C(6)–C(1)–C(2) angle to 114.3 (5)° from the normal 120°. C(1)–C(2)–C(3) and C(5)–C(6)–C(1) are increased to compensate (123.3 (5), 122.4 (5)°). Small decreases (and increases) in angles are known when an electronegative group is para to the phosphorus atom, but the present value is very small.[14] The fluorine atoms are not moved markedly from the plane of the phenyl ring. Only F(4), F(5), and F(6) are significantly out of the ring plane, bent away from the chromium atom (0.024 (4), 0.022 (4), 0.016 (4) Å). The phosphorus atom is bent away from the chromium atom by a larger amount (0.077 (2) Å), consistent with C(1) becoming more sp^3-like. The hydrogen atom mean positions (−0.04 (10) to −0.23 (10) Å) are all toward the chromium atom, but the errors are so large that this cannot be considered significant. All other bond lengths and angles within the phosphine are normal.[15]

(13) (a) Bailey, M. F.; Dahl, L. F. *Inorg. Chem.* **1965**, *4*, 1298–1306; 1314–1319. (b) Allegra, G.; Natta, G. *Atti Accad. Naz. Lincei, Cl. Sci. Fis., Mat. Nat., Rend.* **1961**, *31*, 241. (c) Ibers, J. A. *J. Chem. Phys.* **1964**, *40*, 3129–3130. (d) Keulen, E.; Jellinek, F. *J. Organomet. Chem.* **1966**, *5*, 490–492.

(14) Dreissig, W.; Plieth, K. *Z. Kristallogr.* **1972**, *135*, 294–307.

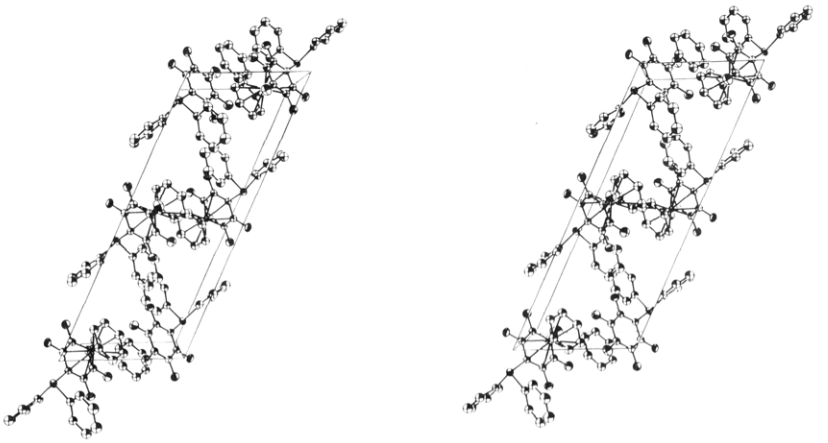

Figure 2. Packing of **2** within the unit cell. *a* and *c** are parallel to the bottom and side of the page and the view is down **b**.

The packing is shown in Figure 2 and is rather surprising. There is no evidence of any dipole–dipole interaction between the $(C_6H_6)Cr(C_6F_5)$ fragments, such as we observed in $(C_6H_6)Cr(C_6F_6)$, presumably because of the blocking by the phenyl rings, nor is there any evidence of any interactions between the aromatic rings such as we have seen many times previously.[15d] Molecules near the *c* face are related in pairs such that H(13) and H(14) approach F(3) and F(4), but the interatomic distances (H(13)–F(4) = 2.8 (1) Å, H(14)–F(3) = 2.7 (1) Å) suggest that hydrogen bonding is very weak or nonexistent. The molecules pack in a very rough hexagonal close packed lattice, the hexagonal layers being at $z = 0$ and $^1/_2$, and the forces are primarily van der Waals.

^{19}F NMR Spectra. The ^{19}F NMR spectra of the molecules **2** and **3** proved to be particularly interesting when compared to those of the corresponding free arenes, viz., $C_6F_5PPh_2$ and its rhodium complex.[16] The ^{19}F nuclei in the fluorochromarenes are known[4c] to exhibit upfield shifts of 40–50 ppm relative to the shifts of the free arenes, and this effect is observed for **2** and **3**. Even more spectacular, however, are the very different fluorine–fluorine coupling constants exhibited by these molecules from those of their noncomplexed analogues. We have previously presented[17] analyses of the six-spin C_6F_5P system in chromium complexes; the coupling constants were evaluated by computer simulation of the 84.66-MHz spectrum and showed unprecedented increases in the $^3J_{FF}$ and $^4J_{FF}$ values compared to those in all other C_6F_5X systems.[18] Coupling constants between ortho fluorines are normally close to −20 Hz,[19] but in the pentafluorochromarenes we have reported that $^3J_{FF}$ can be as large as 109 Hz. We now present the 235-MHz ^{19}F spectrum of **2** (see Figure 3 and Table IV) in which the greater spectral dispersion now allows observation of the weak outer transitions. The data reported here, together with the simulated spectrum (see Figure 3), yielded the coupling constants presented in Table IV; these values supercede those obtained from the 84-MHz spectrum in which the weak outer transitions were not observed owing to peak overlap. Gratifyingly, these

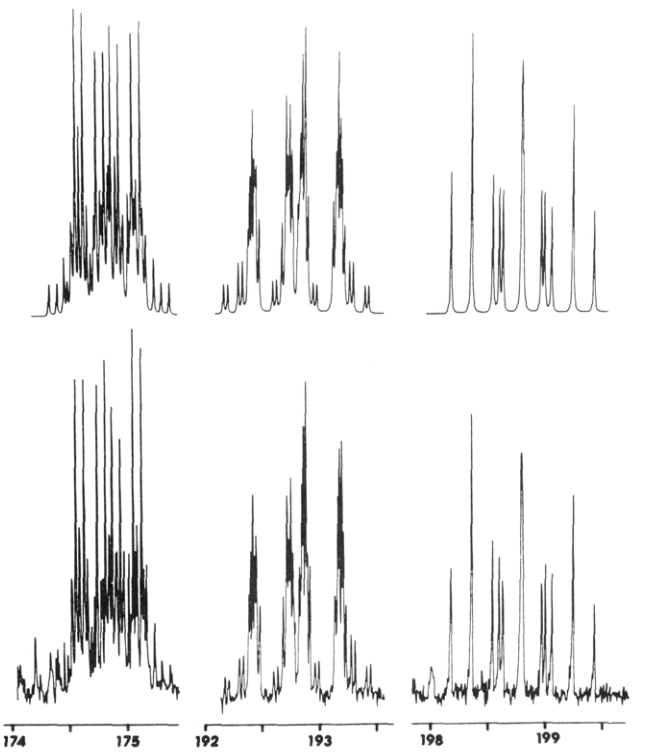

Figure 3. Computer-simulated and experimentally obtained 235-MHz ^{19}F NMR spectra of **2**.

Table IV. ^{19}F and ^{31}P NMR Spectroscopic Data for 2

		$C_6F_5PPh_2$ [a]	$(C_6F_5PPh_2)$-$Cr(C_6H_6)$, **2**
$\delta_{^{19}F}$	ortho	−127.7	−174.7
	meta	−160.9	−192.7
	para	−150.7	−198.7
$\delta_{^{31}P}$		−26.3	−15.0
$^nJ_{PF}$	$^4J_{P-F_2}$	38.0	16.7
	$^4J_{P-F_3}$	<0.5	8.2
	$^5J_{P-F_4}$	<0.5	0
$^nJ_{FF}$	$J_{2,3}$	−24.2	89.9
	$J_{2,4}$	4.0	43.7
	$J_{2,5}$	10.0	−15.4
	$J_{2,6}$	1.6	23.1
	$J_{3,4}$	−20.4	104.8
	$J_{3,5}$	−4.4	42.3

[a] Data from ref 16 and 22.

accurately determined *J* values confirm our earlier assertion of greatly increased coupling constants in the chromarenes relative to the free pentafluoroarenes. These very large increases in J_{FF} values in the chromarenes are

(15) (a) Sobolev, A. N.; Chetkina, L. A.; Romm, I. P.; Gur'yanova, E. N. *J. Struct. Chem.* **1976**, *17*, 83–88. (b) Cameron, T. S.; Miller, K. *Cryst. Struct. Commun.* **1974**, *3*, 489–492. (c) Daly, J. J. *J. Chem. Soc.* **1964**, 3799–3810. (d) Faggiani, R.; Lippert, B.; Lock, C. J. L.; Pfab, R. *Inorg. Chem.* **1981**, *20*, 2381 and references therein.
(16) Nichols, D. I. *J. Chem. Soc. A* **1969**, 1471–1473.
(17) McGlinchey, M. J.; Nguyen Hao; Sayer, B. G.; Tan, T.-S. *J. Organomet. Chem.* **1980**, *194*, 325–330.
(18) Pushkina, L. N.; Stepanov, A. P.; Zhukov, V. S.; Naumov, A. D. *Org. Magn. Reson.* **1972**, *4*, 607–623.
(19) Snyder, L. C.; Anderson, E. W. *J. Chem. Phys.* **1965**, *42*, 3336–3337.

not amenable to a simple explanation, but calculations are currently underway to examine the factors involved. To our knowledge, the only reported instances of such anomalously large coupling constants between aromatic fluorines were those reported by Olah[20] for the fluorobenzenium ions, e.g., $C_6H_5F_2^+$, where J_{FF} = 80 Hz. Clearly, simple electron density considerations are insufficient to account for these changes in J values since Olah's cations presumably have a much different electron density distribution to the chromarenes discussed here. Interestingly, in (fluoroarene)tricarbonylchromium(0) systems the J_{FF} values are less than 10 Hz.[21] We have previously speculated[17] about the possibility of steric restraints brought about by the presence of the diphenylphosphino group; however, the structural data presented herein suggest that steric factors do not play a major role insofar as the fluorines are concerned.

We have previously suggested[1] that the π-$Cr(C_6H_6)$ moiety behaves as a net donor of electron density to fluoroarene rings and thus the phosphine **2** would be expected to be more basic than $C_6F_5PPh_2$ itself. In accordance with these ideas, the chromium-containing rhodium complex **3** exhibits ν_{CO} at 1955 cm^{-1} which is 20 cm^{-1} lower than the value for $(C_6F_5PPh_2)_2Rh(CO)Cl$.

The ^{31}P and ^{19}F NMR spectra of the molecules $(C_6F_5)_nPPh_{3-n}$ have been interpreted[22,23] in terms of a pπ–dπ interaction between the ring and the phosphorus. Complexation of the C_6F_5 ring to chromium in **2** results in a deshielding of the phosphorus by 11 ppm and is presumably a consequence of the enhanced pπ–dπ overlap resulting from the electron donation by the π-$Cr(C_6H_6)$ unit. As is typical[22] when the phosphine is complexed to a metal, the pπ–dπ electron flow from the ring to the phosphorus in **3** must complete with dπ–dπ back-donation from rhodium to phosphorus. The net result is a small upfield shift of the ^{31}P nucleus and the disappearance of all the P–F coupling constants.

We have proposed[24] that the air stability of fluorochromarenes can be correlated with the "internal oxidation" of the molecule; thus, the aerial decomposition (which proceeds via one-electron oxidation of the formally zero-valent chromium) is retarded by the presence of electron-withdrawing substituents in the ring. Indeed, it was predicted[24] that a correlation should exist between the polarographic half-wave potential, $\epsilon^{1/2}$, and the sum of the Hammett meta parameters for the substituents $\sum\sigma_m$; this correlation now has experimental support.[25] The remarkable air stability of the molecules $(C_6H_6)Cr(C_6F_5X)$, where X is $P(C_6H_5)_2$ or SCH_3,[17] is readily rationalized by invoking delocalization of the excess electron density of the fluoroarene ring onto the substituent via pπ–dπ overlap. This picture is also consistent with the ^{31}P NMR spectroscopic data discussed above. A final point to be made in this connection concerns the ^1H and ^{13}C NMR chemical shifts of the C_6H_6 ring in complex **2**, which occur at δ 4.57 and 85.5, respectively. We have previously noted[24] these shifts correlate well with the $\sum\sigma_m$ for the substituents in the fluorinated ring and hence with the oxidative stability of the molecule. We note that these shifts suggest that the Ph_2P substituent is electronically somewhere between a fluorine and a carbethoxy group and thus reinforces the idea of electron delocalisation onto the substituent via a pπ–dπ interaction.

Acknowledgment. We thank the Natural Sciences and Engineering Research Council of Canada for financial support and Professor W. A. G. Graham (University of Alberta) for useful discussions on (pentafluorophenyl)-phosphine complexes.

Registry No. 1, 59930-70-0; 2, 75968-97-7; 3, 83148-20-3.

Supplementary Material Available: Temperature factors for non-hydrogen atoms (Table A), hydrogen atom positional parameters (Table B), bond lengths and angles in phenyl rings (Table C), best planes and dihedral and torsional angles (Table D), and a list of observed and calculated structure factors (Table E) (16 pages). Ordering information is given on any current masthead page.

(20) Olah, G. A.; Kovsky, T. E. *J. Am. Chem. Soc.* **1967**, *89*, 5692–5694.
(21) Unpublished data from this laboratory.
(22) Kemmitt, R. D. W.; Nichols, D. I.; Peacock, R. D. *J. Chem. Soc. A* **1968**, 1898–1902.
(23) Hogben, M. G.; Gay, R. S.; Graham, W. A. G. *J. Am. Chem. Soc.* **1966**, *88*, 3457–3459.
(24) Nguyen Hao; McGlinchey, M. J. *J. Organomet. Chem.* **1978**, *161*, 381–390.
(25) Treichel, P. M.; Essenmacher, G. P.; Efner, H. F.; Klabunde, K. J. *Inorg. Chim. Acta* **1981**, *48*, 41–44.

Trans Addition of Nucleophiles to η^2-Alkyne Complexes of Iron. Crystal and Molecular Structure of $CpFeCO[P(OPh)_3][(Z)$-C(Me)=C(Ph)Me]. Use of Higher Order Organocuprate Reagents

Daniel L. Reger,* Kenneth A. Belmore, Edward Mintz, N. G. Charles, E. A. H. Griffith, and E. L. Amma*

Department of Chemistry, University of South Carolina, Columbia, South Carolina 29208

Received June 15, 1982

The reaction of $[CpFeCO[P(OPh)_3](\eta^2$-MeC≡CMe)]$^+$ with $Ph_2Cu(CN)Li_2$ yields $CpFeCO[P(OPh)_3]$-[(*E*)-C(Me)=C(Me)Ph], whereas the reaction of $[CpFeCO[P(OPh)_3](\eta^2$-PhC≡CMe)]$^+$ with $Me_2Cu(CN)Li_2$ yields $CpFeCO[P(OPh)_3][(Z)$-C(Me)=C(Ph)Me], the product of the latter reaction being characterized by X-ray crystallography. These alkenyl products will not interconvert under the conditions of the reactions. Thus trans addition of these nucleophiles to η^2-alkyne complexes is definitively demonstrated for the first time. Furthermore, for the addition reaction to η^2-PhC≡CMe the regiochemistry is that which places the incoming nucleophile at the alkyne carbon atom bearing the phenyl substituent. Yields in these reactions are high, demonstrating for the first time the usefulness of higher order organocuprate reagents for addition reactions to unsaturated organic ligands π coordinated to transition metals. The structure of $CpFeCO$-$[P(OPh)_3][(Z)$-C(Me)=C(Ph)(Me)] is made up of isolated molecules separated by ordinary van der Waals distances. The Fe atom is four-coordinate with CO, $P(OPh)_3$, Cp, and the fourth coordination site made up of an Fe–C σ bond to the alkenyl group. The Ph substituent is clearly at the β-alkenyl carbon atom and cis to the Fe. The alkenyl group is oriented such that the angle between the normals of the Cp plane and the alkenyl plane is 31.1 (1)°. Crystal data: monoclinic, $P2_1/c$, a = 8.482 (3)Å, b = 36.84 (1) Å, c = 9.939 (3) Å, β = 112.20 (3)°; Z = 4; ρ_{obsd} = 1.33 (1) g/cm^3, ρ_{calcd} = 1.36 g/cm^3; NO = 2545, NV = 361; R_{final} = 0.047. The structure was solved by standard heavy-atom methods and refined by full-matrix least squares including anisotropic temperature, anomalous dispersion corrections, and absorption corrections.

Introduction

We have recently reported[1] that a variety of nucleophiles will add to $[CpFeCO(PPh_3)(\eta^2$-alkyne)]$^+$ complexes as shown in eq 1 for the alkyne equal to 2-butyne. This

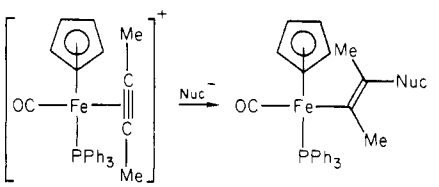

(1)

Nuc = Me, Ph, CN, $CH(CO_2R)_2$, OR, SR

represents an extremely versatile new route to iron–alkenyl complexes. An important aspect of this reaction is the stereochemistry of the addition.[2] In our earlier report, ^{1}H NOE enhancement experiments were used to assign the stereochemistry of the products isolated in these reactions.[3] With the exception of hydride as the nucleophile,[4] the trans configuration was assigned to the products as shown in eq 1. Of considerable importance is the fact that determination of the stereochemistry of the product, isolated in these cases after column chromatography on alumina, does *not* definitively define the mode of addition of the nucleophile because metal–alkenyl complexes have been shown to undergo low-energy cis–trans isomerization reactions.

The best example of this type of isomerization takes place in reaction 2.[5] The initial product of the reaction,

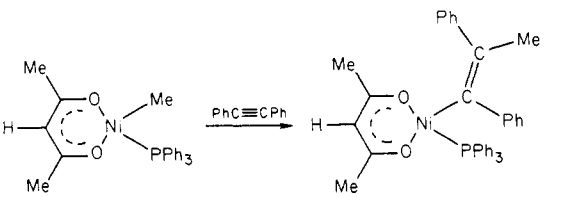

(2)

the *E* isomer, slowly isomerizes to an equilibrium mixture of the *E* and *Z* isomers. A variety of experiments allowed the authors to propose that reaction *2* actually goes by cis addition, followed by a cis–trans isomerization. Thus, determination of the stereochemistry of the product of a reaction that produces a metalloalkenyl complex does not definitively establish the actual mode of addition. Others have proposed similar isomerization processes for other alkenylmetal complexes.[6]

We present here results, both synthetic and structural, that strongly support trans addition of methyl and phenyl substituents delivered from organocuprate reagents. These results include the solid-state structure of $CpFeCO[P$-$(OPh)_3][(Z)$-C(Me)=C(Ph)Me], as determined by X-ray crystallography. We also show that higher order mixed

(1) Reger, D. L.; McElligott, P. J. *J. Am. Chem. Soc.* **1980**, *102*, 5923.
(2) Trans addition of nucleophiles to $[CpFe(CO)_2(\eta^2$-alkene)]$^+$ complexes has been previously demonstrated: (a) Nicholas, K. M.; Rosan, A. M. *J. Organomet. Chem.* **1975**, *84*, 351. (b) Sanders, A.; Magatti, C. V.; Giering, W. P. *J. Am. Chem. Soc.* **1974**, *96*, 1610.
(3) These NOE experiments have not proven to be readily reproducible for $CpFeCO[P(OPh)_3]$(alkenyl) complexes. Slight decomposition of the complexes could place paramagnetic iron in solution. This would diminish the observed NOE enhancements. This point and other NMR methods for determining the stereochemistry of these iron–alkenyl complexes will be discussed in a later publication.
(4) The structure of the product of the reaction of $[CpFeCO$-$(PPh_3)(\eta^2$-MeC≡$CCO_2Et)]BF_4$ and L-Selectride, crystallized after purification on alumina, has been determined crystallographically. The added hydride is cis with respect to iron. Atwood, J. L.; personal communication.
(5) Huggins, J. M.; Bergman, R. G. *J. Am. Chem. Soc.* **1981**, *103*, 3002.
(6) (a) Green, M.; Norman, N. C.; Orpen, A. G. *J. Am. Chem. Soc.* **1981**, *103*, 1267. (b) Murray, T. F.; Norton, J. R. *Ibid.* **1979**, *101*, 4107 and references therein.

0276-7333/83/2302-0101$01.50/0

organocuprate reagents of the type $R_2Cu(CN)Li_2$[7] are particularly effective reagents in these reactions.

Experimental Section

General Procedure. All operations on complexes in solution were carried out under an atmosphere of prepurified nitrogen using solvents that were purified and degassed before use. Infrared spectra were recorded on a Beckman Model IR 4210 spectrometer. Proton NMR spectra were recorded on a Varian Model EM 390 spectrometer and chemical shifts are reported as δ vs. Me_4Si. Carbon-13 spectra were recorded on a Varian CFT-20 spectrometer using $CDCl_3$ as the solvent and internal standard ($\delta(CDCl_3)$ 76.9). Alkyllithium reagents were purchased from Aldrich, CuCN from Fisher, and $AgBF_4$ from Ozark-Mahoning. $CpFeCO[P(OPh)_3]I$ was prepared by the method of Brown et al.[8] Elemental analyses were performed by Robertson Laboratory.

$CpFeCO[P(OPh)_3][(E)$-C(Me)=C(Me)Ph]. A mixture of $CpFeCO[P(OPh)_3]I$ (1.64 g, 2.8 mmol) and $AgBF_4$ (0.58 g, 3.0 mmol) was stirred in CH_2Cl_2 (25 mL) at room temperature, and after 10 min MeC≡CMe (0.20 g, 0.30 mL, 3.7 mmol) was added. This solution was stirred for 40 min and filtered by using Celite. The solvent was evaporated, yielding a reddish brown fluffy solid. This solid was dissolved in THF (40 mL) prechilled to −78 °C and mixed with a cold THF solution of $Ph_2Cu(CN)Li_2$[5] (made by addition of PhLi (3.9 mL of 1.43 M solution, 5.6 mmol) to CuCN (0.25 g, 2.8 mmol) in the THF (20 mL) previously cooled to −60 °C). This mixture was stirred cold for 30 min and allowed to warm to ambient temperature, and the solvent was then evaporated to yield a green-brown oil. This oil was redissolved in CH_2Cl_2 (20 mL) and filtered by using a short plug of alumina, followed by elution with an additional 40 mL of CH_2Cl_2. Evaporation of the CH_2Cl_2 yielded a yellow-orange oil (1.53 g, 93% based on $CpFeCO[P(OPh)_3]I$): ^1H NMR (δ in $CDCl_3$) 7.1 (20, m, $P(OPh)_3$, Ph), 4.33 (5, s, Cp), 2.20, 2.00 (3, 3; br s; Me's); IR spectrum (cm^{-1} in hexane) ν(CO) 1946; ^{13}C NMR (δ in $CDCl_3$) 219.6 (d, J = 50.7 Hz, CO), 151.8, 129.5, 124.7, 121.8, (d, s, d, d; J = 10.4, 0.8, 3.7 Hz; $P(OPh)_3$), 149.1 (d, J = 3.1 Hz, =*C*(Me)Ph), 141.4, 128.6, 127.8, 121.5 (all s, =C*Ph*), 137.7 (d, J = 34.2 Hz, FeC=), 84.4 (d, J = 1.8 Hz, Cp), 36.1, 29.7, (d, s; J = 4.9 Hz, Me's). Anal. Calcd for $C_{34}H_{31}FeO_4P$: C, 69.16; H, 5.29. Found: C, 68.85; H, 5.25.

$CpFeCO[P(OPh)_3][(Z)$-C(Me)=C(Ph)Me]. This complex was prepared in an manner similar to that outlined above by using MeC≡CPh and $Me_2Cu(CN)Li_2$. The orange oil obtained after CH_2Cl_2 evaporation was dissolved in benzene (20 mL) and stirred with alumina (4 g). This mixture was filtered, followed by elution with benzene (20 mL), and the benzene evaporated (25 °C), yielding an orange oil (1.43 g, 87%): ^1H NMR (δ in benzene-d_6) 7.3–6.7 (20, m, $P(OPh)_3$, Ph), 4.18 (5, s, Cp), 2.55, 2.23 (3, 3; s, s; Me's); IR spectrum (cm^{-1} in hexane) ν(CO) 1951; ^{13}C NMR (δ in $CDCl_3$) 217.4 (d, J = 49.1 Hz, CO), 151.4, 129.4, 124.5, 121.2 (d, s, s, d; J = 10.3, 4.2 Hz; $P(OPh)_3$), 152.4 (s, =*C*(Ph)Me), 142.1, 129.9, 126.9, 121.6 (all s, =C*Ph*), 136.5 (d, J = 37.2 Hz, FeC=), 84.7 (s, Cp), 34.0, 23.8 (d, d; J = 9.1, 3.1 Hz; Me's). Anal. Calcd for $C_{34}H_{31}FeO_4P$: C, 69.16; H, 5.29. Found: C, 68.90; H, 5.19.

X-ray Data. Crystals of $CpFeCO[P(OPh)_3][(Z)$-C(Me)=C(Ph)Me] were grown from hexane solution, isolated, and sealed into thin-walled capillaries and mounted on a CAD-4 diffractometer interfaced to a PDP 11/40 computer. The crystal alignment, data collection techniques, computer programs, etc. used were those previously reported.[9,10] The structure was solved by standard heavy-atom methods and refined by full-matrix least squares including anisotropic temperature factors to a final conventional R of 0.047 with 2545 observed reflections. For details see Table I. No attempt was made to locate the numerous hydrogen atoms, and they were not included in the refinement.

Table I. Cell Data, Data Collection, and Refinement Parameters for $CpFeCO[P(OPh_3)][(Z)$-C(Me)=C(Ph)Me]

Cell Data	
a = 8.482 (3) Å	ρ(obsd) = 1.33 g/cm^3
b = 36.84 (1) Å	ρ(calcd) = 1.36 g/cm^3
c = 9.939 (3) Å	fw 590.4 g/mol
β = 112.20 (3)°	Z = 4

Data Collection

wavelength Mo Kα, λ = 0.710 73 Å
graphite monochromator used, θ = 6.1°
space group $P2_1/c$
$h0l$, $l = 2n + 1$; $0k0$, $k = 2n + 1$ absent
size of crystal = 0.17 × 0.34 × 0.34 mm
μ = 6.4 cm^{-1}
faces of the form {001}, {110}, {010}
absorption corrections made and maximum and minimum transmission factor found were 0.913 and 0.896[14]
P factor = 0.030 in $\sigma(F_o^2) = [\sigma(I_{raw})^2 + (PI_{raw})^2]^{1/2}/Lp$ and $w = 1/\sigma(F_o)^2$
data considered nonzero if $F^2 > 4\sigma(F^2)$, $|F| > 14.0$
8349 independent hkl's measured in ω–2θ mode; 47° < 2θ < 60°, 4000 measured F's, 450 ≠ 0, 2θ(max) = 60°
2545 reflections used to solve and refine structure
variable scan speed with preliminary scan speed of 4°/min (2θ)
25 reflections used in orientation matrix (checked every 24 h)
three standard reflections monitored every 100 reflections, decay less than 2% I
room temp ≈ 18 °C

Refinement Parameters

structure refined by full-matrix least squares,[15] including anisotropic temperature factors and anomalous dispersion corrections with weights based upon intensity statistics, function minimized = $\Sigma_i w_i[|F_c| - |F_o|]^2$
largest shift at end of refinement = 0.02 σ
final least squares performed on Amdahl V6 (f's from international tables V.IV)[15]
no. of variables = 361
final R = 0.047, weighted R = 0.062
error of observn of unit weight = 2.05

A listing of structure factors is available as supplementary material. Table II contains the atomic positional and thermal parameters. Interatomic distances and angles are found in Table III, and relevant dihedral angles and selected nonbonded distances are in Table IV. An ORTEP drawing of an individual molecule is shown in Figure 1. Figure 2 shows an ORTEP drawing of the unit cell contents.

Results and Discussion

Two isomers of the formula $CpFeCO[P(OPh)_3][\sigma$-C(Me)=C(Me)Ph] can be prepared as shown in eq 3 and 4. The products of these reactions were clearly established

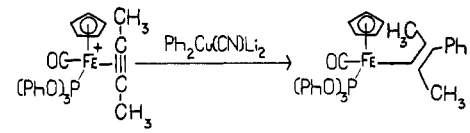

(3)

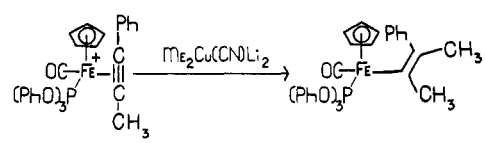

(4)

by NMR (^1H and ^{13}C) spectroscopy to be different compounds of the basic structural type indicated. Of importance is the fact that these two compounds do not interconvert over a period of weeks in solution at room temperature and decompose above 90 °C. The structure of

(7) Lipshutz, B. H.; Kozlowski, J.; Wilhelm, R. S. *J. Am. Chem. Soc.* **1982**, *104*, 2305.
(8) Brown, D. A.; Lyons, H. J.; Manning, A. R.; Rowley, J. M. *Inorg. Chim. Acta* **1969**, *3*, 346.
(9) Griffith, E. A. H.; Charles, N. G.; Amma, E. L. *Acta Crystallogr., Sect.* B **1982**, *B38*, 262.
(10) Reger, D. L.; McElligott, P. J.; Charles, N. G.; Griffith, E. A. H.; Amma, E. L. *Organometallics* **1982**, *1*, 443.

Table II. Positional and Thermal[a] Parameters and Their Estimated Deviations for CpFeCO[P(OPh)$_3$][(*Z*)-C(Me)=C(Ph)Me]

atom	*x*	*y*	*z*	*B*, Å^2	atom	*x*	*y*	*z*	*B*, Å^2
Fe	0.0900 (1)	0.35133 (2)	0.29792 (9)	2.75 (3)	C(3P3)	0.833 (1)	0.4206 (3)	0.7038 (8)	4.6 (4)
P	0.2648 (2)	0.39435 (4)	0.3391 (2)	2.59 (7)	C(4P3)	0.822 (1)	0.4571 (3)	0.7290 (8)	4.6 (4)
O(1)	0.4150 (5)	0.3971 (1)	0.2764 (4)	3.1 (2)	C(5P3)	0.667 (1)	0.4750 (2)	0.6757 (8)	4.7 (3)
O(2)	0.1946 (5)	0.4355 (1)	0.2980 (5)	3.8 (2)	C(6P3)	0.5180 (9)	0.4554 (2)	0.5979 (8)	3.8 (3)
O(3)	0.3838 (5)	0.3975 (1)	0.5078 (4)	3.3 (2)	C(1P1)	0.3885 (8)	0.3971 (2)	0.1281 (7)	3.6 (3)
O(4)	−0.0838 (8)	0.3724 (2)	−0.0014 (6)	5.7 (3)	C(2P1)	0.456 (1)	0.3672 (3)	0.0822 (9)	5.3 (5)
C(1)	−0.0113 (9)	0.3637 (2)	0.1157 (8)	3.4 (3)	C(3P1)	0.448 (1)	0.3683 (4)	−0.064 (1)	7.3 (7)
C(1C)	−0.125 (1)	0.3237 (2)	0.307 (1)	4.8 (4)	C(4P1)	0.370 (1)	0.3977 (4)	−0.153 (1)	7.2 (7)
C(2C)	−0.124 (1)	0.3615 (2)	0.3549 (9)	4.6 (4)	C(5P1)	0.305 (1)	0.4269 (4)	−0.103 (1)	7.3 (7)
C(3C)	0.029 (1)	0.3656 (2)	0.4783 (9)	4.5 (4)	C(6P1)	0.312 (1)	0.4266 (3)	0.0411 (9)	5.1 (5)
C(4C)	0.121 (1)	0.3326 (2)	0.5066 (9)	4.8 (4)	C(1V)	0.2559 (8)	0.3168 (2)	0.2607 (7)	3.2 (3)
C(5C)	0.024 (1)	0.3063 (2)	0.3989 (9)	4.7 (3)	C(2V)	0.2290 (9)	0.2960 (2)	0.1432 (8)	4.0 (3)
C(1P2)	0.0284 (8)	0.4467 (2)	0.2719 (7)	3.3 (3)	C(3V)	0.364 (1)	0.2699 (3)	0.127 (1)	6.8 (5)
C(2P2)	−0.018 (1)	0.4562 (2)	0.3863 (8)	4.2 (3)	C(4V)	0.4270 (9)	0.3125 (2)	0.3890 (8)	4.5 (3)
C(3P2)	−0.181 (1)	0.4689 (2)	0.358 (1)	5.5 (5)	C(1P4)	0.0640 (9)	0.2937 (2)	0.0138 (8)	3.7 (3)
C(4P2)	−0.297 (1)	0.4730 (3)	0.215 (1)	6.2 (5)	C(2P4)	0.054 (1)	0.3055 (2)	−0.1227 (8)	4.7 (4)
C(5P2)	−0.247 (1)	0.4638 (3)	0.103 (1)	6.0 (5)	C(3P4)	−0.097 (1)	0.3038 (3)	−0.2432 (9)	5.6 (4)
C(6P2)	−0.082 (1)	0.4507 (2)	0.1289 (9)	4.5 (3)	C(4P4)	−0.243 (1)	0.2880 (3)	−0.2283 (9)	5.2 (4)
C(1P3)	0.5315 (8)	0.4188 (2)	0.5735 (7)	3.0 (3)	C(5P4)	−0.232 (1)	0.2760 (2)	−0.094 (1)	5.0 (4)
C(2P3)	0.6858 (9)	0.4007 (2)	0.6240 (8)	4.2 (3)	C(6P4)	−0.0797 (9)	0.2785 (2)	0.0272 (8)	4.0 (3)

atom	*U*(1,1)	*U*(2,2)	*U*(3,3)	*U*(1,2)	*U*(1,3)	*U*(2,3)
Fe	0.0322 (4)	0.0367 (5)	0.0342 (4)	−0.0036 (5)	0.0108 (4)	−0.0019 (5)
P	0.0316 (8)	0.0374 (9)	0.0290 (8)	−0.0033 (7)	0.0113 (7)	−0.0010 (7)
O(1)	0.034 (2)	0.056 (3)	0.031 (2)	−0.004 (2)	0.014 (2)	−0.000 (2)
O(2)	0.036 (2)	0.043 (3)	0.065 (3)	0.003 (2)	0.019 (2)	0.003 (2)
O(3)	0.041 (2)	0.053 (3)	0.030 (2)	−0.014 (2)	0.012 (2)	−0.006 (2)
O(4)	0.092 (4)	0.053 (4)	0.045 (3)	0.010 (3)	−0.004 (3)	0.002 (3)
C(1)	0.049 (4)	0.026 (3)	0.049 (4)	0.004 (3)	0.014 (3)	−0.004 (3)
C(1C)	0.060 (5)	0.063 (6)	0.078 (6)	−0.020 (4)	0.048 (5)	−0.011 (4)
C(2C)	0.055 (5)	0.067 (6)	0.069 (5)	−0.015 (4)	0.043 (4)	−0.014 (4)
C(3C)	0.054 (5)	0.073 (6)	0.058 (5)	−0.014 (4)	0.037 (4)	−0.010 (4)
C(4C)	0.077 (6)	0.062 (6)	0.057 (5)	−0.014 (5)	0.043 (4)	0.004 (4)
C(5C)	0.064 (5)	0.061 (5)	0.063 (5)	−0.014 (4)	0.034 (4)	0.012 (4)
C(1P2)	0.041 (4)	0.034 (4)	0.051 (4)	−0.003 (3)	0.017 (3)	−0.004 (3)
C(2P2)	0.060 (5)	0.051 (5)	0.055 (5)	0.009 (4)	0.030 (4)	0.000 (4)
C(3P2)	0.074 (6)	0.060 (6)	0.090 (7)	0.009 (4)	0.047 (6)	−0.002 (5)
C(4P2)	0.064 (6)	0.076 (7)	0.093 (7)	0.010 (5)	0.029 (6)	−0.006 (6)
C(5P2)	0.050 (5)	0.084 (7)	0.077 (6)	0.014 (5)	0.003 (5)	−0.002 (5)
C(6P2)	0.050 (4)	0.056 (5)	0.055 (5)	0.007 (4)	0.011 (4)	−0.003 (4)
C(1P3)	0.040 (4)	0.045 (4)	0.028 (3)	−0.007 (3)	0.013 (3)	0.000 (3)
C(2P3)	0.045 (4)	0.064 (5)	0.046 (4)	−0.000 (4)	0.012 (3)	0.005 (4)
C(3P3)	0.043 (4)	0.074 (6)	0.053 (5)	−0.010 (4)	0.011 (4)	0.001 (4)
C(4P3)	0.058 (5)	0.079 (6)	0.035 (4)	−0.023 (5)	0.013 (4)	−0.003 (4)
C(5P3)	0.065 (5)	0.065 (5)	0.044 (4)	−0.018 (4)	0.017 (4)	−0.009 (4)
C(6P3)	0.052 (4)	0.044 (4)	0.047 (4)	−0.006 (3)	0.016 (3)	−0.010 (3)
C(1P1)	0.034 (3)	0.070 (5)	0.034 (3)	−0.014 (3)	0.013 (3)	−0.002 (4)
C(2P1)	0.062 (5)	0.095 (7)	0.060 (5)	−0.031 (5)	0.039 (4)	−0.028 (5)
C(3P1)	0.091 (7)	0.14 (1)	0.070 (6)	−0.043 (7)	0.051 (6)	−0.033 (7)
C(4P1)	0.067 (6)	0.16 (1)	0.054 (6)	−0.036 (7)	0.031 (5)	0.001 (7)
C(5P1)	0.053 (6)	0.17 (1)	0.058 (6)	−0.014 (6)	0.023 (5)	0.026 (7)
C(6P1)	0.044 (4)	0.096 (7)	0.051 (5)	−0.010 (4)	0.016 (4)	0.022 (4)
C(1V)	0.037 (4)	0.037 (4)	0.043 (4)	0.005 (3)	0.011 (3)	−0.000 (3)
C(2V)	0.040 (4)	0.055 (5)	0.051 (4)	0.005 (3)	0.013 (3)	−0.012 (4)
C(3V)	0.064 (6)	0.084 (7)	0.099 (7)	0.028 (5)	0.020 (5)	−0.039 (6)
C(4V)	0.040 (4)	0.055 (5)	0.053 (4)	0.011 (4)	−0.008 (3)	0.005 (4)
C(1P4)	0.047 (4)	0.039 (4)	0.051 (4)	0.000 (3)	0.015 (3)	−0.010 (3)
C(2P4)	0.060 (5)	0.065 (6)	0.053 (5)	−0.007 (4)	0.022 (4)	−0.010 (4)
C(3P4)	0.077 (6)	0.077 (6)	0.054 (5)	−0.011 (5)	0.021 (5)	−0.009 (4)
C(4P4)	0.061 (5)	0.073 (6)	0.052 (5)	−0.007 (4)	0.008 (4)	−0.013 (4)
C(5P4)	0.056 (5)	0.059 (6)	0.067 (6)	−0.012 (4)	0.013 (4)	−0.010 (4)
C(6P4)	0.046 (4)	0.042 (4)	0.058 (5)	−0.007 (3)	0.014 (3)	−0.014 (3)

[a] The form of the anisotropic thermal parameter is $\exp(-2\pi^2(U(1,1)h^2a^2 + U(2,2)k^2b^2 + U(3,3)l^2c^2 + 2U(1,2)hkab \cos\gamma + 2U(1,3)hlac \cos\beta + 2U(2,3)klbc \cos\alpha))$.

the *Z* isomer formed in reaction 4 has been definitively established by a single-crystal X-ray structural determination.

The structure may be described as isolated molecules, Figure 1, separated by ordinary van der Waals distances, Figure 2. Figure 1 shows an ORTEP drawing of the molecule, establishing both the regio- and stereochemical consequences of reaction 4. The nucleophile adds to the alkyne carbon atom bearing the phenyl substituent. The same regiochemistry is observed with similar η^2-styrene derivatives.[11] It is clear that the Fe atom and the phenyl group are on the same side of the ethylene linkage, thus establishing the complex as the *Z* isomer. If the center of the Cp ring is considered a coordination site, the local geometry about the Fe atom is that of a distorted tetrahedron. As expected, the Cp(center)–Fe–L, where L = C(1V), P, or C(1), angles of 119.5 (5)–126.0 (5)° are greater

(11) Lennon, P.; Rosan, A. M.; Rosenblum, M. *J. Am. Chem. Soc.* **1977**, *99*, 8426.

Table III. Bonded Distances (Å) and Angles (Deg) with Esd's in Parentheses for CpFeCO[P(OPh)$_3$][(*Z*)-C(Me)=C(Ph)Me]

Bond Distances

Fe-P	2.102 (2)	O(1)-C(1P1)	1.404 (8)	C(3P2)-C(4P2)	1.40 (1)
Fe-C(1)	1.746 (7)	O(2)-C(1P2)	1.396 (9)	C(4P2)-C(5P2)	1.37 (2)
Fe-C(1V)	2.031 (8)	O(3)-C(1P3)	1.411 (8)	C(5P2)-C(6P2)	1.40 (1)
Fe-C(1C)	2.12 (1)	C(1C)-C(2C)	1.47 (1)	C(6P2)-C(1P2)	1.384 (9)
Fe-C(2C)	2.13 (1)	C(2C)-C(3C)	1.42 (1)	C(1P3)-C(2P3)	1.38 (1)
Fe-C(3C)	2.11 (1)	C(3C)-C(4C)	1.41 (1)	C(2P3)-C(3P3)	1.40 (1)
Fe-C(4C)	2.107 (9)	C(4C)-C(5C)	1.45 (1)	C(3P3)-C(4P3)	1.38 (1)
Fe-C(5C)	2.120 (9)	C(5C)-C(1C)	1.40 (1)	C(4P3)-C(5P3)	1.39 (1)
Fe-center[a]	1.736 (9)	C(1P1)-C(2P1)	1.39 (1)	C(5P3)-C(6P3)	1.41 (1)
C(1)-O(4)	1.138 (9)	C(2P1)-C(3P1)	1.43 (2)	C(6P3)-C(1P3)	1.38 (1)
C(1V)-C(4V)	1.536 (8)	C(3P1)-C(4P1)	1.40 (2)	C(1P4)-C(2P4)	1.40 (1)
C(1V)-C(2V)	1.34 (1)	C(4P1)-C(5P1)	1.39 (2)	C(2P4)-C(3P4)	1.38 (1)
C(2V)-C(3V)	1.55 (1)	C(5P1)-C(6P1)	1.41 (1)	C(3P4)-C(4P4)	1.42 (1)
C(2V)-C(1P4)	1.503 (9)	C(6P1)-C(1P1)	1.39 (1)	C(4P4)-C(5P4)	1.37 (1)
P-O(1)	1.619 (5)	C(1P2)-C(2P2)	1.38 (1)	C(5P4)-C(6P4)	1.40 (1)
P-O(2)	1.623 (5)	C(2P2)-C(3P2)	1.38 (1)	C(6P4)-C(1P4)	1.39 (1)
P-O(3)	1.602 (4)				

Bond Angles

P-Fe-C(1)	92.3 (2)	C(3V)-C(2V)-C(1P4)	111.3 (7)	C(1P2)-C(2P2)-C(3P2)	119.5 (7)
P-Fe-C(1V)	91.2 (2)	Fe-C(1)-O(4)	176.6 (8)	C(2P2)-C(3P2)-C(4P2)	120 (1)
P-Fe-center[a]	126.0 (5)	C(5C)-C(1C)-C(2C)	109.3 (7)	C(3P2)-C(4P2)-C(5P2)	119.1 (9)
C(1)-Fe-C(1V)	94.5 (3)	C(1C)-C(2C)-C(3C)	105.7 (7)	C(4P2)-C(5P2)-C(6P2)	121.5 (8)
C(1)-Fe-center[a]	124.5 (5)	C(2C)-C(3C)-C(4C)	109.5 (7)	C(5P2)-C(6P2)-C(1P2)	117.9 (9)
C(1V)-Fe-center[a]	119.5 (5)	C(3C)-C(4C)-C(5C)	108.4 (6)	C(6P3)-C(1P3)-C(2P3)	122.4 (6)
Fe-P-O(1)	124.9 (2)	C(4C)-C(5C)-C(1C)	107.1 (7)	C(1P3)-C(2P3)-C(3P3)	118.1 (7)
Fe-P-O(2)	119.4 (2)	P-O(1)-C(1P1)	124.5 (4)	C(2P3)-C(3P3)-C(4P3)	120.5 (7)
Fe-P-O(3)	112.2 (2)	P-O(2)-C(1P2)	124.8 (4)	C(3P3)-C(4P3)-C(5P3)	120.8 (7)
O(1)-P-O(2)	96.4 (3)	P-O(3)-C(1P3)	128.5 (4)	C(4P3)-C(5P3)-C(6P3)	119.4 (8)
O(1)-P-O(3)	97.0 (2)	C(6P1)-C(1P1)-C(2P1)	124.5 (8)	C(5P3)-C(6P3)-C(1P3)	118.8 (7)
O(2)-P-O(3)	102.8 (2)	C(1P1)-C(2P1)-C(3P1)	116.3 (8)	C(6P4)-C(1P4)-C(2P4)	118.8 (6)
Fe-C(1V)-C(4V)	114.6 (5)	C(2P1)-C(3P1)-C(4P1)	120.(1)	C(1P4)-C(2P4)-C(3P4)	121.7 (9)
Fe-C(1V)-C(2V)	127.9 (5)	C(3P1)-C(4P1)-C(5P1)	122.(1)	C(2P4)-C(3P4)-C(4P4)	119.0 (9)
C(2V)-C(1V)-C(4V)	117.4 (6)	C(4P1)-C(5P1)-C(6P1)	119.(1)	C(3P4)-C(4P4)-C(5P4)	119.4 (7)
C(1V)-C(2V)-C(3V)	123.6 (6)	C(5P1)-C(6P1)-C(1P1)	118.2 (9)	C(4P4)-C(5P4)-C(6P4)	121.0 (9)
C(1V)-C(2V)-C(1P4)	125.0 (7)	C(6P2)-C(1P2)-C(2P2)	121.5 (7)	C(5P4)-C(6P4)-C(1P4)	120.2 (8)

[a] Center of cyclopentadiene ring. Esd's are approximate.

Table IV. Least-Squares Planes and Angles between Planes and Some Selected Nonbonded Distances

	atoms in plane	max dev.
I	ring 1 C(1P1)···C(6P1)	0.009 (3)
II	ring 2 C(1P2)···C(6P2)	0.010 (3)
III	ring 3 C(1P3)···C(6P3)	0.008 (3)
IV	ring 4 C(1P4)···C(6P4)	0.012 (3)
V	Cp C(1C)···C(5C)	0.003 (3)
VI	Fe, C(1V), C(2V), C(3V), C(4V), C(1P4)	0.05 (1)

Angles between Planes, Deg

IV-VI	67.3 (1)	[center*, Fe, C(1)]-VI	59.3 (1)
V-VI	31.1 (1)	VI-[C(1V), Fe, P]	55.4 (1)

Nonbonded Distances, Å

C(4V)-C(4C)	3.31 (1)	C(2P4)-O(4)	3.15 (1)
C(4V)-C(5C)	3.46 (1)	C(6P4)-C(1C)	3.39 (1)
C(2P4)-C(3P1)	3.92 (2)	C(2P4)-C(1)	3.39 (1)

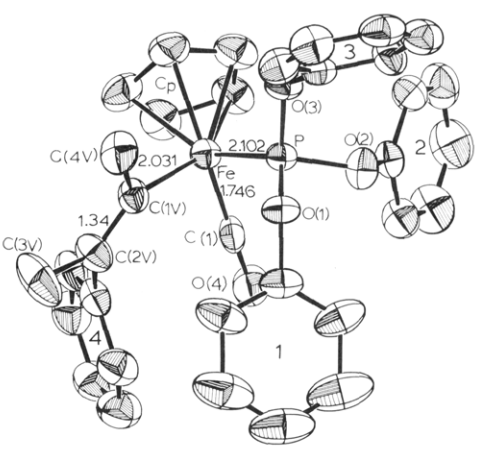

Figure 1. An ORTEP[13] drawing of an individual molecule of CpFeCO[P(OPh)$_3$][*Z*]-C(Me)=C(Ph)Me] with the more important distances. An important feature to be noted is the cis relationship of Fe to Ph. The ellipsoids are drawn at the 50% probability level. The notation for the rings are consistent with the tables and are as follows. For the Cp ring, C(4C) is closest to the viewer and then in a counterclockwise fashion C(5C) is closest to C(4V), then C(1C)···C(3C). For ring 4, C(1P4) is bound to C(2V) and then in a clockwise fashion toward ring 1, C-(2P4)···C(6P4). For ring 1, C(1P1) is bound to O(1) and then in a counterclockwise rotation C(2P1)···C(6P1). For ring 2, C(1P2) is bound to O(2) and then in a clockwise fashion toward ring 3, C(2P2)···C(6P2). For ring 3, C(1P3) is bound to O(3) and then in clockwise fashion up toward the viewer C(2P3), C(3P3)···C(6P3).

than the tetrahedral angle, whereas the L–Fe–L angles are 91.2 (2)–94.5 (3)° (Table III). The P–O distances are essentially equal and are less than three standard deviations from the average of 1.614 Å. The Fe–C(1V) distance of 2.031 (8) Å is almost identical with that observed by us recently in a similar compound[10] and is indicative of an Fe–C single bond to an sp^2-hybridized carbon. In general, the bond distances and angles and nonbonded interactions, both inter- and intramolecular, are normal.

The orientation of the alkenyl moiety is determined by nonbonded repulsions between the Cp ring and the C(4V) methyl group of the alkene, see distances of C(4V)–C(4C) and C(4V)–C(5C) (Table IV), and molecular packing in the crystal. This is also demonstrated by the angle between the alkene plane and the Cp plane of 31.1 (1)° (Table IV). Rotation around the Fe–C(IV) single bond would bring either the phenyl group or the methyl group geminal to the iron in close proximity to the Cp ligand. It is interesting to note that although the ethylene moiety and its bonded atoms are coplanar (σ = 0.03), the angle between phenyl ring 4 and the ethylene plane is 67.3 (1)°. This is no doubt due to nonbonded repulsions between the methyl

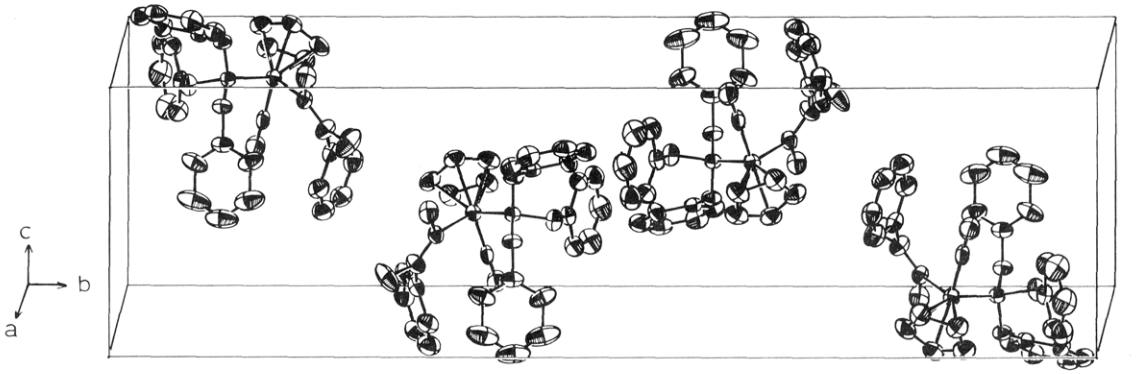

Figure 2. An ORTEP drawing, with probability level as above, of the contents of the unit cell. The origin is in the back lower left-hand corner with axes as indicated.

group C(3V) and phenyl ring 4. In addition, all the C–C bonds from the ethylene carbon atoms are relatively long, C(4V), C(3V), C(1P4) at 1.536 (8), 1.55 (1) Å, and 1.503 (9) Å, respectively (Table III).

It is interesting to note that in $CpFe(CO)(PPh_3)[\sigma$-$C(CO_2Et)=CMe_2]$ the nonbonded interactions of the substituted ethylene with the phosphine phenyl rings and with the cyclopentadiene ring restricted the orientation of the substituted ethylene to a cleft in the molecule.[10] However, by the substitution of triphenyl phosphite for triphenylphosphine the possibility of rotation about the Fe–C(IV) bond in solution is very real. However, molecular packing considerations make rotation about this bond unlikely in the solid state.

This structure characterizes the product of reaction 4 as the *Z* isomer. Due to the similarity of the synthetic method and the spectral data, the product of reaction 3 is clearly the *E* isomer of the same formula. These two isomers do not interconvert vide supra under the conditions of these reactions and subsequent isolations. Thus, these isomers are the primary products of the reactions. This establishes trans addition as the mode of nucleophilic addition. Note that the preparation of both isomers and proof that they do not interconvert under the reaction conditions was necessary for this conclusion. This represents the first definitive proof of trans addition of a nucleophile to an η^2-alkyne complex.

The yields in reactions 3 and 4 are exceedingly high. These reactions are actually carried out in two steps from $CpFeCO[P(OPh)_3]I$, using $AgBF_4$ in CH_2Cl_2 to remove I^- and allow the alkyne to fill the vacant coordination site. The intermediate η^2-alkyne complex is used after filtration and solvent evaporation. We have switched to this triphenyl phosphite system from our original report shown in eq 1 because the starting material is easier to prepare and the intermediate η^2-alkyne complex more stable. In this system, the normal R_2CuLi type organocuprate reagents that we used previously produced variable yields. The use of the higher order mixed organocuprate reagents, $R_2Cu(CN)Li_2$, overcame these problems. We feel that reagents of this type offer promise in the important general area of addition of nucleophiles to unsaturated organic ligands π coordinated to transition metals.[12] Further work in this area continues.

Acknowledgment is made to the National Science Foundation for its support of this research through Grant CHE 8019513 (D.L.R.). We thank the University of South Carolina for funds used to purchase the diffractometer. We also thank Professor Timothy L. MacDonald for useful discussions on higher order cuprates.

Registry No. $CpFeCO[P(OPh)_3][(E)$-$C(Me)=C(Me)Ph]$, 83096-09-7; $CpFeCO[P(OPh)_3][(Z)$-$C(Me)=C(Ph)Me]$, 83149-30-8; $CpFeCO[P(OPh)_3]I$, 31988-05-3; $Ph_2Cu(CN)Li_2$, 80473-66-1; $Me_2Cu(CN)Li_2$, 80473-70-7; $[CpFeCO[P(OPh)_3](\eta^2$-$MeC{\equiv}CMe]^+$, 83096-10-0; $[CpFeCO(P(OPh)_3](\eta^2$-$PhC{\equiv}CMe]^+$, 83096-11-1.

Supplementary Material Available: Listings of structural factor amplitudes for $CpFeCO[P(OPh)_3][(Z)$-$C(Me)=C(Ph)Me]$ (15 pages). Ordering information is given on any current masthead page.

(12) (a) Trost, B. M. *Acc. Chem. Res.* **1980**, *13*, 385; (b) Birch, A. J.; Jenkins, I. D. "Transition Metal Organometallics In Organic Synthesis"; Alper, H., Ed.; Academic Press: New York, 1976; Vol. I, Chapter 1.

(13) Johnson, C. K. ORTEP II, Report ORNL-3794 1970, Oak Ridge National Laboratory, Oak Ridge, TN.

(14) Frenz, B. A. "Enraf-Nonius Structure Determination Package", Version 17, with local modification for the PDP-11/40, 1980.

(15) Stewart, J. M., Ed. "The X-ray System", Technical Report TR-445, Computer Science Center, University of Maryland, College Park, MD, 1979.

Geminal Bis(haloorganostannanes) and Their Complexation as Mono- and Bidentate Lewis Acids with Dimethyl Sulfoxide

Thomas J. Karol, John P. Hutchinson, Jeffrey R. Hyde, Henry G. Kuivila,* and Jon A. Zubieta*

Department of Chemistry, State University of New York at Albany, Albany, New York 12222

Received June 1, 1982

Six (chloromethylstannyl)methanes with structures $CH_2(SnMe_nCl_{3-n})(SnMe_mCl_{3-m})$ with n = 0–3 and m = 0–2 have been prepared by chlorine–methyl exchange from bis(trimethylstannyl)methane or bis(trivinylstannyl)methane. Four 2,2-bis(chloromethylstannyl)propanes have been similarly prepared from 2,2-bis(trimethylstannyl)propane. Correlations between ^1H and ^{13}C magnetic resonance parameters have been examined. The effects of dimethyl sulfoxide (Me_2SO) on the ^1H NMR parameters of the chlorostannanes have been examined as a source of information on complexation. Seven complexes with Me_2SO have been prepared, and the structures of $CH_2(SnMeCl_2)$–$(SnMe_2Cl)(Me_5SO)^4_\lambda$, $CH_2(SnMeCl_2)_2(2Me_2SO)^5_\lambda$, and $CH_2(SnCl_3)_2(4Me_2SO)^7_\lambda$ have been determined by X-ray diffraction. In the first of these, the oxygen of the Me_2SO bridges the two tins which display distorted trigonal-bipyramidal geometry; in the second, the oxygens of each Me_2SO act as bridges between the tins which display distorted octahedral geometry; in the third, the oxygens do not bridge and the CH_2 group serves as a common apex for the octehedra of two hexacoordinate tins. Pertinent features of the structures are discussed. Compound **4** crystallizes in the space group $P\bar{1}$ with a = 7.551 (2) Å, b = 7.945 (2) Å, c = 13.354 (3) Å, α = 80.63 (2)°, β = 89.13 (2)°, γ = 72.96 (2)°, and Z = 2. The structure solution and refinement were based on 1609 reflections with $F_o > 6\sigma(F_o)$ to give a discrepancy factor of 0.045. Compound **5** crystallizes in the orthorhombic space group $Pbnm$ with a = 9.821 (2) Å, b = 12.411 (2) Å, c = 15.540 (3) Å, and Z = 4. Refinement based on 1109 reflections with $F_o > 6\sigma(F_o)$ converged at 0.048. Compound **7** crystallizes in the monoclinic space group $C2/c$ with a = 20.998 (5) Å, b = 7.925 (3) Å, c = 16.535 (4) Å, β = 98.79 (3)°, and Z = 4. Refinement using 1277 reflections with $F_o > 6\sigma(F_o)$ yielded R = 0.034.

A great majority of known organotin compounds contain a single tin atom. The most common of those that contain more than one tin atom have the tins bonded to each other as in the ditins and the polymeric compounds of the formula $(R_2Sn)_x$.[1] Those in which the tin atoms are separated by one or more carbon atoms in polymers[2,3] and in simpler compounds such as distannylmethanes[4-10] and higher homologues are less familiar. Yet such species should be readily prepared by known synthetic procedures, and they might display novel and useful properties. With this idea in mind we have begun a study of the preparation and properties of compounds containing more than one tin atom separated by one or more carbon atoms. In this paper we report results of studies on the simplest members of this class, namely, those with a single Sn–C–Sn structural unit. Preparations of chlorotins are described along with studies on complexation with dimethyl sulfoxide and physical properties of interest.

Bis(halostannyl)methanes. The obvious precursor of this series compound **1** was first obtained "quantitatively" by Kraus and Neal[4] by the reaction of (trimethylstannyl)sodium with methylene chloride (eq 1) in liquid ammonia. The preparation has been repeated[5] and has also been carried out in other solvents and by other methods.[6-10] We have prepared **1** in liquid ammonia routinely in 89% yield and in tetraglyme in 65% yield. Replacement of one or more of the methyl groups of **1** with halogen or other labile group would provide a functional center at tin for elaborating the structure. Kaesz[2] has reported that treatment of **1** with hydrogen chloride leads to the formation of tetramethylstannane and trimethylchlorostannane (eq 2) by cleavage of a methylene–tin bond rather than the desired methyl–tin bond.

$$2Me_3SnNa + CH_2Cl_2 \rightarrow \underset{\mathbf{1}}{CH_2(SnMe_3)_2} + 2NaCl \quad (1)$$

$$CH_2(SnMe_3)_2 + HCl \rightarrow CH_3SnMe_3 + ClSnMe_3 \quad (2)$$

Scheme I

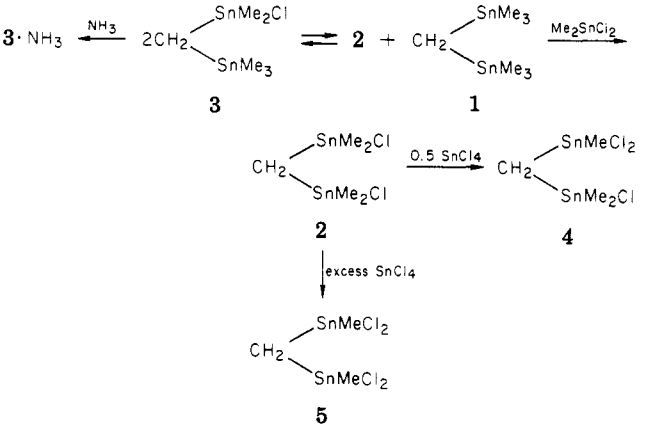

We have found that treatment with bromine in methanol–carbon tetrachloride at −60 °C followed by warming yielded trimethylbromostannane and dibromodimethylstannane as major cleavage products. Iodine similarly yielded a mixture of products.

The desired mode of cleavage was achieved by reaction of **1** with dichlorodimethylstannane (Scheme I). The trimethylchlorostannane formed could be removed at reduced pressure in 95% yield, and the residue was bis(di-

(1) Sawyer, A. K. "Organotin Compounds"; Marcel Dekker: New York, 1972; Vol. II, p 823.
(2) Henry, M. C.; Davidsohn, W. E. In "Organotin Compounds"; Sawyer, A. K., Ed.; Marcel Dekker: New York, 1972; Vol. III, p 975.
(3) Subramanian, R. V.; Garg, B. K. *Polym.—Plast. Technol. Eng.* **1978**, *11*, 81.
(4) Kraus, C. A.; Neal, A. M. *J. Am. Chem. Soc.* **1930**, *52*, 4426.
(5) Kaesz, H. D. *J. Am. Chem. Soc.* **1961**, *83*, 1514.
(6) Kuivila, H. G.; DiStefano, F. V. *J. Organomet. Chem.* **1976**, *122*, 171.
(7) Buyakov, A. A.; Gar, T. K.; Mironov, V. F. *Zh. Obsch. Khim.* **1973**, *43*, 801.
(8) Takai, K.; Hotta, Y.; Oshima, K.; Nozaki, H. *Tetrahedron Lett.* **1978**, 2417.
(9) Mitchell, T. N.; El-Behairy, M. *J. Organomet. Chem.* **1979**, *172*, 293.
(10) Dessy, R. E.; Pohl, R. L.; King, R. B. *J. Am. Chem. Soc.* **1966**, *88*, 5121.

0276-7333/83/2302-0106$01.50/0

Scheme II

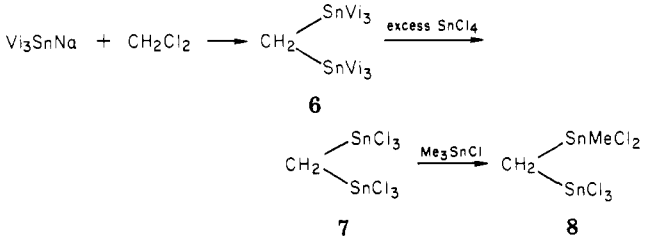

methylchlorostannyl)methane (**2**) of high purity. This dichloride could then be converted in quantitative yield to the diiodide by reaction with potassium iodide in acetone.

Attempted preparation of the monochloride, (trimethylstannyl)(chlorodimethylstannyl)methane (**3**) by reaction of 1 mol of dichlorodimethylstannane with **1** resulted in a mixture of **1**, **2**, and **3** in the ratio of about 1:1:2. This was established to be an equilibrium composition, for the same mixture of the three compounds was obtained upon mixing equimolar amounts of **1** and **2**. It was possible to obtain **3** as its ammonia complex (**3**·NH_3) by extracting the equilibrium mixture in pentane with water and immediately passing ammonia through the pentane solution, whereupon **3**·NH_3 precipitated. This complex was stable with respect to methyl–chlorine exchange. It lost ammonia if exposed to the air but was stable in an ammonia atmosphere.

Stepwise replacement of a methyl group on each tin atom of **2** could be achieved routinely in 95% yield. (Chlorodimethylstannyl)(dichloromethylstannyl)methane (**4**) was obtained by reaction of 1 mol of **2** with 0.5 mol of tetrachlorostannane. Replacement of a methyl group on each of the tins of **2** was most easily realized by treatment with excess tetrachlorostannane in methylene chloride to provide bis(dichloromethylstannyl)methane (**5**).

Exchange of the third methyl group on the tins to form the trichlorostannyl derivatives could not be achieved by simple reaction with tin tetrachloride. It has been shown that vinyl groups undergo exchange with chlorine of chlorostannanes with great facility.[11-13] For example, trichlorovinylstannane can be prepared from tetravinylstannane by exchange with tetrachlorostannane at temperatures of 100 °C or lower.[11,12] We exploited these observations by first preparing bis(trivinylstannyl)methane (**8**) by the reaction of (trivinylstannyl)sodium with methylene chloride in liquid ammonia in 70% yield (Scheme II). Treatment of **8** with tetrachlorostannane provided bis(trichlorostannyl)methane (**7**) in 87% yield. Treatment of **7**, in turn, with 1 mol of trimethylchlorostannane gave (trichlorostannyl)(dichloromethyl)stannane (**6**).

2,2-Bis(halostannyl)propanes. The "supernucleophilic"[9,10] behavior of (trimethylstannyl)sodium as reflected in the facility with which it reacted with methylene chloride prompted an examination of the reaction with the more hindered 2,2-dichloropropane. Reaction occurred readily and in high yield at −33 °C in liquid ammonia providing 2,2-bis(trimethylstannyl)propane (**9**) (eq 3). Treatment of **9** with 2 mol of dichlorodimethylstannane at 60 °C yielded 95% of 2,2-bis(chlorodimethylstannyl)propane (**10**) (eq 4). Replacement of a

$$Me_2CCl_2 + 2Me_3SnNa \rightarrow \underset{\mathbf{9}}{Me_2C(SnMe_3)_2} \qquad (3)$$

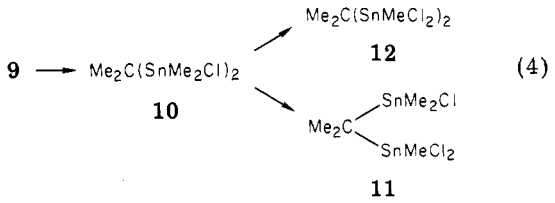

(4)

methyl on each tin was achieved by treatment with excess tetrachlorostannane to form 2,2-bis(dichloromethylstannyl)propane (**12**). When 1 mol of **10** was treated with 0.5 mol of tetrachlorostannane, the product was 2-(chloromethylstannyl)-2-(dichloromethylstannyl)propane (**11**) isolated in 75% yield (eq 4).

NMR Spectra. Values of proton chemical shifts and ^{119}Sn–^{1}H coupling constants are given in the Experimental Section and those for ^{13}C in Table I for the compounds described above. Both sets of parameters show the expected qualitative trends. Replacement of methyl groups by chlorine atoms decreases chemical shifts and increases the coupling constants. However, simple additivity trends are not discernible.

Comparison of compounds **1**–**6** shows an unexpected effect of replacing methyl by chlorine. On going from **1** to **5** replacement of two methyls of a trimethylstannyl group by chlorines causes a downfield shift of the methyl carbon by 16.6 ppm, whereas replacement of two trimethylstannyl groups on the methylene by the dichloromethylstannyl groups shifts the carbon signal downfield by 23.5 ppm. But replacement of the third methyls by chlorines causes an additional downfield shift by only 3.8 ppm.

Good correlations between ^{1}H and ^{13}C parameters are observed. For example the chemical shifts for the CH_2 protons of bis(trimethylstannyl)methane, **1**, and its chloro analogues are plotted vs. the values for ^{13}C in Figure 4. The parameters for the methyl groups do not show a similar correlation.

Previous investigators have examined the relationship between $^{2}J(^{119}Sn-^{1}H)$ and $^{1}J(^{119}Sn-^{13}C)$ and have reported approximate linear correlations.[15-17] These do not pass through the origin leading to the conclusion that factors other than the Fermi contact interaction are involved in the coupling between the tin and proton or carbon nucleus, or both.[15] In Figure 5 are plotted our data, along with those of Petrosyan et al.,[16] Singh,[17] and Mathiasch.[18] The correlation line drawn for the first three sets of data, excluding that for hexamethylditin, has a correlation coefficient of 0.996 and the intercept on the carbon axis of −98.3 Hz. The Petrosyan data intersect at −51 Hz. The cluster of points that fall above the line at the lower end are for ditins, the diamonds for cyclic derivatives, and the square for hexamethylditin. These deviant data further demonstrate that caution should be used in inferring values of one of the coupling constants from that of the other unless quite similar structures are involved.[17]

Complexation of Chlorostannanes with Dimethyl Sulfoxide in Solution. Molecules bearing more than one Lewis base function serve as valuable tools in many aspects of coordination chemistry. The chlorostannanes described above have the potential of playing a complementary role as bidentate Lewis acids. We have examined the behavior of these chlorides in solution with dimethyl sulfoxide

(11) Seyferth, D.; Stone, F. G. A. *J. Am. Chem. Soc.* **1957**, *79*, 515.
(12) Rosenberg, S. D.; Gibbons, A. J., Jr. *J. Am. Chem. Soc.* **1957**, *79*, 2138.
(13) Rosenberg, S. D.; Gibbons, A. J., Jr.; Ramsden, H. E. *J. Am. Chem. Soc.* **1957**, *79*, 2137.
(14) Kuivila, H. G.; Reeves, W. G. *Bull. Soc. Chim. Belg.* **1980**, *89*, 801.
(15) McFarlane, W. *J. Chem. Soc. A* **1967**, 528.
(16) Petrosyan, V. S.; Permin, A. B.; Reutov, O. A.; Roberts, J. D. *J. Magn. Reson.* **1980**, *40*, 511.
(17) Singh, G. *J. Organomet. Chem.* **1975**, *99*, 251.
(18) Mathiasch, B. *J. Organomet. Chem.* **1977**, *141*, 295.

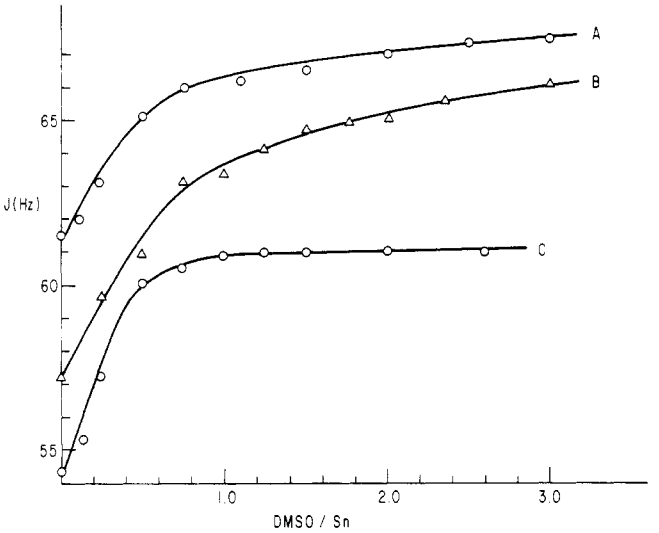

Figure 1. Effect of Me_2SO on $^2J(^{119}Sn-^1H)$ of methyltin protons in methylene chloride: A, 0.30 M bis(chlorodimethylstannyl)-methane, **2**; B, 0.63 M chlorotrimethylstannane; C, 0.58 M 2,2-bis(chlorodimethylstannyl)propane, **10**.

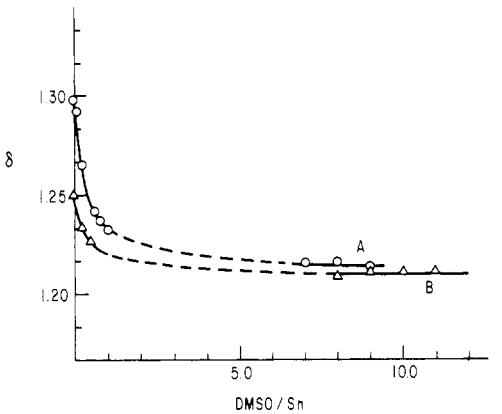

Figure 2. Effect of Me_2SO on chemical shifts of methyltin protons in acetone-d_6: A, 0.29 M bis(dichloromethylstannyl)-methane, **5**; B, 0.25 M 2,2-bis(dichloromethylstannyl)propane, **11**.

(Me_2SO), a donor whose complexation with simple organotin halides and other derivatives has been studied from several perspectives during the past two decades. In general the halides R_3SnX tend to form pentacoordinate complexes[19-21] while R_2SnX_2 and $RSnX_3$ tend to form hexacoordinate complexes.[21-24] We used proton magnetic resonance spectroscopy (^1H NMR) for this study because of its convenience. The observed magnitudes of changes in parameters were not deemed great enough for accurate quantitative work. Nonetheless, the changes in chemical shifts and/or coupling constants on the methyltin protons of the chlorotins upon addition of increments of Me_5SO were sufficient to provide useful information about complexation.

Results for chlorotrimethylstannane, **2**, and **10** are shown in Figure 1. In each case a large initial slope in the plot decreases fairly rapidly and approaches zero. The values of the coupling constants are taken to represent weighted

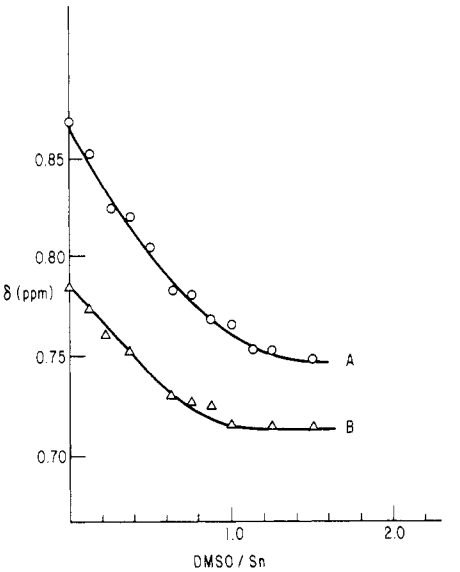

Figure 3. Effect of Me_2SO on the chemical shifts of the dichloromethyl ($MeCl_2Sn$) protons in methylene chloride: A, 0.29 M (dichloromethylstannyl)(chlorodimethylstannyl)methane, **4**; B, 0.39 M 2-(chlorodimethylstannyl)-2-(dichloromethylstannyl)propane, **10**.

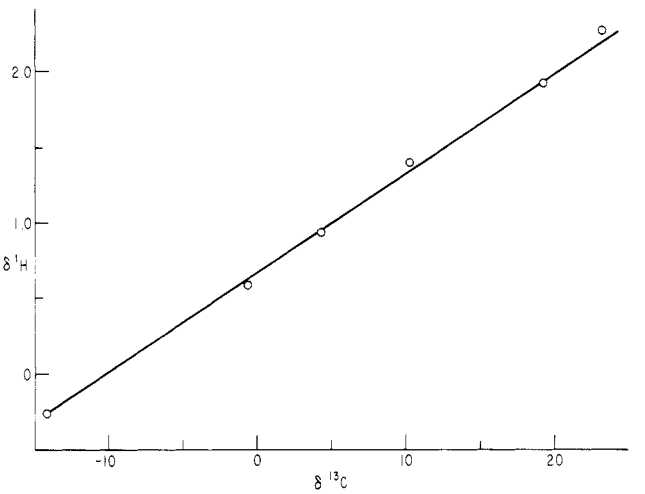

Figure 4. Relationship between proton and ^{13}C chemical shifts in methylene chloride or carbon tetrachloride.

means for species in rapidly established equilibria such as those represented in eq 5 and 6. Extrapolations of the

$$2 + Me_2SO \rightarrow 2(Me_2SO) \quad (5)$$

$$2(Me_2SO) + Me_2SO \rightarrow 2(2Me_2SO) \text{ etc.} \quad (6)$$

nearly linear initial and final portions of the plots for **2** and **10** intersect at a Me_2SO/Sn ratio near 0.5, indicating that 1/1 complexes ($2(Me_2SO)$ and $10(Me_2SO)$) are particularly stable, but additional coordination may occur at higher Me_2SO concentrations. By contrast the break in the plot for chlorotrimethylstannane is less pronounced than that in the others, and a similar extrapolation suggests intersection nearer a 1/1 molecular ratio. The chemical shifts of the methyl protons also changes, but the change in the same experiments for **10** was only 2 Hz (0.03 ppm) upfield.

Similar plots for **5** and **11** are shown in Figure 2. Due to the low solubility of the complexes in methylene chloride, acetone-d_6 was used as the solvent. Even then, ^1H NMR data (chemical shifts of the tin methyl protons) could not be obtained when Me_2SO/SN fell between 1 and 7 due to precipitation of the complex. At higher concentrations of Me_2SO the complex was soluble. Inspection

(19) Kawasaki, Y.; Hori, M.; Uenaka, K. *Bull. Chem. Soc. Jpn.* **1967**, *40*, 2463.
(20) Petrosyan, V. S.; Yashina, N. S.; Reutov, O. A. *J. Organomet. Chem.* **1973**, *52*, 315.
(21) Petrosyan, V. S.; Yashina, N. S.; Reutov, O. A. *Adv. Organomet. Chem.* **1976**, *14*.
(22) Langer, H. D.; Blut, A. H. *J. Organomet. Chem.* **1967**, *5* 288.
(23) Clark, H. C.; Goel, R. C. *J. Organomet. Chem.* **1967**, *7*, 263.
(24) Isaacs, N. W.; Kennard, C. H. L. *J. Chem. Soc.* **1970**, 1257.

Table I. Carbon-13 Magnetic Resonance Parameters[a,b]

	carbons							
	w		x		y		z	
	δ	$^n(J)$[c]	δ	$^n(J)$[c]	δ	$^n(J)$[c]	δ	$^n(J)$[c]
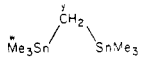 **1**	−7.4	^{1}(330)			−14.2	^{1}(287)		
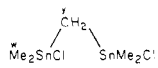 **2**	1.5	^{1}(400)			4.2	^{1}(295)		
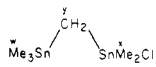 **3**[d]	−7.5	^{1}(344)	−6.0	^{1}(361)	−0.06	$^w1$(236) $^x1$(287)		
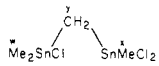 **4**	1.1	^{1}(409)	9.7	^{1}(508)	10.2	$^w1$(261) $^x1$(385)		
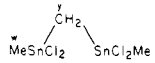 **5**	9.2	^{1}(547)			19.3	^{1}(403)		
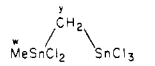 **6**								
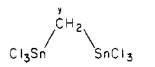 **7**					23.1	^{1}(698)		
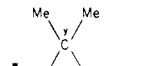 **9**	−18.8	^{1}(299)			10.1	^{1}(341)	26.3	^{2}(18)
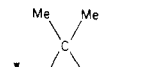 **10**	−1.8	^{1}(340)			29.8	^{1}(361)	23.8	^{2}(24)
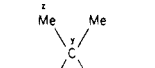 **11**	−1.9	^{1}(365)	7.8	^{1}(389)	31.2	*e*	23.1	$^w2$(15) $^x2$(29)
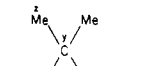 **12**	6.9	^{1}(430)			49.2	^{1}(466)	22.6	^{2}(24)

[a] Solvent and internal. [b] Chemical shifts in ppm downfield from Me_4Si obtained by using CH_2Cl_2 as secondary reference (δ 53.486). [c] $^nJ = {}^nJ(^{119}Sn-^{13}C)$; $^wn(J)$ or $^xn(J)$ coupling to carbon w or x. [d] In pyridine. [e] Not detected due to weak signal from tetrasubstituted carbon.

of the plots suggests that the complex with a Me_2SO/Sn ratio of unity or less is particularly stable.

The intermediate trichloro analogues **4** and **13** both yielded plots with somewhat less definite changes in slopes, but indicate intersections near unity. The pentachloro and hexachloro analogues **8** and **7**, respectively, formed complexes which were so insoluble that similar ^1H NMR studies could not be made.

Isolation of Me_2SO Complexes. Complexes with Me_5SO were prepared from all of the chlorostannanes except **3**. These were obtained by adding the chlorostannane and Me_2SO to carbon tetrachloride. All were crystalline solids but varied in composition as follows: **2**(Me_2SO); **4**(Me_2SO); **5**($2Me_2SO$); **8**($3Me_2SO$); **7**($4Me_2SO$); **10**(Me_2SO); **12**(Me_2SO); **11**($2Me_2SO$). These may not be the most stable complexes formed but are those whose stability constants and solubility in carbon tetrachloride are such that they crystallize most readily.

Structures of Me_2SO Complexes. The structures of three of the complexes were determined by X-ray diffraction. That of **6**($3Me_2SO$) could not be solved due to disorder. Schematics of the structures are shown in Figure 6, together with relevant bridging parameters.[25] Data on bond lengths and angles are gathered in Table II.

Compound **5**($2Me_2SO$) consists of discrete dimers, each tin atom enjoying pseudooctahedral geometry. The tin

(25) A preliminary communication on these structures has been published: Hyde, J. R.; Karol, T. J.; Hutchinson, J. P.; Kuivila, H. G.; Zubieta, J. A. *Organometallics* **1982**, *1*, 404.

(26) Coghi, L.; Nardelli, M.; Pelizzi, C.; Pelizzi, G. *Gazz. Chim. Ital.* **1975**, *105*, 1187.

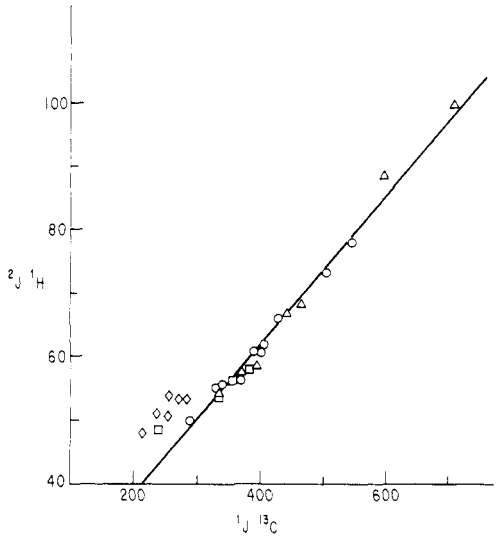

Figure 5. Plot of coupling constants of ^{119}Sn with protons and ^{13}C in methylene chloride or carbon tetrachloride for proton spectra and deuteriochloroform/methylene chloride for ^{13}C: O, this work; △, ref 16; □, ref 17; ◇, ref 18.

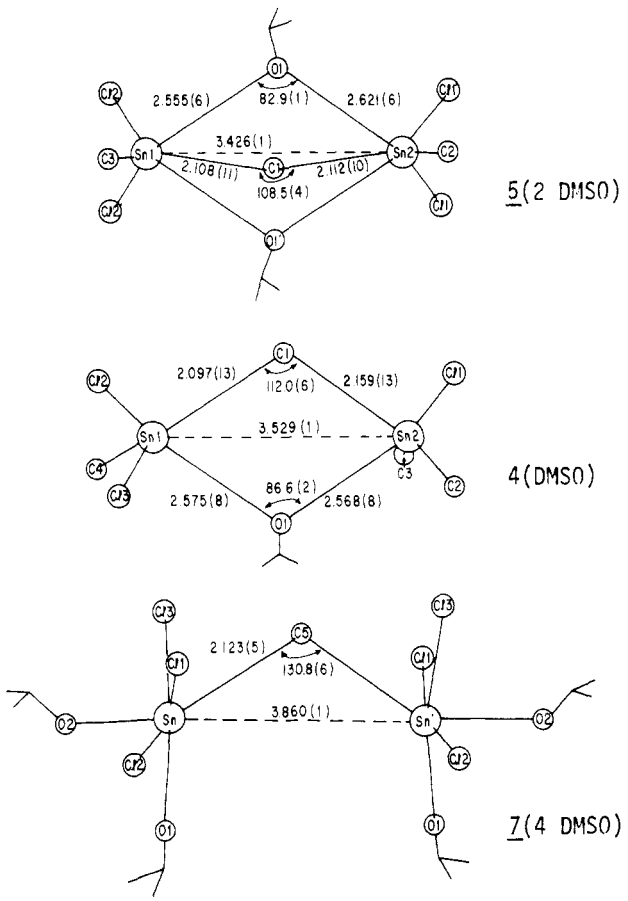

Figure 6. Schematics of structures of Me_2SO complexes.

octahedra share a common face through the bridging methylene groups and the oxygens of the Me_2SO groups. A crystallographic mirror plane passes through Sn1, Sn2, C2, and C3. As anticipated, the average Sn–O(Me_2SO) bridging distance of 2.588 (6) Å is significantly longer than that observed for Sn–O(Me_2SO) terminal bonding in $[SnCl_2Ph_2(Me_2SO)_2]$,[25] 2.318 (5) Å, or in 7(4Me_2SO), 2.118 (6) Å. The significant lengthening of the Sn–O(Me_2SO) bond distance in $[SnCl_2CH_2(Me_2SO)_2]$ as compared to 7(4Me_2SO) presumably reflects the steric constraints imposed by the phenyl groups in this species. The $(Me_2SO)_2$

Table II. Selected Bond Lengths (Å) and Angles (Deg) for the Bis(stannyl)methanes

(a) $[Sn_2(CH_2)(CH_3)_2Cl_4(Me_2SO)_2]$

Bond Distances

Sn1···Sn2	3.426 (1)	Sn2-C1	2.112 (10)
Sn1-Cl2	2.419 (3)	Sn2-C2	2.117 (15)
Sn1-C1	2.108 (11)	Sn2-O1	2.621 (6)
Sn1-C3	2.115 (15)	S1-O1	1.527 (6)
Sn1-O1	2.555 (6)	S1-C4	1.79 (1)
Sn2-Cl1	2.411 (3)	S1-C5	1.79 (1)

Bond Angles

O1-Sn1-O1	82.0 (3)	O1-Sn2-O1′	79.5 (2)
O1-Sn1-C1	72.2 (2)	O1-Sn2-C1	70.8 (2)
O1-Sn1-C3	87.1 (3)	O1-Sn2-C2	83.1 (3)
O1-Sn1-Cl2	88.5 (1)	O1-Sn2-Cl1	90.4 (1)
O1-Sn1-Cl2′	168.2 (2)	O1-Sn2-Cl1′	168.4 (2)
C1-Sn1-C3	152.3 (5)	C1-Sn2-C2	145.7 (5)
C1-Sn1-Cl2	98.3 (2)	C1-Sn2-Cl1	100.6 (2)
C3-Sn1-Cl2	99.4 (3)	C1-Sn2-Cl1	101.5 (3)
Sn1-C1-Cl2′	100.1 (1)	C2-Sn2-Cl1′	99.1 (1)
Sn1-O1-Sn2	82.9 (2)	O1-S1-C4	105.3 (4)
Sn1-C1-Sn2	108.5 (4)		
Sn1-O1-S1	131.1 (3)	O1-S1-C5	105.8 (4)
Sn2-O1-S1	145.6 (3)	C4-S1-C5	97.7 (5)

(b) $[Sn_2(CH_2)(CH_3)Cl_3(Me_2SO)]$

Bond Distances

Sn1···Sn2	3.529 (1)	Sn2-O1	2.568 (8)
Sn1-Cl2	2.410 (4)	Sn2-Cl	2.159 (3)
Sn1-Cl3	2.372 (4)	Sn2-C2	2.136 (13)
Sn1-O1	2.572 (8)	Sn2-C3	2.152 (18)
Sn1-C1	2.097 (13)	S-O1	1.526 (8)
Sn1-C4	2.140 (17)	S1-C5	1.82 (2)
Sn2-Cl1	2.453 (4)	S1-C6	1.80 (2)

Bond Angles

O1-Sn1-C1	77.9 (4)	O1-Sn2-C1	77.0 (4)
O1-Sn1-Cl2	174.2 (3)	O1-Sn2-Cl1	175.7 (2)
O1-Sn1-Cl3	81.5 (2)	O1-Sn2-C2	88.4 (5)
O1-Sn1-C4	83.8 (4)	O1-Sn2-C3	82.4 (5)
C1-Sn1-Cl2	99.9 (3)	C1-Sn2-Cl1	98.0 (3)
C1-Sn1-Cl3	109.6 (4)	C1-Sn2-C2	115.2 (6)
C1-Sn1-C4	134.9 (6)	Cl1-Sn2-C3	120.4 (6)
Cl2-Sn1-Cl3	94.4 (1)	Cl1-Sn2-C2	97.3 (4)
Cl2-Sn1-C4	101.4 (4)	Cl1-Sn2-C3	97.1 (4)
Cl3-Sn1-C4	107.9 (4)	C2-Sn2-C3	119.5 (6)
Sn1-O1-Sn2	86.6 (2)	O1-S1-C5	106.3 (6)
Sn1-O1-Sn2	112.0 (6)		
Sn1-O1-S1	130.6 (5)	O1-S1-C6	103.4 (6)
Sn2-O1-Sn	134.4 (5)	C5-S1-C6	97.7 (8)

(c) $[Sn_2(CH_2)Cl_6(Me_2SO)_4$

Bond Distances

Sn···Sn	3.860 (1)	S1-O1	1.550 (6)
Sn-Cl1	2.46 (2)	S1-C1	1.770 (9)
SnCl2	2.447 (2)	S1-C2	1.784 (9)
Sn-Cl3	2.475 (3)	S2-O2	1.547 (7)
Sn-O1	2.109 (5)	S2-C3	1.753 (15)
Sn-C5	2.123 (5)	S2-C4	1.726 (15)

Bond Angles

Cl1-Sn-Cl2	167.2 (1)	O1-Sn-C5	101.8 (3)
Cl1-Sn-Cl3	91.5 (1)	O2-Sn-C5	174.8 (3)
Cl1-Sn-O1	88.9 (1)	Sn-C5-Sn′	130.8 (6)
Cl1-Sn-O2	80.9 (2)	Sn-O1-S1	128.7 (3)
Cl1-Sn-C5	94.8 (1)	O1-S1-C1	100.5 (4)
Cl2-Sn-Cl3	93.0 (1)	O1-S1-C2	103.0 (4)
Cl2-Sn-O1	83.9 (2)	C1-S1-C2	100.2 (4)
Cl2-Sn-O2	87.6 (2)	Sn-O2-S2	123.8 (3)
Cl2-Sn-C5	97.0 (1)	O2-S2-C3	102.7 (7)
Cl3-Sn-O1	165.9 (2)	O2-S2-C4	105.1 (6)
Cl3-Sn-C5	84.9 (2)	C3-S2-C4	97.1 (9)
Cl3-Sn-C5	92.3 (3)		
O1-Sn-O2	81.2 (2)		

compounds of pseudooctahedral Sn adopt cis configurations for the structurally characterized examples $[SnCl_2Me_2(Me_2SO)_2]$,[24] $[SnCl_2Ph_2(Me_2SO_2]$, 4(Me_2SO), and 5(2Me_2SO). Steric arguments[27] would suggest that pointed monodentate groups preferentially adopt the cis pattern.

In contrast, structure 4(Me_2SO) is doubly bridged by the methylene carbon and the oxygen of the (Me_2SO) group, with each Sn atom displaying distorted trigonal-bipyramidal geometry. The bridging methylene group is in the equatorial position in both the Sn1 and Sn2 coordination while the bridging oxygen atom occupies an axial position in both cases. The equatorial positions for Sn1 are completed by C4 and C13, while the equatorial plane of Sn2 is defined by C2 and C3, in addition to the bridging methylene group. The second apical position is occupied by a Cl atom for both Sn1 and Sn2, Cl2 and Cl1, respectively. The equatorial Sn1–Cl3 distance of 2.372 (4) Å is significantly shorter than the average of the Sn–Cl–axial distances Sn1–Cl2 and Sn2–Cl1, 2.434 (4) Å average. The Sn–O distances, 2.572 (8) Å average, are essentially identical with those observed in 4, where the Me_2SO groups are likewise bridging.

The single bridged compound 7(4Me_2SO) displays distorted octahedral geometry about the crystallographically identical Sn atoms. The single-bridged geometry may reflect the coordinative saturation of the Sn atoms, precluding additional bridging through the Me_2SO groups, which would render the Sn atom seven-coordinate.

Figure 6 illustrates the trend in the Sn···Sn distances and the concomitant increase in the Sn–C–Sn angle in passing from triply bridged 5(2Me_2SO) to double bridged 4-(Me_2SO) and finally to singly bridged 7(4Me_2SO) species.

Experimental Section

General Data. Proton nuclear resonance spectra were obtained at 60 MHz by using a Varian A-60A or EM360A instrument. Chemical shifts are reported in parts per million downfield from tetramethylsilane followed in parentheses by the multiplicity, number of protons, coupling constant, and assignment. Proton–tin-119 coupling constants are reported as $^nJ(^{119}Sn–H)$ with the superscript donoting the number of bonds intervening between nuclei. Carbon-13 NMR spectra were obtained by using a Bruker WH-90 spectrometer with a B-NC-12 data system. All spectra were recorded in chloroform-*d* as solvent and as internal lock, and chemical shifts are in parts per million from internal tetramethylsilane. Gas chromatographic analyses were performed on an F & M Hewlett-Packard Model 5750 or an F & M 720 instrument using a thermal conductivity detector. All analyses were performed on a 6 ft or 17 ft × 0.25 in. copper column packed with 15% SE-30 on Chromosorb W, 60–80 mesh. Melting points and boiling points are uncorrected. Carbon–hydrogen analyses were done by Instranal of Rensselaer, New York. Mass spectra were recorded on an AEI MS 902 mass spectrometer using the heated inlet or direct insertion methods. The spectra were run at 70 eV with an accelerating potential of 8 kV. Values are reported for the peak of highest intensity in the highest *m/e* cluster observed.

Bis(trimethylstannyl)methane (1). Method I. Trimethylchlorostannane (149 g, 750 mmol) and 100 mL of pentane were transferred into a 1-L, 3-neck flask, fitted with a mechanical stirrer, a Dry ice cooled cold finger, and nitrogen bubbler. Ammonia was condensed into the flask until two-thirds full. The mixture was stirred while sodium (34.6 g, 1.51 mol) in small pieces was added over a period of 5 min. The mixture was stirred 10 min longer. Methylene chloride (31.6 g) was added slowly with stirring by syringe through a septum in one neck of the flask. The ammonia was then allowed to evaporate, and the resulting mixture was extracted with 200 mL of pentane and 500 mL of water. The organic layer was washed with 500 mL of 0.1 M sulfuric acid and then with 500 mL of water. The organic layer was dried over $MgSO_4$, filtered, concentrated, and distilled into a liquid-nitrogen-cooled trap at 0.01 torr while being stirred at room temperature to yield 97.4 g (89%) of 1: ^1H NMR (CCl_4) δ –0.25 (s, 2, $^2J(^{119}Sn–H)$ = 63.0 Hz, $SnCH_2Sn$), 0.02 (s, 9, $^2J(^{119}Sn–H)$ = 54.5 Hz, CH_3Sn).

Method II. (Trimethylstannyl)sodium was prepared in a 3-neck, 250-mL round-bottom flask equipped with a wire stirrer by reaction of trimethylchlorostannane (54.9 g, 275.5 mmol) and sodium (17.0 g, 741 mmol) in 225 mL of TG or THF under nitrogen at 0 °C. The yield was 91.5% as determined by reaction of an aliquot with bromobenzene. Methylene chloride (8.81 g, 104 mmol) was added slowly by syringe with stirring at 0 °C. The product was extracted after 5 min by adding 500 mL of water and 100 mL of petroleum ether. The organic layer was washed with 500 mL of water, dried over $MgSO_4$, and rotary evaporated to afford 29.0 g of crude product which was distilled at 12 torr: bp 70–75 °C; 23.0 g (65%).

3-(Trimethylstannyl)-2,2,4,4,6,6-hexamethyl-2,4,6-tristannaheptane (18). This tetratin compound was isolated as a by-product in the previous experiments. From method II the residue (6.05 g, 21% total weight) was primarily 18 with roughly 5% of 1 present by GC analysis. From method I, the residue (7.7 g, 7% of total weight, 7% yield overall) was 18 with less than 1% of 1.

Compound 18 was distilled at 0.01 torr through a short path by heating with a steam bath. Compound 1 was an impurity in the distillate and was removed by warming at 50 °C and 0.01 torr with stirring overnight. The residual 18 had the following properties: mp 29–30 °C; mass spectrum, *m/e* 652 (M – 15), M_2(calcd) 667; ^1H NMR (CCl_4) δ –0.75 (s, 1, $^2J(^{119}Sn–CH)$ = 62.0 Hz, $SnCH(Sn)_2$), –0.25 (s, 2, $^2J(^{119}Sn–CH)$ = 62.0 Hz, $SnCH_2Sn$), 0.07 (s, 6, $^2J(^{119}Sn–CH)$ = 52.0 Hz, $CSn(Me_2)C$), 0.12 (s, 18, $^2J(^{119}Sn–CH)$ = 52.0 Hz, $Me_3SnCSnC(SnMe_3)_2$). Anal. Calcd for $C_{13}H_{36}Sn_4$: C, 23.40; H, 5.45. Found: C, 23.96; H, 5.47.

Bis(chlorodimethylstannyl)methane (2). Bis(trimethylstannyl)methane (3.04 g, 8.9 mmol) was placed in a round-bottom, 1-neck flask with dimethyldichlorostannane (3.91 g, 17.8 mmol). The flask was heated at 60 °C for 12 h. The trimethylchlorostannane formed was collected by distillation by warming with steam at 12–15 torr in 95% yield (98% pure). Following further heating at 0.01 torr, the product remaining contained less than 1% of trimethylchlorostannane.

A portion of the product was recrystallized from benzene for analysis: mp 59–60 °C; ^1H NMR (Cl_2CH_2) δ 0.78 (s, 12, $^2J(^{119}Sn–CH)$ = 61.0 Hz, $SnMe_2$), 0.93 (s, 2, $^2J(^{119}Sn–CH)$ = 61.0, $SnCH_2Sn$). Anal. Calcd for $C_5H_{14}Sn_2Cl_2$: C, 15.70; H, 3.70. Found: C, 15.49; H, 3.63.

Bis(iododimethylstannyl)methane. Into a 250-mL round-bottom flask were placed bis(dimethylchlorostannyl)methane (7.76 g, 20.29 mmol), potassium iodide (7.94 g, 27.8 mmol), and 100 mL of acetone. The mixture was stirred overnight, concentrated an oil, and then treated with 25 mL of methylene chloride. The solution was filtered to remove sodium chloride and then rotary evaporated. The product was then placed under 0.01 torr by slowly reducing the pressure while the mixture was stirred, leaving an oil which solidified on standing (8.7 g, 98% yield). The H NMR of the product indicated that it contained about 1% trimethyliodostannane. It was further purified by dissolving in petroleum ether (150 mL) with warming, filtered, and concentrated to about 20 mL by rotary evaporation. This afforded a portion of the product recrystallized (5.3 g, 60% yield): mp 33.5–34.0 °C; ^1H NMR (CH_2Cl_2) δ 0.98 (s, 12, $^2J(^{119}Sn–CH)$ = 58.9 Hz, SnMe), 1.30 (s, 2, $^2J(^{119}Sn–CH)$ = 60.0 Hz, $SnCH_2Sn$).

(Trimethylstannyl)(chlorodimethylstannyl)methane (3). Equimolar amounts of bis(dimethylchlorostannyl)methane (5.5 g, 25 mmol) and bis(trimethylstannyl)methane (8.6 g, 25 mmol) were placed into a 100-mL flask and warmed at 60 °C for 12 h. The product was mixed with 100 mL of pentane and extracted with several 200-mL portions of water to remove unreacted dichloro compound. The pentane solution was then filtered, and ammonia was immediately passed through it with stirring. A white complex which formed was filtered, washed with pentane saturated with ammonia, and dried in a current of ammonia. The unreacted dichloro compound was recovered from the water extract by saturating with sodium chloride and extraction with several 50-mL portions of ether (roughly 80% recovery). The unreacted bis(trimethylstannyl)methane was recovered quantitatively from the pentane by flash evaporation. The yield of the ammonia complex

(27) Zahrobsky, R. F. *J. Am. Chem. Soc.* **1971**, *93*, 3313.

Table III. Summary of Experimental Details and Crystal Data for the Structural Study

	$[Sn_2(CH_2)(CH_3)_2Cl_4\text{-}(Me_2SO)_2]$	$[Sn_2(CH_2)(CH_3)_3Cl_3\text{-}(Me_2SO)]$	$[Sn_2(CH_2)Cl_6\text{-}(Me_2SO)_4]$
(A) Crystal Parameters[a] at 23 °C			
a, Å	9.821 (2)	7.551 (2)	20.998 (5)
b, Å	12.411 (2)	7.945 (2)	7.925 (3)
c, Å	15.540 (3)	13.354 (3)	16.535 (4)
α, deg	90.00	80.63 (2)	90.00
β, deg	90.00	89.13 (2)	98.79 (3)
γ, deg	90.00	77.96 (2)	90.00
V, Å^3	1894.2	755.3	2719.3
space group	$Pbnm$	$P\bar{1}$	$C2/c$
Z	4	2	4
D(calcd), g cm^{-3}	2.03	2.11	1.90
(B) Measurement of Intensity Data			
cryst dimens, mm	0.20 × 0.18 × 0.22	0.24 × 0.16 × 0.26	0.21 × 0.23 × 0.20
instrument	Nicolet R3m		
radiation	Mo Kα graphite monochromator (equatorial mode)		
scan mode	coupled θ(crystal)-2θ(counter)		
scan rate	variable within the limits 3.0°/min and 30.0°/min		
scan length, deg	$[2\theta(K\alpha_1) - 1.0]$ to $[2\theta(K\alpha_1) + 1.0]$		
bkgd measurements	three reflections every 100 data reflections		
no. of reflctns collected	1498	1932	1837
scan range, deg	$0 < 2\theta \leq 45$	$0 < 2\theta \leq 45$	$0 \leq 2\theta < 45$
(C) Treatment of Intensity Data, Structure Solution, and Refinement[b]			
reduction to F_o^2 and $\sigma(F_o)^2$	data corrected for background, attenuators, and Lorentz-polarization in the usual manner		
abs coeff, cm^{-1}	34.2	39.6	27.5
abs correction	based on Ψ scans for five medium intensity reflections with χ angles near 90°		
obsd unique data $F_o > 6\sigma(F_o)$	1109	1609	1277
structure soln[c,d]	tin positions located on three-dimensional Patterson maps; all other non-hydrogen atoms located on subsequent difference Fourier maps; hydrogen atoms were introduced as fixed contributors in the final stages of refinement; Block-diagonal least-squares refinement of positional and thermal parameters in the usual fashion		
final discrepancy factors: R, R_w[e]	0.048, 0.047	0.045, 0.055	0.034, 0.038

[a] From a least-squares fitting of the setting angle of 25 reflections. [b] All calculations were performed on a Data General Nova 3 computer with 32K of 16-bit words using versions of the Nicolet SHELXTL interactive crystallographic softward package as described in GM Sheldrick, "Nicolet SHELXTL Operations Manual", Nicolet XRD Corp., Cupertino, CA, 1979. [c] Cromer, D. T.; Mann, J. B. *Acta Crystallogr., Sect. A* **1968**, *24A*, 321. [d] "International Tables for X-ray Crystallography", Kynoch Press: Birmingham, England, 1962; Vol. III. [e] $R = \Sigma ||F_o| - |F_c||/\Sigma |F_o|$; $R_w = \{\Sigma w(|F_o| - |F_o|)^2/\Sigma |F_o|^2\}^{1/2}$; $w = 1/\sigma^2(F)$.

based on starting bis(dimethylchlorostannyl)methane was 50% assuming a 1:1 complex: ^{1}H NMR (pyridine) δ 0.28 (s, 9, ^2J(^{119}Sn–CH) = 54.7 Hz, $SnMe_3$), 0.59 (s, 2, ^2J(^{119}Sn–CH) = 73.0 to SnCl and 57.5 to $SnMe_3$, $SnCH_2Sn$), 0.90 (s, 6, ^2J(^{119}Sn–CH) = 67.2, $SnMe_2Cl$).

(Chlorodimethylstannyl)(dichloromethylstannyl)methane (4). Into a 100-mL, round-bottom flask was placed 9.6 g (25.1 mmol) of bis(dimethylchlorostannyl)methane with 2 mL of methylene chloride and 3.27 g (12.5 mmol) of tetrachlorostannane. The solution was warmed and the solvent removed by rotary evaporation. The flask was then heated at 60 °C for 36 h. Dimethyldichlorostannane was removed by reducing the pressure to 0.01 torr with stirring and warming to 60 °C, leaving 9.4 g (24.0 mmol, 93% yield) of product of ca. 95% purity by ^{1}H NMR analysis. A portion was recrystallized from CCl_4 (mp 66–67 °C) for analysis: ^{1}H NMR (CH_2Cl_2) δ 0.85 (s, 6, ^2J(^{119}Sn–CH) = 62.0 Hz, Sn(Cl)Me_2), 1.30 (s, 3, ^2J(^{119}Sn–CH) = 73.6 Hz, Sn(Cl_2)Me), 1.40 (s, 2, ^2J(^{119}Sn–CH) = 75.9 Hz for CH_2SnCl_2Me and 60.0 Hz for $CH_2SnClMe_2$). Anal. Calcd $C_4H_{11}Sn_2Cl_3$: C, 11.92; H, 2.76. Found: C, 11.88; H, 2.78.

2,2-Bis(trimethylstannyl)propane (9). (Trimethylstannyl)sodium was prepared under nitrogen from sodium (15.2 g, 660 mmol) and trimethylchlorostannane (58.59 g, 294.2 mmol) in 100 mL of pentane and 250 mL of liquid ammonia in a 3-neck 1-L round-bottom flask, equipped with a mechanical stirrer and cold finger Dry Ice–acetone cooled condenser. The flask was fitted with a septum through which 2,2-dichloropropane (15.6 g, 139 mmol) was slowly added with stirring by syringe. After the ammonia was allowed to boil off, the product was extracted with 200 mL of pentane and 700 mL of water and the pentane layer washed once with water. The pentane was removed in a rotary evaporator, and the product was treated with a solution of 2 mL of 30% hydrogen peroxide in 100 mL of acetone and stirred for several minutes (to remove hexamethyldistannane). The product was immediately treated with 200 mL of pentane and washed twice with 500-mL portions of water. The pentane layer was dried over $MgSO_4$, filtered, and concentrated. The product was distilled at room temperature into a liquid-nitrogen-cooled trap at 0.01 torr. This afforded 46.4 g of material (90% yield (98+% purity)): ^{1}H NMR (CCl_4) δ 0.02 (s, 18, ^2J(^{119}Sn–CH) = 50.0 Hz, $SnMe_3$), 1.47 (s, 6, ^3J(^{119}Sn–CH) = 77.5 Hz, SnC(Me_2)Sn). Anal. Calcd for $C_9H_{24}Sn_2$: C, 29.23; H, 6.56. Found: C, 29.68; H, 6.32.

2,2-Bis(chlorodimethylstannyl)propane (10). 2,2-Bis(trimethylstannyl)propane (46.85 g, 126.7 mmol) was placed in a 200-mL round-bottom flash with dimethyldichlorostannane (56.5 g, 257 mmol). The flask was heated at 60 °C overnight at which time the contents were entirely liquid. The bulk of the byproduct trimethylchlorostannane was removed with stirring at 15–20 torr into an ice-cooled receiver by using a steam bath temperature. The remaining byproduct was removed by warming at 0.01 torr to 100 °C. ^{1}H NMR analysis of the product indicated 1% or less of the byproduct trimethylchlorostannane remained after the high vacuum treatment. This afforded the product (49.8 g, 120 mmol), a 95% yield on the controversion. Further purification was accomplished by recrystallization from CCl_4: mp 110–111 °C; ^{1}H NMR (Cl_2CH_2) δ 0.70 (s, 12, ^2J(^{119}Sn–CH) = 55.5 Hz, SnMeCl, 1.73 (s, 6, ^3J(^{119}Sn–CH) = 94.5 Hz, SnC(Me_2)Sn). Anal. Calcd for $C_7H_{18}Sn_2Cl_2$: C, 20.33; H, 5.12. Found: C, 20.23; H, 4.82.

2-(Chlorodimethylstannyl)-2-(dichloromethylstannyl)-propane (11). Into a 100-mL, round-bottom flask was placed 13.02 g (31.50 mmol) of 2,2-bis(dimethylchlorostannyl)propane along with 2 mL of methylene chloride and 4.0 g (15.4 mmol) of tetrachlorostannane. The solution was warmed and the solvent removed by rotary evaporation. The flask was warmed and the solvent removed by rotary evaporation. The flask was warmed to 60 °C overnight. Dimethyldichlorostannane was removed at 0.01 torr with stirring at 60 °C, leaving 13.0 g (30.0 mmol, 95%) of product of ca. 95% purity by ^{1}H NMR analysis. The product was recrystallized from petroleum ether to afford 10.3 g (24.0 mmol, 75%)d of product: mp 50–51 °C; ^{1}H NMR (Cl_2CH_2) δ 0.78 (s, 6, $^2J(^{119}Sn–CH)$ = 56.0 Hz, Sn(Cl)Me_2), 1.23 (s, 3, $^2J(^{119}Sn–CH)$ = 61.0 Hz, Sn(Cl_2)Me), 1.78 (s, 3, $^3J(^{119}Sn–CCH$ = 139.3 Hz for Me_2CSnCl_2*Me* and 83.2 Hz for Me_2CSnCl*Me*$_2$). Anal. Calcd for $C_6H_{15}Sn_2Cl_3$: C, 16.72; H, 3.56. Found: C, 16.74; H, 3.59.

Bis(dichloromethylstannyl)methane (5) and 2,2-Bis(dichloromethylstannyl)propane (12). Into a 100-mL round-bottom flask were placed 12–13 mmol of bis(dimethylchlorostannyl)methane or 2,2-bis(dimethylchlorostannyl)propane. An excess of tetrachlorostannane (5–7 g, 19–27 mmol) was added slowly after the addition of 5 mL of methylene chloride. The solution was agitated for 5 min and then concentrated by rotary evaporation. The product was heated at 60 °C overnight. The reaction was shown to be complete by the disappearance of methyltin peaks in the region: δ 0.5–0.8 (R-Sn(Me_2)Cl. The dimethyldichlorostannane, methyltrichlorostannane, and unreacted tetrachlorostannane were removed by slowly reducing the pressure to 0.01 torr and warming to 60 °C for 0.5 h. The residue was recrystallized from CCl_4 to afford 70% of product in each case.

2,2-Bis(dichloromethylstannyl)propane (11): mp 96–98 °C; ^{1}H NMR (Cl_2CH_2) δ 1.38 (s, 6, $^2J(^{119}Sn–CH)$ = 66.0 Hz, SnMe), 1.93 (2, 6, $^3J(^{119}Sn–CCH)$ = 128.0 Hz, $(Sn)_2CMe_2$). Anal. Calcd for $C_5H_{12}Sn_2Cl_4$: C, 13.30; H, 2.69. Found: C, 13.20; H, 2.64.

Bis(dichloromethylstannyl)methane (5): mp 62–64 °C; ^{1}H NMR (Cl_2OH_2) δ 1.44 (s, 6, $^2J(^{119}Sn–CH)$ = 78.0 Hz, $SnMeCl_2$), 1.93 (s, 2, $^2J(^{119}Sn–CH$ = 68.0 Hz, $SnCH_2Sn$). Anal. Calcd for $C_3H_8Sn_2Cl_4$: C, 8.51; H, 1.91. Found: C, 8.43; H, 2.06.

Bis(trivinylstannyl)methane (6). Into a 500-mL, 3-neck, round-bottom flask, equipped with a stirrer, a serum cap, and Dry ice cap, and Dry ice–acetone condenser was placed 25.5 g (108 mmol) of trivinylchlorostannane along with 100 mL of petroleum ether under an atmosphere of nitrogen. Ammonia (200 mL) was condensed into the flask with stirring. Sodium (5.2 g, 226 mmol) was added over a period of 3–5 min as stirring was continued. To the resulting pale yellow solution was added 4 mL (5.2 g, 61 mmol) of methylene chloride slowly by syringe.

The ammonia was allowed to boil off, and 100 mL of petroleum ether was added with stirring. The mixture was filtered and the solvent removed by rotary evaporation, and the product was pot-to-pot distilled into a liquid-nitrogen-cooled receiver at 0.01 torr, with warming with steam. The distillate was stirred for 10 min at 1 torr to remove traces of solvent and lower boiling impurities affording 15.3 g (38 mmol, 70% yield) of product of ca.d 95% purity by GC analysis. A portion of the product was GC purified for characterization: ^{1}H NMR (CCl_4) δ 0.05 (s, 2, $^2J(^{119}Sn–CH)$ = 61.0 Hz, $SnCH_2Sn$), 5.37–6.63 (m, 18, Sn*CH*=*CH*$_2$). Anal. Calcd for $C_{13}H_{20}Sn_2$: C, 37.74; H, 5.03. Found: C, 37.77; H, 5.03.

Bis(trichlorostannyl)methane (7). Into a 250-mL, round-bottom flask was placed 26.1 g (63.1 mmol) of bis(trivinylstannyl)methane along with 200 mL of methylene chloride. The solution was cooled to 0 °C and 25 mL (56.5 g, 217 mmol) of tetrachlorostannane was added cautiously. After 5 min the solvent was removed by rotary evaporation, and the solution was cooled to 0 °C, and 25 mL of $SnCl_4$ (56.5 g, 217 mmol) was added. It was warmed to 60 °C for 72 h, the flask cooled to room temperature, and the pressure slowly reduced to 0.01 torr and held at this pressure for 15 min with slight warming. The product was removed, treated with 2 g of activated charcoal in 50 mL of CCl_4 with stirring for 10 min, and filtered. Removal of the solvent by rotary evaporation afforded 27.7 g (95 mmol) of crude product. This was treated in 200 mL of warm petroleum ether which was decanted from a dark oil. The solvent was removed by rotary evaporation and the product distilled pot-to-pot at 0.01 torr by warming with steam, affording 25.2 g (87%) of product: mp 63–65 °C; ^{1}H NMR (CCl_4) δ 2.28 (s, 2, $^2J(^{119}Sn–CH)$ = 93.0 Hz, $Cl_3SnCH_2SnCl_3$). Anal. Calcd for $CH_2Sn_2Cl_6$: C, 2.59; H, 0.44. Found: C, 2.72; H, 0.99.

(Trichlorostannyl)(dichloromethylstannyl)methane (6). Into a 10-mL test tube were placed 3.92 g (8.4 mmol) of bis(trichlorostannyl)methane, 1.06 (5.34 mmol) of trimethylchlorostannane, and 5 mL of methylene chloride. The mixture was shaken and then allowed to stand 1 week. The solvent was removed by rotary evaporation and the product heated at 75 °C at 0.01 torr for 0.5 h. The residue was recrystallized from petroleum ether to afford 1.0 g (43%) of product: mp 68–70 °C; ^{1}H NMR (CH_2Cl_2) δ 1.44 (s, 3, $^2J(^{119}Sn–CH)$ = 78.0 Hz, SnMe), 2.08 (s, 2, $^2J(^{119}Sn–CH)$ = 105.5 Hz to CH_2SnCl_3 and 62.5 Hz to $CHSnCl_2Me$). Anal. Calcd for $C_2H_5Sn_2Cl_5$: C, 5.41; H, 1.14. Found: C, 4.91; H, 1.40.

^{1}H NMR Studies of Complexation between the Halotins and Dimethyl Sulfoxide. To 0.50 mL of a solution of the chlorostannane (0.20–0.30 M) in CH_2Cl_2 or acetone-d_6 were added increments of Me_2SO, and the spectra were scanned at the normal probe temperature after each addition. Plots of proton chemical shifts or $^2J(^{119}Sn–^1H)$ or both vs. Me_2SO concentration are shown in the figures.

Organohalostannane–Dimethyl Sulfoxide Complexes. In a typical procedure 0.367 g (0.96 mmol) of bis(dimethylchlorostannyl)methane, **2**, was dissolved in 3 mL of CCl_4 and 0.068 mL (1 mmol) of Me_2SO was added. An oil which separated solidified upon standing at 5 °C. The solvent was decanted, and 0.5 mL of warm CH_2Cl_2 was used to dissolve the oil. Cooling to room temperature followed by storage at −22 °C provided crystals, mp

Table IV. Final Positional Parameters for the Structural Studies of $Sn_2(CH_2)(CH_3)_2Cl_4(Me_2SO)_2$, $Sn_2(CH_2)(CH_3)_3Cl_3(Me_2SO)$, and $Sn_2(CH_2)Cl_6(Me_2SO)_4$

atom	*x*	*y*	*z*
	(a) $Sn_2(CH_2)(CH_3)_2Cl_4(Me_2SO)_2$		
Sn1	0.81308 (7)	0.59388 (6)	0.75000
Sn2	1.15277 (7)	0.65657 (6)	0.75000
Cl1	1.2974 (2)	0.6937 (2)	0.6319 (2)
Cl2	0.7209 (2)	0.4921 (1)	0.8693 (2)
S1	0.9187 (2)	0.7485 (1)	0.5545 (1)
O1	0.9554 (5)	0.7009 (4)	0.8579 (4)
C1	1.0112 (9)	0.5285 (8)	0.7500
C2	1.1787 (12)	0.8259 (10)	0.7500
C3	0.6755 (13)	0.7250 (12)	0.7500
C4	1.0511 (9)	0.8433 (7)	0.9688 (7)
C5	0.9651 (13)	0.6487 (8)	1.0229 (7)
	(b) $Sn_2(CH_2)(CH_3)_3(Me_2SO)$		
Sn1	0.08444 (9)	0.47585 (8)	0.29397 (7)
Sn2	0.29589 (10)	0.27512 (9)	0.08809 (7)
Cl1	0.2836 (5)	0.4160 (5)	−0.0903 (3)
Cl2	−0.0662 (5)	0.7816 (5)	0.3115 (3)
Cl3	0.3043 (5)	0.4266 (5)	0.4287 (3)
S1	0.4048 (5)	0.0092 (5)	0.3544 (3)
O1	0.2767 (9)	0.1558 (9)	0.2774 (6)
C1	0.2099 (16)	0.5154 (16)	0.1544 (10)
C2	0.5865 (17)	0.1411 (18)	0.1002 (13)
C3	0.1044 (18)	0.1262 (19)	0.0720 (13)
C4	−0.1218 (18)	0.3507 (18)	0.3484 (11)
C5	0.2594 (20)	−0.0467 (20)	0.4569 (11)
C6	0.4396 (19)	−0.1879 (17)	0.2974 (12)
	(c) $Sn_2(CH_2)Cl_6(Me_2SO)_4$		
Sn	0.41333 (3)	0.29665 (7)	0.69082 (3)
Cl1	0.4307 (1)	0.2167 (3)	0.5521 (1)
Cl2	0.3807 (1)	0.4247 (3)	0.8127 (1)
Cl3	0.3509 (1)	0.0361 (3)	0.7045 (1)
S1	0.4767 (1)	0.6078 (3)	0.5962 (1)
S2	0.2649 (1)	0.4283 (3)	0.6622 (2)
O1	0.4440 (3)	0.5433 (5)	0.6682 (3)
O2	0.3260 (3)	0.3901 (6)	0.6237 (3)
C1	0.4850 (5)	0.7921 (11)	0.8598 (5)
C2	0.4114 (5)	0.6997 (16)	0.5289 (5)
C3	0.2515 (8)	0.6430 (16)	0.6401 (10)
C4	0.2016 (7)	0.3511 (16)	0.5931 (9)
C5	0.5000	0.1852 (15)	0.7500

72-74 °C. Anal. Calcd for $C_7H_{20}Sn_2Cl_2SO$: C, 18.25; H, 4.39. Found: C, 18.05; H, 4.36.

This general procedure was followed for the other complexes listed below. The products were analytically pure after a single recrystallization, but some isolated yields were low due to the solubility of the complexes.

2,2-Bis(chlorodimethylstannyl)propane-dimethyl sulfoxide: from CH_2Cl_2; mp 116-117 °C. Anal. Calcd for $C_9H_{24}Sn_2Cl_2SO$: C, 22.12; H, 4.96. Found: C, 22.21; H, 4.96.

Bis(dichloromethylstannyl)methane-bis(dimethyl sulfoxide): from methanol; mp 150-153 °C. Anal. Calcd for $C_7H_{20}Sn_2Cl_4S_2O_2$: C, 14.51; H, 3.49. Found: C, 14.59; H, 3.57.

2,2-Bis(dichloromethylstannyl)propane-bis(dimethyl sulfoxide): from methanol; mp 149-154 °C. Anal. Calcd for $C_9H_{24}Sn_2Cl_4S_2O_2$: C, 17.79; H, 3.99. Found: C, 17.86, H, 4.11.

(Chlorodimethylstannyl)(dichloromethylstannyl)-methane-dimethyl sulfoxide: from CCl_4; mp 107-108 °C. Anal. Calcd for $C_6H_{17}Sn_2Cl_3SO$: C, 14.98; H, 3.57. Found: C, 14.76; H, 3.65.

2-(Chlorodimethylstannyl)-2-(dichloromethylstannyl)-propane-dimethyl sulfoxide: from CCl_4; 91% yield; mp 112-113 °C. Anal. Calcd for $C_8H_{21}Sn_2Cl_3SO$: C, 18.87; H, 4.17. Found: C, 19.11; H, 4.25.

(Trichlorostannyl)(dichloromethylstannyl)methane-tris(dimethyl sulfoxide): from Me_2SO/CH_2Cl_2, 49%; mp 171-173 °C. Anal. Calcd for $C_8H_{23}Sn_2S_3O_3Cl_5$: C, 14.70; H, 3.4. Found: C, 14.07; H, 3.26.

Bis(trichlorostannyl)methane-tetrakis(dimethyl sulfoxide): from CCl_4/Me_2SO, 4/1; CH_2Cl_2 washing, 42% yield; mp 169-173 °C. Anal. Calcd for $C_9H_{26}Sn_2S_4O_4Cl_6$: C, 14.01; H, 3.38. Found: C, 14.30; H, 3.47.

Crystallographic Data Collection and Structure Refinement and Solution. The details for the crystallographic study of the compounds are summarized in Table III and the supplementary material. Full details of the routine crystallographic procedures are described in ref 28.

Acknowledgment. We are grateful for support of this research by the National Science Foundation (Grants CHE 780075402 and CHE 8105020) and by the National Institutes of Health (partially by Grant GM 22566 and funding for the diffractometer from Grant GM 27459). Acknowledgement is also made to the donors of Petroleum Research Fund, administered by the American Chemical Society, for partial support.

Registry No. 1, 16812-43-4; 2, 83135-39-1; 2 dimethyl sulfoxide, 83135-49-3; 3, 83135-40-4; 4, 79992-67-9; 4 dimethyl sulfoxide, 79992-49-7; 5, 79992-66-8; 5 bis(dimethyl sulfoxide), 83198-38-3; 6, 83135-41-5; 6 tris(dimethyl sulfoxide), 83135-51-7; 7, 79992-68-0; 7 tetrakis(dimethyl sulfoxide), 83198-39-4; 8, 83135-42-6; 9, 83135-43-7; 10, 83135-44-8; 10 dimethyl sulfoxide, 83135-50-6; 11, 83135-45-9; 11 dimethyl sulfoxide, 83152-02-7; 12, 83135-46-0; 12 bis(dimethyl sulfoxide), 83152-01-6; 18, 83135-47-1; Me_3SnCl, 1066-45-1; CH_2Cl_2, 75-09-2; Me_3SnNa, 16643-09-7; Me_2SnCl_2, 753-73-1; KI, 7681-11-0; $SnCl_4$, 7646-78-8; 2,2-dichloropropane, 594-20-7; bis(iododimethylstannyl)methane, 83135-48-2; chlorotrivinylstannane, 10008-90-9.

Supplementary Material Available: Tables of anisotropic thermal parameters and calculated and observed structure factors for compounds 4-6 (30 pages). Ordering information is given on any current masthead page.

(28) Bruce, A.; Corbin, J. L.; Dahlstrom, P. L.; Hyde, J. R.; Minelli, M.; Stiefel, E. I.; Spence, J. T.; Zubieta, J. A. *Inorg. Chem.* **1982**, *21*, 917.

Pentacarbonyl[tris(phenylethynyl)phosphine]chromium(0), $Cr(CO)_5P(C{\equiv}CPh)_3$: Spectral, Structural, and MO Characteristics

Axel Hengefeld, Jürgen Kopf, and Dieter Rehder*

Institut für Anorganische Chemie der Universität Hamburg, D 2000-Hamburg 13, Federal Republic of Germany

Received June 17, 1982

The crystal and molecular structures of $Cr(CO)_5P(C{\equiv}CPh)_3$ have been determined (R_w = 0.057). The complex crystallizes in space group $P\bar{1}$ with a = 1095.8 (6) pm, b = 1656.2 (8) pm, c = 1689.4 (8) pm, α = 101.34 (4)°, β = 108.97 (4)°, and γ = 105.76 (5)°. The ligand strength (σ donor and π acceptor capability) of $P(C{\equiv}CPh)_3$ relative to that of PPh_3 and $P(OPh)_3$ is discussed on the basis of structural data, spectroscopic parameters (IR, ^{31}P NMR of $W(CO)_5P(C{\equiv}CPh)_3$), and SCCCMO calculations carried out on $C{\equiv}CH^-$ and $P(C{\equiv}CH)_3$. $P(C{\equiv}CPh)_3$ is considered a strong σ-interacting ligand (mainly via $P(3p_z)$) but only a moderate π acceptor for Cr → P(3d) delocalization. An approach is made to explain structural and spectral features through direct $\pi^*(CO) \rightarrow \pi^*(C{\equiv}C)$ interaction.

Introduction

There is continuing interest in correlations between structural data and spectral parameters in a series of similar complexes. In transition-metal carbonyl complexes, variations in ligand properties such as the π-acceptor and σ-donor power induce, inter alias, changes in the π^* occupation of the carbonyl set, which are reflected in the M-(CO) and C-O stretching modes of the vibrational spectra. On the other hand, the extent to which the originally degenerate metal d orbitals are split by varying interactions with ligands of differing integral strengths (and, correspondingly, the quality and quantity of electron population in the resulting molecular orbitals) is parallelled by changes in NMR parameters such as the nuclear shielding and the scalar interaction of the atoms participating in the metal-ligand bond. It is commonly accepted that excessive steric strains are closely related to unusual bond parameters as obtained from an X-ray structural analysis (this has recently again been shown by comparing the two complexes $W(CO)_5PMe_3$[1] and $W(CO)_5P(t\text{-}Bu)_3$[2]).

(1) Cotton, F. A.; Darensbourg, D. J.; Kolthammer, B. W. S. *Inorg. Chem.* **1981**, *20*, 4440.

(2) von Pickardt, J.; Rösch, L.; Schumann, H. Z. *Z. Anorg. Allg. Chem.* **1976**, *426*, 66.

0276-7333/83/2302-0114$01.50/0

72-74 °C. Anal. Calcd for $C_7H_{20}Sn_2Cl_2SO$: C, 18.25; H, 4.39. Found: C, 18.05; H, 4.36.

This general procedure was followed for the other complexes listed below. The products were analytically pure after a single recrystallization, but some isolated yields were low due to the solubility of the complexes.

2,2-Bis(chlorodimethylstannyl)propane-dimethyl sulfoxide: from CH_2Cl_2; mp 116-117 °C. Anal. Calcd for $C_9H_{24}Sn_2Cl_2SO$: C, 22.12; H, 4.96. Found: C, 22.21; H, 4.96.

Bis(dichloromethylstannyl)methane-bis(dimethyl sulfoxide): from methanol; mp 150-153 °C. Anal. Calcd for $C_7H_{20}Sn_2Cl_4S_2O_2$: C, 14.51; H, 3.49. Found: C, 14.59; H, 3.57.

2,2-Bis(dichloromethylstannyl)propane-bis(dimethyl sulfoxide): from methanol; mp 149-154 °C. Anal. Calcd for $C_9H_{24}Sn_2Cl_4S_2O_2$: C, 17.79; H, 3.99. Found: C, 17.86, H, 4.11.

(Chlorodimethylstannyl)(dichloromethylstannyl)-methane-dimethyl sulfoxide: from CCl_4; mp 107-108 °C. Anal. Calcd for $C_6H_{17}Sn_2Cl_3SO$: C, 14.98; H, 3.57. Found: C, 14.76; H, 3.65.

2-(Chlorodimethylstannyl)-2-(dichloromethylstannyl)-propane-dimethyl sulfoxide: from CCl_4; 91% yield; mp 112-113 °C. Anal. Calcd for $C_8H_{21}Sn_2Cl_3SO$: C, 18.87; H, 4.17. Found: C, 19.11; H, 4.25.

(Trichlorostannyl)(dichloromethylstannyl)methane-tris(dimethyl sulfoxide): from Me_2SO/CH_2Cl_2, 49%; mp 171-173 °C. Anal. Calcd for $C_8H_{23}Sn_2S_3O_3Cl_5$: C, 14.70; H, 3.4. Found: C, 14.07; H, 3.26.

Bis(trichlorostannyl)methane-tetrakis(dimethyl sulfoxide): from CCl_4/Me_2SO, 4/1; CH_2Cl_2 washing, 42% yield; mp 169-173 °C. Anal. Calcd for $C_9H_{26}Sn_2S_4O_4Cl_6$: C, 14.01; H, 3.38. Found: C, 14.30; H, 3.47.

Crystallographic Data Collection and Structure Refinement and Solution. The details for the crystallographic study of the compounds are summarized in Table III and the supplementary material. Full details of the routine crystallographic procedures are described in ref 28.

Acknowledgment. We are grateful for support of this research by the National Science Foundation (Grants CHE 780075402 and CHE 8105020) and by the National Institutes of Health (partially by Grant GM 22566 and funding for the diffractometer from Grant GM 27459). Acknowledgement is also made to the donors of Petroleum Research Fund, administered by the American Chemical Society, for partial support.

Registry No. 1, 16812-43-4; 2, 83135-39-1; 2 dimethyl sulfoxide, 83135-49-3; 3, 83135-40-4; 4, 79992-67-9; 4 dimethyl sulfoxide, 79992-49-7; 5, 79992-66-8; 5 bis(dimethyl sulfoxide), 83198-38-3; 6, 83135-41-5; 6 tris(dimethyl sulfoxide), 83135-51-7; 7, 79992-68-0; 7 tetrakis(dimethyl sulfoxide), 83198-39-4; 8, 83135-42-6; 9, 83135-43-7; 10, 83135-44-8; 10 dimethyl sulfoxide, 83135-50-6; 11, 83135-45-9; 11 dimethyl sulfoxide, 83152-02-7; 12, 83135-46-0; 12 bis(dimethyl sulfoxide), 83152-01-6; 18, 83135-47-1; Me_3SnCl, 1066-45-1; CH_2Cl_2, 75-09-2; Me_3SnNa, 16643-09-7; Me_2SnCl_2, 753-73-1; KI, 7681-11-0; $SnCl_4$, 7646-78-8; 2,2-dichloropropane, 594-20-7; bis(iododimethylstannyl)methane, 83135-48-2; chlorotrivinylstannane, 10008-90-9.

Supplementary Material Available: Tables of anisotropic thermal parameters and calculated and observed structure factors for compounds 4-6 (30 pages). Ordering information is given on any current masthead page.

(28) Bruce, A.; Corbin, J. L.; Dahlstrom, P. L.; Hyde, J. R.; Minelli, M.; Stiefel, E. I.; Spence, J. T.; Zubieta, J. A. *Inorg. Chem.* **1982**, *21*, 917.

Pentacarbonyl[tris(phenylethynyl)phosphine]chromium(0), $Cr(CO)_5P(C{\equiv}CPh)_3$: Spectral, Structural, and MO Characteristics

Axel Hengefeld, Jürgen Kopf, and Dieter Rehder*

Institut für Anorganische Chemie der Universität Hamburg, D 2000-Hamburg 13, Federal Republic of Germany

Received June 17, 1982

The crystal and molecular structures of $Cr(CO)_5P(C{\equiv}CPh)_3$ have been determined (R_w = 0.057). The complex crystallizes in space group $P\bar{1}$ with a = 1095.8 (6) pm, b = 1656.2 (8) pm, c = 1689.4 (8) pm, α = 101.34 (4)°, β = 108.97 (4)°, and γ = 105.76 (5)°. The ligand strength (σ donor and π acceptor capability) of $P(C{\equiv}CPh)_3$ relative to that of PPh_3 and $P(OPh)_3$ is discussed on the basis of structural data, spectroscopic parameters (IR, ^{31}P NMR of $W(CO)_5P(C{\equiv}CPh)_3$), and SCCCMO calculations carried out on $C{\equiv}CH^-$ and $P(C{\equiv}CH)_3$. $P(C{\equiv}CPh)_3$ is considered a strong σ-interacting ligand (mainly via $P(3p_z)$) but only a moderate π acceptor for Cr → P(3d) delocalization. An approach is made to explain structural and spectral features through direct $\pi^*(CO) \rightarrow \pi^*(C{\equiv}C)$ interaction.

Introduction

There is continuing interest in correlations between structural data and spectral parameters in a series of similar complexes. In transition-metal carbonyl complexes, variations in ligand properties such as the π-acceptor and σ-donor power induce, inter alias, changes in the π^* occupation of the carbonyl set, which are reflected in the M-(CO) and C-O stretching modes of the vibrational spectra. On the other hand, the extent to which the originally degenerate metal d orbitals are split by varying interactions with ligands of differing integral strengths (and, correspondingly, the quality and quantity of electron population in the resulting molecular orbitals) is parallelled by changes in NMR parameters such as the nuclear shielding and the scalar interaction of the atoms participating in the metal-ligand bond. It is commonly accepted that excessive steric strains are closely related to unusual bond parameters as obtained from an X-ray structural analysis (this has recently again been shown by comparing the two complexes $W(CO)_5PMe_3$[1] and $W(CO)_5P(t\text{-}Bu)_3$[2]).

(1) Cotton, F. A.; Darensbourg, D. J.; Kolthammer, B. W. S. *Inorg. Chem.* **1981**, *20*, 4440.

(2) von Pickardt, J.; Rösch, L.; Schumann, H. Z. *Z. Anorg. Allg. Chem.* **1976**, *426*, 66.

0276-7333/83/2302-0114$01.50/0

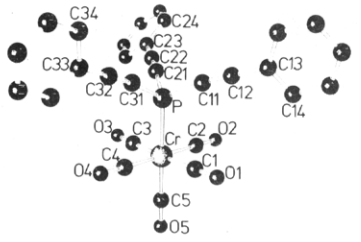

Figure 1. SCHAKAL drawing and numbering of atoms for one of the molecules in the asymmetric unit. For the second molecule, 50 is to be added.

Whether there is a corresponding relation arising from factors primarily electronic in nature has not yet been investigated satisfactorily.

In this paper, we describe the molecular structure and spectral properties of $Cr(CO)_5P(C{\equiv}CPh)_3$ and related compounds. The data are compared with those on $Cr(CO)_5PPh_3$ and $Cr(CO)_5P(OPh)_3$, reported 10 years ago by Grim and co-workers.[3] We will further focus on (i) MO theoretical predictions of the "strength" of the ligand triethynylphosphine and (ii) the implications of direct (intramolecular) ligand-to-ligand interaction.

Results

The Structure of $Cr(CO)_5P(C{\equiv}CPh)_3$. Fractional coordinates are given in Table I and selected data in Table II. Figure 1 is a SCHAKAL drawing of the molecule. There are two independent molecules in the asymmetric unit, numbered 1–33 and 51–83, respectively. The complex crystallizes in the triclinic space group $P\bar{1}$. Crystallographic parameters are as follows: a = 1095.8 (6) pm, b = 1656.2 (8) pm, c = 1689.4 (8) pm, α = 101.34 (4)°, β = 108.97 (4), γ = 105.76 (5)°; $C_{29}H_{15}CrO_5P$ (M = 526.41); V = 2650.3 × 10^6 pm^3, Z = 4; Q = 1.32 g cm^{-3} (calculated); μ = 4.78 cm^{-1}; λ = 70.926 pm.

Vibrational and NMR Data. In Table III, selected data for the complexes $Cr(CO)_5L$ (L = $P(C{\equiv}CPh)_3$, **1**; L = $P(OPh)_3$, **2**; L = PPh_3, **3**) are collected together with bond lengths and bond angles. For the metal-to-phosphorus coupling constants, the data of the corresponding tungsten complexes are listed. Comparison of the data reveals the following main features. (i) For L = $P(C{\equiv}CPh)_3$, the Cr–P distance, d(CrP), is shorter than for L = PPh_3; but it compares to that for L = $P(OPh)_3$, suggesting comparatively strong Cr–P interaction in **1** and **2**. (ii) The $d[Cr(CO)_{cis}]$ distances are slightly longer in **1** and **2** than in **3**, while the $d[Cr(CO)_{trans}]$ distances are approximately the same. (iii) Correspondingly, the $d(CO)_{cis}$ bond lengths are larger in **3** then in **1** and **2**; but there is no clear distinction between the $d(CO)_{trans}$ bond lengths of the three complexes. (iv) Throughout, the $d(CO)_{cis}$ distances are shorter than the $d(CO)_{trans}$ distances and $d[Cr(CO)_{cis}]$ distances are longer than $d[Cr(CO)_{trans}]$ distances, showing that all three phoshine ligands are weaker π-accepting ligands than CO.

(i) and (iii) are in accord with the assumption that PPh_3 is a comparatively weak π acceptor, while $P(OPh)_3$ and $P(C{\equiv}CPh)_3$ should be considered strong acceptors, giving rise to a decreased π^*(CO) population and a strengthening of the chromium-phosphorus bond in **1** and **2**. This effect

Table I. Fractional Coordinates for $Cr(CO)_5P(C{\equiv}CPh)_3$

atom	x/a	y/b	z/c
Cr1	0.2698 (1)	0.4322 (1)	0.0870 (1)
P1	0.3840 (1)	0.4950 (1)	0.2390 (1)
C1	0.3960 (6)	0.5292 (4)	0.0763 (4)
O1	0.4723 (5)	0.5855 (3)	0.0699 (3)
C2	0.3941 (6)	0.3719 (4)	0.0861 (4)
O2	0.4682 (5)	0.3365 (3)	0.0843 (3)
C3	0.1477 (5)	0.3338 (4)	0.1003 (4)
O3	0.0747 (4)	0.2770 (3)	0.1089 (3)
C4	0.1515 (5)	0.4955 (3)	0.0908 (3)
O4	0.0824 (4)	0.5343 (2)	0.0951 (2)
C5	0.1784 (6)	0.3841 (4)	−0.0346 (4)
O5	0.1227 (5)	0.3540 (3)	−0.1095 (3)
C11	0.5613 (5)	0.5129 (3)	0.2808 (3)
C12	0.6788 (5)	0.5230 (3)	0.2993 (3)
C13	0.8215 (5)	0.5337 (3)	0.3215 (3)
C14	0.8654 (6)	0.5175 (4)	0.2540 (4)
C15	1.0057 (7)	0.5267 (5)	0.2769 (5)
C16	1.0944 (6)	0.5497 (4)	0.3616 (5)
C17	1.0495 (5)	0.5648 (4)	0.4289 (4)
C18	0.9109 (5)	0.5664 (4)	0.4087 (4)
C21	0.3238 (5)	0.4380 (3)	0.3036 (3)
C22	0.2735 (5)	0.3917 (3)	0.3381 (3)
C23	0.2125 (6)	0.3327 (3)	0.3792 (4)
C24	0.2818 (6)	0.3444 (4)	0.4682 (4)
C25	0.2231 (8)	0.2845 (5)	0.5066 (4)
C26	0.0955 (9)	0.2170 (5)	0.4544 (6)
C27	0.0246 (8)	0.2055 (5)	0.3658 (6)
C28	0.0843 (7)	0.2652 (4)	0.3259 (4)
C31	0.3834 (5)	0.6002 (3)	0.2805 (3)
C32	0.3727 (5)	0.6694 (4)	0.2989 (3)
C33	0.3573 (7)	0.7547 (4)	0.3197 (4)
C34	0.4761 (7)	0.8278 (4)	0.3793 (4)
C35	0.4609 (11)	0.9116 (6)	0.3969 (6)
C36	0.3355 (14)	0.9158 (7)	0.3576 (7)
C37	0.2146 (11)	0.8435 (7)	0.2976 (6)
C38	0.2257 (8)	0.7579 (4)	0.2777 (4)
Cr51	0.5701 (1)	0.2231 (0)	0.3526 (0)
P51	0.5243 (1)	0.0983 (1)	0.2399 (1)
C51	0.4432 (6)	0.2469 (3)	0.2636 (3)
O51	0.3615 (4)	0.2577 (2)	0.2087 (3)
C52	0.4220 (6)	0.1618 (3)	0.3778 (3)
O52	0.3319 (4)	0.1271 (3)	0.3932 (3)
C53	0.6942 (6)	0.1922 (4)	0.4379 (4)
O53	0.7681 (5)	0.1720 (3)	0.4870 (3)
C54	0.7182 (6)	0.2872 (3)	0.3281 (3)
O54	0.8050 (4)	0.3256 (3)	0.3136 (3)
C55	0.5940 (5)	0.3267 (4)	0.4324 (3)
O55	0.6057 (4)	0.3916 (3)	0.4779 (3)
C61	0.3465 (5)	0.0364 (3)	0.1866 (3)
C62	0.2239 (6)	0.0104 (3)	0.1589 (3)
C63	0.0768 (5)	−0.0176 (3)	0.1269 (3)
C64	0.0188 (6)	0.0398 (5)	0.1510 (6)
C65	−0.1313 (9)	0.0130 (8)	0.1171 (7)
C66	−0.2120 (9)	−0.0682 (7)	0.0640 (7)
C67	−0.1511 (9)	−0.1208 (6)	0.0400 (7)
C68	−0.0045 (6)	−0.0974 (4)	0.0722 (6)
C71	0.5693 (5)	0.1238 (3)	0.1542 (3)
C72	0.6104 (5)	0.1536 (3)	0.1058 (3)
C73	0.6618 (5)	0.1942 (3)	0.0497 (3)
C74	0.7359 (5)	0.2851 (3)	0.0803 (3)
C75	0.7832 (5)	0.3251 (3)	0.0247 (4)
C76	0.7600 (6)	0.2752 (4)	−0.0595 (4)
C77	0.6867 (6)	0.1837 (4)	−0.0893 (4)
C78	0.6384 (6)	0.1428 (3)	−0.0337 (3)
C81	0.6008 (5)	0.0199 (3)	0.2597 (3)
C82	0.6636 (5)	−0.0267 (3)	0.2754 (3)
C83	0.7397 (6)	−0.0856 (4)	0.2927 (4)
C84	0.8750 (7)	−0.0506 (4)	0.3563 (4)
C85	0.9470 (7)	−0.1110 (5)	0.3702 (5)
C86	0.8807 (9)	−0.2006 (5)	0.3213 (5)
C87	0.7471 (9)	−0.2334 (4)	0.2603 (5)
C88	0.6716 (6)	0.1770 (4)	0.2433 (4)

(3) Plastas, H. J.; Stewart, J. M.; Grim, S. O.; *Inorg. Chem.* **1973**, *12*, 265.
(4) Mootz, D.; Sassmannhausen, G. *Z. Anorg. Allg. Chem.* **1967**, *335*, 200.
(5) Delbeke, F. T.; Claeys, E. G.; de Caluwe, R. M. van der Kelen, G. P. *J. Organomet. Chem.* **1970**, *23*, 505.
(6) Barnett, G. H.; Cooper, M. K. *Inorg. Chim. Acta* **1975**, *14*, 223.
(7) Magee, T. A.; Matthews, C. N.; Wang, T. S.; Wotiz, J. H. *J. Am. Chem. Soc.* **1961**, *83*, 3200.
(8) Cotton, F. A. *Inorg. Chem.* **1964**, *3*, 702.
(9) Young, F. R., III; Levenson, R. A.; Memering, M. N.; Dobson, G. R. *Inorg. Chim. Acta* **1974**, *8*, 61.

Table II. Selected Structural Data for $Cr(CO)_5P(C{\equiv}CPh)_3$

Bond Lengths (pm)

Cr1-P1	232.2 (1)	Cr51-P51	232.6 (1)	P1-C11	175.3 (6)	P51-C61	175.2 (2)
Cr1-C1	189.6 (7)	Cr51-C51	197.7 (6)	P1-C21	174.8 (6)	P51-C71	176.4 (6)
Cr1-C2	189.7 (7)	Cr51-C52	189.0 (6)	P1-C31	174.8 (6)	P51-C81	175.5 (6)
Cr1-C3	191.1 (6)	Cr51-C53	189.1 (6)	C11-C12	117.7 (8)	C61-C62	118.6 (8)
Cr1-C4	188.4 (6)	Cr51-C54	189.0 (6)	C21-C22	117.7 (8)	C71-C72	118.0 (8)
Cr1-C5	185.6 (6)	Cr51-C55	185.7 (6)	C31-C32	117.4 (8)	C81-C82	118.0 (9)
C1-O1	112.2 (9)	C51-O51	114.4 (7)	C12-C13	143.4 (8)	C62-C63	142.7 (8)
C2-O2	112.8 (9)	C52-O52	113.6 (8)	C22-C23	144.8 (9)	C72-C73	143.4 (8)
C3-O3	112.5 (8)	C53-O53	113.0 (8)	C32-C33	145.7 (9)	C82-C83	145.9 (9)
C4-O4	112.8 (7)	C54-O54	111.9 (8)				
C5-O5	114.3 (7)	C55-O55	114.0 (7)				

Bond Angles (Deg)

P1-Cr1-C5	178.8 (2)	P51-Cr51-C55	173.3 (2)	P1-C11-C12	172.6 (5)	P51-C61-C62	166.2 (5)
C1-Cr1-C2	88.0 (3)	C51-Cr51-C52	88.8 (3)	P1-C21-C22	172.2 (4)	P51-C71-C72	169.8 (4)
C1-Cr1-C3	178.1 (3)	C51-Cr51-C53	176.7 (2)	P1-C31-C32	172.4 (4)	P51-C81-C82	173.9 (4)
C1-Cr1-C4	90.6 (3)	C51-Cr51-C54	90.6 (3)	C11-C12-C13	179.0 (5)	C61-C62-C63	177.9 (6)
C2-Cr1-C3	90.4 (3)	C52-Cr51-C53	90.3 (3)	C21-C22-C23	178.3 (7)	C71-C72-C73	177.1 (5)
C2-Cr1-C4	178.0 (2)	C52-Cr51-C54	178.6 (3)	C31-C32-C33	178.7 (5)	C81-C82-C83	178.7 (5)
C3-Cr1-C4	91.0 (3)	C53-Cr51-C54	90.3 (3)	Cr1-C(1-5)-O(1-5)	178.7 (6)	Cr51-C(51-55)-O(51-55)	177.7 (5)
Cr1-P1-C11	114.7 (2)	Cr51-P51-C61	111.2 (2)				
Cr1-P1-C21	117.3 (1)	Cr51-P51-C71	113.1 (2)				
Cr1-P1-C31	115.0 (2)	Cr51-P51-C81	121.6 (2)				
C11-P1-C21	103.4 (3)	C61-P51-C71	103.5 (2)				
C11-P1-C31	102.1 (2)	C61-P51-C81	104.3 (2)				
C21-P1-C31	102.4 (3)	C71-P51-C81	101.1 (3)				

Best Planes (Deviations in pm)

(1)	Cr1(−17.4)-C1(2.0)-C2(6.6)-C3(2.1)-C4(6.7)
(1′)	Cr51(12.9)-C51(−40.0)-C52(33.6)-C53(−39.3)-C54(32.8)
(2a)	Cr1(−9.9)-P1(4.4)-C1(0.1)-C5(−5.5)
(2a′)	Cr51(−8.5)-P51(4.2)-C51(0.6)-C55(5.1)
(2b)	Cr1(−10.2)-P1(4.5)-C2(0.1)-C5(5.6)
(2b′)	Cr51(79.8)-P51(−35.1)-C52(−0.6)-C55(−44.0)
(3)	Cr1(−13.6)-P1(6.07)-C5(7.6)-C11(0.0)
(3′)	Cr51(67.6)-P51(−33.0)-C55(−37.2)-C61(2.6)
(4a)	C13(6.7)-C14(−4.4)-C15(−0.7)-C16(3.5)-C17(−1.3)-C18(−3.8)
(5)	C12(−4.1)-C13(12.7)-C14(−4.3)-C18(−4.3)
(5′)	C62(−3.4)-C63(10.6)-C64(−3.5)-C68(−3.7)

Angles between Normals to Planes

(1)/(4a)	(2a)/(4a)	(2b)/(4a)	(3)/(1)	(2b)/(2a)	(5)/(1)
76.6	55.6	39.9	91.4	88.0	76.6
(1)/(4b)	(2a)/(4b)	(2b)/(4b)	(3)/(2)	(2b)/(3)	(5)/(2a)
45.9	14.4	88.0	56.9	31.1	14.4
(1)/(4c)	(2a)/(4c)	(2b)/(4c)	(3)/(4a)	(2b)/(5)	(5)/(3)
82.9	79.3	134.0	8.9	88.0	57.9
			(3)/(5)		(6)/(4a)
			58.0		34.0

is more pronounced in the CO trans to the phosphine, where there is a more effective competition for the metal d_π orbitals than for the CO groups in the equatorial plane.[10,11] The high acceptor ability of $P(OPh)_3$ results from the large electronegativity of the OPh groups attached to P; the acceptor strength of $P(C{\equiv}CPh)_3$ might be explained either by π delocalization into π^* orbitals associated with the CC triple bond or by enhanced delocalization into the phenyl ring systems via the ethynyl groups.

While this interpretation of the structure parameters is consistent with the size of the CO stretching force constants k_2 and k_1 (Table III) in the case for **2** and **3**, there is an apparent discrepancy in the case for **1**: k_1 (which is assigned the axial CO group trans to L) is significantly smaller as one would expect if L were a strong π-accepting ligand. Furthermore, contrasting **2** and **3**, the E and $A_1{}^1$ modes are no longer degenerate accidentally.

This is *one* point we shall keep in mind for the discussion of the bonding situation encountered with $P(C{\equiv}CPh)_3$. Another striking feature is the almost identical metal-to-phosphorus coupling constant for **1** and **3**, which seems to place PPh_3 and $P(C{\equiv}CPh)_3$ into the same category of either weak σ donors or—synergetically—weak π acceptors, while the very effective interaction of the nuclear spins in **2** is indicative of $P(OPh)_3$ being a very good acceptor.[12]

Hence, $P(C{\equiv}CPh)_3$ may be considered either a strong π acceptor (as anticipated by structural data, the E mode in the IR spectrum, and k_2) comparable to $P(OPh)_3$ or a relatively weak π acceptor comparable to PPh_3 (as suggested by the overall IR results and the NMR spectroscopic coupling constant). Before this question is further elucidated, the ligand is viewed in the light of its electronic properties as obtained by molecular orbital calculations of the SCC, CNDO/2, and MINDO/3 type.

Molecular Orbital Calculations. For practical purposes (number of atoms to be considered), the calculations were carried out on $P(C{\equiv}CH)_3$ rather than on $P(C{\equiv}CPh)_3$ itself. Comparison of the bond lenghts and bond angles

(10) Graham, W. A. G. *Inorg. Chem.* **1968**, *7*, 315.
(11) Cotton, F. A.; Kraihanzel, C. S. *J. Am. Chem. Soc.* **1962**, *84*, 4432.
(12) Rehder, D.; Dorn, W. L.; Schmidt, J. *Transition Met. Chem. (Weinheim, Ger.)* **1976**, *1*, 233.

Table III. Selected Structural and Spectral Data for $Cr(CO)_5L$ Complexes and for $P(C{\equiv}CPh)_3$

	$Cr(CO)_5P(C{\equiv}CPh)_3$ (1)[a]		$Cr(CO)_5P(OPh)_3$ (2)	$Cr(CO)_5PPh_3$ (3)	$P(C{\equiv}CPh)_3$[b]
	Structural Data[c]				
Cr-P	232.2 (1)	232.6 (1)	230.9 (1)	242.2 (1)	
$Cr-(CO)_{cis}$	189.7	188.9	189.6	188.0	
$Cr-(CO)_{trans}$	185.6 (6)	185.7 (6)	186.1 (4)	184.5 (4)	
$(C{\equiv}O)_{cis}$	112.6	113.2	113.1	114.7	
$(C{\equiv}O)_{trans}$	114.3 (6)	114.0 (7)	113.6 (6)	115.4 (5)	
C≡C	117.6	118.2			119.7 (14)
∡Cr-P-E	115.7	115.3	117.8	115.6	
∡E-P-E	102.6	103.0	100.0	102.6	100.7 (5)
∡P-E-C	172.4	170.0	126.7		174.6 (11)
	Vibrational Data[d,e]				
ν(CO) A_1^2	2071		2080 m	2066 m	
ν(CO) B_1	1984[f]		2000 sh	1988 w	
ν(CO) E	1956		1960 vs	1944 s	
ν(CO) A_1^1	1925		1960	1944	
k_2	1600		1610	1585	
k_1	1504		1574	1554	
k_c, $k_{c'}$, k_t	33, 23, 56		27, 32, 59	25, 35, 60	
ν(C≡C)	2174.5				2169, 2137
ν(Cr-C)	473, 458, 404,[g] 395			543, 468,[g] 405,[g] 393[g]	
δ(Cr-C-O)	667, 662, 643,[g] 536[g]		651	670, 654, 616	
ν(Cr-P)	189[g]			186[g]	
ν(P-C)	857 vs, 850 sh				840, 832
	NMR Data				
$^1J(^{183}W-^{31}P)$[h]	262		411	280	

[a] Structure data for the two independent molecules. [b] Reference 4. [c] 2 and 3 from ref 3. Bond lengths in pm, bond angles in degrees; E = C (1 and 3) or O (2). [d] Force constants k in Nm^{-1} calculated according to ref 5; not corrected for anharmonicity (error arising from this simplification is ±5 Nm^{-1} [6]). [e] Data for 2 and 3 from ref 7-9. [f] Raman spectrum: 1991.7 cm^{-1}. [g] Raman data. [h] In Hz, for $W(CO)_5L$.

Table IV. Eigenvalues, Eigenvectors,[a,b] and Electron Populations[b] of $P(C{\equiv}CH)_3$

	eigenvector																	
	phosphorus									$(HC{\equiv}C^-)^1$			$(HC{\equiv}C^-)^2$			$(HC{\equiv}C^-)^3$		
eigenvalues, aJ	s	p_x	p_y	p_z	d_{xy}	d_{yz}	d_{xz}	$d_{x^2-y^2}$	d_{z^2}	σ	π_h*	π_v*	σ	π_h*	π_v*	σ	π_h*	π_v*
2e, −0.9962[c]	0	−17	−843	0	−215	−221	0	0	0	0	0	0	−317	0	0	310	0	0
2e, −0.9966[c]	0	845	−17	0	0	0	221	−215	0	−360	0	0	175	0	0	187	0	0
$2a_1$, −1.0240[d]	53	0	0	995	0	0	0	0	5	−36	0	14	−34	0	14	−34	0	14
1e, −1.0844	0	328	−412	0	173	180	−145	139	0	377	29	10	219	−33	6	−599	6	−14
1e, −1.0844	0	−410	−329	0	139	144	181	−174	0	−472	23	−13	564	14	15	−89	−35	−5
$1a_1$, −2.2167	860	0	0	1	0	0	0	0	0	120	0	0	120	0	0	120	0	0

	electron pop.										
	phosphorus										
	s	p_x	p_y	p_z	d_{xy}	d_{yz}	d_{xz}	$d_{x^2-y^2}$	$(HC{\equiv}C^-)^1$	$(HC{\equiv}C^-)^2$	$(HC{\equiv}C^-)^3$
2e			1.387		0.116	0.124				0.190	0.182
2e		1.393					0.122	0.115	0.245	0.058	0.066
$2a_1$	0.002			1.987					0.003	0.003	0.003
1e		0.228	0.361		0.082	0.092	0.060	0.053	0.290	0.098	0.729
1e		0.358	0.231		0.053	0.058	0.092	0.083	0.453	0.648	0.016
$1a_1$	1.689								0.104	0.104	0.104
e	1.691	0.586	0.592	1.987	0.135	0.150	0.152	0.136	0.850	0.851	0.852

[a] Eigenvectors ×10^3. [b] For numbering of the ethynyl ligands, see Figure 1. [c] LUMO. [d] HOMO. [e] Gross population for the complete molecule.

of the two phosphines[4,13] shows that the effect imparted by the phenyl group may be neglected in this context. The SCCCMO results (eigenvalues and eigenvectors) are listed in Table IV (for the overlap matrix see Experimental Section). Figure 2 illustrates the choice of the respective coordinate systems for phosphorus and the ethynyl groups, and Figure 3 is a graphical representation of the MO scheme. The calculations were carried out with a basis set comprised of the phosphorus valence orbitals 3s (a_1), $3p_z$

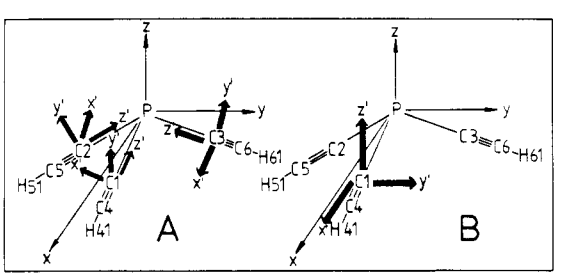

Figure 2. Coordinate systems for P (x, y, z) and the three $HC{\equiv}C^-$ (x', y', z'): A, SCCC; B, CNDO; MINDO.

(13) Krohn, J.; Hulscher, J. B.; Peerdeman, A. F. *J. Mol. Struct.* **1971**, 7, 217.

Table V. Selected CNDO/2 (A), MINDO/3 (B), and SCCC (C) Results

	eigenvalues		eigenvectors of the σ-donor orbital						
	π acceptor	σ donor	s	p_x	p_y	p_z	d_{z^2}	$d_{x^2-y^2}$	d_{xy}
A[a] I	+0.3579	−1.9129	−0.498	+0.295	+0.582	−0.656	−0.173		
II	+0.3518	−1.9403	−0.506				+0.066	+0.091	+0.107
B	+0.3558	−1.3583	−0.306			−0.629			
C	−0.9966	−1.0240	+0.053			+0.995	+0.005		

[a] Eigenvalues in aJ. I, idealized structure (C_{3v} symmetry); II, structure data from ref 13.

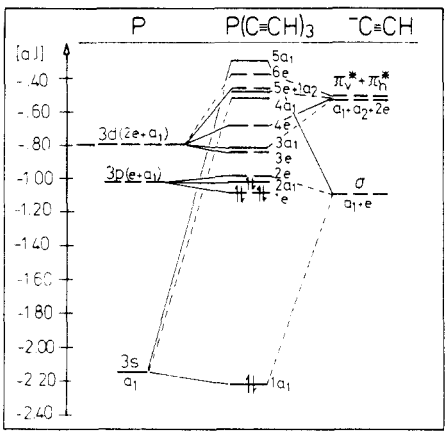

Figure 3. SCCC MO scheme of $P(C{\equiv}CH)_3$.

Table VI. CO Stretching Force Constants for $M(CO)_5P(C{\equiv}CR)_nPh_{3-n}$

complex	k_1	k_2	ref
$Cr(CO)_5P(C{\equiv}CPh)_3$	1504	1600	*b*
$Cr(CO)_5P(C{\equiv}CPh)_2Ph$	1503	1597	23
$Cr(CO)_5P(C{\equiv}CPh)Ph_2$	1501	1595	23
$Cr(CO)_5PPh_3$	1554	1585	11
$Cr(CO)_5P(C{\equiv}CCMe_3)_3$[a]	1508	1595	24
$Mo(CO)_5P(C{\equiv}CPh)_3$	1511	1607	23
$Mo(CO)_5PPh_3$	1552	1596	11
$Mo(CO)_5P(C{\equiv}CCMe_3)_3$[a]	1522	1606	24
$W(CO)_5P(C{\equiv}CPh)_3$	1498	1597	23
$W(CO)_5PPh_3$	1541	1587	11
$W(CO)_5P(C{\equiv}CCMe_3)_3$[a]	1505	1601	24

[a] Cotton-Kraihanzel approximation. [b] This work.

(a_1), $3p_{x,y}$ (e), $3d_{z^2}$ (a_1), $3d_{xy,x^2-y^2}$ (e), and $3d_{xz,yz}$ (e) and the molecular orbitals of $C{\equiv}CH^-$, $\sigma(a_1 + e)$, $\pi_h(a_2 + e)$, and $\pi_v(a_1 + e)$, obtained from seperate calculations on the acetylide anion (see Experimental Section).

Since the HOMO ($2a_1$, −1.0240 aJ) is close to that of the chromium 3d system (−0.963 aJ for Cr(0); −1.25 aJ for Cr(0.3+); calculated according to ref[14]), $P(C{\equiv}CH)_3$ is expected to be a good or even excellent σ donor. An analogous conclusion can be drawn for the LUMO (2e, −0.9966 aJ), which is a π*-type orbital. In these terms, $P(C{\equiv}CH)_3$ should be a better σ donor than CN^- (5σ = −1.2703 aJ) and a better π acceptor than CO (2π = −1.3807 aJ).[15] There are, however, two restrictions to this hypothesis. First, as Wensky pointed out,[16] the SCCC calculations (which are based on Cusach's approach) compress the orbital energies by a factor of 2/3 (i.e., the interacting σ and π orbitals of the ligand are less stable than anticipated by our calculations), and second, the choice of the p(3d) orbital energy for the calculation of the Coulomb integrals (−0.7945 aJ; interpolated between the 3d valence orbital ionization potentials of neutral Ti and V[14]) might be considered somewhat arbitrary. The π orbital of $P(C{\equiv}CH)_3$ is destabilized (the π-acceptor power diminished) if smaller (less negative) values for P(3d) are employed; the σ donor orbital is not effected to a great extent.

Consequently, while $P(C{\equiv}CPh)_3$ will remain a good σ donor despite of these restrictions, the energy calculated for the LUMO is a lower limit and the π acceptor ability may be less than predicted. In any case, the SCCC results are more suitable in discussing the σ/π characteristics of this ligand than the data obtained from CNDO/2 and MINDO/3 (compare Table V).

Discussion

Direct ligand-to-ligand donation between carbonyl groups and a phosphine, amine, or halogen ligand has been discussed previously to explain IR results and descrepancies between data obtained from IR, on one hand, and NMR and MO, on the other hand.[17-21]

In $Cr(CO)_5P(C{\equiv}CPh)_3$, the orbitals of the phosphine ligand which might participate in ligand–ligand interaction are (i) the 3d orbitals on phosphorus (or corresponding accepting π-type molecular orbitals of dominant P character) with components directed toward π*(CO) and (ii) π* orbitals associated with the ethynyl group. Interaction between P(3d) and π*(C≡C) may also occur.

Direct π*(CO) → π*(C≡C) donation will release the π*(CO) orbitals and thus strengthen the C≡O bond of the equatorial CO ligands. This may account for the high k_2 value. According to the X-ray structure of **1**, the ethynyl group is slightly bent (the average PCC angle is 171.2°) toward the equatorial plane $Cr-(CO)_1-(CO)_2-(CO)_3-(CO)_4$. Some of the electron density can then be transferred into P(3d) orbitals (with the restrictions mentioned below), weakening the acceptor ability of the phosphine and simultaneously the C≡O bond of the CO trans to it; hence a low k_1. The calculated (CNDO) P–C bond order is 1.13 and seems to support P(3d)– π*(C≡C) overlap. This effect should, however, not be overestimated: due to the nonlinearity of the P–C–C bond, the overlap will probably not occur to a great extent. It may also be counteracted by Cr → P(3d) → π*(C≡C) delocalization. A σ interaction is more likely to infer a sizable effect (vide infra).

There are two "symmetrical" possibilities for matching the threefold symmetry of PR_3 and the fourfold symmetry of the $Cr(CO)_5$ moiety. The actual geometry is quite close to A, leaving one of the equatorial CO groups, $(CO)_1$ and $(CO)_{51}$, respectively, in a position where the $(CO)_1-(C{\equiv}C)$ interaction is minimized. Differences in the corresponding bond lengths (113.3/188.6 pm for $Cr(CO)_{1,51}$ and 112.8/189.6 pm for $Cr(CO)_{2-4,52-54}$) are not clearly significant, though.

An increase of the π*(C≡C) population by direct electron transfer from suitable equatorial CO groups should

(14) Basch, H.; Viste, A.; Gray, H. B. *Theor. Chim. Acta* **1965**, *3*, 458.
(15) Schmidt, H.; Rehder, D. *Transition Met. Chem. (Weinhein, Ger.)* **1980**, *5*, 214.
(16) Wensky, D. A. *J. Chem. Phys.* **1974**, *60*, 1.
(17) Brown, R. A.; Dobson, G. R. *Inorg. Chim. Acta* **1972**, *6*, 65.
(18) Jolly, W. L., private communication.
(19) Fenske, R. F.; DeKock, R. . *Inorg. Chem.* **1972**, *11*, 437.
(20) Talay, R.; Rehder, D. *Chem. Ber.* **1978**, *111*, 1978.
(21) Bechthold, H.-Ch.; Kececi, A.; Rehder, D.; Schmidt, H.; Siewing, M. *Z. Naturforsch; B: Anorg. Chem., Org. Chem.* **1982**, *37B*, 631.

Table VII. SCCC MO Data on $C{\equiv}CH^-$

	overlap integrals[a]			
	$\sigma_s(C_b)$	$\sigma_{p_z}(C_b)$	$\pi(C_b)$	$\sigma(H)$
$\sigma_s(C_a)$	0.5440	0.5224		0.0802
$\sigma_{p_z}(C_a)$	−0.5224	−0.1673		0.0998
$\pi(C_a)$			0.4166	
$\sigma_s(C_b)$				0.4153
$\sigma_{p_z}(C_b)$				−0.4704

Energy Eigenvalues (aJ)[b]

2π	−0.5265 (LUMO)	1π	−1.0676 (HOMO)	5σ	−1.0927

	eigenvectors and electron pop.[b,c]						
	$s(C_a)$	$p_z(C_a)$	$\pi(C_a)$	$s(C_b)$	$p_z(C_b)$	$\pi(C_b)$	s(H)
2π	0	0	−0.9701	0	0	0.8756	0
1π	0	0	0.5186	0	0	0.6659	0
5σ	0.3506	0.6952	0	−0.3048	−0.1856	0	0.5193
I	0.0966	1.1586		0.1594	0.1349		0.4648
II	1.533	1.243	1.650	1.477	0.559	2.349	1.189
overlap pop.			−0.254[d]				

[a] The indices a and b correspond to the carbon atoms carrying the lone pair (C_a) and the hydrogen (C_b), respectively. [b] 2π, the π-accepting orbital (LUMO) is antibonding, 1π is the HOMO, and 5σ (which is slightly antibonding) is the σ-donating orbital. [c] Eigenvectors for 2π, 1π, and 5σ; populations are given for the two electrons in 5σ (I) and for all the ten electrons of the acetylide ligand (II). [d] Electron density in the bond C_a–C_b corresponding to 5σ; the respective value calculated from CNDO/2 is −0.088.

result in a decrease of $\nu(C{\equiv}C)$ relative to the free ligand. The contrary is true, however (the stretching modes are 2174.5 cm^{-1} for the complex and 2169 (A_1)/2137 (E) cm^{-1} for the uncordinated phosphine). This may partly result from a release of $\pi^*(C{\equiv}C)$ through $\pi^*(C{\equiv}C) \rightarrow P(3d)$ donation (see above), but a more substantial effect should arise from P–(C≡C) σ interaction: Since the donor orbital of the acetylide is slightly antibonding (5σ, see Experimental Section), σ delocalization into σ-accepting P(3d) orbitals will strengthen the C–C bond. This enhanced σ donation may be induced synergetically by direct (C-O)–(C≡C) π interaction. The net effect is a comparatively high electron density on phosphorus and a strong metal–phosphorus σ bond.

Finally, we shall briefly comment on the ^{183}W–^{31}P coupling. The magnitude of scalar coupling constants is dominated by the Fermi contact term;[22] it is proportional to (i) the σ(s) density in the bond between the coupling nuclei and (ii) the valences electron densities $|S(0)|_{ns}^2$ at the respective nuclei. σ(s), according to our SCCC calculations, is small (it is mostly the $P(3p_z)$ orbital that contributes to the donor MO; the coefficients are 0.995 for $\sigma(p_z)$ and 0.053 for σ(s)), and the $|S(0)|^2$ values decrease for a weak π acceptor relative to a strong one.[12] Hence, the coupling of W to $P(C{\equiv}CPh)_3$ is only about 0.6 of that to $P(OPh)_3$.

Conclusion

Although there is strong mutual interaction along the preferential axis of the molecule ($(CO)_5$–Cr–$P(C{\equiv}CPh)_3$), which leads to a short Cr–P bond of mainly σ character, $P(C{\equiv}CPh)_3$ seemingly is not a very good π acceptor for direct metal–phosphorus π interaction. The overall electronic situation is, however, stabilized by (CO) → (C≡C) π^* interaction. This situation is maintained as long as at least one ethynyl group is attached to phosphorus, and it is independent of the group R in $P(C{\equiv}CR)_{3-n}Ph_n$ complexes. This is demonstrated by the CO force constants k_1 and k_2 for the various complexes contained in Table VI.

Experimental Section

Preparation of Complexes. $Cr(CO)_5P(C{\equiv}CPh)_3$ (1). A 1.98-g (9.0-mmol) sample of $Cr(CO)_6$ and 3.01 g of (9.6 mmol) $P(C{\equiv}CPh)_3$ (prepared as described in ref 25), dissolved in 170 mL of THF, were irradiated for 24 h (high-pressure mercury lamp Hanau TQ 81 fitted in a cooled quartz immersion well). After this time, the main product was 1, but the di- and trisubstituted products and unreacted hexacarbonyl were also present. The yellow-orange solution was stirred at room temperature for 3 h (upon which it became lighter), and the solvent was evaporated in vacuo. For removal of the main portion of unreacted $Cr(CO)_6$, the yellow-brown oil thus obtained was subjected to sublimation (323 K (0.01 torr)). The sticky residue was then chromatographed on silica gel (column dimensions 2.5 × 40 cm), starting with ethyl acetate–*n*-hexane, 1/9. The eluant was gradually enriched with ethyl acetate during this procedure. The second, yellow fraction was drawn off, concentrated to 5 mL, chromatographed a second time, filtered through a short column filled with acidic alumina (ca. 3 cm), and evaporated to dryness. The product was recrystallized from *n*-hexane and dried under high vacuum (4 h at room temperature and exclusion of light) to yield 0.86 g (18%) of yellow, crystalline 1. The complex is soluble in polar solvents and slightly soluble in nonpolar solvents. It is stable toward air and moisture, F_p = 368 K. Anal. Calcd for $C_{29}H_{15}CrO_5P$ (M_r = 526.4): C, 66.17; H, 2.87; Cr, 9.88; P, 5.88. Found: C, 66.52; H, 2,88; Cr, 9.82; P, 6.10.

$W(CO)_5P(C{\equiv}CPh)_3$ was prepared accordingly by irradiation (THF, 6 h) of 4.70 g of $W(CO)_6$ (13.4 mmol) and 6.23 g of $P(C{\equiv}CPh)_3$ (18.6 mmol) to yield 2.00 g (23%) of a yellow-brown complex, F_p = 374 K (with decomposition). Anal. Calcd for $C_{29}H_{15}O_5PW$ (M_r = 658.3): C, 52.92; H, 2.30; P, 4.71; W, 27.93. Found: C, 53.68; H, 2.34; P, 4.50; W, 27.20.

Crystal Structure Determination. Single crystals of 1 were grown by allowing a saturated hexane solution to stand at 273 K for 1 week. The structure determination was carried out on a Hilger & Watts (Y 290) diffractometer (graphite monochromator, Mo K_α; $\theta/2\theta$ scan method, $2\theta_{max}$ = 44° (scattering at higher values of 2θ was inefficient)). A total of 6953 significant ($F_o < 3\sigma(F_o)$) reflections were collected; the calculations were carried out with the program systems SHELX 76[26] and MULTAN 78.[27] The final

(22) Webb, G. A. In "NMR and the Periodic Table"; Harris, R. K., Mann, B. E., Eds.; Academic Press: London, 1978.
(23) Hengefeld, A. Ph.D. Thesis, Hamburg 1980.
(24) George, A. D.; George, T. A.; Wiebers, D. O. *J. Coord. Chem.* **1974**, *4*, 27.
(25) Carty, A. J.; Hota, N. K.; Ng, T. W.; Patel, H. A.; O'Connor, T. J. *Can. J. Chem.* **1971**, *49*, 2706.
(26) Sheldrick, G. M. SHELX 76, Program for Crystal Structure Determination, University of Cambridge, England, 1976.

Table VIII. Overlap Matrix for $P(C{\equiv}CH)_2$

$(HC{\equiv}C^-)^1$					$(HC{\equiv}C^-)^2$					$(HC{\equiv}C^-)^3$					
σ	π_h	π_v	π_h^*	π_v^*	σ	π_h	π_v	π_h^*	π_v^*	σ	π_h	π_v	π_h^*	π_v^*	
															phosphorus
0	−0.1548	0	−0.1860	0	0.0867	0.0774	0.0608	0.0930	0.0732	−0.0867	0.0774	−0.0608	0.0930	−0.0732	d_{xy}
0	0.0788	0	0.0948	0	0.0844	−0.0934	−0.0883	−0.0474	−0.1063	−0.0884	−0.0394	−0.0883	−0.0474	0.1063	d_{yz}
−0.1020	0	0.1020	0	0.1226	0.0510	−0.0683	−0.0510	0.0820	−0.0613	0.0510	−0.0683	−0.0510	−0.0820	−0.0613	d_{xz}
0.1000	0	0.0702	0	0.0844	−0.0500	0.1340	−0.0351	0.1610	−0.0422	−0.0500	−0.1340	−0.0351	−0.1610	−0.0422	$d_{x^2-y^2}$
−0.0278	0	−0.1217	0	−0.1463	−0.0278	0	−0.1217	0	−0.1463	−0.0278	0	−0.1217	0	−0.1463	d_{z^2}
0.3359	0	0	0	0	0.3359	0	0	0	0	0.3359	0	0	0	0	s
0.0360	0	0.0038	0	0.0064	−0.0180	−0.0073	−0.0019	−0.0121	−0.0032	−0.0180	0.0073	−0.0019	0.0121	0.0032	p_x
0	−0.0084	0	−0.0140	0	−0.0314	0.0042	−0.0033	0.0070	−0.0055	0.0314	0.0042	0.0033	0.0070	0.0055	p_y
−0.0184	0	0.0075	0	0.0125	−0.0184	0	0.0075	0	0.0125	−0.0184	0	0.0075	0	0.0125	p_z
															$(HC{\equiv}C^-)^1$
1	0	0	0	0	0.0947	−0.0258	−0.0203	−0.0354	−0.0281	0.0947	0.0258	−0.0203	0.0354	−0.0281	σ
	1	0	0	0	0.0258	−0.0345	0.0115	0.0383	−0.0108	−0.0258	−0.0345	−0.0115	0.0383	0.0108	π_h
		1	0	0	−0.0203	−0.0115	0.0288	0.0108	−0.0331	−0.0203	0.0115	0.0288	−0.0108	−0.0331	π_v
			1	0	0.0354	0.0383	−0.0108	−0.0455	−0.0111	−0.0354	0.0383	0.0108	−0.0455	0.0111	π_h^*
				1	−0.0281	0.0108	−0.0331	0.0111	0.0402	−0.0281	−0.0108	−0.0331	−0.0111	0.0402	π_v^*
															$(HC{\equiv}C^-)^2$
					1	0	0	0	0	0.0947	−0.0258	−0.0203	−0.0354	−0.0281	σ
						1	0	0	0	0.0258	−0.0345	0.0115	0.0383	−0.0108	π_h
							1	0	0	−0.0203	−0.0115	0.0288	0.0108	−0.0331	π_v
								1	0	0.0354	0.0383	−0.0108	−0.0455	−0.0111	π_h^*
									1	−0.0281	0.0108	−0.0331	0.0111	0.0402	π_v^*
															$(HC{\equiv}C^-)^3$
										1	0	0	0	0	σ
											1	0	0	0	π_h
												1	0	0	π_v
													1	0	π_h^*
														1	π_v^*

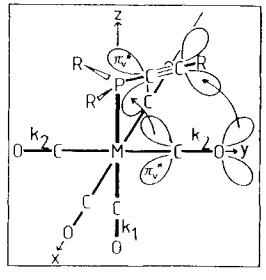

Figure 4. Interaction between the π^* orbitals of the carbonyl and the ethynyl ligand.

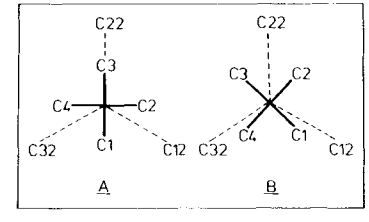

Figure 5. The "symmetrical" arrangements of the two sets $(CO)_{1-4}$ and $C_{11-31}{\equiv}C_{12-32}Ph$.

R value was 0.063 (weighted ≡ 0.057). The final ΔF map contained no peaks higher than 0.5 e/Å^3. For the drawing (Figure 1), the SCHAKAL program[28] was employed.

MO Calculations. The following program systems were employed: ACIWERTE[29] and ACMORS;[30] CNDO/2 and QCPE No. 91; MINDO/3 and QCPE No. 279.

Parameters for overlap calculations: bond distances, d(C≡C) = 117, d(C–H) = 90, d(C–P) = 175 pm; bond angles in P(C≡CH)$_3$, idealized C_{3v} symmetry, 101° (adapted from ref 13); atomic orbital coefficients for valence orbitals, H(s), C(s), C(p), P(s), and P(p) Clementi's double-ζ's[31] and P(d) Richardson's 3d coefficients for V(0).[32] The overlap matrices for C≡CH$^-$ and P(C≡CH)$_3$ are given in Tables VII and VIII. To calculate the overlap integrals for P(C≡CH)$_3$, collective C≡CH$^-$ orbitals were used: σ[H(s), C_a(s), C_b(s), $C_a(p_z)$, $(C_b(p_z)]$; π_v*[$C_a(p_y)$, $C_b(p_y)$]; π_h*[$C_a(p_x)$, $C_b(p_x)$] (the indices a and b refer to the carbon carrying the negative charge, C_a, and the hydrogen, C_b). Bonding π(C≡CH$^-$) orbitals were excluded on the grounds of negligible interaction with P orbitals.

For the SCCC calculations on C≡CH$^-$, valence orbital ionization potentials (VOIPs) of Basch, Viste, and Gray[14] for two limiting configurations ($2s^2p^2$ and $2sp^3$ in the case of C) and the electron distributions were fed into the program. The program first caculates Coulomb integrals and exchange integrals (on the basis of Cusachs' approach[33]) and then eigenvectors and eigenvalues, and finally a Mulliken population analysis is undertaken. This procedure is maintained until self-consistency is achieved. For the results, see Table VII. In the case of P(C≡CH)$_3$, the following starting parameters were employed: P(3s) and P(3p), VOIPs by Basch, Viste, and Gray; P(3d), –0.7945 aJ (–40 × 10^3 cm^{-1}; this is the mean value of the VOIPs for the 3d orbitals of Ti(0) and V(0)); C≡CH$^-$, –1.0927 (σ) and –0.5265 aJ (π) (cf. Table VII).

Spectra. Instruments: IR, Perkin-Elmer 325 and 225 spectrophotometers in cyclohexane (ν(CO) region) and CsI; FIR, Digilab FTS 14 spectrophotometer in polyethylene; Raman, Cary 82 (Varian) spectrophotometer, fitted with Kr or Ar laser (Spectra Physics), neat samples. For a complete set of all of the IR and Raman data of P(C≡CPh)$_3$ and the complexes see ref 23. ^{31}P NMR of W(CO)$_5$P(C≡CPh)$_3$: bruker WH 90 spectrometer in 7.5-mm vials at 306 K relative to 80% H_3PO_4, ca. 0.02 M THF solution; δ(^{31}P) –41.2 (central line and ^{183}W satellite doublet, intensity ratio 7.1/1).

Registry No. 1, 83136-71-4; W(CO)$_5$P(C≡CPh)$_3$, 83152-07-2.

Supplementary Material Available: Tables of thermal parameters, best planes, and structure factor amplitudes for Cr(CO)$_5$P(C≡CPh)$_3$ (75 pages). Ordering information is given on any current masthead page.

(27) Main, P.; Hull, S. E.; Lessinger, L.; Germain, G.; Declerq, J. P.; Woolfson, M. M. MULTAN 78, A System of Computer Programs for the Automatic Solution of Crystal Structures from X-ray Diffraction Data, University of York, England, 1978.
(28) Keller, E. SCHAKAL, University of Freiburg, 1980.
(29) Schmidt, J. ACIWERTE, University of Hamburg, 1973.
(30) Dorn, W. L. ACMORS, University of Hamburg, 1973.
(31) Clementi, E. IBM Research Paper RJ-256, 1963.
(32) Richardson, J. W.; Nieuwpoort, W. C.; Powell, R. R; Edgell, W. F. *J. Chem. Phys.* **1962**, *36*, 1057.
(33) Cusachs, L. C. *J. Chem. Phys.* **1965**, *43*, S157 L.C. Cusachs, L. C.; Cusachs, B. B. *Ibid.* **1967**, *71*, 1060.

Oxidative Demethylation of Methylcobalamin by Hexachloroiridate(IV)

Yueh-Tai Fanchiang*

Gray Freshwater Biological Institute, College of Biological Sciences, University of Minnesota, Navarre, Minnesota 55392

Received May 17, 1982

The stoichiometries and kinetics of the demethylation of CH_3-B_{12} by $IrCl_6^{2-}$ in aqueous solution have been examined. In the presence of excess $IrCl_6^{2-}$, this reaction occurs with a 2:1 ($IrCl_6^{2-}$:CH_3-B_{12}) stoichiometry, producing H_2O-B_{12}^+, CH_3Cl, and $IrCl_6^{3-}$/$IrCl_5(H_2O)^{2-}$. With deficient $IrCl_6^{2-}$, the reaction occurs with a ~1.3:1 ($IrCl_6^{2-}$:CH_3-B_{12}) stoichiometry, producing H_2O-B_{12}^+, $IrCl_6^{3-}$, and C_2H_6 (the major demethylation product). The demethylation follows a second-order rate expression: first order in CH_3-B_{12} and first order in $IrCl_6^{2-}$. This second-order rate constant is pH dependent in acidic solution, which is interpreted in terms of protonation of the 5,6-dimethylbenzimidazole moiety and its resulting base-on to base-off conversion. $IrCl_6^{3-}$ inhibits the demethylation, while Cl^- pronouncedly enhances the rate. The mechanism is described as a one-electron transfer from CH_3-B_{12} to $IrCl_6^{2-}$ (rate-determining step), yielding a transient CH_3-B_{12}^+ intermediate. This intermediate rapidly releases a methyl radical which either abstracts a chlorine atom from a second $IrCl_6^{2-}$ molecule to produce CH_3Cl or combines to yield C_2H_6.

Introduction

The cleavage of the Co–C bonds in organocobalt compounds is a subject of considerable interest in B_{12}-dependent biological reactions,[1] as well as in various homogeneous catalytic processes.[2] Several modes of reagent-induced cleavage of the Co–C bond of methylcobalamin (CH_3-B_{12}) have already been described.[3] The reactions between CH_3-B_{12} and the electrophile are generally characterized as a direct displacement of the Co atom. However, some recent experiments on the methyl transfer from CH_3-B_{12} to platinum,[4] gold,[5] and tetracyanoethylene[6] in-

*To whom correspondence should be addressed at the Department of Biochemistry, Medical School, University of Minnesota, Minneapolis, Minnesota 55455.

(1) (a) Hogenkamp, H, P. C. *Annu. Rev. Biochem.* **1968**, *37*, 225. (b) Abeles, R. H. *Adv. Chem. Ser.* **1900**, *No. 100*, 346. (c) Barker, H. A., *Annu. Rev. Biochem.* **1972**, *41*, 55.
(2) Halpern, J. *Adv. Chem. Ser.* **1968**, *No. 70*, 1.
(3) Wood, J. M.; Fanchiang, Y.-T. "Vitamin B_{12}"; Zagalak, B., Friedrich, W., Eds.; Walter de Gruyer and Co.: Berlin, 1979; p 539.
(4) (a) Taylor, R. T.; Hanna, M. L. *Bioinorg. Chem.* **1976**, *6*, 281. (b) Fanchiang, Y.-T.; Ridley, W. P.; Wood, J. M. *J. Am. Chem. Soc.* **1979**, *101*, 1442. (c) Fanchiang, Y.-T.; Pignatello, J. J.; Wood, J. M., to be submitted for publication.

0276-7333/83/2302-0121$01.50/0

R value was 0.063 (weighted ≡ 0.057). The final ΔF map contained no peaks higher than 0.5 e/Å^3. For the drawing (Figure 1), the SCHAKAL program[28] was employed.

MO Calculations. The following program systems were employed: ACIWERTE[29] and ACMORS;[30] CNDO/2 and QCPE No. 91; MINDO/3 and QCPE No. 279.

Parameters for overlap calculations: bond distances, d(C≡C) = 117, d(C–H) = 90, d(C–P) = 175 pm; bond angles in P(C≡CH)$_3$, idealized C_{3v} symmetry, 101° (adapted from ref 13); atomic orbital coefficients for valence orbitals, H(s), C(s), C(p), P(s), and P(p) Clementi's double-ζ's[31] and P(d) Richardson's 3d coefficients for V(0).[32] The overlap matrices for C≡CH$^-$ and P(C≡CH)$_3$ are given in Tables VII and VIII. To calculate the overlap integrals for P(C≡CH)$_3$, collective C≡CH$^-$ orbitals were used: σ[H(s), C_a(s), C_b(s), $C_a(p_z)$, $(C_b(p_z)]$; π_v*[$C_a(p_y)$, $C_b(p_y)$]; π_h*[$C_a(p_x)$, $C_b(p_x)$] (the indices a and b refer to the carbon carrying the negative charge, C_a, and the hydrogen, C_b). Bonding π(C≡CH$^-$) orbitals were excluded on the grounds of negligible interaction with P orbitals.

For the SCCC calculations on C≡CH$^-$, valence orbital ionization potentials (VOIPs) of Basch, Viste, and Gray[14] for two limiting configurations ($2s^2p^2$ and $2sp^3$ in the case of C) and the electron distributions were fed into the program. The program first caculates Coulomb integrals and exchange integrals (on the basis of Cusachs' approach[33]) and then eigenvectors and eigenvalues, and finally a Mulliken population analysis is undertaken. This procedure is maintained until self-consistency is achieved. For the results, see Table VII. In the case of P(C≡CH)$_3$, the following starting parameters were employed: P(3s) and P(3p), VOIPs by Basch, Viste, and Gray; P(3d), –0.7945 aJ (–40 × 10^3 cm^{-1}; this is the mean value of the VOIPs for the 3d orbitals of Ti(0) and V(0)); C≡CH$^-$, –1.0927 (σ) and –0.5265 aJ (π) (cf. Table VII).

Spectra. Instruments: IR, Perkin-Elmer 325 and 225 spectrophotometers in cyclohexane (ν(CO) region) and CsI; FIR, Digilab FTS 14 spectrophotometer in polyethylene; Raman, Cary 82 (Varian) spectrophotometer, fitted with Kr or Ar laser (Spectra Physics), neat samples. For a complete set of all of the IR and Raman data of P(C≡CPh)$_3$ and the complexes see ref 23. ^{31}P NMR of W(CO)$_5$P(C≡CPh)$_3$: bruker WH 90 spectrometer in 7.5-mm vials at 306 K relative to 80% H_3PO_4, ca. 0.02 M THF solution; δ(^{31}P) –41.2 (central line and ^{183}W satellite doublet, intensity ratio 7.1/1).

Registry No. 1, 83136-71-4; W(CO)$_5$P(C≡CPh)$_3$, 83152-07-2.

Supplementary Material Available: Tables of thermal parameters, best planes, and structure factor amplitudes for Cr(CO)$_5$P(C≡CPh)$_3$ (75 pages). Ordering information is given on any current masthead page.

(27) Main, P.; Hull, S. E.; Lessinger, L.; Germain, G.; Declerq, J. P.; Woolfson, M. M. MULTAN 78, A System of Computer Programs for the Automatic Solution of Crystal Structures from X-ray Diffraction Data, University of York, England, 1978.
(28) Keller, E. SCHAKAL, University of Freiburg, 1980.
(29) Schmidt, J. ACIWERTE, University of Hamburg, 1973.
(30) Dorn, W. L. ACMORS, University of Hamburg, 1973.
(31) Clementi, E. IBM Research Paper RJ-256, 1963.
(32) Richardson, J. W.; Nieuwpoort, W. C.; Powell, R. R; Edgell, W. F. *J. Chem. Phys.* **1962**, *36*, 1057.
(33) Cusachs, L. C. *J. Chem. Phys.* **1965**, *43*, S157 L.C. Cusachs, L. C.; Cusachs, B. B. *Ibid.* **1967**, *71*, 1060.

Oxidative Demethylation of Methylcobalamin by Hexachloroiridate(IV)

Yueh-Tai Fanchiang*

Gray Freshwater Biological Institute, College of Biological Sciences, University of Minnesota, Navarre, Minnesota 55392

Received May 17, 1982

The stoichiometries and kinetics of the demethylation of CH_3-B_{12} by $IrCl_6^{2-}$ in aqueous solution have been examined. In the presence of excess $IrCl_6^{2-}$, this reaction occurs with a 2:1 ($IrCl_6^{2-}$:CH_3-B_{12}) stoichiometry, producing H_2O-B_{12}^+, CH_3Cl, and $IrCl_6^{3-}$/$IrCl_5(H_2O)^{2-}$. With deficient $IrCl_6^{2-}$, the reaction occurs with a ~1.3:1 ($IrCl_6^{2-}$:CH_3-B_{12}) stoichiometry, producing H_2O-B_{12}^+, $IrCl_6^{3-}$, and C_2H_6 (the major demethylation product). The demethylation follows a second-order rate expression: first order in CH_3-B_{12} and first order in $IrCl_6^{2-}$. This second-order rate constant is pH dependent in acidic solution, which is interpreted in terms of protonation of the 5,6-dimethylbenzimidazole moiety and its resulting base-on to base-off conversion. $IrCl_6^{3-}$ inhibits the demethylation, while Cl^- pronouncedly enhances the rate. The mechanism is described as a one-electron transfer from CH_3-B_{12} to $IrCl_6^{2-}$ (rate-determining step), yielding a transient CH_3-B_{12}^+ intermediate. This intermediate rapidly releases a methyl radical which either abstracts a chlorine atom from a second $IrCl_6^{2-}$ molecule to produce CH_3Cl or combines to yield C_2H_6.

Introduction

The cleavage of the Co–C bonds in organocobalt compounds is a subject of considerable interest in B_{12}-dependent biological reactions,[1] as well as in various homogeneous catalytic processes.[2] Several modes of reagent-induced cleavage of the Co–C bond of methylcobalamin (CH_3-B_{12}) have already been described.[3] The reactions between CH_3-B_{12} and the electrophile are generally characterized as a direct displacement of the Co atom. However, some recent experiments on the methyl transfer from CH_3-B_{12} to platinum,[4] gold,[5] and tetracyanoethylene[6] in-

*To whom correspondence should be addressed at the Department of Biochemistry, Medical School, University of Minnesota, Minneapolis, Minnesota 55455.

(1) (a) Hogenkamp, H, P. C. *Annu. Rev. Biochem.* **1968**, *37*, 225. (b) Abeles, R. H. *Adv. Chem. Ser.* **1900**, *No. 100*, 346. (c) Barker, H. A., *Annu. Rev. Biochem.* **1972**, *41*, 55.
(2) Halpern, J. *Adv. Chem. Ser.* **1968**, *No. 70*, 1.
(3) Wood, J. M.; Fanchiang, Y.-T. "Vitamin B_{12}"; Zagalak, B., Friedrich, W., Eds.; Walter de Gruyer and Co.: Berlin, 1979; p 539.
(4) (a) Taylor, R. T.; Hanna, M. L. *Bioinorg. Chem.* **1976**, *6*, 281. (b) Fanchiang, Y.-T.; Ridley, W. P.; Wood, J. M. *J. Am. Chem. Soc.* **1979**, *101*, 1442. (c) Fanchiang, Y.-T.; Pignatello, J. J.; Wood, J. M., to be submitted for publication.

0276-7333/83/2302-0121$01.50/0

dicate that an electron transfer may be involved in these reactions. It is important, therefore, to explore electron-transfer reactions of CH_3-B_{12}.

Hexachloroiridate(IV) is well-known as a one-electron oxidant capable of participating in both outer-sphere and inner-sphere processes.[7] More recently, Halpern et al. have shown that organobis(dioximato)cobalt(III) complexes can be oxidized to organocobalt(IV) by $IrCl_6^{2-}$, followed by a nucleophile-induced heterolytic cleavage of the Co–C bond to yield Co(II) ions.[8] Oxidative cleavage of metal–carbon bonds of organometals such as R'HgR, R_4Pb, and R_2PtL_2 by $IrCl_6^{2-}$ has also been described by Kochi et al.[9] A remarkable and noteworthy point lies in the fact that the oxidized organocobaloxime intermediate undergoes a nucleophilic displacement, while R_2Hg^+ or R_4Pb^+ releases an organic radical.

We report here the reaction of CH_3-B_{12} with $IrCl_6^{2-}$. It is described in terms of a one-electron oxidative demethylation. However, unlike alkylcobaloximes, the oxidized CH_3-B_{12} intermediate releases a methyl radical which undergoes further reactions.

Experimental Section

Materials. $Na_2IrCl_6 \cdot 6H_2O$ and $Na_3IrCl_6 \cdot 12H_2O$ were obtained from Goldsmith Inc. Their purity was checked with the published molar absorptivities. $^{13}CH_3I$ (90% enriched) was obtained from Stohler, Inc. CH_3-B_{12} and $^{13}CH_3$-B_{12} were synthesized in the dark from cyanocobalamin and CH_3I or $^{13}CH_3I$.[10] Cob(II)alamin (B_{12r}) was generated by reducing H_2O-B_{12}^+ with equimolar amounts of Eu^{2+} under an atmosphere of Ar. Concentrations of CH_3-B_{12}, H_2O-B_{12}^+, and B_{12r} were determined from their absorption spectra.[11] All other chemicals were reagent grade.

Base-On and Base-Off Equilibrium Constants of CH_3-B_{12}. Protonation of the 5,6-dimethylbenzimidazole moiety and the resulting base-on and base-off conversion can be expressed as in eq 1. pK_2 is taken as 4.7—the pK_a of free 5,6-dimethylbenz-

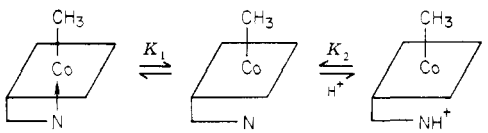

(1)

imidazole.[12] pK_1 at 1.0 M $NaClO_4$ and NaCl has been previously determined to be 0.90 and 1.74, respectively (23 °C).[5]

Stoichiometries and Products. The consumption ratios of $IrCl_6^{2-}$:CH_3-B_{12} were determined by spectrophotometric titration with a Cary 15 or GCA/McPherson spectrophotometer. When the reaction was performed with a large ratio of $IrCl_6^{2-}$ over CH_3-B_{12}, the titration was done at 487.5 nm (absorbance maximum for $IrCl_6^{2-}$) with an identical concentration of H_2O-B_{12}^+ in the reference cell to eliminate the B_{12} product absorption. When the reaction was performed with excess CH_3-B_{12}, the titration was done at 351 nm (γ band for H_2O-B_{12}^+) with an identical concentration of $IrCl_6^{3-}$ in the reference cell. The B_{12} products were identified spectrophotometrically. Organic products were examined by a gas chromatograph or a Brüker 250-MHz ^{13}C NMR at low temperature. The identity of the reduced Ir species was determined spectrophotometrically at pH 1. The reaction solution was oxidized with Cl_2. After removal of the excess chlorine, the spectrum was recorded and analyzed with respect to the $IrCl_6^{2-}/IrCl_5(H_2O)^-$ composition by using published spectral data.[13] An identical concentration of H_2O-B_{12}^+ (treated with Cl_2[14] was used in the reference cell to eliminate the B_{12} spectrum.

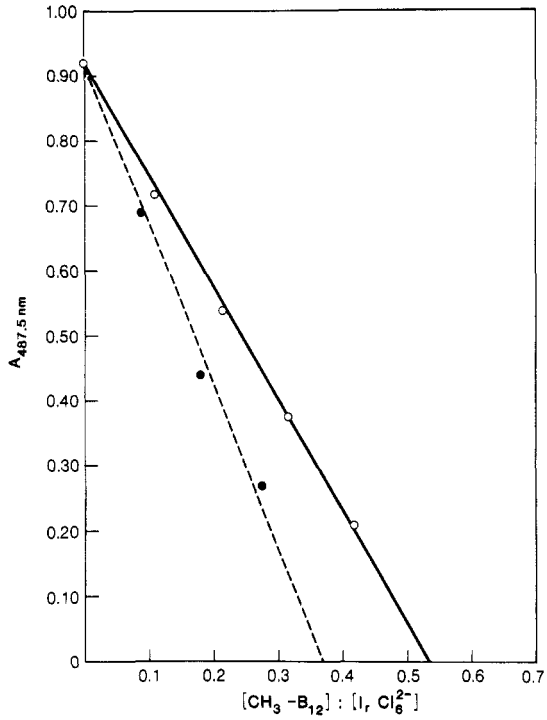

Figure 1. Spectrophotometric titration of 1.8×10^{-4} M $IrCl_6^{2-}$ with deficient amounts of CH_3-B_{12} at 487.5 nm (pH 2.91). An identical concentration of H_2O-B_{12}^+ was used in the reference cell to eliminate the absorbance of H_2O-B_{12}^+ produced during the reaction: (○), in 1.0 M NaCl; (●), in 1.0 M $NaClO_4$.

Kinetic Measurements. The rates for demethylation of CH_3-B_{12} by $IrCl_6^{2-}$ were estimated by the absorption increase at 351 nm at 23 °C under a dim light. Ionic strength was maintained at 1.0 M with $NaClO_4$ and/or NaCl throughout. The pH was controlled in the range of 0–3 with $HClO_4$.

Results

Preliminary Observations of the Oxidative Demethylation of CH_3-B_{12}. Similar to that of the B_{12} model compounds,[8] CH_3-B_{12} can be demethylated by a broad variety of oxidants. These include Fe^{3+}, $IrCl_6^{2-}$, Ce(IV), and Br_2. Several noteworthy aspects of the oxidative demethylation of CH_3-B_{12} were observed. (1) Fe^{3+} demethylates CH_3-B_{12} extremely slowly in perchloric acid solution. However, rapid demethylation occurs in the presence of Cl^-. This reaction is first order in both CH_3-B_{12} and Fe^{3+} at low [Fe^{3+}] but approaches zero order in Fe^{3+} as its concentration is increased. (2) Similarly, appreciable demethylation of CH_3-B_{12} by Ce(IV) only occurs in the presence of Cl^-. However, mixing 1 equiv of Ce(IV) with CH_3-B_{12} at pH 7 (in the absence of Cl^-) results in a quantitative base-on to base-off conversion. (3) Br_2 rapidly demethylates CH_3-B_{12}. This reaction is complicated by

(5) Fanchiang, Y.-T. *Inorg. Chem.* **1982**, *21*, 2344.
(6) Fanchiang, Y.-T., unpublished results. A mixture of CH_3-B_{12} and tetracyanoethylene (TCNE) in CH_3OH/H_2O solution displays a sharp new absorption band at 420 nm, with ϵ 1.1×10^4 M^{-1} cm^{-1} and formation constant = 3.9×10^2 M^{-1} (23 °C). This band indicates the formation of a charge-transfer complex between corrin π orbitals and TCNE.
(7) (a) Halpern, J.; Legare, R. J.; Lumry, R. *J. Am. Chem. Soc.* **1963**, *85*, 680. (b) Halpern, J.; Pribanic, M. *Ibid.* **1968**, *90*, 5942. (c) Abley, P.; Halpern, J. *Chem. Commun.* **1971**, 1238.
(8) (a) Abley, P.; Dockal, E. R.; Halpern, J. *J. Am. Chem. Soc.* **1972**, *94*, 659. (b) Halpern, J.; Chan, M. S.; Hanson, J.; Roche, T. S.; Topich, J. A. *Ibid.* **1975**, *97*, 1606. (c) Halpern, J.; Chan, M. S.; Roche, T. S.; Tom, G. M. *Acta Chem. Scand., Ser. A* **1979**, *33A*, 141. (d) Topich, J.; Halpern, J. *Inorg. Chem.* **1980**, *18*, 1339. (e) Halpern, J. "B_{12}", Dophin, D., Ed.; Wiley: New York, 1982; Vol. 1, p 501.
(9) (a) Gardner, H. C.; Kochi, J. K. *J. Am. Chem. Soc.* **1975**, *97*, 1855. (b) Chen, J. Y.; Gardner, H. C.; Kochi, J. K. *Ibid.* **1976**, *98*, 6150. (c) Kochi, J. K. "Organometals and Organometalloids"; Brinkman, F. E., Bellama, J. M., Eds.; Washington, DC, 1978; *ACS Symp. Ser. No. 82*, p 205.
(10) Dolphin, D. *Methods Enzymol.* **1971**, *18C*, 34.
(11) Pratt, J. M. "Inorganic Chemistry of Vitamin B_{12}"; Academic Press: London, 1972, p 44.
(12) Davies, M. T.; Mamalis, P.; Petrow, V.; Sturgeon, B. *J. Pharm. Pharmacol.* **1951**, *3*, 420.
(13) Chang, J. C.; Garner, C. W. *Inorg. Chem.* **1965**, *4*, 209.
(14) Treatment of H_2O-B_{12}^+ with Cl_2 results in an immediate color change from red to orange and in some cases the decomposition of cobalamin.

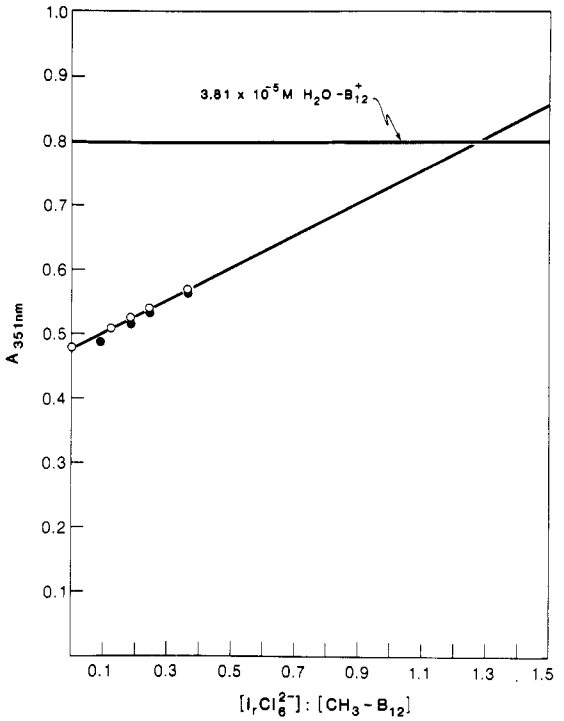

Figure 2. Spectrophotometric titration of 3.81×10^{-5} M CH_3-B_{12} with deficient amounts of $IrCl_6^{2-}$ at 351 nm (pH 2.91). An identical concentration of $IrCl_6^{3-}$ was used in the reference cell to eliminate the absorbance of $IrCl_6^{3-}$ produced during the reaction: (○), in 1.0 M NaCl; (●), in 1.0 M $NaClO_4$.

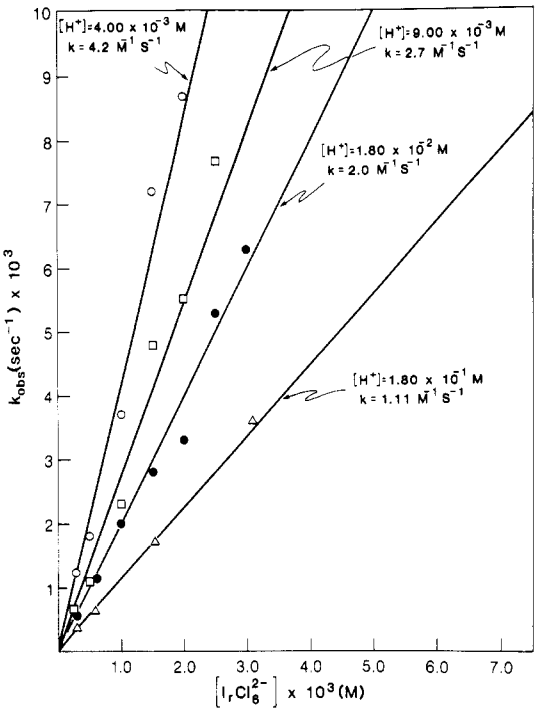

Figure 3. Kinetic data for the demethylation of CH_3-B_{12} by $IrCl_6^{2-}$ ($[CH_3\text{-}B_{12}] = (1\sim3) \times 10^{-5}$ M; μ = 1.0 M ($HClO_4$ + $NaClO_4$); temperature, 23 °C): (○), $[H^+] = 4.00 \times 10^{-3}$ M; (□), $[H^+] = 9.00 \times 10^{-3}$ M; (●), $[H^+] = 1.80 \times 10^{-2}$ M; (△), $[H^+] = 1.80 \times 10^{-1}$ M.

the Br_2 oxidation of the corrin ring.[15] Detailed stoichiometric and kinetic data of the oxidative demethylation of CH_3-B_{12} by $IrCl_6^{2-}$ are presented below.

Stoichiometries and Reaction Products. CH_3-B_{12} (3.5×10^{-5} M) was quantitatively demethylated to H_2O-B_{12}^+ by a sixfold excess of $IrCl_6^{2-}$ in 1.0 M $NaClO_4$ solution. This reaction proceeded with a half-life of ~13 min (pH 3; 23 °C) with isosbestic points at 515, 364, and 335 nm. Reactions performed under Ar yielded the same B_{12} product with no significant change in the demethylation rate. H_2O-B_{12}^+ was produced under all experimental conditions (i.e., with $IrCl_6^{2-}$ in excess over CH_3-B_{12} or vice versa, aerobic or anaerobic). No B_{12r} was detected. $IrCl_6^{2-}$ rapidly oxidized B_{12r} to H_2O-B_{12}^+. H_2O-B_{12}^+ does not react with $IrCl_6^{2-}$.

In 1.0 M NaCl solution, consumption ratio of $[IrCl_6^{2-}]$:$[CH_3\text{-}B_{12}]$ was determined to be 1.95:1 when $IrCl_6^{2-}$ used was in large excess over CH_3-B_{12} (Figure 1).[16] Spectrophotometric titration in perchlorate solution with excess $IrCl_6^{2-}$ is also shown in Figure 1. The results in perchlorate solution are less satisfactory, with $[IrCl_6^{2-}]$:$[CH_3\text{-}B_{12}] \approx 2.7$:1. We failed to identify the cause. The results of spectrophotometric titration with CH_3-B_{12} in excess over $IrCl_6^{2-}$ are shown in Figure 2. The consumption ratios of $[IrCl_6^{2-}]$:$[CH_3\text{-}B_{12}]$ measured under this condition are considerably smaller than 2. As shown in Figure 2, $[IrCl_6^{2-}]$:$[CH_3\text{-}B_{12}]$ was found to be ~1.3:1 in both the Cl^- and ClO_4^- media.

The ^{13}C resonance of methyl-transfer product appeared at 26.0 ppm (relative to external Me_4Si) when the reaction of $^{13}CH_3$-B_{12} with a large ratio of $IrCl_6^{2-}$ was complete. This indicates that with a large excess of $IrCl_6^{2-}$, CH_3Cl is the main organic product generated under all experimental conditions (i.e., in the presence and absence of Cl^- or pyridine, aerobic or anaerobic). No other organic products are detected either by gas chromatograph or by ^{13}C NMR analyses. However, CH_3OH is not definitely ruled out. When reactions were carried out with deficient $IrCl_6^{2-}$ in perchlorate solution, C_2H_6 is the major organic product (^{13}C resonance appeared at 6.027 ppm relative to external Me_4Si). A minor amount of CH_3Cl was also generated. The generation of C_2H_6 under this condition is confirmed by GC analysis of the vapor above the reaction solution (the reaction flask (2 cm^3) was sealed with a serum cap and warmed to ~40 °C).[17]

With $IrCl_6^{2-}$ in excess over CH_3-B_{12}, 1 equiv of $IrCl_6^{3-}$ and $IrCl_5(H_2O)^{2-}$ is generated for each equivalent of CH_3-B_{12} consumed. With deficient $IrCl_6^{2-}$, $IrCl_6^{3-}$ is the main Ir product. No significant amount of $IrCl_5(H_2O)^{2-}$ was found under this condition.

In summary, the demethylation of CH_3-B_{12} by an excess of $IrCl_6^{2-}$ can be expressed in eq 2. With deficient $IrCl_6^{2-}$, the main reaction is eq 3.

$$CH_3\text{-}B_{12} + 2IrCl_6^{2-} + 2H_2O \rightarrow H_2O\text{-}B_{12}^+ + CH_3Cl + IrCl_6^{3-} + IrCl_5(H_2O)^{2-} \quad (2)$$

$$CH_3\text{-}B_{12} + IrCl_6^{2-} + H_2O \rightarrow H_2O\text{-}B_{12}^+ + {}^1/_2C_2H_6 + IrCl_6^{3-} \quad (3)$$

Kinetic Measurements. An excess of $IrCl_6^{2-}$ over CH_3-B_{12} was used in all the rate measurements so that $[IrCl_6^{2-}]$ remained essentially constant. The range of $[CH_3\text{-}B_{12}]$ was $(1\text{–}3) \times 10^{-5}$ M. Plots of log $(A_\infty - A_t)$ vs. time gave straight lines for more than 90% of the reactions. Reproducibility was found to be better than 7%. Kinetics data at various pH values are plotted in Figure 3. The

(15) Bonnett, R.; Cannon, J. R.; Clark, U. M.; Johnson, A. W.; Parker, L. F. J.; Smith, E. L.; Todd, A. *J. Chem. Soc.* **1957**, 1158.

(16) The 2:1 stoichiometry was confirmed by calculation with ϵ 5.1 × 10^3 M^{-1} cm^{-1} for $IrCl_6^{2-}$ at 487.5 nm.

(17) Reaction of CH_3-B_{12} with a deficient amount of $IrCl_6^{2-}$ in CH_3OH/H_2O media presaturated with $CHCl_3$ yields a small amount of CH_4 at the expense of C_2H_6. However, CH_3OH production is not ruled out. Furthermore, we failed to obtain a quantitative measurement because of experimental difficulties.

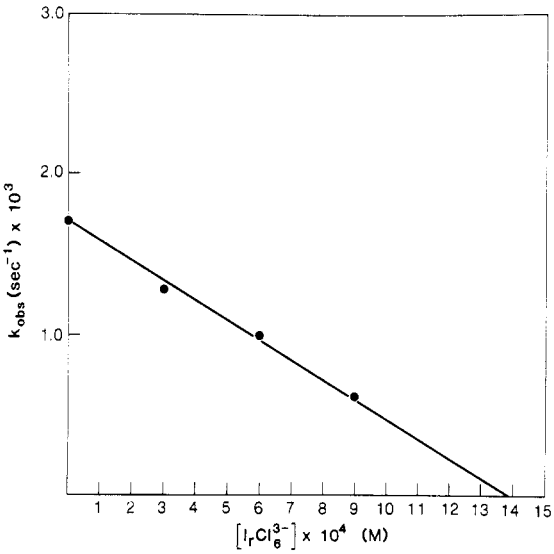

Figure 4. Effect of addition of $IrCl_6^{3-}$ on the kinetic measurements of the demethylation of CH_3-B_{12} by $IrCl_6^{2-}$ ($[IrCl_6^{2-}] = 1.55 \times 10^{-3}$ M; $[H^+] = 0.18$ M; $\mu = 1.0$ M ($HClO_4$ + $NaClO_4$); temperature, 23 °C).

reaction was found to be first order in CH_3-B_{12} and first order in $IrCl_6^{2-}$ according to eq 4 at all pH values. The

$$\frac{d[H_2O\text{-}B_{12}^+]}{dt} = k[IrCl_6^{2-}][CH_3\text{-}B_{12}] \quad (4)$$

values of k are pH dependent. Considering eq 1, rate law 5 is obtained. Here k' represents the reaction path of

$$k = \frac{k'K_2 + k''K_1[H^+]}{K_2 + K_1K_2 + K_1[H^+]} \quad (5)$$

base-on CH_3-B_{12}, while k'' represents the path of the protonated base-off form. We have neglected the unprotonated base-off form, since its concentration is extremely small. Under the present experimental conditions, rate law 5 can be simplified into rate law 6. Plots of k vs. $[H^+]^{-1}$ yielded $k' = 83$ M^{-1} s^{-1} and $k'' = 1.1$ M^{-1} s^{-1} ($\mu = 1.0$ M ($HClO_4$ + $NaClO_4$); 23 °C).

$$\frac{d[H_2O\text{-}B_{12}^+]}{dt} = \frac{k'K_2 + k''K_1[H^+]}{K_1[H^+]}[IrCl_6^{2-}][CH_3\text{-}B_{12}] \quad (6)$$

Addition of large amounts of $IrCl_6^{3-}$ inhibits the demethylation at low pH. This is plotted in Figure 4. Addition of $IrCl_6^{3-}$ ($(1.56 \sim 7.84) \times 10^{-3}$ M) at $[H^+] = 0.0040$ M does not affect the kinetic measurements. The Cl^- effect on the reaction rates at a constant ionic strength is shown in Figure 5. This experiment was carried out at pH 0.74 so that rate law 6 can be simplified into eq 7. This is necessary because Cl^- anion has a pronounced effect on the value of K_1. The Cl^- effect can be expressed in eq 8. Plots of k'' vs. $[Cl^-]$ yield $k''_1 = 0.97$ M^{-1} s^{-1} (i.e., perchlorate path) and $k''_2 = 24$ M^{-1} s^{-1} (i.e., chloride path).

$$\frac{d[H_2O\text{-}B_{12}^+]}{dt} = k''[IrCl_6^{2-}][CH_3\text{-}B_{12}] \quad (7)$$

$$k'' = k''_1 + k''_2[Cl^-] \quad (8)$$

Discussion

The reactions of $IrCl_6^{2-}$ with $RCo(DH)_2H_2O$[8] and with R_2Hg or R_4Pb[9] have been described in terms of a one-electron transfer mechanism. A similar mechanism is adopted here for the reaction between CH_3-B_{12} and $IrCl_6^{2-}$, which is depicted in Scheme I.

Scheme I

$$CH_3\text{-}B_{12} + IrCl_6^{2-} \overset{k}{\rightleftharpoons} CH_3\text{-}B_{12}^+ + IrCl_6^{3-} \quad (9)$$

with excess $IrCl_6^{2-}$

$$CH_3\text{-}B_{12}^+ + IrCl_6^{2-} + 2H_2O \xrightarrow{\text{fast}} H_2O\text{-}B_{12}^+ + CH_3Cl + IrCl_5(H_2O)^{2-} \quad (10)$$

with deficient $IrCl_6^{2-}$

$$CH_3\text{-}B_{12}^+ + H_2O \xrightarrow{\text{fast}} H_2O\text{-}B_{12}^+ + {}^1/_2C_2H_6 \quad (11)$$

An alternative path for the demethylation is a direct electrophilic attack at the carbon atom. However, this mechanism is not likely to occur. Electrophilic attack is essentially a one-step reaction. The stoichiometry and $IrCl_6^{3-}$ inhibition on the demethylation of CH_3-B_{12} virtually eliminate this mechanism.

The $IrCl_6^{3-}$ inhibition on the $IrCl_6^{2-}$ oxidation of $RCo(DH)_2(H_2O)$ and the redox potential measurements have allowed Halpern et al. to estimate rates of the electron transfer and of the cleavage of Co–C bonds for these reactions.[8] Although a similar $IrCl_6^{3-}$ effect was observed on the reaction of $IrCl_6^{2-}$ with CH_3-B_{12} at low pH, this effect cannot be interpreted in terms of the reverse reaction of electron transfer from CH_3-B_{12} to $IrCl_6^{2-}$. This is because the 2:1 stoichiometry at the experimental conditions of kinetic measurements and the high flux of C_2H_6 when the reactions were performed with deficient $IrCl_6^{2-}$ demand that the rate of cleavage of Co–C of CH_3-B_{12}^+ to be much larger than the electron-transfer rate under all experimental conditions. The retardation by $IrCl_6^{3-}$ is also unlikely due to an inverse salt effect, because all the rate measurements were performed in 1.0 M ClO_4^- media ($HClO_4$ + $NaClO_4$). Therefore, we propose that the $IrCl_6^{3-}$ retardation can be interpreted in the framework of Scheme II, which involves a preequilibrium between CH_3-B_{12} and

Scheme II

$$CH_3\text{-}B_{12} + IrCl_6^{2-} \overset{K}{\rightleftharpoons} \underset{\mathbf{a}}{CH_3\text{-}B_{12}, IrCl_6^{2-}} \quad (12)$$

$$CH_3\text{-}B_{12} + IrCl_6^{3-} \overset{K'}{\rightleftharpoons} \underset{\mathbf{b}}{CH_3\text{-}B_{12}, IrCl_6^{3-}} \quad (13)$$

$$\underset{\mathbf{a}}{CH_3\text{-}B_{12}, IrCl_6^{2-}} \overset{k_{et}}{\rightleftharpoons} CH_3\text{-}B_{12}^+ + IrCl_6^{3-} \quad (14)$$

$IrCl_6^{2-}$. In the presence of stoichiometric amounts of $IrCl_6^{3-}$, complex **b**, which is inert to the electron-transfer reaction, would compete with complex **a** and retardation by $IrCl_6^{3-}$ would result.

In a recent paper,[5] we have demonstrated that the reaction between CH_3-B_{12} and AuX_4^- is zero order in AuX_4^- at high gold concentration. This kinetic behavior is interpreted as "complexation" between CH_3-B_{12} and AuX_4^- prior to the electron-transfer reaction. "Complexation" has also been demonstrated in the methyl transfer from CH_3-B_{12} to Pt^{IV}/Pt^{II} systems (in which an electron transfer is involved) by kinetic and spectroscopic methods.[4] On the basis of these experiences, the suggestion of "complexation" between CH_3-B_{12} and $IrCl_6^{2-}$ in Scheme II seems to be reasonable. It is noteworthy that the reaction rates of $IrCl_6^{2-}$ with organometals such as R_4Sn were found to be faster than that estimated from an outer-sphere model.[18]

It has been shown that the base-on CH_3-B_{12} has a much larger formation constant than the base-off form when

(18) Wong, C. L.; Kochi, J. K. *J. Am. Chem. Soc.* **1979**, *101*, 5593.

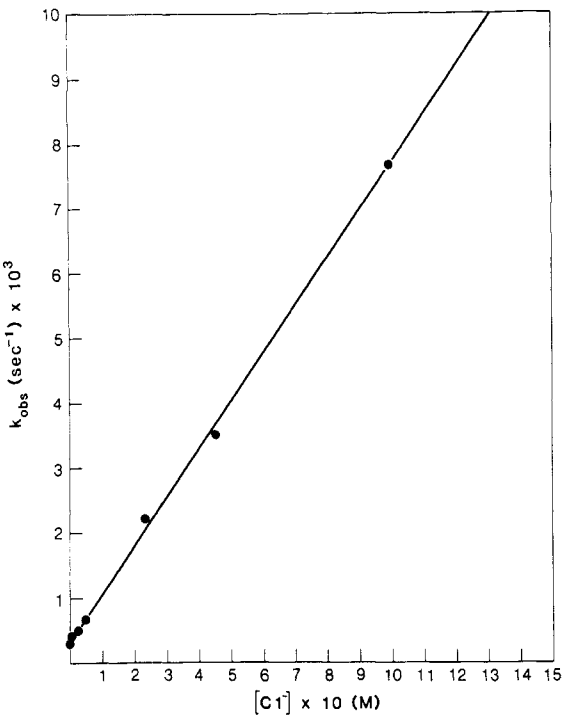

Figure 5. Cl^- effect on the kinetic measurements of demethylation of CH_3-B_{12} by $IrCl_6^{2-}$ ($[CH_3\text{-}B_{12}] = (1\sim3) \times 10^{-6}$ M; $[IrCl_6^{2-}] = 3.2 \times 10^{-4}$ M; $[H^+] = 0.18$ M; $\mu = 1.0$ M (maintained with $NaClO_4$); 23 °C).

complexing with platinum or gold complexes.[4,5] Similarly, k' ($= k_{et}K$) is found to be ~80-fold larger than k''. This suggests that K for the base-on CH_3-B_{12} is larger than that for the base-off form. However, since k_{et} is not separated from K in the present study, this suggestion should remain tentative for the $IrCl_6^{2-}$ oxidation of CH_3-B_{12}.

Figure 5 shows that Cl^- has a pronounced effect on the $IrCl_6^{2-}$ oxidation rate, with $k''_{Cl^-}/k''_{ClO_4^-} = 24$. Indeed. the Cl^--assisted demethylation of CH_3-B_{12} by electrophile has been frequently observed. This includes Fe^{3+}, Ce(IV), Pt(IV)/Pt(II),[4] and Au(III).[5] In cases of platinum and gold complexes in which k_{et} and K can be separated,[19] it is found that $[Cl^-]$ does not affect k_{et}, while K is significantly larger at high Cl^- concentration.

Anion-assisted outer-sphere electron-transfer reactions between $Co(en)_3^{3+}$, $Co(NH_3)_6^{3+}$, $Co(phen)_3^{3+}$, and Cr^{2+} or V^{2+} and between Fe^{3+} and $Co(phen)_3^{2+}$ have been thoroughly investigated.[20] This assistance is interpreted in terms of the orbital symmetries of the electron donor, electron acceptor, and the anion. More recently, Burdett has developed a molecular orbital model to rationalize the counterion effect.[21] This effect is suggested to be threefold: (i) acting as an electrostatic glue, (ii) reducing the barrier to reaction, and (iii) ensuring adiabatic behavior. This argument can be applied to the bridging inner-sphere reactions as well. The accelerating effect of Cl^- on the electron transfer between CH_3-B_{12} and $IrCl_6^{2-}$ can be readily interpreted by this molecular orbital model. However, it should be noted that CH_3-B_{12} is basically a neutral molecule. Thus, we suggest that the Cl^- anion interacts with the π orbitals of corrin ring to increase the formation constant (K) of the "complex" between CH_3-B_{12} and $IrCl_6^{2-}$. It should also be noted that the chloride acceleration is unlikely due to the reversibility in eq 14 in competition to nucleophilic attack of Cl^- on CH_3-B_{12}^+,[8] because CH_3-B_{12}^+ undergoes a homolytic scission of the Co–C bond to generate a $CH_3\cdot$ radical, even the reaction was performed in 1.0 M Cl^- media (vide infra).

A key question that should be asked about the oxidation of organometals is how does the metal–carbon bond of the oxidized intermediate cleave? Two modes are readily available for CH_3-B_{12}^+. One is a nucleophilic displacement resulting in the production of B_{12r}, $IrCl_6^{3-}$ and CH_3OH (with H_2O as the nucleophile) or CH_3Cl (with Cl^- as the nucleophile), or N-methylated pyridine (with pyridine as the nucleophile). Two lines of evidence are against this mechanism. First, when a large excess of $IrCl_6^{2-}$ is used, CH_3Cl is the only detectable organic product generated under all experimental conditions. Second, $IrCl_5(H_2O)^{2-}$ is produced with excess $IrCl_6^{2-}$. We have shown that the reaction between B_{12r} and $IrCl_6^{2-}$ yields H_2O-B_{12}^+ and $IrCl_6^{3-}$, thus the production of $IrCl_5(H_2O)^{2-}$ can be considered as a compelling evidence for the generation of $CH_3\cdot$ radical as described below.

The other mode of cleavage is for CH_3-B_{12}^+ to release a transient $CH_3\cdot$ radical, which then quickly abstracts a chlorine atom from a second $IrCl_6^{2-}$ molecule to form CH_3Cl and $IrCl_5(H_2O)^{2-}$. The rate of the $CH_3\cdot$ extraction of a chlorine atom from $IrCl_6^{2-}$ in aqueous solution has been determined to be 1.15×10^9 M^{-1} s^{-1} (22 ± 2 °C, pH 4–6).[22] In the absence of excess $IrCl_6^{2-}$, $CH_3\cdot$ combines to generate C_2H_6. This mode is remarkably similar to the homolytic scission of CH_3–Co bonds in cations derived from the macrocyclic complexes $(CH_3)_2Co(DpnH)$.[23] In this respect, $(CH_3)_2Co(DpnH)$ is more closely related to CH_3-B_{12} than that of methylcobaloximes. It should be noted that photolysis of CH_3-B_{12} in the presence of O_2 yields H_2O-B_{12}^+ and HCHO as the major products; traces of CH_3OH, CH_4 and C_2H_6 are also formed.[24] This photolysis is generally believed to involve homolysis of Co–C bond to yield $CH_3\cdot$ and B_{12r} as the initial products. The remarkable point that should be stressed in the $IrCl_6^{2-}$ oxidation of CH_3-B_{12} is that it generates a high flux of C_2H_6 with deficient $IrCl_6^{2-}$.

The high flux of C_2H_6 can be interpreted in terms of the relative ease of electron transfer from CH_3-B_{12} to $IrCl_6^{2-}$ and the very fast cleavage of Co–C bond of CH_3-B_{12}^+. In particular, our recent discovery that CH_3-B_{12} forms a head-to-head dimer in aqueous solution at a $[CH_3\text{-}B_{12}] > 10^{-3}$ M[25] greatly enhances the chance of generating C_2H_6 from $CH_3\cdot$ by confining them close together. The high flux of C_2H_6 has also been observed in the cations derived from $(CH_3)_2Co(DpnH)$.[23]

In summary, $IrCl_6^{2-}$ oxidation of CH_3-B_{12} involves a one-electron transfer from CH_3-B_{12} to $IrCl_6^{2-}$ as the rate-determining step. The transient CH_3-B_{12}^+ intermediate then releases a $CH_3\cdot$ radical which either abstracts a chlorine atom from a second $IrCl_6^{2-}$ molecule or combines with another $CH_3\cdot$ radical to generate C_2H_6. $IrCl_6^{3-}$ inhibits the $IrCl_6^{2-}$ oxidation, while Cl^- significantly enhances the rate of reaction.

Acknowledgment. This research was performed during my postdoctoral period at Gray Freshwater Biological Institute, University of Minnesota. It was supported by a grant from NIH, No. AM 18101.

Registry No. Na_2IrCl_6, 16941-25-6; Na_3IrCl_6, 15702-05-3; CH_3-B_{12}, 13422-55-4; $^{13}CH_3$-B_{12}, 43184-67-4.

(19) These reactions all involve an electron-transfer mechanism.
(20) Przystas, T. J.; Sutin, N. *J. Am. Chem. Soc.* **1973**, *95*, 5545.
(21) Burdett, J. K. *Inorg. Chem.* **1978**, *17*, 2537.
(22) Steenken, S.; Neta, P. *J. Am. Chem. Soc.* **1982**, *104*, 1244.
(23) Tamblyn, W. H.; Klingler, R. J.; Hwang, W. S.; Kochi, J. K. *J. Am. Chem. Soc.* **1981**, *103*, 3161.
(24) (a) Hogenkamp, H. P. C. *Biochemistry* **1966**, *5*, 417. (b) Hogenkamp, H. P. C. "B_{12}" Dolphin, D., Ed.; New York, 1982; Vol. 1, p 295.
(25) Pignatello, J. J.; Fanchiang, Y.-T., to be submitted for publication.

Solution Dynamics of (μ-alkyne)$Co_2(CO)_4$DPM

Brian E. Hanson* and Judith S. Mancini

Department of Chemistry, Virginia Polytechnic Institute, Blacksburg, Virginia 24061

Received July 15, 1982

A novel fluxional process is postulated for (μ-alkyne)$Co_2(CO)_4$DPM (DPM = bis(diphenylphosphino)methane) complexes. The motion generates an effective mirror plane on the NMR time scale that contains the cobalt–cobalt bond. When the bridging alkyne is C_2Ph_2, the activation energy for the process is estimated to be 11.0 kcal mol^{-1}. For the unsymmetrical alkyne HCCPh, there is no evidence that rotation of the alkyne can occur in such a manner that the C–C bond becomes parallel to the Co–Co bond.

Introduction

In the course of an investigation of the chemisty of $Co_2(CO)_6$DPM and its derivatives (DPM = bis(diphenylphospino)methane) it was noticed that these compounds showed simpler NMR spectra than their solid-state structures would predict.[1] Ambient-temperature NMR data on some of these derivatives and many similar molecules had been previously reported[2] although nothing was mentioned about the implied dynamic behavior. Variable-temperature NMR studies have now been carried out on $Co_2(CO)_6$DPM, **1**,[3] (μ-C_2H_2)$Co_2(CO)_4$DPM, **2**,[2] (μ-C_2Ph_2)$Co_2(CO)_4$DPM, **3**,[4] and (μ-HCCPh)$Co_2(CO)_4$DPM, **4**. We report these results in the context of the unique fluxional behavior recently observed in the chiral dimer (η^5-C_5H_5)$NiCo(CO)_3$(μ-alkyne).[5]

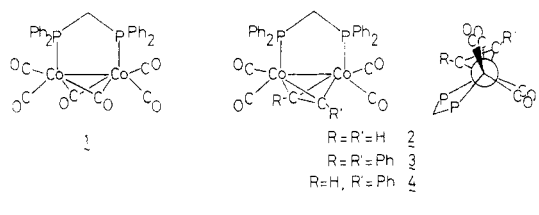

The structure of each of the DPM compounds is derived from $Co_2(CO)_8$, **6**,[6] where two terminal carbonyls have been replaced by DPM and the two bridging sites are occupied by CO or alkyne. These molecules can be considered to have a "vacant" bridging site. This is readily apparent from a comparison of the structure of $Co_2(CO)_8$ with $Fe_2(CO)_9$;[7] one can visualize the bridged $Co_2(CO)_8$ structure by removing one bridging carbonyl from the $Fe_2(CO)_9$ structure. The observed fluxional process described here utilizes the "vacant" bridging site.

Results and Discussion

The NMR results for compounds **1–4** are presented in Table I. Schematic structures for the compounds are shown above. A crystal structure has been reported only for (μ-C_2Ph_2)$Co_2(CO)_4$DPM, **3**.[4] Infrared data for the other alkyne derivatives **2** and **4** suggest an identical structure. The structure assigned to **1** above is based on the crystal structure of the related molecule $Co_2(CO)_6$(ffars),[8] ffars = o-$C_4F_4(AsMe_2)_2$, and the structural requirements for bridging a DPM ligand.[9]

Each molecule has a mirror plane bisecting the cobalt–cobalt bond. No other symmetry elements are present. The alkyne derivatives should show two types of carbonyl in the ^{13}C NMR spectrum provided the same structure persists in solution. Also the methylene protons of the DPM ligand should give an ABX_2 pattern in the ^1H NMR spectrum (X = ^{31}P). These results are obtained only for compound **4** which has an unsymmetrical alkyne.

When bridging alkyne is C_2Ph_2, **3**, the expected ^{13}C NMR spectrum in the carbonyl region is obtained at −55 °C. As the temperature is raised, the two carbonyl peaks coalesce at −35 °C and finally a single sharp peak is observed at room temperature. In the ^1H NMR spectrum a triplet is observed in the methylene region ($J(^{31}P-^1H)$ = 10.1 Hz) at 25 °C. Cooling to −55 °C collapses the triplet, but the expected ABX_2 pattern is not resolved.

When C_2H_2 occupies the bridging position, the slow-exchange limit for carbonyl exchange could not be reached even at −94 °C. In the ^{13}C NMR spectrum significant broadening of the single carbonyl resonance occurs at −85 °C.

For the parent compound, $Co_2(CO)_6$DPM, carbonyl exchange remained fast at −105 °C.

The observed NMR spectra for the alkyne derivatives can be easily explained by the occurrence of a novel motion of the bridging alkyne only. (The same motion can explain the simple ^1H NMR spectrum reported for (μ-C_2Ph_2)-$Co_2(CO)_4$(ffars).[2] The movement of the alkyne is depicted in Figure 1.

When the bridging alkyne is symmetrically substituted, as in the case of **2** and **3**, the postulated motion generates a time-averaged mirror plane containing the two P atoms and the two Co atoms. This is strictly true only if the envelope configuration of the DPM ligand is rapidly flip-flopping as expected.[8] The mirror plane would then make equivalent the two carbonyls on one cobalt and the two protons of the methylene bridge.

For a simple two-site-exchange process the activation barrier can be readily estimated: compound **2**, R = R′ = H, $E_a \leq 7.5$ kcal mol^{-1}; compound **3**, R = R′ = C_6H_5, E_a = 11.4 kcal mol^{-1}.[10]

It is reasonable to assume, in the light of the results for **2** and **3**, that a similar motion is also rapid in **4** where the alkyne is unsymmetrically substituted. Importantly, for

(1) Hanson, B. E.; Fanwick, P. E.; Mancini, J. S. *Inorg. Chem.*, in press.
(2) Chia, L. S.; Cullen, W. R.; Franklin, M.; Manning, A. R. *Inorg. Chem.* **1975**, *14*, 2521.
(3) Fukumoto, T.; Matsumura, Y.; Okawara, R. *J. Organomet. Chem.* **1974**, *69*, 437.
(4) Bird, P. H.; Fraser, A. R.; Hall, D. N. *Inorg. Chem.* **1977**, *16*, 1923.
(5) Jaouen, G.; Marinetti, A.; Saillard, J. Y.; Sayer, B. G.; McGlinchey, M. J. *Organometallics* **1982**, *1*, 225.
(6) Sumner, G. G.; Klug, H. P.; Alexander, L. L. *Acta Crystallogr.* **1964**, *17*, 732.
(7) Cotton, F. A.; Troup, J. M. *J. Chem. Soc., Dalton Trans.* **1974**, 800.
(8) Harrison, W.; Trotter, J. *J. Chem. Soc. A* **1971**, 1607.
(9) Cotton, F. A.; Troup, J. M. *J. Am. Chem. Soc.* **1974**, *96*, 4422.
(10) The coalescence temperature was estimated to be −35 °C for **3** and ≤−110 °C for **2**. Activation energies were estimated from the Arrhenius equation.

0276-7333/83/2302-0126$01.50/0

Table I. NMR Results for 1-5[a]

compd	^{13}C NMR carbonyl region[b]	^{1}H NMR methylene region	^{1}H NMR alkyne region
1	204.3 (s) (−105 to +22 °C)	3.15 (t, $J(^{31}P-^1H)$ = 9.9 Hz) (−105 to +22 °C)	
2	202.2 (s) (25 °C)	3.40 (t, $J(^{31}P-^1H)$ = 10.0 Hz) (25 °C)	5.75 (t, $J(^{31}P-^1H)$ = 3.1 Hz) (25 °C)
	202.2 (br) (−94 °C)	3.40 (br) (−98 °C)	5.75 (t) (−98 °C)
3	205.0 (s) (22 °C)	3.30 (t, $J(^{31}P-^1H)$ = 10.1 Hz) (22 °C)	
	207.0 (s), 203.0 (s) (−55 °)	3.30 (br) (−40 °C)	
4	207.1 (s), 203.0 (s) (22 °C)	3.32 (ABX_2, $J(^{31}P-^1H)$ = 10.5 Hz, $J(^1H-^1H)$ = 13.5 Hz) (30 °C)	5.78 (t, $J(^{31}P-^1H)$ = 7 Hz) (30 °C)

[a] Chemical shifts are in parts per million relative to Me_4Si. [b] $^{31}P-^{13}CO$ couplings were not resolved.

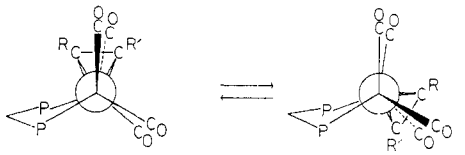

Figure 1. Proposed motion for the μ-alkyne ligand. R equals Ph or H as indicated in the text. The view is down the cobalt–cobalt bond. The empty vertex of the trigonal bipyramid is trans to the center of the alkyne ligand.

an unsymmetric alkyne the postulated motion cannot generate a second mirror plane. Thus the carbonyls and the protons remain unique even when the rocking of the alkyne is rapid. This is consistent with the observed ^{13}C and ^{1}H NMR spectra for **5** (Table I).

Observation of the "frozen" spectrum for **5** at room temperature reflects the static nature of the Co_2C_2 tetrahedron with respect to alkyne rotation relative to the cobalt–cobalt bond. The ^{1}H NMR spectrum persists to 60 °C with no detectable line broadening. This is not surprising since such a rotation is symmetry forbidden. Molecular orbital calculations have been reported for several μ-alkyne complexes, including (μ-C_2H_2)$CO_2(CO)_6$.[11,12] The results are applicable here since the DPM derivatives have the same eclipsed structure. In particular for (μ-C_2H_2)$Co_2(CO)_6$ the HOMO has a_2 symmetry,[11] and as the alkyne rotates, the HOMO is significantly destabilized.[12] The results obtained here contrast the dynamic behavior of the heterobimetallic compounds (μ-alkyne)(η^5-C_5H_5)NiCo(CO)$_3$ and (μ-alkyne)(η^5-C_5H_5)NiMo(CO)$_2$.[5]

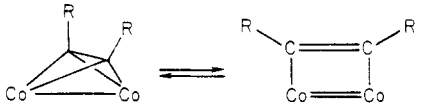

In these complexes the alkyne was found to rotate formally with respect to the metal–metal bond. For the former compound the free energy of activation was reported to be 20.5 kcal mol^{-1}. With regard to the mechanism of exchange Jaouen et al.[5] propose an alternative pathway in which the dimer opens up to form an intermediate butterfly-type structure. From a symmetry point of view this is to be preferred over alkyne rotation. The butterfly mechanism is unavailable to the DPM derivatives due to the constraint imposed by the DPM ligand.

In the butterfly mechanism the tetrahedral M_2C_2 unit is considered a nido cluster on the basis of a trigonal bipyramid with M_2 occupying an apical and an equatorial site.[5] The empty vertex is the other apical site. The rocking motion proposed here may also be viewed by using this formalism. Now the missing vertex is in the equatorial plane, and the cobalt atoms occupy apical sites. The alkyne may thus be viewed as sliding to occupy two of the three equatorial sites.[13]

With regard to formal alkyne rotation relative to the metal–metal bond recent calculations show that when $CpCo^-$ replaces Co(CO)$_3$, the estimated barrier to rotation is significantly reduced.[14] Since $CpCo^-$ is isoelectronic, with CpNi alkyne rotation in (η^5-C_5H_5)NiCo(CO)$_3$(μ-alkyne)[5] is probably more favorable than in the cobalt carbonyl derivatives **2–4** reported here. In the related chiral tetrahedral compound $Co_3(CCO_2CHMe)(CO)_7$(arphos) racemization was found to occur with an activation energy of 13.1 kcal mol^{-1}.[5] The arphos ligand, $Ph_2PCH_2CH_2AsPh_2$, apparently has sufficient flexibility to allow the deformation of the tetrahedron to a butterfly-type intermediate.

The mechanism shown in Figure 1 for compounds **2–4** appears to be unique for derivatives of cobalt carbonyl. In the molybdenum dimers (μ-alkyne)(η^5-C_5H_5)$_2Mo_2(CO)_4$,[15-17] the observed dynamic behavior is readily explained by a static Mo_2C_2 framework and rotation of the (C_5H_5)Mo(CO)$_2$ groups relative to one another. (The mechanism proposed here can also explain the observed behavior of the molybdenum dimers. However, the necessary intermediates in such a process are rather unrealistic, and therefore this mechanism is an unattractive alternative to rotation about the Mo–Mo bond. Rotation about the Co–Co bond in **2–4** is unlikely due to the presence of the bridging ligand.) Recently, alkyne dissociation from one metal has been observed in the molybdenum dimers at high temperatures.[18] Such a process could explain the dynamic behavior of the heterobitmetallic complexes but clearly is not taking place in the cobalt dimers reported here as demonstrated by the persistence of the ABX_2 pattern in the ^{1}H NMR spectrum of **4** at 60 °C.

In the cobalt dimers an important feature is the availability of a vacant bridging site. This site is intimately involved in the postulated mechanism since its presence allows the alkyne to move.

Experimental Section

All NMR spectra were obtained on a JEOL FX200 NMR spectrometer (proton, 200 MHz, carbon, 50 MHz). Solvents were either $CDCl_3$ for spectra above −50 °C or $CDCl_3/CH_2Cl_2$ (25:75) for spectra below −50 °C. All solutions were freeze–pump–thaw degassed before recording the NMR spectrum.

To obtain ^{13}C NMR spectra, it was necessary to enrich the samples in ^{13}CO. This was done by preparing a solution of

(11) Thorn, D. L.; Hoffman, R. *Inorg. Chem.* **1978**, *17*, 126.
(12) Anderson, A. B. *Inorg. Chem.* **1976**, *15*, 2598.
(13) We are grateful to a reviewer for bringing this point to our attention.
(14) Hoffman, D. M.; Hoffman, R.; Fisel, C. R. *J. Am. Chem. Soc.* **1982**, *104*, 3858.
(15) Bailey, W. I., Jr.; Chisholm, M. H.; Cotton, F. A.; Rankel, L. A. *J. Am. Chem. Soc.* **1978**, *100*, 5764.
(16) Bailey, W. I., Jr.; Cotton, F. A.; Jamerson, J. D.; Kolb, J. R. *J. Organomet. Chem.* **1976**, *121*, C23.
(17) Bailey, W. I., Jr.; Collins, D. M.; Cotton, F. A. *J. Organomet. Chem.* **1977**, *135*, C53.
(18) Slater, S.; Muetterties, E. L. *Inorg. Chem.* **1980**, *19*, 3337.

$Co_2(CO)_6DPM$, 1, in CH_2Cl_2 and stirring in the presence of 90% ^{13}CO and 5% Pd/charcoal. Enriched samples of 1 were then used to prepare 2-5 by literature methods.[1,3] The level of enrichment was estimated by infrared spectroscopy to be ca. 20%.

Acknowledgment. We thank the Research Corp. and the State of Virginia for support of this research. We thank Mr. Tom Glass for assistance in obtaining the low-temperature NMR data.

Registry No. 1, 52615-19-7; 2, 55925-97-8; 3, 52659-27-5; 4, 82864-95-7.

Synthesis of Some Ring-Substituted [1]Ferrocenophanes and the Structure of Four Representative Examples

Ian R. Butler,[1a] William R. Cullen,*[1a] Frederick W. B. Einstein,[1b] Steven J. Rettig,[1a] and Anthony J. Willis[1b]

Chemistry Departments, University of British Columbia, Vancouver, British Columbia, and Simon Fraser University, Burnaby, British Columbia, Canada

Received June 30, 1982

The reaction of 1,1′-dilithioferrocenes $(\eta^5\text{-}C_5H_4Li)Fe(\eta^5\text{-}C_5H_3R^1Li)$ [R^1 = H, $CHMeNMe_2$, or $CH(CHMe_2)NMe_2$] with Cl_2PPh, I_2AsPh, and $Cl_2P\text{-}t\text{-}Bu$ [X_2ER^2] affords the appropriate [1]ferrocenophanes $(\eta^5\text{-}C_5H_4)Fe(\eta^5\text{-}C_5H_3R^1ER^2)$. The crystal structures of four such complexes have been determined: R^1 = H, E = P, R^2 = Ph; *Pbca*, a = 7.3427 (8) Å, b = 27.078 (4) Å, c = 12.682 (2) Å, Z = 8, R = 0.045 for 1544 reflections; R^1 = H, E = P, R^2 = *t*-Bu; $P2_1/n$, a = 6.1007 (5) Å, b = 20.1851 (8) Å, c = 10.2303 (9) Å, β = 93.284 (4)°, Z = 4, R = 0.036 for 2427 reflections; R^1 = $CH(CHMe_2)NMe_2$, E = P, R^2 = Ph; $P2_1/c$, a = 8.2775 (9) Å, b = 15.4055 (8), c = 15.7558 (19) Å, β = 103.908 (5)°, Z = 4, R = 0.030 for 2730 reflections; R^1 = $CHMeNMe_2$, E = As, R^2 = Ph; $P\bar{1}$, a = 9.0873 (8) Å, b = 10.2776 (7) Å, c = 11.0240 (8) Å, α = 65.974 (7)°, β = 66.451 (6)°, γ = 76.959 (6)°, Z = 2, R = 0.024 for 3404 reflections. In the three phosphorus-bridged [1]ferrocenophanes, the mean tilt of the cyclopentadienyl rings is 27.0 (1)°, and the mean bridgehead angle at phosphorus is 90.8 (4)°. The corresponding parameters for the arsenic derivatives are 22.9 and 87.90 (7)°, respectively. The mean Fe–(cyclopentadienyl ring centroid) distance for all four molecules is 1.636 (6) Å.

Introduction

There has been considerable interest in reactions catalyzed by ferrocenyl phosphine derivatives of metals such as Ni, Pd, and Rh.[2-11] It is clear that rather dramatic changes in reaction products and yields can be achieved by changes in the metal and ligand. For example, it has been found that the dialkylphosphine 1 [R = $P(C(CH_3)_3)_2$] affords rhodium(I) complexes which are unexpectedly effective as asymmetric hydrogenation catalysts.[5] Complexes of the related diphenylphosphine 1 [R = $P(C_6H_5)_2$] are actually less effective in some cases. Kumada and co-workers[11] have shown that the regeo chemistry of Grignard cross coupling reactions can be varied by using either the nickel or palladium derivatives of 2 [R = $P(C_6H_5)_2$] as catalysts.

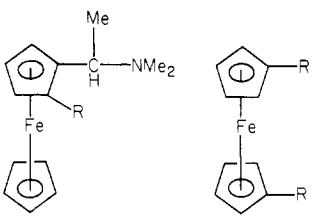

1 2

In order to extend this chemistry, it is desirable to have available a range of compounds related to 1 and 2 with a variety of substituents and stereochemistries. The reported[12] cleavage reaction of the bridged ferrocene derivative 3 (eq 1) appeared to offer a general convenient synthetic route as indicated in eq 2. This route has been found to be viable.[12,13]

This paper describes the structure determination of bridged phosphines and arsines related to 3 which are synthetically useful starting materials for ligand preparation. The structure determination of 3 was reported[14] during the course of this study but as our own results for

(1) (a) University of British Columbia. (b) Simon Fraser University.
(2) Hayashi, T.; Yamamoto, K; Kumada, M. *Tetrahedron Lett.* **1974**, 4405. Hayashi, T., Mise, T., Mitachi, S., Yamamoto, K., Kumada, M. *Ibid.* **1976**, 1133.
(3) Cullen, W. R.; Einstein, F. W. B.; Huang, C.-H.; Willis, A. C.; Yeh, E.-S. *J. Am. Chem. Soc.* **1980**, *102*, 988.
(4) Yamamoto, K.; Wakatsuki, J.; Sugimoto, R. *J. Chem. Soc. Jpn.* **1980**, *53*, 1132.
(5) Cullen, W. R.; Woolins, J. D. *Can. J. Chem.* **1982**, *60*, 1973.
(6) Hayashi, T.; Katsumura, A.; Konishi, M.; Kumada, M. *Tetrahedron Lett.* **1979**, 425.
(7) Hayashi, T.; Konishi, M.; Kumada, M. *Tetrahedron Lett.* **1979**, 1871.
(8) Hayashi, T.; Tajika, M.; Tameo, K.; Kumada, M. *J. Am. Chem. Soc.* **1976**, *98*, 3718.
(9) Zembayashi, M.; Tameo, K.; Hayashi, T.; Mise, T.; Kumada, M. *Tetrahedron* **1977**, *21*, 1799.
(10) Hayashi, T.; Kunishi, M.; Kumada, M. *J. Organomet. Chem.* **1980**, *186*, C1.
(11) Kumada, M.; Hayashi, T.; Konishi, M. Proceedings of 10th International Conference on Organometallic Chemistry, Toronto, Canada, Aug 1981, Abstract 4A12, p 119.
(12) Seyferth, D.; Withers, H. P. *J. Organomet. Chem.* **1980**, *185*, C1.
(13) Cullen, W. R.; Butler, I. R., unpublished results.
(14) Stoeckli-Evans, H.; Osborne, A. G.; Whiteley, R. H. *J. Organomet. Chem.* **1980**, *194*, 91.

0276-7333/83/2302-0128$01.50/0

$Co_2(CO)_6DPM$, 1, in CH_2Cl_2 and stirring in the presence of 90% ^{13}CO and 5% Pd/charcoal. Enriched samples of 1 were then used to prepare 2-5 by literature methods.[1,3] The level of enrichment was estimated by infrared spectroscopy to be ca. 20%.

Acknowledgment. We thank the Research Corp. and the State of Virginia for support of this research. We thank Mr. Tom Glass for assistance in obtaining the low-temperature NMR data.

Registry No. 1, 52615-19-7; 2, 55925-97-8; 3, 52659-27-5; 4, 82864-95-7.

Synthesis of Some Ring-Substituted [1]Ferrocenophanes and the Structure of Four Representative Examples

Ian R. Butler,[1a] William R. Cullen,*[1a] Frederick W. B. Einstein,[1b] Steven J. Rettig,[1a] and Anthony J. Willis[1b]

Chemistry Departments, University of British Columbia, Vancouver, British Columbia, and Simon Fraser University, Burnaby, British Columbia, Canada

Received June 30, 1982

The reaction of 1,1′-dilithioferrocenes $(\eta^5\text{-}C_5H_4Li)Fe(\eta^5\text{-}C_5H_3R^1Li)$ [R^1 = H, $CHMeNMe_2$, or $CH(CHMe_2)NMe_2$] with Cl_2PPh, I_2AsPh, and $Cl_2P\text{-}t\text{-}Bu$ [X_2ER^2] affords the appropriate [1]ferrocenophanes $(\eta^5\text{-}C_5H_4)Fe(\eta^5\text{-}C_5H_3R^1ER^2)$. The crystal structures of four such complexes have been determined: R^1 = H, E = P, R^2 = Ph; *Pbca*, a = 7.3427 (8) Å, b = 27.078 (4) Å, c = 12.682 (2) Å, Z = 8, R = 0.045 for 1544 reflections; R^1 = H, E = P, R^2 = *t*-Bu; $P2_1/n$, a = 6.1007 (5) Å, b = 20.1851 (8) Å, c = 10.2303 (9) Å, β = 93.284 (4)°, Z = 4, R = 0.036 for 2427 reflections; R^1 = $CH(CHMe_2)NMe_2$, E = P, R^2 = Ph; $P2_1/c$, a = 8.2775 (9) Å, b = 15.4055 (8), c = 15.7558 (19) Å, β = 103.908 (5)°, Z = 4, R = 0.030 for 2730 reflections; R^1 = $CHMeNMe_2$, E = As, R^2 = Ph; $P\bar{1}$, a = 9.0873 (8) Å, b = 10.2776 (7) Å, c = 11.0240 (8) Å, α = 65.974 (7)°, β = 66.451 (6)°, γ = 76.959 (6)°, Z = 2, R = 0.024 for 3404 reflections. In the three phosphorus-bridged [1]ferrocenophanes, the mean tilt of the cyclopentadienyl rings is 27.0 (1)°, and the mean bridgehead angle at phosphorus is 90.8 (4)°. The corresponding parameters for the arsenic derivatives are 22.9 and 87.90 (7)°, respectively. The mean Fe–(cyclopentadienyl ring centroid) distance for all four molecules is 1.636 (6) Å.

Introduction

There has been considerable interest in reactions catalyzed by ferrocenyl phosphine derivatives of metals such as Ni, Pd, and Rh.[2-11] It is clear that rather dramatic changes in reaction products and yields can be achieved by changes in the metal and ligand. For example, it has been found that the dialkylphosphine 1 [R = $P(C(CH_3)_3)_2$] affords rhodium(I) complexes which are unexpectedly effective as asymmetric hydrogenation catalysts.[5] Complexes of the related diphenylphosphine 1 [R = $P(C_6H_5)_2$] are actually less effective in some cases. Kumada and co-workers[11] have shown that the regeo chemistry of Grignard cross coupling reactions can be varied by using either the nickel or palladium derivatives of 2 [R = $P(C_6H_5)_2$] as catalysts.

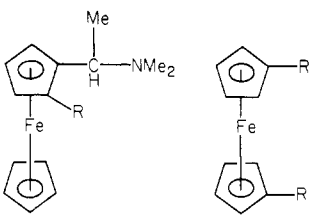

1 2

In order to extend this chemistry, it is desirable to have available a range of compounds related to 1 and 2 with a variety of substituents and stereochemistries. The reported[12] cleavage reaction of the bridged ferrocene derivative 3 (eq 1) appeared to offer a general convenient synthetic route as indicated in eq 2. This route has been found to be viable.[12,13]

This paper describes the structure determination of bridged phosphines and arsines related to 3 which are synthetically useful starting materials for ligand preparation. The structure determination of 3 was reported[14] during the course of this study but as our own results for

(1) (a) University of British Columbia. (b) Simon Fraser University.
(2) Hayashi, T.; Yamamoto, K; Kumada, M. *Tetrahedron Lett.* **1974**, 4405. Hayashi, T., Mise, T., Mitachi, S., Yamamoto, K., Kumada, M. *Ibid.* **1976**, 1133.
(3) Cullen, W. R.; Einstein, F. W. B.; Huang, C.-H.; Willis, A. C.; Yeh, E.-S. *J. Am. Chem. Soc.* **1980**, *102*, 988.
(4) Yamamoto, K.; Wakatsuki, J.; Sugimoto, R. *J. Chem. Soc. Jpn.* **1980**, *53*, 1132.
(5) Cullen, W. R.; Woolins, J. D. *Can. J. Chem.* **1982**, *60*, 1973.
(6) Hayashi, T.; Katsumura, A.; Konishi, M.; Kumada, M. *Tetrahedron Lett.* **1979**, 425.
(7) Hayashi, T.; Konishi, M.; Kumada, M. *Tetrahedron Lett.* **1979**, 1871.
(8) Hayashi, T.; Tajika, M.; Tameo, K.; Kumada, M. *J. Am. Chem. Soc.* **1976**, *98*, 3718.
(9) Zembayashi, M.; Tameo, K.; Hayashi, T.; Mise, T.; Kumada, M. *Tetrahedron* **1977**, *21*, 1799.
(10) Hayashi, T.; Kunishi, M.; Kumada, M. *J. Organomet. Chem.* **1980**, *186*, C1.
(11) Kumada, M.; Hayashi, T.; Konishi, M. Proceedings of 10th International Conference on Organometallic Chemistry, Toronto, Canada, Aug 1981, Abstract 4A12, p 119.
(12) Seyferth, D.; Withers, H. P. *J. Organomet. Chem.* **1980**, *185*, C1.
(13) Cullen, W. R.; Butler, I. R., unpublished results.
(14) Stoeckli-Evans, H.; Osborne, A. G.; Whiteley, R. H. *J. Organomet. Chem.* **1980**, *194*, 91.

0276-7333/83/2302-0128$01.50/0

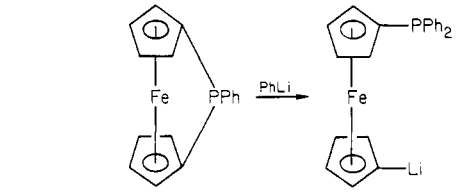

(1)

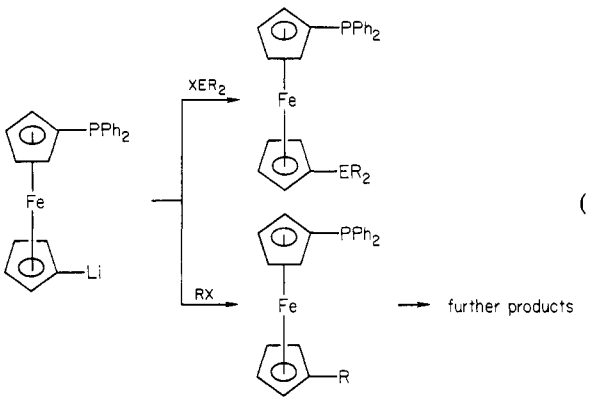

(2)

this compound afford slightly better residuals these are also included.

Compounds such as **3**, in which the cyclopentadienyl rings of the ferrocene moiety are connected by a single atom bridge, are known as [1]ferrocenophanes. The preparation and characterization of a number of these compounds with Si, Ge, and As as bridging atoms have been recently reported.[12,15-17] X-ray structure determinations have been published for three such compounds: 1,1′-ferrocenediyldiphenylsilane,[18] 1,1′-ferrocenediyldiphenylgermane,[14] and, as mentioned above, 1,1′-ferrocenediylphenylphosphine, **3**.[14]

Experimental Section

All manipulations were performed under an atmosphere of dry nitrogen. Microanalyses were performed by Mr. P. Borda of the Chemistry Department, University of British Columbia. ^{1}H NMR spectra were recorded on either a Bruker W.P. 80 operating at 80 MHz, a Varian XL100 at 100 MHz, or a Bruker WM 400 at 400 MHz. All solvents were predried and freshly distilled.

Preparation of 1,1′-Ferrocenediylphenylphosphine (3),[17] 1,1′-Ferrocenediyl-*tert*-butylphosphine (4), and 1,1′-Ferrocenediylphenylarsine (5).[12] The compounds **3** and **5** were prepared according to the published procedures.[12,17,19] Compound **4** was prepared by a similar method using *tert*-butyldichlorophosphine.[20] Careful chromatography is required in the latter preparation to separate the red 1,1′-ferrocenediyl-*tert*-butylphosphine from a white phosphine byproduct.

1,1′-Ferrocenediyl-*tert*-butylphosphine: red needles, decomp pt >95 °C yield 46%; ^{1}H NMR δ 4.10–5.10 (m, 8), 1.40 (d, 9). Anal. Calcd for $C_{14}H_{17}FeP$: C, 61.80; H, 6.30. Found: C, 61.82; H, 6.50.

Preparation of [2-(α-Dimethylamino)ethyl)-1,1′-ferrocenediyl]phenylphosphine (6) and [2-(α-(Dimethylamino)-β-methylpropyl)-1,1′-ferrocenediyl]phenylphosphine (7). (a) Isolation of the Dilithioferrocenyl Tetramethylethylenediamine Adducts. α-R-*N*,*N*-dimethyl-α-ferrocenylmethylamine derivatives (**6a**, R = CH_3, and **7a**, R = *i*-C_3H_7) were prepared by the published procedures.[21-23]

A solution of *n*-butyllithium in hexane (18 mL, 1.6 M) was added dropwise to a well stirred solution of **6a** or **7a** (7.20 g, 7.98 g, 28 mmol) in *n*-hexane (30 mL) and diethyl ether (50 mL). The solution was stirred for 1 h before a mixture of *n*-butyllithium (19 mL, 1.6 M) and tetramethylethylenediamine (TMED) (3.48 g, 30 mmol) was added dropwise. The solution was stirred for a further 10 h. A pale orange precipitate of 1,1′-dilithio-2-(α-R-α-(dimethylamino)methylferrocene–tetramethylethylenediamine (**6b**, R = Me, and **7b**, R = *i*-Pr) formed. This adduct was isolated by filtration and washed several times with *n*-hexane. The yield of the pyrophoric adducts is 70–80%.

(b) Reaction of the Adducts with Chlorophosphines. To a well-stirred suspension of **6b** or **7b** (1.80 g, 1.88 g, 4.7 mmol) in diethyl ether (50 mL), maintained at −78 °C, was added *P*,*P*-dichlorophenylphosphine (0.9 g, 5 mmol) in diethyl ether (10 mL). The solution was allowed to warm to room temperature slowly and was stirred for a further 1 h. The product mixture was hydrolyzed (H_2O, 20 mL), the ethereal layer separated and dried over anhydrous $MgSO_4$, and the solution volume reduced to approximately 10 mL. The resulting red oil was chromatographed on neutral alumina, eluting with diethyl ether. The second deep red band was collected, the solution volume reduced to approximately 10 mL, and *n*-hexane (5 mL) added. The solution was then cooled to −20 °C overnight. Red crystals were obtained, yield 40–60%. **6**, R = Me: mp 113–114 °C; ^{1}H NMR δ 7.10–7.90 (m, 5), 4.00–4.70 (m, 7), 3.05 (q, 1), 1.85 (s, 6), 1.90 (d, 3). Anal. Calcd for $C_{20}H_{22}FeNP$: C, 66.10; H, 6.06; N, 3.85. Found: C, 66.70; H, 6.20; N, 3.76. **7**, R = *i*-Pr: mp 128–129 °C; ^{1}H NMR δ 7.10–7.70 (m, 5), 4.00–4.80 (m, 8), 3.72 (m, 1), 2.05 (s, 6), 1.56 (2d, 3, 3). Anal. Calcd for $C_{22}H_{26}FeNP$: C, 67.88; H, 6.90; N, 3.60. Found: C, 67.53; H, 6.70; N, 3.58.

Preparation of [2-α-Dimethylamino)ethyl)-1,1′-ferrocenediyl]-*tert*-butylphosphine (8) and [2-(α-(Dimethylamino)ethyl)-1,1′-ferrocenediyl]phenylarsine (9). A procedure identical with that of the preceding preparations was used employing *tert*-butyldichlorophosphine[20] and *As*,*As*-diiodophenylarsine, respectively, in place of *P*,*P*-dichlorophenylphosphine; yields 45–65%. **8**: mp 91.5–92.5 °C ^{1}H NMR δ, 4.25–4.80 (m, 7), 4.08 (m, 1), 2.10 (s, 6), 1.54 (d, 3), 1.40 (d, 9). Anal. Calcd for $C_{18}H_{26}FeNP$: C, 62.99; H, 7.64; N, 4.08. Found: C, 63.09; H, 7.68; N, 4.07. **9**: decomp pt >108 °C; ^{1}H NMR δ 7.25–7.70 (m, 5), 4.00–4.50 (m, 8), 2.18 (s, 6), 1.56 (d, 3). Anal. Calcd for $C_{20}H_{22}AsFeN$: C, 58.91; H, 5.45; N, 3.44. Found: C, 58.86; H, 5.52; N, 3.45.

X-ray Crystallographic Analyses of 3, 4, 7, and 9. Crystallographic data for all four compounds are given in Table I. Space groups were determined from preliminary X-ray photographs (Cu Kα, λ = 1.5418 Å, or Mo Kα radiation, λ = 0.710 73 Å). Crystals of **3** were mounted on an automated Picker FACS-I diffractometer and crystals of **4**, **7**, and **9** on an Enraf-Nonius CAD4-F diffractometer; all in nonspecific orientations. Final unit-cell dimensions were obtained by least squares from the setting angles of 28 accurately centered reflections (with $25 < 2\theta < 31°$) for **3** and by least squares on 2 (sin θ)/λ values for 25 reflections (with $40 < 2\theta < 50°$, $35 < 2\theta < 49°$, and $45 < 2\theta < 49°$ for **4**, **7**, and **9**, respectively) measured with Mo $K\alpha_1$ radiation (λ = 0.709 30 Å).

For **3**, two standards were measured after every 80 reflections and showed small, almost sinusoidal, variations in intensity (maximum of 4% from mean). A five-point smoothed curve was derived from the standards and used to rescale the data. The peak profiles of 2236 independent relections yielded 1544 reflections with $I > 2.3\sigma(I)$ which were regarded as observed and were used in the structure solution and refinement. Background counts of 0.1 × (scan time) were taken at each side of the very scan. Intensities and their associated errors were derived by a peak profile analysis.[24]

For **4**, **7**, and **9** the intensities of three check reflections were measured every hour throughout the data collections, showing only random fluctuations for **7** and **9**, and a uniform decrease of 7.9% in the case of **4** was accounted for by application of an isotropic decay correction. Totals of 3664, 4459, and 4989 in-

(15) Osborne, A. G., Whiteley, R. H. *J. Organomet. Chem.* **1975**, *101*, C27.
(16) Osborne, A. B.; Whiteley, R. H.; Hollands, R. E. Proceedings of the 9th International Conference on Organometallic Chemistry, Dijon, France, Sept. 1979, P14T.
(17) Osborne, A. G.; Whiteley, R. H.; Meads, R. E. *J. Organomet. Chem.* **1980**, *193*, 345.
(18) Stoeckli-Evans, Osborn, A. G.; Whiteley, R. H. *Helv. Chim. Acta* **1976**, *59*, 2402.
(19) Seyferth, D.; Withers, H. P. *Organometallics* **1982**, *1*, 1275.
(20) Fild, M.; Stelzer, O.; Schmutzler, R. *Inorg. Synth.* **1973**, *14*, 4.
(21) Gokel, G. V.; Ugi, I. K. *J. Chem. Educ.* **1972**, *49*, 294.
(22) Hauser, C. R.; Lindsay, J. K. *J. Org. Chem.* **1957**, *22*, 906.
(23) **6a** is a low-melting (34.5–35.0 °C) solid, cf. lit.,[21] red oil.
(24) Grant, D. F.; Gabe, E. J. *J. Appl. Crystallogr.* **1978**, *11*, 114.

Table I. Crystallographic Data[a]

	3	4	7	9
formula	$C_{16}H_{13}FeP$	$C_{14}H_{17}FeP$	$C_{22}H_{26}FeNP$	$C_{20}H_{22}AsFeN$
fw	292.10	272.11	391.28	407.17
cryst system	orthorhombic	monoclinic	monoclinic	triclinic[b]
space group	*Pbca*	$P2_1/n$[c]	$P2_1/c$	$P\bar{1}$
a, Å	7.3427 (8)	6.1007 (5)	8.2775 (9)	9.0873 (8)
b, Å	27.078 (4)	20.1851 (8)	15.4055 (8)	10.2776 (7)
c, Å	12.682 (2)	10.2303 (9)	15.7558 (19)	11.0240 (8)
α, deg	90	90	90	65.974 (7)
β, deg	90	93.284 (4)	103.908 (5)	66.451 (6)
γ, deg	90	90	90	76.959 (6)
V, Å^3	2521.5 (6)	1257.7 (2)	1950.2 (3)	859.6 (1)
Z	8	4	4	2
D_{calcd}, g cm^{-3}	1.539	1.437	1.333	1.573
F(000)	1200	568	824	416
cryst dimens, mm	0.30 × 0.14 × 0.47	0.34 × 0.36 × 0.44	0.24 × 0.25 × 0.31	0.11 × 0.43 × 0.43
μ(Mo Kα), cm^{-1}	12.96	12.93	8.56	27.81
transmission factors	0.66-0.84	0.61-0.69	0.80-0.83	0.51-0.77
scan type	ω-2θ	ω-θ	ω-$^4/_3\theta$	ω-2θ
ω scan speed, deg min^{-1}	1.00	1.55-10.06	1.34-10.06	1.34-10.06
scan range (deg in ω)[d]	0.80 + 0.35 tan θ	0.65 + 0.35 tan θ	0.65 + 0.35 tan θ	0.60 + 0.35 tan θ
data collected	*h*,*k*,*l*	*h*,*k*,±*l*	±*h*,*k*,*l*	*h*,±*k*,±*l*
$2\theta_{max}$, deg	50	60	55	60
cryst decay	negligible	7.9%	negligible	negligible
unique reflctns	2236	3664	4459	4989
observed reflctns	1544	2427	2730	3404
no. of variables	216	213	330	296
R(observed reflctns)	0.045	0.036	0.030	0.024
R_w(observed reflctns)	0.062	0.050	0.034	0.030
R(all data)		0.067	0.058	0.052
error in observn of unit weight		1.000	1.938	1.329

[a] Temperature 21 ± 1 °C; Mo Kα radiation, graphite monochromator, λ = 0.709 30 Å (α_1), 0.713 59 Å (α_2); function minimized: $\Sigma w(|F_o| - |F_c|)^2$, $R = \Sigma||F_o| - |F_c||/\Sigma|F_o|$, $R_w = (\Sigma w(|F_o| - |F_c|)^2)^{1/2}$, $w = 1/(\sigma^2(F) + 0.0004F^2)$ for **3** and $w = 1/\sigma^2(F)$. $\sigma^2(I) = S + 2B + [0.04(S - B)]^2$ (S = scan count; B = background count) for **4**, **7**, and **9**. [b] Lattice constants refer to reduced cell. [c] Nonstandard setting of $P2_1/c$, equivalent positions ±(x, y, z; $^1/_2 - x$, $^1/_2 + y$, $^1/_2 - z$). [d] For **4**, **7** and **9** the scan range was extended by 25% on each side for background measurement.

dependent data were measured and processed for **4**, **7**, and **9**, respectively. Of these, 2427, 2730, and 3404 had $I > 3\sigma(I)$ and were used in the solution and refinement of the structures. Absorption corrections were applied to all four data sets, transmission factor ranges appearing in Table I.

The structures were all solved by conventional heavy-atom techniques; all atoms (including hydrogen) not located from the Patterson function were positioned from successive difference maps. In the case of **9**, the centrosymmetric space group $P\bar{1}$ was indicated by the Patterson function and was verified by the subsequent successful refinement. All non-hydrogen atoms were refined with anisotropic thermal parameters and hydrogen atoms with isotropic thermal parameters. An extinction parameter[25] was included in the refinement of **3**. Neutral-atom scattering factors and anomalous scattering corrections (for As, Fe, and P) were taken from ref 26.

Maximum parameter shifts on the last cycles of refinement corresponded to 0.10σ, 0.28σ, 1.8σ, and 1.1σ for **3**, **4**, **7**, and **9**, respectively; for **7** and **9** the maximum shifts were associated with hydrogen atom parameters, those for non-hydrogen atoms all being less than 0.10σ. Final difference maps showed no unusual features. Refinement of **3** was by block-diagonal (Gauss-Siedel) least squares. All calculations for **3** involved computer programs[27] run on an in-house PDP-8e computer. Full-matrix least-squares refinement was employed for **4**, **7**, and **9**, calculations being performed on an Amdahl 470/V8 computer using programs listed in ref 28. Final positional and isotropic (or equivalent isotropic, U_{eq} = 1/3 trace U) thermal parameters are given for **3**, **4**, **7**, and **9** in Tables II–V, respectively. Anisotropic thermal parameters (Tables VI–IX) and measured and calculated structure factors for the four structures are included as supplementary material.

Table II. Final Positional (Fractional, ×10^4; Fe and P, ×10^5; H, ×10^3) and Isotropic Thermal Parameters (U × 10^3 Å^2) with Estimated Standard Deviations in Parentheses for 1,1'-Ferrocenediylphenylphosphine (**3**)

atom	*x*	*y*	*z*	U_{eq}/U_{iso}
Fe	21415 (9)	7520 (2)	49700 (4)	44
P	46793 (16)	13839 (4)	40731 (9)	49
C(1)	2820 (6)	995 (2)	3549 (3)	49
C(2)	3060 (7)	467 (2)	3603 (3)	58
C(3)	1351 (8)	248 (2)	3835 (3)	67
C(4)	55 (7)	624 (2)	3900 (3)	62
C(5)	926 (6)	1076 (2)	3729 (3)	51
C(6)	3998 (6)	1234 (2)	5441 (3)	48
C(7)	4454 (6)	749 (2)	5824 (4)	58
C(8)	3039 (8)	578 (2)	6476 (3)	68
C(9)	1700 (7)	946 (2)	6521 (3)	63
C(10)	2264 (6)	1352 (2)	5897 (3)	49
C(11)	3743 (6)	1996 (2)	3879 (3)	47
C(12)	3910 (6)	2369 (2)	4637 (3)	52
C(13)	3338 (6)	2844 (2)	4416 (4)	60
C(14)	2613 (6)	2959 (2)	3453 (4)	62
C(15)	2419 (7)	2598 (2)	2702 (4)	60
C(16)	2982 (6)	2120 (2)	2908 (3)	53
H(2)	414 (5)	29 (1)	356 (3)	42 (10)
H(3)	136 (6)	−6 (1)	391 (3)	71 (13)
H(4)	−120 (5)	59 (1)	408 (3)	61 (12)
H(5)	48 (6)	139 (1)	381 (3)	61 (12)
H(7)	551 (5)	60 (2)	564 (3)	64 (12)
H(8)	304 (6)	23 (1)	678 (3)	70 (14)
H(9)	60 (5)	94 (1)	688 (3)	62 (12)
H(10)	166 (4)	163 (1)	576 (2)	34 (9)
H(12)	433 (5)	229 (1)	529 (3)	42 (10)
H(13)	356 (6)	312 (2)	495 (2)	59 (13)
H(14)	223 (5)	328 (1)	328 (3)	56 (12)
H(15)	190 (6)	268 (2)	211 (4)	82 (15)
H(16)	284 (5)	188 (1)	235 (3)	60 (12)

Bond lengths and angles for the four structures are given in Tables X and XI, respectively. Important structural parameters for **3**,

(25) Zachariasen, W. H. *Acta Crystallogr.* **1967**, *23*, 558.
(26) "International Tables for X-ray Crystallography"; Kynoch Press: Birmingham; 1974; Vol. IV.
(27) Larson, A. C.; Gabe, E. J. "Computing in Crystallography"; Schenk, H., et al., Eds.; Delft University Press: Holland, 1978.
(28) Fryzuk, M. D.; MacNeil, P. A.; Rettig, S. J.; Secco, A. S.; Trotter, J. *Organometallics* **1982**, *1*, 918.

Table III. Final Positional (Fractional, $\times 10^4$; Fe and P, $\times 10^5$; H, $\times 10^3$) and Isotropic Thermal Parameters ($U \times 10^3$ Å^2) with Estimated Standard Deviations in Parentheses for 1,1′-Ferrocenediyl-*tert*-butylphosphine (4)

atom	*x*	*y*	*z*	U_{eq}/U_{iso}
Fe	21270 (7)	45294 (2)	30336 (4)	32
P	38307 (14)	36407 (5)	13059 (10)	43
C(1)	2350 (6)	4440 (2)	1116 (3)	40
C(2)	129 (6)	4584 (2)	1414 (3)	45
C(3)	87 (7)	5209 (2)	2059 (4)	50
C(4)	2243 (7)	5458 (2)	2165 (4)	52
C(5)	3644 (7)	5008 (2)	1582 (4)	48
C(6)	3193 (6)	3604 (2)	3054 (4)	45
C(7)	1073 (7)	3641 (2)	3587 (4)	49
C(8)	1174 (8)	4057 (2)	4717 (4)	57
C(9)	3365 (8)	4280 (2)	4909 (4)	56
C(10)	4605 (7)	4007 (2)	3916 (4)	50
C(11)	2247 (6)	2972 (2)	408 (4)	46
C(12)	2985 (11)	3007 (3)	−998 (5)	71
C(13)	3043 (10)	2326 (2)	1052 (6)	67
C(14)	−244 (8)	3005 (3)	372 (7)	69
H(2)	−121 (8)	430 (2)	120 (5)	70 (14)
H(3)	−120 (7)	541 (2)	239 (4)	50 (11)
H(4)	256 (8)	583 (3)	251 (5)	73 (15)
H(5)	524 (7)	504 (2)	148 (4)	47 (11)
H(7)	−18 (6)	344 (2)	324 (4)	41 (10)
H(8)	−10 (8)	417 (2)	519 (5)	71 (15)
H(9)	399 (7)	453 (2)	561 (5)	65 (13)
H(10)	593 (6)	410 (2)	381 (3)	32 (9)
H(12a)	467 (10)	298 (2)	−106 (5)	83 (16)
H(12b)	224 (11)	265 (4)	−151 (7)	126 (24)
H(12c)	254 (10)	338 (3)	−135 (6)	94 (21)
H(13a)	255 (11)	230 (4)	207 (7)	131 (25)
H(13b)	246 (9)	201 (3)	67 (6)	86 (18)
H(13c)	457 (8)	230 (2)	111 (5)	65 (14)
H(14a)	−71 (10)	297 (3)	120 (6)	97 (21)
H(14b)	−79 (8)	339 (3)	−6 (5)	66 (15)
H(14c)	−89 (8)	260 (3)	−17 (5)	83 (16)

4, **7**, and **9**, are compared with those of other [1] ferrocenophanes in Table XII. Bond distances and angles involving hydrogen atoms and torsion angles (Tables XIII–XXIII) are included as supplementary material.

Results and Discussion

The previously known [1]ferrocenophanes **3** and **5** were prepared from 1,1′-dilithioferrocene by the literature procedure (eq 3, R^1 = H, X_2ER^2 = I_2AsPh, Cl_2PPh). A

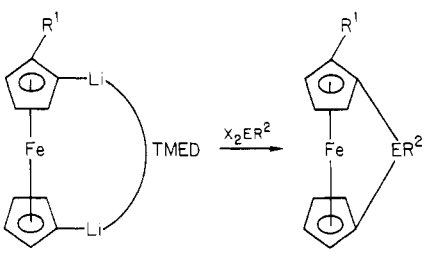

10

3, R^1 = H, R^2 = Ph, E = P
4, R^1 = H, R^2 = *t*-Bu, E = P
5, R^1 = H, R^2 = Ph, E = As
6, R^1 = CH(Me)NMe_2, R^2 = Ph, E = P
7, R^1 = CH($CHMe_2$)NMe_2, R^2 = Ph, E = P
8, R^1 = CH(Me)NMe_2, R^2 = *t*-Bu, E = P
9, R^1 = CH(Me)NMe_2, R^2 = Ph, E = As

simple extension using Cl_2P-*t*-Bu allows the isolation of the previously unknown **4**. Best yields are obtained when the isolated TMED adduct is used. An excess of X_2ER^2 should be avoided because of a reaction of this with the ferrocenophane product.

Table IV. Final Positional (Fractional, $\times 10^4$; Fe and P, $\times 10^5$; H, $\times 10^3$) and Isotropic Thermal Parameters ($U \times 10^3$ Å^2) with Estimated Standard Deviations in Parentheses for [2-(α-(Dimethylamino)-β-methylpropyl)-1,1′-ferrocenediyl]phenylphosphine (7)

atom	*x*	*y*	*z*	U_{eq}/U_{iso}
Fe	33666 (4)	28659 (2)	35932 (2)	33
P	53454 (8)	41943 (4)	44538 (4)	32
N	5670 (3)	4614 (1)	1948 (1)	43
C(1)	5552 (3)	3388 (1)	3599 (1)	30
C(2)	4474 (3)	3479 (2)	2721 (1)	31
C(3)	4019 (3)	2621 (2)	2415 (2)	37
C(4)	4794 (4)	2018 (2)	3061 (2)	44
C(5)	5748 (3)	2480 (2)	3782 (2)	38
C(6)	3435 (3)	3654 (2)	4604 (2)	38
C(7)	1947 (3)	3823 (2)	3933 (2)	41
C(8)	976 (3)	3057 (2)	3772 (2)	51
C(9)	1798 (4)	2411 (2)	4346 (2)	55
C(10)	3302 (4)	2763 (2)	4857 (2)	45
C(11)	6984 (3)	3835 (2)	5384 (2)	34
C(12)	6725 (3)	3658 (2)	6200 (2)	41
C(13)	8052 (4)	3459 (2)	6892 (2)	48
C(14)	9645 (4)	3438 (2)	6783 (2)	54
C(15)	9922 (4)	3624 (2)	5976 (2)	61
C(16)	8615 (3)	3823 (2)	5282 (2)	52
C(17)	4158 (3)	4323 (2)	2212 (2)	34
C(18)	7021 (4)	4883 (3)	2659 (2)	54
C(19)	6277 (5)	4012 (3)	1382 (3)	66
C(20)	2677 (3)	4283 (2)	1399 (2)	42
C(21)	1031 (4)	4136 (3)	1645 (2)	61
C(22)	2563 (5)	5116 (3)	849 (3)	68
H(3)	331 (4)	251 (2)	188 (2)	48 (8)
H(4)	467 (3)	143 (2)	298 (2)	43 (7)
H(5)	638 (3)	223 (1)	432 (1)	23 (6)
H(7)	174 (3)	435 (2)	365 (2)	40 (8)
H(8)	−11 (3)	303 (2)	339 (2)	44 (7)
H(9)	134 (4)	185 (2)	444 (2)	64 (9)
H(10)	403 (3)	247 (2)	524 (2)	27 (6)
H(12)	556 (4)	366 (2)	632 (2)	51 (8)
H(13)	786 (4)	330 (2)	744 (2)	74 (10)
H(14)	1055 (4)	334 (2)	727 (2)	66 (9)
H(15)	1102 (4)	362 (2)	589 (2)	48 (8)
H(16)	882 (4)	394 (2)	476 (2)	78 (11)
H(17)	395 (2)	479 (1)	260 (1)	17 (5)
H(18a)	669 (4)	523 (2)	301 (2)	60 (11)
H(18b)	736 (4)	518 (2)	247 (2)	50 (8)
H(18c)	765 (4)	444 (2)	302 (2)	65 (10)
H(19a)	538 (5)	393 (2)	91 (3)	83 (13)
H(19b)	724 (5)	427 (2)	123 (2)	81 (11)
H(19c)	668 (4)	349 (2)	171 (2)	76 (12)
H(20)	283 (3)	384 (2)	107 (2)	29 (7)
H(21a)	14 (4)	408 (2)	113 (2)	75 (11)
H(21b)	101 (3)	362 (2)	202 (2)	61 (9)
H(21c)	89 (4)	462 (2)	205 (2)	69 (11)
H(22a)	171 (4)	507 (2)	32 (2)	65 (9)
H(22b)	243 (5)	557 (3)	130 (3)	106 (15)
H(22c)	349 (5)	517 (3)	68 (2)	92 (14)

The monolithiation of α-dimethylamino ferrocenes is well-known to be stereospecific. Dilithiation easily affords the substituted 1,1′-dilithioferrocenes **6b** and **7b** (**10**, R = CH(Me)NMe_2, CH($CHMe_2$)NMe_2) which can be isolated as TMED adducts. These compounds also react as shown in eq 3, giving the substituted ferrocenophanes **6**–**9**.

The reaction of these ferrocenophanes have been investigated according to the scheme shown in eq 2. This chemistry and the use of the derived ligands in catalytic hydrogenation reactions will be described in forthcoming publications.

The remainder of this paper is concerned with a description of the structures of a representative selection of the ferrocenophanes.

The crystal structures of **3**, **4**, **7**, and **9** each consist of discrete molecules separated by normal van der Waals

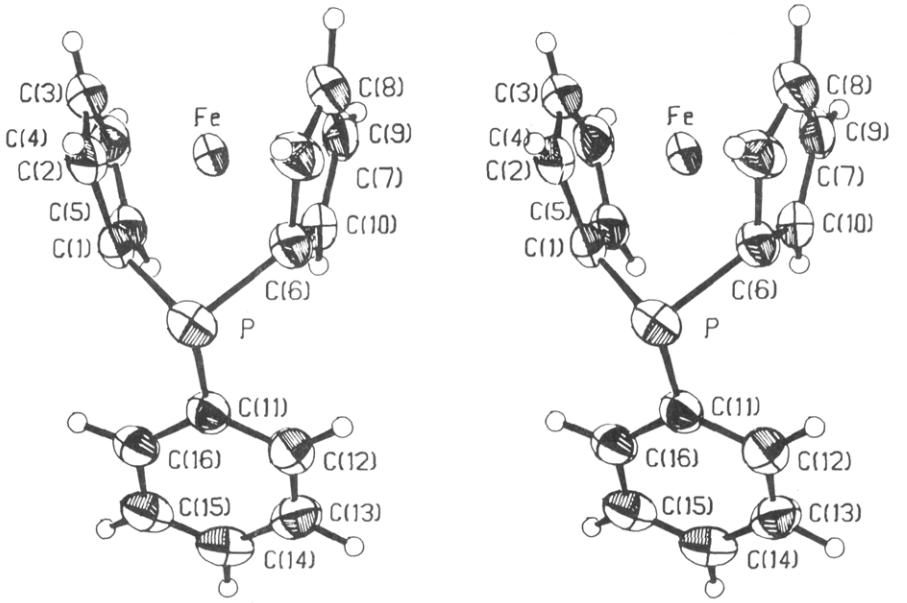

Figure 1. Stereoview of the structure of the ferrocenophane **3**.

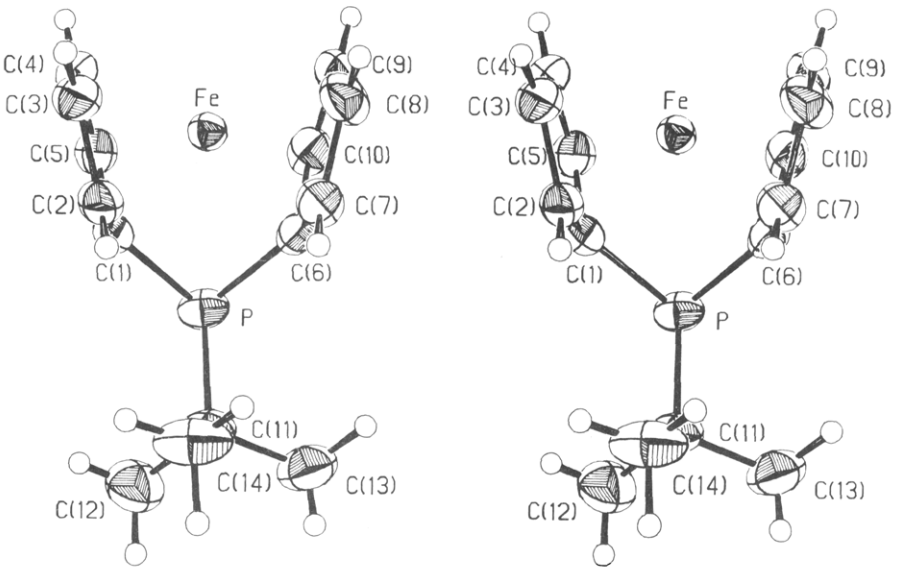

Figure 2. Stereoview of the structure of the ferrocenophane **4**.

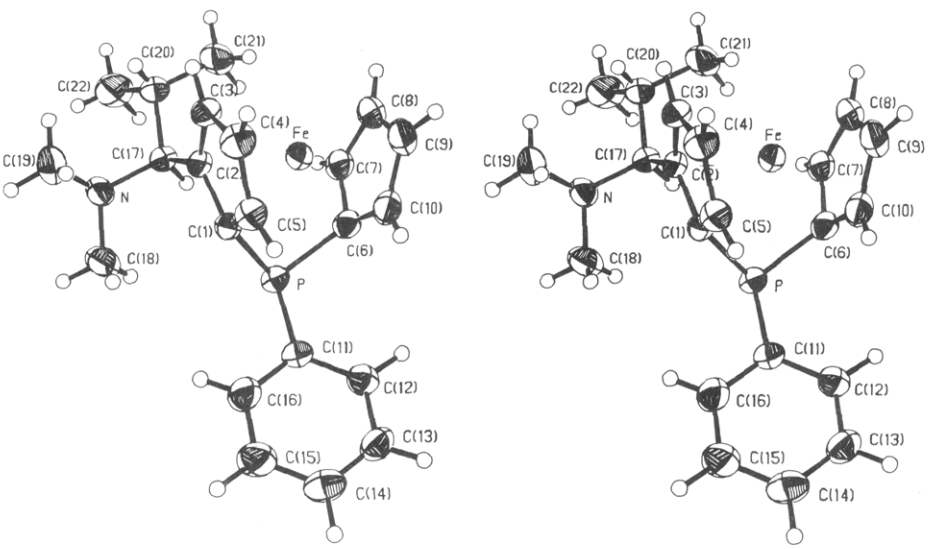

Figure 3. Stereoview of the structure of the ferrocenophane **7**.

distances. Stereoscopic views of the four molecules are shown in Figure 1–4. The unsubstituted molecules **3** and **4** have approximate mirror symmetry, the plane of symmetry containing atoms Fe, P, and C(11).

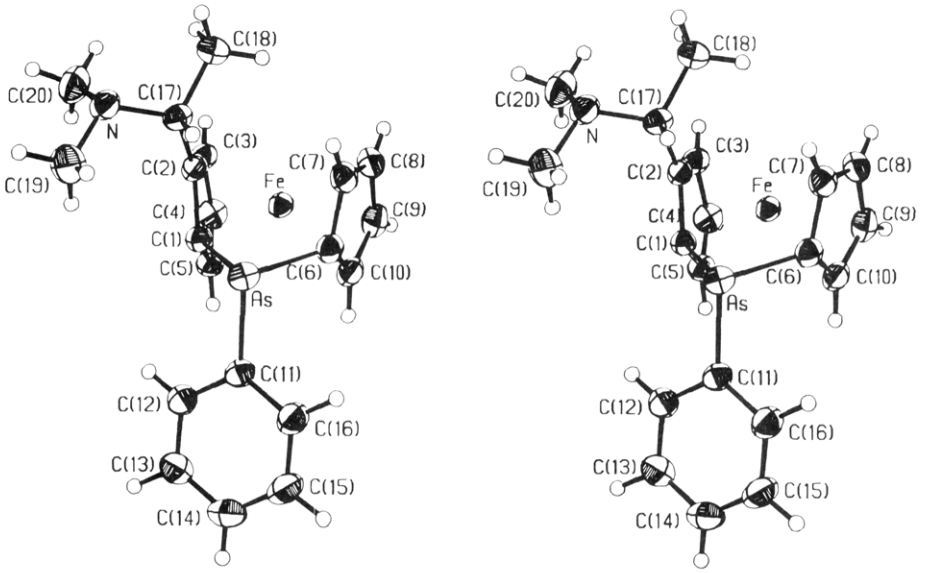

Figure 4. Stereoview of the structure of the ferrocenophane **9**.

Table V. Final Positional (Fractional, ×10⁴; As and Fe, ×10⁵; H, ×10³) and Isotropic Thermal Parameters ($U \times 10^3$ Å²) with Estimated Standard Deviations in Parentheses for [2-(α-(Dimethylamino)ethyl)-1,1′-ferrocenediyl]phenylarsine (9)

atom	*x*	*y*	*z*	U_{eq}/ U_{iso}
As	59259 (2)	40160 (2)	70728 (2)	33
Fe	74152 (3)	15753 (3)	62550 (3)	30
N	2049 (2)	1856 (2)	7473 (2)	40
C(1)	5580 (2)	1948 (2)	7873 (2)	30
C(2)	4988 (2)	1414 (2)	7130 (2)	30
C(3)	5768 (2)	33 (2)	7210 (2)	35
C(4)	6830 (3)	−311 (2)	7977 (2)	39
C(5)	6716 (2)	861 (2)	8381 (2)	35
C(6)	7885 (2)	3619 (2)	5571 (2)	35
C(7)	7603 (3)	3356 (2)	4494 (2)	40
C(8)	8762 (3)	2278 (3)	4113 (2)	44
C(9)	9788 (3)	1874 (3)	4920 (2)	46
C(10)	9252 (2)	2682 (2)	5817 (2)	40
C(11)	6815 (2)	4104 (2)	8374 (2)	34
C(12)	6161 (3)	3351 (2)	9820 (2)	41
C(13)	6638 (3)	3565 (3)	10768 (2)	48
C(14)	7759 (3)	4539 (3)	10286 (3)	50
C(15)	8398 (3)	5286 (3)	8863 (3)	51
C(16)	7948 (3)	5069 (2)	7904 (2)	43
C(17)	3702 (2)	2168 (2)	6473 (2)	34
C(18)	3964 (3)	1871 (3)	5152 (2)	47
C(19)	1564 (4)	2469 (4)	8570 (3)	63
C(20)	1746 (3)	354 (3)	8100 (3)	56
H(3)	565 (3)	−41 (3)	681 (3)	47 (7)
H(4)	749 (3)	−125 (3)	828 (3)	48 (6)
H(5)	722 (3)	91 (3)	890 (3)	46 (6)
H(7)	676 (3)	377 (3)	416 (3)	43 (6)
H(8)	894 (4)	187 (3)	353 (3)	54 (8)
H(9)	1074 (3)	113 (3)	488 (3)	39 (6)
H(10)	971 (3)	267 (3)	646 (3)	57 (8)
H(12)	540 (3)	277 (2)	1012 (2)	36 (5)
H(13)	606 (4)	315 (3)	1178 (3)	49 (8)
H(14)	806 (3)	467 (3)	1091 (3)	55 (8)
H(15)	919 (3)	592 (3)	851 (3)	57 (7)
H(16)	840 (3)	560 (3)	687 (3)	56 (7)
H(17)	370 (3)	323 (3)	620 (3)	52 (7)
H(18a)	381 (3)	86 (3)	537 (3)	53 (7)
H(18b)	507 (4)	212 (4)	445 (4)	83 (10)
H(18c)	310 (4)	234 (3)	473 (3)	62 (8)
H(19a)	222 (4)	199 (3)	922 (3)	65 (8)
H(19b)	40 (5)	241 (4)	911 (4)	81 (10)
H(19c)	164 (4)	346 (4)	810 (3)	66 (8)
H(20a)	204 (4)	−7 (4)	740 (4)	87 (11)
H(20b)	227 (4)	−29 (4)	879 (4)	83 (10)
H(20c)	67 (5)	27 (4)	854 (4)	83 (10)

Table X. Bond Lengths (Å) for 3, 4, 7, and 9 with Estimated Standard Deviations in Parentheses (E = P or As)

bond	3	4	7	9
Fe-C(1)	1.982 (4)	1.983 (3)	1.978 (2)	2.000 (2)
Fe-C(2)	2.014 (4)	2.003 (3)	2.056 (2)	2.039 (2)
Fe-C(3)	2.067 (4)	2.069 (4)	2.089 (3)	2.077 (2)
Fe-C(4)	2.076 (5)	2.078 (4)	2.069 (3)	2.075 (2)
Fe-C(5)	2.011 (4)	2.038 (4)	2.011 (3)	2.014 (2)
Fe-C(6)	1.979 (4)	1.978 (4)	1.992 (2)	2.005 (2)
Fe-C(7)	2.014 (4)	1.998 (4)	2.036 (3)	2.033 (2)
Fe-C(8)	2.075 (4)	2.081 (4)	2.086 (3)	2.073 (2)
Fe-C(9)	2.062 (4)	2.083 (4)	2.080 (3)	2.075 (2)
Fe-C(10)	2.007 (4)	2.015 (4)	2.011 (3)	2.020 (2)
E-C(1)	1.849 (5)	1.854 (3)	1.870 (2)	1.987 (2)
E-C(6)	1.850 (5)	1.854 (3)	1.851 (2)	1.986 (2)
E-C(11)	1.811 (4)	1.870 (4)	1.827 (2)	1.946 (2)
C(1)-C(2)	1.443 (6)	1.435 (5)	1.462 (3)	1.453 (2)
C(1)-C(5)	1.426 (6)	1.456 (5)	1.431 (4)	1.436 (3)
C(2)-C(3)	1.419 (7)	1.424 (5)	1.427 (3)	1.421 (3)
C(3)-C(4)	1.396 (8)	1.406 (6)	1.412 (4)	1.422 (3)
C(4)-C(5)	1.399 (7)	1.405 (6)	1.410 (4)	1.416 (3)
C(6)-C(7)	1.440 (6)	1.434 (6)	1.440 (3)	1.444 (3)
C(6)-C(10)	1.435 (7)	1.447 (5)	1.441 (4)	1.435 (3)
C(7)-C(8)	1.406 (7)	1.427 (6)	1.416 (4)	1.418 (3)
C(8)-C(9)	1.401 (8)	1.414 (6)	1.406 (5)	1.421 (3)
C(9)-C(10)	1.415 (6)	1.413 (6)	1.418 (4)	1.417 (3)
C(11)-C(12)	1.398 (6)	1.532 (6)	1.381 (4)	1.392 (3)
C(11)-C(16)	1.393 (6)		1.397 (4)	1.389 (3)
C(12)-C(13)	1.382 (6)		1.383 (3)	1.386 (3)
C(13)-C(14)	1.369 (7)		1.371 (4)	1.385 (3)
C(14)-C(15)	1.372 (7)		1.375 (4)	1.372 (4)
C(15)-C(16)	1.385 (6)		1.376 (4)	1.383 (3)
C(11)-C(13)		1.529 (6)		
C(11)-C(14)		1.520 (6)		
N-C(17)			1.480 (3)	1.477 (3)
N-C(18/20)			1.441 (4)	1.452 (3)
N-C(19)			1.457 (4)	1.457 (3)
C(2)-C(17)			1.517 (3)	1.517 (2)
C(17)-C(20/18)			1.547 (3)	1.524 (3)
C(20)-C(21)			1.520 (4)	
C(20)-C(22)			1.538 (4)	

The geometry of the bridged ferrocene moiety in each of the three phosphorus-bridged species is essentially the same as that reported earlier for **3**.[14] The parameters listed in Table XII are virtually identical for **3** and **4**, the only significant difference being the shorter Fe···P distance in **4**, a result consistent with the slightly larger value of β in **4**. In the substituted molecule **7** the values of $\bar{\beta}$ and θ are slightly larger than those in **3** and **4** resulting in a small

Table XI. Bond Angles (deg) for 3, 4, 7, and 9 with Estimated Standard Deviations in Parentheses (E = P or As)

atoms	3	4	7	9
C(1)-E-C(6)	90.7 (2)	90.48 (15)	91.28 (10)	87.90 (7)
C(1)-E-C(11)	101.1 (2)	110.0 (2)	101.43 (11)	100.13 (7)
C(6)-E-C(11)	103.1 (2)	108.3 (2)	104.73 (11)	102.34 (8)
E-C(1)-C(2)	117.2 (3)	127.9 (3)	118.5 (2)	117.54 (13)
E-C(1)-C(5)	125.1 (3)	113.5 (3)	122.0 (2)	122.56 (13)
C(2)-C(1)-C(5)	105.4 (4)	105.8 (3)	107.4 (2)	106.9 (2)
C(1)-C(2)-C(3)	108.4 (4)	108.6 (3)	106.4 (2)	107.21 (15)
C(1)-C(2)-C(17)			124.8 (2)	125.8 (2)
C(3)-C(2)-C(17)			128.2 (2)	126.9 (2)
C(2)-C(3)-C(4)	108.1 (4)	108.1 (4)	109.2 (2)	109.3 (2)
C(3)-C(4)-C(5)	108.5 (4)	108.9 (4)	108.6 (2)	107.6 (2)
C(4)-C(5)-C(1)	109.6 (4)	108.5 (4)	108.4 (2)	109.0 (2)
E-C(6)-C(7)	117.0 (3)	127.5 (3)	115.6 (2)	115.62 (14)
E-C(6)-C(10)	124.7 (3)	114.5 (3)	126.0 (2)	124.85 (14)
C(7)-C(6)-C(10)	105.9 (4)	104.9 (4)	105.5 (2)	106.3 (2)
C(6)-C(7)-C(8)	109.0 (4)	109.9 (4)	109.2 (3)	108.6 (2)
C(7)-C(8)-C(9)	108.0 (4)	107.3 (4)	108.0 (3)	108.1 (2)
C(8)-C(9)-C(10)	108.9 (4)	108.5 (4)	108.5 (3)	108.2 (2)
C(9)-C(10)-C(6)	108.2 (4)	109.4 (4)	108.8 (3)	108.8 (2)
E-C(11)-C(12)	112.2 (3)	104.9 (3)	123.7 (2)	120.22 (15)
E-C(11)-C(16/13)	119.5 (3)	105.2 (3)	117.6 (2)	120.28 (15)
P-C(11)-C(14)		118.0 (3)		
C(12)-C(11)-C(16/13)	118.0 (4)	109.9 (4)	118.4 (2)	118.9 (2)
C(12)-C(11)-C(14)		108.8 (4)		
C(13)-C(11)-C(14)		109.9 (4)		
C(11)-C(12)-C(13)	120.4 (4)		120.4 (2)	120.3 (2)
C(12)-C(13)-C(14)	120.8 (4)		120.8 (3)	120.2 (2)
C(13)-C(14)-C(15)	119.8 (4)		119.4 (3)	119.5 (2)
C(14)-C(15)-C(16)	120.3 (4)		120.5 (3)	120.9 (2)
C(15)-C(16)-C(11)	120.8 (4)		120.6 (3)	120.2 (2)
C(17)-N-C(20/18)			114.8 (2)	114.7 (2)
C(17)-N-C(19)			114.7 (2)	112.3 (2)
C(19)-N-C(20/18)			110.0 (3)	110.4 (2)
N-C(17)-C(2)			111.0 (2)	113.48 (15)
N-C(17)-C(20/18)			109.6 (2)	109.4 (2)
C(2)-C(17)-C(20/18)			113.9 (2)	113.0 (2)
C(17)-C(20)-C(21)			112.0 (2)	
C(17)-C(20)-C(22)			111.2 (2)	
C(21)-C(20)-C(22)			109.3 (3)	

Table XII. Selected Structural Data for [1]Ferrocenophanes [(η^5-C_5H_4)(η^5-C_5H_3R)Fe]X

	a	*b*	3[b]	3[c]	4[c]	7[c]	9[c]
X	$Si(C_6H_5)_2$	$Ge(C_6H_5)_2$	PC_6H_5	PC_6H_5	P(*t*-C_4H_9)	PC_6H_5	AsC_6H_5
R	H	H	H	H	H	$CH[N(CH_3)_2]C_3H_7$	$CH(CH_3)N(CH_3)_2$
mean Fe-Cp[d]	1.65	1.63	1.63	1.632 (3)	1.631 (2)	1.642 (2)	1.641 (1)
mean Fe-C	2.054	2.029	2.028	2.029	2.033	2.041	2.041
Fe···X[e]	2.636 (5)	2.744 (3)	2.774 (3)	2.774 (1)	2.763 (1)	2.764 (1)	2.8760 (3)
C(1)···C(6)	2.86 (1)	2.858 (14)	2.619 (12)	2.632 (6)	2.633 (5)	2.661 (3)	2.758 (3)
Cp-Fe-Cp	167	170	160	159.8	159.8	160.1	162.5
α[f]	19.2	16.6	26.7	26.9	27.1	27.0	22.9
$\bar{\beta}$[f]	40	38	32.5	32.3	32.8	33.1	32.8
θ[f]	99.1 (3)	93.6 (4)	90.6 (3)	90.7 (2)	90.5 (2)	91.3 (1)	87.90 (7)
mean Fe-C(1,6)	2.014 (11)	2.001 (14)	1.979 (4)	1.981 (2)	1.980 (3)	1.985 (7)	2.002 (3)
mean Fe-C(2,5,7,10)	2.030 (7)	2.031 (13)	2.013 (8)	2.012 (3)	2.014 (17)	2.029 (12)	2.026 (12)
mean Fe-C(3,4,8,9)	2.098 (16)	2.042 (7)	2.067 (14)	2.070 (7)	2.078 (6)	2.081 (9)	2.075 (2)

[a] Reference 18. [b] Reference 14. [c] This work. [d] Cp refers to centroid of cyclopentadienyl ring. [e] X refers to bridging atom here. [f] Defined in ref 14: α = tilt angle between Cp rings, $\bar{\beta}$ = mean angle between Cp plane and Cp-X bond, and θ = C(1)-X-C(6).

but significant increase in the C(1)···C(6) separation. The Fe···P distances in **4** and **7** are equal.

The mean Fe–Cp distances for all of the complexes listed in Table XVIII are near the expected value of 1.64 Å.[14] It is noteworthy, however, that the mean Fe–Cp distances in the two substituted complexes **7** and **9** are slightly longer than those in the unsubstituted molecules **3** and **4**. The arsine complex **9** displays structural parameters (Table XII) which are more similar to those of the phosphine analogues than to the germanium derivative even though the covalent radii of As and Ge are nearly identical. Strain is thus relieved in different ways in these compounds. In the silicon and germanium analogues the $\bar{\beta}$ values are large, indicating that most of the strain occurs at atoms C(1) and C(6). The phosphorus and arsenic derivatives have smaller (and in fact equal) values of $\bar{\beta}$, additional strain being compensated for by larger ring tilts (α) and smaller bridgehead angles θ. The smaller values of θ for the phosphorus and arsenic compounds are a result of the presence of the lone pair of electrons, bond angles at tervalent P or As commonly being substantially less than the tetrahedral angle. The θ angle in **9** at 87.90 (7)° is the smallest yet observed for a [1]ferrocenophane and the Fe···As distance of 2.8760 (3) Å the longest distance between the iron and the bridging atom. The most significant difference between the phosphorus and arsenic compounds is in the ring tilt α, the value of 22.9° observed for the arsine being intermediate between the mean of 27.0

(1)° for the phosphorus-bridged and the values of 19.2 and 16.6° for the silicon- and germanium-bridged analogues, respectively. The C(1)···C(6) distance and the Cp–Fe–Cp angle in **9** are also intermediate between the corresponding values observed for the phosphorus and the silicon/germanium derivatives (see Table XII).

The cyclopentadienyl and phenyl rings in all four compounds are planar to within ±0.01 Å although seven of the eleven rings exhibit statistically significant deviations from planarity (χ^2 values for the C(1) and C(6) cyclopentadienyl rings are 11.7 and 2.3 for **3**, 16.6 and 3.9 for **4**, 38.0 and 26.0 for **7**, and 0.4 and 13.6 for **9**; χ^2 = 4.3, 15.0, and 11.5, respectively, for the phenyl rings in **3**, **7**, and **9**). The mean displacements of the P or As atoms from the mean planes of the cyclopentadienyl rings are 0.988 (1), 1.004 (4), 1.015 (6), and 1.075 (4) Å for **3**, **4**, **7**, and **9**, respectively. The mean libration-corrected[29,30] distance in the cyclopentadienyl rings of 1.428 Å is in excellent agreement with the accepted value of 1.429 Å.[31] The cyclopentadienyl rings all display substituent-induced geometrical distortions, the mean bond length involving the P- or As-substituted carbon atom being 1.445 (9) Å, adjacent C–C bonds averaging 1.419 (8) Å, and the unique bonds (across the ring from the substituted atom) averaging 1.414 (9) Å. The pattern of C–C bond length variation in the 1,2-disubstituted cyclopentadienyl rings differs somewhat (see Table X), the longest distances (1.464 (3) Å in **7**, and 1.445 (2) A in **9**) being between the substituted carbon atoms. Ring bond angles at the substituted carbon atoms are contracted from the "ideal" 108.0° to 104.9 (4)–106.3 (2)° for monosubstituted 106.4 (2)–107.4 (2)° for disubstituted rings with corresponding increases in the angles at the unsubstituted carbons. Substituent-induced ring distortions for the P- and As-substituted phenyl rings are as expected.[32]

The mean bond angles at phosphorus are 98.3, 102.9, and 99.2° in **3**, **4**, and **7**, respectively, and the mean angle at As in **9** is 96.8°, all of these values being substantially smaller than the tetrahedral angle (vide supra). The mean angles at nitrogen (113.2° for **7**, 112.5° for **9**), in contrast, are larger than the tetrahedral angle, indicating some delocalization of the lone pair.

Acknowledgment. Computing funds for the structure analyses of **4**, **7**, and **9** were provided by grants from the Xerox Corp. of Canada and the U.B.C. Computing Centre. Financial assistance in the form of operating grants from NSERC, Canada, to W.R.C. and F.W.B.E. is gratefully acknowledged.

Registry No. **3**, 72954-06-4; **4**, 83547-83-5; **5**, 72954-08-6; **6**, 83560-65-0; **6a**, 31904-34-4; **6b**, 83547-84-6; **7**, 83547-85-7; **7a**, 83601-98-3; **7b**, 83560-64-9; **8**, 83547-86-8; **9**, 83547-87-9; TMED, 110-18-9; *tert*-butyldichlorophosphine, 25979-07-1; *As,As*-diiodophenylarsine, 6380-34-3; *P,P*-dichlorophenylphosphine, 644-97-3.

Supplementary Material Available: Tables of anisotropic thermal parameters, measured and calculated thermal parameters, bond distances and angles involving hydrogen atoms and torsion angles, and structure factor amplitudes (Tables VI–IX and XIII–XXIII) (77 pages). Ordering information is given on any current masthead page.

(29) Schomaker, V.; Trueblood, K. N. *Acta Crystallogr., Sect. B* **1968**, *B24*, 63.
(30) Cruickshank, D. W. J. *Acta Crystallogr.* **1956**, *9*, 747, 754; **1961**, *14*, 896.
(31) Churchill, M. R.; Karla, K. L. *Inorg. Chem.* **1973**, *12*, 1650.
(32) Domenicano, A.; Vaciago, A.; Coulson, C. A. *Acta Crystallogr., Sect. B* **1975**, *B31*, 221, 234.

An η^2-Arene Complex of Rhenium: Synthesis, Characterization, and Activation of the Aromatic Carbon–Hydrogen Bonds

James R. Sweet and William A. G. Graham*

Department of Chemistry, University of Alberta, Edmonton, Alberta, Canada T6G 2G2

Received July 2, 1982

Investigations of a cationic η^2-arene complex of rhenium having activated aromatic carbon–hydrogen bonds are described. $[(\eta\text{-}C_5H_5)Re(NO)(CO)(3,4\text{-}\eta^2\text{-}C_6H_5CHPh_2)][PF_6]$ (**2**·PF_6) forms as yellow microcrystals from the reaction of Ph_3CPF_6 with $(\eta\text{-}C_5H_5)Re(NO)(CO)H$ in CH_2Cl_2 at −78 °C; the solid is stable at room temperature for limited periods, but solutions begin to decompose at a significant rate above −40 °C. The triphenylmethane ligand is readily displaced by PPh_3 to form $[(\eta\text{-}C_5H_5)Re(NO)(CO)(PPh_3)][PF_6]$. In CH_2Cl_2 at −78 °C, **2**·PF_6 is deprotonated by Et_3N affording para and meta isomers of $(\eta\text{-}C_5H_5)Re(NO)(CO)(\eta^1\text{-}C_6H_4CHPh_2)$. ^1H NMR spectra indicate that **2** is stereochemically nonrigid over the range studied (−40 to −70 °C). Migration of the rhenium group about the coordinated ring is proposed to occur via intermediate η^1-arenium structures, a model related to that of electrophilic aromatic substitution. Formation of these intermediates in solution accounts for activation of the carbon–hydrogen bonds toward deprotonation.

Arene molecules coordinated in η^2 fashion to a transition metal have often been suggested as intermediates in the activation of carbon–hydrogen bonds or other catalytic processes.[1] The η^2-arene bonding mode is well established for d^{10} metals such as Cu^+ and Ag^+,[2] and there are several examples involving transition metals with perfluoro- or perfluoroalkyl-substituted derivatives;[3] the latter cannot be regarded as typical arenes, however. The crystal structure of a (1,2-η^2-anthracene)nickel(0) complex[4] ap-

(1) References to the original literature are cited in the following reviews: (a) Parshall, G. W. *Acc. Chem. Res.* **1970**, *3*, 139. (b) *Ibid.* **1975**, *8*, 113. (c) "Homogeneous Catalysis"; Wiley: New York, 1980; Chapter 7. (d) Muetterties, E. L.; Bleeke, J. R. *Acc. Chem. Res.* **1979**, *12*, 325.
(2) Silverthorne, W. E. *Adv. Organomet. Chem.* **1975**, *13*, 47.
(3) (a) Browning, J.; Green, M.; Penfold, B. R.; Spencer, J. L.; Stone, F. G. A. *J. Chem. Soc., Chem. Commun.* **1973**, 31. (b) Cobbledick, R. E.; Einstein, F. W. B. *Acta Crystallogr., Sect. B.* **1978**, *B34*, 1849. (c) Cook, D. J.; Green, M.; Mayne, N.; Stone, F. G. A. *J. Chem. Soc. A* **1968**, 1771.

0276-7333/83/2302-0135$01.50/0

(1)° for the phosphorus-bridged and the values of 19.2 and 16.6° for the silicon- and germanium-bridged analogues, respectively. The C(1)···C(6) distance and the Cp–Fe–Cp angle in **9** are also intermediate between the corresponding values observed for the phosphorus and the silicon/germanium derivatives (see Table XII).

The cyclopentadienyl and phenyl rings in all four compounds are planar to within ±0.01 Å although seven of the eleven rings exhibit statistically significant deviations from planarity (χ^2 values for the C(1) and C(6) cyclopentadienyl rings are 11.7 and 2.3 for **3**, 16.6 and 3.9 for **4**, 38.0 and 26.0 for **7**, and 0.4 and 13.6 for **9**; χ^2 = 4.3, 15.0, and 11.5, respectively, for the phenyl rings in **3**, **7**, and **9**). The mean displacements of the P or As atoms from the mean planes of the cyclopentadienyl rings are 0.988 (1), 1.004 (4), 1.015 (6), and 1.075 (4) Å for **3**, **4**, **7**, and **9**, respectively. The mean libration-corrected[29,30] distance in the cyclopentadienyl rings of 1.428 Å is in excellent agreement with the accepted value of 1.429 Å.[31] The cyclopentadienyl rings all display substituent-induced geometrical distortions, the mean bond length involving the P- or As-substituted carbon atom being 1.445 (9) Å, adjacent C–C bonds averaging 1.419 (8) Å, and the unique bonds (across the ring from the substituted atom) averaging 1.414 (9) Å. The pattern of C–C bond length variation in the 1,2-disubstituted cyclopentadienyl rings differs somewhat (see Table X), the longest distances (1.464 (3) Å in **7**, and 1.445 (2) A in **9**) being between the substituted carbon atoms. Ring bond angles at the substituted carbon atoms are contracted from the "ideal" 108.0° to 104.9 (4)–106.3 (2)° for monosubstituted 106.4 (2)–107.4 (2)° for disubstituted rings with corresponding increases in the angles at the unsubstituted carbons. Substituent-induced ring distortions for the P- and As-substituted phenyl rings are as expected.[32]

The mean bond angles at phosphorus are 98.3, 102.9, and 99.2° in **3**, **4**, and **7**, respectively, and the mean angle at As in **9** is 96.8°, all of these values being substantially smaller than the tetrahedral angle (vide supra). The mean angles at nitrogen (113.2° for **7**, 112.5° for **9**), in contrast, are larger than the tetrahedral angle, indicating some delocalization of the lone pair.

Acknowledgment. Computing funds for the structure analyses of **4**, **7**, and **9** were provided by grants from the Xerox Corp. of Canada and the U.B.C. Computing Centre. Financial assistance in the form of operating grants from NSERC, Canada, to W.R.C. and F.W.B.E. is gratefully acknowledged.

Registry No. **3**, 72954-06-4; **4**, 83547-83-5; **5**, 72954-08-6; **6**, 83560-65-0; **6a**, 31904-34-4; **6b**, 83547-84-6; **7**, 83547-85-7; **7a**, 83601-98-3; **7b**, 83560-64-9; **8**, 83547-86-8; **9**, 83547-87-9; TMED, 110-18-9; *tert*-butyldichlorophosphine, 25979-07-1; *As,As*-diiodophenylarsine, 6380-34-3; *P,P*-dichlorophenylphosphine, 644-97-3.

Supplementary Material Available: Tables of anisotropic thermal parameters, measured and calculated thermal parameters, bond distances and angles involving hydrogen atoms and torsion angles, and structure factor amplitudes (Tables VI–IX and XIII–XXIII) (77 pages). Ordering information is given on any current masthead page.

(29) Schomaker, V.; Trueblood, K. N. *Acta Crystallogr., Sect. B* **1968**, *B24*, 63.
(30) Cruickshank, D. W. J. *Acta Crystallogr.* **1956**, *9*, 747, 754; **1961**, *14*, 896.
(31) Churchill, M. R.; Karla, K. L. *Inorg. Chem.* **1973**, *12*, 1650.
(32) Domenicano, A.; Vaciago, A.; Coulson, C. A. *Acta Crystallogr., Sect. B* **1975**, *B31*, 221, 234.

An η^2-Arene Complex of Rhenium: Synthesis, Characterization, and Activation of the Aromatic Carbon–Hydrogen Bonds

James R. Sweet and William A. G. Graham*

Department of Chemistry, University of Alberta, Edmonton, Alberta, Canada T6G 2G2

Received July 2, 1982

Investigations of a cationic η^2-arene complex of rhenium having activated aromatic carbon–hydrogen bonds are described. $[(\eta\text{-}C_5H_5)Re(NO)(CO)(3,4\text{-}\eta^2\text{-}C_6H_5CHPh_2)][PF_6]$ (**2**·PF_6) forms as yellow microcrystals from the reaction of Ph_3CPF_6 with $(\eta\text{-}C_5H_5)Re(NO)(CO)H$ in CH_2Cl_2 at −78 °C; the solid is stable at room temperature for limited periods, but solutions begin to decompose at a significant rate above −40 °C. The triphenylmethane ligand is readily displaced by PPh_3 to form $[(\eta\text{-}C_5H_5)Re(NO)(CO)(PPh_3)][PF_6]$. In CH_2Cl_2 at −78 °C, **2**·PF_6 is deprotonated by Et_3N affording para and meta isomers of $(\eta\text{-}C_5H_5)Re(NO)(CO)(\eta^1\text{-}C_6H_4CHPh_2)$. ^1H NMR spectra indicate that **2** is stereochemically nonrigid over the range studied (−40 to −70 °C). Migration of the rhenium group about the coordinated ring is proposed to occur via intermediate η^1-arenium structures, a model related to that of electrophilic aromatic substitution. Formation of these intermediates in solution accounts for activation of the carbon–hydrogen bonds toward deprotonation.

Arene molecules coordinated in η^2 fashion to a transition metal have often been suggested as intermediates in the activation of carbon–hydrogen bonds or other catalytic processes.[1] The η^2-arene bonding mode is well established for d^{10} metals such as Cu^+ and Ag^+,[2] and there are several examples involving transition metals with perfluoro- or perfluoroalkyl-substituted derivatives;[3] the latter cannot be regarded as typical arenes, however. The crystal structure of a (1,2-η^2-anthracene)nickel(0) complex[4] ap-

(1) References to the original literature are cited in the following reviews: (a) Parshall, G. W. *Acc. Chem. Res.* **1970**, *3*, 139. (b) *Ibid.* **1975**, *8*, 113. (c) "Homogeneous Catalysis"; Wiley: New York, 1980; Chapter 7. (d) Muetterties, E. L.; Bleeke, J. R. *Acc. Chem. Res.* **1979**, *12*, 325.
(2) Silverthorne, W. E. *Adv. Organomet. Chem.* **1975**, *13*, 47.
(3) (a) Browning, J.; Green, M.; Penfold, B. R.; Spencer, J. L.; Stone, F. G. A. *J. Chem. Soc., Chem. Commun.* **1973**, 31. (b) Cobbledick, R. E.; Einstein, F. W. B. *Acta Crystallogr., Sect. B.* **1978**, *B34*, 1849. (c) Cook, D. J.; Green, M.; Mayne, N.; Stone, F. G. A. *J. Chem. Soc. A* **1968**, 1771.

0276-7333/83/2302-0135$01.50/0

pears to provide the only direct evidence for η^2-coordination of a representative aromatic hydrocarbon to a transition metal. Thus, (η^2-arene)metal complexes of d^n configuration ($n < 10$) are a little known but credible species about which information is required, as was recently pointed out by Muetterties and Bleeke.[1d]

We have prepared and characterized a cationic triphenylmethane complex in which one of the phenyl rings is η^2 coordinated to rhenium(I). The compound is prepared by addition of (η-C_5H_5)Re(NO)(CO)H[5,6] (**1**) to 1 mol of $Ph_3C^+PF_6^-$ in dichloromethane at low temperature[7] and is formulated on the basis of chemical and spectroscopic studies as [(η-C_5H_5)Re(NO)(CO)(3,4-η^2-$C_6H_5CHPh_2$)]-[PF_6] (**2**·PF_6). Although cation **2** is stable in solution (CH_2Cl_2) only at temperatures below −40 °C, the pale yellow microcrystalline hexafluorophosphate salt can be isolated in analytical purity and survives for several hours at room temperature without noticeable decomposition. Previous work in this and other laboratories has shown the ability of the rhenium group, (η-C_5H_5)Re(NO)(CO), to form complexes of exceptional stability with organic functional groups and small molecules;[5,8] the present results provide a further striking example.

An important aspect of **2** is that aromatic carbon–hydrogen bonds of the η^2-coordinated ring have been activated to such an extent that hydrogen can be removed as a proton by triethylamine. The products of deprotonation are isomers of the neutral substituted phenyl derivative (η-C_5H_5)Re(NO)(CO)($C_6H_4CHPh_2$). Moreover, low-temperature ^{1}H NMR spectroscopy has established that **2** is nonrigid. The intermediate in this dynamic process, as well as in the deprotonation reactions, is proposed to have the η^1-cyclohexadienyl cation structure of the type established in electrophilic aromatic substitution.

Results and Discussion

In recent studies of (η-C_5H_5)Re(NO)(CO)H (**1**), we were unable to demonstrate any Lowry–Brønsted acidity, but found that it reacted readily with the strong hydride acceptor cations tropylium ($C_7H_7^+$) and trityl (Ph_3C^+). Reaction with $C_7H_7^+$ (eq 1a) gave a 1,2-η^2-C_7H_8 cation in which cycloheptatriene (produced by hydride abstraction) formed the ligand.[8b] Reaction with Ph_3C^+ (eq 1b) in donor solvents led to rhenium cations having solvent molecules as ligands.[5b] In both reactions, the hypothetical 16-electron cation [(η-C_5H_5)Re(NO)(CO)]$^+$, which would be the formal product of abstraction of the hydride ligand, is converted to the observed coordinatively saturated product by ligands which are present.

We were intrigued with the possibility of generating and perhaps isolating the reactive species [(η-C_5H_5)Re(NO)-(CO)]$^+$ and supposed that the reaction of eq 1b, carried out in the generally non-coordinating solvent dichloro-

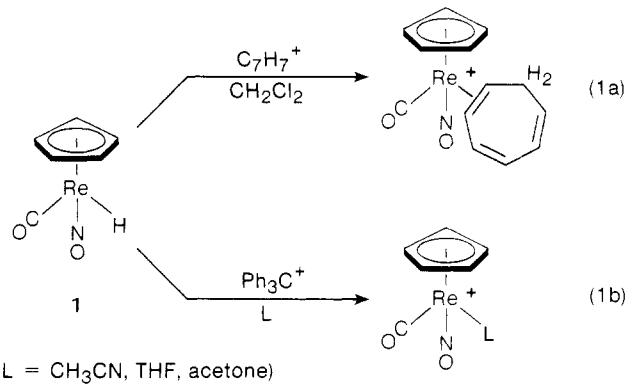

methane, would provide a route to this potentially useful intermediate. In view of the work of Beck and Schloter[9] on the reaction of (η-C_5H_5)$M(CO)_3H$ (M = Mo, W) with $Ph_3C^+X^-$ (X^- = BF_4^-, PF_6^-), it seemed possible that the species we sought would emerge as a "lightly stabilized" complex with coordinated CH_2Cl_2 or counterion. However, the work described here shows that the course of events in the rhenium system is both unanticipated and unprecedented.

Reaction of (η-C_5H_5)Re(NO)(CO)H (1) with Ph_3CPF_6. Although the reaction at 25 °C was unpromising,[10] slow addition of solid **1** to an equimolar amount of Ph_3CPF_6 in CH_2Cl_2 at −78 °C produced a yellow, microcrystalline precipitate after a short interval. The color, solubility, and infrared spectra (ν_{CO} 2026 cm^{-1}, ν_{NO} 1765 cm^{-1}) of this air-stable solid were consistent with a carbonylnitrosylrhenium cation; reproducible analyses for C, H, and N led to its formation as [(η-C_5H_5)Re(NO)(CO)-(Ph_3CH)][PF_6] (**2**·PF_6).[11] The reaction may be written as in eq 2, in which the product incorporates 1 mol of triphenylmethane.

$$(\eta\text{-}C_5H_5)Re(NO)(CO)H + Ph_3CPF_6 \xrightarrow[-78\ ^\circ C]{CH_2Cl_2} [(\eta\text{-}C_5H_5)Re(NO)(CO)(Ph_3CH)][PF_6] \quad (2)$$

1 → **2**·PF_6

Complex **2**·PF_6 decomposes rapidly above −40 °C in dichloromethane to give unidentified η-C_5H_5 products and 1 mol of Ph_3CH; the latter confirms the formulation. As a solid **2**·PF_6 exhibits much higher thermal stability, with fairly slow decomposition at room temperature.[12]

Keeping in mind the 18-electron formalism, two plausible structures **2a** and **2b** may be considered for the tri-

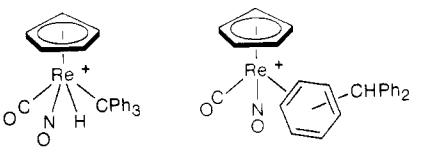

2a **2b**

phenylmethane cation. Both are consistent with properties so far described for **2**·PF_6. The hydridoalkyl structure **2a** could form by direct attack of trityl cation at the metal center.[13] The η^2-arene structure **2b** could arise as does

(4) Brauer, D. J.; Krüger, C. *Inorg. Chem.* **1977**, *16*, 884.
(5) (a) Stewart, R. P.; Okamoto, N.; Graham, W. A. G. *J. Organomet. Chem.* **1972**, *42*, C32. (b) Sweet, J. R.; Graham, W. A. G. *Organometallics*, **1982**, *1*, 982.
(6) The prefix η used alone implies that all the atoms in a ring or chain, or all the multiply bonded ligand atoms, are bound to the central atom: International Union of Pure and Applied Chemistry, "Nomenclature of Inorganic Chemistry", 2nd ed. (Definitive Rules 1970); Butterworths: London, 1971. Cf. also: *Pure Appl. Chem.* **1971**, *28*, 1.
(7) The conditions are critical in this reaction. Under other conditions (room temperature, reverse addition, 0.5 mol of Ph_3C^+) the product is [(η-C_5H_5)$_2$$Re_2(NO)_2$CO)$_2$H][$PF_6$]: Sweet, J. R.; Graham, W. A. G., manuscript in preparation.
(8) (a) Sweet, J. R.; Graham, W. A. G. *J. Organomet. Chem.* **1979**, *173*, C9. (b) *Ibid.* **1981**, *217*, C37. (c) *J. Am. Chem. Soc.* **1982**, *104*, 2811. (d) Casey, C. P.; Andrews, M. A.; McAlister, D. R.; Rinz, J. E. *Ibid.* **1980**, *102*, 1927. (e) Tam, W.; Lin, G.-Y.; Wong, W.-K.; Kiel, W. A.; Wong, V. K.; Gladysz, J. A. *Ibid.* **1982**, *104*, 141.
(9) Beck, W.; Schloter, K. *Z. Naturforsch., B.: Anorg. Chem., Org. Chem.* **1978**, *33B*, 1214.
(10) A black solution formed from which no carbonyl-containing products were isolated; ^{1}H NMR monitoring showed the presence of Ph_3CH and several unidentified η-cyclopentadienyl products.
(11) In particular, the high carbon and hydrogen content excludes such a priori possibilities as [(η-C_5H_5)Re(NO)(CO)CH_2Cl_2]PF_6 or (η-C_5H_5)-Re(NO)(CO)PF_6.
(12) Solid **2**·PF_6 darkens noticeably after a few hours under nitrogen at room temperature, but excellent microanalytical results are obtained 2–3 h after a freshly prepared sample has reached room temperature.

the η^2-cycloheptatriene complex of eq 1a: initial hydride abstraction from 1 followed by coordination of the 16-electron rhenium moiety to one double bond of Ph_3CH.

In the following sections we discuss the evidence bearing on the structure of cation **2**, first examining its chemical reactions and then the ^1H NMR data.

Reaction of 2·PF$_6$ with Ph$_3$P. One equivalent of Ph_3P reacts with a CH_2Cl_2 solution of **2**·PF_6 at low temperature forming the new complex $[(\eta\text{-}C_5H_5)Re(NO)(CO)(PPh_3)][PF_6]$ (**3**) in 96% yield as stable yellow crystals which have been fully characterized.[14] The reaction also forms 1 equiv of Ph_3CH and may therefore be written as eq 3.

$$\mathbf{2}\cdot PF_6 + Ph_3P \xrightarrow[-78 \text{ to } 25\ ^\circ C]{CH_2Cl_2} \underset{\mathbf{3}}{[(\eta\text{-}C_5H_5)Re(NO)(CO)(PPh_3)][PF_6]} + Ph_3CH \quad (3)$$

This facile reaction might reasonably be expected for either of the structures proposed for **2**. For **2a**, the process would be visualized as a ligand-assisted reductive elimination, while displacement of the η^2-arene ligand would be expected to occur readily, although there is of course no exact precedent.

Reaction of 2·PF$_6$ with Et$_3$N. The reaction with Et_3N was expected to be more informative. A cation having structure **2a** might lose a proton to this base forming the neutral complex $(\eta\text{-}C_5H_5)Re(NO)(CO)(\eta^1\text{-}CPh_3)$ or the products of its decomposition. It was less clear whether deprotonation of **2b** would occur, but η^2-coordination to the metal cation might activate the carbon–hydrogen bonds of the arene sufficiently for this to occur; the product would then be a neutral (η^1-aryl)rhenium derivative.

Reaction of **2**·PF_6 with Et_3N occurred readily at −78 °C in CH_2Cl_2 affording a red, air-stable crystalline product. The color, solubility, and IR (hexane, ν_{CO} 1982 cm^{-1}, ν_{NO} 1731 cm^{-1}) indicated a neutral $(\eta\text{-}C_5H_5)Re(NO)(CO)$ derivative. Mass spectroscopy and analysis indicated the composition $(C_5H_5)Re(NO)(CO)(C_{19}H_{15})$. The 400-MHz ^1H NMR spectrum was more complex than expected if the $C_{19}H_{15}$ residue had been a CPh_3 group; in particular, *two* $(\eta\text{-}C_5H_5)$ resonances in 55:45 ratio were observed and it became evident that two isomers had been formed. After separation by multiple fractional crystallization, these were characterized as the para (**4**) and meta (**5**) forms of $(\eta\text{-}C_5H_5)Re(NO)(CO)(C_6H_4CHPh_2)$. The ^1H NMR spectra with assignments are shown in Figure 1 and justified in the Experimental Section. It is noteworthy that protons ortho to the rhenium group are shifted to lower field than the other aromatic protons.

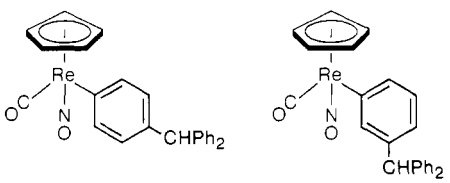

4

5

The deprotonation products from the Et_3N reaction are consistent with the η^2-arene structure **2b**. It is significant that no ortho isomer was formed in the reaction; the isolated yield of unseparated para and meta isomers was 89%, and the para:meta ratio in the initial product mixture was 55:45. The products imply that it is the para and meta C–H bonds of the η^2-aryl ligand that are being activated. This would suggest that in **2**, the $(\eta\text{-}C_5H_5)Re(NO)(CO)^+$ group is attached to C_3 and C_4 of the coordinated phenyl group. On this argument, **2b** could be more precisely formulated as $[(\eta\text{-}C_5H_5)Re(NO)(CO)(3,4\text{-}\eta^2\text{-}C_6H_5CHPh_2)]^+$. We shall consider this point in more detail below.

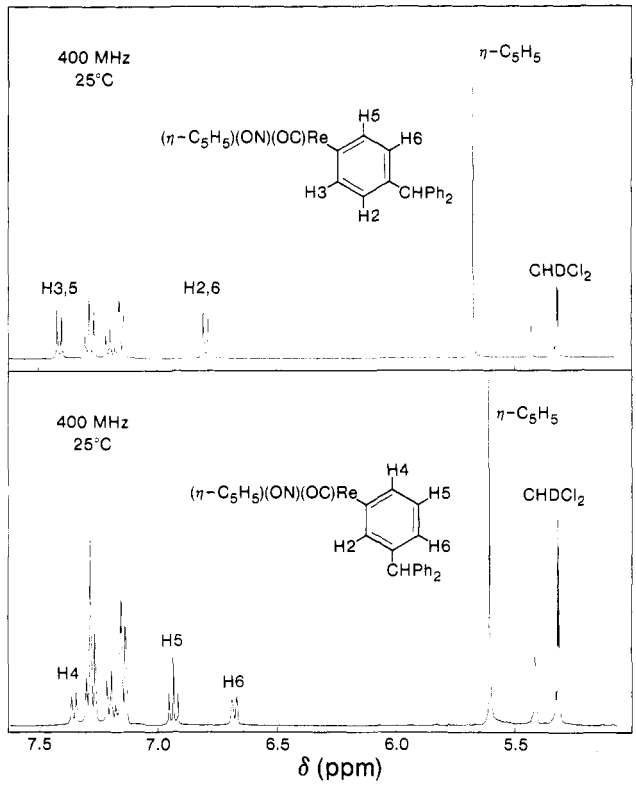

Figure 1. ^1H NMR spectra (400 MHz, CD_2Cl_2) of para (**4** upper spectrum) and meta (**5**, lower spectrum) isomers of $(\eta\text{-}C_5H_5)Re(NO)(CO)(C_6H_4CHPh_2)$.

Deprotonation of the triphenylmethane cation **2** is reversible. Reaction of the 55:45 mixture of **4** and **5** with $HBF_4\cdot OEt_2$ at −78 °C afforded $[(\eta\text{-}C_5H_5)Re(NO)(CO)(Ph_3CH)][BF_4]$ in 82% yield, and the ^1H NMR of cation **2** formed in this way was the same as that of **2** formed in eq 2. Protonation of pure para (**4**) and meta (**5**) isomers *separately* gave the same result.

Reaction of 2·PF$_6$ with PMe$_2$Ph. In the reaction of **2** with Ph_3P, triphenylmethane displacement occurred (eq 3). With the more basic Et_3N, deprotonation of the triphenylmethane ligand was the exclusive pathway. Both of these reaction modes are exhibited in the reaction of **2**·PF_6 with phenyldimethylphosphine. In CH_2Cl_2 at −78 °C, the products consisted of an approximately 1:1:2 mixture of **4**, **5**, and the new phosphine cation $[(\eta\text{-}C_5H_5)Re(NO)(CO)(PMe_2Ph)][PF_6]$ (**6**).[15] Stable, yellow **6** was isolated in good yield and fully characterized. A noteable feature of its ^1H NMR is the nonequivalence of the (diastereotopic) methyl groups, a consequence of the chirality of the metal center.

^{1}H NMR Studies of 2·PF$_6$. The foregoing chemical investigations are suggestive of the η^2-$C_6H_5CHPh_2$ (**2b**) structure and more specifically the 3,4-η^2-$C_6H_5CHPh_2$ isomer. As we shall see, the results of ^1H NMR studies are generally in agreement with this picture but permit an elaboration of considerable interest.

(13) A related but *neutral* complex which definitely has the hydridoalkyl structure is $(\eta\text{-}C_5H_5)Re(CO)_2(H)(\eta^1\text{-}CH_2Ph)$: Fischer, E. O.; Frank, A. *Chem. Ber.* **1978**, *111*, 3740.

(14) Spectroscopic parameters of **3** are similar to those of $[(\eta\text{-}C_5H_5)Re(NO)(CO)(CH_3CN)][PF_6]$.[5b] Preparation of the cation of **3** as its BF_4^- salt has very recently been reported.[8e]

(15) The exact product ratio in this reaction is somewhat temperature dependent. At −78 °C, the yield of **6** is about 60%, dropping at higher temperatures to about 50%. The ratio of **4** to **5** remains constant and equal to that obtained on deprotonation with Et_3N.

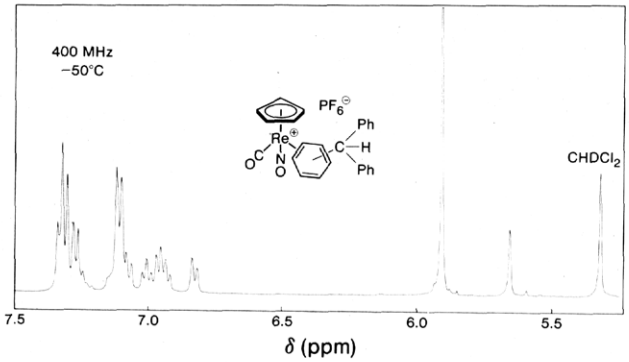

Figure 2. ^{1}H NMR spectrum (400 MHz, CD_2Cl_2, −50 °C) of $[(\eta\text{-}C_5H_5)Re(NO)(CO)(\eta^2\text{-}C_6H_5CHPh_2)][PF_6]$.

Efforts to obtain ^{1}H NMR data of high quality were hampered by the low thermal stability of **2** and by its low solubility in CD_2Cl_2. No other suitable solvent was found. Very long acquisition times were required. It was advantageous to react **1** with Ph_3CPF_6 in the NMR tube, thereby generating a supersaturated solution which only slowly precipitated **2**·PF_6. Spectra of these solutions were identical with those of samples prepared by dissolving solid **2**·PF_6 at low temperature.

The 400-MHz ^{1}H NMR spectrum of **2**·PF_6 is shown in Figure 2. The spectrum was invariant over the −70 to −40 °C range, above which decomposition became quite rapid. Major features are the η-C_5H_5 signal at δ 5.90 (5 H), a value typical of cations in this system, a series of complex multiplets in the aromatic region (15 H), and a singlet at δ 5.65 (1 H). The latter singlet enables a clear choice to be made between possibilities **2a** and **2b** for the structure of the cation. For **2a**, the resonance of the hydridic hydrogen would be expected at very much higher field.

The observed position at δ 5.65 is more consistent with the aliphatic hydrogen of the η^2-$C_6H_5CHPh_2$ group; it is only slightly shifted to *lower field* from its position in free Ph_3CH (δ 5.56 in CD_2Cl_2). Moreover, at higher amplitude, the δ 5.65 singlet exhibits ^{13}C satellites with $^1J(^{13}C\text{–}H)$ = 128 Hz, a normal value for a C(sp^3)–H bond.

In the aromatic region, again consistent with the structure **2b**, several small multiplets appear shifted upfield from the phenyl multiplets. These are assigned to the unique phenyl ring which is bonded to the metal center. Coordination to rhenium would be expected to shift the resonances of these protons to higher fields.

Further evidence for the structure of cation **2** and for the mechanism by which it is formed comes from studies with the deuteride[5b] $(\eta\text{-}C_5H_5)Re(NO)(CO)D$ (**7**). The reaction product of **7** with Ph_3CPF_6 has a ^{1}H NMR spectrum that is the same as that of **2** (Figure 2) except for the singlet at δ 5.65 which is absent in the deuterated complex. Finally, deprotonation of deuterated **2** prepared in this way forms deuterated **4** and **5**, with deuterium in the aliphatic position as shown in eq 4 (where the $(\eta\text{-}C_5H_5)Re(NO)(CO)$ group is represented for simplicity by Re). These observations directly confirm that the proton is removed from an sp^2 carbon atom, demonstrating the extent to which the coordinated arene ring has been activated in the complex **2**.

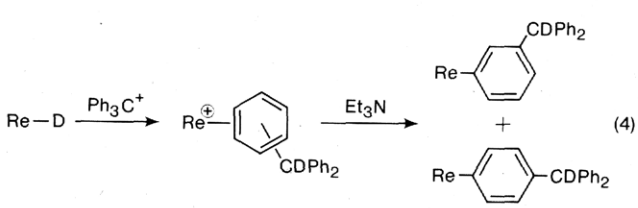

(4)

The evidence discussed so far for the structure of **2** points to the coordination of one phenyl ring of triphenylmethane. The 18-electron rule suggests that the coordination is of the η^2-type, while deprotonation to para and meta products suggests that C3 and C4 are bonded to rhenium. The structure most consistent with these observations is **2c**.

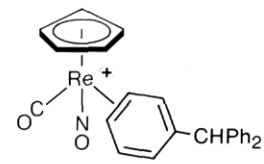

2c

Stereochemical Aspects and the Nonrigidity of 2 in Solution. As reasonable as the arguments to this point may appear, the single static structure **2c** does not fully explain the ^{1}H NMR spectrum of **2**. It is well-known that coordination of a metal to an unsymmetrical olefin imparts chirality to the system,[16] and when the metal center is chiral as is the case with the $(\eta\text{-}C_5H_5)Re(NO)(CO)$ group, two diastereomers will result. We have demonstrated[8b] that the diastereomers of the olefin cation $[(\eta\text{-}C_5H_5)Re(NO)(CO)(1,2\text{-}\eta^2\text{-}C_7H_8)]^+$ are readily distinguished by their ^{1}H NMR spectra, and the same would be anticipated for **2**.

The diastereomers expected for the triphenylmethane cation **2** are shown as **2d** and **2e** (only one enantiomer is shown for each). Yet the single η-C_5H_5 signal of Figure

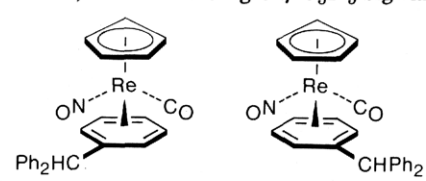

2d **2e**

2 does not indicate the presence of diastereomers nor do the signals of the coordinated phenyl ring. It is possible that by coincidence these signals differ so little from one diastereomer to the other as to be unresolvable; it is also possible that only one diastereomer has been formed in an asymmetric synthesis. We think it more likely that the diastereomers are interconverted by a process which is rapid on the NMR time scale.[17a] The observed ^{1}H NMR spectrum of **2** would thus reflect the average environment of each of the protons in the two distinct structures. An observation to be mentioned later enabled us to conclude that reversible dissociation of the η^2-Ph_3CH ligand is *not* occurring rapidly on NMR time scale, so other interconversion pathways must be considered.

If we exclude inversion at rhenium on the grounds that the activation energy is likely to be high,[17b] the simplest intramolecular process that would interconvert **2d** and **2e** is migration of the rhenium group from the 3,4-η^2 to the adjacent 4,5-η^2 position on the same face of the phenyl ring. We now direct attention to the question of possible in-

(16) Paiaro, G.; Panunzi, A. *J. Am. Chem. Soc.* **1964**, *86*, 5148. Panunzi, A.; Paiaro, G. *Ibid.* **1966**, *88*, 4843.

(17) (a) On the assumption that the η-C_5H_5 ^{1}H NMR signals of the diastereomers of **2** would be separated by 16 Hz as they are in $[(\eta\text{-}C_5H_5)Re(NO)(CO)(1,2\text{-}\eta^2\text{-}C_7H_8)]^+$,[8b] the rate of interconversion at −70 °C must exceed 35.5 s^{-1}, leading to an upper limit on $\Delta G^{\ddagger}_{203}$ of 10.3 kcal. (b) Inversion clearly does not occur at ambient temperature in the olefin cation $[(\eta\text{-}C_5H_5)Re(NO)(CO)(1,2\text{-}\eta^2\text{-}C_7H_8)]^+$ since diastereomers are observed[8b] nor in the Me_2PPh cation **6** where diastereotopic methyls are observed. In $(\eta\text{-}C_5H_5)Re(NO)(CO)(\eta^1\text{-}C_7H_7)$, the rhenium centre is configurationally stable on the NMR time scale to at least 130 °C.[8b]

termediates in this migration process. This is an important point because it may be the intermediate, not the ground state of the η^2-Ph_3CH cation, that actually undergoes deprotonation. We shall examine two models.

The Hydridoaryl Intermediate. This possibility derives from the early suggestion of Chatt and Davidson[18] of the tautomeric equilibrium shown in eq 5 (dmpe = $Me_2PCH_2CH_2PMe_2$). Only the hydridoaryl form **9** was observed in solution, and it was also found in the solid state.[19] The η^2-naphthalene form **8** was proposed to account for the chemical reactions, especially the release of naphthalene on pyrolysis.

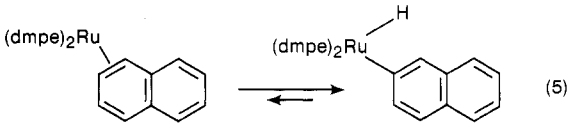

(5)

8 **9**

Application of an equilibrium of this sort to the interconversion of diastereomers of **2** is shown in Figure 3. Although deprotonation of **11** or **13** should lead to the correct products, careful interpretation of the arene resonances in the ^1H NMR spectrum enables hydridoaryl intermediates to be excluded.

The ^1H NMR spectrum of **2** (Figure 2) has small multiplets at δ 6.83 (d, 1 H), 6.95 (m, 2 H), and 7.01 (t, 1 H). Decoupling established that these protons were on the same ring (clearly the coordinated phenyl) and that the δ 6.95 multiplet involved two different protons. The signal due to the fifth proton of this ring must be at another position where it is obscured. The conclusion that there are five separate signals for the coordinated ring requires that the process which interconverts diastereomers does not interchange any of the protons of this ring. However, in the hydridoaryl intermediate **11**, free rotation about the rhenium–phenyl bond would interchange two pairs of protons, and three signals at most would be observed. Thus, rapid interconversion of the structures shown in Figure 3 does not properly account for the observed spectrum of **2**.[20]

The Arenium Intermediate.[21] A second type of intermediate through which diastereomers of **2** could interconvert is the arenium ion **2f**, and this pathway is shown

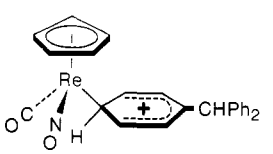

2f

in Figure 4. The η^2 to η^1 conversions proposed here are reminiscent of the π complex to arenium ion sequence of electrophilic aromatic substitution[22] (eq 6), the last two steps of which provide a model for the deprotonation of **2**.

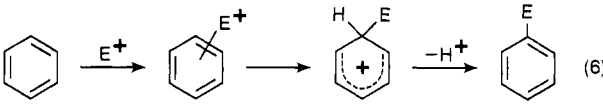

(6)

The sequences of Figure 4 are consistent with the ^1H NMR spectrum of **2**. In every structure the five protons of the coordinated ring are nonequivalent, and in particular in the intermediate **2f**, proton pairs on opposite sides of the ring are diastereotopic. Thus five different signals, each a weighted average, would be expected in the absence of accidental degeneracies. While one cannot predict the appearance of the averaged spectrum in an exact way, contributions from the arenium structures would be expected to shift the hydrogens of the rhenium-bonded ring to considerably higher field than in free triphenylmethane. The overall similarity of the ^1H NMR spectrum of **2** to that of free Ph_3CH (only small upfield shifts of protons in the coordinated ring) suggests that the η^2-bonded form is dominant. This conclusion is in agreement with the chemical shift of the η-C_5H_5 group and the carbonyl and nitrosyl stretching frequencies, both of which we have found to be sensitive indicators of positive charge localized on the rhenium atom.[23] If significant quantities of the arenium structures had been present in solution, their IR bands would have been clearly observable.

Deprotonation of **2** would presumably occur from the arenium intermediates. The para and meta arenium ions of Figure 4 would form **4** and **5**, respectively. The lack of an ortho phenyl product from deprotonation may reflect an absence of the appropriate ortho arenium precursor; this would be reasonable on steric grounds. We note that Figure 4 could be extended to include 2,3-η^2-Ph_3CH structures, although this is not required by the experimental evidence.

Conclusions. From its chemical reactions and spectroscopic properties, we conclude that **2** contains an η^2-coordinated phenyl group. Furthermore, the probe provided by the chiral rhenium center shows that the complex is stereochemically nonrigid, and a pathway for migration of the rhenium group is proposed which involves an arenium ion intermediate. The proposed intermediate accounts for the activation of the aromatic hydrogens in the complex to the extent that they can be removed as protons by triethylamine. The concepts of electrophilic aromatic substitution provide a model for this and vice versa.

The thermal stability of **2** is much less than that of an η^2 complex of a nonaromatic system, for which [(η-C_5H_5)Re(NO)(CO)(1,2-η^2-C_7H_8)]$^+$ serves as an example.[8b] The η^2-Ph_3CH is also much more readily displaced as shown by the low temperature reaction with Ph_3P.[24] These observations indicate a substantial difference in the energetics of η^2-olefin and η^2-arene coordination; one likely rationale for this is the loss of aromatic stabilization when the arene coordinates.

(18) Chatt, J.; Davidson, J. M. *J. Chem. Soc.* **1965**, 843. This seminal paper appears to contain the first suggestion of an aromatic system as a two-electron donor, "after the manner of a mono-olefin", to a transition metal not involving a d^{10} configuration: an η^2-arene complex in present terminology. Inherent in it was the notion that activation of an aromatic C–H bond involved an intermediate η^2-arene complex.

(19) Gregory, U. A.; Ibekwe, S. D.; Kilbourn, B. T.; Russell, D. R. *J. Chem. Soc. A*, **1971**, 1118.

(20) The same observation also excludes interconversion of diastereomers on the NMR time scale by reversible dissociation of the triphenylmethane ligand.

(21) We utilize the nomenclature which has been proposed for carbocations of the cyclohexadienyl type: Olah, G. A. *J. Am. Chem. Soc.* **1972**, *94*, 808.

(22) March, J. "Advanced Organic Chemistry"; McGraw-Hill: New York, 1979; p 453.

(23) Values of ν_{CO} and ν_{NO} for **2** (2026, 1765 cm^{-1}) fall in the range of cationic complexes of more traditional ligands: [(η-C_5H_5)Re(NO)(CO)-(PPh_3)]$^+$ (**6**), 2023, 1767 cm^{-1}; [(η-C_5H_5)Re(NO)(CO)(CH_3CN)]$^+$, 2030, 1769 cm^{-1};[5b] [(η-C_5H_5)Re(NO)(CO)(η^2-C_7H_8)]$^+$, 2050, 1774 cm^{-1}.[8b] Frequencies in the arenium structures where positive charge is mainly localized in the ring would be expected to fall nearer the range of such derivatives as (η-C_5H_5)Re(NO)(CO)CH_3[5a,8c] (1963, 1696 cm^{-1}) or **4** and **5** (1976, 1715 cm^{-1}). To facilitate comparison with the ionic derivatives, values listed here for the neutral complexes were also measured in CH_2Cl_2; in the latter solvent they are shifted to lower frequency by 6–19 cm^{-1} from their values in hexane.

(24) [(η-C_5H_5)Re(NO)(CO)(1,2-η^2-C_7H_8)][BF_4] does not react with Ph_3P in CH_2Cl_2 at temperatures up to 25 °C.

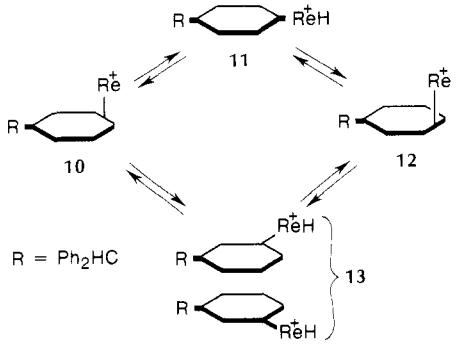

Figure 3. A possible mechanism for interconversion of diastereomers **10** and **12** via hydridoaryl intermediates **11** and **13**. Two equivalent orientations of **13** are shown. The chiral (η-C_5H_5)-Re(NO)(CO) group is represented by Re. This pathway is inconsistent with observed ^{1}H NMR spectra (see text).

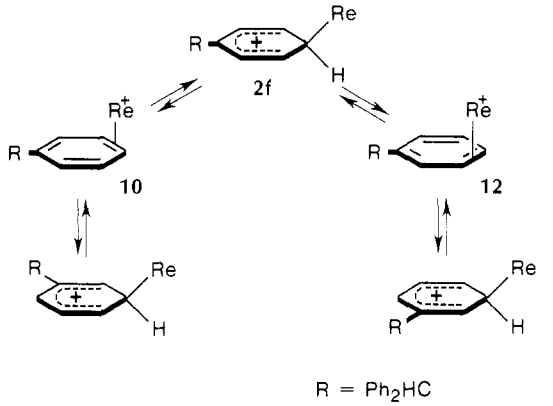

Figure 4. Interconversion of diastereomers **10** and **12** via the arenium intermediate **2f**. The para and meta arenium ions shown would form **4** and **5** upon deprotonation. The chiral (η-C_5H_5)-Re(NO)(CO) group is represented by Re.

The characteristics of the triphenylmethane cation **2** (low solubility, low stability, complex ^{1}H NMR) present problems in the determination of its structure. Simpler arene derivatives of this system should be advantageous, and we are seeking to prepare other [(η-C_5H_5)Re(NO)-(CO)(arene)]$^+$ complexes to gain further insight into the nature of this important class of compounds.

Experimental Section

All reactions were carried out under an atmosphere of nitrogen. Solvents were dried by using standard procedures and distilled immediately before use. Rhenium carbonyl was purchased from Strem Chemicals, Inc., and triphenylcarbenium hexafluorophosphate from Aldrich; (η-C_5H_5)Re(NO)(CO)H (**1**) was prepared as previously described.[5b] Infrared spectra were measured by using a Nicolet MX-1 fourier transform instrument and ^{1}H NMR spectra by using a Bruker WH-200 or WH-400 Fourier transform spectrometers.

Preparation of [(η-C_5H_5)Re(NO)(CO)(Ph_3CH)][PF_6] (2·PF_6). Triphenylcarbenium hexafluorophosphate (0.125 g, 0.32 mmol) was dissolved in 10 mL of CH_2Cl_2 and cooled to −78 °C. Solid **1** (0.100 g, 0.32 mmol) was added in four equal portions over about 15 min. The solution turned reddish yellow and within 0.5 h a yellow precipitate appeared. The solution was filtered at −78 °C and the solid washed with cold CH_2Cl_2 (2 × 5 mL) to afford **2**·PF_6 as yellow microcrystals (0.21 g, 93%): IR (cm^{-1}; CH_2Cl_2) ν_{CO} 2026 (s), ν_{NO} 1765 (s); ^{1}H NMR see Results and Discussion and Figure 2. Anal. Calcd for $C_{25}H_{21}NO_2RePF_6$: C, 42.98; H, 3.12; N, 2.00. Found: C, 42.96; H, 3.02; N, 2.11.

Reaction of 2·PF_6 with Triphenylphosphine. A solution of Ph_3CPF_6 (0.125 g, 0.32 mmol) in 10 mL of CH_2Cl_2 was cooled to −78 °C, and solid **1** (0.100 g, 0.32 mmol) was added in four equal portions over 15 min. Triphenylphosphine (0.085 g, 0.32 mmol) was added, and the resulting yellow solution was stirred at −78 °C for 1 h before being warmed to room temperature. Addition of diethyl ether afforded a precipitate which was collected and washed with ether (3 × 10 mL) to give [(η-C_5H_5)Re(NO)(CO)-(PPh_3)][PF_6] (**3**) as yellow microcrystals (0.22 g, 96%): IR (cm^{-1}; CH_2Cl_2) ν_{CO} 2023 (s), ν_{NO} 1767 (s); ^{1}H NMR (CD_2Cl_2) δ 5.83 (5 H), 7.5 (m, 15 H). Anal. Calcd for $C_{24}H_{20}NO_2P_2F_6Re$: C, 40.23; H, 2.81; N, 1.95. Found: C, 40.29; H, 2.80; N, 1.92.

Reaction of 2·PF_6 with Triethylamine. Triethylamine (0.90 mL, 6.47 mmol) was added to a solution of 2·PF_6 (1.61 mmol, prepared as above) in 10 mL of CH_2Cl_2 maintained at −78 °C. After being stirred at −78 °C for 1 h, the solution was warmed to room temperature and solvent removed at reduced pressure, leaving a red solid. This solid was extracted into hexane, and the extracts were filtered and cooled to −78 °C, affording pink crystals of **4** and **5** (total yield 0.79 g, 89%). Isomers **4** and **5** were separated by repeated fractional crystallizations from CH_2Cl_2–hexane. Para isomer (**4**): IR (cm^{-1}; hexane) ν_{CO} 1982 (s), ν_{NO} 1731 (s): mass spectrum, (24 eV, 120 °C, m/e), M^+, $(M - CO)^+$, $(M - CO - NO)^+$. Anal. Calcd for $C_{25}H_{20}NO_2Re$: C, 54.33; H, 3.65; N, 2.53. Found: C, 54.04; H, 3.65; N, 2.57. Meta Isomer (**5**): IR (cm^{-1}; hexane) ν_{CO} 1982 (s), ν_{NO} 1731 (s): MS (20 eV, 120 °C, m/e) M^+, $(M - CO)^+$, $(M - CO - NO)^+$. Anal. Calcd for $C_{25}H_{20}O_2NRe$: C, 54.33; H, 3.65; N, 2.53. Found: C, 54.09; H, 3.64; N, 2.59.

^{1}H NMR Spectrum of 4. Singlets at δ 5.67 (5 H) and 5.46 (1 H) are assigned to the η-C_5H_5 ring and the aliphatic C*H*Ph_2 proton (Figure 1). A series of multiplets centered ca. δ 7.2 (10 H) are assigned to the monosubstituted phenyls. Bracketing these multiplets are doublets at δ 6.82 (2 H) and 7.43 (2 H); decoupling at δ 6.82 caused collapse of the δ 7.43 doublet. This AA'XX' pattern is only consistent with para disubstitution. The δ 6.82 and 7.43 signals are assigned to $H_{2,6}$ and $H_{3,5}$, respectively (numbering as in Fig 1), based on the fact that irradiation at δ 5.46 eliminated a small coupling on the δ 6.82 doublet. A NOE experiment complemented this result by confirming the close proximity of the C*H*Ph_2 proton to the protons at δ 6.82.

^{1}H NMR Spectrum of 5. Singlets at δ 5.60 (5 H) and 5.44 (1 H) are assigned to η-C_5H_5 and C*H*Ph_2. In the aromatic region, decoupling the triplet at δ 6.96 (1 H) collapsed the doublets at both δ 6.71 (1 H) and 7.40 (1 H). This coupling pattern implies meta substitution and leads to the assignment of the δ 6.96 triplet to H5 with J(H4–H5) $\simeq$ J(H5,H6) = 7.3 Hz. The δ 6.71 and 7.40 doublets are assigned to H6 and H4, respectively; each component of these doublets is a triplet (J = 1.5 Hz) due to meta coupling. H2 is obscured by the C_6H_5 multiplets at ca. δ 7.2 (10 H).

Reaction of 2·PF_6 with Phenyldimethylphosphine. Phenyldimethylphosphine (0.25 mL, 1.69 mmol) was added to a solution of 2·PF_6 (1.61 mmol, prepared as above) in 10 mL of CH_2Cl_2 maintained at −78 °C. The resulting orange solution was stirred for 1 h at −78 °C and then warmed to room temperature. Addition of ether gave a precipitate which was washed with ether (3 × 20 mL) affording [(η-C_5H_5)Re(NO)(CO)(PMe_2Ph)][PF_6] (**6**) as yellow microcrystals (0.55 g, 58%, see Results and Discussion): IR (cm^{-1}) (CH_2Cl_2) ν_{CO} 2022 (s), ν_{NO} 1771 (s): ^{1}H NMR (CD_2Cl_2) δ 5.83 (5 H), 7.68 (m, 5 H), 2.285 (d, 3 H), 2.291 (d, 3 H); J-[$(CH_3)_a$–P] $\simeq$ J[$(CH_3)_b$–P] = 10.7 Hz. Anal. Calcd for $C_{14}H_{16}F_6NO_2P_2Re$: C, 28.38; H, 2.72; N, 2.36. Found: C, 28.34; H, 2.69; N, 2.43.

Protonation of 4 and 5. A mixture of isomers **4** and **5** (0.100 g, 0.18 mmol, prepared in 55:45 molar ratio by reaction of 2·PF_6 with Et_3N as described above) was dissolved in CH_2Cl_2 and cooled to −78 °C. Addition of excess HBF_4·Et_2O (Aldrich) formed a yellow-orange solution from which a yellow solid slowly precipitated. The solid was collected by filtration at −78 °C and washed with cold CH_2Cl_2 (2 × 5 mL); IR and ^{1}H NMR of the solid identified it as 2·BF_4 (0.116 g, 82%).

Acknowledgment. We thank the Natural Sciences and Engineering Research Council of Canada for financial support and a scholarship to J.R.S. and T. Nakashima and G. Bigham for their cooperation in measuring NMR spectra.

Registry No. **1**, 38814-46-9; **2**$^+$ PF_6^-, 83585-32-4; **2**$^+$ BF_4^-, 83585-33-5; **3**, 79919-50-9; **4**, 83572-98-9; **5**, 83572-99-0; **6**, 83573-01-7; triphenylcarbenium hexafluorophosphate, 437-17-2; triethylamine, 121-44-8.

Nucleophilic Attack on η^2-Coordinated Dithio Acids by Hydride Ion. A Preliminary Step in the Formation of a Variety of Nickel Complexes

Claudio Bianchini,* Carlo Mealli, Andrea Meli, and Giancarlo Scapacci

Istituto per lo Studio della Stereochimica ed Energetica dei Composti di Coordinazione, C.N.R., 50132 Firenze, Italy

Received June 14, 1982

The nickel(II) complexes $[(triphos)Ni(S_2CPEt_3)](BPh_4)_2$, $[(triphos)Ni(S_2CSMe)]BPh_4$, $[(triphos)Ni(S_2COEt)]BPh_4$, and $[(triphos)Ni(S_2CNEt_2)]BPh_4$ (triphos = 1,1,1-tris((diphenyphosphino)methyl)ethane) react with $NaBH_4$ to give the complexes $[(triphos)Ni\{S_2C(H)PEt_3\}]BPh_4$, $[(triphos)Ni(\pi\text{-}CS_2)]$, $[(triphos)Ni(CO)]$, and $[(triphos)Ni(SH)]$, respectively. The formation of all of these compounds is suggested to proceed via nucleophilic attack by the hydride ion from $NaBH_4$ on the electrophilic CS_2 carbon atom, followed by rearrangement of the resultant adduct. In some cases the reaction is accompanied by a lowering of the metal oxidation state by one or two units.

Introduction

Increasing attention has been directed recently toward the reactivity of (η^2-dithio acid)metal complexes (I) with nucleophiles. Reactions of η^2-metal-linked S_2C–X groups include ligand substitution to give complexes with different dithio acid ligands,[1-3] and nucleophile addition to give 1,1-dithiolate complexes.[4,5] The η^2-coordination of dithio acid ligands enhances the electrophilicity of the CS_2 carbon atom, which consequently can be attacked by nucleophiles.

In recent papers were showed that the hydride ion from $NaBH_4$ attacks the metal-coordinated S_2C–PEt_3 zwitterion (II) and transforms it into the dithioformate or the phosphonium adduct of dithioformate.[1,4]

I, L = ancillary ligand II

Now we show that the reactivity of (η^2-dithio acid)metal complexes with $NaBH_4$ is in general a chemical feature of these disulfido ligands. The reactions of a number of nickel(II) complexes of formula $[(triphos)Ni(S_2C\text{–}X)](BPh_4)_n$ (III) and $NaBH_4$ are summarized in Scheme I.

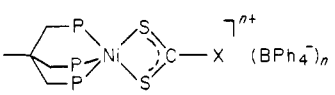

III, X = SMe, OEt, NEt_2; n = 1
X = PEt_3; n = 2

The product obtainable from each of these reactions depends on the nature of the X substituent. Beside addition reactions, the hydride ion may cause the fragmentation of the chelated dithioacid, thus generating metal complexes with a variety of smaller ligands such as CS_2, CO, and HS^-. These reactions are often accompanied by a decrease of the metal oxidation number by one or two units.

Scheme I

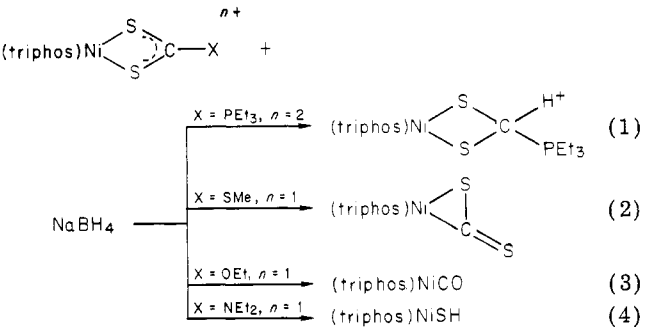

Experimental Section

All chemicals and solvents employed were reagent grade and were used without further purification. All the reactions described were carried out under an atmosphere of dry nitrogen. The solid complexes were collected on a sintered-glass frit and washed successively with ethanol and petroleum ether (bp 40–70 °C) before being dried in a stream of dry nitrogen. Infrared spectra were recorded with a Perkin-Elmer 283 spectrophotometer using samples mulled in Nujol. ^{31}P NMR spectra were taken on a Varian CFT 20 spectrometer. Chemical shifts are downfield (+) from external H_3PO_4. The methods used for the magnetic and molar conductance measurements and the recording of the UV–visible spectra have been described previously.[6]

Syntheses. $[(triphos)Ni\{S_2C(H)PEt_3\}]BPh_4$ (1). A solution of $[(triphos)Ni(S_2CPEt_3)](BPh_4)_2$[4] (0.45 g, 0.3 mmol) in acetone (25 mL) was treated with $NaBH_4$ (0.02 g, 0.5 mmol) in ethanol (10 mL). There was an immediate color change from dark green to orange. By addition of *n*-butanol (20 mL) to the solution and partial evaporation an orange microcrystalline solid was obtained; yield 85%.

Anal. Calcd for $C_{72}H_{75}BNiP_4S_2$: C, 72.18; H, 6.31; Ni, 4.90; P, 10.34. Found: C, 71.97; H, 6.24; Ni, 4.85; P, 10.45.

$[(triphos)Ni(\pi\text{-}CS_2)]$ (2). A solution of $NaBH_4$ in ethanol was added dropwise to a suspension of $[(triphos)Ni(S_2CSMe)]BPh_4$[7] (0.34 g, 0.3 mmol) in acetone (30 mL) until the suspended compound dissolved to give a red brown solution. Ethanol (10 mL) then was added. Dark brown crystals precipitated in a short time: yield 90%; IR (cm^{-1}) ν(C=S) 1145, ν(CS) 630.

Anal. Calcd for $C_{42}H_{39}NiP_3S_2$: C, 66.41; H, 5.17; Ni, 7.73; S, 8.44. Found: C, 66.25; H, 5.14; Ni, 7.64; S, 8.35.

(1) (a) Bianchini, C.; Meli, A.; Orlandini, A.; Scapacci, G. *J. Organomet. Chem.* **1981**, *215*, C59. (b) Bianchini, C.; Innocenti, P.; Meli, A.; Orlandini, A.; Scapacci, G. *Ibid.* **1982**, *233*, 233.

(2) Bianchini, C.; Mealli, C.; Meli, A.; Scapacci, G. *J. Chem. Soc., Dalton Trans.* **1982**, 799.

(3) Fackler, J. P., Jr.; Seidel, W. C. *Inorg. Chem.* **1969**, *8*, 1631.

(4) (a) Bianchini, C.; Meli, A.; Orlandini, A. *Angew. Chem., Int. Ed. Engl.* **1982**, *21*, 197. (b) Bianchini, C.; Meli, A.; Orlandini, A. *Inorg. Chem.*, in press.

(5) Bianchini, C.; Meli, A.; Nuzzi, F.; Dapporto, P. *J. Organomet. Chem.* **1982**, *236*, 245.

(6) Sacconi, L.; Bertini, I.; Mani, F. *Inorg. Chem.* **1968**, *7*, 1417.

(7) Unpublished results of this laboratory. The $[(triphos)Ni(S_2CSMe)]BPh_4$ complex was synthetized by treatment under nitrogen of a solution of $[(triphos)Ni(S_2CS)]$ (0.5 mmol)[2] in CH_2Cl_2 (20 mL) with $MeOSO_2F$ (0.55 mmol), followed by addition of $NaBPh_4$ (0.5 mmol) in ethanol (30 mL).

0276-7333/83/2302-0141$01.50/0

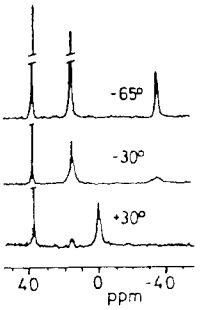

Figure 1. Variable-temperature $^{31}P\{^1H\}$ NMR spectra of [(triphos)Ni{$S_2C(H)PEt_3$}]BPh_4 in acetone.

[(triphos)Ni(CO)] (3). An acetone (30 mL) suspension of [(triphos)Ni(S_2COEt)]BPh_4[8] (0.34 g, 0.3 mmol) was treated with a large excess of $NaBH_4$ in ethanol (20 mL) which caused the solid to dissolve, giving a yellow brown solution. When left standing for 1 h, the solution gave yellow crystals: yield 50%; IR (cm^{-1}) ν(CO) 1890.

Anal. Calcd for $C_{42}H_{39}NiOP_3$: C, 70.91; H, 5.52; Ni, 8.25. Found: C, 70.81; H, 5.60; Ni, 8.19.

[(triphos)Ni(SH)] (4). $NaBH_4$ (0.05 g, 1 mmol) in ethanol (20 mL) was allowed to react with a solution of [(triphos)Ni(S_2CNEt_2)]BPh_4[8] (0.34 g, 0.3 mmol) in acetone (30 mL). Within a few minutes a light brown solution was obtained. Yellow crystals precipitated in a short time; yield 40%.

Anal. Calcd for $C_{41}H_{40}NiP_3S$: C, 68.73; H, 5.62; Ni, 8.19; S, 4.47. Found: C, 68.68; H, 5.58; Ni, 8.12; S, 4.39.

Results and Discussion

When $NaBH_4$ was reacted with [(triphos)Ni(S_2CPEt_3)]$(BPh_4)_2$ (triphos = 1,1,1-tris((diphenylphosphino)methyl)ethane) in acetone–alcohol, the color of the solution turns to orange and a microcrystalline orange solid of empirical formula [(triphos)Ni{$S_2C(H)PEt_3$}]BPh_4 (**1**) precipitates. This complex is diamagnetic and air stable in the solid state. It is soluble in all common organic solvents, in which it behaves as a 1:1 electrolyte (molar conductance in 10^{-3} nitroethane solution: 46 cm^2 Ω^{-1} mol^{-1}). The reflectance spectrum, with no band at frequencies <15 000 cm^{-1}, is typical of the square-planar nickel(II) complexes or of the low-spin square-pyramidal complexes, in which the metal atom undergoes a weak apical interaction.[9] The IR spectrum shows no bands attributable to C=S stretching modes. The structure of **1** has been unambiguously ascertained by means of variable-temperature ^{31}P NMR spectra. The ^{31}P NMR spectra for the temperature range +30 to −65 °C are presented in Figure 1. At −65 °C the spectrum indicates a "frozen" structure in which the triphos ligand is functioning as a bidentate ligand, one of the arms leading to a phosphine group being not coordinated to the metal. The most likely structure is illustrated in IV. The ^{31}P NMR assignments

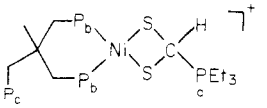

IV

are as follows: $\delta(P_a)$ 38.90, $\delta(P_b)$ 16.72, and $\delta(P_c)$ −31.77. As the temperature increases, the uncoordinated Ph_2P group c begins to switch its position with the other two arms of the tripod ligand as shown by the simultaneous broadening of the above resonances. At +30 °C they give rise essentially to a broad absorption at ca. 1 ppm. The temperature increases induces only a very small high-field shift of the resonance due to the phosphorus atom of the PEt_3 group (from 38.90 ppm at −65 °C to 38.03 ppm at +30 °C). Conversely when the temperature is decreased to −80 °C (not shown), the resonance due to the uncoordinated phosphorus atom P_c and to the phosphorus atom P_a are split into two signals at 39.38 and 39.02 ppm and at 31.73 and 32.45 ppm, respectively. This splitting may be attributed to the presence of isomeric structures which at higher temperature rapidly interconvert as shown in eq 1. The phosphonium adduct of dithioformate $S_2C(H)PEt_3$

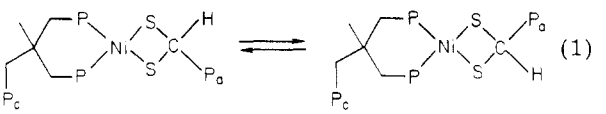

(1)

has been recently found in the three complexes of general formula [(triphos)$MS_2C(H)PEt_3$]$(BPh_4)_n$ (M = Fe,[10] n = 1; M = Co,[4] n = 1 or 2). These have been assigned a distorted square-pyramidal geometry around the metal center at variance with structure **1** where the triphos ligand acts as bidentate ligand. Likely, the latter compound receives extra stability from the well-known electronic factors which favor the formation of the low-spin d^8 square-planar complexes.

Reaction of [(triphos)Ni(S_2CSMe)]BPh_4 or [(triphos)-Ni(S_2COEt)]BPh_4 with $NaBH_4$ produces dark brown or yellow crystals of [(triphos)Ni(π-CS_2)], **2**, or [(triphos)-Ni(CO)], **3**, respectively. Analytical and spectroscopic data

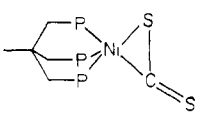

2

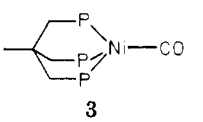

3

agree well with the representations given for **2** and **3**. These compounds have been previously synthetized by different routes.[11,12]

Both reactions which lead to the formation of **2** and **3** can be envisaged as involving in a first step the attack by the hydride ion from $NaBH_4$ on the electrophilic carbon atom of the CS_2 moiety of the methyl trithiocarbonate or xanthate ligands.

Nucleophilic attack by hydride ion on the CS_2 carbon atom of a 1,1-dithio ligand has been reported to occur in the reactions of $NaBH_4$ with metal complexes containing the chelated zwitterion Et_3P–CS_2 (see Introduction). More recently, we observed that $NaBH_4$ reacts with acetone solutions of the [(triphos)Co(S_2CSMe)]BPh_4, and [(triphos)Co(S_2COEt)]BPh_4 complexes to give the compounds V and VI, which can be isolated in good yield.[10]

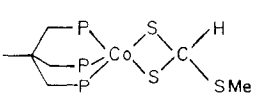

V

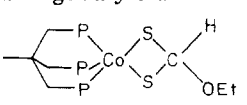

VI

The reaction mechanism for the formation of **2** may proceed by an initial attack of H^- on the CS_2 carbon atom of the trithiocarbonate complex to give an intermediate of type V. This intermediate could then interconvert directly to the final product by expelling methyl mercaptan, followed by a rearrangement of the CS_2 group. On

(8) Unpublished results of this laboratory. The [(triphos)Ni(S_2CX)]BPh_4 (X = OEt, NEt_2) complexes were synthetized by adding under nitrogen KS_2COEt or NaS_2CNEt_2 (1 mmol) in ethanol (10 mL) to a mixture of $Ni(BF_4)_2 \cdot 6H_2O$ (1 mmol) in ethanol (20 mL), triphos (1 mmol) in CH_2Cl_2 (20 mL), and $NaBPh_4$ (1 mmol) in acetone (10 mL).

(9) Lever, A. B. P. "Inorganic Electron Spectroscopy"; Elsevier: Amsterdam, 1968, and references therein.

(10) Unpublished results.

(11) Dapporto, P.; Midollini, S.; Orlandini, A.; Sacconi, L. *Inorg. Chem.* **1976**, *15*, 2768.

(12) Chatt, J.; Hart, F. A. *J. Chem. Soc.* **1965**, 812.

the basis of the above considerations, the reaction mechanism for compound **3** may be tentatively rationalized in terms of the formation of the unstable carbonyl sulfide, intermediate VII, which then converts to the carbonyl derivative **3**. As a confirmation of this mechanism we

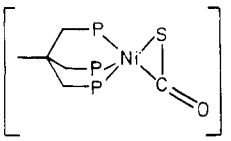

VII

found that the nickel (0) complex [Ni(triphos)$_2$] reacts with COS to give **3** in good yield. Moreover, Werner et al. reported that the carbonyl complex [(C_5H_5)Co(PMe_3)CO] is obtainable from the reaction of [(C_5H_5)Co$(PMe_3)_2$] with COS via an unstable COS intermediate.[13] The sulfur atom can be easily removed from the COS group by action of the phosphine ligand, a fact already ascertained in the reactions of some phosphine–rhodium compounds with COS, which give carbonyl complexes and phosphine sulfides.[14] However, we have not been successful in isolating any phosphine sulfide.

An acetone solution of the dithiocarbamate complex [(triphos)Ni(S_2CNEt_2)]BPh_4 reacts with $NaBH_4$, giving a light brown solution from which yellow crystals of empirical formula [(triphos)Ni(SH)], **4**, are precipitated. Compound **4** is air stable in the solid state but decomposes in solution even in an inert atmosphere. For this reason the compound has not been studied in solution. The room-temperature magnetic moment has a value of 2.11 μ_B, corresponding to a doublet ground state. The reflectance spectrum with absorption maxima at 8700 (sh), 10 400, and 22 200cm^{-1} is comparable with those of distorted tetrahedral nickel (I) complexes.[15] No band that could be attributed to the S–H stretching vibration has been detected in the IR spectrum. Indeed, this is rarely observed, probably due to its low intensity.[16] A preliminary X-ray analysis has confirmed the structure proposed for **4**. The nickel atom is coordinated by the three

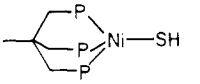

4

phosphorus atoms of the triphos ligand and by the sulfur atom, which form a distorted tetrahedral environment.

While we do not have enough information to propose a plausible mechanism for the formation of this thiolo complex from the starting dithiocarbamate compound, it is useful to report the presence of some secondary products in the reaction mixture. Alkyl mercaptans and hydrogen sulfide are indeed detected when the [(triphos)Ni$(S_2C$–X)]BPh_4 (X = SMe, OEt, NEt_2) complexes are treated with $NaBH_4$.

Indeed, tripod-like poly(tertiary phosphines) such as triphos can stabilize mercapto complexes of transition metals.[17] In particular, the nickel complexes are limited to the μ-S dinuclear complex [(triphos)Ni(μ-S)Ni(triphos)]$(BPh_4)_2$,[18] obtained through reaction of nickel(II) aquocations with H_2S in the presence of triphos and $NaBPh_4$. Up to date the dithiocarbamate reaction seems to be the only way of obtaining compound **4**.

Acknowledgment. Thanks are expressed to Mr. F. Cecconi, F. Nuzzi, and D. Masi for technical assistance and to Mr. P. Innocenti for recording NMR spectra.

Registry No. **1**, 83561-90-4; **2**, 60294-99-7; **3**, 14876-51-8; **4**, 83561-91-5; [(triphos)Ni(S_2CPEt_3)]$(BPh_4)_2$, 83561-93-7; [(triphos)Ni(S_2CSMe)]BPh_4, 83561-95-9; [(triphos)Ni(S_2COEt)]BPh_4, 83561-97-1; [(triphos)Ni(S_2CNEt_2)]BPh_4, 83561-99-3; $NaBH_4$, 16940-66-2; (triphos)Ni(S_2CS), 83562-00-9; $MeOSO_2F$, 421-20-5; KS_2COEt, 151-01-9; NaS_2CNEt_2, 148-18-5; $Ni(BF_4)_2$, 14708-14-6; triphos, 22031-12-5; $NaBPh_4$, 143-66-8.

(13) Werner, H.; Kolb, O. *Angew. Chem., Int. Ed. Engl.* **1979**, *18*, 865.
(14) Datta, S.; Pandey, K. K.; Agarwala, U. C. *Inorg. Chim. Acta* **1980**, *40*, 65.
(15) Sacconi, L.; Midollini, S. *J. Chem. Soc., Dalton Trans.* **1972**, 1213.
(16) Collman, J. P.; Rothrock, R. R.; Stark, R. A. *Inorg. Chem.* **1977**, *16*, 1437.
(17) Ghilardi, C. A.; Mealli, C.; Midollini, S.; Nefedov, V. I.; Orlandini, A.; Sacconi, L. *Inorg. Chem.* **1980**, *19*, 2454 and references therein.
(18) Mealli, C.; Midollini, S.; Sacconi, L. *J. Chem. Soc., Chem. Commun.* **1975**, 765.

Effects of Ligand Substitution on the Metal–Metal Bonding in Triosmium Carbonyl Clusters. The Crystal and Molecular Structures of $Os_3(\mu_3\text{-}S)_2(CO)_9$ and $Os_3(\mu_3\text{-}S)_2(CO)_8PMe_2Ph$

Richard D. Adams,* István T. Horváth, Brigitte E. Segmüller, and Li-Wu Yang

Department of Chemistry, Yale University, New Haven, Connecticut 06511

Received July 9, 1982

The molecular structures of the compounds $Os_3(\mu_3\text{-}S)_2(CO)_9$, I, and $Os_3(\mu_3\text{-}S)_2(CO)_8PMe_2Ph$, II, have been determined by single-crystal X-ray diffraction methods. For I: space group $P\bar{1}$, a = 6.745 (2) Å, b = 9.503 (2) Å, c = 13.592 (3) Å, α = 82.42 (2)°, β = 84.58 (2)°, γ = 69.61 (2)°; V = 808.4 (4) Å^3, Z = 2, ρ_{calcd} = 3.64 g/cm^3. The structure was solved by a combination of Patterson and difference Fourier techniques. Full-matrix least-squares refinement on 2137 reflections ($F_o^2 \geq 3.0\sigma(F)^2$) yielded the final residuals R_F = 0.032 and R_{wF} = 0.038. The molecule contains an open triangular cluster of three metal atoms with two equivalent metal–metal bonds Os(1)–Os(2) = 2.814 (1) Å and Os(1)–Os(3) = 2.812 (1) Å. There are two inequivalent triply bridging sulfido ligands, and each metal atom has three linear terminal carbonyl ligands. For II: space group $P\bar{1}$, a = 9.316 (2) Å, b = 11.346 (1) Å, c = 13.592 (3) Å, α = 71.65 (1)°, β = 71.63 (2)°, γ = 79.67 (1)°, V = 1164.5 (3) Å^3, Z = 2, ρ_{calcd} = 2.84 g/cm^3. This structure was solved by a combination of Patterson and difference Fourier techniques. Full-matrix least-squares refinement on 2834 reflections ($F_o^2 \geq 3.0\sigma(F)_2$) yielded the final residuals R_F = 0.040 and R_{wF} = 0.041. The structure of II is similar to that of I except that a PMe_2Ph ligand has been substituted for an equatorially positioned carbonyl ligand on one of the exterior metal atoms of the cluster in a position trans to one of the metal–metal bonds. The two metal–metal bonds are significantly different. The one trans to the phosphine ligand is 2.856 (1) Å while the other is 2.770 (1) Å. The structures of I and II are compared with that of $Os_3(\mu_3\text{-}S)_2(CO)_8CS$, III, which shows distortions in the metal–metal bonding that are similar to II. The cause of these distortions is attributed to a trans influence of the substituted ligand and is believed to be largely σ inductive in nature.

Introduction

The concept of the metal–metal bonding in molecular complexes[1,2] is one that has now grown from the simple two-center two-electron model used to explain the bonding in $Mn_2(CO)_{10}$ to the highly complex, delocalized models used to explain metal–metal multiple bonding[1] and the bonding in clusters.[3-5] To this one would like to add an understanding of the effects of ligand substitution on the metal–metal bonding and the reactivity at the sites of neighboring metal atoms.[6,7]

It has been observed that phosphine substitution in the clusters $Me_3(CO)_{12}$ (M = Fe,[8] Ru,[9] Os[10]) causes a net increase in the M–M internuclear separations. This has been attributed variously to the decreased π acidity of phosphines compared to CO[8,9,11] or to ligand packing effects.[10,11] We have recently synthesized the clusters $Os_3(\mu_3\text{-}S)_2(CO)_9$, I and $Os_3(\mu_3\text{-}S)_2(CO)_8PMe_2Ph$, II and have now examined their molecular structures by X-ray crystallographic methods. The latter compound contains an equatorially substituted phosphine ligand and shows significant distortions in the metal–metal bonding of the cluster. In this report the molecular structures of I and II will be described and discussed and compared with that of the related compound $(Os_3(\mu_3\text{-}S)_2(CO)_8(CS)$, III.[13]

Results

$Os_3(\mu_3\text{-}S)_2(CO)_9$, I. An ORTEP diagram of the molecular structure of I is shown in Figure 1. Final positional and thermal parameters are listed in Table I. Complete lists of interatomic distances and angles are given in Tables II and III. Structurally II is very similar to the related compounds $Fe_3(\mu_3\text{-}S)_2(CO)_9$[14] and $Fe_3(\mu_3\text{-}Se)_2(CO)_9$.[15] The molecule consists of an "open" cluster of three metal atoms with two metal–metal bonds, Os(1)–Os(2) = 2.814 (1) Å and Os(1)–Os(3) = 2.812 (1) Å, which are slightly shorter than those in $Os_3(CO)_{12}$, Os–Os = 2.877 (3) Å.[16] The Os(2)···Os(3) separation at 3.662 (1) Å is similar to the 3.644 Å observed in the related compound $Os_3(\mu_3\text{-}S)_2(CO)_8CS$, III, and is clearly nonbonding. Overall, I has C_s symmetry (not crystallographically imposed) such that the three atoms S(1), Os(2), and S(2) and the carbonyl ligand C(2)–O(2) lie in the reflection plane. There are two triply bridging sulfido ligands. The Os–S distances to the central seven-coordinate metal atom Os(1), Os(1)–S(1) = 2.454 (2) Å and Os(1)–S(2) = 2.434 (2) Å, are slightly longer than those to the external six-coordinate metal atoms Os(2) and Os(3), 2.390 (2)–2.415 (2) Å. A similar pattern was also observed for II (see below) and III.[13] The sulfido ligands are chemically inequivalent, and curiously each metal–sulfur bonding distance to S(1) is slightly longer than the corresponding distance to S(2). This was also observed in II and III. Each metal atom contains three linear terminal carbonyl ligands. The shortest intermolecular

(1) Cotton, F. A., Wilkinson, G. "Advanced Inorganic Chemistry"; Wiley: New York, 1980; Chapter 26.
(2) Vahrenkamp, H. *Angew Chem. Int. Ed. Engl.* **1978**, *17*, 379.
(3) Johnson, B. F. G.; Benfield, R. E. "Topics in Inorganic and Organometallic Stereochemistry"; *Geoffroy*, G., *Ed*; Wiley: New York, 1981.
(4) Wade, K. In "Transition Metal Clusters"; Johnson, B. F. G., Ed.; Wiley: New York, 1980.
(5) Lauher, J. *J. Am. Chem. Soc.* **1978**, *100*, 5305.
(6) Karel, K. J.; Norton, J. R. *J. Am. Chem. Soc.* **1974**, *96*, 6812.
(7) Drago, R. S.; Long, J. R.; Cosmano, R. *Inorg. Chem.* **1981**, *20*, 2920.
(8) Dahm, D. J.; Jacobson, R. A. *J. Am. Chem. Soc.* **1968**, *90*, 5106.
(9) Forbes, E. J.; Goodhand, N.; Jones, D. L.; Hamor, T. A. *J. Organomet. Chem.* **1979**, *182*, 143.
(10) Benfield, R. E.; Johnson, B. F. G.; Raithby, P. R.; Sheldrick, G. M. *Acta Crystallogr., Sect. B.* **1978**, *B34*, 666.
(11) The structure of $Os_6(CO)_{17}[P(OMe)_3]_4$ shows similar M–M lengthening effects.[12]
(12) Goudsmit, R. J.; Johnson, B. F. G.; Lewis, J.; Raithby, P. R.; Whitmire, K. H. *J. Chem. Soc., Chem. Commun.* **1982**, 640.
(13) Broadhurst, P. V.; Johnson, B. F. G.; Lewis, J.; Raithby, P. R. *J. Organomet. Chem.* **1980**, *194*, C35.
(14) Wei, C. H.; Dahl, L. F. *Inorg. Chem.* **1965**, *48* 493.
(15) Dahl, L. F.; Sutton, P. *Inorg. Chem.* **1963**, *2*, 1067.
(16) Churchill, M. R.; DeBoer, B. G. *Inorg. Chem.* **1977**, *16*, 878.

0276-7333/83/2302-0144$01.50/0

Table I. Positional and Thermal Parameters and Their Estimated Standard Deviations for $Os_3(\mu_3\text{-}S)_2(CO)_9$, I[a]

atom	x	y	z	B(1,1)	B(2,2)	B(3,3)	B(1,2)	B(1,3)	B(2,3)
Os(1)	0.41680 (9)	0.30293 (7)	0.34111 (4)	2.45 (2)	2.37 (2)	1.79 (2)	−0.85 (2)	−0.27 (2)	0.00 (2)
Os(2)	0.29615 (10)	0.59770 (7)	0.24291 (4)	2.84 (2)	1.97 (2)	2.23 (2)	−0.84 (2)	−0.10 (2)	−0.26 (2)
Os(3)	0.33095 (10)	0.24057 (7)	0.15623 (4)	2.84 (2)	2.05 (2)	1.94 (2)	−0.82 (2)	−0.16 (2)	−0.32 (2)
S(1)	0.0919 (6)	0.4318 (4)	0.2517 (2)	2.3 (1)	2.4 (1)	2.3 (1)	−0.6 (1)	−0.2 (1)	−0.3 (1)
S(2)	0.5536 (6)	0.3807 (4)	0.1788 (3)	2.7 (1)	2.7 (2)	2.3 (1)	−1.0 (1)	0.3 (1)	−0.3 (1)

atom	x	y	z	B, Å²	atom	x	y	z	B, Å²
O(1)	0.236 (2)	0.464 (2)	0.5286 (9)	5.8 (3)	C(1)	0.309 (3)	0.397 (2)	0.458 (1)	4.3 (4)
O(2)	0.868 (2)	0.183 (1)	0.4109 (9)	5.2 (3)	C(2)	0.699 (2)	0.226 (2)	0.385 (1)	3.2 (3)
O(3)	0.347 (2)	0.001 (1)	0.4126 (9)	5.0 (3)	C(3)	0.375 (3)	0.117 (2)	0.364 (1)	3.6 (3)
O(4)	−0.033 (2)	0.811 (1)	0.3782 (8)	4.5 (3)	C(4)	0.089 (2)	0.731 (2)	0.328 (1)	3.2 (3)
O(5)	0.161 (2)	0.786 (1)	0.0452 (9)	5.1 (3)	C(5)	0.201 (3)	0.722 (2)	0.123 (1)	3.5 (3)
O(6)	0.628 (2)	0.741 (1)	0.2711 (9)	5.3 (3)	C(6)	0.504 (3)	0.686 (2)	0.260 (1)	4.0 (4)
O(7)	0.198 (2)	0.374 (1)	−0.0530 (8)	4.6 (3)	C(7)	0.236 (2)	0.320 (2)	0.027 (1)	2.9 (3)
O(8)	0.696 (2)	−0.031 (1)	0.0911 (9)	5.1 (3)	C(8)	0.562 (2)	0.067 (2)	0.118 (1)	3.2 (3)
O(9)	0.036 (2)	0.052 (1)	0.1930 (9)	5.0 (3)	C(9)	0.147 (2)	0.125 (2)	0.177 (1)	3.3 (3)

[a] The form of the anisotropic thermal parameter is $\exp[-1/4(h^2a^{*2}B(1,1) + k^2b^{*2}B(2,2) + l^2c^{*2}B(3,3) + 2hka^*b^*B(1,2) + 2hla^*c^*B(1,3) + 2klb^*c^*B(2,3)]$.

Table II. Interatomic Distances (Å) with Esds for $Os_3(\mu_3\text{-}S)_2(CO)_9$, I

Os(1)-Os(2)	2.814 (1)	Os(2)-C(6)	1.91 (1)
Os(1)-Os(3)	2.812 (1)	Os(3)-C(7)	1.90 (1)
Os(2)···Os(3)	3.662 (1)	Os(3)-C(8)	1.93 (1)
Os(1)-S(1)	2.454 (2)	Os(3)-C(9)	1.91 (1)
Os(1)-S(2)	2.434 (2)	C(1)-O(1)	1.20 (1)
Os(2)-S(1)	2.415 (2)	C(2)-O(2)	1.14 (1)
Os(2)-S(2)	2.392 (2)	C(3)-O(3)	1.20 (1)
Os(3)-S(1)	2.402 (2)	C(4)-O(4)	1.15 (1)
Os(3)-S(2)	2.390 (2)	C(5)-O(5)	1.16 (1)
Os(1)-C(1)	1.88 (1)	C(6)-O(6)	1.16 (1)
Os(1)-C(2)	1.91 (1)	C(7)-O(7)	1.15 (1)
Os(1)-C(3)	1.90 (1)	C(8)-O(8)	1.12 (1)
Os(2)-C(4)	1.93 (1)	C(9)-O(9)	1.17 (1)
Os(2)-C(5)	1.90 (1)		

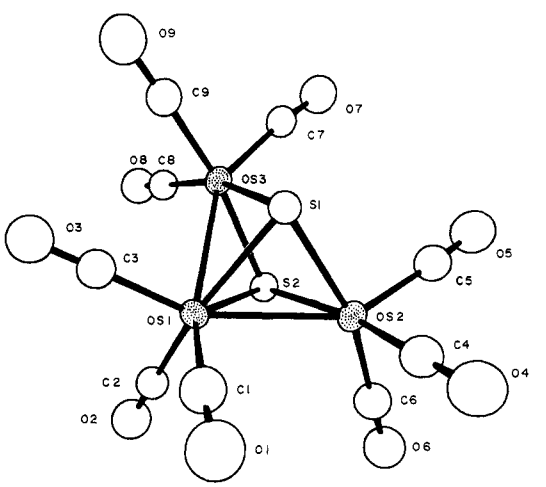

Figure 1. An ORTEP diagram of $Os_3(\mu_3\text{-}S)_2(CO)_9$, I, showing 50% probability thermal motion ellipsoids.

contacts were between carbonyl oxygen atoms at 3.06–3.09 Å.

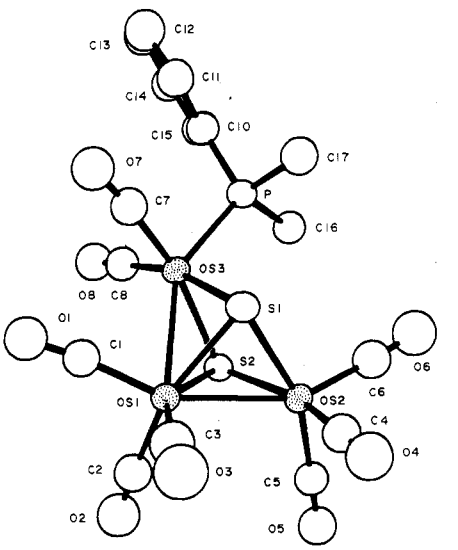

Figure 2. An ORTEP diagram of $Os_3(\mu_3\text{-}S)_2(CO)_8PMe_2Ph$, II, showing 50% probability thermal motion ellipsoids.

$Os_3(\mu_3\text{-}S)_2(CO)_8PMe_2Ph$, II. An ORTEP diagram of the molecular structure of II is shown in Figure 2. Final positional and thermal parameters are listed in Table IV. Complete lists of interatomic distances and angles are given in Tables V and VI. The gross structure of II is essentially the same as that of I, but a PMe_2Ph ligand has been substituted for one of the "equatorially" positioned carbonyl ligands on one of the external metal atoms of the cluster. Unlike I, the Os–Os bonding distances in II differ quite significantly. The Os(1)–Os(3) bond which is essentially trans to the phosphine ligand has increased to 2.856 (1) Å while the Os(1–Os(2) distance has contracted by an equal amount to 2.770 (1) Å. The average value, 2.813 Å, is the same as that in I. A similar change in the metal–metal bonding was observed in III which is analo-

Table III. Interatomic Angles (deg) with Esds for $Os_3(\mu_3\text{-}S)_2(CO)_9$, I

Os(2)-Os(1)-Os(3)	81.21 (1)	Os(1)-Os(2)-S(2)	55.02 (6)	Os(1)-S(2)-Os(2)	71.35 (6)
Os(2)-Os(1)-S(1)	54.04 (6)	Os(1)-Os(2)-C(4)	108.5 (3)	Os(1)-S(2)-Os(3)	71.31 (7)
Os(2)-Os(1)-S(2)	53.63 (6)	Os(1)-Os(2)-C(5)	146.0 (3)	Os(2)-S(2)-Os(3)	99.95 (9)
Os(2)-Os(1)-C(1)	85.5 (4)	Os(1)-Os(2)-C(6)	109.3 (3)	Os(1)-C(1)-O(1)	176.4 (10)
Os(2)-Os(1)-C(2)	114.9 (3)	Os(1)-Os(3)-S(1)	55.47 (5)	Os(1)-C(2)-O(2)	178.7 (10)
Os(2)-Os(1)-C(3)	153.2 (3)	Os(1)-Os(3)-S(2)	55.07 (5)	Os(1)-C(3)-O(3)	178.9 (9)
Os(3)-Os(1)-S(1)	53.75 (5)	Os(1)-Os(3)-C(7)	146.6 (3)	Os(2)-C(4)-O(4)	179.7 (6)
Os(3)-Os(1)-S(2)	53.62 (6)	Os(1)-Os(3)-C(8)	107.8 (3)	Os(2)-C(5)-O(5)	172.4 (10)
Os(3)-Os(1)-C(1)	147.4 (4)	Os(1)-Os(3)-C(9)	109.1 (3)	Os(2)-C(6)-O(6)	179.1 (9)
Os(3)-Os(1)-C(2)	120.1 (3)	Os(1)-S(1)-Os(2)	70.63 (7)	Os(3)-C(7)-O(7)	172.2 (9)
Os(3)-Os(1)-C(3)	82.1 (3)	Os(1)-S(1)-Os(3)	70.77 (7)	Os(3)-C(8)-O(8)	177.0 (9)
Os(1)-Os(2)-S(1)	55.33 (6)	Os(2)-S(1)-Os(3)	98.97 (8)	Os(3)-C(9)-O(9)	177.7 (9)

Table IV. Table of Positional and Thermal Parameters and Their Estimated Standard Deviations for $Os_3(\mu_3\text{-}S)_2(CO)_8PMe_2Ph$, II[a]

atom	x	y	z	B(1,1)	B(2,2)	B(3,3)	B(1,2)	B(1,3)	B(2,3)	B(EQV)
Os(1)	0.06727 (7)	0.19466 (5)	0.09926 (6)	2.62 (2)	2.83 (2)	3.48 (2)	−0.29 (2)	−1.30 (2)	−0.28 (2)	3.01 (1)
Os(2)	0.29160 (7)	0.27803 (5)	0.15209 (5)	2.99 (2)	2.89 (2)	3.14 (2)	−0.62 (2)	−1.03 (2)	−0.56 (2)	2.98 (1)
Os(3)	0.17542 (7)	−0.04136 (5)	0.23210 (5)	2.81 (2)	2.63 (2)	2.98 (2)	−0.44 (2)	−1.06 (2)	−0.20 (2)	2.85 (1)
S(1)	0.1033 (4)	0.1446 (3)	0.2997 (3)	3.5 (2)	3.5 (1)	2.8 (2)	−0.3 (1)	−0.6 (1)	−0.7 (1)	3.3 (1)
S(2)	0.3295 (4)	0.1040 (3)	0.0705 (3)	2.6 (1)	3.2 (1)	2.9 (2)	−0.3 (1)	−0.8 (1)	−0.5 (1)	2.95 (9)
P	0.3312 (4)	−0.1459 (3)	0.3512 (4)	3.3 (2)	3.3 (2)	3.3 (2)	−0.4 (1)	−1.2 (1)	−0.2 (1)	3.4 (1)

atom	x	y	z	B, Å²	atom	x	y	z	B, Å²
O(1)	−0.173 (1)	0.026 (1)	0.131 (1)	6.0 (3)	C(5)	0.396 (2)	0.383 (1)	0.002 (1)	4.1 (3)
O(2)	0.134 (1)	0.288 (1)	−0.172 (1)	6.7 (3)	C(6)	0.457 (2)	0.248 (1)	0.217 (2)	5.2 (4)
O(3)	−0.150 (2)	0.416 (1)	0.147 (1)	8.5 (4)	C(7)	0.011 (2)	−0.124 (1)	0.342 (1)	4.5 (4)
O(4)	0.137 (1)	0.505 (1)	0.238 (1)	6.5 (3)	C(8)	0.228 (2)	−0.164 (1)	0.143 (1)	4.2 (4)
O(5)	0.453 (1)	0.447 (1)	−0.089 (1)	5.3 (3)	C(10)	0.327 (2)	−0.314 (1)	0.401 (1)	4.1 (3)
O(6)	0.559 (1)	0.224 (1)	0.261 (1)	7.1 (3)	C(11)	0.205 (2)	−0.368 (1)	0.491 (1)	4.9 (4)
O(7)	−0.100 (1)	−0.171 (1)	0.404 (1)	5.9 (3)	C(12)	0.208 (2)	−0.501 (2)	0.524 (2)	6.1 (5)
O(8)	0.262 (1)	−0.234 (1)	0.089 (1)	5.4 (3)	C(13)	0.319 (2)	−0.570 (2)	0.470 (2)	5.7 (4)
C(1)	−0.076 (2)	0.085 (1)	0.122 (1)	4.5 (4)	C(14)	0.443 (2)	−0.519 (1)	0.379 (1)	4.8 (4)
C(2)	0.101 (2)	0.253 (1)	−0.070 (2)	5.1 (4)	C(15)	0.447 (2)	−0.391 (1)	0.344 (1)	4.1 (3)
C(3)	−0.068 (2)	0.331 (2)	0.124 (2)	6.2 (5)	C(16)	0.533 (2)	−0.117 (1)	0.274 (1)	4.2 (4)
C(4)	0.195 (2)	0.419 (1)	0.206 (1)	4.5 (4)	C(17)	0.293 (2)	−0.100 (1)	0.488 (1)	4.8 (4)

[a] The form of the anisotropic thermal parameter is $\exp[-1/4(h^2a^{*2}B(1,1) + k^2b^{*2}B(2,2) + l^2c^{*2}B(3,3) + 2hka^*b^*B(1,2) + 2hla^*c^*B(1,3) + 2klb^*c^*B(2,3)]$.

Table V. Interatomic Distances (Å) with Esds for $Os_3(\mu_3\text{-}S)_2(CO)_8PMe_2Ph$, II

Os(1)-Os(2)	2.770 (1)	P-C(10)	1.82 (1)
Os(1)-Os(3)	2.856 (1)	P-C(16)	1.86 (1)
Os(2)···Os(3)	3.713 (1)	P-C(17)	1.81 (1)
Os(1)-S(1)	2.452 (3)	C(10)-C(11)	1.39 (1)
Os(1)-S(2)	2.446 (2)	C(10)-C(15)	1.43 (1)
Os(2)-S(1)	2.426 (2)	C(11)-C(12)	1.43 (2)
Os(2)-S(2)	2.405 (2)	C(12)-C(13)	1.32 (2)
Os(3)-S(1)	2.413 (2)	C(13)-C(14)	1.40 (2)
Os(3)-S(2)	2.389 (2)	C(14)-C(15)	1.38 (1)
Os(3)-P	2.298 (3)	C(1)-O(1)	1.18 (1)
Os(1)-C(1)	1.89 (1)	C(2)-O(2)	1.14 (1)
Os(1)-C(2)	1.90 (1)	C(3)-O(3)	1.17 (1)
Os(1)-C(3)	1.86 (1)	C(4)-O(4)	1.15 (1)
Os(2)-C(4)	1.90 (1)	C(5)-O(5)	1.15 (1)
Os(2)-C(5)	1.91 (1)	C(6)-O(6)	1.19 (1)
Os(2)-C(6)	1.89 (1)	C(7)-O(7)	1.18 (1)
Os(3)-C(7)	1.86 (1)	C(8)-O(8)	1.13 (1)
Os(3)-C(8)	1.93 (1)		

gous to II but has a thiocarbonyl ligand in the site occupied by the phosphine ligand in II. In III the Os–Os bond trans to the substituent has increased to 2.830 (2) Å while the other Os–Os bond has decreased to 2.780 (2) Å. The Os–S distances to the triply bridging sulfido ligands are very similar to those in I and III and as observed in I and III each Os–S distance to S(1) is slightly longer than the corresponding distance to S(2). There are eight linear terminal carbonyl ligands distributed in the 3:3:2 pattern as shown in Figure 2. The phosphine ligand has no unusual distortions. The Os(3)–P distance of 2.298 (3) Å is similar to the 2.307 (2) Å observed in the related "open" cluster $Os_3(\mu_3\text{-}S)(\mu_3\text{-}SCH_2)(CO)_8PMe_2Ph$.[17] The shortest intermolecular contacts are between carbonyl oxygen atoms at 3.15 (1) Å.

Discussion

Closed Clusters. Crystallographic analyses have been performed on the monosubstituted clusters $Fe_3(CO)_{11}PPh_3$, IV,[8] $Ru_3(CO)_{11}PPh_3$, V,[9] and $Os_3(CO)_{11}P(OMe)_3$, VI.[10] Each cluster contains a closed triangle (three metal–metal bonds) of three metal atoms with a phosphorus ligand in an equatorial coordination site. Each of these

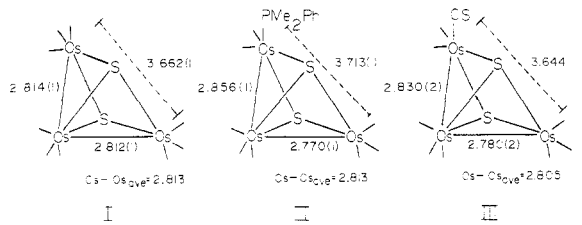

Figure 3.

compounds shows a general increase in the metal–metal internuclear separations when compared with those of the parent binary carbonyl clusters. This is mitigated somewhat in IV by the presence of bridging carbonyl ligands, but the net result in each case is an increase in the overall size of the M_3 grouping. In V the M–M separations are on the average 0.04 Å longer than those in $Ru_3(CO)_{12}$.[9] In VI the average increase is 0.02 Å over that in $Os_3(CO)_{12}$.[10,16] Although the Ru–Ru bond cis to the phosphine ligand in V is significantly longer than the other two Ru–Ru bonds, it is clear that both in V and VI all three metal–metal bonds have been lengthened and in VI there is no selectivity in the lengthening. A noticeable expansion of a Ru_3 cluster has also been observed when a PPh_2OEt ligand was substituted for a carbonyl ligand in the compound $HRu_3(CO)_9(C{\equiv}C\text{-}t\text{-}Bu)$.[18]

The reason for the expansion of the M_3 core has not been unambiguously established. It was proposed that the substitution of a poor π acceptor for a good one results in an increase in electron density on the metal atoms, perhaps, in antibonding orbitals, and this causes the cluster to expand.[8,9] Alternatively, it has been proposed that due to the effects of ligand packing, the substitution of a bulky ligand for a nonbulky one leads to expansions of the ligand sphere and the cluster than expands to maintain the optimum overall molecular geometry.[10]

Open Clusters. In this category only the clusters I, II, and III, which have only two metal–metal bonds between the three metal atoms and do not contain bridging hydride ligands, will be considered. Comparisons of the metal–metal bonding in I, II, and III are shown in Figure 3. Since these clusters are opened and thus naturally expanded

(17) Adams, R. D.; Golembeski, N. M.; Selegue, J. P. *J. Am. Chem. Soc.* **1981**, *103*, 546.

(18) Carty, A. J.; MacLaughlin, S. A.; Taylor, N. J.; Sappa, E. *Inorg. Chem.* **1981**, *20*, 4437.

Table VI. Interatomic Angles (deg) with Esds for $Os_3(\mu_3\text{-}S)_2(CO)_8PMe_2Ph$, II

Os(2)-Os(1)-Os(3)	82.57 (2)	Os(1)-Os(3)-S(1)	54.68 (6)	C(16)-P-C(17)	103.9 (5)
Os(2)-Os(1)-S(1)	54.97 (6)	Os(1)-Os(3)-S(2)	54.73 (6)	P-C(10)-C(11)	120.0 (8)
Os(2)-Os(1)-S(2)	54.49 (6)	Os(1)-Os(3)-P	146.54 (6)	P-C(10)-C(15)	120.1 (8)
Os(2)-Os(1)-C(1)	155.7 (3)	Os(1)-Os(3)-C(7)	109.0 (3)	C(11)-C(10)-C(15)	119.9 (9)
Os(2)-Os(1)-C(2)	106.9 (3)	Os(1)-Os(3)-C(8)	112.1 (3)	C(10)-C(11)-C(12)	117 (1)
Os(2)-Os(1)-C(3)	93.1 (4)	Os(1)-S(1)-Os(2)	69.19 (7)	C(11)-C(12)-C(13)	122 (1)
Os(3)-Os(1)-S(1)	53.43 (6)	Os(1)-S(1)-Os(3)	71.89 (7)	C(12)-C(13)-C(14)	123 (1)
Os(3)-Os(1)-S(2)	52.88 (5)	Os(2)-S(1)-Os(3)	100.19 (9)	C(13)-C(14)-C(15)	118 (1)
Os(3)-Os(1)-C(1)	75.3 (3)	Os(1)-S(2)-Os(2)	69.62 (7)	C(14)-C(15)-C(10)	121 (1)
Os(3)-Os(1)-C(2)	127.0 (3)	Os(1)-S(2)-Os(3)	72.39 (7)	Os(1)-C(1)-O(1)	174 (1)
Os(3)-Os(1)-C(3)	140.0 (4)	Os(2)-S(2)-Os(3)	101.49 (9)	Os(1)-C(2)-O(2)	174 (1)
Os(1)-Os(2)-S(1)	55.84 (6)	Os(3)-P-C(10)	115.0 (4)	Os(1)-C(3)-O(3)	175 (1)
Os(1)-Os(2)-S(2)	55.89 (6)	Os(3)-P-C(16)	112.1 (4)	Os(2)-C(4)-O(4)	180 (1)
Os(1)-Os(2)-C(4)	104.0 (3)	Os(3)-P-C(17)	114.5 (4)	Os(2)-C(5)-O(5)	178 (1)
Os(1)-Os(2)-C(5)	104.0 (3)	C(10)-P-C(16)	105.5 (5)	Os(2)-C(6)-O(6)	177 (1)
Os(1)-Os(2)-C(6)	151.3 (3)	C(10)-P-C(17)	104.8 (5)	Os(3)-C(7)-O(7)	174 (1)
				Os(3)-C(8)-O(8)	178 (1)

around the M_3 framework, it would seem that ligand packing effects should be less important than in the closed clusters. Accordingly, the average value of the Os–Os bonding distance for the three compounds is essentially the same. However, the nonbonding Os···Os distance in II is significantly longer than that in I and III. This could be due to a small crowding effect caused by the phosphine ligand.

The most obvious and important effect of the ligand substitution is a pronounced increase in the metal–metal bond distance trans to the substituted ligand both in II and III. Since the thiocarbonyl ligand in III is essentially sterically identical with CO, we believe that the notion of the ligand packing is not a viable explanation for this effect.

Let us next consider the notion of the effect of the π acidity of the substituent. It is widely accepted that phosphine ligands are poorer π acceptors than CO, and on the the other hand, considerable evidence has been accumulated to show that CS is a better π acceptor than CO. Thus, since the π activity properties are in opposite directions, it would seem unlikely that they would produce the same result (i.e., trans bond lengthening).

Another factor which could be important is the σ-donor capacity of the substituent. Phosphines and thiocarbonyl[19] are both believed to be better σ donors than CO, and it is generally agreed that the σ-inductive effect does play a major role in trans influence.[20] Thus, a trans influence strongly dominated by σ-inductive effects would seem to be a plausible explanation for the trans bond lengthening observed in these clusters.

The other interesting feature of the metal–metal bonding is the pronounced shortening of the second metal–metal bond, 2.770 (1) Å in II and 2.780 (2) Å in III. This is probably a consequence of the weakening of the first metal–metal bond. This weakening and its accompanying decrease in metal–metal orbital overlap could, in turn, permit a greater degree of orbital overlap and thus strengthening of the metal–metal bond between the second and third metal atoms.

In conclusion, the comparisons of the structures of I, II, and III show that ligand substitutions can have a significant influence on the metal–metal bonding in cluster compounds. The observed effects can be fully interpreted in terms of a trans influence which is largely σ inductive in character. This trans influence leads to a weakening of the metal–metal bond directly opposite the substituent and a strengthening of the metal–metal bond one metal atom removed. Such a pattern is not apparent in the closed clusters, but this could be due to delocalization of their σ bonding.[21]

Facile perturbation of the metal–metal bonding could have implications in reactivity, and it has recently been shown that the related cluster $Fe_3(\mu_3\text{-}Te)_2(CO)_9$ readily adds donors via cleavage of a metal–metal bond.[22]

As a note of caution, we add that the observations and conclusions presented here may not apply to clusters containing bridging hydride ligands. Indeed, in the related open cluster $H_2Os_3(\mu_3\text{-}S)_2(CO)_7CS$ which has a thiocarbonyl ligand in an equatorial site on one of the exterior metal atoms and hydride ligands bridging each of the two metal–metal bonds, the Os–Os bonds are not significantly different.[23] However, it has been proposed that in the presence of bridging hydride ligands, direct metal–metal interactions do not exist.[24] It would be interesting to see if the thiocarbonyl ligand in $H_2Os_3(\mu_3\text{-}S)_2(CO)_7CS$ significantly influences the metal–hydrogen bond distances.

Experimental Section

$Os_3(\mu_3\text{-}S)_2(CO)_9$ was prepared as reported previously.[25] PMe_2Ph was purchased from Strem Chemicals, Inc., and was used without further purification. Reagent grade solvents were used without further purification. IR spectra were recorded on a Nicolet 7199 FT-IR. The ^1H NMR spectrum of II was recorded on a Bruker HX-270 spectrometer.

Preparation of $Os_3(\mu_3\text{-}S)_2(CO)_8PMe_2Ph$, II. Under an N_2 atmosphere 5.0 mg of $Os_3(\mu_3\text{-}S)_2(CO)_9$ was dissolved in 10 mL of hexane in a round-bottom flask at room temperature. A 1.1-μL sample of PMe_2Ph was added via syringe. After the mixture was stirred 3 h, the solvent was removed in vacuo. The residue was dissolved and chromatographed on silica TLC plates with hexane/CH_2Cl_2 (95/5) solvent. The yellow product was recrystallized from hexane: yield 5.0 mg, 88%; IR (ν(CO) in hexane) 2083 (w), 2065 (m), 2050 (s), 2018 (m), 2008 (vs), 1995 (m), 1974 (w), 1962 (vw) cm^{-1}. ^1H NMR (in $CDCl_3$) δ 7.40–7.72 (m, 5 h), 2.51 (d, 6 H, $J_{P\text{-}H}$ = 11.0 Hz).

Crystallographic Analyses. Crystals of I and II were grown by slow evaporation of solvent from hexane solutions at room temperature. The crystals were mounted in thin-walled glass capillaries. Diffraction measurements were made on an Enraf-Nonius CAD-4 fully automated diffractometer by using graphite-monochromatized Mo $K_{\bar{\alpha}}$ radiation. Unit cells were determined and refined from 25 randomly selected reflections obtained by using the CAD-4 automatic search, center, index, and

(19) (a) Butler, I. S. *Acc. Chem. Res.* **1977**, *10*, 359. (b) Yaneff, P. V. *Coord. Chem. Rev.* **1977**, *23*, 183.

(20) (a) Appleton, T. G.; Clark, H. C.; Manzer, L. E. (*Coord. Chem. Rev.* **1973**, *10*, 335. (b) Mason, R.; Towl, A. D. C. *J. Chem. Soc. A* **1970**, 1601.

(21) Schilling, B. E. R.; Hoffman, R. *J. Am. Chem. Soc.* **1979**, *101*, 3456.

(22) Lesch, D. A.; Rauchfuss, T. B. *Organometallics* **1982**, *1*, 499.

(23) Broadhurst P. V.; Johnson, B. F. G.; Lewis, J.; Orpen, A. G.; Raithby, P. R.; Thornback, J. R. *J. Organomet. Chem.* **1980**, *187*, 141.

(24) Johnson, B. F. G.; Lewis, J.; Pippard, D.; Raithby, P. R.; Sheldrick, G. M.; Rouse, K. D. *J. Chem. Soc., Dalton Trans.* **1979**, 616.

(25) Adams, R. D.; Yang, L. W. *J. Am. Chem. Soc.* **1982**, *104*, 4115.

Table VII. Crystallographic Data for X-ray Diffraction Studies

	I	II
	(A) Crystal Data	
formula	$Os_3S_2O_9C_9$	$Os_3S_2PO_8C_{16}H_{11}$
temp, ±5 °C	23	25
space group	$P\bar{1}$	$P\bar{1}$
a, Å	6.745 (2)	9.361 (2)
b, Å	9.503 (2)	11.346 (1)
c, Å	13.592 (3)	12.221 (2)
α, deg	82.42 (2)	71.65 (1)
β, deg	84.58 (2)	71.63 (2)
γ, deg	69.61 (2)	79.67 (1)
V, Å^3	808.4 (4)	1164.5 (3)
mol wt	886.8	997.0
ρ_{calcd}, g/cm^3	3.64	2.84
Z	2	2
	(B) Measurement of Intensity Data	
radiation	Mo K$\bar{\alpha}$ (0.710 73 Å)	Mo K$\bar{\alpha}$ (0.710 73 Å)
monochromator	graphite	graphite
detector aperture, mm		
horizontal (A + B tan θ)		
A	3.0	3.0
B	1.0	1.0
vertical	4.0	4.0
cryst faces	$0\bar{1}0$, 010, 001, $00\bar{1}$, 100, $\bar{1}00$	010, 010, 101, $\bar{1}0\bar{1}$, 100, $\bar{1}00$
crystal size, mm	0.33 × 0.05 × 0.11	0.21 × 0.20 × 0.53
crystal orientation; direction, deg from ϕ axis	normal to 211; 8.0	normal to $1\bar{1}2$; 10.5
reflctns measd	$h,\pm k,\pm l$	$h,\pm k,\pm l$
max 2θ, deg	50	50
scan type	moving crystal-stationary counter	moving crystal-stationary counter
ω-scan width, A + 0.347 tan θ, deg	A = 0.85	A = 0.95
background	$^1/_4$ additional scan at each end of scan	$^1/_4$ additional scan at each end of scan
max/min, deg	10	10
min/min, deg	1.3	1.4
no. of reflctns measd	2807	4044
data used ($F^2 \geq 3.0\sigma(F)^2$)	2137	2834
	(C) Treatment of Data	
absorption correction		
coefficient, cm^{-1}	252.9	166.31
grid	14 × 6 × 8	8 × 8 × 14
transmission coeff		
max	0.316	0.183
min	0.0852	0.057
P factor	0.010	0.01
final residuals R	0.032	0.040
R_w	0.038	0.041
esd of unit weight	2.70	2.602
largest shift/error value on final cycle	0.01	0.39

least-squares routines. The triclinic space group $P\bar{1}$ was selected for both compounds and confirmed by the successful solution and refinement of the structures. Crystal data and data collection parameters are listed in Table VII. All data processing was performed on a Digital Equipment Corp. PDP 11/45 computer using the Enraf Nonius SDP program library (version 16). Absorption corrections of a Gaussian integration type were done for both structures. Neutral atom scattering factors were calculated by the standard procedures.[26a] Anomalous dispersion corrections were applied to all non-hydrogen atoms.[26b] Full-matrix least-squares refinements minimized the function $\sum_{hkl} w(|F_o| - |F_c|)^2$ where $w = 1/\sigma(F)^2$, $\sigma(F) = \sigma(F_o^2)/2F_o$, and $\sigma(F_o^2) = [\sigma(I_{raw})^2 + (PF_o^2)^2]^{1/2}/Lp$.

Both structures were solved by the combination of Patterson and difference Fourier techniques. Only atoms heavier than oxygen were refined anisotropically. The positions of hydrogen atoms were calculated assuming idealizing geometry. Their contributions were added to the structure factor calculations, but their positions were not refined. Positional and thermal parameters for the structures are listed in Table I and IV. Interatomic distances and angles with errors obtained from the inverse matrix obtained on the final cycle of refinement for each structure are listed in Tables II, III, V, and VI. Structure factor amplitudes are available.[27]

Acknowledgment. We wish to thank the National Science Foundation for support of this research through Grant No. CHE 80-19041 and the Alfred P. Sloan Foundation for a fellowship to R.D.A. NMR studies were supported in part under Grant No. CHE-7916210 from the Chemistry Division of the National Science Foundation. We also wish to thank Engelhard Industries for a loan of osmium tetroxide.

Registry No. I, 72282-40-7; II, 83632-56-8.

Supplementary Material Available: Tables of structure factor amplitudes for both structures (23 pages). Ordering information is given on any current masthead page.

(26) "International Tables for X-ray Crystallography"; Kynoch Press: Birmingham, England, 1975; Vol. IV: (a) Table 2.2B, pp 99–101; (b) Table 2.3.1, pp 149–150.

(27) See supplementary material.

The Oligomerization of Clusters. The Synthesis and Crystal and Molecular Structure of $[(\mu\text{-H})_2(\mu_4\text{-S})Ru_3(CO)_8]_3$

Richard D. Adams,* Detlef Männig, and Brigitte E. Segmüller

Department of Chemistry, Yale University, New Haven, Connecticut 06511

Received September 9, 1982

Thermolysis of $(\mu\text{-H})_2(\mu_3\text{-S})Ru_3(CO)_9$, I, in refluxing heptane or photolysis in octane at room temperature leads to loss of 1 mol of CO and formation of the cyclic trimer $[(\mu\text{-H})_2(\mu_4\text{-S})Ru_3(CO)_8]_3$, II, in yields of 25 and 27%, respectively. II has been characterized by IR, ^1H NMR, and a single-crystal X-ray diffraction analysis: space group $P\bar{1}$ at 27 °C; a = 11.368 (2) Å, b = 12.670 (4) Å, c = 19.134 (7) Å, α = 77.77 (3)°, β = 72.32 (2)°, γ = 63.94 (2)°, V = 2349 (1) Å^3, Z = 2, ρ_{calcd} = 2.38 g/cm^3. The structure was solved by a combination of direct methods (MULTAN) and difference Fourier techniques. Refinement on 3697 reflections ($F^2 \geq 3.0\sigma(F^2)$) yielded the final residuals R = 0.042 and R_w = 0.041. II is a cyclotrimer of $(\mu\text{-H})_2(\mu_3\text{-S})Ru_3(CO)_8$ formed by the head-to-tail coupling (S → Ru) of three monomers. The six-membered S–Ru–S–Ru–S–Ru ring has C_3 symmetry and is slightly puckered into a chairlike conformation. The metal–metal and metal–sulfur bonds in the monomeric units are very similar to those in I. The Ru–S bonds that link the clusters are slightly longer than those within the monomeric units. Crystallographically, the two hydride ligands in each monomeric unit are inequivalent, and this is supported by the ^1H NMR spectrum at room temperature. However, at elevated temperature the hydride resonances average (T_c = 370 K). This could be explained by scrambling of the hydride ligands about the individual monomeric triruthenium units or by chair-to-chair inversions of the six-membered ring. Under an atmosphere of CO, II is converted back into I quantitatively.

Introduction

In recent years much attention has been focused on the synthesis of high nuclearity transition-metal carbonyl cluster compounds.[1,2] Commonly employed synthetic routes involve the condensation of unsaturated species formed by pyrolytic decarbonylation[2-5] or redox condensation in which metal complexes in different oxidation states are coupled (e.g., metal carbonyl anion with a neutral metal carbonyl complex).[3-8] Recently, we have been investigating the syntheses of high nuclearity clusters through the condensation of low nuclearity heteronuclear transition-metal carbonyl cluster compounds.[9,10] Heteroatoms from the main-group elements such as sulfur, phosphorus, arsenic, etc. containing a lone pair of electrons could facilitate the linking of two cluster units via the formation of a donor–acceptor bond. This approach has already been used successfully in the syntheses of a variety of small clusters.[11,12]

$(\mu\text{-H})_2(\mu_3\text{-S})Ru_3(CO)_9$, I, contains a triangular cluster of three ruthenium atoms with a triply bridging sulfido ligand that contains one lone pair of electrons.[13] We have now discovered that I loses 1 mol of CO when heated and condenses to form the cyclic trimer $[(\mu\text{-H})_2(\mu_4\text{-S})Ru_3(CO)_8]_3$.

Results

When $(\mu\text{-H})_2(\mu_3\text{-S})Ru_3(CO)_9$, I, is refluxed in heptane solvent for 3 h under a slow purge of N_2, it loses 1 mol of CO and is converted into the trimer $[(\mu\text{-H})_2(\mu_4\text{-S})Ru_3(CO)_8]_3$, II which can be isolated in 25% yield by TLC. Compound II can also be obtained in 27% yield by UV photolysis of octane solutions. It was characterized by a combination of IR and ^1H NMR spectroscopies and a single-crystal X-ray diffraction analysis.

An ORTEP drawing of the molecule with the hydride ligands omitted is shown in Figure 1. Another view showing only the $[(\mu_4\text{-S})Ru_3]_3$ core is shown in Figure 2. As can be seen, three monomeric units of the species $(\mu\text{-H})_2(\mu_3\text{-S})Ru_3(CO)_8$ have been coupled in a head-to-tail fashion to form a 1,3,5-trithia-2,4,6-triruthenacyclohexane ring through the formation of coordinate bonds between a sulfido donor in one cluster unit and a ruthenium acceptor in an adjacent cluster. Overall, the molecule has C_3 symmetry (not crystallographically imposed) which can be seen clearly by the projection along the C_3 axis shown in Figure 2. The six-membered ring is slightly puckered producing a chairlike conformation which can be seen more clearly in Figure 3. Six of the nine ruthenium atoms are outside the six-membered ring. Three of these, Ru(3), Ru(6), and Ru(8), lie in "axial" positions while the other three, Ru(2), Ru(5), and Ru(7) lie in "equatorial" positions. The alternating S–Ru–S–Ru–S–Ru arrangement in the six-membered ring or the head-to-tail coupling of the monomers is dictated by the intrinsic donor–acceptor character of the S→Ru linking bonds.

Each monomeric Ru_3S unit contains a triangular group of three metal atoms with a triply bridging sulfido ligand and two edge bridging hydride ligands. The metal–metal bonding is very similar to that in I; however, in II the hydride-bridged metal–metal bonds are inequivalent (Figure 3), and this produces an observable effect on the internuclear separations. Hydrides H(1), H(3), and H(5) bridge metal–metal bonds between the ring metal atoms and the "equatorial" metal atoms. The Ru–Ru separations are 2.885 (1), 2.888 (1), and 2.866 (1) Å, average 2.880 Å. H(2), H(4), and H(6) bridge metal–metal bonds between the ring metal atoms and the "axial" metal atoms. The Ru–Ru separations at 2.921 (1), 2.922 (1), and 2.909 (1) Å,

(1) Chini, P. *Gazz. Chim. Ital.* **1979**, *109*, 225.
(2) Lewis, J.; Johnson, B. F. G. *Pure Appl. Chem.* **1982**, *54*, 97.
(3) (a) Chini, P. *J. Organomet. Chem.* **1980**, *200*, 37. (b) Chini, P.; Longoni, G.; Albano, V. G. *Adv. Organomet. Chem.* **1976**, *14*, 285.
(4) King, R. B. *Prog. Inorg. Chem.* **1972**, *15*, 287.
(5) Johnston, R. D. *Adv. Inorg. Chem. Radiochem.* **1970**, *13*, 471.
(6) Chini, P.; Ciani, G.; Martinengo, S.; Sironi, A.; Longhetti, L.; Heaton, B. T. *J. Chem. Soc., Chem. Commun.* **1979**, 188.
(7) Pfeffer, M.; Fischer, J.; Mitschler, A.; Ricard, L. *J. Am. Chem. Soc.* **1980**, *102*, 6338.
(8) Braunstein, P.; Matt, D.; Bars, O.; Louer, M.; Grandjean, D.; Fischer, J.; Mitschler, A. *J. Organomet. Chem.* **1981**, *213*, 79.
(9) Adams, R. D.; Dawoodi, Z.; Foust, D. F. *Organometallics* **1982**, *1*, 411.
(10) Adams, R. D.; Horvath, I. T.; Yang, L. W. *J. Am. Chem. Soc.*, submitted for publication.
(11) (a) Marko, L. *Gazz. Chim. Ital.* **1979**, *109*, 247. (b) Vahrenkamp, H. *Angew. Chem., Int. Ed. Engl.* **1975**, *14*, 322.
(12) (a) Richter, F.; Vahrenkamp, H. *Angew. Chem., Int. Ed. Engl.* **1980**, *19*, 65. (b) Richter, F.; Vahrenkamp, H. *Ibid.* **1979**, *18*, 531. (c) Vahrenkamp, H.; Wucherer, E. J. *Ibid.* **1981**, *20*, 680.
(13) Adams, R. D.; Katahira, D. A. *Organometallics* **1982**, *1*, 53.

0276-7333/83/2302-0149$01.50/0

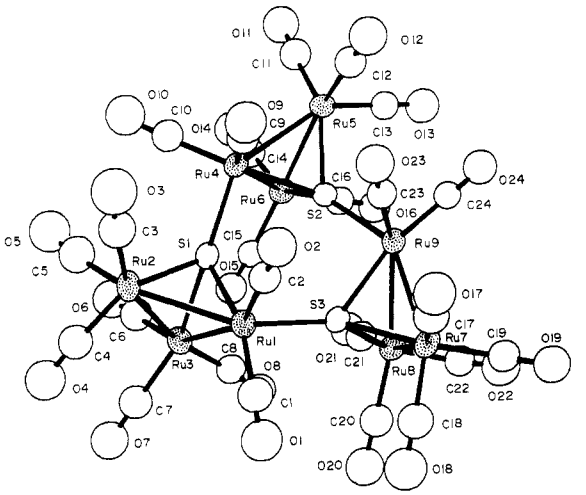

Figure 1. An ORTEP diagram of $[(\mu\text{-H})_2(\mu_4\text{-S})Ru_3(CO)_8]_3$, II, showingf 50% probability thermal motion ellipsoids. Hydride ligands are not shown.

Table I. Crystallographic Data for X-ray Diffraction Study

(A) Crystal Data

formula	$Ru_9S_3O_{24}C_{24}H_6$
temp, ±3 °C	27
space group	$P\bar{1}$
a, Å	11.368 (2)
b, Å	12.670 (4)
c, Å	19.134 (7)
α, deg	77.77 (3)
β, deg	72.32 (2)
γ, deg	63.94 (2)
V, Å^3	2349 (1)
mol wt	1684.12
Z	2
ρ_{calcd}, g/cm^3	2.38

(B) Measurement of Intensity Data

radiation	Mo K$\bar{\alpha}$ (0.710 73 Å)
monochromator	graphite
detector aperture, mm	
horizontal ($A + B \tan \theta$)	
A	3.0
B	1.0
vertical	4.0
cryst faces	$00\bar{1}$, 001, $0\bar{1}\bar{2}$, 012, $\bar{2}\bar{1}\bar{1}$, 211
crystal size	0.13 × 0.12 × 0.14
crystal orientatn directn; deg from ϕ axis	normal to 211; 7.3°
reflectns measd	$h, \pm k, \pm l$
$2\theta_{max}$, deg	45
scan type	moving crystal-stationary counter
ω scan width	
$A + 0.347 \tan \theta$	$A = 0.95$
bkgd	1/4 additional scan at each end of scan
ω scan rate (variable)	
max/min, deg	10.0
min/min, deg	1.5
no. of reflctns measd	6051
data used ($F^2 \geq 3.0\sigma(F)^2$)	3697

(C) Treatment of Data

P factor	0.010
final residuals	
R	0.042
R_w	0.041
esd of unit weight	2.358
largest shift/error value on final cycle	0.01
largest peaks in final diff fourier, e/Å^3	0.87-0.94

average 2.917 Å, are approximately 0.03 Å longer than those between the ring and equatorial metal atoms. The

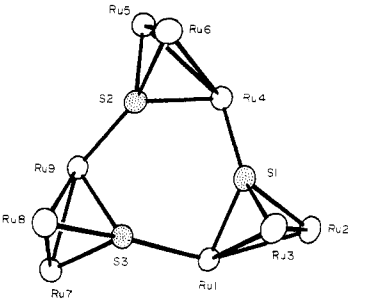

Figure 2. An ORTEP diagram of the $[(\mu_4\text{-S})Ru_3]_3$ core of compound II viewed along the C_3 axis.

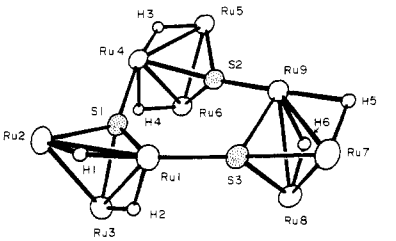

Figure 3. An ORTEP diagram of compound II without the carbonyl ligands.

Table II. Interatomic Distances (Å) with Esds for $[(\mu\text{-H})_2(\mu_4\text{-S})Ru_3(CO)_8]_3$, II

Ru(1)-Ru(2)	2.885 (1)	Ru(6)-C(14)	1.88 (1)
Ru(1)-Ru(3)	2.921 (1)	Ru(6)-C(15)	1.90 (1)
Ru(2)-Ru(3)	2.758 (1)	Ru(6)-C(16)	1.90 (1)
Ru(4)-Ru(5)	2.888 (1)	Ru(7)-C(17)	1.92 (1)
Ru(4)-Ru(6)	2.922 (1)	Ru(7)-C(18)	1.88 (1)
Ru(5)-Ru(6)	2.756 (1)	Ru(7)-C(19)	1.87 (1)
Ru(7)-Ru(8)	2.768 (1)	Ru(8)-C(20)	1.85 (1)
Ru(7)-Ru(9)	2.866 (1)	Ru(8)-C(21)	1.92 (1)
Ru(8)-Ru(9)	2.909 (1)	Ru(8)-C(22)	1.89 (1)
Ru(1)-S(1)	2.373 (2)	Ru(9)-C(23)	1.88 (1)
Ru(2)-S(1)	2.341 (2)	Ru(9)-C(24)	1.84 (1)
Ru(3)-S(1)	2.367 (3)	C(1)-O(1)	1.15 (1)
Ru(4)-S(1)	2.413 (3)	C(2)-O(2)	1.16 (1)
Ru(4)-S(2)	2.372 (2)	C(3)-O(3)	1.16 (1)
Ru(5)-S(2)	2.328 (3)	C(4)-O(4)	1.15 (1)
Ru(6)-S(2)	2.362 (2)	C(5)-O(5)	1.17 (1)
Ru(9)-S(2)	2.399 (2)	C(6)-O(6)	1.15 (1)
Ru(1)-S(3)	2.423 (2)	C(7)-O(7)	1.14 (1)
Ru(7)-S(3)	2.354 (2)	C(8)-O(8)	1.15 (1)
Ru(8)-S(3)	2.368 (2)	C(9)-O(9)	1.14 (1)
Ru(9)-S(3)	2.376 (3)	C(10)-O(10)	1.17 (1)
Ru(1)-C(1)	1.89 (1)	C(11)-O(11)	1.16 (1)
Ru(1)-C(2)	1.87 (1)	C(12)-O(12)	1.14 (1)
Ru(2)-C(3)	1.91 (1)	C(13)-O(13)	1.17 (1)
Ru(2)-C(4)	1.88 (1)	C(14)-O(14)	1.19 (1)
Ru(2)-C(5)	1.85 (1)	C(15)-O(15)	1.14 (1)
Ru(3)-C(6)	1.90 (1)	C(16)-O(16)	1.16 (1)
Ru(3)-C(7)	1.89 (1)	C(17)-O(17)	1.16 (1)
Ru(3)-C(8)	1.94 (1)	C(18)-O(18)	1.14 (1)
Ru(4)-C(9)	1.90 (1)	C(19)-O(19)	1.19 (1)
Ru(4)-C(10)	1.85 (1)	C(20)-O(20)	1.19 (1)
Ru(5)-C(11)	1.90 (1)	C(21)-O(21)	1.15 (1)
Ru(5)-C(12)	1.93 (1)	C(22)-O(22)	1.16 (1)
Ru(5)-C(13)	1.86 (1)	C(23)-O(23)	1.15 (1)
		C(24)-O(24)	1.17 (1)

hydride-bridged metal–metal bonds in I are 2.879 (1) and 2.882 (1) Å.[13] As expected,[14] the non-hydride-bridged metal–metal bonds are considerably shorter, Ru(2)–Ru(3) = 2.758 (1), Ru(5)–Ru(6) = 2.756 (1), and Ru(7)–Ru(8) = 2.768 (1) Å, and are similar to that in I, 2.760 (1) Å.[13]

Each sulfido ligand is actually a quadruple bridge which serves as a triple bridge within the monomeric unit while

(14) (a) Churchill, M. R. *Adv. Chem. Ser.* **1978**, *No. 167*, 36. (b) Churchill, M. R.; DeBoer, B. G.; Rottella, F. J. *Inorg. Chem.* **1976**, *15*, 1843.

Table III. Interatomic Angles (deg) with Esds for $[(\mu\text{-}H)_2(\mu_4\text{-}S)Ru_3(CO)_8]_3$, II

Ru(2)-Ru(1)-Ru(3)	56.70 (3)	S(1)-Ru(3)-S(2)	93.10 (8)	C(20)-Ru(8)-C(21)	94.6 (5)
Ru(1)-Ru(2)-Ru(3)	62.30 (3)	S(1)-Ru(4)-C(9)	92.7 (3)	C(20)-Ru(8)-C(22)	91.9 (5)
Ru(1)-Ru(3)-Ru(2)	61.00 (3)	S(1)-Ru(4)-C(10)	95.5 (3)	C(21)-Ru(8)-C(22)	94.7 (5)
Ru(5)-Ru(4)-Ru(6)	56.62 (3)	S(2)-Ru(4)-C(9)	101.3 (3)	Ru(7)-Ru(9)-S(2)	147.28 (7)
Ru(4)-Ru(5)-Ru(6)	62.30 (3)	S(2)-Ru(4)-C(10)	165.5 (3)	Ru(7)-Ru(9)-S(3)	52.37 (6)
Ru(4)-Ru(6)-Ru(5)	61.08 (3)	C(9)-Ru(4)-C(10)	90.0 (4)	Ru(7)-Ru(9)-C(23)	96.9 (3)
Ru(8)-Ru(7)-Ru(9)	62.14 (3)	Ru(4)-Ru(5)-S(2)	52.78 (6)	Ru(7)-Ru(9)-C(24)	118.3 (3)
Ru(7)-Ru(8)-Ru(9)	60.59 (3)	Ru(4)-Ru(5)-C(11)	111.2 (3)	Ru(8)-Ru(9)-S(2)	103.03 (6)
Ru(7)-Ru(9)-Ru(8)	57.27 (3)	Ru(4)-Ru(5)-C(12)	100.4 (3)	Ru(8)-Ru(9)-S(3)	52.06 (6)
Ru(2)-Ru(1)-S(1)	51.75 (6)	Ru(4)-Ru(5)-C(13)	150.2 (3)	Ru(8)-Ru(9)-C(23)	149.0 (3)
Ru(2)-Ru(1)-S(3)	147.06 (7)	Ru(6)-Ru(5)-S(2)	54.58 (6)	Ru(8)-Ru(9)-C(24)	114.0 (3)
Ru(2)-Ru(1)-C(1)	116.4 (3)	Ru(6)-Ru(5)-C(11)	97.9 (3)	S(2)-Ru(9)-S(3)	95.01 (8)
Ru(2)-Ru(1)-C(2)	99.0 (3)	Ru(6)-Ru(5)-C(12)	157.0 (3)	S(2)-Ru(9)-C(23)	90.5 (3)
Ru(3)-Ru(1)-S(1)	51.87 (6)	Ru(6)-Ru(5)-C(13)	95.9 (3)	S(2)-Ru(9)-C(24)	93.0 (3)
Ru(3)-Ru(1)-S(3)	102.58 (6)	S(2)-Ru(5)-C(11)	151.5 (4)	S(3)-Ru(9)-C(23)	99.6 (3)
Ru(3)-Ru(1)-C(1)	111.9 (3)	S(2)-Ru(5)-C(12)	103.4 (3)	S(3)-Ru(9)-C(24)	165.3 (3)
Ru(3)-Ru(1)-C(2)	151.5 (3)	S(2)-Ru(5)-C(13)	98.5 (3)	C(23)-Ru(9)-C(24)	92.7 (4)
S(1)-Ru(1)-S(3)	95.51 (8)	C(11)-Ru(5)-C(12)	102.8 (5)	Ru(1)-S(1)-Ru(2)	75.49 (8)
S(1)-Ru(1)-C(1)	162.6 (3)	C(11)-Ru(5)-C(13)	90.8 (5)	Ru(1)-S(1)-Ru(3)	76.09 (8)
S(1)-Ru(1)-C(2)	102.5 (3)	C(12)-Ru(5)-C(13)	93.8 (4)	Ru(1)-S(1)-Ru(4)	131.78 (10)
S(3)-Ru(1)-C(1)	94.4 (3)	Ru(4)-Ru(6)-S(2)	52.05 (6)	Ru(2)-S(1)-Ru(3)	71.71 (7)
S(3)-Ru(1)-C(2)	91.0 (3)	Ru(4)-Ru(6)-C(14)	109.6 (3)	Ru(2)-S(1)-Ru(4)	130.17 (10)
C(1)-Ru(1)-C(2)	91.6 (5)	Ru(4)-Ru(6)-C(15)	105.6 (13)	Ru(3)-S(1)-Ru(4)	144.26 (11)
Ru(1)-Ru(2)-S(1)	52.76 (6)	Ru(4)-Ru(6)-C(16)	147.4 (3)	Ru(4)-S(2)-Ru(5)	75.82 (7)
Ru(1)-Ru(2)-C(3)	101.6 (3)	Ru(5)-Ru(6)-S(2)	53.46 (6)	Ru(4)-S(2)-Ru(6)	76.22 (7)
Ru(1)-Ru(2)-C(4)	110.9 (3)	Ru(5)-Ru(6)-C(14)	95.6 (3)	Ru(4)-S(2)-Ru(9)	131.33 (10)
Ru(1)-Ru(2)-C(5)	149.7 (4)	Ru(5)-Ru(6)-C(15)	165.3 (3)	Ru(5)-S(2)-Ru(6)	71.96 (7)
Ru(3)-Ru(2)-S(1)	54.59 (6)	Ru(5)-Ru(6)-C(16)	94.4 (3)	Ru(5)-S(2)-Ru(9)	128.78 (11)
Ru(3)-Ru(2)-C(3)	158.0 (4)	S(2)-Ru(6)-C(14)	148.1 (3)	Ru(6)-S(2)-Ru(9)	145.35 (11)
Ru(3)-Ru(2)-C(4)	101.8 (3)	S(2)-Ru(6)-C(15)	114.4 (3)	Ru(7)-S(3)-Ru(8)	71.76 (7)
Ru(3)-Ru(2)-C(5)	94.1 (4)	S(2)-Ru(6)-C(16)	96.7 (3)	Ru(7)-S(3)-Ru(9)	74.59 (7)
S(1)-Ru(2)-C(3)	104.1 (4)	C(14)-Ru(6)-C(15)	94.9 (4)	Ru(7)-S(3)-Ru(1)	130.96 (10)
S(1)-Ru(2)-C(4)	154.7 (3)	C(14)-Ru(6)-C(16)	92.8 (5)	Ru(8)-S(3)-Ru(9)	75.63 (7)
S(1)-Ru(2)-C(5)	98.7 (4)	C(15)-Ru(6)-C(16)	95.4 (4)	Ru(8)-S(3)-Ru(1)	146.31 (11)
C(3)-Ru(2)-C(4)	98.1 (5)	Ru(8)-Ru(7)-S(3)	54.35 (6)	Ru(9)-S(3)-Ru(1)	129.55 (10)
C(3)-Ru(2)-C(5)	94.8 (5)	Ru(8)-Ru(7)-C(17)	157.9 (3)	Ru(1)-C(1)-O(1)	177 (1)
C(4)-Ru(2)-C(5)	91.5 (5)	Ru(8)-Ru(7)-C(18)	99.0 (3)	Ru(1)-C(2)-O(2)	178 (1)
Ru(1)-Ru(3)-S(1)	52.04 (6)	Ru(8)-Ru(7)-C(19)	97.8 (3)	Ru(2)-C(3)-O(3)	176 (1)
Ru(1)-Ru(3)-C(6)	150.7 (3)	Ru(9)-Ru(7)-S(3)	53.04 (6)	Ru(2)-C(4)-O(4)	175 (1)
Ru(1)-Ru(3)-C(7)	107.7 (3)	Ru(9)-Ru(7)-C(17)	99.2 (3)	Ru(2)-C(5)-O(5)	173 (1)
Ru(1)-Ru(3)-C(8)	103.3 (3)	Ru(9)-Ru(7)-C(18)	152.7 (3)	Ru(3)-C(6)-O(6)	178 (1)
Ru(2)-Ru(3)-S(1)	53.70 (6)	Ru(9)-Ru(7)-C(19)	109.4 (3)	Ru(3)-C(7)-O(7)	178 (1)
Ru(2)-Ru(3)-C(6)	97.5 (3)	S(3)-Ru(7)-C(17)	105.7 (3)	Ru(3)-C(8)-O(8)	173 (1)
Ru(2)-Ru(3)-C(7)	91.3 (4)	S(3)-Ru(7)-C(18)	100.3 (3)	Ru(4)-C(9)-O(9)	176 (1)
Ru(2)-Ru(3)-C(8)	163.2 (3)	S(3)-Ru(7)-C(19)	150.8 (3)	Ru(4)-C(10)-O(10)	178 (1)
S(1)-Ru(3)-C(6)	99.8 (4)	C(17)-Ru(7)-C(18)	93.8 (5)	Ru(5)-C(11)-O(11)	178 (1)
S(1)-Ru(3)-C(7)	144.2 (4)	C(17)-Ru(7)-C(19)	99.8 (4)	Ru(5)-C(12)-O(12)	178 (1)
S(1)-Ru(3)-C(8)	112.9 (3)	C(18)-Ru(7)-C(19)	91.7 (5)	Ru(5)-C(13)-O(13)	180 (1)
C(6)-Ru(3)-C(7)	91.3 (5)	Ru(7)-Ru(8)-S(3)	53.90 (6)	Ru(6)-C(14)-O(14)	177 (1)
C(6)-Ru(3)-C(8)	94.8 (5)	Ru(7)-Ru(8)-C(20)	94.5 (3)	Ru(6)-C(15)-O(15)	176 (1)
C(7)-Ru(3)-C(8)	99.8 (5)	Ru(7)-Ru(8)-C(21)	166.0 (3)	Ru(6)-C(16)-O(16)	178 (1)
Ru(5)-Ru(4)-S(1)	144.22 (6)	Ru(7)-Ru(8)-C(22)	95.6 (3)	Ru(7)-C(17)-O(17)	175 (1)
Ru(5)-Ru(4)-S(2)	51.40 (6)	Ru(9)-Ru(8)-S(3)	52.30 (6)	Ru(7)-C(18)-O(18)	177 (1)
Ru(5)-Ru(4)-C(9)	98.2 (3)	Ru(9)-Ru(8)-C(20)	148.3 (3)	Ru(7)-C(19)-O(19)	178 (1)
Ru(5)-Ru(4)-C(10)	118.4 (3)	Ru(9)-Ru(8)-C(21)	107.0 (3)	Ru(8)-C(20)-O(20)	178 (1)
Ru(6)-Ru(4)-S(1)	100.18 (6)	Ru(9)-Ru(8)-C(22)	108.7 (3)	Ru(8)-C(21)-O(21)	174 (1)
Ru(6)-Ru(4)-S(2)	51.72 (6)	S(3)-Ru(8)-C(20)	97.9 (4)	Ru(8)-C(22)-O(22)	176 (1)
Ru(6)-Ru(4)-C(9)	150.3 (3)	S(3)-Ru(8)-C(21)	114.2 (3)	Ru(9)-C(23)-O(23)	178 (1)
Ru(6)-Ru(4)-C(10)	115.0 (3)	S(3)-Ru(8)-C(22)	148.4 (3)	Ru(9)-C(24)-O(24)	178 (1)

additionally serving as a bridge to link two monomers. The metal–sulfur distances within the monomeric units range from 2.328 (3) to 2.376 (3) Å and are similar to those in I, but these are all slightly shorter than the metal–sulfur bonds which link the clusters, 2.413 (3), 2.399 (2), and 2.423 (2) Å.

The bonding around the sulfido ligands can be viewed as distorted tetrahedral where the Ru–S–Ru angles within the monomeric units are fairly acute, 71.76 (7)–76.22 (7)°, and those between clusters are fairly large, 129.55 (10)–146.41 (11)°. The former are very similar to those in I, 71.64 (4)–75.04 (4)°.[13]

Overall, there are 24 linear terminal carbonyl ligands. Each monomeric unit has eight carbonyls arranged in a three:three:two pattern with the metal atom in the six-membered ring having only two. The hydride ligands are shown where they were observed in difference Fourier maps in Figure 3. Complete lists of bond distances and angles are given in Tables II and III. The shortest intermolecular contacts were between carbonyl oxygen atoms at 3.02–3.08 Å.

The ^{1}H NMR spectrum of II shows two resonances δ −18.39 and −21.00 at room temperature due to the hydride ligands which are arranged into two inequivalent groups of three ligands. As the temperature is raised, the resonances broaden, reversibly, collapse into the base line and exist as a broad singlet at 380 K (the maximum temperature attempted). A dynamical process, $\Delta G^*_{370} = 16.4 \pm 0.3$ kcal/mol (calculated from $T_c = 370 \pm 5$ K), which averages the environments of the hydride ligands is in-

Table IV. Positional and Thermal Parameters and Their Estimated Standard Deviations[a] for $[(\mu\text{-H})_2(\mu_4\text{-S})Ru_3(CO)_8]_3$, II

atom	x	y	z	B(1,1)	B(2,2)	B(3,3)	B(1,2)	B(1,3)	B(2,3)
Ru(1)	0.5243 (1)	0.90265 (9)	0.18175 (6)	0.0089 (1)	0.00425 (8)	0.00212 (3)	−0.0052 (1)	−0.0032 (1)	0.00073 (9)
Ru(2)	0.3748 (1)	1.08587 (9)	0.28099 (6)	0.0112 (1)	0.00404 (8)	0.00309 (4)	−0.0052 (2)	−0.0038 (1)	−0.00039 (9)
Ru(3)	0.5557 (1)	0.87451 (9)	0.33141 (6)	0.0100 (1)	0.00580 (9)	0.00249 (4)	−0.0065 (2)	−0.0044 (1)	0.00029 (9)
Ru(4)	0.1684 (1)	0.85431 (9)	0.32678 (6)	0.0071 (1)	0.00441 (8)	0.00234 (4)	−0.0027 (2)	−0.0027 (1)	−0.00007 (9)
Ru(5)	0.0810 (1)	0.66920 (10)	0.33368 (6)	0.0069 (1)	0.00623 (9)	0.00273 (4)	−0.0058 (2)	−0.0017 (1)	−0.00071 (10)
Ru(6)	0.2725 (1)	0.62399 (9)	0.40889 (6)	0.0084 (1)	0.00538 (9)	0.00210 (4)	−0.0050 (2)	−0.0026 (1)	0.00111 (9)
Ru(7)	0.6738 (1)	0.60903 (10)	0.05009 (6)	0.0096 (1)	0.00577 (9)	0.00213 (4)	−0.0051 (2)	−0.0008 (1)	−0.00101 (9)
Ru(8)	0.7072 (1)	0.49915 (9)	0.18829 (6)	0.0078 (1)	0.00477 (9)	0.00288 (4)	−0.0029 (2)	−0.0030 (1)	−0.00012 (10)
Ru(9)	0.4383 (1)	0.61038 (9)	0.16135 (6)	0.0076 (1)	0.00442 (8)	0.00199 (3)	−0.0041 (1)	−0.0027 (1)	−0.00003 (8)
S(1)	0.3623 (3)	0.9028 (3)	0.2945 (2)	0.0082 (4)	0.0042 (2)	0.0023 (1)	−0.0033 (5)	−0.0031 (3)	−0.0002 (3)
S(2)	0.2955 (3)	0.6666 (3)	0.2804 (2)	0.0075 (3)	0.0048 (2)	0.0022 (1)	−0.0052 (5)	−0.0024 (3)	0.0004 (3)
S(3)	0.5817 (3)	0.7023 (3)	0.1600 (2)	0.0074 (3)	0.0044 (3)	0.0022 (1)	−0.0034 (5)	−0.0021 (3)	−0.0001 (3)

atom	x	y	z	B, Å²	atom	x	y	z	B, Å²
O(1)	0.7711 (11)	0.9214 (9)	0.0692 (6)	7.0 (3)	C(4)	0.464 (1)	1.186 (1)	0.2680 (8)	5.2 (4)
O(2)	0.3519 (10)	1.0044 (9)	0.0704 (6)	6.2 (3)	C(5)	0.278 (2)	1.131 (1)	0.3743 (9)	6.3 (4)
O(3)	0.1462 (12)	1.2475 (11)	0.2049 (7)	8.8 (4)	C(6)	0.480 (1)	0.890 (1)	0.4339 (8)	5.5 (4)
O(4)	0.5266 (10)	1.2413 (9)	0.2575 (6)	7.0 (3)	C(7)	0.673 (1)	0.945 (1)	0.3294 (8)	5.7 (4)
O(5)	0.2121 (11)	1.1512 (10)	0.4341 (7)	8.4 (4)	C(8)	0.675 (1)	0.709 (1)	0.3441 (8)	4.6 (4)
O(6)	0.4325 (11)	0.8987 (10)	0.4957 (6)	8.2 (3)	C(9)	0.105 (1)	0.948 (1)	0.2438 (8)	4.8 (4)
O(7)	0.7450 (11)	0.9868 (9)	0.3265 (6)	7.2 (3)	C(10)	0.057 (11)	0.978 (1)	0.3841 (8)	5.1 (4)
O(8)	0.7565 (10)	0.6147 (8)	0.3473 (5)	5.8 (3)	C(11)	−0.065 (1)	0.676 (1)	0.4168 (8)	5.3 (4)
O(9)	0.0714 (10)	1.0075 (9)	0.1936 (6)	7.2 (3)	C(12)	−0.005 (1)	0.726 (1)	0.2528 (8)	4.9 (4)
O(10)	−0.0180 (11)	1.0563 (10)	0.4200 (6)	7.9 (3)	C(13)	0.121 (1)	0.512 (1)	0.3275 (8)	4.2 (3)
O(11)	−0.1524 (11)	0.6774 (10)	0.4674 (6)	7.4 (3)	C(14)	0.158 (1)	0.625 (1)	0.5031 (8)	4.9 (4)
O(12)	−0.0546 (10)	0.7611 (9)	0.2041 (6)	6.8 (3)	C(15)	0.415 (1)	0.622 (1)	0.4423 (7)	4.0 (3)
O(13)	0.1469 (10)	0.4128 (9)	0.3233 (6)	6.4 (3)	C(16)	0.340 (1)	0.457 (1)	0.4102 (8)	4.7 (4)
O(14)	0.0812 (10)	0.6304 (9)	0.5619 (6)	6.8 (3)	C(17)	0.588 (1)	0.723 (1)	−0.0220 (8)	5.3 (4)
O(15)	0.4946 (9)	0.6233 (8)	0.4661 (5)	5.6 (3)	C(18)	0.834 (1)	0.634 (1)	0.0153 (8)	5.6 (4)
O(16)	0.3842 (10)	0.3555 (8)	0.4093 (5)	5.9 (3)	C(19)	0.750 (1)	0.473 (1)	0.0005 (8)	4.5 (4)
O(17)	0.5292 (10)	0.7892 (9)	−0.0643 (6)	7.1 (3)	C(20)	0.872 (1)	0.506 (1)	0.1753 (8)	5.6 (4)
O(18)	0.9275 (11)	0.6543 (10)	−0.0053 (6)	7.8 (3)	C(21)	0.686 (1)	0.451 (1)	0.2919 (8)	5.1 (4)
O(19)	0.7997 (10)	0.3846 (9)	−0.0290 (6)	6.2 (3)	C(22)	0.791 (1)	0.344 (1)	0.1598 (8)	4.9 (4)
O(20)	0.9759 (11)	0.5141 (10)	0.1665 (6)	7.5 (3)	C(23)	0.311 (1)	0.736 (1)	0.1155 (7)	3.9 (3)
O(21)	0.6747 (10)	0.4129 (9)	0.3527 (6)	6.5 (3)	C(24)	0.368 (1)	0.505 (1)	0.1591 (7)	3.7 (3)
O(22)	0.8361 (11)	0.2502 (10)	0.1407 (6)	8.0 (3)	H(3)	0.0547	0.7910	0.3555	4.0
O(23)	0.2349 (10)	0.8112 (9)	0.0857 (6)	6.3 (3)	H(6)	0.5820	0.4785	0.1855	4.0
O(24)	0.3240 (9)	0.4370 (8)	0.1599 (5)	5.7 (3)	H(2)	0.6094	0.8535	0.2539	4.0
C(1)	0.676 (1)	0.915 (1)	0.1102 (8)	5.4 (4)	H(4)	0.2500	0.7500	0.4219	4.0
C(2)	0.419 (1)	0.963 (1)	0.1127 (8)	4.3 (3)	H(1)	0.4707	0.0410	0.2031	4.0
C(3)	0.233 (1)	1.190 (1)	0.2344 (9)	5.9 (4)	H(5)	0.5547	0.5410	0.0664	4.0

[a] The form of the anisotropic thermal parameter is $\exp[-(B(1,1)h^2 + B(2,2)k^2 + B(3,3)l^2 + B(1,2)hk + B(1,3)hl + B(2,3)kl)]$. Estimated standard deviations in the least significant digits are shown in parentheses. The hydrogen atoms were not refined.

dicated. Intramolecular mechanisms which could accomplish this are hydride scrambling or an inversion in the configuration of the six-membered ring. Rapid movement of bridging hydride ligands between metal–metal bonds in cluster complexes is not unusual,[15] and ^{13}C NMR studies of I have shown the existence of dynamical processes which could be explained by movement of the hydride ligands around the cluster.[16] Alternatively, an inversion of configuration of the six-membered ring similar to that which rapidly occurs in cyclohexane would also lead to an averaging of the hydride ligands.[17] This process could involve some bond cleavages in the ring. Although the mechanisms cannot be distinguished with the present data, it can be concluded that chair-to-chair ring inversion in II is not rapidly occurring at room temperature.

The mechanism of the formation of II is also obscure. It could be formed by the cyclotrimerization of an intermediate such as $(\mu\text{-H})_2(\mu_3\text{-S})Ru_3(CO)_8$, III, formed by the decarbonylation of I; however, ^1H NMR spectra of samples of I at various stages of pyrolysis showed only the two hydride containing species I and II.

Under an atmosphere of CO at room temperature, compound II is converted back into I quantitatively over a period of 4 h (eq 1). As with the forward reaction, ^1H NMR spectra of the reverse reaction taken at various stages of completion showed the presence of only I and II. Even though it was not detected, it seems most likely under the conditions used that the reaction occurs via a short-lived intermediate like III, and the oligomerization or deoligomerization, once it begins, is rapid. We found no evidence for cyclodimers or cyclotetramers, etc. of III. The absence of dimers could be attributed to strain in the four-membered ring which would probably be most important at the sulfido ligand.

$$3\underset{\text{I}}{(\mu\text{-H})_2(\mu_3\text{-S})Ru_3(CO)_9} \underset{\text{1 atm/room temp}}{\overset{\text{100 °C, -3CO}}{\rightleftharpoons}} \underset{\text{II}}{[(\mu\text{-H})_2(\mu_4\text{-S})Ru_3(CO)_8]_3} \quad (1)$$

Although the cyclotrimerization of clusters is quite rare, it is not without precedent. For example, the clusters $(\mu_3\text{-E})Co_3(CO)_9$, E = P, As, also lose CO and form cyclotrimers.[11a,18] Indeed, the reaction, eq 2, lies heavily on the side of the cyclotrimer, and for the case E = P, it cannot be reversed even under a pressure of 200 atm of CO.

$$3(\mu_3\text{-E})Co_3(CO)_9 \underset{+3CO}{\overset{-3CO}{\rightleftharpoons}} [(\mu_4\text{-E})Co_3(CO)_8]_3 \quad (2)$$

E = P, As

Experimental Section

All operations were performed under an inert atmosphere. $(\mu\text{-H})_2(\mu_3\text{-S})Ru_3(CO)_9$ was prepared from $Ru_3(CO)_{12}$ (Strem Chemicals) by reaction with H_2S.[13] Reagent grade solvents were used. Heptane was dried over Na wire and purged with N_2 before use. CO was purified by passing through a column of KOH. IR spectra were recorded on a Nicolet 7199 FT-IR. ^1H NMR spectra were recorded on a JEOL JNM-FX90Q or Bruker HX-270 FT-NMR equipped with a variable-temperature accessory.

Thermolysis of $(\mu\text{-H})_2(\mu_3\text{-S})Ru_3(CO)_9$ (I). A solution of I (140 mg, 0.24 mmol) in heptane solvent was refluxed for 3 h under a slow purge of N_2. During this time the solution changed from yellow to orange. (Prolonged heating may lead to decomposition as evidenced by formation of a ruthenium mirror.) The solvent was removed in vacuo. The residue was taken up in CH_2Cl_2 and applied to thin-layer silica plates. Elution with hexane yielded two bands. The first was **I**. The second yellow-orange band was the product $[(\mu\text{-H})_2(\mu_4\text{-S})Ru_3(CO)_8]_3$, II: yield 35 mg, 25%; mp 160 °C dec; IR (ν(CO) in hexane) 2087 (vs), 2075 (vs), 2062 (m), 2027 (s), 2017 (m) cm^{-1}; ^1H NMR (ppm in $CDCl_3$ at 23 °C) δ −18.39 s (3 H), −21.00 s, 3 H). Variable-temperature studies were done in toluene-d_8 solvent. Once it is isolated, II is air stable. Solutions of II exposed to air showed no change in their IR spectra over a period of 24 h.

Photolysis of I. A 70-mg sample of **I** was placed in 40 mL of octane in a Pyrex flask and irradiated with UV radiation from a high-pressure mercury lamp for 9 h under a slow purge of N_2. The solvent was removed in vacuo, and the product II (11.4 mg) was isolated by TLC, as described above. A 29-mg sample of I was recovered. Yield of II: 27% (based on amount of I consumed).

Addition of CO to II. A sample of II was dissolved in C_6D_6 in an NMR tube. The solution was purged with CO, and spectra were taken periodically. Only resonances due to the formation of I and residual of II were observed. The addition was complete in 4 h at room temperature.

Crystallographic Analysis. Crystals of II suitable for diffraction measurements were obtained by cooling hexanes solutions to −20 °C. These were mounted in thin-walled glass capillaries. Diffraction measurements were made on an Enraf-Nonius CAD-4 fully automated diffractometer using graphite-monochromatized Mo K$\bar{\alpha}$ radiation. The unit cell was determined and refined from 25 randomly selected reflections obtained by using the CAD-4 automatic search, center, index, and least-squares routines.

The space group $P\bar{1}$ was selected and confirmed by the successful solution and refinement of the structure. Crystal data and data collection parameters are listed in Table I. All data processing was performed on a Digital Equipment Corp. PDP 11/45 computer using the Enraf Nonius SDP program library (version 18). The absorption coefficient for II is 29.6 cm^{-1}. No absorption correction was applied. Neutral atom scattering factors were calculated by the standard procedures.[19a] Anomalous dispersion corrections were applied to all non-hydrogen atoms.[19b] Full-matrix least-squares refinements minimized the function $\sum_{hkl} w(|F_o| - |F_c|)^2$ where $w = 1/\sigma(F)^2$, $\sigma(F) = \sigma(F_o^2)/2F_o$, and $\sigma(F_o^2) = [\sigma(I_{raw})^2 + (PF_o^2)^2]^{1/2}/Lp$.

The structure was solved by a combination of direct methods and difference Fourier techniques. The nine metal atoms were located in an electron density map based on the phasing (MULTAN) of 280 reflections ($E_{min} \geq 1.72$). Only the ruthenium and sulfur atoms were refined anisotropically. Tables II and III list interatomic distances and angles with errors obtained from the inverse matrix obtained on the final cycle of refinement. Table IV lists final positional and thermal parameters.

Acknowledgment. We wish to thank the National Science Foundation for support of this research through Grant No. CHE 80-19041 and the Alfred P. Sloan Foundation for a fellowship to R.D.A. NMR studies were supported by Grant No. CHE-7916210 from the National Science Foundation.

Registry No. I, 32574-35-9; II, 83380-28-3.

Supplementary Material Available: A listing of structure factor amplitudes (16 pages). Ordering information is given on any current masthead page.

(15) Band, E.; Muetterties, E. L. *Chem. Rev.* **1978**, *78*, 639.
(16) Forster, A.; Johnson, B. F. G.; Lewis, J.; Matheson, T. W. *J. Organomet. Chem.* **1976**, *104*, 225.
(17) Anet, F. A. L.; Anet, R. In "Dynamical Nuclear Magnetic Resonance Spectroscopy"; Jackman, L. M., Cotton, F. A. Eds.; Academic Press: New York, 1975.
(18) Vizi-Orosz, A.; Galamb, V.; Pályi, G.; Marko, L.; Bor, G.; Natile, G. *J. Organomet. Chem.* **1976**, *107*, 235.
(19) "International Tables for X-ray Crystallography"; Kynoch Press: Birmingham, England, 1975; Vol. IV: (a) Table 2.2B, pp 99–101; (b) Table 2.3.1., pp 149–150.

Synthesis and Structure of $Zr_2[(CH_2)_2P(CH_3)_2]_4[\mu\text{-}CP(CH_3)_3]_2$. A Molecule with Unusually Short Zirconium–Carbon Bonds

Gary W. Rice,*[1a] Gerald B. Ansell,[1b] Michelle A. Modrick,[1b] and Susan Zentz[1b]

Exxon Research and Engineering Company, Linden, New Jersey 07036

Received June 24, 1982

The title compound has been prepared from $Zr(CH_2CMe_3)_4$ and excess Me_3PCH_2, and its structure has been determined. It crystallizes in space group $P\bar{1}$ with a = 10.288 (6) Å, b = 10.132 (9) Å, c = 10.330 (7) Å, α = 106.50 (6)°, β = 118.64 (5)°, γ = 74.19 (5)°, V = 894 (2) Å^3, and Z = 1. The structure has discrete molecules which rest upon a crystallographic inversion center but have approximate C_{2h} symmetry. Each zirconium is bonded to six carbon atoms with the bonding distorted from the octahedral bonding angles by the presence of one Zr_2C_2 and two ZrC_2P rings. The zirconium coordination sphere has three pairs of chemically equivalent bonds. The bridging carbons have very short Zr–C distances of 2.156 (4) Å, while the Zr–C bonds trans to these are long, 2.614 (5) Å, and the axial Zr–C bonds are intermediate, 2.454 (5) Å.

Introduction

Several years ago, Schmidbaur and co-workers[2] showed that trimethyl(methylene)phosphorane and the anions derived from it by deprotonation are a versatile set of ligands for preparing stable compounds with metal–carbon bonds. At least six bonding modes are now known for these ligands. Neutral Me_3PCH_2 can coordinate through the methylene carbon.[2a] The monoanion $[Me_2P(CH_2)_2]^-$ can bond through both methylenes to chelate one metal or bridge two.[2a] The isomeric monoanion $[Me_3PCH]^-$ has been found as a terminal ligand on zirconium[3] and as a bridging one between two titaniums[2b] while the dianion $[Me_3PC]^{2-}$ has also been found to bridge two titaniums.[2b]

Although several phosphoranyl complexes of the group 4 metals have been reported, all to date have included additional ligands such as chloride,[2,3] cyclopentadienyl,[3,4] and dimethyl amide.[2b] The reaction of $ZrCl_4$ with 4 equiv of $Li(CH_2)_2PMe_2$ apparently does not yield a binary complex,[2b] nor does the reaction of $ZrCl_4$ with eight Me_3PCH_2 give one.[5] We have found, however, that $Zr(CH_2CMe_3)_4$ reacts smoothly with Me_3PCH_2 to yield the dimeric complex $Zr_2[(CH_2)_2PMe_2]_4(\mu\text{-}CPMe_3)_2$, I. The crystal and molecular structure of the product has been determined.

Results and Discussion

The reaction of $Zr(CH_2CMe_3)_4$ with excess Me_3PCH_2 proceeds rapidly and exothermically according to eq 1 to give pale red solutions from which I is isolated by cooling.

$$Zr(CH_2CMe_3)_4 + 3Me_3PCH_2 \xrightarrow[\text{or ether}]{\text{benzene}} 4CMe_4 + {}^1/_2Zr_2[(CH_2)_2PMe_2]_4(\mu\text{-}CPMe_3)_2 \quad (1)$$

Yellow crystals of I are triclinic with one molecule in the centrosymmetric unit cell. The final atomic positions are given in Table I, while the atom numbering scheme is shown in Figure 1. Selected bond lengths and angles are collected in Table II. The only crystallographically imposed symmetry is the inversion center, which forces the Zr_2C_2 ring to be planar. However, there is only slight distortion from molecular C_{2h} symmetry, with a 2-fold axis through the zirconium atoms and a perpendicular mirror plane containing the C(1)–P(1) bond; the data in Table II have been grouped to emphasize this fact. P(1) is out of the Zr_2C_2 plane by 0.60 Å. The view in Figure 2 is along the pseudo 2-fold axis.

The structure of I is a variation of that found for dimeric (trimethylsilyl)methylidyne-bridged niobium,[6] tungsten,[7] and rhenium[8] molecules with the formula $M_2(CH_2SiMe_3)_4(\mu\text{-}CSiMe_3)_2$. Each of those molecules has the metals in oxidation state +5 with metal–metal bond orders of 0 (Nb), 1 (W), and 2 (Re) and with each metal coordinated to two terminal and two bridging carbons arranged in a distorted tetrahedron. The structure of I is qualitatively the same for the metals and the bridging ligands, but the reamining ligands chelate as $[Me_2P(CH_2)_2]^-$ to produce a distorted octahedral coordination of zirconium rather than binding as terminal $[Me_3PCH]^-$ to fully mimic the silyls.

The most significant questions regarding I are the orders of the zirconium–carbon bonds and of the phosphorus–carbon bonds for those carbons coordinated to zirconium. Zirconium–element multiple bonds are quite uncommon in zirconium chemistry.[9,10] The available data from this work, taken with bond distances from other structures, suggest that the Zr–C(1) bond order in I is significantly greater than one. The metal–carbon bond distances from I and from the $M_2(CH_2SiMe_3)_4(\mu\text{-}CSiMe_3)_2$[6-8] molecules are collected in Table III. The silyl complexes have, as internal references, metal–carbon single bonds to which the bridge bonds can be compared. For all three of these, the single bond lengths are approximately those that would be predicted from summing covalent radii, while the bridge bonds are 0.15–0.22 Å shorter than the terminal ones. In I there is no such internal standard. However, the zirco-

(1) (a) Corporate Research Science Laboratory. (b) Analytical and Information Department.

(2) (a) Schmidbaur, H. *Acc. Chem. Res.* **1975**, *8*, 62–70 and references therein. (b) Schmidbaur, H.; Scharf, W.; Füller, H. J. *Z. Naturforsch., B: Anorg. Chem., Org. Chem.* **1977**, *32B*, 858–862.

(3) Gell, K. I.; Schwartz, J. *Inorg. Chem.* **1980**, *19*, 3207–3211.

(4) Manzer, L. E. *Inorg. Chem.* **1976**, *15*, 2567–2569.

(5) This reaction might be expected to eliminate Me_4PCl, in the same manner that we have found in the synthesis of $Cp_2ZrCl(CHPMe_3)$ from Cp_2ZrCl_2 and Me_3PCH_2. The $ZrCl_4$ reaction does not, however, yield a tractable product.

(6) Hug, F.; Mowat, W.; Skapski, A. C.; Wilkinson, G. *J. Chem. Soc., Chem. Commun.* **1971**, 1477–1478.

(7) Chisholm, M. H.; Cotton, F. A.; Extine, M. W.; Murillo, C. A. *Inorg. Chem.* **1978**, *17*, 696–698.

(8) Bochmann, M.; Wilkinson, G.; Galas, A. M. R.; Hursthouse, M. B.; Malik, K. *M.* A. *J. Chem. Soc., Dalton Trans.* **1980**, 1797–1799.

(9) Wailes, P. C.; Coutts, R. S. P.; Weigold, H. "Organometallic Chemistry of Titanium, Zirconium and Hafnium"; Academic Press: New York, 1974.

(10) Larsen, E. M. *Adv. Inorg. Chem. Radiochem.* **1970**, *13*, 1–133.

(11) Dean, J. A., Ed. "Lange's Handbook of Chemistry", 12th ed.; McGraw-Hill: New York, 1979; pp 3–120. The values of the radii need not be accurate, for this argument, so long as the differences between them are correct.

0276-7333/83/2302-0154$01.50/0

Table I. Positional and Thermal Parameters and Their Estimated Standard Deviations[a]

atom	x	y	z	B(1,1)	B(2,2)	B(3,3)	B(1,2)	B(1,3)	B(2,3)
Zr(1)	−0.04620 (6)	0.12726 (6)	0.11163 (6)	0.00787 (5)	0.00637 (5)	0.00764 (5)	−0.00115 (8)	0.00921 (7)	0.00031 (9)
P(1)	−0.1059 (2)	0.1954 (2)	−0.2243 (2)	0.0105 (2)	0.0083 (2)	0.0097 (2)	−0.0011 (3)	0.0098 (2)	0.0051 (3)
P(2)	0.2004 (2)	0.2813 (2)	0.3817 (2)	0.0114 (2)	0.0086 (2)	0.0091 (2)	−0.0036 (3)	0.0080 (3)	−0.0016 (3)
P(3)	−0.3756 (2)	0.2229 (2)	0.0680 (2)	0.0086 (2)	0.0109 (2)	0.0119 (2)	−0.0001 (3)	0.0122 (2)	0.0012 (3)
C(1)	−0.0772 (6)	0.0820 (6)	−0.1175 (6)	0.0088 (6)	0.0066 (6)	0.0077 (6)	0.000 (1)	0.0079 (8)	0.0031 (9)
C(2)	0.0550 (9)	0.2698 (9)	−0.1855 (9)	0.0147 (9)	0.0160 (9)	0.0198 (10)	−0.010 (1)	0.0095 (14)	0.0163 (14)
C(3)	−0.1746 (12)	0.1339 (10)	−0.4265 (9)	0.0379 (17)	0.0180 (11)	0.0097 (9)	−0.026 (2)	0.0121 (18)	0.0046 (15)
C(4)	−0.2413 (10)	0.3526 (9)	−0.2196 (10)	0.0247 (11)	0.0147 (10)	0.0330 (12)	0.019 (2)	0.0398 (15)	0.0296 (16)
C(5)	0.1170 (7)	0.3006 (7)	0.1946 (7)	0.0118 (7)	0.0099 (7)	0.0101 (7)	−0.008 (1)	0.0092 (10)	−0.0007 (12)
C(6)	0.0652 (8)	0.2259 (8)	0.4000 (7)	0.0137 (7)	0.0132 (9)	0.0106 (7)	−0.007 (1)	0.0129 (10)	−0.0003 (13)
C(7)	0.3578 (9)	0.1421 (9)	0.4076 (10)	0.0116 (9)	0.0119 (10)	0.0174 (12)	0.001 (2)	0.0073 (16)	0.0034 (18)
C(8)	0.2815 (11)	0.4338 (9)	0.5177 (9)	0.0261 (14)	0.0121 (9)	0.0105 (10)	−0.018 (2)	0.0061 (19)	−0.0043 (16)
C(9)	−0.2611 (7)	0.3384 (8)	0.1044 (8)	0.0106 (7)	0.0099 (8)	0.0180 (9)	0.000 (1)	0.0173 (11)	0.0007 (15)
C(10)	−0.2541 (7)	0.0730 (7)	0.1310 (8)	0.0100 (6)	0.0099 (8)	0.0194 (8)	0.001 (1)	0.0180 (10)	0.0086 (13)
C(11)	−0.4838 (9)	0.1792 (11)	−0.1318 (9)	0.0146 (10)	0.0219 (14)	0.0130 (10)	−0.009 (2)	0.0091 (15)	0.0026 (20)
C(12)	−0.5178 (8)	0.2887 (11)	0.1399 (9)	0.0132 (7)	0.0183 (13)	0.0260 (11)	0.001 (2)	0.0295 (11)	−0.0012 (21)

[a] The form of the anisotropic thermal parameter is $\exp[-(B(1,1)h^2 + B(2,2)k^2 + B(3,3)l^2 + B(1,2)hk + B(1,3)hl + B(2,3)kl)]$.

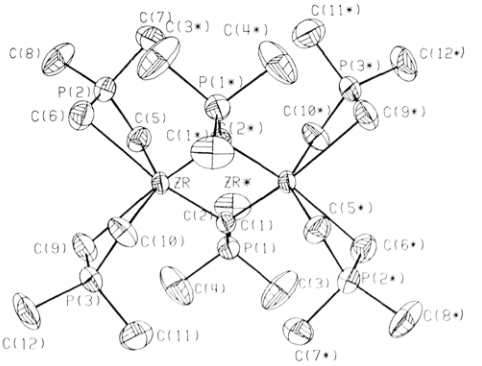

Figure 1. An ORTEP drawing of the molecule showing the atom numbering scheme. Thermal ellipsoids enclose 50% of the electron density. Starred atoms are related to the unstarred ones by the inversion center.

Figure 2. A stereographic projection of the molecule along its pseudo 2-fold axis.

Table II. Selected Interatomic Distances and Angles[a]

(a) Bond Lengths (Å)

Zr-C(1)	2.158 (4)	C(1)-P(1)	1.688 (4)
-C(1)′	2.155 (4)	C(5)-P(2)	1.744 (5)
-C(5)	2.451 (4)	C(10)-P(3)	1.744 (5)
-C(10)	2.456 (5)	C(6)-P(2)	1.739 (5)
-C(6)	2.617 (5)	C(9)-P(3)	1.724 (5)
-C(9)	2.612 (5)	Zr···Zr′	3.203

(b) Bond Angles (deg)

Zr-C(1)-Zr′	96.0 (2)	C(1)-Zr-C(5)	94.4 (2)
Zr-C(1)-P(1)	128.0 (2)	C(1)′-Zr-C(10)	94.6 (2)
Zr′-C(1)-P(1)	129.6 (2)	C(1)-Zr-C(10)	111.8 (2)
Zr-C(5)-P(2)	93.4 (2)	C(1)-Zr-C(5)	112.1 (2)
Zr-C(10)-P(3)	93.7 (2)	C(1)-Zr-C(6)	159.5 (2)
Zr-C(6)-P(2)	88.0 (2)	C(1)′-Zr-C(9)	160.3 (2)
Zr-C(9)-P(3)	88.9 (2)	C(1)-Zr-C(9)	101.3 (2)
C(5)-P(2)-C(6)	104.4 (2)	C(1)′-Zr-C(6)	98.9 (2)
C(9)-P(3)-C(10)	105.3 (2)	C(5)-Zr-C(9)	86.6 (2)
C(1)-Zr-C(1)′	84.0 (2)	C(6)-Zr-C(10)	88.3 (2)
C(5)-Zr-C(10)	144.6 (2)	C(5)-Zr-C(6)	65.7 (2)
C(6)-Zr-C(9)	82.8 (2)	C(9)-Zr-C(10)	65.8 (2)

[a] The remaining P-C bond lengths and C-P-C bond angles are available as supplementary material.

Table III. Comparison of $Zr_2[(CH_2)_2PMe_2]_4(\mu\text{-}CPMe_3)_2$ to $M_2(CH_2SiMe_3)_4(\mu\text{-}CSiMe_3)_2$[a]

metal	covalent[a] radius	$r_m + r_c$[a]	$d(M\text{-}C_t)$[b]	$d(M\text{-}C_b)$[b]	$d(M\text{-}C_t) - d(M\text{-}C_b)$
Zr	1.45	2.22	2.45 (1)	2.16 (1)	0.29
			2.61 (1)		0.45
Nb	1.34	2.11	2.16 (1)	1.97 (1)	0.19
W	1.30	2.07	2.10 (3)	1.88 (3)	0.22
Re	1.28	2.05	2.08 (1)	1.93 (1)	0.15

[a] Metal radii from ref 11; carbon single bond radius = 0.77 Å. [b] Distances to terminal and bridging carbons are averaged values. Uncertainties are those for individual distances included in the averages.

nium covalent radius is about 0.11 Å greater than that of niobium, predicting a zirconium–carbon single bond length of about 2.27 Å; the observed lengths[12] of 2.28 and 2.29 Å

Table IV. NMR Data (ppm) for $Zr_2[CH_2PMe_2]_4(\mu\text{-}CPMe_3)_2$ [a]

	^1H, τ ($^2J_{PH}$, Hz)	^{13}C ($^1J_{PC}$, Hz)	^{31}P
$Me_2P\text{-}(CH_2)_2$	8.46 (12.2, Me_2), 9.59 (10.5, $(CH_2)_2$)	23.32 (35.3, Me_2), 14.19 (41.4, $(CH_2)_2$)	8.16 (P)
$Me_3\text{-}P\text{-}C$	8.67 (11.4, Me_3)	23.05 (59.8, Me_3), not observed for C	−50.53 (P)

[a] All spectra in toluene-d_8.

in Cp_2ZrR_2, R = CH_2SiMe_3 and CH_2CMe_3, respectively, validate the comparison. The Zr–C(1) bonds are thus 0.11–0.13 Å shorter than expected for single bonds, but the estimated contraction is less than that observed in the μ-(trimethylsilyl)methylidyne complexes. Both ESCA[13] and PES[14] data suggest that the ylidic formulation, $Me_3P^+\text{–}^-CH_2$, best represents free phosphoranes, but the phosphonium center must reduce the availability of the carbon pπ electrons to the metal. Although the P(1)–C(1) bond length of 1.688 (4) Å is the shortest in the molecule, it is longer, by a statistically small margin, than the P–CH_2 bond of 1.661 (8) Å in neutral Ph_3PCH_2.[15] The lower lying metal dπ levels would be expected to reduce the already weak carbon 2pπ–phosphorus 3dπ contribution to the carbon–phosphorus bond.

It should be noted that the bond lengths around C(1) are quite similar to those observed in $Cp_2ZrCl(CHPPh_3)$.[25] The Zr–C bond length of 2.152 (8) Å in that molecule is statistically the same as the bridge bonds in I. The unique P–C bond was 1.708 (6) Å, somewhat longer than found here. We also note that the reaction of Cp_2ZrCl_2 with CH_2PPh_3 was found to require several days to obtain complete conversion to $Cp_2ZrCl(CHPPh_3)$.[25] We have found that the corresponding reaction of Cp_2ZrCl_2 with 2 equiv of CH_2PMe_3 is complete in a few minutes, with near quantitative yield of the $Cp_2ZrCl(CHPMe_3)$ complex first reported by Gell and Schwartz.[3] This is in contrast to the report that the same reaction at −78 °C yields only $[Cp_2Zr(CH_2PMe_3)_2]Cl_2$.[2b]

A final point regarding the structure is that the zirconium to methylene carbon bonds fall into two pairs of very different lengths, and all are longer than the expected single bond length. However, it has been shown that the molybdenum–carbon bonds in $Mo_2[(CH_2)_2PMe_2]_4$ (2.31 Å[16]) are 0.18 Å longer than those in $Mo_2(CH_2SiMe_3)_6$ (2.13 Å[17]). Adding the difference to the observed single bond length of 2.28 Å[12] in a zirconium silyl *or* adding the 0.15-Å difference in zirconium and molybdenum radii[11] to the bond length from the molybdenum phosphoranyl indicates that the zirconium–carbon bonds of 2.45-Å length are about what one would expect for the ligand. Only the bonds of 2.61-Å length unusually long, and these are presumably lengthened by the trans influence of the strongly bound bridging carbons.

Recently, Wengrovius and Schrock[18] have shown that zirconium neopentyl complexes are not amenable to α-hydrogen abstraction reactions. They suggested that the methylene hydrogen must be activated by an adjacent electrophilic center, such as is present in the M–CH_2–CR_3 (M = Ta, Nb) moiety but is not in Zr–CH_2–CR_3. Although the detailed mechanism is unknown, generation of the bridging ligands in I should involve sequential α-hydrogen abstraction, from a transient Zr–CH_2–PMe_3 moiety, by neopentyl groups from the same zirconium or an adjacent one. Evidently, the loss in methylene hydrogen reactivity in M–CH_2–CR_3 upon replacing tantalum or niobium with zirconium is at least partly recovered by substituting the more electrophilic phosphorus for the adjacent carbon.

Table V. Crystal Data and Data Collection

mol formula	$Zr_2P_6C_{24}H_{58}$
mol wt	714.99
a, Å	10.288 (6)
b, Å	10.132 (9)
c, Å	10.330 (7)
α, deg	106.50 (6)
β, deg	118.65 (5)
γ, deg	74.19 (5)
V, Å^3	894 (2)
Z	1
d_{cald}, g cm^{-3}	1.33
space group	$P\bar{1}$
abs coeff μ(Mo Kα), cm^{-1}	8.5
dimens, mm	0.4 × 0.4 × 0.7 [a]
diffractometer	Enraf-Nonius CAD-4
method	ω-2θ scan
scan speed, deg/min	4–20
scan width, deg	Mo Kα_1 − 0.5 to Mo Kα_2 + 0.5
bkgd time	half scan time
stds	3 every 100 min
2θ limits, deg	$0 < 2\theta \leq 50°$
no. of total data	3460
no. of data used ($I > 2\sigma(I)$)	2571 [b]
final no. of variables	145

[a] Apparent dimensions of crystal/epoxy interface. The actual crystal was smaller. The long dimension of the crystal lay along the ϕ direction. [b] Reference 22.

The NMR data for I are given in Table IV. Observation of only one doublet for all the methylene protons indicate that the molecule is fluxional in solution. The phosphorous–carbon coupling constants for the two types of ligand are quite similar to those seen, for similarly bound ligands, by Gell and Schwartz[3] in the $[Me_2P(CH_2)_2]^-$ and $[Me_3PCH]^-$ isomers of $Cp_2Zr(Cl)(PC_4H_{10})$. The signal for the unique bridging carbon was unfortunately not observed for I.

The observed infrared bands are collected in the Experimental Section. Comparison of the spectrum to those of $Cp_2Zr(Cl)CHPMe_3$,[3] Me_4PCl, Me_3PCH_2, and $LiMe_2P\text{-}(CH_2)_2$ indicates that the strong band at 603 cm^{-1} is a stretching mode involving the bridging carbon. By comparison, the ν(Zr–C) frequency in $Zr(CH_2SiMe_3)_4$ has been reported at 470 cm^{-1}.[24]

Experimental Section

Preparative work was done under nitrogen atmosphere by using Schlenk techniques or a Vacuum Atmospheres drybox. The $Zr(CH_2CMe_3)_4$[19] and Me_3PCH_2[20] were prepared by literature

(12) Jeffery, J.; Lappert, M. F.; Luong-Thi, N. T.; Webb, M.; Atwood J. L.; Hunter, W. E. *J. Chem. Soc., Dalton Trans.* **1981**, 1593–1605.
(13) Avanzino, S. C.; Jolly, W. L.; Lazarus, M. S.; Perry, W. B.; Rietz, R. R.; Schaaf, T. F. *Inorg. Chem.* **1975**, *14*, 1595–1597.
(14) Starzewski, K. A. O.; Bock. H. *J. Am. Chem. Soc.* **1976**, *98*, 8486–8494.
(15) Bart, J. C. J. *J. Chem. Soc. B* **1969**, 350–365.
(16) Cotton, F. A.; Hanson, B. E.; Ilsley, W. H.; Rice, G. W. *Inorg. Chem.* **1979**, *18*, 2713–2717.
(17) Hug, F.; Mowat, W.; Shortland, A.; Skapski, A. C.; Wilkinson, G. *Chem. Commun.* **1971**, 1079–1080.
(18) Wengrovius, J. H.; Schrock, R. R. *J. Organomet. Chem.* **1981**, *205*, 319–327.
(19) Mowat, W.; Wilkinson, G. *J. Chem. Soc., Dalton Trans.* **1973**, 1120–1124.

methods. Solvents were dried with NaK alloy.

In a typical preparation, 4.9 mmol of $Zr(CH_2CMe_3)_4$ in 20 mL of ether was treated with 20 mmol of Me_3PCH_2 in 30 mL of ether. The solution changed from colorless to red and yielded yellow crystals of I upon cooling to −40 °C. Elemental analysis was satisfactory.[21]

NMR data were collected on a JEOL FX-90Q spectrometer with a multinuclear insert. Infrared spectra were taken with a Perkin-Elmer 283B spectrophotometer. Observed bands for I: 1289 (m), 1270 (m), 1057 (m), 1020 (vs), 981 (m), 960 (w), 940 (s), 922 (m), 886 (m), 841 (w), 817 (s), 750 (s), 729 (s), 701 (m), 654 (m), 603 (s), 506 (m), 420 (w) cm^{-1}.

X-ray Crystallography. Crystals of air-sensitive I were examined under a layer of degassed Nujol. A selected crystal was mounted in an 0.5-mm glass capillary in an epoxy matrix. Details of data collection are given in Table V. Standard Lorentz and polarization corrections were applied to the data.[23] Correction was also made for a total linear decrease in intensity of the standards of about 13% by using program CHORTA.[23] Because the precise crystal dimensions were unknown and the absorption coefficient was small, no absorption correction was applied. Since anisotropic refinement produced no unusual thermal parameters, the omission of this correction was deemed acceptable.

The structure was solved for the heavy atoms from a Patterson map and completed by standard Fourier and least-squares procedures to final discrepancy indices $R = \sum||F_o| - |F_c||/|F_o| = 0.059$ and $R_w = (\sum||F_o| - |F_c||^2/\sum|F_o|^2)^{1/2} = 0.082$ and an esd of an observation of unit weight of 2.48.

Registry No. I, 83603-93-4; $Zr(CH_2CMe_3)_4$, 38010-72-9; Me_3PCH_2, 14580-91-7.

Supplementary Material Available: Listings of anisotropic thermal parameters, additional bond distances and angles, and observed and calculated structure factors (16 pages). Ordering information is given on any current masthead page.

(20) Schmidbaur, H.; Tronich, W. *Inorg. Synth.* **1978**, *18*, 137-138.
(21) Analysis by Schwarzkopf Microanalytical Laboratory, Woodside, NY, 11377, gave an empirical formula of $ZrP_{3.0}C_{12.1}H_{29.0}$ with four elements totaling 99% of the material.
(22) $I = S(C - RB)$ and $\sigma(I) = [S^2(C + R^2B) + \kappa I^2]^{1/2}$, where C = total counts, R = twice the ratio of scanning time to total background B, S is the scan rate, and $\kappa = 0.05$, a factor to reflect instrument stability.
(23) All computing was done on a PDP 11/60 using the 1980 Enraf-Nonius SDP package.
(24) Collier, M. R.; Lappert, M. F.; Pearce, R. *J. Chem. Soc., Dalton Trans.* **1973**, 445-451.
(25) Baldwin, J. C.; Keder, N. L.; Strouse, C. E.; Kaska, W. C. *Z. Naturforsch., B: Anorg. Chem., Org. Chem.* **1980**, *35B*, 1289-1297.

Photolytic Cleavage and Isomerization Reactions of (1-σ,4-6-η³-Organo)tricarbonyliron Complexes Involving an (η⁴-Diene)(η²-olefin)Fe(CO)₂ Intermediate. Quantum Yields and Mechanistic Studies

Takeo Akiyama, Friedrich-Wilhelm Grevels,* Johannes G. A. Reuvers, and Peter Ritterskamp

Max-Planck-Institut für Strahlenchemie, D-4330 Mülheim a.d. Ruhr, Federal Republic of Germany

Received April 22, 1982

Photolysis of two isomeric (1-σ,4-6-η³-organo)$Fe(CO)_3$ complexes (**1a**/**1b**)—the organic moiety being an adduct of methyl acrylate and 2,3-dimethylbutadiene—results in the interconversion of the two isomers and in the cleavage of the initially formed carbon–carbon bond leading to (η⁴-2,3-dimethylbutadiene)$Fe(CO)_3$ (**2**) and methyl acrylate. The quantum yields are in the range of 0.03 (**1** → **2**), 0.07 (**1a** → **1b**), and 0.20 (**1b** → **1a**). (η⁴-2,3-Dimethylbutadiene)(η²-methyl acrylate)$Fe(CO)_2$ is the key intermediate in these processes. The thermal reactions of the analogous (1-σ,4-6-η³-organo)$Fe(CO)_2P(C_6H_5)_3$ complex (**5**) parallel the above photoreactions of **1**.

Introduction

Prolonged irradiation of pentacarbonyliron in the presence of 1,3-dienes and methyl acrylate[1] or other olefins[2] results in carbon–carbon bond formation to give products in which a monoolefin–diene adduct is 1,4-6-η-coordinated to the $Fe(CO)_3$ moiety. The reaction proceeds via either the (η²-olefin)$Fe(CO)_4$ or (η⁴-diene)$Fe(CO)_3$ complexes (cf. ref 3–6), as monitored by infrared spectroscopy and confirmed by separate irradiations starting from the respective reactants.[1] Irradiation of (η⁴-diene)$Fe(CO)_3$/fluoroalkyne mixtures yields analogous products.[7,8]

Scheme I

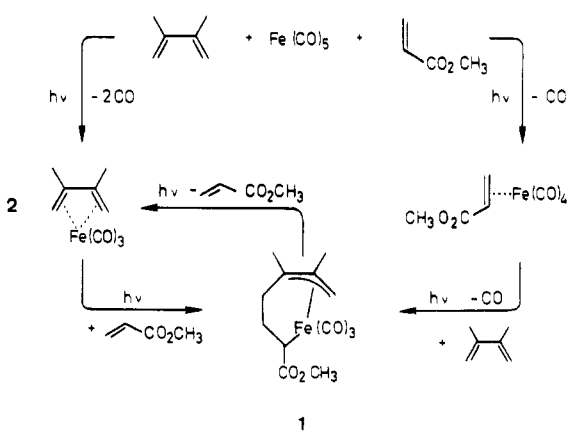

1

(1) Grevels, F.-W.; Feldhoff, U.; Leitich, J.; Krüger, C. *J. Organomet. Chem.* **1976**, *118*, 79. In relation to the η³-allyl group the ester group of **1a** is exo and that of **1b** endo: Chiang, A.-P.; Krüger, C., unpublished results (X-ray structure analysis of **1b**).
(2) Grevels, F.-W.; Salama, I., unpublished results.
(3) Whitesides, T. H.; Shelly, J. "Abstracts of Papers", 169th National Meeting of the Americal Chemical Society, Philadelphia, PA, Apr 1975; Americal Chemical Society: Washington, DC, 1975; ORGN-86.
(4) Bond, A.; Lewis, B.; Green, M. *J. Chem. Soc., Dalton Trans.* **1975**, 1109.
(5) Green, M.; Lewis, B.; Daly, J. J.; Sanz, F. *J. Chem. Soc., Dalton Trans.* **1975**, 1118.
(6) Kerber, R. C.; Koerner von Gustorf, E. A. *J. Organomet. Chem.* **1976**, *110*, 345.

0276-7333/83/2302-0157$01.50/0

methods. Solvents were dried with NaK alloy.

In a typical preparation, 4.9 mmol of $Zr(CH_2CMe_3)_4$ in 20 mL of ether was treated with 20 mmol of Me_3PCH_2 in 30 mL of ether. The solution changed from colorless to red and yielded yellow crystals of I upon cooling to −40 °C. Elemental analysis was satisfactory.[21]

NMR data were collected on a JEOL FX-90Q spectrometer with a multinuclear insert. Infrared spectra were taken with a Perkin-Elmer 283B spectrophotometer. Observed bands for I: 1289 (m), 1270 (m), 1057 (m), 1020 (vs), 981 (m), 960 (w), 940 (s), 922 (m), 886 (m), 841 (w), 817 (s), 750 (s), 729 (s), 701 (m), 654 (m), 603 (s), 506 (m), 420 (w) cm^{-1}.

X-ray Crystallography. Crystals of air-sensitive I were examined under a layer of degassed Nujol. A selected crystal was mounted in an 0.5-mm glass capillary in an epoxy matrix. Details of data collection are given in Table V. Standard Lorentz and polarization corrections were applied to the data.[23] Correction was also made for a total linear decrease in intensity of the standards of about 13% by using program CHORTA.[23] Because the precise crystal dimensions were unknown and the absorption coefficient was small, no absorption correction was applied. Since anisotropic refinement produced no unusual thermal parameters, the omission of this correction was deemed acceptable.

The structure was solved for the heavy atoms from a Patterson map and completed by standard Fourier and least-squares procedures to final discrepancy indices $R = \sum||F_o| - |F_c||/|F_o| = 0.059$ and $R_w = (\sum||F_o| - |F_c||^2/\sum|F_o|^2)^{1/2} = 0.082$ and an esd of an observation of unit weight of 2.48.

Registry No. I, 83603-93-4; $Zr(CH_2CMe_3)_4$, 38010-72-9; Me_3PCH_2, 14580-91-7.

Supplementary Material Available: Listings of anisotropic thermal parameters, additional bond distances and angles, and observed and calculated structure factors (16 pages). Ordering information is given on any current masthead page.

(20) Schmidbaur, H.; Tronich, W. *Inorg. Synth.* **1978**, *18*, 137-138.
(21) Analysis by Schwarzkopf Microanalytical Laboratory, Woodside, NY, 11377, gave an empirical formula of $ZrP_{3.0}C_{12.1}H_{29.0}$ with four elements totaling 99% of the material.
(22) $I = S(C - RB)$ and $\sigma(I) = [S^2(C + R^2B) + \kappa I^2]^{1/2}$, where C = total counts, R = twice the ratio of scanning time to total background B, S is the scan rate, and $\kappa = 0.05$, a factor to reflect instrument stability.
(23) All computing was done on a PDP 11/60 using the 1980 Enraf-Nonius SDP package.
(24) Collier, M. R.; Lappert, M. F.; Pearce, R. *J. Chem. Soc., Dalton Trans.* **1973**, 445-451.
(25) Baldwin, J. C.; Keder, N. L.; Strouse, C. E.; Kaska, W. C. *Z. Naturforsch., B: Anorg. Chem., Org. Chem.* **1980**, *35B*, 1289-1297.

Photolytic Cleavage and Isomerization Reactions of (1-σ,4-6-η³-Organo)tricarbonyliron Complexes Involving an (η⁴-Diene)(η²-olefin)Fe(CO)₂ Intermediate. Quantum Yields and Mechanistic Studies

Takeo Akiyama, Friedrich-Wilhelm Grevels,* Johannes G. A. Reuvers, and Peter Ritterskamp

Max-Planck-Institut für Strahlenchemie, D-4330 Mülheim a.d. Ruhr, Federal Republic of Germany

Received April 22, 1982

Photolysis of two isomeric (1-σ,4-6-η³-organo)$Fe(CO)_3$ complexes (**1a**/**1b**)—the organic moiety being an adduct of methyl acrylate and 2,3-dimethylbutadiene—results in the interconversion of the two isomers and in the cleavage of the initially formed carbon–carbon bond leading to (η⁴-2,3-dimethylbutadiene)$Fe(CO)_3$ (**2**) and methyl acrylate. The quantum yields are in the range of 0.03 (**1** → **2**), 0.07 (**1a** → **1b**), and 0.20 (**1b** → **1a**). (η⁴-2,3-Dimethylbutadiene)(η²-methyl acrylate)$Fe(CO)_2$ is the key intermediate in these processes. The thermal reactions of the analogous (1-σ,4-6-η³-organo)$Fe(CO)_2P(C_6H_5)_3$ complex (**5**) parallel the above photoreactions of **1**.

Introduction

Prolonged irradiation of pentacarbonyliron in the presence of 1,3-dienes and methyl acrylate[1] or other olefins[2] results in carbon–carbon bond formation to give products in which a monoolefin–diene adduct is 1,4-6-η-coordinated to the $Fe(CO)_3$ moiety. The reaction proceeds via either the (η²-olefin)$Fe(CO)_4$ or (η⁴-diene)$Fe(CO)_3$ complexes (cf. ref 3–6), as monitored by infrared spectroscopy and confirmed by separate irradiations starting from the respective reactants.[1] Irradiation of (η⁴-diene)$Fe(CO)_3$/fluoroalkyne mixtures yields analogous products.[7,8]

Scheme I

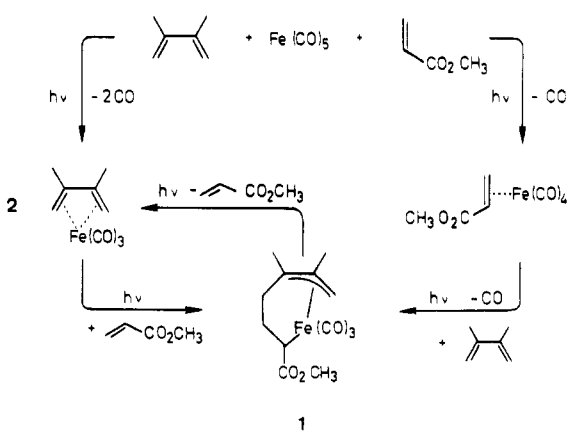

1

(1) Grevels, F.-W.; Feldhoff, U.; Leitich, J.; Krüger, C. *J. Organomet. Chem.* **1976**, *118*, 79. In relation to the η³-allyl group the ester group of **1a** is exo and that of **1b** endo: Chiang, A.-P.; Krüger, C., unpublished results (X-ray structure analysis of **1b**).
(2) Grevels, F.-W.; Salama, I., unpublished results.
(3) Whitesides, T. H.; Shelly, J. "Abstracts of Papers", 169th National Meeting of the Americal Chemical Society, Philadelphia, PA, Apr 1975; Americal Chemical Society: Washington, DC, 1975; ORGN-86.
(4) Bond, A.; Lewis, B.; Green, M. *J. Chem. Soc., Dalton Trans.* **1975**, 1109.
(5) Green, M.; Lewis, B.; Daly, J. J.; Sanz, F. *J. Chem. Soc., Dalton Trans.* **1975**, 1118.
(6) Kerber, R. C.; Koerner von Gustorf, E. A. *J. Organomet. Chem.* **1976**, *110*, 345.

0276-7333/83/2302-0157$01.50/0

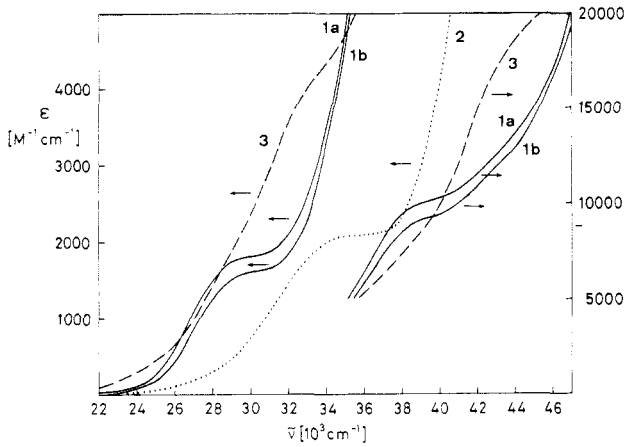

Figure 1. Electronic spectra of the complexes **1a**, **1b**, **2**, and **3**, in *n*-hexane.

Scheme II

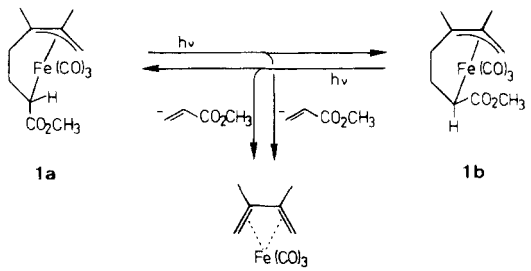

Scheme I summarizes the photochemical synthesis of the (2,3-dimethylbutadiene/methyl acrylate)$Fe(CO)_3$ adduct **1** in *n*-hexane or diethyl ether at ambient temperature. Two stereoisomers, **1a** and **1b**, are formed which differ in

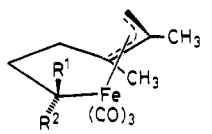

1a: $R^1 = H$, $R^2 = CO_2CH_3$
1b: $R^1 = CO_2CH_3$, $R^2 = H$

the orientation of the ester group.[1] As the reaction proceeds, (η^2-methyl acrylate)$Fe(CO)_4$ is consumed almost completely whereas, even after extended irradiation, substantial amounts of (η^4-2,3-dimethylbutadiene)$Fe(CO)_3$ (**2**) are remaining present in the reaction mixture. At first glance, this could be attributed to internal light filter effects (see electronic spectra, Figure 1). However, preliminary experiments have shown that the adducts **1**, upon irradiation, release methyl acrylate with reformation of **2**.[1] It seemed worthwhile to study this photolytic reaction in some detail since, beyond our interest in this particular case, a more comprehensive knowledge of the mechanism of such a facile metal-assisted reversible C–C coupling of di- and monoolefins may be of general relevance to transition-metal catalysis.[9]

Results and Discussion

Irradiation of the two isomeric (σ,η^3-allyl)$Fe(CO)_3$ complexes **1a** or **1b** in both cases not only brings about the formation of (η^4-2,3-dimethylbutadiene)$Fe(CO)_3$ (**2**) with loss of methyl acrylate but also concomitantly, isomerization, **1a** ⇄ **1b**, is observed (Scheme II). No other products are detected if the photolysis is performed under a carbon monoxide atmosphere. Figure 2 shows the course of two experiments which have been carried out on a preparative scale. The extent of photolytic cleavage yielding **2** is nearly the same for each of the two starting materials **1a** and **1b**. However, as a notable difference, the isomerization **1b** $\xrightarrow{h\nu}$ **1a** (Figure 2B) is more efficient than

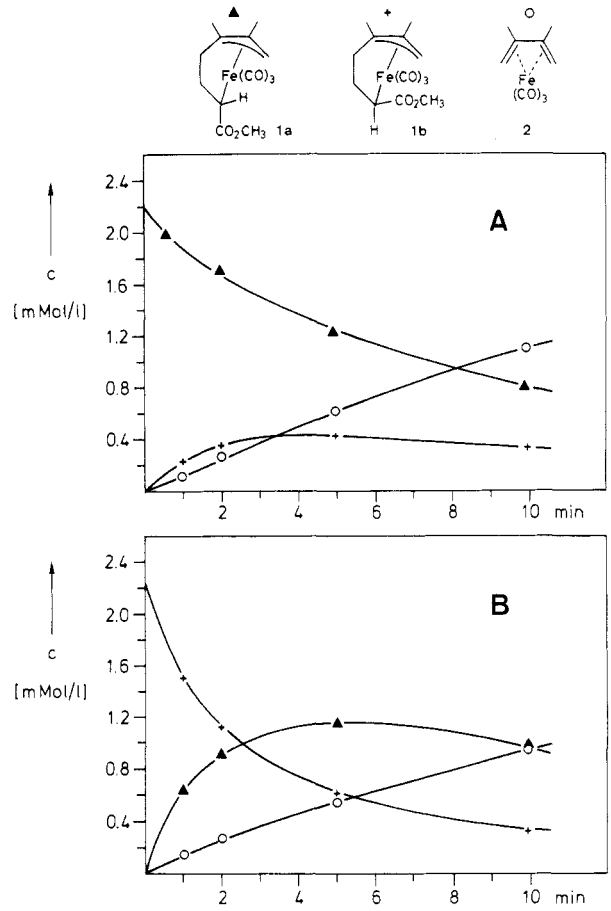

Figure 2. Irradiation of 2.2×10^{-3} M solutions of the adducts **1a** (A) and **1b** (B) in *n*-hexane at ambient temperature (immersion lamp apparatus, solidex glass, Hg lamp, Philips HPK, 125 W).

Table I. Quantum Yields[a] for the Photolytic Cleavage and Isomerization of 1a and 1b

	expt no.	ϕ_{-1a}	ϕ_{1b}	ϕ_2
1a	1	0.109	0.069	0.033
	2	0.121	0.083	0.025
	3[b]	0.106	0.076	0.023
	4	0.097	0.056	0.033
	5	0.083	0.063	0.019
	6	0.109	0.056	0.024
	7[c]	0.132	0.083	0.028
	8[c]	0.111	0.066	0.027
	av	0.109	0.069	0.028
	expt no.	ϕ_{-1b}	ϕ_{1a}	ϕ_2
1b	9	0.260	0.213	0.033
	10[b]	0.204	0.188	0.028
	av	0.232	0.201	0.031

[a] At 340 nm (29 400 cm^{-1}), in *n*-hexane under CO atmosphere; 22 °C; 20% conversion, for details see Experimental Section. [b] Light intensity reduced, as compared to no. 1 + 2 and 9, respectively, by using a 32% transmission wire guaze. [c] Light intensity reduced, as compared to no. 4-6, by using a 14% transmission neutral density filter.

(7) Bottrill, M.; Goddard, R.; Green, M.; Hughes, R. P.; Lloyd, M. K.; Lewis, B.; Woodward, P. *J. Chem. Soc., Chem. Commun.* **1975**, 253.
(8) Bottrill, M.; Davies, R.; Goddard, R.; Green, M.; Hughes, R. P.; Lewis, B.; Woodward, P. *J. Chem. Soc., Dalton Trans.* **1977**, 1252.
(9) Julémont, M.; Teyssié, Ph. *Aspects Homogeneous Catal.* **1981**, *4*, 99.

Scheme III

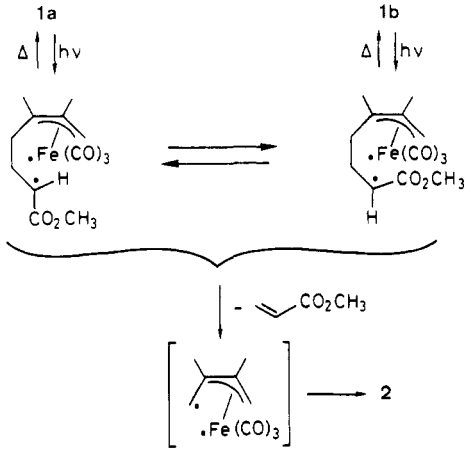

Scheme IV

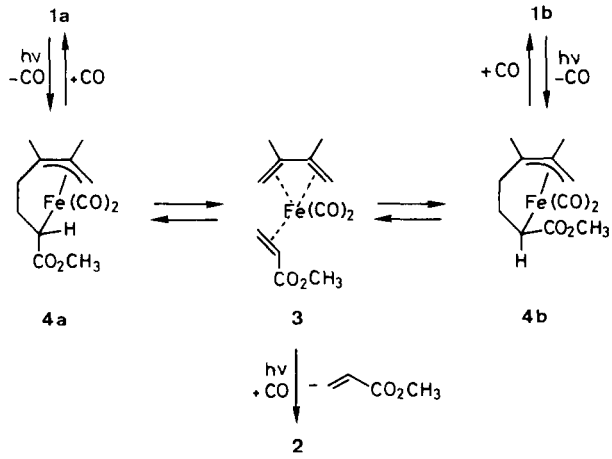

the reverse reaction (Figure 2A).

These trends are confirmed by the quantum yields (Table I) which indicate an equal, albeit moderate, efficiency for the formation of **2** in each case ($\phi_2 \approx 0.03$). On the other hand, the quantum yields for the formation of the respective isomer differ by a factor of about 2.5–3. The sum of the product quantum yields is in excellent accord with the value for the disappearance of the respective starting material.

In regard to the mechanism two alternatives may be considered for the initial photolytic step: either homolysis of the metal–carbon σ bond (Scheme III) or dissociation of one carbon monoxide ligand. Spectroscopic studies at low-temperature matrix isolation conditions[10] at 10–12 K have shown that detachment of CO is the only detectable primary photoreaction under those circumstances; there is no indication of an isomerization, **1a** ($h\nu$) ⇄ **1b** ($h\nu$) in either direction.

If the photolysis in solution is carried out under an inert-gas atmosphere an additional product (**3**) can be observed. Enrichment of the solution with this product, such that it can be isolated, is favored by low temperatures and by removal of liberated carbon monoxide. It is identified as (η^4-2,3-dimethylbutadiene)(η^2-methyl acrylate)-$Fe(CO)_2$ (**3**), which has previously been prepared[11] from (η^2-methyl acrylate)$Fe(CO)_4$ and 2,3-dimethylbutadiene. At ambient temperature—without irradiation—**3** readily takes up one carbon monoxide molecule to yield a mixture of the isomeric adducts **1a** and **1b** in a ~2.5:1 ratio.[11] No (η^4-2,3-dimethylbutadiene)$Fe(CO)_3$ (**2**) is formed under these conditions. However, irradiation of **3** under CO atmosphere in *n*-hexane solution at −45 °C —where the thermal reaction yielding **1** is almost negligible—results in complete displacement of methyl acrylate by carbon monoxide yielding **2**.

From these results we conclude that **3** is the key intermediate in the reactions depicted in Scheme II, namely, the photochemical interconversion of **1a** and **1b** and the photolytic formation of **2** as well. As outlined in Scheme IV the photolytic dissociation of one carbonyl ligand from **1a** or **1b**, with retention of the carbon skeleton of the organic moiety, yields the 16-electron intermediates **4a** or **4b** which have been observed in low-temperature matrices.[10] At ambient temperature these coordinatively unsaturated species can be expected to undergo spontaneous reductive cleavage to form the 18-electron complex **3**. The diradical type intermediate shown in Scheme III cannot entirely be excluded. However, a contribution from this alternative pathway ought to be small in view of the fact that the **1a**:**1b** ratio in the course of the photolysis (Figure 2) approaches the same value as that obtained in the thermal reaction of **3** with carbon monoxide.[11]

Bearing in mind that two consecutive photochemical steps are involved in the conversion **1** → **2** (Scheme IV) one might expect the efficiency of this process to depend on the intensity of light. At the outset of this study first preparative data seemed in fact to indicate such a light intensity effect,[12] i.e., that higher intensities would reduce the yield of **1** by favoring the cleavage back to **2**. However, the quantum yield determinations at 340 nm (29 400 cm^{-1})—where the absorbances of **1a**/**1b** and the intermediate **3** are not much different (Figure 1)—showed such an effect to be within the experimental error limits (Table I), if at all existing. A solid interpretation of this result requires a more detailed knowledge of the kinetics governing the delicate balance of the reactions involving the species **3** and **4a**/**4b** (Scheme IV). We are anticipating this information from forthcoming kinetic studies using flash photolysis and fast infrared techniques.

Starting from **3** not only carbon monoxide but also other ancillary ligands such as phosphines or isonitriles[13] are able to bring about the oxidative cyclization as long as these ligands are not too bulky. The triphenylphosphine complex **5** (Scheme V) is moderately stable and can be isolated from a concentrated solution containing excess triphenylphosphine. In dilute *n*-hexane solutions the metal carbonyl bands of **5** (1993 and 1935 cm^{-1}) gradually disappear. Complex **3** is formed intermediately and reacts further to yield (η^4-2,3-dimethylbutadiene)(triphenylphosphine)$Fe(CO)_2$ (**6**) as the final product. This thermal reaction sequence parallels nicely the photochemical conversion

$$1 \underset{\Delta}{\overset{h\nu}{\rightleftharpoons}} 3 \xrightarrow{h\nu} 2$$

thus confirming our formulation of the reductive cleavage as a thermal process subsequent to the initial loss of an ancillary ligand (Scheme IV). If **5** is allowed to decompose under carbon monoxide atmosphere or in the presence of, e.g., trimethyl phosphite the (σ,η^3-allyl)iron complexes **1a**/**1b** or **7**[13] are obtained (Scheme V). Further detailed investigations concerning the ligand-induced oxidative cyclization of type **3** complexes are in progress. Although

(10) Grevels, F.-W.; Klotzbücher, W. E. *Inorg. Chem.* **1981**, *20*, 3002.
(11) Grevels, F.-W.; Schneider K. *Angew. Chem.* **1981**, *93*, 417; *Angew. Chem. Int. Ed. Engl.* **1981**, *20*, 410.
(12) Akiyama, T.; Grevels, F.-W.; Salama, I., Proceedings of the International Conference on Organometallic Chemistry, 9th, Dijon/France, Sept 1979, Abstract D2.
(13) Grevels, F.-W., et al., unpublished results.

Scheme V

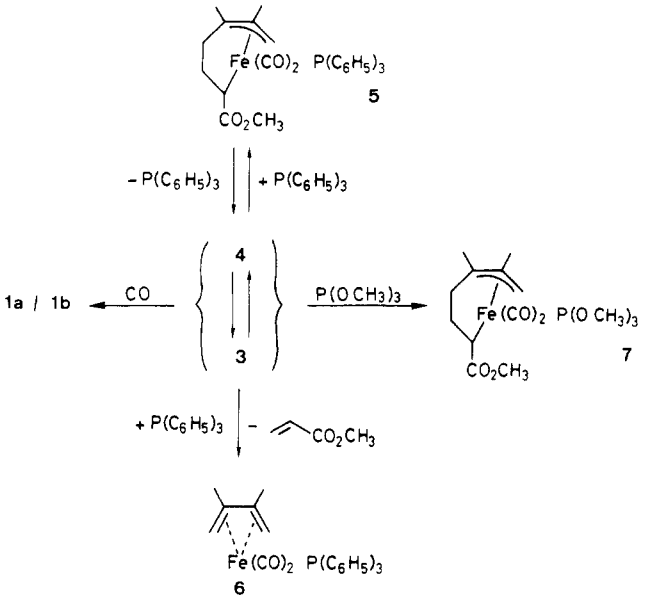

such a metal-assisted C–C bond formation between a diene and a monoolefin has been classified as a symmetry-forbidden process,[14] the reaction proceeds under rather mild conditions in case of the carbonyliron complex **3**.

Experimental Section

All reactions and manipulations were carried out, unless noted otherwise, under argon and in argon-saturated solvents. Irradiations were performed in an immersion lamp apparatus (solidex glass, $\lambda \geq 280$ nm) by using a mercury lamp Philips HPK 125 W. Spectra were recorded by using the following instruments: IR, Perkin-Elmer 580; UV–visible, Bruins Instruments MIT 20. Melting points were determined on a Reichert Kofler apparatus. Microanalysis was performed by Dornis & Kolbe, Mülheim a.d. Ruhr. Analytical grade solvents (Merck, Darmstadt) and reagents (Merck and Fluka) were used as received. Complexes **1a/1b**,[1] **2** (by analogy to ref 15), and **3**[11] were prepared according to published procedures.

(1) Photolysis of Complexes 1a/1b. (a) Solutions of 0.120 g (0.39 mmol) of **1a** or **1b** in 170 mL of *n*-hexane, purged with carbon monoxide for 5 min, were irradiated. Samples were drawn after 1, 2, 5, and 10 min and analyzed by quantitative infrared spectroscopy using the CO stretching bands at 2006/2062 (**1a**), 1998.5/2057 (**1b**), and 2049 (**2**) cm^{-1}; appropriate corrections were made in order to account for tail absorptions of the respective other components. The results are displayed in Figure 2.

(b) Quantum Yield Determinations. An electronically integrating actinometer was used (described elsewhere)[16] which was calibrated by ferrioxalate actinometry.[17] Solutions of **1a** or **1b** ($\sim 2 \times 10^{-3}$ M) in *n*-hexane were prepared under argon and subsequently saturated with carbon monoxide. The 3-mL samples were irradiated at 340 nm in quartz cuvettes ($d = 1$ cm) by using a Hanovia 1000-W Hg–Xe lamp in connection with a Schoeffel Instruments GM 250 single-grating monochromator. Light intensities were in the order of $(4–30) \times 10^{-8}$ einstein min^{-1}. All experiments were carried out at ambient temperature (22 ± 2 °C). Concentrations of **1a**, **1b**, and **2** were determined, at 10–20% conversion, by quantitative infrared spectroscopy (see above).

(c) Isolation of (η^4-2,3-Dimethylbutadiene)(η^2-methyl acrylate)Fe(CO)$_2$ (3). A solution of **1a** (3.70 g, 12 mmol) in 200 mL of diethyl ether was irradiated at −30 °C for 14.5 h. Carbon monoxide was removed by an argon stream. The solvent was evaporated under vacuum at −30 °C and the residue chromatographed on silica gel (Merck, Darmstadt; Kieselgel 60, 230–400 mesh). The column (5 × 35 cm) was operated at −30 °C. Elution with pentane gave **2** (1.06 g, 40%); **3** was eluted with pentane–diethyl ether (7:3). The crude product (1.37 g, 41%) was recrystallized from hexane at −80 °C and identified[11] by its melting point, infrared and ^{1}H NMR spectroscopy, and mass spectrometry. A third fraction, eluted with diethyl ether, contained **1a** and other, unidentified, products.

(2) Photoreaction of 3 with Carbon Monoxide. A solution of **3** (0.24 g, 0.86 mmol) in 180 mL of *n*-hexane was cooled to −45 °C and saturated with carbon monoxide. Samples were drawn after 10 min and 1 h, degassed, and warmed up to ambient temperature. The infrared spectra showed **3** and minor amounts of **1a/1b** but no **2**. The solution of **3**, under carbon monoxide at −45 °C, was then irradiated for 0.25 h. The infrared spectrum showed the almost exclusive formation of (η^4-2,3-dimethylbutadiene)Fe(CO)$_3$ (**2**), and only trace amounts of **1a/1b** were detectable.

(3) Reaction of 3 with Triphenylphosphine. A solution of **3** (0.21 g, 0.75 mmol) in 1.5 mL of *n*-hexane was added to a solution of triphenylphosphine (0.40 g, 1.5 mmol) in 19 mL of *n*-hexane at 0 °C. Yellow crystals started to precipitate after 25 min and were isolated after 1.5 h by inverse filtration, washed twice with 0.5 mL of *n*-hexane, and dried under vacuum: yield 0.40 g of **5** (98%): mp 75–77 °C; infrared spectrum (KBr) $\tilde{\nu}$(CO) 1981 and 1924 cm^{-1}, $\tilde{\nu}$(ester carbonyl) 1681 cm^{-1}. Anal. Calcd for $C_{30}H_{31}FeO_4P$: C, 66.43; H, 5.76; Fe, 10.30; P, 5.71. Found: C, 65.98; H, 6.29; Fe, 10.48; P, 5.78.

(4) Reactions of Complex 5. (a) Complex **5** (10.2 mg, 0.019 mmol) was dissolved in 10 mL of *n*-hexane. As monitored by infrared spectroscopy, ca. 40% of **5** was converted immediately to **3**. When the mixture was left standing at ambient temperature, the metal carbonyl bands of (η^4-2,3-dimethylbutadiene)(triphenylphosphine)Fe(CO)$_2$ (**6**, identified by comparison with an authentic sample[13]) gradually appeared while the concentration of **3** remained nearly constant for about 2 h. After 6.5 h the formation of **6** was almost complete, and only trace amounts of **5**, **3**, and **1a/1b** were detectable.

(b) With Carbon Monoxide. Complex **5** (11.3 mg, 0.021 mmol) was dissolved in 10 mL of *n*-hexane. When the mixture was left standing under carbon monoxide, **5** was converted into **1a/1b** (ca. 5–10:1 ratio). At ambient temperature the reaction was complete after 4–5 h; at 0 °C 1.5 days were required. **3** was not observed as an intermediate, and neither **6** nor **2** was detected.

(c) With Trimethyl Phosphite. A solution of **5** (4.8 mg, 0.0089 mmol) and trimethyl phosphite (42.7 mg, 0.34 mmol) in 10 mL of *n*-hexane was allowed to stand at ambient temperature. The CO stretching bands of **5** gradually disappeared, and those of the analogous trimethyl phosphite complex **7** grew in. After 2.5 h the conversion was complete. **7** was identified by comparison with an authentic sample,[13] the structure of which was determined by X-ray crystallography.[18]

Acknowledgment. We thank the staff of the spectroscopic laboratories of this institute for their help and Miss H. Nowak, Mrs. R. Schrader, and Mr. K. Schneider for able technical assistance.

Registry No. **1a**, 61950-05-8; **1b**, 61867-50-3; **2**, 31741-56-7; **3**, 77257-30-8; **5**, 83399-55-7; **6**, 74753-27-8; **7**, 83399-56-8.

(14) Pearson, A. G. "Symmetry Rules for Chemical Reactions"; Wiley-Interscience: New York, 1976; p 427.
(15) Koerner von Gustorf, E.; Pfajfer, Z.; Grevels, F.-W. *Z. Naturforsch., B: Anorg. Chem., Org. Chem., Biochem., Biophys., Biol.* **1971**, *26*, 66.
(16) Amrein, W.; Gloor, J.; Schaffner, K. *Chimia* **1974**, *28*, 185.
(17) Hatchard, C. G.; Parker, C. A. *Proc. R. Soc. London, Ser. A* **1956**, *235*, 518. Murov, S. L. In "Handbook of Photochemistry"; Marcel Dekker: New York, 1976; p 119.
(18) Chiang, A.-P.; Krüger, C., to be submitted for publication.

Communications

Catalytic C–H Activation in Early Transition-Metal Dialkylamides and Alkoxides†

William A. Nugent,* Derick W. Ovenall, and Steven J. Holmes[1]

Central Research and Development Department
E. I. du Pont de Nemours and Company
Experimental Station, Wilmington, Delaware 19898

Received July 1, 1982

Summary: Labeling studies provide evidence for reversible cyclometalaton in d^0 dialkylamido complexes (140–180 °C) and in d^0 alkoxo complexes (180–220 °C). In contrast to the facile α-metalation of dimethylamine, catalytic metalation occurs exclusively at the β-position of ethanol. Such a cyclometalation process serves as the basis for the catalytic aminomethylation of terminal olefins and may also be involved in the stereoselective isomerization of 3-buten-1-ol to *cis*-crotyl alcohol.

Cyclometalation of coordinated ligands is a common feature in low-valent transition-metal complexes[2] but has rarely been observed in d^0 early transition-metal compounds.[3,4] However, we wish to report evidence that, at elevated temperatures, facile reversible cyclometalation occurs in both d^0 dialkylamido[5] and alkoxo[6] complexes.

Treatment of dimethylamine-*N*-*d* with early transition-metal dimethylamides at 140–180 °C caused rapid incorporation of deuterium into the methyl group (Table I).

$$(CH_3)_2ND \xrightleftharpoons{M(NMe_2)_n} (CH_3)(CH_2D)NH \qquad (1)$$

The Ta and Zr catalysts could be recovered unchanged after the reaction. The Nb and W amides were reduced to as yet unidentified active catalyst species.[7] The reaction could be conveniently monitored by gas-phase IR spectroscopy by following the disappearance of the N–D bending mode at 1243 cm^{-1} and the concomitant increase in the C–D band at 2085 cm^{-1}. For selected runs, the results were confirmed by ^2H NMR spectroscopy. Using the isotopic shift, we found that exclusive monodeuteration of the methyl group occurs at low conversions. Equation 1 is presumed to involve the reversible metalation of the dimethylamide ligand as shown in eq 2. Azametalla-

Table I. Catalysts for H-D Exchange in Me_2ND and for Addition of Me_2NH to 1-Pentene[a]

catalyst	% H-D exchange[c]	insertn (turnovers)[d]
$Ti(NMe_2)_4$	0[e]	0.0
$Zr(NMe_2)_4$	37	0.0
$Hf(NMe_2)_4$	0[e]	
$Nb(NMe_2)_5$	67	4.5
$Ta(NMe_2)_5$	26	0.3
$W(NMe_2)_n$[b]	57	7.0
$Sn(NMe_2)_4$	0[e]	0.0

[a] All runs in evacuated sealed tubes 14 h at 160 °C. [b] Catalyst was 2:1 adduct of $W_2(NMe_2)_6/W(NMe_2)_6$ prepared by method of Chisholm.[17] [c] Percent decrease in 1243-cm^{-1} band. All runs contained 0.25 mmol of catalyst and 12.5 mmol of Me_2ND in 5 mL of decalin. [d] Yield of hexylmethylamines in mol/mol of catalyst. All runs contained 0.25 mmol of catalyst, 12.5 mmol of 1-pentene, and 12.5 mmol of dimethylamine in 5 mL of decalin. [e] None detected under conditions where as little as 3% exchange could be observed.

Scheme I

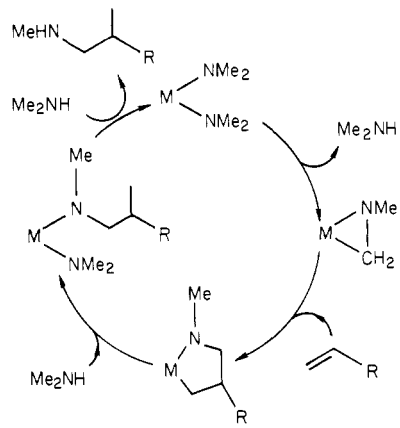

$$\text{M(NMe}_2\text{)(NMe}_2\text{)} \rightleftharpoons \text{M(NMe)(CH}_2\text{)} + \text{Me}_2\text{NH} \qquad (2)$$

cyclopropanes related to those in eq 2 are reported to be formed during thermolysis of diethylamido complexes.[8]

The intermediate azametallacyclopropanes in eq 2 can apparently be trapped by terminal olefins. Thus, heating an equimolar mixture of 1-pentene and dimethylamine with 2 mol % of metal dimethylamide resulted in the catalytic aminomethyaltion[9] of the pentene (eq 3). The

$$Me_2NH + CH_2{=}CHC_3H_7 \xrightarrow{\text{cat.}} MeHNCH_2C(CH_3)HC_3H_7 \qquad (3)$$

† Contribution No. 3079.

(1) Du Pont student summer employee.

(2) Parshall, G. W. *Acc. Chem. Res.* **1975**, *8*, 113–117. Bruce, M. I. *Angew. Chem., Int. Ed. Engl.* **1977**, *16*, 73–86.

(3) Bennett, C. R.; Bradley, D. C. *J. Chem. Soc., Chem. Commun.* **1974**, 29–30. Sharp, P. R.; Astruc, D.; Schrock, R. R. *J. Organomet. Chem.* **1979**, *182*, 477–488. Rausch, M. D.; Mintz, E. A. *Ibid.* **1980**, *190*, 65–72. Gal, A. W.; van der Heijden, H. *Angew. Chem., Int. Ed. Engl.* **1981**, *21*, 978–980.

(4) For a related metalation in an f^0 organoactinide system see: Simpson, S. J.; Turner, H. W.; Andersen, R. A. *J. Am. Chem. Soc.* **1979**, *101*, 7728–7729.

(5) Lappert, M. F.; Power, P. P.; Sanger, A. R.; Srivastava, R. C. "Metal and Metalloid Amides"; Wiley: New York, 1980.

(6) Bradley, D. C.; Mehrotra, R. C.; Gaur, D. P. "Metal Alkoxides"; Academic Press: London, 1978.

(7) This initial stoichiometric reduction proceeded with formation of methane (0.15 mol/mol of Nb). The catalyst could be isolated at the completion of the run and was fully active in a subsequent run.

(8) (a) Takahashi, Y.; Onoyama, N.; Ishikawa, Y.; Motojima, S.; Sugiyama, K. *Chem. Lett.* **1978**, 525–528. Airoldi, C.; Bradley, D. C.; Vuru, G. *Transition Met. Chem. (Weinheim, Ger.)* **1979**, *4*, 64. (b) The X-ray crystal structure of a d^0 azametallacyclopropane derivative prepared in a different manner has been reported: Chiu, K. W.; Jones, R. A.; Wilkinson, G.; Galas, A. M. R.; Hursthouse, M. B. *J. Chem. Soc., Dalton Trans.* **1981**, 2088–2097. See also: Wolczanski, P. T.; Bercaw, J. E. *J. Am. Chem. Soc.* **1979**, *101*, 6450–6452.

0276-7333/83/2302-0161$01.50/0

Table II. H-D Exchange in CH_3CH_2OD Catalyzed by Transition-Metal Ethoxides[a]

catalyst	temp, °C	% H-D exchange[c]	distributn of ^2H label,[b] %		
			CH_2D	CD_2H	CD_3
$Ti(OEt)_4$	180	0[e]			
$Zr(OEt)_4$	200	14	5	25	70
$Nb_2(OEt)_{10}$	200	18	27	41	32
$Ta_2(OEt)_{10}$	180	9			
$Ta_2(OEt)_{10}$	200	23	28	39	33
$Ta_2(OEt)_{10}$	220	47			
$Ta_2(OEt)_{10}$ + C_6H_5N[d]	200	55	38	39	23
$Ta_2(OEt)_{10}$ + Et_3N[d]	200	50			
$W(OEt)_6$	200	0[e,f]			

[a] All runs involved 0.5 mmol of catalyst in 50 mmol of ethanol-*d* for 14 h in evacuated glass tubes. [b] Relative areas of d^1, d^2, d^3 resonances (at δ 0.98, 0.96, and 0.94, respectively) in the 61.4-MHz ^1H-decoupled ^2H NMR. [c] Percent of starting OD incorporated into methyl group determined by area of OH resonance in 90-MHz ^1H NMR. [d] Run additionally contains 2.0 mmol of amine additive. [e] Catalyst decomposed to white insolubles; no exchange detected under conditions where 1% exchange could be observed. [f] Ethanol was disproportionated to diethyl ether and H_2O.

activity of the various metal amides for the reaction shown in eq 3 (Table I) roughly parallels their efficacy for H–D exchange. The regiochemistry of 1-pentene insertion varied somewhat with reaction conditions, but the product always consisted of >90% *N*-methyl-*N*-(2-methylpentyl)amine, the remainder being *N*-methyl-*N*-hexylamine. We propose that the mechanism of this reaction is that shown in the Scheme I. The proposed insertion of the olefin into the strained azametallacyclopropane intermediate has precedent in the analogous reaction of an oxametallacyclopropane recently reported by Erker.[10]

H–D exchange in ethanol-*d* was catalyzed by metal ethoxides at somewhat higher temperatures (180–220 °C). ^2H NMR studies indicate that deuterium is incorporated exclusively into the methyl group of ethanol.[11] Even at low conversions, much of the product consists of di- and trideuterated ethanols (Table II). The reaction with $Zr(OEt)_4$ is first-order in catalyst at 185 °C, while that with $Ta_2(OEt)_{10}$ at 180 °C appears half-order in catalyst.[12] The rate of the H–D exchange in ethanol is enhanced by addition of triethylamine or pyridine.

Incorporation of deuterium exclusively into the β-position of ethanol can be rationalized in terms of the preferential formation of an oxametallacyclobutane intermediate[13] (eq 4). The predominance of multiply deuterated

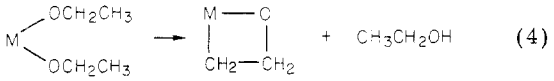

(4)

products, especially from the Zr catalyst, suggests that further metalation of the intermediate metallacycle is fast compared with the reverse of eq 4.[14] It is noteworthy in this regard that Andersen has recently observed such an effect in the *stoichiometric* cyclometalation of Zr and Hf amides. Thermal elimination of alkane from the complexes $R_2M[N(SiMe_3)_2]_2$ proceeded with loss of two hydrogens from the same methyl group to afford bridging carbene derivatives, e.g., $\{ZrCHSiMe_2NSiMe_3[N(SiMe_3)_2]\}_2$.[15] Elimination of two hydrogens from the same methyl group has also been observed in metal alkyl chemistry.[16]

We have not to date demonstrated the intermolecular insertion of olefins into the C–H bond of ethanol. We have, however, observed that isomerization of 3-butenol is catalyzed by $Ta_2(OEt)_{10}$ at 200 °C. At 5% conversion, the product crotyl alcohol consisted >99% of the cis isomer. This stereospecificity suggests the possibility that the isomerization involves a cyclometalation of the type shown in eq 4, followed by ring enlargement to a oxametallacyclohexene intermediate.

Acknowledgment. The skilled technical assistance of D. M. Lattomus and J. C. Center are gratefully acknowledged. We also thank Professor Andersen for a preprint of ref 15.

Registry No. Me_2ND, 917-72-6; Me_2NH, 124-40-3; $Zr(NMe_2)_4$, 19756-04-8; $Nb(NMe_2)_5$, 19824-58-9; $Ta(NMe_2)_5$, 19824-59-0; $W_2(NMe_2)_6$, 54935-70-5; $W(NMe_2)_6$, 68941-84-4; CH_3CH_2OD, 925-93-9; $Zr(OEt)_4$, 18267-08-8; $Nb_2(OEt)_{10}$, 3236-82-6; $Ta_2(OEt)_{10}$, 6074-84-6; 1-pentene, 109-67-1.

(9) Noteworthy in this regard is a claim in the patent literature that insertion of olefins into the α C–H bonds of dialkylamines is promoted by a variety of transition-metal species including $NbCl_5$. German Patent 2748293 (to ANIC S.p.A.)

(10) Erker, G.; Rosenfeldt, F. *J. Organomet. Chem.* **1982**, *224*, 29–42.

(11) In contrast, exclusive deuteration of the methylene carbon of ethanol by low-valent group 8 catalysts has been reported: Regan, S. L. *J. Org. Chem.* **1974**, *39*, 260–261. Sasson, Y.; Blum, J. *J. Chem. Soc., Chem. Commun.* **1974**, 309–310.

(12) The degree of aggregation of tantalum ethoxide in refluxing ethanol has been determined as 1.78 (vs. 1.98 in refluxing benzene). Bradley, D. C.; Chakravarti, B. N.; Wardlaw, W. *J. Chem. Soc.* **1956**, 2381–2384.

(13) Given eq 4, it is intriguing that in no case have we observed the formation of ethylene, which would be the expected product of Wittig-type cleavage of the cyclometalated intermediate.

(14) An alternative explanation which we cannot exclude is that deuterium incorporation occurs in a reactive *intermediate* in which both cyclometalation and its reverse reaction are fast relative to alkoxide exchange with solvent. However, it is known that alkoxide exchange with free alcohol is very rapid in the homoleptic transition-metal alkoxides (see ref 6).

(15) Planalp, R. P.; Andersen, R. A.; Zalkin, A., submitted for publication.

(16) Fellmann, J. D.; Turner, H. W.; Schrock, R. R. *J. Am. Chem. Soc.* **1980**, *102*, 6608–6609. Sharp, P. R.; Holmes, S. J.; Schrock, R. R.; Churchill, M. R.; Wasserman, H. J. *Ibid.* **1981**, *103*, 965–966. Wengrovis, J. H.; Sancho, J.; Schrock, R. R. *Ibid.* **1981**, *103*, 3932–3934.

(17) Chisholm, M. H.; Cotton, F. A.; Extine, M. W.; Stults, B. R. *J. Am. Chem. Soc.* **1976**, *98*, 4477–4485.

Synthesis of a Binuclear Hafnium Hydride Complex Which Incorporates Hybrid Multidentate Ligands

Michael D. Fryzuk* and Hugh David Williams

Department of Chemistry, University of British Columbia Vancouver, British Columbia, Canada V6T 1Y6

Received August 4, 1982

Summary: Disproportionation of $HfCl[N(SiMe_2CH_2PMe_2)_2]_2$ by excess $HfCl_4$ results in the formation of the "mono" amide complex $HfCl_3[N(SiMe_2CH_2PMe_2)_2]HfCl_4$ which can be converted to $Hf(BH_4)_3[N(SiMe_2CH_2PMe_2)_2]$ and $Hf(BH_4)_4$ by reaction with excess $LiBH_4$. The reaction of Lewis bases with $Hf(BH_4)_3[N(SiMe_2CH_2PMe_2)_2]$ generates the new binuclear

0276-7333/83/2302-0162$01.50/0

Table II. H-D Exchange in CH_3CH_2OD Catalyzed by Transition-Metal Ethoxides[a]

catalyst	temp, °C	% H-D exchange[c]	distributn of ^2H label,[b] %		
			CH_2D	CD_2H	CD_3
$Ti(OEt)_4$	180	0[e]			
$Zr(OEt)_4$	200	14	5	25	70
$Nb_2(OEt)_{10}$	200	18	27	41	32
$Ta_2(OEt)_{10}$	180	9			
$Ta_2(OEt)_{10}$	200	23	28	39	33
$Ta_2(OEt)_{10}$	220	47			
$Ta_2(OEt)_{10}$ + C_6H_5N[d]	200	55	38	39	23
$Ta_2(OEt)_{10}$ + Et_3N[d]	200	50			
$W(OEt)_6$	200	0[e,f]			

[a] All runs involved 0.5 mmol of catalyst in 50 mmol of ethanol-*d* for 14 h in evacuated glass tubes. [b] Relative areas of d^1, d^2, d^3 resonances (at δ 0.98, 0.96, and 0.94, respectively) in the 61.4-MHz ^1H-decoupled ^2H NMR. [c] Percent of starting OD incorporated into methyl group determined by area of OH resonance in 90-MHz ^1H NMR. [d] Run additionally contains 2.0 mmol of amine additive. [e] Catalyst decomposed to white insolubles; no exchange detected under conditions where 1% exchange could be observed. [f] Ethanol was disproportionated to diethyl ether and H_2O.

activity of the various metal amides for the reaction shown in eq 3 (Table I) roughly parallels their efficacy for H–D exchange. The regiochemistry of 1-pentene insertion varied somewhat with reaction conditions, but the product always consisted of >90% *N*-methyl-*N*-(2-methylpentyl)amine, the remainder being *N*-methyl-*N*-hexylamine. We propose that the mechanism of this reaction is that shown in the Scheme I. The proposed insertion of the olefin into the strained azametallacyclopropane intermediate has precedent in the analogous reaction of an oxametallacyclopropane recently reported by Erker.[10]

H–D exchange in ethanol-*d* was catalyzed by metal ethoxides at somewhat higher temperatures (180–220 °C). ^2H NMR studies indicate that deuterium is incorporated exclusively into the methyl group of ethanol.[11] Even at low conversions, much of the product consists of di- and trideuterated ethanols (Table II). The reaction with $Zr(OEt)_4$ is first-order in catalyst at 185 °C, while that with $Ta_2(OEt)_{10}$ at 180 °C appears half-order in catalyst.[12] The rate of the H–D exchange in ethanol is enhanced by addition of triethylamine or pyridine.

Incorporation of deuterium exclusively into the β-position of ethanol can be rationalized in terms of the preferential formation of an oxametallacyclobutane intermediate[13] (eq 4). The predominance of multiply deuterated

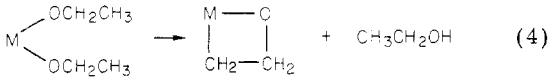

(4)

products, especially from the Zr catalyst, suggests that further metalation of the intermediate metallacycle is fast compared with the reverse of eq 4.[14] It is noteworthy in this regard that Andersen has recently observed such an effect in the *stoichiometric* cyclometalation of Zr and Hf amides. Thermal elimination of alkane from the complexes $R_2M[N(SiMe_3)_2]_2$ proceeded with loss of two hydrogens from the same methyl group to afford bridging carbene derivatives, e.g., $\{ZrCHSiMe_2NSiMe_3[N(SiMe_3)_2]\}_2$.[15] Elimination of two hydrogens from the same methyl group has also been observed in metal alkyl chemistry.[16]

We have not to date demonstrated the intermolecular insertion of olefins into the C–H bond of ethanol. We have, however, observed that isomerization of 3-butenol is catalyzed by $Ta_2(OEt)_{10}$ at 200 °C. At 5% conversion, the product crotyl alcohol consisted >99% of the cis isomer. This stereospecificity suggests the possibility that the isomerization involves a cyclometalation of the type shown in eq 4, followed by ring enlargement to a oxametallacyclohexene intermediate.

Acknowledgment. The skilled technical assistance of D. M. Lattomus and J. C. Center are gratefully acknowledged. We also thank Professor Andersen for a preprint of ref 15.

Registry No. Me_2ND, 917-72-6; Me_2NH, 124-40-3; $Zr(NMe_2)_4$, 19756-04-8; $Nb(NMe_2)_5$, 19824-58-9; $Ta(NMe_2)_5$, 19824-59-0; $W_2(NMe_2)_6$, 54935-70-5; $W(NMe_2)_6$, 68941-84-4; CH_3CH_2OD, 925-93-9; $Zr(OEt)_4$, 18267-08-8; $Nb_2(OEt)_{10}$, 3236-82-6; $Ta_2(OEt)_{10}$, 6074-84-6; 1-pentene, 109-67-1.

(9) Noteworthy in this regard is a claim in the patent literature that insertion of olefins into the α C–H bonds of dialkylamines is promoted by a variety of transition-metal species including $NbCl_5$. German Patent 2748293 (to ANIC S.p.A.)

(10) Erker, G.; Rosenfeldt, F. *J. Organomet. Chem.* **1982**, *224*, 29–42.

(11) In contrast, exclusive deuteration of the methylene carbon of ethanol by low-valent group 8 catalysts has been reported: Regan, S. L. *J. Org. Chem.* **1974**, *39*, 260–261. Sasson, Y.; Blum, J. *J. Chem. Soc., Chem. Commun.* **1974**, 309–310.

(12) The degree of aggregation of tantalum ethoxide in refluxing ethanol has been determined as 1.78 (vs. 1.98 in refluxing benzene). Bradley, D. C.; Chakravarti, B. N.; Wardlaw, W. *J. Chem. Soc.* **1956**, 2381–2384.

(13) Given eq 4, it is intriguing that in no case have we observed the formation of ethylene, which would be the expected product of Wittig-type cleavage of the cyclometalated intermediate.

(14) An alternative explanation which we cannot exclude is that deuterium incorporation occurs in a reactive *intermediate* in which both cyclometalation and its reverse reaction are fast relative to alkoxide exchange with solvent. However, it is known that alkoxide exchange with free alcohol is very rapid in the homoleptic transition-metal alkoxides (see ref 6).

(15) Planalp, R. P.; Andersen, R. A.; Zalkin, A., submitted for publication.

(16) Fellmann, J. D.; Turner, H. W.; Schrock, R. R. *J. Am. Chem. Soc.* **1980**, *102*, 6608–6609. Sharp, P. R.; Holmes, S. J.; Schrock, R. R.; Churchill, M. R.; Wasserman, H. J. *Ibid.* **1981**, *103*, 965–966. Wengrovis, J. H.; Sancho, J.; Schrock, R. R. *Ibid.* **1981**, *103*, 3932–3934.

(17) Chisholm, M. H.; Cotton, F. A.; Extine, M. W.; Stults, B. R. *J. Am. Chem. Soc.* **1976**, *98*, 4477–4485.

Synthesis of a Binuclear Hafnium Hydride Complex Which Incorporates Hybrid Multidentate Ligands

Michael D. Fryzuk* and Hugh David Williams

Department of Chemistry, University of British Columbia Vancouver, British Columbia, Canada V6T 1Y6

Received August 4, 1982

Summary: Disproportionation of $HfCl[N(SiMe_2CH_2PMe_2)_2]_2$ by excess $HfCl_4$ results in the formation of the "mono" amide complex $HfCl_3[N(SiMe_2CH_2PMe_2)_2]HfCl_4$ which can be converted to $Hf(BH_4)_3[N(SiMe_2CH_2PMe_2)_2]$ and $Hf(BH_4)_4$ by reaction with excess $LiBH_4$. The reaction of Lewis bases with $Hf(BH_4)_3[N(SiMe_2CH_2PMe_2)_2]$ generates the new binuclear

0276-7333/83/2302-0162$01.50/0

hydride derivative $\{Hf[N(SiMe_2CH_2PMe_2)_2]\}_2(H)_3(BH_4)_3$.

Transition-metal hydrides constitute a very reactive class of organometallic complexes. This is certainly true of the group 4B metals Zr and Hf for which the unique reactivity of $(\eta^5\text{-}C_5H_5)_2Zr(H)Cl$ and $(\eta^5\text{-}C_5Me_5)_2ZrH_2$ with olefins, acetylenes, carbon monoxide, and isocyanides has generated new vistas in organic and organometallic chemistry.[1,2] To extend the potentially rich chemistry of the group 4B hydrides, we have undertaken a study aimed at the synthesis of new complexes of zirconium and hafnium which incorporate hydride ligands stabilized by ancillary "hybrid" multidentate ligands[3] of the type **1**. These particular ancillary ligands were specifically designed to generate new types of electronic and steric environments at the metal center by combining the *hard* amido donor, $^-NR_2$, with *soft* phosphine donors into a chelating array (**1**). Herein we describe the synthesis of a new dimeric hafnium hydride complex which contains tetrahydroborate ($^-BH_4$) ligands.

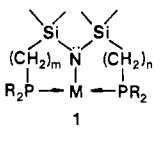

1

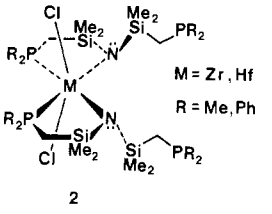

2

Previously,[4] we reported the synthesis of zirconium(IV) and hafnium(IV) complexes which contain two hybrid multidentate ligands and have the molecular formula $MCl_2[N(SiMe_2CH_2PR_2)_2]_2$ **2**. Although the solution and solid-state structures were of stereochemical interest, these complexes were surprisingly unreactive toward strong nucleophiles (RMgX, RLi, $LiBH_4$). We attributed this lack of reactivity to overcrowding at the metal center due to the incorporation of two bulky amidophosphine chelate ligands. However, we have since discovered that these complexes undergo a facile disproportionation reaction in the presence of the starting metal tetrahalide to generate "mono" derivatives which contain only one tridentate hybrid ligand per metal; this engenders a sterically less encumbered metal center which, as a result, is very reactive to strong nucleophiles.

The reaction of $HfCl_4$ (≥9 equiv) with the "bis" derivative $HfCl_2[N(SiMe_2CH_2PMe_2)_2]_2$ (**2**, M = Hf, R = Me) in toluene results in the formation of a yellow, sparingly soluble complex with the analytical formula $Hf_2Cl_7[N(SiMe_2CH_2PMe_2)_2]$[5] (**3**). Although the low solubility of

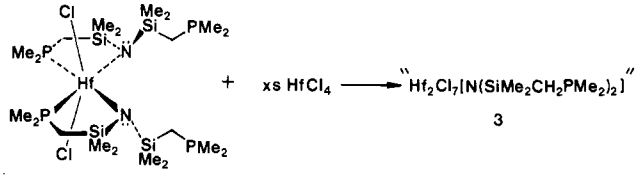

3

3 has precluded accurate molecular weight measurement,[5] the reactivity of this species suggests an empirical formula of $HfCl_3[N(SiMe_2CH_2PMe_2)_2]\cdot HfCl_4$; that is, the genuine "mono" derivative $HfCl_3[N(SiMe_2CH_2PMe_2)_2]$ with an associated $HfCl_4$ molecule, presumably through chloride bridges. The use of a stoichiometric amount (1 equiv) of $HfCl_4$ results in an oily mixture of products. We had previously attempted to generate this type of species by the slow addition of $LiN(SiMe_2CH_2PMe_2)_2$ to 3 equiv of $HfCl_4$; however, only the "bis" derivative **2** (M = Hf, R = Me) was isolated. By increasing the amount of $HfCl_4$ to 5 equiv, the one-step synthesis of **3** from $LiN(SiMe_2CH_2PMe_2)_2$ is effective if long reaction times are used; presumably, initial formation of the "bis" derivative followed by disproportionation occurs. The above reaction also proceeds with zirconium, but because the analogous "mono" derivative appears to be somewhat thermally sensitive, we have concentrated our efforts on hafnium.

The reaction of excess $LiBH_4$ (≥8 equiv) with **3** produces two hafnium-containing compounds: the volatile $Hf(BH_4)_4$ (identified by IR[6]) and a new tetrahydroborate derivative, $Hf(BH_4)_3[N(SiMe_2CH_2PMe_2)_2]$[7] (**4**). Colorless crystals of

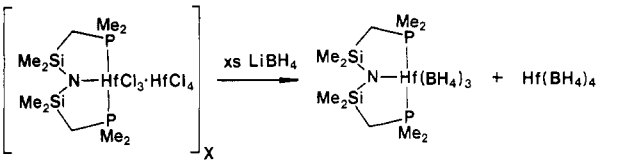

3 **4**

4 are monomeric[7] in benzene solution and contain bidentate[8] $^-BH_4$ ligands as evidenced from the IR (hexane, cm^{-1}): 2470, 2420 ($\nu(B\text{-}H^t)$); 2110, 1950 ($\nu(B\text{-}H^b)$); 1345 ($\delta(B\text{-}H)$). The ^1H NMR[7] shows virtual triplets for the phosphorus methyl protons and the methylene protons (PCH_2Si) which indicates a trans[9] disposition of the phosphorus nuclei in the complex; the B–H resonance appears as a very broad quartet ($^1J_{11B}$ = 88 Hz) suggesting rapid interchange of bridging and terminal B–H bonds. The structure of **4** is not obvious in the absence of crystallographic information; in solution the spectroscopic data are consistent with the tridentate "hybrid" ligand coordinated in a meridional fashion, leaving the three bidentate $^-BH_4$ ligands in two nonequivalent sites by symmetry: one $^-BH_4$ ligand trans to the amido donor and the remaining two cis to the amido ligand (assuming a basic octahedral geometry). However, the ^{11}B NMR consists only of a single broad quintet at room temperature[7] suggesting exchange between the two nonequivalent $^-BH_4$ sites.

In certain cases, the reaction of Lewis bases such as tertiary amines (NR_3) with a transition-metal tetrahydroborate derivative will remove BH_3 (as $H_3B{\leftarrow}NR_3$) and generate a metal hydride. For example, both $(\eta^5\text{-}C_5H_5)_2Zr(H)BH_4$ and $[(\eta^5\text{-}C_5H_5)_2ZrH_2]_2$ can be generated from $(\eta^5\text{-}C_5H_5)_2Zr(BH_4)_2$ by the use of appropriate stoichiometries of NMe_3.[10] In the analogous reaction of NEt_3 with the tris(tetrahydroborate) complex **4**, a more com-

(1) (a) Schwartz, J.; Labinger, J. A. *Angew. Chem., Int. Ed. Engl.* **1976**, *15*, 333. (b) Carr, D. B.; Schwartz, J. *J. Am. Chem. Soc.* **1979**, *101*, 3521. (c) Fachinetti, G.; Floriani, C.; Roselli, A.; Pucci, S. *J. Chem. Soc., Chem. Commun.* **1978**, 269.

(2) (a) Bercaw, J. E. *Adv. Chem. Ser.* **1978**, *No. 167*, 136. (b) Wolczanski, P. T.; Bercaw, J. E. *Acc. Chem. Res.* **1980**, *13*, 121.

(3) Fryzuk, M. D.; MacNeil, P. A. *J. Am. Chem. Soc.* **1981**, *103*, 3592.

(4) Fryzuk, M. D.; Williams, H. D.; Rettig, S. J., submitted for publication in *Inorg. Chem.*

(5) **3**: mp 167.5–168.5 °C; ^1H NMR (C_6D_6, ppm) 0.99 (t, $P(CH_3)_2$, J_{app} = 5.0 Hz), 0.87 (t, PCH_2Si, J_{app} = 5.6 Hz), 0.22 (s, $Si(CH_3)_2$); $^{31}P\{^1H\}$ NMR (C_6D_6, ppm relative to $P(OMe)_3$ at 141.0) −3.86 (s). Anal. Calcd for $C_{10}H_{28}NCl_7Hf_2P_2Si_2$: C, 13.56; H, 3.18; N, 1.58; Cl, 28.02. Found: C, 13.88; H, 3.25; N, 1.47; Cl, 28.30. Preliminary solution molecular weight measurements by the Signer method (isothermal distillation) give values of 1500 which is between the monomeric (885) and dimeric (1770) formulations.

(6) Marks, T. J.; Kolb, J. R. *Chem. Rev.* **1977**, *77*, 263.

(7) **4**: mp 119 °C dec; molecular weight (Signer, C_6D_6, 25 °C) 481, theoretical 503; ^1H NMR (C_6D_6, ppm) 1.17 (t, $P(CH_3)_2$, J_{app} = 4.0 Hz), 0.94 (t, PCH_2Si, J_{app} = 6.0 Hz), 0.31 (s, $Si(CH_3)_2$), 2.9 (br q, BH_4, $J_{^{11}B}$ = 88 Hz); $^{31}P\{^1H\}$ NMR (C_6D_6, ppm relative to external $P(OMe)_3$ at 141.0) −20.03 (s); ^{11}B NMR (C_6D_6, ppm relative to external $B(OMe)_3$ at −18.1) −27.2 (q, $^1J_{^1H}$ = 88 Hz); low-temperature spectra are broad and uninformative. Anal. Calcd for $C_{10}H_{40}NB_3HfP_2Si_2$: C, 24.93; H, 8.36; N, 2.90. Found: C, 24.60; H, 8.30; N, 2.77.

(8) Johnson, P. L.; Cohen, S. A.; Marks, T. J.; Williams, J. M. *J. Am. Chem. Soc.* **1978**, *100*, 2709 and ref 6.

(9) Shaw, B. L.; Brookes, P. R. *J. Chem. Soc. A* **1967**, 1079.

(10) James, B. D.; Nanda, R. K.; Wallbridge, M. G. H. *Inorg. Chem.* **1967**, *6*, 1979.

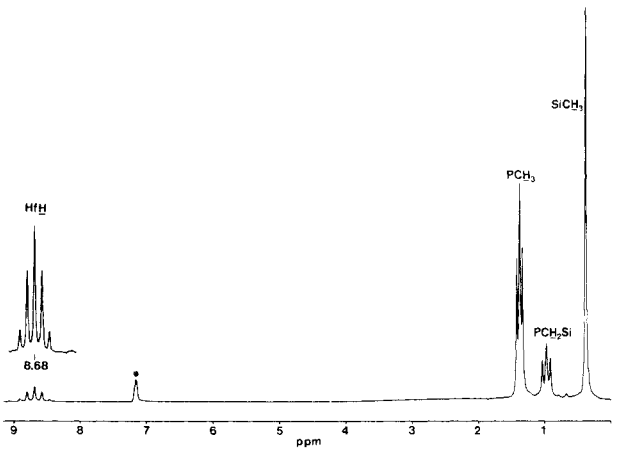

Figure 1. 80-MHz ^1H NMR of $\{Hf[N(SiMe_2CH_2PMe_2)_2]\}_2(H)_3(BH_4)_3$ (**5**). The $^-BH_4$ resonances appear as a broad hump at ~2 ppm. The C_6D_5H peak is marked by an asterisk.

plicated sequence ensues. The addition of excess NEt_3 to a toluene solution of **4** results in the quantitative production (by ^1H NMR) of a dimeric hafnium hydride with the molecular formula $\{Hf[N(SiMe_2CH_2PMe_2)_2]\}_2(H)_3(BH_4)_3$[11] (**5**). Separation of **5** from the borane adduct $H_3B{\leftarrow}NEt_3$ is difficult; however, the use of PMe_3 as the Lewis base provides >65% recrystallized yields of **5** by fractional crystallization from hexane. Less basic amines such as pyridine and ethers such as tetrahydrofuran do not remove BH_3 from **4** suggesting that a minimum bascity is required for this transformation. Further reaction of the remaining $^-BH_4$ ligands of **5** is not observed even with tetramethylethylenediamine and longer reaction times.

The dimeric nature of **5** is evident from the ^1H NMR (Figure 1) wherein the hydride resonance appears as a binomial quintet at 8.68 ppm due to coupling with *four* equivalent phosphorus nuclei; a solution molecular weight confirms this dimeric formulation. That there are *three*

$$4 \xrightarrow{PMe_3} \underset{5}{\{Hf[N(SiMe_2CH_2PMe_2)_2]\}_2(H)_3(BH_4)_3} + H_3B{\leftarrow}PMe_3$$

hydrides per dimer is evident from the quartet observed in the ^{31}P NMR when the methylene and phosphorus-methyl protons are selectively decoupled. As with **4**, the structure of **5** is ambiguous solely on the basis of solution spectroscopic techniques. Once again, the ^1H NMR spectrum is consistent with the hybrid ligand arranged in a meridional bonding mode on each hafnium in solution; however, the relative orientation of the planar tridentate ligands on each hafnium (parallel or skew) is unknown. In addition, the quintet observed for the hydride protons suggests fluxional,[12] bridging hydrides as is observed for $Ta_2Cl_4(PMe_3)_4H_2$.[13] Unfortunately, little information is available on both the position and the binding mode of the remaining three tetrahydroborate ligands. The high symmetry of the complex in solution, as suggested by the ^1H NMR spectrum, is perhaps a result of exchange of the three $^-BH_4$ moieties between the two hafnium centers; this would require a bridging[14] $^-BH_4$ ligand at some point in the exchange process. One possible formulation is $\{[(Me_2PCH_2SiMe_2)_2N]Hf(BH_4)\}_2(\mu\text{-}H)_3(\mu\text{-}BH_4)$; one bridging $^-BH_4$ and two "terminal" $^-BH_4$ groups. The broad ^1H NMR resonances and complex IR spectrum of **5** make such a formulation speculative.[15]

The formation of the dimeric hydride **5** and the borane adduct proceeds via a complicated mechanism involving stepwise removal of BH_3 by the Lewis base and at some point, a dimerization. Although we have been unable to isolate or identify any intermediates as yet, some are observable by $^{31}P\{^1H\}$ and ^1H NMR and are under investigation at present.

The hydrides of **5** do not exchange with D_2 (4 atm); in addition **5** is not a hydrogenation catalyst for 1-hexene even at 100 atm of H_2. This lack of reactivity may be due to the fact that each hafnium is formally nine-coordinate (assuming bidentate $^-BH_4$ ligation) and perhaps inaccessible to substrates.[16] Synthetic routes to tetrahydroborate-free hafnium hydrides are in progress.

Acknowledgment. Financial support for this research was generously provided by the Department of Chemistry and the Natural Sciences and Engineering Research Council of Canada. We also thank Dr. G. M. Williams for valuable discussions.

Registry No. **2**, 83634-64-4; **3**, 83634-65-5; **4**, 83634-66-6; **5**, 83634-67-7; $HFCl_4$, 13499-05-3; $LiBH_4$, 16949-15-8; NEt_3, 121-44-8; PMe_3, 594-09-2.

Supplementary Material Available: Full experimental details for the synthesis of **3**, **4**, and **5** and the infrared spectra of **4** and **5** (4 pages). Ordering information is given on any current masthead page.

(11) **5**: mp 134-136 °C; molecular weight (Signer, C_6D_6, 25 °C) 980, theoretical 965; ^1H NMR (C_7D_8, ppm) 8.68 (q, HfH, J_P = 8.6 Hz), 1.37 (t, $P(CH_3)_2$, J_{app} = 3.4 Hz), 0.94 (t, PCH_2Si, J_{app} = 4.9 Hz), 0.37 (s, $Si(CH_3)_2$); $^{31}P\{^1H\}$ NMR (C_6D_6, ppm relative to external $(P(OMe)_3$ at 141.0) -16.16 (s); ^{11}B NMR (C_6D_6, ppm relative to external $B(OMe)_3$ at -18.1) -49.2 (br q, $J_{^1H} \approx 95$ Hz); IR (hexane, cm^{-1}) 2520 (w), 2425 (s), 2400 (w, sh), 2144 (s), 1545 (s) (B-H and Hf-H modes). Anal. Calcd for $C_{20}H_{71}N_2B_3Hf_2P_4Si_4$: C, 24.88; H, 7.41; N, 2.90; B, 3.36; P, 12.83. Found: C, 25.00; H, 7.08; N, 3.20; B, 3.69; P, 12.96.

(12) Variable-temperature ^1H NMR studies on **5** have been inconclusive; broadening of all resonances as the temperature is lowered is observed, but no limiting low-temperature spectrum has been as yet obtained. The singlet observed[11] in the $^{31}P\{^1H\}$ NMR broadens as the temperature is lowered (<-50 °C) to a complicated, unsymmetrical multiplet pattern which we have not been able to analyze.

(13) Wilson, B. R., Jr.; Sattelberger, A. P.; Huffman, J. C. *J. Am. Chem. Soc.* **1982**, *104*, 858.

(14) Bridging $^-BH_4$ ligands are not well established; see: Holah D. G.; Hughes, A. N.; Hui, B. C. *Can. J. Chem.* **1975**, *53*, 3669.

(15) The single-crystal X-ray analysis of **5** is in progress. Preliminary results (S. J. Rettig, personal communication) show an unsymmetrical structure of the form $[(Me_2PCH_2SiMe_2)_2N]Hf(BH_4)_2(\mu\text{-}H)_3Hf(BH_4)[N(SiMe_2CH_2PMe_2)_2]$; one hafnium contains two bidentate $^-BH_4$ groups while the other hafnium has one tridentate $^-BH_4$ ligand. Structural parameters for **5**: triclinic, $P\bar{1}$; α = 13.333 (3) Å, b = 18.722 (3) Å, c = 9.690 (3) Å, α = 94.02 (2)°, β = 107.04 (2); γ = 109.14 (2)°; Z = 2; current R = 0.042 (R_w = 0.056) for 7675 reflections with $I \geq 3\sigma(I)$.

(16) Wolczanski, P. T.; Bercaw, J. E. *Organometallics* **1982**, *1*, 793.

Dihydrido(triethylsilyl)iridium(V) Complexes

Maria-Jesus Fernandez and Peter M. Maitlis*

Department of Chemistry, The University Sheffield S3 7HF, England

Received August 18, 1982

Summary: Reaction of $[(C_5Me_5Ir)_2Cl_4]$ with Et_3SiH gives first $[(C_5Me_5Ir)_2H_2Cl_2]$, then $[C_5Me_5Ir^V(H)_2(Cl)SiEt_3]$, and finally $[C_5Me_5Ir(H)_2(SiEt_3)_2]$. The reaction $[(C_5Me_5Ir)_2H_2Cl_2] + 2Et_3SiH \rightarrow 2[C_5Me_5Ir(H)_2(SiEt_3)Cl]$ is formally an Ir(III) → Ir(V) oxidative addition.

We recently reported[1] that $[(C_5Me_5Rh)_2Cl_4]$ (**1a**) and other rhodium complexes were effective catalysts for the

(1) Millan, A.; Towns, E.; Maitlis, P. M. *J. Chem. Soc., Chem. Commun.* **1981**, 673.

0276-7333/83/2302-0164$01.50/0

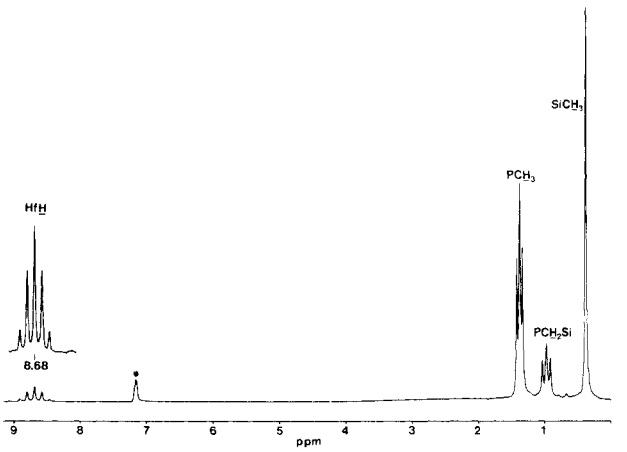

Figure 1. 80-MHz ^1H NMR of $\{Hf[N(SiMe_2CH_2PMe_2)_2]\}_2(H)_3(BH_4)_3$ (**5**). The $^-BH_4$ resonances appear as a broad hump at ~2 ppm. The C_6D_5H peak is marked by an asterisk.

plicated sequence ensues. The addition of excess NEt_3 to a toluene solution of **4** results in the quantitative production (by ^1H NMR) of a dimeric hafnium hydride with the molecular formula $\{Hf[N(SiMe_2CH_2PMe_2)_2]\}_2(H)_3(BH_4)_3$[11] (**5**). Separation of **5** from the borane adduct $H_3B{\leftarrow}NEt_3$ is difficult; however, the use of PMe_3 as the Lewis base provides >65% recrystallized yields of **5** by fractional crystallization from hexane. Less basic amines such as pyridine and ethers such as tetrahydrofuran do not remove BH_3 from **4** suggesting that a minimum bascity is required for this transformation. Further reaction of the remaining $^-BH_4$ ligands of **5** is not observed even with tetramethylethylenediamine and longer reaction times.

The dimeric nature of **5** is evident from the ^1H NMR (Figure 1) wherein the hydride resonance appears as a binomial quintet at 8.68 ppm due to coupling with *four* equivalent phosphorus nuclei; a solution molecular weight confirms this dimeric formulation. That there are *three*

$$4 \xrightarrow{PMe_3} \underset{5}{\{Hf[N(SiMe_2CH_2PMe_2)_2]\}_2(H)_3(BH_4)_3} + H_3B{\leftarrow}PMe_3$$

hydrides per dimer is evident from the quartet observed in the ^{31}P NMR when the methylene and phosphorus-methyl protons are selectively decoupled. As with **4**, the structure of **5** is ambiguous solely on the basis of solution spectroscopic techniques. Once again, the ^1H NMR spectrum is consistent with the hybrid ligand arranged in a meridional bonding mode on each hafnium in solution; however, the relative orientation of the planar tridentate ligands on each hafnium (parallel or skew) is unknown. In addition, the quintet observed for the hydride protons suggests fluxional,[12] bridging hydrides as is observed for $Ta_2Cl_4(PMe_3)_4H_2$.[13] Unfortunately, little information is available on both the position and the binding mode of the remaining three tetrahydroborate ligands. The high symmetry of the complex in solution, as suggested by the ^1H NMR spectrum, is perhaps a result of exchange of the three $^-BH_4$ moieties between the two hafnium centers; this would require a bridging[14] $^-BH_4$ ligand at some point in the exchange process. One possible formulation is $\{[(Me_2PCH_2SiMe_2)_2N]Hf(BH_4)\}_2(\mu\text{-}H)_3(\mu\text{-}BH_4)$; one bridging $^-BH_4$ and two "terminal" $^-BH_4$ groups. The broad ^1H NMR resonances and complex IR spectrum of **5** make such a formulation speculative.[15]

The formation of the dimeric hydride **5** and the borane adduct proceeds via a complicated mechanism involving stepwise removal of BH_3 by the Lewis base and at some point, a dimerization. Although we have been unable to isolate or identify any intermediates as yet, some are observable by $^{31}P\{^1H\}$ and ^1H NMR and are under investigation at present.

The hydrides of **5** do not exchange with D_2 (4 atm); in addition **5** is not a hydrogenation catalyst for 1-hexene even at 100 atm of H_2. This lack of reactivity may be due to the fact that each hafnium is formally nine-coordinate (assuming bidentate $^-BH_4$ ligation) and perhaps inaccessible to substrates.[16] Synthetic routes to tetrahydroborate-free hafnium hydrides are in progress.

Acknowledgment. Financial support for this research was generously provided by the Department of Chemistry and the Natural Sciences and Engineering Research Council of Canada. We also thank Dr. G. M. Williams for valuable discussions.

Registry No. **2**, 83634-64-4; **3**, 83634-65-5; **4**, 83634-66-6; **5**, 83634-67-7; $HFCl_4$, 13499-05-3; $LiBH_4$, 16949-15-8; NEt_3, 121-44-8; PMe_3, 594-09-2.

Supplementary Material Available: Full experimental details for the synthesis of **3**, **4**, and **5** and the infrared spectra of **4** and **5** (4 pages). Ordering information is given on any current masthead page.

(11) **5**: mp 134-136 °C; molecular weight (Signer, C_6D_6, 25 °C) 980, theoretical 965; ^1H NMR (C_7D_8, ppm) 8.68 (q, HfH, J_P = 8.6 Hz), 1.37 (t, $P(CH_3)_2$, J_{app} = 3.4 Hz), 0.94 (t, PCH_2Si, J_{app} = 4.9 Hz), 0.37 (s, $Si(CH_3)_2$); $^{31}P\{^1H\}$ NMR (C_6D_6, ppm relative to external $(P(OMe)_3$ at 141.0) -16.16 (s); ^{11}B NMR (C_6D_6, ppm relative to external $B(OMe)_3$ at -18.1) -49.2 (br q, $J_{^1H} \approx 95$ Hz); IR (hexane, cm^{-1}) 2520 (w), 2425 (s), 2400 (w, sh), 2144 (s), 1545 (s) (B-H and Hf-H modes). Anal. Calcd for $C_{20}H_{71}N_2B_3Hf_2P_4Si_4$: C, 24.88; H, 7.41; N, 2.90; B, 3.36; P, 12.83. Found: C, 25.00; H, 7.08; N, 3.20; B, 3.69; P, 12.96.

(12) Variable-temperature ^1H NMR studies on **5** have been inconclusive; broadening of all resonances as the temperature is lowered is observed, but no limiting low-temperature spectrum has been as yet obtained. The singlet observed[11] in the $^{31}P\{^1H\}$ NMR broadens as the temperature is lowered (<-50 °C) to a complicated, unsymmetrical multiplet pattern which we have not been able to analyze.

(13) Wilson, B. R., Jr.; Sattelberger, A. P.; Huffman, J. C. *J. Am. Chem. Soc.* **1982**, *104*, 858.

(14) Bridging $^-BH_4$ ligands are not well established; see: Holah D. G.; Hughes, A. N.; Hui, B. C. *Can. J. Chem.* **1975**, *53*, 3669.

(15) The single-crystal X-ray analysis of **5** is in progress. Preliminary results (S. J. Rettig, personal communication) show an unsymmetrical structure of the form $[(Me_2PCH_2SiMe_2)_2N]Hf(BH_4)_2(\mu\text{-}H)_3Hf(BH_4)[N(SiMe_2CH_2PMe_2)_2]$; one hafnium contains two bidentate $^-BH_4$ groups while the other hafnium has one tridentate $^-BH_4$ ligand. Structural parameters for **5**: triclinic, $P\bar{1}$; α = 13.333 (3) Å, b = 18.722 (3) Å, c = 9.690 (3) Å, α = 94.02 (2)°, β = 107.04 (2); γ = 109.14 (2)°; Z = 2; current R = 0.042 (R_w = 0.056) for 7675 reflections with $I \geq 3\sigma(I)$.

(16) Wolczanski, P. T.; Bercaw, J. E. *Organometallics* **1982**, *1*, 793.

Dihydrido(triethylsilyl)iridium(V) Complexes

Maria-Jesus Fernandez and Peter M. Maitlis*

Department of Chemistry, The University Sheffield S3 7HF, England

Received August 18, 1982

Summary: Reaction of $[(C_5Me_5Ir)_2Cl_4]$ with Et_3SiH gives first $[(C_5Me_5Ir)_2H_2Cl_2]$, then $[C_5Me_5Ir^V(H)_2(Cl)SiEt_3]$, and finally $[C_5Me_5Ir(H)_2(SiEt_3)_2]$. The reaction $[(C_5Me_5Ir)_2H_2Cl_2] + 2Et_3SiH \rightarrow 2[C_5Me_5Ir(H)_2(SiEt_3)Cl]$ is formally an Ir(III) → Ir(V) oxidative addition.

We recently reported[1] that $[(C_5Me_5Rh)_2Cl_4]$ (**1a**) and other rhodium complexes were effective catalysts for the

(1) Millan, A.; Towns, E.; Maitlis, P. M. *J. Chem. Soc., Chem. Commun.* **1981**, 673.

0276-7333/83/2302-0164$01.50/0

hydrosilylation–dehydrogenation reaction of α-olefins with silicon hydrides to give vinylic and allylic silanes as well as for normal hydrosilylation reactions. The corresponding iridium complex $[(C_5Me_5Ir)_2Cl_4]$ (**1b**)[2] was, however, quite inactive for either reaction though it did promote the addition of Si–H to alkynes.[3] The lack of reactivity of other iridium complexes in olefin hydrosilylation has previously been noted.[4]

Separate experiments showed that the isomerization of 1-hexene was only very slowly catalyzed by **1b** and Et_3SiH and that rapid formation of internal hexene isomers was not the reason why **1b** was a poor catalyst.

Under conditions reasonably similar to those used in the hydrosilylation reactions (CH_2Cl_2 solvent, 20 °C) **1b** reacted directly and quickly with Et_3SiH to give a new colorless complex (70% yield) that was shown to be the iridium(V) silyl hydride $[C_5Me_5Ir(H)_2Cl(SiEt_3)]$ (**3**)[5] [IR ν(Ir–H) 2135, ν(Ir–Cl, terminal) 305 cm^{-1}; ^1H NMR (CD_2Cl_2) δ −12.6 (s, IrH_2), 0.8 (q, J = 7.5 Hz, $SiCH_2$), 0.94 (t, J = 7.5 Hz, $SiCH_2CH_3$), 1.91 (s, C_5Me_5)]. Extended reaction converted **3** into $[C_5Me_5Ir(H)_2(SiEt_3)_2]$ (**4**)[5] that was more conveniently prepared by reaction of **1b** (30% yield) or **2** (40% yield) with Et_3SiH in the presence of triethylamine in refluxing benzene. [IR ν(Ir–H) 2160 cm^{-1}; mass spectrum, m/e 556, 558 $(M-1)^+$; ^1H NMR ($CDCl_3$) δ −17.4 (s, IrH_2), 0.67 (q, J = 8 Hz, $SiCH_2$), 0.82 (t, J = 8 Hz, $SiCH_2CH_3$), 1.97 (s, C_5Me_5)].

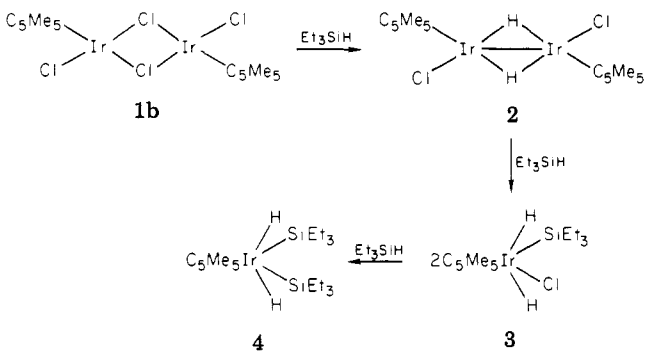

Complex **4** is the analogue of the rhodium(V) complex $[C_5Me_5Rh(H)_2(SiEt_3)_2]$ that we recently reported,[6] and X-ray photographs show them to be isomorphous. Although a number of iridium(V) hydrides L_2IrH_5[7] and one iridium(V) organometallic $C_5Me_5IrMe_4$[8] have been prepared, **3** and **4** are the first organosilyls in this oxidation state. In fact even some Ir(I) complexes only add $R_3Si–H$ with reluctance.[9]

We are investigating details of these and related reactions further, but we note (a) that the dinuclear dihydride complex **2**[10] is intermediate[11] in the reaction of **1b** to give **3** and (b) that **2** reacts directly with Et_3SiH to give **3**. This latter reaction is, formally at least, an example of the rather rare oxidative addition Ir(III) → Ir(V) ($d^6 \rightarrow d^4$).

Acknowledgment. We thank the SERC for supporting this work, Johnson Matthey Ltd for the loan of iridium salts, and Dr. P. M. Bailey for the X-ray measurement.

(2) For a review of these complexes, see Maitlis, P. M. *Chem. Soc. Rev.* **1981**, *10*, 1.
(3) Millan, A. Ph.D. Thesis, University of Sheffield, 1981.
(4) Haszeldine, R. N.; Parish, R. V.; Parry, D. J. *J. Chem. Soc. A* **1969**, 683.
(5) Satisfactory microanalyses were obtained for all new complexes.
(6) Fernandez, M.-J.; Maitlis, P. M. *J. Chem. Soc., Chem. Commun.* **1982**, 310.
(7) Mann, B. E.; Masters, C.; Shaw, B. L. *J. Inorg. Nucl. Chem.* **1971**, *33*, 2195.
(8) Isobe, K.; Bailey, P. M.; Maitlis, P. M. *J. Chem. Soc., Chem. Commun.* **1981**, 808.
(9) Chalk, A. J.; Harrod, J. F. *J. Am. Chem. Soc.* **1965**, *87*, 16, but see Blackburn, S. N.; Haszeldine, R. N.; Parish, R. V.; Setchfield, J. H. *J. Chem. Res., Synop.* **1980**, 170.
(10) Gill, D. S.; Maitlis, P. M. *J. Organomet. Chem.* **1975**, *87*, 359.
(11) The dihydride **2** is unique amongst C_5Me_5–Ir complexes in being deep blue. We have therefore interpreted the transient blue color seen during reaction of **1b** with Et_3SiH as evidence that **2** is the intermediate. This is, of course, supported by the direct reaction of **2** to give **3**.

Metal–Metal Multiple Bonds in Rational Cluster Synthesis.[1] Novel Isomerism in Iron–Molybdenum–Sulfur Clusters and a Molybdenum–Sulfur Cubane. Structure of $(\eta^5\text{-}CH_3C_5H_4)_2Mo_2Fe_2(\mu_3\text{-}S)_2(CO)_6(\mu\text{-}CO)_2$

P. Douglas Williams, M. David Curtis,* D. Neil Duffy, and William M. Butler
Department of Chemistry, The University of Michigan Ann Arbor, Michigan 48109

Received June 28, 1982

Summary: Reaction of $R_2Mo_2(CO)_4(Mo{\equiv}Mo)$, R = Cp, Cp′, or η^5-$CH_3C_5H_4$ (**1**), with $Fe_2S_2(CO)_6$ generates a pair of isomeric iron–molybdenum–sulfur clusters with different $Fe_2Mo_2S_2$ frameworks. Although both isomers have a 62-cluster-electron count, different formal oxidation states must be assigned to the metals in order for them to achieve an 18-electron count. Also, the Mo≡Mo bond of **1** displaces propylene from $Cp_2Mo_2(SC_3H_5S)_2$ to give the cluster $Cp_2Cp'_2Mo_4S_4$. These reactions demonstrate the utility of the Mo≡Mo triple bond in the rational synthesis of metal–sulfur clusters.

Interest in metal sulfides has resulted in part from their importance as catalysts.[2] Iron–molybdenum–sulfur compounds in particular are interesting as possible models of hydrodesulfurization catalysts[3,4] and the nitrogenase cofactor.[5] Here we report a rational approach to the synthesis of molybdenum–sulfur clusters and an unprecedented system of isomeric iron–molybdenum–sulfur clusters.

The utility of sulfur ligands in the stabilization of metal clusters has already been demonstrated.[6] Of particular utility in the preparation of iron–sulfur clusters is the compound $Fe_2S_2(CO)_6$ which has been shown to react with a variety of metal carbonyls and low-valent metal complexes.[7–13]

(1) Part 11 of Metal–Metal Multiple Bonds. Part 10: Curtis, M. D.; Fotinos, N. A.; Han, K. R.; Butler, W. M. *J. Am. Chem. Soc.*, in press.
(2) Mitchell, P. C. H. *Catalysis (London)* **1977**, *1*, 204–233.
(3) Furimsky, E. *Catal. Rev.—Sci. Eng.* **1980**, *22*, 371.
(4) (a) DuBois, M. R.; Haltiwanger, R. C.; Miller, D. J.; Glatzmaier, G. *J. Am. Chem. Soc.* **1979**, *101*, 5245. (b) DuBois, M. R.; VanDerveer, M. C.; DuBois, D. L.; Haltiwanger, R. C.; Miller, W. K. *Ibid.* **1980**, *102*, 7456.
(5) (a) Coucouvanis, D. *Acc. Chem. Res.* **1981**, *14*, 20. (b) Müller, A.; Diemann, E.; Jostes, R.; Bögge, H. *Angew. Chem., Int. Ed. Engl.* **1981**, *20*, 934.
(6) Vahrenkamp, H. *Angew. Chem., Int. Ed. Engl.* **1975**, *14*, 322.
(7) Khattab, S. A.; Marko, L.; Bor, G.; Marko, B. *J. Organomet. Chem.* **1964**, *1*, 373.
(8) Seyferth, D.; Henderson, R. S.; Gallagher, M. K. *J. Organomet. Chem.* **1980**, *193*, C75.
(9) Braunstein, P.; Sappa, E.; Tiripicchio, A.; Camellini, M. T. *Inorg. Chim. Acta* **1980**, *45*, L191.
(10) Vahrenkamp, H.; Wucherer, E. J. *Angew. Chem., Int. Ed. Engl.* **1981**, *20*, 680.
(11) Seyferth, D.; Henderson, R. S.; Fackler, J. D., Jr.; Majany, A. M. *J. Organomet. Chem.* **1981**, *213*, C21.
(12) Braunstein, P.; Tiripicchio, Camellini, M. T.; Sappa, E. *Inorg. Chem.* **1981**, *20*, 3586.
(13) Day, V. W.; Leach, D. A.; Rauchfuss, T. B. *J. Am. Chem. Soc.* **1982**, *104*, 1290.

0276-7333/83/2302-0165$01.50/0

hydrosilylation–dehydrogenation reaction of α-olefins with silicon hydrides to give vinylic and allylic silanes as well as for normal hydrosilylation reactions. The corresponding iridium complex $[(C_5Me_5Ir)_2Cl_4]$ (**1b**)[2] was, however, quite inactive for either reaction though it did promote the addition of Si–H to alkynes.[3] The lack of reactivity of other iridium complexes in olefin hydrosilylation has previously been noted.[4]

Separate experiments showed that the isomerization of 1-hexene was only very slowly catalyzed by **1b** and Et_3SiH and that rapid formation of internal hexene isomers was not the reason why **1b** was a poor catalyst.

Under conditions reasonably similar to those used in the hydrosilylation reactions (CH_2Cl_2 solvent, 20 °C) **1b** reacted directly and quickly with Et_3SiH to give a new colorless complex (70% yield) that was shown to be the iridium(V) silyl hydride $[C_5Me_5Ir(H)_2Cl(SiEt_3)]$ (**3**)[5] [IR ν(Ir–H) 2135, ν(Ir–Cl, terminal) 305 cm^{-1}; ^1H NMR (CD_2Cl_2) δ −12.6 (s, IrH_2), 0.8 (q, J = 7.5 Hz, $SiCH_2$), 0.94 (t, J = 7.5 Hz, $SiCH_2CH_3$), 1.91 (s, C_5Me_5)]. Extended reaction converted **3** into $[C_5Me_5Ir(H)_2(SiEt_3)_2]$ (**4**)[5] that was more conveniently prepared by reaction of **1b** (30% yield) or **2** (40% yield) with Et_3SiH in the presence of triethylamine in refluxing benzene. [IR ν(Ir–H) 2160 cm^{-1}; mass spectrum, m/e 556, 558 $(M-1)^+$; ^1H NMR ($CDCl_3$) δ −17.4 (s, IrH_2), 0.67 (q, J = 8 Hz, $SiCH_2$), 0.82 (t, J = 8 Hz, $SiCH_2CH_3$), 1.97 (s, C_5Me_5)].

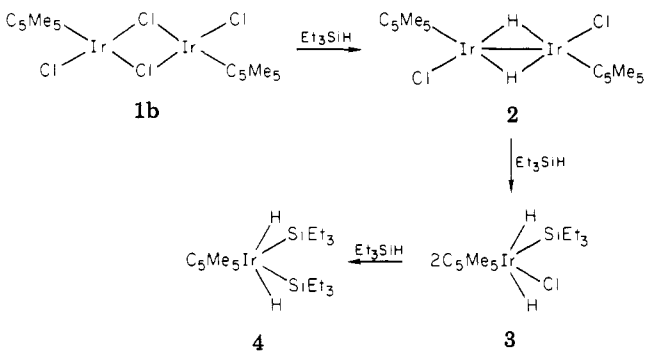

Complex **4** is the analogue of the rhodium(V) complex $[C_5Me_5Rh(H)_2(SiEt_3)_2]$ that we recently reported,[6] and X-ray photographs show them to be isomorphous. Although a number of iridium(V) hydrides L_2IrH_5[7] and one iridium(V) organometallic $C_5Me_5IrMe_4$[8] have been prepared, **3** and **4** are the first organosilyls in this oxidation state. In fact even some Ir(I) complexes only add $R_3Si–H$ with reluctance.[9]

We are investigating details of these and related reactions further, but we note (a) that the dinuclear dihydride complex **2**[10] is intermediate[11] in the reaction of **1b** to give **3** and (b) that **2** reacts directly with Et_3SiH to give **3**. This latter reaction is, formally at least, an example of the rather rare oxidative addition Ir(III) → Ir(V) ($d^6 \rightarrow d^4$).

Acknowledgment. We thank the SERC for supporting this work, Johnson Matthey Ltd for the loan of iridium salts, and Dr. P. M. Bailey for the X-ray measurement.

(2) For a review of these complexes, see Maitlis, P. M. *Chem. Soc. Rev.* **1981**, *10*, 1.
(3) Millan, A. Ph.D. Thesis, University of Sheffield, 1981.
(4) Haszeldine, R. N.; Parish, R. V.; Parry, D. J. *J. Chem. Soc. A* **1969**, 683.
(5) Satisfactory microanalyses were obtained for all new complexes.
(6) Fernandez, M.-J.; Maitlis, P. M. *J. Chem. Soc., Chem. Commun.* **1982**, 310.
(7) Mann, B. E.; Masters, C.; Shaw, B. L. *J. Inorg. Nucl. Chem.* **1971**, *33*, 2195.
(8) Isobe, K.; Bailey, P. M.; Maitlis, P. M. *J. Chem. Soc., Chem. Commun.* **1981**, 808.
(9) Chalk, A. J.; Harrod, J. F. *J. Am. Chem. Soc.* **1965**, *87*, 16, but see Blackburn, S. N.; Haszeldine, R. N.; Parish, R. V.; Setchfield, J. H. *J. Chem. Res., Synop.* **1980**, 170.
(10) Gill, D. S.; Maitlis, P. M. *J. Organomet. Chem.* **1975**, *87*, 359.
(11) The dihydride **2** is unique amongst C_5Me_5–Ir complexes in being deep blue. We have therefore interpreted the transient blue color seen during reaction of **1b** with Et_3SiH as evidence that **2** is the intermediate. This is, of course, supported by the direct reaction of **2** to give **3**.

Metal–Metal Multiple Bonds in Rational Cluster Synthesis.[1] Novel Isomerism in Iron–Molybdenum–Sulfur Clusters and a Molybdenum–Sulfur Cubane. Structure of $(\eta^5\text{-}CH_3C_5H_4)_2Mo_2Fe_2(\mu_3\text{-}S)_2(CO)_6(\mu\text{-}CO)_2$

P. Douglas Williams, M. David Curtis,* D. Neil Duffy, and William M. Butler
Department of Chemistry, The University of Michigan Ann Arbor, Michigan 48109

Received June 28, 1982

Summary: Reaction of $R_2Mo_2(CO)_4(Mo{\equiv}Mo)$, R = Cp, Cp′, or η^5-$CH_3C_5H_4$ (**1**), with $Fe_2S_2(CO)_6$ generates a pair of isomeric iron–molybdenum–sulfur clusters with different $Fe_2Mo_2S_2$ frameworks. Although both isomers have a 62-cluster-electron count, different formal oxidation states must be assigned to the metals in order for them to achieve an 18-electron count. Also, the Mo≡Mo bond of **1** displaces propylene from $Cp_2Mo_2(SC_3H_5S)_2$ to give the cluster $Cp_2Cp'_2Mo_4S_4$. These reactions demonstrate the utility of the Mo≡Mo triple bond in the rational synthesis of metal–sulfur clusters.

Interest in metal sulfides has resulted in part from their importance as catalysts.[2] Iron–molybdenum–sulfur compounds in particular are interesting as possible models of hydrodesulfurization catalysts[3,4] and the nitrogenase cofactor.[5] Here we report a rational approach to the synthesis of molybdenum–sulfur clusters and an unprecedented system of isomeric iron–molybdenum–sulfur clusters.

The utility of sulfur ligands in the stabilization of metal clusters has already been demonstrated.[6] Of particular utility in the preparation of iron–sulfur clusters is the compound $Fe_2S_2(CO)_6$ which has been shown to react with a variety of metal carbonyls and low-valent metal complexes.[7–13]

(1) Part 11 of Metal–Metal Multiple Bonds. Part 10: Curtis, M. D.; Fotinos, N. A.; Han, K. R.; Butler, W. M. *J. Am. Chem. Soc.*, in press.
(2) Mitchell, P. C. H. *Catalysis (London)* **1977**, *1*, 204–233.
(3) Furimsky, E. *Catal. Rev.—Sci. Eng.* **1980**, *22*, 371.
(4) (a) DuBois, M. R.; Haltiwanger, R. C.; Miller, D. J.; Glatzmaier, G. *J. Am. Chem. Soc.* **1979**, *101*, 5245. (b) DuBois, M. R.; VanDerveer, M. C.; DuBois, D. L.; Haltiwanger, R. C.; Miller, W. K. *Ibid.* **1980**, *102*, 7456.
(5) (a) Coucouvanis, D. *Acc. Chem. Res.* **1981**, *14*, 20. (b) Müller, A.; Diemann, E.; Jostes, R.; Bögge, H. *Angew. Chem., Int. Ed. Engl.* **1981**, *20*, 934.
(6) Vahrenkamp, H. *Angew. Chem., Int. Ed. Engl.* **1975**, *14*, 322.
(7) Khattab, S. A.; Marko, L.; Bor, G.; Marko, B. *J. Organomet. Chem.* **1964**, *1*, 373.
(8) Seyferth, D.; Henderson, R. S.; Gallagher, M. K. *J. Organomet. Chem.* **1980**, *193*, C75.
(9) Braunstein, P.; Sappa, E.; Tiripicchio, A.; Camellini, M. T. *Inorg. Chim. Acta* **1980**, *45*, L191.
(10) Vahrenkamp, H.; Wucherer, E. J. *Angew. Chem., Int. Ed. Engl.* **1981**, *20*, 680.
(11) Seyferth, D.; Henderson, R. S.; Fackler, J. D., Jr.; Majany, A. M. *J. Organomet. Chem.* **1981**, *213*, C21.
(12) Braunstein, P.; Tiripicchio, Camellini, M. T.; Sappa, E. *Inorg. Chem.* **1981**, *20*, 3586.
(13) Day, V. W.; Leach, D. A.; Rauchfuss, T. B. *J. Am. Chem. Soc.* **1982**, *104*, 1290.

0276-7333/83/2302-0165$01.50/0

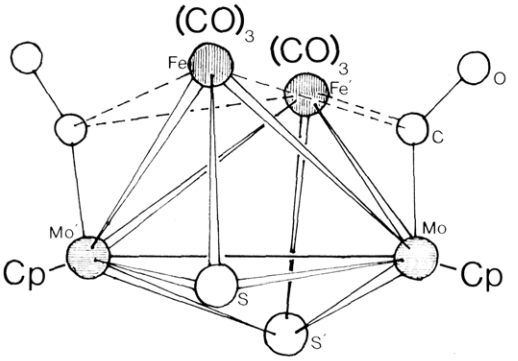

Figure 1. Molecular structure of $Cp_2Mo_2Fe_2(\mu_3\text{-}S)_2(CO)_6(\mu_3\text{-}CO)_2$ (**4a**) (Fe···Fe distance is nonbonding).

The reactive site afforded by multiple metal–metal bonds has also been useful in the synthesis of new metal cluster complexes.[14-18] Since the Mo≡Mo triple bond in $Cp_2Mo_2(CO)_4$ (**1a**) has been shown to add organic disulfides,[18] and since Seyferth et al.[19] have elegantly demonstrated the similarity of the reactivity of the S–S bonds in $Fe_2S_2(CO)_6$ (**2**) and organic disulfides, it seemed highly likely that a combination of these approaches would allow for a rational cluster synthesis. In fact, **1** and **2** react completely at room temperature in less than 0.5 h to give essentially quantitative yields of $Mo_2Fe_2S_2$ clusters according to the stoichiometry of eq 1 (toluene solvent). The Cp′ complexes are somewhat more soluble than the unsubstituted, Cp complexes.

$$\begin{aligned} &2R_2Mo_2(CO)_4(Mo{\equiv}Mo) + Fe_2S_2(CO)_6 \rightarrow \\ &\quad \textbf{1a}, R = Cp \\ &\textbf{1b}, R = Cp' \text{ or } \eta^5\text{-}CH_3C_5H_4 \\ &\quad Cp_2Mo_2(CO)_6 + R_2Mo_2Fe_2(\mu_3\text{-}S)_2(CO)_6(\mu\text{-}CO)_2 + \\ &\qquad\qquad \textbf{3a}, R = Cp\ (20\%) \\ &\qquad\qquad \textbf{3b}, R = Cp'\ (20\%) \\ &\qquad\qquad R_2Mo_2Fe_2(\mu_3\text{-}S)_2(CO)_6(\mu_3\text{-}CO)_2 \quad (1) \\ &\qquad\qquad\qquad \textbf{4a}, R = Cp\ (80\%) \\ &\qquad\qquad\qquad \textbf{4b}, R = Cp'\ (80\%) \end{aligned}$$

A mixture of **3** and **4** precipitates as dark brown, air-stable crystals. These complexes are separable on a Florisil column with CH_2Cl_2 as the eluent. While this work was in progress, Braunstein and co-workers published the synthesis and structure of complex **4a**.[20] This complex was shown to possess the butterfly geometry expected for a 62-electron cluster.[21] The structure of **4a** is depicted in Figure 1, and pertinent bond distances and angles are given in Table I.

The second cluster, **3**, has been shown to be a centrosymmetric isomer of **4** with a planar Mo_2Fe_2 skeleton (Figure 2).[22-24] Although butterfly clusters have been shown to exhibit a range of fold angles and bond distances, depending on the electron count,[26] planar 62-electron clusters are exceedingly rare.[27] Only two other planar, mixed-metal M_4 clusters are known: $Mo_2M_2(CO)_6L_2$ (M = Pd, Pt; L = Et_3P).[28] With M = Pd or Pt, these 58-

Table I. Important Bond Lengths (Å) and Angles (deg) in 3b and 4a[a]

3b		4a	
Mo-Mo′	2.821 (1)	Mo-Mo′	2.846 (5)
Mo-Fe	2.776 (1)	Mo-Fe	2.818 (5)
Mo-Fe′	2.805 (1)	Mo-Fe′	2.815 (5)
Mo-S′	2.344 (1)	Mo-S	2.335 (9)
Mo-S	2.381 (1)	Mo-S′	2.327 (9)
Fe-S′	2.213 (2)	Fe-S	2.165 (8)
Mo-C(μ)	2.025 (6)	Mo-C(μ)	1.90 (4)
Fe-C(μ)	2.270 (6)	Fe′-C(μ)	2.62 (3)
Mo-C(ring)$_{av}$	2.357 (12)	Fe′-C(μ)	2.64 (3)
Fe-Mo-Mo′	60.14 (3)	Fe-Mo-Fe′	85.8 (1)
Fe-Mo′-Mo	59.14 (3)	Fe-Mo-Mo′	59.6 (1)
		Fe-Mo′-Mo	59.7 (1)
Mo-S′-Mo	73.30 (4)	Mo-S-Mo′	75.3 (3)
Fe-S′-Mo	75.00 (5)	Fe-S-Mo	77.4 (3)
Fe-S′-Mo′	75.14 (5)	Fe-S-Mo′	77.5 (3)
Mo-C-O	152.24 (50)	Mo-C-O	159 (3)
		Fe-C-O	119 (2)
		Fe-CO-O	116 (2)

[a] Lengths and angles for **4a** found in ref 20.

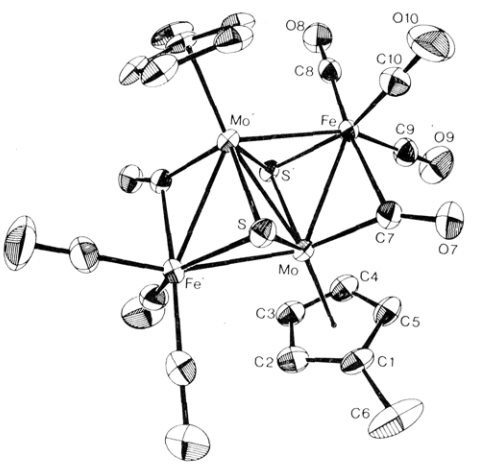

Figure 2. ORTEP plot of $Cp'_2Mo_2Fe_2(\mu_3\text{-}S)_2(CO)_6(\mu\text{-}CO)_2$ (**3b**).

(14) Curtis, M. D.; Messerle, L.; Fotinos, N. A.; Gerlach, R. F. In "Reactivity of Metal-Metal Bonds", Chisholm, M. H., Ed.; Washington: D.C., 1981; *ACS* Symp. *Ser. No. 155*, pp 221–258.
(15) Chisholm, M. H.; Errington, R. J., Folting, K.; Huffman, J. C. *J. Am. Chem. Soc.* **1982**, *104*, 2025.
(16) Curtis, M. D.; Butler, W. M. *J. Chem. Soc., Chem. Commun.* **1980**, 998.
(17) McGinnis, R. N.; Ryan, T. R.; McCarley, R. E. *J. Am. Chem. Soc.* **1978**, *100*, 7900.
(18) Curtis, M. D.; Klingler, R. J. *J. Organomet. Chem.* **1978**, *161*, 23.
(19) Seyferth, D.; Henderson, R. S.; Song, L.-C. *Organometallics* **1982**, *1*, 125.
(20) Braunstein, P.; Jud, J. M.; Tiripicchio, A.; Tiripicchio-Camellini, M.; Sappa, E. *Angew. Chem., Int. Ed. Engl.* **1982**, *21*, 307.
(21) Lauher, J. W. *J. Am. Chem. Soc.* **1978**, *100*, 5305 and references therein.
(22) $Cp'_2Mo_2Fe_2(\mu_3\text{-}S)_2(CO)_6(\mu\text{-}CO)_2$ (**3b**): mp 188 °C; IR (KBr) 2005 (s), 1955 (s), 1935 (s), 1800 (m) cm^{-1}; ^1H NMR ($CDCl_3$, δ 7.24) 2.06 (6 H), 5.25 (8 H) ppm.
(23) $Cp'_2Mo_2Fe_2(\mu_3\text{-}S)_2(CO)_6(\mu_3\text{-}CO)_2$ (**4b**): mp 222 °C; IR (KBr) 2040 (m), 2005 (s), 1975 (s), 1955 (m), 1940 (s), 1795 (s) cm^{-1}; ^1H NMR ($CDCl_3$, δ 7.24) 2.15 (6 H), 5.10 (8 H). Anal. Calcd for $[C_{20}H_{14}Fe_2Mo_2O_8S_2]$: C, 32.03; H, 1.88; Fe, 14.89; Mo, 25.58; S, 8.55. Found: C, 32.06; H, 1.95; Fe, 15.87; Mo, 25.20; S, 8.74. Our unit cell data for **4a** agrees within experimental error with those reported in ref 20.
(24) Dark brown crystals of **3b** were obtained from CH_2Cl_2/hexane. All measurements were performed on a Syntex $P2_1$ four-circle diffractometer at ambient temperature with graphite-filtered Mo Kα radiation. **3b** crystallizes in the triclinic space group $P\bar{1}$, Z = 1, a = 9.219 (2) Å, b = 6.899 (2) Å, c = 10.441 (2) Å, α = 73.34 (2)°, β = 113.68 (2)°, γ = 95.98 (2)°, V = 582.5 (3) Å^3, ρ_{calcd} = 2.14 g/cm^3, and ρ_{obsd} = 2.12 g/cm^3 (flotation). The prismatic crystal had the dimensions 0.221 × 0.184 × 0.191 mm. The heavy atoms were located by direct methods (MULTAN) and light atoms were located in subsequent difference maps. The structure was refined to least-squares, anisotropic convergence on all nonhydrogen atoms using 2357 reflections with $I > 3\sigma(I)$; final R value was 0.047 and the weighted R value was 0.063. A description of the computing programs used can be found in ref 25. The standard reduced cell has the values a, b, c, α, β, and γ = 6.899 Å, 9.219 Å, 10.441 Å, 66.32°, 73.34°, and 94.02°, respectively.
(25) Curtis, M. D.; Green, J.; Butler, W. M. *J. Organomet. Chem.* **1979**, *164*, 371.
(26) Carty, A. J.; MacLaughlin, S. A.; Wagner, J. V.; Taylor, N. J. *Organometallics* **1982**, *1*, 1013.
(27) $Re_4(CO)_{16}^{2-}$: Churchill, M. R.; Bau, R. *Inorg. Chem.* **1968**, *7*, 2606.

electron clusters are electronically equivalent to the 62-electron Mo_2Fe_2 clusters described here.[21,29] Given the range of observed geometries, electron counts,[15,26] and isomers within a given electron count,[15] it would appear that any attempt to predict structures and stoichiometries of M_4 clusters on the basis of *any* cluster counting scheme should proceed with utmost caution.

Localized electron counting arguments can also be used to derive an 18-electron configuration at each metal center in complexes **3** and **4**; but, rather surprisingly, different formal oxidation states must be assigned in order to do so. Assuming each M–M bond and each μ-CO contribute one electron each to the metal, Cp^- contributes six, and each M–S and terminal M–CO bond contribute two, then for **3** we assign oxidation states of S^{-2}, Cp^-, Fe^{+1}, and Mo^{+2}. Because of the different roles played by the carbonyl bonded to Mo in the two isomers, the formal oxidation states in **4** are Fe^0 and Mo^{+3}.[30] These complexes will be the subject of a planned Mössbauer study.

A comparison of the M–M and M–S distances in Table I show that the M–M bonds are shorter by 0.02–0.03 Å and the M–S bonds longer by 0.01–0.05 Å, in the butterfly **4a** vs. the planar **3b**. In both structures, the Mo–Mo bond is surprisingly short compared to the Mo–Fe bond (a difference of about 0.2 Å might be expected on the basis of atomic radii). Apparently the *double* sulfide bridge of the Mo–Mo bond imparts additional bonding character to its orbital makeup.[31]

The generality of the reaction between metal sulfur complexes and metal–metal multiple bonds in rational cluster synthesis is shown by the reaction of **5** with the Mo≡Mo bond of **1b** (eq 2). In the formation of the Mo_4S_4

$$\underset{\mathbf{5}}{CpMo(SCH_2CH(Me)S)_2MoCp} + \mathbf{1b} \rightarrow \underset{\mathbf{6}}{Cp_2Cp'_2Mo_4S_4} + C_3H_6 \quad (2)$$

cluster, **6**,[32] the displacement of propylene from **5** by the Mo≡Mo bonds presumably parallels the analogous displacement of C_3H_6 by the C≡C bonds of acetylenes.[4a]

Acknowledgment. We thank the National Science Foundation for support through Grant No. CHE79-07748-02. P.D.W. thanks the Department of Chemistry and the donors of the Samuel H. Baer Fellowship for support. We are also grateful to Dr. P. Braunstein for helpful comments.

Registry No. **1b**, 83587-35-3; **2**, 14243-23-3; **3b**, 83587-36-4; **4b**, 83603-89-8; **5**, 81423-61-2; **6**, 83587-37-5; Mo, 7439-98-7; Fe, 7439-89-6.

Supplementary Material Available: Tables of fractional coordinates, thermal factor, and observed and calculated structure factors for **3b** (12 pages). Ordering information is given on any current masthead page.

(28) Bender, R.; Braunstein, P.; Dusausoy, Y.; Protas, J. *Angew. Chem., Int. Ed. Engl.* **1978**, *17*, 596; *J. Organomet. Chem.* **1979**, *172*, C51.
(29) Lauher, J. W. *J. Organomet. Chem.* **1981**, *213*, 25.
(30) In this assignment, it is assumed that the "μ_3-CO" in **4** contributes two electrons to Mo and none to Fe. This carbonyl is best assigned a role as "semibridging" since its ^{13}C resonance falls at 238 ppm, well within the range for "terminal" Mo–CO carbonyls.
(31) Rives, A. B.; Xiao-Zang, Y.; Fenske, R. F. *Inorg. Chem.* **1982**, *21*, 2286.
(32) Complex **6** is generated by heating of a toluene solution of **1b** and **5** to 65 °C for 48 h followed by cooling and filtering off the product as a violet powder. **6** decomposes in chlorinated solvents after several hours and is sparingly soluble in most common organic solvents. X-ray structure characterization of this species is planned. $Cp_2Cp'_2Mo_4S_4$ (**6**): mp ca. 330 °C; ^1H NMR ($CDCl_3$, δ 7.24) 2.02 (6 H), 5.11 (8 H), 5.17 (10 H) ppm; mass spectrum, *m/e* $(P)^+$ 800, $(P - CH_3)^+$ 785, $(P - CH_3C_5H_4)^+$721.

Synthesis, Structure, and Spectral Properties of $Mo(CO)(RC{\equiv}CR')L_2X_2$ Complexes

Paul B. Winston, Sharon J. Nieter Burgmayer, and Joseph L. Templeton*

Department of Chemistry, University of North Carolina Chapel Hill, North Carolina 27514

Received July 7, 1982

Summary: The preparation of $Mo(CO)(R^1C{\equiv}CR^2)(PEt_3)_2Br_2$ (R^1 = Ph, R^2 = H, **1**; $R^1 = R^2$ = Me, **2**) and the structure of **1** are reported as the first members of a new class of formal 16-electron Mo(II) complexes, $Mo(CO)(RC{\equiv}CR)L_2X_2$. The unique NMR chemical shifts of π-donor alkyne ligands have been supplemented by visible spectroscopy and cyclic voltammetry, both convenient probes for studying other electron-deficient complexes with π-donor ligands in the coordination sphere.

Monomeric metal alkyne complexes display a rich chemistry that is inconsistent with an alkyne bonding model which neglects the second alkyne π system.[1] Communications describing five-coordinate Mo(II) alkyne complexes,[2] structures of alkyne ligands as two- and four-electron donors in closely related complexes ($[Co(C_2Ph_2)L_3]^+$ and $[Co(C_2Ph_2)L_3(CH_3CN)]^+$)[3] and formation of a coordinated alkyne from coupling of carbon monoxide and methylidyne ligands[4] have been reported in the first half of 1982 alone. We wish to report here the preparation of a new class of alkyne complexes, $Mo(CO)(R^1C{\equiv}CR^2)L_2X_2$, which hold promise as versatile reagents for expanding the chemistry of group 6 alkyne complexes.

A deep blue methylene chloride solution of $Mo(CO)_2(PEt_3)_2Br_2$[5] with a threefold excess of phenylacetylene was heated at 40 °C for 18 h to yield a dark green-brown solution. Solvent removal and extraction of the residue with diethyl ether produced a light green solution of $Mo(CO)(PhC{\equiv}CH)(PEt_3)_2Br_2$ (**1**). Subsequent recrystallization from ether/toluene yielded analytically pure forest green crystals of **1**. An analogous synthesis utilizing a tenfold excess of 2-butyne yielded $Mo(CO)(MeC{\equiv}CMe)(PEt_3)_2Br_2$ (**2**).

The ^1H NMR spectrum of **1** revealed a resonance at 13.0 ppm which was assigned to the acetylenic proton in accord with previous NMR observations for six-coordinate terminal (alkyne)molybdenum(II) complexes.[6] In conjunction with the single ν(CO) infrared absorption at 1950 cm^{-1}[7] and molecular orbital guidelines[8] established for d^4

(1) Tatsumi, K.; Hoffmann, R.; Templeton, J. L. *Inorg. Chem.* **1982**, *21*, 466.
(2) (a) Kamata, M.; Yoshida, T.; Otsuka, S.; Hirotsu, K.; Higuchi, T.; Kido, M.; Tatsumi, K.; Hoffmann, R. *Organometallics* **1982**, *1*, 227. (b) The structure of a square-pyramidal molybdenum(II) alkyne has also been recently communicated by: De Cian, A.; Colin, J.; Schappacher, M.; Ricard, L.; Weiss, R. *J. Am. Chem. Soc.* **1981**, *103*, 1850.
(3) Capelle, B.; Beauchamp, A. L.; Dartiguenave, M.; Dartiguenave, Y. *J. Chem. Soc., Chem. Commun.* **1982**, 566.
(4) Churchill, M. R.; Wasserman, H. J.; Holmes, S. J.; Schrock, R. R. *Organometallics* **1982**, *1*, 766.
(5) Moss, J. R.; Shaw, B. L. *J. Chem. Soc. A* **1970**, 595.
(6) (a) McDonald, J. W.; Newton, W. E.; Creedy, C. T. C.; Corbin, J. L. *J. Organomet. Chem.* **1975**, *92*, C25. (b) Templeton, J. L.; Ward, B. C.; Chen, G. J.-J.; McDonald, J. W.; Newton, W. E. *Inorg. Chem.* **1981**, *20*, 1248.

0276-7333/83/2302-0167$01.50/0

electron clusters are electronically equivalent to the 62-electron Mo_2Fe_2 clusters described here.[21,29] Given the range of observed geometries, electron counts,[15,26] and isomers within a given electron count,[15] it would appear that any attempt to predict structures and stoichiometries of M_4 clusters on the basis of *any* cluster counting scheme should proceed with utmost caution.

Localized electron counting arguments can also be used to derive an 18-electron configuration at each metal center in complexes **3** and **4**; but, rather surprisingly, different formal oxidation states must be assigned in order to do so. Assuming each M–M bond and each μ-CO contribute one electron each to the metal, Cp^- contributes six, and each M–S and terminal M–CO bond contribute two, then for **3** we assign oxidation states of S^{-2}, Cp^-, Fe^{+1}, and Mo^{+2}. Because of the different roles played by the carbonyl bonded to Mo in the two isomers, the formal oxidation states in **4** are Fe^0 and Mo^{+3}.[30] These complexes will be the subject of a planned Mössbauer study.

A comparison of the M–M and M–S distances in Table I show that the M–M bonds are shorter by 0.02–0.03 Å and the M–S bonds longer by 0.01–0.05 Å, in the butterfly **4a** vs. the planar **3b**. In both structures, the Mo–Mo bond is surprisingly short compared to the Mo–Fe bond (a difference of about 0.2 Å might be expected on the basis of atomic radii). Apparently the *double* sulfide bridge of the Mo–Mo bond imparts additional bonding character to its orbital makeup.[31]

The generality of the reaction between metal sulfur complexes and metal–metal multiple bonds in rational cluster synthesis is shown by the reaction of **5** with the Mo≡Mo bond of **1b** (eq 2). In the formation of the Mo_4S_4

$$\underset{\mathbf{5}}{CpMo(SCH_2CH(Me)S)_2MoCp} + \mathbf{1b} \rightarrow \underset{\mathbf{6}}{Cp_2Cp'_2Mo_4S_4} + C_3H_6 \quad (2)$$

cluster, **6**,[32] the displacement of propylene from **5** by the Mo≡Mo bonds presumably parallels the analogous displacement of C_3H_6 by the C≡C bonds of acetylenes.[4a]

Acknowledgment. We thank the National Science Foundation for support through Grant No. CHE79-07748-02. P.D.W. thanks the Department of Chemistry and the donors of the Samuel H. Baer Fellowship for support. We are also grateful to Dr. P. Braunstein for helpful comments.

Registry No. **1b**, 83587-35-3; **2**, 14243-23-3; **3b**, 83587-36-4; **4b**, 83603-89-8; **5**, 81423-61-2; **6**, 83587-37-5; Mo, 7439-98-7; Fe, 7439-89-6.

Supplementary Material Available: Tables of fractional coordinates, thermal factor, and observed and calculated structure factors for **3b** (12 pages). Ordering information is given on any current masthead page.

(28) Bender, R.; Braunstein, P.; Dusausoy, Y.; Protas, J. *Angew. Chem., Int. Ed. Engl.* **1978**, *17*, 596; *J. Organomet. Chem.* **1979**, *172*, C51.
(29) Lauher, J. W. *J. Organomet. Chem.* **1981**, *213*, 25.
(30) In this assignment, it is assumed that the "μ_3-CO" in **4** contributes two electrons to Mo and none to Fe. This carbonyl is best assigned a role as "semibridging" since its ^{13}C resonance falls at 238 ppm, well within the range for "terminal" Mo–CO carbonyls.
(31) Rives, A. B.; Xiao-Zang, Y.; Fenske, R. F. *Inorg. Chem.* **1982**, *21*, 2286.
(32) Complex **6** is generated by heating of a toluene solution of **1b** and **5** to 65 °C for 48 h followed by cooling and filtering off the product as a violet powder. **6** decomposes in chlorinated solvents after several hours and is sparingly soluble in most common organic solvents. X-ray structure characterization of this species is planned. $Cp_2Cp'_2Mo_4S_4$ (**6**): mp ca. 330 °C; ^1H NMR ($CDCl_3$, δ 7.24) 2.02 (6 H), 5.11 (8 H), 5.17 (10 H) ppm; mass spectrum, *m/e* $(P)^+$ 800, $(P - CH_3)^+$ 785, $(P - CH_3C_5H_4)^+$721.

Synthesis, Structure, and Spectral Properties of $Mo(CO)(RC{\equiv}CR')L_2X_2$ Complexes

Paul B. Winston, Sharon J. Nieter Burgmayer, and Joseph L. Templeton*

Department of Chemistry, University of North Carolina Chapel Hill, North Carolina 27514

Received July 7, 1982

Summary: The preparation of $Mo(CO)(R^1C{\equiv}CR^2)(PEt_3)_2Br_2$ (R^1 = Ph, R^2 = H, **1**; $R^1 = R^2$ = Me, **2**) and the structure of **1** are reported as the first members of a new class of formal 16-electron Mo(II) complexes, $Mo(CO)(RC{\equiv}CR)L_2X_2$. The unique NMR chemical shifts of π-donor alkyne ligands have been supplemented by visible spectroscopy and cyclic voltammetry, both convenient probes for studying other electron-deficient complexes with π-donor ligands in the coordination sphere.

Monomeric metal alkyne complexes display a rich chemistry that is inconsistent with an alkyne bonding model which neglects the second alkyne π system.[1] Communications describing five-coordinate Mo(II) alkyne complexes,[2] structures of alkyne ligands as two- and four-electron donors in closely related complexes ($[Co(C_2Ph_2)L_3]^+$ and $[Co(C_2Ph_2)L_3(CH_3CN)]^+$)[3] and formation of a coordinated alkyne from coupling of carbon monoxide and methylidyne ligands[4] have been reported in the first half of 1982 alone. We wish to report here the preparation of a new class of alkyne complexes, $Mo(CO)(R^1C{\equiv}CR^2)L_2X_2$, which hold promise as versatile reagents for expanding the chemistry of group 6 alkyne complexes.

A deep blue methylene chloride solution of $Mo(CO)_2(PEt_3)_2Br_2$[5] with a threefold excess of phenylacetylene was heated at 40 °C for 18 h to yield a dark green-brown solution. Solvent removal and extraction of the residue with diethyl ether produced a light green solution of $Mo(CO)(PhC{\equiv}CH)(PEt_3)_2Br_2$ (**1**). Subsequent recrystallization from ether/toluene yielded analytically pure forest green crystals of **1**. An analogous synthesis utilizing a tenfold excess of 2-butyne yielded $Mo(CO)(MeC{\equiv}CMe)(PEt_3)_2Br_2$ (**2**).

The ^1H NMR spectrum of **1** revealed a resonance at 13.0 ppm which was assigned to the acetylenic proton in accord with previous NMR observations for six-coordinate terminal (alkyne)molybdenum(II) complexes.[6] In conjunction with the single ν(CO) infrared absorption at 1950 cm^{-1}[7] and molecular orbital guidelines[8] established for d^4

(1) Tatsumi, K.; Hoffmann, R.; Templeton, J. L. *Inorg. Chem.* **1982**, *21*, 466.
(2) (a) Kamata, M.; Yoshida, T.; Otsuka, S.; Hirotsu, K.; Higuchi, T.; Kido, M.; Tatsumi, K.; Hoffmann, R. *Organometallics* **1982**, *1*, 227. (b) The structure of a square-pyramidal molybdenum(II) alkyne has also been recently communicated by: De Cian, A.; Colin, J.; Schappacher, M.; Ricard, L.; Weiss, R. *J. Am. Chem. Soc.* **1981**, *103*, 1850.
(3) Capelle, B.; Beauchamp, A. L.; Dartiguenave, M.; Dartiguenave, Y. *J. Chem. Soc., Chem. Commun.* **1982**, 566.
(4) Churchill, M. R.; Wasserman, H. J.; Holmes, S. J.; Schrock, R. R. *Organometallics* **1982**, *1*, 766.
(5) Moss, J. R.; Shaw, B. L. *J. Chem. Soc. A* **1970**, 595.
(6) (a) McDonald, J. W.; Newton, W. E.; Creedy, C. T. C.; Corbin, J. L. *J. Organomet. Chem.* **1975**, *92*, C25. (b) Templeton, J. L.; Ward, B. C.; Chen, G. J.-J.; McDonald, J. W.; Newton, W. E. *Inorg. Chem.* **1981**, *20*, 1248.

0276-7333/83/2302-0167$01.50/0

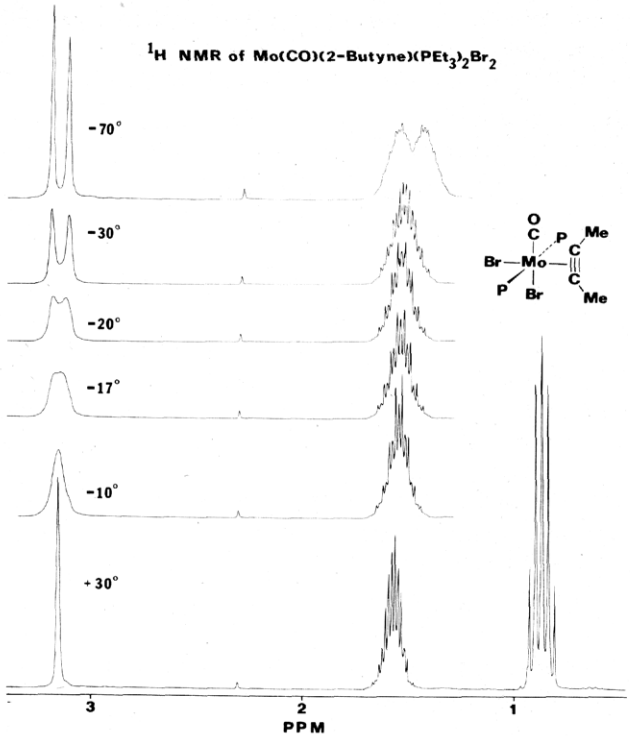

Figure 1. Variable-temperature ^{1}H NMR spectra of Mo(CO)(MeC≡CMe)(PEt$_3$)$_2$Br$_2$ (**2**).

monocarbonyl alkyne derivatives a cis colinear Mo(CO)(PhC≡CH) fragment was indicated. The two alkyne carbons in **1** appear as triplets in the ^{13}C spectrum with $^2J_{P-Mo-C}$ coupling constants typical of *cis*-P–Mo–C geometries while ^{31}P coupling to the carbonyl carbon is too small to resolve (δ 224.7 (t, J = 5.2 Hz, Ph*C*≡CH), 224.8 (t, J = 5.2 Hz, PhC≡*C*H), 230.9 (br s, J = <4 Hz, CO). The average alkyne ^{13}C chemical shift of 224.8 ppm suggests substantial donation from the second alkyne filled π orbital, $\pi_\perp$, into the vacant metal dπ orbital.[9] The equivalence of the phosphine ligands and the *cis*–PMoC coupling constants led us to anticipate a *trans*-bis(triethylphosphine)-*cis*-dibromocarbonyl(alkyne)molybdenum(II) isomer reminiscent of the structure of W(CO)(CHCMe$_3$)(PR$_3$)$_2$Cl$_2$[10] but with the alkyne of **1** or **2** in place of the neopentylidene ligand. Only one orientation of the PhC≡CH ligand was evident in NMR studies of **1**. The symmetrical 2-butyne ligand in **2** exhibited a barrier to rotation of 13.0 kcal mol^{-1} for the two-site methyl exchange process reflected in a variable-temperature ^{1}H study (Figure 1). Note that a sharp singlet at δ +9.1 is the only ^{31}P signal observed as low as −90 °C for **2**, again in accord

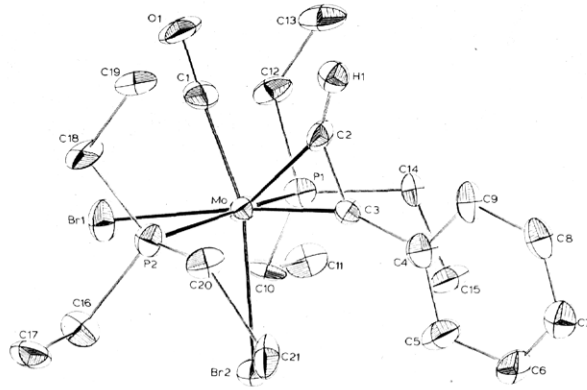

Figure 2. An ORTEP view of Mo(CO)(PhC≡CH)(PEt$_3$)$_2$Br$_2$ (**1**) showing the atomic labeling scheme.

with a rigid trans phosphine fragment.

The disposition of the ligands in **1** was subsequently demonstrated by X-ray crystallography (see Figure 2 and Table I).[11] The molecule adopts a distorted octahedral geometry with the bromides, carbonyl, and the alkyne, including its phenyl ring, coplanar. Alternatively one can consider each alkyne carbon as an independent ligating atom so that the molecular structure corresponds to a pentagonal bipyramid with phosphine ligands occupying both axial positions. The bonding description for **1** and **2** is elaborated below, but one reflection of the three-center two-electron bond postulated from a single filled metal dπ orbital to carbonyl and alkyne π^* orbitals is the slippage of the alkyne toward the carbonyl carbon which generates a C1···C2 distance of only 2.29 Å.

Both **1** and **2** exhibit a low-energy absorption in the visible spectrum (**1**, λ_{max} 666 nm (ϵ 265 M^{-1} cm^{-1}); **2**, λ_{max} 615 nm (ϵ 50 M^{-1} cm^{-1})). We believe this transition is localized within the dπ manifold of these complexes. The coordinate system shown

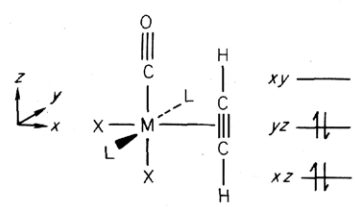

leaves d_{xy} as the LUMO which is destabilized by alkyne $\pi_\perp$ donation. The remaining two dπ levels then house the four metal electrons with d_{xz} lying below d_{yz} due to overlap of alkyne $\pi_\parallel^*$ with the d_{xz} + CO(π^*p_x) combination. Extended Hückel calculations support the hypothesis that the d_{xy} LUMO energy responds to alkyne $\pi_\perp$ donation while the d_{yz} HOMO is dominated by CO π^* acceptance and is independent of the alkyne to first order since the δ overlap of d_{yz} with $\pi_\perp^*$ is negligible. Stronger π-donor alkynes should increase the LUMO energy and indeed the observed transition energy for the electron-rich butyne ligand is about 1400 cm^{-1} greater than the analogous phenylacetylene electronic transition. An exhaustive study of M(CO)(RC≡CR)(S$_2$CNR$^1_2$)$_2$ electronic spectra as a function of R has confirmed this interplay between π donation and the transition energy.[12] Lippard's MoL$_4$-

(7) The π acidity of PhC≡CH can be gauged by comparison with the average of the two ν(CO) absorptions in Mo(CO)$_2$(PEt$_3$)$_2$Br$_2$, 1904 cm^{-1} (1948, 1860 cm^{-1}).

(8) (a) Ricard, L.; Weiss, R.; Newton, W. E.; Chen, G. J.-J.; McDonald, J. W. *J. Am. Chem. Soc.* **1978**, *100*, 1318. (b) Braterman, P. S.; Davidson, J. L.; Sharp, D. W. A. *J. Chem. Soc., Dalton Trans.* **1976**, 241. (c) Howard, J. A. K.; Stansfield, R. F. D.; Woodward, P. *Ibid.* **1976**, 246. (d) Ward, B. C.; Templeton, J. L. *J. Am. Chem. Soc.* **1980**, *102*, 1532.

(9) (a) Templeton, J. L.; Ward, B. C. *J. Am. Chem. Soc.* **1980**, *102*, 3288. (b) This value is low even for "four-electron donor" alkynes and suggests very little additional π donation from the ancillary L$_2$X$_2$ ligands. In contrast the alkyne carbon signals of Mo(CNR)$_2$(SR)$_2$(RC≡CR) complexes appear in the range of 171–184 ppm,[2a] suggesting that π donation from the thiolate ligands substantially decreases $\pi_\perp$ donation from the alkyne ligand; the alkyne can be viewed as a "three-electron donor" ligand in view of the single vacant dπ b_1 orbital which overlaps with both the filled alkyne $\pi_\perp$ b_1 and a b_1 thiolate lone pair combination in a three-center four-electron bonding scheme.

(10) Wengrovius, J. H.; Schrock, R. R.; Churchill, M. R.; Wasserman, H. J. *J. Am. Chem. Soc.* **1982**, *104*, 1739.

(11) The crystal selected was monoclinic of space group $P2_1/n$ with unit cell dimensions of a = 7.995 (3) Å, b = 14.559 (4) Å, c = 22.209 (10) Å, β = 98.04 (3)°, and Z = 4. Of the 4878 reflections monitored, 1660 independent reflections with $I > 3\sigma(I)$ were used in the structure solution and refinement which converged to 4.8 and 3.5% for R and R_w, respectively. Hydrogen atom positions were calculated and not refined with the exception of the acetylenic hydrogen which was located on a difference Fourier map and refined.

Table I. Selected Bond Distances (Å) and Angles (deg) for $Mo(CO)(PhC{\equiv}CH)(PEt_3)_2Br_2$ (1)

Bond Distances			
Mo-C1	1.939 (10)	Mo-Br1	2.673 (1)
Mo-C2	1.988 (10)	Mo-Br2	2.700 (1)
Mo-C3	1.982 (9)	C2-C3	1.273 (11)
Mo-P1	2.547 (3)	C2-H1	1.099 (74)
Mo-P2	2.538 (3)		
Bond Angles			
C2-Mo-C3	37.40 (32)	C2-Mo-Br1	147.11 (29)
C1-Mo-C2	71.24 (40)	C3-Mo-Br1	175.41 (29)
Br1-Mo-Br2	85.35 (4)	C2-C3-C4	134.00 (93)
P1-Mo-P2	163.50 (10)	C3-C2-H1	139 (4)
C1-Mo-Br2	161.24 (31)		

$(RHNC{\equiv}CNRH)X^+$[13] complexes display a band between 500 and 570 nm assigned as a $d\pi$–$d\pi$ transition ($\epsilon \sim 600$ M^{-1} cm^{-1}), and we have found that a low-energy visible transition with an extinction coefficient on the order of 10^2 M^{-1} cm^{-1} is characteristic of other formal 16-electron complexes including $Mo(CO)_2L_2X_2$,[5,14] $Mo(CO)_2(S_2CNR_2)_2$,[15] and $Mo(CO)(RC{\equiv}CR)(S_2CNR_2)_2$[6a] that contain both π-acceptor and π-donor ligands in the coordination sphere.[16] Addition of a seventh ligand invariably causes this band to disappear. Thus the variety of vivid blue, purple, and green colors typical of this class of compounds result from a window between high-energy absorptions and the visible $d\pi$ transition into the vacant LUMO that would be filled for related 18-electron complexes.

Both 1 and 2 exhibit reduction waves (1, –0.99 V, and 2, –1.18 V, vs. SSCE in 0.10 M n-Bu_4NClO_4, CH_3CN). No reversible oxidations were observed, but both 1 and 2 show the onset of oxidative processes near +0.87 V. The reduction of the relatively electron-rich butyne derivative 2 is 0.19 V more negative than for 1 in accord with a higher energy $d\pi$ LUMO for 2 and also comparable in magnitude to the blue shift of 0.17 V in the visible absorption in going from 1 to 2. In contrast the similarity of the oxidative processes of 1 and 2 are compatible with a $d\pi$ HOMO that is roughly independent of alkyne. The absorption and electrochemical measurements dovetail nicely here to reinforce the bonding description that has evolved for these systems. Furthermore both of these techniques offer convenient probes of the $d\pi$ interactions in other formal 16-electron complexes. We believe that experimental assessment of these bonding schemes is essential for fine tuning the reactivity of unsaturated intermediates.

Acknowledgment. We are grateful to the donors of the Petroleum Research Fund, administered by the American Chemical Society, for support of this research.

Registry No. 1, 83801-84-7; 2, 83801-85-8; $Mo(CO)_2(PEt_3)_2Br_2$, 25685-65-8; phenylacetylene, 536-74-3; 2-butyne, 503-17-3.

Supplementary Material Available: A table of positional and thermal parameters for 1 (2 pages). Ordering information is given on any current masthead page.

(12) Templeton, J. L.; Herrick, R. S.; Morrow, J. R., manuscript in preparation.
(13) Giandomenico, C. M.; Lam, C. T.; Lippard, S. J. *J. Am. Chem. Soc.* **1982**, *104*, 1263.
(14) Drew, M. G. B.; Tomkins, I. B.; Colton, R. *Aust. J. Chem.* **1970**, *23*, 2517.
(15) (a) Templeton, J. L.; Ward, B. C. *J. Am. Chem. Soc.* **1980**, *102*, 6568. (b) Colton, R.; Scollary, G. R.; Tomkins, I. B. *Aust. J. Chem.* **1968**, *21*, 15.
(16) Templeton, J. L.; Winston, P. B.; Ward, B. C. *J. Am. Chem. Soc.* **1981**, *103*, 7713.

Reversible Intramolecular Isomerization of Mixed Carbonyl–Alkyl Isocyanide Complexes of Molybdenum: An Electrochemical Investigation

Kay A. Conner and Richard A. Walton*
Department of Chemistry, Purdue University
West Lafayette, Indiana 47907

Received August 30, 1982

Summary: Cyclic voltammetry and coulometry have been used to examine the isomerism of $Mo(CO)_2(CNC_6H_{11})_4$ and several complexes of the type $Mo(CO)_2(CNR)_2(PR_3)_2$ following their electrochemical oxidation. Products have been characterized by ESR and IR spectroscopy, and a possible mechanism for the isomerization is suggested.

The complexes $Mo(CO)_2(CNR)_2(PR'_3)_2$ and $Mo(CO)_2(CNR)_4$ (R = CH_3, CMe_3, or C_6H_{11} and PR'_3 = PEt_3, P-n-Pr_3, $PMePh_2$, or $PEtPh_2$), formed by the phosphine-assisted elimination of allyl chloride from $(\eta^3$-$C_3H_5)$-$MoCl(CO)_2(CNR)_2$, have recently been prepared in this laboratory.[1] On the basis of spectroscopic properties, these complexes were shown to have structures I and II. In subsequent studies directed at exploring the redox chemistry of these complexes, we have discovered that they undergo a rapid intramolecular isomerization to the all-trans species III and IV, respectively. Since these results have an important bearing upon studies carried out by other workers on related systems[2–5] and are of relevance to problems relating to the electrochemical activation of organometallic molecules, we herein communicate preliminary details of these results.

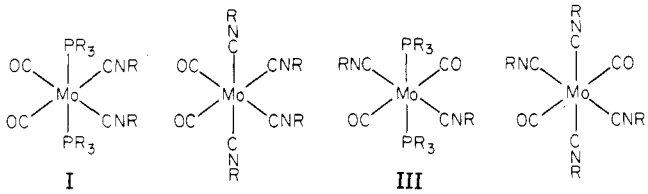

Electrochemistry has been found to be an extremely sensitive technique for studying cis–trans isomerization in complexes of the type $Mo(CO)_4(PR_3)_2$,[2] $Mo(CO)_2(P{-}P)_2$, where P–P represents $Ph_2P(CH_2)_nPPh_2$ (n = 1, 2, or 3),[3] and $Mo(CO)_4(carbene)_2$,[4] following their oxidation to the related 17-electron monocations. On the basis of kinetic and thermodynamic measurements,[2–6] these isomerizations are believed to occur via a trigonal-prismatic intermediate through a nondissociative rearrangement commonly referred to as the "Bailar twist".[7] Although this twist mechanism can easily account for isomerization in the MX_2Y_4 systems, two separate twists are required to convert an $MX_2Y_2Z_2$ complex with one pair of trans ligands (as in I) to the all-trans isomer (III).

The electrochemical properties were investigated by cyclic voltammetry and controlled potential electrolysis.

(1) Deaton, J. C.; Walton, R. A. *J. Organomet. Chem.* **1981**, *219*, 187.
(2) Bond, A. M.; Darensbourg, D. J.; Mocellin, E.; Stewart, B. J. *J. Am. Chem. Soc.* **1981**, *103*, 6827.
(3) (a) Wimmer, F. L.; Snow, M. R.; Bond, A. M. *Inorg. Chem.* **1974**, *13*, 1617. (b) Bond, A. M.; Colton, R.; Jackowski, J. J. *Ibid.* **1975**, *14*, 2526. (c) Bond, A. M.; Graberic, B. S.; Jackowski, J. J. *Ibid.* **1978**, *17*, 2153.
(4) Riecke, R. D.; Kojima, H.; Ofele, K. *J. Am. Chem. Soc.* **1976**, *98*, 6735.
(5) Darensbourg, D. J. *Inorg. Chem.* **1979**, *18*, 14.
(6) Datta, S.; Dezube, B.; Kouba, J. K.; Wreford, S. S. *J. Am. Chem. Soc.* **1978**, *100*, 4404.
(7) Bailar, J. C. *J. Inorg. Nucl. Chem.* **1958**, *8*, 165.

0276-7333/83/2302-0169$01.50/0

Table I. Selected Bond Distances (Å) and Angles (deg) for $Mo(CO)(PhC{\equiv}CH)(PEt_3)_2Br_2$ (1)

Bond Distances			
Mo-C1	1.939 (10)	Mo-Br1	2.673 (1)
Mo-C2	1.988 (10)	Mo-Br2	2.700 (1)
Mo-C3	1.982 (9)	C2-C3	1.273 (11)
Mo-P1	2.547 (3)	C2-H1	1.099 (74)
Mo-P2	2.538 (3)		
Bond Angles			
C2-Mo-C3	37.40 (32)	C2-Mo-Br1	147.11 (29)
C1-Mo-C2	71.24 (40)	C3-Mo-Br1	175.41 (29)
Br1-Mo-Br2	85.35 (4)	C2-C3-C4	134.00 (93)
P1-Mo-P2	163.50 (10)	C3-C2-H1	139 (4)
C1-Mo-Br2	161.24 (31)		

$(RHNC{\equiv}CNRH)X^+$[13] complexes display a band between 500 and 570 nm assigned as a $d\pi$–$d\pi$ transition ($\epsilon \sim 600$ M^{-1} cm^{-1}), and we have found that a low-energy visible transition with an extinction coefficient on the order of 10^2 M^{-1} cm^{-1} is characteristic of other formal 16-electron complexes including $Mo(CO)_2L_2X_2$,[5,14] $Mo(CO)_2(S_2CNR_2)_2$,[15] and $Mo(CO)(RC{\equiv}CR)(S_2CNR_2)_2$[6a] that contain both π-acceptor and π-donor ligands in the coordination sphere.[16] Addition of a seventh ligand invariably causes this band to disappear. Thus the variety of vivid blue, purple, and green colors typical of this class of compounds result from a window between high-energy absorptions and the visible $d\pi$ transition into the vacant LUMO that would be filled for related 18-electron complexes.

Both 1 and 2 exhibit reduction waves (1, –0.99 V, and 2, –1.18 V, vs. SSCE in 0.10 M n-Bu_4NClO_4, CH_3CN). No reversible oxidations were observed, but both 1 and 2 show the onset of oxidative processes near +0.87 V. The reduction of the relatively electron-rich butyne derivative 2 is 0.19 V more negative than for 1 in accord with a higher energy $d\pi$ LUMO for 2 and also comparable in magnitude to the blue shift of 0.17 V in the visible absorption in going from 1 to 2. In contrast the similarity of the oxidative processes of 1 and 2 are compatible with a $d\pi$ HOMO that is roughly independent of alkyne. The absorption and electrochemical measurements dovetail nicely here to reinforce the bonding description that has evolved for these systems. Furthermore both of these techniques offer convenient probes of the $d\pi$ interactions in other formal 16-electron complexes. We believe that experimental assessment of these bonding schemes is essential for fine tuning the reactivity of unsaturated intermediates.

Acknowledgment. We are grateful to the donors of the Petroleum Research Fund, administered by the American Chemical Society, for support of this research.

Registry No. 1, 83801-84-7; 2, 83801-85-8; $Mo(CO)_2(PEt_3)_2Br_2$, 25685-65-8; phenylacetylene, 536-74-3; 2-butyne, 503-17-3.

Supplementary Material Available: A table of positional and thermal parameters for 1 (2 pages). Ordering information is given on any current masthead page.

(12) Templeton, J. L.; Herrick, R. S.; Morrow, J. R., manuscript in preparation.
(13) Giandomenico, C. M.; Lam, C. T.; Lippard, S. J. *J. Am. Chem. Soc.* **1982**, *104*, 1263.
(14) Drew, M. G. B.; Tomkins, I. B.; Colton, R. *Aust. J. Chem.* **1970**, *23*, 2517.
(15) (a) Templeton, J. L.; Ward, B. C. *J. Am. Chem. Soc.* **1980**, *102*, 6568. (b) Colton, R.; Scollary, G. R.; Tomkins, I. B. *Aust. J. Chem.* **1968**, *21*, 15.
(16) Templeton, J. L.; Winston, P. B.; Ward, B. C. *J. Am. Chem. Soc.* **1981**, *103*, 7713.

Reversible Intramolecular Isomerization of Mixed Carbonyl–Alkyl Isocyanide Complexes of Molybdenum: An Electrochemical Investigation

Kay A. Conner and Richard A. Walton*
Department of Chemistry, Purdue University
West Lafayette, Indiana 47907

Received August 30, 1982

Summary: Cyclic voltammetry and coulometry have been used to examine the isomerism of $Mo(CO)_2(CNC_6H_{11})_4$ and several complexes of the type $Mo(CO)_2(CNR)_2(PR_3)_2$ following their electrochemical oxidation. Products have been characterized by ESR and IR spectroscopy, and a possible mechanism for the isomerization is suggested.

The complexes $Mo(CO)_2(CNR)_2(PR'_3)_2$ and $Mo(CO)_2(CNR)_4$ (R = CH_3, CMe_3, or C_6H_{11} and PR'_3 = PEt_3, P-n-Pr_3, $PMePh_2$, or $PEtPh_2$), formed by the phosphine-assisted elimination of allyl chloride from $(\eta^3$-$C_3H_5)$-$MoCl(CO)_2(CNR)_2$, have recently been prepared in this laboratory.[1] On the basis of spectroscopic properties, these complexes were shown to have structures I and II. In subsequent studies directed at exploring the redox chemistry of these complexes, we have discovered that they undergo a rapid intramolecular isomerization to the all-trans species III and IV, respectively. Since these results have an important bearing upon studies carried out by other workers on related systems[2–5] and are of relevance to problems relating to the electrochemical activation of organometallic molecules, we herein communicate preliminary details of these results.

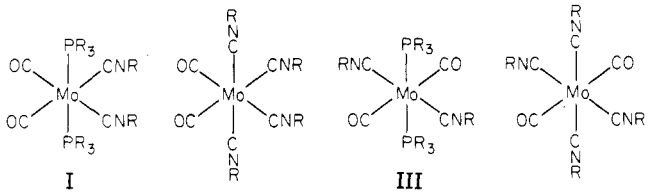

Electrochemistry has been found to be an extremely sensitive technique for studying cis–trans isomerization in complexes of the type $Mo(CO)_4(PR_3)_2$,[2] $Mo(CO)_2(P{-}P)_2$, where P–P represents $Ph_2P(CH_2)_nPPh_2$ (n = 1, 2, or 3),[3] and $Mo(CO)_4(carbene)_2$,[4] following their oxidation to the related 17-electron monocations. On the basis of kinetic and thermodynamic measurements,[2–6] these isomerizations are believed to occur via a trigonal-prismatic intermediate through a nondissociative rearrangement commonly referred to as the "Bailar twist".[7] Although this twist mechanism can easily account for isomerization in the MX_2Y_4 systems, two separate twists are required to convert an $MX_2Y_2Z_2$ complex with one pair of trans ligands (as in I) to the all-trans isomer (III).

The electrochemical properties were investigated by cyclic voltammetry and controlled potential electrolysis.

(1) Deaton, J. C.; Walton, R. A. *J. Organomet. Chem.* **1981**, *219*, 187.
(2) Bond, A. M.; Darensbourg, D. J.; Mocellin, E.; Stewart, B. J. *J. Am. Chem. Soc.* **1981**, *103*, 6827.
(3) (a) Wimmer, F. L.; Snow, M. R.; Bond, A. M. *Inorg. Chem.* **1974**, *13*, 1617. (b) Bond, A. M.; Colton, R.; Jackowski, J. J. *Ibid.* **1975**, *14*, 2526. (c) Bond, A. M.; Graberic, B. S.; Jackowski, J. J. *Ibid.* **1978**, *17*, 2153.
(4) Riecke, R. D.; Kojima, H.; Ofele, K. *J. Am. Chem. Soc.* **1976**, *98*, 6735.
(5) Darensbourg, D. J. *Inorg. Chem.* **1979**, *18*, 14.
(6) Datta, S.; Dezube, B.; Kouba, J. K.; Wreford, S. S. *J. Am. Chem. Soc.* **1978**, *100*, 4404.
(7) Bailar, J. C. *J. Inorg. Nucl. Chem.* **1958**, *8*, 165.

0276-7333/83/2302-0169$01.50/0

Table I. Voltammetric $E_{1/2}$ Values for CH_2Cl_2 Solutions of Mixed Carbonyl-Alkyl Isocyanide Complexes of Molybdenum[a]

complex	$E_{1/2}$(I or II)	$E_{1/2}$(III or IV)
$Mo(CO)_2(CN\text{-}t\text{-}Bu)_2(PEt_3)_2$	−0.25	−0.50
$Mo(CO)_2(CN\text{-}t\text{-}Bu)_2(P\text{-}n\text{-}Pr_3)_2$	−0.26	−0.51
$Mo(CO)_2(CN\text{-}t\text{-}Bu)_2(PMePh_2)_2$	−0.065	−0.31
$Mo(CO)_2(CNC_6H_{11})_4$	−0.065	−0.295
$[Mo(CO)_2(CN\text{-}t\text{-}Bu)_2(PMePh_2)_2]^+$[b]		−0.31

[a] In volts vs. SCE at a Pt bead working electrode and 0.2 M tetra-*n*-butylammonium hexafluorophosphate (TBAH) as supporting electrolyte. [b] Generated chemically by using $C_7H_7^+PF_6^-$ as the oxidant.

CV measurements were made on degassed dichloromethane, acetonitrile, and acetone solutions containing 0.2 M tetra-*n*-butylammonium hexafluorophosphate (TBAH) as supporting electrolyte at a platinum bead electrode.[8] The redox behavior of the complexes was found to be similar in all three solvents. Voltammetric half-wave potentials (vs. SCE in CH_2Cl_2 at 22 ± 2 °C and uncorrected for junction potentials) are presented in Table I.

Figure 1a shows a CV typical of those exhibited by these complexes; a scan to positive potentials starting from 0 V reveals an irreversible oxidation at $E_{p,a} \sim +1.3$ V[9] and two couples at negative potentials (i.e., $E_{1/2}$ values of −0.26 and −0.51 V in the case of $Mo(CO)_2(CN\text{-}t\text{-}Bu)_2(P\text{-}n\text{-}Pr_3)_2$) corresponding to an oxidation and a reduction, respectively. If the scan is started at a potential between these two couples and carried out in a negative direction (Figure 1b), it is observed that the species responsible for the more negative couple is not present and in fact is produced only after the first oxidation has occurred.

Bulk electrolysis carried out at potentials more positive than those corresponding to the first couple (i.e., $E_{1/2}$ (I or II) in Table I) converted the pale yellow solutions to bright orange and produced voltammograms (Figure 1c) with just one couple ($E_{1/2}$(III or IV) in Table I). The oxidation was shown by coulometry to be a one-electron process ($n = 1 \pm 0.1$) and the couple $E_{1/2}$(III or IV) was characterized by values for $E_{p,a} - E_{p,c}$ of 70–90 mV and $i_{p,a}/i_{p,c}$ ratios that were close to unity for sweep rates ranging from 50 to 500 mV s^{-1}. These orange solutions could be electrochemically reduced back to the parent species (exhibiting CV's identical with Figure 1a) at potentials more negative than those listed as $E_{1/2}$(III or IV) in Table I with little apparent decomposition as measured by peak currents.

The potentials listed in Table I for the oxidation of the $Mo(CO)_2(CNR)_2(PR_3)_2$ complexes and $Mo(CO)_2(CNC_6H_{11})_4$ are, as expected, intermediate between those for the oxidation of neutral carbonyl complexes $Mo(CO)_4(PR_3)_2$, $Mo(CO)_4$(P–P), and $Mo(CO)_4$(carbene)$_2$,[2-4] on the one hand, and the much more readily oxidizable isocyanide species $Mo(CNR)_2(Ph_2PCH_2CH_2PPh_2)_2$,[10] on the other. This trend follows from the general order of σ-donor abilities CO < CNR < PR_3. In any event, the $E_{1/2}$ values in Table I imply that a chemical oxidation is feasible, and such a process has been investigated by using tropylium

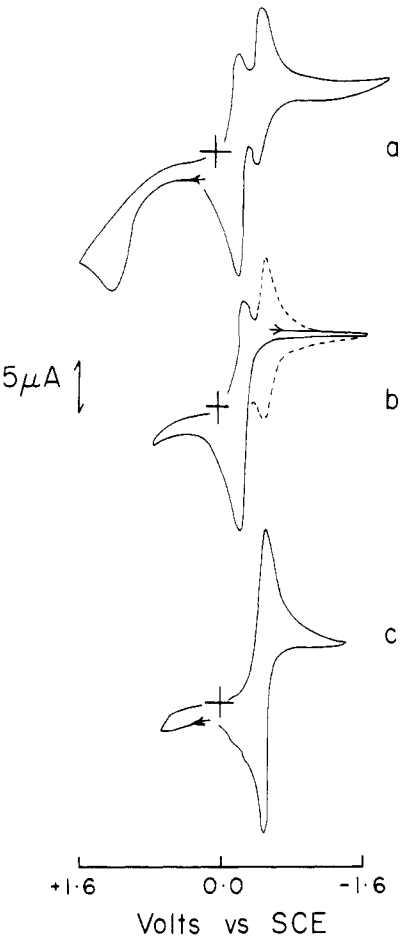

Figure 1. Cyclic voltammograms in 0.2 M TBAH–dichloromethane of $Mo(CO)_2(CN\text{-}t\text{-}Bu)_2(P\text{-}n\text{-}Pr_3)_2$: (a) positive scan starting at 0.0 V; (b) negative scan starting at −0.4 V (dotted line shows the second scan); (c) after controlled potential electrolysis at +0.1 V.

hexafluorophosphate as the oxidant.[11] Upon its addition to yellow CH_2Cl_2 solutions of the complex $Mo(CO)_2(CN\text{-}t\text{-}Bu)_2(PMe_2Ph)_2$ an orange color was immediately generated. The resulting solutions gave X-band ESR spectra identical with those of the electrochemically generated cations (vide infra). Thus far the product has only been obtained as an oil that quickly decomposes, but its IR spectrum confirms that there has been a structure change. Whereas the neutral complex has two ν(CO) and two ν(CN) bands,[1] the cation has only one of each,[12] an observation that is in accord with an all-trans geometry.

The X-band ESR spectra of frozen CH_2Cl_2 solutions of the electrochemical and chemical oxidation products reveal species with approximate tetragonal symmetry possessing a single unpaired electron with $g_\perp > g_\parallel$.[13] In the case of the $[Mo(CO)_2(CNC_6H_{11})_4]^+$ cation, this is consistent with the proposed trans structure (Figure 2a). Hyperfine splitting due to ^{95}Mo and ^{97}Mo (combined abundance 25.15%, $I = {}^5/_2$) accounts for the apparent asymmetry in

(8) Full details of our electrochemical procedure are described elsewhere; see: Zietlow, T. C.; Klendworth, D. D.; Nimry, T.; Salmon, D. J.; Walton, R. A. *Inorg. Chem.* **1981**, *20*, 947.

(9) This oxidation may correspond to the process $[Mo(CO)_2(CNR)_2(PR_3)_2]^+ \rightarrow [Mo(CO)_2(CNR)_2(PR_3)_2]^{2+} + e$. The lack of electrochemical reversibility could follow from the structure changes that are expected to be associated with the formation of such a 16-electron species; see: Kubacek, P.; Hoffmann, R. *J. Am. Chem. Soc.* **1981**, *103*, 4320.

(10) Chatt, J.; Elson, C. M.; Pombeiro, A. J. L.; Richards, R. L.; Royston, G. H. D. *J. Chem. Soc., Dalton Trans.* **1978**, 165.

(11) Solutions of $C_7H_7^+PF_6^-$ in 0.2 M TBAH–CH_2Cl_2 are characterized by a reduction at $E_{p,c} = -0.13$ V vs. SCE at $\nu = 200$ mV/s; in 0.1 M TBAH–CH_3CN the corresponding $E_{p,c}$ value is −0.19 V.

(12) The IR spectrum of $Mo(CO)_2(CN\text{-}t\text{-}Bu)_2(PMePh_2)_2$ recorded as a Nujol mull, for example, has ν(CO) at 1855 and 1810 cm^{-1} and ν(CN) at 2125 and 2100 cm^{-1} (see ref 1), while for $[Mo(CO)_2(CN\text{-}t\text{-}Bu)_2(PMePh_2)_2]PF_6$, ν(CO) = 1880 (s) cm^{-1} and ν(CN) = 2130 (s) cm^{-1} for a Nujol mull and ν(CO) = 1885 (s) cm^{-1} and ν(CN) = 2125 cm^{-1} for a CH_2Cl_2 solution.

(13) Appropriate g values are as follows: $[Mo(CO)_2(CNC_6H_{11})_4]^+$, $g_\perp = 2.121$, $g_\parallel = 1.984$; $[Mo(CO)_2(CN\text{-}t\text{-}Bu)_2(PEt_3)_2]^+$, $g_\perp = 2.079$, $g_\parallel = 1.981$; $[Mo(CO)_2(CN\text{-}t\text{-}Bu)_2(PMe_2Ph)_2]^+$, $g_\perp = 2.076$, $g_\parallel = 1.976$.

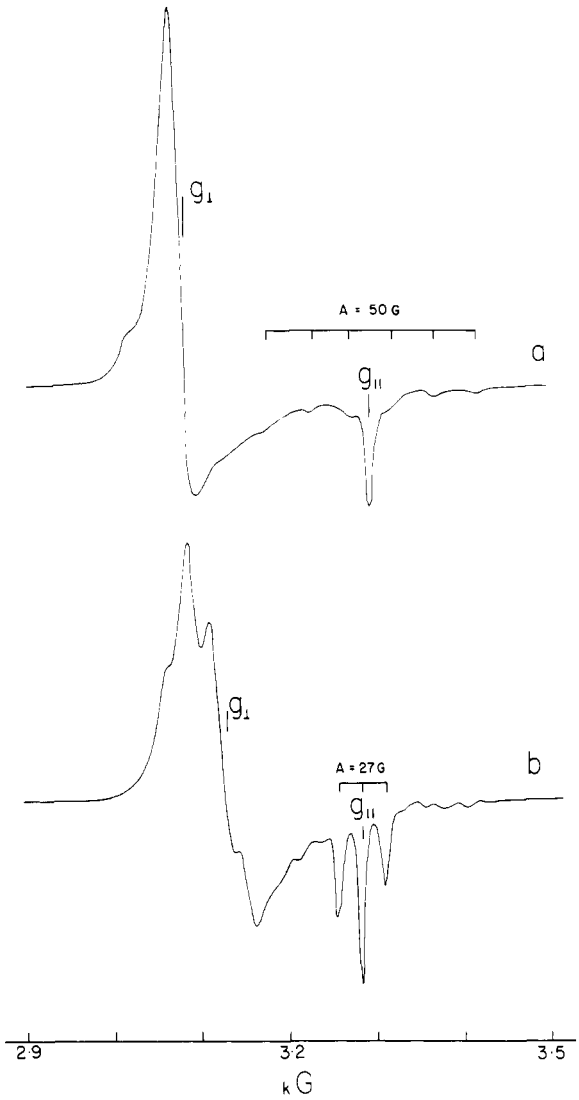

Figure 2. X-band ESR spectra of frozen CH_2Cl_2 solutions at −160 °C of (a) $[Mo(CO)_2(CNC_6H_{11})_4]^+$ and (b) $[Mo(CO)_2(CN\text{-}t\text{-}Bu)_2(PMePh_2)_2]^+$.

Scheme I

$$Mo(CO)_2(CNR)_2(PR_3)_2 \underset{E_{1/2}(I)}{\overset{-e}{\rightleftharpoons}} [Mo(CO)_2(CNR)_2(PR_3)_2]^+$$
I

$k_2 \uparrow\downarrow k_{-2}$ $\qquad$ $k_{-1} \uparrow\downarrow k_1$

$$Mo(CO)_2(CNR)_2(PR_3)_2 \underset{E_{1/2}(III)}{\overset{-e}{\rightleftharpoons}} [Mo(CO)_2(CNR)_2(PR_3)_2]^+$$
III

the $g_\perp$ signal. The hyperfine lines in the $g_\parallel$ region are well resolved with A = 50 G. Figure 2b shows an ESR spectrum that is typical of the $[Mo(CO)_2(CNR)_2(PR_3)_2]^+$ cations. For the phosphine complexes, the "perpendicular" signal is broader and also more structured, but only one g value is clearly resolved. The 1:2:1 triplet in $g_\parallel$ results from the interaction of the unpaired electron with two equivalent ^{31}P atoms ($I = {}^1/_2$).

On the basis of the ESR evidence for equivalent phosphines and IR data which suggest that the two carbonyl ligands are trans as are also the two isocyanides, the structure of $[Mo(CO)_2(CNR)_2(PR_3)_2]^+$ is concluded to be all-trans. The electrochemical and spectroscopic data for $[Mo(CO)_2(CNR)_2(PR_3)_2]^{0,1+}$ are in accord with Scheme I.

Oxidation of isomer I is followed by rapid isomerization to the all-trans cation (possessing structure III) that in turn isomerizes back to I upon its electrochemical reduction to

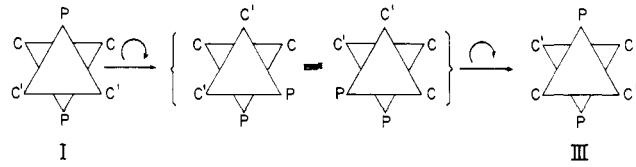

Figure 3. Schematic representation of two sequential twists that could convert I to III without bond breaking: C = CO; C′ = CNR, and P = PR_3.

the neutral 18-electron species. From our studies it is clear that the order of rates is $k_1 > k_2$.[14] The similarity of the electrochemical behavior in various solvents as well as the reversibility established by the coulometric experiments support the notion that the structural rearrangement is nondissociative. Figure 3 illustrates a possible mechanism for the intramolecular conversion of I to III.

Our work provides the first examples of the electrochemically induced isomerization of complexes of the type $MX_2Y_2Z_2$ that contain a $M(CO)_2$ unit, where M represents a group 6 metal. We hope to expand the scope of these investigations to include a wider range of isocyanide and phosphine ligands, in particular focusing upon the constraints imposed by chelating phosphines of the type $Ph_2P(CH_2)_nPPh_2$, since the latter will ensure that the isomerization will be different from that which has been studied so far (I ⇄ III).

Acknowledgment. Support from the National Science Foundation (Grant CHE82-06117) is gratefully acknowledged.

Registry No. $Mo(CO)_2(CN\text{-}t\text{-}Bu)_2(PEt_3)_2$, 80215-95-8; $Mo(CO)_2(CN\text{-}t\text{-}Bu)_2(P\text{-}n\text{-}Pr_3)_2$, 80215-96-9; $Mo(CO)_2(CN\text{-}t\text{-}Bu)_2(PMePh_2)_2$, 80215-97-0; $Mo(CO)_2(CNC_6H_{11})_4$, 80215-99-2; $[Mo(CO)_2(CN\text{-}t\text{-}Bu)_2(PMePh_2)_2]^+$, 83897-56-7; $C_7H_7^+PF_6^-$, 29663-54-5; $[Mo(CO)_2(CNC_6H_{11})_4]^+$, 83897-57-8; $[Mo(CO)_2(CN\text{-}t\text{-}Bu)_2(PMePh_2)_2]PF_6$, 83897-58-9; $[Mo(CO)_2(CN\text{-}t\text{-}Bu)_2(PEt_3)_2]^+$, 83897-59-0.

(14) Note that for the so-called cross redox reaction

$$I^+ + III \underset{k_{-3}}{\overset{k_3}{\rightleftharpoons}} I + III^+$$

the order $k_3 > k_{-3}$ holds; for the appropriate theory see: Feldberg, S. W.; Jeftic, L. *J. Phys. Chem.* **1972**, *76*, 2439.

New Stable Dianions from the Electrochemical Reduction of Conjugated Bis(phenyltricarbonylchromium) Groups

Stuart N. Milligan and Reuben D. Rieke*

Department of Chemistry, University of Nebraska—Lincoln, Nebraska 68588

Received August 13, 1982

Summary: Bis(tricarbonylchromium) complexes of arene compounds with two conjugated phenyl rings reduce electrochemically in a two-electron fashion. The process is chemically reversible as shown by cyclic voltammetry and coulometry.

(Arene)tricarbonylchromium complexes exhibit redox properties that vary as a function of the arene ligand. When benzene or substituted benzene rings are present, reduction is a two-electron process[1-3] yielding a highly

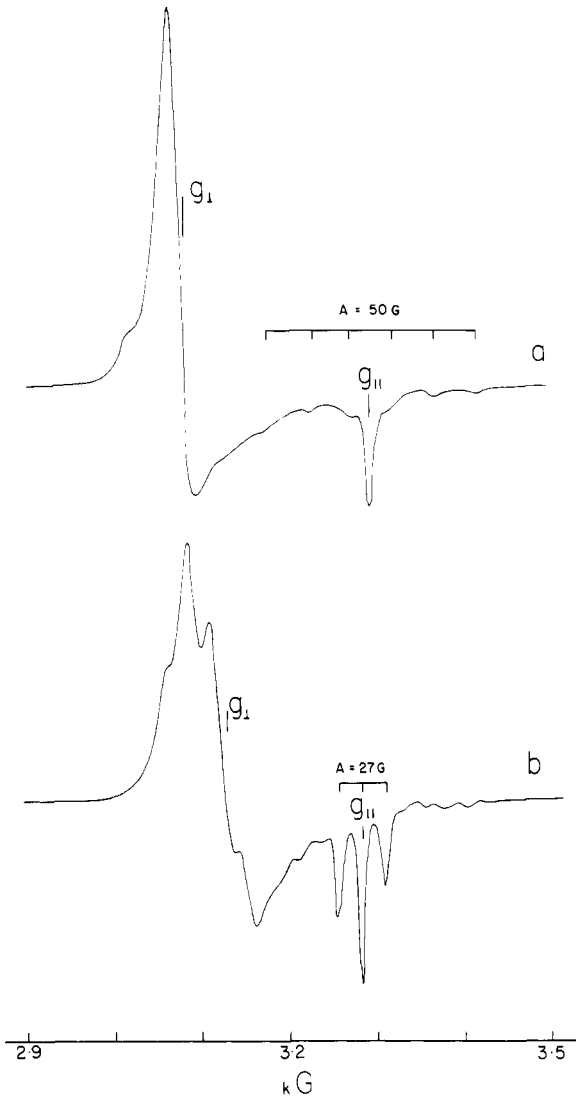

Figure 2. X-band ESR spectra of frozen CH_2Cl_2 solutions at −160 °C of (a) $[Mo(CO)_2(CNC_6H_{11})_4]^+$ and (b) $[Mo(CO)_2(CN\text{-}t\text{-}Bu)_2(PMePh_2)_2]^+$.

Scheme I

$$Mo(CO)_2(CNR)_2(PR_3)_2 \underset{E_{1/2}(I)}{\overset{-e}{\rightleftharpoons}} [Mo(CO)_2(CNR)_2(PR_3)_2]^+$$
I

$k_2 \uparrow\downarrow k_{-2}$ $\qquad$ $k_{-1} \uparrow\downarrow k_1$

$$Mo(CO)_2(CNR)_2(PR_3)_2 \underset{E_{1/2}(III)}{\overset{-e}{\rightleftharpoons}} [Mo(CO)_2(CNR)_2(PR_3)_2]^+$$
III

the $g_\perp$ signal. The hyperfine lines in the $g_\parallel$ region are well resolved with A = 50 G. Figure 2b shows an ESR spectrum that is typical of the $[Mo(CO)_2(CNR)_2(PR_3)_2]^+$ cations. For the phosphine complexes, the "perpendicular" signal is broader and also more structured, but only one g value is clearly resolved. The 1:2:1 triplet in $g_\parallel$ results from the interaction of the unpaired electron with two equivalent ^{31}P atoms ($I = {}^1/_2$).

On the basis of the ESR evidence for equivalent phosphines and IR data which suggest that the two carbonyl ligands are trans as are also the two isocyanides, the structure of $[Mo(CO)_2(CNR)_2(PR_3)_2]^+$ is concluded to be all-trans. The electrochemical and spectroscopic data for $[Mo(CO)_2(CNR)_2(PR_3)_2]^{0,1+}$ are in accord with Scheme I.

Oxidation of isomer I is followed by rapid isomerization to the all-trans cation (possessing structure III) that in turn isomerizes back to I upon its electrochemical reduction to

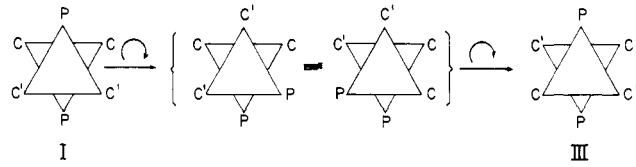

Figure 3. Schematic representation of two sequential twists that could convert I to III without bond breaking: C = CO; C′ = CNR, and P = PR_3.

the neutral 18-electron species. From our studies it is clear that the order of rates is $k_1 > k_2$.[14] The similarity of the electrochemical behavior in various solvents as well as the reversibility established by the coulometric experiments support the notion that the structural rearrangement is nondissociative. Figure 3 illustrates a possible mechanism for the intramolecular conversion of I to III.

Our work provides the first examples of the electrochemically induced isomerization of complexes of the type $MX_2Y_2Z_2$ that contain a $M(CO)_2$ unit, where M represents a group 6 metal. We hope to expand the scope of these investigations to include a wider range of isocyanide and phosphine ligands, in particular focusing upon the constraints imposed by chelating phosphines of the type $Ph_2P(CH_2)_nPPh_2$, since the latter will ensure that the isomerization will be different from that which has been studied so far (I ⇄ III).

Acknowledgment. Support from the National Science Foundation (Grant CHE82-06117) is gratefully acknowledged.

Registry No. $Mo(CO)_2(CN\text{-}t\text{-}Bu)_2(PEt_3)_2$, 80215-95-8; $Mo(CO)_2(CN\text{-}t\text{-}Bu)_2(P\text{-}n\text{-}Pr_3)_2$, 80215-96-9; $Mo(CO)_2(CN\text{-}t\text{-}Bu)_2(PMePh_2)_2$, 80215-97-0; $Mo(CO)_2(CNC_6H_{11})_4$, 80215-99-2; $[Mo(CO)_2(CN\text{-}t\text{-}Bu)_2(PMePh_2)_2]^+$, 83897-56-7; $C_7H_7^+PF_6^-$, 29663-54-5; $[Mo(CO)_2(CNC_6H_{11})_4]^+$, 83897-57-8; $[Mo(CO)_2(CN\text{-}t\text{-}Bu)_2(PMePh_2)_2]PF_6$, 83897-58-9; $[Mo(CO)_2(CN\text{-}t\text{-}Bu)_2(PEt_3)_2]^+$, 83897-59-0.

(14) Note that for the so-called cross redox reaction

$$I^+ + III \underset{k_{-3}}{\overset{k_3}{\rightleftharpoons}} I + III^+$$

the order $k_3 > k_{-3}$ holds; for the appropriate theory see: Feldberg, S. W.; Jeftic, L. *J. Phys. Chem.* **1972**, *76*, 2439.

New Stable Dianions from the Electrochemical Reduction of Conjugated Bis(phenyltricarbonylchromium) Groups

Stuart N. Milligan and Reuben D. Rieke*

Department of Chemistry, University of Nebraska—Lincoln, Nebraska 68588

Received August 13, 1982

Summary: Bis(tricarbonylchromium) complexes of arene compounds with two conjugated phenyl rings reduce electrochemically in a two-electron fashion. The process is chemically reversible as shown by cyclic voltammetry and coulometry.

(Arene)tricarbonylchromium complexes exhibit redox properties that vary as a function of the arene ligand. When benzene or substituted benzene rings are present, reduction is a two-electron process[1-3] yielding a highly

Table I. Electrochemical Results

compd[a]	$E_{1/2}$,[b] V	$E_{3/4} - E_{1/4}$, mV	i_d, μA
(biphenyl)$Cr(CO)_3$	−1.948	40	2.72
(biphenyl)$[Cr(CO)_3]_2$	−1.606	30	2.68
(9,10-dihydrophenanthrene)-$Cr(CO)_3$	−1.982	33	2.52
(9,10-dihydrophenanthrene)-$[Cr(CO)_3]_2$	−1.663	31	2.76
(*trans*-stilbene)$Cr(CO)_3$	−1.656	37	1.83
(*trans*-stilbene)$[Cr(CO)_3]_2$	−1.385	26	2.82
(*cis*-stilbene)$Cr(CO)_3$	−1.673	24	2.48
(*cis*-stilbene)$[Cr(CO)_3]_2$	−1.395	17[c]	2.78

[a] Approximately 1 mM in THF, 0.2 M TBAP, 0 °C, on the DME. [b] Vs. the Ag/AgCl, saturated NaCl (aq) reference electrode, ±0.005 V. [c] The slope of the log plot is 23 mV.

reactive dianion as shown by the irreversibility of the cyclic voltammograms. Naphthalene complexes, on the other hand, also reduce with two electrons, but the dianion is extremely persistent.[1] Phenyl ketone complexes undergo only one-electron reduction, but the odd electron is localized primarily on the ketone functionality of the ligand.[4-7]

Except for the phenyl ketone systems, which do not really involve the tricarbonylchromium group, all (arene)tricarbonylchromium complexes reduce in a characteristic two-electron per chromium atom manner. We report here reductive electrochemical studies demonstrating that bis(tricarbonylchromium) complexes of aromatic compounds containing two conjugated phenyl rings reduce with a total of two electrons. This is formally one electron per chromium atom. In addition, the dianions produced are very persistent.

Mono- and bis(tricarbonylchromium) complexes of biphenyl, 9,10-dihydrophenanthrene, and *cis*- and *trans*-stilbene were chosen because the two phenyl rings are conjugated. As expected, the mono complexes exhibit reductive characteristics that are analogous to the tricarbonylchromium complexes of substituted benzenes. They generally reduce at about the same potential as (benzene)tricarbonylchromium with some allowance for extra conjugation. The reduction products are also quite reactive. The cyclic voltammograms are irreversible until scan rates in excess of 1 V/s at which point a very small anodic peak begins to appear.

The redox properties of the bis(tricarbonylchromium) complexes associated with these conjugated ligands stand in marked contrast to their mono counterparts. Each of the bis complexes is reduced approximately 300 mV positive of its corresponding mono complex (see Table I). This significant decrease in reduction potential suggests coupling between the tricarbonylchromium moieties in the same way that extended conjugation in an organic molecule lowers the reduction potential. The two phenyl rings must be conjugated to experience this shift since dimethylbis(phenyltricarbonylchromium)tin reduces at approximately

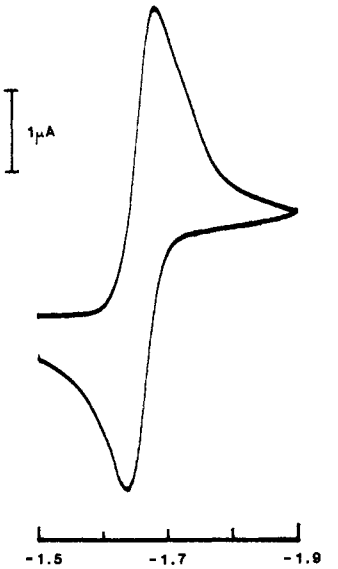

Figure 1. A cyclic voltammogram of (9,10-dihydrophenanthrene)bis(tricarbonylchromium) in THF (0.2 M TBAP, 0 °C, 50 mV/s, HMDE).

Table II. Infrared Carbonyl Bands

compd	CO bands	Cr ox. state
(biphenyl)$[Cr(CO)_3]_2$	1963, 1899	0
	1881, 1788, 1765	−1
(9,10-dihydrophenanthrene)-$[Cr(CO)_3]_2$	1960, 1895	0
	1878, 1785, 1765	−1
(*trans*-stilbene)$[Cr(CO)_3]_2$	1962, 1895	0
	1888, 1797, 1777	−1
(*cis*-stilbene)$[Cr(CO)_3]_2$	1964, 1898	0
	1896, 1802 1780	−1

the same potential as (benzene)tricarbonylchromium.

The longevity of the resulting dianions of the bis complexes contrasts with the high reactivity of the dianions derived from the mono complexes. An anodic to cathodic current ratio of unity in the cyclic voltammograms is observed for the bis complexes even with scan rates as low as 20 mV/s (see Figure 1). They also appear to have half-lives on the order of several hours when bulk coulometric studies are performed. In this respect the bis complexes are similar to (naphthalene)tricarbonylchromium.[1]

Polarographic, voltammetric, and coulometric studies all indicate that the reduction process of bis complexes of arene ligands with conjugated phenyl rings involves a total of two electrons.[14] This one electron per chromium atom reduction distinguishes this class of tricarbonylchromium complexes from benzene[1-3] and naphthalene[1] complexes.

Studies of the carbonyl stretching bands were also performed (see Table II). The bands of the unreduced bis complexes are quite similar to those of other (arene)tricarbonylchromium complexes; two sharp bands are usually observed at approximately 1960 and 1895 cm^{-1} in THF solutions. Exhaustive electrochemical reduction results in the disappearance of these original bands and the appearance of new ones at about 1885, 1790, and 1770 cm^{-1}. The small peaks remaining at the original positions are most likely due to trace amounts of oxygen introduced upon transfer of the dianion. When exhaustive reoxidation is performed on the solution either electrochemically or by air, the low wavenumber bands disappear and the or-

(1) Rieke, R. D.; Arney, J. S.; Rich, W. E.; Willeford, B. R.; Poliner, B. S. *J. Am. Chem. Soc.* **1975**, *97*, 5951-5953.
(2) Dessey, R. E.; Story, F. E.; King, R. B.; Waldrop, M. *J. Am. Chem. Soc.* **1966**, *88*, 471-476.
(3) Dessey, R. E.; King, R. B.; Waldrop, M. *J. Am. Chem. Soc.* **1966**, *88*, 5112-5117.
(4) Khandkarova, V. S.; Gubin, S. P. *J. Organomet. Chem.* **1970**, *22*, 149-152.
(5) Gubin, S. P. *Pure Appl. Chem.* **1970**, *23*, 463-487.
(6) Ceccon, A.; Corvaja, C.; Giacometti, G.; Venzo, A. *J. Chim. Phys.* **1975**, *72*, 23-24.
(7) Ceccon, A.; Corvaja, C.; Giacometti, G.; Venzo, A. *J. Chem. Soc., Perkin Trans. 2* **1978**, 283-288.

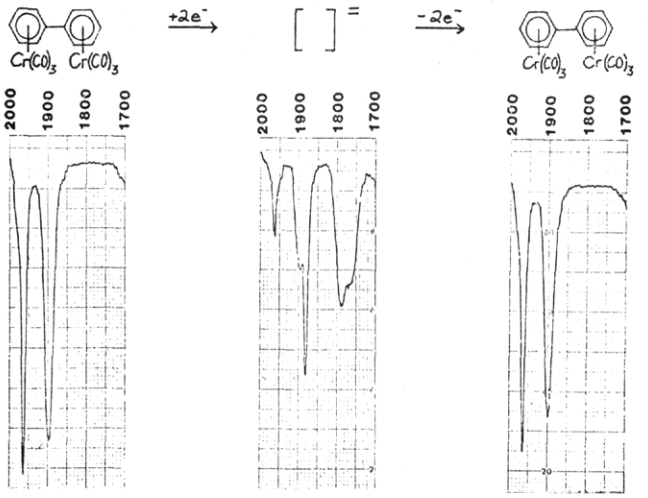

Figure 2. Infrared carbonyl stretching bands for (biphenyl)-bis(tricarbonylchromium): left; before reduction; center; after electrochemical reduction; right, after electrochemical reoxidation.

iginal carbonyl stretching bands are seen once again (see, for example, Figure 2).

The carbonyl stretching bands for the dianions of the bis complexes were compared to values for other chromium carbonyl compounds obtained in our research group[8] and by Hayter.[9] The results indicate that both chromium atoms are formally in the −1 oxidation state. No mixed-valance interactions are indicated, and this further confirms a strong coupling between the tricarbonylchromium moieties.

We propose that the following mechanism occurs during the reduction of these complexes. This mechanism is of the ECE type which is usually associated with two-electron processes. Beginning with the neutral bis complex of biphenyl, a one-electron reduction forms the radical anion making one tricarbonylchromium group a 19-electron moiety. This unfavorable situation can be relieved with an isomerization step. It is proposed that this occurs by changing from η^6 to η^5 bonding in the 19-electron metal portion. This chromium would now be bound to five carbons, which is a pentadienide system and leaves carbon 1 no longer bonded to the chromium atom. Thus this chromium atom returns to the stable 18-electron configuration. However, this has left an unpaired electron in a benzylic position with regard to the unreduced ring. Resonance structures can be drawn so as to pair up this electron with the electron on the carbon 1′ position. This leads to η^5 bonding of the unreduced chromium atom and therefore a 17-electron species. Immediate reduction by a second electron occurs by virtue of the applied potential being quite negative of what is required to reduce this 17-electron species. The final result is that each chromium atom is part of an 18-electron system, bound to the ring in a η^5 fashion and in the −1 oxidation state. A carbon–carbon double bond is postulated to form between the phenyl rings. Precisely the same mechanism can be used to explain reduction of the (stilbene)tricarbonylchromium complexes except that a butadiene moiety forms between the phenyl rings (see Scheme I).

The proposed η^5 bonding has several precedents. Cyclopentadienyltricarbonylchromium complexes have been known for some time.[10,11] Semmelhack and co-

Scheme I

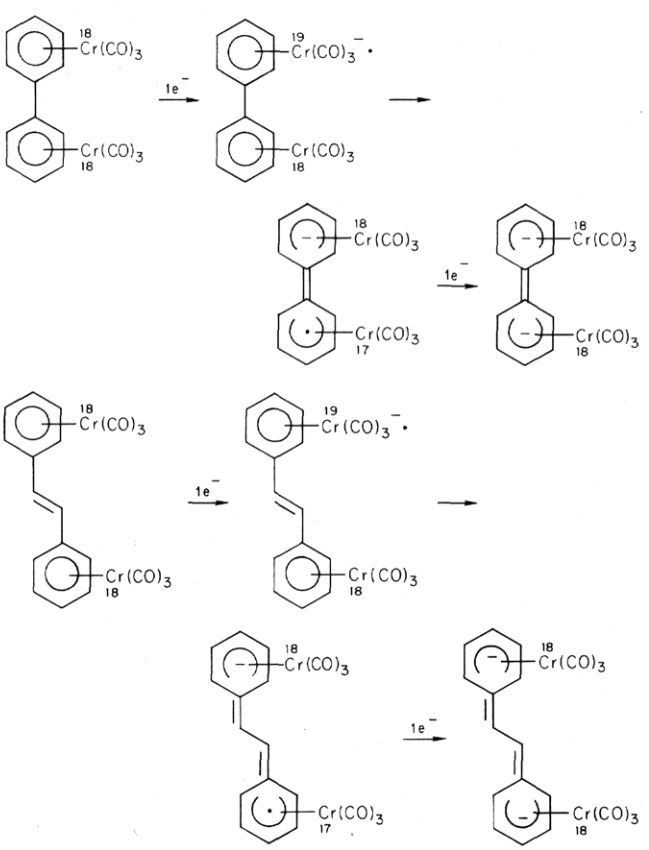

worker[12] have demonstrated the existence of a η^5-bound species in work on nucleophilic substitution of (benzene)tricarbonylchromium. Recently, the compound with the structure shown below was reported[13] that is analogous to the proposed structure of the dianion.

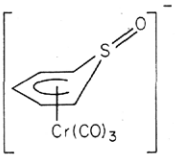

We are presently attempting to isolate the dianions so as to characterize them further. We are also exploring the chemistry associated with these dianions.

Acknowledgment. We gratefully acknowledge support of this work by the National Science Foundation, Grant No. CHE78-06661. We also like to acknowledge a duPont Fellowship administered by the University of Nebraska Chemistry Department to SNM. Dr. Indu Tucker synthesized (9,10-dihydrophenanthrene)bis(tricarbonylchromium). The mono- and bis(tricarbonylchromium) complexes of *cis*- and *trans*-stilbene were supplied by Dr. Bennett R. Willeford.

Registry No. (biphenyl)$Cr(CO)_3$, 12111-60-3; (biphenyl)$[Cr(CO)_3]_2$, 33010-84-3; (9,10-dihydrophenanthrene)$Cr(CO)_3$, 12094-55-2; (9,10-dihydrophenanthrene)$[Cr(CO)_3]_2$, 57395-32-1; (*trans*-stilbene)$Cr(CO)_3$, 12155-45-2; (*trans*-stilbene)$[Cr(CO)_3]_2$, 83861-09-0; (*cis*-stilbene)$Cr(CO)_3$, 12155-44-1; (*cis*-stilbene)$[Cr(CO)_3]_2$, 83861-10-3.

(8) Rieke, R. D.; Arney, J. S.; Henry, W. P., unpublished results.
(9) Hayter, R. G. *J. Am. Chem. Soc.* **1966**, *88*, 4376–4382.
(10) Nesmayanov, A. N.; Ustynyuk, N. A.; Novikova, L. N.; Andrianov, V. G.; Struchkov, Y. T.; Ustynyuk, Y. A.; Oprunenko, Y. F.; Luzikov, Y. N. *J. Organomet. Chem.* **1982**, *226*, 239–250 and references therein.
(11) Piper, T. S.; Wilkinson, G. *J. Inorg. Nucl. Chem.* **1956**, *3*, 104–124.
(12) Semmelhack, M. F.; Hall, H. T.; Yoshifuji, M. *J. Am. Chem. Soc.* **1976**, *98*, 6387–6389.
(13) Weber, L.; Wewers, D. *Z. Naturforsch., B: Anorg. Chem., Org. Chem.* **1982**, *37*, 68–72.
(14) Polarographic and voltammetric experiments were performed by using *iR* feedback compensation.

Silicon–Carbon Unsaturated Compounds. 15. Synthesis and Molecular Structure of Stable Disilacyclopropanes

Mitsuo Ishikawa,*[1a] Hiroshi Sugisawa,[1a] Makoto Kumada,*[1a] Taiichi Higuchi,*[1b] Koji Matsui,[1b] Ken Hirotsu,[1b] and Jun Iyoda[1c]

Department of Synthetic Chemistry, Faculty of Engineering Kyoto University, Kyoto 606, Japan
Department of Chemistry, Faculty of Science Osaka City University, Sugimotocho Sumiyoshi-ku, Osaka, Japan
and Government Industrial Research Institute Osaka Ikeda, Osaka 563, Japan

Received September 28, 1982

Summary: Two stable disilacyclopropanes 1,1,2,2-tetramesityl-3-[bis(trimethylsilyl)methylene]- and 1,1,2,2-tetramesityl-3-[phenyl(trimethylsilyl)methylene]-1,2-disilacyclopropane (**3** and **7**) have been prepared by addition of dimesitylsilylene to 1,1-dimesityl-3,3-bis(trimethylsilyl)-1-silapropadiene and 1,1-dimesityl-3-phenyl-3-(trimethylsilyl)-1-silapropadiene, respectively. Preliminary results of an X-ray diffraction study of **3** are described.

All efforts to prepare disilacyclopropanes had been unsuccessful until in 1976 Seyferth and Duncan provided chemical evidence that a disilacyclopropane derivative was formed in the reaction of 1-chloro-2-(bromonorcaranyl)-tetramethyldisilane with butyllithium.[2] The presence of the disilacyclopropane was inferred on the basis of its reaction with methanol to give the product arising from cleavage of the silicon–silicon bond.[3] It could not be isolated or even detected spectroscopically. In this paper, we report the first synthesis of two stable disilacyclopropanes 1,1,2,2-tetramesityl-3-bis(trimethylsilyl)methylene- and 1,1,2,2-tetramesityl-3-[phenyl(trimethylsilyl)methylene]-1,2-disilacyclopropane and preliminary results of X-ray diffraction study of the latter compound and of ab initio MO calculations for simplified model compounds.

When a solution of 0.8105 g (1.86 mmol) of 1,1-dimesityl-2,2,2-trimethyl-1-[(trimethylsilyl)ethynyl]disilane[4] (**1**) and 1.6317 g (3.95 mmol) of 2,2-dimesitylhexamethyltrisilane (**2**) in 120 mL of dry hexane was photolyzed by irradiation with a low-pressure mercury lamp bearing a Vycor filter for 7 h at −40 to −20 °C,[5] yellow crystals identified as 1,1,2,2-tetramesityl-3-[bis(trimethylsilyl)-methylene]-1,2-disilacyclopropane (**3**) [0.3199 g (25% yield); mp 158 °C dec; UV λ_{max} (ϵ) 288 (22450), 364 (8970), 415 nm (5640)] were formed, which could be readily isolated by column chromatography, in addition to 20% yield of 1,1-dimesityl-2,3-bis(trimethylsilyl)-1-silacyclopropene (**4**), with 30% of the starting material **1** being unchanged. Since it has been well established recently that the photolysis of **1** affords silacyclopropene **4** and 1,1-dimesityl-3,3-bis(trimethylsilyl)-1-silapropadiene[4,6] (**5**), while **2** yields

Scheme I

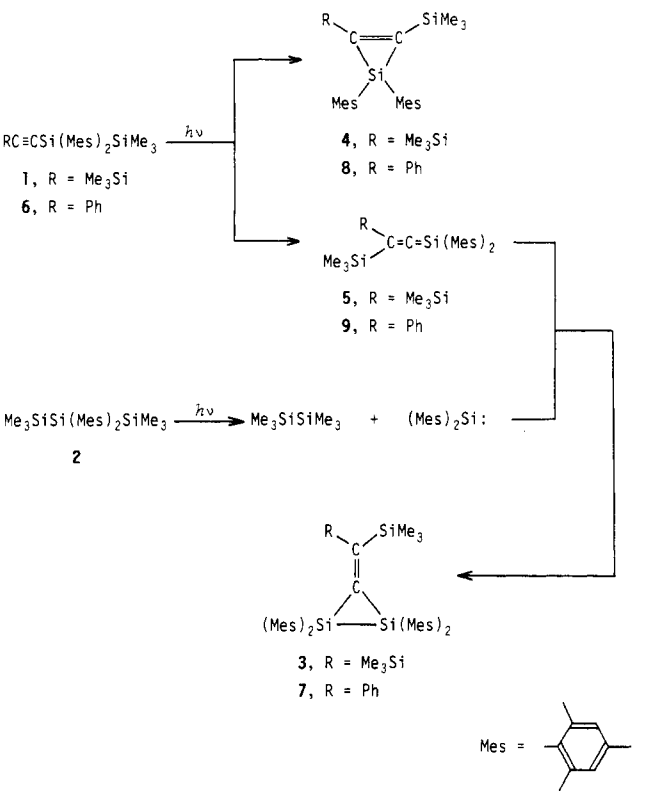

dimesitylsilylene,[7] the formation of **3** can be explained in terms of the reaction of **5** with dimesitylsilylene (Scheme I). Because photochemical degradation of **1** also involves the extrusion of dimesitylsilylene,[4] **3** was expected to be formed in the photolysis of **1** in the absence of **2**. However, we could not isolate **3** from this reaction mixture, although a trace amount of **3** could be detected by TLC.

The structure of **3** was confirmed by spectroscopic analysis [^{1}H NMR δ 0.01 (s, 18 H, Me_3Si), 2.15 (s, 12 H, *p*-CH_3), 2.25 (s, 24 H, *o*-CH_3), 6.50 (br s, 8 H, ring protons); ^{29}Si NMR δ (upfield from tetramethylsilane) −6.5 ($SiMe_3$), −48.5 ($SiMes_2$); mass spectrum, M^+ 702] as well as elemental analysis.[8]

Similar irradiation of a mixture of 0.9620 g (2.18 mmol) of 1,1-dimesityl-2,2,2-trimethyl-1-(phenylethynyl)disilane (**6**) and 0.3328 g (0.81 mmol) of **2** in 100 mL of hexane for 3.5 h at room temperature yielded 0.2158 g (14% yield) of yellow crystals of 1,1,2,2-tetramesityl-3-[phenyl(trimethylsilyl)methylene]-1,2-disilacyclopropane[9] (**7**) (mp 203 °C dec; UV λ_{max} (ϵ) 284 (18180), 316 (13500), 382 nm (5180)), in addition to 62% yield of 1,1-dimesityl-2-phenyl-3-(trimethylsilyl)-1-silacyclopropene (**8**). Here again, **7** may result from the addition of dimesitylsilylene to the 1-silapropadiene intermediate **9**.[10] In a previous paper,[4] we reported this yellow compound to be 1,1,2,2-tetramesityl-2-phenyl-3-(trimethylsilyl)-1,2-disilacyclobutane. However, this has turned out to be an erroneous assignment.[11]

(1) (a) Kyoto University. (b) Osaka City University. (c) Government Industrial Research Institute Osaka.
(2) Seyferth, D.; Duncan, D. P. *J. Organomet. Chem.* **1976**, *111*, C21.
(3) Intermediary formation of disilacyclopropanes has been reported, for example: (a) Roark, D. N.; Peddle, G. J. D. *J. Am. Chem. Soc.* **1972**, *94*, 5837. (b) Wulff, W. D.; Goure, W. F.; Barton, T. J. *Ibid.* **1978**, *100*, 6236. (c) Chen, T.-S.; Cohen, B, H.; Gaspar, P. P. *J. Organomet. Chem.* **1980**, *195*, C1.
(4) Ishikawa, M.; Nishimura, K.; Sugisawa, H.; Kumada, M. *J. Organomet. Chem.* **1980**, *194*, 147.
(5) The photolysis of the same mixture at room temperature gave **3** only in a trace amount.
(6) Paper 14 in this series: Ishikawa, M.; Nishimura, K.; Ochiai, H.; Kumada, M. *J. Organomet. Chem.* **1982**, *236*, 7.
(7) West, R.; Fink, M. J. *Science (Washington, DC)* **1981**, *214*, 1343.
(8) For **3**. Anal. Calcd for $C_{44}H_{62}Si_4$: C, 75.14; H, 8.89. Found: C, 75.09; H, 8.73.
(9) For **7**: ^{1}H NMR δ −0.13 (s, 9 H, Me_3Si), 2.00 (s, 12 H, *o*-CH_3), 2.11 (s, 6 H, *p*-CH_3), 2.16 (s, 6 H, *p*-CH_3), 2.36 (s, 12 H, *o*-CH_3), 6.38 (s, 4 H, mesityl ring protons), 6.56 (s, 4 H, mesityl ring protons, 6.6–7.2 (m, 5 H, phenyl ring protons); ^{29}Si δ (upfield from Me_4Si) −5.7 ($SiMe_3$), −56.0 ($Si(Mes)_2$), −63.3 ($Si(Mes)_2$). Anal. Calcd for $C_{47}H_{58}Si_3$: C, 79.82; H, 8.27. Found: C, 80.01; H, 8.32.
(10) The yield of 1-silapropadiene **9** was determined to be ca. 20% from the photolysis of **6** in the presence of methanol.

0276-7333/83/2302-0174$01.50/0

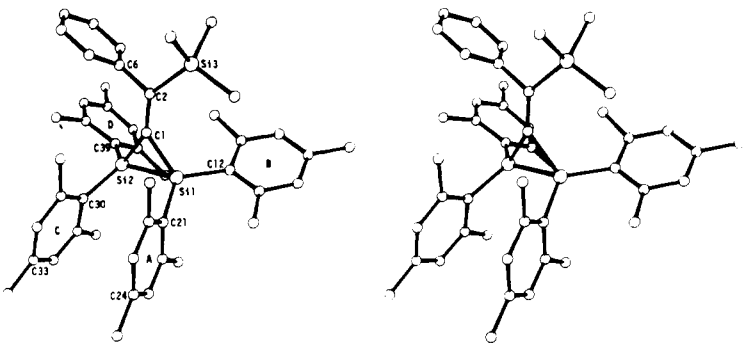

Figure 1. Stereoscopic view of 1,1,2,2-tetramesityl-3-[phenyl(trimethylsilyl)methylene]-1,2-disilacyclopropane (7).

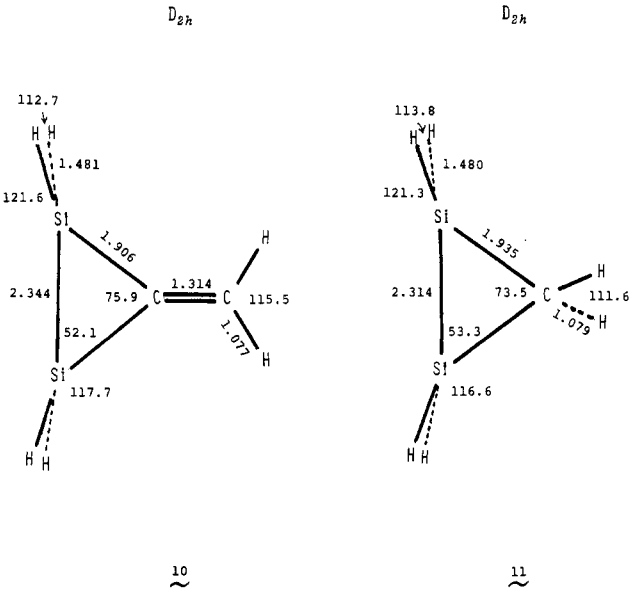

Figure 2. Geometries of 3-methylene-1,2-disilacyclopropane (**10**) and disilacyclopropane (**11**).

In contrast to the photolysis of **1**, when **6** was photolyzed in the absence of **2**, compound **7** was obtained in 8% yield,[11] together with 1-silacyclopropene **8** (65% yield). Both disilacyclopropanes **3** and **7** are stable toward atmospheric oxygen and moisture. They do not react with alcohols at room temperature.

The structure of **7** was determined by X-ray diffraction study. We also carried out ab initio MO calculations for 3-(methylene)-1,2-disilacyclopropane (**10**) and disilacyclopropane (**11**).[12,13] The crystals of **7** are triclinic of space group $P\bar{1}$ with cell dimensions a = 16.710 (3) Å, b = 13.150 (2) Å, c = 11.268 (3) Å, α = 70.96 (2)°, β = 66.94 (2)°, γ = 69.87 (2)°; V = 2085.6 (7) Å^3, and D_x = 1.171 Kg M^{-3} (Z = 2). The structure was solved by direct method.[15] Only the 3491 reflections with $I > 2\sigma(I)$ were used in the least-squares refinement (R = 0.053). Figure 1 shows a stereoscopic view of a single molecule. The disilacyclopropane ring and a plane consisting of Si(3), C(2), and C(6) atoms are almost coplanar with the dihedral angle of 7.6°. The sum of the bond angles of C(21)–Si(1)–Si(2), C(12)–Si(1)–Si(2), and C(12)–Si(1)–C(21) is 355.1° which is consistent with the corresponding values obtained from MO calculations for **10** (355.9°) and for **11** (356.4°), while the sum of the bond angles of C(39)–Si(2)–Si(1), C(30)–Si(2)–Si(1), and C(30)–Si(2)–C(39) is 343.4°. These results suggest that Si(1), C(12), C(21), Si(2), C(30), and C(39) atoms lie in almost the same plane. Two mesityl groups on Si(1) and Si(2) atoms, A and C rings, are fairly parallel to each other. The inter-ring distances C(21)–C(30) and C(24)–C(33) are 3.38 and 4.25 Å, respectively. The bond lengths of Si–Si (2.327 (2) Å) and two Si–C bonds (1.907 (4) Å (average)) in the disilacyclopropane ring are consistent with those of the respective normal bond. The bond angles of Si–C–Si and C–Si–Si in the ring are 75.2 (2) and 52.4 (1)° (average), respectively. Interestingly, these values are in good agreement with those obtained from MO calculations for **10** but not for **11** as shown in Figure 2.

The chemical behavior of the disilacyclopropanes is currently being examined and will be reported elsewhere.

Acknowledgment. We are grateful to Dr. K. Kitaura of Osaka City University for useful discussions and the MO calculations. We are also indebted to the Crystallographic Research Center, Institute for Protein Research, Osaka University, and Institute for Molecular Science for the use of computers.

Registry No. **1**, 75529-54-3; **2**, 79184-72-8; **3**, 83846-02-0; **4**, 75529-57-6; **6**, 75529-55-4; **7**, 83846-03-1; **8**, 75535-87-4; **10**, 83846-04-2; **11**, 51130-21-3.

Supplementary Material Available: A listing of observed and calculated structure factor amplitudes and tables of positional and anisotropic thermal parameters and bond lengths and angles (17 pages). Ordering information is given on any current masthead page.

(11) All spectral data for the previous compound were identical with those of **7**.

(12) The ab initio MO calculations for **10** and **11** were carried out by using a 3-21G basis set.[14] The geometries were optimized with the energy gradient technique.

(13) Morokuma, K.; Kato, S.; Kitaura, K.; Ohmine, I.; Sakai, S.; Obara, S. IMS Computer Center Program Library, The Institute for Molecular Science, 1980; Program No. 0372.

(14) (a) Gorden, M. S.; Binkley, J. S.; Pople, J. A.; Pietre, W. J.; Hehre, W. J. *J. Am. Chem. Soc.* **1982**, *104*, 2797. (b) Binkley, J. S.; Pople, J. A.; Hehre, W. J. *Ibid.* **1980**, *102*, 939.

(15) Germain, G.; Woolfson, M. M. *Acta Crystallog., Sect. B* **1968**, *B24*, 91.

Macrocycles Containing Tin. Two Syntheses of 1,1,6,6,11,11,16,16-Octaphenyl-1,6,11,16-tetrastannacycloeicosane and a Synthesis of 1,1,6,6-Tetraphenyl-1,6-distannacyclodecane

Martin Newcomb,*[1] Yutaka Azuma, and Arlene R. Courtney

Department of Chemistry, Texas A&M University College Station, Texas 77843

Received September 1, 1982

Summary: The title syntheses are described. The synthetic and purification and analytical methods employed are of general utility for the preparation and functionalization of members of this class of compounds.

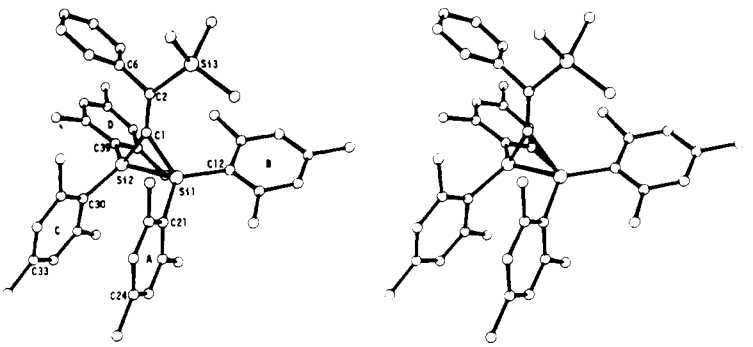

Figure 1. Stereoscopic view of 1,1,2,2-tetramesityl-3-[phenyl(trimethylsilyl)methylene]-1,2-disilacyclopropane (7).

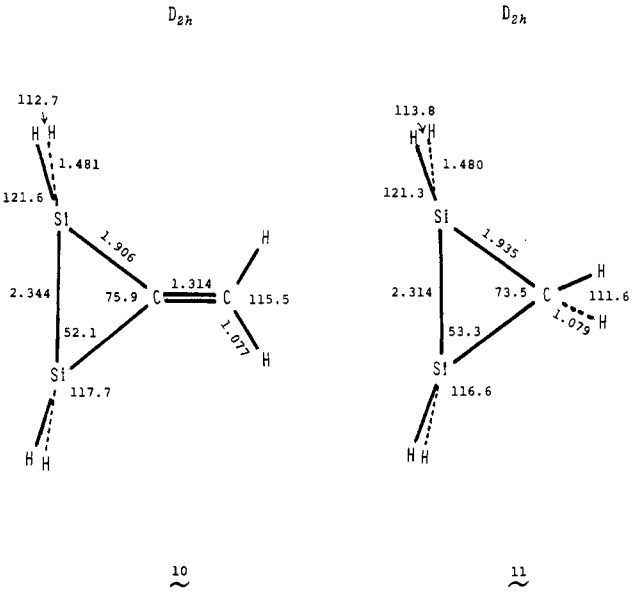

Figure 2. Geometries of 3-methylene-1,2-disilacyclopropane (**10**) and disilacyclopropane (**11**).

In contrast to the photolysis of **1**, when **6** was photolyzed in the absence of **2**, compound **7** was obtained in 8% yield,[11] together with 1-silacyclopropene **8** (65% yield). Both disilacyclopropanes **3** and **7** are stable toward atmospheric oxygen and moisture. They do not react with alcohols at room temperature.

The structure of **7** was determined by X-ray diffraction study. We also carried out ab initio MO calculations for 3-(methylene)-1,2-disilacyclopropane (**10**) and disilacyclopropane (**11**).[12,13] The crystals of **7** are triclinic of space group $P\bar{1}$ with cell dimensions a = 16.710 (3) Å, b = 13.150 (2) Å, c = 11.268 (3) Å, α = 70.96 (2)°, β = 66.94 (2)°, γ = 69.87 (2)°; V = 2085.6 (7) Å^3, and D_x = 1.171 Kg M^{-3} (Z = 2). The structure was solved by direct method.[15] Only the 3491 reflections with $I > 2\sigma(I)$ were used in the least-squares refinement (R = 0.053). Figure 1 shows a stereoscopic view of a single molecule. The disilacyclopropane ring and a plane consisting of Si(3), C(2), and C(6) atoms are almost coplanar with the dihedral angle of 7.6°. The sum of the bond angles of C(21)–Si(1)–Si(2), C(12)–Si(1)–Si(2), and C(12)–Si(1)–C(21) is 355.1° which is consistent with the corresponding values obtained from MO calculations for **10** (355.9°) and for **11** (356.4°), while the sum of the bond angles of C(39)–Si(2)–Si(1), C(30)–Si(2)–Si(1), and C(30)–Si(2)–C(39) is 343.4°. These results suggest that Si(1), C(12), C(21), Si(2), C(30), and C(39) atoms lie in almost the same plane. Two mesityl groups on Si(1) and Si(2) atoms, A and C rings, are fairly parallel to each other. The inter-ring distances C(21)–C(30) and C(24)–C(33) are 3.38 and 4.25 Å, respectively. The bond lengths of Si–Si (2.327 (2) Å) and two Si–C bonds (1.907 (4) Å (average)) in the disilacyclopropane ring are consistent with those of the respective normal bond. The bond angles of Si–C–Si and C–Si–Si in the ring are 75.2 (2) and 52.4 (1)° (average), respectively. Interestingly, these values are in good agreement with those obtained from MO calculations for **10** but not for **11** as shown in Figure 2.

The chemical behavior of the disilacyclopropanes is currently being examined and will be reported elsewhere.

Acknowledgment. We are grateful to Dr. K. Kitaura of Osaka City University for useful discussions and the MO calculations. We are also indebted to the Crystallographic Research Center, Institute for Protein Research, Osaka University, and Institute for Molecular Science for the use of computers.

Registry No. **1**, 75529-54-3; **2**, 79184-72-8; **3**, 83846-02-0; **4**, 75529-57-6; **6**, 75529-55-4; **7**, 83846-03-1; **8**, 75535-87-4; **10**, 83846-04-2; **11**, 51130-21-3.

Supplementary Material Available: A listing of observed and calculated structure factor amplitudes and tables of positional and anisotropic thermal parameters and bond lengths and angles (17 pages). Ordering information is given on any current masthead page.

(11) All spectral data for the previous compound were identical with those of **7**.

(12) The ab initio MO calculations for **10** and **11** were carried out by using a 3-21G basis set.[14] The geometries were optimized with the energy gradient technique.

(13) Morokuma, K.; Kato, S.; Kitaura, K.; Ohmine, I.; Sakai, S.; Obara, S. IMS Computer Center Program Library, The Institute for Molecular Science, 1980; Program No. 0372.

(14) (a) Gorden, M. S.; Binkley, J. S.; Pople, J. A.; Pietre, W. J.; Hehre, W. J. *J. Am. Chem. Soc.* **1982**, *104*, 2797. (b) Binkley, J. S.; Pople, J. A.; Hehre, W. J. *Ibid.* **1980**, *102*, 939.

(15) Germain, G.; Woolfson, M. M. *Acta Crystallog., Sect. B* **1968**, *B24*, 91.

Macrocycles Containing Tin. Two Syntheses of 1,1,6,6,11,11,16,16-Octaphenyl-1,6,11,16-tetrastannacycloeicosane and a Synthesis of 1,1,6,6-Tetraphenyl-1,6-distannacyclodecane

Martin Newcomb,*[1] Yutaka Azuma, and Arlene R. Courtney

Department of Chemistry, Texas A&M University College Station, Texas 77843

Received September 1, 1982

Summary: The title syntheses are described. The synthetic and purification and analytical methods employed are of general utility for the preparation and functionalization of members of this class of compounds.

Scheme I

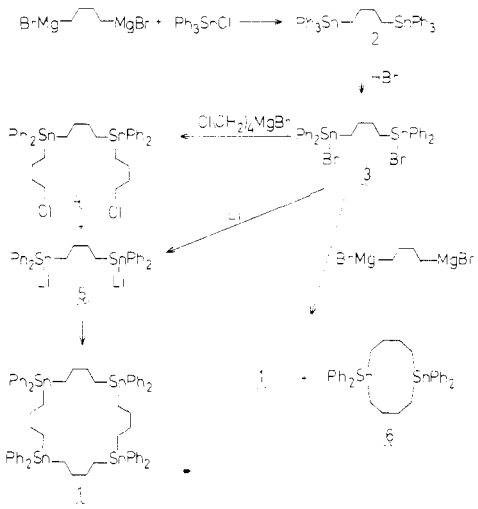

Macrocyclic, polydentate cation-complexing ligands (crown ethers, cryptands, etc.) have enjoyed a broad and useful chemistry during the past decade and a half, but their counterparts, anion-complexing macrocycles, have received relatively little attention. Recent advances in anion complexation, including structural selectivity, by macrocyclic polyammonium ligands suggest that this will be a fertile area of study.[2] Reasoning that polystanna macrocycles may be appropriately substituted to give *Lewis acid* complexing ligands that are direct analogues of crown ethers or cryptands, we have developed synthetic procedures for this class of compounds represented by the title compound **1**. Two approaches (Scheme I) have yielded the target 20-membered ring compound. The synthetic methods and purification techniques described herein are generally applicable for this class of compounds and also furnish tin functionalized macrocycles. We are unaware of other neutral macrocycles with the potential for anion complexation.

All reactions were run in argon or nitrogen atmospheres. Treatment of the diGrignard reagent from 1,4-dibromobutane with triphenylstannyl chloride in tetrahydrofuran (THF) gave 1,4-bis(triphenylstannyl)butane[3a,b] (**2**, mp 148.5–149 °C) in 77% isolated yield after recrystallization from hexane–dichloromethane (2:1, v:v). Unacceptably low selectivity was observed in several attempted conversions of **2** to 1,4-bis(bromodiphenylstannyl)butane (**3**) with various reagents and conditions; a second phenyl group was readily replaced, giving the dibromophenylstannyl moiety. However, treatment of **2** with 2.1 molar equiv of hydrogen bromide in dry dichloromethane at −78 °C followed by slow warming to room temperature gave, after recrystallization (dry ether), **3**[3a] in 75% yield (mp 88–90 °C). The dibromide **3** was treated with excess (4-chlorobutyl)magnesium bromide in THF at −10 °C for 1.5 h followed by warming to room temperature (7 h) to give 1,14-dichloro-5,5,10,10-tetraphenyl-5,10-distannatetradecane (**4**)[3a] that was purified by reverse-phase chromatography (C-18, methanol elution) in 62% yield (oil).

Table I. Spectroscopic Data for Isolated Products[a,b]

compd	^{1}H NMR, δ	^{1}H-decoupled ^{13}C NMR, δ	mol wt calcd	mol wt found[c]
2	7.10–7.53 (30 H, m)	138.9, 137.0, 128.7	755	734
	1.65–1.90 (4 H, m)	128.4, 31.3, 10.6		
	1.30–1.60 (4 H, m)			
3	7.17–7.67 (20 H, m)			
	1.71–1.93 (8 H, m)			
4	7.20–7.57 (20 H, m)			
	3.47 (4 H, t, J = 6 Hz)			
	1.57–1.87 (12 H, m)			
	1.03–1.40 (8 H, m)			
1	7.17–7.50 (40 H, m)	140.3, 136.7, 128.4	1315	1341
	1.53–1.87 (16 H, m)	128.2, 31.6, 10.4		
	1.17–1.47 (16 H, m)			
6	7.23–7.60 (20 H, m)	140.6, 136.5, 128.4	657	654
	1.57–2.03 (8 H, m)	128.2, 29.3, 10.1		
	1.37–1.50 (8 H, m)			

[a] NMR spectra of $CDCl_3$ solutions; chemical shifts are reported relative to Me_4Si. [b] Relatively featureless IR spectra (Nujol) were recorded for each compound; a characteristic Sn–Ph band at 1070 cm^{-1} was present in each spectrum. [c] Determined with chloroform solutions using a Hewlett-Packard Model 302B vapor pressure osmometer.

The two component macrocyclization was accomplished at high dilution. The dibromide **3** was added to excess lithium metal in THF to give the dilithium reagent **5** (total base = 63% of theory). A THF solution of **5** (diluted to 0.037 M) was added slowly (2 h) to a THF solution of **4** (1.0 molar equiv, 0.02 M) at 0 °C followed by warming to room temperature (12 h). After a conventional workup,[4] the crude product was purified by reverse-phase chromatography (C-18) with THF–acetonitrile elution (1:3, v:v) to give the desired macrocycle **1**[3] in 43% isolated yield (mp 107.5–108 °C from hexane–ether, 3:1).

Alternatively, macrocycle **1** was also obtained in lower yield from a high dilution, four-component macrocyclization reaction. Thus, the diGrignard reagent from 1,4-dibromobutane in THF (0.07 M) was added over 2 h to 1 molar equiv of dibromide **3** in THF (0.034 M) at 0 °C. After 12 h at room temperature, the reaction was quenched and worked up. The crude products were purified by preparative reverse-phase chromatography as above to give, after recrystallization, the desired macrocycle **1** in 16% yield and 1,1,6,6-tetraphenyl-1,6-distannacyclodecane[3a,b] (**6**, mp 114–114.5 °C, lit.[5] mp 96–98 °C) in 10%

(1) Camille and Henry Dreyfus Teacher-Scholar, 1980–1985.

(2) Dietrich, B.; Hosseini, M. W.; Lehn, J. M.; Sessions, R. B. *J. Am. Chem. Soc.* **1981**, *103*, 1282. Hosseini, M. W.; Lehn, J. M. *Ibid.* **1982**, *104*, 3525 and references therein.

(3) (a) The compound was characterized by ^{1}H NMR spectroscopy. (b) The compound was characterized by ^{1}H-decoupled ^{13}C NMR spectroscopy and by osmometric molecular weight determination. (c) A satisfactory elemental analysis (±0.4% for C and H) was obtained; see Table I for details of the spectroscopic characterization.[4]

(4) The workup of each reaction involving an organomagnesium or organolithium reagent was the same. At the completion of the reaction period the reaction mixture (a THF solution of 30–150 mL) was treated with 50 mL of saturated aqueous NH_4Cl solution. Phases were separated, and the aqueous phase was extracted with ether (2 × 50 mL). The combined organic phases were washed with 50 mL of saturated aqueous NaCl solution and dried with $MgSO_4$, and the solvent was removed in vacuo. The crude products were recrystallized or purified by chromatography as indicated in the text. Yields of isolated products 1–4 and 6 are given in the text.

yield. Compound 6 has been prepared by a different route.[5]

The macrocycles 1 and 6 may be analyzed readily by analytical HPLC (reverse phase, C-18) with methanol elution; the 10-membered ring compound 6 elutes before 1. However, for preparative chromatography, the solubilities of 1 and 6 in methanol are inconveniently low. Thus, chromatography with the mixed-solvent system THF–acetonitrile was developed. We found that analytical HPLC on 10 μm Spherisorb ODS columns correlated well with preparative chromatography on 40 μm ODS supplied by J. T. Baker Co.; the analytical phase retained material about 1.5 times as long as the preparative phase in terms of column volumes.

The procedures described above are generally useful for the preparation and functionalization of other tin-containing macrocycles. For example, the reactions of the 6-, 8-, and 10-carbon analogues of 3 with the corresponding chain-length α,ω-diGrignard reagents gave the 14-, 18-, and 22-membered ring analogues of the distanna compound 6, respectively, as well as low yields of the 28-, 36-, and 44-membered ring analogues of tetrastanna compound 1, respectively. All separations were accomplished by reverse-phase chromatography. Further, when the selective bromination procedure was applied to macrocycle 6, we obtained 1,6-dibromo-1,6-diphenyl-1,6-distannacyclodecane;[3a] this reaction exemplifies a critically important functionalization of the macrocycles. Finally, preparative reverse-phase chromatography of the intermediate tin bromides is also possible on a C-18 column with THF–acetonitrile elution if *dry* solvents are used.

As in any macrocyclization reaction, the high dilution methods we used required careful technique. However, in our minds, the key steps to obtaining macrocycle 1 were the selective bromination of 2 and our development of a preparative chromatography method. The two-component macrocyclization route and reverse-phase preparative chromatography permit the synthesis of 1 in gram batches. With the methods at hand we plan to prepare and functionalize several members of this class of compounds and explore their application in anion coordination chemistry.

Acknowledgment. This work was supported by the Office of Naval Research.

Registry No. 1, 83802-01-1; 2, 5274-40-8; 3, 83815-91-2; 4, 83815-92-3; 5, 83802-02-2; 6, 68970-21-8; $Br(CH_2)_4Br$, 110-52-1; Ph_3SnCl, 639-58-7; $Cl(CH_2)_4Br$, 6940-78-9.

(5) Davies, A. G.; Tse, M.-W.; Kennedy, J. D.; McFarlane, W.; Pyne, G. S.; Ladd, M. F. C.; Povey, D. C. *J. Chem. Soc., Chem. Commun.* **1978**, 791.

Investigations of Polymer-Supported Complexes of Platinum(II) by High-Resolution Solid-State ^{31}P NMR Spectroscopy Employing Magic-Angle Spinning and Cross-Polarization Techniques

H. C. Clark, J. A. Davies, C. A. Fyfe,* P. J. Hayes, and R. E. Wasylishen[1]

The Guelph-Waterloo Centre for Graduate Work in Chemistry
Department of Chemistry, University of Guelph
Guelph, Ontario, N1G 2W1 Canada

Received April 6, 1982

Summary: Solid-state ^{31}P NMR spectroscopy employing high-power proton decoupling, cross-polarization, and magic-angle spinning has been used to characterize various polymer-supported phosphines and their platinum complexes The reduction of polymer (polystyrene cross-linked with divinylbenzene) bound phosphine oxide, to the tertiary phosphine, and the immobilization of a platinum complex via the bound phosphine were monitored by these NMR techniques. The polymer-supported complex was synthesized by an alternate route, and the success of this process was confirmed by this NMR method. Platinum complexes were coordinated to poly(4-vinyl)pyridine, through the pyridine nitrogen, and the outcome of this process was elucidated from the solid-state ^{31}P NMR spectra of triphenylphosphine ligands which were coordinated to the platinum but which were not part of the polymer support.

In recent years there has been considerable research on polymer-bound transition-metal catalysts[2-7] but as yet little success has been achieved in determining either their general structure or the structure at the active site.

Theoretically, ^{31}P NMR spectroscopy is an attractive technique with which to investigate metal complexes which are bound to polymers via phosphine ligands. Research has been done on these systems employing high-resolution solution ^{31}P NMR[8,9] to study solvent-swollen polymers, but no resonances were observed for the immobilized catalyst. Solid-state ^{31}P NMR spectroscopy employing cross-polarization[10] with magic-angle spinning[11] (CP/MAS) has been used to study transition-metal phosphine complexes.[12,13] We have recently reported a thorough study[14] of tertiary phosphines, transition-metal phosphine complexes, and their analogues immobilized on glass and silica surfaces.

In the present study we have examined metal complexes supported on organic polymers, functionalized with tertiary phosphine and pyridine moieties utilizing solid-state CP/MAS ^{31}P NMR and high-resolution solution ^{31}P NMR spectroscopy in solution.

In the past polymer-immobilized catalysts have been prepared by first fixing a phosphine ligand to the polymer surface and then reacting this functionalized polymer with a metal complex. Two general methods have been used to synthesize such functionalized polymers: the first involves performing a chemical reaction on the polymer[15,16]

(1) Department of Chemistry, Dalhousie University, Halifax, Nova Scotia, Canada.
(2) Grubbs, R. H. *CHEMTECH* **1977**, 512.
(3) Hartley, F. R., Vezey, P. N. *Adv. Organomet. Chem.* **1977**, *15*, 189.
(4) Pittman, C. U., Jr.; Evans, G. O. *Chemtech.* **1973**, 560.
(5) Collman, R. P.; Hegedus, L. S. "Principles and Applications of Organotransition Metal Chemistry"; University Science Books: California, 1980; p 370.
(6) Bailar, J. D. *Catal. Rev.* **1974**, *10*, 17.
(7) Chauvin, Y.; Commereuc, D.; Dawans, F. *Prog. Polym. Sci.* **1977**, *5*, 95.
(8) Grubbs, R. H.; Su, S. G.-H. *Prepr. Div. Pet. Chem. Am. Chem. Soc.* **1977**, *22*, 1193.
(9) Naaktgeboren, A. J.; Nolte, R. J. M.; Drenth, W. *J. Am. Chem. Soc.* **1980**, *102*, 3350.
(10) Pines, A.; Gibby, M. G., Waugh, J. S. *J. Chem. Phys.* **1972**, *56*, 1776; **1973**, *59*, 569.
(11) Andrew, E. R. *Prog. Nucl. Magn. Reson. Spectrosc.* **1971**, *8*, 1.
(12) Maciel, G. E.; O'Donnell, D. J.; Greaves, R. *Adv. Chem. Ser.* **1982**, *No. 196*, 389.
(13) Diesveld, J. W.; Menger, E. M.; Edzes, H. T.; Veeman, W. S. *J. Am. Chem. Soc.* **1980**, *102*, 7935.
(14) Bemi, L.; Clark, H. C.; Davies, J. A.; Drexler, D.; Fyfe, C. A.; Wasylishen, R. E. *J. Organomet. Chem.* **1982**, *224*, C5.
(15) Collman, J. P.; Hegedus, L. S.; Cooke, M. P.; Norton, J. R.; Dolcetti, G.; Marquardt, D. N. *J. Am. Chem. Soc.* **1972**, *94*, 1789.
(16) Evans, G. O.; Pittman, C. U., Jr.; McMillan, R.; Beach, R. T.; Jones, R. *J. Organomet. Chem.* **1974**, *67*, 295.

0276-7333/83/2302-0177$01.50/0

yield. Compound 6 has been prepared by a different route.[5]

The macrocycles 1 and 6 may be analyzed readily by analytical HPLC (reverse phase, C-18) with methanol elution; the 10-membered ring compound 6 elutes before 1. However, for preparative chromatography, the solubilities of 1 and 6 in methanol are inconveniently low. Thus, chromatography with the mixed-solvent system THF–acetonitrile was developed. We found that analytical HPLC on 10 μm Spherisorb ODS columns correlated well with preparative chromatography on 40 μm ODS supplied by J. T. Baker Co.; the analytical phase retained material about 1.5 times as long as the preparative phase in terms of column volumes.

The procedures described above are generally useful for the preparation and functionalization of other tin-containing macrocycles. For example, the reactions of the 6-, 8-, and 10-carbon analogues of 3 with the corresponding chain-length α,ω-diGrignard reagents gave the 14-, 18-, and 22-membered ring analogues of the distanna compound 6, respectively, as well as low yields of the 28-, 36-, and 44-membered ring analogues of tetrastanna compound 1, respectively. All separations were accomplished by reverse-phase chromatography. Further, when the selective bromination procedure was applied to macrocycle 6, we obtained 1,6-dibromo-1,6-diphenyl-1,6-distannacyclodecane;[3a] this reaction exemplifies a critically important functionalization of the macrocycles. Finally, preparative reverse-phase chromatography of the intermediate tin bromides is also possible on a C-18 column with THF–acetonitrile elution if *dry* solvents are used.

As in any macrocyclization reaction, the high dilution methods we used required careful technique. However, in our minds, the key steps to obtaining macrocycle 1 were the selective bromination of 2 and our development of a preparative chromatography method. The two-component macrocyclization route and reverse-phase preparative chromatography permit the synthesis of 1 in gram batches. With the methods at hand we plan to prepare and functionalize several members of this class of compounds and explore their application in anion coordination chemistry.

Acknowledgment. This work was supported by the Office of Naval Research.

Registry No. 1, 83802-01-1; 2, 5274-40-8; 3, 83815-91-2; 4, 83815-92-3; 5, 83802-02-2; 6, 68970-21-8; $Br(CH_2)_4Br$, 110-52-1; Ph_3SnCl, 639-58-7; $Cl(CH_2)_4Br$, 6940-78-9.

(5) Davies, A. G.; Tse, M.-W.; Kennedy, J. D.; McFarlane, W.; Pyne, G. S.; Ladd, M. F. C.; Povey, D. C. *J. Chem. Soc., Chem. Commun.* **1978**, 791.

Investigations of Polymer-Supported Complexes of Platinum(II) by High-Resolution Solid-State ^{31}P NMR Spectroscopy Employing Magic-Angle Spinning and Cross-Polarization Techniques

H. C. Clark, J. A. Davies, C. A. Fyfe,* P. J. Hayes, and R. E. Wasylishen[1]

The Guelph-Waterloo Centre for Graduate Work in Chemistry
Department of Chemistry, University of Guelph
Guelph, Ontario, N1G 2W1 Canada

Received April 6, 1982

Summary: Solid-state ^{31}P NMR spectroscopy employing high-power proton decoupling, cross-polarization, and magic-angle spinning has been used to characterize various polymer-supported phosphines and their platinum complexes The reduction of polymer (polystyrene cross-linked with divinylbenzene) bound phosphine oxide, to the tertiary phosphine, and the immobilization of a platinum complex via the bound phosphine were monitored by these NMR techniques. The polymer-supported complex was synthesized by an alternate route, and the success of this process was confirmed by this NMR method. Platinum complexes were coordinated to poly(4-vinyl)pyridine, through the pyridine nitrogen, and the outcome of this process was elucidated from the solid-state ^{31}P NMR spectra of triphenylphosphine ligands which were coordinated to the platinum but which were not part of the polymer support.

In recent years there has been considerable research on polymer-bound transition-metal catalysts[2-7] but as yet little success has been achieved in determining either their general structure or the structure at the active site.

Theoretically, ^{31}P NMR spectroscopy is an attractive technique with which to investigate metal complexes which are bound to polymers via phosphine ligands. Research has been done on these systems employing high-resolution solution ^{31}P NMR[8,9] to study solvent-swollen polymers, but no resonances were observed for the immobilized catalyst. Solid-state ^{31}P NMR spectroscopy employing cross-polarization[10] with magic-angle spinning[11] (CP/MAS) has been used to study transition-metal phosphine complexes.[12,13] We have recently reported a thorough study[14] of tertiary phosphines, transition-metal phosphine complexes, and their analogues immobilized on glass and silica surfaces.

In the present study we have examined metal complexes supported on organic polymers, functionalized with tertiary phosphine and pyridine moieties utilizing solid-state CP/MAS ^{31}P NMR and high-resolution solution ^{31}P NMR spectroscopy in solution.

In the past polymer-immobilized catalysts have been prepared by first fixing a phosphine ligand to the polymer surface and then reacting this functionalized polymer with a metal complex. Two general methods have been used to synthesize such functionalized polymers: the first involves performing a chemical reaction on the polymer[15,16]

(1) Department of Chemistry, Dalhousie University, Halifax, Nova Scotia, Canada.
(2) Grubbs, R. H. *CHEMTECH* **1977**, 512.
(3) Hartley, F. R., Vezey, P. N. *Adv. Organomet. Chem.* **1977**, *15*, 189.
(4) Pittman, C. U., Jr.; Evans, G. O. *Chemtech.* **1973**, 560.
(5) Collman, R. P.; Hegedus, L. S. "Principles and Applications of Organotransition Metal Chemistry"; University Science Books: California, 1980; p 370.
(6) Bailar, J. D. *Catal. Rev.* **1974**, *10*, 17.
(7) Chauvin, Y.; Commereuc, D.; Dawans, F. *Prog. Polym. Sci.* **1977**, *5*, 95.
(8) Grubbs, R. H.; Su, S. G.-H. *Prepr. Div. Pet. Chem. Am. Chem. Soc.* **1977**, *22*, 1193.
(9) Naaktgeboren, A. J.; Nolte, R. J. M.; Drenth, W. *J. Am. Chem. Soc.* **1980**, *102*, 3350.
(10) Pines, A.; Gibby, M. G., Waugh, J. S. *J. Chem. Phys.* **1972**, *56*, 1776; **1973**, *59*, 569.
(11) Andrew, E. R. *Prog. Nucl. Magn. Reson. Spectrosc.* **1971**, *8*, 1.
(12) Maciel, G. E.; O'Donnell, D. J.; Greaves, R. *Adv. Chem. Ser.* **1982**, *No. 196*, 389.
(13) Diesveld, J. W.; Menger, E. M.; Edzes, H. T.; Veeman, W. S. *J. Am. Chem. Soc.* **1980**, *102*, 7935.
(14) Bemi, L.; Clark, H. C.; Davies, J. A.; Drexler, D.; Fyfe, C. A.; Wasylishen, R. E. *J. Organomet. Chem.* **1982**, *224*, C5.
(15) Collman, J. P.; Hegedus, L. S.; Cooke, M. P.; Norton, J. R.; Dolcetti, G.; Marquardt, D. N. *J. Am. Chem. Soc.* **1972**, *94*, 1789.
(16) Evans, G. O.; Pittman, C. U., Jr.; McMillan, R.; Beach, R. T.; Jones, R. *J. Organomet. Chem.* **1974**, *67*, 295.

0276-7333/83/2302-0177$01.50/0

(e.g., polystyrene cross-linked with divinylbenzene) to attach the phosphorus group (for example see eq 1). The second method employs a functionalized monomer in a copolymerization with styrene and divinylbenzene[17] (see eq 2).

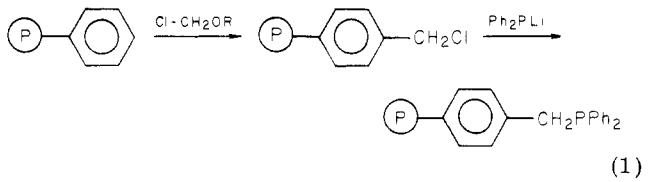

(1)

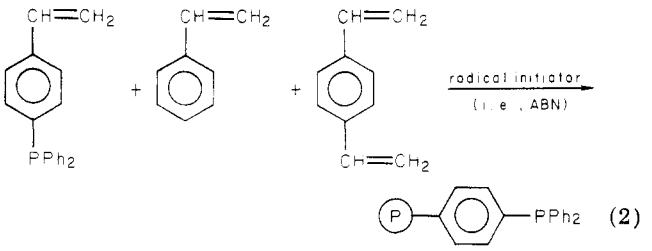

(2)

Functionalized polymer samples, prepared by both methods, were analyzed by solid-state CP/MAS ^{31}P NMR and also by high-resolution solution ^{31}P NMR spectroscopy. The solid-state CP/MAS ^{31}P NMR spectrum of a commercial sample of polymer-supported triphenylphosphine, prepared via the first method, showed two resonances (see Figure 1A). The resonance at −5.3 ppm (relative to external 85% H_3PO_4) could be identified, by comparison with the spectrum of *p*-styryldiphenylphosphine, as due to polymer-immobilized triphenylphosphine. (In accordance with IUPAC convention a negative chemical shift signifies an upfield shift.) The other resonance, appearing at approximately 25 ppm, could be attributed to the presence of phosphine oxide as confirmed by comparison with the solid-state CP/MAS ^{31}P NMR spectrum of *p*-styryldiphenylphosphine oxide. Samples of functionalized polymers, prepared by the copolymerization method, displayed resonances in the solid-state CP/MAS ^{31}P NMR spectra, similar to those of polymers prepared by the first method.

In order to ensure the success of the reaction between functionalized polymer and complex, it was necessary to convert all immobilized phosphine oxide to tertiary phosphine. Usually silane reagents (e.g., trichlorosilane) are reacted with the oxide to accomplish this, and considerable work has been done on the reduction[18,19] of free phosphine oxides. No report of the reduction of polymer-bound phosphine oxides has previously been made, but recently we have reported the reduction of phosphine oxides immobilized on glass.[14] Samples of functionalized polymers with high phosphine oxide content were subjected to trichlorosilane treatment, and in most cases a virtually quantitative disappearance of the phosphine oxide resonance, in the solid-state CP/MAS ^{31}P NMR spectrum, was observed.

The final step in the preparation of the polymer-bound catalysts, the reaction between a metal complex and a functionalized polymer, was monitored by both solid-state CP/MAS ^{31}P NMR and high-resolution solution ^{31}P NMR spectroscopy. Polymer samples, before and after treatment with trichlorosilane, were reacted with $[PtCl_2(NCPh)_2]$. Those which had not been treated with trichlorosilane displayed only a single resonance due to phosphine oxide in the solid-state CP/MAS ^{31}P spectrum. The trichlorosilane-treated samples, however, displayed a pattern of resonances similar to those found in the high-resolution solution ^{31}P NMR spectrum of the analogous free metal complex after exchange with $[PtCl_2(NCPh)_2]$. It was noted

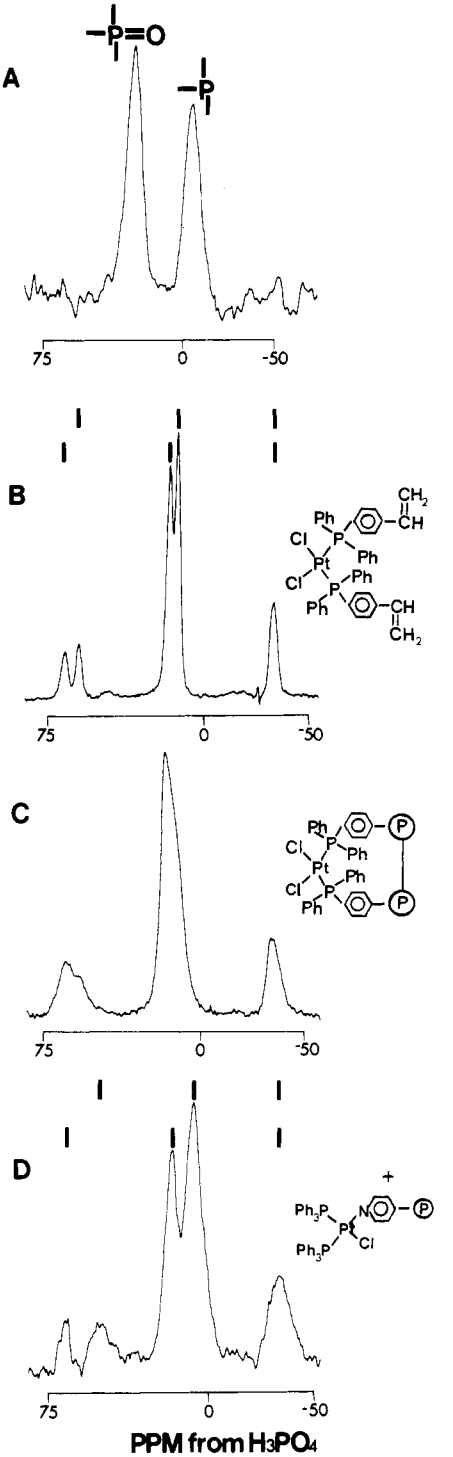

Figure 1. (A) Solid-state CP/MAS ^{31}P NMR spectrum of a commercial samples of polymer-bound (polystyrene cross-linked with 2% divinylbenzene) triphenylphosphine (2870 scans and 50-Hz line broadening). (B) Solid-state CP/MAS ^{31}P NMR spectrum of *cis*-$[PtCl_2(PPh_2C_6H_4CH{=}CH_2)_2]$ (1774 scans and no line broadening). (C) Solid-state CP/MAS ^{31}P NMR spectrum of a copolymer of 65% styrene, 31% divinylbenzene and 4% *cis*-$[PtCl_2(PPh_2C_6H_4CH{=}CH_2)_2]$ after Soxhlet extraction (36 196 scans and 10-Hz line broadening). (D) Solid-state CP/MAS ^{31}P NMR spectrum of *cis*-$[PtCl(PPh_3)_2(py\text{-}Ⓟ)]^+(ClO_4)^-$ after Soxhlet extraction (17 142 scans and 25-Hz line broadening).

(17) (a) McKinley, S. V.; Rakshys, J. W. U.S. Patent 3 708 462, 1973. (b) Rabinowitz, R.; Marcus, R.; Pellon, J. *J. Polym. Sci., Part A* **1964**, *2*, 1241.
(18) Fritzsche, H.; Hasserodt, U.; Korte, F. *Chem. Ber.* **1964**, *97*, 1988.
(19) Fritzsche, H.; Hasserodt, U.; Korte, F. *Chem. Ber.* **1965**, *98*, 1681.

that a mild, initial reaction of the complex with the functionalized polymer yielded a product whose spectrum confirmed the success of the immobilization but a resonance due to unreacted phosphine, at −5.4 ppm, indicated that the reaction was not complete. Comparison with high-resolution solution ^{31}P NMR spectra of analogous free complexes indicated that resonances at 11.8 and 20.9 ppm were due to the immobilized complex. The appearance, however, of more than one resonance in this region, along with associated ^{195}Pt–^{31}P satellites, suggests that a complex mixture of products exists. The spectrum could not be interpreted without ambiguity, and species other than *cis*- and *trans*-$[PtCl_2(PR_3)_2]$ and free PR_3 units may be present.

The initially reacted polymer was again reacted with $[PtCl_2(NCPh)_2]$ but in this instance more rigorous conditions were employed. The resonance, in the solid-state CP/MAS ^{31}P NMR due to the uncomplexed phosphine, disappeared, thus confirming the completion of the reaction. The high-resolution solution ^{31}P NMR spectrum of this product showed only a broad featureless resonance. This failure to observe any large, relatively sharp resonance due to the complexed phosphine, while a relatively sharp peak was observed prior to coordination, has been attributed in previous work,[8] to an increase in the relaxation rate of the phosphorus upon coordination. A general explanation[20] may be that coordination severely restricts the mobility of the immobilized phosphines and thus prevents their quantitative detection by high-resolution solution NMR techniques.

Elemental analyses, to determine the percentage of phosphorous by weight, were performed on samples of immobilized ligand before and after treatment with the metal complex. Prior to treatment, 1.3% P was found in the sample (expected 2.0% P from 8% phosphine ligand by molar ratio polymerized with styrene and DVB) while after final treatment this value dropped to 0.9% of P.

The success of the preparation of the functionalized polymer by the copolymerization method and other previous studies[21-23] suggested that the polymer-immobilized complex might be synthesized by copolymerizing a metal complex containing *p*-styryldiphenylphosphine ligands with styrene and divinylbenzene rather than reacting a functionalized polymer with a metal complex (see eq 3).

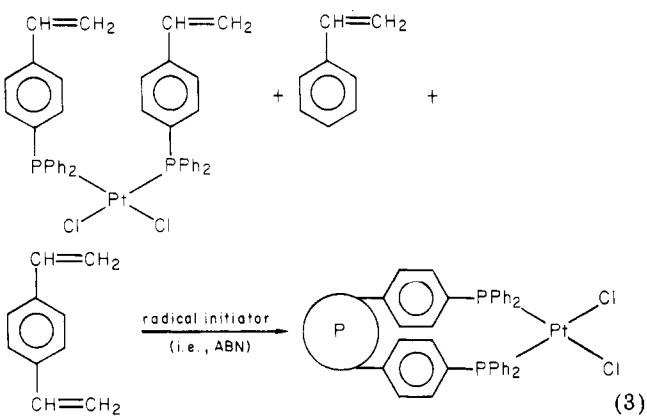

(3)

The complex to be copolymerized *cis*-$[PtCl_2(PPh_2C_6H_4CH{=}CH_2)_2]$ was analyzed by high-resolution solution ^{31}P NMR and solid-state CP/MAS ^{31}P NMR spectroscopy. The high-resolution solution spectrum of the complex consisted of a single, central resonance at 13.6 ppm, but the solid-state CP/MAS spectrum showed central resonances due to two types of phosphorus nuclei at 11.8 and 15.6 ppm (see Figure 1B). The freezing in of a fixed conformation (the equivalence in solution resulting from rotation about the Pt–P bonds), which minimizes the steric effects of the bulky ligands, could explain two inequivalent phosphorus nuclei.

This hypothesis is confirmed by a recent X-ray crystal structure of *cis*-$[PtCl_2(PPh_3)_2]$.[24] Copolymers of 2%, 15%, and 30% cross-linking were prepared and analyzed by solid-state CP/MAS ^{31}P NMR. The 15% and 30% cross-linked samples were subjected to rigorous Soxhlet extraction, and their ^{31}P spectra (see Figure 1C) afterward confirmed the success of the incorporation, and, by comparison with the spectrum of the complex prior to incorporation, it was observed that the complex remained in the cis geometry.

High-resolution solution ^{31}P NMR spectra were run of the cross-linked samples of the copolymerized complex, and these were compared to spectra of similarly cross-linked samples of trichlorosilane-treated, functionalized polymers. For the three functionalized polymers there was a broadening of the single resonance, due to the immobilized phosphine, indicating that as the degree of cross-linking increases, the mobility of the phosphorus nuclei decrease. For samples of identical degrees of cross-linking, the resonances were much broader in the spectra of the copolymerized complexes than in the spectra of the corresponding functionalized polymers, in agreement with the earlier conclusion[20] that when the immobilized phosphine is coordinated, its mobility is greatly restricted.

Results of elemental analysis for phosphorus yielded values for the immobilized ligands of 1.3% P (2% DVB), 1.3% P (15% DVB), and 1.5% P (30% DVB), expected 2.0% P. The results for the polymers prepared by direct incorporation of metal complex were less reliable: 2.50% P (2% DVB; it was not possible to Soxhlet extract this material), 2.4% P (15% DVB), and 1.45% P (30% DVB). In all of these cases values of 1.2% P were expected (4% *cis*-$[PtCl_2(CH_2{=}CHC_6H_4PPh_2)_2]$ (by molar ratio, copolymerized with styrene and DVB).

The solid-state CP/MAS ^{31}P NMR technique may also be used to characterize polymer-immobilized catalysts in systems which do not employ a phosphine ligand as a link between polymer and complex but where a phosphine ligand is still present as a probe of the molecular structure. Poly(4-vinyl)pyridine beads (cross-linked) were reacted with both neutral and cationic halide-bridged dimeric platinum complexes such that the nitrogen of the pyridine was directly coordinated to the platinum center (see eq 4 and 5). Solid-state CP/MAS ^{31}P NMR spectra of the

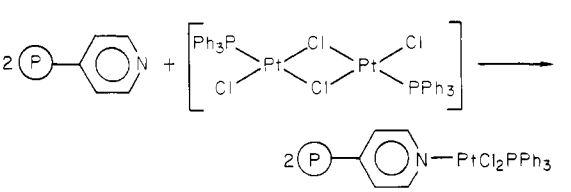

(4)

poly(4-vinyl)pyridine complexes were almost identical with the solid-state CP/MAS ^{31}P NMR spectrum of analogous free metal complexes. The poly(4-vinyl)pyridine complexes were Soxhlet extracted after reaction so the similarity between the spectra indicates that the immobilization was successful. The solid-state CP/MAS ^{31}P NMR

(20) Fritschel, S. J.; Ackerman, J. J. H.; Keyser, T.; Stille, J. K. *J. Org. Chem.* **1979**, *44*, 3152.
(21) Pittman, C. U., Jr., In "Organometallic Polymers"; Academic Press: New York, 1978; p 1.
(22) Imperial Chemical Industries, French Patent 2030134.
(23) Imperial Chemical Industries, French Patent 2013481.
(24) Anderson, G. K.; Clark, H. C.; Davies, J. A.; Ferguson, G.; Parvez, M. *J. Cryst. Spectrosc. Reson.*, **1982**, *12*, 449.

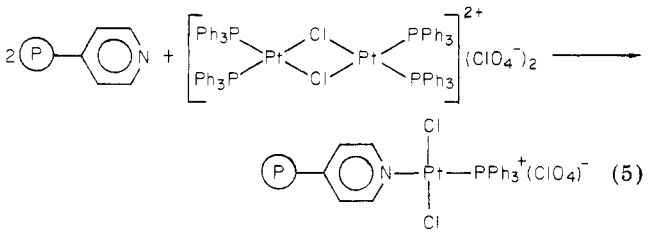

(5)

spectrum of the polymeric cationic pyridine complex (see Figure 1D) shows central resonances due to two different phosphorus nuclei (elemental analysis 0.42% P). The nonequivalence, in this case, is due to the fact that each phosphorus is trans to a different ligand. The solid-state CP/MAS ^{31}P NMR spectrum of the polymeric neutral complex indicated that both cis and trans isomers of $[PtCl_2(PPh_3)(py\text{-}Ⓟ)]$ were formed (elemental analysis 0.27% P).

Further investigations, employing solid-state CP/MAS ^{31}P NMR spectroscopy, of the polymer-supported complexes are underway at the present time.

Acknowledgment. We acknowledge the financial support of the Natural Science and Engineering Research Council of Canada in the form of operating grants (H.C.C., C.A.F., and R.E.W.) and Johnson Matthey Limited for a very generous loan of platinum metal salts. They also thank Reilly Tar and Chemical Corp. for a gift of poly(4-vinyl)pyridine and Dr. R.L. Dudley for his assistance. R.E.W. thanks the University of Winnipeg for the granting of a sabbatical leave. Chemical analyses were carried out by Huffman Laboratories, Wheat Ridge, CO, 80033.

Registry No. *p*-(Diphenylphosphino)styrene styrene *p*-divinylbenzene copolymer, 83816-34-6; *cis*-$[PtCl_2(PPh_2C_6H_4CH{=}CH_2)_2]$, 83831-00-9; *cis*-$[PtCl_2(PPh_2C_6H_4CH{=}CH_2)_2]\cdot PhCH{=}CH_2{\cdot}CH_2{=}CHC_6H_4CH{=}CH_2$ copolymer, 83844-73-9.

Syntheses of the First Mixed-Metal Clusters with $Ph_2PCH_2PPh_2$. Crystal Structures of the Metalloligated Triangulo Clusters $Pd_2Co_2(CO)_7(Ph_2PCH_2PPh_2)_2$ and $Pt_2Mo_2(\eta^5\text{-}C_5H_5)_2(CO)_6(Ph_2PCH_2CH_2PPh_2)$[1]

Pierre Braunstein* and Jean-Marc Jud

Laboratoire de Chimie de Coordination, ERA 670 CNRS
Institut Le Bel, Université Louis Pasteur
F-67070 Strasbourg Cédex, France

Yves Dusausoy

Laboratoire de Minéralogie-Cristallographie, ERA 162 CNRS
Université de Nancy 1, C.O. 140
F-54037 Nancy, France

Jean Fischer

Laboratoire de Cristallochimie, ERA 08 CNRS
Institut Le Bel, Université Louis Pasteur
F-67070 Strasbourg Cédex, France

Received September 23, 1982

Summary: The first heterometallic palladium–cobalt, –molybdenum, –tungsten clusters containing the $Ph_2PCH_2PPh_2$ (dppm) ligand have been prepared from reactions between $[PdCl(dppm)]_2$ and $Co(CO)_4^-$, $Mo(CO)_3Cp^-$, and $W(CO)_3Cp^-$, respectively. The structure of the metalloligated $Pd_2Co_2(CO)_7(dppm)_2$ cluster has been established by X-ray diffraction. Reaction of *trans*-$Pt[Mo(CO)_3Cp]_2(PhCN)_2$ with $Ph_2PCH_2CH_2PPh_2$ affords the metalloligated $Pt_2Mo_2Cp_2(CO)_6(dppe)$ cluster, whose structure was determined by X-ray diffraction.

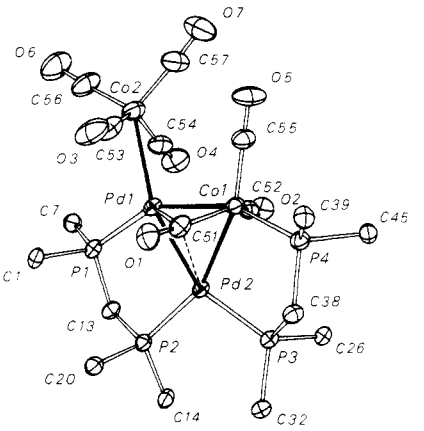

Figure 1. Diagram of the molecular structure of $Pd_2Co_2(CO)_7(dppm)_2$ (1). Principal dimensions are given in Table I.

The stereochemical influence of the $Ph_2PCH_2PPh_2$ (dppm) ligand on the synthesis, structure, and reactivity of homobimetallic transition metal complexes has aroused a considerable interest in the past few years. This is motivated by the remarkable and unique properties of these complexes for the unusual coordination of small molecules, their activation and catalytic transformations, which is notable in but not limited to CO chemistry.[2,3] One can expect that if analogous systems were available with metal atoms of a different nature, a new dimension could be introduced into the reactivity and catalytic applications of these molecules, parallel to that observed on going from homo- to heteropolymetallic clusters.[4] Surprisingly, the first example of an heterobimetallic complex containing the dppm ligand(s): $PdPtCl_2(dppm)_2$ has only been reported very recently,[5] but until now no mixed-metal *cluster* with this ligand has been structurally described.

Two strategies can be considered for the preparation of mixed-metal clusters containing phosphine ligands. Method a involves the reaction of a metal complex containing the desired ligand with another metal fragment in the sequence [ML] + [M′] → [MM′L]. The second method

(1) Organometallic Complexes with Metal-Metal Bonds. Part 20. Part 19, see ref 6.

(2) See, for example: (a) Cotton, F. A.; Troup, J. M. *J. Am. Chem. Soc.* **1974**, *96*, 4422. (b) Cotton, F. A.; Shive, L. W.; Stults, B. R. *Inorg. Chem.* **1976**, *15*, 2239. (c) Holloway, R. G.; Penfold, B. R.; Colton, R.; McCormick, M. J. *J. Chem. Soc., Chem. Commun.* **1976**, 485. (d) Kubiak, C. P.; Eisenberg, R. *J. Am. Chem. Soc.* **1977**, *99*, 6129. (e) Olmstead, M. M.; Hope, H.; Benner, L. S.; Balch, A. L. *Ibid.* **1977**, *99*, 5502. (f) Brown, M. P.; Puddephatt, R. J.; Rashidi, M.; Seddon, K. R. *J. Chem. Soc., Dalton Trans.* **1977**, 951. (g) Chin, C. S.; Sennett, M. S.; Wier, P. J.; Vaska, L. *Inorg. Chim. Acta* **1978**, *31*, L443. (h) Brown, M. P.; Cooper, J. S.; Puddephatt, R. J.; Thomson, M. A.; Seddon, K. R. *J. Chem. Soc., Chem. Commun.* **1979**, 1117. (i) Balch, A. L.; Benner, L. S.; Olmstead, M. M. *Inorg. Chem.* **1979**, *18*, 2996. (j) Balch, A. L.; Lee, C. L.; Lindsay, C. H.; Olmstead, M. M. *J. Organomet. Chem.* **1979**, *177*, C22. (k) Brown, M. P.; Fischer, J. R.; Manojlović-Muir, L.; Muir, K. W.; Puddephatt, R. J.; Thomson, M. A.; Seddon, K. R. *J. Chem. Soc., Chem. Commun.* **1979**, 931, 1117. (l) Kubiak, C. P.; Eisenberg, R. *Inorg. Chem.* **1980**, *19*, 2726, 2733. (m) Hoffman, D. M.; Hoffmann, R. *Ibid.* **1981**, *20*, 3543. (n) Frew, A. A.; Hill, R. H.; Manojlović-Muir, L.; Muir, K. W.; Puddephatt, R. J. *J. Chem. Soc., Chem. Commun.* **1982**, 198.

(3) Benner, L. S.; Balch, A. L. *J. Am. Chem. Soc.* **1978**, *100*, 6099.

(4) Gladfelter, W. L.; Geoffroy, G. L. *Adv. Organomet. Chem.* **1980**, *18*, 207.

(5) Pringle, P. G.; Shaw, B. L. *J. Chem. Soc., Chem. Commun.* **1982**, 81.

0276-7333/83/2302-0180$01.50/0

Laboratoire de Chimie de Coordination was supported by the CNRS (Greco-CO).

Registry No. 1, 83704-63-6; 3, 83704-64-7; 4, 83704-65-8; 5, 83704-66-9; Co, 7440-48-4; Mo, 7439-98-7; $[PdCldppm]_2$, 83704-67-0; $NaCo(CO)_4$, 14878-28-5; $NaMo(CO)_3Cp$, 12107-35-6; $NaW(CO)_3Cp$, 12107-36-7; *trans*-$Pt[Mo(CO)_3Cp]_2(PhCN)_2$, 83704-68-1; $PtCl_2(dppe)$, 14647-25-7; W, 7440-33-7; Pd, 7440-05-3; Pt, 7440-06-4.

Supplementary Material Available: Tables of the positional and thermal parameters and their estimated standard deviations for compounds 1 and 5 (6 pages). Ordering information is given on any current masthead page.

Basic Cluster Reactions. 3.[1] Hetero Site Reactivities in $Ru_2Co_2(CO)_{13}$

Eckehart Roland and Heinrich Vahrenkamp*

Institut für Anorganische Chemie der Universität Freiburg D-7800 Freiburg, Germany

Received July 8, 1982

Summary: Two metal-specific reactions have been observed for the tetrahedral cluster $Ru_2Co_2(CO)_{13}$ under very mild conditions. Hydrogen reacts at the ruthenium atoms to form $H_2Ru_2Co_2(CO)_{12}$. Alkynes insert between the cobalt atoms to form $Ru_2Co_2(CO)_{11}(R_2C_2)$.

The advantages of mixed-metal clusters in studying cluster reactivity and molecular dynamics as well as their catalytic potential due to the their possible different site reactivities have been stressed.[2,3] However, few reactions of mixed-metal clusters have been found yet to underline this.[2,4] In particular, we are not aware of such a cluster for which reactions with simple substrates at different specific locations in the cluster core have been reported.[5] We have now observed that the ternary metal carbonyl $Ru_2Co_2(CO)_{13}$[6] possesses hetero site reactivity.

The two reagents chosen were hydrogen and internal acetylenes, both well established in cluster chemistry.[7,8] From their different reactivities toward simple clusters of cobalt and ruthenium one could expect that hydrogen would prefer the ruthenium sites and acetylenes would prefer the cobalt sites in a mixed cobalt–ruthenium cluster. This was observed. Both reactions proceeded in *n*-hexane at 45–50 °C. Stirring of $Ru_2Co_2(CO)_{13}$ for 3 h under an atmosphere of H_2 produced black **1**,[9] isolated in 78% yield by crystallization from toluene. Reaction of $Ru_2Co_2(CO)_{13}$ with diphenylacetylene for 4 h yielded dark green **2**,[10] isolated in 76% yield by cooling the solution to 4 °C. 3-Hexyne reacted equivalently.

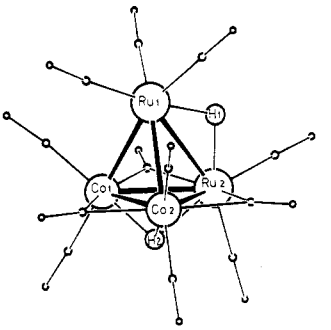

Figure 1. Molecular structure of $H_2Ru_2Co_2(CO)_{12}$ (1): small circles, CO ligands. H atoms were located but not refined. Bond lengths (pm): Ru1–Ru2 = 290.4 (1), Ru1–Co1 = 266.6 (1), Ru1–Co2 = 266.3 (1), Ru2–Co1 = 264.3 (1), Ru2–Co2 = 265.3 (1), Co1–Co2 = 254.6 (1), Ru1–H1 = 190, Ru2–H1 = 177, Ru2–H2 = 196, Co1–H2 = 173, Co2–H2 = 180.

$H_2Ru_2Co_2(CO)_{12}$ **1** $\qquad$ $Ru_2Co_2(CO)_{11}(Ph_2C_2)$ **2**

The compositions of both new clusters were determined by FD mass spectra. The reaction sites were deduced for 1 from NMR data[11] and established for 1 and 2 by crystal structure analyses.[12] The hydrogen positions in 1 were located from difference Fourier maps as well as by Orpen's H searching program.[13] Figures 1 and 2 give the overall molecular structures and important bond lengths. The cluster core geometries and ligand distributions are normal in both cases. There is a striking similarity (including unit cell dimensions) between 1 and $Co_4(CO)_{12}$[14] or $HFeCo_3(CO)_{12}$,[15] whereas 2 is intermediate between $Co_4(CO)_{10}(R_2C_2)$[16] and $Ru_4(CO)_{12}(R_2C_2)$.[17]

The structures show that the preferred reaction sites have been used. The acetylene in 2 has been inserted between the two cobalt atoms, thereby opening the cluster and forming a closo $Ru_2Co_2C_2$ core. The hydrogen atoms in 1 are associated with the ruthenium atoms, one of them

(1) Part 2: Vahrenkamp, H.; Wolters, D. *Organometallics* **1982**, *1*, 874.
(2) Gladfelter, W. L.; Geoffroy, G. L. *Adv. Organomet. Chem.* **1980**, *18*, 207.
(3) Vahrenkamp, H. *Philos. Trans. R. Soc. London*, in press.
(4) Cf. Richter, F.; Vahrenkamp, H. *Organometallics* **1982**, *1*, 756.
(5) Among the few reactions of mixed-metal clusters with different substrates are the nonspecific reactions of $H_2FeRu_3(CO)_{13}$ with H_2 and alkynes: Knox, S. A. R.; Koepke, J. W.; Andrews, M. A.; Kaesz, H. D. *J. Am. Chem. Soc.* **1975**, *97*, 3942. Fox, J. R.; Gladfelter, W. L.; Geoffroy, G. L.; Tavanaiepour, I.; Abdel-Mequid, S.; Day, V. W. *Inorg. Chem.* **1981**, *20*, 3230.
(6) Roland, E.; Vahrenkamp, H. *Angew. Chem.* **1981**, *93*, 714; *Angew. Chem., Int. Ed. Engl.* **1981**, *20*, 679.
(7) Humphries, H. P.; Kaesz, H. D. *Prog. Inorg. Chem.* **1979**, *25*, 145.
(8) Deeming, A. J., In "Transition Metal Clusters"; Johnson, B. F. G., Ed.; Wiley: New York, 1980; p 391.
(9) $H_2Ru_2Co_2(CO)_{12}$ (1): black crystals; mp 175 °C dec; IR ($CHCl_3$) 2112 (vw), 2082 (s), 2058 (vs), 2050 (sh), 2032 (sh), 1880 (w), 1868 (sh) cm^{-1}; ^1H NMR (CD_2Cl_2) broad resonance at −18.8 ppm. Anal. Calcd for $[C_{12}H_2Co_2O_{12}Ru_2]$: C, 21.90; H, 0.31. Found: C, 22.22; H, 0.08.
(10) $Ru_2Co_2(CO)_{11}(Ph_2C_2)$ (2): green-black crystals; mp 194 °C dec; IR (cyclohexane) 2090 (w), 2052 (vs), 2047 (s), 2019 (m), 2006 (w), 1881 (w), 1861 (w) cm^{-1}; ^1H NMR ($CDCl_3$) multiplet centered at 7.07 ppm. Anal. Calcd for $[C_{25}H_{10}Co_2O_{11}Ru_2]$: C, 37.24; H, 1.25. Found: C, 36.94; H, 0.80.
(11) Upon cooling of CD_2Cl_2 solutions of 1 the broad ^1H NMR resonance sharpens and moves to high field. At −60 °C when the low solubility of 1 limits further cooling there is a sharp signal at −20.36 ppm which we associate with a Ru–Ru edge bridging hydrogen because of the strong broadening effect of the quadrupolar cobalt nuclei. The second signal to be expected to the low field side of this which would have to be associated with a Ru/Co or Co/Co bridging hydrogen is too broad to be observed.
(12) Crystals of 1 were obtained from toluene and those of 2 from hexane. The crystal quality was checked by Weissenberg photographs; all other measurements were done on a Nonius CAD 4 diffractometer. 1: monoclinic, space group $P2_1/c$, $Z = 4$, $a = 930.4$ (1) pm, $b = 1153.0$ (2) pm, $c = 1664.2$ (4) pm, $\beta = 91.28$ (2)°. 2: monoclinic, space group $P2_1/c$, $Z = 4$, $a = 922.6$ (4) pm, $b = 1168.8$ (1) pm, $c = 2398.1$ (3) pm, $\beta = 93.77$ (2)°. The structures were solved by direct methods. Full matrix refinement (anisotropic for all non-hydrogen atoms, phenyl groups in 2 as rigid bodies with H atoms isotropic, H atoms in 1 located but not refined) using unit weights resulted in R values of 0.040 for 1 and 0.036 for 2. All details of the crystallographic work are documented in the supplementary material: Table A contains all crystallographic data, Tables B and C list all atomic parameters, Tables D and E all bond lengths and angles for both compounds, Tables F and G give the F_o/F_c listings, and Figures A and B show the detailed molecular structures and atom numbering schemes.
(13) Orpen, A. G. *J. Chem. Soc., Dalton Trans.* **1980**, 2509.
(14) Wei, C. H. *Inorg. Chem.* **1969**, *8*, 2384.
(15) Cf. Huie, B. T.; Knobler, C. B.; Kaesz, H. D. *J. Am. Chem. Soc.* **1978**, *100*, 3059.
(16) Dahl, L. F.; Smith, D. L. *J. Am. Chem. Soc.* **1962**, *84*, 2450.
(17) Johnson, B. F. G.; Lewis, J.; Reichert, B. E.; Schorpp, K. T.; Sheldrick, G. M. *J. Chem. Soc., Dalton Trans.* **1977**, 1417.

0276-7333/83/2302-0183$01.50/0

Laboratoire de Chimie de Coordination was supported by the CNRS (Greco-CO).

Registry No. 1, 83704-63-6; 3, 83704-64-7; 4, 83704-65-8; 5, 83704-66-9; Co, 7440-48-4; Mo, 7439-98-7; $[PdCldppm]_2$, 83704-67-0; $NaCo(CO)_4$, 14878-28-5; $NaMo(CO)_3Cp$, 12107-35-6; $NaW(CO)_3Cp$, 12107-36-7; *trans*-$Pt[Mo(CO)_3Cp]_2(PhCN)_2$, 83704-68-1; $PtCl_2(dppe)$, 14647-25-7; W, 7440-33-7; Pd, 7440-05-3; Pt, 7440-06-4.

Supplementary Material Available: Tables of the positional and thermal parameters and their estimated standard deviations for compounds 1 and 5 (6 pages). Ordering information is given on any current masthead page.

Basic Cluster Reactions. 3.[1] Hetero Site Reactivities in $Ru_2Co_2(CO)_{13}$

Eckehart Roland and Heinrich Vahrenkamp*

Institut für Anorganische Chemie der Universität Freiburg D-7800 Freiburg, Germany

Received July 8, 1982

Summary: Two metal-specific reactions have been observed for the tetrahedral cluster $Ru_2Co_2(CO)_{13}$ under very mild conditions. Hydrogen reacts at the ruthenium atoms to form $H_2Ru_2Co_2(CO)_{12}$. Alkynes insert between the cobalt atoms to form $Ru_2Co_2(CO)_{11}(R_2C_2)$.

The advantages of mixed-metal clusters in studying cluster reactivity and molecular dynamics as well as their catalytic potential due to the their possible different site reactivities have been stressed.[2,3] However, few reactions of mixed-metal clusters have been found yet to underline this.[2,4] In particular, we are not aware of such a cluster for which reactions with simple substrates at different specific locations in the cluster core have been reported.[5] We have now observed that the ternary metal carbonyl $Ru_2Co_2(CO)_{13}$[6] possesses hetero site reactivity.

The two reagents chosen were hydrogen and internal acetylenes, both well established in cluster chemistry.[7,8] From their different reactivities toward simple clusters of cobalt and ruthenium one could expect that hydrogen would prefer the ruthenium sites and acetylenes would prefer the cobalt sites in a mixed cobalt–ruthenium cluster. This was observed. Both reactions proceeded in *n*-hexane at 45–50 °C. Stirring of $Ru_2Co_2(CO)_{13}$ for 3 h under an atmosphere of H_2 produced black **1**,[9] isolated in 78% yield by crystallization from toluene. Reaction of $Ru_2Co_2(CO)_{13}$ with diphenylacetylene for 4 h yielded dark green **2**,[10] isolated in 76% yield by cooling the solution to 4 °C. 3-Hexyne reacted equivalently.

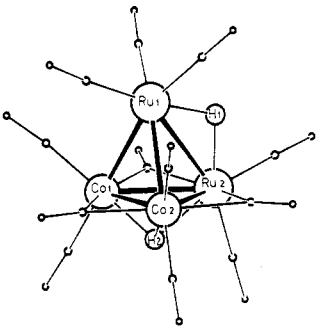

Figure 1. Molecular structure of $H_2Ru_2Co_2(CO)_{12}$ (1): small circles, CO ligands. H atoms were located but not refined. Bond lengths (pm): Ru1–Ru2 = 290.4 (1), Ru1–Co1 = 266.6 (1), Ru1–Co2 = 266.3 (1), Ru2–Co1 = 264.3 (1), Ru2–Co2 = 265.3 (1), Co1–Co2 = 254.6 (1), Ru1–H1 = 190, Ru2–H1 = 177, Ru2–H2 = 196, Co1–H2 = 173, Co2–H2 = 180.

$H_2Ru_2Co_2(CO)_{12}$ **1** $\qquad$ $Ru_2Co_2(CO)_{11}(Ph_2C_2)$ **2**

The compositions of both new clusters were determined by FD mass spectra. The reaction sites were deduced for 1 from NMR data[11] and established for 1 and 2 by crystal structure analyses.[12] The hydrogen positions in 1 were located from difference Fourier maps as well as by Orpen's H searching program.[13] Figures 1 and 2 give the overall molecular structures and important bond lengths. The cluster core geometries and ligand distributions are normal in both cases. There is a striking similarity (including unit cell dimensions) between 1 and $Co_4(CO)_{12}$[14] or $HFeCo_3(CO)_{12}$,[15] whereas 2 is intermediate between $Co_4(CO)_{10}(R_2C_2)$[16] and $Ru_4(CO)_{12}(R_2C_2)$.[17]

The structures show that the preferred reaction sites have been used. The acetylene in 2 has been inserted between the two cobalt atoms, thereby opening the cluster and forming a closo $Ru_2Co_2C_2$ core. The hydrogen atoms in 1 are associated with the ruthenium atoms, one of them

(1) Part 2: Vahrenkamp, H.; Wolters, D. *Organometallics* **1982**, *1*, 874.
(2) Gladfelter, W. L.; Geoffroy, G. L. *Adv. Organomet. Chem.* **1980**, *18*, 207.
(3) Vahrenkamp, H. *Philos. Trans. R. Soc. London*, in press.
(4) Cf. Richter, F.; Vahrenkamp, H. *Organometallics* **1982**, *1*, 756.
(5) Among the few reactions of mixed-metal clusters with different substrates are the nonspecific reactions of $H_2FeRu_3(CO)_{13}$ with H_2 and alkynes: Knox, S. A. R.; Koepke, J. W.; Andrews, M. A.; Kaesz, H. D. *J. Am. Chem. Soc.* **1975**, *97*, 3942. Fox, J. R.; Gladfelter, W. L.; Geoffroy, G. L.; Tavanaiepour, I.; Abdel-Mequid, S.; Day, V. W. *Inorg. Chem.* **1981**, *20*, 3230.
(6) Roland, E.; Vahrenkamp, H. *Angew. Chem.* **1981**, *93*, 714; *Angew. Chem., Int. Ed. Engl.* **1981**, *20*, 679.
(7) Humphries, H. P.; Kaesz, H. D. *Prog. Inorg. Chem.* **1979**, *25*, 145.
(8) Deeming, A. J., In "Transition Metal Clusters"; Johnson, B. F. G., Ed.; Wiley: New York, 1980; p 391.
(9) $H_2Ru_2Co_2(CO)_{12}$ (1): black crystals; mp 175 °C dec; IR ($CHCl_3$) 2112 (vw), 2082 (s), 2058 (vs), 2050 (sh), 2032 (sh), 1880 (w), 1868 (sh) cm^{-1}; ^1H NMR (CD_2Cl_2) broad resonance at −18.8 ppm. Anal. Calcd for $[C_{12}H_2Co_2O_{12}Ru_2]$: C, 21.90; H, 0.31. Found: C, 22.22; H, 0.08.
(10) $Ru_2Co_2(CO)_{11}(Ph_2C_2)$ (2): green-black crystals; mp 194 °C dec; IR (cyclohexane) 2090 (w), 2052 (vs), 2047 (s), 2019 (m), 2006 (w), 1881 (w), 1861 (w) cm^{-1}; ^1H NMR ($CDCl_3$) multiplet centered at 7.07 ppm. Anal. Calcd for $[C_{25}H_{10}Co_2O_{11}Ru_2]$: C, 37.24; H, 1.25. Found: C, 36.94; H, 0.80.
(11) Upon cooling of CD_2Cl_2 solutions of 1 the broad ^1H NMR resonance sharpens and moves to high field. At −60 °C when the low solubility of 1 limits further cooling there is a sharp signal at −20.36 ppm which we associate with a Ru–Ru edge bridging hydrogen because of the strong broadening effect of the quadrupolar cobalt nuclei. The second signal to be expected to the low field side of this which would have to be associated with a Ru/Co or Co/Co bridging hydrogen is too broad to be observed.
(12) Crystals of 1 were obtained from toluene and those of 2 from hexane. The crystal quality was checked by Weissenberg photographs; all other measurements were done on a Nonius CAD 4 diffractometer. 1: monoclinic, space group $P2_1/c$, $Z = 4$, $a = 930.4$ (1) pm, $b = 1153.0$ (2) pm, $c = 1664.2$ (4) pm, $\beta = 91.28$ (2)°. 2: monoclinic, space group $P2_1/c$, $Z = 4$, $a = 922.6$ (4) pm, $b = 1168.8$ (1) pm, $c = 2398.1$ (3) pm, $\beta = 93.77$ (2)°. The structures were solved by direct methods. Full matrix refinement (anisotropic for all non-hydrogen atoms, phenyl groups in 2 as rigid bodies with H atoms isotropic, H atoms in 1 located but not refined) using unit weights resulted in R values of 0.040 for 1 and 0.036 for 2. All details of the crystallographic work are documented in the supplementary material: Table A contains all crystallographic data, Tables B and C list all atomic parameters, Tables D and E all bond lengths and angles for both compounds, Tables F and G give the F_o/F_c listings, and Figures A and B show the detailed molecular structures and atom numbering schemes.
(13) Orpen, A. G. *J. Chem. Soc., Dalton Trans.* **1980**, 2509.
(14) Wei, C. H. *Inorg. Chem.* **1969**, *8*, 2384.
(15) Cf. Huie, B. T.; Knobler, C. B.; Kaesz, H. D. *J. Am. Chem. Soc.* **1978**, *100*, 3059.
(16) Dahl, L. F.; Smith, D. L. *J. Am. Chem. Soc.* **1962**, *84*, 2450.
(17) Johnson, B. F. G.; Lewis, J.; Reichert, B. E.; Schorpp, K. T.; Sheldrick, G. M. *J. Chem. Soc., Dalton Trans.* **1977**, 1417.

0276-7333/83/2302-0183$01.50/0

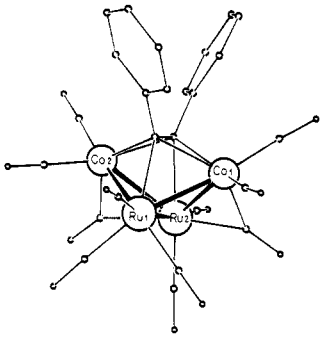

Figure 2. Molecular structure of $Ru_2Co_2(CO)_{11}(Ph_2C_2)$ (2): small circles, CO ligands and C atoms of Ph_2C_2. Bond lengths (pm): Ru1–Ru2 = 275.7 (1), Ru1–Co1 = 260.7 (1), Ru2–Co1 = 258.7 (1), Ru1–Co2 = 261.4 (1), Ru2–Co2 = 257.2 (1), Co1···Co2 = 352.4 (1). Acetylenic ligand distances (pm): Ru1–C = 216.6 (3), Co1–C = 210.1 (3), Co2–C = 210.2 (3) (front C), Ru2–C = 227.8 (3), Co1–C = 204.8 (3), Co2–C = 202.4 (3) (rear C), C–C = 143.2 (5).

occupying the "best" position bridging the Ru–Ru edge and the other one bridging a $RuCo_2$ face.[18] Both reactions are basic steps of substrate activation by clusters. And in both products the reactive sites for the respective reagent are still available.

The relation of these observations to bimetallic catalysis is obvious. Subsequent reactions such as the expulsion of H_2 from **1** by adding CO or the addition of acetylenes to **1** and of hydrogen to **2** suggest themselves. These reactions require more forcing conditions, thereby leading to complicated product mixtures. Further work in optimizing and extending the model character of the Ru_2Co_2 clusters is in progress.

Acknowledgment. This work was supported by the Fonds der Chemischen Industrie and by the Rechenzentrum der Universität Freiburg.

Registry No. **1**, 83830-89-1; **2**, 83830-90-4; $Ru_2Co_2(CO)_{13}$, 78456-90-3; H_2, 1333-74-0; Ph_2C_2, 501-65-5; Co, 7440-48-4; Ru, 7440-18-8; 3-hexyne, 928-49-4.

Supplementary Material Available: Listings of the complete crystallographic details, all positional and anisotropic thermal parameters, all bond lengths and angles, observed and calculated structure factors, and complete molecular drawings with atom numbering for both structures (47 pages). Ordering information is given on any current masthead page.

(18) A "better" position for H2, e.g., Ru–Ru bridging or Ru_2Co bridging, seems unlikely due to steric reasons.

Two Unprecedented Observations In Organocuprate Chemistry: Reversibility of Addition to an Alkyne and Low pK_a of a Stannylcuprate

S. D. Cox and F. Wudl*

Bell Laboratories
Murray Hill, New Jersey 07974

Received August 17, 1982

Summary: The addition of organocuprates to unsaturated carbonyl-substituted systems is assumed always to proceed irreversibly and stereospecifically and to proceed probably via electron transfer. Here we report that stannylcuprates enter into a dynamic equilibrium with ethyl butynoate. The equilibrium can be driven to the product side only with protons as electrophiles. The stannylcuprates are protonated by trifluoroacetic acid (100%) and acetic acid (~50%) but not by methanol. Thus, contrary to intuition, the conjugate acid of a stannylcuprate has a pK_a of ~5.

Piers discovered that stannylcuprates can be added to alkynoate esters.[1,2] When the reaction was carried out at low temperature, it was found to produce the *E* ester (**1**) stereospecifically and exclusively.

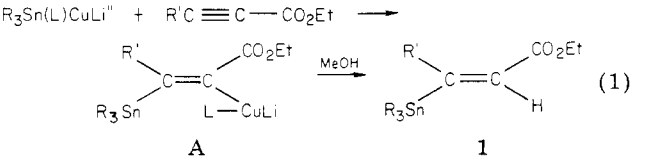

Piers also noted that the quenching reagent (MeOH) could be added concurrently with the alkynoate to the stannylcuprate without sacrifice in yield or stereoselectivity but did not comment further on this observation.

When we tried to apply this reaction to the preparation of compounds of general formula **2**, by addition of an electrophile (Y–Cl or Y–Br) to cuprate A at −78 °C, followed by quenching with methanol, we were surprised to observe the results tabulated in Table I. The salient

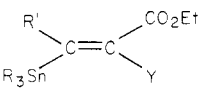

2, Y = Br, R_3Sn, HgCl

features were that (a) only protons seemed to quench A efficiently, something that Piers had also observed when he tried to trap A with various organic electrophiles (CH_3I, ketones, etc),[3] and (b) even though formation of A is essentially complete in ca. 15 min at −78 to −48 °C, substantial amounts of alkynoate were recovered when powerful electrophiles such as bromine or mercuric chloride were used.

To account for these observations, we were forced to suggest two unprecedented phenomena: (1) addition of "$R_3Sn(L)CuLi$" to $CH_3C{\equiv}C{-}CO_2Et$ is reversible and (2) the conjugate acid of "$R_3Sn(L)Cu^-Li^+$" ("$R_3Sn(L)CuH$", R = Me, Bu) is a relatively strong acid (or conversely "$R_3Sn(L)Cu^-Li^+$" is a very weak base in THF). This is depicted in Scheme I.

Scheme I

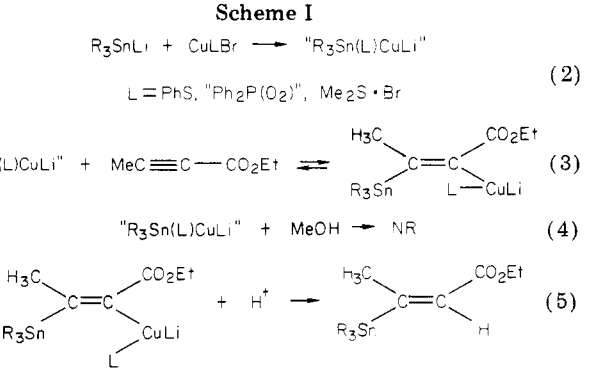

(1) Piers, E.; Morton, H. E. *J. Org. Chem.* **1980**, *45*, 4263.
(2) Piers, E.; Chong, J. M.; Morton, H. E. *Tetrahedron Lett.* **1981**, *22*, 4905.
(3) Piers, E.; Chong, J. M. *J. Org. Chem.* **1982**, *47*, 1602.

*To whom correspondence should be addressed at the Department of Physics, University of California, Santa Barbara, CA 93106.

0276-7333/83/2302-0184$01.50/0

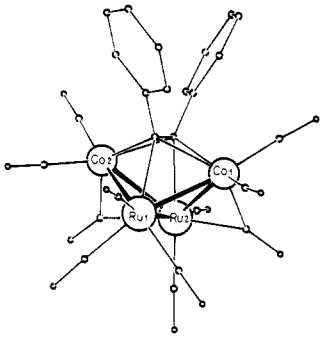

Figure 2. Molecular structure of $Ru_2Co_2(CO)_{11}(Ph_2C_2)$ (2): small circles, CO ligands and C atoms of Ph_2C_2. Bond lengths (pm): Ru1–Ru2 = 275.7 (1), Ru1–Co1 = 260.7 (1), Ru2–Co1 = 258.7 (1), Ru1–Co2 = 261.4 (1), Ru2–Co2 = 257.2 (1), Co1···Co2 = 352.4 (1). Acetylenic ligand distances (pm): Ru1–C = 216.6 (3), Co1–C = 210.1 (3), Co2–C = 210.2 (3) (front C), Ru2–C = 227.8 (3), Co1–C = 204.8 (3), Co2–C = 202.4 (3) (rear C), C–C = 143.2 (5).

occupying the "best" position bridging the Ru–Ru edge and the other one bridging a $RuCo_2$ face.[18] Both reactions are basic steps of substrate activation by clusters. And in both products the reactive sites for the respective reagent are still available.

The relation of these observations to bimetallic catalysis is obvious. Subsequent reactions such as the expulsion of H_2 from **1** by adding CO or the addition of acetylenes to **1** and of hydrogen to **2** suggest themselves. These reactions require more forcing conditions, thereby leading to complicated product mixtures. Further work in optimizing and extending the model character of the Ru_2Co_2 clusters is in progress.

Acknowledgment. This work was supported by the Fonds der Chemischen Industrie and by the Rechenzentrum der Universität Freiburg.

Registry No. **1**, 83830-89-1; **2**, 83830-90-4; $Ru_2Co_2(CO)_{13}$, 78456-90-3; H_2, 1333-74-0; Ph_2C_2, 501-65-5; Co, 7440-48-4; Ru, 7440-18-8; 3-hexyne, 928-49-4.

Supplementary Material Available: Listings of the complete crystallographic details, all positional and anisotropic thermal parameters, all bond lengths and angles, observed and calculated structure factors, and complete molecular drawings with atom numbering for both structures (47 pages). Ordering information is given on any current masthead page.

(18) A "better" position for H2, e.g., Ru–Ru bridging or Ru_2Co bridging, seems unlikely due to steric reasons.

Two Unprecedented Observations In Organocuprate Chemistry: Reversibility of Addition to an Alkyne and Low pK_a of a Stannylcuprate

S. D. Cox and F. Wudl*

Bell Laboratories
Murray Hill, New Jersey 07974

Received August 17, 1982

Summary: The addition of organocuprates to unsaturated carbonyl-substituted systems is assumed always to proceed irreversibly and stereospecifically and to proceed probably via electron transfer. Here we report that stannylcuprates enter into a dynamic equilibrium with ethyl butynoate. The equilibrium can be driven to the product side only with protons as electrophiles. The stannylcuprates are protonated by trifluoroacetic acid (100%) and acetic acid (~50%) but not by methanol. Thus, contrary to intuition, the conjugate acid of a stannylcuprate has a pK_a of ~5.

Piers discovered that stannylcuprates can be added to alkynoate esters.[1,2] When the reaction was carried out at low temperature, it was found to produce the *E* ester (**1**) stereospecifically and exclusively.

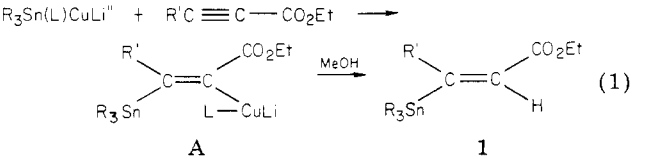

Piers also noted that the quenching reagent (MeOH) could be added concurrently with the alkynoate to the stannylcuprate without sacrifice in yield or stereoselectivity but did not comment further on this observation.

When we tried to apply this reaction to the preparation of compounds of general formula **2**, by addition of an electrophile (Y–Cl or Y–Br) to cuprate A at −78 °C, followed by quenching with methanol, we were surprised to observe the results tabulated in Table I. The salient

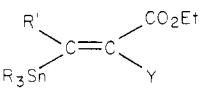

2, Y = Br, R_3Sn, HgCl

features were that (a) only protons seemed to quench A efficiently, something that Piers had also observed when he tried to trap A with various organic electrophiles (CH_3I, ketones, etc),[3] and (b) even though formation of A is essentially complete in ca. 15 min at −78 to −48 °C, substantial amounts of alkynoate were recovered when powerful electrophiles such as bromine or mercuric chloride were used.

To account for these observations, we were forced to suggest two unprecedented phenomena: (1) addition of "$R_3Sn(L)CuLi$" to $CH_3C{\equiv}C{-}CO_2Et$ is reversible and (2) the conjugate acid of "$R_3Sn(L)Cu^-Li^+$" ("$R_3Sn(L)CuH$", R = Me, Bu) is a relatively strong acid (or conversely "$R_3Sn(L)Cu^-Li^+$" is a very weak base in THF). This is depicted in Scheme I.

Scheme I

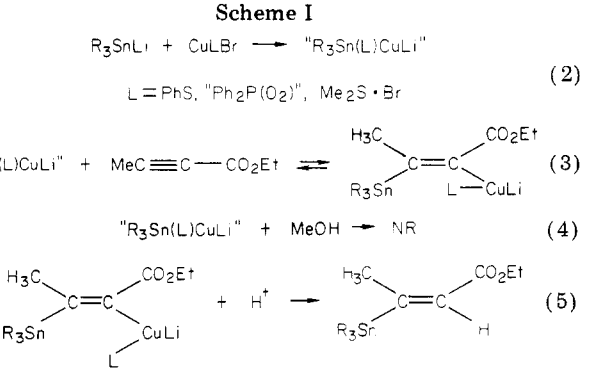

(1) Piers, E.; Morton, H. E. *J. Org. Chem.* **1980**, *45*, 4263.
(2) Piers, E.; Chong, J. M.; Morton, H. E. *Tetrahedron Lett.* **1981**, *22*, 4905.
(3) Piers, E.; Chong, J. M. *J. Org. Chem.* **1982**, *47*, 1602.

*To whom correspondence should be addressed at the Department of Physics, University of California, Santa Barbara, CA 93106.

0276-7333/83/2302-0184$01.50/0

Table I

entry	quenching reagent	reactn time, h	$CH_3C{\equiv}C{-}CO_2Et$, %	$(CH_3)_3Sn(CH_3)C{=}C(H)CO_2Et$, %
1	Br_2	2[a]	60	20
2	$HgCl_2$	2[b]	50	<5[c]
3	Br_2	*e*	0	100
4	$HgCl_2$	*e*	0	100
5	$(CH_3)_3SnCl$	5[a]	0	60–70[d]

[a] −78 °C. [b] −48 °C. [c] About 30% of organomercurials was obtained; the structure of these is currently being determined. [d] 30–40% of (*E*)-distannylcrotonate was formed. This same compound was obtained by Piers when excess stannylcuprate was allowed to react with ethyl butynoate.[3] [e] Reaction of stannylcopper reagent with ethyl butynoate was allowed to proceed for 2 h a small aliquot was quenched with MeOH and worked up.

Table II

entry	quenching reagent	pK_a[d]	addn. time,[a] min	reactn time,[b] min	ratio[c] sm/prod
1	CH_3OH	16	−2	30	30/70
	CH_3OH	16	120	10	5/95
2	CH_3COOH	5	−10	30	45/55
3	CF_3COOH (TFA)	0	−10	30	100/0
4	CF_3COOH (TFA)	0	−0.1	60	85/15
5	CF_3COOH (TFA)	0	0.5	30	55/45
6	CF_3COOH (TFA)	0	120	60	20/80
7	CF_3COOH (TFA)	0	1000	30	25/75

[a] Addition time relative to addition of ethyl 2-butynoate. [b] Reaction time at −45 to −50 °C after last addition. [c] Ratio from integration of methyl peaks in NMR of product mixture, SM, $MeC{=}CCO_2Et$; prod, (*E*)-$Me_3SnC(Me){=}C(H)CO_2Et$. [d] Not determined in THF but for comparison purposes.

The stannylcuprate is in quotations because its structure is unknown. It probably is a cluster compound. Suffice it to say that it has the reactivity pattern of an organocuprate. Whereas R_3SnLi adds to enones,[3] it does not add to ethyl butynoate under the conditions of reaction 1 in the absence of Cu^I; thus, copper^I is essential for this reaction, but the nature of ligands (L)[4] is not nearly as critical but has some effect on stereochemistry.[2]

To learn if indeed the reaction described by eq 3 is an equilibrium, we performed experiments shown as entries 3 and 4 in Table I. That is, if one removes an aliquot from the reaction mixture after addition of the butynoate but before addition of Br_2 or $HgCl_2$ and quenches it with methanol, it shows *no butynoate* left (by GPC only 1 is present). Yet, after the addition of 1 equiv of either electrophile to the original reaction mixture (followed by methanol quench and workup, *there is 60% of butynoate* and *20% 1*! The only explanation consistent with these results is that both reactions 3 and 5 are fast, that (5) is *irreversible*, that (3) is reversible (Br_2 and $HgCl_2$ destroy the stannylcuprate more rapidly than they react with A, thus "driving" the equilibrium to the left), and that the stannylcuprate is stable to methanol so that with a fast and irreversible reaction (eq 5),[2] equilibrium 3 is "driven" to the right by methanol.

The question then arose: how low must the acidity of the medium be before a stannylcuprate is quenched as fast as its addition product A? The surprising answer was that it required trifluoroacetic acid (entries 3 and 4, Table II) to quench the stannylcuprate rapidly. Entries 6 and 7 represent a "snapshot" of the equilibrium mixture of stannylcuprate and A, assuming that TFA reacts as rapidly with A as with the stannylcuprate.

Therefore, on the basis of the experiments presented above and the results shown in the tables, stannylcuprates enter into a fast, reversible reaction with butynoates in THF at −50 to −45 °C and the "pK_a" of "$Me_3SnCu(Me_2S)H$" in THF is close to that of acetic acid in the same solvent.

We have no explanation at this time for the behavior of A toward electrophiles other than protons. Clearly A cannot have a simple structure as drawn by Piers or by us.[5] Furthermore, the stereoselectivity of the formation of the kinetic control[1,2] product **1**, as opposed to thermodynamic control[1,2] product (*Z* isomer of **1**), is dependent not only on the possible equilibrium proposed by Piers but also on equilibrium 3.

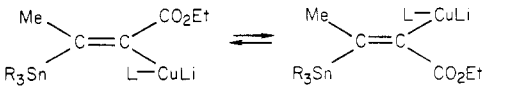

A B

Acknowledgment. We thank Steven H. Bertz and Gary Dabbagh for a sample of $Ph_2PCu{\cdot}O_2$ and numerous important discussions.

Registry No. (*E*)-$(CH_3)_3Sn(CH_3)C{=}C(H)CO_2Et$, 74854-51-6; Me_3SnLi, 17946-71-3; ethyl 2-butynoate, 4341-76-8.

(4) Bertz, S. H.; Dabbagh, G.; Villacorta, G. M., in press.

(5) Marino, J. P.; Linderman, R. J. *J. Org. Chem.* **1981**, *46*, 3696. These authors also found that α-carbethoxyvinyl cuprates do not exhibit the usual reactivity expected of organocuprates and interpreted their results as the basis of equilibrium i ⇄ ii.

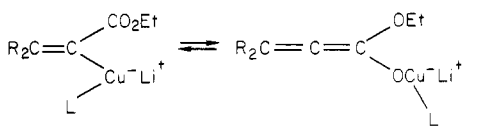

i ii

Coupling of Methylidyne and Carbonyl Ligands on the Triosmium Cluster Framework. Crystal Structure of $(\mu\text{-}H)_2Os_3(CO)_9(\mu_3\text{-}\eta^1\text{-}CCO)$

John R. Shapley,* Debra S. Strickland, and George M. St. George

Department of Chemistry, University of Illinois Urbana, Illinois 61801

Melvyn Rowen Churchill* and Clifford Bueno

Department of Chemistry State University of New York at Buffalo Buffalo, New York 14214

Received July 12, 1982

Summary: The compound $H_2Os_3(CO)_9(CCO)$ is formed more readily from $HOs_3(CO)_{10}(CH)$ than from $Os_3(CO)_{11}(CH_2)$. The crystal structure of $H_2Os_3(CO)_9(CCO)$ shows the CCO ligand to be in an upright rather than a tilted orientation.

Table I

entry	quenching reagent	reactn time, h	$CH_3C{\equiv}C{-}CO_2Et$, %	$(CH_3)_3Sn(CH_3)C{=}C(H)CO_2Et$, %
1	Br_2	2[a]	60	20
2	$HgCl_2$	2[b]	50	<5[c]
3	Br_2	*e*	0	100
4	$HgCl_2$	*e*	0	100
5	$(CH_3)_3SnCl$	5[a]	0	60–70[d]

[a] −78 °C. [b] −48 °C. [c] About 30% of organomercurials was obtained; the structure of these is currently being determined. [d] 30–40% of (*E*)-distannylcrotonate was formed. This same compound was obtained by Piers when excess stannylcuprate was allowed to react with ethyl butynoate.[3] [e] Reaction of stannylcopper reagent with ethyl butynoate was allowed to proceed for 2 h a small aliquot was quenched with MeOH and worked up.

Table II

entry	quenching reagent	pK_a[d]	addn. time,[a] min	reactn time,[b] min	ratio[c] sm/prod
1	CH_3OH	16	−2	30	30/70
	CH_3OH	16	120	10	5/95
2	CH_3COOH	5	−10	30	45/55
3	CF_3COOH (TFA)	0	−10	30	100/0
4	CF_3COOH (TFA)	0	−0.1	60	85/15
5	CF_3COOH (TFA)	0	0.5	30	55/45
6	CF_3COOH (TFA)	0	120	60	20/80
7	CF_3COOH (TFA)	0	1000	30	25/75

[a] Addition time relative to addition of ethyl 2-butynoate. [b] Reaction time at −45 to −50 °C after last addition. [c] Ratio from integration of methyl peaks in NMR of product mixture, SM, $MeC{=}CCO_2Et$; prod, (*E*)-$Me_3SnC(Me){=}C(H)CO_2Et$. [d] Not determined in THF but for comparison purposes.

The stannylcuprate is in quotations because its structure is unknown. It probably is a cluster compound. Suffice it to say that it has the reactivity pattern of an organocuprate. Whereas R_3SnLi adds to enones,[3] it does not add to ethyl butynoate under the conditions of reaction 1 in the absence of Cu^I; thus, copper^I is essential for this reaction, but the nature of ligands (L)[4] is not nearly as critical but has some effect on stereochemistry.[2]

To learn if indeed the reaction described by eq 3 is an equilibrium, we performed experiments shown as entries 3 and 4 in Table I. That is, if one removes an aliquot from the reaction mixture after addition of the butynoate but before addition of Br_2 or $HgCl_2$ and quenches it with methanol, it shows *no butynoate* left (by GPC only 1 is present). Yet, after the addition of 1 equiv of either electrophile to the original reaction mixture (followed by methanol quench and workup, *there is 60% of butynoate* and *20% 1*! The only explanation consistent with these results is that both reactions 3 and 5 are fast, that (5) is *irreversible*, that (3) is reversible (Br_2 and $HgCl_2$ destroy the stannylcuprate more rapidly than they react with A, thus "driving" the equilibrium to the left), and that the stannylcuprate is stable to methanol so that with a fast and irreversible reaction (eq 5),[2] equilibrium 3 is "driven" to the right by methanol.

The question then arose: how low must the acidity of the medium be before a stannylcuprate is quenched as fast as its addition product A? The surprising answer was that it required trifluoroacetic acid (entries 3 and 4, Table II) to quench the stannylcuprate rapidly. Entries 6 and 7 represent a "snapshot" of the equilibrium mixture of stannylcuprate and A, assuming that TFA reacts as rapidly with A as with the stannylcuprate.

Therefore, on the basis of the experiments presented above and the results shown in the tables, stannylcuprates enter into a fast, reversible reaction with butynoates in THF at −50 to −45 °C and the "pK_a" of "$Me_3SnCu(Me_2S)H$" in THF is close to that of acetic acid in the same solvent.

We have no explanation at this time for the behavior of A toward electrophiles other than protons. Clearly A cannot have a simple structure as drawn by Piers or by us.[5] Furthermore, the stereoselectivity of the formation of the kinetic control[1,2] product **1**, as opposed to thermodynamic control[1,2] product (*Z* isomer of **1**), is dependent not only on the possible equilibrium proposed by Piers but also on equilibrium 3.

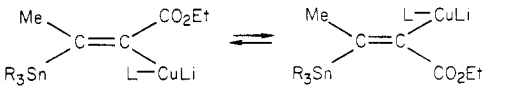

A B

Acknowledgment. We thank Steven H. Bertz and Gary Dabbagh for a sample of $Ph_2PCu{\cdot}O_2$ and numerous important discussions.

Registry No. (*E*)-$(CH_3)_3Sn(CH_3)C{=}C(H)CO_2Et$, 74854-51-6; Me_3SnLi, 17946-71-3; ethyl 2-butynoate, 4341-76-8.

(4) Bertz, S. H.; Dabbagh, G.; Villacorta, G. M., in press.

(5) Marino, J. P.; Linderman, R. J. *J. Org. Chem.* **1981**, *46*, 3696. These authors also found that α-carbethoxyvinyl cuprates do not exhibit the usual reactivity expected of organocuprates and interpreted their results as the basis of equilibrium i ⇄ ii.

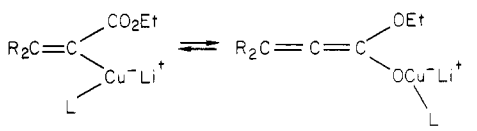

i ii

Coupling of Methylidyne and Carbonyl Ligands on the Triosmium Cluster Framework. Crystal Structure of $(\mu\text{-}H)_2Os_3(CO)_9(\mu_3\text{-}\eta^1\text{-}CCO)$

John R. Shapley,* Debra S. Strickland, and George M. St. George

Department of Chemistry, University of Illinois Urbana, Illinois 61801

Melvyn Rowen Churchill* and Clifford Bueno

Department of Chemistry State University of New York at Buffalo Buffalo, New York 14214

Received July 12, 1982

Summary: The compound $H_2Os_3(CO)_9(CCO)$ is formed more readily from $HOs_3(CO)_{10}(CH)$ than from $Os_3(CO)_{11}(CH_2)$. The crystal structure of $H_2Os_3(CO)_9(CCO)$ shows the CCO ligand to be in an upright rather than a tilted orientation.

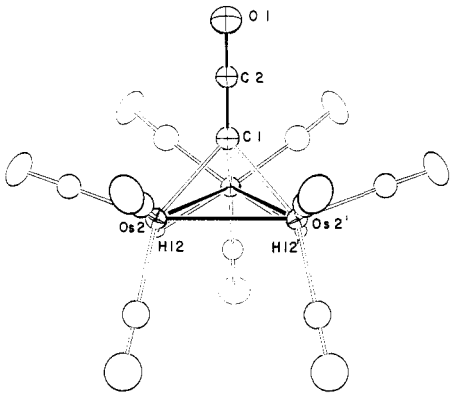

Figure 1. View of molecule A of $(\mu\text{-H})_2Os_3(CO)_9(\mu_3\text{-}\eta^1\text{-CCO})$. The crystallographic plane of symmetry is coincident with atoms C(1), C(2), O(2), Os(1), C(11), and O(11).

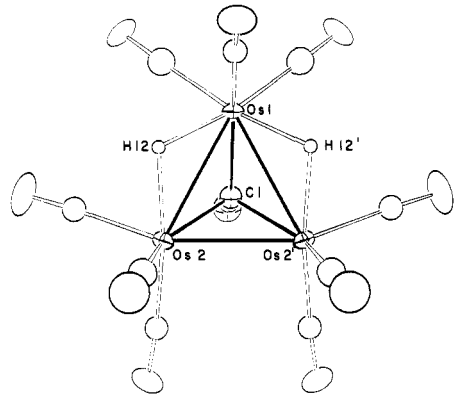

Figure 2. View of molecule A illustrating that the carbonylmethylidyne ligand is orthogonal to the triosmium plane.

A recent report[1] showed that the product resulting from pyrolysis (80–110 °C) of $Os_3(CO)_{11}CH_2$[2,3] should be formulated as $H_2Os_3(CO)_9(CCO)$. One species considered as a possible intermediate in this reaction was $HOs_3(CO)_{10}(CH)$, which has since been synthesized by another route and structurally characterized (see **1**).[4] We now report that $HOs_3(CO)_{10}(CH)$ rearranges to $H_2Os_3(CO)_9(CCO)$ under milder conditions than does $Os_3(CO)_{11}(CH_2)$. This result not only suggests the probable pathway by which $H_2Os_3(CO)_9(CCO)$ is formed but also provides a product uncontaminated with $Os_3(CO)_{12}$, which hindered previous efforts to obtain X-ray quality crystals. By analogy with $H_2Os_3(CO)_9(CCH_2)$[5] the structure of $H_2Os_3(CO)_9(CCO)$ was proposed earlier to have a tilted configuration (**2**); a single-crystal X-ray diffraction study shows, however, that the carbonylmethylidyne (CCO) ligand is in an upright position (**3**).

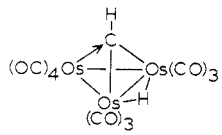

1

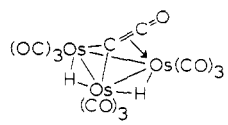

2

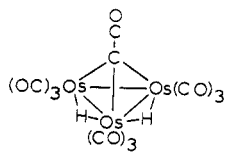

3

The rearrangement of $HOs_3(CO)_{10}(CH)$ to $H_2Os_3(CO)_9(CCO)$ proceeds cleanly in refluxing hexane. More convenient preparatively, however, is to heat solid $HOs_3(CO)_{10}(CH)$ in a sublimation apparatus (85 °C at ca. 0.1 mm), which causes the more volatile $H_2Os_3(CO)_9(CCO)$ to collect on the cold finger. The isolated yield after crystallization (pentane, −15 °C) is 75%.

Crystals of $H_2Os_3(CO)_9(CCO)$ have two independent half molecules in the crystallographic unit.[6] Each molecule thus possesses precise crystallographic C_s symmetry *in the absence of disorder*. Molecule A is ordered with three carbonyl ligands bound to each osmium atom (Figure 1). Bridging hydride ligands, which were located directly from the analysis, span the equivalent Os(1)–Os(2) and Os(1)–Os(2') linkages [Os(1)–H(12) = 1.80 (10) Å, Os(2)–H(12) = 1.92 (9) Å, ∠Os(1)–H(12)–Os(2) = 101.1 (45)°]. The hydrido-bridged Os–Os bonds are 2.870 (1) Å in length, while Os(2)–Os(2') = 2.760 (1) Å.

The most striking feature of the structure is the symmetrically triply bridged CCO fragment lying perpendicularly above the triosmium triangle (Figure 2). The Os–C distances are Os(1)–C(1) = 2.157 (26) Å and Os(2)–C(1) = Os(2')–C(1) = 2.133 (20) Å. The CCO moiety is close to linear [∠C(1)–C(2)–O(1) = 178.6 (24)°] with C(1)–C(2) = 1.264 (37) Å and C(2)–O(1) = 1.154 (34) Å.

Molecule B is disordered, but the pattern of disorder has been resolved and all parameters thereby deduced are consistent with those from molecule A.[7]

The structural features of $H_2Os_3(CO)_9(CCO)$ suggest a valence bond formulation such as $Os_3{\equiv}C^-{-}C{\equiv}O^+$ for the complexed carbonylmethylidyne ligand. This picture is consistent with the ^{13}C NMR data recorded previously,[1] which showed a markedly upfield resonance for the me-

(1) Sievert, A. C.; Strickland, D. S.; Shapley, J. R.; Steinmetz, G. R.; Geoffroy, G. L. *Organometallics* **1982**, *1*, 214.
(2) Steinmetz, G. R.; Geoffroy, G. L. *J. Am. Chem. Soc.* **1981**, *103*, 1278.
(3) Shapley, J. R.; Sievert, A. C.; Churchill, M. R.; Wasserman, H. J. *J. Am. Chem. Soc.* **1981**, *103*, 6975.
(4) Shapley, J. R.; Cree-Uchiyama, M. E.; St. George, G. M.; Churchill, M. R.; Bueno, C. *J. Am. Chem. Soc.*, accepted for publication.
(5) Deeming, A. J.; Underhill, M. *J. Chem. Soc., Dalton Trans.* **1974**, 1415.

(6) Diffraction data were collected with a Syntex $P2_1$ automated four-circle diffractometer. The structure was solved by direct methods (MULTAN) and refined via difference-Fourier and full-matrix least-squares methods. All computations were performed in-house under the SUNY-Buffalo modified Syntex XTL system. For $H_2Os_3(CO)_9(CCO)$: space group $P2_1/m$, a = 9.272 (1) Å, b = 14.227 (2) Å, c = 12.600 (2) Å, β = 92.42 (1)°, V = 1660.7 (4) Å^3, ρ(calcd) = 3.46 g·cm^{-3} for mol wt = 864.7 and Z = 4; R_F = 6.5% and R_{wF} = 6.3% for all 2292 reflections with $4° < 2\theta < 45°$.

(7) Observed Os–Os "distances" in molecule B are Os(1)–Os(2) = Os(1)–Os(2') = 2.813 (1) Å and Os(2)–Os(2') = 2.875 (1) Å. The Os(2)–Os(2') bond length is clearly consistent with the hydrido-bridged distance in molecule A. The other two distances are close to the average of hydrido-bridged and non-hydrido-bridged distances in molecule A [(1/2) (2.870 + 2.760) = 2.815 Å]. We propose a disorder of the type:

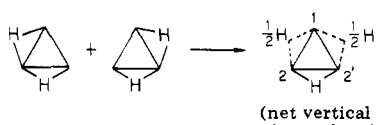

(net vertical mirror plane)

In keeping with this proposal, molecule B has atoms with larger "thermal parameters" than molecule A; equatorial Os–Os–CO angles in molecule B have values intermediate between their components as seen in molecule A; difference-Fourier maps revealed only the site of the ordered hydride ligand. The geometry of the carbonylmethylidyne ligand is unaffected. Appropriate parameters are Os(1)–C(1) = 2.170 (25) Å, Os(2)–C(1) = Os(2')–C(1) = 2.130 (18) Å, ∠C(1)–C(2)–O(1) = 176.6 (25) Å, C(1)–C(2) = 1.285 (38) Å, and C(2)–O(1) = 1.194 (35) Å.

thylidyne carbon (δ 8.6) and a resonance for the carbonyl carbon (δ 160.3) in the same region as for the carbonyls bound to osmium. In the absence of specific isotopic labeling we are unable to attribute one of the IR bands observed in the ν(CO) region to the CCO ligand.[8]

Protonation of $H_2Os_3(CO)_9(CCO)$ leads to $H_3Os_3(CO)_9(CCO)^+$, as indicated by bleaching of the color from yellow to white and by ^1H NMR and IR data.[9] It is probable that both $H_3Os_3(CO)_9(CCO)^+$ and the analogous tricobalt cation $Co_3(CO)_9(CCO)^+$ studied by Seyferth and co-workers[10] have the CCO ligand in an upright position as well. This contrasts with the evidence that both $H_3Os_3(CO)_9(C{=}CH_2)^+$[11] and $Co_3(CO)_9(C{=}CHR)^+$[12] have tilted configurations. A molecular orbital analysis[13] of the preference for a tilted configuration in $Co_3(CO)_9(CCH_2)^+$ attributed it to the empty orbital on the β-carbon interacting differentially with the high-lying, filled e set of metal ring orbitals. This leads to an energy decrease with bending. On the other hand, since the CCO ligand has its p-π^* orbitals in e pairs, there appears to be no incentive for it to tilt away from the perpendicular position in $Co_3(CO)_9(CCO)^+$ or $H_3Os_3(CO)_9(CCO)^+$. It is significant, however, that even when the symmetry of the metal framework is reduced to C_s in $H_2Os_3(CO)_9(CCO)$, an upright orientation is preferred.

The crystal structure of $HOs_3(CO)_{10}(CH)$[4] shows that the bridging methylidyne ligand comes into close contact with an axial carbonyl of the $Os(CO)_4$ unit. This feature suggests that the facile thermal rearrangement of $HOs_3(CO)_{10}(CH)$ into $H_2Os_3(CO)_9(CCO)$ proceeds via an intermediate in which the methylidyne and carbonyl ligands have coupled into a "ketenyl" HC=C=O ligand. Analogous compounds $HM_3(CO)_9(RC{=}C{=}CH_2)$ (M = Ru, Os) with isoelectronic "allenyl" ligands are known,[14] and the coupling of methylidyne and carbonyl ligands on tungsten (mediated by $AlCl_3$) has been observed recently.[15] Related ligands formed from aryl-substituted methylidyne compounds also are known.[16]

$H_2Os_3(CO)_9(CCO)$ reacts slowly with H_2 (1 atm) in refluxing heptane or toluene to provide $H_3Os_3(CO)_9(CH)$[17] as the sole product observed spectroscopically (IR and ^1H NMR) and isolated after TLC in 54% yield. Under similar conditions with a mixture of H_2 and CO (3:1), no reaction is observed. The observed product implies the generation of $HOs_3(CO)_9CH$, which in turn suggests that the methylidyne–carbonyl coupling that leads to $H_2Os_3(CO)_9(CCO)$ is reversible.[18] Further reactions of $H_2Os_3(CO)_9(CCO)$ and $H_3Os_3(CO)_9(CCO)^+$ are being explored.

Acknowledgment. This research was supported at the University of Illinois by NSF Grant CHE 81-00140 (J.R.S.) and at S.U.N.Y.-Buffalo by NSF Grant CHE 80-23448 (M.R.C.).

Registry No. 1, 83573-03-9; 3, 83585-34-6.

Supplementary Material Available: Tables of positional parameters, anisotropic thermal parameters, and observed and calculated structure factors (15 pages). Ordering information is given on any current masthead page.

(8) The weak band at 1644 cm^{-1} observed previously[1] for a Nujol mull of $H_2Os_3(CO)_9(CCO)$ is not observed for a Nujol mull prepared in an inert-atmosphere box. Thus, this band is probably due to a small amount of $H_2Os_3(CO)_9(CCO_2H)$ formed in making the mull.

(9) For $[H_3Os_3(CO)_9(CCO)]BF_4$: ^1H NMR (CH_2Cl_2, 35 °C) δ -19.36 (s); IR (ν(CO), Nujol) 2155 (m), 2125 (s), 2069 (s, br), 2039 (s, br) cm^{-1}.

(10) (a) Seyferth, D.; Hallgren, J. E.; Eschbach, C. S. *J. Am. Chem. Soc.* **1974**, *96*, 1730. (b) Seyferth, D.; Williams, G. H.; Nivert, C. L. *Inorg. Chem.* **1977**, *16*, 758.

(11) Deeming, A. J.; Hasso, S.; Underhill, M.; Canty, A. J.; Johnson, B. F. G.; Jackson, W. G.; Lewis, J.; Matheson, T. W. *J. Chem. Soc., Chem. Commun.* **1974**, 807.

(12) Edidin, R. T.; Norton, J. R.; Mislow, K. *Organometallics* **1982**, *1*, 561.

(13) Schilling, B. E. R.; Hoffman, R. *J. Am. Chem. Soc.* **1979**, *101*, 3456.

(14) (a) Deeming, A. J.; Hasso, S.; Underhill, M. *J. Chem. Soc., Dalton Trans.* **1975**, 1614. (b) Gervasio, G.; Osella, D.; Valle, M. *Inorg. Chem.* **1976**, *15*, 1221.

(15) Churchill, M. R.; Wasserman, H. J.; Holmes, S. J.; Schrock, R. R. *Organometallics* **1982**, *1*, 766.

(16) Kreissl, F. R.; Uedelhoven, W.; Erber, K. *Angew Chem., Int Ed. Engl.* **1978**, *17*, 859. Also see: Martin-Gil, J.; Howard, J. A. K.; Navarro, R.; Stone, F. G. A. *J. Chem. Soc., Chem. Commun.* **1979**, 1168. Orama, O.; Schubert, U.; Kreissel, F. R.; Fischer, E. O. *Z. Naturforsch., B: Anorg. Chem., Org. Chem.* **1980**, *35B*, 82.

(17) Calvert, R. B.; Shapley, J. R. *J. Am. Chem. Soc.* **1977**, *99*, 5225.

(18) An alternative possibility is that $H_2Os_3(CO)_9(CCO)$ reacts with H_2 to form $H_3Os_3(CO)_9(CCHO)$, which subsequently decarbonylates. This strikes us an unlikely, since $Co_3(CO)_9(CCHO)$ is reduced by H_2 exclusively to $Co_3(CO)_9(CCH_3)$.[19] However, we are currently attempting to prepare $H_3Os_3(CO)_9(CCHO)$ in order to check its behavior.

(19) Seyferth, D.; Nestle, M. O. *J. Am. Chem. Soc.* **1981**, *103*, 3320.

Reactive Charge-Transfer Complexes as Precursors for New Organometallic Salts. Synthesis and Structure of $[(\eta^5\text{-}C_5H_5)_2Fe]_{1.5}^+[(NC)_2C{=}C(CN)O]^-$

Brian W. Sullivan and Bruce M. Foxman*

Department of Chemistry, Brandeis University
Waltham, Massachusetts 02254

Received July 20, 1982

Summary: Reaction of the ferrocene–tetracyanoethylene charge-transfer complex in ethyl acetate gives the title complex in excellent yield. Crystals of the new material contain both ferrocene and ferricenium ions; ferrocene and tricyanoethenolate anion form a donor–acceptor stack in the crystal structure, while the ferricenium ions form a nearly linear stack.

In 1964 Rosenblum[1] demonstrated that the reaction of ferrocene with tetracyanoethylene (TCNE)[2] led to a 1:1 charge-transfer complex of the neutral closed-shell components. In that same paper a singular discovery was also presented: the neutral complex decomposed either in solution or in the solid state to yield both the neutral congeners and black needles of the salt ferricenium pentacyanopropenide in low yield.[3] Thus, the reaction proceeds with covalent bond formation to yield an organometallic salt which has not yet been synthesized by alternative means.[4] These results suggested an as-yet-unrealized opportunity, viz., that reactive charge-transfer complexes might be employed as precursors for new and otherwise unavailable organometallic phases. With this goal in mind we felt that a reinvestigation of the reaction chemistry of the ferrocene–TCNE charge-transfer complex was warranted. This communication reports the high-yield synthesis and structure of a previously unknown product, $[(\eta^5\text{-}C_5H_5)_2Fe]_{1.5}^+[(NC)_2C{=}C(CN)O^-]$.

In a typical experiment, equimolar amounts of ferrocene (0.642 g, 3.44 mmol) and TCNE (0.442 g, 3.44 mmol) are dissolved in 15–20 mL of purified, warm (50 °C) ethyl

(1) Rosenblum, M.; Fish, R. W.; Bennett, C. *J. Am. Chem. Soc.* **1964**, *86*, 5166.

(2) Webster, O. W.; Mahler, W.; Benson, R. E. *J. Am. Chem. Soc.* **1962**, *84*, 3678.

(3) This reaction was later observed and reported by other workers: Brandon, R. L.; Osiecki, J. H.; Ottenberg, A. *J. Org. Chem.* **1966**, *31*, 1214.

(4) Sullivan, B. W., unpublished observations. Structural characterization of the salt is underway.

0276-7333/83/2302-0187$01.50/0

thylidyne carbon (δ 8.6) and a resonance for the carbonyl carbon (δ 160.3) in the same region as for the carbonyls bound to osmium. In the absence of specific isotopic labeling we are unable to attribute one of the IR bands observed in the ν(CO) region to the CCO ligand.[8]

Protonation of $H_2Os_3(CO)_9(CCO)$ leads to $H_3Os_3(CO)_9(CCO)^+$, as indicated by bleaching of the color from yellow to white and by ^1H NMR and IR data.[9] It is probable that both $H_3Os_3(CO)_9(CCO)^+$ and the analogous tricobalt cation $Co_3(CO)_9(CCO)^+$ studied by Seyferth and co-workers[10] have the CCO ligand in an upright position as well. This contrasts with the evidence that both $H_3Os_3(CO)_9(C{=}CH_2)^+$[11] and $Co_3(CO)_9(C{=}CHR)^+$[12] have tilted configurations. A molecular orbital analysis[13] of the preference for a tilted configuration in $Co_3(CO)_9(CCH_2)^+$ attributed it to the empty orbital on the β-carbon interacting differentially with the high-lying, filled e set of metal ring orbitals. This leads to an energy decrease with bending. On the other hand, since the CCO ligand has its p-π^* orbitals in e pairs, there appears to be no incentive for it to tilt away from the perpendicular position in $Co_3(CO)_9(CCO)^+$ or $H_3Os_3(CO)_9(CCO)^+$. It is significant, however, that even when the symmetry of the metal framework is reduced to C_s in $H_2Os_3(CO)_9(CCO)$, an upright orientation is preferred.

The crystal structure of $HOs_3(CO)_{10}(CH)$[4] shows that the bridging methylidyne ligand comes into close contact with an axial carbonyl of the $Os(CO)_4$ unit. This feature suggests that the facile thermal rearrangement of $HOs_3(CO)_{10}(CH)$ into $H_2Os_3(CO)_9(CCO)$ proceeds via an intermediate in which the methylidyne and carbonyl ligands have coupled into a "ketenyl" HC=C=O ligand. Analogous compounds $HM_3(CO)_9(RC{=}C{=}CH_2)$ (M = Ru, Os) with isoelectronic "allenyl" ligands are known,[14] and the coupling of methylidyne and carbonyl ligands on tungsten (mediated by $AlCl_3$) has been observed recently.[15] Related ligands formed from aryl-substituted methylidyne compounds also are known.[16]

$H_2Os_3(CO)_9(CCO)$ reacts slowly with H_2 (1 atm) in refluxing heptane or toluene to provide $H_3Os_3(CO)_9(CH)$[17] as the sole product observed spectroscopically (IR and ^1H NMR) and isolated after TLC in 54% yield. Under similar conditions with a mixture of H_2 and CO (3:1), no reaction is observed. The observed product implies the generation of $HOs_3(CO)_9CH$, which in turn suggests that the methylidyne–carbonyl coupling that leads to $H_2Os_3(CO)_9(CCO)$ is reversible.[18] Further reactions of $H_2Os_3(CO)_9(CCO)$ and $H_3Os_3(CO)_9(CCO)^+$ are being explored.

Acknowledgment. This research was supported at the University of Illinois by NSF Grant CHE 81-00140 (J.R.S.) and at S.U.N.Y.-Buffalo by NSF Grant CHE 80-23448 (M.R.C.).

Registry No. 1, 83573-03-9; 3, 83585-34-6.

Supplementary Material Available: Tables of positional parameters, anisotropic thermal parameters, and observed and calculated structure factors (15 pages). Ordering information is given on any current masthead page.

(8) The weak band at 1644 cm^{-1} observed previously[1] for a Nujol mull of $H_2Os_3(CO)_9(CCO)$ is not observed for a Nujol mull prepared in an inert-atmosphere box. Thus, this band is probably due to a small amount of $H_2Os_3(CO)_9(CCO_2H)$ formed in making the mull.

(9) For $[H_3Os_3(CO)_9(CCO)]BF_4$: ^1H NMR (CH_2Cl_2, 35 °C) δ -19.36 (s); IR (ν(CO), Nujol) 2155 (m), 2125 (s), 2069 (s, br), 2039 (s, br) cm^{-1}.

(10) (a) Seyferth, D.; Hallgren, J. E.; Eschbach, C. S. *J. Am. Chem. Soc.* **1974**, *96*, 1730. (b) Seyferth, D.; Williams, G. H.; Nivert, C. L. *Inorg. Chem.* **1977**, *16*, 758.

(11) Deeming, A. J.; Hasso, S.; Underhill, M.; Canty, A. J.; Johnson, B. F. G.; Jackson, W. G.; Lewis, J.; Matheson, T. W. *J. Chem. Soc., Chem. Commun.* **1974**, 807.

(12) Edidin, R. T.; Norton, J. R.; Mislow, K. *Organometallics* **1982**, *1*, 561.

(13) Schilling, B. E. R.; Hoffman, R. *J. Am. Chem. Soc.* **1979**, *101*, 3456.

(14) (a) Deeming, A. J.; Hasso, S.; Underhill, M. *J. Chem. Soc., Dalton Trans.* **1975**, 1614. (b) Gervasio, G.; Osella, D.; Valle, M. *Inorg. Chem.* **1976**, *15*, 1221.

(15) Churchill, M. R.; Wasserman, H. J.; Holmes, S. J.; Schrock, R. R. *Organometallics* **1982**, *1*, 766.

(16) Kreissl, F. R.; Uedelhoven, W.; Erber, K. *Angew Chem., Int Ed. Engl.* **1978**, *17*, 859. Also see: Martin-Gil, J.; Howard, J. A. K.; Navarro, R.; Stone, F. G. A. *J. Chem. Soc., Chem. Commun.* **1979**, 1168. Orama, O.; Schubert, U.; Kreissel, F. R.; Fischer, E. O. *Z. Naturforsch., B: Anorg. Chem., Org. Chem.* **1980**, *35B*, 82.

(17) Calvert, R. B.; Shapley, J. R. *J. Am. Chem. Soc.* **1977**, *99*, 5225.

(18) An alternative possibility is that $H_2Os_3(CO)_9(CCO)$ reacts with H_2 to form $H_3Os_3(CO)_9(CCHO)$, which subsequently decarbonylates. This strikes us an unlikely, since $Co_3(CO)_9(CCHO)$ is reduced by H_2 exclusively to $Co_3(CO)_9(CCH_3)$.[19] However, we are currently attempting to prepare $H_3Os_3(CO)_9(CCHO)$ in order to check its behavior.

(19) Seyferth, D.; Nestle, M. O. *J. Am. Chem. Soc.* **1981**, *103*, 3320.

Reactive Charge-Transfer Complexes as Precursors for New Organometallic Salts. Synthesis and Structure of $[(\eta^5\text{-}C_5H_5)_2Fe]_{1.5}^+[(NC)_2C{=}C(CN)O]^-$

Brian W. Sullivan and Bruce M. Foxman*

Department of Chemistry, Brandeis University
Waltham, Massachusetts 02254

Received July 20, 1982

Summary: Reaction of the ferrocene–tetracyanoethylene charge-transfer complex in ethyl acetate gives the title complex in excellent yield. Crystals of the new material contain both ferrocene and ferricenium ions; ferrocene and tricyanoethenolate anion form a donor–acceptor stack in the crystal structure, while the ferricenium ions form a nearly linear stack.

In 1964 Rosenblum[1] demonstrated that the reaction of ferrocene with tetracyanoethylene (TCNE)[2] led to a 1:1 charge-transfer complex of the neutral closed-shell components. In that same paper a singular discovery was also presented: the neutral complex decomposed either in solution or in the solid state to yield both the neutral congeners and black needles of the salt ferricenium pentacyanopropenide in low yield.[3] Thus, the reaction proceeds with covalent bond formation to yield an organometallic salt which has not yet been synthesized by alternative means.[4] These results suggested an as-yet-unrealized opportunity, viz., that reactive charge-transfer complexes might be employed as precursors for new and otherwise unavailable organometallic phases. With this goal in mind we felt that a reinvestigation of the reaction chemistry of the ferrocene–TCNE charge-transfer complex was warranted. This communication reports the high-yield synthesis and structure of a previously unknown product, $[(\eta^5\text{-}C_5H_5)_2Fe]_{1.5}^+[(NC)_2C{=}C(CN)O^-]$.

In a typical experiment, equimolar amounts of ferrocene (0.642 g, 3.44 mmol) and TCNE (0.442 g, 3.44 mmol) are dissolved in 15–20 mL of purified, warm (50 °C) ethyl

(1) Rosenblum, M.; Fish, R. W.; Bennett, C. *J. Am. Chem. Soc.* **1964**, *86*, 5166.

(2) Webster, O. W.; Mahler, W.; Benson, R. E. *J. Am. Chem. Soc.* **1962**, *84*, 3678.

(3) This reaction was later observed and reported by other workers: Brandon, R. L.; Osiecki, J. H.; Ottenberg, A. *J. Org. Chem.* **1966**, *31*, 1214.

(4) Sullivan, B. W., unpublished observations. Structural characterization of the salt is underway.

0276-7333/83/2302-0187$01.50/0

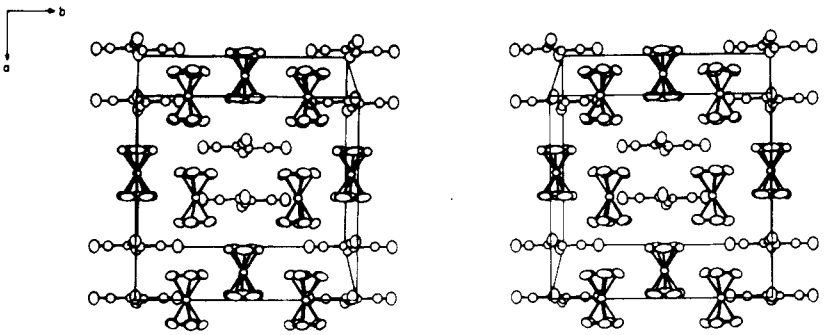

Figure 1. A stereoview of the crystal structure of $[(\eta^5\text{-}C_5H_5)_2Fe]_{1.5}^+[(NC)_2C{=}C(CN)O]^-$ (50% probability ellipsoids). Only one of the two disordered orientations of the tricyanoethenolate anion is shown.

acetate. The initially light green solution is placed in a refrigerator and slowly turns quite dark as it is allowed to stand in air. After intervals of several days, the title complex is collected in the form of highly reflective black crystals (three harvests): 0.771 g (84% based on ferrocene); mp 137–138 °C; IR (KBr) 3112, 2203, 2180, 1595 cm^{-1}; μ = 2.49 μ_B. Anal. Calcd for $C_{40}H_{30}N_6O_2Fe_3$: C, 60.49; H, 3.81; N, 10.58. Found: C, 60.68; H, 4.12; N, 10.63. The analytical and spectroscopic data are consistent with the formulation $[(C_5H_5)_2Fe]_{1.5}^+[C_5N_3O]^-$; since this is an unusual stoichiometry,[5] an X-ray structure determination was carried out.

Crystals of the title complex are monoclinic of space group $C2/m$ with a = 14.105 (3) Å, b = 15.471 (3) Å, c = 8.728 (2) Å, β = 112.84 (2)°, ρ_{obsd} = 1.50 (1) g·cm^{-3},[6] and ρ_{calcd} = 1.51 g·cm^{-3} for Z = 4. Full-matrix least-squares refinement of positional and thermal parameters for all atoms, using 1264 data for which $F > 3.92\sigma(F)$ and $2\theta_{MoK\alpha} < 51°$, gave R = 0.036 and R_w = 0.046. The crystal structure (Figure 1) is composed of one-dimensional segregated stacks of (a) ferricenium ions and (b) alternating 1:2:1 ...ferrocene–bis(tricyanoethenolate)–ferrocene... stacks. The latter stack is probably best viewed as a weak 1:2 donor–acceptor complex between ferrocene and the tricyanoethenolate anion.[7] Formally, this material is to be considered a ternary phase of the type $[D^+][D_{0.5}A^-]$, where D and A are donor and acceptor molecules, respectively. The observed arrangement may by prototypical of this stoichiometry, although we know of no other examples.

The details of the interactions within each stack are as follows. In the ferricenium ion stack, the Fe atoms lie on twofold axes at (0, 0.231, 0) and ($^1/_2$, 0.269, 0); thus, the cations are related by an inversion center at ($^1/_4$, $^1/_4$, 0), and form infinite, zigzag chains along a, with relative displacements in b from one another of 0.59 Å. The intercation ring-to-ring distance is 3.61 Å, very similar to the distance of 3.63 Å reported for 1,1′-dimethylferricenium $(TCNQ)_2$.[8] Individual cations are rigorously eclipsed and have an Fe–ring center distance of 1.700 (2) Å, average Fe–C distance of 2.073 (2) Å, and C_5H_5 rings at an angle of 4.6°.

The 1:2 ferrocene–tricyanoethenolate ion ($TCEA^-$) stack is comprised of *disordered* $TCEA^-$ ions occupying sites of

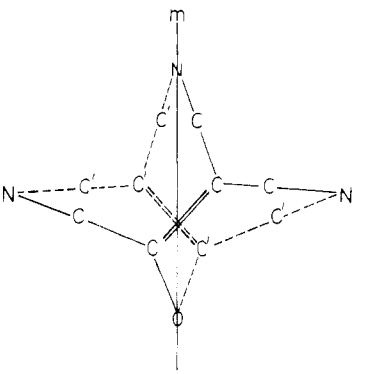

Figure 2. Disorder (1:1) observed for the tricyanoethenolate anion.

m symmetry and *ordered* ferrocene molecules of crystallographic $2/m$ symmetry. Elemental analysis and IR spectra were crucial in establishing the presence of the enolate anion, owing to the complex nature of the disorder (the C=C bond of the $TCEA^-$ anion intersects the mirror plane at an angle of 40° (Figure 2), and a cyano N atom and the O atom trans to it lie on the mirror plane). However, in the final refinement, this disorder has been well resolved; the C=C (1.387 (9) Å) and C—O (1.246 (7) Å) bond lengths indicate that both resonance forms of the anion are important. Unlike the structure of ferrocene, where it is likely that the disordered ferrocene molecules are nearly eclipsed,[9,10] it would appear here that the *ferrocene* molecules are *not* disordered and are staggered. Although the ferrocene C_5H_5 rings show considerable in-plane libration, the location of H atoms strongly suggested a staggered configuration, and refinement proceeded successfully only for this model.

Within the 1:2 stack the interplanar distance between centrosymmetrically related anions is 3.69 Å, and the ferrocene–anion average separation is 3.47 Å, which is longer than the revised interplanar distance,[10] 3.28 Å, in ferrocene–TCNE.[11] However, the value of 3.47 Å is misleading, in that the $TCEA^-$ anion plane is tipped 9.3° *toward* the C_5H_5 rings of ferrocene about an axis perpendicular to the mirror plane. This serves to move the negatively charged O atom away from the C_5H_5 ring plane (3.78 Å) and the trans-C≡N group very near to the plane (3.12 Å). These phenomena are independent of the anion disorder and may account for the observed staggered ar-

(5) Herbstein, F. H. "Perspectives in Structural Chemistry"; Dunitz, J. D., Ibers, J. A., Eds.; Wiley: New York, 1971; Vol. 4, p 166.
(6) Determined by neutral bouyancy in C_6H_6–CCl_4.
(7) In acetonitrile solution 0.1 M in tetrabutylammonium hexafluorophosphate, the TCEA anion exhibits a cathodic peak at −1.56 V relative to the Ag/AgCl electrode in saturated NaCl.
(8) Wilson, S. R.; Corvan, P. J.; Seiders, R. P; Hodgson, D. J.; Brookhart, M.; Hatfield, W. E.; Miller, J. S.; Reis, A. H.; Rogan, P. K.; Gebert, E.; Epstein, A. J. "Molecular Metals"; Hatfield, W. E., Ed.; Plenum Press: New York, 1979; p 407. TCNQ = 7,7,8,8-tetracyano-p-quinodimethane.
(9) Seiler, P.; Dunitz, J. D. *Acta Crystallogr., Sect. B* **1979**, *B35*, 1068. Koetzle, T. F.; Takusagawa, F. *Ibid.* **1979**, *B35*, 1074.
(10) A recent redetermination of the structure of ferrocene–TCNE at room temperature in our laboratories shows that the ferrocene molecule is disordered in a similar manner to that found in ref 9.
(11) Adman, E.; Rosenblum, M.; Sullivan, S.; Margulis, T. N. *J. Am. Chem. Soc.* **1967**, *89*, 4540.

rangement. The ferrocene molecules have an Fe–ring center distance of 1.656 (4) Å and an average Fe–C distance of 2.018 (4) Å.

This material cannot be recrystallized nor can it be assembled from its congeners. These observations are consistent with the solid complex being a kinetically formed phase,[12] likely a decomposition product of ferricenium–TCNE^{-}· which has been shown to be in equilibrium with ferrocene–TCNE. If moisture (but not oxygen) is excluded from the reaction described above, the products include both TCEA^{-} and pentacyanopropenide anions. This latter observation is in excellent agreement with the reactivity pattern observed, e.g., in acetonitrile solutions of the TCNE radical anion.[13]

Acknowledgment. This work was supported in part by the Office of Naval Research. We thank L. Acampora and G. D. Zoski for performing electrochemical measurements and D. J. Sandman, A. Reis, and L. S. Stuhl for helpful discussions.

Registry No. $[(C_5H_5)_2Fe]_{1.5}^{+}[C_5N_3O]^{-}$, 83587-82-0; ferrocenetetracyanoethylene, 12116-72-2.

Supplementary Material Available: Tables of atomic coordinates, thermal parameters, and observed and calculated structure factors (7 pages). Ordering information is given on any current masthead page.

(12) Sandman, D. J. *Mol. Cryst. Liq. Cryst.* **1979**, *50*, 235.
(13) Webster, O. W.; Mahler, W.; Benson, R. E. *J. Am. Chem. Soc.* **1962**, *84*, 3678.

Carbonylation and Amination of μ-η^2-Acetylides in $M_2(CO)_6(\mu$-η^2-C≡CPh)(PPh_2): Synthesis of μ-O=CCHC(Ph)NR_2 Complexes and the X-ray Structure of $Ru_2(CO)_6[\mu$-O=CCHC(Ph)$NEt_2](PPh_2)$

Graham Nigel Mott, Ruthanne Granby, Shane A. MacLaughlin, Nicholas J. Taylor, and Arthur J. Carty*

Guelph-Waterloo Centre for Graduate Work in Chemistry
Waterloo Campus, University of Waterloo
Waterloo, Ontario, Canada N2L 3G1

Received August 18, 1982

Summary: The multisite bound acetylide in $M_2(CO)_6(\mu$-η^2-C≡CPh)$PPh_2)$ (M = Ru, Fe) reacts with CO in the presence of primary and secondary amines NHRR′ to generate via carbonylation and amination the μ-keto compounds $M_2(CO)_6[\mu$-O=CCHC(Ph)NRR′$](PPh_2)$ (**2**). X-ray analyses of **2** (M = Ru, R = R′ = Et) and **2** (M = Fe, R = Ph, R′ = H) revealed the presence of oxygen and carbon bonded acyl groups with regiospecific addition of the amine to the original β-alkynyl carbon atom. These μ-O,C complexes may be closely related to species implicated in the reduction of CO by H_2 to oxygenates in the presence of binuclear catalysts. The possible use of this reductive carbonylation strategy for the elaboration of other multisite bound carbocationic ligands is suggested.

The possible involvement of μ-bound ligands of the general type **1** (e.g., X = OH, OR) in the nucleophilic activation of carbon monoxide has focused increasing attention on the chemistry of bi- and polynuclear carbonyl derivatives containing these moieties.[1] Several examples of attack by amines on coordinated CO in $Ru_3(CO)_{12}$ and $Os_3(CO)_{12}$ have been described,[2] and Kaesz[3] has recently generated edge bridging μ-O=C(X) groups from anionic nucleophiles (NMe_2^{-}, Me^{-}, or OR^{-}) via the proposed intermediacy of η^1-C(=O)X species. Oxygen *and* carbon coordinated CO have also been implicated in the catalytic reduction of CO by binuclear ruthenium systems[4] although the proposed intermediates were not isolated. Intuitively one might expect both η^1- and μ-O=C(X) complexes to be involved in homogeneously catalyzed or stoichiometric reductive carbonylations of organic substrates in the presence of polynuclear compounds. We wish to report the synthesis of the novel, α-substituted μ-acyl complexes $M_2(CO)_6[\mu$-O=CCH=CPhNRR′$](PPh_2)$ (**2**, M = Fe, Ru, R = Ph, R′ = H; M = Ru, R = R′ = Et, *n*-Pr, R, R′ = 2-EtC_5H_9) via the facile carbonylation–amination of the unsaturated alkynyl ligand in $M_2(CO)_6(\mu$-η^2-C≡CPh)-(PPh_2). Our results have relevance to strategies for the elaboration of carbocationic multisite bound unsaturated ligands and to the synthesis of oxygenates from CO.[4] Furthermore trapping of μ-O=CCH=C(Ph)NRR′ ligands in **2** suggests the possible use of binuclear carbonyls in reductive carbonylations of the Reppe-type, reactions that are at present mechanistically obscure.[5]

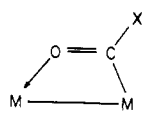

1

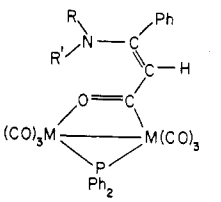

2

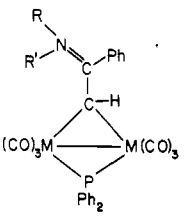

3

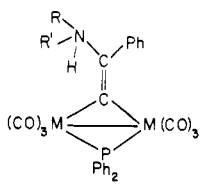

4

The phosphido-bridged binuclear acetylide $Fe_2(CO)_6$-$(\mu$-η^2-C≡CPh$)(PPh_2)$[6] in benzene reacts cleanly with aniline in the presence of carbon monoxide. Infrared monitoring of the reaction mixture showed essentially quantitative replacement of the ν(CO) bands of the precursor with those of a single product[7] of composition $Fe_2(CO)_7$-

(1) See, for example: (a) Lin, Y. C.; Knobler, C. B.; Kaesz, H. D. *J. Am. Chem. Soc.* **1981**, *103*, 1216. (b) Butts, S. B.; Strauss, S. H.; Holt, E. M.; Stimson, R. E.; Alcock, N. W.; Shriver, D. F. *Ibid.* **1980**, *102*, 5093. (c) Marsella, J. A.; Folting, K.; Huffman, J. C.; Caulton, K. G. *Ibid.* **1981**, *103*, 5596. (d) Maata, E. A.; Marks, T. J. *Ibid.* **1981**, *103*, 3576. (e) Wolczanski, P. T.; Bercaw, J. E. *Acc. Chem. Res.* **1980**, *13*, 121.

(2) (a) Azam, K. A.; Choo Yin, C.; Deeming, A. J. *J. Chem. Soc., Dalton Trans.* **1978**, 1201. (b) Szostak, R.; Strouse, C. E.; Kaesz, H. D. *J. Organomet. Chem.* **1980**, *191*, 243. (c) Adams, R. D.; Golembeski, N.; Selegue, J. P. *Inorg. Chem.* **1981**, *20*, 1242.

(3) Mayr, A.; Lin, Y. C.; Boag, N. M.; Kaesz, H. D. *Inorg. Chem.* **1982**, *21*, 1704.

(4) Daroda, R. J.; Blackborow, J. R.; Wilkinson, G. *J. Chem. Soc., Chem. Commun.* **1980**, 1101.

(5) See, for example: Collman, J. P.; Hegedus, L. S. "Principles and Applications of Organotransition Metal Chemistry"; University Science Books: Mill Valley, CA, 1980; Chapter 8.

(6) Smith, W. F.; Yule, J.; Taylor, N. J.; Paik, H. N.; Carty, A. J. *Inorg. Chem.* **1977**, *16*, 1593.

0276-7333/83/2302-0189$01.50/0

rangement. The ferrocene molecules have an Fe–ring center distance of 1.656 (4) Å and an average Fe–C distance of 2.018 (4) Å.

This material cannot be recrystallized nor can it be assembled from its congeners. These observations are consistent with the solid complex being a kinetically formed phase,[12] likely a decomposition product of ferricenium–TCNE^{-}· which has been shown to be in equilibrium with ferrocene–TCNE. If moisture (but not oxygen) is excluded from the reaction described above, the products include both TCEA^{-} and pentacyanopropenide anions. This latter observation is in excellent agreement with the reactivity pattern observed, e.g., in acetonitrile solutions of the TCNE radical anion.[13]

Acknowledgment. This work was supported in part by the Office of Naval Research. We thank L. Acampora and G. D. Zoski for performing electrochemical measurements and D. J. Sandman, A. Reis, and L. S. Stuhl for helpful discussions.

Registry No. $[(C_5H_5)_2Fe]_{1.5}^{+}[C_5N_3O]^{-}$, 83587-82-0; ferrocenetetracyanoethylene, 12116-72-2.

Supplementary Material Available: Tables of atomic coordinates, thermal parameters, and observed and calculated structure factors (7 pages). Ordering information is given on any current masthead page.

(12) Sandman, D. J. *Mol. Cryst. Liq. Cryst.* **1979**, *50*, 235.
(13) Webster, O. W.; Mahler, W.; Benson, R. E. *J. Am. Chem. Soc.* **1962**, *84*, 3678.

Carbonylation and Amination of μ-η^2-Acetylides in $M_2(CO)_6(\mu$-η^2-C≡CPh)(PPh_2): Synthesis of μ-O=CCHC(Ph)NR_2 Complexes and the X-ray Structure of $Ru_2(CO)_6[\mu$-O=CCHC(Ph)$NEt_2](PPh_2)$

Graham Nigel Mott, Ruthanne Granby, Shane A. MacLaughlin, Nicholas J. Taylor, and Arthur J. Carty*

Guelph-Waterloo Centre for Graduate Work in Chemistry
Waterloo Campus, University of Waterloo
Waterloo, Ontario, Canada N2L 3G1

Received August 18, 1982

Summary: The multisite bound acetylide in $M_2(CO)_6(\mu$-η^2-C≡CPh)$PPh_2)$ (M = Ru, Fe) reacts with CO in the presence of primary and secondary amines NHRR′ to generate via carbonylation and amination the μ-keto compounds $M_2(CO)_6[\mu$-O=CCHC(Ph)NRR′$](PPh_2)$ (**2**). X-ray analyses of **2** (M = Ru, R = R′ = Et) and **2** (M = Fe, R = Ph, R′ = H) revealed the presence of oxygen and carbon bonded acyl groups with regiospecific addition of the amine to the original β-alkynyl carbon atom. These μ-O,C complexes may be closely related to species implicated in the reduction of CO by H_2 to oxygenates in the presence of binuclear catalysts. The possible use of this reductive carbonylation strategy for the elaboration of other multisite bound carbocationic ligands is suggested.

The possible involvement of μ-bound ligands of the general type **1** (e.g., X = OH, OR) in the nucleophilic activation of carbon monoxide has focused increasing attention on the chemistry of bi- and polynuclear carbonyl derivatives containing these moieties.[1] Several examples of attack by amines on coordinated CO in $Ru_3(CO)_{12}$ and $Os_3(CO)_{12}$ have been described,[2] and Kaesz[3] has recently generated edge bridging μ-O=C(X) groups from anionic nucleophiles (NMe_2^{-}, Me^{-}, or OR^{-}) via the proposed intermediacy of η^1-C(=O)X species. Oxygen *and* carbon coordinated CO have also been implicated in the catalytic reduction of CO by binuclear ruthenium systems[4] although the proposed intermediates were not isolated. Intuitively one might expect both η^1- and μ-O=C(X) complexes to be involved in homogeneously catalyzed or stoichiometric reductive carbonylations of organic substrates in the presence of polynuclear compounds. We wish to report the synthesis of the novel, α-substituted μ-acyl complexes $M_2(CO)_6[\mu$-O=CCH=CPhNRR′$](PPh_2)$ (**2**, M = Fe, Ru, R = Ph, R′ = H; M = Ru, R = R′ = Et, *n*-Pr, R, R′ = 2-EtC_5H_9) via the facile carbonylation–amination of the unsaturated alkynyl ligand in $M_2(CO)_6(\mu$-η^2-C≡CPh)-(PPh_2). Our results have relevance to strategies for the elaboration of carbocationic multisite bound unsaturated ligands and to the synthesis of oxygenates from CO.[4] Furthermore trapping of μ-O=CCH=C(Ph)NRR′ ligands in **2** suggests the possible use of binuclear carbonyls in reductive carbonylations of the Reppe-type, reactions that are at present mechanistically obscure.[5]

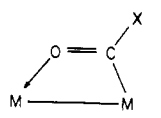

1

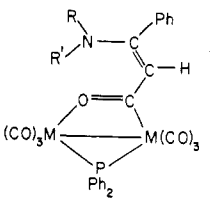

2

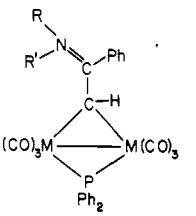

3

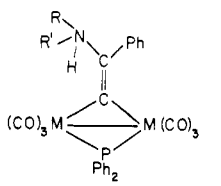

4

The phosphido-bridged binuclear acetylide $Fe_2(CO)_6$-$(\mu$-η^2-C≡CPh$)(PPh_2)$[6] in benzene reacts cleanly with aniline in the presence of carbon monoxide. Infrared monitoring of the reaction mixture showed essentially quantitative replacement of the ν(CO) bands of the precursor with those of a single product[7] of composition $Fe_2(CO)_7$-

(1) See, for example: (a) Lin, Y. C.; Knobler, C. B.; Kaesz, H. D. *J. Am. Chem. Soc.* **1981**, *103*, 1216. (b) Butts, S. B.; Strauss, S. H.; Holt, E. M.; Stimson, R. E.; Alcock, N. W.; Shriver, D. F. *Ibid.* **1980**, *102*, 5093. (c) Marsella, J. A.; Folting, K.; Huffman, J. C.; Caulton, K. G. *Ibid.* **1981**, *103*, 5596. (d) Maata, E. A.; Marks, T. J. *Ibid.* **1981**, *103*, 3576. (e) Wolczanski, P. T.; Bercaw, J. E. *Acc. Chem. Res.* **1980**, *13*, 121.

(2) (a) Azam, K. A.; Choo Yin, C.; Deeming, A. J. *J. Chem. Soc., Dalton Trans.* **1978**, 1201. (b) Szostak, R.; Strouse, C. E.; Kaesz, H. D. *J. Organomet. Chem.* **1980**, *191*, 243. (c) Adams, R. D.; Golembeski, N.; Selegue, J. P. *Inorg. Chem.* **1981**, *20*, 1242.

(3) Mayr, A.; Lin, Y. C.; Boag, N. M.; Kaesz, H. D. *Inorg. Chem.* **1982**, *21*, 1704.

(4) Daroda, R. J.; Blackborow, J. R.; Wilkinson, G. *J. Chem. Soc., Chem. Commun.* **1980**, 1101.

(5) See, for example: Collman, J. P.; Hegedus, L. S. "Principles and Applications of Organotransition Metal Chemistry"; University Science Books: Mill Valley, CA, 1980; Chapter 8.

(6) Smith, W. F.; Yule, J.; Taylor, N. J.; Paik, H. N.; Carty, A. J. *Inorg. Chem.* **1977**, *16*, 1593.

0276-7333/83/2302-0189$01.50/0

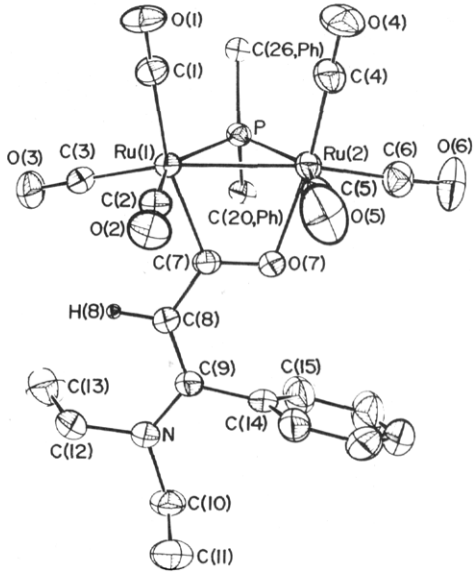

Figure 1. A perspective view of the molecular structure of $Ru_2(CO)_6(\mu\text{-}O{=}CCHC(Ph)NEt_2)(PPh_2)$ drawn so as to emphasize the new ligand.

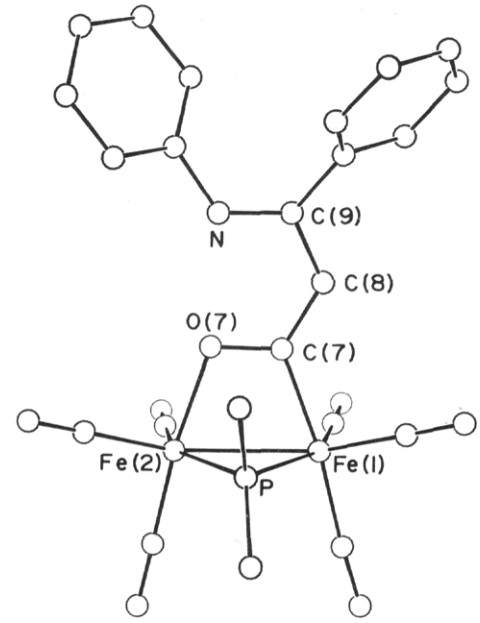

Figure 2. A ball and stick plot of the structure of $Fe_2(CO)_6(\mu\text{-}O{=}CCHC(Ph)NHPh)(PPh_2)$.

$(C_2Ph)(Ph_2P)(PhNH_2)$ (**2**, M = Fe, R = Ph, R′ = H). Minute amounts of this complex had previously been isolated from the reaction of aniline with the parent acetylide where the major product is the zwitterionic μ-alkylidene complex $Fe_2(CO)_6$ [CHC(Ph)NHPh](PPh$_2$). The solution IR spectrum of **2** (M = Fe, R = Ph, R′ = H) exhibited a ν(C=O) band at 1555 cm^{-1} typical of a μ-O=C(X) ligand,[1] and the ^{31}P chemical shift is characteristic of a phosphido group across a metal–metal bond simultaneously bridged by a two atom ligand.[9] In the ^{13}C NMR spectrum a resonance at δ 253.6 can be attributed to the acyl carbon atom. Analogous products were obtained from $Ru_2(CO)_6(\mu\text{-}\eta^2\text{-}C{\equiv}CPh)(PPh_2)$ with $PhNH_2$, Et_2NH, $(n\text{-}Pr)_2NH$, and 2-ethylpiperidine.[10] Structural details, particularly the stereochemistry of the hydrocarbon chain in **2**, were revealed by single-crystal X-ray analyses of a ruthenium (**2**, M = Ru, R = R′ = Et) and an iron (**2**, M = Fe, R = Ph, R′ = H) derivative.[11] Since the two structures are closely related and the ruthenium data set is the more precise, discussion here will center on the ruthenium complex. An ORTEP II plot is shown in Figure 1. The binuclear framework consists of two tricarbonylruthenium moieties joined by a strong Ru–Ru bond (Ru(1)–Ru(2) = 2.7540(5) Å) and a symmetrical bridging phosphido group. As expected from the ^{31}P NMR shift the Ru(1)–P–Ru(2) angle (71.6 (0)°) is acute. The other bridging group is a 3-(diethylamino)-3-phenyl-2-propen-1-al ligand formed via formal insertion of CO into the metal–acetylide bond and cis addition of the secondary amine across the alkyne. The keto group is coordinated to Ru(1) via carbon and to Ru(2) via oxygen in μ-O=C(X) fashion with a C(7)–O(7) bond length (1.275 (6) Å) typical of η^2-bonded carbonyls;[12] the trapezoidal $Ru_2(CO)$ four-membered ring is planar. A least-squares plane through the atoms N, C(9), C(14), C(8), C(7), and O(7)[13] reveals that the entire hydrocarbon skeleton deviates little from planarity. Although the C(8)–C(9) bond (1.394 (6) Å) is formally the olefinic link of the generated enamine, it is clear from the bond lengths[14] that there is some delocal-

(7) $Fe_2(CO)_6(\mu\text{-}\eta^2\text{-}C{\equiv}CPh)(PPh_2)$ (1.0 g) was dissolved in degassed benzene and heated to 60 °C with a slow stream of CO gas at 1 atm passing through the solution. Aniline (1 mL) was added via a serum cap by syringe and the mixture stirred magnetically with periodic IR monitoring of the reaction mixture. Complete conversion took ~10 days. The reaction mixture was concentrated, diluted with heptane, and chromatographed on Florisil. Heptane/benzene (1:1) eluted the product which was obtained from the mother liquor as red crystals on cooling at −10 °C overnight: yield 70%; mp 137 °C; (C_6H_{12}) ν(CO) 2061 (s), 2018 (vs), 1995 (s), 1978 (m), 1968 (m), 1958 (m) 1555 (m) cm^{-1}; ^{31}P NMR (ppm wrt 85% H_3PO_4) +179.0.

(8) Satisfactory elemental analyses have been obtained on all new compounds described herein.

(9) (a) Carty, A. J.; Mott, G. N.; Taylor, N. J.; Yule, J. E. *J. Am. Chem. Soc.* **1978**, *100*, 3051. (b) Carty, A. J. *Adv. Chem. Ser.* **1982**, *No. 196*, 163. (c) Mott, G. N.; Carty A. J., submitted for publication.

(10) **2** (M = Ru, R = R′ = Et): IR (C_6H_{12}) ν(CO) 2066 (s), 2033 (s), 2000 (s), 1986 (m), 1974 (m), 1960 (m), 1518 (m) cm^{-1}; NMR δ(^{31}P) (C_6D_6) +150.7; ^{13}C NMR (proton coupled; CD_2Cl_2) δ 243.6 (d, acyl CO), 203.3 (m), 200.8 (s), 199.7(s), 193.2 (s, CO), 155.7 (s, *C*Ph), 140.8–125.7 (m, ring C), 112.5 (d, CH), 45.0 (t), 43.6 (t), (CH_2), 12.2 (q), 14.4 (q, CH_3). **2** (M = Ru, R = Ph, R′ = H): IR (C_6H_{12}) ν(CO) 2070 (s), 2038 (s), 2007 (s), 1990 (m), 1979 (m), 1970 (m), 1559 (m) cm^{-1}; NMR δ(^{31}P) (C_6D_6) +149.5. **2** (M = Ru, R = R′ = *n*-Pr) IR (C_6H_{12}) ν(CO) 2066 (s), 2033 (s), 2000 (s), 1986 (m), 1975 (m), 1960 (m), 1516 (m) cm^{-1}; NMR δ(^{31}P) (C_6D_6) +150.2. **2** (M = Ru, R, R′ = 2-ethyl-C_5H_9): IR (C_6H_{12}) ν(CO) 2066 (s), 2033 (s), 2000 (s), 1985 (m), 1974 (m), 1959 (m), 1506 (m) cm^{-1}; NMR δ(^{31}P)(C_6D_6) +150.5.

(11) Yellow prisms of $Ru_2(CO)_6[\mu\text{-}O{=}CCHC(Ph)NEt_2](PPh_2)$ are triclinic of space group $P\bar{1}$ with a = 9.580 (2) Å, b = 10.616 (3) Å, c = 16.991 (5) Å, α = 87.85 (2)°, β = 95.83 (2)°, γ = 110.57 (2)°, Z = 2, ρ_{measd} = 1.55 ρ_{calcd} = 1.563 g cm^{-3}, V = 1609.4 (8) Å^3, and μ(Mo Kα) = 10.14 cm^{-1}. The structure was solved by using standard heavy-atom methods and refined by full-matrix least-squares techniques. With 3415 observed intensities ($I \geq 3\sigma(I)$) measured on a Syntex P21 diffractometer with graphite-monochromated Mo Kα radiation, anisotropic refinement of all non-hydrogen atoms gave R and R_w values of 0.027 and 0.030, respectively. All hydrogen atoms were located. Red needles of $Fe_2(CO)_6[\mu\text{-}O{=}CCHC(Ph)NPhH](PPh_2)$ are monoclinic of space group $P2_1/n$ with a = 14.286 (7) Å b = 14.255 (9) Å, c = 15.134 (6) Å, β = 90.35 (4)°, Z = 4, ρ_{measd} = 1.46 g cm^{-3}, ρ_{calcd} = 1.48 g cm^{-3}, V = 3084 (3) Å^3, and μ(Mo Kα) = 10.66 cm^{-1}. In view of the similarities between the iron and ruthenium compounds a data set of 2497 observed (3352 measured to 45°) reflections was collected and partially refined isotropically to R = 0.131 to provide basic structural details only. Pertinent distance (Å) are Fe(1)–Fe(2) = 2.60, Fe(1)–P = 2.22, Fe(2)–P = 2.24, O(7)–C(7) = 1.28, C(7)–C(8) = 1.42, C(8)–C(9) = 1.43, and C(9)–N = 1.34.

(12) Compare for example: C–O = 1.287 (9) Å in $HRu_3(CO)_{10}(\mu\text{-}O{=}CN\,Me_2)$. See ref. 2b.

(13) Atomic displacements from this plane are N (0.029 Å), C(9) (0.013 Å), C(14) (−0.028 Å), C(8) (0.049 Å), C(7) (0.01 Å), and O(7) (0.025 Å). Ru(1) and Ru(2) are displaced by 0.028 and 0.054 Å from this plane.

ization over the C(7)–C(8)–C(9)–N fragment as might be expected for a planar skeleton. In stereochemical terms, addition of the secondary amine across the alkynyl group is *regiospecific*, there being no spectroscopic or synthetic evidence for a 2-diethylamino 3-phenyl isomer. The iron derivative **2** (M = Fe, R = Ph, R′ = H) is also formed regiospecifically via β attack (Figure 2), but in the resulting enamine the addenda are mutually trans. In this case the stereochemistry of the product appears to be controlled by hydrogen bonding between the carbonyl oxygen O(7) and the amine hydrogen atom.[18] The ruthenium–aniline adduct may have similar stereochemistry.

Several features of these reactions and products are notable in the context of CO chemistry. Complexes of type **2** are closely similar to intermediates postulated by Wilkinson and co-workers in CO reductions to oxygenated products catalyzed by binuclear ruthenium catalysts.[4] Moreover the synthesis of **2** from a multisite bound ligand with demonstrated carbocationic character,[19] carbon monoxide, and a base suggests the possibility of accomplishing selective additions to other carbocations in binuclear or cluster compounds. It is particularly noteworthy that the direction of addition, with amine functionalization of the acetylene differs from that observed in Reppe reactions[5] or in stoichiometric carbonylations of acetylenes by metal carbonyls in the presence of added bases where the nucleophile is attached to the carbonyl group.

Possible mechanisms for the carbonylation–amination sequence leading to **2** include direct CO insertion into the metal–acetylide bond of $M_2(CO)_6(\mu\text{-}\eta^2\text{-}C{\equiv}CPh)(PPh_2)$ followed by amine addition across the triple bond or intramolecular coupling of the acetylide and a carboxamide group generated via amine attack on coordinated CO. There is now ample precedent for $\mu\text{-}\eta^2$- or η-bonded carboxamide species in other systems.[1-3] However, the precursors $M_2(CO)_6(\mu\text{-}\eta^2\text{-}C{\equiv}CPh)(PPh_2)$ do not insert CO even under pressure, and in the absence of added CO amine addition to the acetylenic triple bond is extremely facile, there being no spectroscopic evidence for carboxamide species. A more likely mechanism is direct CO insertion into the dipolar μ-alkylidene complex **3**[9] or the μ-vinylidene species **4**[9] formed via amine attack on the triple bond. Such insertions, which are of obvious interest in the context of C–C bond forming processes in hydrocarbon synthesis,[20] are presently under investigation.

Acknowledgment. We are grateful to NSERC and Imperial Oil Ltd. for financial support of this work in the form of grants (A.J.C.) and a scholarship (S.A.M.)

Registry No. **2** (M = Fe, R = Ph, R′ = H), 83802-16-8; **2** (M = Ru, R = Ph, R′ = H), 83802-17-9; **2** (M = Ru, R = R′ = Et), 83802-18-0; **2** (M = Ru, R = R′ = *n*-Pr), 83802-19-1; **2** (M = Ru, R = R′ = 2-EtC_5H_9), 83802-20-4; $Fe_2(CO)_6(\mu\text{-}\eta^2\text{-}C{\equiv}CPh)(PPh_2)$, 52970-25-9; $Ru_2(CO)_6(\mu\text{-}\eta^2\text{-}C{\equiv}CPh)(PPh_2)$, 82647-81-2; Et_2NH, 109-89-7; Pr_2NH, 142-84-7; $PhNH_2$, 1484-80-6; 2-ethylpiperidine, 62-53-3.

Supplementary Material Available: Table I, atomic positions Table II, anisotropic thermal parameters, Table III, bond lengths, Table IV, bond angles, and a listing of observed and calculated structure factor amplitudes for $Ru_2(CO)_6(\mu\text{-}O{=}CCHC(Ph)NEt_2)(PPh_2)$ (25 pages). Ordering information is given on any current masthead page.

(14) The C(8)–C(9) bond length of 1.394(6) Å is somewhat longer than the standard $C(sp^2)$–$C(sp^2)$ double bond length (1.337 (6) Å) in olefins[15] and the C(9)–N distance (1.334 (7) Å) can be compared with corresponding values for >C=N< bond lengths in *N,N*-dimethylisopropylideniminium perchlorate (1.30 (2) Å)[16] or 2,6-dihydroxypyridinium cation (1.346 (3) and 1.335 (3) Å)[17] where there is unquestionably C–N multiple bonding.

(15) Kennard, O., Watson, D. G., Allen, F. H., Isaacs, N. W., Motherwell, W. D. S., Petterson, R. C.; Town, W. G. Eds. "Molecular Structures and Dimensions"; N. V. A. Oosthoek: Utrecht, Vol. A1, p 52.

(16) Trefonas, L. M.; Flurry, R. L., Jr.; Majeste, R.; Mayers, E. A.; Copeland, R. F. *J. Am. Chem. Soc.* **1966**, *88*, 2145.

(17) Mason, S. A.; White, J. C. B.; Woodlock, A. *Tetrahedron Lett.* **1969**, 5219.

(18) In the iron dimer the O(7)–C(7)–C(8)–C(9)–N unit is planar. With an N–H distance of 0.95 Å, the hydrogen atom would be located ~1.80 Å from O(7), a value compatible with a hydrogen bond interaction.

(19) Carty, A. J. *Pure Appl. Chem.* **1982**, *54*, 113.

(20) Dyke, A. F.; Guerchais, J. E.; Knox, S. A. R.; Roue, J.; Short, R. L.; Taylor, G. E.; Woodward, P. *J. Chem. Soc., Chem. Commun.* **1981**, 537.

Allylation of Aldehydes and Ketones in the Presence of Water by Allylic Bromides, Metallic Tin, and Aluminum

Junzo Nokami,* Junzo Otera, Takuzo Sudo, and Rokuro Okawara

Okayama University of Science
Ridai, Okayama 700, Japan

Received July 22, 1982

Summary: Allylation of aldehydes and ketones to give the homoallyl alcohol can be carried out successfully by allyl bromide and metallic tin in the presence of water, and also the allylation by various allylic bromides is successful in the presence of water by using metallic tin and aluminum.

Allylaton at the carbonyl carbon of aldehydes or ketones by di-*n*-butylallyltin chloride,[1a] diallyltin dibromide (**1**)[2] at −70 °C, or its analogues, i.e., tin and $CH_2{=}CHCH_2X$ (X = Br, I),[1b] or $SnCl_2$ and $CH_2{=}CHCH_2I$ at room temperature,[1c] has been reported to give the corresponding homoallyl alcohol. However, we have often encountered difficulties in that the allylation in a nonaqueous solvent at room temperature does not proceed easily. For example, in the reaciton of **1** with benzaldehyde in dry ether, benzene, or ethyl acetate, the yield of the homoallyl alcohol usually was less than 50%, even after a reaction time of 10 h, and the starting materials were recovered after workup with water. As this reaction seemed to be accelerated by the addition of water, we were successful in completing the allylation by carrying out the reaction in the presence of water. An example follows below. Water (2 mL) was added to a solution of benzaldehyde (212 mg, 2 mmol) in ether (2 mL). To this heterogeneous mixture was added **1** (360 mg, 1 mmol), and stirring was continued for 1.5 h at room temperature. The organic layer was separated, washed with brine, and dried over anhydrous sodium sulfate. Removal of ether in vacuo gave the corresponding homoallyl alcohol, 1-phenylbut-3-en-1-ol in 75% yield after column chromatography on silica gel.

From a synthetic point of view, it is desirable to replace **1** by allyl bromide and metallic tin as shown in eq 1.[3] Also,

$$R^1COR^2 + CH_2{=}CHCH_2Br + {}^1/_2Sn \xrightarrow{H_2O} R^1R^2C(OH)CH_2CH{=}CH_2 \quad (1)$$

(1) (a) Peruzzo, V.; Tagliavini, G. *J. Organomet. Chem.* **1978**, *162*, 37–44. Gambaro, A.; Peruzzo, V., Plazzogna, G.; Tagliavini, G. *Ibid.* **1980**, *197*, 45–50. (b) Mukaiyama, T.; Harada, T. *Chem. Lett.* **1981**, 1527–1528. (c) Mukaiyama, T.; Harada, T.; Shoda, S. *Ibid.* **1980**, 1507–1510.

(2) The reaction of allyl bromide with metallic tin is known to give diallyltin dibromide: (a) Vijayaraghavan, K. V. *J. Indian Chem. Soc.* **1945**, *22*, 135–140; *Chem. Abstr.* **1946**, *40*, 2787. (b) Sisido, K.; Takeda, Y. *J. Org. Chem.* **1961**, *26*, 2301–2304.

0276-7333/83/2302-0191$01.50/0

ization over the C(7)–C(8)–C(9)–N fragment as might be expected for a planar skeleton. In stereochemical terms, addition of the secondary amine across the alkynyl group is *regiospecific*, there being no spectroscopic or synthetic evidence for a 2-diethylamino 3-phenyl isomer. The iron derivative **2** (M = Fe, R = Ph, R′ = H) is also formed regiospecifically via β attack (Figure 2), but in the resulting enamine the addenda are mutually trans. In this case the stereochemistry of the product appears to be controlled by hydrogen bonding between the carbonyl oxygen O(7) and the amine hydrogen atom.[18] The ruthenium–aniline adduct may have similar stereochemistry.

Several features of these reactions and products are notable in the context of CO chemistry. Complexes of type **2** are closely similar to intermediates postulated by Wilkinson and co-workers in CO reductions to oxygenated products catalyzed by binuclear ruthenium catalysts.[4] Moreover the synthesis of **2** from a multisite bound ligand with demonstrated carbocationic character,[19] carbon monoxide, and a base suggests the possibility of accomplishing selective additions to other carbocations in binuclear or cluster compounds. It is particularly noteworthy that the direction of addition, with amine functionalization of the acetylene differs from that observed in Reppe reactions[5] or in stoichiometric carbonylations of acetylenes by metal carbonyls in the presence of added bases where the nucleophile is attached to the carbonyl group.

Possible mechanisms for the carbonylation–amination sequence leading to **2** include direct CO insertion into the metal–acetylide bond of $M_2(CO)_6(\mu\text{-}\eta^2\text{-}C{\equiv}CPh)(PPh_2)$ followed by amine addition across the triple bond or intramolecular coupling of the acetylide and a carboxamide group generated via amine attack on coordinated CO. There is now ample precedent for $\mu\text{-}\eta^2$- or η-bonded carboxamide species in other systems.[1-3] However, the precursors $M_2(CO)_6(\mu\text{-}\eta^2\text{-}C{\equiv}CPh)(PPh_2)$ do not insert CO even under pressure, and in the absence of added CO amine addition to the acetylenic triple bond is extremely facile, there being no spectroscopic evidence for carboxamide species. A more likely mechanism is direct CO insertion into the dipolar μ-alkylidene complex **3**[9] or the μ-vinylidene species **4**[9] formed via amine attack on the triple bond. Such insertions, which are of obvious interest in the context of C–C bond forming processes in hydrocarbon synthesis,[20] are presently under investigation.

Acknowledgment. We are grateful to NSERC and Imperial Oil Ltd. for financial support of this work in the form of grants (A.J.C.) and a scholarship (S.A.M.)

Registry No. **2** (M = Fe, R = Ph, R′ = H), 83802-16-8; **2** (M = Ru, R = Ph, R′ = H), 83802-17-9; **2** (M = Ru, R = R′ = Et), 83802-18-0; **2** (M = Ru, R = R′ = *n*-Pr), 83802-19-1; **2** (M = Ru, R = R′ = 2-EtC_5H_9), 83802-20-4; $Fe_2(CO)_6(\mu\text{-}\eta^2\text{-}C{\equiv}CPh)(PPh_2)$, 52970-25-9; $Ru_2(CO)_6(\mu\text{-}\eta^2\text{-}C{\equiv}CPh)(PPh_2)$, 82647-81-2; Et_2NH, 109-89-7; Pr_2NH, 142-84-7; $PhNH_2$, 1484-80-6; 2-ethylpiperidine, 62-53-3.

Supplementary Material Available: Table I, atomic positions Table II, anisotropic thermal parameters, Table III, bond lengths, Table IV, bond angles, and a listing of observed and calculated structure factor amplitudes for $Ru_2(CO)_6(\mu\text{-}O{=}CCHC(Ph)NEt_2)(PPh_2)$ (25 pages). Ordering information is given on any current masthead page.

(14) The C(8)–C(9) bond length of 1.394(6) Å is somewhat longer than the standard $C(sp^2)$–$C(sp^2)$ double bond length (1.337 (6) Å) in olefins[15] and the C(9)–N distance (1.334 (7) Å) can be compared with corresponding values for >C=N< bond lengths in *N,N*-dimethylisopropylideniminium perchlorate (1.30 (2) Å)[16] or 2,6-dihydroxypyridinium cation (1.346 (3) and 1.335 (3) Å)[17] where there is unquestionably C–N multiple bonding.

(15) Kennard, O., Watson, D. G., Allen, F. H., Isaacs, N. W., Motherwell, W. D. S., Petterson, R. C.; Town, W. G. Eds. "Molecular Structures and Dimensions"; N. V. A. Oosthoek: Utrecht, Vol. A1, p 52.

(16) Trefonas, L. M.; Flurry, R. L., Jr.; Majeste, R.; Mayers, E. A.; Copeland, R. F. *J. Am. Chem. Soc.* **1966**, *88*, 2145.

(17) Mason, S. A.; White, J. C. B.; Woodlock, A. *Tetrahedron Lett.* **1969**, 5219.

(18) In the iron dimer the O(7)–C(7)–C(8)–C(9)–N unit is planar. With an N–H distance of 0.95 Å, the hydrogen atom would be located ~1.80 Å from O(7), a value compatible with a hydrogen bond interaction.

(19) Carty, A. J. *Pure Appl. Chem.* **1982**, *54*, 113.

(20) Dyke, A. F.; Guerchais, J. E.; Knox, S. A. R.; Roue, J.; Short, R. L.; Taylor, G. E.; Woodward, P. *J. Chem. Soc., Chem. Commun.* **1981**, 537.

Allylation of Aldehydes and Ketones in the Presence of Water by Allylic Bromides, Metallic Tin, and Aluminum

Junzo Nokami,* Junzo Otera, Takuzo Sudo, and Rokuro Okawara

Okayama University of Science
Ridai, Okayama 700, Japan

Received July 22, 1982

Summary: Allylation of aldehydes and ketones to give the homoallyl alcohol can be carried out successfully by allyl bromide and metallic tin in the presence of water, and also the allylation by various allylic bromides is successful in the presence of water by using metallic tin and aluminum.

Allylaton at the carbonyl carbon of aldehydes or ketones by di-*n*-butylallyltin chloride,[1a] diallyltin dibromide (**1**)[2] at −70 °C, or its analogues, i.e., tin and $CH_2{=}CHCH_2X$ (X = Br, I),[1b] or $SnCl_2$ and $CH_2{=}CHCH_2I$ at room temperature,[1c] has been reported to give the corresponding homoallyl alcohol. However, we have often encountered difficulties in that the allylation in a nonaqueous solvent at room temperature does not proceed easily. For example, in the reaciton of **1** with benzaldehyde in dry ether, benzene, or ethyl acetate, the yield of the homoallyl alcohol usually was less than 50%, even after a reaction time of 10 h, and the starting materials were recovered after workup with water. As this reaction seemed to be accelerated by the addition of water, we were successful in completing the allylation by carrying out the reaction in the presence of water. An example follows below. Water (2 mL) was added to a solution of benzaldehyde (212 mg, 2 mmol) in ether (2 mL). To this heterogeneous mixture was added **1** (360 mg, 1 mmol), and stirring was continued for 1.5 h at room temperature. The organic layer was separated, washed with brine, and dried over anhydrous sodium sulfate. Removal of ether in vacuo gave the corresponding homoallyl alcohol, 1-phenylbut-3-en-1-ol in 75% yield after column chromatography on silica gel.

From a synthetic point of view, it is desirable to replace **1** by allyl bromide and metallic tin as shown in eq 1.[3] Also,

$$R^1COR^2 + CH_2{=}CHCH_2Br + {}^1/_2Sn \xrightarrow{H_2O} R^1R^2C(OH)CH_2CH{=}CH_2 \quad (1)$$

(1) (a) Peruzzo, V.; Tagliavini, G. *J. Organomet. Chem.* **1978**, *162*, 37–44. Gambaro, A.; Peruzzo, V., Plazzogna, G.; Tagliavini, G. *Ibid.* **1980**, *197*, 45–50. (b) Mukaiyama, T.; Harada, T. *Chem. Lett.* **1981**, 1527–1528. (c) Mukaiyama, T.; Harada, T.; Shoda, S. *Ibid.* **1980**, 1507–1510.

(2) The reaction of allyl bromide with metallic tin is known to give diallyltin dibromide: (a) Vijayaraghavan, K. V. *J. Indian Chem. Soc.* **1945**, *22*, 135–140; *Chem. Abstr.* **1946**, *40*, 2787. (b) Sisido, K.; Takeda, Y. *J. Org. Chem.* **1961**, *26*, 2301–2304.

0276-7333/83/2302-0191$01.50/0

Table I. Allylation of Aldehydes and Ketones by Allyl Bromide and Metallic Tin in the Presence of Water[a] at Room Temperature

aldehyde or ketone (mmol)	Sn, mmol	allyl bromide, mmol	reaction time, h	homoallyl alcohol yield,[b] %
PhCHO (1.35)	0.77	1.96	2	73 (75)
$CH_3(CH_2)_4CHO$ (1.46)	0.85	1.96	2	70 (87)
$CH_3CH{=}CHCHO$ (1.30)	0.82	1.96	2	57 (79)
citral (1.37)	0.82	1.90	2	68 (79)
cyclohexanone (1.32)	0.82	1.96	3	76 (70)
2-methylcyclohexanone (1.52)	0.91	2.08	12	45 (59)
$CH_3(CH_2)_5COCH_3$ (1.28)	0.83	1.96	12	58 (61)
$CH_3COCH_2CH_2COOH$ (1.34)	0.82	1.96	12	47[c] (60)
$PhCOCH_3$ (1.43)	0.81	1.96	12	50 (62)

[a] The reaction system consisted of ether (1 mL), water (1 mL), and hydrobromic acid (5%, 0.1 mL). [b] After purification, based on aldehyde or ketone. The yield in parentheses shows that of by using diallyltin dibromide **1** (0.5 molar equiv to aldehyde or ketone). [c] 3-Allyl-4-valerolactone.

Table II. Synthesis of β-Methylhomoallyl Alcohol

aldehyde[a] (mmol)	1-bromobut-2-ene, mmol	metallic Sn, mmol	metallic Al, mmol	solvent (mL)	reaction time, h	yield, % (erythro/threo)[b]
PhCHO (1.42)	1.94	0.81	0.85	Et_2O/H_2O (2/1)	9	87 (60/40)
				THF/H_2O (2/0.2)	2	81 (78/22)
CH_3CHO (20.0)	19.4	8.3	18.0	Et_2O/H_2O (5/3)	15	100 (61/39)
$CH_3(CH_2)_4CHO$ (1.37)	1.84	0.78	1.63	Et_2O/H_2O (2/1)	12	87 (53/47)
				THF/H_2O (2/0.2)	2	97 (60/40)
				$EtOH/H_2O$ (2/0.2)	5	89 (63/37)
$(CH_3)_2CHCHO$ (20.1)	19.4	8.4	19.0	Et_2O/H_2O (5/3)	15	92 (65/35)
$CH_3CH{=}CHCHO$ (1.74)	1.84	0.82	1.82	Et_2O/H_2O (2/1)	12	64 (59/41)
				THF/H_2O (2/0.2)	2	96 (67/33)
citral (1.40)	1.84	0.80	1.90	Et_2O/H_2O (2/1)	9	81 (69/31)
				THF/H_2O (2/0.2)	2	76 (73/27)

[a] Commercially available material was used without purification. [b] The ratio was determined by GPC based on the authentic sample prepared.[7]

in this system, satisfactory results were obtained (Table I). A typical procedure is as follows. The heterogeneous mixture of hexanal (1.46 mmol), allyl bromide (1.96 mmol), commercially available tin powder (200 mesh, 0.85 mmol), ether (1 mL), and water (1 mL)[4] was vigorously stirred at room temperature, and dilute hydrobromic acid (5%, 0.1 mL) was added to this mixture. After 2 h, the organic layer was separated, washed with brine, dried, and distilled (Kugelrohr) to give the homoallyl alcohol non-1-en-4-ol in 70% yield.

In addition, reactions involving metallic tin and a variety of allylic bromides were carried out. In these reactions, we have found that the addition of metallic aluminum (commercially available powder or foil)[5] dramatically improves the yield[6] (Table II). For example, the synthesis of β-methylhomoallyl alcohols[7] will be shown. The mixture of 1-bromobut-2-ene (**2**, 2.62 g, 19.4 mmol) and acetaldehyde (1.0 g, ca. 90%, 20.0 mmol) was dissolved in ether (5 mL), and water (3 mL), tin powder (1 g, 200 mesh, 8.4 mmol), aluminum powder (0.5 g, 200 mesh, 18.5 mmol), and a catalytic amount of hydrobromic acid were added. The mixture was vigorously stirred for 15 h at room temperature. The organic layer was separated, washed with brine, dried, and distilled (Kugelrohr) to give 3-methylpent-1-en-3-ol quantitatively. From Table II, it is clearly shown that the further improvement of the yield can be attained in some cases by changing ether to THF.

Prenyl bromide, methyl 11-bromoundec-9-enoate, and 1-bromohept-2-ene can react with aldehydes, under conditions similar to those shown in Table II, to give the corresponding homoallylic alcohols in fairly satisfactory yield. Also, some larger scale experiments[8] showed satis-

(3) It is known that the reactin of benzyl chloride with metallic tin proceeds in boiling water to give tribenzyltin chloride: Sisido, K.; Takeda, Y.; Kinugawa, Z. *J. Am. Chem. Soc.* **1961**, *83*, 538–541.

(4) We could not observe the product in dry THF or ether by TLC monitoring even when the activated metallic tin[2b] was used. However, the formation of the product could be confirmed after the addition of water into the mixture to workup.

(5) Aluminu chloride, alumnum oxide, or metallic zinc were ineffective.

(6) Among the aldehydes shown in Table II, only benzaldehyde can react with **2** without aluminum to give the product in ca. 60% yield.

(7) Yamamoto, Y.; Yatagai, H.; Naruta, Y.; Maruyama, K. *J. Am. Chem. Soc.* **1980**, *102*, 7107–7109.

(8) For example, to the heterogeneous mixture of allyl bromide (0.1 mol), tin powder (0.05 mol), water (20 mL), and a catalytic amount of hydrobromic acid, cyclohexanone (0.1 mol) was added dropwise during 0.5–1 h with vigorous stirring. After the tin was disappeared, the stirring was continued for additional 2–3 h. The reaction mixture was neutralized with sodium carbonate. The product obtained by steam distillation was extracted with ether and purified by distillation under reduced pressure (63 °C (0.6 torr), 77%).

factory results. Thus a wide applicability of this reaction has been confirmed.

Registry No. 2, 4784-77-4; PhCHO, 100-52-7; $CH_3(CH_2)_4CHO$, 66-25-1; $CH_3CH{=}CHCHO$, 4170-30-3; $CH_3(CH_2)_5COCH_3$, 111-13-7; $CH_3COCH_2CH_2CO_2H$, 123-76-2; $PhCOCH_3$, 98-86-2; $CH_2{=}CHCH_2Br$, 106-95-6; CH_3CHO, 75-07-0; Sn, 7440-31-5; Al, 7429-90-5; H_2O, 7732-18-5; PhCHO homoallyl alcohol, 936-58-3; $CH_3(CH_2)_4CHO$ homoallyl alcohol, 35192-73-5; $CH_3CH{=}CHCHO$ homoallyl alcohol, 5638-26-6; $CH_3(CH_2)_5COCH_3$ homoallyl alcohol, 38564-33-9; $PhCOCH_3$ homoallyl alcohol, 4743-74-2; $(CH_3)_2CHCHO$, 78-84-2; PhCHO (*R**,*S**)-β-methylhomoallyl alcohol, 52922-19-7; PhCHO (*R**,*R**)-β-methylhomoallyl alcohol, 52922-10-8; CH_3CHO (*R**,*R**)-β-methylhomoallyl alcohol, 1538-23-4; CH_3CHO (*R**,*S**)-β-methylhomoallyl alcohol, 1538-22-3; $CH_3(CH_2)_4CHO$ (*R**,*R**)-β-methylhomoallyl alcohol, 52922-22-2; $CH_3(CH_2)_4CHO$ (*R**,*S**)-β-methylhomoallyl alcohol, 52922-27-7; $(CH_3)_2CHCHO$ (*R**,*R**)-β-methylhomoallyl alcohol, 1502-91-6; $(CH_3)_2CHCHO$ (*R**,*S**)-β-methylhomoallyl alcohol, 1502-90-5; $CH_3CH{=}CHCHO$ (*R**,*R**)-β-methylhomoallyl alcohol, 78377-34-1; $CH_3CH{=}CHCHO$ (*R**,*S**)-β-methylhomoallyl alcohol, 78377-32-9; citral homoallyl alcohol, 28897-20-3; cyclohexanone homoallyl alcohol, 1123-34-8; 2-methylcyclohexanone homoallyl alcohol, 24580-51-6; 4-allyl-4-valerolactone, 69492-28-0; citral (*R**,*S**)-β-methylhomoallyl alcohol, 83605-34-9; citral (*R**,*R**)-β-methylhomoallyl alcohol, 83605-35-0; citral, 5392-40-5; cyclohexanone, 108-94-1; 2-methylcyclohexanone, 583-60-8.

Electronic Structure of the Silicon–Silicon Double Bond. Silicon-29 Shielding Anisotropy in Tetramesityldisilene

Kurt W. Zilm, David M. Grant,* and Josef Michl*
Department of Chemistry, University of Utah
Salt Lake City, Utah 84112

Mark J. Fink and Robert West
Department of Chemistry, University of Wisconsin
Madison, Wisconsin 53706

Received August 10, 1982

Summary: The solid ^{29}Si NMR spectrum of tetramesityldisilene (σ_{11} 180, σ_{22} 27, and σ_{33} −15 ppm downfield from Me_4Si) shows an anisotropy comparable to that of the solid ^{13}C spectrum of ethylene (σ_{11} 234, σ_{22} 120, and σ_{33} 24 ppm downfield from Me_4Si). The solid ^{29}Si NMR spectrum of tetramesityldisilane (σ_{11} −37, σ_{22} −56, and σ_{33} −72 ppm downfield from Me_4Si) shows a much smaller anisotropy, similar to that in ^{13}C spectra of alkanes. It is concluded that the electronic structure of the Si=Si double bond bears a close resemblance to that of the C=C double bond.

Within a year, the report[1-3] of the remarkable stability of the first compound with a silicon–silicon double bond, tetramesityldisilene (1), was followed by two additional reports of disilene syntheses.[4,5] Along with the recent isolation of a compound with a carbon–silicon double bond[6] culminating much matrix-isolation and gas-phase work that permitted direct spectroscopic observation of less stabilized members of the silene family,[7] this secured the demise of the time-honored rule concerning the instability—or nonexistence—of multiple bonds involving silicon. In spite of this intense interest, relatively little is known as yet about the detailed nature of the Si=Si moiety. According to an X-ray structure analysis[2] on 1, the four C–Si bonds are approximately coplanar (slightly antipyramidalized) and the Si=Si distance is about 9% shorter than the Si—Si distance in tetramesityldisilane (2) in good agreement with quantum mechanical calculations on Si_2H_4 itself.[8] This evidence suggests a fairly close analogy with the corresponding compounds of carbon.

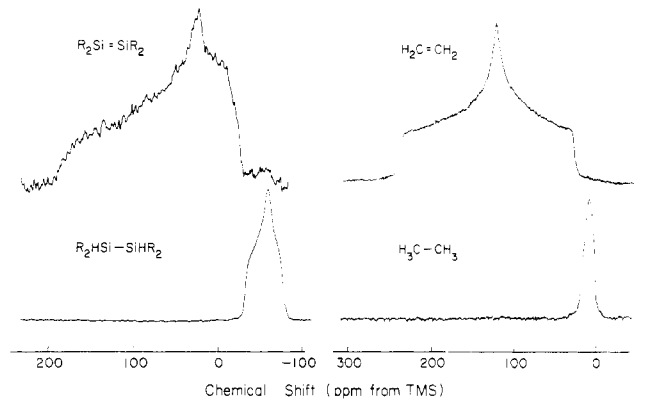

Figure 1. Solid-state ^{29}Si NMR (left) and ^{13}C NMR (right) spectra obtained by the cross-polarization technique. R stands for mesityl (2,4,6-$(CH_3)_3C_6H_2$).

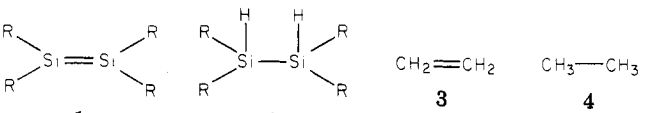

1 2 3 4

R = 2,4,6-$(CH_3)_3C_6H_2$

We now wish to report the measurement of the anisotropy of the ^{29}Si chemical shift in 1. This probe of the finer details of electronic structure permits us to conclude that the Si=Si and C=C double bonds are indeed quite analogous even in intimate detail (Figure 1).

The NMR chemical shift of a nucleus in a molecule is a function of the orientation of the molecule in the magnetic field. For ethylene (3) the principal values measured in parts per million downfield from Me_4Si are 24 for molecules aligned with their plane perpendicular to the magnetic field, 120 for molecules with the C=C bond aligned with the magnetic field, and 234 for molecules with their short in-plane axis aligned with the magnetic field.[9] For ethane (4), the difference of the chemical shifts for molecules whose C–C axis lies along the magnetic field and those whose C–C axis lies perpendicular to the magnetic

(1) West, R.; Fink, M. J.; Michl, J. 15th Organosilicon Symposium, Duke University, Durham, NC, Mar 27–28, 1981.
(2) West, R.; Fink, M. J.; Michl, J. 6th International Symposium on Organosilicon Chemistry, Budapest, Hungary, Aug 23–29, 1981.
(3) West, R.; Fink, M. J.; Michl, J. *Science (Washington, D.C.)* **1981**, *214*, 1343.
(4) Masamune, S.; Hanzawa, Y.; Murakami, S.; Bally, T.; Blount, J. F. *J. Am. Chem. Soc.* **1982**, *104*, 1150.
(5) Boudjouk, P.; Han, B.-H.; Anderson, K. R. *J. Am. Chem. Soc.* **1982**, *104*, 4992.
(6) Brook, A. G.; Abdesaken, F.; Gutekunst, B.; Gutekunst, A.; Kallury, R. K. *J. Chem. Soc., Chem. Commun.* **1981**, 191.
(7) Chapman, O. L.; Chang, C. C.; Kolc, J.; Jung, M. E.; Lowe, J. A.; Barton, T. J.; Turney, M. L. *J. Am. Chem. Soc.* **1976**, *98*, 7844. Chedekel, M. R.; Skogland, M.; Kreeger, R. L.; Schechter, H. *Ibid.* **1976**, *98*, 7846. Nefedov, O. M.; Mal'tsev, A. K.; Khabashesku, V. N.; Korolev, V. A. *J. Organomet. Chem.* **1980**, *201*, 123. Gusel'nikov, L. E.; Volkova, V. V.; Avakyan, V. G.; Nametkin, N. S. *Ibid.* **1980**, *201*, 137. Mahaffy, P. G.; Gutowsky, R.; Montgomery, L. K. *J. Am. Chem. Soc.* **1980**, *102*, 1854. Rosmus, P.; Bock, H.; Solouki, B.; Maier, G.; Mihm, G. *Angew. Chem., Int. Ed. Engl.* **1981**, *20*, 598. Maier, G.; Mihm, G.; Reisenauer, H. P. *Ibid.* **1981**, *20*, 597. Drahnak, T. J.; Michl, J.; West, R. *J. Am. Chem. Soc.* **1981**, *103*, 1845.
(8) Lischka, H.; Köhler, H.-J. *Chem. Phys. Lett.* **1982**, *85*, 467 and references therein.
(9) Zilm, K. W.; Grant, D. M.; Conlin, R. T.; Michl, J. *J. Am. Chem. Soc.* **1978**, *100*, 8038. Zilm, K. W.; Conlin, R. T.; Grant, D. M.; Michl, J. *Ibid.* **1980**, *102*, 6672.

0276-7333/83/2302-0193$01.50/0

factory results. Thus a wide applicability of this reaction has been confirmed.

Registry No. 2, 4784-77-4; PhCHO, 100-52-7; $CH_3(CH_2)_4CHO$, 66-25-1; $CH_3CH{=}CHCHO$, 4170-30-3; $CH_3(CH_2)_5COCH_3$, 111-13-7; $CH_3COCH_2CH_2CO_2H$, 123-76-2; $PhCOCH_3$, 98-86-2; $CH_2{=}CHCH_2Br$, 106-95-6; CH_3CHO, 75-07-0; Sn, 7440-31-5; Al, 7429-90-5; H_2O, 7732-18-5; PhCHO homoallyl alcohol, 936-58-3; $CH_3(CH_2)_4CHO$ homoallyl alcohol, 35192-73-5; $CH_3CH{=}CHCHO$ homoallyl alcohol, 5638-26-6; $CH_3(CH_2)_5COCH_3$ homoallyl alcohol, 38564-33-9; $PhCOCH_3$ homoallyl alcohol, 4743-74-2; $(CH_3)_2CHCHO$, 78-84-2; PhCHO (*R**,*S**)-β-methylhomoallyl alcohol, 52922-19-7; PhCHO (*R**,*R**)-β-methylhomoallyl alcohol, 52922-10-8; CH_3CHO (*R**,*R**)-β-methylhomoallyl alcohol, 1538-23-4; CH_3CHO (*R**,*S**)-β-methylhomoallyl alcohol, 1538-22-3; $CH_3(CH_2)_4CHO$ (*R**,*R**)-β-methylhomoallyl alcohol, 52922-22-2; $CH_3(CH_2)_4CHO$ (*R**,*S**)-β-methylhomoallyl alcohol, 52922-27-7; $(CH_3)_2CHCHO$ (*R**,*R**)-β-methylhomoallyl alcohol, 1502-91-6; $(CH_3)_2CHCHO$ (*R**,*S**)-β-methylhomoallyl alcohol, 1502-90-5; $CH_3CH{=}CHCHO$ (*R**,*R**)-β-methylhomoallyl alcohol, 78377-34-1; $CH_3CH{=}CHCHO$ (*R**,*S**)-β-methylhomoallyl alcohol, 78377-32-9; citral homoallyl alcohol, 28897-20-3; cyclohexanone homoallyl alcohol, 1123-34-8; 2-methylcyclohexanone homoallyl alcohol, 24580-51-6; 4-allyl-4-valerolactone, 69492-28-0; citral (*R**,*S**)-β-methylhomoallyl alcohol, 83605-34-9; citral (*R**,*R**)-β-methylhomoallyl alcohol, 83605-35-0; citral, 5392-40-5; cyclohexanone, 108-94-1; 2-methylcyclohexanone, 583-60-8.

Electronic Structure of the Silicon–Silicon Double Bond. Silicon-29 Shielding Anisotropy in Tetramesityldisilene

Kurt W. Zilm, David M. Grant,* and Josef Michl*
Department of Chemistry, University of Utah
Salt Lake City, Utah 84112

Mark J. Fink and Robert West
Department of Chemistry, University of Wisconsin
Madison, Wisconsin 53706

Received August 10, 1982

Summary: The solid ^{29}Si NMR spectrum of tetramesityldisilene (σ_{11} 180, σ_{22} 27, and σ_{33} −15 ppm downfield from Me_4Si) shows an anisotropy comparable to that of the solid ^{13}C spectrum of ethylene (σ_{11} 234, σ_{22} 120, and σ_{33} 24 ppm downfield from Me_4Si). The solid ^{29}Si NMR spectrum of tetramesityldisilane (σ_{11} −37, σ_{22} −56, and σ_{33} −72 ppm downfield from Me_4Si) shows a much smaller anisotropy, similar to that in ^{13}C spectra of alkanes. It is concluded that the electronic structure of the Si=Si double bond bears a close resemblance to that of the C=C double bond.

Within a year, the report[1-3] of the remarkable stability of the first compound with a silicon–silicon double bond, tetramesityldisilene (1), was followed by two additional reports of disilene syntheses.[4,5] Along with the recent isolation of a compound with a carbon–silicon double bond[6] culminating much matrix-isolation and gas-phase work that permitted direct spectroscopic observation of less stabilized members of the silene family,[7] this secured the demise of the time-honored rule concerning the instability—or nonexistence—of multiple bonds involving silicon. In spite of this intense interest, relatively little is known as yet about the detailed nature of the Si=Si moiety. According to an X-ray structure analysis[2] on 1, the four C–Si bonds are approximately coplanar (slightly antipyramidalized) and the Si=Si distance is about 9% shorter than the Si—Si distance in tetramesityldisilane (2) in good agreement with quantum mechanical calculations on Si_2H_4 itself.[8] This evidence suggests a fairly close analogy with the corresponding compounds of carbon.

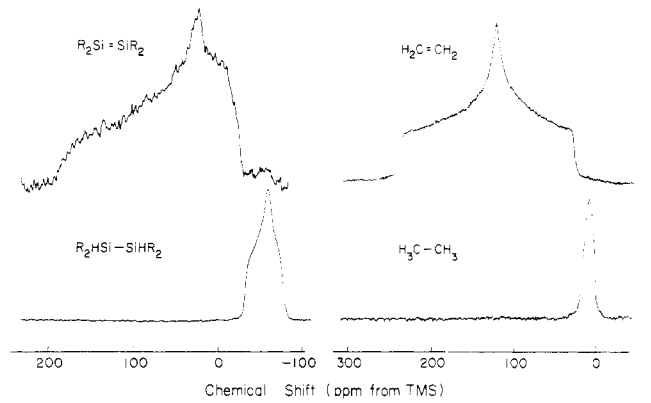

Figure 1. Solid-state ^{29}Si NMR (left) and ^{13}C NMR (right) spectra obtained by the cross-polarization technique. R stands for mesityl (2,4,6-$(CH_3)_3C_6H_2$).

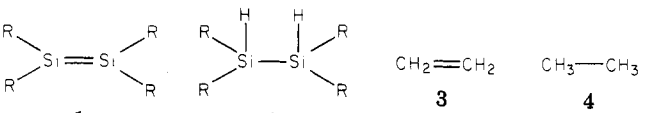

1 2 3 4

R = 2,4,6-$(CH_3)_3C_6H_2$

We now wish to report the measurement of the anisotropy of the ^{29}Si chemical shift in 1. This probe of the finer details of electronic structure permits us to conclude that the Si=Si and C=C double bonds are indeed quite analogous even in intimate detail (Figure 1).

The NMR chemical shift of a nucleus in a molecule is a function of the orientation of the molecule in the magnetic field. For ethylene (3) the principal values measured in parts per million downfield from Me_4Si are 24 for molecules aligned with their plane perpendicular to the magnetic field, 120 for molecules with the C=C bond aligned with the magnetic field, and 234 for molecules with their short in-plane axis aligned with the magnetic field.[9] For ethane (4), the difference of the chemical shifts for molecules whose C–C axis lies along the magnetic field and those whose C–C axis lies perpendicular to the magnetic

(1) West, R.; Fink, M. J.; Michl, J. 15th Organosilicon Symposium, Duke University, Durham, NC, Mar 27–28, 1981.
(2) West, R.; Fink, M. J.; Michl, J. 6th International Symposium on Organosilicon Chemistry, Budapest, Hungary, Aug 23–29, 1981.
(3) West, R.; Fink, M. J.; Michl, J. *Science (Washington, D.C.)* **1981**, *214*, 1343.
(4) Masamune, S.; Hanzawa, Y.; Murakami, S.; Bally, T.; Blount, J. F. *J. Am. Chem. Soc.* **1982**, *104*, 1150.
(5) Boudjouk, P.; Han, B.-H.; Anderson, K. R. *J. Am. Chem. Soc.* **1982**, *104*, 4992.
(6) Brook, A. G.; Abdesaken, F.; Gutekunst, B.; Gutekunst, A.; Kallury, R. K. *J. Chem. Soc., Chem. Commun.* **1981**, 191.
(7) Chapman, O. L.; Chang, C. C.; Kolc, J.; Jung, M. E.; Lowe, J. A.; Barton, T. J.; Turney, M. L. *J. Am. Chem. Soc.* **1976**, *98*, 7844. Chedekel, M. R.; Skogland, M.; Kreeger, R. L.; Schechter, H. *Ibid.* **1976**, *98*, 7846. Nefedov, O. M.; Mal'tsev, A. K.; Khabashesku, V. N.; Korolev, V. A. *J. Organomet. Chem.* **1980**, *201*, 123. Gusel'nikov, L. E.; Volkova, V. V.; Avakyan, V. G.; Nametkin, N. S. *Ibid.* **1980**, *201*, 137. Mahaffy, P. G.; Gutowsky, R.; Montgomery, L. K. *J. Am. Chem. Soc.* **1980**, *102*, 1854. Rosmus, P.; Bock, H.; Solouki, B.; Maier, G.; Mihm, G. *Angew. Chem., Int. Ed. Engl.* **1981**, *20*, 598. Maier, G.; Mihm, G.; Reisenauer, H. P. *Ibid.* **1981**, *20*, 597. Drahnak, T. J.; Michl, J.; West, R. *J. Am. Chem. Soc.* **1981**, *103*, 1845.
(8) Lischka, H.; Köhler, H.-J. *Chem. Phys. Lett.* **1982**, *85*, 467 and references therein.
(9) Zilm, K. W.; Grant, D. M.; Conlin, R. T.; Michl, J. *J. Am. Chem. Soc.* **1978**, *100*, 8038. Zilm, K. W.; Conlin, R. T.; Grant, D. M.; Michl, J. *Ibid.* **1980**, *102*, 6672.

0276-7333/83/2302-0193$01.50/0

field is only ~14 ppm; the signal is centered at 12 ppm (Figure 1). These values are fairly characteristic of alkenes and alkanes in general: the former exhibit huge anisotropies, the latter much smaller ones. This is well understood in a qualitative sense. The NMR experiment probes the electronic structure around a nucleus, in the plane perpendicular to the field direction; thus, in a molecule of **3** whose plane is perpendicular to the magnetic field, it responds only to σ electrons and the corresponding component of the chemical shift tensor lies in the region characteristic of alkanes. In a molecule of **4**, all tensor shielding components depend upon σ electrons so its anisotropy is small. On the other hand, when a molecule of **3** is oriented so that the axes of the atomic p orbitals of the carbons in its π system are perpendicular to the magnetic field, their very different involvement in chemical bonding is reflected in the observed chemical shift values. In this fashion, the anisotropy of the electronic structure of a carbon atom involved in a C=C bond compared with that involved in a C–C bond translates directly into the anisotropy of its chemical shift.

The three principal values of chemical shift can be read off the powder pattern spectra obtained on solid samples. This is shown in Figure 1, which illustrates very clearly the analogy between carbon and silicon. Just as in the case of the ^{13}C NMR spectra of **3** vs. **4**, the ^{29}Si NMR spectrum of disilene **1** displays a large anisotropy and that of **2** a small one. Computer line-shape fitting yields the values σ_{11} 180, σ_{22} 27, and σ_{33} −15 for **1** and σ_{11} −31, σ_{22} −56, and σ_{33} −73 for **2** (ppm downfield from Me_4Si).

We conclude that the electronic structure of the Si=Si double bond bears a close resemblance to that of the C=C double bond.

Acknowledgment. This research was supported by NSF Grants CHE 78-27094 and CHE 80-00256 and the Air Force Office of Scientific Research AF-AFOSR 82-0067. The U.S. Government is authorized to reproduce and distribute reprints for government purposes notwithstanding any copyright notation thereon.

Registry No. 1, 80785-72-4; 2, 74864-45-2; 3, 74-85-1; 4, 74-84-0.

Alkylation and Aldol Reactions of Iron Acyl Enolates

Lanny S. Liebeskind* and Mark E. Welker

Department of Chemistry, Florida State University
Tallahassee, Florida 32306

Received August 24, 1982

Summary: Treatment of the acyliron complex CpFe(CO)(PPh$_3$)COCH$_3$ with lithium diisopropylamide at low temperature in THF generates the corresponding enolate. Reaction of this enolate with alkyl halides gives high yields of C-alkylation products while aldol products result from reaction with carbonyl compounds. Oxidative cleavage of the acyl–iron bond occurs in high yield (NBS, CH_2Cl_2/EtOH) to give esters.

In order to expand the preparative chemistry of certain stoichiometric organometallics in conjunction with their utilization in organic synthesis, we have initiated a research program to explore the synthetic applications of organotransition-metal carbanions. Our first effort in this area has concerned the conversion of iron acyls into iron acyl enolates and their reaction with various electrophiles to produce derivatized iron acyls (eq 1).[1]

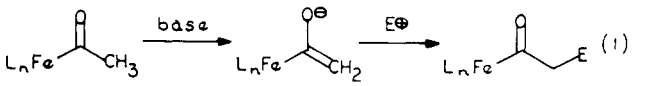

(1)

After our initial attempts to generate the enolate of CpFe(CO)$_2$COCH$_3$[2] **1a** were thwarted by migration of the acyl group to the cyclopentadienyl ring,[3] we found that slow addition of a THF solution of CpFe(CO)(PPh$_3$)-COCH$_3$[4] **1b** to a 0.15 M solution of lithium diisopropylamide (LDA) maintained under N_2 at −42 °C gave a deep red solution of the corresponding lithium enolate **2**. After the mixture was stirred at −42 °C for 1.5 h, the enolate was quenched with various electrophiles to give good to excellent yields of products (Scheme I). For example, treatment of enolate **2b** with MeI, EtBr, allyl bromide, and benzyl bromide gave C-alkylation products **3b–6b** in isolated, purified yields of 78, 81, 78 and 91%, respectively.[5] Aldol reactions with acetone, acetaldehyde, pivaldehyde, and benzaldehyde similarly occurred in good yields to give compounds **7b–10b** with the latter three reactants each giving a ca. 1:1 mixture of diastereomeric products.[5]

In principle, the asymmetric iron atom of the enolate could influence the formation of the new asymmetric carbon atom in aldol products **8–10**. To briefly probe this

(1) After submission of our manuscript, Professor Bergman (Berkeley) reported the successful generation of the enolate of a cobaltacyclopentanone which underwent high yield aldol and alkylation reactions: Theopold, K. H.; Becker, P. N.; Bergman, R. G. *J. Am. Chem. Soc.* **1982**, *104*, 5250.

(2) King, R. B. *J. Am. Chem. Soc.* **1963**, *85*, 1918.

(3) The base-induced migration of organic fragments from metal to a coordinated cyclopentadienyl ring has been observed in a number of systems: Werner, H.; Hofmann, W. *Angew. Chem., Int. Ed. Engl.* **1978**, 17, 464. Berryhill, S. R.; Sharenow, B. *J. Organomet. Chem.* **1981**, *221*, 143.

(4) Bibler, J. P.; Wojcicki, A. *Inorg. Chem.* **1966**, *5*, 889.

(5) Spectral data and elemental analyses. **3b**: orange solid; mp 158–161 °C ($CHCl_3$/petroleum ether); IR ($CHCl_3$, cm^{-1}) 3040, 3010, 2980, 1910, 1605, 1490, 1440, 1100, 1080, 880, 830; ^1H NMR (60 MHz, $CDCl_3$, δ) 7.50–7.13 (m, 15 H), 4.33 (br s, 5 H), 2.93–2.37 (m, 2 H), 0.56 (t, J = 7 Hz, 3 H). Anal. Calcd for $C_{27}H_{25}FeO_2P$: C, 69.25; H, 5.38. Found: C, 69.47; H, 5.48. **4b**: orange solid; mp 157–159 °C ($CHCl_3$/petroleum ether); IR ($CHCl_3$, cm^{-1}) 3020, 2980, 1920, 1608, 1440, 1100; ^1H NMR (60 MHz, $CDCl_3$, δ) 7.50–7.13 (m, 15 H), 4.35 (br s, 5 H), 2.93–2.40 (m, 2 H), 1.43–0.87 (m, 2 H), 0.58 (t, J = 6 Hz, 3 H). Anal. Calcd for $C_{28}H_{27}FeO_2P$: C, 69.72; H, 5.64. Found: C, 69.82; H, 5.80. **5b**: orange solid; mp 115–117 °C ($CHCl_3$/petroleum ether); IR ($CHCl_3$, cm^{-1}) 3040, 3005, 1910, 1600, 1485, 1440, 1100, 910, 820; ^1H NMR (60 MHz, $CDCl_3$, δ) 7.40–7.03 (m, 15 H), 5.70–5.07 (m, 1 H), 4.93–4.50 (m, 2 H), 4.30 (br s, 5 H), 3.00–2.47 (m, 2 H), 2.10–1.57 (m, 2 H). Anal. Calcd for $C_{29}H_{27}FeO_2P$: C, 70.46; H, 5.51. Found: C, 70.36; H, 5.73. **6b**: orange solid; mp 128–131 °C ($CHCl_3$/petroleum ether); IR ($CHCl_3$, cm^{-1}) 3070, 3010, 1920, 1600, 1490, 1440, 1100, 830; ^1H NMR (60 MHz, $CDCl_3$, δ) 7.70–6.70 (m, 20 H), 4.30 (br s, 5 H), 3.20–2.00 (m, 4 H). Anal. Calcd for $C_{33}H_{29}FeO_2P$: C, 72.81; H, 5.37. Found: C, 72.89; H, 5.55. **7b**: yellow-orange solid; mp 130–132 °C ($CHCl_3$/petroleum ether); IR ($CHCl_3$, cm^{-1}) 3420, 3080, 2995, 1920, 1590, 1490, 1440, 1120, 1100, 950; ^1H NMR (60 MHz, $CDCl_3$, δ) 7.67–7.10 (m, 15 H), 4.30 (d, J_{P-H} = 1 Hz, 5 H), 4.00 (br s, 1 H), 3.17 (d, J = 17 Hz, 1 H), 2.70 (d, J = 17 Hz, 1 H), 1.00 (s, 3 H), 0.70 (s, 3 H). Anal. Calcd for $C_{29}H_{29}FeO_3P$: C, 67.98; H, 5.71. Found: C, 67.70; H, 5.69. **8b**: yellow-orange solid; 50/50 mixture of diastereomers; IR ($CHCl_3$, cm^{-1}) 3395, 3078, 3060, 2998, 1918, 1583, 1481, 1435, 1120, 1093, 965, 825; ^1H NMR (60 MHz, C_6D_6, δ) 7.77–6.73 (m, 15 H), 4.16 (m, 5 H), 3.70 (br s, 1 H), 3.33–2.90 (m, 3 H), 1.03, 1.00 (two overlapping doublets, each J = 7 Hz, 3 H total, 50/50 ratio). Anal. Calcd for $C_{28}H_{27}FeO_3P$: C, 67.49; H, 5.46. Found: C, 67.70; H, 5.66. **9b**: yellow-orange solid; 50/50 mixture of diastereomers; IR ($CHCl_3$, cm^{-1}) 3440, 3080, 3020, 2980, 1920, 1585, 1480, 1440, 1095, 1070, 1000, 825; ^1H NMR (60 MHz, $CDCl_3$, δ) 7.50–6.93 (m, 15 H), 4.23 (br s, 5 H), 3.60–2.50 (complex m, 3 H), 2.13 (br s, 1 H), 0.63, 0.60 (two singlets, 9 H total, 50/50 ratio). Anal. Calcd for $C_{31}H_{33}FeO_3P$: C, 68.80; H, 6.16. Found: C, 68.97; H, 5.90. **9d**: yellow orange solid; 60/40 mixture of diastereomers; IR ($CHCl_3$, cm^{-1}) 3400, 2980, 2882, 1915, 1582, 1440, 1383, 1172, 1100, 1039, 1020, 935; ^1H NMR (270 MHz, $CDCl_3$, δ) 7.97–7.81 (m, 4 H), 7.62–7.38 (m, 6 H), 4.24 (m, 5 H), 3.46–2.22 (m, 8 H), 1.10, 0.94 (two triplets, each J = 5 Hz, 6 H total, 40/60 ratio), 0.79, 0.75 (two singlets, 9 H total, 60/40 ratio). Anal. Calcd for $C_{29}H_{38}FeNO_3P$: C, 65.05; H, 7.15. Found: C, 65.23; H, 7.33. **10b**: yellow-orange solid; 50/50 mixture of diastereomers; IR ($CHCl_3$, cm^{-1}) 3407, 3059, 3000, 1919, 1580, 1480, 1434, 1093, 998, 937, 824; ^1H NMR (60 MHz, $CDCl_3$, δ) 7.73–7.07 (m, 20 H), 4.93–4.50 (m, 1 H), 4.40 (m, 5 H), 4.00 (m, 0.5 H, exchanges with D_2O), 3.33–2.67 (m, 2.5 H, 0.5 H exchanges with D_2O).

0276-7333/83/2302-0194$01.50/0

field is only ~14 ppm; the signal is centered at 12 ppm (Figure 1). These values are fairly characteristic of alkenes and alkanes in general: the former exhibit huge anisotropies, the latter much smaller ones. This is well understood in a qualitative sense. The NMR experiment probes the electronic structure around a nucleus, in the plane perpendicular to the field direction; thus, in a molecule of **3** whose plane is perpendicular to the magnetic field, it responds only to σ electrons and the corresponding component of the chemical shift tensor lies in the region characteristic of alkanes. In a molecule of **4**, all tensor shielding components depend upon σ electrons so its anisotropy is small. On the other hand, when a molecule of **3** is oriented so that the axes of the atomic p orbitals of the carbons in its π system are perpendicular to the magnetic field, their very different involvement in chemical bonding is reflected in the observed chemical shift values. In this fashion, the anisotropy of the electronic structure of a carbon atom involved in a C=C bond compared with that involved in a C–C bond translates directly into the anisotropy of its chemical shift.

The three principal values of chemical shift can be read off the powder pattern spectra obtained on solid samples. This is shown in Figure 1, which illustrates very clearly the analogy between carbon and silicon. Just as in the case of the ^{13}C NMR spectra of **3** vs. **4**, the ^{29}Si NMR spectrum of disilene **1** displays a large anisotropy and that of **2** a small one. Computer line-shape fitting yields the values σ_{11} 180, σ_{22} 27, and σ_{33} −15 for **1** and σ_{11} −31, σ_{22} −56, and σ_{33} −73 for **2** (ppm downfield from Me_4Si).

We conclude that the electronic structure of the Si=Si double bond bears a close resemblance to that of the C=C double bond.

Acknowledgment. This research was supported by NSF Grants CHE 78-27094 and CHE 80-00256 and the Air Force Office of Scientific Research AF-AFOSR 82-0067. The U.S. Government is authorized to reproduce and distribute reprints for government purposes notwithstanding any copyright notation thereon.

Registry No. 1, 80785-72-4; 2, 74864-45-2; 3, 74-85-1; 4, 74-84-0.

Alkylation and Aldol Reactions of Iron Acyl Enolates

Lanny S. Liebeskind* and Mark E. Welker

Department of Chemistry, Florida State University
Tallahassee, Florida 32306

Received August 24, 1982

Summary: Treatment of the acyliron complex CpFe(CO)(PPh$_3$)COCH$_3$ with lithium diisopropylamide at low temperature in THF generates the corresponding enolate. Reaction of this enolate with alkyl halides gives high yields of C-alkylation products while aldol products result from reaction with carbonyl compounds. Oxidative cleavage of the acyl–iron bond occurs in high yield (NBS, CH_2Cl_2/EtOH) to give esters.

In order to expand the preparative chemistry of certain stoichiometric organometallics in conjunction with their utilization in organic synthesis, we have initiated a research program to explore the synthetic applications of organotransition-metal carbanions. Our first effort in this area has concerned the conversion of iron acyls into iron acyl enolates and their reaction with various electrophiles to produce derivatized iron acyls (eq 1).[1]

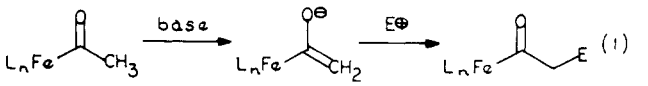

(1)

After our initial attempts to generate the enolate of CpFe(CO)$_2$COCH$_3$[2] **1a** were thwarted by migration of the acyl group to the cyclopentadienyl ring,[3] we found that slow addition of a THF solution of CpFe(CO)(PPh$_3$)-COCH$_3$[4] **1b** to a 0.15 M solution of lithium diisopropylamide (LDA) maintained under N_2 at −42 °C gave a deep red solution of the corresponding lithium enolate **2**. After the mixture was stirred at −42 °C for 1.5 h, the enolate was quenched with various electrophiles to give good to excellent yields of products (Scheme I). For example, treatment of enolate **2b** with MeI, EtBr, allyl bromide, and benzyl bromide gave C-alkylation products **3b–6b** in isolated, purified yields of 78, 81, 78 and 91%, respectively.[5] Aldol reactions with acetone, acetaldehyde, pivaldehyde, and benzaldehyde similarly occurred in good yields to give compounds **7b–10b** with the latter three reactants each giving a ca. 1:1 mixture of diastereomeric products.[5]

In principle, the asymmetric iron atom of the enolate could influence the formation of the new asymmetric carbon atom in aldol products **8–10**. To briefly probe this

(1) After submission of our manuscript, Professor Bergman (Berkeley) reported the successful generation of the enolate of a cobaltacyclopentanone which underwent high yield aldol and alkylation reactions: Theopold, K. H.; Becker, P. N.; Bergman, R. G. *J. Am. Chem. Soc.* **1982**, *104*, 5250.

(2) King, R. B. *J. Am. Chem. Soc.* **1963**, *85*, 1918.

(3) The base-induced migration of organic fragments from metal to a coordinated cyclopentadienyl ring has been observed in a number of systems: Werner, H.; Hofmann, W. *Angew. Chem., Int. Ed. Engl.* **1978**, 17, 464. Berryhill, S. R.; Sharenow, B. *J. Organomet. Chem.* **1981**, *221*, 143.

(4) Bibler, J. P.; Wojcicki, A. *Inorg. Chem.* **1966**, *5*, 889.

(5) Spectral data and elemental analyses. **3b**: orange solid; mp 158–161 °C ($CHCl_3$/petroleum ether); IR ($CHCl_3$, cm^{-1}) 3040, 3010, 2980, 1910, 1605, 1490, 1440, 1100, 1080, 880, 830; ^1H NMR (60 MHz, $CDCl_3$, δ) 7.50–7.13 (m, 15 H), 4.33 (br s, 5 H), 2.93–2.37 (m, 2 H), 0.56 (t, J = 7 Hz, 3 H). Anal. Calcd for $C_{27}H_{25}FeO_2P$: C, 69.25; H, 5.38. Found: C, 69.47; H, 5.48. **4b**: orange solid; mp 157–159 °C ($CHCl_3$/petroleum ether); IR ($CHCl_3$, cm^{-1}) 3020, 2980, 1920, 1608, 1440, 1100; ^1H NMR (60 MHz, $CDCl_3$, δ) 7.50–7.13 (m, 15 H), 4.35 (br s, 5 H), 2.93–2.40 (m, 2 H), 1.43–0.87 (m, 2 H), 0.58 (t, J = 6 Hz, 3 H). Anal. Calcd for $C_{28}H_{27}FeO_2P$: C, 69.72; H, 5.64. Found: C, 69.82; H, 5.80. **5b**: orange solid; mp 115–117 °C ($CHCl_3$/petroleum ether); IR ($CHCl_3$, cm^{-1}) 3040, 3005, 1910, 1600, 1485, 1440, 1100, 910, 820; ^1H NMR (60 MHz, $CDCl_3$, δ) 7.40–7.03 (m, 15 H), 5.70–5.07 (m, 1 H), 4.93–4.50 (m, 2 H), 4.30 (br s, 5 H), 3.00–2.47 (m, 2 H), 2.10–1.57 (m, 2 H). Anal. Calcd for $C_{29}H_{27}FeO_2P$: C, 70.46; H, 5.51. Found: C, 70.36; H, 5.73. **6b**: orange solid; mp 128–131 °C ($CHCl_3$/petroleum ether); IR ($CHCl_3$, cm^{-1}) 3070, 3010, 1920, 1600, 1490, 1440, 1100, 830; ^1H NMR (60 MHz, $CDCl_3$, δ) 7.70–6.70 (m, 20 H), 4.30 (br s, 5 H), 3.20–2.00 (m, 4 H). Anal. Calcd for $C_{33}H_{29}FeO_2P$: C, 72.81; H, 5.37. Found: C, 72.89; H, 5.55. **7b**: yellow-orange solid; mp 130–132 °C ($CHCl_3$/petroleum ether); IR ($CHCl_3$, cm^{-1}) 3420, 3080, 2995, 1920, 1590, 1490, 1440, 1120, 1100, 950; ^1H NMR (60 MHz, $CDCl_3$, δ) 7.67–7.10 (m, 15 H), 4.30 (d, J_{P-H} = 1 Hz, 5 H), 4.00 (br s, 1 H), 3.17 (d, J = 17 Hz, 1 H), 2.70 (d, J = 17 Hz, 1 H), 1.00 (s, 3 H), 0.70 (s, 3 H). Anal. Calcd for $C_{29}H_{29}FeO_3P$: C, 67.98; H, 5.71. Found: C, 67.70; H, 5.69. **8b**: yellow-orange solid; 50/50 mixture of diastereomers; IR ($CHCl_3$, cm^{-1}) 3395, 3078, 3060, 2998, 1918, 1583, 1481, 1435, 1120, 1093, 965, 825; ^1H NMR (60 MHz, C_6D_6, δ) 7.77–6.73 (m, 15 H), 4.16 (m, 5 H), 3.70 (br s, 1 H), 3.33–2.90 (m, 3 H), 1.03, 1.00 (two overlapping doublets, each J = 7 Hz, 3 H total, 50/50 ratio). Anal. Calcd for $C_{28}H_{27}FeO_3P$: C, 67.49; H, 5.46. Found: C, 67.70; H, 5.66. **9b**: yellow-orange solid; 50/50 mixture of diastereomers; IR ($CHCl_3$, cm^{-1}) 3440, 3080, 3020, 2980, 1920, 1585, 1480, 1440, 1095, 1070, 1000, 825; ^1H NMR (60 MHz, $CDCl_3$, δ) 7.50–6.93 (m, 15 H), 4.23 (br s, 5 H), 3.60–2.50 (complex m, 3 H), 2.13 (br s, 1 H), 0.63, 0.60 (two singlets, 9 H total, 50/50 ratio). Anal. Calcd for $C_{31}H_{33}FeO_3P$: C, 68.80; H, 6.16. Found: C, 68.97; H, 5.90. **9d**: yellow orange solid; 60/40 mixture of diastereomers; IR ($CHCl_3$, cm^{-1}) 3400, 2980, 2882, 1915, 1582, 1440, 1383, 1172, 1100, 1039, 1020, 935; ^1H NMR (270 MHz, $CDCl_3$, δ) 7.97–7.81 (m, 4 H), 7.62–7.38 (m, 6 H), 4.24 (m, 5 H), 3.46–2.22 (m, 8 H), 1.10, 0.94 (two triplets, each J = 5 Hz, 6 H total, 40/60 ratio), 0.79, 0.75 (two singlets, 9 H total, 60/40 ratio). Anal. Calcd for $C_{29}H_{38}FeNO_3P$: C, 65.05; H, 7.15. Found: C, 65.23; H, 7.33. **10b**: yellow-orange solid; 50/50 mixture of diastereomers; IR ($CHCl_3$, cm^{-1}) 3407, 3059, 3000, 1919, 1580, 1480, 1434, 1093, 998, 937, 824; ^1H NMR (60 MHz, $CDCl_3$, δ) 7.73–7.07 (m, 20 H), 4.93–4.50 (m, 1 H), 4.40 (m, 5 H), 4.00 (m, 0.5 H, exchanges with D_2O), 3.33–2.67 (m, 2.5 H, 0.5 H exchanges with D_2O).

0276-7333/83/2302-0194$01.50/0

Scheme I

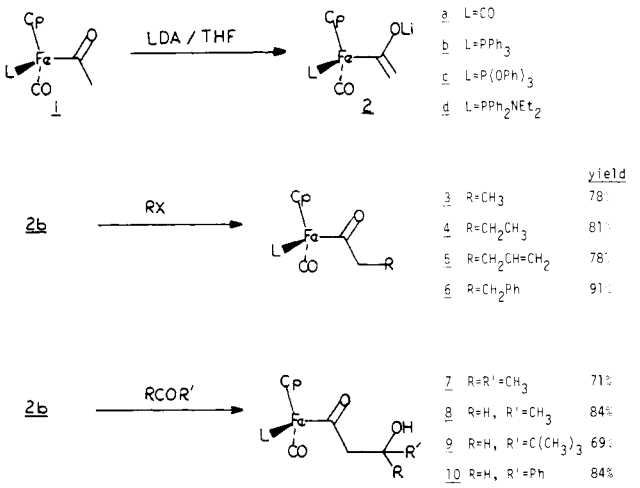

aspect of the chemistry, we prepared iron acyls **1c**[4] and **1d**[6] but found that **1c** did not give a stable enolate and although **1d** formed a stable enolate, reaction with pivaldehyde gave only a 60:40 mixture of diastereomeric aldol products **9d** in 53% yield (31% recovered starting material).[5]

The acyl–iron bond is readily cleaved in these complexes to give high yields of esters. For example, slow addition of a CH_2Cl_2 solution of *N*-bromosuccinimide to a solution of iron acyl **6b** in 1:1 CH_2Cl_2/ethanol at −42 °C resulted in oxidative cleavage, giving ethyl dihydrocinnamate in 89% yield (eq 2).

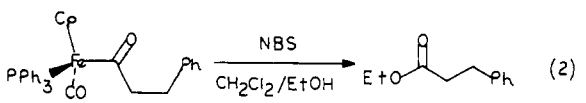

6b

The experimental procedures for the synthesis and subsequent cleavage or iron acyl **6b** are typical. Diisopropylamine (190 μL, 1.36 mmol) was added to a solution of *n*-butyllithium (825 μL of 1.6 M hexane solution, 1.32 mmol) in THF (8 mL) maintained at 0 °C under N_2. After the mixture was stirred at 0 °C for 20 min, the flask was cooled in a dry ice/CH_3CN bath (ca. −42 °C). To this solution of LDA was added a solution of iron acyl **1b** (500 mg, 1.10 mmol) in THF (4 mL) dropwise by syringe. During the addition the initial orange color of **1b** turned to deep red. After the mixture was stirred at −42 °C for 90 min, the enolate was quenched by the addition of benzyl bromide (170 μL, 1.43 mmol) that caused an immediate color change from red to dark orange. The reaction mixture was allowed to warm to room temperature, and after 30 min aqueous ammonium chloride (5%, 30 mL) was added followed by CH_2Cl_2 (30 mL) and 1.2 N HCl (20 mL). After the organic layer was separated, the aqueous layer was extracted with CH_2Cl_2 (2 × 30 mL) and the CH_2Cl_2 extracts were combined and dried over Na_2SO_4. Filtration and removal of volatiles on a rotary evaporator left an orange oil that was chromatographed on activated alumina (2 × 15 cm, CH_2Cl_2) and gave 542 mg (91%) of iron complex **6b** as a deep orange solid: mp 128–131 °C (CH_2Cl_2/petroleum ether); IR ($CHCl_3$, cm^{-1}) 3050, 3010, 1920, 1600, 1490, 1440; 60-MHz ^1H NMR ($CDCl_3$, δ) 7.6–6.8 (m, 20 H), 4.3 (d, J = 2 Hz, 5 H), 3.2–2.0 (m, 4 H). Cleavage of the metal–acyl bond was effected by dissolving iron complex **6b** (389 mg, 0.715 mmol) in CH_2Cl_2 (5 mL) and diluting with an equal volume of EtOH. After the solution was cooled in a dry ice/CH_3CN bath (ca. −42 °C), *N*-bromosuccinimide (142 mg, 0.793 mmol) dissolved in CH_2Cl_2 (5 mL) was added dropwise. The color of the solution slowly changed from orange to deep green. After the addition, the solution was allowed to warm to room temperature and after 45 min was transferred to a separatory funnel with the aid of CH_2Cl_2 and then washed with 1 N NaOH. After the aqueous solution was backextracted with CH_2Cl_2, the combined CH_2Cl_2 layers were dried over Na_2SO_4. Filtration followed by removal of volatiles on a rotary evaporator at room temperature left a green semi-solid residue that was triturated several times with Et_2O. The combined ether fractions were condensed to an oil which after filtration through a short alumina column with petroleum ether gave 114 mg (89%) of ethyl dihydrocinnamate, identical with an authentic sample.

The generation of these iron acyl enolates and their reaction with electrophiles are comparable to the formation and reaction of organic ester enolates under strongly basic, aprotic conditions. Although the chiral iron center, in the present work, did not significantly control the formation of any new asymmetric carbon atoms, further work with conformationally restricted iron acyl enolates may overcome this limitation.

Acknowledgment is made to the National Cancer Institute, D.H.E.W. (Grant CA 26374), for support of this work. We thank Professor John Selegue for an early discussion of this chemistry.

(6) Prepared according to standard procedures[4] from $CpFe(CO)_2CH_3$ and Ph_2PNEt_2.

Octafluorocyclooctatetraene Transition-Metal Compounds. Novel Transannular Ring Closures and a Formal Intramolecular Redox Equilibrium between 1,2,5,6-η and 1,2,3,6-η Ligands

Russell P. Hughes*[1] and Deborah E. Samkoff
Department of Chemistry, Dartmouth College
Hanover, New Hampshire 03755

Raymond E. Davis* and Brian B. Laird
Department of Chemistry, University of Texas at Austin
Austin, Texas 78712

Received September 27, 1982

Summary: Octafluorocyclooctatetraene (OFCOT) reacts with $[Co(CO)_2(\eta\text{-}C_5Me_5)]$ to give $[Co(\eta\text{-}C_5Me_5)(C_8F_8)]$, which is in dynamic redox equilibrium between the 1,2,5,6-η and 1,2,3,6-η forms of coordinated OFCOT. The molecular structure of a cobalt product derived from transannular ring closure of OFCOT is also reported, and structure reassignments for some Pt–OFCOT compounds are proposed.

The recent synthesis[2] and structural characterization[3] of octafluorocyclooctatetraene (OFCOT) have allowed its organometallic chemistry to be compared to that of its thoroughly studied hydrocarbon analogue.[4] We have

(1) Alfred P. Sloan Research Fellow, 1980–1984.
(2) Lemal, D. M.; Buzby, J. M.; Barefoot, A. C., III; Grayston, M. W.; Laganis, E. D. *J. Org. Chem.* **1980**, *45*, 3118–3120.
(3) Laird, B. B.; Davis, R. E. *Acta Crystallogr., Sect. B* **1982**, *B38*, 678–680.
(4) For reviews of cyclooctatetraene chemistry see: Deganello, G. "Transition Metal Complexes of Cyclic Polyolefins"; Academic Press: New York, 1979. Fray, G. I.; Saxton, R. G. "The Chemistry of Cyclooctatetraene and Its Derivatives"; Cambridge University Press: Cambridge, 1978.

0276-7333/83/2302-0195$01.50/0

Scheme I

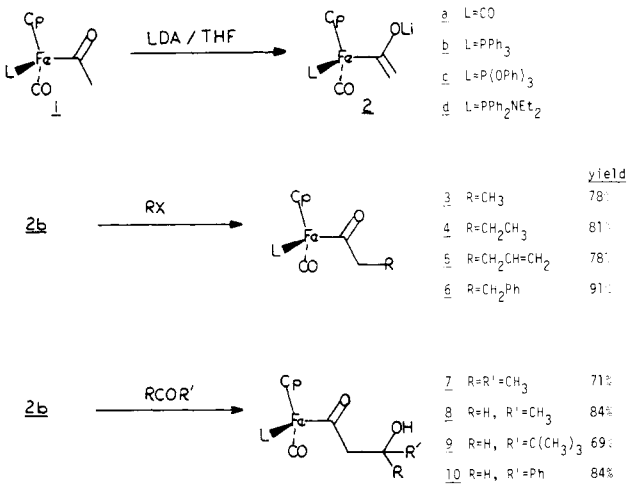

aspect of the chemistry, we prepared iron acyls **1c**[4] and **1d**[6] but found that **1c** did not give a stable enolate and although **1d** formed a stable enolate, reaction with pivaldehyde gave only a 60:40 mixture of diastereomeric aldol products **9d** in 53% yield (31% recovered starting material).[5]

The acyl–iron bond is readily cleaved in these complexes to give high yields of esters. For example, slow addition of a CH_2Cl_2 solution of *N*-bromosuccinimide to a solution of iron acyl **6b** in 1:1 CH_2Cl_2/ethanol at −42 °C resulted in oxidative cleavage, giving ethyl dihydrocinnamate in 89% yield (eq 2).

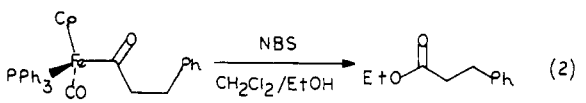

6b

The experimental procedures for the synthesis and subsequent cleavage or iron acyl **6b** are typical. Diisopropylamine (190 μL, 1.36 mmol) was added to a solution of *n*-butyllithium (825 μL of 1.6 M hexane solution, 1.32 mmol) in THF (8 mL) maintained at 0 °C under N_2. After the mixture was stirred at 0 °C for 20 min, the flask was cooled in a dry ice/CH_3CN bath (ca. −42 °C). To this solution of LDA was added a solution of iron acyl **1b** (500 mg, 1.10 mmol) in THF (4 mL) dropwise by syringe. During the addition the initial orange color of **1b** turned to deep red. After the mixture was stirred at −42 °C for 90 min, the enolate was quenched by the addition of benzyl bromide (170 μL, 1.43 mmol) that caused an immediate color change from red to dark orange. The reaction mixture was allowed to warm to room temperature, and after 30 min aqueous ammonium chloride (5%, 30 mL) was added followed by CH_2Cl_2 (30 mL) and 1.2 N HCl (20 mL). After the organic layer was separated, the aqueous layer was extracted with CH_2Cl_2 (2 × 30 mL) and the CH_2Cl_2 extracts were combined and dried over Na_2SO_4. Filtration and removal of volatiles on a rotary evaporator left an orange oil that was chromatographed on activated alumina (2 × 15 cm, CH_2Cl_2) and gave 542 mg (91%) of iron complex **6b** as a deep orange solid: mp 128–131 °C (CH_2Cl_2/petroleum ether); IR ($CHCl_3$, cm^{-1}) 3050, 3010, 1920, 1600, 1490, 1440; 60-MHz ^1H NMR ($CDCl_3$, δ) 7.6–6.8 (m, 20 H), 4.3 (d, J = 2 Hz, 5 H), 3.2–2.0 (m, 4 H). Cleavage of the metal–acyl bond was effected by dissolving iron complex **6b** (389 mg, 0.715 mmol) in CH_2Cl_2 (5 mL) and diluting with an equal volume of EtOH. After the solution was cooled in a dry ice/CH_3CN bath (ca. −42 °C), *N*-bromosuccinimide (142 mg, 0.793 mmol) dissolved in CH_2Cl_2 (5 mL) was added dropwise. The color of the solution slowly changed from orange to deep green. After the addition, the solution was allowed to warm to room temperature and after 45 min was transferred to a separatory funnel with the aid of CH_2Cl_2 and then washed with 1 N NaOH. After the aqueous solution was backextracted with CH_2Cl_2, the combined CH_2Cl_2 layers were dried over Na_2SO_4. Filtration followed by removal of volatiles on a rotary evaporator at room temperature left a green semi-solid residue that was triturated several times with Et_2O. The combined ether fractions were condensed to an oil which after filtration through a short alumina column with petroleum ether gave 114 mg (89%) of ethyl dihydrocinnamate, identical with an authentic sample.

The generation of these iron acyl enolates and their reaction with electrophiles are comparable to the formation and reaction of organic ester enolates under strongly basic, aprotic conditions. Although the chiral iron center, in the present work, did not significantly control the formation of any new asymmetric carbon atoms, further work with conformationally restricted iron acyl enolates may overcome this limitation.

Acknowledgment is made to the National Cancer Institute, D.H.E.W. (Grant CA 26374), for support of this work. We thank Professor John Selegue for an early discussion of this chemistry.

(6) Prepared according to standard procedures[4] from $CpFe(CO)_2CH_3$ and Ph_2PNEt_2.

Octafluorocyclooctatetraene Transition-Metal Compounds. Novel Transannular Ring Closures and a Formal Intramolecular Redox Equilibrium between 1,2,5,6-η and 1,2,3,6-η Ligands

Russell P. Hughes*[1] and Deborah E. Samkoff
Department of Chemistry, Dartmouth College
Hanover, New Hampshire 03755

Raymond E. Davis* and Brian B. Laird
Department of Chemistry, University of Texas at Austin
Austin, Texas 78712

Received September 27, 1982

Summary: Octafluorocyclooctatetraene (OFCOT) reacts with $[Co(CO)_2(\eta\text{-}C_5Me_5)]$ to give $[Co(\eta\text{-}C_5Me_5)(C_8F_8)]$, which is in dynamic redox equilibrium between the 1,2,5,6-η and 1,2,3,6-η forms of coordinated OFCOT. The molecular structure of a cobalt product derived from transannular ring closure of OFCOT is also reported, and structure reassignments for some Pt–OFCOT compounds are proposed.

The recent synthesis[2] and structural characterization[3] of octafluorocyclooctatetraene (OFCOT) have allowed its organometallic chemistry to be compared to that of its thoroughly studied hydrocarbon analogue.[4] We have

(1) Alfred P. Sloan Research Fellow, 1980–1984.
(2) Lemal, D. M.; Buzby, J. M.; Barefoot, A. C., III; Grayston, M. W.; Laganis, E. D. *J. Org. Chem.* **1980**, *45*, 3118–3120.
(3) Laird, B. B.; Davis, R. E. *Acta Crystallogr., Sect. B* **1982**, *B38*, 678–680.
(4) For reviews of cyclooctatetraene chemistry see: Deganello, G. "Transition Metal Complexes of Cyclic Polyolefins"; Academic Press: New York, 1979. Fray, G. I.; Saxton, R. G. "The Chemistry of Cyclooctatetraene and Its Derivatives"; Cambridge University Press: Cambridge, 1978.

0276-7333/83/2302-0195$01.50/0

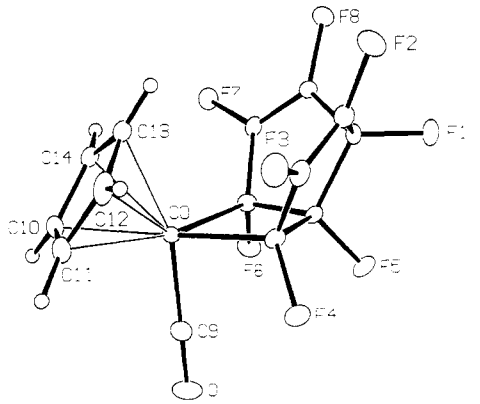

Figure 1. ORTEP drawing of **4**. Selected bond lengths (Å): Co–C4 = 1.993 (2), Co–C6 = 1.986 (2), Co–Cp ring centroid = 1.711, range of Co–Cp carbon = [2.048 (2)–2.117 (2)], C4–C5 = 1.525 (3), C5–C6 = 1.526 (3), C3–C4 = 1.470 (2), C6–C7 = 1.471 (2), C2–C3 = 1.326 (2), C7–C8 = 1.322 (2), C1–C2 = 1.478 (3), C8–C1 = 1.484 (3), and C1–C5 = 1.568 (2). Selected bond angles (deg): C4–Co–C6 = 72.87 (7), C4–Co–C9 = 90.68 (8), and C6–Co–C9 = 91.46 (8). Selected dihedral angles (deg): Cp ring with (Co–C4–C5–C6) = 52.2, (C1–C2–C3–C4–C5) with (Co–C4–C5–C6) = 61.5, (C1–C5–C6–C7–C8) with (Co–C4–C5–C6) = 61.1, and (Co–C4–C6) with (C4–C5–C6) = 4.1.

previously described an intramolecular oxidative addition of OFCOT, which afforded the crystallographically characterized 1,2,3,6-η compound **1** [ML_n = $Fe(CO)_3$].[5] We

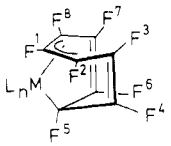

I.

also reported that the reaction of OFCOT with zerovalent platinum compounds afforded products of general formula $[Pt(C_8F_8)L_2]$ (L = PPh_3, PMe_2Ph, PPh_2Me), which on the basis of ^{19}F and ^{31}P NMR data were suggested to have structure **1** (ML_n = PtL_2).[5] This communication outlines some cobalt–OFCOT chemistry that provides the first example of a formal *redox equilibrium* between valence isomers of a cobalt complex and also defines a novel transannular carbon–carbon bond formation that leads to the octafluorobicyclo[3.3.0]octa-2,7-diene-4,6-diyl ligand. A reassignment of the structure of $[PtL_2(C_8F_8)]$ is also described.

Reaction of $[Co(\eta\text{-}C_5Me_5)(CO)_2]$[6] with OFCOT in refluxing hexanes (84 h) afforded, after column chromatography, a mixture of two isomeric $[Co(\eta\text{-}C_5Me_5)(C_8F_8)]$ compounds in 60% overall yield. A combination of spectroscopic techniques clearly identified the structures of these isomers as **2a**[7] and **3**.[8] A comparison of ^{19}F NMR data for **3** and **1** [M = $Fe(CO)_3$] (Table I) shows that fluorines attached to carbons that are directly bound to the metal suffer the greatest chemical shift perturbation on changing the metal.[9] While **2a** and **3** could be separated by preparative TLC, they slowly equilibrated on standing in solution [2–3 days, 20 °C; $K_{eq}(CDCl_3, 20\ °C, \mathbf{2a} \rightleftarrows \mathbf{3})$ = 0.3]. A similar reaction of $[Co(\eta\text{-}C_5H_5)(CO)_2]$ with OFCOT in refluxing *n*-octane (48 h) afforded only poor yields (4–5%) of **2b**.[7] No evidence for any compound with structure analogous to **3** was observed, nor did **2b**

Table I. ^{19}F Chemical Shifts[a]

compd	δ F_1	$F_{2,8}$	$F_{3,7}$	$F_{4,6}$	F_5
4	197.7	138.8	154.7	156.6	144.8
5a	193.3	135.4	159.1	185.9	141.3
3	168.9	182.4	130.3	112.6	216.3
1 [ML_n = $Fe(CO)_3$]	129.3	164.4	127.9	115.4	171.8

[a] ppm upfield from internal $CFCl_3$; in $CDCl_3$; 20 °C.

Table II. Fractional Atomic Coordinates and Thermal Parameters for **4**[a]

atom	*x*	*y*	*z*	*U*, Å^2
Co	2376.5 (3)	1352.9 (2)	1788.3 (3)	152 (1)
F1	2828 (1)	6169 (1)	287 (1)	292 (4)
F2	4759 (1)	6056 (1)	3420 (1)	355 (4)
F3	5884 (1)	3091 (1)	2790 (1)	321 (4)
F4	4503 (1)	1724 (1)	−618 (1)	305 (4)
F5	2410 (1)	3504 (1)	−1564 (1)	297 (4)
F6	146 (1)	2444 (1)	−383 (1)	266 (4)
F7	−490 (1)	4147 (1)	3128 (1)	255 (4)
F8	1332 (1)	6623 (1)	3602 (1)	292 (4)
O	1977 (2)	−608 (1)	−1647 (2)	402 (6)
C1	2773 (2)	5108 (2)	1320 (2)	202 (6)
C2	4177 (2)	4924 (2)	2275 (2)	241 (6)
C3	4681 (2)	3548 (2)	1999 (2)	231 (6)
C4	3738 (2)	2526 (2)	790 (2)	209 (6)
C5	2525 (2)	3520 (2)	225 (2)	192 (6)
C6	1217 (2)	2942 (2)	936 (2)	181 (5)
C7	675 (2)	4214 (2)	2214 (2)	185 (5)
C8	1493 (2)	5366 (2)	2420 (2)	196 (5)
C9	2135 (2)	157 (2)	−313 (2)	251 (6)
C10	1528 (2)	−40 (2)	3302 (2)	237 (6)
C11	3045 (2)	−296 (2)	3203 (2)	280 (7)
C12	3722 (2)	1019 (2)	3960 (3)	327 (7)
C13	2626 (3)	2101 (2)	4478 (2)	302 (7)
C14	1273 (2)	1434 (2)	4110 (2)	261 (6)
H10	80 (2)	−75 (2)	285 (2)	24 (5)
H11	354 (2)	−122 (2)	268 (3)	41 (6)
H12	474 (2)	114 (2)	402 (3)	37 (6)
H13	277 (2)	307 (2)	500 (3)	37 (6)
H14	32 (2)	197 (2)	433 (2)	30 (6)
Cp ring centroid	2439	844	3810	

[a] *U* for H, U_{eq} for non-hydrogen. All values ×10^4 (except for H atoms; ×10^3). Numbers in parentheses indicate estimated standard deviations in last digit shown.

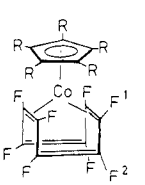

2a. R = Me.
2b. R = H.

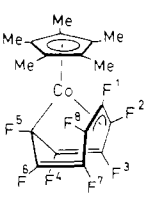

3.

(5) Barefoot, A. C., III; Corcoran, E. W., Jr.; Hughes, R. P.; Lemal, D. M.; Saunders, W. D.; Laird, B. B.; Davis, R. E. *J. Am. Chem. Soc.* **1981**, *103*, 970–972.

(6) (a) Frith, S. A.; Spencer, J. L. *Inorg. Synth.*, submitted for publication. (b) King, R. B.; Bisnette, M. B. *J. Organomet. Chem.* **1967**, *8*, 287–297. (c) King, R. B.; Efraty, A. *J. Am. Chem. Soc.* **1972**, *94*, 3773–3779.

(7) Compound **2a**: ^1H NMR ($CDCl_3$, 20 °C) δ (downfield from Me_4Si) 1.80 (s, C_5Me_5); $^{13}C\{^1H\}$ NMR ($CDCl_3$, 20 °C) δ (downfield from Me_4Si) 105.7 (s, C_5Me_5), 10.0 (quintet, $J_{^{13}C-^{19}F}$ = 2.5 Hz, C_5Me_5); ^{19}F NMR ($CDCl_3$, 20 °C) δ (upfield from $CFCl_3$) 117.1 (F^2), 188.3 (F^1); IR (hexane) $\nu_{C=C}$ 1736 cm^{-1}; mass spectrum, *m/e* 442 (P^+). Anal. C, H. **2b**: ^1H NMR δ 5.29 (s, C_5H_5); ^{19}F NMR δ 114.0 (F^2), 163.9 (F^1); mass spectrum, *m/e* 372 (P^+); IR (hexanes) $\nu_{C=C}$ 1734 cm^{-1}. Anal. C, H.

(8) Compound **3** (all spectral conditions as described in ref 7): ^1H NMR δ 1.70 (s, C_5Me_5); $^{13}C\{^1H\}$ NMR δ 102.5 (s, C_5Me_5), 9.2 (doublet of quartets, J_{CF} = 4 Hz, 1.5 Hz, C_5Me_5); ^{19}F NMR (Table I); IR $\nu_{C=C}$ 1736 cm^{-1}; mass spectrum, *m/e* 442 (P^+). Anal. C, H.

(9) A complete analysis of the ^{19}F NMR spectra will be published separately.

undergo any detectable valence isomerization in solution. The reaction of $[Co(\eta\text{-}C_5H_5)(CO)_2]$ neat with OFCOT (80 °C, 72 h) yielded a second yellow crystalline product in execrable yield (<1%). No unambiguous structure could be assigned on the basis of its spectral properties,[10] but an X-ray crystallographic study characterized the structure as **4**, containing the octafluorobicyclo[3.3.0]octa-2,7-diene-4,6-diyl ligand. An ORTEP drawing of **4**, together with representative bond lengths and angles, is presented in Figure 1.[11] Fractional atomic coordinates and thermal parameters for **4** are assembled in Table II. The cobaltacyclobutane ring in **4** is almost planar, the dihedral angle

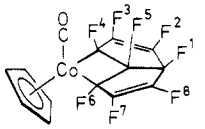

4.

between the planes (Co–C4–C6) and (C4–C5–C6) being 4.1°. The cobalt atom is displaced 0.11 Å out of the (C4–C5–C6) plane, in the direction away from the cavity of the C_8F_8 ligand.

The equilibrium system **2a** ⇌ **3** represents a remarkable example of a formal intramolecular redox reaction with a close thermodynamic balance between the two isomers. When the pentamethylcyclopentadienyl ligand in **2a** is replaced by cyclopentadienyl, the equilibrium clearly lies far to the left, in qualitative agreement with the idea that electron-donating methyl groups should increase the proclivity of the metal toward oxidative addition. The equilibrium described here is in clear contrast to that observed in cobalt analogues containing the hydrocarbon ligand cyclooctatetraene (COT), where the solution equilibrium is $[Co(\eta\text{-}C_5R_5)(1\text{-}4\text{-}\eta\text{-}COT)] \rightleftharpoons [Co(\eta\text{-}C_5R_5)(1,2,5,6\text{-}\eta\text{-}COT)]$.[12] Irreversible isomerizations of kinetically formed $[M(\eta\text{-}C_5Me_5)(1\text{-}4\text{-}\eta\text{-}COT)]$ to give $[M(\eta\text{-}C_5Me_5)(1,2,5,6\text{-}\eta\text{-}COT)]$ (M = Rh, Ir)[13] and $[Os(CO)_3(1,2,3,6\text{-}\eta\text{-}COT)]$ to give $[Os(CO)_3(1\text{-}4\text{-}\eta\text{-}COT)]$[14] have been reported.

The structural characterization of **4** suggested an alternative assignment for the structures of the (OFCOT)Pt complexes originally formulated as **1** $[ML_n = PtL_2]$.[5] ^{19}F NMR data (Table I) provide compelling evidence that these compounds should be reformulated as **5** [L = PPh_3, PMe_2Ph, PPh_2Me]. Comparison of ^{19}F chemical shifts of compounds **5** with those of **4** shows that only one resonance, corresponding to two equivalent fluorines (F_4 and F_6), is shifted significantly (~30 ppm) on changing the metal. Moreover, there is a significant value for $J_{1,5}$ of 14.5 Hz in **7a** and 18.5 Hz in **4**, but there is negligible coupling between F_1 and F_5 in compounds **1** $[ML_n = Fe(CO)_3]$ and **3**.[9]

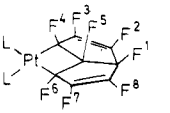

5a. L = PPh_3
5b. L = $PPhMe_2$
5c. L = PPh_2Me

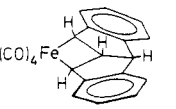

6.

The ferracyclobutane compound **6** has been formed directly by metal insertion into a C–C bond of dibenzosemibullvalene.[15] However, the presence of free octafluorosemibullvalene under our reaction conditions is highly implausible,[16] and we are forced to conclude that the transannular ring closure to produce **4** (or **5**) is metal induced. There is no direct evidence for such a transannular ring closure in the organometallic chemistry of the hydrocarbon COT, although a similar type of ring closure must be an important step in the formation of pentalene ligands from cyclooctatetraene derivatives.[18] Studies of the mechanism of isomerization and transannular ring closure reactions of coordinated OFCOT are in progress.

Acknowledgment. R.P.H. is grateful to the donors of the Petroleum Research Fund, administered by the American Chemical Society, and to the Alfred P. Sloan Foundation for financial support of this work. R.E.D. acknowledges support by the Robert A. Welch Foundation (Grant F-233) and a grant from the National Science Foundation (Grant GP-37028) for purchase of a Syntex $P2_1$ diffractometer. We are also grateful to Dr. John L. Spencer (Bristol University) for a preprint concerning a high yield synthesis of $[Co(CO)_2(\eta\text{-}C_5Me_5)]$.

Registry No. **2a**, 83781-42-4; **2b**, 83781-43-5; **3**, 83781-44-6; **4**, 83781-45-7; **5a**, 76624-82-3; **5b**, 76624-83-4; **5c**, 76654-66-5; **6**, 40806-41-5; OFCOT, 57070-35-6; $[Co(\eta\text{-}C_5Me_5)(CO)_2]$, 12129-77-0; $[Co(\eta\text{-}C_5H_5)(CO)_2$, 12078-25-0.

Supplementary Material Available: A listing of structure factor amplitudes (Supplementary Table I) (17 pages). Ordering information is given on any current masthead page.

(10) Compound **4** (all spectral conditions as described in ref 7): ^1H NMR δ 5.22 (s, C_5H_5); ^{19}F NMR (Table I); IR ν_{CO} 2078 cm^{-1}, $\nu_{C=C}$ 1716, 1703 cm^{-1}.

(11) Crystals of **4** are triclinic of space group $P\bar{1}$ with a = 9.293 (2) Å, b = 9.323 (2) Å, c = 7.688 (2) Å, α = 101.65 (2)°, β = 93.48 (2)°, γ = 87.37 (2)°, and Z = 2. The structure was solved by heavy-atom methods and refined by full-matrix least-squares procedures to final agreement factors $R = \sum||F_o| - |F_c||/\sum|F_o| = 0.029$ and $R_w = [\sum w(|F_o| - |F_c|)^2/\sum w|F_o|^2]^{1/2} = 0.031$ using 3702 reflections with $I \geq 2.00\,\sigma(I)$.

(12) (a) Moraczewski, J.; Geiger, W. E., Jr. *J. Am. Chem. Soc.* **1981**, *103*, 4779–4787. (b) Albright, T. A.; Geiger, W. E., Jr.; Moraczewski, J.; Tulyathan, B. *Ibid.* **1981**, *103*, 4787–4794.

(13) Smith, A. K.; Maitlis, P. M. *J. Chem. Soc., Dalton Trans.* **1976**, 1773–1777.

(14) (a) Bruce, M. I.; Cooke, M.; Green, M.; Westlake, D. L. *J. Chem. Soc. A* **1969**, 987–992. (b) Bruce, M. I.; Cooke, M.; Green, M. *Angew. Chem., Int. Ed. Engl.* **1968**, *7*, 639.

(15) Moriarty, R. M.; Chen, K.-N.; Yeh, C.-L.; Flippen, J. L.; Karle, J. *J. Am. Chem. Soc.* **1972**, *94*, 8944–8946.

(16) No octafluorosemibullvalene is observed on heating OFCOT at 300 °C for 8 h or after flash vacuum pyrolysis at 500 °C followed by rapid quenching to −196 °C.[17]

(17) Grayston, M. W.; Lemal, D. M., unpublished results.

(18) Knox, S. A. R.; Stone, F. G. A. *Acc. Chem. Res.* **1974**, *7*, 321–328.

Novel Parallel Path Mechanism for the Oxidation of Allyl Alcohol by Aqueous Palladium(II) Chloride

K. Zaw,[1] M. Lautens, and P. M. Henry*[1]

Guelph-Waterloo Centre for Graduate Work in Chemistry
University of Guelph
Guelph, Ontario, Canada N1G2W1

Received May 10, 1982

Summary: Allyl alcohol is oxidized by aqueous palladium(II) chloride to a mixture of β-hydroxypropanal, α-hydroxyacetone, and acrolein. Deuterium-labeling studies show that the first two are formed by the normal olefin oxidation route while the acrolein is formed by hydride

(1) Present Address: Department of Chemistry, Loyola University of Chicago, Chicago, IL 60626

0276-7333/83/2302-0197$01.50/0

undergo any detectable valence isomerization in solution. The reaction of $[Co(\eta\text{-}C_5H_5)(CO)_2]$ neat with OFCOT (80 °C, 72 h) yielded a second yellow crystalline product in execrable yield (<1%). No unambiguous structure could be assigned on the basis of its spectral properties,[10] but an X-ray crystallographic study characterized the structure as **4**, containing the octafluorobicyclo[3.3.0]octa-2,7-diene-4,6-diyl ligand. An ORTEP drawing of **4**, together with representative bond lengths and angles, is presented in Figure 1.[11] Fractional atomic coordinates and thermal parameters for **4** are assembled in Table II. The cobaltacyclobutane ring in **4** is almost planar, the dihedral angle

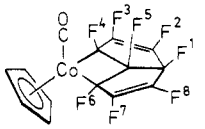

4.

between the planes (Co–C4–C6) and (C4–C5–C6) being 4.1°. The cobalt atom is displaced 0.11 Å out of the (C4–C5–C6) plane, in the direction away from the cavity of the C_8F_8 ligand.

The equilibrium system **2a** ⇌ **3** represents a remarkable example of a formal intramolecular redox reaction with a close thermodynamic balance between the two isomers. When the pentamethylcyclopentadienyl ligand in **2a** is replaced by cyclopentadienyl, the equilibrium clearly lies far to the left, in qualitative agreement with the idea that electron-donating methyl groups should increase the proclivity of the metal toward oxidative addition. The equilibrium described here is in clear contrast to that observed in cobalt analogues containing the hydrocarbon ligand cyclooctatetraene (COT), where the solution equilibrium is $[Co(\eta\text{-}C_5R_5)(1\text{-}4\text{-}\eta\text{-}COT)] \rightleftharpoons [Co(\eta\text{-}C_5R_5)(1,2,5,6\text{-}\eta\text{-}COT)]$.[12] Irreversible isomerizations of kinetically formed $[M(\eta\text{-}C_5Me_5)(1\text{-}4\text{-}\eta\text{-}COT)]$ to give $[M(\eta\text{-}C_5Me_5)(1,2,5,6\text{-}\eta\text{-}COT)]$ (M = Rh, Ir)[13] and $[Os(CO)_3(1,2,3,6\text{-}\eta\text{-}COT)]$ to give $[Os(CO)_3(1\text{-}4\text{-}\eta\text{-}COT)]$[14] have been reported.

The structural characterization of **4** suggested an alternative assignment for the structures of the (OFCOT)Pt complexes originally formulated as **1** $[ML_n = PtL_2]$.[5] ^{19}F NMR data (Table I) provide compelling evidence that these compounds should be reformulated as **5** [L = PPh_3, PMe_2Ph, PPh_2Me]. Comparison of ^{19}F chemical shifts of compounds **5** with those of **4** shows that only one resonance, corresponding to two equivalent fluorines (F_4 and F_6), is shifted significantly (~30 ppm) on changing the metal. Moreover, there is a significant value for $J_{1,5}$ of 14.5 Hz in **7a** and 18.5 Hz in **4**, but there is negligible coupling between F_1 and F_5 in compounds **1** $[ML_n = Fe(CO)_3]$ and **3**.[9]

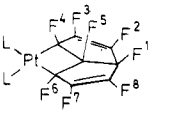

5a. L = PPh_3
5b. L = $PPhMe_2$
5c. L = PPh_2Me

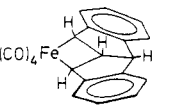

6.

The ferracyclobutane compound **6** has been formed directly by metal insertion into a C–C bond of dibenzosemibullvalene.[15] However, the presence of free octafluorosemibullvalene under our reaction conditions is highly implausible,[16] and we are forced to conclude that the transannular ring closure to produce **4** (or **5**) is metal induced. There is no direct evidence for such a transannular ring closure in the organometallic chemistry of the hydrocarbon COT, although a similar type of ring closure must be an important step in the formation of pentalene ligands from cyclooctatetraene derivatives.[18] Studies of the mechanism of isomerization and transannular ring closure reactions of coordinated OFCOT are in progress.

Acknowledgment. R.P.H. is grateful to the donors of the Petroleum Research Fund, administered by the American Chemical Society, and to the Alfred P. Sloan Foundation for financial support of this work. R.E.D. acknowledges support by the Robert A. Welch Foundation (Grant F-233) and a grant from the National Science Foundation (Grant GP-37028) for purchase of a Syntex $P2_1$ diffractometer. We are also grateful to Dr. John L. Spencer (Bristol University) for a preprint concerning a high yield synthesis of $[Co(CO)_2(\eta\text{-}C_5Me_5)]$.

Registry No. **2a**, 83781-42-4; **2b**, 83781-43-5; **3**, 83781-44-6; **4**, 83781-45-7; **5a**, 76624-82-3; **5b**, 76624-83-4; **5c**, 76654-66-5; **6**, 40806-41-5; OFCOT, 57070-35-6; $[Co(\eta\text{-}C_5Me_5)(CO)_2]$, 12129-77-0; $[Co(\eta\text{-}C_5H_5)(CO)_2$, 12078-25-0.

Supplementary Material Available: A listing of structure factor amplitudes (Supplementary Table I) (17 pages). Ordering information is given on any current masthead page.

(10) Compound **4** (all spectral conditions as described in ref 7): ^1H NMR δ 5.22 (s, C_5H_5); ^{19}F NMR (Table I); IR ν_{CO} 2078 cm^{-1}, $\nu_{C=C}$ 1716, 1703 cm^{-1}.

(11) Crystals of **4** are triclinic of space group $P\bar{1}$ with a = 9.293 (2) Å, b = 9.323 (2) Å, c = 7.688 (2) Å, α = 101.65 (2)°, β = 93.48 (2)°, γ = 87.37 (2)°, and Z = 2. The structure was solved by heavy-atom methods and refined by full-matrix least-squares procedures to final agreement factors $R = \sum||F_o| - |F_c||/\sum|F_o| = 0.029$ and $R_w = [\sum w(|F_o| - |F_c|)^2/\sum w|F_o|^2]^{1/2} = 0.031$ using 3702 reflections with $I \geq 2.00\,\sigma(I)$.

(12) (a) Moraczewski, J.; Geiger, W. E., Jr. *J. Am. Chem. Soc.* **1981**, *103*, 4779–4787. (b) Albright, T. A.; Geiger, W. E., Jr.; Moraczewski, J.; Tulyathan, B. *Ibid.* **1981**, *103*, 4787–4794.

(13) Smith, A. K.; Maitlis, P. M. *J. Chem. Soc., Dalton Trans.* **1976**, 1773–1777.

(14) (a) Bruce, M. I.; Cooke, M.; Green, M.; Westlake, D. L. *J. Chem. Soc. A* **1969**, 987–992. (b) Bruce, M. I.; Cooke, M.; Green, M. *Angew. Chem., Int. Ed. Engl.* **1968**, *7*, 639.

(15) Moriarty, R. M.; Chen, K.-N.; Yeh, C.-L.; Flippen, J. L.; Karle, J. *J. Am. Chem. Soc.* **1972**, *94*, 8944–8946.

(16) No octafluorosemibullvalene is observed on heating OFCOT at 300 °C for 8 h or after flash vacuum pyrolysis at 500 °C followed by rapid quenching to −196 °C.[17]

(17) Grayston, M. W.; Lemal, D. M., unpublished results.

(18) Knox, S. A. R.; Stone, F. G. A. *Acc. Chem. Res.* **1974**, *7*, 321–328.

Novel Parallel Path Mechanism for the Oxidation of Allyl Alcohol by Aqueous Palladium(II) Chloride

K. Zaw,[1] M. Lautens, and P. M. Henry*[1]

Guelph-Waterloo Centre for Graduate Work in Chemistry
University of Guelph
Guelph, Ontario, Canada N1G2W1

Received May 10, 1982

Summary: Allyl alcohol is oxidized by aqueous palladium(II) chloride to a mixture of β-hydroxypropanal, α-hydroxyacetone, and acrolein. Deuterium-labeling studies show that the first two are formed by the normal olefin oxidation route while the acrolein is formed by hydride

(1) Present Address: Department of Chemistry, Loyola University of Chicago, Chicago, IL 60626

0276-7333/83/2302-0197$01.50/0

abstraction from the alcohol carbon.

The oxidation of allyl-, crotyl-, and methylvinyl alcohols by palladium(II) chloride in aqueous solution has been reported to give the corresponding allylic ketone,[2-4] and it has been suggested that these unsaturated ketones arise from the β-hydroxy ketones formed by the normal palladium(II) oxidation route (eq 1).[4] We have found that, in fact, the acrolein product is not formed from dehydration of 1 but arises from a completely different reaction path.

$$CH_2{=}CHCH_2OH + PdCl_4^{2-} \xrightarrow[-4Cl^-]{H_2O} Pd(0) + 2H^+ + \underset{\mathbf{1}}{HOCH_2CH_2CHO} \xrightarrow{-H_2O} CH_2{=}CHCHO \quad (1)$$

With use of GLC analysis, the stoichiometric oxidations of allyl alcohol by aqueous $PdCl_4^{2-}$ at 25 °C gave about a 30% yield of acrolein and a 12–15% yield of α-hydroxyacetone. The quantitative analysis for 1 proved tedious since it mainly exists as a dimer in aqueous solution. The 2,4-dinitrophenylhydrazone of 1 was isolated in 5% yield, and ^1H NMR experiments indicated the monomeric form of 1 was present in 11% yield. A series of other measurements including Fehlings solution titrations, hydroxylamine titrations, and control studies on authentic samples of 1 prepared by hydration of acrolein indicated the total yield of 1 in the form of monomer plus dimer was about 40%.

At 0.1–0.3 M acid concentration no dehydration of 1 was observed during the 10–15-min reaction time. In fact, an earlier study of the rates and equilibrium at various acid concentrations would predict not only that the dehydration would take hours to come to equilibrium but also that the equilibrium would be 90% on the side of 1.[5]

To confirm that acrolein and 1 are formed by two different routes, we prepared samples of allyl-*1,1-*d_2[6] and -*3,3-*d_2 alcohol[7] by literature procedures, and the deuterium distribution of their oxidation products was determined by using ^1H and ^2H NMR spectra. Both samples were isotopically pure with no evidence of the other isomer within the limit of the experiment (<3%). The three deuterated products were separated by column chromatography as the 2,4-dinitrophenylhydrazone derivatives. The deuterium distribution of each of the isolated products was easily determined in an unambiguous fashion by comparison of the ^1H and ^2H NMR spectra of each product.

The α-hydroxyacetone product from $CH_2{=}CHCD_2OH$ (**2a**) was almost exclusively $CH_3C(O)CD_2OH$ while that from $CD_2{=}CHCH_2OH$ (**2b**) was $CD_2HC(O)CH_2OH$. These are the products expected from the route proposed for the formation of acetone from propylene.[8]

More interesting is the deuterium distribution of the β-hydroxypropanal and acrolein products. Both **2a** and **2b** gave the two possible isomers, $HOCD_2CH_2CHO$ (**1a**) and $HOCH_2CHDCDO$ (**1b**) in the same ratio (**1a**/**1b** = 1.9). This is the result expected from a symmetrical intermediate.[4] The surprising result was that **2a** gave 96% $CH_2{=}CHCDO$ (**3a**) and 4% $CD_2{=}CHCHO$ (**3b**) while the oxidation of **2b** gave 96% **3b** and 4% **3a**. The small

Scheme I

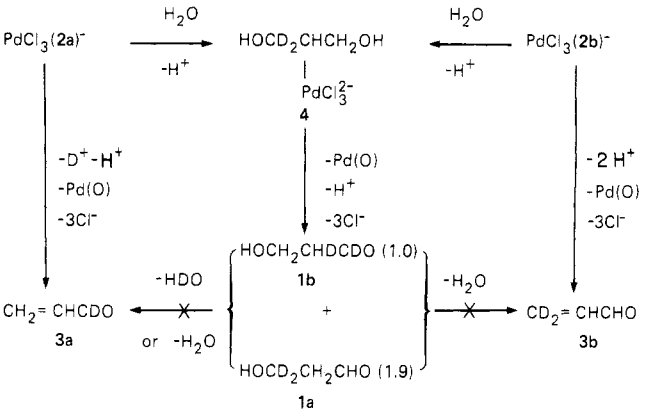

amounts of the other acrolein isomer in each case can be attributed to the Pd(II)-catalyzed isomerization of the starting deuterated allyl alcohol during the course of the oxidation.[9]

The deuterium-labeling results for acrolein and 1 are consistent with the reaction sequence shown in Scheme I. It is assumed that the allyl alcohol π complex $PdCl_3(2)^-$ is an intermediate in both oxidations.

As indicated in Scheme I, formation of 3 cannot involve attack on the olefin to form 1 followed by dehydration but rather direct abstraction of a hydride from the alcohol carbon.

The oxidation of saturated alcohols by palladium(II) salts to aldehydes and ketones was discovered by Berzelius[10] over 150 years ago, and since then the reaction has been studied by several workers.[11-13] Recently, the kinetics of the oxidation of methanol, ethanol, and 2-propanol by palladium(II) chloride in aqueous solution has been studied at temperatures between 66 and 99 °C.[14]

Oxidation of allyl alcohol is much faster than saturated alcohol and must reflect coordination of the C=C bond to palladium(II) (eq 2). The ratio of **1a**/**1b** = 1.9 is a

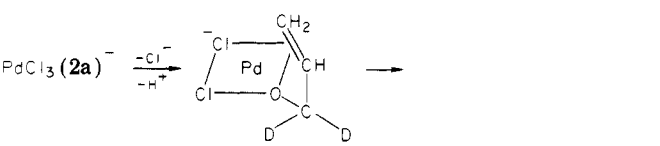

(2)

measure of the isotope effect k_H/k_D. It is in close agreement with value of 1.8 found for ethylene by a similar internal competition experiment using 1,2-ethylene-d_2.[15,16]

Studies are being carried out on other allyl alcohols such as crotyl- and methylvinyl alcohol to determine factors involved in the competition between unsaturated and saturated carbonyl product formation.

Acknowledgment. This investigation was supported by the Natural Sciences and Engineering Research Council

(2) For general discussion and references, see: Henry, P. M. "Palladium Catalyzed Oxidation of Hydrocarbons"; D. Reidel: Dordrecht, Holland 1980.
(3) Smidt, J.; Hafner, W.; Jira, R.; Sieber, R.; Sedlmeier, Jr. *Agnew. Chem.* **1959**, *71*, 176.
(4) Jira, R. *Tetrahedron Lett.* **1971**, 1225.
(5) Hall, R. H.; Stern, E. S. *J. Chem. Soc.* **1950**, 490.
(6) Schuetz, R. D.; Millard, F. W. *J. Org. Chem.* **1959**, *24*, 297.
(7) McMichael, K. D. *J. Am. Chem. Soc.* **1967**, *89*, 2943.
(8) Henry, P. M. *J. Am. Chem. Soc.* **1966**, *88*, 1595.
(9) Gregor, N.; Henry, P. M. *J. Am. Chem. Soc.* **1981**, *103*, 681.
(10) Berzelius, J. J. *Justus Liebigs Ann. Chem.* **1828**, *B13*, 435.
(11) Lloyd, W. G. *J. Org. Chem.* **1967**, *32*, 2816.
(12) Ketley, A. D.; Fisher, L. P. *J. Organomet. Chem.* **1968**, *13*, 243.
(13) Blackburn, T. F.; Schwartz, J. *J. Chem. Soc., Chem. Commun.* **1977**, 157.
(14) Kozhevnikov, I. V.; Taraban'ko, V. E.; Matveev, K. I. *Kinet. Katal.* **1980**, *21*, 940; *Kinet. Catal. (Engl. Transl.)* **1980**, 679.
(15) Henry, P. M. *J. Org. Chem.* **1973**, *38*, 2415.
(16) Kosaki, M.; Isemura, M.; Kitaura, Y.; Shinoda, S.; Saito, Y. *J. Mol. Catal.* **1977**, *2*, 351.

of Canada. We thank Mr. B. McDonald and Dr. R. Lenkinski for the Bruker 400-MHz ^1H and ^2H NMR measurements.

Registry No. Deuterium, 7782-39-0; allyl alcohol, 107-18-6; β-hydroxypropanal, 2134-29-4; α-hydroxyacetone, 116-09-6; acrolein, 107-02-8; hydride, 12184-88-2; $PdCl_4^{2-}$, 14349-67-8.

Silacyclopropene to Vinylsilylene Isomerization in Reactions of Silyl- and Hydridosilylenes with Acetylenes

Thomas J. Barton,* Stephanie A. Burns, and Gary T. Burns

Department of Chemistry, Iowa State University Ames, Iowa 50011

Received July 6, 1982

Summary: Evidence is presented that silacyclopropenes with silyl or hydride substitution on silicon thermally rearrange to vinylsilylenes.

The thermochemistry of silirenes **1** (silacyclopropenes) is a key feature in the longstanding question of the mechanism for disilin **2** formation in the reaction of silylenes (R_2Si:) and acetylenes. Among the several suggested mechanisms[1] for this reaction is the dimerization of initially formed silirenes across the silicon–carbon ring bond.[2] Until 1976 silirenes were unknown, and this

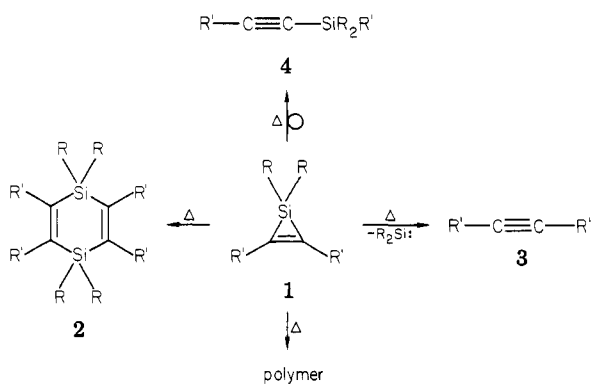

mechanism could not be tested. However, in the intervening 6 years that silirenes have been synthetically available, the reports of their thermal behavior has produced a chaotic picture. Thus, variably substituted silirenes are said to dimerize to disilins **2**,[3] polymerize,[4] extrude silylenes to form acetylenes **3**,[5] and isomerize to silylacetylenes **4**[6]—usually as remarkably clean processes.

It has also been suggested[7] that the reactions of silylenes with terminal acetylenes to produce ethynylsilanes **5** proceed not through direct C–H insertion but by rearrangement of a transient silirene intermediate. However, silirenes have never been observed in these reactions with terminal acetylenes.

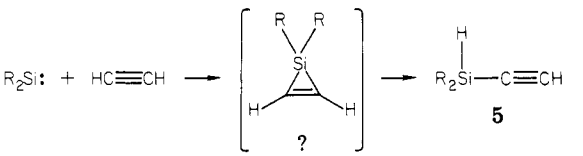

We report here several reactions[8] that demonstrate yet another thermal rearrangement pathway taken by these versatile silirenes. When 2-cyclopropyl-2-methoxyhexamethyltrisilane[9] (**6**) was pyrolyzed at 450 °C in a flow apparatus employing acetylene as the carrier gas, the pyrolysate contained in addition to the expected Me_3SiOMe (from α elimination[10]) only a single product, silane **12** in 52% yield [NMR (CS_2) δ −0.40–0.90 (m, 5 H), 0.16 (s, 9 H), 2.26 (d, 1 H, J = 1 Hz, collapses to s with *hν* at δ 4.23), 4.23 (m, 1 H), 6.68 (d of d, 1 H, J = 20 and 6 Hz, collapses to d, J = 20 Hz with *hν* at 4.23), 6.98 (d, 1 H, J = 20 Hz); calcd for $C_9H_{15}Si_2$ (M − CH_3) m/e 179.071 23, measured m/e 179.071 19]. The formation of **12** corresponds to the addition of expected silylene **7** to two molecules of acetylene. We propose that an initially formed silirene **8** rearranges to vinylsilylene **10**, either through a diradical intermediate or via prior isomerization to 1-silacyclopropene **9**.[11] Silylene **10** then can react with a second molecule of acetylene to form silirene **11** that, not being possessed with a good migrating group on silicon, rearranges to **12** by hydrogen migration to silicon.

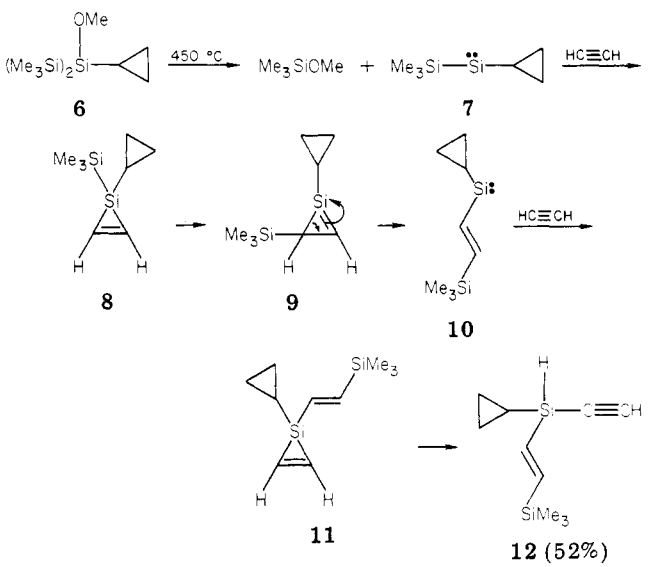

If this mechanistic pathway is correct, it should be operative for other silylsilylene/acetylene reactions, and we find this to be so. Copyrolysis of trisilane **13** and acetylene cleanly afforded the expected 3,6,6-trimethyl-3,5-disilahept-4-en-1-yne (**14**) in 48% yield [NMR (CS_2) δ 0.15 (s, 9 H), 0.29 (d, 3 H, J = 4 Hz, collapses to s with *hν* at δ 4.37), 2.29 (d, 1 H, J = 1 Hz, s with *hν* at δ 4.37), 4.37 (m, 1 H), 6.51 (d of d, 1 H, J = 20 and 6 Hz, collapses to d, J = 20

(1) For a review of the early mechanistic work on this reaction see: Barton, T. J.; Kilgour, J. A. *J. Am. Chem. Soc.* **1976**, *98*, 7746.
(2) Atwell, W. H.; Weyenberg, D. R. *J. Am. Chem. Soc.* **1968**, *90*, 3438.
(3) Isikawa, M.; Fuchikami, T.; Kumada, M. *J. Organomet. Chem.* **1977**, *142*, C45.
(4) Conlin, R. T.; Gaspar, P. P. *J. Am. Chem. Soc.* **1976**, *98*, 3715.
(5) Seyferth, D.; Annerelli, D. C.; Vick, S. C. *J. Am. Chem. Soc.* **1976**, *98*, 6382: and reference 6a.
(6) (a) Ishikawa, M.; Nishimura, K.; Sugisawa, H.; Kumada, M. *J. Organomet. Chem.* **1980**, *194*, 147. (b) Ishikawa, M.; Nakagawa, K.-I.; Kumada, M. *J. Organomet. Chem.* **1980**, *190*, 117.
(7) Haas, C. H.; Ring, M. A. *Inorg. Chem.* **1975**, *14*, 2253.
(8) The pyrolyses reported here were run on a 0.5–1.0-g scale, and yields are absolute by GC.
(9) The synthesis and spectral properties of **6** are being reported elsewhere: Burns, S. A.; Burns, G. T.; Barton, T. J. *J. Am. Chem. Soc.*, in press.
(10) Atwell, W. H.; Weyenberg, D. R. *J. Am. Chem. Soc.* **1968**, *90*, 3438.
(11) Barton, T. J.; Burns, G. T.; Goure, W. F.; Wulff, W. D. *J. Am. Chem. Soc.* **1982**, *104*, 1149.

0276-7333/83/2302-0199$01.50/0

of Canada. We thank Mr. B. McDonald and Dr. R. Lenkinski for the Bruker 400-MHz ^1H and ^2H NMR measurements.

Registry No. Deuterium, 7782-39-0; allyl alcohol, 107-18-6; β-hydroxypropanal, 2134-29-4; α-hydroxyacetone, 116-09-6; acrolein, 107-02-8; hydride, 12184-88-2; $PdCl_4^{2-}$, 14349-67-8.

Silacyclopropene to Vinylsilylene Isomerization in Reactions of Silyl- and Hydridosilylenes with Acetylenes

Thomas J. Barton,* Stephanie A. Burns, and Gary T. Burns

Department of Chemistry, Iowa State University Ames, Iowa 50011

Received July 6, 1982

Summary: Evidence is presented that silacyclopropenes with silyl or hydride substitution on silicon thermally rearrange to vinylsilylenes.

The thermochemistry of silirenes **1** (silacyclopropenes) is a key feature in the longstanding question of the mechanism for disilin **2** formation in the reaction of silylenes (R_2Si:) and acetylenes. Among the several suggested mechanisms[1] for this reaction is the dimerization of initially formed silirenes across the silicon–carbon ring bond.[2] Until 1976 silirenes were unknown, and this

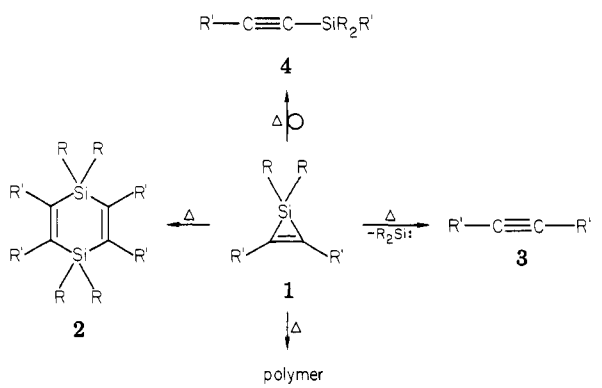

mechanism could not be tested. However, in the intervening 6 years that silirenes have been synthetically available, the reports of their thermal behavior has produced a chaotic picture. Thus, variably substituted silirenes are said to dimerize to disilins **2**,[3] polymerize,[4] extrude silylenes to form acetylenes **3**,[5] and isomerize to silylacetylenes **4**[6]—usually as remarkably clean processes.

It has also been suggested[7] that the reactions of silylenes with terminal acetylenes to produce ethynylsilanes **5** proceed not through direct C–H insertion but by rearrangement of a transient silirene intermediate. However, silirenes have never been observed in these reactions with terminal acetylenes.

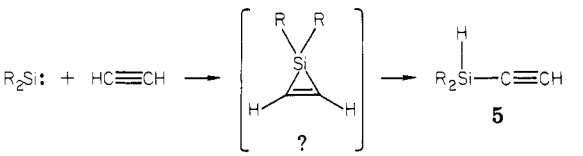

We report here several reactions[8] that demonstrate yet another thermal rearrangement pathway taken by these versatile silirenes. When 2-cyclopropyl-2-methoxyhexamethyltrisilane[9] (**6**) was pyrolyzed at 450 °C in a flow apparatus employing acetylene as the carrier gas, the pyrolysate contained in addition to the expected Me_3SiOMe (from α elimination[10]) only a single product, silane **12** in 52% yield [NMR (CS_2) δ −0.40–0.90 (m, 5 H), 0.16 (s, 9 H), 2.26 (d, 1 H, J = 1 Hz, collapses to s with *hν* at δ 4.23), 4.23 (m, 1 H), 6.68 (d of d, 1 H, J = 20 and 6 Hz, collapses to d, J = 20 Hz with *hν* at 4.23), 6.98 (d, 1 H, J = 20 Hz); calcd for $C_9H_{15}Si_2$ (M − CH_3) m/e 179.071 23, measured m/e 179.071 19]. The formation of **12** corresponds to the addition of expected silylene **7** to two molecules of acetylene. We propose that an initially formed silirene **8** rearranges to vinylsilylene **10**, either through a diradical intermediate or via prior isomerization to 1-silacyclopropene **9**.[11] Silylene **10** then can react with a second molecule of acetylene to form silirene **11** that, not being possessed with a good migrating group on silicon, rearranges to **12** by hydrogen migration to silicon.

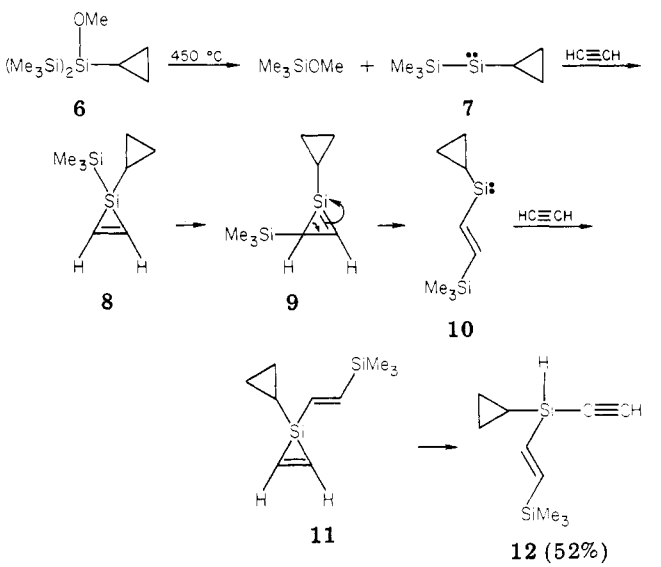

If this mechanistic pathway is correct, it should be operative for other silylsilylene/acetylene reactions, and we find this to be so. Copyrolysis of trisilane **13** and acetylene cleanly afforded the expected 3,6,6-trimethyl-3,5-disilahept-4-en-1-yne (**14**) in 48% yield [NMR (CS_2) δ 0.15 (s, 9 H), 0.29 (d, 3 H, J = 4 Hz, collapses to s with *hν* at δ 4.37), 2.29 (d, 1 H, J = 1 Hz, s with *hν* at δ 4.37), 4.37 (m, 1 H), 6.51 (d of d, 1 H, J = 20 and 6 Hz, collapses to d, J = 20

(1) For a review of the early mechanistic work on this reaction see: Barton, T. J.; Kilgour, J. A. *J. Am. Chem. Soc.* **1976**, *98*, 7746.
(2) Atwell, W. H.; Weyenberg, D. R. *J. Am. Chem. Soc.* **1968**, *90*, 3438.
(3) Isikawa, M.; Fuchikami, T.; Kumada, M. *J. Organomet. Chem.* **1977**, *142*, C45.
(4) Conlin, R. T.; Gaspar, P. P. *J. Am. Chem. Soc.* **1976**, *98*, 3715.
(5) Seyferth, D.; Annerelli, D. C.; Vick, S. C. *J. Am. Chem. Soc.* **1976**, *98*, 6382: and reference 6a.
(6) (a) Ishikawa, M.; Nishimura, K.; Sugisawa, H.; Kumada, M. *J. Organomet. Chem.* **1980**, *194*, 147. (b) Ishikawa, M.; Nakagawa, K.-I.; Kumada, M. *J. Organomet. Chem.* **1980**, *190*, 117.
(7) Haas, C. H.; Ring, M. A. *Inorg. Chem.* **1975**, *14*, 2253.
(8) The pyrolyses reported here were run on a 0.5–1.0-g scale, and yields are absolute by GC.
(9) The synthesis and spectral properties of **6** are being reported elsewhere: Burns, S. A.; Burns, G. T.; Barton, T. J. *J. Am. Chem. Soc.*, in press.
(10) Atwell, W. H.; Weyenberg, D. R. *J. Am. Chem. Soc.* **1968**, *90*, 3438.
(11) Barton, T. J.; Burns, G. T.; Goure, W. F.; Wulff, W. D. *J. Am. Chem. Soc.* **1982**, *104*, 1149.

0276-7333/83/2302-0199$01.50/0

Hz with $h\nu$ at δ 4.37), 6.79 (d, 1 H, J = 20 Hz); calcd for $C_7H_{13}Si_2$ (M − CH_3) m/e 153.0556, measured m/e 153.0559].

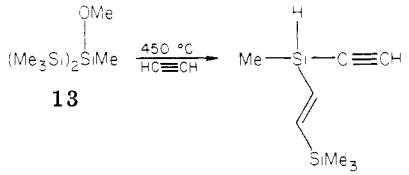

13 14 (48%)

This novel rearrangement of a silirene to a vinylsilylene is not restricted to systems having silicon available as a migrating group. Thus, generation of methylsilylene by the pyrolysis of 1,1,1,2-tetramethyldisilane in an acetylene stream afforded, in addition to Me_3SiH, 3-methyl-3-sila-pent-4-en-1-yne (**17**) in 26% yield [NMR (D_6C_6) δ 0.22 (d, 3 H, J = 4 Hz, s with $h\nu$ at δ 4.44), 2.12 (d, 1 H, J = 1.2 Hz, s with $h\nu$ at δ 4.44), 4.44 (m, 1 H, SiH), 5.92 (s, 3 H); m/e 96 (M^+, 25%), calcd for C_5H_7Si (M − H) m/e 95.0317, measured m/e 95.0314]. Thus, it appears that hydrogen migration from silicon to carbon occurs to transform silirene **15** to vinylsilylene **16** followed by the same addition–rearrangement sequence as before (vide supra). Independent generation of vinylsilylene **16** in an acetylene stream by the pyrolysis of vinyldisilane **18** was conducted to determine the viability of the intermediacy of **16** in this reaction. Me_3SiOMe and **17** were the sole volatile products.

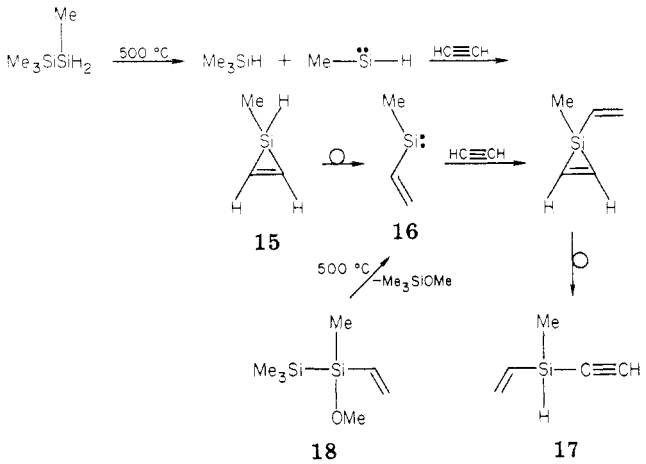

15 **16** **18** **17**

In order to demonstrate that these rearrangements were not unique to reactions of parent acetylene, copyrolysis of tetramethyldisilane and propyne was undertaken. Thus, generation of methylsilylene in a stream of propyne produced a remarkably clean reaction affording two products, **19** and **20**, in a combined yield of 73% (ca. 3:1). Structural assignments were made on the basis of spectral data [**19**: NMR ($DCCl_3$) δ 0.29 (d, 3 H, J = 4 Hz, s with $h\nu$ at δ 4.21), 1.83 (d of d, 3 H, J = 6 and 1 Hz), 1.91 (s, 3 H), 4.21 (m, 1 H, SiH), 5.59 (d of d of q, 1 H, J = 18, 3 and 1 Hz, d of d with $h\nu$ at δ 1.83), 6.29 (d of q, 1 H, J = 18 and 6 Hz, d of J = 18 Hz with $h\nu$ at δ 1.83); calcd for $C_7H_{12}Si$ (M^+, 39%) m/e 124.07083, measured m/e 124.07105. **20**: NMR ($DCCl_3$) δ 0.34 (d, 3 H, J = 4 Hz, s with $h\nu$ at δ 4.21), 1.87 (m, 6 H, overlapped allylic and acetylenic methyls), 4.21 (m, 1 H, SiH), 5.49 (m, 1 H, d of J = 4 Hz with $h\nu$ at δ 1.87), 5.68 (m, 1 H, d of J = 4 Hz with $h\nu$ at δ 1.87); mass spectrum virtually identical with that of **19**].

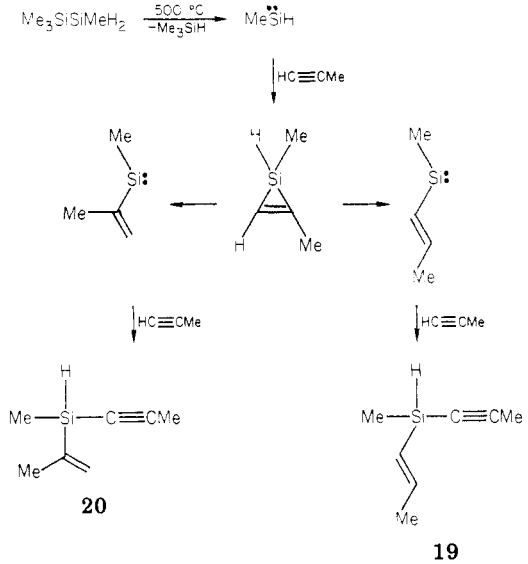

20 **19**

It is of interest to speculate that vinylsilylenes and appropriately substituted silirenes are in equilibrium at our thermal conditions. Methylvinylsilylene (**16**) is known to isomerize to 3-sila-1-butyne (**22**), and it has been suggested that this occurs through the intermediacy of silirene **15**.[11]

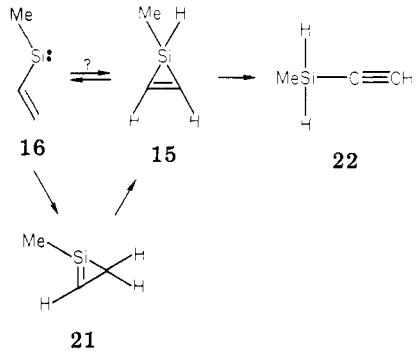

16 **15** **22** **21**

This work establishes a link between **15** and **16**, and, thus, lends strength to that proposal as it seems inevitable that **15** would in the absence of traps be bled from the equilibrium as **22**. The interesting question of whether 1-silacyclopropene **21** is an intermediate in an equilibrium between **15** and **16** has not been experimentally attacked in this work. However, the recent calculations of Gordon[12] suggest that **21** may be a thermodynamically unreasonable expectation.

Acknowledgment. The support of this research by the National Science Foundation is gratefully acknowledged.

Registry No. **6**, 83268-89-7; **7**, 83802-32-8; **12**, 83802-27-1; **13**, 69545-89-7; **14**, 83802-28-2; **17**, 83802-29-3; **19**, 83802-30-6; **20**, 83802-31-7; HC≡CH, 74-86-2; Me_3SiOMe, 1825-61-2; $Me_3SiSi(Me)H_2$, 81633-92-3; Me_3SiH, 993-077; HC≡CMe, 74-99-7; Methylsilylene, 55544-30-4.

(12) Gordon, M. S.; Koob, R. D. *J. Am. Chem. Soc.* **1981**, *103*, 2939.